

## Combination Therapy for Cancer Treatment

### Technical Field

[0001] This invention relates to the treatment of cancer with a Poly(ADP-ribose) polymerase (PARP) inhibitor and a topoisomerase inhibitor.

### Background

[0002] Liposomal irinotecan and PARP inhibitors are therapies useful in the treatment of cancer. Liposome encapsulated irinotecan formulations of the topoisomerase inhibitor irinotecan provide sustained exposure of irinotecan and the metabolite SN-38 in a tumor. ONIVYDE (irinotecan liposome injection) is an example of liposomal irinotecan recently approved in the United States for the treatment of patients with metastatic adenocarcinoma of the pancreas after disease progression following gemcitabine-based therapy. Poly(ADP-ribose) polymerases are a family of enzymes involved in DNA repair believed to act via two mechanisms: catalytic inhibition and trapping of PARP-DNA complexes, and inhibition of this repair pathway can result in cell death following DNA damage. PARP inhibitors are a new class of chemotherapeutic agents currently in development for the treatment of various cancer types.

[0003] While certain combinations of PARP and topoisomerase inhibitors have shown to be synergistic in in vitro assays, the clinical development of PARP inhibitor and topoisomerase inhibitor combinations has been limited due to increased toxicities and resultant dose reductions, thereby limiting the potential clinical utility of the combination. For example, significant myelosuppression was seen in a dose-escalation study of veliparib and topotecan, wherein the maximum tolerated dose was exceeded at the first planned dose level. Most PARP inhibitors are being developed to date solely as monotherapies. As a result, there is a need for methods to safely and effectively combine a PARP inhibitor with a Top1 inhibitor to treat cancer.

### Summary

[0004] The present disclosure provides methods of treating cancer by administering a topoisomerase inhibitor and a PARP inhibitor with reduced peripheral toxicity. This can be accomplished by administering the topoisomerase inhibitor in a form (e.g., liposomal irinotecan) that prolongs accumulation of the topoisomerase inhibitor in a tumor relative to sites outside the tumor, and then subsequently administering the PARP inhibitor(s) to the patient after an interval between the administration of the topoisomerase inhibitor and the PARP inhibitor. The interval can be selected to provide enough time for the topoisomerase

inhibitor (e.g., irinotecan and/or its metabolite SN-38) to clear plasma or tissue outside of the tumor to a greater extent than inside the tumor. Preferably, the interval is an effective topoisomerase-1 inhibitor plasma clearing interval. As used herein, the term “effective topoisomerase-1 inhibitor plasma clearing interval” (e.g., irinotecan plasma clearing interval) is that interval between concluding the administration of a topoisomerase-1 inhibitor formulation (e.g., liposomal irinotecan) and initiating the administration of one or more PARP inhibitors, where the time interval is selected to allow sufficient clearance of the topoisomerase-1 inhibitor (e.g., irinotecan or its active metabolite SN-38) from the blood plasma (or peripheral tissue) but allows an effective quantity of the topoisomerase-1 inhibitor (e.g., irinotecan and/or SN38) to remain in one or more tumors within the patient during the subsequent administration of the PARP inhibitor in an amount effective to provide a desired effect on the tumor (e.g., heightened combined toxicity localized within the tumor). Preferably, the PARP inhibitor is administered after an irinotecan plasma clearing interval of 3-5 days (e.g., 3, 4 or 5 days) after completing the administration of liposomal irinotecan on days 1 and 15 during each of one or more 28-day treatment cycles.

**[0005]** Methods of treating cancer disclosed herein include the treatment of solid tumors. In certain examples, the cancer treated can be selected from the group consisting of cervical cancer, ovarian cancer, triple negative breast cancer, non-small cell lung cancer, small cell lung cancer, gastrointestinal stromal tumors gastric cancer, pancreatic cancer, colorectal cancer, and a neuroendocrine cancer. Preferably, the cancer is cervical cancer.

**[0006]** The topoisomerase inhibitor can be provided as a liposome formulation. Preferably, the topoisomerase inhibitor is a liposomal irinotecan. The liposomal irinotecan can provide an irinotecan terminal elimination half-life of 26.8 hours and a maximal irinotecan plasma concentration of 38.0 micrograms/ml. In some examples, the liposomal irinotecan can include irinotecan sucrose octasulfate encapsulated within phospholipid vesicles having a size of about 110 nm. For example, the liposomal irinotecan can be the product ONIVYDE® (irinotecan liposome injection) (Merrimack Pharmaceuticals, Inc, Cambridge, MA), previously designated “MM-398.” The PARP inhibitor can include one or more compounds selected from the group consisting of niraparib, olaparib, veliparib, and rucaparib, preferably veliparib or olaparib.

**[0007]** The topoisomerase-1 inhibitor is preferably a liposomal irinotecan (e.g., MM-398), which can be administered at dose of 80 mg/m<sup>2</sup> (salt) irinotecan once every 2 weeks in combination with a PARP inhibitor (e.g., veliparib, olaparib, niraparib or rucaparib) administered daily during each two week cycle starting 3-5 days after administration of

liposomal irinotecan without administering the PARP inhibitor on days when the liposomal irinotecan is administered (e.g., without administering the PARP inhibitor 1, 2 or 3 days before the next liposomal irinotecan administration). Preferably, the PARP inhibitor is not administered within 3 days of (i.e., neither 3 days after nor 3 days before) the administration of liposomal irinotecan.

**[0008]** Specific methods of treating a cancer provided herein include administering an antineoplastic therapy consisting of the administration of liposomal irinotecan every 2 weeks (e.g., on days 1 and 15 of a 28-day treatment cycle), and the administration of a PARP inhibitor one or more times per day (e.g., twice per day) for one or more days (e.g., 7-9 days) starting at least 3 days (e.g., 3, 4 or 5 days) after each administration of the liposomal irinotecan, without administering other antineoplastic agents during the antineoplastic therapy. For example, one antineoplastic therapy is a 28-day treatment cycle consisting of: administering 70 mg/m<sup>2</sup> MM-398 liposomal irinotecan (free base) on days 1 and 15, and administering a therapeutically effective amount of the PARP inhibitor (e.g., 50-400 mg twice per day for veliparib) on each of days 5-12 and days 19-25 of the treatment cycle, where no other antineoplastic agent is administered during the treatment cycle. Another antineoplastic therapy is a 28-day treatment cycle consisting of: administering 70 mg/m<sup>2</sup> MM-398 liposomal irinotecan (free base) on days 1 and 15, and administering a therapeutically effective amount of the PARP inhibitor (e.g., 50-400 mg twice per day for veliparib) on each of days 3-12 and days 17-25 of the treatment cycle, where no other antineoplastic agent is administered during the treatment cycle.

**[0009]** In some examples, liposomal irinotecan and a PARP inhibitor can be combined in an antineoplastic therapy for the treatment of a solid tumor, comprising a 28-day antineoplastic therapy treatment cycle consisting of: administering the liposomal irinotecan on days 1 and 15 of the treatment cycle, and administering the PARP inhibitor on one or more days starting at least 3 days after the liposomal irinotecan and ending at least 1 day prior to administration of additional liposomal irinotecan. In some examples, the PARP inhibitor is not administered for at least 3 days after the administration of liposomal irinotecan. For example, the PARP inhibitor can be administered on one or more of days 5-12 of the antineoplastic therapy treatment cycle, and administered on one or more of days 19-25 of the antineoplastic therapy treatment cycle. In some examples, the PARP inhibitor is administered on one or more of days 3-12 of the antineoplastic therapy treatment cycle, and administered on one or more of days 17-25 of the antineoplastic therapy treatment cycle. In

some examples, the PARP inhibitor is not administered within 3 days before or after the administration of the liposomal irinotecan.

In addition, therapeutically effective doses of the topoisomerase inhibitor and PARP inhibitor compounds are provided herein. In some examples, each administration of liposomal irinotecan is administered at a dose of 80 mg/m<sup>2</sup> (salt) of MM-398. In some examples, each administration of the PARP inhibitor is administered at a dose of from about 20 mg/day to about 800 mg/day. Each administration of the PARP inhibitor can be administered once or twice daily at a dose of from about 20 mg/day to about 400 mg/day.

#### **Brief Description of the Drawings**

**[0010]** Figure 1A is a graph showing the results of a cell viability *in vitro* measurement of ME-180 human cervical cancer cells treated with the topoisomerase 1 inhibitor SN-38 and various PARP inhibitors.

**[0011]** Figure 1B is a graph showing the results of a cell viability *in vitro* measurement of MS-751 human cervical cancer cells treated with the topoisomerase 1 inhibitor SN-38 and various PARP inhibitors.

**[0012]** Figure 1C is a graph showing the results of a cell viability *in vitro* measurement of C-33A human cervical cancer cells treated with the topoisomerase 1 inhibitor SN-38 and various PARP inhibitors.

**[0013]** Figure 1D is a graph showing the results of a cell viability *in vitro* measurement of SW756 human cervical cancer cells treated with the topoisomerase 1 inhibitor SN-38 and various PARP inhibitors.

**[0014]** Figure 1E is a graph showing the results of a cell viability *in vitro* measurement of SiHa human cervical cancer cells treated with the topoisomerase 1 inhibitor SN-38 and various PARP inhibitors.

**[0015]** Figure 2A is a graph showing the results of *in vitro* measurement of % cell number over time for DMS-114 small cell lung cancer cells treated with the topoisomerase inhibitor SN-38 and the PARP inhibitor rucaparib.

**[0016]** Figure 2B is a graph showing the results of *in vitro* measurement of % cell number over time for NCI-H1048 small cell lung cancer cells treated with the topoisomerase inhibitor SN-38 and the PARP inhibitor rucaparib.

**[0017]** Figure 2C is a graph showing the results of *in vitro* measurement of % cell number over time for CFPAC-1 pancreatic cancer cells treated with the topoisomerase inhibitor SN-38 and the PARP inhibitor rucaparib.



**[0018]** Figure 2D is a graph showing the results of *in vitro* measurement of % cell number over time for BxPC-3 pancreatic cancer cells treated with the topoisomerase inhibitor SN-38 and the PARP inhibitor rucaparib.

**[0019]** Figure 2E is a graph showing the results of *in vitro* measurement of % cell number over time for MDA-MB-231 triple negative breast cancer (TNBC) cancer cells treated with the topoisomerase inhibitor SN-38 and the PARP inhibitor rucaparib.

**[0020]** Figure 3A is a graph showing the results of *in vitro* measurement of cell survival for BT-20 triple negative breast cancer (TNBC) cancer cells treated with the topoisomerase inhibitor SN-38 and the PARP inhibitor talazoparib.

**[0021]** Figure 3B is a graph showing the results of *in vitro* measurement of cell survival for HCC38 triple negative breast cancer (TNBC) cancer cells treated with the topoisomerase inhibitor SN-38 and the PARP inhibitor talazoparib.

**[0022]** Figure 4 depicts a graphical representation of a murine tolerability study design comparing MM-398 and olaparib as a monotherapy or in combination using a fixed dose of MM-398 and varying doses of olaparib, with various dosing schedules for different groups.

**[0023]** Figure 5A is a graph showing the results of a murine tolerability study of a combination of MM-398 and veliparib, measuring % change in bodyweight after administration of 15 mg/kg of MM-398 on day 1, and 50 mg/kg of veliparib on days 2, 3, and 4.

**[0024]** Figure 5B is a graph showing the results of a murine tolerability study of a combination of MM-398 and veliparib, measuring % change in bodyweight after administration of 28 mg/kg of MM-398 on day 1, and 50 mg/kg of veliparib on days 3, 4, and 5.

**[0025]** Figure 5C is a graph showing the results of a murine tolerability study of a combination of MM-398 and veliparib, measuring % change in bodyweight after administration of 50 mg/kg of MM-398 on day 1, and 50 mg/kg of veliparib on days 4, 5, and 6.

**[0026]** Figure 6A is a graph comparing the results of a murine tolerability study measuring % change in bodyweight after administration of 10 mg/kg of MM-398 (+PBS); 200 mg/kg/day of Olaparib; 10 mg/kg of MM-398 (+PBS) with 200 mg/kg/day of Olaparib on days 1-4; and 10 mg/kg of MM-398 (+PBS) with 200 mg/kg/day of Olaparib on days 1-5.

**[0027]** Figure 6B is a graph comparing the results of a murine tolerability study measuring % change in bodyweight after administration of 10 mg/kg of MM-398 (+PBS) and 200 mg/kg/day of Olaparib.

[0028] Figure 6C is a graph comparing the results of a murine tolerability study measuring % change in bodyweight after administration of 10 mg/kg of MM-398 (+PBS); 10 mg/kg of MM-398 (+PBS) with 200 mg/kg/day of Olaparib on days 1-4; and 10 mg/kg of MM-398 (+PBS) with 200 mg/kg/day of Olaparib on days 1-5.

[0029] Figure 6D is a graph comparing the results of a murine tolerability study measuring % change in bodyweight after administration of 10 mg/kg of MM-398 (+PBS); 10 mg/kg of MM-398 (+PBS) with 200 mg/kg/day of Olaparib on days 1-5; 10 mg/kg of MM-398 (+PBS) with 150 mg/kg/day of Olaparib on days 1-5; and 10 mg/kg of MM-398 (+PBS) with 265 mg/kg/day of Olaparib on days 3-5.

[0030] Figure 7A is a graph showing data from a mouse xenograft study using MS751 cervical cancer cells in a murine model treated with liposomal irinotecan (5 mg/kg MM398) and/or the PARP inhibitor veliparib on days 4-6 after administration of MM398.

[0031] Figure 7B is a graph showing data from a mouse xenograft study using MS751 cervical cancer cells in a murine model treated with liposomal irinotecan (2 mg/kg MM398) and/or the PARP inhibitor veliparib on days 4-6 after administration of MM398.

[0032] Figure 8A is a graph that depicts the *in vivo* tolerability of 50 mg/kg dose of MM-398 in combination with 50 mg/kg veliparib given on days 1, 2, and 3; or 2, 3, and 4; or 3, 4, and 5 after administration of the MM-398.

[0033] Figure 8B is a graph that depicts the *in vivo* tolerability of 28 mg/kg dose of MM-398 in combination with 50 mg/kg veliparib given on days 1, 2, and 3; or 2, 3, and 4; or 3, 4, and 5 after administration of the MM-398.

[0034] Figure 9A is a graph showing data from a mouse xenograft study using MS751 cervical cancer cells in a murine model treated with liposomal irinotecan (5 mg/kg MM398) and/or the PARP inhibitor veliparib (50 mpk) on days 3-5 starting after administration of MM398.

[0035] Figure 9B is a graph showing survival data from a mouse xenograft study using MS751 cervical cancer cells in a murine model treated with liposomal irinotecan (5 mg/kg MM398) and/or the PARP inhibitor veliparib (50 mpk) on days 3-5 starting after administration of MM398.

[0036] Figure 9C is a graph that depicts the effect of MM-398 in combinations with veliparib in MS751 xenograft murine model treated with liposomal irinotecan (5 mg/kg MM398) and/or the PARP inhibitor veliparib (50 mpk) on days 3-5 starting after administration of MM398.

[0037] Figure 10 is a graph showing data from a mouse xenograft study using C33 cervical cancer cells in a murine model treated with liposomal irinotecan (2 mg/kg MM398) and/or the PARP inhibitor veliparib (50 mpk) on days 3-5 starting after administration of MM398.

[0038] Figure 11 is a graph showing survival data from a mouse xenograft study using C33 cervical cancer cells in a murine model treated with liposomal irinotecan (5 mg/kg MM398) and/or the PARP inhibitor veliparib (50 mpk) on days 3-5 starting after administration of MM398.

[0039] Figure 12 depicts the effect of MM-398 in combination with veliparib in C33A xenograft model and body weight, where veliparib was dosed 72 h following liposomal irinotecan (5 mg/kg MM398) and/or the PARP inhibitor veliparib (50 mpk) on days 3-5 starting after administration of MM398.

[0040] Figure 13A is a graph showing the *in vitro* activity (IC<sub>50</sub>) for multiple cervical cancer cell lines treated with veliparib and SN38, added together or with the veliparib added 24 hours after the SN38.

[0041] Figure 13B is a graph showing the cell viability (CTG assay) in nude mice with cervical cancer tumors, injected with a single dose of MM-398 (10 mg/kg) followed by measurement of irinotecan and SN38 content in the tumor measured by LC-MS.

[0042] Figure 14 is a graphical representation of a phase I study design employing the combinations of MM-398 (nal-IRI) and veliparib.

[0043] Figure 15A is a schematic showing a use of ferumoxytol (FMX) as a predictive biomarker for cancer treatment with liposomal irinotecan (e.g., MM-398).

[0044] Figure 15B is a graph showing FMX concentration of individual patient lesions was calculated using a standard curve from MR images obtained 24h post-FMX injection.

[0045] Figure 15C is a graph showing FMX signal from lesions at 24h are grouped relative to the median value observed in the FMX MRI evaluable lesions and compared to the best change in lesion size based on CT scans (data available from 9 patients; total of 31 lesions).

[0046] Figure 16A is a graph showing the tumor SN-38 (nmol/L) measured in tumors after administration of free (non-liposomal) irinotecan (CPT-11) at 50 mg/kg or 100 mg/kg, compared to the administration of MM-398 (5 mg/kg, 10 mg/kg or 20 mg/kg).

[0047] Figure 16B is a graph showing levels of tumor growth inhibition as a function of time of SN-38 concentration required to yield tumor response.

### Detailed Description

[0048] The present disclosure provides for methods of administering a combination of a topoisomerase-1 (Top1) inhibitor (e.g., irinotecan and/or its metabolite SN-38) and a PARP inhibitor to a tumor with reduced peripheral toxicity. The Top1 inhibitor can be administered in a liposome formulation resulting in the prolonged accumulation of the Top1 inhibitor in a solid tumor compared to peripheral plasma and/or healthy organs. Subsequently, a PARP inhibitor can be administered after a period of time permitting a reduction in the amount of the Top1 inhibitor outside the tumor relative to the amount of Top1 inhibitor within the tumor. Preferably, the Top1 inhibitor is administered as a liposomal irinotecan that provides SN-38 to a solid tumor.

[0049] Methods of treating a cancer are provided, as well as therapeutic uses of PARP inhibitor compounds in combination with liposomal irinotecan formulations for the treatment of cancer, particularly cancer comprising solid tumors. These uses and methods can provide a treatment regimen comprising: (a) administering to a patient in need thereof an effective amount of an irinotecan liposomal formulation; and (b) after completion of the administration of the Top1 inhibitor, administering to the patient an effective amount of a PARP inhibitor, wherein the PARP inhibitor is administered to the patient following an interval that allows for a reduction in peripheral toxicity as compared to simultaneous administration of the Top1 inhibitor and the PARP inhibitor. The interval can be selected to provide time for sufficient clearance of the Top1 inhibitor (e.g., either or both of irinotecan and SN-38) from the blood plasma to avoid peripheral toxicity due to the synergistic toxic effects of the combination of Top1 inhibitor and PARP inhibitor, while allowing an effective quantity of Top1 inhibitor to remain in one or more tumors within the patient for the subsequent administration of the PARP inhibitor to have a desired synergistic therapeutic effect. This treatment regimen can preferably provide one or more attributes, which may include increased efficacy of the combination as compared to single agent treatment; reduced side effects, dosing the drugs at a higher dose compared with administration of the combination of a PARP inhibitor and a non-liposomal Top1 inhibitor.

[0050] The uses and methods disclosed herein are based in part on experiments evaluating the combination of a topoisomerase 1 inhibitor (e.g., liposomal irinotecan or SN-38) and a PARP inhibitor in both pre-clinical and human clinical studies. The topoisomerase 1 inhibitor was administered in certain *in vitro* animal models using a formulation delivering a more prolonged exposure of the topoisomerase 1 inhibitor (e.g., irinotecan and/or the irinotecan active metabolite designated SN-38) within solid tumors than in peripheral tissue

and plasma outside the tumor. Combinations of the topoisomerase 1 inhibitor SN38 and/or irinotecan and PARP inhibitor compounds were tested in various *in vitro* experiments. As detailed in Example 1, the *in vitro* testing of multiple combinations of a topoisomerase 1 inhibitor (SN38) and various PARP inhibitors in more than 20 different cancer cell lines (including cervical, breast, ovarian, colorectal, pancreatic, and small cell lung cancer cell lines) all demonstrated decreased cancer cell line viability (Figures 1A, 1B, 1C, 1D, 1E, 2A, 2B, 2C, 2D, 2E, and 13A). The liposomal irinotecan (MM398) demonstrated greater tumor volume reduction than non-liposomal (free) irinotecan (CPT11) in mouse xenograft studies across multiple types of cancer cell lines (including breast, ovarian, colorectal and pancreatic cancer cell lines).

**[0051]** As detailed in Example 2, the tolerability of a topoisomerase 1 inhibitor (liposomal irinotecan) administered in combination with various PARP inhibitors was evaluated by measuring the change in animal (mouse) body weight in multiple murine models by comparing various dosing schedules. In some experiments, both liposomal irinotecan and a PARP inhibitor were administered together on the same day (day 1). In other experiments, the PARP inhibitor was first administered daily starting 2, 3 or 4 days after each administration of the liposomal irinotecan. The PARP inhibitor was administered for multiple consecutive days (e.g., 3 consecutive days), and not administered on the same day as the topoisomerase 1 inhibitor. As detailed in multiple experiments herein, administration of the PARP inhibitor at least one day after the liposomal irinotecan resulted in improved tolerability of comparable combined doses of the PARP inhibitor and liposomal irinotecan (MM-398) as measured by change in percent bodyweight in the animal (e.g., Figures 6A, 6B, 6C, 6D, 8A, and 8B). Delaying the administration of the PARP inhibitor 2, 3 or 4 days after administration of the liposomal irinotecan led to greater overall tolerability of a combined administration of the liposomal irinotecan and the PARP inhibitor, compared to the administration of the liposomal irinotecan and the PARP inhibitor on the same day. For example, administration of veliparib on days 2, 3 and 4 after administration of liposomal irinotecan on day 1 resulted in successively increased tolerability (measured as higher percent mouse bodyweight) of the combination of these two drugs (observed at 15 mg/kg liposomal irinotecan dose on day 1 followed by veliparib dosing on days 2, 3 and 4 (Figure 5A); at 28 mg/kg liposomal irinotecan dosage on day 1 followed by veliparib dosing on days 3, 4, and 5 (Figures 5B and 8B), or followed by veliparib dosing on days 2, 3 and 4 (Figure 8B); and at 50 mg/kg liposomal irinotecan dose on day 1 followed by veliparib dosing on days 4, 5 and 6 (Figure 5C), or followed by veliparib dosing on days 2, 3 and 4 or followed by veliparib

dosing on days 3, 4, and 5 (Figure 8A)). Similarly, administering olaparib starting on days 2 or 3 after MM398 resulted in comparable or improved tolerability compared to administration of both agents on day 1. For example, administering a 200 mg/kg dose of olaparib to mice on days 2, 3, 4 and 5 after administration of 10 mg/kg MM398 liposomal irinotecan on day 1 resulted in a lower reduction in bodyweight than administering the same doses of both MM398 and olaparib on days 1, 2, 3 and 4.

**[0052]** Combinations of a topoisomerase 1 inhibitor (SN38 and/or irinotecan) and PARP inhibitor compounds were tested in various preclinical *in vivo* experiments to evaluate the effectiveness of the administration of various PARP inhibitors starting 3 or 4 days after administration of the liposomal topoisomerase 1 inhibitor MM398. As detailed in Example 3, the administration of liposomal irinotecan (MM398) on day 1 followed by the PARP inhibitor veliparib on either days 3, 4 and 5 or days 4, 5, and 6, resulted in decreased tumor volume and extended percent survival in mouse xenograft models of cervical cancer using two different cell lines (MS751 and C33A) (Figures 7A, 7B, 9A, 9B, 10 and 11).

**[0053]** Based in part on these experiments, methods of treating human cancer include the administration of a PARP inhibitor one or more days (preferably 2, 3, 4, 5 or 6 days) after the administration of liposomal topoisomerase inhibitor such as liposomal irinotecan. Preferably, the PARP inhibitor and the liposomal irinotecan are not administered on the same day. Example 5 provides preferred embodiments for the use of liposomal irinotecan and one or more PARP inhibitors for the treatment of human cancer, such as cervical cancer, while other embodiments (e.g., Table 3) are also provided.

*Topoisomerase Inhibitors, Including Liposomal Irinotecan and Camptothecin Conjugates*

**[0054]** The topoisomerase inhibitor can be administered in any form that provides for the prolonged retention of a topoisomerase-1 inhibitor activity within a tumor compared to outside the tumor, after administration of the topoisomerase inhibitor. For example, the topoisomerase inhibitor can be a formulation that delivers SN-38 to a tumor cell *in vivo*, administered in an amount and manner providing a higher concentration of the SN-38 within the tumor than outside the tumor for a period of time after administration of the topoisomerase inhibitor. Suitable formulations of topoisomerase inhibitors include conjugate molecules of a topoisomerase inhibitor (e.g., camptothecin conjugated to a polymer or antibody), liposomes containing a topoisomerase inhibitor or other targeted release formulation technologies. The Top1 inhibitor is preferably formulated to provide prolonged accumulation in a tumor site, compared to accumulation in healthy (non-cancer) tissue

outside the tumor site (e.g., in the plasma and/or healthy organs such as colon, duodenum, kidney, liver, lung and spleen). Various Top1 inhibitor liposomal formulations are described in U.S. Patent No. 8,147,867 and U.S. Patent Application Publication No. 2015/0005354, both of which are incorporated herein by reference.

**[0055]** In one embodiment, the topoisomerase inhibitor is SN-38, camptothecin or a compound that is converted to SN-38 within the body, such as irinotecan. Irinotecan and SN-38 are examples of Top1 inhibitors. Irinotecan is converted by esterase enzymes into the more active metabolite, SN-38. The chemical name of irinotecan is (*S*)-4,11-diethyl-3,4,12,14-tetrahydro-4-hydroxy-3,14-dioxo1*H*-pyrano[3',4':6,7]-indolizino[1,2-*b*]quinolin-9-yl-[1,4'-bipiperidine]-1'-carboxylate. Irinotecan hydrochloride trihydrate is also referred to by the name CPT-11 and by the trade name CAMPTOSAR®.

**[0056]** The topoisomerase inhibitor can be camptothecin conjugated to a biocompatible polymer such as a cyclodextrin or cyclodextrin analog (e.g., sulfonated cyclodextrins). For example, the topoisomerase inhibitor can be a cyclodextrin-containing polymer chemically bound to a camptothecin, irinotecan, SN-38 or other topoisomerase 1 inhibitor compound. A cyclodextrin-camptothecin conjugated topoisomerase 1 inhibitor can be administered at a pharmaceutically acceptable dose including 6, 12, or 18 mg/m<sup>2</sup> weekly administration, or 12, 15 or 18 mg/m<sup>2</sup> biweekly administration. Examples of camptothecin-cyclodextrin conjugate topoisomerase 1 inhibitors (e.g., the cyclodextrin-containing polymer conjugate with camptothecin designated "CRLX101"), and related intermediates for preparing the same, are disclosed, for example, in Greenwald et al., *Bioorg. Med. Chem.*, 1998, 6, 551-562, as well as United States Patent Application 2010/0247668, United States Patent Application 2011/0160159 and United States Patent Application 2011/0189092

**[0057]** The topoisomerase inhibitor can also be a liposomal formulation of a topoisomerase inhibitor such as irinotecan, camptothecin or topotecan. Liposomal irinotecan (e.g., MM-398, also called "nal-IRI") is a highly stabilized liposomal formulation of irinotecan that provides for sustained exposure of irinotecan, and the active metabolite SN-38 in the tumor to a higher proportion of cells during the more sensitive S-phase of the cell cycle. MM-398 is a liposomal irinotecan that has shown promising preclinical and clinical activity in a range of cancer types, and was recently approved in the United States in combination with 5-FU/LV for patients with metastatic adenocarcinoma of the pancreas after disease progression following gemcitabine-based therapy. Compared with free irinotecan, nal-IRI has an extended PK profile with prolonged local tumor exposure of MM-398 and SN-38. Since SN-38 is cleared more quickly from normal tissues than from tumor, it is

hypothesized that delayed dosing of veliparib relative to MM-398 will allow for the expected window of maximum irinotecan-induced toxicity to pass in the absence of concurrent veliparib toxicity. However, the tumor levels of SN-38 are predicted to be sustained upon subsequent veliparib dosing, therefore maintaining the ability of both drugs to act on tumor tissue simultaneously and maintain synergy.

**[0058]** One suitable liposomal Top1 inhibitor formulation is liposomal irinotecan available under the brand name ONIVYDE® (irinotecan liposome injection) (Merrimack Pharmaceuticals, Inc, Cambridge, MA), previously designated “MM-398” prior to FDA approval, and liposomal irinotecan products that are bioequivalent to ONIVYDE. The ONIVYDE/MM-398 (irinotecan liposome injection) includes irinotecan as an irinotecan sucrosfate salt encapsulated in liposomes for intravenous use. The drug product liposome is a small unilamellar lipid bilayer vesicle, approximately 110 nm in diameter, which encapsulates an aqueous space which contains irinotecan in a gelated or precipitated state, as the sucrosfate salt. The liposome carriers are composed of 1,2-distearoyl-sn-glycero-3-phosphocholine (DSPC), 6.81 mg/mL; cholesterol, 2.22 mg/mL; and methoxy-terminated polyethylene glycol (MW 2000)-distearoylphosphatidylethanolamine (MPEG-2000-DSPE), 0.12 mg/mL. Each mL also contains 2-[4-(2-hydroxyethyl)piperazin-1-yl]ethanesulfonic acid (HEPES) as a buffer, 4.05 mg/mL; sodium chloride as isotonicity reagent, 8.42 mg/mL. ONIVYDE/MM-398 is believed to include about 80,000 molecules of irinotecan in a gelated or precipitated state as a sucrosfate salt encapsulated in a liposome of about 100 nm in diameter.

**[0059]** As used herein, unless otherwise indicated, the dose of irinotecan in ONIVYDE/MM-398 refers to the dose of irinotecan based on the molecular weight of irinotecan hydrochloride trihydrate (i.e., “(salt)” dose), unless clearly indicated otherwise. Alternatively, the irinotecan dose in ONIVYDE/MM-398 may also be expressed as the irinotecan free base (i.e., “(base)” dose). Converting a dose based on irinotecan (salt) dose to an irinotecan (base) dose based on irinotecan free base is accomplished by multiplying the dose based on irinotecan hydrochloride trihydrate with the ratio of the molecular weight of irinotecan free base (586.68 g/mol) and the molecular weight of irinotecan hydrochloride trihydrate (677.19 g/mol). This ratio is 0.87 which can be used as a conversion factor. For example, the 80 mg/m<sup>2</sup> irinotecan (salt) dose of ONIVYDE/MM-398 refers to the amount of irinotecan based on irinotecan hydrochloride trihydrate, and is equivalent to a 69.60 mg/m<sup>2</sup> irinotecan (base) dose of ONIVYDE/MM-398 based on irinotecan free base (80 x 0.87). In the clinic this is rounded to 70 mg/m<sup>2</sup> to minimize any potential dosing errors. Similarly, a



clinical dose of 120 mg/m<sup>2</sup> (salt) dose of ONIVYDE/MM-398 (based on the corresponding amount of irinotecan hydrochloride trihydrate providing the same amount of irinotecan free base) is equivalent to 100 mg/m<sup>2</sup> (base) dose of ONIVYDE/MM-398 (based on the actual amount of irinotecan free base administered in the liposomal irinotecan).

[0060] ONIVYDE/MM-398 has been shown to improve the pharmacokinetic and safety profile of the free irinotecan, through high retention of the irinotecan molecules within the liposome, by extending the half-life of irinotecan in the plasma, and increased exposure of tumor cells to irinotecan compared with other organs. Table 1 below provides a summary of median (%IQR)<sup>\*</sup> total irinotecan and SN-38 pharmacokinetic parameters observed in patients with solid tumors after administration of ONIVYDE/MM-398 at a dose of 80 mg/m<sup>2</sup> irinotecan (salt) dose administered once every 2 weeks.

**Table 1**

Dose (mg/m <sup>2</sup> )	Total Irinotecan					SN-38		
	C <sub>max</sub> [μg/ml]	t <sub>1/2</sub> [h] <sup>†</sup>	AUC <sub>0-∞</sub> [h·μg/ml] <sup>†</sup>	V <sub>d</sub> [L/m <sup>2</sup> ] <sup>†</sup>	CL [L h/m <sup>2</sup> ] <sup>†</sup>	C <sub>max</sub> [ng/ml]	t <sub>1/2</sub> [h] <sup>†</sup>	AUC <sub>0-∞</sub> [h·ng/ml] <sup>†</sup>
80 (n=25)	38.0 (36%)	26.8 (110%)	1030 (169%)	2.2 (55%)	0.077 (143%)	4.7 (89%)	49.3 (103%)	587 (69%)

\* %IQR: % Interquartile Ratio =  $\frac{\text{Interquartile-range}}{\text{Median}} \cdot 100\%$

† t<sub>1/2</sub>, AUC<sub>0-∞</sub> and V<sub>d</sub> were only calculated for a subset of patients with sufficient number of samples in the terminal phase: n=23 for total irinotecan; n=13 for SN-38.

C<sub>max</sub>: Maximum plasma concentration

t<sub>1/2</sub>: Terminal elimination half-life

AUC<sub>0-∞</sub>: Area under the plasma concentration curve extrapolated to time infinity

V<sub>d</sub>: Volume of distribution

[0061] For ONIVYDE/MM-398, over the dose range of 60 to 180 mg/m<sup>2</sup>, the maximum concentrations of both total irinotecan and SN-38 increase linearly with dose. The AUCs of total irinotecan increase linearly with dose; the AUCs of SN-38 increase less than proportionally with dose. The half-lives of both total irinotecan and SN-38 do not change with dose. In a pooled analysis from 353 patients, higher plasma SN-38 C<sub>max</sub> was associated with increased likelihood of experiencing neutropenia, and higher plasma total irinotecan C<sub>max</sub> was associated with increased likelihood of experiencing diarrhea. Direct measurement of liposomal irinotecan shows that 95% of irinotecan remains liposome-encapsulated during circulation. The volume of distribution of MM-398 80 mg/m<sup>2</sup> is 2.2 L/m<sup>2</sup>. The volume of distribution of Irinotecan HCl is between 110 L/m<sup>2</sup> (dose=125mg/m<sup>2</sup>) and 234 L/m<sup>2</sup> (dose=340 mg/m<sup>2</sup>). The plasma protein binding of MM-398 is <0.44% of the total irinotecan

in MM-398. The plasma protein binding of irinotecan HCl is 30% to 68% and approximately 95% of SN-38 is bound to human plasma proteins. The plasma clearance of total irinotecan from MM-398 80 mg/m<sup>2</sup> is 0.077 L/h/m<sup>2</sup> with a terminal half live of 26.8 h. Following administration of irinotecan HCl 125 mg/m<sup>2</sup>, the plasma clearance of irinotecan is 13.3 L/h/m<sup>2</sup> with a terminal half live of 10.4 h.

**[0062]** Examples of an effective amount of liposomal irinotecan provided as MM-398 include doses (salt) from about 60 mg/m<sup>2</sup> to about 120 mg/m<sup>2</sup>, including doses of 70, 80, 90, 100, 110 or 120 mg/m<sup>2</sup> (based on the weight of irinotecan hydrochloride trihydrate salt) and doses of 50, 60, 70, 80, 95, and 100 mg/m<sup>2</sup> (based on the weight of irinotecan free base), each given once every two (2) weeks (e.g., on days 1 and 15 of a 28 day antineoplastic treatment cycle). In some embodiments, the effective amount of MM-398 is about 80 mg/m<sup>2</sup> (salt), optionally administered in combination with 400 mg/m<sup>2</sup> of leucovorin over 30 minutes, followed by intravenous administration of 2400 mg/m<sup>2</sup> of 5-fluorouracil as an infusion over 46 hours. In some embodiments, the effective amount of MM-398 is about 90 mg/m<sup>2</sup> (free base).

**[0063]** Liposomal irinotecan MM-398 extends the tumor exposure of the topoisomerase 1 inhibitor SN-38. MM-398 liposomal irinotecan was found to be more active than irinotecan in multiple murine xenograph models. The duration of tumor exposure to the topoisomerase 1 inhibitor SN-38 above a threshold minimum concentration (e.g., 120 nM) correlated with anti-tumor activity of the liposomal irinotecan. In addition, MM-398 liposomal irinotecan can provide prolonged SN-38 tumor durations that exceed those provided by non-liposomal irinotecan. For example, Figure 13B depicts tumor content of SN-38 in multiple murine cervical cancer models. Nude mice bearing cervical tumors were injected with a single dose of MM-398 at 10 mg/kg and tumor content of CPT-11 and SN-38 were measured by LC-MS. Figure 16A is a graph showing the tumor SN-38 (nmol/L) measured in tumors after administration of free (non-liposomal) irinotecan (CPT-11) at 50 mg/kg or 100 mg/kg, compared to the administration of MM-398 (5 mg/kg, 10 mg/kg or 20 mg/kg). The graph depicts the prolonged accumulation of SN-38 (concentration) measured in a tumor after liposomal irinotecan (MM-398) administration compared to other organs, obtained using HT-29 colorectal cancer (CRC) tumor xenograft-bearing mice. Figure 16B is a graph showing levels of tumor growth inhibition as a function of time of SN-38 concentration required to yield tumor response. Levels of SN-38 of 120 nM were identified as the SN-38 tumor concentration required to yield tumor response. The in vitro IC<sub>50</sub> for SN-38 effect on cell line can be used as an in vivo threshold (GI<sub>50</sub> for HT-29 was observed to be about 60

nM). MM-398 liposomal irinotecan was observed to prolong the duration of SN-38 exposure at doses of 10 mg/kg and 20 mg/kg.

*PARP Inhibitors*

**[0064]** PARPs are a family of enzymes involved in DNA repair that act via two mechanisms: catalytic inhibition and trapping of PARP-DNA complexes, and inhibition of this repair pathway can result in cell death following DNA damage. In preferred embodiments, combining PARP inhibitors with Top1 inhibitors results in increased efficacy in the clinic compared to either agent alone. While it has been demonstrated that synergism between PARP inhibitors and Top1 inhibitors is due to PARP catalytic inhibition, and does not involve PARP trapping, this promising preclinical activity has given rise to unacceptable toxicity in the clinic for these combinations.

**[0065]** The PARP inhibitor can be selected from compounds that inhibit Poly(ADP-ribose) polymerase (PARP), a family of enzymes involved in DNA repair. Preferably, the PARP inhibitor is a compound that acts via two mechanisms: catalytic inhibition and trapping of PARP-DNA complexes. The PARP inhibitor can be one or more clinically available PARP inhibitor compounds (e.g. talazoparib, niraparib, olaparib, and veliparib, among others), including compounds that can act via both mechanisms, although to different degrees. For example, niraparib is much more potent at PARP trapping than veliparib, whereas they both exhibit similar PARP catalytic activity. The PARP inhibitor can be selected from one or more compounds selected from the group consisting of talazoparib, niraparib, olaparib, veliparib, iniparib, rucaparib, CEP 9722 or BGB-290. In a further embodiment, the PARP inhibitor is veliparib, olaparib, rucaparib or niraparib. In another embodiment, the PARP inhibitor is veliparib, or olaparib. The PARP inhibitor can be veliparib administered after liposomal irinotecan. The PARP inhibitor can be olaparib administered after liposomal irinotecan

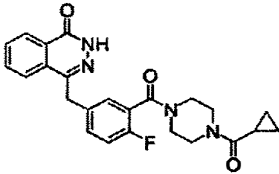
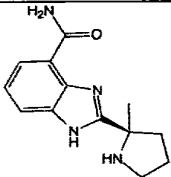
**[0066]** Olaparib is indicated as monotherapy in patients with deleterious or suspected deleterious germline BRCA mutated (as detected by an FDA-approved test) advanced ovarian cancer who have been treated with three or more prior lines of chemotherapy. The recommended dose of olaparib for this indication is 400 mg (eight 50 mg capsules) taken twice daily, for a total daily dose of 800 mg. Patients taking olaparib are instructed to avoid concomitant use of strong and moderate CYP3A inhibitors and consider alternative agents with less CYP3A inhibition. If the inhibitor cannot be avoided, reduce the Lynparza dose to 150 mg (three 50 mg capsules) taken twice daily for a strong CYP3A inhibitor or 200 mg

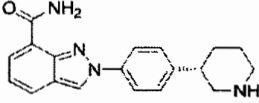
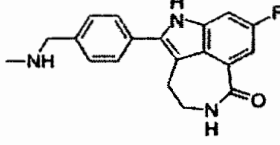
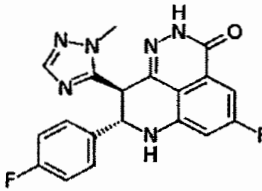
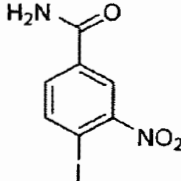
(four 50 mg capsules) taken twice daily for a moderate CYP3A inhibitor.

**[0067]** The PARP inhibitor can inhibit PARP 1 and/or PARP 2. For example, the PARP inhibitor can be a PARP ½ inhibitor with IC50 of 5nM/1nM in cell-free assays and 300-times less effective against tankyrase-1 (e.g., olaparib). The PARP inhibitor can be an inhibitor of PARP 1 and PARP2 with Ki of 5.2 nM and 2.9 nM respectively in cell-free assays, and inactive to SIRT2 (e.g., veliparib). The PARP inhibitor can be an inhibitor of PARP1 with a Ki of 1.4 nM in a cell-free assay, and can also show binding affinity for other PARP domains (e.g., rucaparib). The PARP inhibitor can be effective against triple negative breast cancer (TNBC) alone or in combination with other agents. The PARP inhibitor can be a PARP1 inhibitor with an IC50 of 0.58 nM in a cell free assay that does not inhibit PARG and is sensitive to a PTEN mutation (e.g., talazoparib). The PARP inhibitor can be a potent and selective tankyrase inhibitor with an IC50 of 46 nM and 25 nM for TNKS 1/2, respectively (e.g., G007-LK). The PARP inhibitor can be a potent inhibitor of PARP 1 with a Ki of less than about 5nM in a cell free assay (e.g., AG-14361). The PARP inhibitor can be a selective inhibitor of PARP 2 with an IC50 of 0.3 micromolar, and can be about 27-fold selective against PARP 1 (e.g., UPF-1069). The PARP inhibitor can be a potent and selective inhibitor with an IC50 for PARP 3 of about 0.89 micromolar, and about 7-fold selectivity over PARP 1 (e.g., ME0328). The PARP inhibitor can be an inhibitor of PARP 1 and PARP2 with Ki values of 1 nM and 1.5 nM, respectively.

**[0068]** Preferred examples of PARP inhibitors are provided in the table 2A below, as well as pharmaceutically acceptable prodrugs, salts (e.g., tosylates) and esters thereof.

**Table 2A: Examples of PARP inhibitors**

Olaparib (AZD-2281)	
Veliparib (ABT-888)	

Niraparib (MK04827)	
Rucaparib (AG 014699)	
Talazoparib (BMN-673)	
Iniparib (BSI-201)	

**[0069]** The dose of the PARP inhibitor and the frequency of dosing can be selected based on various characteristics of the PARP inhibitor, including the pharmacokinetic properties of the compound (e.g., half-life), prior dosing regimens and patient characteristics. Parameters that can be used in selecting the PARP inhibitor dose include those listed in Table 2B below.

**[0070]** In addition, patients can be selected to receive treatment combining a topoisomerase inhibitor and a PARP inhibitor. For example, patients can be selected based on their status in BRCA (e.g. BRCA1, BRCA2), Homologous Recombination Deficiency (HRD), BROCA-HR or other genetic risk panel analysis of a patient.

**Table 2B Characteristics of Some PARP inhibitors**

Characteristic	Veliparib	Olaparib	Rucaparib	Niraparib	Talazoparib
Molecular Weight	244.3	434.5	323.4	320.4	380.4
PARP1 IC50	4.73-5.2	1.94-5	1.4-1.98	2.1-3.8	0.57-1.2
PAR EC50	5.9	3.6	4.7		2.5
Monotherapy dosing	200-400 mg BID	300 mg BID	240-600 mg BID	300 mg QD	1 mg QD
CDx	BRCA	BRCA, HRD	HRD	BRCA, HR	HRD, HR

**[0071]** In the methods of this disclosure, the PARP inhibitor is administered at a therapeutically effective dose (e.g., a dose selected for the PARP inhibitor monotherapy, such as from about 200 mg/day to about 800 mg/day for veliparib). In a further embodiment, the PARP inhibitor is administered twice daily at a dose of from about 100 to about 400 mg for veliparib, rucaparib or olaparib. In some embodiments, 200 mg BID dose of veliparib is administered to patients after (e.g., 3-5 days after) each administration of liposomal irinotecan.

*Uses in the Treatment of Cancer*

**[0072]** In the methods of this disclosure, the PARP inhibitor is preferably administered after an "effective irinotecan plasma clearing interval," as defined above. The effective plasma clearing interval in the methods of this disclosure is from about 24 to about 168 hours, including 48 hours to about 168 hours. In a further embodiment, the effective plasma clearing interval is from about 48 to about 96 hours. In a further embodiment, the effective plasma clearing interval is 24 hours or 2, 3, 4 or 5 days.

**[0073]** In certain embodiments, the MM-398 and the PARP inhibitor are administered in at least one cycle. A cycle comprises the administration of a first agent (e.g., a first prophylactic or therapeutic agents) for a period of time, followed by the administration of a second agent (e.g., a second prophylactic or therapeutic agents) for a period of time, optionally followed by the administration of a third agent (e.g., a third prophylactic or therapeutic agents) for a period of time and so forth, and repeating this sequential administration, i.e., the cycle. In one embodiment, the combination of MM-398 and a PARP inhibitor is administered for at least one cycle. In one embodiment the cycle is a 2 week cycle. In another embodiment, the cycle is a 3 week cycle. In another embodiment, the cycle

is a 4 week cycle. In one embodiment MM-398 is administered at the beginning of the cycle and administration of a PARP inhibitor (e.g., veliparib) is delayed until at least about 24, 48, 72, 96, or 120 hours, after the administration of MM-398. In one embodiment, MM-398 is administered as part of a 28 day cycle on days 1 and 15 and the PARP inhibitor is administered on days 3-12 and on days 17-25. In another embodiment, MM-398 is administered as part of a 28 day cycle on days 1 and 15 and the PARP inhibitor is administered on days 5-12 and days 19-25.

**[0074]** In some examples, including the protocols in Table 3, the PARP inhibitor is not administered within 3 days of the administration of liposomal topoisomerase 1 inhibitor such as MM-398 liposomal irinotecan (i.e., the PARP inhibitor is only administered on days that are both at least 2, 3, 4 or 5 days after the administration of the liposomal topoisomerase 1 inhibitor, and 2, 3, 4 or 5 days prior to the next administration of the liposomal topoisomerase 1 inhibitor). Table 3 shows dose timing protocols for administering a therapeutically effective amount of a PARP inhibitor and liposomal irinotecan on certain days of a 28-day antineoplastic treatment cycle.

**Table 3: Examples of 28-day Treatment Cycles**

Protocol	PARP inhibitor given on days	Liposomal Irinotecan given on days
1	3-12; 17-25	1, 15
2	4-12; 17-25	1, 15
3	5-12; 17-25	1, 15
4	6-12; 17-25	1, 15
5	3-12; 18-25	1, 15
6	4-12; 18-25	1, 15
7	5-12; 18-25	1, 15
8	6-12; 18-25	1, 15
9	3-12; 19-25	1, 15
10	4-12; 19-25	1, 15
11	5-12; 19-25	1, 15
12	6-12; 19-25	1, 15

**[0075]** In some examples, the PARP inhibitor is administered on one or more of days of a 28-day antineoplastic treatment cycle. For example, the PARP inhibitor can be administered on one or more of days 3, 4, 5, 6, 7, 8, 9, 10, 11 and 12 and 19, 20, 21, 22, 23, 24 and 25 of the 28-day antineoplastic treatment cycle when the liposomal irinotecan (e.g., MM-398) is administered once every two weeks, or on days 1 and 15 of the 28-day antineoplastic treatment cycle.

**[0076]** Methods of treatment and therapeutic uses of PARP inhibitors and topoisomerase inhibitors (e.g., liposomal irinotecan) disclosed herein are useful in the treatment of various forms of cancer. Preferably, the cancer includes a diagnosed solid tumor. In some examples, the cancer (e.g., solid tumor) is of a tumor type with one or more DNA repair pathway deficiencies, such as breast and ovarian tumors with BRCA1 or BRCA2 mutations.

**[0077]** In the methods of this disclosure, the cancer is cervical cancer, ovarian cancer, breast cancers including triple negative breast cancer (TNBC), non-small cell lung cancer (NSCLC), small cell lung cancer (SCLC), gastric cancer, pancreatic cancer, colorectal cancer, or a neuroendocrine tumor.

**[0078]** The methods of this disclosure can further comprise administering to the patient one or more additional agents including, but not limited, to anti-emetics such as a 5-HT3 antagonist; agents for treating of diarrhea, such as loperamide; dexamethasone; or other chemotherapeutic agents.

**[0079]** In one embodiment, the methods of the present disclosure result in a pathologic complete response (pCR), complete response (CR), partial response (PR) or stable disease (SD). In another embodiment the combination therapy with MM-398 and a PARP inhibitor, e.g., veliparib, results in therapeutic synergy.

**[0080]** Further aspects include providing an existing standard of care therapy to the patients, which may or may not include treatment with appropriate single agents. In some instances, the standard of care may include administration of a PARP inhibitor compound.

**[0081]** Thus, in one aspect, the present disclosure provides a method of treating a patient with cancer and having a tumor, the method comprising:

- i. parenterally (e.g., intravenously) administering to the patient an effective amount of an irinotecan liposomal formulation; and
- ii. administering to the patient an effective amount of a PARP inhibitor wherein the PARP inhibitor is administered after an effective irinotecan plasma clearing interval.

**[0082]** The present disclosure provides a method of treating a patient with cancer and having a tumor, the method comprising a treatment regimen that may be repeated at weekly or longer intervals (e.g., Q2W, Q3W, or Q4W), each instance of the treatment comprising:

- i. intravenously administering to the patient an effective amount of an irinotecan liposomal formulation of a Top1 inhibitor such as irinotecan, topotecan, lurtotecan, indotecan, and indimitecan; and



ii. administering to the patient and effective amount of a PARP inhibitor wherein the PARP inhibitor is administered after an interval following completion of the administration of the Top1 inhibitor, e.g., an effective irinotecan plasma clearing interval.

**[0083]** In a further embodiment, the method comprises:

i. intravenously administering to the patient an effective amount of an irinotecan liposomal formulation having a terminal elimination half-life of about 26.8 hours and a maximal irinotecan plasma concentration of about 38.0 micrograms/ml; and

ii. administering to the patient and effective amount of a PARP inhibitor wherein the PARP inhibitor is administered after an interval of 24 hours or up to three days following completion of the administration of the irinotecan.

#### **Examples**

**[0084]** The following non-limiting examples illustrate the methods of the present disclosure.

#### **Example 1: In Vitro Studies**

**[0085]** *In vitro* studies were performed testing combinations of various PARP inhibitors and topoisomerase inhibitors liposomal irinotecan and SN-38.

**[0086]** Figures 1A-1D show line graphs that depict cervical cancer cell viability following treatment with SN-38 and/or various PARP inhibitors. Unless otherwise indicated, the data in each of these figures was obtained by measuring cell viability of 5 different cervical cancer cells (ME-180 in Figure 1A, MS-751 in Figure 1B, C-33A in Figure 1C, SW756 in Figure 1D and SiHa in Figure 1E) with 1000 cells/well in a 384 well plate treated with SN-38 (topoisomerase 1 inhibitor) and/or one of 3 different PARP inhibitors (veliparib, niraparib, or olaparib) at 0.33 micrograms/mL) for 24 hours, followed by washing and incubation for an additional 72 hours with fresh media.

**[0087]** The combination of the topoisomerase 1 inhibitor SN-38 and various PARP inhibitors (veliparib, olaparib and rucaparib) were tested in vitro with various small cell lung cancer (SCLC), pancreatic cancer and breast cancer cell lines. At 2nM SN-38 concentration, an additive/synergistic growth inhibition of the cancer cells was observed in combination with olaparib, veliparib and rucaparib (with veliparib observed to be slightly less potent in the combination with SN-38 than olaparib and rucaparib). At all concentrations tested, the static growth of the cancer cell population was achieved. Figures 2A-2E are graphs showing the results of in vitro experiments evaluating combinations of the topoisomerase 1 inhibitor SN38 with various PARP inhibitors, formatted according to the tables 4-5 below (plates of 5,000

cells/well, 100 microliters per well; drugs added with 20x at 10 microliters per drug, top up to 100 microliters total with DMEM; then initiate scan every 4 hours up to 68 hours).

**Table 4**

Treatment	Small Cell Lung Cancer		Pancreatic Cancer		TNBC
	DMS-114	NCI-H1048	CFPAC-1	BxPC-3	MDA-MB-231
SN-38 & Olaparib	Plate 1	Plate 2	Plate 3	Plate 4	Plate 5
SN-38 & Rucaparib	Plate 1	Plate 2	Plate 3	Plate 4	Plate 5
SN-38 & Veliparib	Plate 1	Plate 2	Plate 3	Plate 4	Plate 5

**Table 5**

Target Concentrations				
Drug	Active Range based on XTC068	Estimated tumor range (nM)	Dose Level	Conc' (nM)
SN-38	1-50 nM	3-163 nM (350); IRI < 2000nM	S1	2
			S2	5
			S3	10
			S4	20
			S5	50
Olaparib	1000-10000 nM	8000nM	O1	2000
			O2	4000
			O3	8000
Veliparib	1000-10000 nM	> 2000 nM	V1	2000
			V2	4000
			V3	8000
Rucaparib	1-100 nM (Panc)	< 8000 nM	R1	2000
			R2	4000
			R3	8000

[0088] Additive/synergistic effects were observed between SN-38 at 2nM combined with the tested PARP inhibitors olaparib, veliparib and rucaparib with DMS-114 SCLC cells. Figure 2A is a graph showing the results of *in vitro* measurement of % cell number over time for DMS-114 small cell lung cancer cells treated with the topoisomerase inhibitor SN-38 and the PARP inhibitor rucaparib.

[0089] The NCI-H1048 SCLC cells were slow-growing and very sensitive to combinations of olaparib and rucaparib with SN-38 at 2nM. Figure 2B is a graph showing the results of *in vitro* measurement of % cell number over time for NCI-H1048 small cell

lung cancer cells treated with the topoisomerase inhibitor SN-38 and the PARP inhibitor rucaparib.

[0090] Additive/synergistic effects were observed between SN-38 at 2nM combined with the tested PARP inhibitors olaparib, veliparib and rucaparib with CFPAC-1 pancreatic cancer cells. Figure 2C is a graph showing the results of *in vitro* measurement of % cell number over time for CFPAC-1 pancreatic cancer cells treated with the topoisomerase inhibitor SN-38 and the PARP inhibitor rucaparib.

[0091] Figure 2D is a graph showing the results of *in vitro* measurement of % cell number over time for BxPC-3 pancreatic cancer cells treated with the topoisomerase inhibitor SN-38 and the PARP inhibitor rucaparib. Figure 2E is a graph showing the results of *in vitro* measurement of % cell number over time for MDA-MB-231 triple negative breast cancer (TNBC) cancer cells treated with the topoisomerase inhibitor SN-38 and the PARP inhibitor rucaparib.

[0092] Figure 13A depicts the *in vitro* activity of SN-38 in cervical models. Cervical cells lines were treated with veliparib and SN-38 at either the same time or with scheduling with Veliparib being added 24 h after SN-38, and cell viability was measured using CTG assay.

#### **Example 2: Pre-Clinical Dose Tolerability Studies**

[0093] Various pre-clinical *in vivo* experiments were conducted to evaluate delayed dosing of veliparib relative to liposomal irinotecan can alleviate systemic toxicity, including a pre-clinical dose tolerability study. The combination of veliparib and irinotecan has been plagued by dose-limiting toxicities that have prevented this combination from being dosed at high (effective) doses of each drug, thereby limiting its clinical utility. To address this problem, pre-clinical studies evaluated administering a liposomal preparation of a topoisomerase 1 inhibitor, followed by the administration of a PARP inhibitor at least 1 day (preferably 2-3 days) after the day on which the liposomal topoisomerase 1 inhibitor was administered.

[0094] The advantage of dosing with MM-398 compared to free irinotecan is the extended PK profile and prolonged local tumor exposure of MM-398. Since SN-38 is cleared more quickly from normal tissues than from tumor, delayed dosing of veliparib (e.g. starting veliparib dosing a few days after MM-398 administration) allows for the window of maximum irinotecan-induced toxicity to pass in the absence of concurrent veliparib toxicity. However, the tumor levels of SN-38 are sustained longer than in healthy tissue, such that

upon PARP inhibitor dosing subsequent to liposomal Top1 inhibitor (e.g., MM-398) administration, both drugs will act on tumor tissue simultaneously.

**[0095]** To demonstrate that delayed dosing of veliparib relative to nal-IRI can alleviate systemic toxicity, a pre-clinical dose tolerability study was performed. Mice were dosed chronically with nal-IRI once weekly at various doses on Day 1, while veliparib was dosed once daily at a fixed dose for 3 consecutive days each week (either on Days 2-4, Days 3-5, or Days 4-6), and body weight was followed as a gross measure of toxicity. All mice were dosed chronically once weekly on day 1, with veliparib subsequently dosed for 3 consecutive days either on days 2-4, days 3-5, or days 4-6. Mice were weighed daily and % bodyweight gain is indicated on the Y-axis. Weight loss is indicative of intolerability of the combination. Notably, the highest (50 mg/kg) dose of MM-398 liposomal irinotecan was best tolerated (i.e., lowest measured reduction in % bodyweight observed over the experiment) when the veliparib was administered on days 4, 5 and 6 (Figure 5C). Similarly, the combination of veliparib and MM-398 was best tolerated at lower MM-398 liposomal irinotecan doses when the veliparib was only administered on days 4, 5, and 6 after MM-398 administration. Toxicity of the combination was seen at the highest doses of MM-398 when given in close proximity to the veliparib doses (Figure 5A). However, this toxicity could be alleviated either by dose reducing MM-398 or delaying the start of veliparib dosing, whereby the highest dose of MM-398 could be successfully dosed with veliparib if given on Days 4-6 following Day 1 dosing of MM-398. The Day 4-6 veliparib dosing schedule (following day 1 dosing of MM398) was followed in subsequent efficacy studies which demonstrated synergy of the combination in two cervical cancer tumor xenograft models, in which veliparib alone was not efficacious (Figure 7A) and a second model in which neither MM-398 or veliparib were efficacious as single agents (Figure 7B), however the combination demonstrated tumor growth inhibition (Figure 7B).

**[0096]** To exemplify an embodiment demonstrating that delayed dosing of olaparib relative to MM-398 can alleviate systemic toxicity, a pre-clinical dose tolerability study was performed. Figure 4 depicts a graphical representation of a murine tolerability study design comparing MM-398 and olaparib as a monotherapy or in combination using a fixed dose of MM-398 and varying doses of olaparib, with various dosing schedules for different groups: Group 1: MM-398 alone IV (10 mg/kg); Group 2: olaparib alone oral (200 mg/kg); Group 3: MM-398 (d1) + olaparib (200 mg/kg, d1-5); Group 4: MM-398 (d1) + olaparib (150 mg/kg, d1-5); Group 5: MM-398 (d1) + olaparib (200 mg/kg, d1-4); Group 6: MM-398 (d1) + olaparib (200 mg/kg, d2-5); Group 7: MM-398 (d1) + olaparib (265 mg/kg, d3-5); group 8:

DMSO alone oral (Figures 6A-6D). Mice that received monotherapy of MM-398, olaparib were dosed 5x weekly. Mice that received a combination of a constant concentration of MM-398 (10 mg/kg) and varying concentration of olaparib were dosed in varying schedules: Group 3: MM-398 (d1) + olaparib (200 mg/kg, d1-5); Group 4: MM-398 (d1) + olaparib (150 mg/kg, d1-5); Group 5: MM-398 (d1) + olaparib (200 mg/kg, d1-4); Group 6: MM-398 (d1) + olaparib (200 mg/kg, d2-5); Group 7: MM-398 (d1) + olaparib (200 mg/kg, d3-5). Mice were monitored for treatment dependent toxicities by charting body weight and percent survival. Addition of olaparib seemed to be more toxic as compared to monotherapy, however delaying start of olaparib administration to d3 seemed to decrease olaparib specific toxicity as compared to concurrent therapy. Mice were dosed chronically with MM-398 once weekly at various doses on Day 1, while olaparib was dosed once daily at a weekly fixed dose for 5, 4 or 3 consecutive days each week (either on Days 1-5, Days 1-4, Days 2-5 or Days 3-5), and body weight and percent survival were followed as a gross measure of toxicity. Toxicity of the combination was seen at the highest doses of MM-398 when given in close proximity to the olaparib doses (Figure 4). However, this toxicity could be alleviated either by delaying the start of olaparib dosing, whereby the highest dose of MM-398 could be successfully dosed with olaparib if given on Days 3-5 following Day 1 dosing of MM-398.

[0097] Mice were dosed chronically with MM-398 once weekly at various doses on Day 1, while veliparib was dosed once daily at a fixed dose for 3 consecutive days each week (either on Days 2-4, Days 3-5, or Days 4-6) and body weight was followed as a gross measure of toxicity. Toxicity of the combination was seen at the highest doses of nal-IRI when given in close proximity to the veliparib doses. However, this toxicity could be alleviated either by dose reducing nal-IRI or delaying the start of veliparib dosing. This dosing schedule was followed in subsequent mouse efficacy studies which demonstrated synergy of the combination in two cervical cancer tumor xenograft models, in which veliparib alone was not efficacious, and a second model in which neither nal-IRI or veliparib were efficacious as single agents, however the combination demonstrated tumor growth inhibition.

[0098] The tolerability of the combination of MM398 in a mouse model on day 1 was evaluated in combination with the administration of veliparib on days 1-3, days 2-4 and days 3-5. The tolerability of the combined regimen in mice (measured by change in percent bodyweight over 20 days) increased as the first administration of the veliparib occurred on day 2 and day 3, with day 3 initial veliparib dosing providing the most tolerated dosing schedule. Figure 8A is a graph that further depicts the in vivo tolerability of the 50

milligrams/kilogram (mpk) dose of MM-398 on day 1 in combination with 50 mg/kg veliparib given on days 1, 2, and 3; or days 2, 3, and 4; or days 3, 4, and 5 after administration of the MM-398, as reflected in percent change in body weight with an adjusted lower limit. Figure 8B is a graph that further depicts the *in vivo* tolerability of the 28 mpk dose of MM-398 on day 1 in combination with 50 mg/kg veliparib given on days 1, 2, and 3; or days 2, 3, and 4; or days 3, 4, and 5 after administration of the MM-398, as reflected in percent change in body weight with an adjusted lower limit.

[0099] Figure 12 is a graph showing that treatment of mice with the combination of MM-398 with veliparib in C33A xenograft model described in Example 4 also lead to decreases in body weight as compared to administration of either drug alone.

[00100] These studies demonstrated that this toxicity could be alleviated by delaying the start of PARP inhibitor dosing, preferably by 2-3 days after the day on which liposomal irinotecan was administered. A dosing schedule where the PARP inhibitor was only administered on days subsequent to administration of liposomal irinotecan was followed in mouse efficacy studies (Example 3) demonstrating therapeutic synergy of the combination of a PARP inhibitor and liposomal irinotecan in two cervical cancer tumor xenograft models (in which veliparib alone was not efficacious, and a second model in which neither MM-398 or veliparib were efficacious as single agents, however the combination demonstrated tumor growth inhibition).

### **Example 3: Pre-Clinical Efficacy of Liposomal Irinotecan**

[00101] *In vivo* tumor xenograft studies demonstrated that the efficacy of liposomal irinotecan is greater than free irinotecan. In addition, *in vivo* tumor xenograft studies demonstrated MM-398 is related to high CES activity and/or high tumor levels of CPT-11 following dosing with MM-398. Additionally, MM-398 has demonstrated superior activity compared to equivalent dosing of free irinotecan in several pre-clinical models including breast, colon, ovarian, and pancreatic tumor xenograft models.

[00102] Liposomal irinotecan (MM-398) has greater efficacy in various cancer models, compared to non-liposomal irinotecan. Cancer cells were implanted subcutaneously in mice; when tumors were well established and had reached mean volumes of 200 mm<sup>3</sup>, IV treatment with free irinotecan, MM-398 or control was initiated. The doses of free and nanoliposomal irinotecan used in each study are indicated above, with dose time points indicated by arrows. Tumor permeability as well as tumor tissue carboxylesterase (CES) activity, which is responsible for the enzymatic conversion of CPT-11 to SN-38, are predicted to be critical factors for local tumor exposure of SN-38 following MM-398 dosing. *In vivo* tumor

xenograft studies have demonstrated that efficacy of MM-398 is related to high CES activity and/or high tumor levels of CPT-11 following dosing with MM-398. Additionally, MM-398 has demonstrated superior activity compared to equivalent dosing of free irinotecan in several pre-clinical models including breast, colon, ovarian, and pancreatic tumor xenograft models.

**Example 4: Pre-Clinical Activity of Liposomal Irinotecan and PARP inhibitors**

**[00103]** Referring to Figure 7A and Figure 7B, the antitumor activity of MM-398 was studied in combinations with veliparib (PARPi) in multiple cervical xenograft models. In this study, MS-751 and C33A xenograft models of cervical cancer were employed to probe the effect of administering suboptimal doses of MM-398 in combination with the PARP inhibitor veliparib. Differential tissue levels of MM-398 at 24 and 72 hours indicated that MM-398 and the active metabolite SN-38 cleared faster from the liver, spleen, colon, and plasma, than from tumors. The combination of veliparib and MM-398 gave improvements in key PD biomarkers (cleaved caspase and  $\gamma$ H2AX) when compared to veliparib or MM-398 alone. Figures 7A and 7B show that the combination of MM-398 + veliparib is synergistic. Two different cervical cancer xenograft models were utilized to study the efficacy of MM-398 dosed once weekly on Day 1 (arrows), veliparib dosed at 50 mg/kg orally once daily for 3 consecutive days on Days 4-6 of each week, or the combination dosed on the same schedule as the single agent treatments combined. (A) MS751 cervical cancer xenograft model using MM-398 dosed at 5 mg/kg and (B) C33A cervical cancer xenograft model using MM-398 dosed at 2 mg/kg. In the study, control mice were the same strain, and were harvested prior to tested mice (slightly younger). Data is not presented for mice removed from study for weight loss or for mice removed unintentionally before end date.

*Cervical MS-751 Xenograft Model*

**[00104]** The MS-751 Xenograft Model details are summarized in Table 6.

**Table 6**

Mouse strain:	Nude (Tacoma)			
Tumor	Cervical MS-751, C33A			
Inoculation:	5*10 <sup>6</sup> (s.c.) in 30% MG			
Drug:	MM-398 (iv) + Veliparib (oral)			
Groups:		Animal per group:	Dose (mpk)	
1	Saline	10		
2	MM-398	10	5	
3	veliparib/oral	10	50	3/4/5th day
4	MM-398 +veliparib	10	5+50	3/4/5th day

[00105] Figure 9A shows that tumor volume decreased when MM-398 (5 mpk dose) was administered in combinations with veliparib in the MS751 xenograft model ( $p = 0.03$ ) as compared to administration of either drug alone. Figure 9B shows that percent survival was better for mice treated with MM-398 (5 mpk dose) in combinations with veliparib in MS751 xenograft model as compared to treatment with either drug alone either drug administered alone. Figure 9C shows that treatment with the combination of MM-398 with veliparib in MS751 xenograft model lead to decreases in body weight as compared to administration of either drug alone.

*C33A Cervical Xenograft Model*

[00106] The C33A Xenograft Model details are summarized in Table 7.

**Table 7**

Mice:	Female, Ncr Nudes (Taconic), 5-6 weeks.	
Cell Lines:	C33 A	
Tumor Inoculation: 5×10 <sup>6</sup> in 100 µl Matrigel (30 vol%) sc		
15 mice per a cell line		
<u>Groups:</u>	<u>Dose, mpk:</u>	
MM-398 alone	2	
Veliparib alone	50	
MM-398 + Veliparib (3-4-5 d)	2+60	
<u>End-life Collection: 72 h after first injection</u>		
Frozen (Tumor, Liver, Spleen, Plasma)		
FFPA (Tumor)		



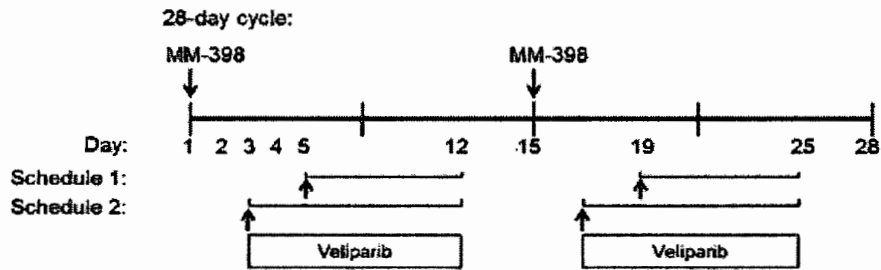
<u>Analysis:</u>	
gamma H2AX and cleaved caspase/Tunnel in FFPE (Lia)	
CPT-11 and SN-38 in all tissues for MM-398 flash frozen only (Roswell)	

[00107] Figure 10 shows that the combination of MM-398 with veliparib in the C33A xenograft model leads to decreases in tumor volume as compared to either drug alone administered alone. Figure 11 shows that percent survival was better for mice MM-398 (5 mpk dose) in combinations with veliparib in C33A xenograft model as compared to either drug administered alone.

**Example 5: Clinical Use of Liposomal Irinotecan and PARP inhibitors**

*Clinical Use of Liposomal Irinotecan and Veliparib*

[00108] This is a Phase 1 human dose escalation study to characterize the safety, tolerability, MTD and PK of MM-398 in combination with veliparib in order to determine an optimal combination dose and schedule that will be identified as the recommended Phase 2 dose. The following schematic outlines two different schedules of veliparib dosing that will be explored in combination with MM-398 bi-weekly dosing:



[00109] MM-398 will be administered by intravenous (IV) infusion over 90 minutes at a dose of 80 mg/m<sup>2</sup> every two weeks. MM-398 is administered by intravenous (IV) infusion over 90 minutes at a dose of 80 mg/m<sup>2</sup> (salt) irinotecan once every two weeks (days 1 and 15 of each 28-day treatment cycle). Veliparib is co-administered orally twice daily by the patient at home according to the following schedule:

**Table 8**

<b>Dose Level<sup>1</sup></b>	<b>Veliparib Dose (mg BID)</b>	<b>Veliparib Dose Days</b>	<b>MM-398 Dose (salt) (mg/m<sup>2</sup> q2w)</b>
1	100	Day 5-12; 19-25	80, Day 1, 15
2	200	Day 5-12; 19-25	80, Day 1, 15
3	200	Day 5-12; 17-25	80, Day 1, 15
4	300	Day 5-12; 19-25	80, Day 1, 15
5	400	Day 5-12; 19-25	80, Day 1, 15

<sup>1</sup>Additional dose levels and alternate dosing schedules may be explored upon agreement of Sponsor, Medical Monitor and Investigators.

\*\* After the MTD is reached, and for the first cycle only, we plan to enroll approximately 18 patients obtain tumor biopsies according to the schema outlined in the correlates section below.

**[00110]** The study will enroll 3 patients per dose cohort following a traditional 3 + 3 dose escalation design. Dose limiting toxicities (DLTs) will be evaluated during the first cycle of treatment (28 days) in order to determine the MTD. If there are no DLTs within the safety evaluation period, then the next cohort can be initiated following agreement between the Investigators and Medical Monitor. If a DLT occurs, then the cohort will be expanded to 6 patients. If 2 or more patients have DLTs within a given dose level, then the dose will not be escalated further; however, lower doses may be explored. Additional dosing schedules may also be explored depending on the safety, tolerability, and PK observed.

**[00111]** Given that these individual therapies have been studied in previous clinical trials, it is important that the safety assessment takes into account the expected safety profile of the standard dose regimens. For all treatment regimens, any toxicity that is related to disease progression will not be considered a DLT. The following events, occurring during cycle 1 of the study combination, will be considered DLTs if deemed drug-related:

grade 3 or 4 neutropenia complicated by fever  $\geq 38.5$  °C (i.e. febrile neutropenia) and/or documented infection;

grade 4 neutropenia that does not resolve within 7 days despite optimal therapy (withholding study drug and GCSF administration);

grade 4 thrombocytopenia that does not resolve within 7 days or any grade 3-4 thrombocytopenia complicated with hemorrhage;

grade 4 anemia that does not resolve within 7 days despite optimal therapy (withholding study drug and red blood cell transfusions);

inability to begin subsequent treatment course within 14 days of the scheduled date, due to study drug toxicity;

any grade 3-4 non-hematologic toxicity (except fatigue/asthenia < 2 weeks in duration; vomiting or diarrhea lasting less than 72 hours whether treated with an optimal anti-emetic or anti-diarrheal regimen or not; or alkaline phosphatase changes).

≥ grade 2 seizure

**[00112]** Patients will be treated until disease progression as determined by RECIST v1.1 criteria evaluated by CT scan every 8 weeks from first dose of study drug. The inclusion and exclusion criteria for the clinical trial are summarized in the table 9 below.

**Table 9**

<u>Inclusion Criteria</u>	<u>Exclusion Criteria</u>
<ul style="list-style-type: none"> <li>• Patients must have histologic or cytologic confirmation of cancer for which there is no known standard therapy capable of extending life expectancy.</li> <li>• ECOG Performance Status 0 or 1</li> <li>• Tumor lesion(s) amenable to multiple pass percutaneous biopsies and patient willing to undergo required pre- and post-treatment biopsies</li> <li>• Must have adequate:</li> <li>• Bone marrow function                             <ul style="list-style-type: none"> <li>○ ANC &gt; 1,500 cells/<math>\mu</math>l without the use of hematopoietic growth factors</li> <li>○ Platelet count &gt; 100,000 cells/<math>\mu</math>l</li> <li>○ Hemoglobin &gt; 9 g/dL</li> </ul> </li> <li>• Hepatic function                             <ul style="list-style-type: none"> <li>○ Normal serum total bilirubin</li> <li>○ AST and ALT <math>\leq</math> 2.5 x ULN (<math>\leq</math> 5 x ULN is acceptable if liver metastases are present)</li> </ul> </li> <li>• Renal function                             <ul style="list-style-type: none"> <li>○ Serum creatinine <math>\leq</math> 1.5 x ULN</li> </ul> </li> <li>• Normal ECG</li> <li>• <math>\geq</math>18 years of age</li> <li>• Able to understand and sign informed consent</li> <li>• Prior PARP inhibitor therapy is allowed</li> <li>• Willing to undergo pre-treatment ferumoxytol MRI (patients will be excluded from undergoing ferumoxytol MRI if they have evidence of iron overload, a known hypersensitivity to ferumoxytol or any other IV iron product, a documented history of multiple drug</li> </ul>	<ul style="list-style-type: none"> <li>• Active CNS metastasis</li> <li>• Clinically significant GI disorders, including history of small bowel obstruction unless the obstruction was a surgically treated remote episode</li> <li>• Prior irinotecan therapy; or topotecan therapy or bevacizumab therapy within 6 months of first dose of study treatment</li> <li>• Prior chemotherapy or biological therapy within 3 weeks, or within a time interval less than 5 half-lives of the agent, prior to first dose of study treatment</li> <li>• Prior radiotherapy within 4 weeks of first dose of study treatment</li> <li>• Patients who have had radiation to the pelvis or other bone marrow-bearing sites will be considered on a case by case basis and may be excluded if the bone marrow reserve is not considered adequate (i.e. radiation to &gt;25% of bone marrow)</li> <li>• Known hypersensitivity to MM-398</li> <li>• Active infection</li> <li>• Pregnant or breast feeding</li> </ul>

<u>Inclusion Criteria</u>	<u>Exclusion Criteria</u>
allergies, or those for whom MRI is otherwise contraindicated, including claustrophobia or anxiety related to undergoing MRI)	

[00113] The dose escalation portion of the trial may require up to 30 patients if 6 patients are required at each of 5 dose levels. An additional 18 patients may be used to explore the effect of veliparib on the biologic correlates. Thus, the accrual ceiling will be set at 48 patients.

[00114] The study is proposed to include all solid tumor types, however, particular indications that are of high interest for this study includes the following: cervical cancer, ovarian cancer, triple negative breast cancer (TNBC), non-small cell lung cancer (NSCLC), small cell lung cancer (SCLC), gastric cancer, pancreatic cancer, and neuroendocrine tumors.

[00115] The methods and uses herein can also be applied to other tumor suitable types including those noted for increased frequency of DNA damage response (DDR) pathway deficiencies (or ‘BRCAness’) found in sporadic tumors, which are predicted to be sensitive to PARP inhibitors. As mentioned previously, BRCA1 or BRCA2 deficiencies, found particularly in triple negative breast cancer and high-grade serous ovarian cancer, sensitize cells to PARP-inhibitors . Likewise, loss of function of other genes and proteins involved in DDR pathways, including the endonuclease XPF-ERCC1, the homologous recombination repair proteins meiotic recombination protein 11 (MRE11) and Fanconi anemia pathway (FANC) proteins, also sensitize cells to PARP inhibitors. Fanconi anemia pathway deficiencies have been demonstrated in lung, cervical, and breast and ovarian cancers. These and other DDR pathway deficiencies may be predictive biomarkers for PARP inhibitor therapy, and will be explored retrospectively in this study. Veliparib, specifically, has also demonstrated clinical activity in a number of indications, including BRCA-positive and BRCA wild-type breast and ovarian cancer, as well as gastric cancer in combination with FOLFIRI. For the proposed study, indications were chosen not only for their high unmet medical need, but for potential sensitivity to irinotecan and/or veliparib based on the aforementioned pre-clinical and/or clinical experience. While the PARP inhibitor olaparib has recently been FDA approved as a monotherapy in BRCA+ ovarian cancer, this study will not limit treatment in the ovarian patient population to BRCA+ patients, as this is a phase I study of a combination therapy and may retrospectively identify patients with other DDR pathway deficiencies in addition to BRCA.

*Use of Liposomal Irinotecan and Olaparib*

[00116] MM-398 is administered by intravenous (IV) infusion over 90 minutes at a dose of 80 mg/m<sup>2</sup> (based on the corresponding amount of irinotecan hydrochloride trihydrate, equivalent to 70 mg/m<sup>2</sup> irinotecan free base) every two weeks. Olaparib is co-administered orally twice daily by the patient at home according to the following schedule (Table 10).

**Table 10**

Dose Level <sup>1</sup>	Olaparib Dose (mg BID)	Olaparib Dose Days	MM-398 Dose (mg/m <sup>2</sup> q2w)*
1	100	Day 5-12; 19-25	80, Day 1, 15
2	200	Day 5-12; 19-25	80, Day 1, 15
3	200	Day 5-12; 17-25	80, Day 1, 15
4	300	Day 5-12; 19-25	80, Day 1, 15
5	400	Day 5-12; 19-25	80, Day 1, 15

\*= The 80 mg/m<sup>2</sup> MM-398 dose is based on the corresponding amount of irinotecan hydrochloride trihydrate (equivalent to 70 mg/m<sup>2</sup> based on irinotecan free base).

**Example 6: Measuring phosphorylated H2AX in Tumor Biopsies**

[00117] Phosphorylated H2AX ( $\gamma$ -H2AX) plays an important role in the recruitment and/or retention of DNA repair and checkpoint proteins such as BRCA1, MRE11/RAD50/NBS1 complex, MDC1 and 53BP1. DNA damage has been shown to increase H2AX phosphorylation in cancer cells following exposure to camptothecins. If the PARP inhibitor compound(s) is/are able to increase the degree of DNA damage due to irinotecan from MM-398, it may be detectable by measurement of H2AX phosphorylation. An immunofluorescence assay was used in previous clinical studies. Patient peripheral blood mononuclear cells (PBMCs), hair follicles, and/or tumor biopsy samples will be collected if there is readily accessible disease. The association between the pharmacodynamic response measured by  $\gamma$ -H2AX level can be assessed by Fisher's test or the Wilcoxon rank sum test, as appropriate; this evaluation will be done at the MTD +/- a maximum of 2 dose levels (Figure 14).

**Table 11. Schedule for biopsies and surrogate samples**

Dose Level		PARPi Dose (mg BID)	PARPi Dose Days	MM-398 Dose (mg/m <sup>2</sup> q2w)	Biopsy in am for PD marker
1		100	Day 5-12; 19-25	80, Day 1, 15	--
2		200	Day 5-12; 19-25	80, Day 1, 15	--
3		200	Day 3-12; 17-25	80, Day 1, 15	Days 1, 5, 19
4		300	Day 3-12; 17-25	80, Day 1, 15	Days 1, 5, 19
5		400	Day 3-12; 17-25	80, Day 1, 15	Days 1, 5, 19
Confirm	A	MTD	Day 3-12; 19-25	80, Day 1, 15	Days 1, 5, 19
	B	MTD	Day 5-12; 17-25	80, Day 1, 15	Days 1, 5, 19

**Example 7: Administering and Detecting Ferumoxytol to Predict Deposition of Topoisomerase Inhibitor from Liposomal Irinotecan**

[00118] Figures 15A-15C show that FMX MRI may be a predictive tool for tumor response to MM-398. Figure 15A is a schematic showing that MM-398 and FMX have similar properties, including 1) extended PK, 2) the ability to deposit in tumor tissues through the EPR effect (i.e. leaky vasculature), and 3) uptake by macrophages. Therefore, visualization of FMX on MRI may be able to predict MM-398 deposition. (B) FMX concentration of individual patient lesions was calculated using a standard curve from MR images obtained 24h post-FMX injection. (C) FMX signal from lesions at 24h are grouped relative to the median value observed in the FMX MRI evaluable lesions and compared to the best change in lesion size based on CT scans (data available from 9 patients; total of 31 lesions).

[00119] The phase I study of MM-398 also examined the feasibility of magnetic resonance (MR) imaging to predict tumor-associated macrophage (TAM) content and MM-398 deposition. TAMs appear to play a key role in the deposition, retention and activation of MM-398 within the tumor microenvironment. In this clinical study, ferumoxytol (FMX) a microparticulate preparation of a superparamagnetic iron oxide coated with polyglucose sorbitol carboxymethylether) was used as an imaging contrast agent and MR images were obtained at 1h, 24h, and 72h following FMX injection. FMX is an approved therapy that is indicated for the treatment of iron deficiency anemia in adult patients with chronic kidney disease; however a growing number of cancer patients without iron deficiency are being administered FMX as an imaging agent to visualize macrophage content and vasculature. Like MM-398, FMX is also a nanoparticle with a diameter of approximately 17-31 nm. As

tumor permeability was predicted to be an important factor in MM-398 efficacy, FMX was also investigated for use as a surrogate for liposome deposition (Figure 15A). A benefit of FMX is that this agent helps to identify patients that are less likely to respond to MM-398 because of poor drug uptake. Ferumoxytol as a diagnostic test enables the detection of a patient population that would significantly benefit from MM-398 that would otherwise be uncategorized.

**[00120]** The MRI results from a human clinical trial study demonstrated that the amount of FMX depositing in tumor lesions was able to be quantified (Figure 15B), and it was subsequently shown that a correlation existed between tumor lesion ferumoxytol uptake by MRI and response to MM-398 (Figure 15C). This correlation is now being studied further in an expansion of the Phase 1 study, and is included as a correlative imaging study for a trial of MM-398 + veliparib.

**[00121]** FMX is an iron replacement product indicated for the treatment of iron deficiency anemia in adult patients with chronic kidney disease. Although not approved as an indication, ferumoxytol has also been used as an imaging agent in cancer patients and will be utilized as such in this study. At least 2 days prior to Cycle 1 Day 1 (maximum of 8 days prior) a single dose of 5 mg/kg FMX will be administered by intravenous injection. The total single dose will not exceed 510 mg, the maximum approved single dose of FMX. This dosing schedule is less intense than the approved label, which recommends two doses of 510 mg 3 to 8 days apart; however since FMX is being used as imaging agent in this study as opposed to a replacement product for iron deficiency, a lower dose is more appropriate. Three MRIs will be performed for each patient over 2 days. All patients will have a baseline image acquired prior to the FMX infusion, and a second image acquired 1-4 h after the end of FMX administration. All patients will return the following day for a 24 h FMX-MRI using the same protocol and sequences as previously. Each patient will be required to complete their FMX-MRIs on the same scanner to reduce inter-scan variability. The body area to be scanned will be determined by the location of the patient's disease. Each MRI study will be evaluated for image quality and signal characteristics of tumors and reference tissue on T1-, T2- and T2\*-weighted sequences. Once a completed set of images from each patient has been received, a qualitative review will be performed and sent to a quantitative lab for analysis. The data will be analyzed in a similar fashion as described above.

**Imaging Correlates Table 12**

<b>Correlative Objective</b>	<b>Imaging Technique</b>	<b>Organ(s) Scanned and Timing of Scans</b>
Ferumoxytol (FMX) uptake	MRI	Sites of disease; 3 scans completed approximately 2-6 days prior to Cycle 1 Day 1. Scan time points: -baseline (immediately prior to FMX infusion) -1h (post-FMX infusion) -24h (post-FMX infusion)
Histone gamma-H2AX (Pommier, DTB-CCR; Doroshow, Leidos)	Immunofluorescence microscopy ELISA (in development)	- Tumor biopsy before treatment, and during treatment. - Hair follicles during treatment. PBMC before treatment and during treatment

Imaging Correlate Study

**[00122]** Patients will be eligible to participate in the FMX imaging study if they do not meet any of the following criteria:

- Evidence of iron overload as determined by:
  - Fasting transferrin saturation of >45% and/or
  - Serum ferritin levels >1000 ng/ml
- A history of allergic reactions to any of the following:
  - compounds similar to ferumoxytol or any of its components as described in full prescribing information for ferumoxytol injection
  - any IV iron replacement product (e.g. parenteral iron, dextran, iron-dextran, or parenteral iron polysaccharide preparations)
  - multiple drugs
- Unable to undergo MRI or for whom MRI is otherwise contraindicated (e.g. presence of errant metal, cardiac pacemakers, pain pumps or other MRI incompatible devices; or history claustrophobia or anxiety related to undergoing MRI)

**[00123]** If a patient consents to FMX-MRI, the patient will receive ferumoxytol infusion and undergo the required FMX-MRI scans approximately 2-6 days prior to beginning MM-398 treatment (the FMX period). FMX will be administered at a dose of 5 mg/kg up to a maximum of 510 mg. All other aspects of administration will be consistent with the latest ferumoxytol prescribing information. A detailed FMX-MRI protocol will be included in the study imaging manual. Briefly, each patient will be required to complete their FMX-MRIs on the same scanner to reduce inter-scan variability. Each MRI study will be evaluated for image quality and signal characteristics of tumors and reference tissue on T1-, T2- and T2\*-



weighted sequences. Once a completed set of images from each patient has been received, the images will be loaded onto the viewing workstation for qualitative review and then sent to a quantitative lab (handled by central imaging CRO) for analysis.

**[00124]** Multiple MR images will be collected on Day 1-Day 2 of the FMX period at various time points: a baseline image acquired prior to the FMX infusion, a second image occurring 1-4 h after the end of FMX administration, and a third image at approximately 24 h post-FMX, using the same protocol and sequences as on Day 1. The body areas to be scanned will be determined by the location of the patient's disease; detailed instructions will be described in the study imaging manual.

**Example 8: Clinical Use of Liposomal Irinotecan in Combination with 5-fluorouracil and leucovorin**

**[00125]** Clinical efficacy of MM-398 has also been demonstrated in gemcitabine-refractory metastatic pancreatic cancer patients: in a randomized, Phase 3, international study (NAPOLI-1), MM-398 was given in combination with 5-fluorouracil/leucovorin (5-FU/LV) and significantly prolonged overall survival (OS) compared to 5-FU/LV treatment alone. The median OS for the MM-398-containing arm was 6.1 months compared to 4.2 months for the control arm (HR=0.67, p=0.0122). Because the active pharmaceutical ingredient in MM-398 is irinotecan, the safety profile was, as anticipated, qualitatively similar to irinotecan, where the most common adverse events ( $\geq 30\%$ ) are nausea, vomiting, abdominal pain, diarrhea, constipation, anorexia, neutropenia, leukopenia (including lymphocytopenia), anemia, asthenia, fever, body weight decreasing, and alopecia (irinotecan package insert). Table 14 provides a summary of Grade 3 or higher safety data of patients treated with MM-398 plus 5-FU/LV from the NAPOLI-1 study. Table 13 provides toxicities observed in the Phase I monotherapy study, for comparison.

**Table 13. Summary of the most common (>10%) grade 3 or greater adverse events from the 13 patients treated with MM-398 monotherapy at a dose of 80 mg/m<sup>2</sup> every 2 weeks during the phase I study.**

Adverse Events $\geq$ Grade 3 in Study MM-398-01-01-02	
	n (%)
Diarrhea	4 (30.8)
Hypokalemia	3 (23.1)
Abdominal pain	2 (15.4)
Anemia	2 (15.4)
Nausea	2 (15.4)
Neutropenia	2 (15.4)

**Table 14 Summary of Grade 3 or higher AEs from the NAPOLI-1 phase III study.**

	MM-398 + 5-FU/LV <sup>1</sup> (N=117)	5-FU/LV <sup>2</sup> (N=134)
GRADE $\geq$ 3 NON-HEMATOLOGIC AEs IN $>$ 5% PATIENTS, % <sup>3</sup>	%	%
Fatigue	14	4
Diarrhea	13	5
Vomiting	11	3
Nausea	8	3
Asthenia	8	7
Abdominal pain	7	6
Decreased appetite	4	2
Hypokalemia	3	2
Hypernatremia	3	2
GRADE $\geq$ 3 HEMATOLOGIC AES BASED ON LABORATORY VALUES, % <sup>3,4</sup>		
Neutrophil count decreased	20	2
Hemoglobin decreased	6	5
Platelet count decreased	2	0

<sup>1</sup> Dose: 80 mg/m<sup>2</sup> MM-398 + 2400 mg/m<sup>2</sup> over 46 h/400 mg/m<sup>2</sup> 5-FU/LV q2w

<sup>2</sup> Dose: 2000 mg/m<sup>2</sup> over 24 h/200 mg/m<sup>2</sup> 5-FU/LV weekly x 4, q6w

<sup>3</sup> Per CTCAE Version 4

<sup>4</sup> Includes only patients who had at least one post-baseline assessment

**[00126] Example 9: Cell survival for various TNBC cell lines following SN-38 and PARP inhibitor combination treatment.**

**[00127]** Tables 15a, 15b, 16a, and 16b provide the results of *in vitro* measurements of cell survival for various triple negative breast cancer (TNBC) cancer cell lines to determine the cell viability following treatment with SN-38 and/or a PARP inhibitor. Tables 15a and 15b provide IC50 data, and Tables 16a and 16b provide Maximum Kill data.

**Table 15a: IC50 log10 ( $\mu$ M)**

Exp. 1	Treatment	Cell Line		
		BT20	SUM159PT	HCC38
	SN38	-0.18	-2.35	-2.80
	Niraparib	2.14	0.35	1.23
	SN38 & Niraparib (3ug/ml)	-0.67	-3.99	-0.12
	SN38 & Niraparib (1ug/ml)	-0.70	-3.42	-4.09
	SN38 & Niraparib (0.3ug/ml)	-0.71	-2.85	-4.23

	SN38 & Niraparib (0.1ug/ml)	-0.61	-2.87	-4.05
Exp. 2	Treatment	Cell Line		
		BT20	SUM149PT	SUM159PT
	SN38	-0.69	0.24	-2.39
	Olaparib	1.24	2.40	0.18
	SN38 & Olaparib (3ug/ml)	-1.48	-0.19	-3.70
	SN38 & Olaparib (1ug/ml)	-1.49	-0.34	-3.31
	SN38 & Olaparib (0.3ug/ml)	-1.44	-0.18	-2.92
	SN38 & Olaparib (0.1ug/ml)	-1.29	-0.11	-2.92
Exp. 3	Treatment	Cell Line		
		BT20	SUM149PT	SUM159PT
	SN38	-0.37	0.27	-2.66
	Rucaparib	1.27	1.68	-0.07
	SN38 & Rucaparib (3ug/ml)	-1.33	-0.16	-3.64
	SN38 & Rucaparib (1ug/ml)	-1.47	-0.23	-3.28
	SN38 & Rucaparib (0.3ug/ml)	-1.48	-0.49	-3.23
	SN38 & Rucaparib (0.1ug/ml)	-1.24	-0.10	-3.11
Exp. 4	Treatment	Cell Line		
		BT20	SUM159PT	HCC38
	SN38	-0.24	-2.33	-2.75
	Talazoparib	1.45	-1.03	-1.23
	SN38 & Talazoparib (3ug/ml)	-1.88	-4.01	-3.41
	SN38 & Talazoparib (1ug/ml)	-1.70	-4.01	-4.01
	SN38 & Talazoparib (0.3ug/ml)	-1.10	-4.01	-5.46
	SN38 & Talazoparib (0.1ug/ml)	-1.36	-4.01	-2.87

Table 15b: IC50 log10 ( $\mu$ M)

Exp. 1	Treatment	Cell Line		
		HCC1187	HCC1806	BT549
	SN38	-0.68	-2.08	-0.10
	Niraparib	2.11	1.27	2.03
	SN38 & Niraparib (3ug/ml)	-1.58	-2.80	-0.39
	SN38 & Niraparib (1ug/ml)	-1.45	-2.62	-0.64

	SN38 & Niraparib (0.3ug/ml)	-1.61	-2.55	-0.74
	SN38 & Niraparib (0.1ug/ml)	-1.41	-2.52	-0.55
Exp. 2	Treatment	Cell Line		
		HCC70	HCC1187	BT549
	SN38	-0.07	-0.64	-0.04
	Olaparib	-4.2 x10 <sup>7</sup>	2.41	2.04
	SN38 & Olaparib (3ug/ml)	-0.58	-1.77	-0.55
	SN38 & Olaparib (1ug/ml)	-0.49	-1.67	-0.48
	SN38 & Olaparib (0.3ug/ml)	-0.50	-1.35	-0.35
	SN38 & Olaparib (0.1ug/ml)	-0.48	-1.56	-0.04
Exp. 3	Treatment	Cell Line		
		HCC38	HCC1954	BT549
	SN38	-2.89	-0.97	-0.05
	Rucaparib	-0.07	1.60	1.75
	SN38 & Rucaparib (3ug/ml)	4.93	-1.22	-0.48
	SN38 & Rucaparib (1ug/ml)	-3.88	-1.33	-0.57
	SN38 & Rucaparib (0.3ug/ml)	-4.01	-1.51	-0.49
	SN38 & Rucaparib (0.1ug/ml)	-3.29	-1.57	-0.52
Exp. 4	Treatment	Cell Line		
		HCC1187	HCC1954	SKBR3
	SN38	-0.98	-0.65	-1.38
	Talazoparib	2.28	3.64	-2.8 x 10 <sup>4</sup>
	SN38 & Talazoparib (3ug/ml)	-1.79	-1.64	-2.05
	SN38 & Talazoparib (1ug/ml)	-1.79	-1.51	-2.65
	SN38 & Talazoparib (0.3ug/ml)	-1.94	-1.45	-2.23
	SN38 & Talazoparib (0.1ug/ml)	-1.92	-1.29	-2.41

**Table 16a: Maximum Kill Percent**

Exp. 1	Treatment	Cell Line		
		BT20	SUM159PT	HCC38
	SN38	100	97	96
	Niraparib	100	97	100
	SN38 & Niraparib (3ug/ml)	100	100	

	SN38 & Niraparib (1ug/ml)	100	100	93
	SN38 & Niraparib (0.3ug/ml)	100	99	100
	SN38 & Niraparib (0.1ug/ml)	100	100	100
<b>Exp. 2</b>	<b>Treatment</b>	<b>Cell Line</b>		
		<b>BT20</b>	<b>SUM149PT</b>	<b>SUM159PT</b>
	SN38	100	96	97
	Olaparib	98	100	94
	SN38 & Olaparib (3ug/ml)	98	97	100
	SN38 & Olaparib (1ug/ml)	99	96	97
	SN38 & Olaparib (0.3ug/ml)	100	98	99
	SN38 & Olaparib (0.1ug/ml)	100	96	99
<b>Exp. 3</b>	<b>Treatment</b>	<b>Cell Line</b>		
		<b>BT20</b>	<b>SUM149PT</b>	<b>SUM159PT</b>
	SN38	100	95	99
	Rucaparib	100	99	97
	SN38 & Rucaparib (3ug/ml)	92	97	99
	SN38 & Rucaparib (1ug/ml)	100	97	99
	SN38 & Rucaparib (0.3ug/ml)	94	95	100
	SN38 & Rucaparib (0.1ug/ml)	96	100	97
<b>Exp. 4</b>	<b>Treatment</b>	<b>Cell Line</b>		
		<b>BT20</b>	<b>SUM159PT</b>	<b>HCC38</b>
	SN38	100	96	92
	Talazoparib	100	94	92
	SN38 & Talazoparib (3ug/ml)	100		
	SN38 & Talazoparib (1ug/ml)	90		
	SN38 & Talazoparib (0.3ug/ml)	93		
	SN38 & Talazoparib (0.1ug/ml)	93		

**Table 16b: Maximum Kill Percent**

Exp. 1	Treatment	Cell Line		
		HCC1187	HCC1806	BT549
	SN38	90	93	95
	Niraparib	98	100	100
	SN38 & Niraparib (3ug/ml)	89	91	94
	SN38 & Niraparib (1ug/ml)	93	92	92
	SN38 & Niraparib (0.3ug/ml)	89	92	92

	SN38 & Niraparib (0.1ug/ml)	89	93	94
Exp. 2	Treatment	Cell Line		
		HCC70	HCC1187	BT549
	SN38	97	100	93
	Olaparib	50	87	100
	SN38 & Olaparib (3ug/ml)	98	100	
	SN38 & Olaparib (1ug/ml)	100	91	96
	SN38 & Olaparib (0.3ug/ml)	100	99	94
	SN38 & Olaparib (0.1ug/ml)	100	99	96
Exp. 3	Treatment	Cell Line		
		HCC38	HCC1954	BT549
	SN38	92	94	94
	Rucaparib	87	100	100
	SN38 & Rucaparib (3ug/ml)		96	93
	SN38 & Rucaparib (1ug/ml)	98	94	92
	SN38 & Rucaparib (0.3ug/ml)	98	95	93
	SN38 & Rucaparib (0.1ug/ml)	97	93	94
Exp. 4	Treatment	Cell Line		
		HCC1187	HCC1954	SKBR3
	SN38	88	100	88
	Talazoparib		100	
	SN38 & Talazoparib (3ug/ml)	89	93	90
	SN38 & Talazoparib (1ug/ml)	89	94	89
	SN38 & Talazoparib (0.3ug/ml)	89	94	100
	SN38 & Talazoparib (0.1ug/ml)	100	96	87

[00128] The experiments that generated these data were performed in 384 well format. Cells were plated at 1000 cells/well and then incubated for 24 hours. Then SN-38 and/or one of four different PARP inhibitors (talazoparib niraparib, olaparib or rucaparib) was added and incubated for an additional 24 hours then the wells were washed with PBS to remove the drug and fresh media was added back into the wells. The plates were then allowed to incubate for 72 hours period. After the 72 hour incubation period the media was removed and cell viability was determined using the CellTiter-Glo® cell viability assay (Promega, Madison WI) according to the product instructions. Figures 3A and 3B are line graphs that depict cell

viability in BT20 and HCC38 breast cancer cell lines, respectively, following treatment with SN-38 and/or talazoparib.

**[00129]** While the invention has been described in connection with specific embodiments thereof, it will be understood that it is capable of further modifications and this application is intended to cover any variations, uses, or adaptations of the invention following, in general, the principles of the invention and including such departures from the present disclosure that come within known or customary practice within the art to which the invention pertains and may be applied to the essential features set forth herein. The disclosure of each and every U.S., international or other patent or patent application or publication referred to herein is hereby incorporated herein by reference in its entirety.

### Claims

1. Use of liposomal irinotecan in combination with a Poly(ADP-ribose) Polymerase (PARP) inhibitor in an antineoplastic therapy for the treatment of a solid tumor, wherein the liposomal irinotecan is repeatedly administered once every two weeks and the PARP inhibitor is administered daily for 3 to 10 days between consecutive administrations of the liposomal irinotecan, without administering the PARP inhibitor within 3 days of the liposomal irinotecan.
2. The use of claim 1, wherein the PARP inhibitor is administered on each of consecutive days 3 to 10 between the days when the liposomal irinotecan is administered.
3. Use of liposomal irinotecan and a Poly(ADP-ribose) Polymerase (PARP) inhibitor in an antineoplastic therapy for the treatment of a solid tumor, the use comprising a 28-day antineoplastic therapy treatment cycle consisting of: administering the liposomal irinotecan on days 1 and 15 of the treatment cycle, and administering the PARP inhibitor on one or more days starting at least 3 days after the liposomal irinotecan and ending at least 1 day prior to administration of additional liposomal irinotecan.
4. The use of claim 3, wherein the PARP inhibitor is not administered for at least 3 days after the administration of liposomal irinotecan.
5. The use of any one of claims 3-4, wherein the PARP inhibitor is not administered for at least 3 days prior to the next administration of liposomal irinotecan.
6. The use of any one of claims 1-5, wherein the PARP inhibitor is administered on one or more of days 5-12 of the antineoplastic therapy treatment cycle.
7. The use of any one of claims 1-6, wherein the PARP inhibitor is administered on one or more of days 19-25 of the antineoplastic therapy treatment cycle.
8. The use of any one of claims 1-7, wherein the PARP inhibitor is administered on one or more of days 3-12 of the antineoplastic therapy treatment cycle.
9. The use of any one of claims 1-8, wherein the PARP inhibitor is administered on one or more of days 17-25 of the antineoplastic therapy treatment cycle.
10. The use of any one of claims 1-9, wherein the liposomal irinotecan has an irinotecan terminal elimination half-life of 26.8 hours and a maximal irinotecan plasma concentration of 38.0 micrograms/ml.



11. The use of any one of claims 1-10, wherein the PARP inhibitor is not administered within 3 days before or after the administration of the liposomal irinotecan.
12. The use of any one of claims 1-11, wherein each administration of liposomal irinotecan is administered at a dose of  $80 \text{ mg/m}^2$  (salt) or  $70 \text{ mg/m}^2$  (free base).
13. The use of any one of claims 1-12, wherein each administration of the PARP inhibitor is administered at a dose of from about 20 mg/day to about 800 mg/day.
14. The use of any one of claims 1-13, wherein each administration of the PARP inhibitor is administered once or twice daily at a dose of from about 20 mg/day to about 400 mg/day.
15. The use of any one of claims 1-14, wherein the PARP inhibitor is selected from the group consisting of niraparib, olaparib, veliparib, rucaparib and talazoparib.
16. The use of any one of claims 1-15, wherein the cancer is cervical cancer, ovarian cancer, triple negative breast cancer, non-small cell lung cancer, small cell lung cancer, gastrointestinal stromal tumors gastric cancer, pancreatic cancer, colorectal cancer, or a neuroendocrine cancer.
17. The use of any one of claims 1-16, wherein the cancer is cervical cancer and the PARP inhibitor is veliparib.
18. The use of any one of claims 1-17, wherein the cancer is cervical cancer and the PARP inhibitor is olaparib.
19. The use of any one of claims 1-18, further comprising the use of ferumoxytol as an imaging agent to select patients to receive the liposomal irinotecan and PARP inhibitor.
20. The use of claim 19, further comprising administering ferumoxytol and then obtaining a MRI image of the patient 24 hours after ferumoxytol administration.

ME-180 cells viability (1000cells/well in 384-well plate) treated with SN-38 and with different PARP inhibitors (0.33 ug/ml) for 24hrs, washed and incubated for additional 72hrs with fresh media

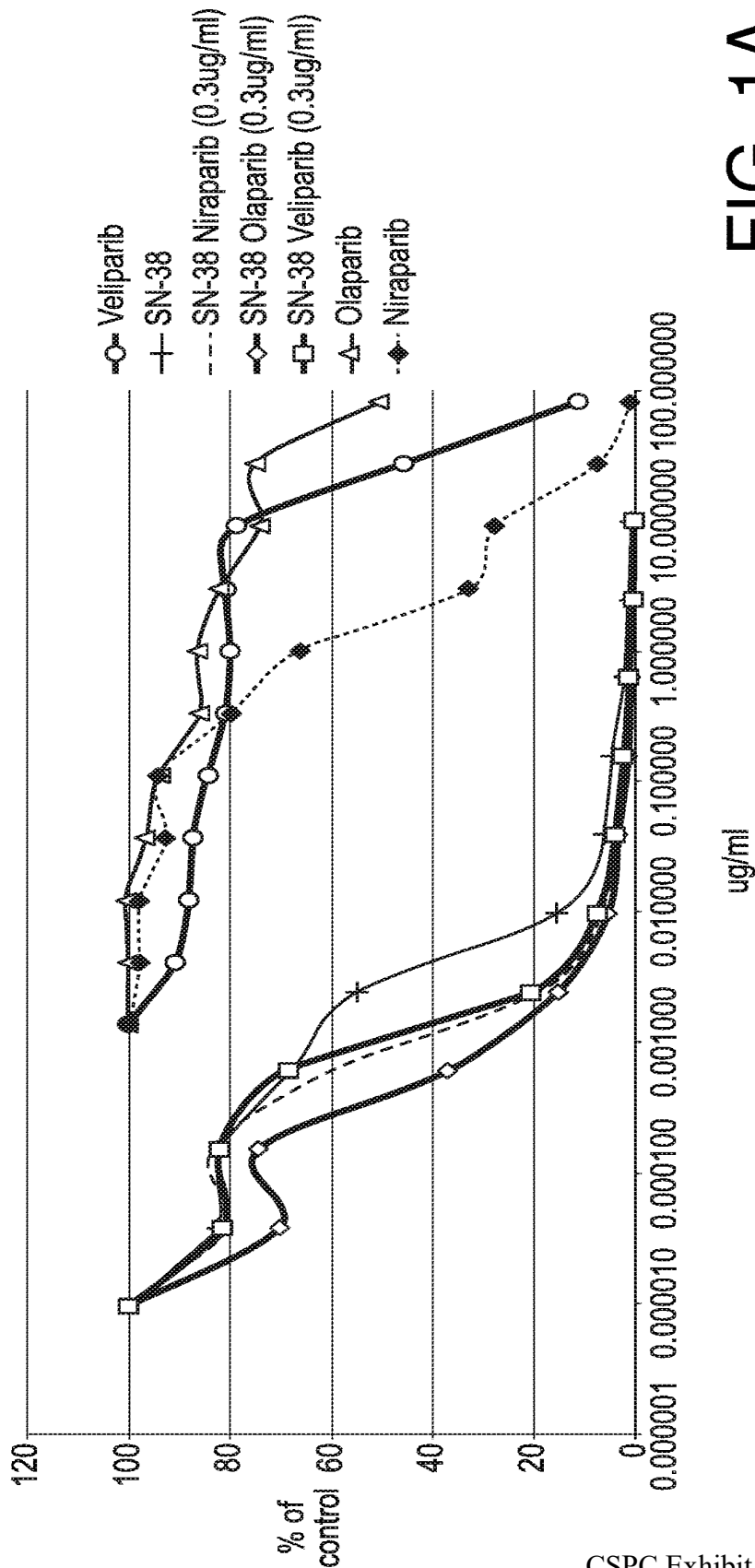
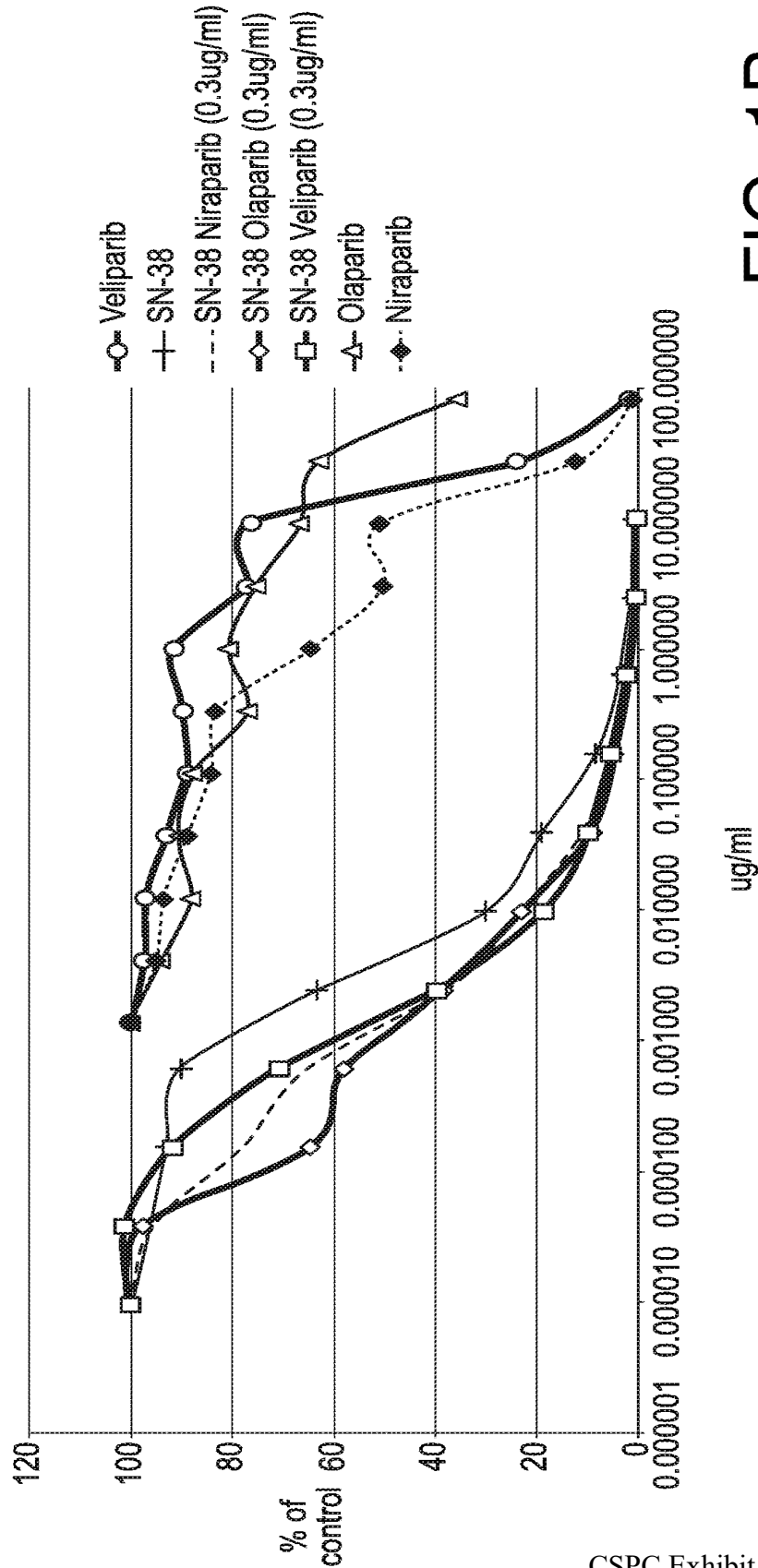


FIG. 1A

**MS-751 cells viability (1000cells/well in 384-well plate) treated with SN-38 and with different PARP inhibitors (0.33 ug/ml) for 24hrs, washed and incubated for additional 72hrs with fresh media**



**FIG. 1B**

**C-33A cells viability (1000cells/well in 384-well plate) treated with SN-38 and with different PARP inhibitors (0.33 ug/ml) for 24hrs, washed and incubated for additional 72hrs with fresh media**

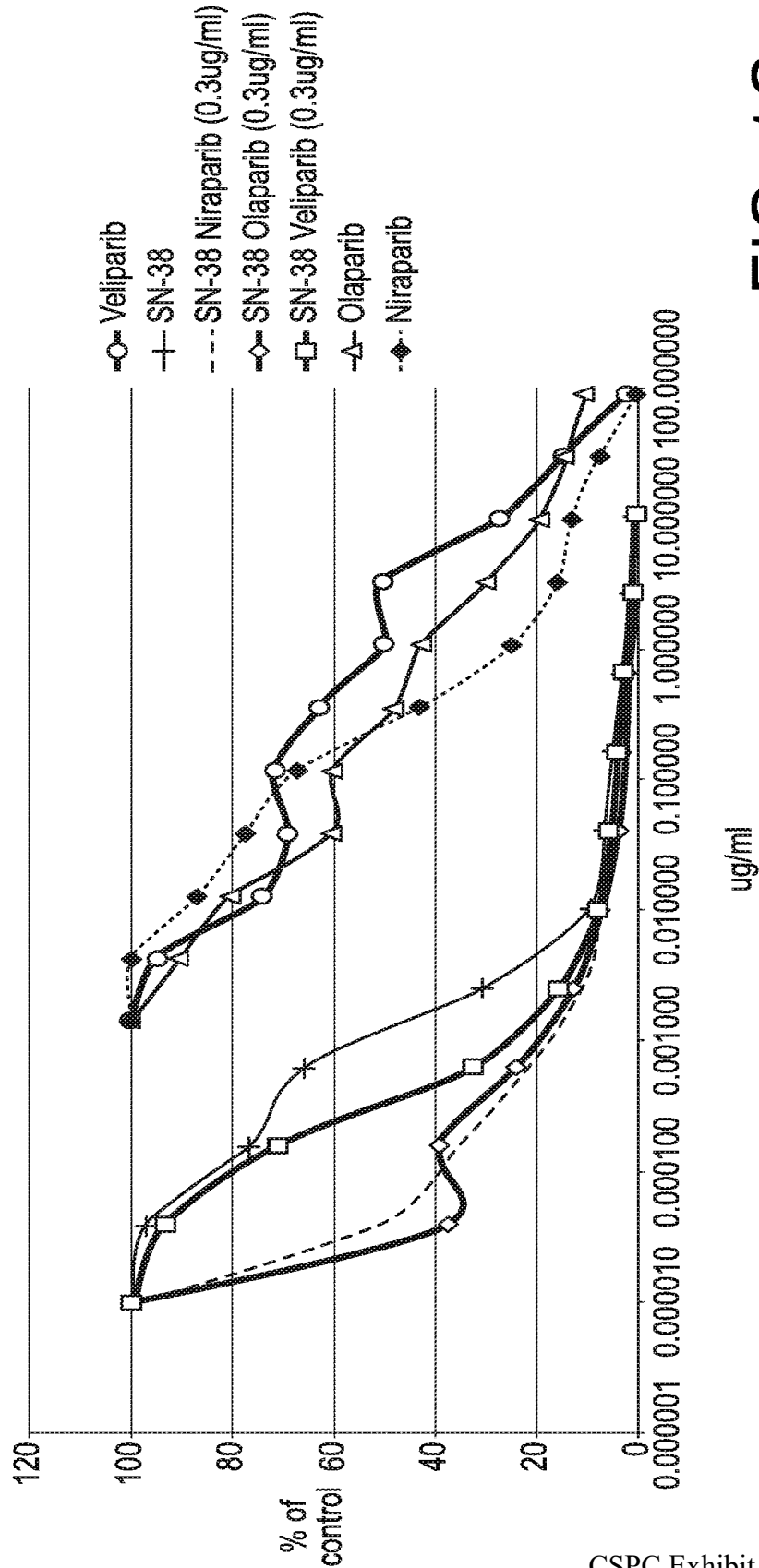


**FIG. 1C**

SW756 cells viability (1000cells/well in 384-well plate) treated with SN-38 and with different PARP inhibitors (0.33 ug/ml) for 24hrs, washed and incubated for additional 72hrs with fresh media

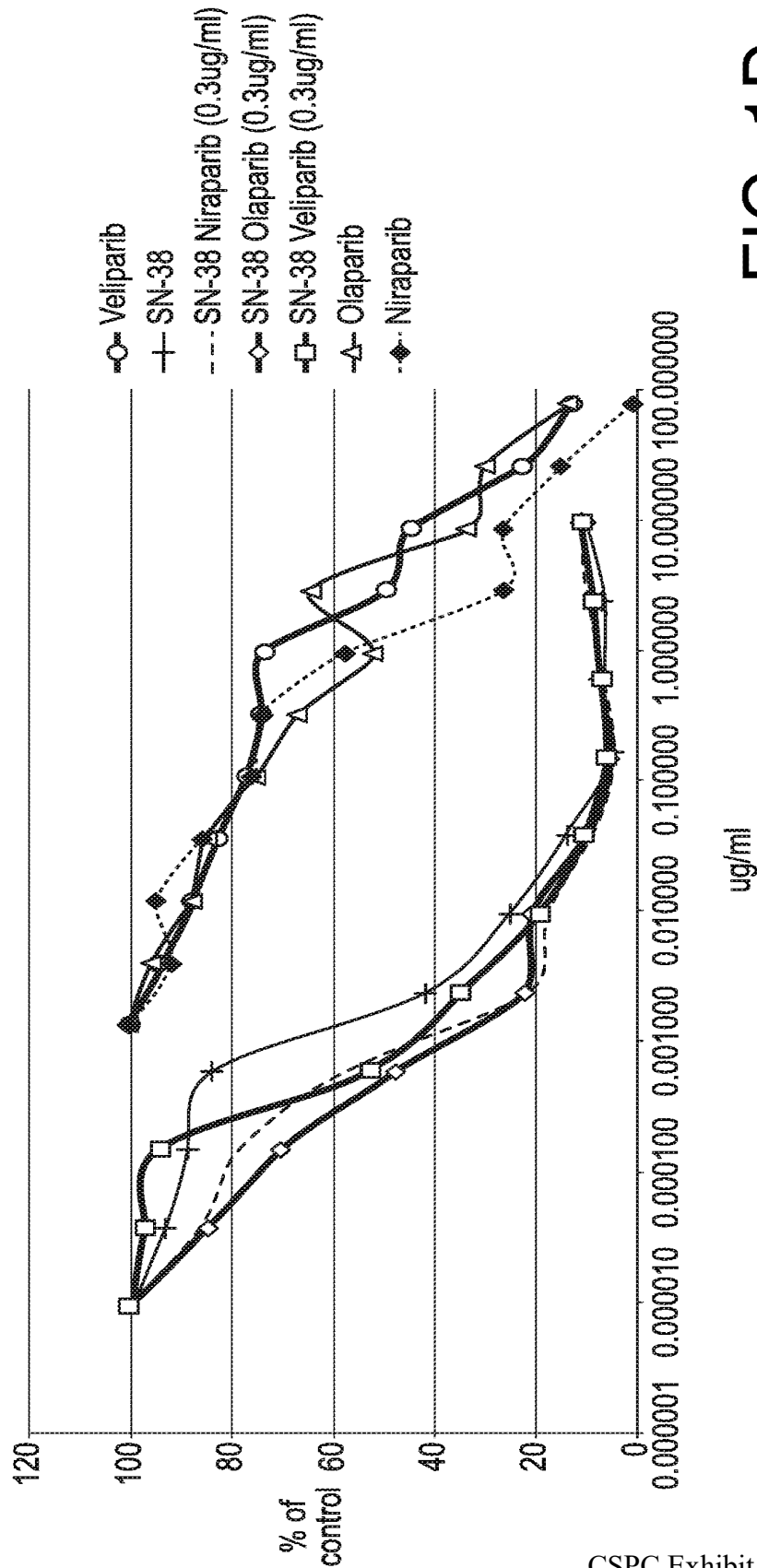


FIG. 1D

SiHa cells viability (1000cells/well in 384-well plate) treated with SN-38 and with different PARP inhibitors (0.33 ug/ml) for 24hrs, washed and incubated for additional 72hrs with fresh media

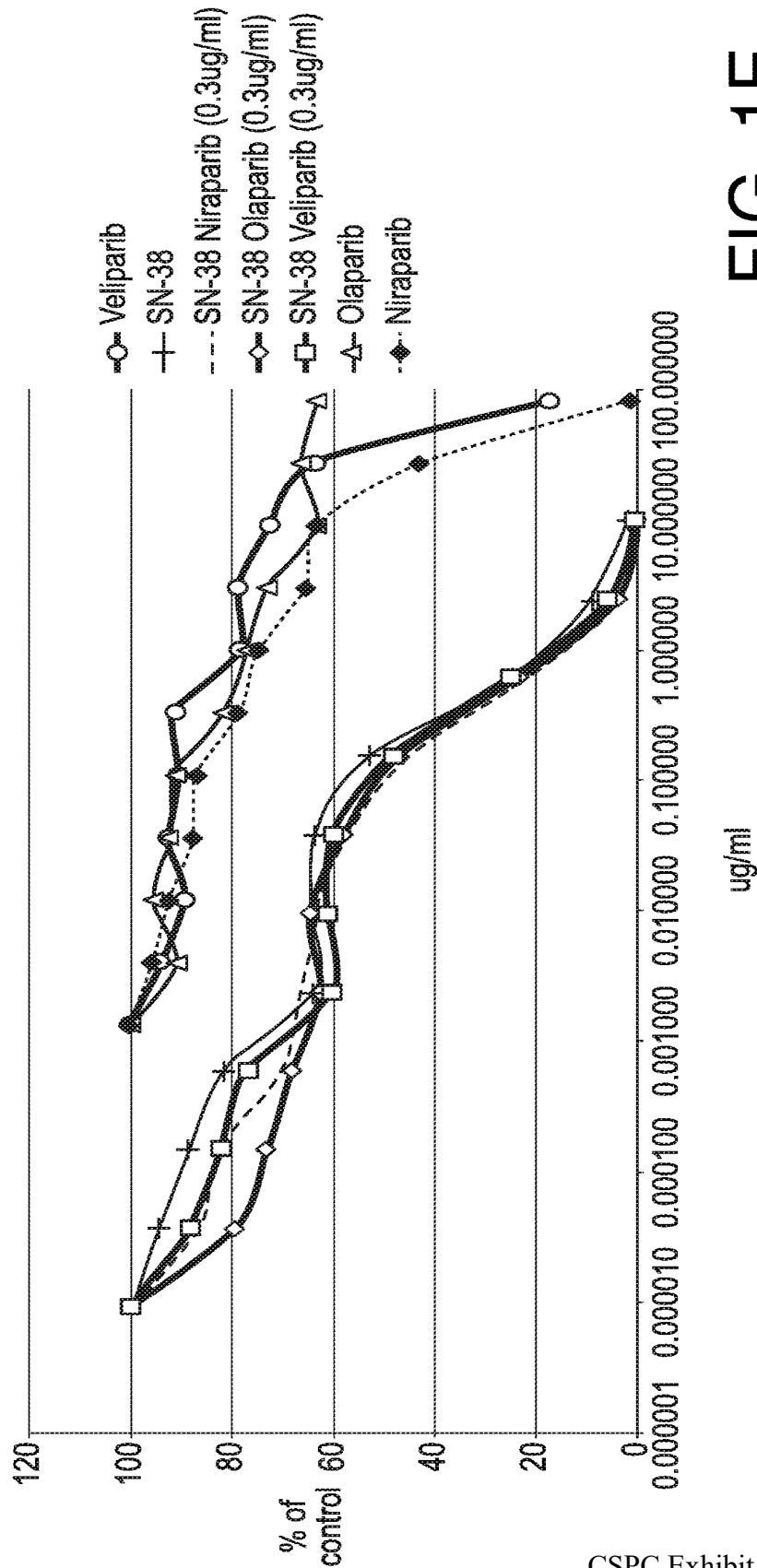


FIG. 1E

### DMS-114\_Rucaparib: SN-38 (2nM)

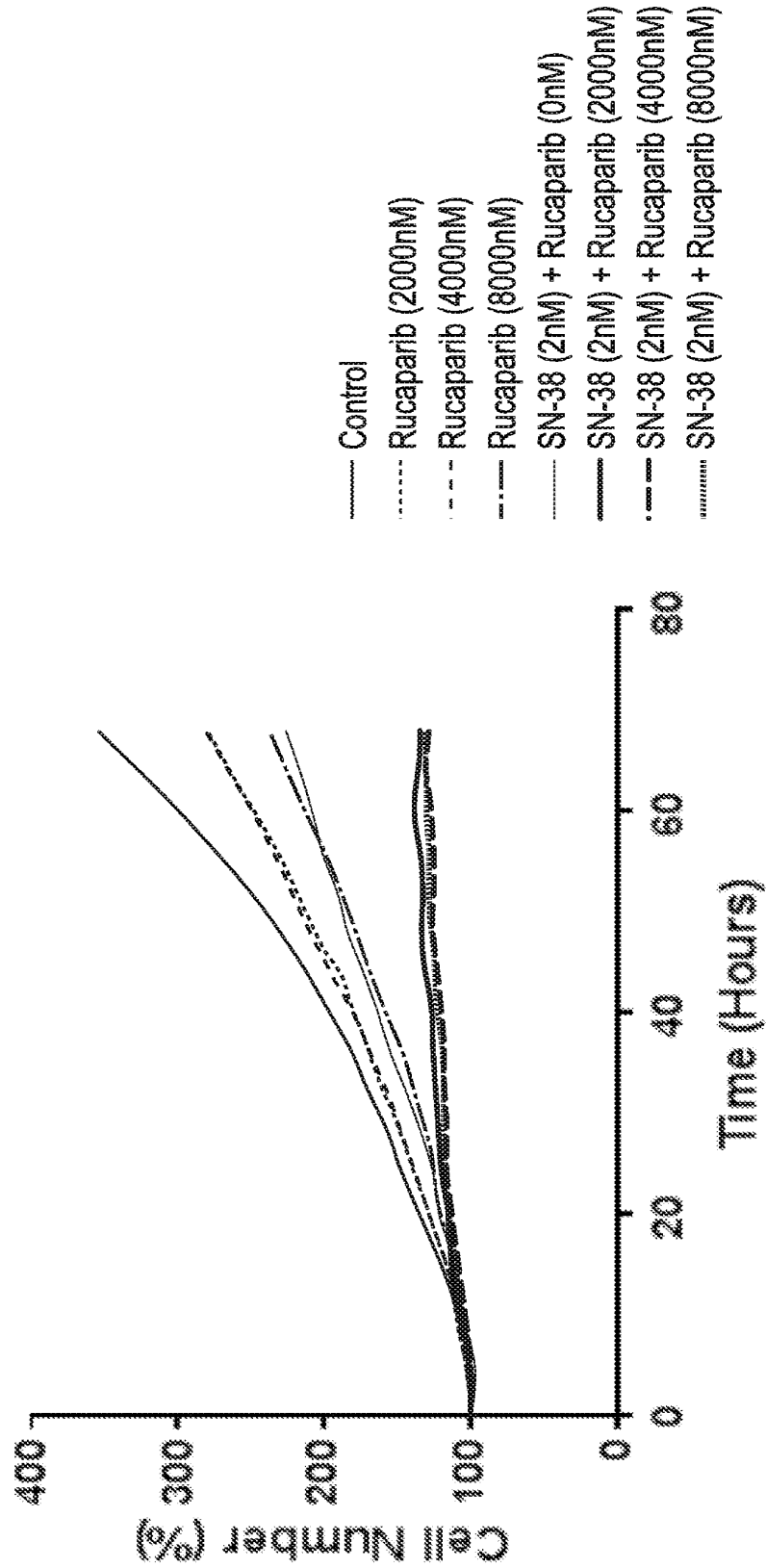


FIG. 2A

### NCI-H1048\_Rucaparib: SN-38 (2nM)

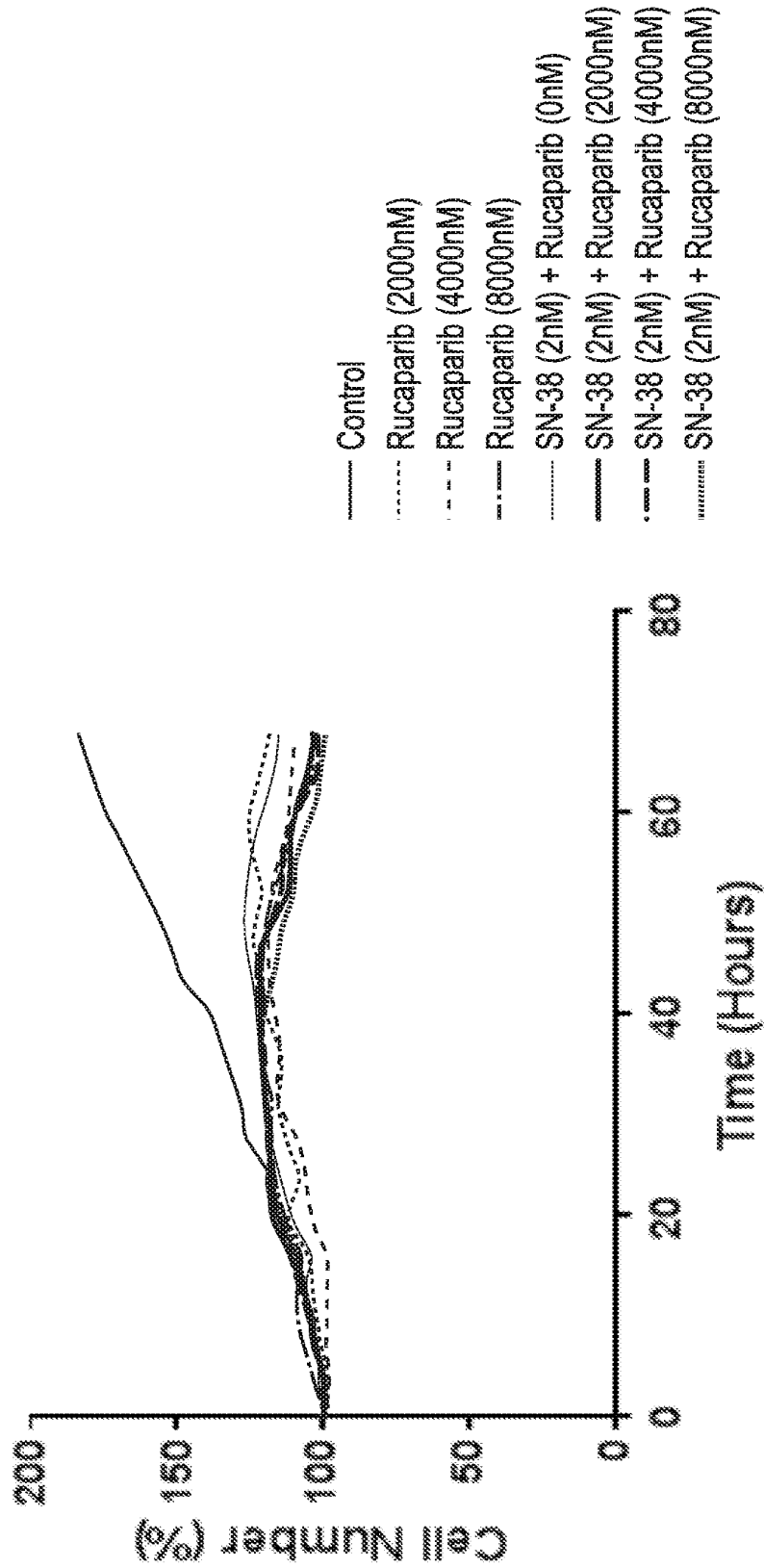


FIG. 2B



### CFPAC-1\_Rucaparib: SN-38 (2nM)

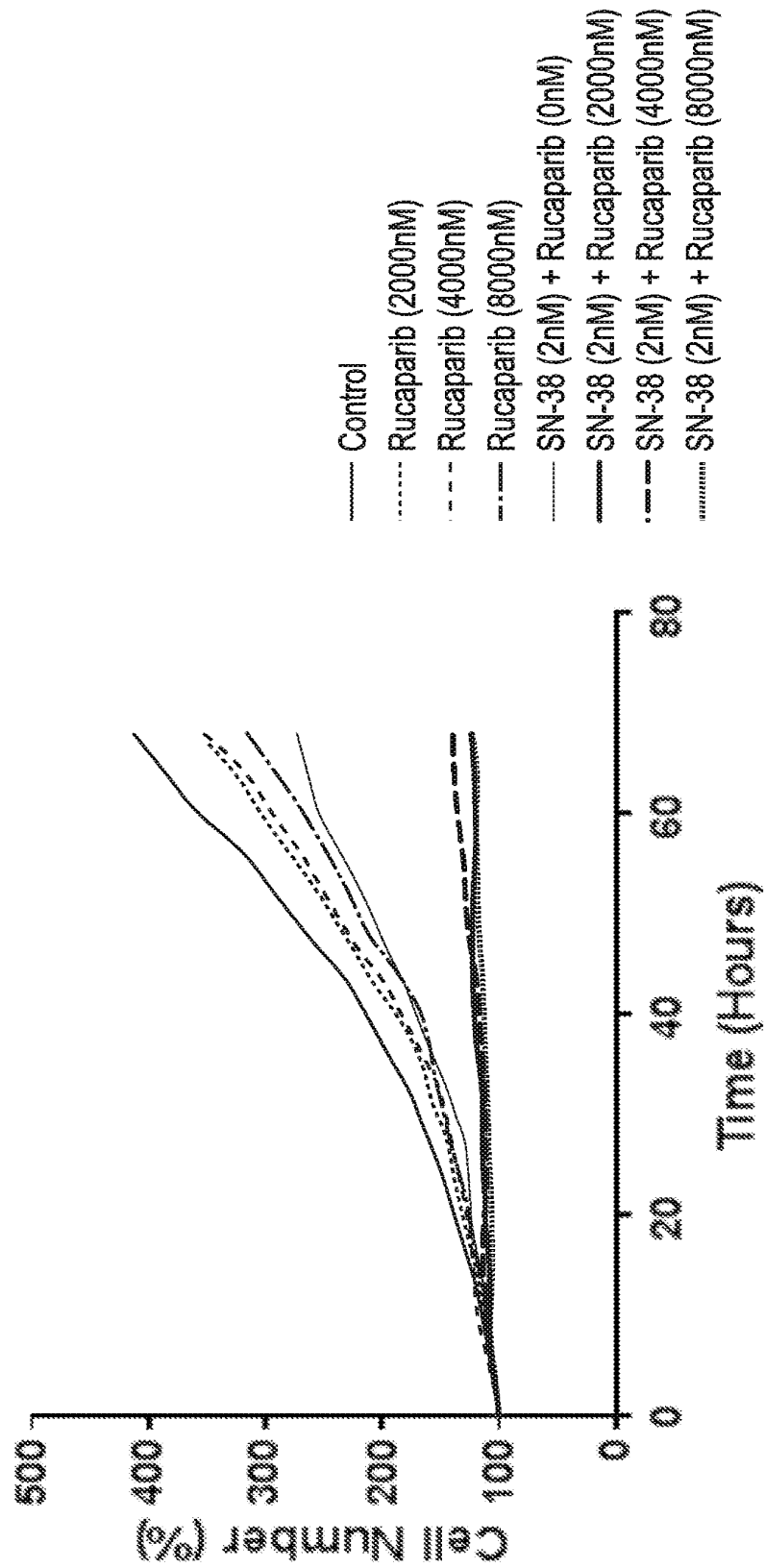


FIG. 2C

### BxPC-3\_Rucaparib: SN-38 (2nM)

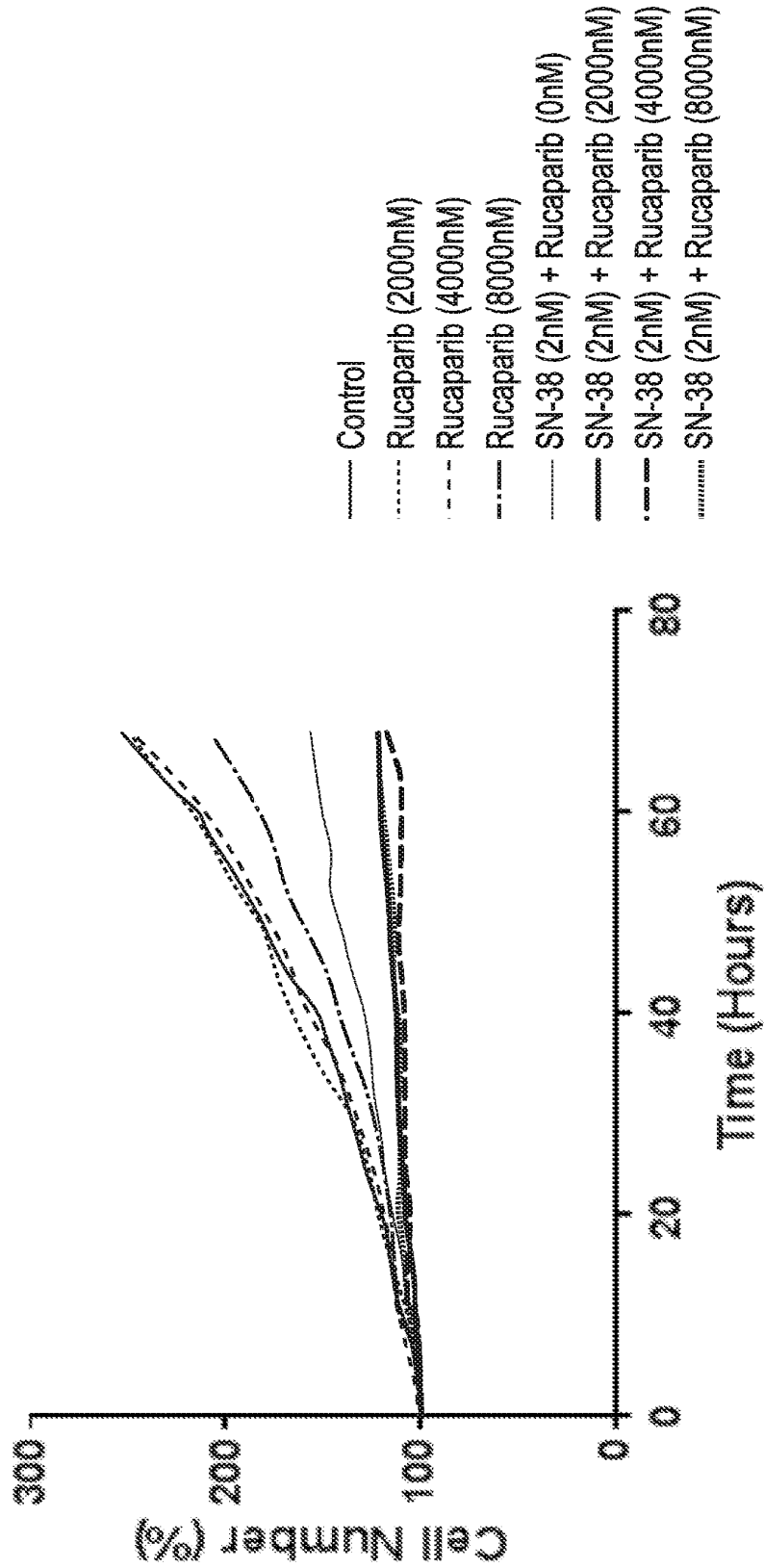
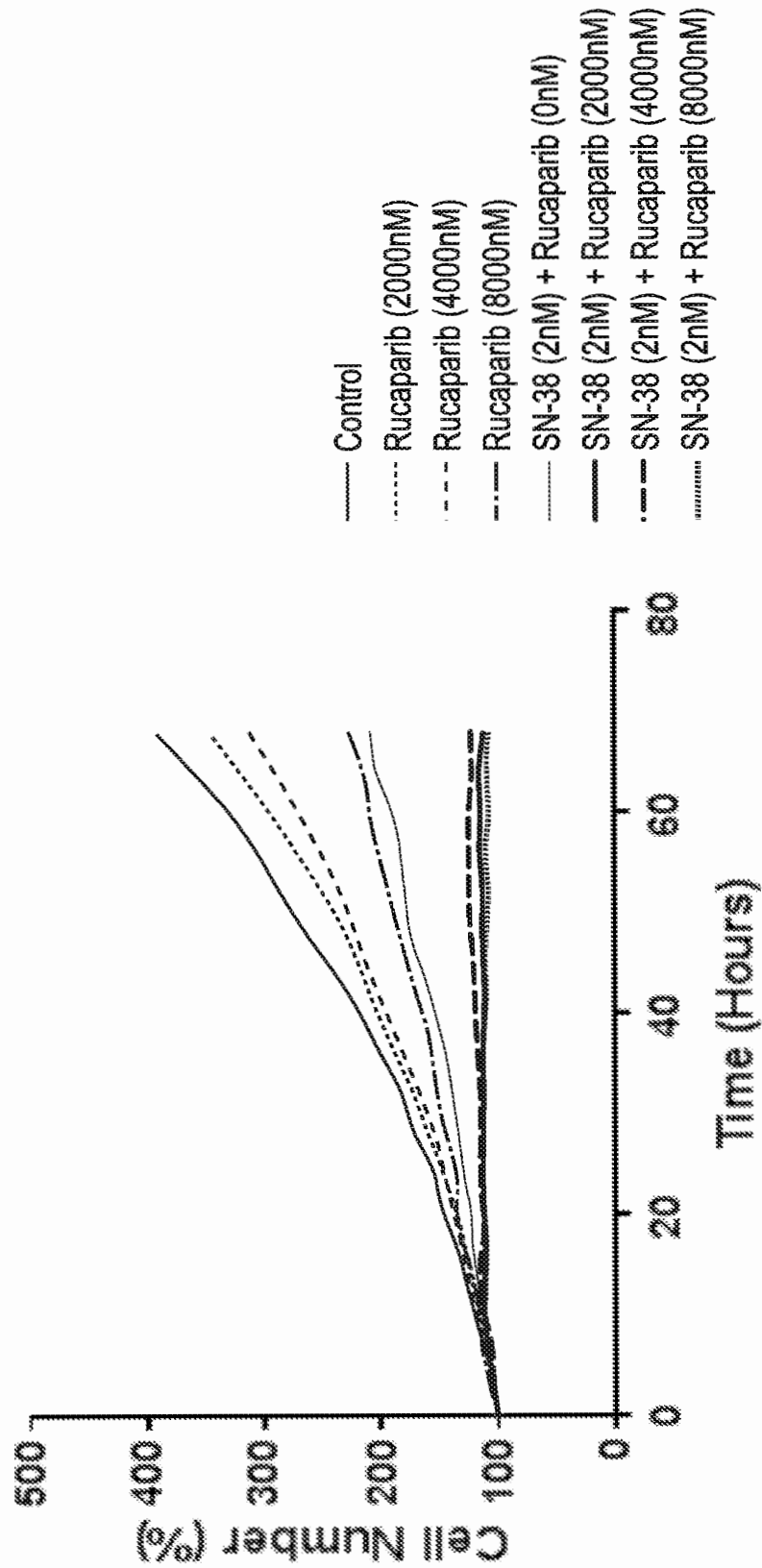


FIG. 2D

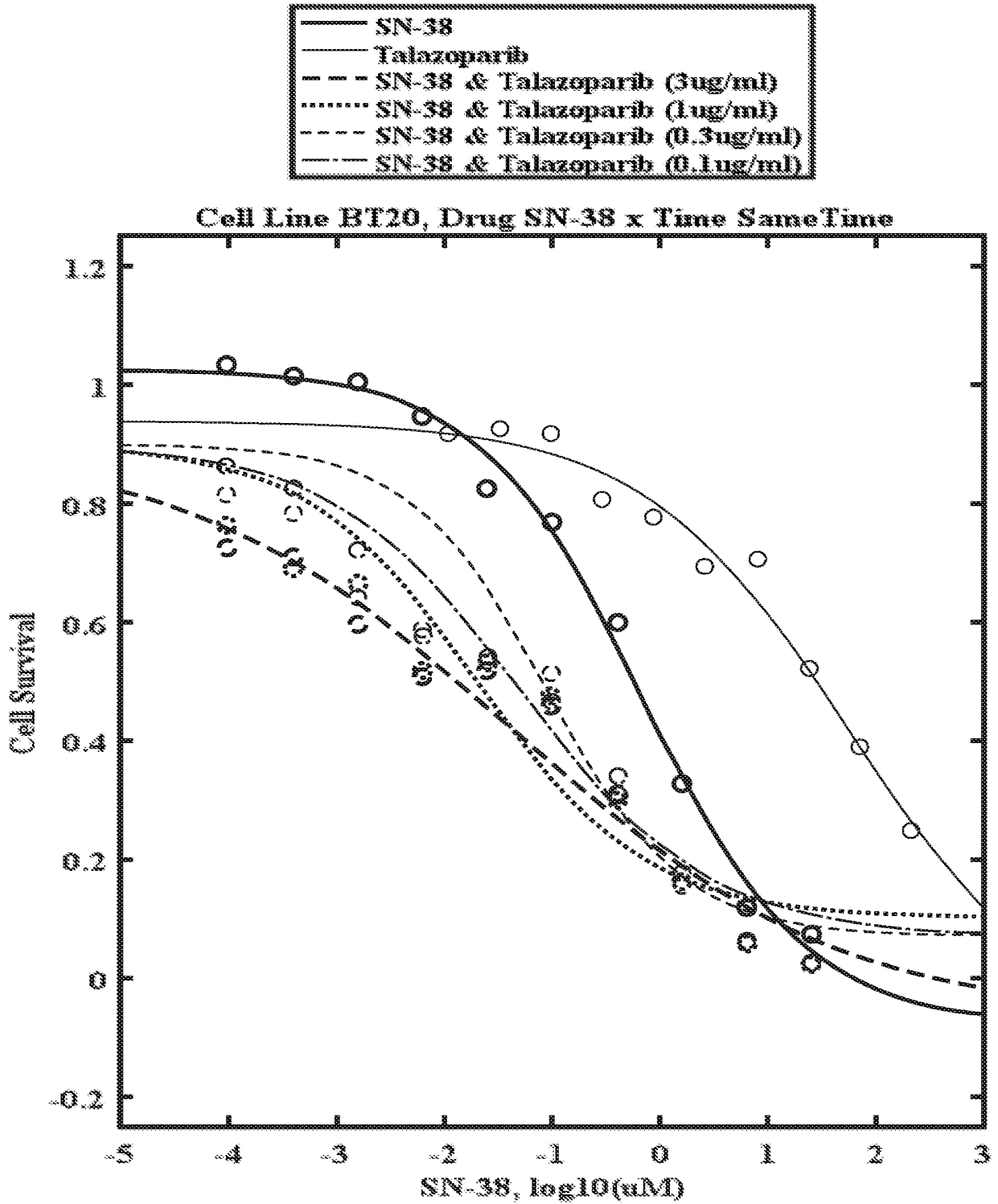
**MDA-MB-231\_Rucaparib: SN-38 (2nM)**



**FIG. 2E**

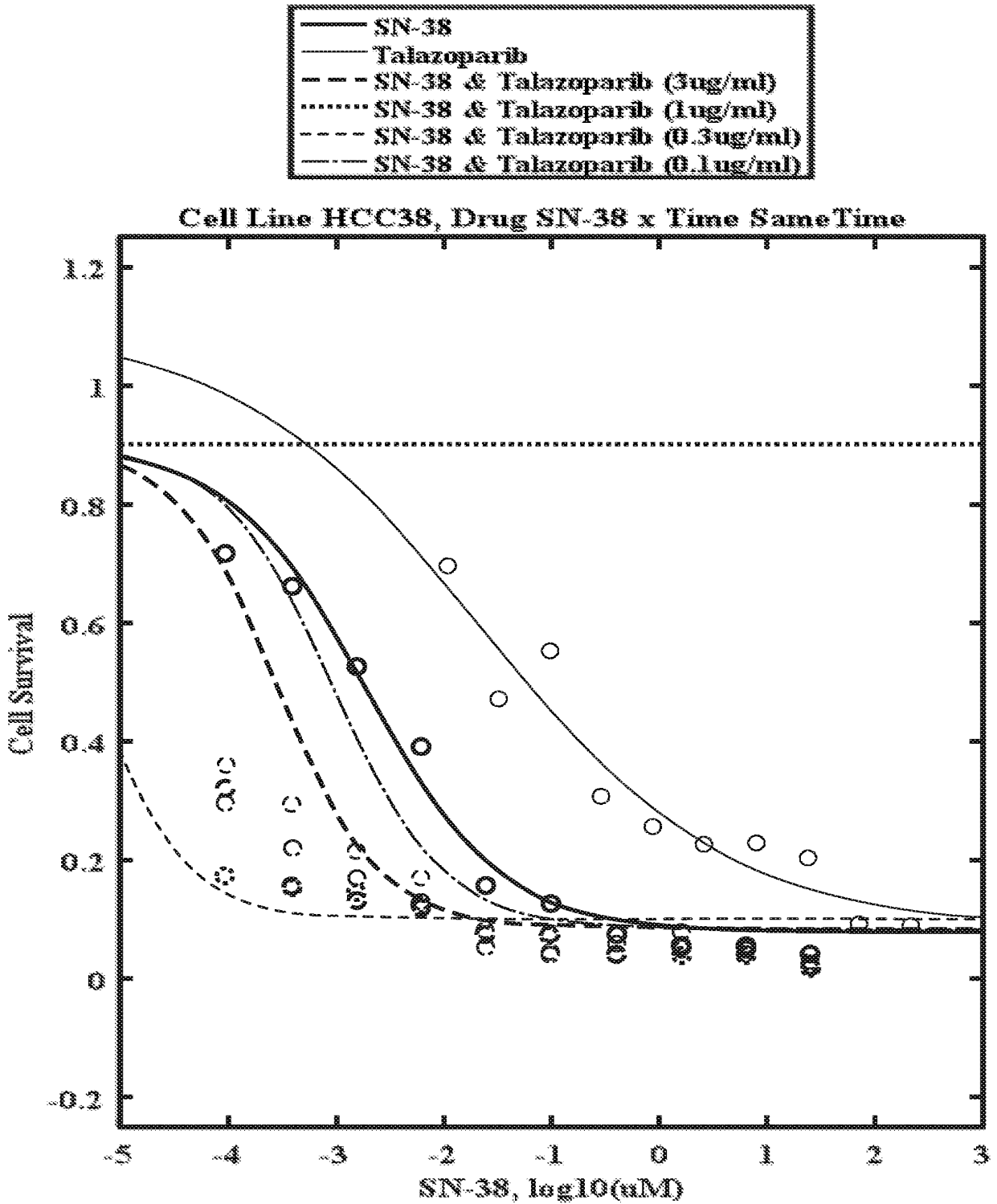
### BT20 cell survival treated with SN-38 and Talazoparib

# FIG. 3A



### HCC38 cell survival treated with SN-38 and Talazoparib

## FIG. 3B



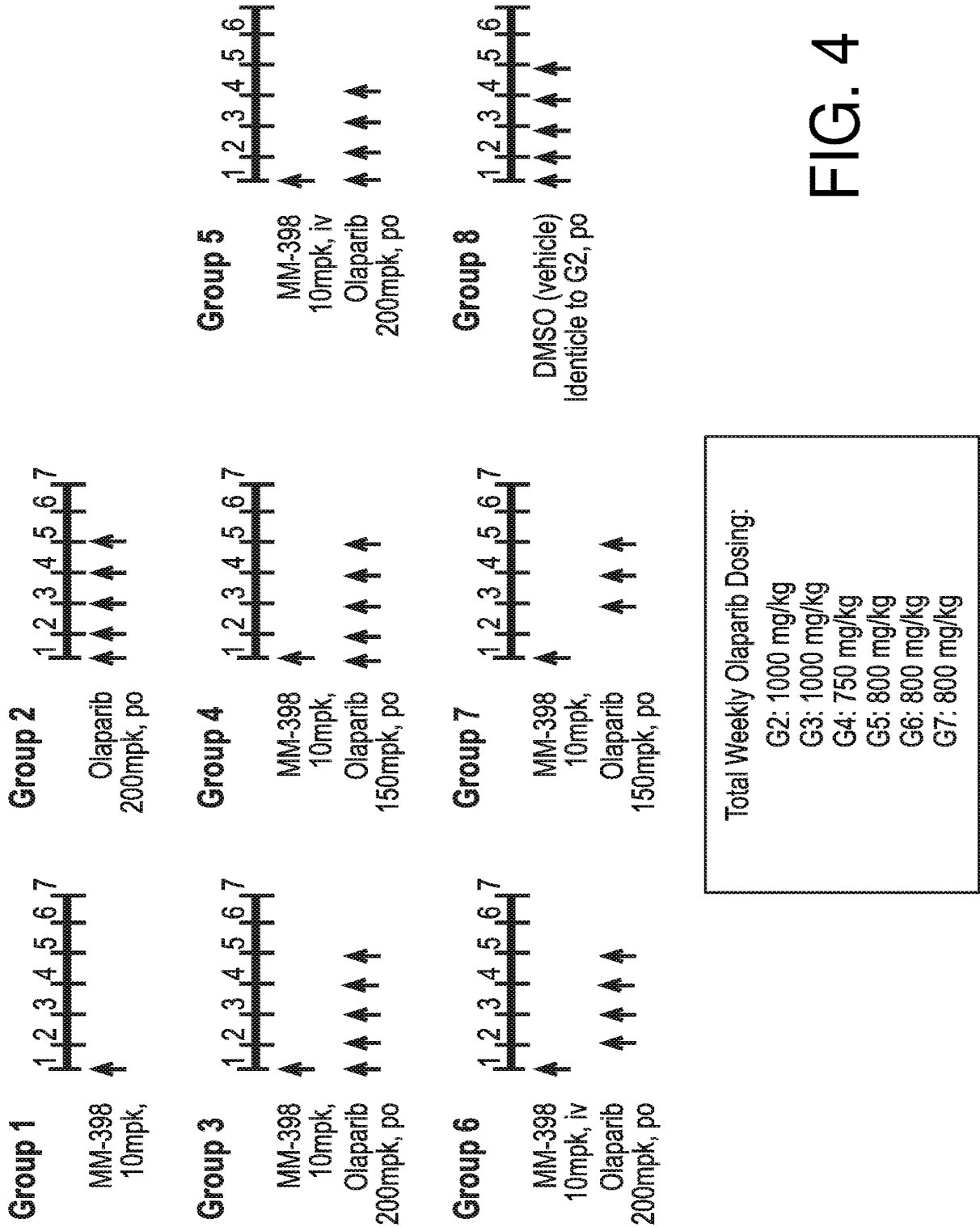


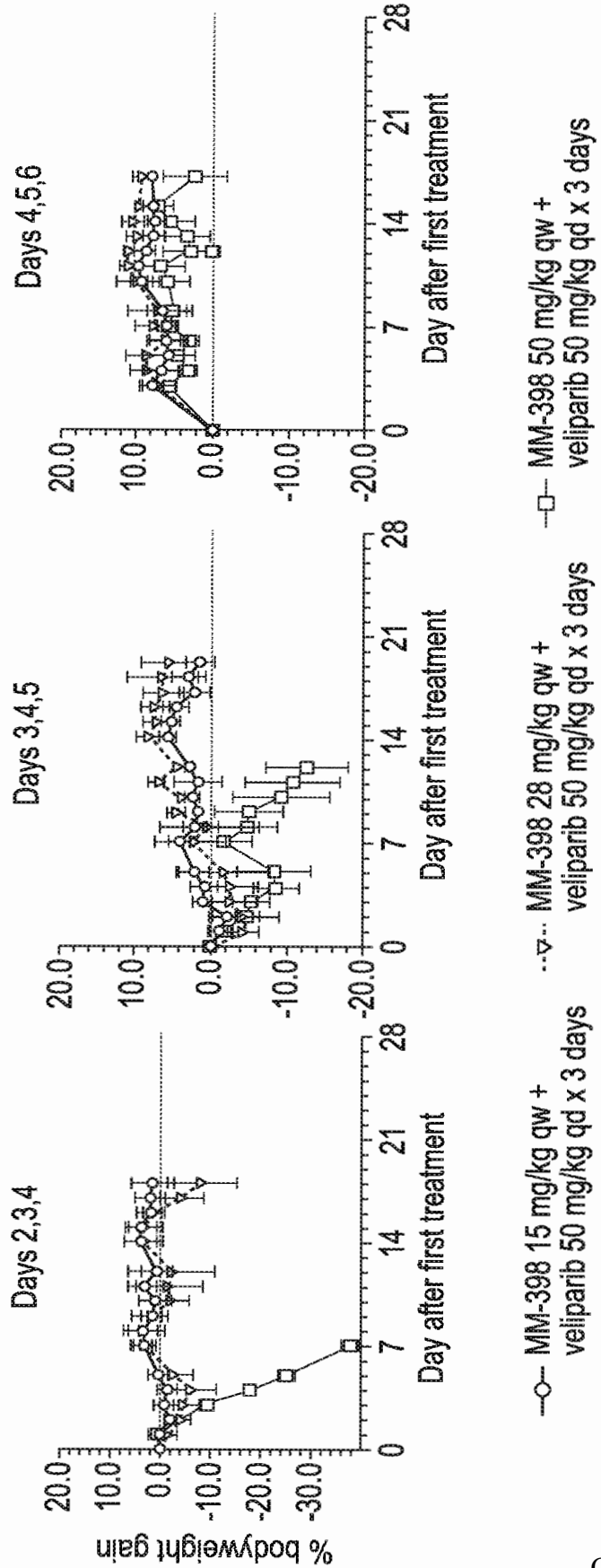
FIG. 4

100.1084WO01

FIG. 5C

FIG. 5B

FIG. 5A



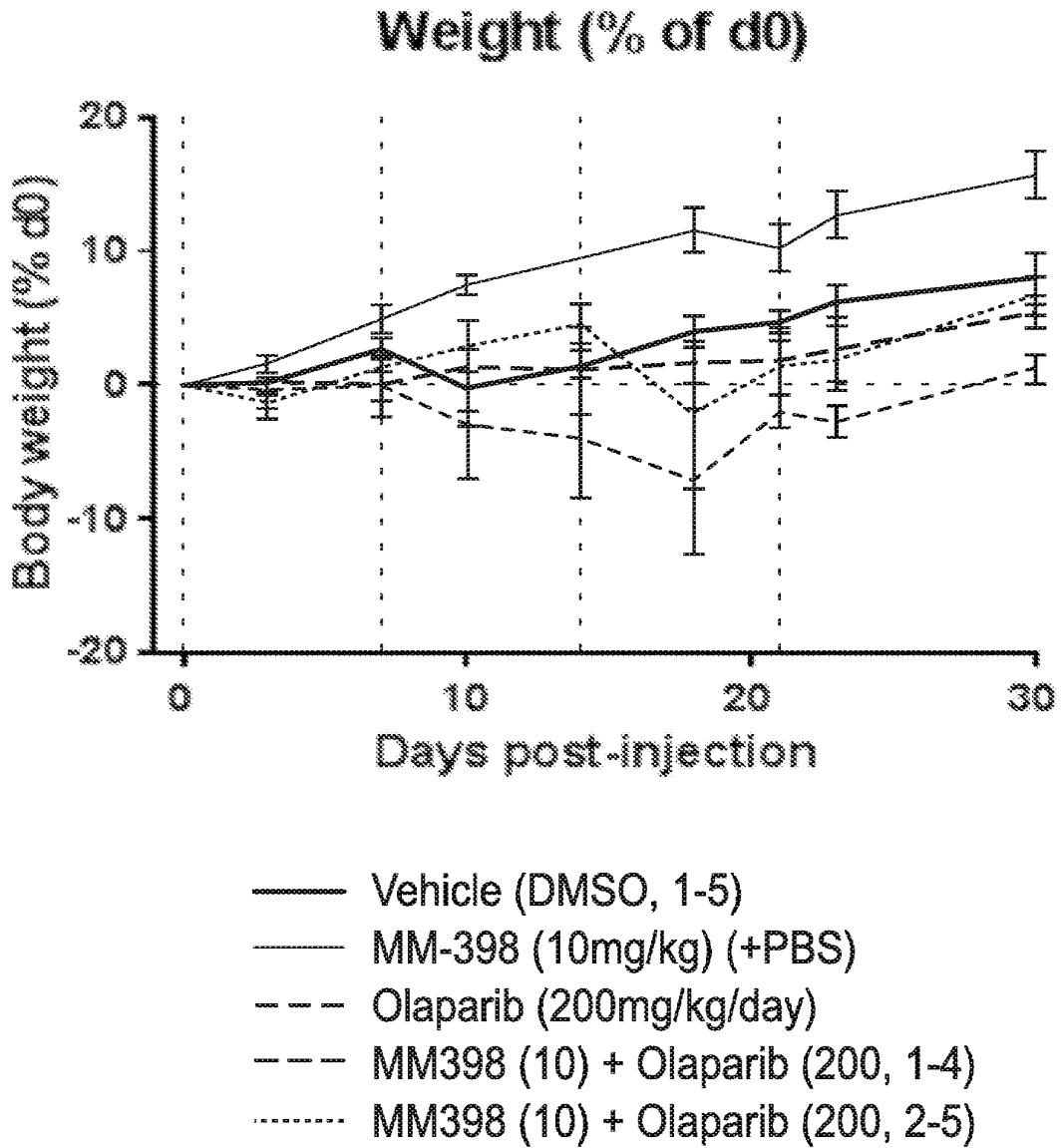


FIG. 6A



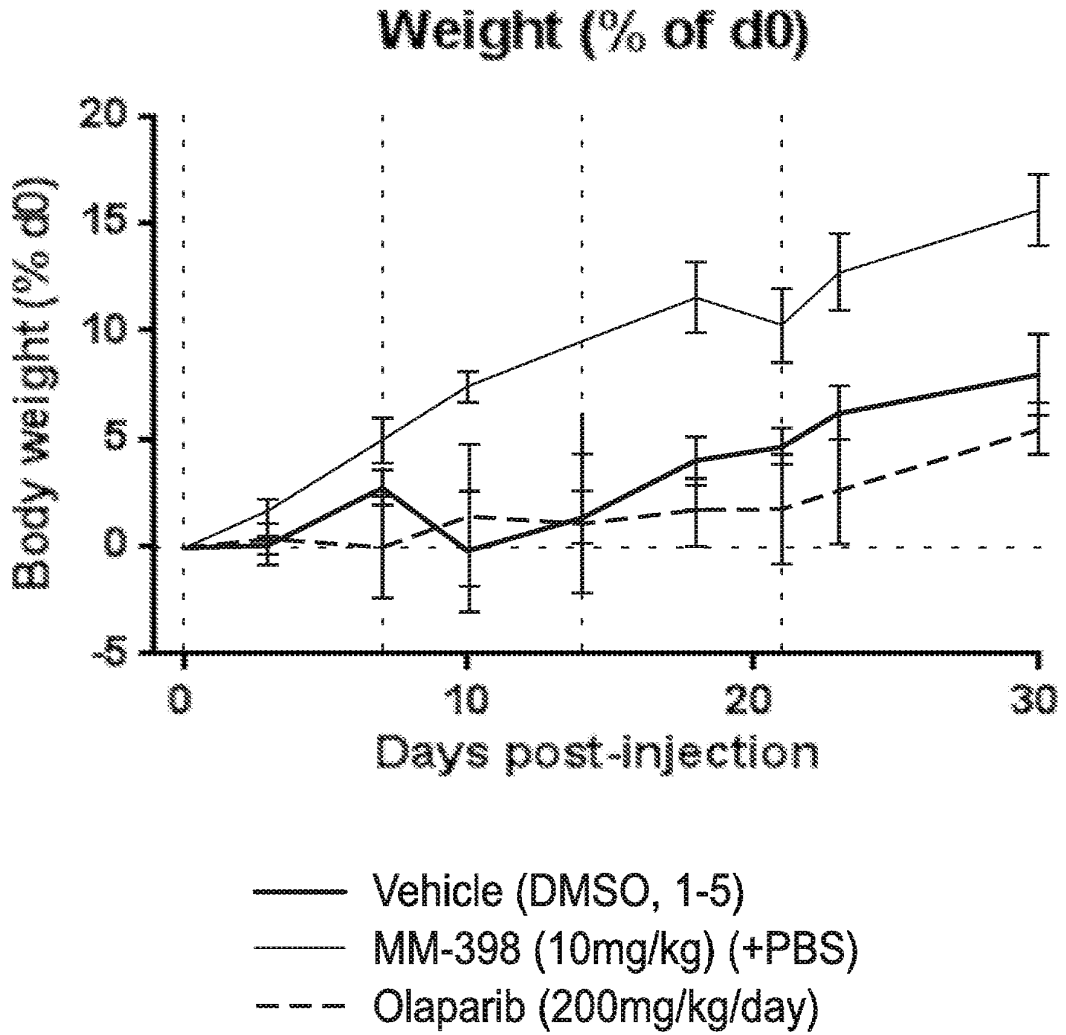


FIG. 6B

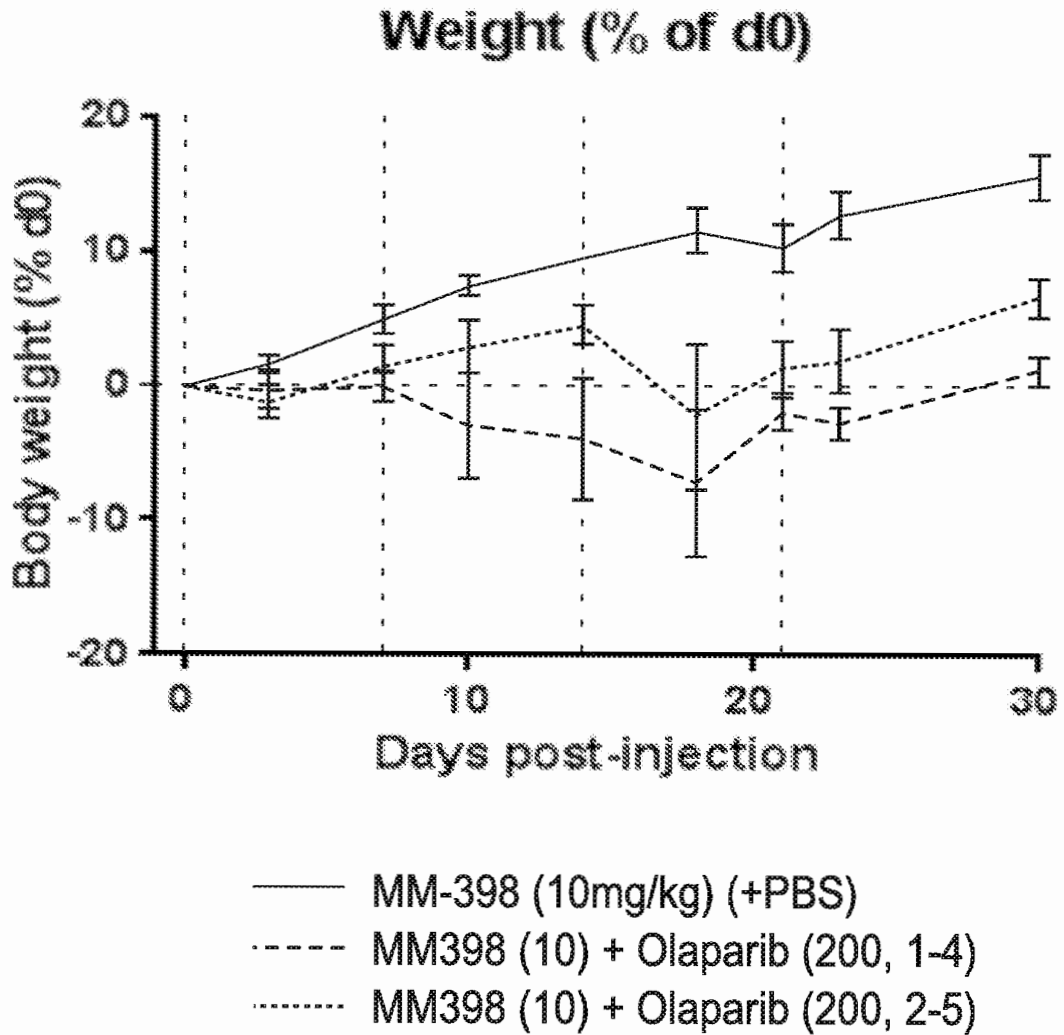


FIG. 6C

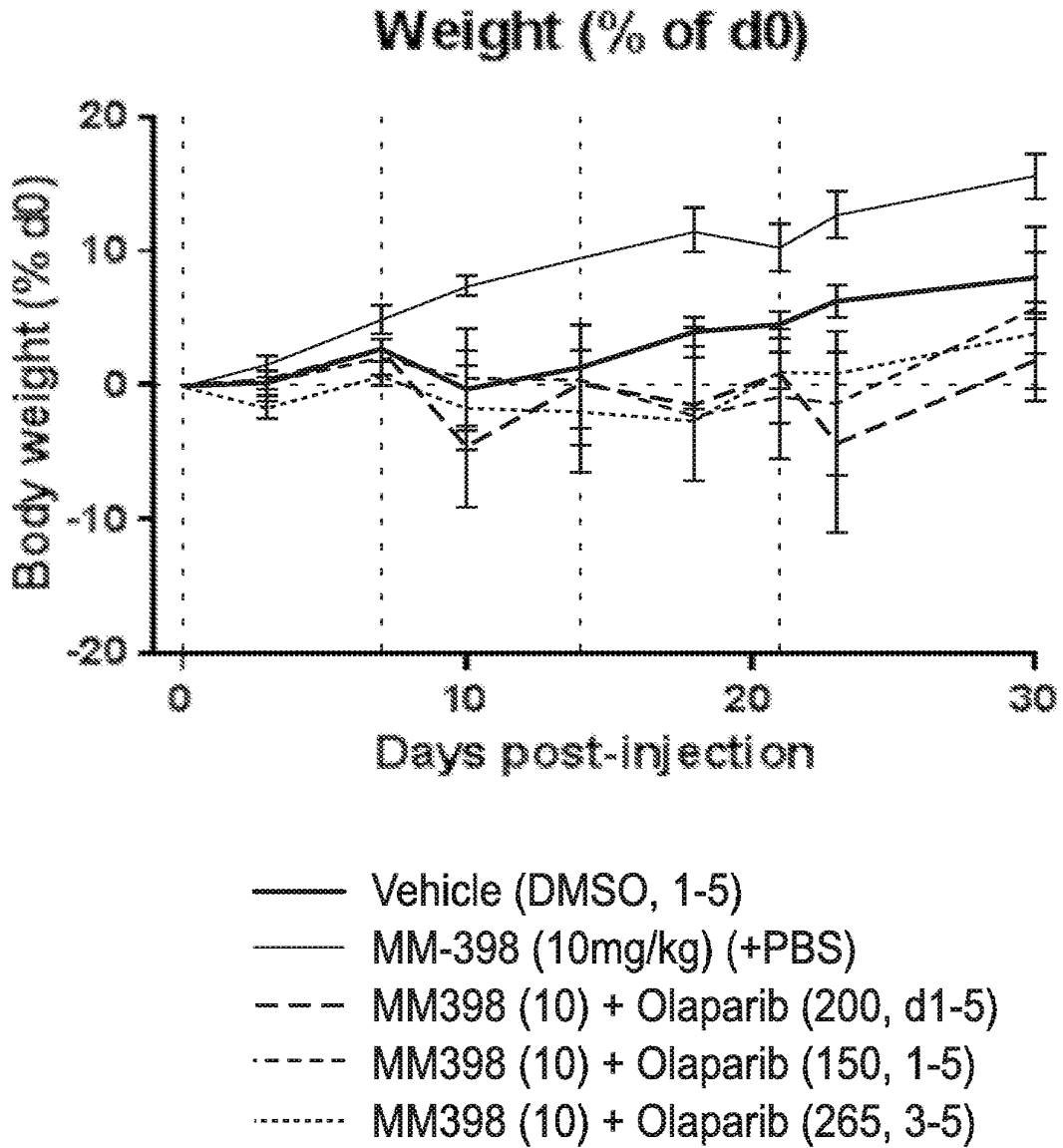


FIG. 6D

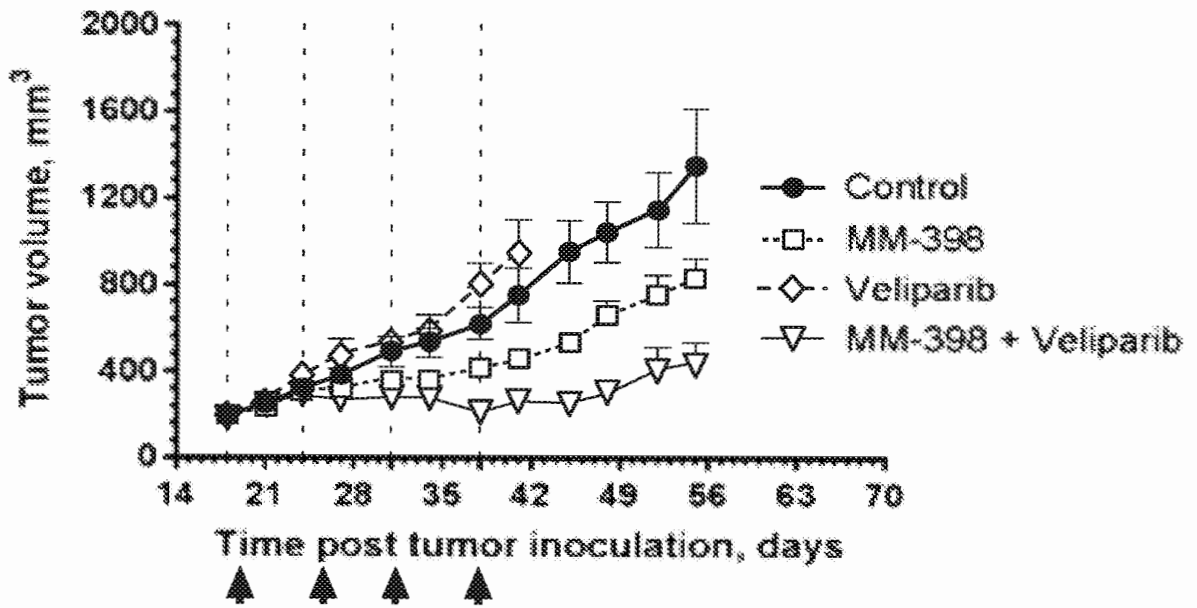


FIG. 7A

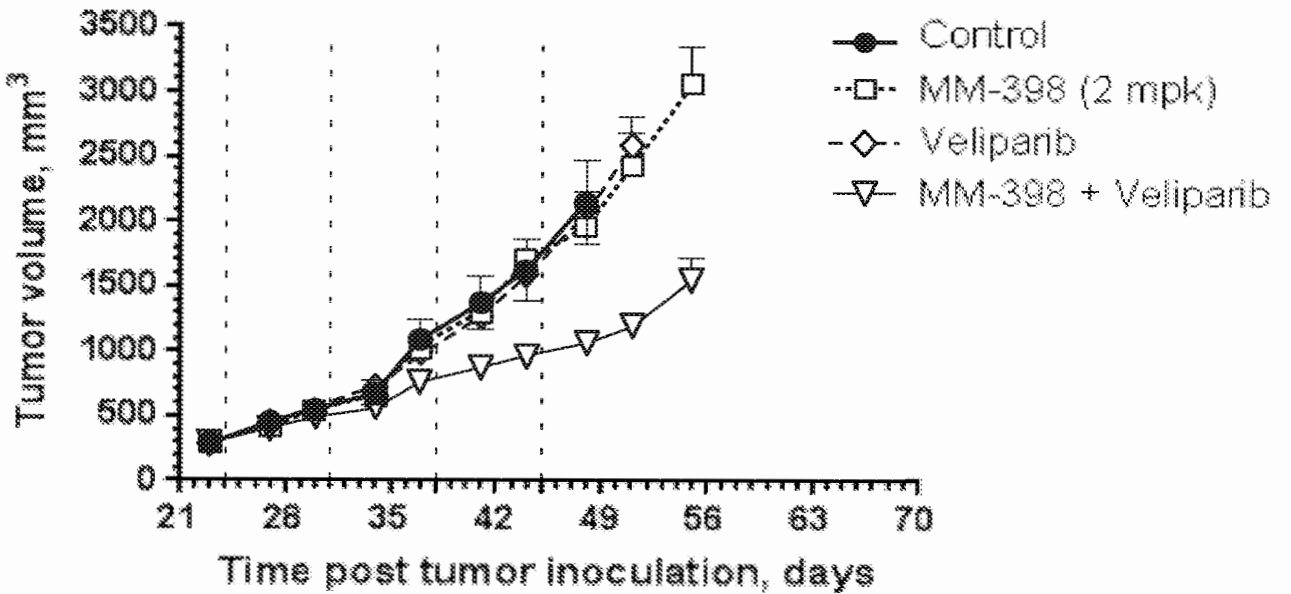
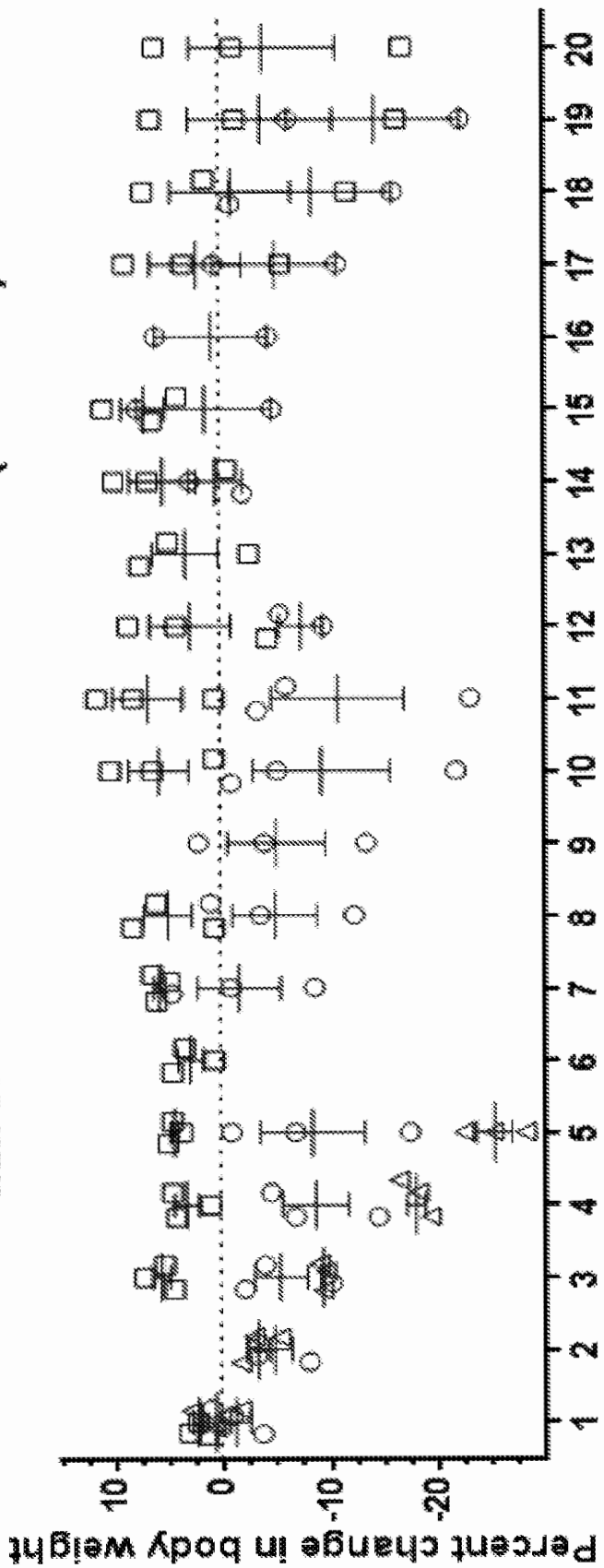


FIG. 7B

### MM-398 in combination with PARPi (ATB-888)



Day

- MM-398/50 mpk + PARPi/345
- MM-398/50 mpk + PARPi/234
- △ MM-398/50 mpk + PARPi/123

FIG. 8A

**MM-398 in combination with PARPi (ATB-888)**

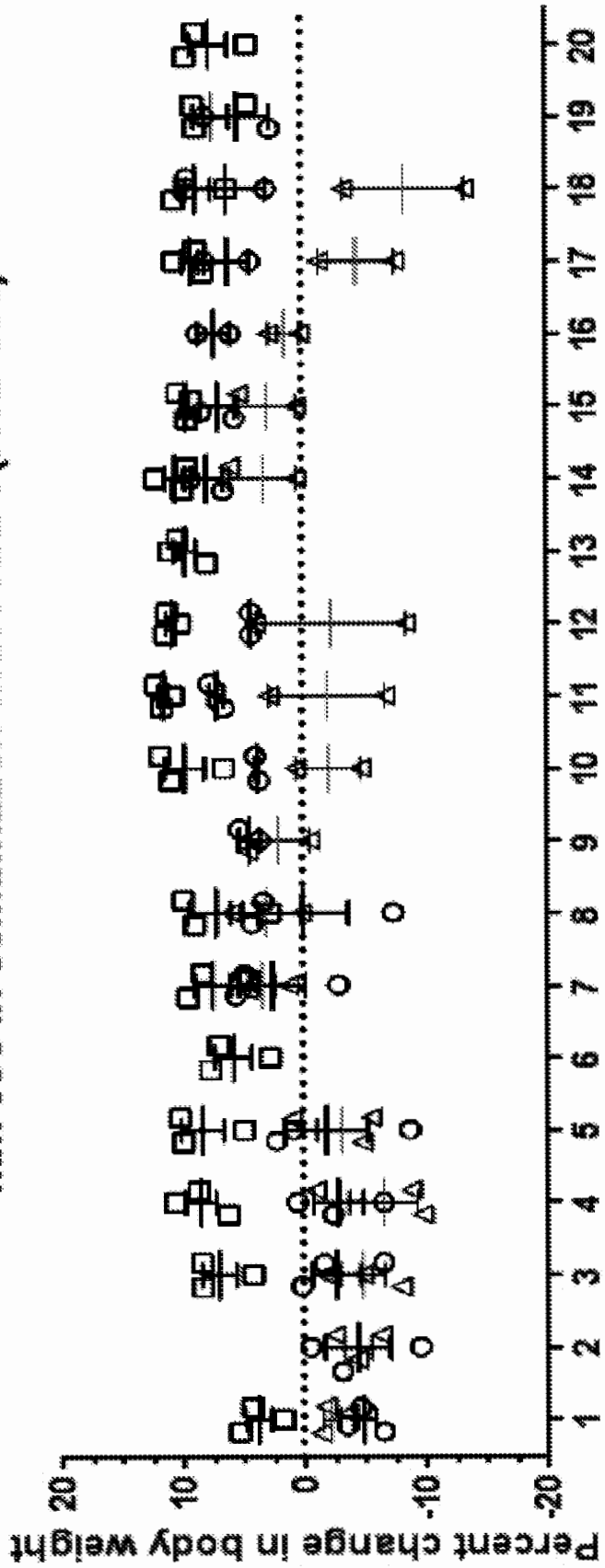


**FIG. 8B**

**Day**

- MM-398/28 mpk + PARPi/345
- MM-398/28 mpk + PARPi/234
- △ MM-398/28 mpk + PARPi/123

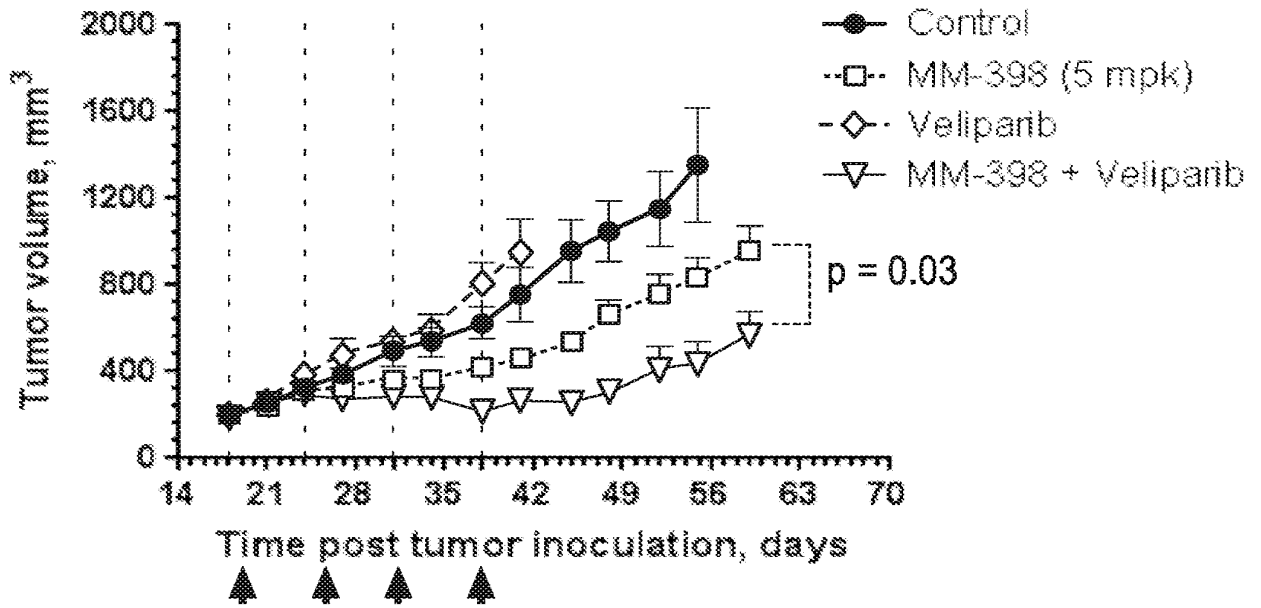


FIG. 9A

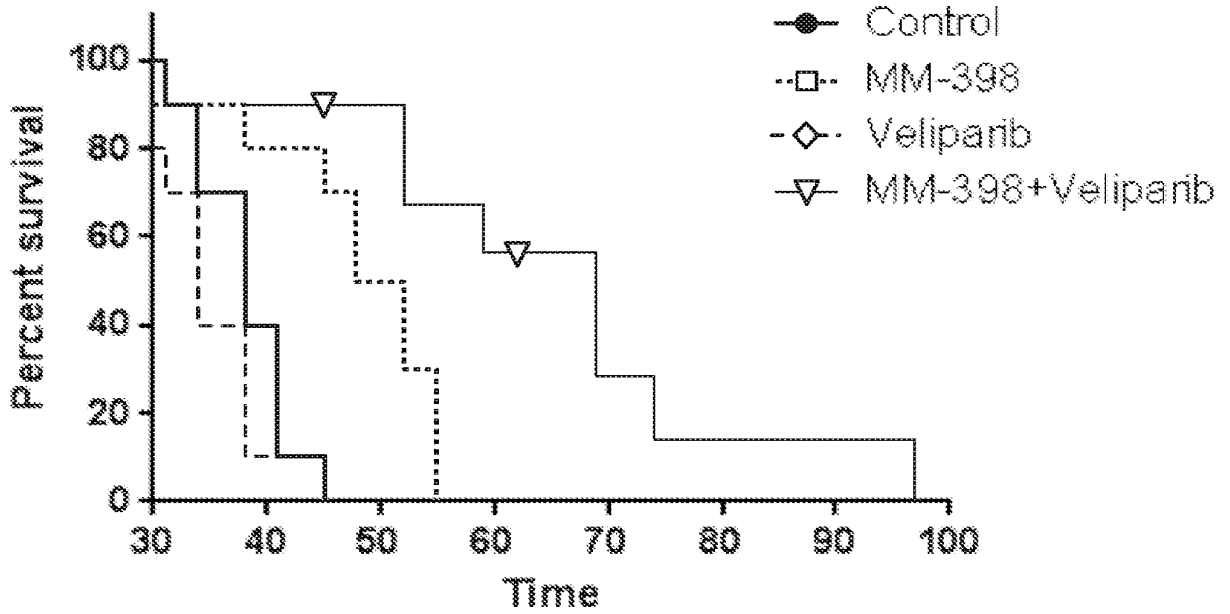


FIG. 9B

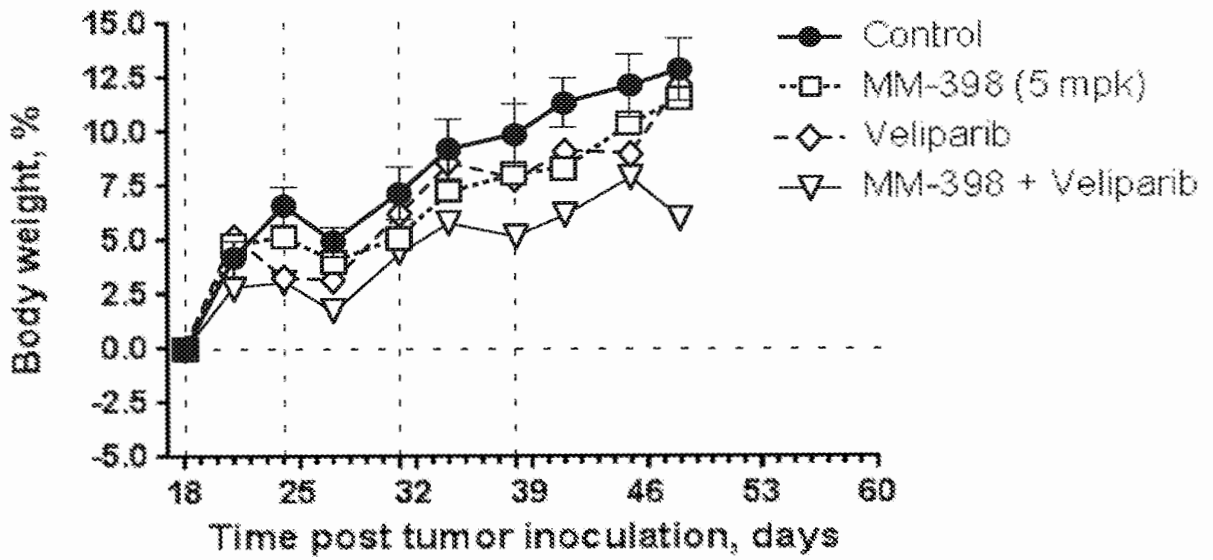


FIG. 9C

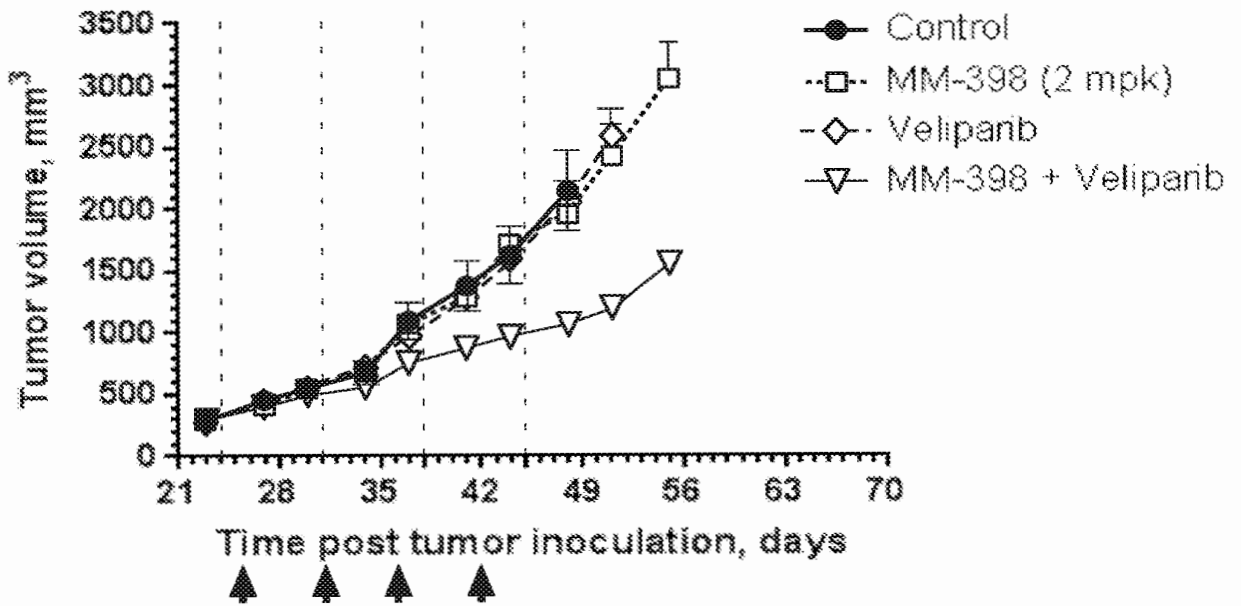


FIG. 10



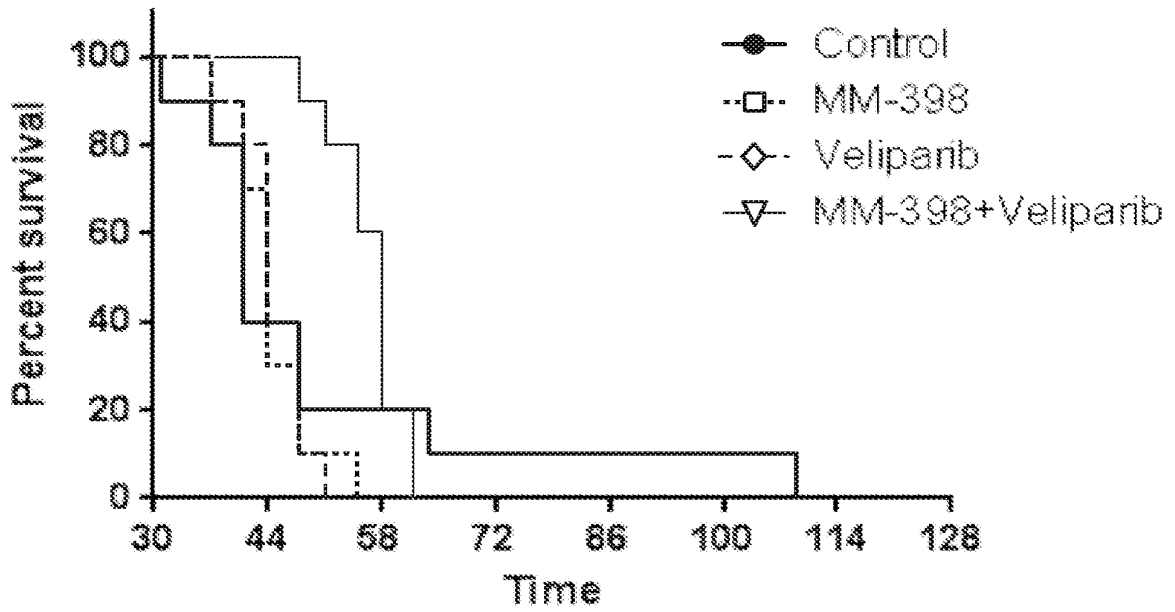


FIG. 11

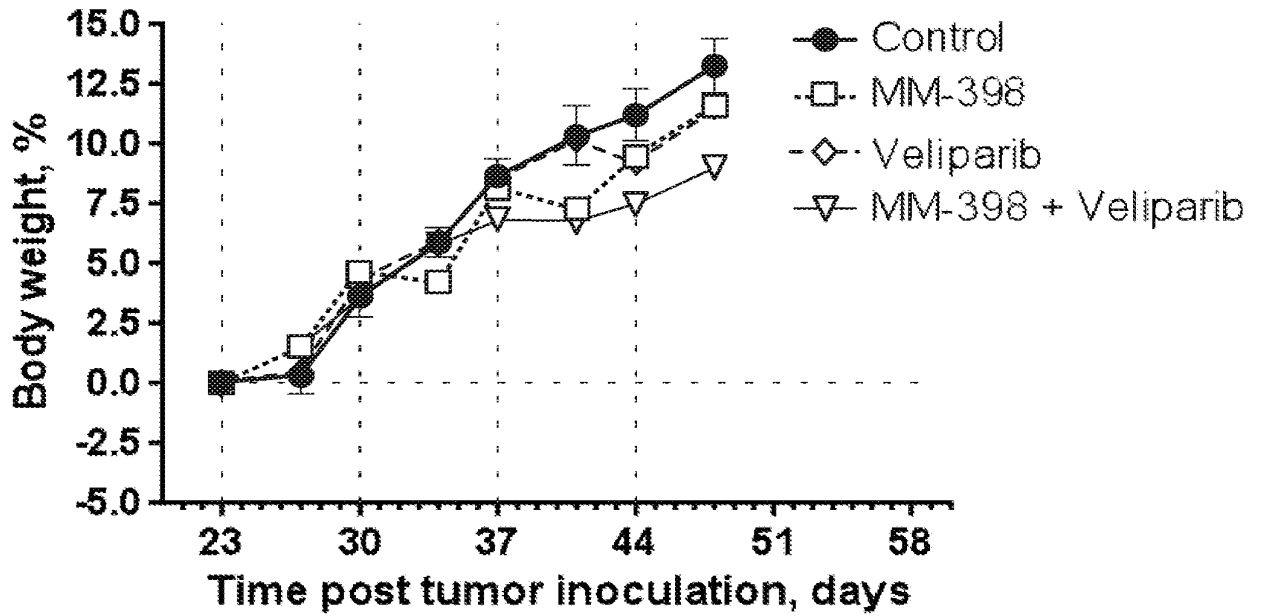


FIG. 12

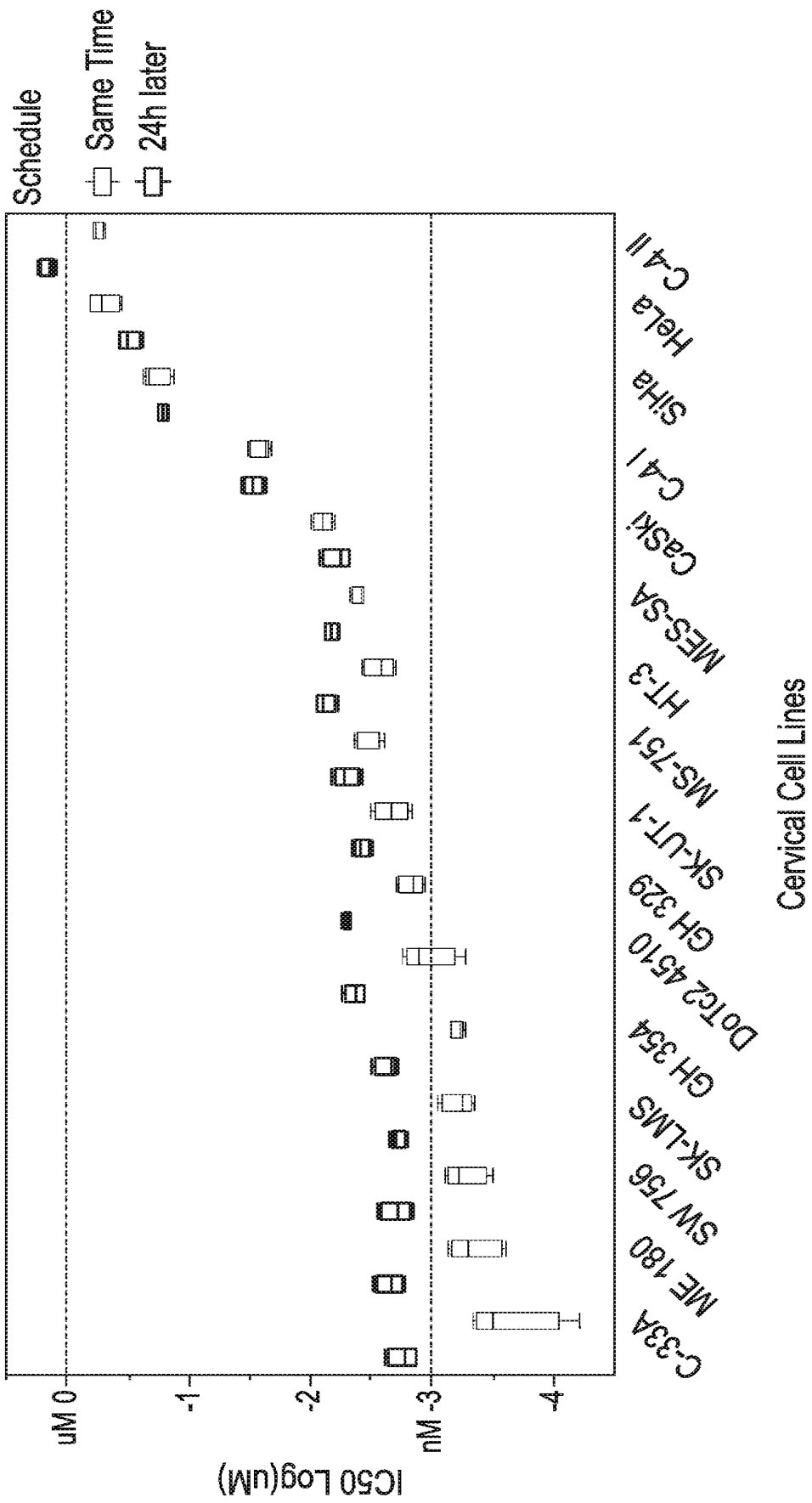


FIG. 13A

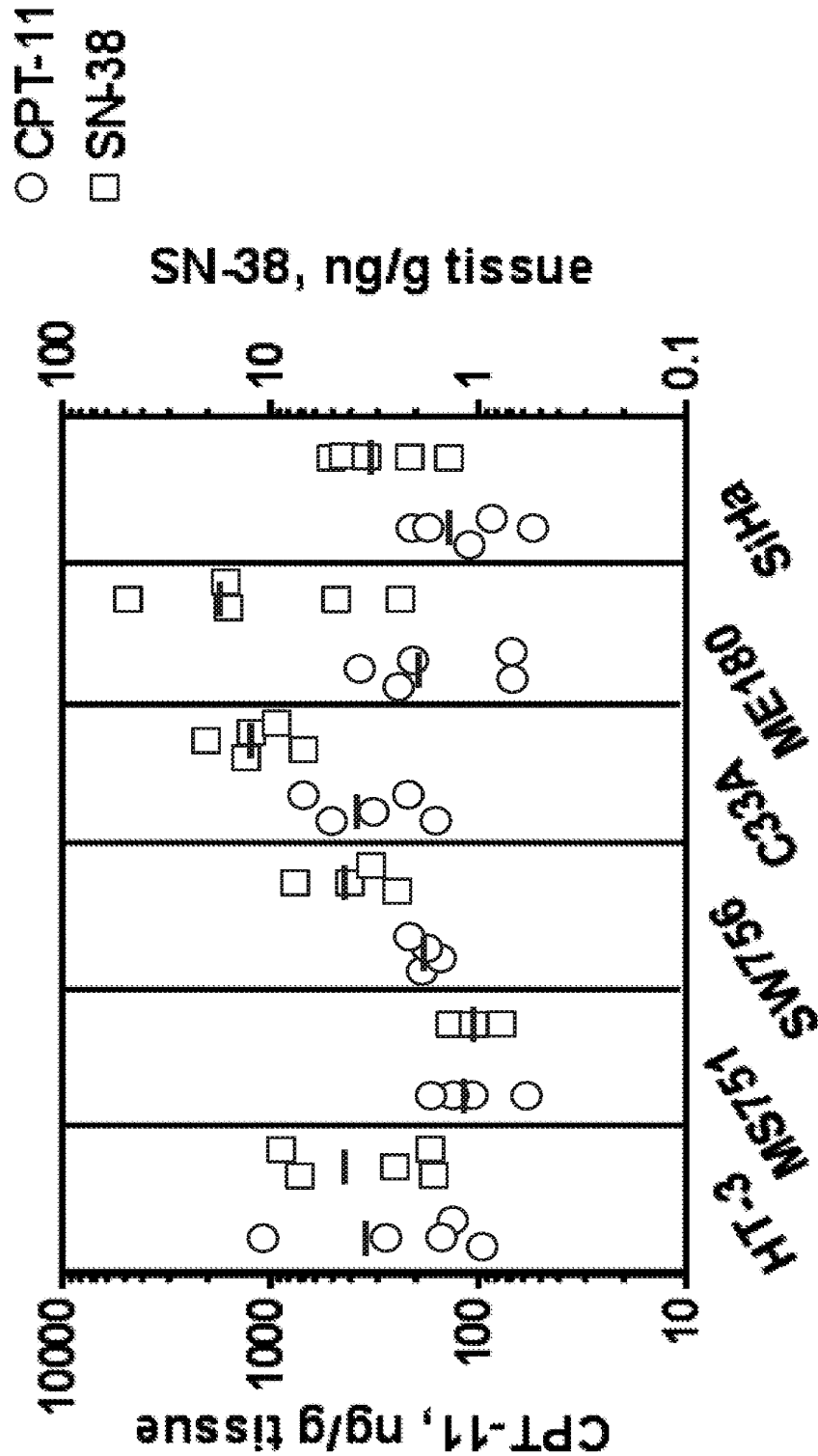
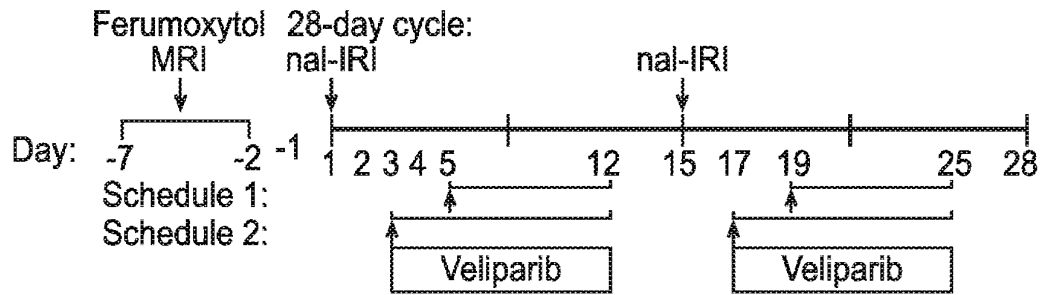


FIG. 13B

TRIAL DESIGN



Dose Escalation Cohorts			
Dose Level	Veliparib Dose (mg BID)	Veliparib Start Day	nal-IRI Dose (salt) (mg/m <sup>2</sup> q2w)
1	100	Day 5	80
2	200	Day 5	80
3	200	Day 3	80
4	300	Day 3	80
5	400	Day 3	80

FIG. 14

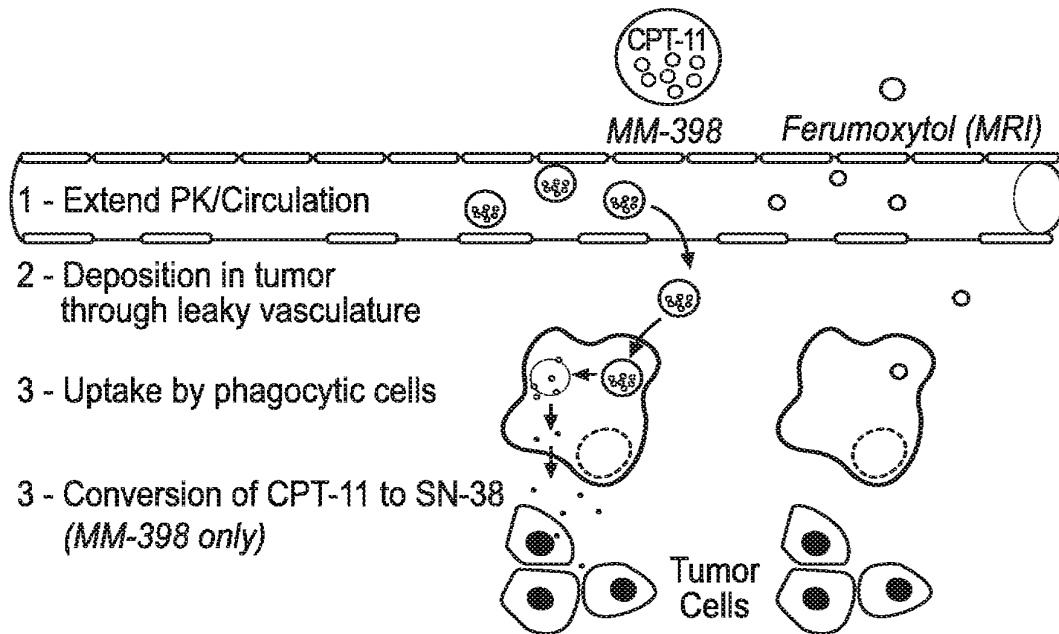


FIG. 15A

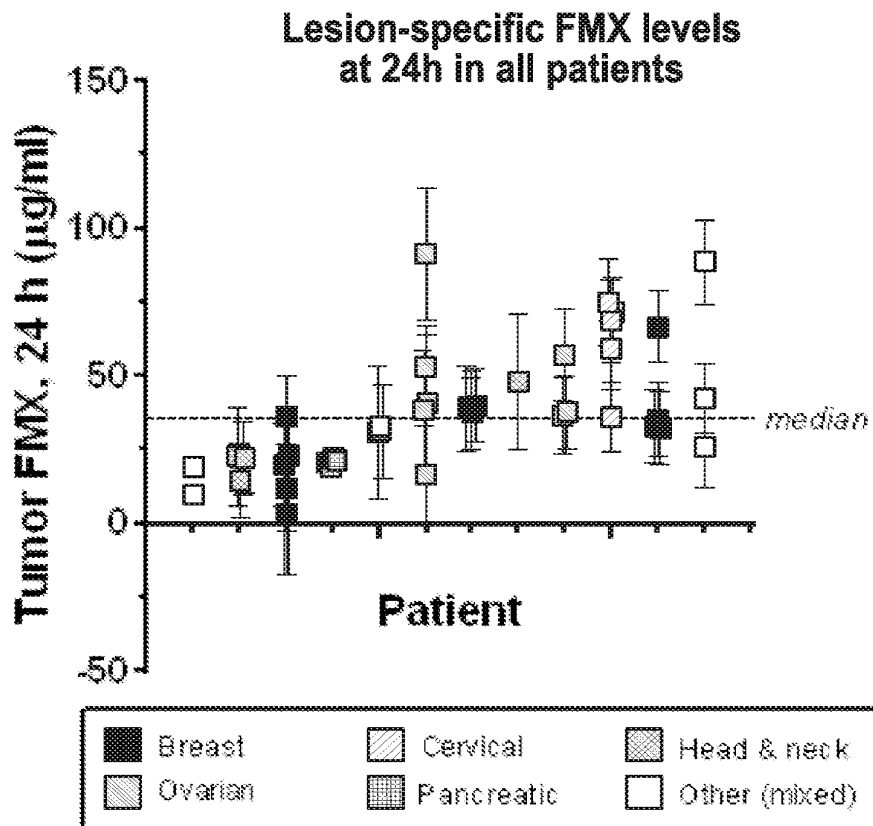


FIG. 15B

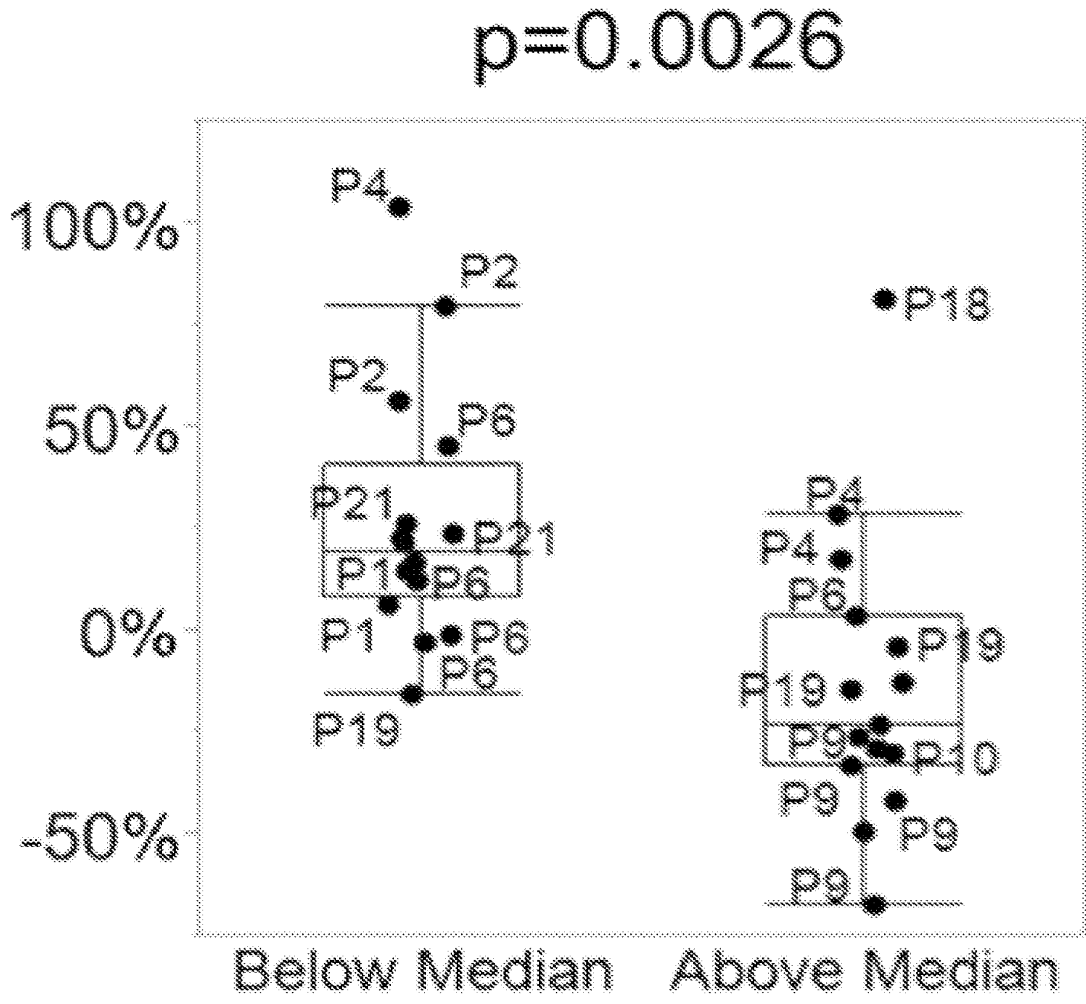


FIG. 15C

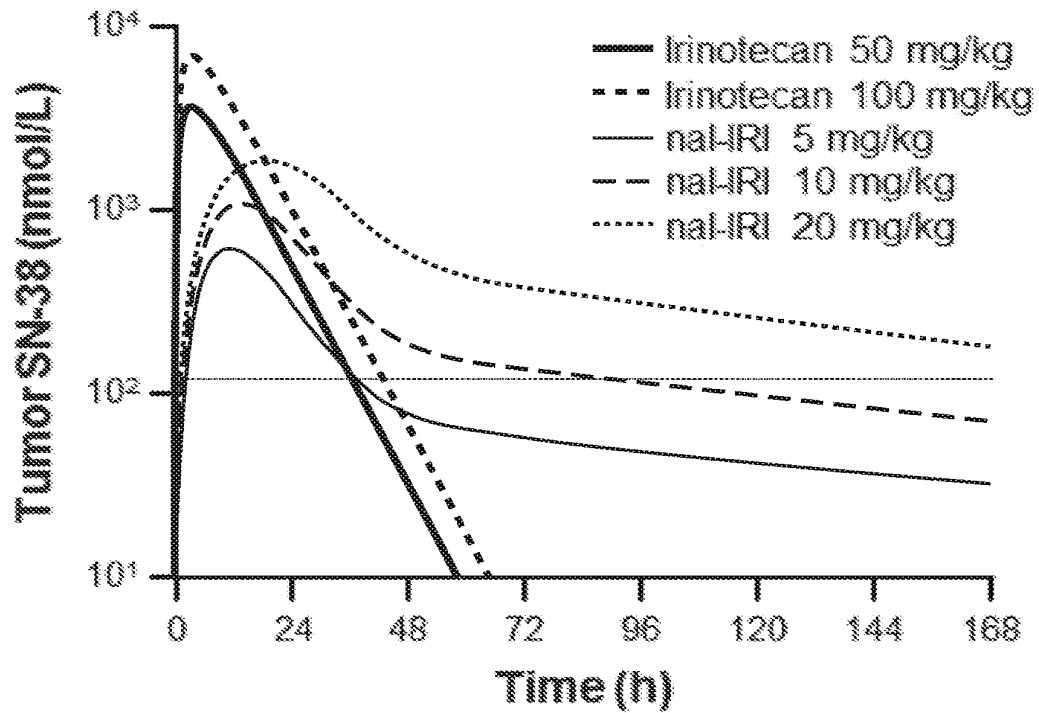


FIG. 16A

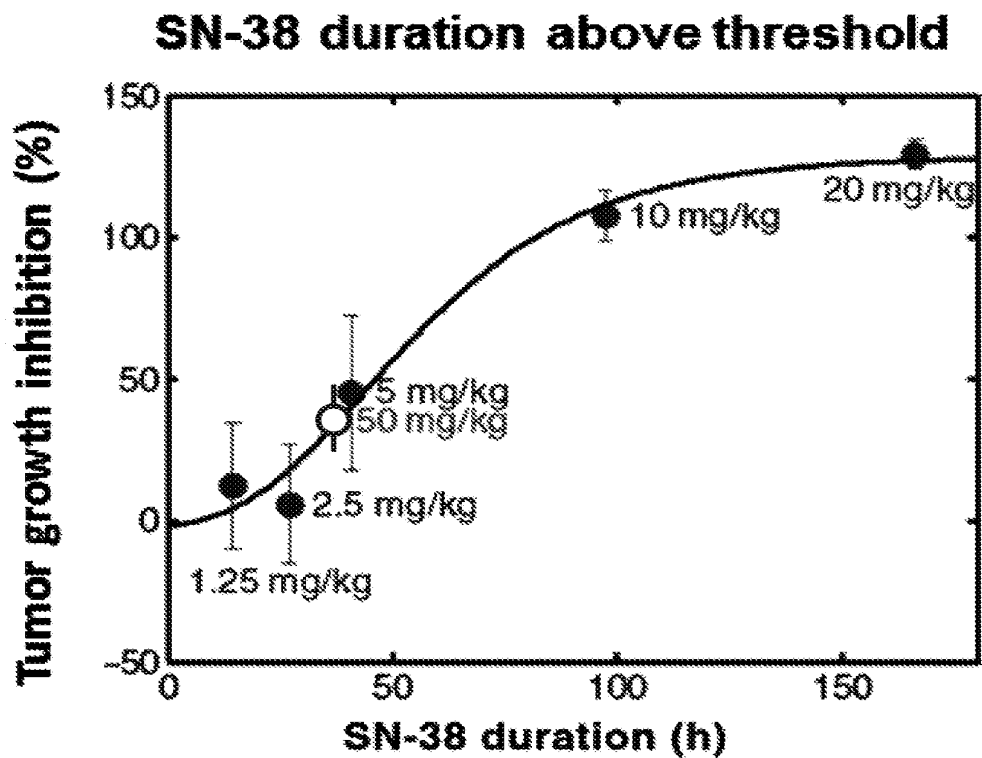


FIG. 16B

INTERNATIONAL SEARCH REPORT

International application No  
PCT/US2016/047827

A. CLASSIFICATION OF SUBJECT MATTER

INV. A61K31/04 A61K31/166 A61K31/416 A61K31/4184 A61K31/436  
A61K31/4745 A61K31/475 A61K31/502 A61K31/55 A61K9/127  
A61K47/06 A61P35/00

According to International Patent Classification (IPC) or to both national classification and IPC

B. FIELDS SEARCHED

Minimum documentation searched (classification system followed by classification symbols)  
A61K

Documentation searched other than minimum documentation to the extent that such documents are included in the fields searched

Electronic data base consulted during the international search (name of data base and, where practicable, search terms used)

EPO-Internal

C. DOCUMENTS CONSIDERED TO BE RELEVANT

Category*	Citation of document, with indication, where appropriate, of the relevant passages	Relevant to claim No.
Y	MESSERER CORRIE LYNN ET AL: "Liposomal irinotecan: formulation development and therapeutic assessment in murine xenograft models of colorectal cancer", CLINICAL CANCER RESEARCH : AN OFFICIAL JOURNAL OF THE AMERICAN ASSOCIATION FOR CANCER RESEARCH, vol. 10, no. 19, 1 October 2004 (2004-10-01), pages 6638-6649, XP002763354, ISSN: 1078-0432 the whole document ----- -/--	1-20

Further documents are listed in the continuation of Box C.

See patent family annex.

\* Special categories of cited documents :

- "A" document defining the general state of the art which is not considered to be of particular relevance
- "E" earlier application or patent but published on or after the international filing date
- "L" document which may throw doubts on priority claim(s) or which is cited to establish the publication date of another citation or other special reason (as specified)
- "O" document referring to an oral disclosure, use, exhibition or other means
- "P" document published prior to the international filing date but later than the priority date claimed

"T" later document published after the international filing date or priority date and not in conflict with the application but cited to understand the principle or theory underlying the invention

"X" document of particular relevance; the claimed invention cannot be considered novel or cannot be considered to involve an inventive step when the document is taken alone

"Y" document of particular relevance; the claimed invention cannot be considered to involve an inventive step when the document is combined with one or more other such documents, such combination being obvious to a person skilled in the art

"&" document member of the same patent family

Date of the actual completion of the international search

25 October 2016

Date of mailing of the international search report

17/11/2016

Name and mailing address of the ISA/

European Patent Office, P.B. 5818 Patentlaan 2  
NL - 2280 HV Rijswijk  
Tel. (+31-70) 340-2040,  
Fax: (+31-70) 340-3016

Authorized officer

Engl, Brigitte



## INTERNATIONAL SEARCH REPORT

International application No

PCT/US2016/047827

C(Continuation). DOCUMENTS CONSIDERED TO BE RELEVANT

Category*	Citation of document, with indication, where appropriate, of the relevant passages	Relevant to claim No.
Y	SYBIL M GENTHER WILLIAMS ET AL: "Treatment with the PARP inhibitor, niraparib, sensitizes colorectal cancer cell lines to irinotecan regardless of MSI/MSS status", CANCER CELL INTERNATIONAL, vol. 15, no. 1, 14, 4 February 2015 (2015-02-04), pages 1-11, XP021213062, BIOMED CENTRAL, LONDON, GB ISSN: 1475-2867, DOI: 10.1186/S12935-015-0162-8 the whole document	1-20
Y	----- DAVIDSON DAVID ET AL: "The PARP inhibitor ABT-888 synergizes irinotecan treatment of colon cancer cell lines", INVESTIGATIONAL NEW DRUGS, vol. 31, no. 2, April 2013 (2013-04), pages 461-468, XP002763355, ISSN: 1573-0646 the whole document	1-20
Y	----- DOUILLARD J ET AL: "Irinotecan combined with fluorouracil compared with fluorouracil alone as first-line treatment for metastatic colorectal cancer: a multicentre randomised trial", THE LANCET, vol. 355, no. 9209, 25 March 2000 (2000-03-25), pages 1041-1047, XP004814762, THE LANCET PUBLISHING GROUP, GB ISSN: 0140-6736, DOI: 10.1016/S0140-6736(00)02034-1 the whole document	1-20
Y	----- HARE JENNIFER I ET AL: "Treatment of colorectal cancer using a combination of liposomal irinotecan (Irinophore C(TM)) and 5-fluorouracil", PLOS ONE, vol. 8, no. 4, E62349, 23 April 2013 (2013-04-23), pages 1-12, XP002763356, ISSN: 1932-6203, DOI: 10.1371/journal.pone.0062349 the whole document -----	1-20



(51) International Patent Classification:

A61K 31/4745 (2006.01) A61K 9/127 (2006.01)  
A61P 35/00 (2006.01)

(21) International Application Number:

PCT/IB2017/000681

(22) International Filing Date:

17 May 2017 (17.05.2017)

(25) Filing Language:

English

(26) Publication Language:

English

(30) Priority Data:

62/337,961	18 May 2016 (18.05.2016)	US
62/345,178	03 June 2016 (03.06.2016)	US
62/362,735	15 July 2016 (15.07.2016)	US
62/370,449	03 August 2016 (03.08.2016)	US
62/394,870	15 September 2016 (15.09.2016)	US
62/414,050	28 October 2016 (28.10.2016)	US
62/415,821	01 November 2016 (01.11.2016)	US
62/422,807	16 November 2016 (16.11.2016)	US
62/433,925	14 December 2016 (14.12.2016)	US
62/455,823	07 February 2017 (07.02.2017)	US
62/474,661	22 March 2017 (22.03.2017)	US

(71) Applicant: **IPSEN BIOPHARM LTD.** [GB/GB]; Ash Road, Wrexham Industrial Estate, Wrexham GB LL13 9UF (GB).

(72) Inventors: **ADIWIJAYA, Bambang**; 16 Brighton Street, Belmont, MA 02478 (US). **FITZGERALD, Jonathan, Basil**; 32 Magnolia Street, Arlington, MA 02474 (US).

LEE, Helen; 120 Rindge Avenue, Apt. 100, Cambridge, MA 02140 (US).

(74) Agent: **CARPMAELS & RANSFORD**; One Southampton Row, London WC1B 5HA (GB).

(81) Designated States (unless otherwise indicated, for every kind of national protection available): AE, AG, AL, AM, AO, AT, AU, AZ, BA, BB, BG, BH, BN, BR, BW, BY, BZ, CA, CH, CL, CN, CO, CR, CU, CZ, DE, DJ, DK, DM, DO, DZ, EC, EE, EG, ES, FI, GB, GD, GE, GH, GM, GT, HN, HR, HU, ID, IL, IN, IR, IS, JP, KE, KG, KH, KN, KP, KR, KW, KZ, LA, LC, LK, LR, LS, LU, LY, MA, MD, ME, MG, MK, MN, MW, MX, MY, MZ, NA, NG, NI, NO, NZ, OM, PA, PE, PG, PH, PL, PT, QA, RO, RS, RU, RW, SA, SC, SD, SE, SG, SK, SL, SM, ST, SV, SY, TH, TJ, TM, TN, TR, TT, TZ, UA, UG, US, UZ, VC, VN, ZA, ZM, ZW.

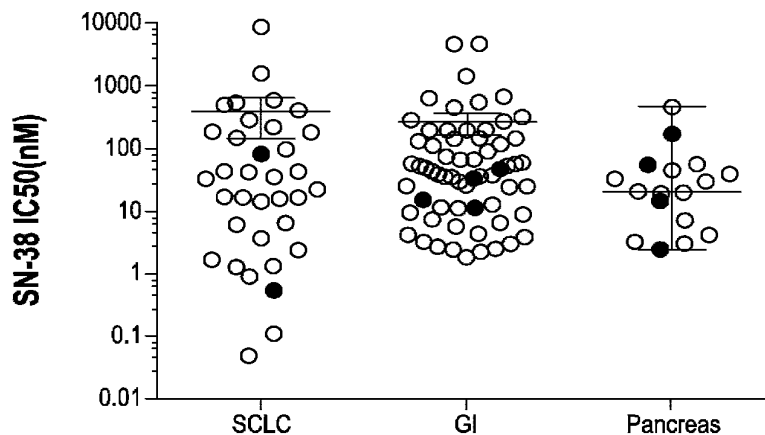
(84) Designated States (unless otherwise indicated, for every kind of regional protection available): ARIPO (BW, GH, GM, KE, LR, LS, MW, MZ, NA, RW, SD, SL, ST, SZ, TZ, UG, ZM, ZW), Eurasian (AM, AZ, BY, KG, KZ, RU, TJ, TM), European (AL, AT, BE, BG, CH, CY, CZ, DE, DK, EE, ES, FI, FR, GB, GR, HR, HU, IE, IS, IT, LT, LU, LV, MC, MK, MT, NL, NO, PL, PT, RO, RS, SE, SI, SK, SM, TR), OAPI (BF, BJ, CF, CG, CI, CM, GA, GN, GQ, GW, KM, ML, MR, NE, SN, TD, TG).

Published:

— with international search report (Art. 21(3))

(54) Title: NANOLIPOSOMAL IRINOTECAN FOR USE IN TREATING SMALL CELL LUNG CANCER

FIG. 1



(57) Abstract: Novel therapies for the treatment of small cell lung cancer (SCLC) include the administration of an antineoplastic therapy consisting of liposomal irinotecan administered once every two weeks, optionally including the administration of other non-antineoplastic agents to the patient such as the administration of a corticosteroid and an anti-emetic to the patient prior to the administration of the irinotecan liposome.



## NANOLIPOSOMAL IRINOTECAN FOR USE IN TREATING SMALL CELL LUNG CANCER

**Cross-Reference to Related Applications**

[001] This application claims the benefit of priority of U.S. Provisional Application No.62/337,961 (filed May 18, 2016), U.S. Provisional Application No. 62/345,178 (filed June 3, 2016), U.S. Provisional Application No. 62/362,735 (filed July 15, 2016), U.S. Provisional Application No.62/370,449 (filed August 3, 2016), U.S. Provisional Application No. 62/394,870 (filed September 15, 2016), U.S. Provisional Application No. 62/414,050 (filed October 28, 2016), U.S. Provisional Application No. 62/415,821 (filed November 1, 2016), U.S. Provisional Application No. 62/422,807 (filed November 16, 2016), U.S. Provisional Application No. 62/433,925 (filed December 14, 2016), U.S. Provisional Application No. 62/455,823 (filed February 7, 2017), and U.S. Provisional Application No. 62/474,661 (filed March 22, 2017), each of which is incorporated herein by reference in its entirety.

**Technical Field**

[002] The present invention relates to the treatment of patients diagnosed with small cell lung cancer (SCLC), including patients with SCLC disease progression after treatment with a platinum-based therapy.

**Background**

[003] Small-cell lung cancer (SCLC) is a highly malignant cancer that most commonly arises within the lung, although it can arise in other body sites. SCLC usually presents as large, rapidly developing lesions arising from the centrally located tracheobronchial airways and invading the mediastinum. Typically, patients present with a cough or dyspnea, wheezing, and/or chest pain. Weight loss, fatigue and anorexia occur in up to one third of the patients. At the time of diagnosis, two thirds of the patients with SCLC have one or more clinically detectable distant metastases.

[004] Initial (first line) treatment of SCLC can include administration of a platinum-based therapy such as 4-6 treatment cycles of cisplatin or carboplatin, in combination with etoposide or irinotecan. Current subsequent (second line) therapy upon SCLC disease progression (after first line therapy) has been reported to provide overall survival of about 7.7 months (sensitive patients) and 5.4 months (refractory patients) based on (Owonikoko, TK, et al., J Thorac Oncol. 2012 May;7(5):866-72). One second line therapy is the administration of topotecan (e.g., HYCAMTIN, topotecan hydrochloride injection), reported in certain regimens to provide an overall survival of 7.8 months (9.9 months in sensitive patients, 5.7

months in refractory patients) (Owonikoko, TK, et al., J Thorac Oncol. 2012 May;7(5):866-72). For example, of second line SCLC treatment with topotecan at 1.5 mg/m<sup>2</sup> administered on days 1-5 once in a three (3)-week treatment cycle provided overall response rates of about 7-24%, progression free survival (PFS) of about 3.1-3.7 months, and overall survival (OS) of 5.0-8.9 months (accompanied by grade 3 or greater neutropenia rates of 28-88% and grade 3 or greater diarrhea of less than about 5%) (PMIDs 16481389, 17135646, 17513814, 9164222, 10080612, 25385727). Another reported SCLC second line therapy is the administration of non-liposomal irinotecan at 300 mg/m<sup>2</sup> once every three (3) weeks, providing mixed overall response rates of 0-33%, PFS of 1.7-2.8 months, and OS of 4.6-6.9 months (accompanied by grade 3 or greater neutropenia rates of 21-23% and grade 3 or greater diarrhea of less than about 0-13%) (PMID 19100647, 1321891).

[005] Irinotecan is an active agent in the treatment of SCLC (e.g., listed in NCCN and ESMO guidelines) but it is not approved in the US or EU. Furthermore, it failed in a PHASE III registration-directed study in combination with a platinum in first line SCLC (PMID: 16648503). No targeted treatment has been successful to date in significantly improving the outcome of patients. The research of novel treatments for this disease is therefore urgently needed.

### Summary

[006] The present disclosure provides methods of treating patients with small cell lung cancer after disease progression following platinum-based therapy, by administering a therapeutically effective amount of liposomal irinotecan. In particular, a liposomal irinotecan such as MM-398 (ONIVYDE), can be administered once every two weeks to patients diagnosed with SCLC after disease progression following platinum-based therapy. In some embodiments, the liposomal irinotecan can be administered to patients diagnosed with SCLC disease progression on or after first-line platinum based chemotherapy (carboplatin or cisplatin), immunotherapy, and/ or chemo-radiation including platinum-based chemotherapy for treatment of limited or extensive stage SCLC.

[007] A human patient diagnosed with small cell lung cancer (SCLC) after disease progression following platinum-based therapy for the SCLC can be treated once every two weeks with an antineoplastic therapy consisting of a single dose of 90 mg/m<sup>2</sup> of irinotecan (free base) encapsulated in irinotecan liposomes. In another embodiment, a human patient who is known to be homozygous for the UGT1A1\*28 allele and is diagnosed with small cell lung cancer (SCLC) after disease progression following platinum-based therapy for the SCLC can be treated with an antineoplastic therapy consisting of a single reduced dose (e.g.,

50-70 mg/m<sup>2</sup>, including 50 mg/m<sup>2</sup> or 70 mg/m<sup>2</sup>) of irinotecan (free base) encapsulated in liposomes, administered once every two weeks. In another embodiment, a human patient who has previously experienced a Grade 3+ adverse event while or after receiving liposomal irinotecan after being diagnosed with small cell lung cancer (SCLC), and after disease progression following platinum-based therapy for the SCLC, can be treated with an antineoplastic therapy consisting of a single reduced dose (e.g., 50-70 mg/m<sup>2</sup>, including 50 mg/m<sup>2</sup> or 70 mg/m<sup>2</sup>) of irinotecan (free base) encapsulated in liposomes, administered once every two weeks.

[008] The liposomal irinotecan can be a pharmaceutically acceptable liposome formulation of irinotecan, comprising irinotecan in a delivery form having a diameter of about 100 nm, such as a liposomal irinotecan (Example 1). Various suitable liposomal irinotecan preparations can be manufactured as disclosed herein (Example 8). Preferably, the liposomal irinotecan is the product MM-398 (ONIVYDE®) (Example 9). In the present disclosure MM-398 is used interchangeably with MM-398 liposomal irinotecan.

#### **Brief Description of the Drawings**

[009] Figure 1 is a graph showing the drug sensitivity data to SN-38 from the Sanger database were plotted for SCLC, gastrointestinal, and pancreatic cancer cell lines (Example 2).

[010] Figures 2A and 2B are kinetic growth curves of DMS114 and NCI-H1048 SCLC cell lines acquired on an Incucyte instrument over 88 hours at various SN-38 concentrations

[011] Figure 3 is a graph showing the anti-tumor activity of MM-398 in the DMS114 xenograft model of SCLC. MM-398 was administered IV at 10 or 20 mg/kg irinotecan hydrochloride trihydrate starting on Day 23 and given weekly for 4 weeks and compared to saline control (black circles).

[012] Figure 4 is a Kaplan-Meier Plot of overall survival by quartiles of unencapsulated SN-38 (uSN38) time above threshold in the MM-398+5FU/LV arm of NAPOLI-1. Q1-Q4 represent the quartiles of uSN38 time above threshold. Q1 represents the shortest time and Q4 represents the longest time.

[013] Figure 5 is a graph showing the association between best response and duration of uSN38>0.03ng/mL for MM-398+5FU/LV arm in NAPOLI-1.

[014] Figure 6A is a graph showing the association between unencapsulated SN-38 C<sub>max</sub> and Neutropenia Grade≥3 in patients treated with MM-398.

[015] Figure 6B is a graph showing the association between total irinotecan C<sub>max</sub> and Diarrhea grade ≥3 in patients treated with MM-398.

[016] Figure 7A is a graph showing carboxylesterase (CES) activity; increased tumor SN-38 levels were associated with increased tumor deposition, as assessed by tumor CPT-11 at 24 h post administration in SCLC mouse xenograft models.

[017] Figure 7B is a graph showing carboxylesterase (CES) activity; SCLC PDX tumors have CES activity comparable to other indications in which irinotecan is active.

[018] Figure 7C is a graph showing cell sensitivity; Nal-IRI tumor deposition is consistent with range of SN-38 sensitivity in H1048 SCLC cells.

[019] Figure 7D is a graph showing cell sensitivity; cytotoxicity of Topo1 inhibitors increases with exposure.

[020] Figure 7E is a chart showing that topotecan administration is severely limited by toxicity, thus limiting sustained inhibition of topo1 in comparison to Onivyde mediated prolonged SN-38 exposure.

[021] Figure 8A shows the anti-tumor activity of MM-398 in the DMS-53 xenograft model of SCLC.

[022] Figure 8B shows the anti-tumor activity of MM-398 in the HCl-H1048 xenograft model of SCLC.

[023] Figure 8C shows the percent survival of rats in the H841 rat orthotopic xenograft model of SCLC that are treated with control, Onivyde (30 or 50 mg/kg salt), irinotecan (25 mg/kg) or topotecan (4 mg/kg) at days post inoculation.

[024] Figures 9A and 9B are graphs showing the tumor metabolite levels in SCLC xenograft models treated with MM-398 and nonliposomal Irinotecan. At 24 hours post-injection, (Figure 9A) CPT-11 and (Figure 9B) active metabolite SN-38 in tumors were significantly higher for mice treated with MM-398 at 16 mg/kg (salt) compared to nonliposomal irinotecan at 30 mg/kg (salt).

[025] Figures 10A and 10B are graphs showing that Nal-IRI is superior to all comparator treatment arms in treatment naïve SCLC xenograft models: Figure 10A is a graph showing Treatment Naïve SCLC Model NCI-H1048 (Nal-IRI 16 mg/kg clinically equivalent dose per BSA = 1x ~90mg/m<sup>2</sup> MM-398; Topotecan 0.83 mg/kg/wk, D1-2, q2w clinically equivalent dose per BSA = 1x ~1.5mg/m<sup>2</sup> Topotecan, q3w, D1-5); Figure 10B shows the number of complete response (Nal-IRI). NCI-H1048 is a chemo-sensitive model (established from pleural effusion metastases of SCLC). All nal-IRI-treated animals have complete response (CR) after 2-3 doses – but dose response is observed at early time-point. IRI-treated animals progress after initially responding to treatment; while nal-IRI treated animals remain CR to date.

[026] Figures 11A and 11B describe a 2L SCLC xenograft model created through treatment with Carboplatin + Etoposide. Figure 11C is a graph showing Treatment Naïve SCLC Model NCI-H1048 (Topotecan 0.83 mg/kg/wk, D1-2, q2w clinically equivalent dose per BSA = 1x ~1.5mg/m<sup>2</sup> Topotecan, q3w, D1-5; 1L Etoposide (25 mg/kg) & Carbo (30 mg/kg) clinically equivalent dose per BSA = 1x ~ 100 mg/m<sup>2</sup> Etoposide D1-3+ AUC6 Carbo D1, q4w); 11B is a schematic of 1L and 2L treatments. 1L regimen results in similar anti-tumor activity as topotecan treatment at clinically relevant doses (based on BSA/BW calculation). After 3 cycles of 1L treatment, mice were randomized for further 2L treatments.

[027] Figure 12 is a graph showing that Nal-IRI remains effective in platinum-treated SCLC tumors and is superior to topotecan and irinotecan: 2L SCLC Model: NCI-H1048. In platinum-treated SCLC tumors: Nal-IRI remains active and is trending towards complete response; IRI treatment is active but after 3rd cycle some tumors are trending regrowth; Topotecan (at 2x clinically relevant dose) seems to be active after 1-2 cycles but progress quickly after 3rd dose; Etoposide + carboplatin is not tolerable by the 5th cycle.

[028] Figures 13A and 13B are graphs showing that Nal-IRI is also superior to topotecan and irinotecan in another SCLC xenograft model (DMS-114): Figure 13A is a graph showing DMS-114 SCLC Mouse Xenograft (s.c.); Figure 13B is a chart showing Nal-IRI (Day 74) tumor volume change. Nal-IRI is superior to irinotecan and topotecan at clinically relevant doses. SCLC tumors respond to irinotecan early on but became less responsive after 2-3 cycles.

[029] Figures 14A-4C are graphs showing SCLC tumors treated with TOP1 inhibitors remain responsive to nal-IRI. Figure 14A. DMS-114: Treatment Naïve; Figure 14B. DMS-114: Topotecan-Treated; Figure 14C. DMS-114: Irinotecan-Treated. DMS114 tumors treated with topotecan are responsive to nal-IRI (16 mg/kg) but not irinotecan (33 mg/kg).

[030] Figures 15A-15C are graphs showing that duration of exposure maybe crucial for TOP1 inhibitor activity. Figure 15A is DMS-114 SCLC Mouse Xenograft (s.c.); Figure 15B is Hypothesized Tumor Exposure; Figure 15C is NCI-H1048 Mouse Xenograft. At the same dose intensity, bolus (given on day 1) topotecan has less anti-tumor activity compared to fractionated topotecan (days 1 & 2). This may be indicative that prolonged exposure of TOP1 inhibitor above a therapeutic threshold is more beneficial than high C<sub>max</sub> because irinotecan is a pro-drug (CPT-11), the active metabolite SN-38 may also have a longer duration than topotecan.

[031] Figures 16A-16D show NCI-H1048 SCLC Mouse Xenograft (s.c.) Figure 16A. Tumor Volume; Figure 16B. Survival; Figure 16C. Body Weight Change; Figure 16D. Response at Day 98.

[032] Figures 17A-7C show NDMC-53 SCLC Mouse Xenograft (s.c.) Figure 17A. Tumor Volume; Figure 17B. Survival; Figure 17C response at Day 98 post inoculation with control, NaI-IRI (16 mg/kg salt) or topotecan (0.83 mg/kg/wk, D1-2)

[033] Figures 18A and 18B are graphs showing that Nal-IRI increases exposure and sustains delivery of irinotecan and SN-38 (active metabolite) in BxPC-3 mouse xenograft tumors: Figure 18A. Plasma; Figure 18B. Tumor.

[034] Figure 19 is a graph showing that Nal-IRI effectively delivers irinotecan to tumors in preclinical models of SCLC.

[035] Figures 20A and 20B are graphs showing SCLC Tumors treated with TOP1 inhibitors remain responsive to nal-IRI: Figure 20A. DMS-114: Topotecan-Treated; Figure 20B. DMS-114: Treatment Naïve. DMS114 tumors treated with topotecan are responsive to nal-IRI (16 mg/kg) but not irinotecan (33 mg/kg).

[036] Figures 21A and 21B are graphs showing that Nal-IRI remains effective in platinum-treated SCLC tumors and is superior to topotecan and irinotecan in a 2L SCLC Model: NCI-H1048. Figure 21A shows the change in Tumor Volume; Figure 21B is a survival graph.

[037] Figures 22A-22D are graphs showing pre-clinical evidence that MM-398 has improved circulation and tumor circulation in a HT29 CRC xenograft model - MM-398 40mg/kg: Figure 22A CPT-11 plasma (sustained plasma levels), Figure 22B. SN-38 plasma (moderately sustained plasma levels), Figure 22C CPT-11 tumor (sustained intra-tumor levels), and Figure 22D SN-38 tumor (enhanced intra-tumor activation to SN38).

[038] Figures 23A-23F are graphs showing Nal-IRI has greater anti-tumor activity than irinotecan and topotecan. NOD/SCID mice with subcutaneous (Figure 23A) DMS-53, (Figure 23B) DMS-114 or (Figure 23C) NCI-H1048. SCLC xenograft tumors were treated with IV nal-IRI (16 mg/kg; triangles), IV irinotecan (33 mg/kg; diamonds), IP topotecan (0.83 mg/kg/wk days 1-2; squares) or vehicle control (circles). For DMS-114 and NCI-H1048 all groups have n=10; for DMS-53 n=4, 5 and 5 for control, topotecan and nal-IRI, respectively. Balb/c nude mice bearing subcutaneous patient-derived xenografts (Figure 23D) LUN-182, (Figure 23E) LUN-081 and (Figure 24F) LUN-164 were treated with IV nal-IRI (16 mg/kg; triangles), IV irinotecan (33 mg/kg; diamonds), IP topotecan (0.83 mg/kg/wk days 1-2;



squares) or vehicle control (circles). For all PDX models n=5 for all groups. Vertical dotted lines indicate start of weekly dosing and error bars indicate standard error of the mean.

### Detailed Description

[039] MM-398 is a liposomal encapsulation of irinotecan that provides sustained tumor exposure of SN-38 and therefore provides certain advantages over nonliposomal irinotecan. The approved regimen of MM-398 in patients with pancreatic cancer is in combination with 5-FU/LV. However, 5-FU is not an active agent used in the treatment of SCLC. To date, the treatment of patients with SCLC with MM-398 has not been disclosed. Applicants have discovered certain methods and uses of MM-398 monotherapy in patients with SCLC, including the methods and uses disclosed herein.

[040] The discovery of these methods and uses of MM-398 for use in patients with SCLC was based in part on preclinical data and clinical pharmacology analysis described herein. The methods and uses are designed to balance increased efficacy with increased toxicity predicted at higher doses. Preclinical data herein indicate the activity of MM-398 in models of SCLC. Clinical pharmacology analysis supports increased toxicity at increased doses and specifically supports the safety profile of the 90 mg/m<sup>2</sup> dose. Finally, preclinical efficacy data at mouse dose levels equivalent to 90 mg/m<sup>2</sup> in humans are shown to be superior to topotecan.

[041] A human patient diagnosed with small cell lung cancer (SCLC) after disease progression following platinum-based therapy for the SCLC can be treated with an antineoplastic therapy consisting of a single dose of a therapeutically effective amount of irinotecan encapsulated in liposomes. The liposomal irinotecan can be a pharmaceutically acceptable liposome formulation of irinotecan, comprising irinotecan in a delivery form having a diameter of about 100 nm, such as an liposomal irinotecan (Example 1), including PEGylated liposomes. Various suitable liposomal irinotecan preparations can be manufactured as disclosed herein (Example 8). Preferably, the liposomal irinotecan is the product MM-398 (ONIVYDE) (Example 9).

[042] As used herein, 90 mg/m<sup>2</sup> irinotecan refers to the free base, encapsulated in liposomes (dose based on the amount of irinotecan free base) and is equivalent to 100 mg/m<sup>2</sup> of the irinotecan hydrochloride anhydrous salt). Converting a dose based on irinotecan hydrochloride trihydrate to a dose based on irinotecan free base is accomplished by multiplying the dose based on irinotecan hydrochloride trihydrate with the ratio of the molecular weight of irinotecan free base (586.68 g/mol) and the molecular weight of irinotecan hydrochloride trihydrate (677.19 g/mol). This ratio is 0.87 which can be used as a

conversion factor. For example, an 80 mg/m<sup>2</sup> dose based on irinotecan hydrochloride trihydrate is equivalent to a 69.60 mg/m<sup>2</sup> dose based on irinotecan free base (80 x 0.87). In the clinic this is rounded to 70 mg/m<sup>2</sup> to minimize any potential dosing errors.

[043] Doses of nal-IRI in some studies were calculated based on the equivalent dose of irinotecan hydrochloride trihydrate (salt); in this specification, unless specified otherwise, the doses are based on irinotecan as the free base. Accordingly, 50 mg/m<sup>2</sup> based on irinotecan as free base is equivalent to 60 mg/m<sup>2</sup> based on irinotecan as the hydrochloride trihydrate, 70 mg/m<sup>2</sup> based on irinotecan as free base is equivalent to 80 mg/m<sup>2</sup> based on irinotecan as the hydrochloride trihydrate, 90 mg/m<sup>2</sup> based on irinotecan as free base is equivalent to 100 mg/m<sup>2</sup> based on irinotecan as the hydrochloride trihydrate, and 100 mg/m<sup>2</sup> based on irinotecan as free base is equivalent to 120 mg/m<sup>2</sup> based on irinotecan as the hydrochloride trihydrate, in accordance with Table 1.

Table 1

Salt	Free base
180	150
120	100
100	90
80	70
60	50
50	45
40	35

[044] The pharmacokinetic parameters of total Irinotecan and total SN-38 following administration of MM-398 90 mg/m<sup>2</sup> as a single agent or part of combination chemotherapy are presented in Table 2.

Table 2: Total Irinotecan and Total SN-38

Pharmacokinetic Parameters in Patients with Solid Tumors.

Dose (mg/m <sup>2</sup> )	Total Irinotecan			Total SN-38	
	C <sub>max</sub> [µg/mL]	AUC <sub>0-∞</sub> [h·µg/mL]	t <sub>1/2</sub> [h]	C <sub>max</sub> [ng/mL]	t <sub>1/2</sub> [h]
Max (125%)	60.5	2216.5	25.8	8.8	67.8
90	48.4	1773.2	25.8	7.0	67.8

Min (80%)	38.7	1418.6	25.8	5.6	67.8
--------------	------	--------	------	-----	------

[045] Over the dose range of 50 to 150 mg/m<sup>2</sup>, the C<sub>max</sub> and AUC of total irinotecan increases with dose. Additionally, the C<sub>max</sub> of total SN-38 increases proportionally with dose; however, the AUC of total SN-38 increases less than proportionally with dose. Higher plasma SN-38 C<sub>max</sub> was associated with increased likelihood of experiencing neutropenia.

[046] The C<sub>max</sub> of SN-38 increases proportionally with liposomal irinotecan dose but the AUC of SN-38 increases less than proportionally with dose, enabling new methods of dosage adjustment. For example, the value of the parameter associated with adverse effects (C<sub>max</sub>) decreases by a relatively greater extent than the value of the parameter associated with the effectiveness of treatment (AUC). Accordingly, when an adverse effect is seen, a reduction in the dosing of the liposomal irinotecan can be implemented that maximizes the difference between the reduction in C<sub>max</sub> and in AUC. The discovery means that in treatment regimens, a given SN-38 AUC can be achieved with a surprisingly low SN-38 C<sub>max</sub>. Likewise, a given SN-38 C<sub>max</sub> can be achieved with a surprisingly high SN-38 AUC.

[047] Direct measurement of irinotecan liposome showed that 95% of irinotecan remains liposome encapsulated, and the ratios between total and encapsulated forms did not change with time from 0 to 169.5 hours post-dose.

[048] In some embodiments, the liposomal irinotecan can be characterized by the parameters in Table 2. In some embodiments, the liposomal irinotecan can be MM-398 or a product that is bioequivalent to MM-398. In some embodiments, the liposomal irinotecan can be characterized by the parameters in Table 3, including a C<sub>max</sub> and/or AUC value that is 80-125% of the corresponding value in Table 2. The pharmacokinetic parameters of total irinotecan for various alternative liposomal irinotecan formulations administering 90 mg/m<sup>2</sup> irinotecan free base once every two weeks is provided in Table 3.

Table 3

Total Irinotecan Pharmacokinetic Parameters in Alternative Liposomal Irinotecan Formulations

Dose (mg/m <sup>2</sup> )	Total Irinotecan	
	C <sub>max</sub> [µg/mL] (n=25)	AUC <sub>0-∞</sub> [h·µg/mL] (n=23)
90	38.7- 60.5	1418.6-2216.5

$C_{max}$ : Maximum plasma concentration

$AUC_{0-\infty}$ : Area under the plasma concentration curve extrapolated to time infinity

$t_{1/2}$ : Terminal elimination half-life

[049] The activity of the active metabolite of irinotecan, SN-38, against various SCLC cell lines was investigated in *in vitro* growth and viability assays (Example 2). An analysis of this data indicated that SCLC cell lines have similar sensitivity to SN-38 as pancreatic and gastrointestinal cancer cell lines (Figure 1). In addition, SN-38 induced a decrease in cell viability of > 90% in four tested SCLC cell lines, the IC50 was variable and spanned several orders of magnitude. Figures 2A and 2B show the cell growth inhibition kinetics of SN-38 in 2 SCLC cell lines, as described in Example 2.

[050] The activity of MM-398 as a single agent was investigated in xenograft models of SCLC (Example 3). As shown in Figure 3, anti-tumor activity was seen at all dose levels tested in the DMS-114 model.

[051] The estimated association between MM-398 exposure and efficacy was evaluated in pancreatic cancer patients (Example 4). The relationship between OS and quartiles of time ( $uSN38 > 0.03$  ng/mL) for the MM-398+5FU/LV is provided in Figure 4.

[052] As described in Examples 6 and 7, an antineoplastic therapy consisting of liposomal irinotecan in a pharmaceutically acceptable injectable form can be administered once every two weeks to patients with SCLC disease that has progressed after having received previous antineoplastic therapy (e.g., prior platinum-based therapies alone or with other chemotherapeutic agents). The dose of liposomal irinotecan (e.g., 50-90 mg/m<sup>2</sup> irinotecan (free base) encapsulated in irinotecan liposomes) and dose frequency (e.g., once every 2 weeks) of liposomal irinotecan can be selected or modified for certain patients. The dose can be selected to provide a tolerable patient dose, including a dose providing acceptably low levels of grade 3 or greater neutropenia (Figure 6A) and/or diarrhea (Figure 6B), as described in Example 6. During the antineoplastic therapy, the patient may receive other agents that are not antineoplastic agents, such as anti-emetic agents. The antineoplastic therapy can be administered in the absence of topotecan.

[053] In some embodiments, the invention is a method of treating a human patient diagnosed with small cell lung cancer (SCLC) after disease progression following platinum-based therapy for the SCLC, the method comprising administering to the human patient an antineoplastic therapy once every two weeks, the antineoplastic therapy consisting of a single dose of liposomal irinotecan providing 90 mg/m<sup>2</sup> (free base) of irinotecan encapsulated in

irinotecan liposomes. In some embodiments, the invention is a method of treating a human patient diagnosed with small cell lung cancer (SCLC) after disease progression following platinum-based therapy for the SCLC, the method comprising administering to the human patient an antineoplastic therapy once every two weeks, the antineoplastic therapy consisting of a single dose of liposomal irinotecan providing 70 mg/m<sup>2</sup> (free base) of irinotecan encapsulated in irinotecan liposomes. In some embodiments, the invention is a method of treating a human patient diagnosed with small cell lung cancer (SCLC) after disease progression following platinum-based therapy for the SCLC, the method comprising administering to the human patient an antineoplastic therapy once every two weeks, the antineoplastic therapy consisting of a single dose of liposomal irinotecan providing 50 mg/m<sup>2</sup> (free base) of irinotecan encapsulated in irinotecan liposomes.

[054] The methods of treatment can include determining whether a patient meets one or more inclusion criteria specified in Example 7, and then administering the antineoplastic therapy consisting of liposomal irinotecan. For example, an antineoplastic therapy can consist of administering a therapeutically effective dose (e.g., 50-90 mg/m<sup>2</sup> irinotecan (free base) encapsulated in liposomes) and dose frequency (e.g., once every 2 weeks) of liposomal irinotecan to a patient who has been treated for SCLC with a platinum-based therapy (e.g., cisplatin and/or carboplatin alone or in combination with etoposide).

[055] In addition, the methods of treatment can include determining whether a patient meets one or more exclusion criteria specified in Example 7, and not administering the antineoplastic therapy consisting of liposomal irinotecan. Methods of treating SCLC disclosed herein can include administering the antineoplastic therapy to a patient who does not meet one or more exclusion criteria in Example 7. For example, an antineoplastic therapy can consist of administering a therapeutically effective dose (e.g., 50-90 mg/m<sup>2</sup> irinotecan (free base) encapsulated in liposomes) and dose frequency (e.g., once every 2 weeks) of liposomal irinotecan to a patient who has not been treated for SCLC with irinotecan or topotecan.

[056] Certain subgroup of patients diagnosed with SCLC may optionally be treated with a reduced dose of the liposomal irinotecan, including patients who have higher levels of bilirubin or patients with UGT1A1\*28 7/7 homozygous allele. The reduced dose refers to a dose of less than 90 mg/m<sup>2</sup> of irinotecan (free base) encapsulated in liposomes administered once every two weeks to the patient receiving the reduced dose. In some examples, the reduced dose can be a dose of 50-90 mg/m<sup>2</sup>, including a reduced dose of 50 mg/m<sup>2</sup>, a reduced dose of 60 mg/m<sup>2</sup>, a reduced dose of 70 mg/m<sup>2</sup> or a reduced dose of 80 mg/m<sup>2</sup> irinotecan

(free base) administered once every two weeks to patients diagnosed with SCLC and receiving the reduced dose. For those patients who start with 70 mg/m<sup>2</sup>, the first dose reduction should be to 50 mg/m<sup>2</sup> and then to 43 mg/m<sup>2</sup>. The exact determination of the appropriate dose will be dependent on the observed pharmacokinetics, efficacy, and safety in that subpopulation.

[057] In some examples, the liposomal irinotecan can be administered to patients diagnosed with SCLC disease progression on or after immunotherapy and/or after first-line platinum based chemotherapy (carboplatin or cisplatin) or chemo-radiation including platinum-based chemotherapy for treatment of limited or extensive stage SCLC. In some examples, the patient can receive some form of immunotherapy for SCLC prior to administration of the liposomal irinotecan. Examples of immunotherapy can include atezolizumab, avelimumab, nivolumab, pembrolizumab, ipilimumab, tremelimumab and/or durvalumab. In one example, a patient receives nivolumab for SCLC (e.g., according to a treatment regimen in NCT02481830) prior to receiving the liposomal irinotecan as disclosed herein. In one example, a patient receives ipilimumab for SCLC (e.g., according to a treatment regimen in NCT01331525, NCT02046733, NCT01450761, NCT02538666 or NCT01928394) prior to receiving the liposomal irinotecan as disclosed herein. The immunotherapy can include molecules that bind to CTLA4, PDL1, PD1, 41BB and/or OX40 including the publicly available compounds in the Table 4 below or other compounds that bind to the same epitope or have the same or similar biological functions.

Table 4

Antibody	Antibody Sequence (literature reference)
$\alpha$ -PDL1	10F.9G2, Bioxcell
$\alpha$ -41BB	LOB12.3, Bioxcell
$\alpha$ -CTLA4	9H10, Bioxcell
$\alpha$ -OX40	OX-86, Bioxcell

[058] The use of a combination of liposomal irinotecan and an immunotherapy can be used for the treatment of cancer in a host in need thereof, in an amount and in a schedule of administration that is therapeutically synergistic in the treatment of said cancer. The immunotherapy can be an antibody or combination of antibodies binding to and/or acting upon alpha-PDL1, alpha-41BB, alpha-CTLA4, alpha-OX40 and/or PD1.

[059] In some embodiments, the treatment of cancer in a host in need thereof comprises the administration of MM-398 without the administration of steroids.

[060] The treatment schedule can comprise administering MM-398 once every two or three weeks or two out of three weeks at 43, 50, 70, 80 or 90 mg/m<sup>2</sup> liposomal irinotecan (free base) in combination with an immunotherapy (e.g., in combination with an antibody to alpha-PDL1, PD1, alpha-41BB, alpha-CTLA4 and/or alpha-OX40). For example, the treatment schedule can comprise administering a (e.g., 28-day) treatment cycle to a human host diagnosed with SCLC, where the treatment cycle includes administration of: a total of 43, 50, 70, 80 or 90 mg/m<sup>2</sup> liposomal irinotecan (free base) followed by the administration of 3 mg/kg nivolumab, once every two weeks; and repeating said treatment cycle until a progression or an unacceptable toxicity is observed. In another example, the treatment schedule can comprise administering a (e.g., 28-day) treatment cycle to a human host diagnosed with SCLC, where the treatment cycle includes administration of: a total of 43, 50, 70, 80 or 90 mg/m<sup>2</sup> liposomal irinotecan (free base) once every two or three weeks or two out of three weeks, followed by the administration of 2 mg/kg pembrolizumab, once every two or three weeks (where the first dose of liposomal irinotecan and pembrolizumab are given on the same day); and repeating said treatment cycle until a progression or an unacceptable toxicity is observed. The treatment schedule can comprise administering MM-398 once every two weeks at 90 mg/m<sup>2</sup> liposomal irinotecan (free base).

[061] A method of treating a human patient diagnosed with small cell lung cancer (SCLC) after disease progression following platinum-based therapy for the SCLC, can consist of administering to the human patient an antineoplastic therapy once every two weeks, the antineoplastic therapy consisting of a single dose of liposomal irinotecan providing 50, 70 or 90 mg/m<sup>2</sup> (free base) of irinotecan encapsulated in irinotecan liposomes. When the patient is known to be homozygous for the UGT1A1\*28 allele, each dose of irinotecan liposome can be reduced (e.g., 50, or 70 mg/m<sup>2</sup>). When the patient is not homozygous for the UGT1A1\*28 allele, and is not otherwise reduced, each dose of irinotecan liposome can be 90 mg/m<sup>2</sup>. The method can further comprise administering a corticosteroid and an anti-emetic to the patient prior to the administration of the irinotecan liposome.

[062] A method of treating a human patient not homozygous for the UGT1A1\*28 allele and diagnosed with small cell lung cancer (SCLC) after disease progression following prior therapy for the SCLC, can comprise administering to the human patient an antineoplastic therapy once every two weeks, the antineoplastic therapy consisting of a single dose of liposomal irinotecan providing 90 mg/m<sup>2</sup> of irinotecan (free base) encapsulated in a irinotecan liposomes. The method can further comprise administering a corticosteroid and an anti-emetic to the patient prior to the administration of the irinotecan liposome.

[063] Prior to receiving the antineoplastic therapy of liposomal irinotecan, the patient can be a patient who has progressed on a platinum-based regimen and who has also (optionally) received a single line of immunotherapy either in maintenance or 2L setting. The patient can be a patient who was not treated with topotecan for the SCLC prior to receiving the liposomal irinotecan antineoplastic therapy. The patient can previously receive immunotherapy induction, followed and/or accompanied by one or more maintenance doses of chemotherapy, prior to administration of the liposomal irinotecan.

[064] The treatment schedule can comprise administering MM-398 once every three weeks at 100-130 mg/m<sup>2</sup> liposomal irinotecan (free base) in combination with an immunotherapy (e.g., in combination with an antibody to alpha-PDL1, PD1, alpha-41BB, alpha-CTLA4 and/or alpha-OX40). For example, the treatment schedule can comprise administering a treatment cycle to a human host diagnosed with SCLC, where the treatment cycle includes administration of: a total of 100, 110, 120, or 130 mg/m<sup>2</sup> liposomal irinotecan (free base) followed by the administration of 3 mg/kg nivolumab, once every three weeks; and repeating said treatment cycle until a progression or an unacceptable toxicity is observed. The treatment schedule can comprise administering a treatment cycle to a human host diagnosed with SCLC, where the treatment cycle includes administration of: a total of 100, 110, 120, or 130 mg/m<sup>2</sup> liposomal irinotecan (free base) once every three weeks combined with the administration of 3 mg/kg nivolumab, once every two or three weeks (where the first dose of liposomal irinotecan and nivolumab are given on the same day); and repeating said treatment cycle until a progression or an unacceptable toxicity is observed. In another example, the treatment schedule can comprise administering a treatment cycle to a human host diagnosed with SCLC, where the treatment cycle includes administration of: a total of 100, 110, 120, or 130 mg/m<sup>2</sup> liposomal irinotecan (free base) followed by the administration of 2 mg/kg pembrolizumab, once every three weeks; and repeating said treatment cycle until a progression or an unacceptable toxicity is observed. The treatment schedule can comprise administering a treatment cycle to a human host diagnosed with SCLC, where the treatment cycle includes administration of: a total of 100, 110, 120, or 130 mg/m<sup>2</sup> liposomal irinotecan (free base) once every three weeks combined with the administration of 2 mg/kg pembrolizumab, once every two or three weeks (where the first dose of liposomal irinotecan and pembrolizumab are given on the same day); and repeating said treatment cycle until a progression or an unacceptable toxicity is observed. The treatment schedule can comprise administering a treatment cycle to a human host diagnosed with SCLC, where the treatment cycle includes administration of: a total of 100, 110, 120, or



130 mg/m<sup>2</sup> liposomal irinotecan (free base) once every two out of three weeks combined with the administration of 2 mg/kg pembrolizumab, once every two or three weeks (where the first dose of liposomal irinotecan and pembrolizumab are given on the same day); and repeating said treatment cycle until a progression or an unacceptable toxicity is observed. The treatment schedule can comprise administering MM-398 once every three weeks at 110 mg/m<sup>2</sup> liposomal irinotecan (free base), in combination with a therapeutically effective amount of an immunotherapy (e.g., in combination with an antibody to alpha-PDL1, PD1, alpha-41BB, alpha-CTLA4 and/or alpha-OX40). The treatment schedule can comprise administering MM-398 once every three weeks at 100 mg/m<sup>2</sup> liposomal irinotecan (free base), in combination with a therapeutically effective amount of an immunotherapy (e.g., in combination with an antibody to alpha-PDL1, PD1, alpha-41BB, alpha-CTLA4 and/or alpha-OX40). The treatment schedule can comprise administering MM-398 once every three weeks at 120 mg/m<sup>2</sup> liposomal irinotecan (free base), in combination with a therapeutically effective amount of an immunotherapy (e.g., in combination with an antibody to alpha-PDL1, PD1, alpha-41BB, alpha-CTLA4 and/or alpha-OX40). The treatment schedule can comprise administering MM-398 once every three weeks at 130 mg/m<sup>2</sup> liposomal irinotecan (free base), in combination with a therapeutically effective amount of an immunotherapy (e.g., in combination with an antibody to alpha-PDL1, PD1, alpha-41BB, alpha-CTLA4 and/or alpha-OX40).

[065] In some embodiments, liposomal irinotecan is administered after disease progression following platinum-based therapy for the SCLC in combination with one or more of prexasertib, aldoxorubicin, lurbinectedin and Rova-T. In some embodiments the liposomal irinotecan can be administered to a patient who has previously received a PD-1 directed therapeutic (e.g., nivolumab, pembrolizumab), a PD-L1 directed therapeutic (e.g., atezolizumab or durvalumab), or a Notch ADC compound (e.g., Rova-T) as a first-line (1L) therapy for the SCLC. In some embodiments the liposomal irinotecan can be administered in combination with a Chk1 directed therapeutic (e.g., prexasertib), a Topo-2 directed therapeutic (e.g., aldoxorubicin), a DNA inhibitor (e.g., lurbinectedin) or a Notch ADC compound (e.g., Rova-T). In other embodiments the liposomal irinotecan can be administered in the absence (i.e., without) a Chk1 directed therapeutic (e.g., prexasertib), a Topo-2 directed therapeutic (e.g., aldoxorubicin), a DNA inhibitor (e.g., lurbinectedin) or a Notch ADC compound (e.g., Rova-T). In some embodiments the liposomal irinotecan can be administered to a patient who has previously received cisplatin or carboplatin for SCLC, and

the liposomal irinotecan is administered in the absence of (i.e., without) cisplatin or carboplatin (for second or subsequent lines of therapy).

[066] In some embodiments, methods of treating SCLC can comprise administering a treatment cycle to a human host diagnosed with SCLC, where the treatment cycle includes administration of: a total of 90 mg/m<sup>2</sup> liposomal irinotecan (free base) or 120 mg/m<sup>2</sup> liposomal irinotecan (free base) once every three weeks combined with the administration of 3 mg/kg nivolumab once every two weeks starting on the same day as the first administration of the liposomal irinotecan, and repeating said treatment cycle until a progression or an unacceptable toxicity is observed. In another example, the treatment schedule can comprise administering a treatment cycle to a human host diagnosed with SCLC, where the treatment cycle includes administration of: a total of 90 mg/m<sup>2</sup> liposomal irinotecan (free base) or 120 mg/m<sup>2</sup> liposomal irinotecan (free base) once every three weeks combined with the administration of 2 mg/kg pembrolizumab once every three weeks starting on the same day as the first administration of the liposomal irinotecan; and repeating said treatment cycle until a progression or an unacceptable toxicity is observed.

[067] The patient can be administered antineoplastic therapy for treatment of SCLC comprising 90 mg/m<sup>2</sup> liposomal irinotecan once every two weeks, without the administration of another antineoplastic agent (e.g., without the administration of topotecan).

[068] Preferably, the antineoplastic therapy for previously treated (e.g. second line) SCLC provides a median time to progression of progression free survival of greater than 15 weeks (e.g., at least about 20-25 weeks, including about 21-24 weeks, about 22-24 weeks, about 23 weeks or about 24 weeks), a median overall survival of greater than 30 weeks (e.g., at least about 30-50 weeks, including about 40-50 weeks, about 44-48 weeks, about 45-47 weeks, about 46 weeks or about 47 weeks), with a hazard ratio of less than 1, and preferably less than 0.7, 0.6 or 0.5 (e.g., including hazard ratio of about 0.6-0.7). Preferably, the antineoplastic therapy provides a major adverse event (grade 3+) occurring in >5% of the population of less than 50% for neutropenia (e.g., about 10-50%, including about 20%), less than 50% for thrombocytopenia (e.g., less than 10%, including 1-10%, 1-5%, less than 5%, and about 2%, about 3% and about 4%), and less than 30% for anemia (e.g., less than 10%, including 1-10%, 1-8%, less than 8%, and about 5-7%, about 6% and about 5%).

[069] A method of treating a human patient diagnosed with small cell lung cancer (SCLC) after disease progression following platinum-based therapy for the SCLC, can consist of administering to the human patient an antineoplastic therapy once every two weeks, the antineoplastic therapy consisting of a single dose of liposomal irinotecan

providing 90 mg/m<sup>2</sup> (free base) of irinotecan encapsulated in irinotecan liposomes (or reduced doses of 50-70 g/m<sup>2</sup> (free base) of irinotecan as the liposomal irinotecan to patients who have experienced adverse events during or after a prior administration of liposomal irinotecan and/or patients known to be homozygous for the UGT1A1\*28 allele), where the antineoplastic therapy in a clinical trial of at least 300 patients (e.g., about 400-450 patients), where the antineoplastic therapy in a clinical trial of at least 300 patients (e.g., about 400-450 patients) results in major adverse event (grade 3+) occurring in >5% of the population of less than 50% for neutropenia (e.g., about 10-50%, including about 20%), less than 50% for thrombocytopenia (e.g., less than 10%, including 1-10%, 1-5%, less than 5%, and about 2%, about 3% and about 4%), and less than 30% for anemia (e.g., less than 10%, including 1-10%, 1-8%, less than 8%, and about 5-7%, about 6% and about 5%).

[070] A method of treating a human patient diagnosed with small cell lung cancer (SCLC) after disease progression following platinum-based therapy for the SCLC, can consist of administering to the human patient an antineoplastic therapy once every two weeks, the antineoplastic therapy consisting of a single dose of liposomal irinotecan providing 90 mg/m<sup>2</sup> (free base) of irinotecan encapsulated in irinotecan liposomes (or reduced doses of 50-70 g/m<sup>2</sup> (free base) of irinotecan as the liposomal irinotecan to patients who have experienced adverse events during or after a prior administration of liposomal irinotecan and/or patients known to be homozygous for the UGT1A1\*28 allele), where the antineoplastic therapy in a clinical trial of at least 300 patients (e.g., about 400-450 patients) results in one or more of the following: median time to progression of progression free survival of greater than 15 weeks (e.g., at least about 20-25 weeks, including about 21-24 weeks, about 22-24 weeks, about 23 weeks or about 24 weeks), a median overall survival of greater than 30 weeks (e.g., at least about 30-50 weeks, including about 40-50 weeks, about 44-48 weeks, about 45-47 weeks, about 46 weeks or about 47 weeks), with a hazard ratio of less than 1, and preferably less than 0.7, 0.6 or 0.5 (e.g., including hazard ratio of about 0.6-0.7).

[071] When the patient is known to be homozygous for the UGT1A1\*28 allele, each dose of irinotecan liposome can be reduced (e.g., 50, or 70 mg/m<sup>2</sup>). When the patient is not homozygous for the UGT1A1\*28 allele, and is not otherwise reduced, each dose of irinotecan liposome can be 90 mg/m<sup>2</sup>. The method can further comprise administering a corticosteroid and an anti-emetic to the patient prior to the administration of the irinotecan liposome.

[072] In some embodiments, the liposomal irinotecan can be administered to patients diagnosed with small cell lung cancer (SCLC) disease progression following treatment with

one or more camptothecin compounds or topoisomerase I (Topo-1) inhibitors. Examples of camptothecin compounds or topoisomerase I (Topo-1) inhibitors include, but are not limited to, camptothecin, 9-aminocamptothecin, 7-ethylcamptothecin, 10-hydroxycamptothecin, 7-ethyl 10-hydroxy camptothecin, 9-nitrocamptothecin, 10,11-methylenedioxcamptothecin, 9-amino-10,11-methylenedioxcamptothecin, 9-chloro-10,11-methylenedioxcamptothecin, irinotecan (CPT-11), topotecan, lurtotecan, silatecan, etirinotecan pegol, rubitecan, exatecan, FL118, belotecan, gimatecan, indotecan, indimitecan, (7-(4-methylpiperazinomethylene)-10,11-ethylenedioxy-20(S)-camptothecin, 7-(4-methylpiperazinomethylene)-10,11-methylenedioxy-20(S)-camptothecin, and 7-(2-N-isopropylamino)ethyl)-(20S)-camptothecin.

[073] In some embodiments the liposomal irinotecan can be administered to patients diagnosed with SCLC disease progression following treatment with irinotecan (CPT-11), topotecan, or both. In some embodiments the liposomal irinotecan can be administered to patients diagnosed with SCLC disease progression following treatment with irinotecan (CPT-11). In some embodiments the liposomal irinotecan can be administered to patients diagnosed with SCLC disease progression following treatment with topotecan. In some embodiments the liposomal irinotecan can be administered to patients diagnosed with SCLC disease progression following treatment with non-liposomal irinotecan.

[074] In some embodiments, the platinum-based therapy is administered in combination with etoposide or non-liposomal irinotecan. In some embodiments, the platinum-based therapy is administered in combination with etoposide. In some embodiments, the platinum-based therapy is administered in combination with non-liposomal irinotecan.

One embodiment is a method of treating a human patient diagnosed with small cell lung cancer (SCLC) following disease progression on or after camptothecin-based therapy for the SCLC, the method comprising administering to the human patient an antineoplastic therapy once every two weeks, the antineoplastic therapy consisting of a  $90 \text{ mg/m}^2$  (free base) dose of MM-398 liposomal irinotecan. In some embodiments, the camptothecin-based therapy comprises the prior, discontinued administration of topotecan or non-liposomal irinotecan to treat the human patient diagnosed with SCLC. In some embodiments, the camptothecin-based therapy comprises the prior, discontinued administration of non-liposomal irinotecan administered to the human patient at a  $300 \text{ mg/m}^2$  dose once every three weeks. In some embodiments, the camptothecin-based therapy comprises the prior, discontinued administration of non-liposomal irinotecan administered to the human patient at a  $1.5 \text{ mg/m}^2$  dose of topotecan on days 1, 2, 3, 4, and 5 in a three week treatment cycle.

[075] In some embodiments, the human patient diagnosed with SCLC is platinum sensitive. In some embodiments the human patient diagnosed with SCLC is platinum resistant.

[076] A first aspect of the present disclosure is a method of treating a human patient diagnosed with small cell lung cancer (SCLC) following disease progression on or after first-line platinum-based therapy for the SCLC. One embodiment of the first aspect is a method of treating a human patient diagnosed with small cell lung cancer (SCLC) following disease progression on or after first-line platinum-based therapy for the SCLC, the method comprising administering to the human patient an antineoplastic therapy once every two weeks, the antineoplastic therapy consisting of a 90 mg/m<sup>2</sup> (free base) dose of MM-398 liposomal irinotecan.

[077] In one embodiment of the first aspect the platinum-based therapy comprises the prior, discontinued administration of cisplatin or carboplatin to treat the human patient diagnosed with SCLC. In another embodiment the human patient has a blood ANC greater than 1,500 cells/microliter without the use of hematopoietic growth factors, prior to the administration of the MM-398 liposomal irinotecan. Another embodiment is a method of treating a human patient diagnosed with small cell lung cancer (SCLC) following disease progression on or after first-line platinum-based therapy for the SCLC. Yet another embodiment is a method of treating a human patient diagnosed with small cell lung cancer (SCLC) following disease progression on or after first-line platinum-based therapy for the SCLC, the method comprising administering to the human patient an antineoplastic therapy once every two weeks, the antineoplastic therapy consisting of a 90 mg/m<sup>2</sup> (free base) dose of MM-398 liposomal irinotecan wherein the human patient has a blood platelet count of greater than 100,000 cells per microliter, prior to the administration of the MM-398 liposomal irinotecan.

[078] In some embodiments of the first aspect the human patient has a blood hemoglobin greater than 9 g/dL, prior to the administration of the MM-398 liposomal irinotecan. In some embodiments the human patient has a serum creatinine of less than or equal to 1.5xULN and a creatinine clearance of greater than or equal to 40 mL/min prior to the administration of the MM-398 liposomal irinotecan.

[079] In some of the embodiments of the first aspect the human patient has not received a topoisomerase I inhibitor prior to administration of the MM-398 liposomal irinotecan. In yet other embodiments of the first aspect the human patient has not received more than a single platinum-based therapy prior to administration of the MM-398 liposomal irinotecan.

[080] Embodiments of the first aspect may comprise a method wherein the antineoplastic therapy comprises the steps of: (a) preparing a pharmaceutically acceptable injectable composition by combining dispersion of MM-398 liposomal irinotecan containing 4.3 mg irinotecan free base/mL of the dispersion with a 5% Dextrose Injection (D5W) or 0.9% Sodium Chloride Injection to obtain the injectable composition having a final volume of 500 mL and 90 mg/m<sup>2</sup> (free base) of the MM-398 liposomal irinotecan ( $\pm 5\%$ ); and (b) administering the injectable composition from step (a) containing the MM-398 irinotecan liposome to the patient in a 90-minute infusion.

[081] In any embodiment of the first aspect the method may further comprise administering to the human patient dexamethasone and a 5-HT<sub>3</sub> blocker prior to each administration of the antineoplastic therapy, and optionally further administering an antiemetic to the human patient.

[082] A second aspect of the present disclosure is a method of treating a human patient who is not homozygous for the UTG1A1\*28 allele and is diagnosed with small cell lung cancer (SCLC) following disease progression on or after first-line platinum-based therapy for the SCLC. One embodiment of the second aspect is a method of treating a human patient who is not homozygous for the UTG1A1\*28 allele and is diagnosed with small cell lung cancer (SCLC) following disease progression on or after first-line platinum-based therapy for the SCLC, the method comprising administering to the human patient an antineoplastic therapy once every two weeks in a six-week cycle, the antineoplastic therapy consisting of a 90 mg/m<sup>2</sup> (free base) dose of MM-398 liposomal irinotecan.

[083] In some embodiments of the second aspect the platinum-based therapy comprises the prior, discontinued administration of cisplatin or carboplatin to treat the human patient diagnosed with SCLC.

[084] One embodiment of the second aspect is a method of treating a human patient who is not homozygous for the UTG1A1\*28 allele and is diagnosed with small cell lung cancer (SCLC) following disease progression on or after first-line platinum-based therapy for the SCLC, wherein the method comprises administering to the human patient an antineoplastic therapy once every two weeks in a six-week cycle, the antineoplastic therapy consisting of a 90 mg/m<sup>2</sup> (free base) dose of MM-398 liposomal irinotecan, wherein the human patient has one or more of the following prior to the administration of the MM-398 liposomal irinotecan: (a) a blood ANC greater than 1,500 cells/microliter without the use of hematopoietic growth factors; (b) a blood platelet count of greater than 100,000 cells per microliter; (c) a blood

hemoglobin greater than 9 g/dL; and (d) a serum creatinine of less than or equal to 1.5xULN and a creatinine clearance of greater than or equal to 40 mL/min.

[085] In some embodiments of the second aspect the human patient has not received a topoisomerase I inhibitor prior to administration of the MM-398 liposomal irinotecan; and the human patient has not received a more than a single platinum-based therapy prior to administration of the MM-398 liposomal irinotecan. In some embodiments the method comprises administering the antineoplastic therapy for at least three six-week cycles.

[086] In some embodiments of the second aspect the antineoplastic therapy comprises the steps of: (a) preparing a pharmaceutically acceptable injectable composition by combining dispersion of MM-398 liposomal irinotecan containing 4.3 mg irinotecan free base/mL of the dispersion with a 5% Dextrose Injection (D5W) or 0.9% Sodium Chloride Injection to obtain the injectable composition having a final volume of 500 mL and 90 mg/m<sup>2</sup> (free base) of the MM-398 liposomal irinotecan ( $\pm 5\%$ ); and (b) administering the injectable composition from step (a) containing the MM-398 irinotecan liposome to the patient in a 90-minute infusion. This embodiment may further comprise administering to the human patient dexamethasone and a 5-HT<sub>3</sub> blocker prior to each administration of the antineoplastic therapy, and optionally further administering an antiemetic to the human patient.

[087] A third aspect of the disclosure provides methods of treating a human patient diagnosed with small cell lung cancer (SCLC) following disease progression on or after a first-line platinum-based therapy for the SCLC selected from the group consisting of cisplatin or carboplatin. One embodiment of the third aspect is a method of treating a human patient diagnosed with small cell lung cancer (SCLC) following disease progression on or after a first-line platinum-based therapy for the SCLC selected from the group consisting of cisplatin or carboplatin. the method comprising administering to the human patient an antineoplastic therapy once every two weeks for a total of at least three six-week cycles, the antineoplastic therapy consisting of a 90 mg/m<sup>2</sup> (free base) dose of MM-398 liposomal irinotecan; wherein the human patient is not homozygous for the UTG1A1\*28 allele and has the following prior to the administration of each antineoplastic therapy of MM-398 liposomal irinotecan: (a) a blood ANC greater than 1,500 cells/microliter without the use of hematopoietic growth factors; (b) a blood platelet count of greater than 100,000 cells per microliter; (c) a blood hemoglobin greater than 9 g/dL; and (d) a serum creatinine of less than or equal to 1.5xULN and a creatinine clearance of greater than or equal to 40 mL/min. In some embodiments of the third aspect the human patient has not received a topoisomerase I inhibitor prior to

administration of the MM-398 liposomal irinotecan and has not received a more than a single platinum-based therapy prior to administration of the MM-398 liposomal irinotecan; and the method further comprises administering to the human patient dexamethasone and a 5-HT3 blocker prior to each administration of the antineoplastic therapy, and optionally further administering an antiemetic to the human patient.

[088] In one embodiment of the third aspect the antineoplastic therapy comprises the steps of: (a) preparing a pharmaceutically acceptable injectable composition by combining dispersion of MM-398 liposomal irinotecan containing 4.3 mg irinotecan free base/mL of the dispersion with a 5% Dextrose Injection (D5W) or 0.9% Sodium Chloride Injection to obtain the injectable composition having a final volume of 500 mL and 90 mg/m<sup>2</sup> (free base) of the MM-398 liposomal irinotecan ( $\pm 5\%$ ); and (b) administering the injectable composition from step (a) containing the MM-398 irinotecan liposome to the patient in a 90-minute infusion.

[089] **Examples**

[090] **Example 1: Liposomal Irinotecan**

[091] The liposomal irinotecan composition preferably comprises or consists of phosphatidylcholine, cholesterol, and a polyethyleneglycol-derivatized phosphatidylethanolamine. The liposomal irinotecan can include unilamellar lipid bilayer vesicles comprising the phosphatidylcholine and cholesterol, encapsulating irinotecan sucrose octasulfate. The irinotecan liposomes in the liposomal irinotecan composition have a diameter of 110 nm ( $\pm 20\%$ ). The liposomal irinotecan can comprise irinotecan sucrose octasulfate encapsulated in liposomes having a unilamellar lipid bilayer vesicle, approximately 110 nm in diameter, which encapsulates an aqueous space containing irinotecan in a gelled or precipitated state as the sucrose octasulfate salt; wherein the vesicle is composed of 1,2-distearoyl-sn-glycero-3-phosphocholine (DSPC) (e.g., about 6.8 mg/mL), cholesterol (e.g., about 2.2 mg/mL), and methoxy-terminated polyethylene glycol (MW 2000)-distearoylphosphatidyl ethanolamine (MPEG-2000-DSPE) (e.g., about 0.1 mg/mL). Each mL also contains 2-[4-(2-hydroxyethyl) piperazin-1-yl]ethanesulfonic acid (HEPES) as a buffer (e.g., about 4.1 mg/mL) and sodium chloride as an isotonicity reagent (e.g., about 8.4 mg/mL).

[092] The lipid membrane of the liposomal irinotecan can be composed of phosphatidylcholine, cholesterol, and a polyethyleneglycol-derivatized phosphatidylethanolamine in a suitable molar ratio (e.g., of about 3:2:0.015, and/or in the amount of approximately one polyethyleneglycol (PEG) molecule for 200 phospholipid molecules). ONIVYDE® (also referred to herein as MM-398 or nal-IRI) is a preferred liposomal



irinotecan, comprising small unilamellar lipid bilayer vesicle (SUV), approximately 110 nm in diameter that encapsulates an aqueous space which contains irinotecan in a gelated or precipitated state as the sucrosolate salt. The ONIVYDE liposomal irinotecan comprises irinotecan sucrose octasulfate encapsulated in liposomes having a unilamellar lipid bilayer vesicle, approximately 110 nm in diameter, which encapsulates an aqueous space containing irinotecan in a gelated or precipitated state as the sucrose octasulfate salt; wherein the vesicle is composed of 1,2-distearoyl-sn-glycero-3-phosphocholine (DSPC) (6.8 mg/mL), cholesterol (2.2 mg/mL), and methoxy-terminated polyethylene glycol (MW 2000)-distearoylphosphatidyl ethanolamine (MPEG-2000-DSPE) (0.1 mg/mL). Each mL also contains 2-[4-(2-hydroxyethyl) piperazin-1-yl]ethanesulfonic acid (HEPES) as a buffer (4.1 mg/mL) and sodium chloride as an isotonicity reagent (8.4 mg/mL). ONIVYDE is a sterile, white to slightly yellow opaque isotonic liposomal dispersion.

[093] The liposomal irinotecan can be supplied as a sterile, white to slightly yellow, opaque liposomal dispersion in a 10 mL single use glass vial, containing 43 mg/10 mL irinotecan free base. The liposomal dispersion in the vial can be diluted prior to intravenous infusion over 90 minutes.

[094] The present disclosure provides for use of liposomal irinotecan (e.g., ONIVYDE described in Example 9) for the treatment of SCLC once every two weeks at a total dose of 90 mg/m<sup>2</sup> irinotecan (free base), encapsulated in liposomes (dose based on the amount of irinotecan free base; equivalent to 100 mg/m<sup>2</sup> of the irinotecan hydrochloride anhydrous salt) IV over 90 minutes, every 2 weeks (preferably, in a 6-week cycle). The recommended starting dose of ONIVYDE in patients known to be homozygous for the UGT1A1\*28 allele is 50 mg/m<sup>2</sup> (free base) administered by intravenous infusion over 90 minutes. The dose of ONIVYDE may be increased to 70 mg/m<sup>2</sup> as tolerated in subsequent cycles. There is no recommended dose of ONIVYDE for patients with serum bilirubin above the upper limit of normal.

[095] **Example 2**

[096] Topoisomerase I inhibition has potent effects on a wide range of cancer cell lines. Reference data in the Wellcome Trust Sanger Institute database of the “Genomics of Drug Sensitivity in Cancer” project are available for 663 cancer cell lines screened for sensitivity to SN-38 (URL [www.cancerrxgene.org/translation/Drug/1003](http://www.cancerrxgene.org/translation/Drug/1003)). An analysis of this data indicated that SCLC cell lines have similar sensitivity to SN-38 as pancreatic and gastrointestinal cancer cell lines (Figure 1). Within this dataset, cancer cell lines of gastrointestinal (HT-29, HCT-116, LoVo, MKN45) or pancreatic (AsPC-1, BxPC3, CFPAC-

1, MiaPaCa-2) origin for which significant *in vivo* anti-tumor efficacies of MM-398 have been observed are highlighted by filled circles. SCLC cell lines DMS114 and NCI-H1048 (see below) are also shown as filled circles.

[097] The activity of the active metabolite of irinotecan, SN-38, against various SCLC cell lines was investigated in *in vitro* growth and viability assays. SN-38 induced a decrease in cell viability of > 90% in four tested SCLC cell lines (DMS53, DMS114, NCI-H1048, SW1271), the IC<sub>50</sub> was variable and spanned several orders of magnitude. Figures 2A and 2B show the cell growth inhibition kinetics of SN-38 in 2 SCLC cell lines (DMS-114 and NCI-H1048) using an IncuCyte® ZOOM System over a time-course of 88 hours. Effective cell growth inhibition was observed between 1-10 nM, while cell killing was observed after prolonged incubation times at concentrations  $\geq 10$ nM. This range of SN-38 therapeutic threshold coincides with the amount of SN-38 measured from patient tumor biopsies at 72h post- MM-398 administration (range: 3 - 163 nM). These data suggest that the prolonged duration of SN-38 in tumors as a result of MM-398 pharmacological characteristics would provide effective activity in SCLC. Preclinical experiments have demonstrated that MM-398 greatly increased the availability of SN-38 in the tumor and showed dose-dependent anti-tumor efficacy at much lower doses than non-liposomal irinotecan.

[098] **Example 3**

[099] The activity of MM-398 as a single agent was investigated in xenograft models of SCLC. DMS114 cells were inoculated subcutaneously in NCR nu/nu mice. When tumors reached  $\sim 300$  mm<sup>3</sup> in volume, mice were treated with 10 or 20 mg/kg of MM-398 irinotecan hydrochloride, administered intravenously on a weekly basis for 4 weeks. Dose levels were selected to correspond to what is believed to be the clinically relevant mouse dose, based on PK modeling and comparison with clinical PK data. As shown in Figure 3, anti-tumor activity was seen at all dose levels tested in the DMS114 model. Animals with tumors receiving 10 or 20 mg/kg showed tumor regression that was sustained for approximately 20-27 days past the last dose of MM-398 (2/5 and 4/5 complete regressions at 10 and 20 mg/kg dose, respectively).

[0100] **Example 4:** Association between exposure and efficacy.

[0101] While the association between MM-398 exposure and efficacy is to be studied in SCLC, data analysis in pancreatic cancer patients indicates benefits in increased exposure to SN-38. In the MM-398+5FU/LV treatment arm of NAPOLI-1, longer overall survival (OS) and progression free survival (PFS) were associated with longer time uSN38 >0.03 ng/mL and higher C<sub>avg</sub> of tIRI, tSN38 and uSN38, with the highest association observed for the

time when uSN38 >0.03 ng/mL. C<sub>max</sub> of tIRI, tSN38, or uSN38 was not predictive of OS (P=0.81-0.92). The relationship between OS and quartiles of time (uSN38>0.03 ng/mL) for the MM-398+5FU/LV is provided in Figure 4. Longer duration of uSN38>0.03 ng/mL was associated with a higher probability of achieving objective response in the MM-398+5FU/LV arm (Figure 5) This association was not observed in the MM-398 monotherapy arm dosed at 100 mg/m<sup>2</sup> every 3 weeks (P=0.62). The lack of association in the monotherapy arm may be attributed partly in the difference of the dose intervals (MM-398 dose in the monotherapy arm is 100 mg/m<sup>2</sup> every 3 weeks, MM-398 dose in the MM-398+5-FU/LV arm is 70 mg/m<sup>2</sup> every 2 weeks).

[0102] **Example 5:** Association between exposure and safety with MM-398

[0103] The association between exposure and safety was evaluated based on data in 353 patients treated with Onivyde. Higher un-encapsulated SN-38 C<sub>max</sub> was associated with higher probability of both incidence and severity of neutropenia treatment-emergent adverse events (Figure 6A). Higher total irinotecan C<sub>max</sub> was associated with higher probability of observing grade 3+ diarrhea (Figure 6B). Moreover, different probabilities of observing grade 3+ neutropenia were seen with and without co-administration with 5FU/LV. These associations were used to evaluate the predicted safety with alternative dose regimens to be tested in SCLC.

[0104] **Example 6:** Prediction of safety for a dose of 90 mg/m<sup>2</sup>

[0105] Based on these exposure-safety associations for neutropenia (Figure 6A) and diarrhea (Figure 6B), the predicted rate of grade 3+ neutropenia and diarrhea is provided in Table 5. Compared to a dose of 70 mg/m<sup>2</sup> (free base) as monotherapy, a dose of 90 mg/m<sup>2</sup> (free base) is predicted to increase grade 3+ neutropenia from 8.4% to 11.1% and diarrhea from 14.3% to 20.0%. These rates were derived based on data with the majority (73%) of patients with pancreatic cancer disease who may have higher risk of diarrhea as compared to patients with SCLC.

Table 5

Predicted neutropenia and diarrhea grade 3 or Higher by Irinotecan Liposome Injection Dose

Adverse Event code	Dose (mg/m <sup>2</sup> )	Predicted rates
Neutropenia grade >=3	70	8.4%
	90	11.1%
	100	13.9%

Adverse Event code	Dose (mg/m <sup>2</sup> )	Predicted rates
Diarrhea grade $\geq 3$	70	14.3%
	90	20.0%
	100	25.8%

[0106] **Example 7:** A Randomized, Open Label Phase 3 Study of nal-IRI (ONIVYDE® or MM-398) in Patients with Small Cell Lung Cancer Who have Progressed On or After Platinum-based First-Line Therapy

[0107] **Overview of Study Design.** This is an open label, randomized Phase 3 study of irinotecan liposome injection *versus* IV topotecan in patients with small cell lung cancer who have progressed on or after platinum-based first line therapy. The study will be conducted in two parts.

[0108] **Part 1:**

[0109] **Part 1a** The objectives of Part 1a are to: 1) describe the safety and tolerability of irinotecan liposome injection monotherapy administered every 2 weeks and 2) to determine the irinotecan liposome injection monotherapy dose (90 mg/m<sup>2</sup> or 70 mg/m<sup>2</sup> administered every two weeks) for the Part 1b and Part 2 of this study.

[0110] **Part 1b** is a parallel study of nal-IRI (N= 25) and IV topotecan (N=25) for the purpose of characterizing preliminary efficacy and safety of irinotecan liposome injection and IV topotecan. The objectives of Part 1b are to describe the 1) progression free survival rate at 12 weeks, 2) objective response rate (ORR), 3) progression free survival (PFS), 4) overall survival (OS), and 5) safety profile.

[0111] **Part 2:** a randomized, efficacy study of the nal-IRI (N=210) *versus* topotecan (N=210). The primary objective of Part 2 is to compare overall survival following treatment with irinotecan liposome injection with overall survival following treatment with IV topotecan.

[0112] The secondary objectives of Part 2 are to compare the following between the treatment arms: 1) progression free survival (PFS), 2) objective response rate (ORR), 3) proportion of patients with symptom improvement in cough, in dyspnea and in fatigue as measured by the European Organization for Research and Treatment of Cancer Quality of Life Questionnaire (EORTC QLQ-C30) and Lung Cancer 13 (LC13) and 4) safety profile.

[0113] Exploratory Objectives (Part 1 and Part 2) include: 1) To describe QTcF following treatment with irinotecan liposome injection (Part 1 only), 2) To explore the biomarkers associated with efficacy and safety following treatment with irinotecan liposome

injection, 3) To describe the association between UGT1A1 genotype, SN-38 concentration (irinotecan liposome injection treated patients only) and safety, 4) To evaluate the relationship between plasma pharmacokinetics of irinotecan liposome injection and efficacy and safety in this patient population, 5) To compare the rate of development/time to development of CNS progression and development of new CNS metastases, 6) To compare time to treatment failure (TTF) between treatment arms and 7) To compare patient-reported outcomes (PROs) between treatment arms using EORTC-QLQ-C30, EORTC-QLQ-LC13 and EQ-5D-5L.

[0114] Both Part 1 and Part 2 will consist of three phases: a screening phase, a Treatment/Active follow-up phase and a long term follow-up phase. The Treatment/Active follow-up phase is the period for the first dose of the study drug through the decision to permanently discontinue study drug treatment. The Long Term follow-up phase is a monthly follow-up for overall survival.

[0115] **Part 1a**

[0116] The initial number of patients to be enrolled in the Part 1a safety run-in is 6 patients evaluable for safety. This initial cohort of patients will be treated with irinotecan liposome injection 70 mg/m<sup>2</sup> every 2 weeks. Dose limiting toxicities (DLTs) will be evaluated during the first 28 days of treatment (or 14 days after the 2nd dose of study treatment if there is a treatment delay) to determine if the dose is tolerable. If 2 or more patients receiving irinotecan liposome injection 70 mg/m<sup>2</sup> every 2 weeks have DLTs then the dose will be declared not tolerable. In all other cases an additional cohort of 6 patients treated with irinotecan liposome injection starting at 90 mg/m<sup>2</sup> will be enrolled. The 90 mg/m<sup>2</sup> cohort will only be enrolled if the overall experience in the initial 6 patients treated in the 70 mg/m<sup>2</sup> cohort is judged to be safe enough to reasonably expect that the 90 mg/m<sup>2</sup> dose will be tolerable in the assessment of the Part 1 investigators and the Sponsor. Evaluation of DLTs will follow the same guidelines as the first cohort. If 2 or more patients have DLTs at the 90 mg/m<sup>2</sup> dose then that dose will be considered to exceed the optimal safety and tolerability criteria, and 70 mg/m<sup>2</sup> will be designated as the dose for Part 1b and Part 1b will initiate administering 70 mg/m<sup>2</sup> of irinotecan liposome injection. If there is 0 or 1 DLT within the safety evaluation period with the 90 mg/m<sup>2</sup> dose, then the decision of which dose to use for Part 1b will be made by Part 1 investigators and the Sponsor based on the entire safety experience of both cohorts.

- All patients who received study drug will be evaluable for DLT and safety. The following adverse events should be considered as DLTs if they occur during the first

28 days of treatment (or 14 days after the 2nd dose of study treatment if there is a treatment delay according to section 6.2) and are deemed related to the study treatment by the investigator: Grade 4 neutropenia or thrombocytopenia that does not resolve within 7 days and grade 4 anemia of any duration

- Inability to begin subsequent treatment course within 14 days of the scheduled date, due to drug-related toxicity
- Grade 3-4 neutropenia complicated by fever  $\geq 38.5$  °C (i.e. febrile neutropenia) and/or by infection
- Any grade 4 non-hematologic toxicity with the exception of the following:
  - Fatigue/asthenia  $< 2$  weeks
  - Nausea and vomiting lasting  $\leq 3$  days duration (only considered dose limiting if they last  $> 72$  hours after treatment with an optimal anti-emetic treatment)
  - Diarrhea  $\leq 3$  days duration (only considered dose limiting if diarrhea lasts  $> 72$  hours after treatment with an optimal anti-diarrheal regimen)
- Grade 3 non-hematologic toxicity with the exception of the following:
  - Any gastrointestinal disorder and dehydration (with associated signs and symptoms) unless grade 3 toxicity persists despite optimal medical management for  $> 72$  hours,
  - Pain unless grade 3 toxicity persists despite optimal medical management,
  - Fatigue, fever, flu like symptoms, infections and infestations
  - Infusion reaction (and associated symptoms) unless it occurs following steroid premedication
  - Hepatic and kidney function abnormalities, and electrolyte abnormalities if they persist, despite optimal medical management

[0117] The determination whether an adverse event is considered a DLT will be made following discussion between the investigators and the Sponsor and confirmed by the safety review committee (i.e. the Part 1a Investigators and the Medical Monitor(s) of the Sponsor). Other adverse events that are deemed related to study treatment can also be considered a DLT event at the discretion of the safety review committee. Safety review meetings between investigators and sponsor will occur regularly during Part 1a of the study with at least monthly meetings, or more frequently, if required.

[0118] **Part 1b**

[0119] Following the determination of the nal-IRI dose in Part 1a, Part 1b of the study will be initiated. In Part 1b, approximately 50 eligible patients will be randomized in a 1:1

ratio between the experimental arm (Arm 1a: 90 mg/m<sup>2</sup> of nal-IRI, every 2 weeks), and the control arm (Arm 1b: topotecan 1.5 mg/m<sup>2</sup> IV for 5 days, every 21 days). Patients will be randomized to the treatment arms using an Interactive Web Response System (IWRS) at a central location. In order to reduce imbalance with regard to prognostic factors used for stratification in the randomization for Part 2, randomization in Part 1b will use a minimization procedure accounting for the Part 2 stratification factors.

[0120] Platinum resistant patients are defined as patients with disease that either progressed during first-line platinum containing therapy or within 90 days of its completion. Platinum sensitive patients are defined as patients with disease that progressed after 90 days of completion of first line platinum containing therapy. To retain a distribution of platinum sensitivity to first-line treatment groups in accordance with previously published studies (von Pawel, 2014), no more than 30 patients will be randomized from either platinum sensitive or platinum resistant patients in Part 1b.

[0121] Safety and efficacy results from Part 1b will determine if the study proceeds (or not) to Part 2. The study will be stopped if both of the following stopping criteria are met:

[0122] PFS (based on investigator assessment) rate at 12 weeks for irinotecan liposome injection is less than 50% AND PFS (based on investigator assessment) rate at 12 weeks for IV topotecan exceeds that of irinotecan liposome injection by at least 5 percentage points

[0123] If the stopping criteria are not met, the final decision to proceed to Part 2 will be made by the Sponsor in consultation with the academic steering committee of the study after consideration of all available efficacy and safety data from Part 1 of the study.

[0124] **Part 2:**

[0125] If the stopping criteria from Part 1b are not met and the decision is made to proceed to Part 2 of the study, approximately 420 eligible patients will be randomized in a 1:1 ratio between the experimental arm (Arm 2a: 90 mg/m<sup>2</sup> of irinotecan liposome injection), and the control arm (Arm 2b: IV topotecan). Patients will be randomized to the treatment arms using an Interactive Web Response System (IWRS) at a central location.

Randomization will be stratified, based on the following factors:

- Disease stage (limited vs extensive) at diagnosis
- Region (North America vs Asia vs Other)
- Platinum sensitivity (sensitive vs resistant)
- Performance status (ECOG 0 vs. 1)
- Prior immunotherapy (yes vs. no)

[0126] Only region and platinum sensitive vs. resistant will be used for the efficacy analysis.

[0127] Tumor responses will be measured and recorded, every 6 weeks (+/- 1 week) by using the RECIST guidelines (version 1.1). The tumor assessment at baseline is CT with contrast (chest/abdomen required and pelvis if clinically indicated) and brain MRI with contrast (CT of brain is acceptable). Each follow-up tumor assessment should use the same assessment as performed at baseline, unless medically contraindicated. All patients will have imaging of the brain at baseline and at each assessment. Patients who discontinue study treatment, for reasons other than objective disease progression, should continue to be followed-up until radiological documentation of progressive disease. The Sponsor will collect and store all tumor measurement images on all patients throughout the study; however, local radiologist and/or PI assessment will determine disease progression. A review of the scans may be performed by the Sponsor for an independent analysis, including analysis of PFS and/or ORR. All patients will be followed at least monthly until death or study closure, whichever occurs first.

[0128] A quality of life assessment will be performed using the EORTC-QLQ-C30, EORTC-QLQ-LC13, and the EuroQoL five-dimension, five level health status questionnaire (EQ-5D-5L) in Part 1b and Part 2 only. Both instruments will be administered before randomization and prior to dosing at 6 week intervals following start of treatment and at treatment discontinuation and at the 30-day follow-up visit.

[0129] Adverse events (AEs) will be evaluated according to the National Cancer Institute's Common Terminology Criteria for Adverse Events version 4.03 (CTCAE v4.03). For summary of AEs, events will be coded using the latest MedDRA dictionary version.

[0130] The primary analysis is planned when at least 333 OS events have occurred. An interim analysis for futility is planned to occur at 30% information time, after at least 100 OS events have occurred. In the event that the trial continues, an interim analysis will be conducted when at least 210 OS events (63% information time, at 50% of anticipated death events) have occurred to assess the potential for early stopping due to efficacy of the experimental treatment regimen.

[0131] A regular review of safety data will be conducted for Part 2 by an independent Data Monitoring Committee (DMC). The DMC will consist of oncology and statistical experts independent of the Sponsor. The first safety review of the DMC will take place in Part 2 after the 30th patient is treated for at least one cycle or after the 30th patient discontinued study drug, whichever occurs first. The timing and details of subsequent data



reviews will be detailed in the DMC charter. Items reviewed on a regular basis will include (but not limited to) safety events, results of PK testing, and UGT1A1\*28 genotype from central testing with particular attention to determine whether any study procedure needs to be modified for patients who are homozygous for UGT1A1\*28.

[0132] **Pharmacokinetics**

[0133] Plasma samples for PK will be collected in Cycle 1 only at the following time points:

[0134] Part 1a, and Part 1b, Arm 1a (nal-IRI arm; cycle 1 only):

[0135] - Day 1: Pre-dose

[0136] - Day 1: End of nal-IRI infusion

[0137] - Day 2: Approximately 24 hours after end of infusion

[0138] - Day 8: Cycle 1, Day 8 (+/- 1 day), at any time of day

[0139] - Day 15: Pre-dose

[0140] - Day 15: End of nal-IRI infusion

[0141] Part 1b, Arm 1b (topotecan arm; cycle 1 only):

[0142] - Day 1: Pre-dose

[0143] - Day 1: End of topotecan infusion

[0144] - Day 1, 2 or 3: Two additional samples between 1.5 and 4 hours after the start of infusion. Each sample must be collected at least 1 hour apart. It is preferred to collect these samples on day 1; however these two additional samples can be collected on day 2 or day 3.

[0145] Part 2, Arm 2a (irinotecan liposome injection arm; cycle 1 only):

[0146] - Day 1: Pre-dose

[0147] - Day 1: End of irinotecan liposome injection infusion

[0148] - Day 1: Between 2.5 and 6 hours after the start of infusion

[0149] - Day 2-6 (Optional): anytime between 1 and 5 days after the start of infusion

[0150] - Day 8: Cycle 1 Day 8 (+/- 1 day), at any time of day.

[0151] **Study Population**

[0152] **Inclusion Criteria**

[0153] **Disease Specific Inclusion Criteria** 1) histopathologically or cytologically confirmed small cell lung cancer according to the International Association for the Study of Lung Cancer (IASLC) histopathological classification. Mixed or combined subtypes according to the IASLC are not allowed; 2) Evaluable disease as defined by RECIST v1.1 guidelines (patients with non-target lesions only are eligible) 3) Progression on or after first-

line platinum based chemotherapy (carboplatin or cisplatin) or chemo-radiation including platinum-based chemotherapy for treatment of limited or extensive stage SCLC; and 4) Recovered from the effects of any prior chemotherapy, surgery, radiotherapy or other anti-neoplastic therapy (recovered to grade 1 or better, with the exception of alopecia).

[0154] **Hematologic, Biochemical and Organ Function Inclusion Criteria:** Adequate bone marrow reserves as evidenced by:

- ANC > 1,500 cells/ $\mu$ l without the use of hematopoietic growth factors; and
- Platelet count > 100,000 cells/ $\mu$ l; and
- Hemoglobin > 9 g/dL; transfusions are allowed

[0155] Adequate hepatic function as evidenced by:

- Serum total bilirubin within normal range for the institution
- Aspartate aminotransferase (AST) and alanine aminotransferase (ALT)  $\leq 2.5 \times$  ULN ( $\leq 5 \times$  ULN is acceptable if liver metastases are present)

[0156] Adequate renal function as evidenced by a serum creatinine  $\leq 1.5 \times$  ULN and creatinine clearance  $\geq 40$  mL/min. Actual body weight should be used for calculating creatinine clearance using the Cockcroft-Gault Equation(except for patients with body mass index (BMI)>30 kg/m<sup>2</sup> when lean body weight should be used instead):

$$\text{Serum Creatinine (mg/min)} = \frac{(140 - \text{Age (years)}) \times (\text{Weight (kg)})}{72 \times \text{Serum Creatinine (mg/dL)}} \times \text{Sex}$$

[0157] Where Sex =1 for males and 0.85 for females.

[0158] ECG without any clinically significant findings

[0159] Recovered from the effects of any prior chemotherapy, surgery, radiotherapy or other anti-neoplastic therapy

[0160] Required to participate in the translational research component of the trial, unless prohibited by local regulations, and provide archived tumor tissue (if available)

[0161] At least 18 years of age

[0162] Able to understand and sign an informed consent (or have a legal representative who is able to do so)

[0163] Patients must meet all the inclusion criteria listed above and none of the following exclusion criteria:

[0164] **General Exclusion Criteria**

[0165] 1) Any medical or social condition deemed by the Investigator to be likely to interfere with a patient's ability to sign informed consent, cooperate and participate in the study, or interfere with the interpretation of the results;

[0166] 2) Pregnant or breast feeding; females of child-bearing potential must test negative for pregnancy at the time of enrollment based on a urine or serum pregnancy test. Both male and female patients of reproductive potential must agree to use a highly effective method of birth control, during the study and for 4 months following the last dose of study drug.

[0167] **Disease Specific Exclusion Criteria**

[0168] 1) Prior treatment regimens with irinotecan, topotecan or any other topoisomerase I inhibitor including investigational topoisomerase I inhibitors;

[0169] 2) Patients with large cell neuroendocrine carcinoma;

[0170] 3) Patients who have had more than one regimen of prior cytotoxic chemotherapy

[0171] 4) More than one line of immunotherapy (e.g. nivolumab, pembrolizumab, ipilimumab, atezolizumab, tremelimumab and/or durvalumab). One line of immunotherapy is defined as the following: monotherapy or combination of immunotherapy agents given as either (i) in combination with chemotherapy followed by immunotherapy maintenance in the first line setting, (ii) only as a maintenance following response to first-line chemotherapy or (iii) immunotherapy given as second line treatment following progression;

[0172] 5) Patients with a history of immunotherapy induced colitis;

[0173] 6) Any prior systemic treatment other than 1 line of platinum-containing regimen or immunotherapy as described above;

[0174] 7) Patients with the following CNS metastasis:

[0175] i) Patients who have developed new or progressive brain metastasis following prophylactic and/or therapeutic cranial radiation (whole brain stereotactic radiation).

[0176] ii) Patients with symptomatic CNS metastasis (a patient with brain metastasis who received cranial radiotherapy is eligible if asymptomatic for neurological symptoms for  $\geq 2$  weeks after cranial radiotherapy and is off corticosteroids for treatment of CNS metastasis. Patients with asymptomatic brain metastases are eligible to be enrolled directly to the study).

[0177] iii) Patients with carcinomatous meningitis;

[0178] 8) Unable to discontinue the use of strong CYP3A4 or UGT1A1 inhibitors at least 1 week or strong CYP3A4 inducers at least 2 weeks prior to receiving the first dose of irinotecan liposome injection;

[0179] 9) Presence of another active malignancy; or

[0180] 10) Investigational therapy administered within 4 weeks, or within a time interval less than at least 5 half-lives of the investigational agent, whichever is less, prior to the first scheduled day of dosing in this study.

[0181] Hematologic, Biochemical and Organ Function Exclusion Criteria

[0182] 1) Severe arterial thromboembolic events (e.g. myocardial infarction, unstable angina pectoris, stroke) less than 6 months before inclusion; 2) NYHA Class III or IV congestive heart failure, ventricular arrhythmias, or uncontrolled blood pressure; 3) Active infection (e.g. acute bacterial infection, tuberculosis, active hepatitis B or active HIV) which in the investigator's opinion might compromise the patient's participation in the trial or affect the study outcome; 4) Known hypersensitivity to any of the components of irinotecan liposome injection, other liposomal products, or topotecan; or Clinically significant gastrointestinal disorder including hepatic disorders, bleeding, inflammation, occlusion, or diarrhea > grade 1.

[0183] **Length of Study**

[0184] It is intended that patients will be treated until disease progression or unacceptable toxicity. Following treatment discontinuation, patients will return to the study site for a 30 day follow up visit. After this visit, patients will continue to be followed for overall survival status by phone or a visit to the study site once every month until death or study closure, whichever occurs first.

[0185] **Method of Assigning Patients to Treatment Groups**

[0186] **Part 1a:**

[0187] After all screening assessments have been completed and the first patient reported outcome assessment has been completed, eligible patients will enter Part 1a.

[0188] **Part 1b:**

[0189] Part 1b will be initiated following dose selection in Part 1a.

[0190] After all screening assessments have been completed and the first patient reported outcome assessment has been completed, eligible patients will be randomized using a computerized interactive web response system (IWRS), in a 1:1 ratio, to one of the following treatment arms: Randomization in Part 1b will use a minimization procedure (McEntegart, 2003) accounting for the Part 2 stratification factors.

[0191] **Arm 1a** (experimental arm): irinotecan liposome injection

[0192] **Arm 1b** (control arm): IV topotecan

[0193] Randomization must occur within 7 days of planned dosing.

[0194] **Part 2:**

[0195] Part 2 will be initiated upon passing the stopping criteria and based on the decision of the Sponsor in consultation with the academic steering committee.

[0196] After all screening assessments have been completed and the first patient reported outcome assessment has been completed, eligible patients will be randomized using a computerized interactive web response system (IWRS), in a 1:1 ratio, to one of the following treatment arms:

[0197] **Arm 2a** (experimental arm): irinotecan liposome injection

[0198] **Arm 2b** (control arm): IV topotecan

[0199] Randomization must occur within 7 days of planned dosing. The randomization will be stratified based on the following prognostic factors:

[0200] - Region (North America vs. Asia vs. Other)

[0201] - Platinum sensitivity (sensitive vs. resistant)

[0202] - Disease stage (limited vs. extensive) at diagnosis

[0203] - Performance status (ECOG 0 vs. 1)

[0204] - Prior immunotherapy (yes vs. no)

[0205] Platinum resistant patients are defined as patients with disease that either progressed during first-line platinum containing therapy or within 90 days of its completion. Platinum sensitive patients are defined as patients with disease that progressed after 90 days of completion of first line platinum containing therapy.

[0206] **Administration of Irinotecan Liposome Injection**

[0207] **Part 1a:**

[0208] Irinotecan liposome injection will be administered at a dose of 70 mg/m<sup>2</sup> (strength expressed based on irinotecan free base; approximately equivalent to 80 mg/m<sup>2</sup> of the anhydrous salt) IV over 90 minutes, every 2 weeks in a 6-week cycle. Should the 70 mg/m<sup>2</sup> dose be deemed tolerable and 90 mg/m<sup>2</sup> is explored, irinotecan liposome injection should be administered at 90 mg/m<sup>2</sup> (strength expressed based on irinotecan free base; approximately equivalent to 100 mg/m<sup>2</sup> of the anhydrous salt) IV over 90 minutes, every 2 weeks in a 6-week cycle.

[0209] **Part 1b & 2:**

[0210] Irinotecan liposome injection will be administered at a dose of 90 mg/m<sup>2</sup> (strength expressed based on irinotecan free base; approximately equivalent to 100 mg/m<sup>2</sup> of the anhydrous salt): IV over 90 minutes, every 2 weeks in a 6-week cycle (unless deemed unacceptable in Part 1).

[0211] Prior to administration, the appropriate dose of irinotecan liposome injection must be diluted in 5% Dextrose Injection (D5W) or 0.9% Sodium Chloride Injection to a final volume of 500 mL. Care should be taken not to use any diluents other than D5W or 0.9% sodium chloride.

[0212] **UGT1A1\*28 Monitoring**

[0213] UGT1A1\*28 genotype will be collected on all patients and assessed centrally. Results will be provided to the site and to the Sponsor. Sites will also be asked to include the result from the UGT1A1\*28 genotyping on the SAE reporting form.

[0214] All patients treated with irinotecan liposome injection, regardless of the results of the UGT1A1\*28 genotype, will be treated with the same starting dose of irinotecan liposome injection and will follow the same dose reduction rules. During the regular safety monitoring of patients during the study, as will be conducted by the sponsor medical monitor(s) and by the DMC (in Part 2), the safety and PK of UGT1A1\*28 homozygous patients will be compared to those who are non-homozygous for UGT1A1\*28 to determine whether any different dosing strategy (such as a lower starting dose and/or different dose reduction for irinotecan liposome injection) is required for patients who are homozygous for UGT1A1\*28. The first safety DMC meeting will occur after the 30th patient completed once cycle of treatment or discontinued treatment, whichever occurs first. No association between UGT1A1\*28 and safety is expected in patients treated with topotecan.

[0215] **Study Treatments**

[0216] **Irinotecan liposome injection:**

[0217] **Part 1a: (Safety Run-in)**

[0218] Irinotecan liposome injection 70 mg/m<sup>2</sup> (strength expressed as irinotecan free base; approximately equivalent to 80 mg/m<sup>2</sup> of the anhydrous salt) IV over 90 minutes, every 2 weeks in a 6 week cycle) OR irinotecan liposome injection 90 mg/m<sup>2</sup> (strength expressed as irinotecan free base; approximately equivalent to 100 mg/m<sup>2</sup> of the anhydrous salt) IV over 90 minutes, every 2 weeks in a 6 week cycle.

[0219] **Part 1b and Part 2:**

[0220] **Arm 1a and 2a (Experimental Arm):**

[0221] Irinotecan liposome injection 90 mg/m<sup>2</sup> (strength expressed as irinotecan free base; approximately equivalent to 100 mg/m<sup>2</sup> of the anhydrous salt): IV over 90 minutes, every 2 weeks in a 6 week cycle (unless deemed unacceptable in Part 1).

[0222] **Arm 1b and 2b (Control Arm):**

[0223] Topotecan 1.5 mg/m<sup>2</sup>: IV over 30 minutes daily for 5 consecutive days, every 3 weeks in a 6 week cycle.

[0224] **Irinotecan liposome injection:**

[0225] **Part 1a, Part 1b Arm 1a and Part 2 Arm 2a:**

[0226] Supportive care measures should follow the guidelines outlined in the prescribing information for ONIVYDE®. Up to two dose reductions of irinotecan liposome injection are permitted for toxicities. The use of prophylactic G-CSF (both short and long acting growth factor is acceptable, based on investigator preference) with the second or later doses of irinotecan liposome injection is allowed, based on investigator judgment.

[0227] **Topotecan:**

[0228] **Part 1b Arm 1b and Part 2 Arm 2b (IV Topotecan)**

[0229] The intended dose for topotecan is 1.5 mg/m<sup>2</sup> IV for 5 consecutive days every 3 weeks. The dose, administration and dose reductions should follow the guidance as outlined in the prescribing information for IV topotecan.

[0230] Patients randomized to treatment with topotecan should be considered for prophylactic G-CSF in all cycles starting 24 hours following the last dose (both short and long acting growth factor is acceptable, based on investigator preference). Up to two dose reductions of topotecan per patient are permitted for toxicities. Dose delays are permitted to allow recovery from treatment-associated toxicities. Prophylactic antibiotics are recommended for patients at high risk of infectious complications.

[0231] **Investigational Product:**

[0232] Irinotecan liposome injection (also known as nal-IRI, pegylated liposomal irinotecan hydrochloride trihydrate, MM-398, PEP02, BAX2398 and ONIVYDE®) is a sterile, white to slightly yellow opaque isotonic liposomal dispersion. Each 10 mL single-dose vial contains 43 mg irinotecan free base at a concentration of 4.3 mg/mL. The liposome is a unilamellar lipid bilayer vesicle, approximately 110 nm in diameter, which encapsulates an aqueous space containing irinotecan in a gelated or precipitated state as the sucrose octasulfate salt. It will be supplied as sterile, single-use vials containing 43 mg irinotecan free base at a concentration of 4.3 mg/mL. Irinotecan liposome injection must be stored refrigerated (2 to 8°C, 36 to 46°F) with protection from light. Do not freeze.

[0233] **Part 1a**

[0234] A dose will be decided to be acceptable for proceeding to Part 1b if the number of patients with DLTs does not exceed 1 in a cohort of 6 patients. Based on this rule, the

probabilities to proceed to Part 1b at a dose as a function of true DLT probability rate are shown in Table 6.

Table 6

True rate of unacceptable Toxicity	Probability to advance to randomization
0.05	0.97
0.10	0.89
0.15	0.77
0.20	0.65
0.25	0.53
0.30	0.42
0.35	0.32
0.40	0.23

[0235] **Part 1b**

[0236] The purpose of Part 1b is to provide a pilot sample of safety and efficacy data in a randomized setting. The sample size for Part 1b was selected for practical purposes to enable curtailment of the study if irinotecan liposome injection is observed to be substantially inferior to topotecan with regard to benefit/risk.

[0237] An efficacy rule, based on the observed PFS rate at 12 weeks, is implemented in this protocol as a formal stopping rule, while additional data will also be considered and may also result in a decision to not proceed to Part 2. The operating characteristics of the formal stopping rule, given the study design in Part 1b, are described below.

[0238] Using a binomial distribution to approximate and assuming the true proportion of progression-free patients at 12 weeks within the control group is 0.55, the probability that the study would be stopped, as a function of the true rate for the irinotecan liposome injection arm, is shown in Table 7.

Table 7

<b>Irinotecan liposome injection PFS rate at 12 weeks</b>	<b>Absolute <math>\Delta</math> to control</b>	<b>Probability stop given rules</b>
0.75	0.20	0.002



0.70	0.15	0.011
0.65	0.10	0.038
0.60	0.05	0.101
0.55	0	0.211
0.50	-0.05	0.363
0.45	-0.10	0.536
0.40	-0.15	0.698
0.35	-0.20	0.827

[0239] A final treatment comparison of PFS will be carried out via a log-rank test when tumor assessments have been completed for all patients in Part 1b. If the censoring rate is assumed to be 10%, it is expected that 45 events would have occurred at the time of the final analysis. If the PFS hazard ratio is 0.64 (e.g. irinotecan liposome injection extends median PFS from 3.5 to 5.5 months), then this analysis would have approximate 75% power to detect the treatment difference with a one-sided level 0.20 test.

[0240] **Part 2**

[0241] The primary endpoint is overall survival (OS).

[0242] A total of 420 patients will be randomized in a 1:1 ratio to the two treatment arms. Follow-up until at least 333 OS events are observed across the two treatment arms provides at least 85% power to detect a true hazard ratio of  $HR \leq 0.714$  (mOS: 7.5 v 10.5 months) using a stratified log-rank test (stratified by region (North America vs. Asia vs. Other) and platinum sensitivity (sensitive vs. resistant)) with overall 1-sided significance level of 0.025 (adjusted for interim analyses).

[0243] Assuming enrollment over 25 months with a ramp-up to 21 patients per month and lost-to-follow-up rate of 5% across both treatment arms, the timing of the primary analysis is expected to be at 39 months.

[0244] An interim analysis for futility will be conducted when approximately 30% of the planned final number of OS events (i.e., 100 of 333 OS events) has been observed in the intent-to-treat (ITT) population. In the event that the study proceeds, a second interim analysis will occur to evaluate both futility and efficacy when approximately 210 OS events (63% of planned OS events and 50% of expected events in the entire study population) have occurred.

[0245] **General:**

[0246] Categorical variables will be summarized by frequency distributions (number and percentages of patients) and continuous variables will be summarized by descriptive statistics (mean, standard deviation, median, minimum, maximum).

[0247] The efficacy and safety of nal-IRI in Part 1 will be reported descriptively using the same outcome measures as in Part 2. In addition, adverse events occurring in Part 1 of the study will be described in detail.

[0248] Patients enrolled and treated with study drug in Part 1 will comprise the Part 1 safety population. The safety and efficacy of these patients will be presented descriptively.

[0249] Patients randomized in Part 2 will comprise the intent-to-treat (ITT) population. This will be the population that is evaluated in comparison to evaluate the efficacy of the experimental arm. In the ITT analyses of efficacy, each patient will be considered according to the randomized treatment assignment. Patients who received any part of any study drug will define the Part 2 safety population.

[0250] For stratified analyses, stratification factors will be the randomization stratification factors of region (North America, Asia, Other) and platinum sensitivity (sensitive, resistant). Classification of stratification factors will be according to the randomization.

[0251] **Primary Efficacy Analysis (Part 2):**

[0252] OS is defined as the number of months from the date of randomization to the date of death. Patients without observed death at the time of the primary analysis will have OS censored according to the last recorded date alive.

[0253] The primary analysis will be performed using a stratified log-rank test comparing the OS difference between two treatment arms with 1-sided level of significance at 0.025. Stratification factors will include the randomization stratification factors and classification will be according to the randomization. Kaplan-Meier methods will be used to estimate median OS (with 95% confidence intervals) and to display OS time graphically. A stratified Cox proportional hazards model will be used to estimate hazard ratio and its corresponding 95% confidence interval. Sensitivity analyses for OS will be described in the Statistical Analysis Plan (SAP).

[0254] **Key Secondary Analyses (Part 2):**

[0255] Key secondary endpoints are PFS, ORR, proportion of patients with symptom improvement in dyspnea, in cough, and in fatigue.

[0256] Key secondary endpoints will be tested no more than once. If the primary endpoint of OS is statistically significant at the interim, testing of secondary endpoints will be tested at the interim. Otherwise secondary endpoints will be tested at the final OS analysis if OS is found to be statistically significant at that analysis. Hypothesis testing of key secondary endpoints will be conducted in a stage wise hierarchical manner (Glimm, E, et al., *Statistics in Medicine* 2010 29:219-228).

[0257] The nominal level for comparison of PFS will depend on whether the test is performed at the interim or at the planned final analysis and will incorporate an  $\alpha$ -spending function similar to that used for OS. If OS and PFS are both significant, then ORR and EORTC-QLQ symptoms will be tested at 1-sided 0.025 level (nominal  $\alpha$  adjusted based on spending function, as described for PFS) with each p-value adjusted using the Benjamini-Hochberg correction (Benjamini & Hochberg, *J. Royal Statistical Soc. B* 2005 57, 289-300) for one-sided  $\alpha$  level testing of 4 planned comparisons. Adjusted p-values will be reported, using SAS PROC MULTTEST with FDR option or equivalent algorithm. Any parameter which is not statistically significant will be regarded as descriptive and exploratory.

[0258] **Progression-free survival:**

[0259] Progression-free survival is the time from randomization to the first documented objective disease progression (PD) using RECIST v1.1 or death due to any cause, whichever occurs first. Determination of PFS will be per investigator assessment. If neither death nor progression is observed, data will be censored on the date of the last observed tumor assessment date. Patients without a valid tumor response evaluation at randomization will be censored on the date of randomization. Patients starting a new anti-cancer treatment prior to documented PD will be censored at the date of the last observed tumor assessment prior to start of the new treatment. Patients with documented PD or death after an unacceptable long interval (i.e., 2 or more missed or indeterminate scheduled assessments) will be censored at the time of the last observed non-PD tumor assessment date prior to progression or death.

[0260] The difference in PFS between treatments will be evaluated using a stratified log-rank test. Kaplan-Meier methods will be used to estimate median PFS (with 95% confidence intervals) and to display PFS time graphically. A stratified Cox proportional hazards model will be used to estimate the PFS hazard ratio and its corresponding 95% confidence interval.

[0261] The difference in PFS between treatments will be evaluated using a stratified log-rank test (stratified by region and platinum sensitivity). Kaplan-Meier methods will be used to estimate median PFS (with 95% confidence intervals) and to display PFS time graphically. A stratified Cox proportional hazards model will be used to estimate the PFS hazard ratio and

its corresponding 95% confidence interval. Sensitivity analyses for PFS will be described in the SAP.

[0262] **Objective Response:**

[0263] Objective response rate (ORR) is the proportion of patients who achieve partial response or complete response according to RECIST v1.1 guidelines. An estimate of the ORR and its 95% CI will be calculated. The difference in ORR between treatment groups will be compared using Cochran-Mantel-Haenszel method, stratified by region and platinum sensitivity.

[0264] Proportion of patients with improvement of lung cancer symptoms:

[0265] This secondary analysis will consider the patient-reported EORTC-QLQ-LC13 symptom scales for cough, dyspnea, and fatigue, as these are considered most clearly to be disease-related and evaluable for treatment impact with regard to the proportion of patients with improvement. The remaining EORTC-QLQ symptom domains will be assessed in exploratory analyses.

[0266] Symptom improvement is defined as achievement and 6-week maintenance of symptom subscale scores at least 10 percentage points of scale (following transformation to 0-100 scale) below baseline. Response classifications will be tabulated by treatment group and statistical analyses will compare the proportions of responders for a given symptom.

[0267] For each symptom, the proportion of patients with improvement will be tabulated by treatment group with 95% confidence intervals based on a Normal approximation. The difference in the proportion of patients with symptom improvement will be presented with corresponding 95% confidence intervals. The proportion of patients with improvement in a symptom will be compared between treatment regimens using Cochran-Mantel-Haenszel method, stratified by region and platinum sensitivity.

[0268] **Safety Analysis:**

[0269] Safety analyses (adverse events and laboratory analyses) will be performed using the safety population, defined as all patients receiving any study drug. Treatment assignment will be according to actual treatment received. Adverse events will be coded using the latest MedDRA dictionary. Severity will be graded according to the NCI CTCAE version 4.03.

[0270] Treatment-emergent adverse events (TEAEs) are defined as any adverse events reported from the date of first study drug exposure to 30 days after the last date of study drug exposure. Frequency and percentages of patients will be summarized for: any grade TEAE, grade 3 or higher TEAE, study-drug related TEAE, serious TEAE, TEAE leading to dose modification, and TEAE leading to study drug discontinuation. Adverse events will be

summarized by System Organ Class and preferred term. All adverse event data will be listed by patient.

[0271] Laboratory data will be summarized according to parameter type. Where applicable, toxicity grading for laboratory safety parameters will be assigned based on NCI CTCAE version 4.03 criteria.

[0272] **QTcF Analyses:**

The potential of QTcF prolongation with irinotecan liposome injection treatment will be evaluated in patients receiving irinotecan liposome injection in Part 1 of this study. For the primary QTcF prolongation analysis, the predicted changes in QTcF will be obtained from the exposure-QTcF relationship using mixed-effect modeling. Sensitivity analyses will be conducted by evaluating by time point and categorical analyses.

[0273] **EORTC-QLQ outcomes**

[0274] Analysis of the EORTC-QLQ-C30 questionnaires will be performed in accordance with the EORTC guidelines (Fayers, 2001). The subscales of the EORTC QLQ-C30 and the QLQ-LC13 will be scored based on the EORTC scoring manual. Scores will be standardized such that higher scores on the EORTC QLQ-C30 or the QLQ-LC13 will represent higher (“better”) levels of functioning and/or a higher (“worse”) level of symptoms.

[0275] Analysis methods for the proportion of patients with symptom improvement are as described in Key Secondary Analysis (section 11.5.2.3).

[0276] Frequency tables by treatment group will be reported for the proportion of patients with symptom improvement for each QLQ-C30 and QLQ-LC13 subscale. Details of additional EORTC-QLQ analyses will be provided in the Statistical Analysis Plan.

[0277] Raw standardized subscale scores and changes from baseline in over time will be reported. Mean change scores will be compared between treatment groups descriptively and may be explored via longitudinal modeling (i.e., covariate analysis and repeated measures modeling)

[0278] **EQ-5D-5L:**

[0279] Raw score and change from baseline in over time will be reported. Mean change scores will be compared between treatment groups descriptively and explored via longitudinal modeling (i.e., covariate analysis and repeated measures modeling).

[0280] **Time to CNS progression:**

[0281] Is defined as time from randomization to development of CNS progression as defined by the RANO-BM working group (Lin et al Lancet Oncology 2015). Time to CNS

progression will be described by Kaplan-Meier methods and treatments will be compared using stratified log-rank test.

[0282] **Pharmacokinetics (PK) and Pharmacodynamics (PD) Analysis:**

[0283] Plasma pharmacokinetics (PK) of total irinotecan, SN-38, and topotecan will be quantified from the concentration samples using nonlinear mixed effect modeling. The initial PK analysis will use the empirical Bayesian estimation, however, additional covariate analyses will be performed to evaluate alternative baseline factors specific to SCLC. The resulting PK estimates will be used to evaluate the association between PK and PD (efficacy and safety endpoints). Topotecan PK will be used to provide additional data to understand the results from Part 1b, by comparing the distribution and the association of PK to efficacy/safety in this study to historical values.

[0284] **Dose Modifications**

[0285] All dose modifications should be based on worst preceding toxicity.

[0286] Table 8: Recommended Dose Modifications for Irinotecan Liposome Injection

Toxicity NCI CTCAE v4.03 Grade <sup>b</sup>	Occurrence	Starting Dose	
		70 mg/m <sup>2</sup>	90 mg/m <sup>2</sup>
<b>Neutropenia, leukopenia, or thrombocytopenia Grade 3 or 4</b> <b>Neutropenic fever</b>	First occurrence	50 mg/m <sup>2</sup>	70 mg/m <sup>2</sup>
	Second occurrence	43 mg/m <sup>2</sup>	50 mg/m <sup>2</sup>
	Third occurrence	Discontinue treatment	
<ul style="list-style-type: none"> <li>• A new cycle of therapy should not begin until the absolute neutrophil count is <math>\geq 1500/\text{mm}^3</math> (<math>1.5 \times 10^9/\text{L}</math>)</li> <li>• A new cycle of therapy should not begin until the platelet count is <math>\geq 100,000/\text{mm}^3</math> (<math>100 \times 10^9/\text{L}</math>)</li> </ul>			
<b>Nonhematological toxicities:</b>			
<b>All nonhematological toxicities (except asthenia and anorexia):</b> <b>Grade 3 or 4</b>	Withhold ONIVYDE. Initiate loperamide for late onset diarrhea of any severity. Administer intravenous or subcutaneous atropine 0.25 to 1 mg (unless clinically contraindicated) for early onset diarrhea of any severity. Upon recovery to < Grade 1, resume ONIVYDE as below:		
	First occurrence	50 mg/m <sup>2</sup>	70 mg/m <sup>2</sup>
	Second occurrence	43 mg/m <sup>2</sup>	50 mg/m <sup>2</sup>
	Third occurrence	Discontinue treatment	

<ul style="list-style-type: none"> <li>• A new cycle of therapy should not begin until serum chemistry parameters resolve to <math>\leq</math> Grade 1</li> <li>• A new cycle of therapy should not begin until nonhematological toxicities resolve to <math>\leq</math> Grade 1</li> <li>• For Grade <math>\geq</math> 3 nausea and vomiting, reduce dose only if occur despite optimal anti-emetic therapy</li> <li>• Asthenia and Grade 3 anorexia do not require any dose modifications</li> </ul>		
<b>Interstitial lung disease</b>	<b>First occurrence</b>	Discontinue treatment
<b>Severe hypersensitivity reaction</b>	<b>First occurrence</b>	Discontinue treatment

<sup>a</sup> All doses mentioned are based on irinotecan free base

<sup>b</sup> National Cancer Institute Common Terminology Criteria for Adverse Events, version 4.03

[0287] Topotecan for Injection

[0288] Topotecan should only be started in patients with a baseline neutrophil count of greater than or equal to 1,500/mm<sup>3</sup> (1.5x10<sup>9</sup>/L) and a platelet count greater than or equal to 100,000/mm<sup>3</sup> (100x10<sup>9</sup>/L).

[0289] Topotecan should not be administered in subsequent cycles unless the neutrophil count is  $\geq 1 \times 10^9/l$ , the platelet count is  $\geq 100 \times 10^9/l$ , and the hemoglobin level is  $\geq 9$  g/dl (after transfusion if necessary). Treatment should be delayed to allow sufficient time for recovery and upon recovery, treatment should be administered according to the guidelines in Table 9 below.

[0290] Dose reduction of topotecan should occur in case of the following toxicities:

[0291] - Grade 4 neutropenia (ANC < 500/mm<sup>3</sup> or <0.5x10<sup>9</sup>/L);

[0292] - Grade 4 thrombocytopenia (platelet count <25,000/mm<sup>3</sup> or <0.5x10<sup>9</sup>/L)

[0293] - Grade 3 or 4 non-hematological toxicity except nausea and vomiting. In case of nausea and vomiting, dose reduction should occur if Grade 3 or 4 toxicity occurs despite optimal medical management

[0294] Dose reduction decisions should be based on worst preceding toxicity. Moving from dose level 0 to dose level 2 is permitted. Prophylactic antibiotics are recommended for patients at high risk of infectious complications.

[0295] Up to two dose reductions of topotecan per patient are permitted for toxicities as shown in Table 9. If a third dose reduction is needed to manage a toxicity, topotecan treatment should be discontinued.

**Table 9: Recommended topotecan Dose Modification Scheme for Subsequent Cycles**

Dose Level	Dose Modifications
0	1.5 mg/m <sup>2</sup> IV days 1-5
-1	1.25 mg/m <sup>2</sup> IV days 1-5
-2	1.0 mg/m <sup>2</sup> IV days 1-5

[0296] The dose of topotecan in patients should be reduced to 0.75 mg/m<sup>2</sup>/day for five consecutive days if the creatinine clearance is between 20 and 39 mL/min.

[0297] Topotecan should be discontinued if a new diagnosis of interstitial lung disease is confirmed.

[0298] **Example 8:** Liposomal irinotecan manufacturing

[0299] The liposomal irinotecans can be prepared in a multi-step process. First, lipids are dissolved in heated ethanol. The lipids can include DSPC, cholesterol and MPEG-2000-DSPE combined in a 3:2:0.015 molar ratio. Preferably, the liposomes can encapsulate irinotecan sucrose octasulfate (SOS) encapsulated in a vesicle consisting of DSPC, cholesterol and MPEG-2000-DSPE combined in a 3:2:0.015 molar ratio. The resulting ethanol-lipid solution is dispersed in an aqueous medium containing substituted amine and polyanion under conditions effective to form a properly sized (e.g. 80-120 nm) essentially unilamellar liposome containing the substituted amine (in the ammonium form) and polyanion encapsulated within a vesicle formed from the dissolved lipids. The dispersing can be performed, e.g., by mixing the ethanolic lipid solution with the aqueous solution containing a substituted amine and polyanion at the temperature above the lipid transition temperature, e.g., 60-70 °C, and extruding the resulting hydrated lipid suspension (multilamellar liposomes) under pressure through one or more track-etched, e.g. polycarbonate, membrane filters with defined pore size, e.g. 50 nm, 80 nm, 100 nm, or 200 nm. The substituted amine can be triethylamine (TEA) and the polyanion can be sucrose octasulfate (SOS) combined in a stoichiometric ratio (e.g., TEA8SOS) at a concentration of about 0.4-0.5N. All or substantially all non-entrapped TEA or SOS is then removed (e.g., by gel-filtration, dialysis or ultrafiltration) prior to contacting the liposome with irinotecan under conditions effective to allow the irinotecan to enter the liposome in exchange with TEA leaving the liposome. The conditions can include one or more conditions selected from the group consisting of: addition of the osmotic agent (e.g., 5% dextrose) to the liposome external medium to balance the osmolality of the entrapped TEA-SOS solution and/or



prevent osmotic rupture of the liposomes during the loading, adjustment and/or selection of the pH (e.g. to 6.5) to reduce the drug and/or lipid degradation during the loading step, and increase of the temperature above the transition temperature of the liposome lipids (e.g., to 60-70 °C) to accelerate the transmembrane exchange of TEA and irinotecan. The loading of irinotecan by exchange with TEA across the liposome preferably continues until all or substantially all of the TEA is removed from the liposome, thereby exhausting its concentration gradient across the liposome. Preferably, the irinotecan liposome loading process continues until the gram-equivalent ratio of irinotecan to sucrooctasulfate is at least 0.9, at least 0.95, 0.98, 0.99 or 1.0 (or ranges from about 0.9-1.0, 0.95-1.0, 0.98-1.0 or 0.99-1.0). Preferably, the irinotecan liposome loading process continues until the TEA is at least 90%, at least 95%, at least 98%, at least 99% or more of the TEA is removed from the liposome interior. The irinotecan can form irinotecan sucrosofate within the liposome, such as irinotecan and sucrose octasulfate in a molar ratio of about 8:1. Next, any remaining extra-liposomal irinotecan and TEA is removed to obtain the irinotecan liposome using, e.g., gel (size exclusion) chromatography, dialysis, ion exchange, or ultrafiltration methods. The liposome external medium is replaced with injectable, pharmacologically acceptable fluid, e.g., buffered isotonic saline. Finally, the liposome composition is sterilized, e.g., by 0.2-micron filtration, dispensed into dose vials, labeled and stored, e.g., upon refrigeration at 2-8 °C, until use. The liposome external medium can be replaced with pharmacologically acceptable fluid at the same time as the remaining extra-liposomal irinotecan and TEA is removed. The extra-liposomal pH of the composition can be adjusted or otherwise selected to provide a desired storage stability property (e.g., to reduce formation of the lyso-PC within the liposome during storage at 4 °C over 180 days), for example by preparing the composition at a pH of about 6.5-8.0, or any suitable pH value there between (including, e.g., 7.0-8.0, and 7.25). Irinotecan liposomes with the extra-liposomal pH values, irinotecan free base concentration (mg/mL) and various concentrations of sucrose octasulfate can be prepared as provided in more detail as described herein.

[0300] DSPC, cholesterol (Chol), and PEG-DSPE were weighed out in amounts that corresponded to a 3:2:0.015 molar ratio, respectively (e.g., 1264 mg/412.5 mg/22.44 mg). The lipids were dissolved in chloroform/methanol (4/1 v/v), mixed thoroughly, and divided into 4 aliquots (A-D). Each sample was evaporated to dryness using a rotary evaporator at 60 °C. Residual chloroform was removed from the lipids by placing under vacuum (180 μtorr) at room temperature for 12 h. The dried lipids were dissolved in ethanol at 60°C, and pre-warmed TEA8SOS of appropriate concentration was added so that the final alcohol content

was 10% (v/v). The lipid concentration was 75 mM. The lipid dispersion was extruded at about 65°C through 2 stacked 0.1 µm polycarbonate membranes (Nucleopore) 10 times using Lipex thermobarrel extruder (Northern Lipids, Canada), to produce liposomes with a typical average diameter of 95-115 nm (determined by quasielastic light scattering). The pH of the extruded liposomes was adjusted with 1 N NaOH to pH 6.5 as necessary. The liposomes were purified by a combination of ion-exchange chromatography and size-exclusion chromatography. First, Dowex™ IRA 910 resin was treated with 1 N NaOH, followed by 3 washes with deionized water and then followed by 3 washes of 3 N HCl, and then multiple washes with water. The liposomes were passed through the prepared resin, and the conductivity of the eluted fractions was measured by using a flow-cell conductivity meter (Pharmacia, Upsalla, Sweden). The fractions were deemed acceptable for further purification if the conductivity was less than 15 µS/cm. The liposome eluate was then applied to a Sephadex G-75 (Pharmacia) column equilibrated with deionized water, and the collected liposome fraction was measured for conductivity (typically less than 1 µS/cm). Cross-membrane isotonicity was achieved by addition of 40% dextrose solution to a final concentration of 5% (w/w) and the buffer (Hepes) added from a stock solution (0.5 M, pH 6.5) to a final concentration of 10 mM.

[0301] A stock solution of irinotecan was prepared by dissolving irinotecan•HCl trihydrate powder in deionized water to 15 mg/mL of anhydrous irinotecan-HCl, taking into account water content and levels of impurities obtained from the certificate of analysis of each batch. Drug loading was initiated by adding irinotecan at 500g/mol liposome phospholipid and heating to  $60 \pm 0.1$  °C for 30 min in a hot water bath. The solutions were rapidly cooled upon removal from the water bath by immersing in ice cold water. Extraliposomal drug was removed by size exclusion chromatography, using Sephadex G75 columns equilibrated and eluted with Hepes buffered saline (10 mM Hepes, 145 mM NaCl, pH 6.5). The samples were analyzed for irinotecan by HPLC and phosphate by the method of Bartlett (see Phosphate Determination). For storage, the samples were divided into 4 mL aliquots and the pH was adjusted as indicated in the Results using 1 N HCl or 1 N NaOH, sterile filtered under aseptic conditions, and filled into sterile clear glass vials that were sealed under argon with a Teflon® lined threaded cap and placed in a thermostatically controlled refrigerator at 4 °C. At defined time points, an aliquot was removed from each sample and tested for appearance, size, drug/lipid ratio, and drug and lipid chemical stability. The liposome size was determined in the diluted samples by dynamic light scattering using

Coulter Nano-Sizer at 90 degree angle, and presented as Mean  $\pm$  Standard deviation (nm) obtained by the method of cumulants.

[0302] **Example 9:** ONIVYDE (MM-398) Liposomal Irinotecan

[0303] One preferred example of a storage stable liposomal irinotecan described herein is the product that will be marketed as ONIVYDE (irinotecan liposome injection). ONIVYDE is a topoisomerase inhibitor, formulated with irinotecan hydrochloride trihydrate into a liposomal dispersion, for intravenous use. ONIVYDE indicated for the treatment of metastatic adenocarcinoma of the pancreas after disease progression following gemcitabine-based therapy.

[0304] ONIVYDE is a storage stabilized liposome having a pH of about 7.25. The ONIVYDE product contains irinotecan sucrosfate encapsulated in a liposome, obtained from an irinotecan hydrochloride trihydrate starting material. The chemical name of irinotecan is (S)-4,11-diethyl-3,4,12,14-tetrahydro-4-hydroxy-3,14-dioxo1H-pyrano[3',4':6,7]-indolizino[1,2-b]quinolin-9-yl-[1,4'bipiperidine]-1'-carboxylate. The dosage of ONIVYDE can be calculated based on the equivalent amount of irinotecan trihydrate hydrochloride starting material used to prepare the irinotecan liposomes, or based on the amount of irinotecan in the liposome. There are about 866 mg of irinotecan per gram of irinotecan trihydrate hydrochloride. For example, an ONIVYDE dose of 80 mg based on the amount of irinotecan hydrochloride trihydrate starting material actually contains about  $0.866 \times (80 \text{ mg})$  of irinotecan free base in the final product (i.e., a dose of  $80 \text{ mg/m}^2$  of ONIVYDE based on the weight of irinotecan hydrochloride starting material is equivalent to about  $70 \text{ mg/m}^2$  of irinotecan free base in the final product). ONIVYDE is a sterile, white to slightly yellow opaque isotonic liposomal dispersion. Each 10 mL single-dose vial contains 43 mg irinotecan free base at a concentration of 4.3 mg/mL. The liposome is a unilamellar lipid bilayer vesicle, approximately 110 nm in diameter, which encapsulates an aqueous space containing irinotecan in a gelated or precipitated state as the sucrose octasulfate salt. The vesicle is composed of 1,2-distearoyl-sn-glycero-3-phosphocholine (DSPC) 6.81 mg/mL, cholesterol 2.22 mg/mL, and methoxy-terminated polyethylene glycol (MW 2000)-distearoylphosphatidyl ethanolamine (MPEG-2000-DSPE) 0.12 mg/mL. Each mL also contains 2-[4-(2-hydroxyethyl) piperazin-1-yl]ethanesulfonic acid (HEPES) as a buffer 4.05 mg/mL and sodium chloride as an isotonicity reagent 8.42 mg/mL. Each vial of ONIVYDE contains 43 mg/10 mL irinotecan free base as a white to slightly yellow, opaque, liposomal dispersion in a single-dose vial.

[0305] In one example, an ONIVYDE unit dosage form is a pharmaceutical composition comprising an amount of irinotecan encapsulated liposomes that provide a total amount of about  $90 \text{ mg/m}^2$  of irinotecan free base, or an amount of irinotecan equivalent to  $100 \text{ mg/m}^2$  irinotecan hydrochloride trihydrate. The unit dosage form can be an intravenous formulation obtained by diluting a unit dosage form (e.g., a vial) at a concentration of about  $4.3 \text{ mg irinotecan free base/mL}$  injectable fluid into a total volume of about  $500 \text{ mL}$ . ONIVYDE is prepared for administering by diluting the isotonic liposomal dispersion from the vial as follows: withdraw the calculated volume of ONIVYDE from the vial. ONIVYDE is diluted into  $500 \text{ mL}$  5% Dextrose Injection, USP or 0.9% Sodium Chloride Injection, USP and mix diluted solution by gentle inversion; protect diluted solution from light and administer diluted solution within 4 hours of preparation when stored at room temperature or within 24 hours of preparation when stored under refrigerated conditions [ $2^\circ\text{C}$  to  $8^\circ\text{C}$  ( $36^\circ\text{F}$  to  $46^\circ\text{F}$ )].

[0306] **Example 10:** The ability of Nal-IRI to deliver irinotecan and SN-38 to tumors was evaluated in SCLC cell-line derived xenograft (CDX) models (NCI-H1048, DMS-114, H841) in comparison to patient-derived xenograft (PDX) models (CRC, SCLC and pancreatic). Irinotecan liposome injection was administered intravenously to mice bearing xenograft tumors. At 24 hours post administration, mice were sacrificed and tumors were harvested. Irinotecan and SN-38 in tumors were measured by high performance liquid chromatography (HPLC). Data were normalized to injected dose per tumor weight. Figure 7A shows the increased tumor SN-38 levels were associated with increased tumor deposition, as assessed by tumor CPT-11 at 24 hours post administration in SCLC mouse xenograft models (H841, H1048 and DMS-53). Figure 7B shows the carboxylesterase (CES) activity in CRC, SCLC, and pancreatic PDX tumors showing that SCLC PDX tumors have CES activity comparable to other indications in which irinotecan is active. Treatment with SN-38 decreased cell viability by  $> 90\%$  in SCLC cell lines (DMS114, NCI-H1048). As shown in Figure 7C (for NCI-H1048 cells) effective cell growth inhibition was observed between  $1\text{-}10 \text{ nM}$ , with increased cell killing with increased time of exposure over a time-course of up to 88 hours. The concentration range of SN-38 in which cell killing begins to occur coincides with the amount of SN-38 measured from tumor biopsies taken from patients with various solid tumors 72 hours after administration of irinotecan liposome injection (range:  $3\text{-}163 \text{ nM}$ ; Ramanathan et al., Eur. J. Cancer, 2014 Nov; 50:87) is overlaid on the time-dependent SN-38 growth inhibition curves (shown in the area within the dashed lines). Similar effects were seen in DMS-114 cells. Cell growth inhibition kinetics of SN-38 in the cell lines was determined using IncuCyte® ZOOM System. Figure 7D is a graph showing cell sensitivity;

cytotoxicity of Topo1 inhibitors increases with exposure. Figure 7E is a chart showing that topotecan administration is severely limited by toxicity, thus limiting sustained inhibition of topo1 in comparison to Onivyde mediated prolonged SN-38 exposure.

[0307] **Example 11.** Preclinical Support for Evaluation of irinotecan liposome injection (nal-IRI, MM-398) in Patients with Small Cell Lung Cancer

[0308] Anti-tumor activity of nal-IRI as a monotherapy was evaluated in DMS-53 and NCI-H1048 xenograft models. Cells were implanted subcutaneously into right flanks of NOD-SCID mice; treatments were initiated when tumors had reached approximately 280 mm<sup>3</sup>. Nal-IRI was dosed at 16 mg/kg salt, q1w, which is equivalent to a proposed clinical dose of 90 mg/m<sup>2</sup> free base, q2w. Topotecan was dosed at 0.83 mg/kg/week, Day 1-2 every 7 days, which approximates a clinical dose intensity of 1.5 mg/m<sup>2</sup> (Day 1-5 every 21 days). Tumor metabolite levels of nal-IRI and non-liposomal irinotecan were measured at 24 hours post-injection, using previously established high performance liquid chromatography methods. The results for the monotherapy treatment in DMS-53 are shown in Figure 8A and the results in NCI-H1048 are shown in Figure 8B. In Figures 8A and 8B the vertical dotted lines indicate days of dosing and the response rates are determined based on tumor volume change from base line: CR: change in tumor volume (TV) < -95%; PR: -95% ≤ change in TV < -30%; SD: -30% ≤ change in TV < 30%; PD: change in TV ≥ 30%. Nal-IRI displayed significantly greater anti-tumor activity than topotecan based on tumor growth kinetics and overall survival. Furthermore, 7 out of 7 mice in NCI-H1048 model treated with nal-IRI experienced complete tumor regressions after 4 cycles of treatment and maintained for at least 50 days after last dose, compared to 0 out of 7 mice treated with topotecan.

[0309] Carboxylesterase activity and sensitivity to SN-38 in SCLC models were comparable to that in indications where nal-IRI or irinotecan HCl has proven to be efficacious clinically (e.g. pancreatic cancer, colorectal cancer). Nal-IRI was found to deliver irinotecan to tumors in SCLC tumors to a similar or greater extent than other tumor types. The tumor irinotecan and SN-38 levels of nal-IRI (16 mg/kg salt) were 12 to 57-fold and 5 to 20-fold higher than nonliposomal irinotecan (30 mg/kg salt), respectively. Nal-IRI demonstrated anti-tumor activity in both xenograft models of SCLC at clinically relevant dose levels, and resulted in complete or partial responses after 4 cycles of treatment, compared to topotecan which have limited tumor growth control.

[0310] The anti-tumor activity of MM-398 (Onivyde) in the H841 rat orthotopic xenograft model of SCLC is shown in Figure 8C which is a graph showing the percent survival of rats treated with control, Onivyde (30 or 50 mg/kg salt), irinotecan (25 mg/kg) or

topotecan (4 mg/kg) for days post inoculation. Rats treated with Onivyde at both 30 and 50 mg/kg showed longer survival times than those treated with control, irinotecan or topotecan. MM-398 has anti-tumor activity in multiple SCLC xenograft models. At clinically relevant doses (16 mg/kg/wk MM-398, 0.8 mg/kg/wk topotecan), MM-398 had greater anti-tumor activity and prolonged survival than topotecan.

[0311] These studies demonstrated that nal-IRI is more active than topotecan at clinically relevant doses in SCLC preclinical models, and thus support a proposed randomized Phase 3 trial of nal-IRI versus topotecan in patients with SCLC that have progressed on prior platinum-based therapy.

[0312] **Example 12**

[0313] Tumor metabolites levels of nal-IRI were compared to non-liposomal irinotecan in SCLC tumor bearing xenograft models DMS-53 and NCI-H1048 (Figures 9A and 9B). Based on body-surface area dosing and scaled to body weight, the clinically-relevant doses of nal-IRI and non-liposomal irinotecan HCl in mice are approximately 16 mg/kg (salt) and 30 mg/kg (salt), respectively. Nal-IRI dosed at 16 mg/kg salt (q1w) is equivalent to a proposed clinical dose of 90 mg/m<sup>2</sup> free base, q2w. Irinotecan HCl dosed at 30 mg/kg, q1w, approximates a clinical dose intensity of 300 mg/m<sup>2</sup>, q3w, which resulted in similar efficacy as topotecan (current standard of care) in second-line SCLC patients (Zhao ML, Bi Q, Ren HX, Tian Q, Bao ML. Clinical observation of irinotecan or topotecan as second-line chemotherapy on treating 43 patients with small-cell lung cancer. *Chin Oncol.* 2011;21:156–158).

[0314] Using high performance liquid chromatography methods, tumor levels of CPT-11 (Figure 9A) and the active metabolites SN-38 (Figure 9B) were measured at 24 hours post-injection (intravenous via tail vein). In both SCLC models, nal-IRI delivered irinotecan to tumors to a greater extent than non-liposomal irinotecan HCl. The tumor CPT-11 and SN-38 levels of nal-IRI (16 mg/kg salt) were 12 to 57-fold and 5 to 20-fold higher than non-liposomal irinotecan (30 mg/kg salt), respectively. The increased tumor CPT-11 and SN-38 delivered by nal-IRI is attributed to the extended circulation as a result of liposomal encapsulation, as well as local activation of liposomal-irinotecan in the tumors (PMID 25273092: Preclinical activity of nanoliposomal irinotecan is governed by tumor deposition and intratumor prodrug conversion. Kalra AV1, Kim J1, Klinz SG1, Paz N1, Cain J1, Drummond DC1, Nielsen UB1, Fitzgerald JB)

[0315]

[0316] **Example 13:** Irinotecan Liposome Injection-mediated Tumor Delivery of Irinotecan and SN-38 *In Vivo*

[0317] The ability of MM-398 to deliver irinotecan and SN-38 to tumors was evaluated in SCLC cell-line derived xenograft (CDX) models (NCI-H1048, DMS-114, H841) in comparison to CDX and patient-derived xenograft (PDX) models of other tumor types. Irinotecan liposome injection was administered intravenously to mice bearing xenograft tumors. At 24 hours post administration, mice were sacrificed and tumors were harvested. Irinotecan and SN-38 in tumors were measured by high performance liquid chromatography (HPLC). Data were normalized to injected dose per tumor weight. As shown in Figure 19, tumors derived from SCLC cell lines have similar or higher levels of irinotecan liposome injection deposition, as assessed by irinotecan content, than other tumor types. Furthermore, analysis of SN-38 levels indicates that increased irinotecan delivery was associated with increased levels of SN-38. These findings are consistent with a proposed mechanism of liposome deposition and local conversion of irinotecan to SN-38 within the tumor.

[0318] **Example 14:** Anti-tumor Activity of Irinotecan Liposome Injection, Non-Liposomal Irinotecan and Topotecan in a Preclinical Model of Second Line SCLC

[0319] Nal-IRI is designed for extended circulation relative to non-liposomal irinotecan and to exploit leaky tumor vasculature for enhanced drug delivery to tumors. Following tumor deposition, nal-IRI is taken up by phagocytic cells followed by irinotecan release and conversion to its active metabolite, SN-38, in the tumors. Sustained inhibition of topoisomerase 1 (TOP1) by extended SN-38 delivery is hypothesized to enable superior anti-tumor activity compared to traditional TOP1 inhibitors. Topotecan, a TOP1 inhibitor, is currently a standard of care for second-line treatment of small cell lung cancer (SCLC).

[0320] As described below, mice bearing NCI-H1048 SCLC tumors were treated with a carboplatin plus etoposide, a first line regimen in SCLC. Once the tumors escaped growth control by carboplatin plus etoposide, mice were randomized to either continue treatment with carboplatin plus etoposide or switch to second line treatment with either irinotecan liposome injection, non-liposomal irinotecan or topotecan.

[0321] NOD/SCID mice with NCIH1048 SCLC xenograft tumors were treated weekly with the combination of 30 mg/kg carboplatin plus 25 mg/kg etoposide. When tumor reached approximately 1200 mm<sup>3</sup>, mice were randomized to receive weekly treatment with topotecan (1.66 mg/kg/wk administered IP in equal fractions on days 1 and 2), non-liposomal irinotecan (33 mg/kg/wk administered IV on day 1) irinotecan liposome injection (16 mg/kg/wk administered IV on day 1), continue treatment with carboplatin plus etoposide or vehicle

control. Vertical dotted lines indicate start of weekly dosing. Irinotecan liposome injection dose is shown on irinotecan HCl basis. After tumors progressed on first-line treatment with carboplatin plus etoposide, irinotecan liposome injection displayed significant anti-tumor activity compared to topotecan and irinotecan ( $p=0.0002$  on day 70 and  $p=0.0002$  on day 84 for topotecan and irinotecan, respectively). In carboplatin plus etoposide -treated SCLC tumors: Nal-IRI remains active and is trending towards complete response; non-liposomal irinotecan treatment is active but after 3rd cycle some tumors are trending regrowth; Topotecan (at 2x clinically relevant dose) seems to be active after 1-2 cycles but progress quickly after 3rd dose; carboplatin plus etoposide is not tolerable by the 5th cycle. As shown in Figure 21A, irinotecan liposome injection had anti-tumor activity in the second line setting and, furthermore, had significantly greater anti-tumor activity than both non-liposomal irinotecan and topotecan. Figure 21B is a survival graph for mice on each of the treatments.

[0322] **Example 15: Irinotecan Liposome Injection Has Improved Anti-Tumor Activity as Compared to Non-liposomal Irinotecan HCl and Topotecan *in Vivo*.**

[0323] The activity of irinotecan liposome injection, non-liposomal irinotecan and topotecan were directly compared at clinically relevant doses in two CDX models (DMS-114 and NCI-H1048) and the activity of irinotecan liposome injection and topotecan in one CDX model (DMS-53). Clinically relevant doses were calculated by using standard surface area to weight ratios conversion per NCI guidelines.

[0324] Figure 23 presents tumor growth kinetics of mice bearing SCLC xenograft tumors that were treated weekly with irinotecan liposome injection, topotecan and non-liposomal irinotecan (two of the three). In the DMS-114 and NCI-H1048 models, irinotecan liposome injection displayed significantly greater anti-tumor activity than both non-liposomal irinotecan and topotecan. In the DMS-53 model, irinotecan liposome injection displayed significantly greater anti-tumor activity than did topotecan. Furthermore, 10 out of 10 mice treated in NCI-H1048 model treated with irinotecan liposome injection experienced complete regressions of their tumors as compared to 0 out of 10 mice treated with topotecan.

[0325] Figure 23 shows the data obtained from NOD/SCID mice with subcutaneous (Figure 23A) DMS-53, (Figure 23B) DMS-114 or (Figure 23C) NCI-H1048. SCLC xenograft tumors were treated with IV nal-IRI (16 mg/kg; triangles), IV irinotecan (33 mg/kg; diamonds), IP topotecan (0.83 mg/kg/wk days 1-2; squares) or vehicle control (circles). For DMS-114 and NCI-H1048 all groups have  $n=10$ ; for DMS-53  $n=4$ , 5 and 5 for control, topotecan and nal-IRI, respectively. Vertical dotted lines indicate start of weekly dosing and error bars indicate standard error of the mean. Irinotecan liposome injection dose is shown on



irinotecan HCl basis. Following treatment, irinotecan liposome injection displayed significant anti-tumor activity compared to topotecan ( $p < 0.0001$  for DMS-114 on day 52 and  $p < 0.0001$  for NCI-H1048 on day 59; non-parametric t-test) and irinotecan ( $p < 0.0001$  for DMS-114 on day 65 and  $p < 0.0001$  for NCI-H1048 on day 84; non-parametric t-test).

[0326] In addition to the CDX models PDX models were also examined using subcutaneous patient-derived xenografts.

[0327] Balb/c nude mice bearing subcutaneous patient-derived xenografts (Figure 23D) LUN-182, (Figure 23E) LUN-081 and (Figure 24F) LUN-164 were treated with IV nal-IRI (16 mg/kg; triangles), IV irinotecan (33 mg/kg; diamonds), IP topotecan (0.83 mg/kg/wk days 1-2; squares) or vehicle control (circles). For all PDX models  $n=5$  for all groups. Vertical dotted lines indicate start of weekly dosing and error bars indicate standard error of the mean.

## CLAIMS

We claim:

1. A method of treating a human patient diagnosed with small cell lung cancer (SCLC) following disease progression on or after first-line platinum-based therapy for the SCLC, the method comprising administering to the human patient an antineoplastic therapy once every two weeks, the antineoplastic therapy consisting of a 90 mg/m<sup>2</sup> (free base) dose of MM-398 liposomal irinotecan.
2. The method of claim 1, wherein the platinum-based therapy comprises the prior, discontinued administration of cisplatin or carboplatin to treat the human patient diagnosed with SCLC.
3. The method of claim 1, wherein the human patient has a blood ANC greater than 1,500 cells/microliter without the use of hematopoietic growth factors, prior to the administration of the MM-398 liposomal irinotecan.
4. The method of any one of claims 1 to 3, wherein the human patient has a blood platelet count of greater than 100,000 cells per microliter, prior to the administration of the MM-398 liposomal irinotecan.
5. The method of any one of claims 1 to 3, wherein the human patient has a blood hemoglobin greater than 9 g/dL, prior to the administration of the MM-398 liposomal irinotecan.
6. The method of any one of claims 1 to 3, wherein the human patient has a serum creatinine of less than or equal to 1.5xULN and a creatinine clearance of greater than or equal to 40 mL/min prior to the administration of the MM-398 liposomal irinotecan.
7. The method of any one of claims 1 to 7, wherein the human patient has not received a topoisomerase I inhibitor prior to administration of the MM-398 liposomal irinotecan.
8. The method of any one of claims 1 to 8, wherein the human patient has not received a more than a single platinum-based therapy prior to administration of the MM-398 liposomal irinotecan.
9. The method of any one of claims 1 to 9, wherein the antineoplastic therapy comprises the steps of:
  - (a) preparing a pharmaceutically acceptable injectable composition by combining dispersion of MM-398 liposomal irinotecan containing 4.3 mg irinotecan free base/mL of the dispersion with a 5% Dextrose Injection (D5W) or 0.9% Sodium Chloride Injection to obtain

the injectable composition having a final volume of 500 mL and 90 mg/m<sup>2</sup> (free base) of the MM-398 liposomal irinotecan ( $\pm 5\%$ ); and

(b) administering the injectable composition from step (a) containing the MM-398 irinotecan liposome to the patient in a 90-minute infusion.

10. The method of any one of claims 1 to 9, further comprising administering to the human patient dexamethasone and a 5-HT<sub>3</sub> blocker prior to each administration of the antineoplastic therapy, and optionally further administering an antiemetic to the human patient.

11. A method of treating a human patient who is not homozygous for the UTG1A1\*28 allele and is diagnosed with small cell lung cancer (SCLC) following disease progression on or after first-line platinum-based therapy for the SCLC, the method comprising administering to the human patient an antineoplastic therapy once every two weeks in a six-week cycle, the antineoplastic therapy consisting of a 90 mg/m<sup>2</sup> (free base) dose of MM-398 liposomal irinotecan.

12. The method of claim 11, wherein the platinum-based therapy comprises the prior, discontinued administration of cisplatin or carboplatin to treat the human patient diagnosed with SCLC.

13. The method of claim 12, wherein the human patient has one or more of the following prior to the administration of the MM-398 liposomal irinotecan:

- (a) a blood ANC greater than 1,500 cells/microliter without the use of hematopoietic growth factors;
- (b) a blood platelet count of greater than 100,000 cells per microliter;
- (c) a blood hemoglobin greater than 9 g/dL; and
- (d) a serum creatinine of less than or equal to 1.5xULN and a creatinine clearance of greater than or equal to 40 mL/min.

14. The method of claim 13, wherein the human patient has not received a topoisomerase I inhibitor prior to administration of the MM-398 liposomal irinotecan; and the human patient has not received a more than a single platinum-based therapy prior to administration of the MM-398 liposomal irinotecan.

15. The method of claim 13, wherein the method comprises administering the antineoplastic therapy for at least three six-week cycles.

16. The method of claim 11, wherein the antineoplastic therapy comprises the steps of:

- (a) preparing a pharmaceutically acceptable injectable composition by combining dispersion of MM-398 liposomal irinotecan containing 4.3 mg irinotecan free base/mL of the

dispersion with a 5% Dextrose Injection (D5W) or 0.9% Sodium Chloride Injection to obtain the injectable composition having a final volume of 500 mL and 90 mg/m<sup>2</sup> (free base) of the MM-398 liposomal irinotecan ( $\pm 5\%$ ); and

(b) administering the injectable composition from step (a) containing the MM-398 irinotecan liposome to the patient in a 90-minute infusion.

17. The method of claim 16, further comprising administering to the human patient dexamethasone and a 5-HT<sub>3</sub> blocker prior to each administration of the antineoplastic therapy, and optionally further administering an antiemetic to the human patient.

18. A method of treating a human patient diagnosed with small cell lung cancer (SCLC) following disease progression on or after a first-line platinum-based therapy for the SCLC selected from the group consisting of cisplatin or carboplatin, the method comprising administering to the human patient an antineoplastic therapy once every two weeks for a total of at least three six-week cycles, the antineoplastic therapy consisting of a 90 mg/m<sup>2</sup> (free base) dose of MM-398 liposomal irinotecan;

wherein the human patient is not homozygous for the UTG1A1\*28 allele and has the following prior to the administration of each antineoplastic therapy of MM-398 liposomal irinotecan:

- (a) a blood ANC greater than 1,500 cells/microliter without the use of hematopoietic growth factors;
- (b) a blood platelet count of greater than 100,000 cells per microliter;
- (c) a blood hemoglobin greater than 9 g/dL; and
- (d) a serum creatinine of less than or equal to 1.5xULN and a creatinine clearance of greater than or equal to 40 mL/min.

19. The method of claim 18, wherein:

(a) the human patient has not received a topoisomerase I inhibitor prior to administration of the MM-398 liposomal irinotecan and has not received a more than a single platinum-based therapy prior to administration of the MM-398 liposomal irinotecan; and

(b) the method further comprises administering to the human patient dexamethasone and a 5-HT<sub>3</sub> blocker prior to each administration of the antineoplastic therapy, and optionally further administering an antiemetic to the human patient.

20. The method of claim 19, wherein the antineoplastic therapy comprises the steps of:

(a) preparing a pharmaceutically acceptable injectable composition by combining dispersion of MM-398 liposomal irinotecan containing 4.3 mg irinotecan free base/mL of the dispersion with a 5% Dextrose Injection (D5W) or 0.9% Sodium Chloride Injection to obtain

the injectable composition having a final volume of 500 mL and 90 mg/m<sup>2</sup> (free base) of the MM-398 liposomal irinotecan ( $\pm 5\%$ ); and

(b) administering the injectable composition from step (a) containing the MM-398 irinotecan liposome to the patient in a 90-minute infusion.



FIG. 1

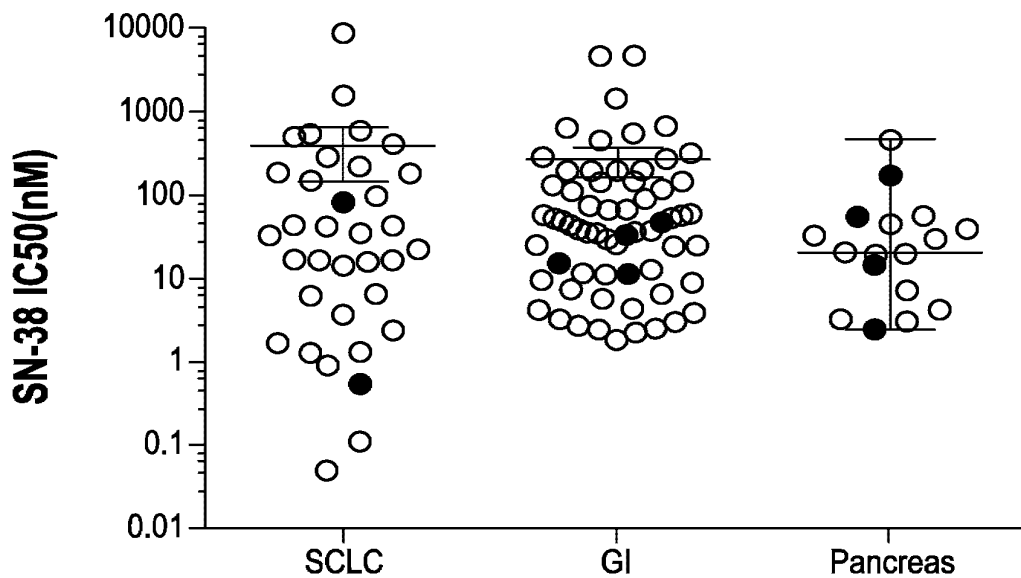




FIG. 2A

### DMS-114 (SCLC)

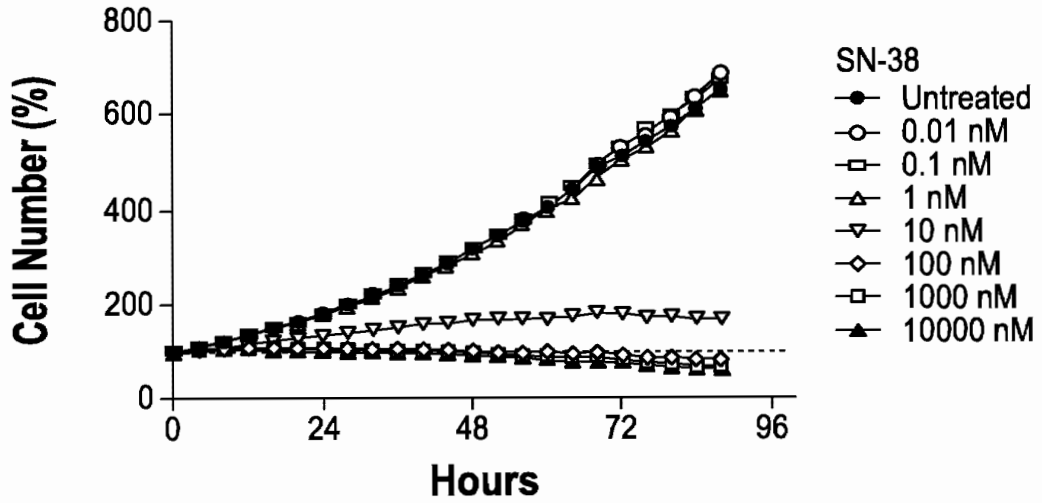


FIG. 2B

### NCI-H1048 (SCLC)

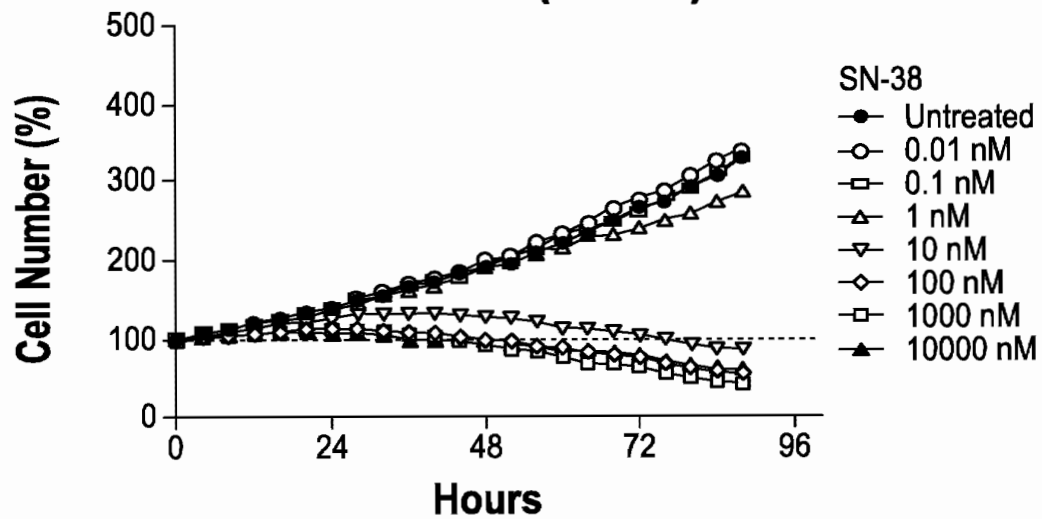




FIG. 3

### DMS114

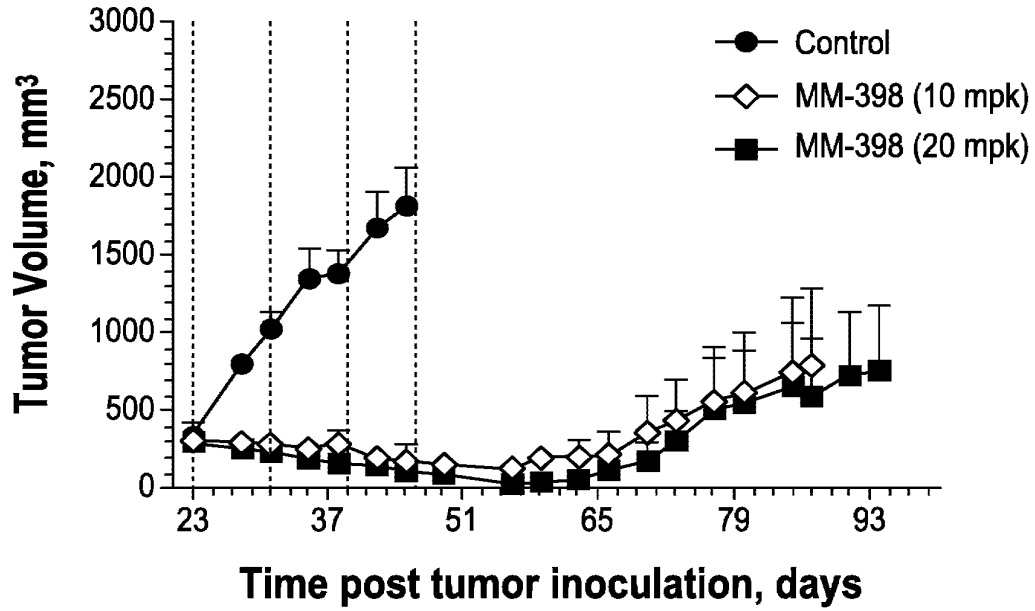




FIG. 4

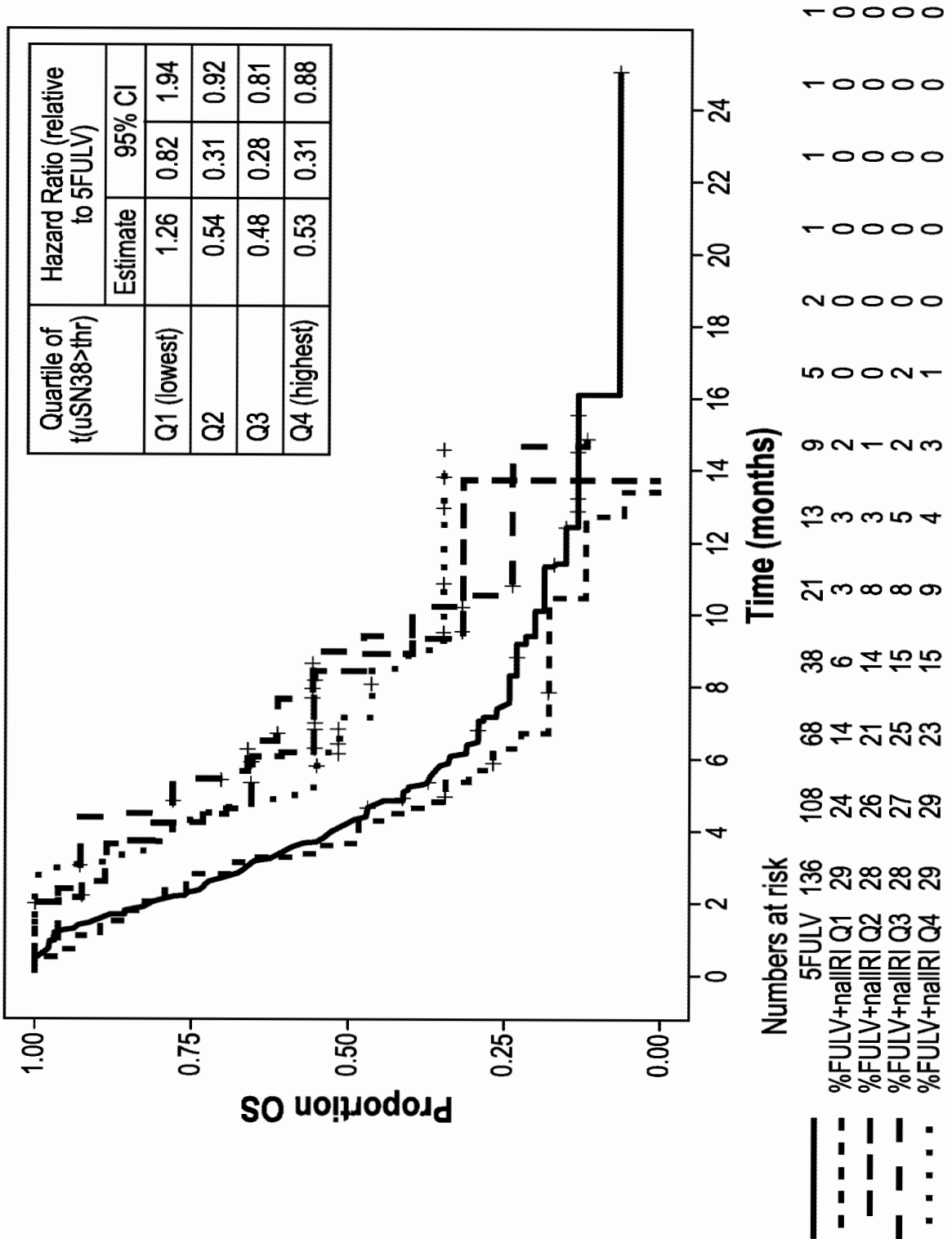


FIG. 5

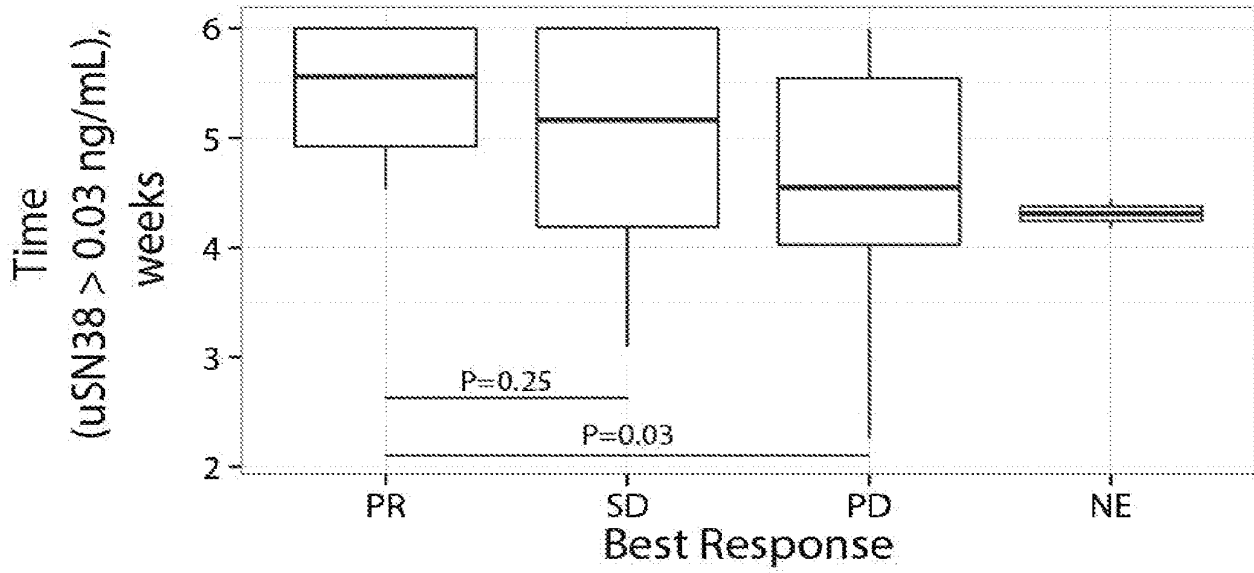




FIG. 6A

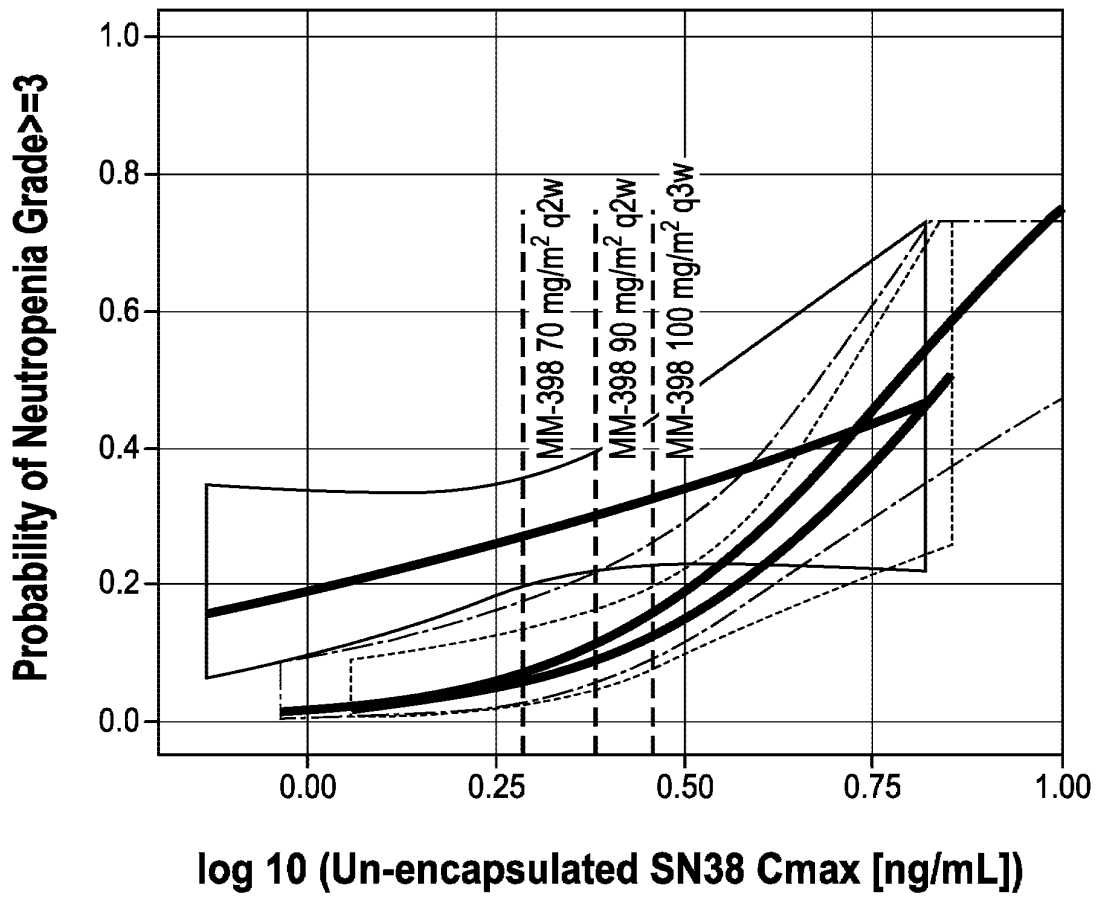




FIG. 6B

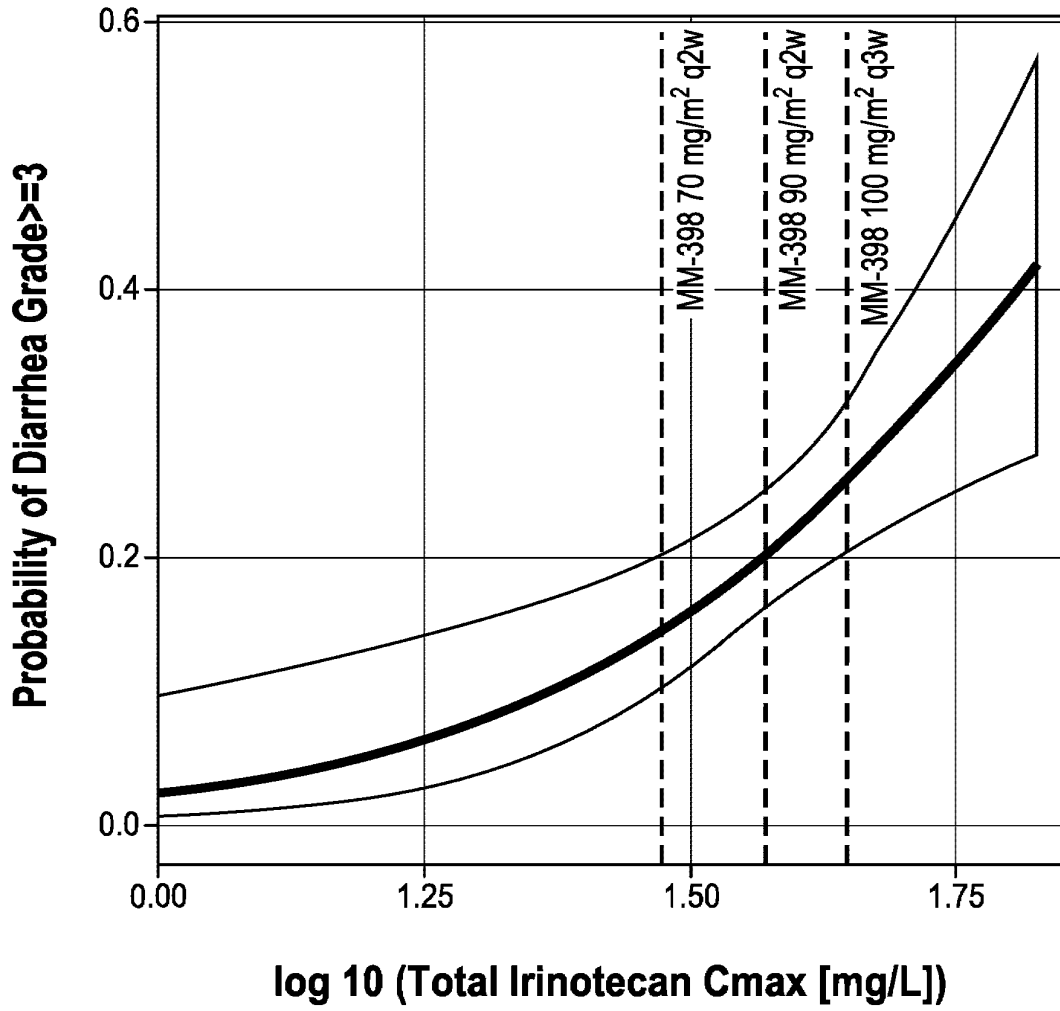




FIG. 7A

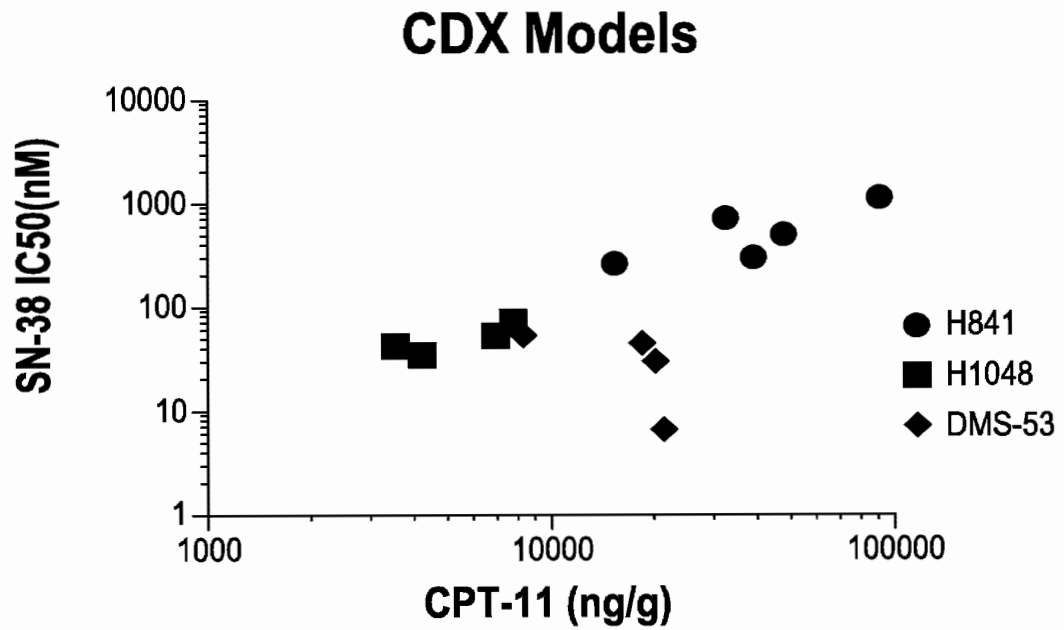


FIG. 7B

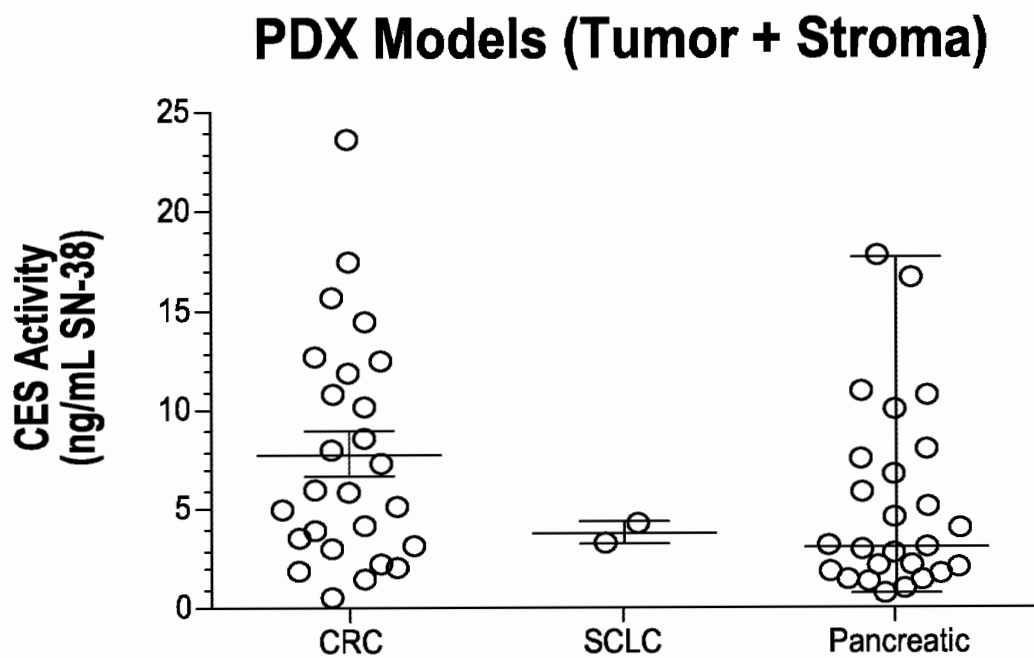




FIG. 7C

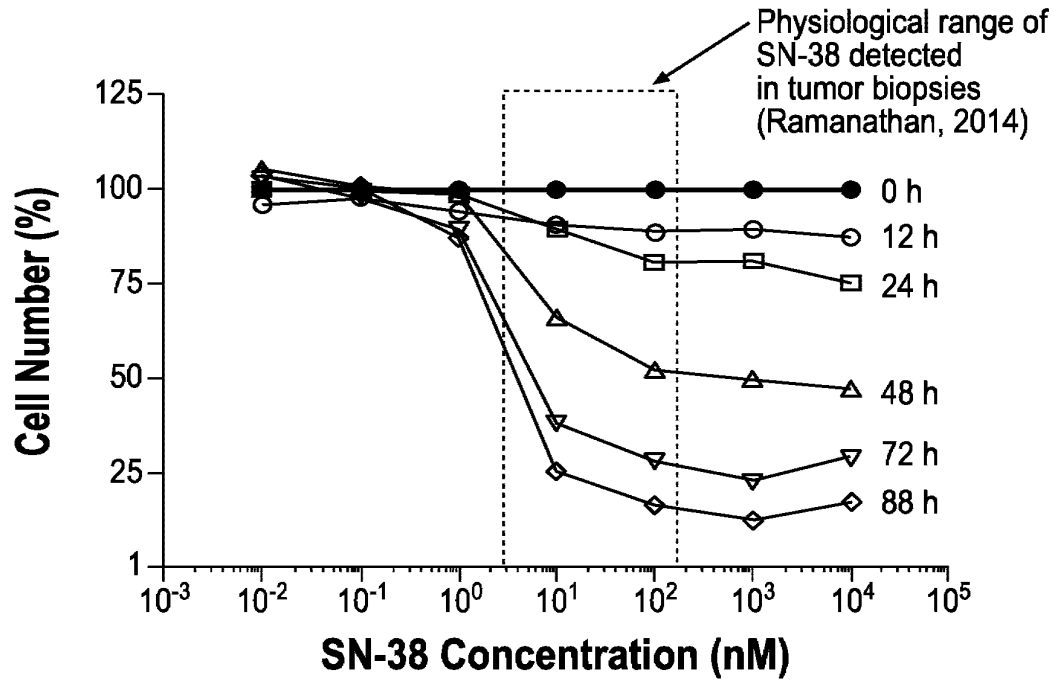


FIG. 7D

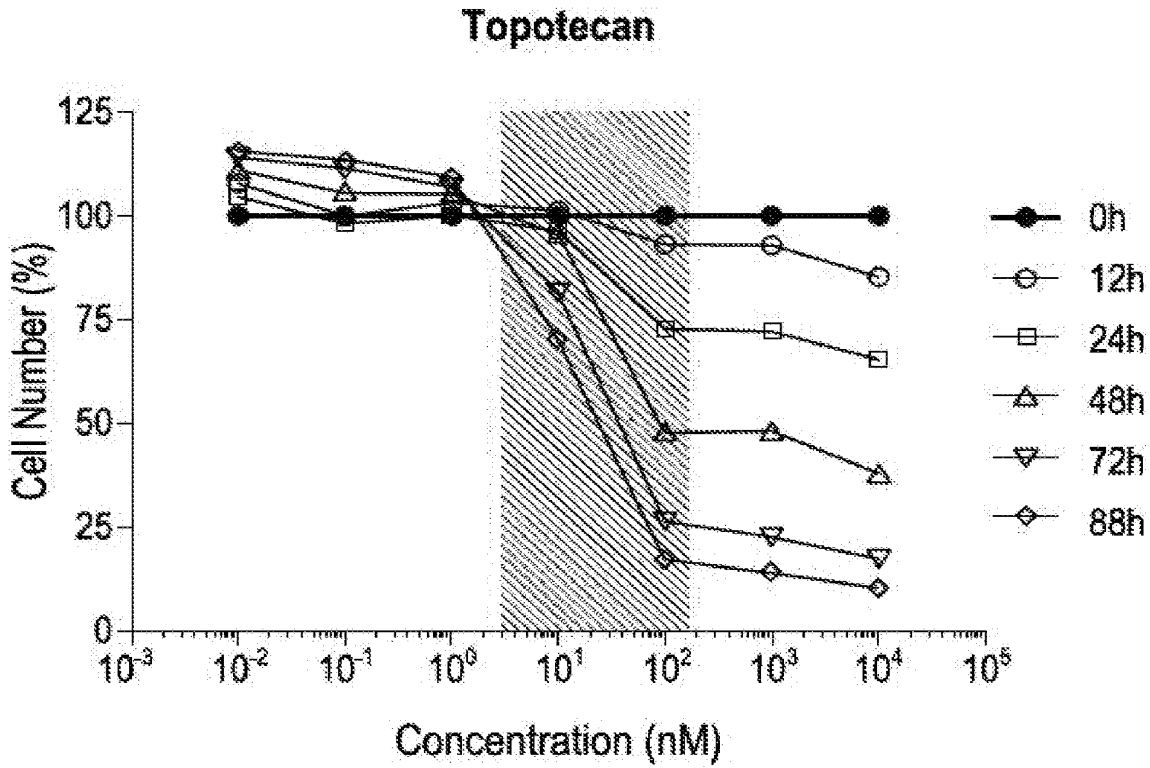


FIG. 7E

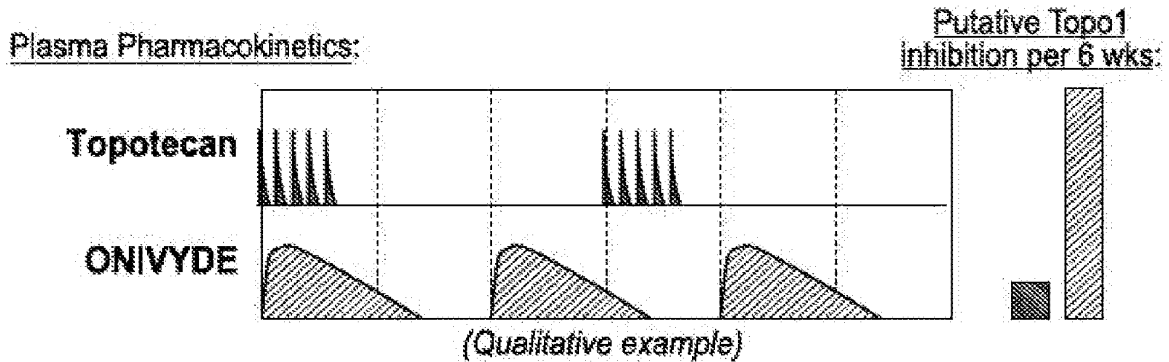
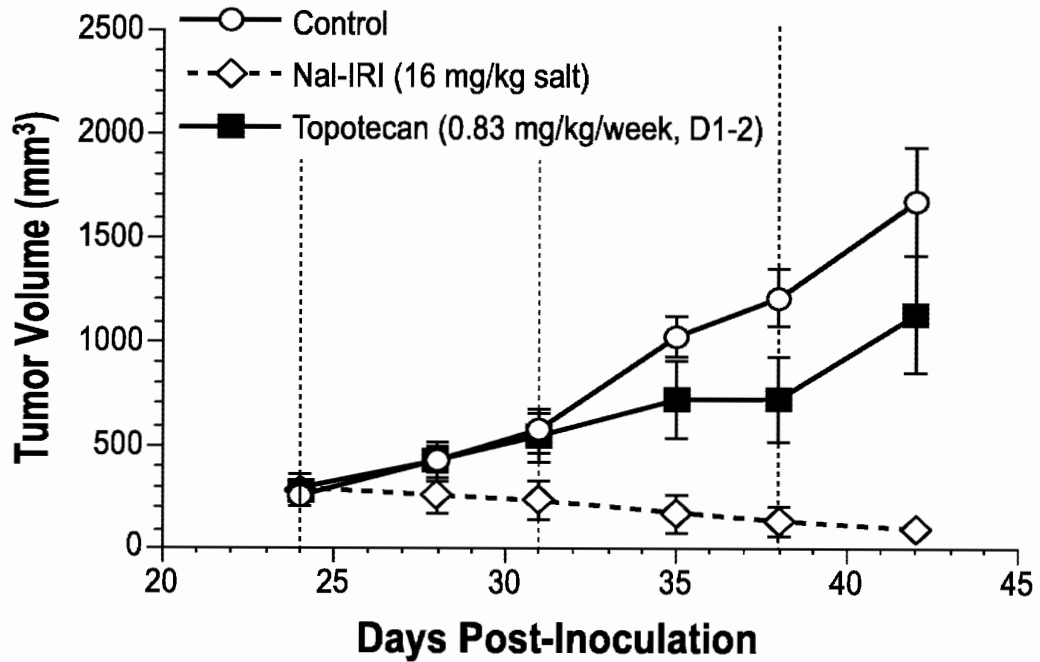




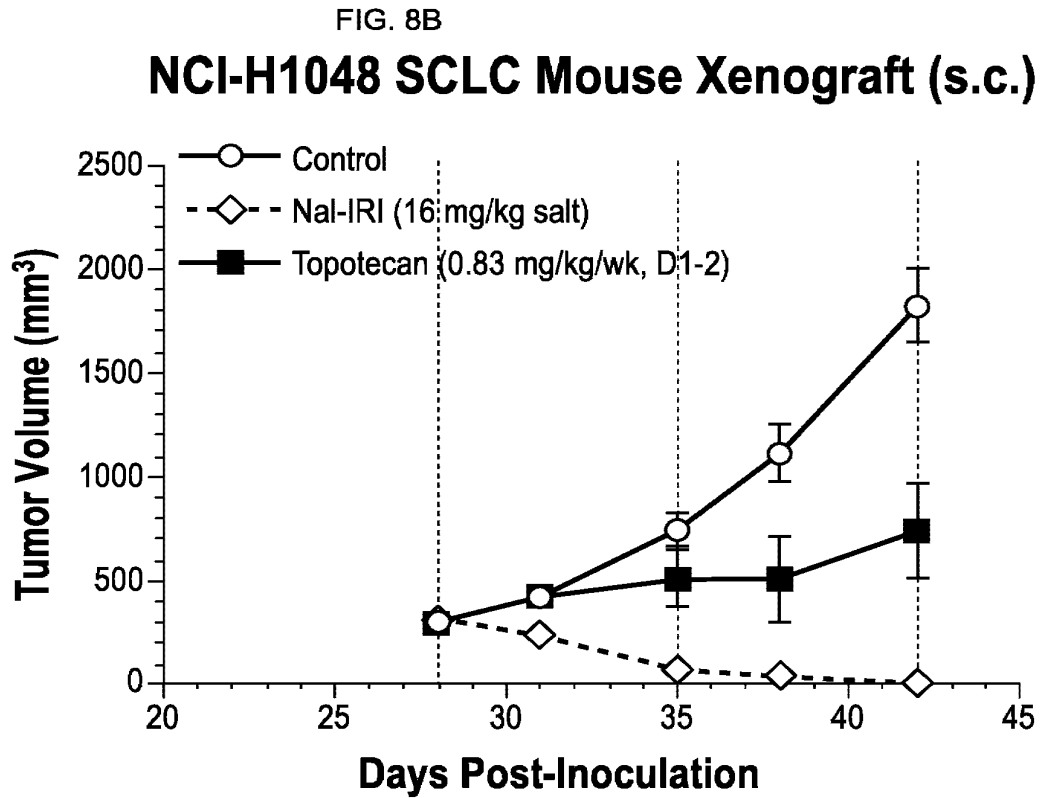
FIG. 8A  
**DMS-53 SCLC Mouse Xenograft (s.c.)**



Response @ Day 42**	PD	SD	PR	CR
Control	100% (5/5)	0% (0/5)	0% (0/5)	0% (0/5)
Nal-IRI	0% (0/5)	0% (0/5)	100% (5/5)	0% (0/5)
Topotecan	100% (5/5)	0% (0/5)	0% (0/5)	0% (0/5)







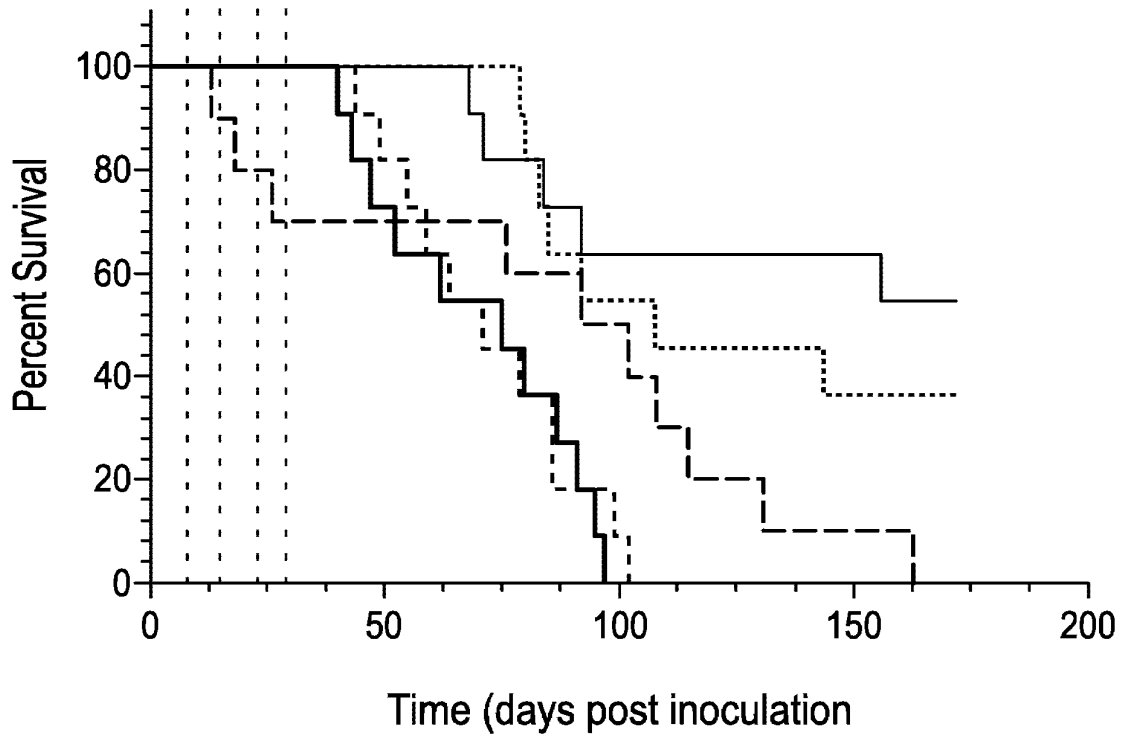
Response @ Day 42**	PD	SD	PR	CR
Control	100% (6/6)	0% (0/6)	0% (0/6)	0% (0/6)
Nal-IRI	0% (0/7)	0% (0/7)	0% (0/7)	100% (7/7)
Topotecan	86% (6/7)	14% (1/7)	0% (0/7)	0% (0/7)





FIG. 8C

### Rat Orthotopic SCLC model (H841)



- control
- ..... ONIVYDE (30 mg/kg salt)
- ONIVYDE (50 mg/kg salt)
- · · · · Irinotecan (25 mg/kg)
- · - · - Topotecan (4 mg/kg)



FIG. 9A

### Tumor CPT-11 (24 h.p.i.)

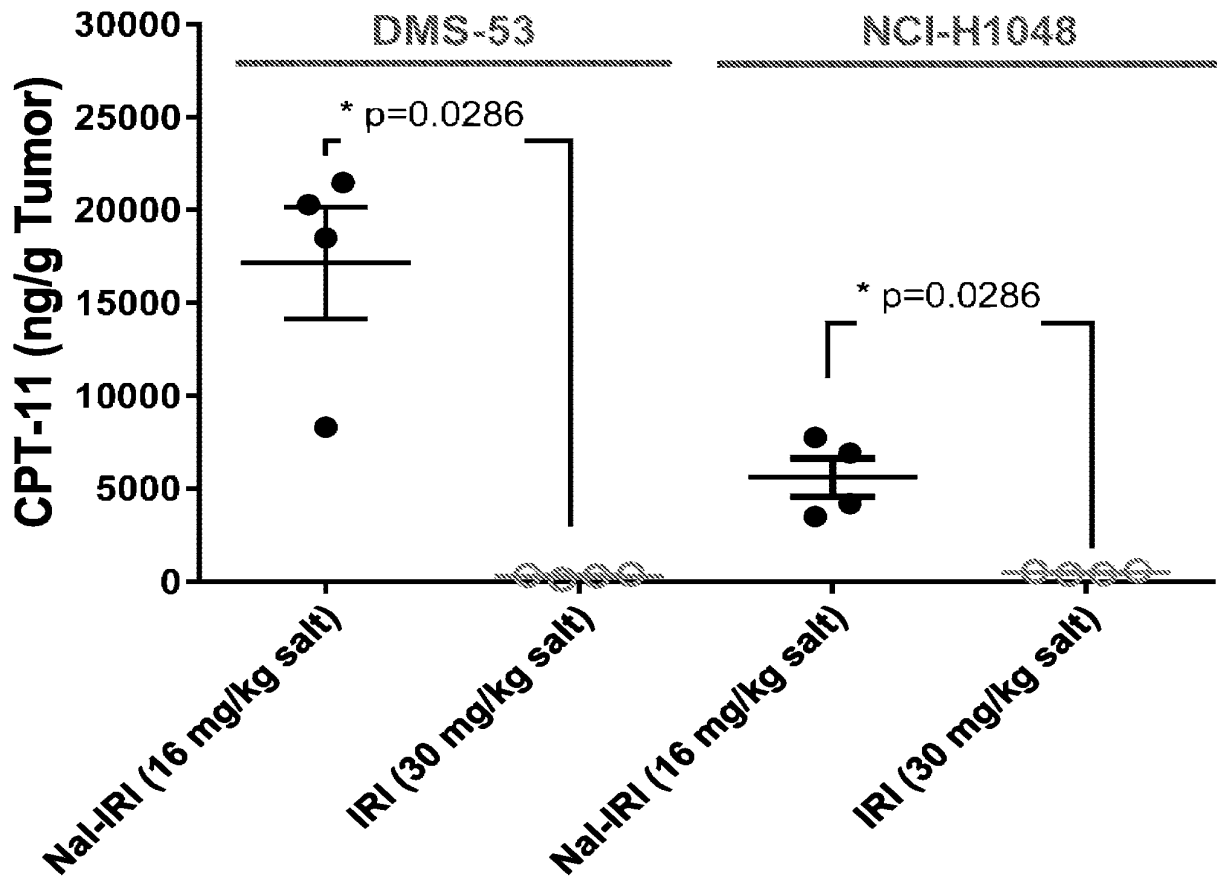


FIG. 9B

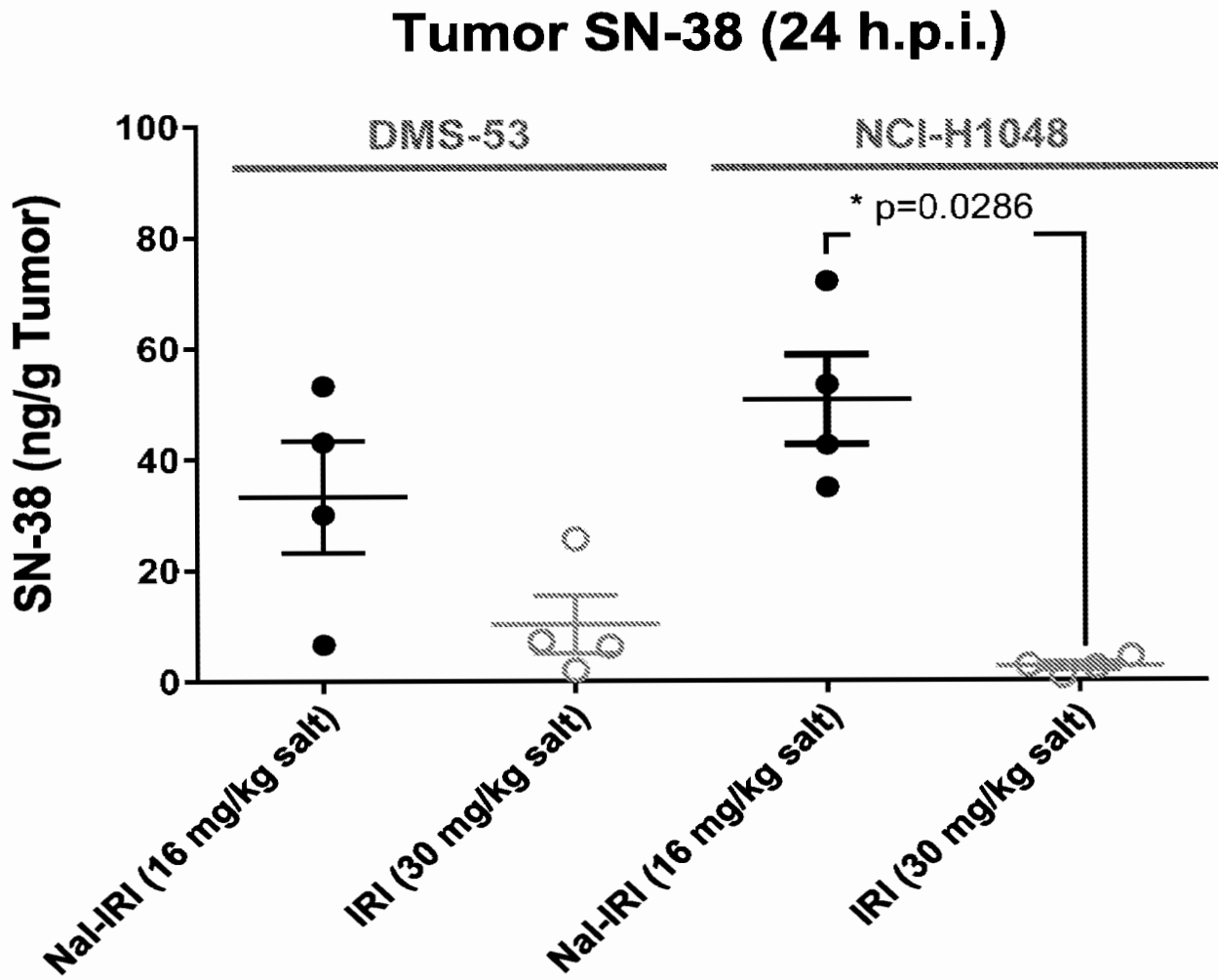


FIG. 10A

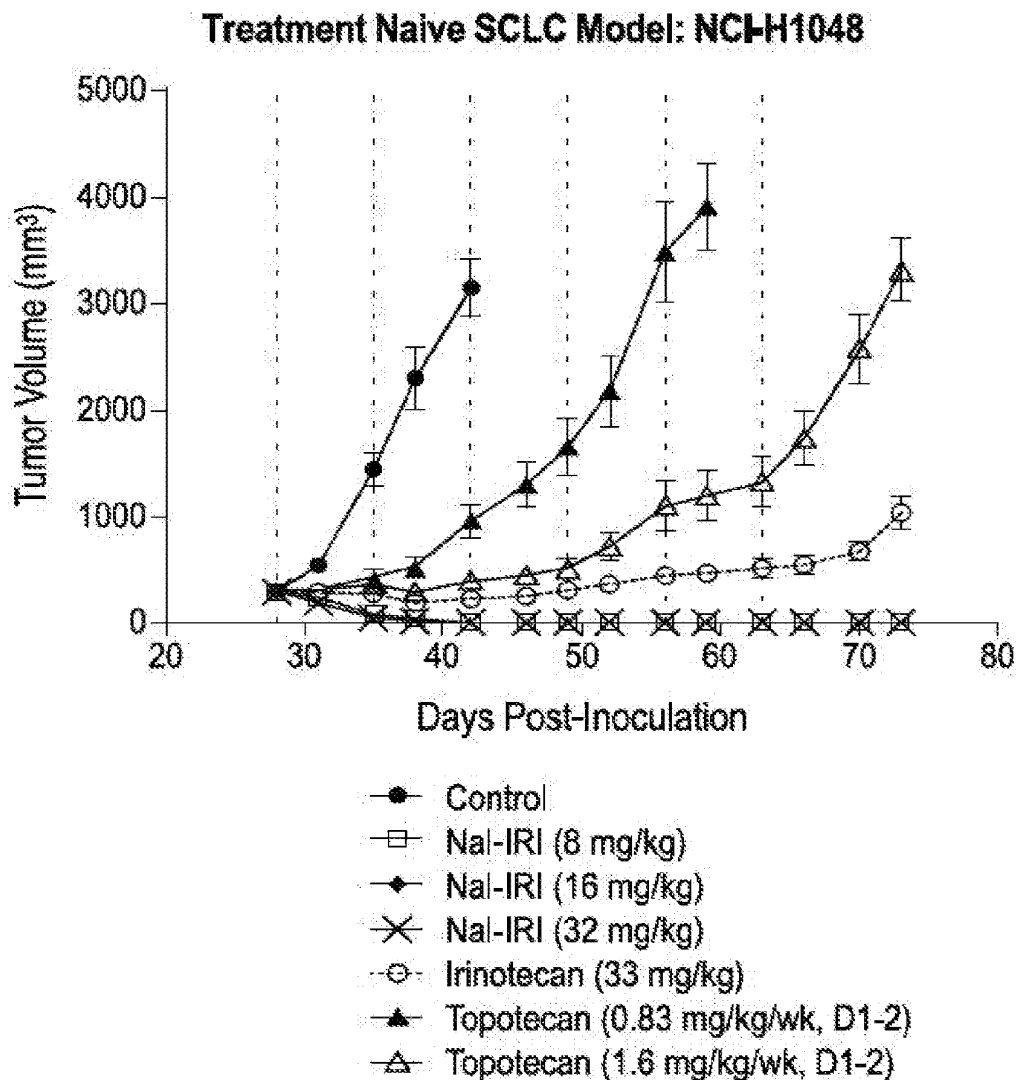


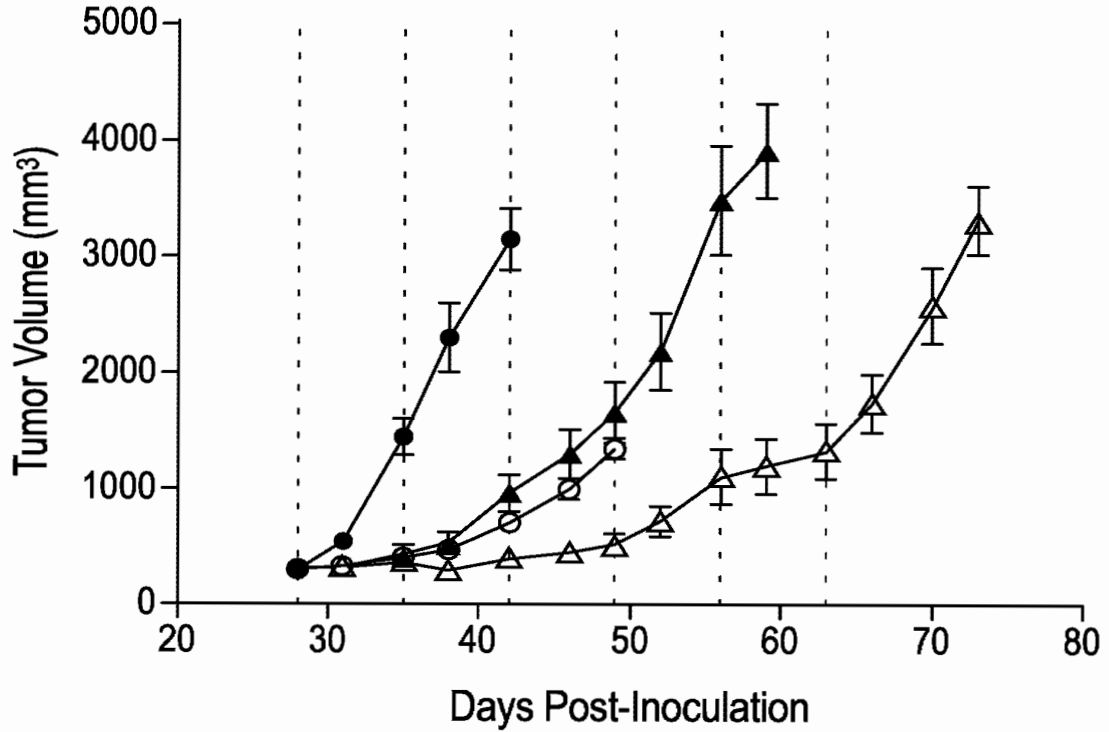
FIG. 10B

Number of complete response (Nal-IRI)			
Nal-IRI Dose:	8 mg/kg	16 mg/kg	32 mg/kg
Day 38	0/10 (0%)	1/10 (10%)	5/10 (50%)
Day 42	8/10 (80%)	9/10 (90%)	9/10 (90%)
Day 46	10/10 (100%)	10/10 (100%)	10/10 (100%)



FIG. 11A

**Treatment Naive SCLC Model: NCI-H1048**



- Control
- ▲ Topotecan (0.83 mg/kg/wk, D1-2)
- △ Topotecan (1.6 mg/kg/wk, D1-2)
- 1L: Etop (25 mg/kg) & Carbo (30 mg/kg)

FIG. 11B

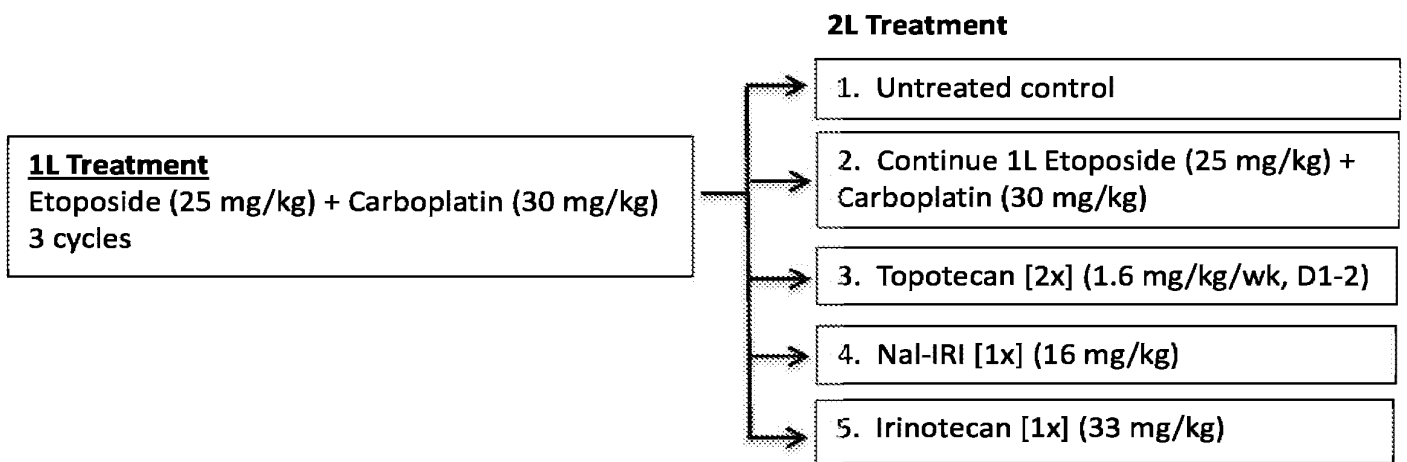


FIG. 12

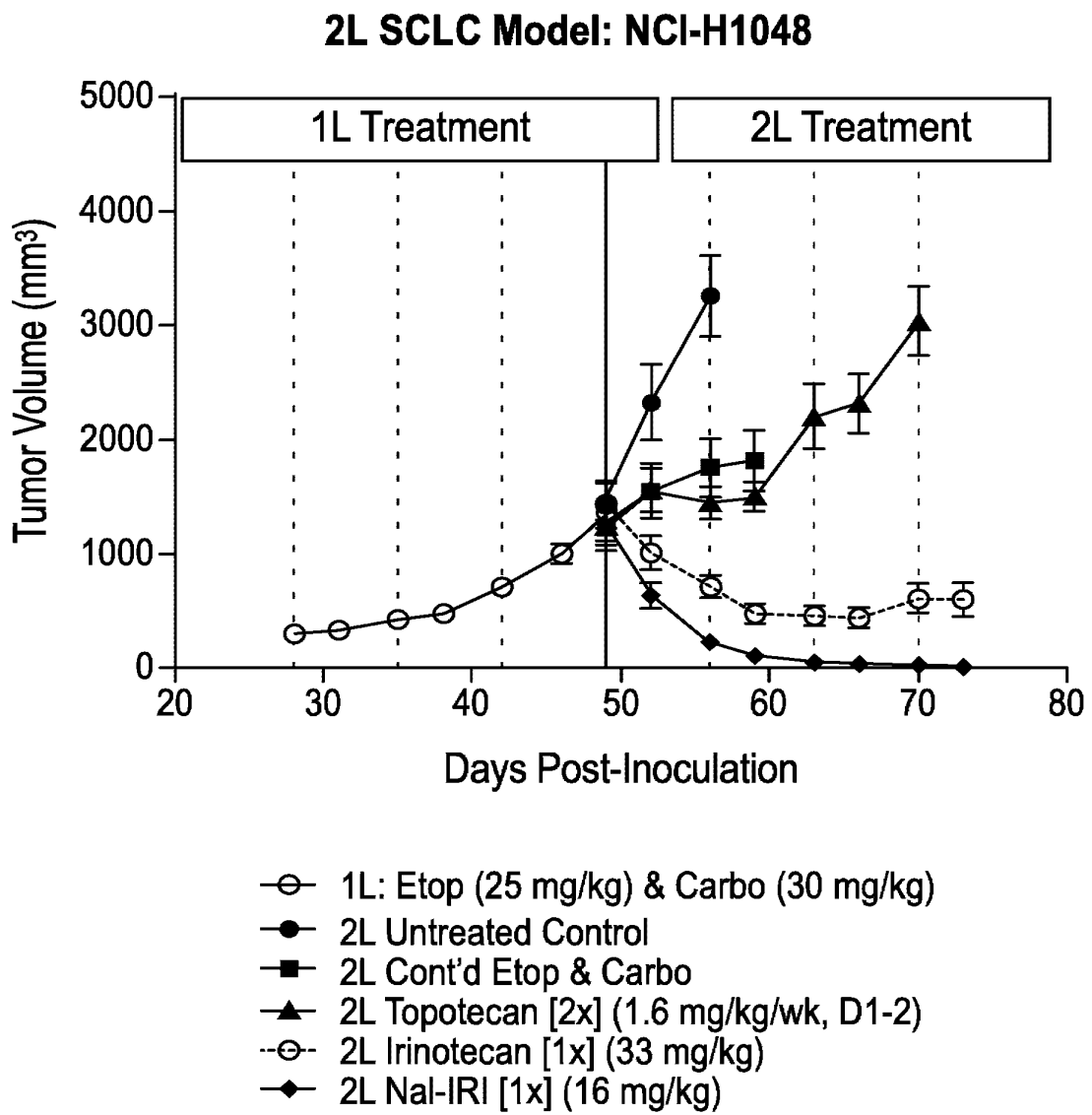
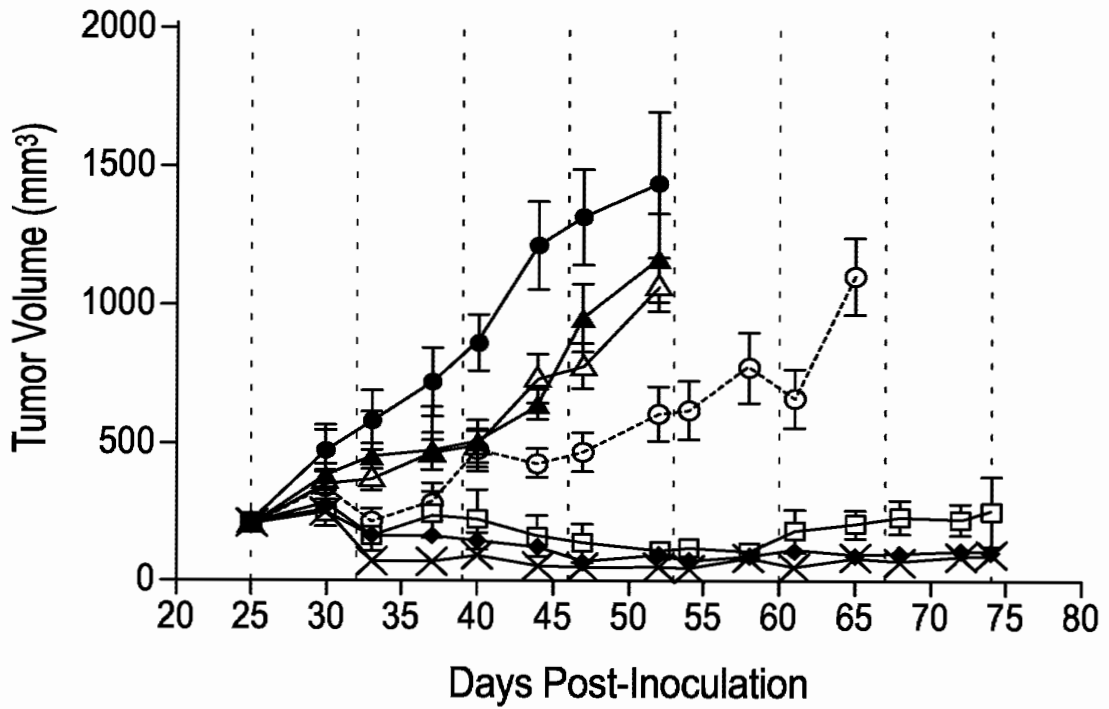






FIG. 13A

**DMS-114 SCLC Mouse Xenograft (s.c.)**



- Control
- ▲ Topotecan 1X (0.83 mg/kg/wk, D1-2)
- △ Topotecan 2X (1.6 mg/kg/wk, D1-2)
- Irinotecan (33 mg/kg)
- Nal-IRI 0.5X (8 mg/kg)
- ◆ Nal-IRI 1X (16 mg/kg)
- × Nal-IRI 2X (32 mg/kg)



FIG. 13B

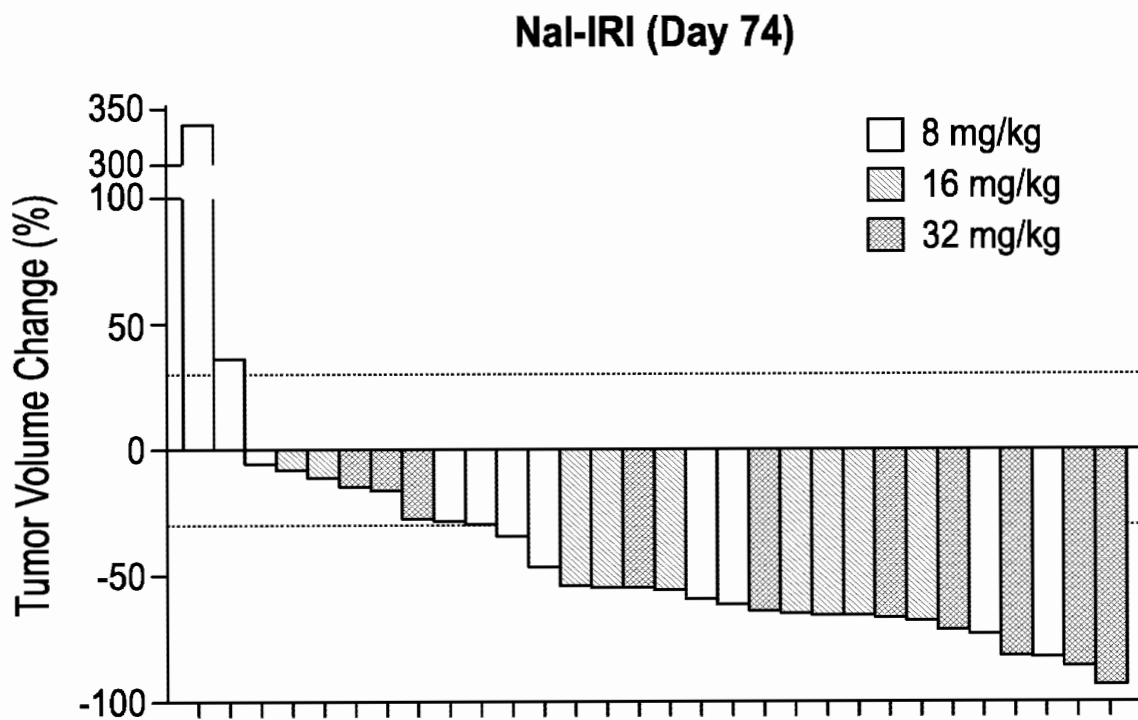




FIG. 14A

**DMS-114: Treatment Naive**

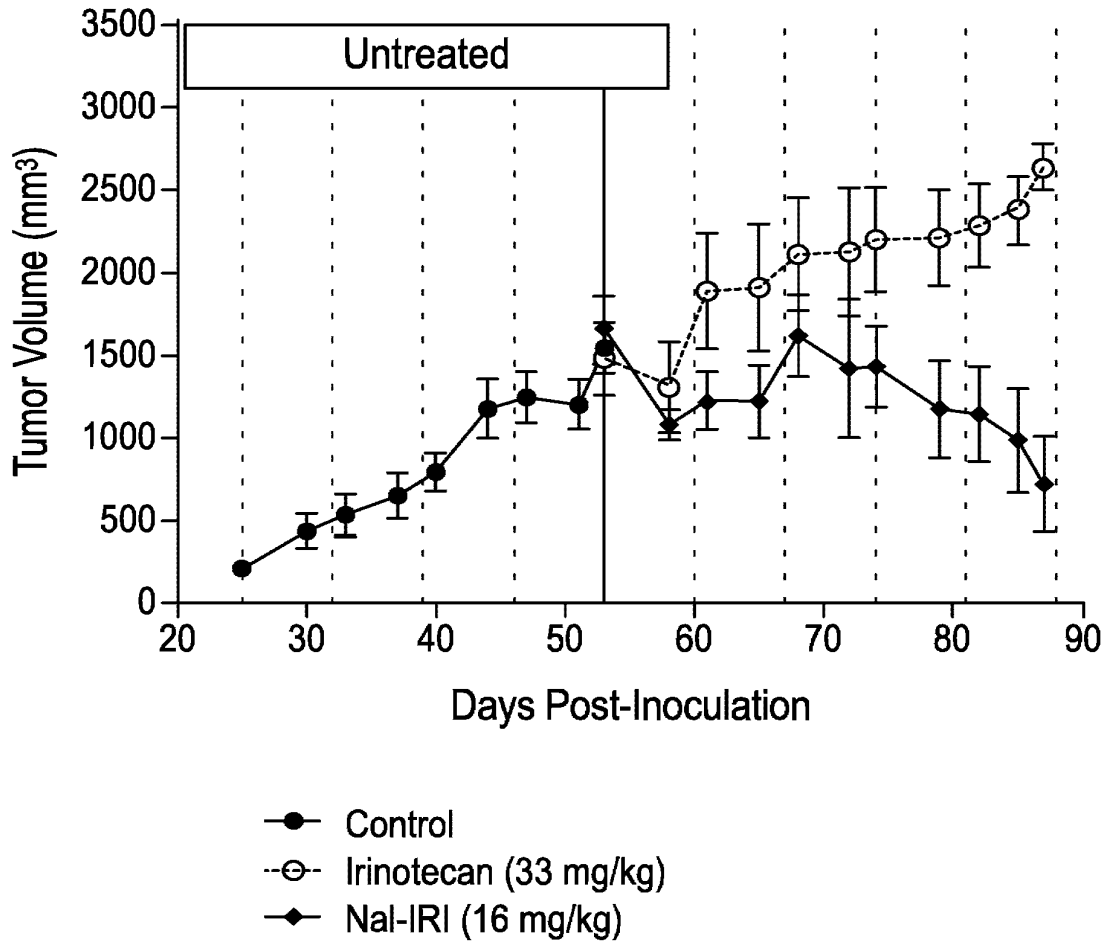
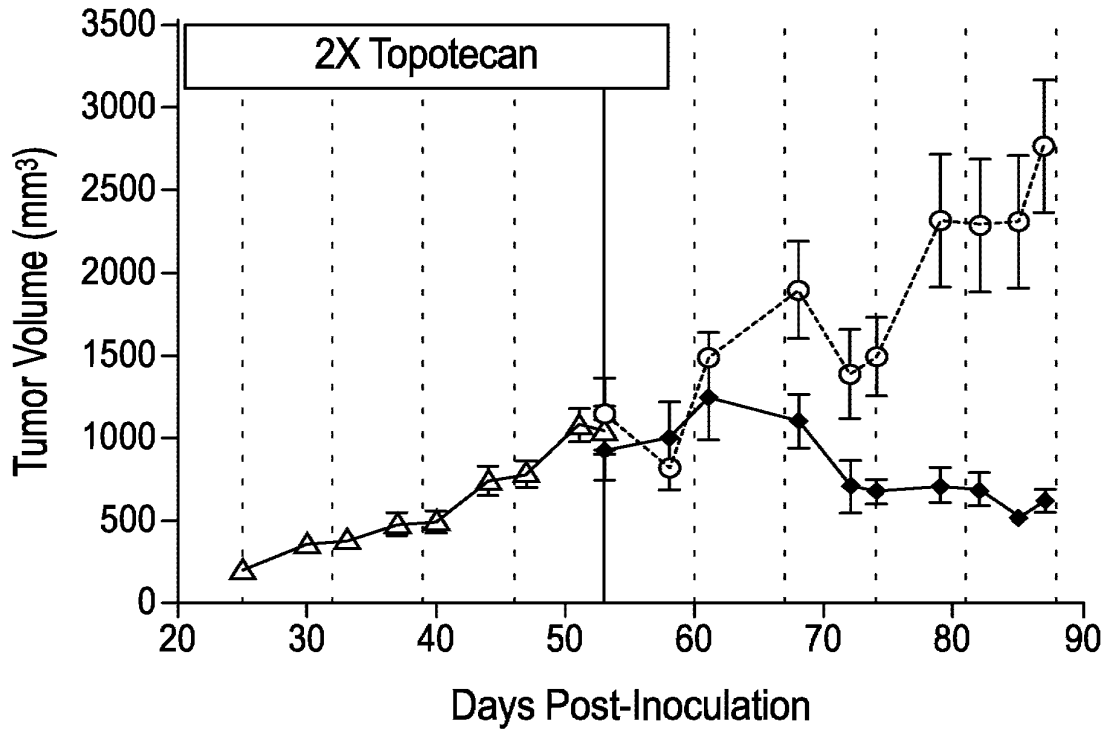




FIG. 14B

### DMS-114: Topotecan-Treated



- △— Topotecan (1.6 mg/kg/wk, D1-2)
- -○- - Irinotecan (33 mg/kg)
- ◆— Nal-IRI (16 mg/kg)





FIG. 14C

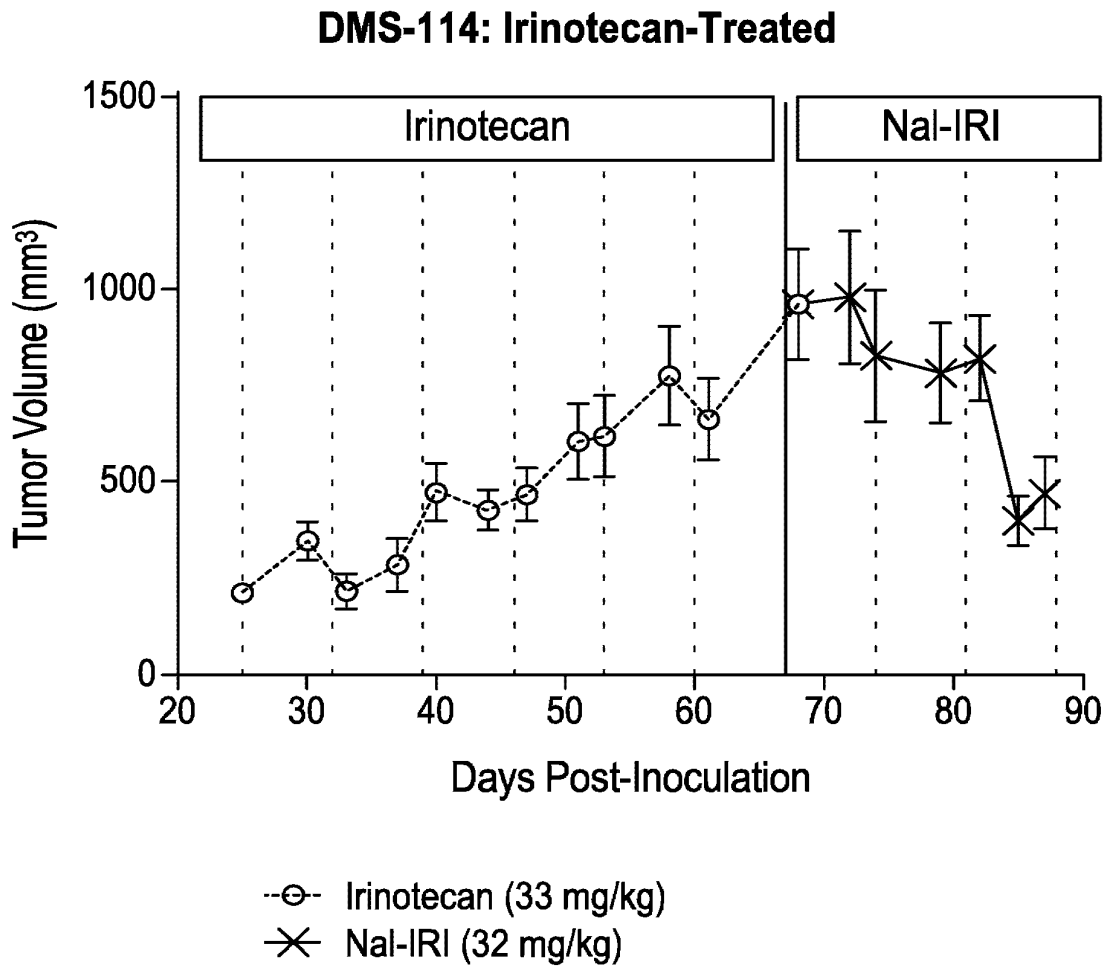


FIG. 15A

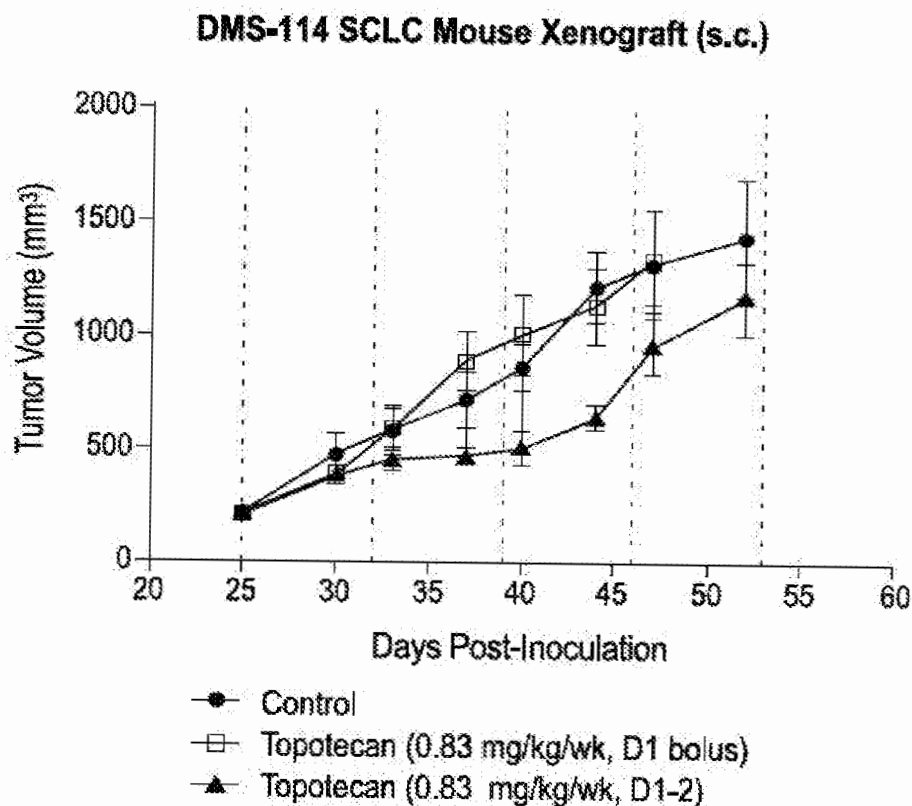


FIG. 15B

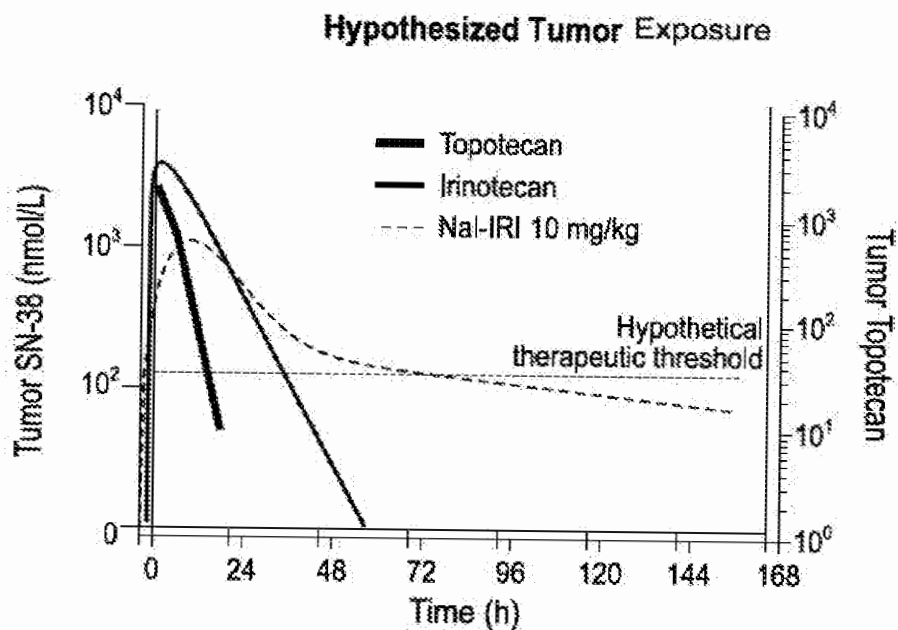
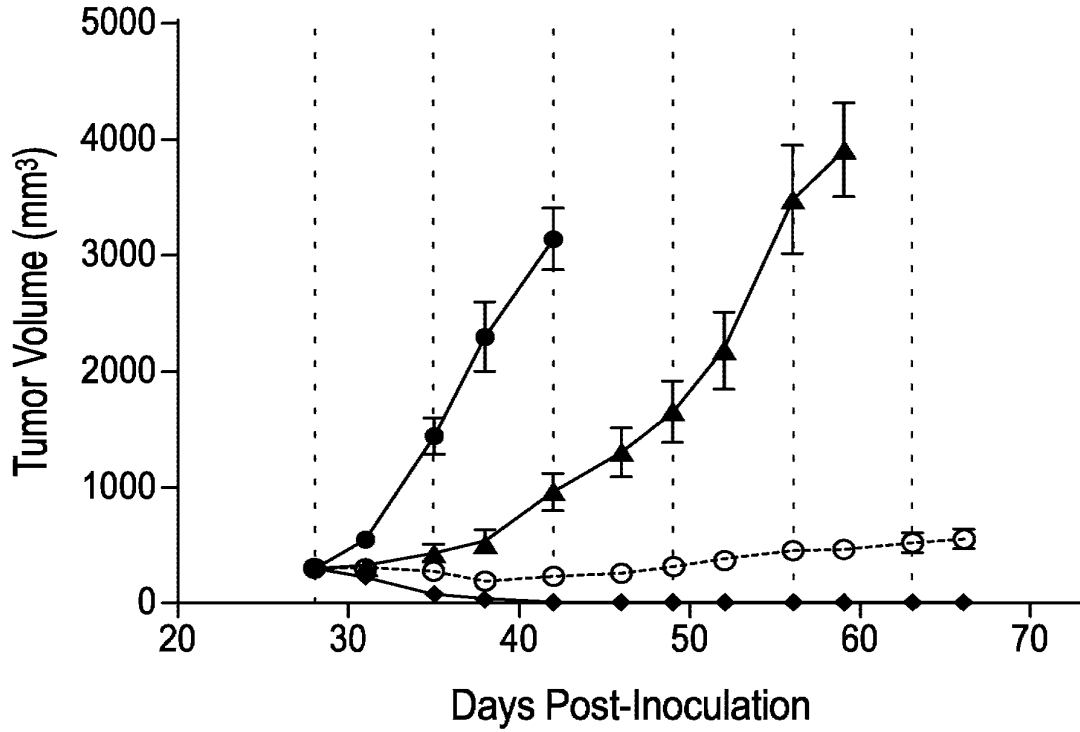




FIG. 15C

### NCI-H1048 Mouse Xenograft



- Control
- ▲ Topotecan (0.83 mg/kg/wk, D1-2)
- Irinotecan (33 mg/kg)
- ◆ Nal-IRI (16 mg/kg)



FIG. 16A

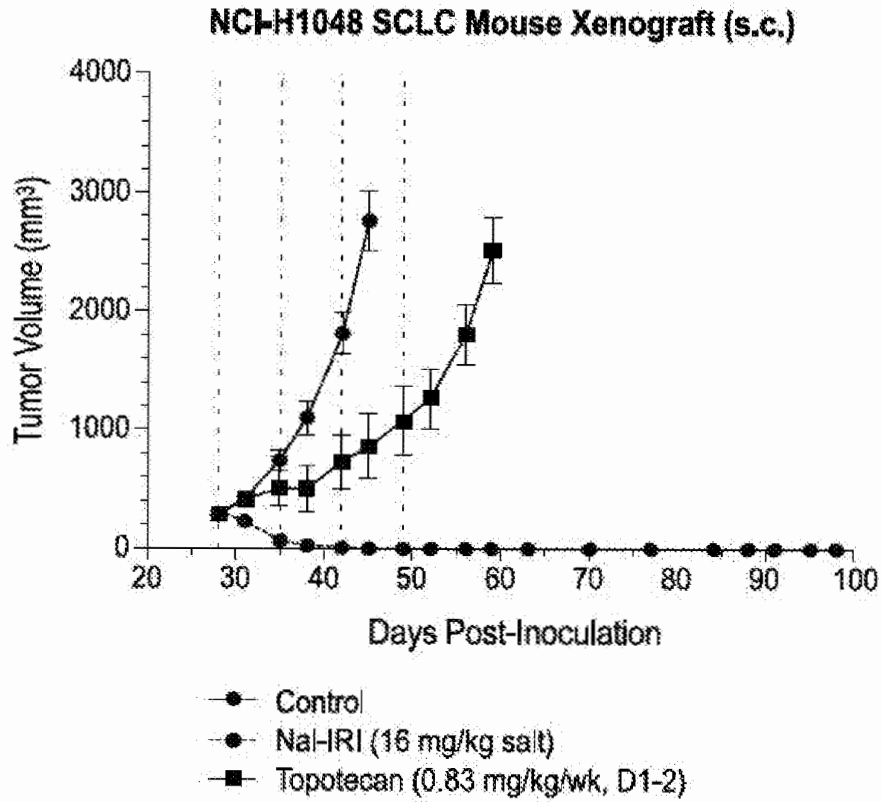


FIG. 16B

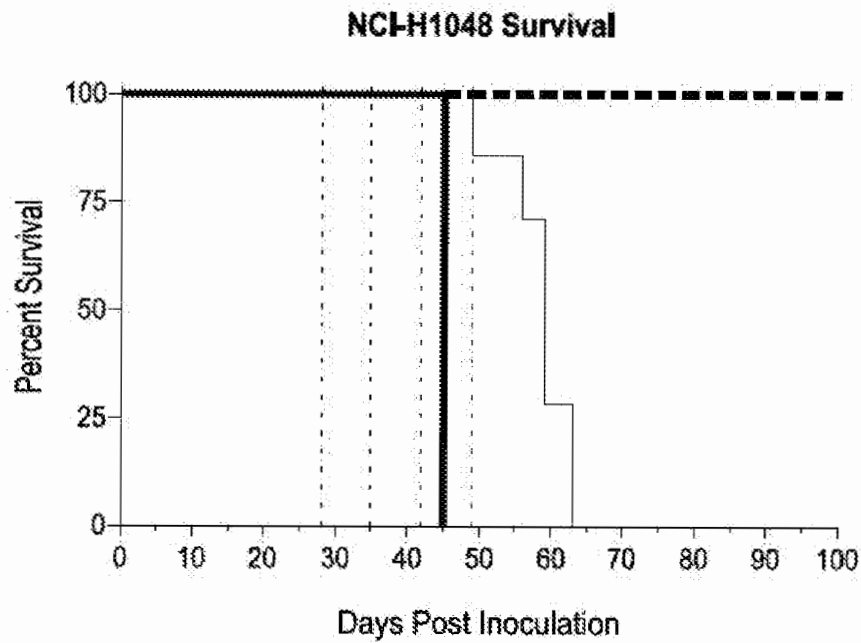






FIG. 16C

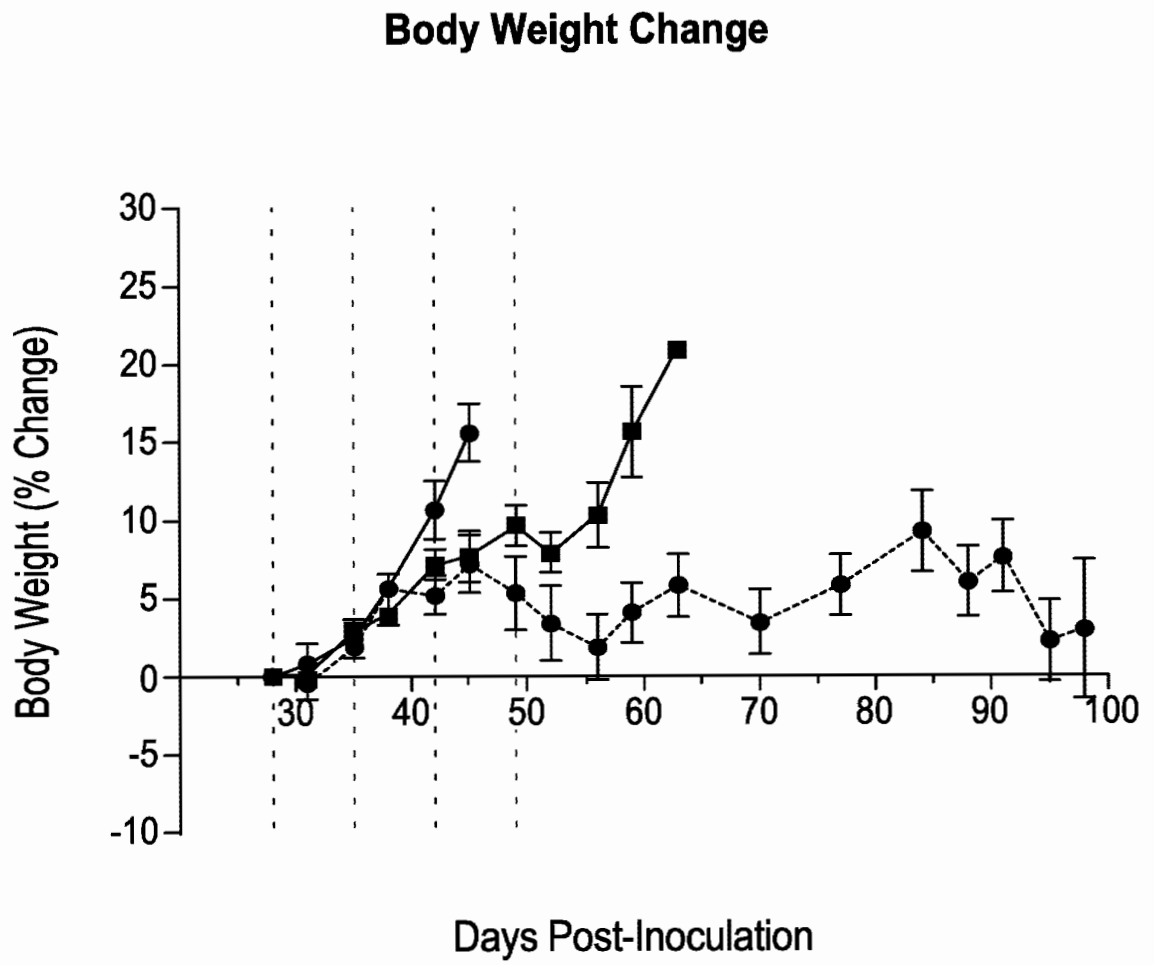


FIG. 16D

<b>Response at Day 98**</b>	<b>CR</b>	<b>PR</b>	<b>SD</b>	<b>PD</b>
<b>Control</b>	<b>0% (0/6)</b>	<b>0% (0/6)</b>	<b>0% (0/6)</b>	<b>100% (6/6)</b>
<b>Nal-IRI</b>	<b>100% (7/7)</b>	<b>0% (0/7)</b>	<b>0% (0/7)</b>	<b>0% (0/7)</b>
<b>Topotecan</b>	<b>0% (0/7)</b>	<b>0% (0/7)</b>	<b>0% (0/7)</b>	<b>100% (7/7)</b>

\*\* Response rates determined based on tumor volume change from baseline:

CR:  $\Delta TV < -95\%$

PR:  $-95\% \leq \Delta TV < -30\%$

SD:  $-30\% \leq \Delta TV < 30\%$

PD:  $\Delta TV \geq 30\%$

FIG. 17A

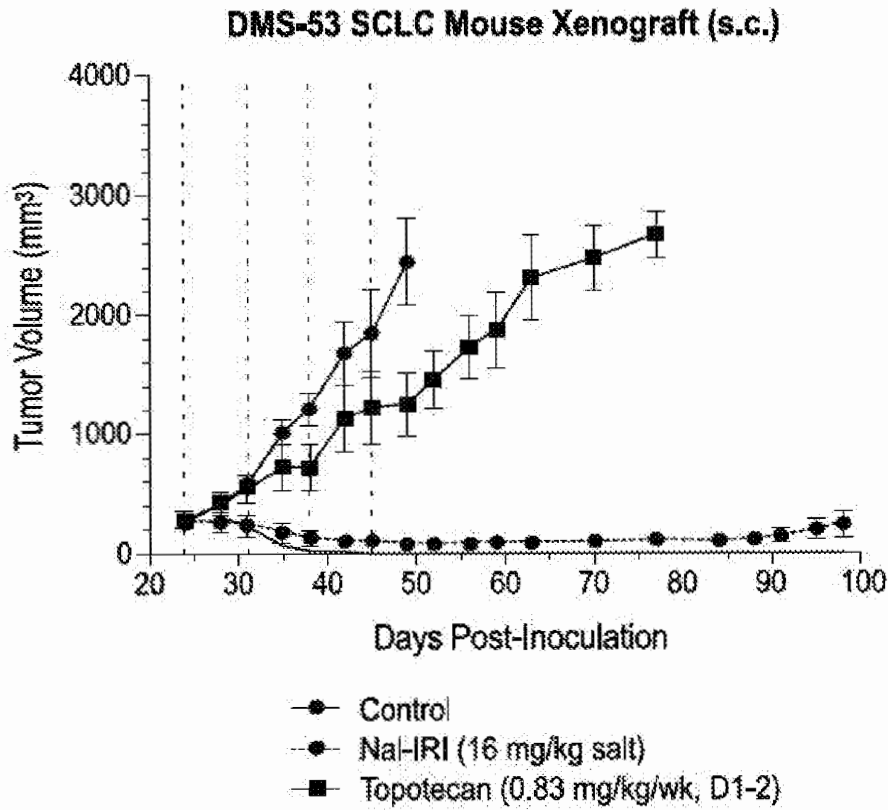


FIG. 17B

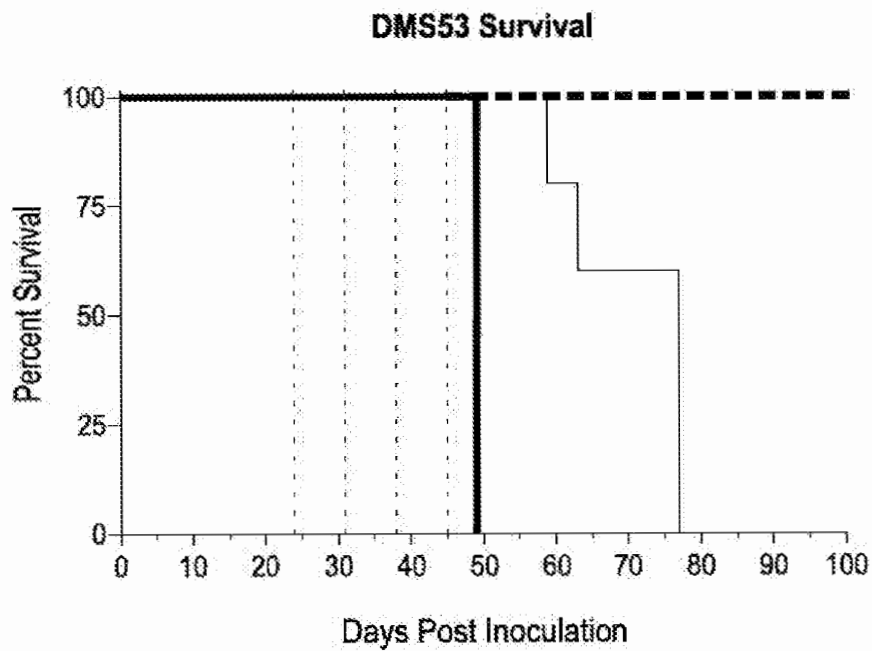


FIG. 17C

<b>Response at Day 98**</b>	<b>CR</b>	<b>PR</b>	<b>SD</b>	<b>PD</b>
<b>Control</b>	<b>0% (0/5)</b>	<b>0% (0/5)</b>	<b>0% (0/5)</b>	<b>100% (5/5)</b>
<b>Nal-IRI</b>	<b>0% (0/5)</b>	<b>60% (3/5)</b>	<b>40% (2/5)</b>	<b>0% (0/5)</b>
<b>Topotecan</b>	<b>0% (0/5)</b>	<b>0% (0/5)</b>	<b>0% (0/5)</b>	<b>100% (5/5)</b>

\*\* Response rates determined based on tumor volume change from baseline:

CR:  $\Delta TV < -95\%$

PR:  $-95\% \leq \Delta TV < -30\%$

SD:  $-30\% \leq \Delta TV < 30\%$

PD:  $\Delta TV \geq 30\%$

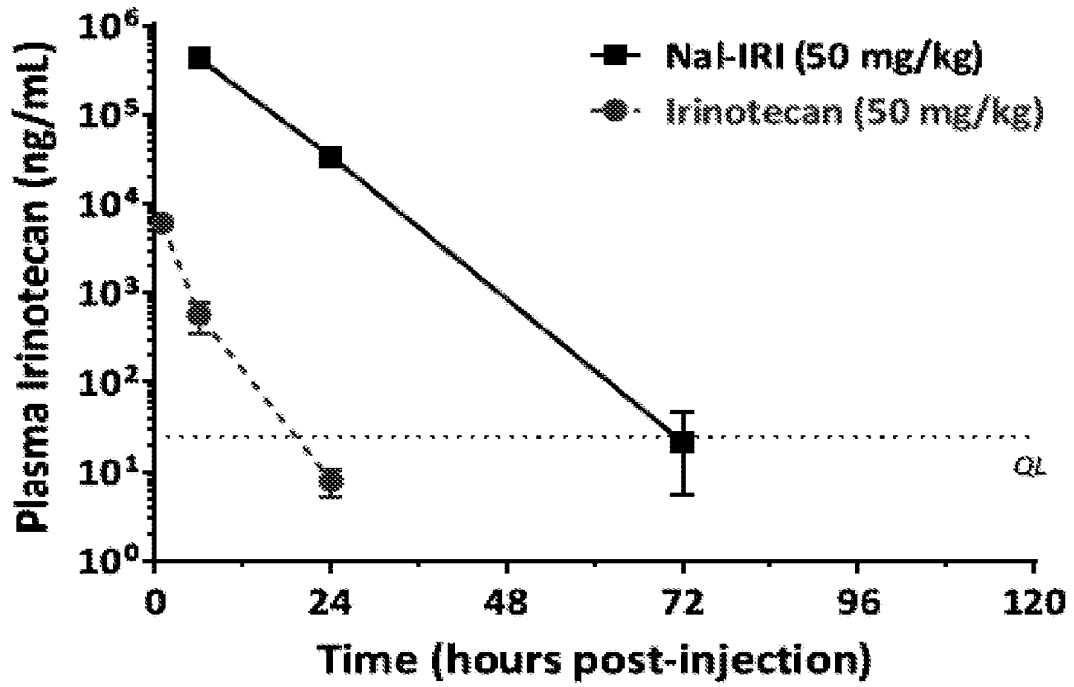


FIG. 18A

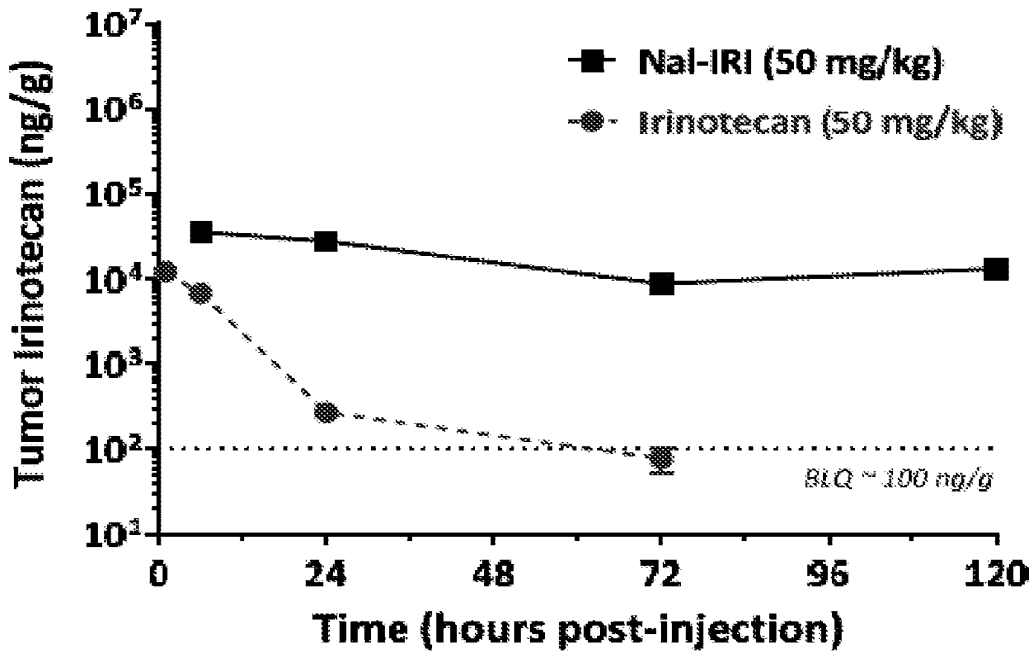


FIG. 18B



# Tumor Irinotecan @ 24 h (%ID/g)

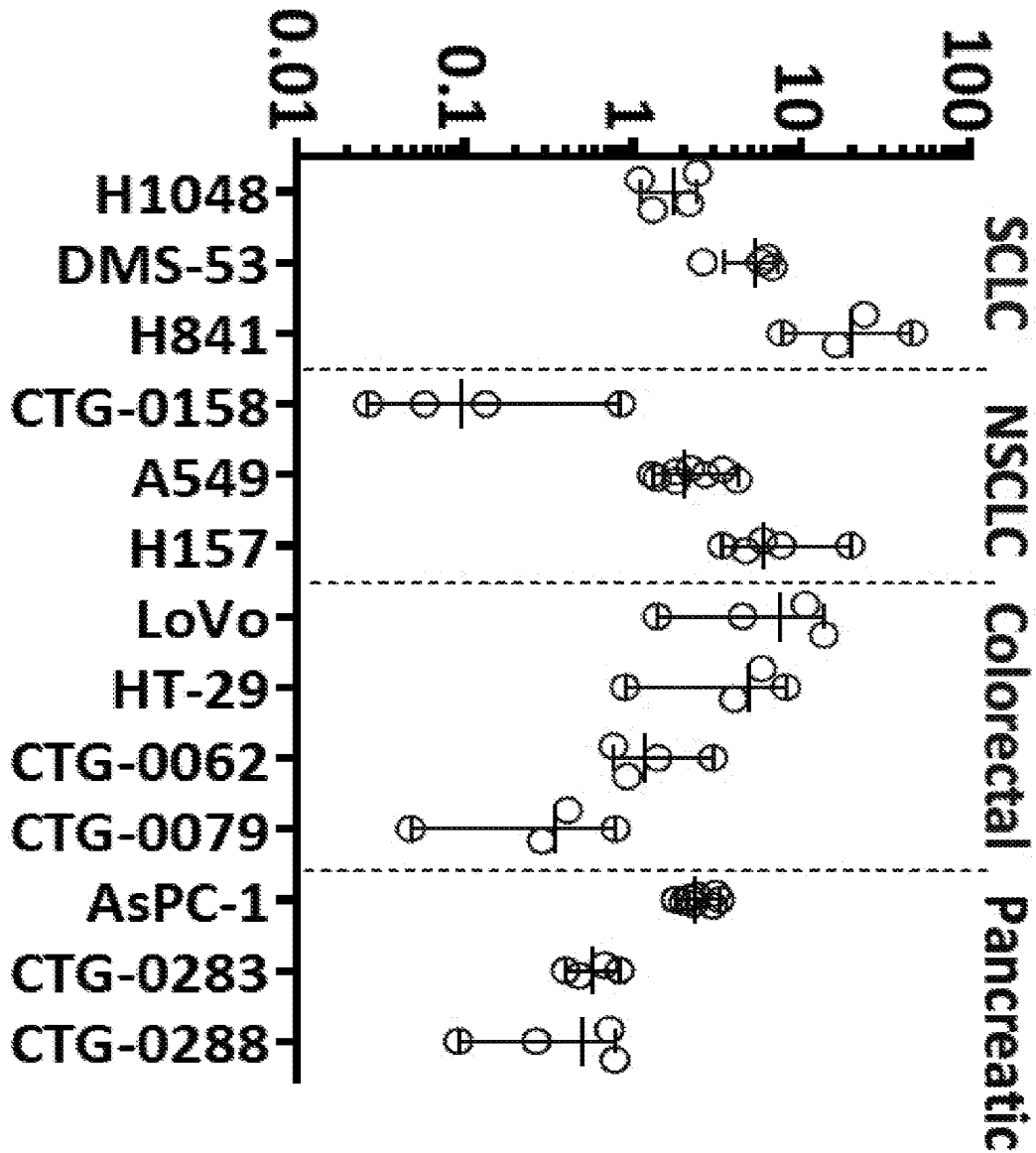
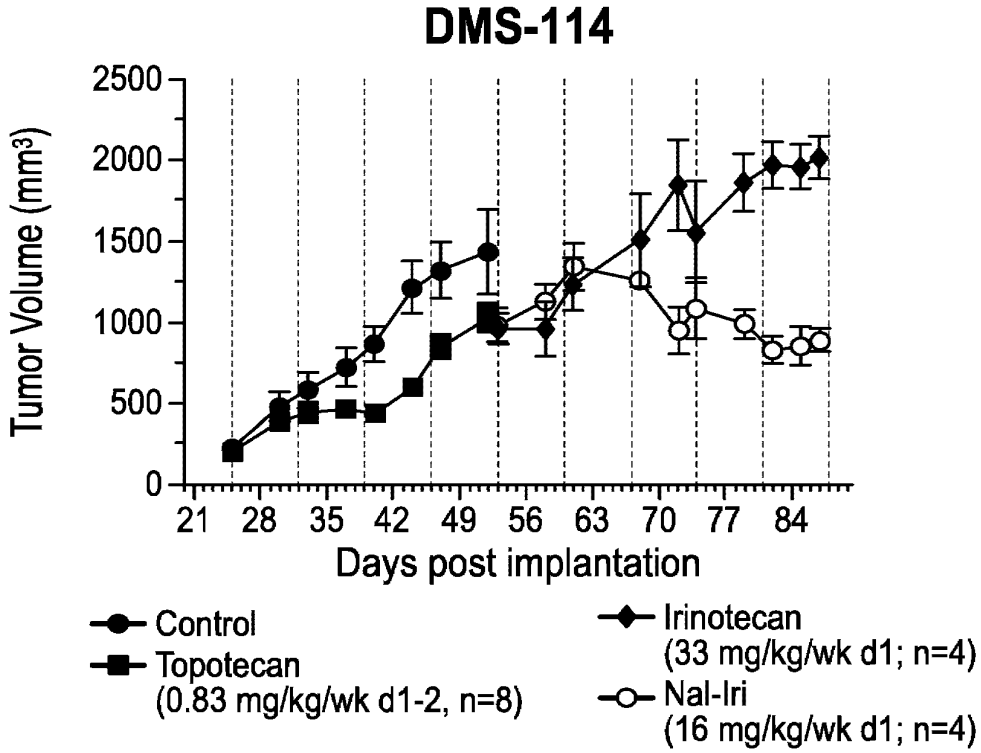
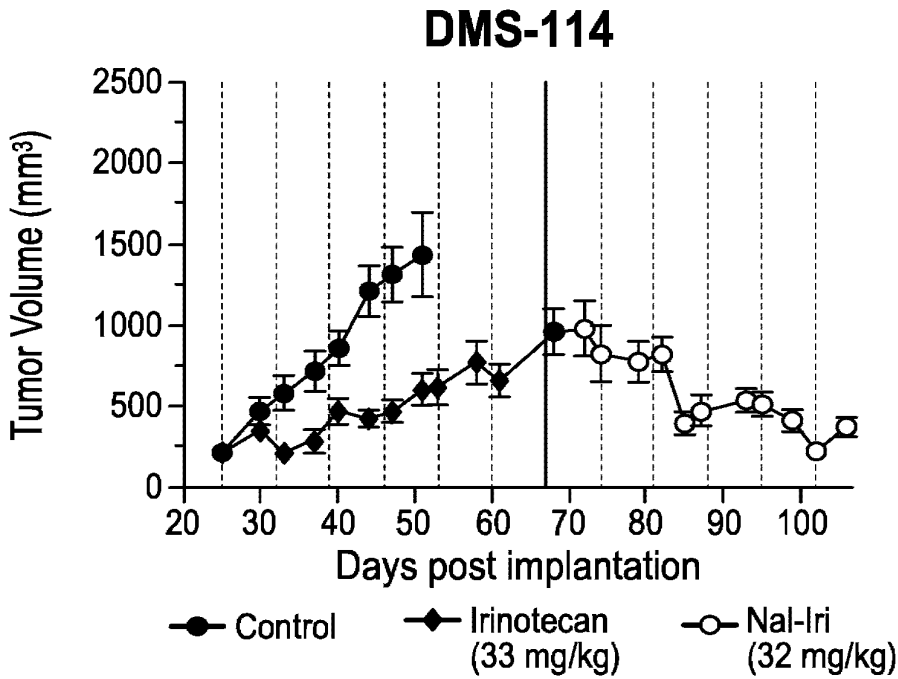


FIG. 19



**FIG. 20A**



**FIG. 20B**

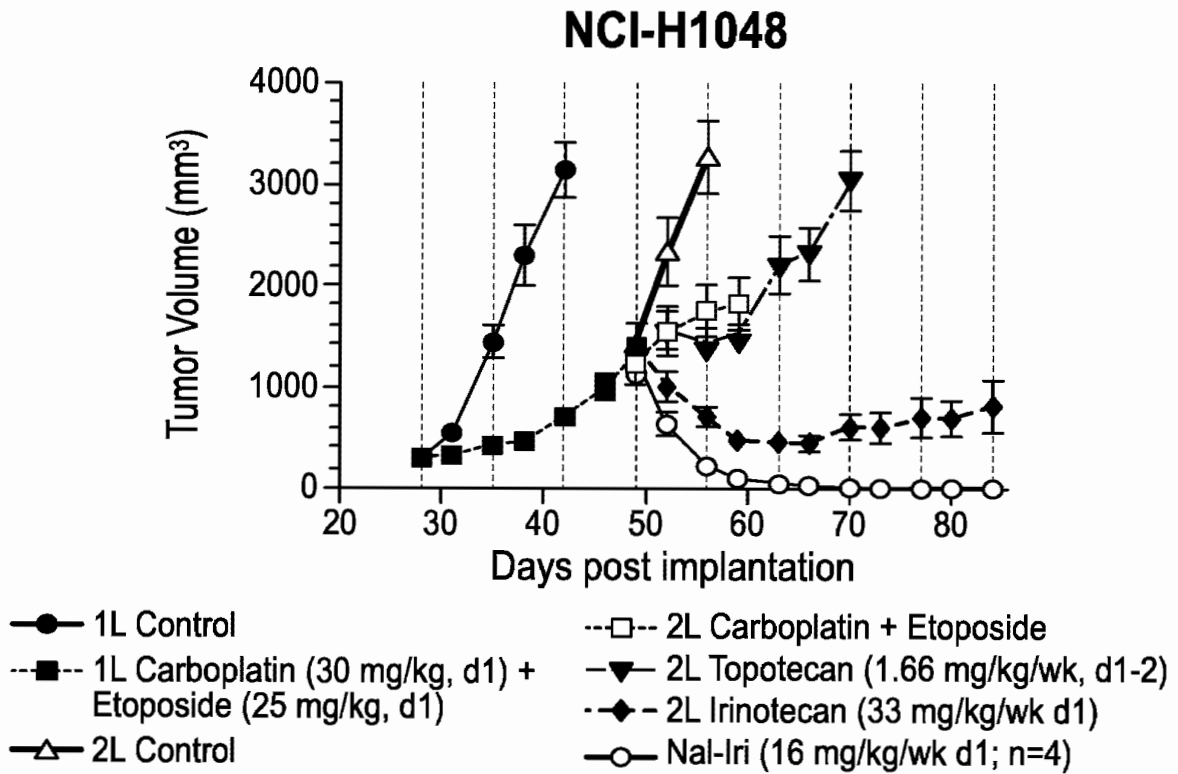


**FIG. 21A**

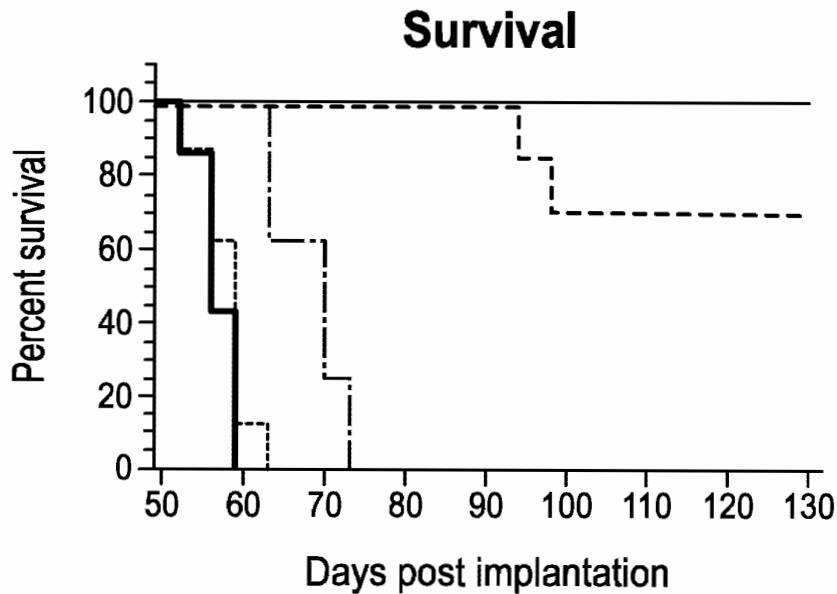


**FIG. 21B**



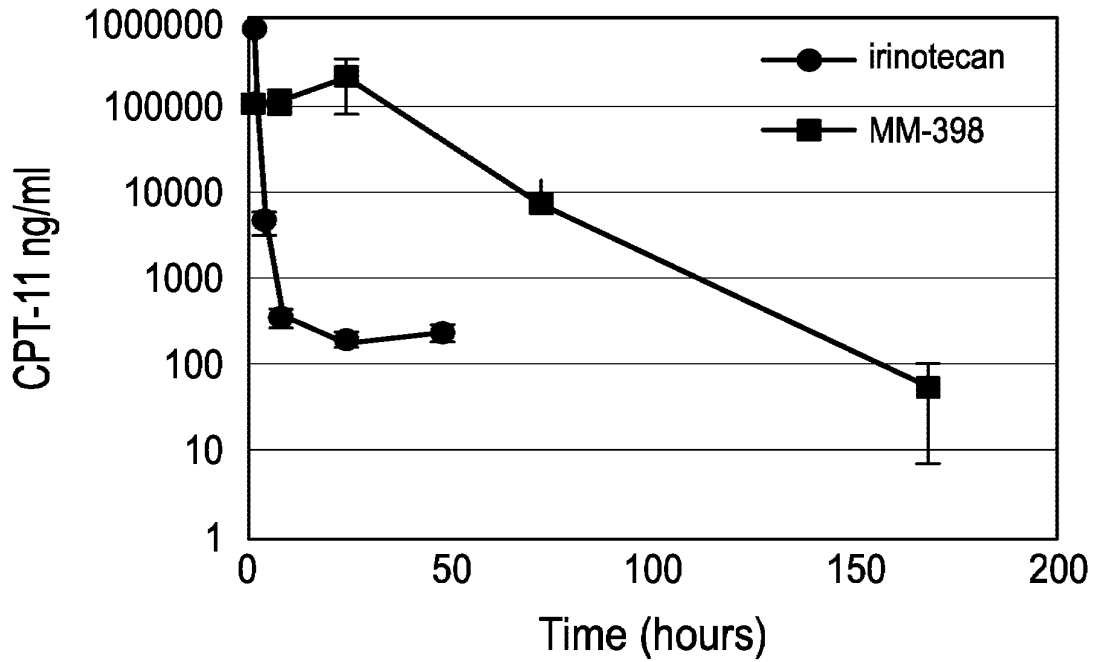


FIG. 22A

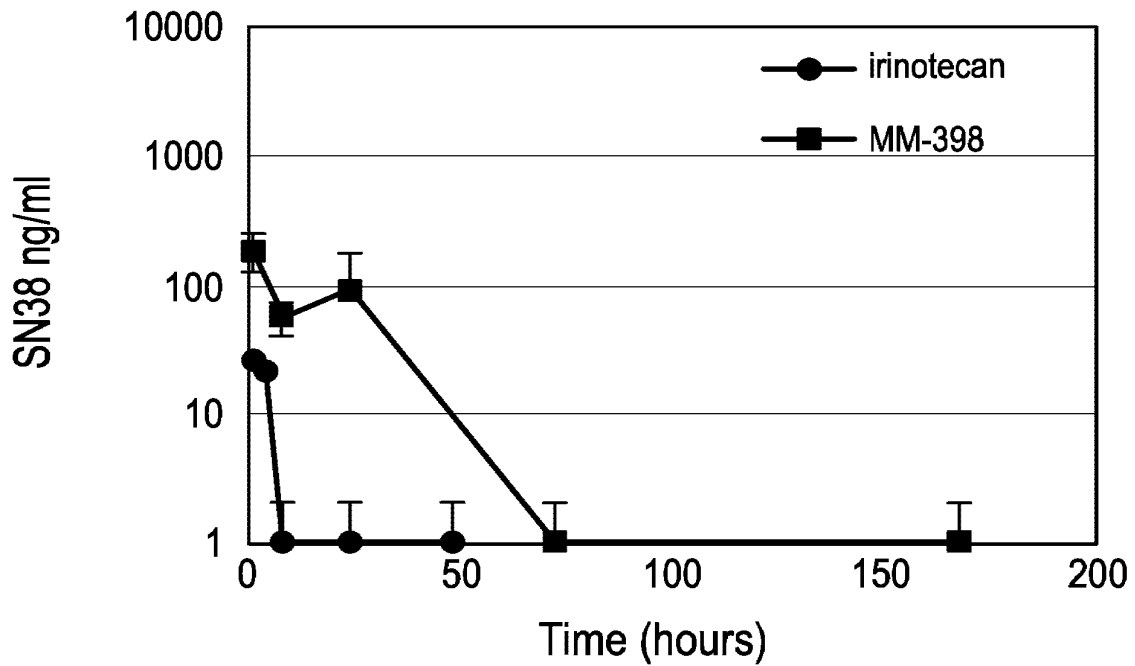


FIG. 22B

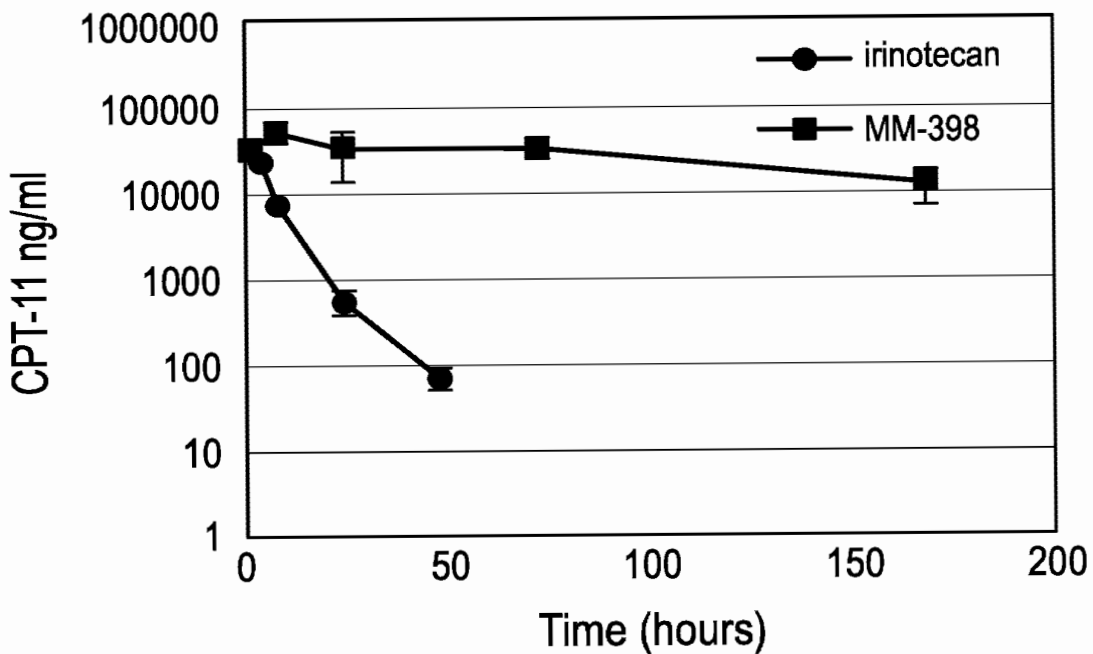


FIG. 22C

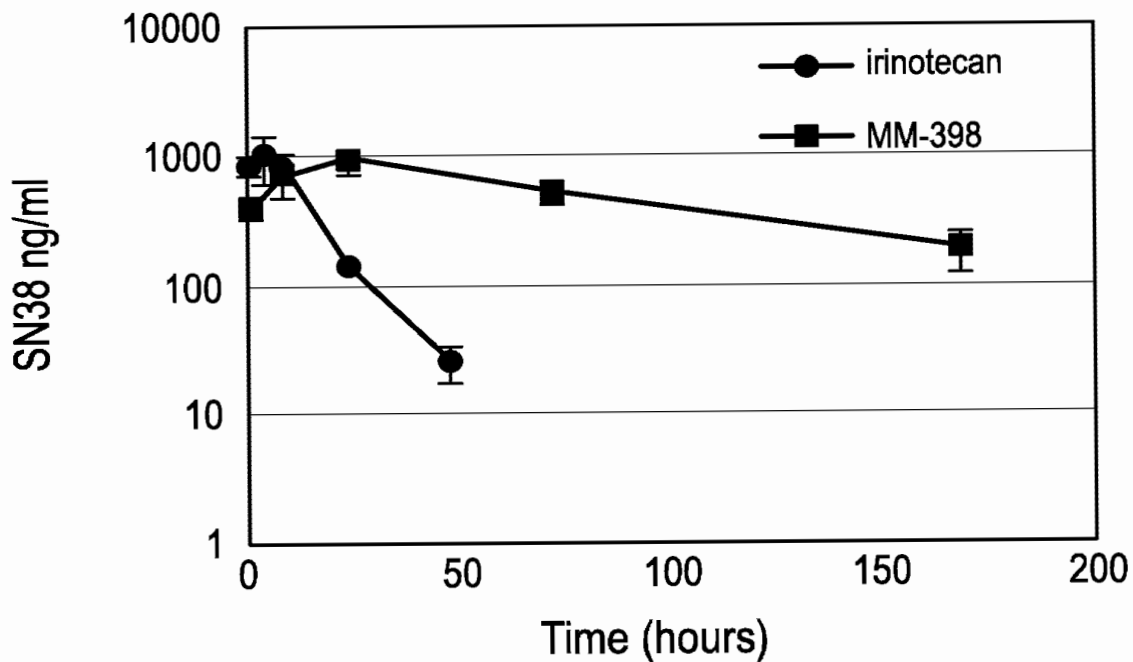


FIG. 22D

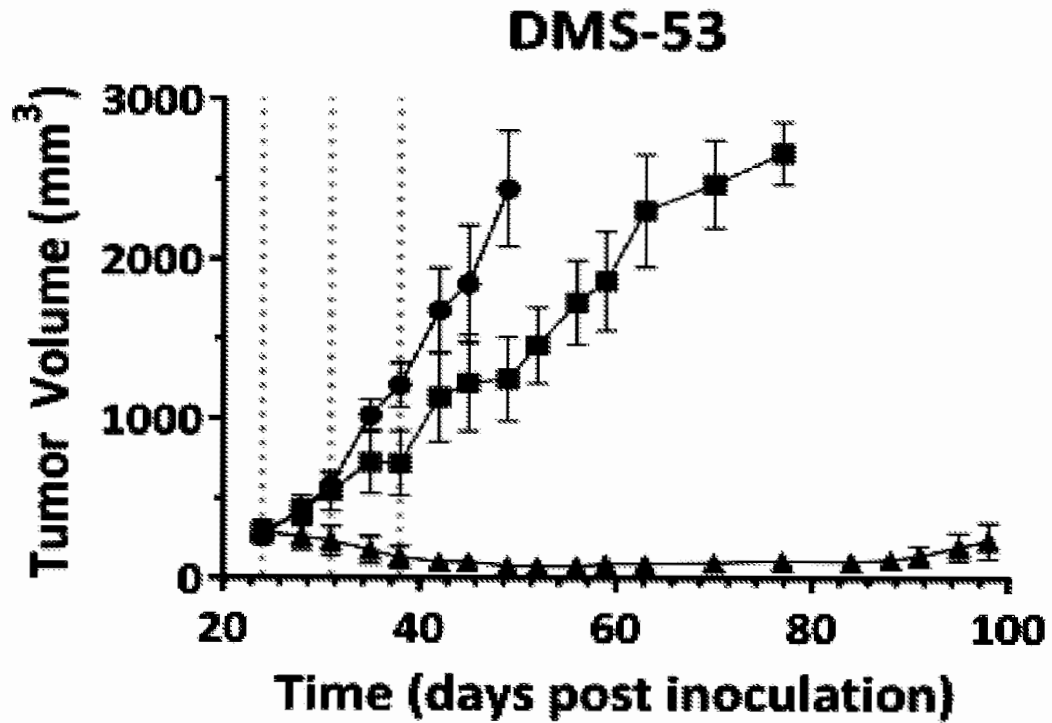


FIG. 23A

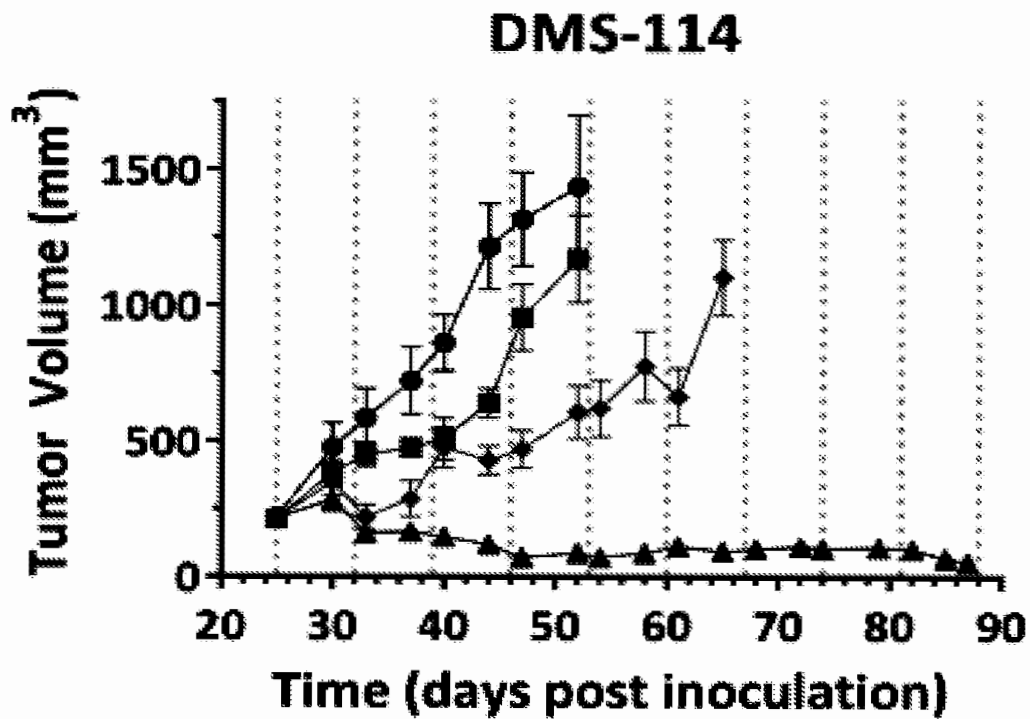


FIG. 23B

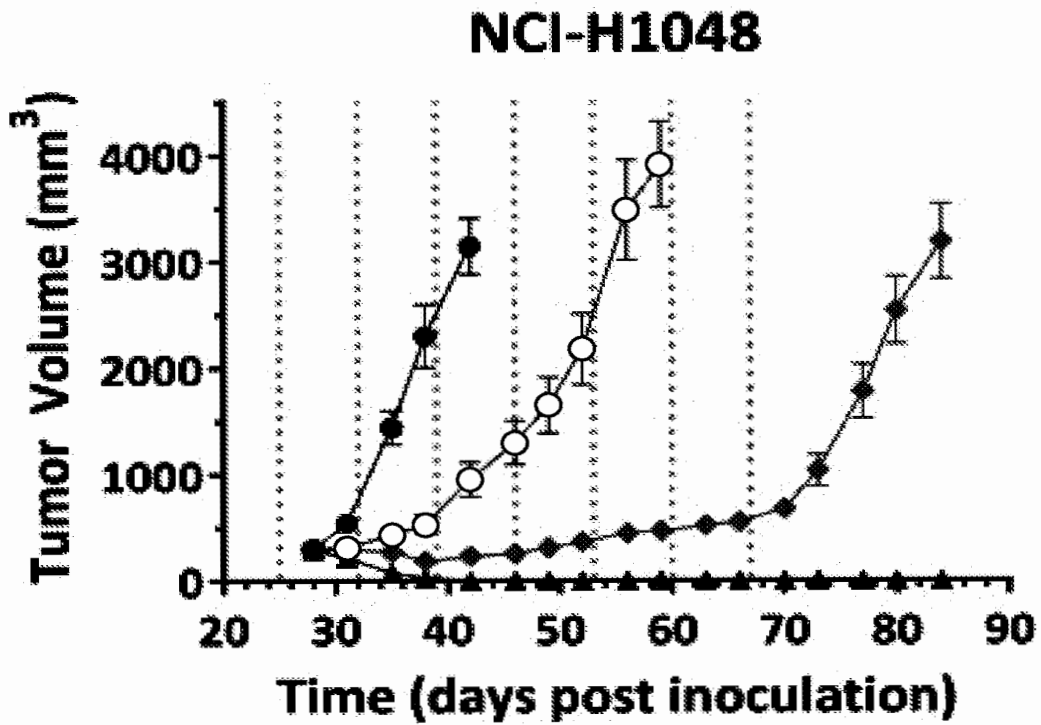


FIG. 23C

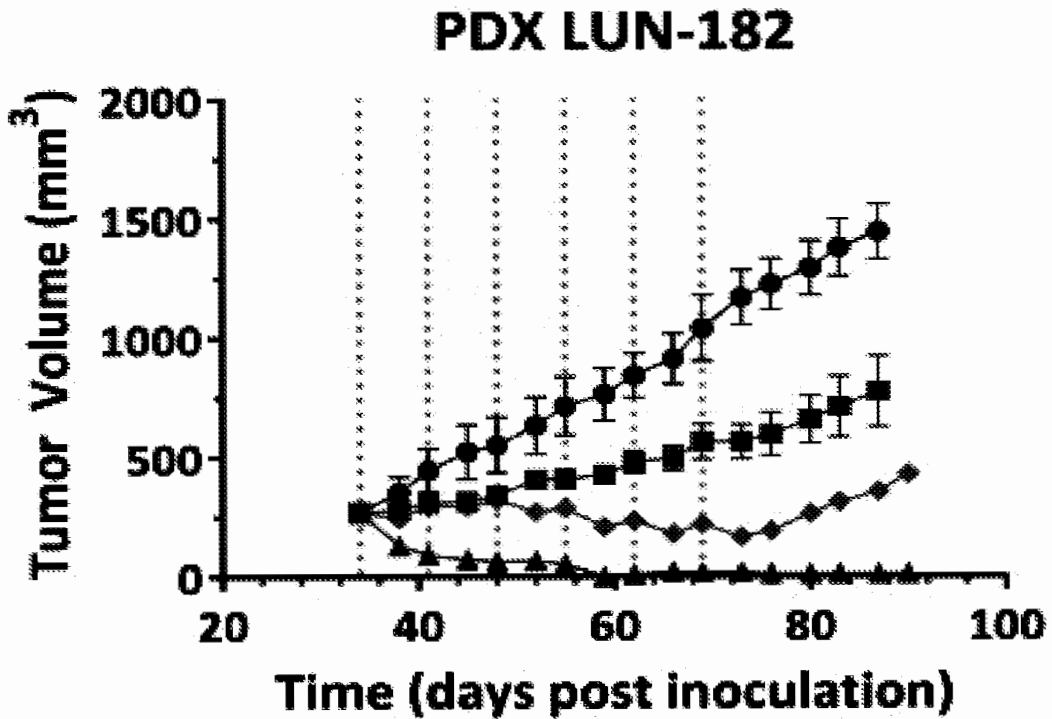


FIG. 23D

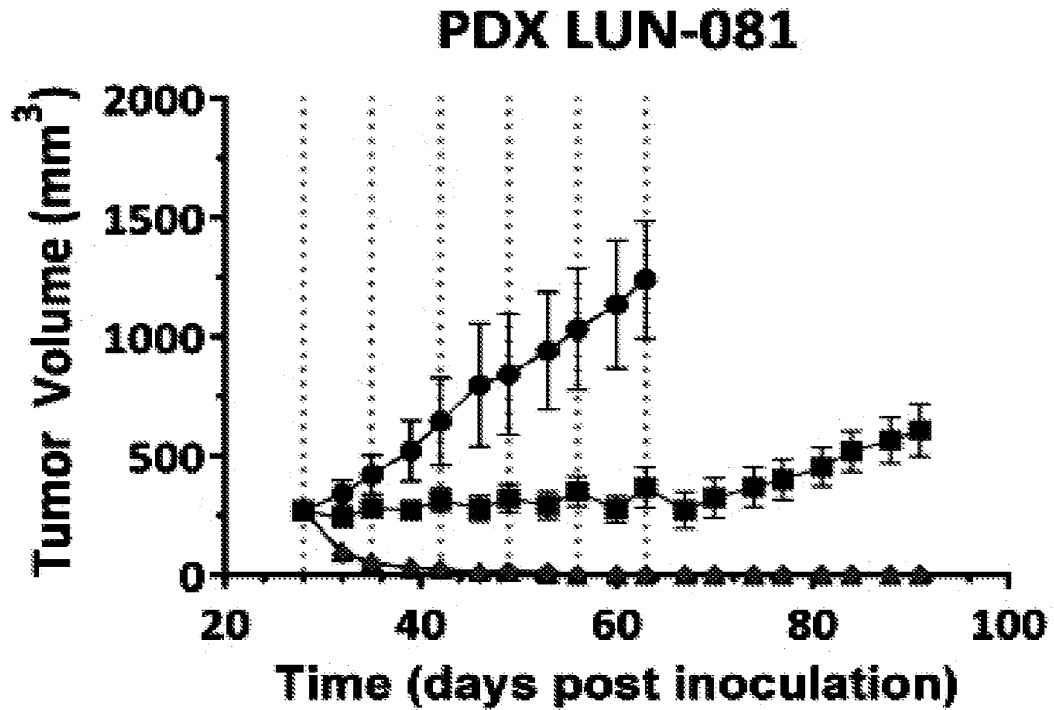


FIG. 23E

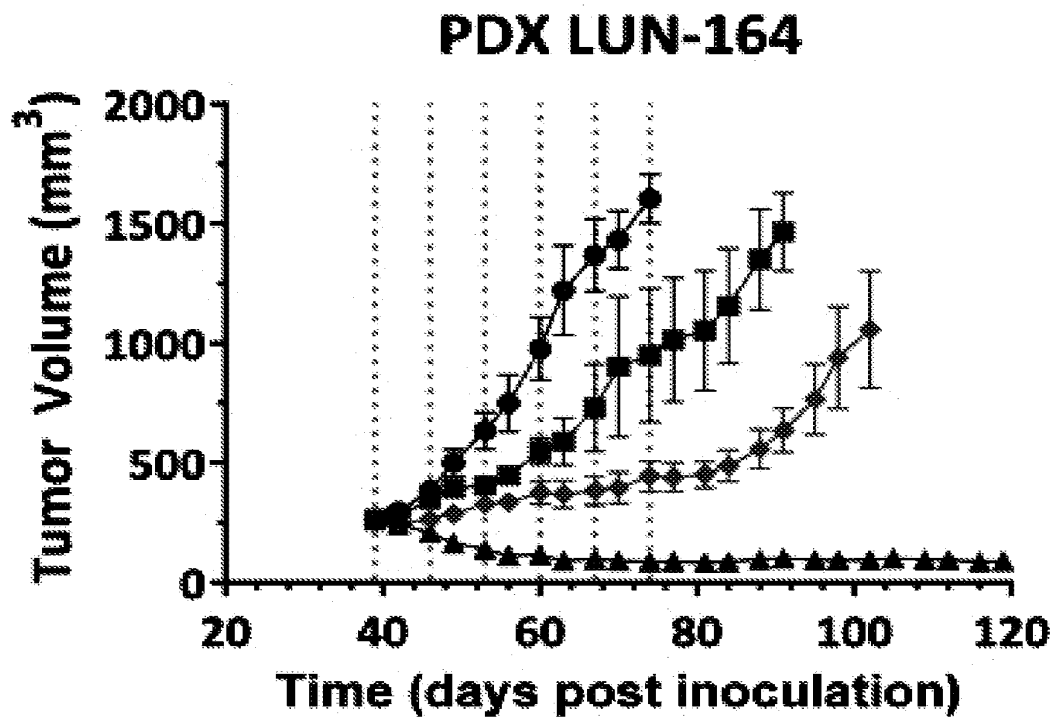


FIG. 23F

## INTERNATIONAL SEARCH REPORT

International application No

PCT/IB2017/000681

A. CLASSIFICATION OF SUBJECT MATTER  
 INV. A61K31/4745 A61P35/00 A61K9/127  
 ADD.

According to International Patent Classification (IPC) or to both national classification and IPC

## B. FIELDS SEARCHED

Minimum documentation searched (classification system followed by classification symbols)

A61K

Documentation searched other than minimum documentation to the extent that such documents are included in the fields searched

Electronic data base consulted during the international search (name of data base and, where practicable, search terms used)

EPO-Internal, BIOSIS, EMBASE, FSTA, INSPEC, WPI Data

## C. DOCUMENTS CONSIDERED TO BE RELEVANT

Category*	Citation of document, with indication, where appropriate, of the relevant passages	Relevant to claim No.
Y	<p>CHAN DANIEL C ET AL: "Abstract 4626: Evaluating the pharmacodynamics and pharmacokinetic effects of MM-398, a nanoliposomal irinotecan (nal-IRI) in subcutaneous xenograft tumor models of human squamous cell carcinoma and small cell lung cancers",            CANCER RESEARCH            ,            vol. 74            1 October 2014 (2014-10-01), XP002772684,            &amp; 105TH ANNUAL MEETING OF THE AMERICAN-ASSOCIATION-FOR-CANCER-RESEARCH (AACR); SAN DIEGO, CA, USA; APRIL 05 -09, 2014            DOI: 10.1158/1538-7445.AM2014-4626            Retrieved from the Internet:            URL:http://cancerres.aacrjournals.org/content/74/19_Supplement/4626</p> <p style="text-align: center;">-/--</p>	1-20

Further documents are listed in the continuation of Box C.

See patent family annex.

## \* Special categories of cited documents :

"A" document defining the general state of the art which is not considered to be of particular relevance

"E" earlier application or patent but published on or after the international filing date

"L" document which may throw doubts on priority claim(s) or which is cited to establish the publication date of another citation or other special reason (as specified)

"O" document referring to an oral disclosure, use, exhibition or other means

"P" document published prior to the international filing date but later than the priority date claimed

"T" later document published after the international filing date or priority date and not in conflict with the application but cited to understand the principle or theory underlying the invention

"X" document of particular relevance; the claimed invention cannot be considered novel or cannot be considered to involve an inventive step when the document is taken alone

"Y" document of particular relevance; the claimed invention cannot be considered to involve an inventive step when the document is combined with one or more other such documents, such combination being obvious to a person skilled in the art

"&" document member of the same patent family

Date of the actual completion of the international search

2 August 2017

Date of mailing of the international search report

25/08/2017

Name and mailing address of the ISA/

European Patent Office, P.B. 5818 Patentlaan 2  
 NL - 2280 HV Rijswijk  
 Tel. (+31-70) 340-2040,  
 Fax: (+31-70) 340-3016

Authorized officer

Baurand, Petra

## INTERNATIONAL SEARCH REPORT

International application No

PCT/IB2017/000681

C(Continuation). DOCUMENTS CONSIDERED TO BE RELEVANT

Category*	Citation of document, with indication, where appropriate, of the relevant passages	Relevant to claim No.
Y	<p>[retrieved on 2017-07-31] abstract</p> <p>-----</p> <p>KALRA ASHISH V ET AL: "Preclinical Activity of Nanoliposomal Irinotecan Is Governed by Tumor Deposition and Intratumor Prodrug Conversion", CANCER RESEARCH, vol. 74, no. 23, December 2014 (2014-12), pages 7003-7013, XP002772685, ISSN: 0008-5472 page 7004, right-hand column, "Antitumor activity studies" page 7004, right-hand column, "Characterizing tumors" figure 6C</p>	1-20
Y	<p>-----</p> <p>Anonymous: "Merrimack Pharmaceuticals Initiates Cross-Tumor Study to Investigate Potential Predictive Response Markers for a Developmental Nanotherapeutic Chemotherapy", Internet  , 19 December 2012 (2012-12-19), XP002772686, Retrieved from the Internet: URL:http://files.shareholder.com [retrieved on 2017-07-31] page 1, paragraph 4 - paragraph 5</p>	1-20
Y	<p>-----</p> <p>TARDI PAUL G ET AL: "Drug ratio-dependent antitumor activity of irinotecan and cisplatin combinations in vitro and in vivo", MOLECULAR CANCER THERAPEUTICS, vol. 8, no. 8, August 2009 (2009-08), pages 2266-2275, XP002772687, ISSN: 1535-7163 figure 2A page 2266, abstract</p> <p>-----</p>	1-20

# DNA Repair and Resistance to Topoisomerase I Inhibitors: Mechanisms, Biomarkers and Therapeutic Targets

M. Alagoz<sup>1</sup>, D.C. Gilbert<sup>2</sup>, S. El-Khamisy<sup>1</sup> and A.J. Chalmers<sup>\*3</sup>

<sup>1</sup>Genome Damage and Stability Centre, Science Park Road, University of Sussex, Falmer, Brighton BN1 9RQ; <sup>2</sup>Sussex Cancer Centre, Royal Sussex County Hospital, Eastern Road, Brighton BN2 5BE; <sup>3</sup>Institute of Cancer Sciences, University of Glasgow, Glasgow G12 8QQ, UK

**Abstract:** Irinotecan and topotecan are derivatives of the naturally occurring cytotoxic compound camptothecin that are used in the treatment of patients with colorectal cancer, either as single agents or in combination with radiotherapy and/or other chemotherapy drugs. They are inhibitors of DNA topoisomerase I (Top I) and exert their cytotoxic effects in replicating cells by inducing DNA strand breaks. A wide range of DNA repair proteins is involved in the recognition and repair of these breaks, and depletion or inhibition of some of these proteins increases the cytotoxic effects of Top I inhibitors. Building on these laboratory observations, ongoing translational research is aiming to establish whether this mechanistic information can be used to improve the treatment of patients with certain types of cancer. Two potential strategies are under investigation: (1) individualising treatment by evaluating levels and/or patterns of expression of DNA repair proteins that predict clinical response to Top I inhibitors, and (2) developing small molecule inhibitors of these repair enzymes to overcome tumour resistance and improve outcomes. This review summarises the current status of these research endeavours, focusing on the key roles of tyrosyl DNA phosphodiesterase 1 (Tdp1) and poly(ADP-ribose) polymerase (PARP), and examines the pre-clinical and clinical data that support the potential value of these and other DNA repair proteins as predictive markers and therapeutic targets. Since irinotecan is increasingly being combined with radiotherapy, the potential for these proteins to act as predictive biomarkers for both Top I inhibitors and radiation is proposed, and the possibility of synergistic potentiation of chemoradiation regimes by Tdp1 and/or PARP inhibitors is considered.

**Keywords:** Topoisomerase I, tyrosyl DNA phosphodiesterase 1, poly(ADP-ribose) polymerase, colorectal cancer, irinotecan, radiation therapy, chemoradiation, biomarkers.

## 1. DNA TOPOISOMERASES

DNA topoisomerases are essential enzymes that regulate the topological modification of supercoiled DNA, during important cellular processes such as transcription, replication, recombination and repair. Topoisomerase activity is mediated through a transient break introduced by a nucleophilic tyrosine of the enzyme into the phosphodiester bond of a DNA strand. This reversible covalent interaction promotes DNA relaxation by rotation of the DNA ends through the nicks followed ligation of DNA ends. Since the first discovery of topoisomerase by Jim Wang in 1971 several families of the two types of DNA topoisomerases (I and II) have been identified [1]. Topoisomerase I (Top I) catalyzes the relaxation of superhelical DNA by generating a transient single stranded break allowing the intact strand through the broken strand (Topo IA) or leaving the broken strand free to rotate around the intact strand (Topo IB). Topoisomerase II (Top II) mediates the ATP-dependent induction of nicks in both strands of the DNA duplex, followed by crossing of another double stranded DNA molecule through the transiently broken duplex [2, 3]. Their ability to relax positively supercoiled DNA allows them to play a major role both in DNA replication and transcription [4].

### The Role of DNA Topoisomerases During Replication

DNA replication in eukaryotic organisms is regulated by assembly and organization of specific protein complexes on the origins of DNA replication. DNA topoisomerases are required for the initiation of replication at the ori C of *Escherichia coli* [5] and this topological status is regulated by the opposing activities of Topo IA and a DNA gyrase [6, 7]. Direct involvement of Top I *via* interaction with the relevant origin-specific binding protein has been shown for the activation of origins of the viral genomes of SV40 [8], EBV [9] and BPV [10]. During initiation of DNA replication in eukaryotes the topoisomerase associates with the origin of replication, regulating topological modification prior to

origin activation. For example, the human DNA replication origin located in the lamin B2 gene interacts with the DNA topoisomerases I and II and the ORC2 subunit of the pre-replication complex. This interaction is modulated in a cell cycle specific manner and inhibition of topoisomerase I activity abolishes origin firing of lamin B2 [11]. The role of DNA topoisomerases during initiation of replication *via* origin firing may function to facilitate DNA unwinding and to increase accessibility of the replication initiation proteins.

Topoisomerases are also required for replication fork progression, during which they release torsional stress ahead of the replication machinery. Different subfamilies of topoisomerases contribute to the replication elongation. For example, DNA gyrase and/or Topo IV fulfil this role in bacteria [12-15], whereas in eukaryotes Topo IB and Topo II $\alpha$  are responsible for relaxation of positive supercoils [16]. As replication forks progress, the un-replicated regions between emerging forks need to be resolved before chromosome segregation. Type II topoisomerase untangles these linked regions of DNA [17-21].

Based on *in vivo* and *in vitro* studies, Top IA and Top II have been suggested to play roles in replication termination [19, 22-25]. In eukaryotes, Top II coordinates replication fork progression and fusion at termination regions to resolve torsional stress thus counteracting abnormal genomic transitions. In *S. cerevisiae*, Top II appears to facilitate fork progression at termination elements [26].

### DNA Topoisomerases During Transcription

The other important cellular role of topoisomerases is to relax the accumulation of superhelical tension during transcription. As transcription proceeds, DNA in front of the transcription bubble becomes positively supercoiled whereas behind the bubble it becomes negatively supercoiled. This change in DNA topology has functional consequences in the cell, such as the activation or repression of transcription and the successful progression of replication forks [27-31]. The topological changes occurring as a consequence of transcription are released by topoisomerases. Top IB relaxes positive supercoils in front of the transcribing polymerase in eukaryotes [32-35]. Furthermore, Top IIA has been

\*Address correspondence to this author at the Institute of Cancer Sciences, University of Glasgow, Glasgow G12 8QQ, UK; Tel: +44 141 301 7097; Fax: +44 141 301 7095; E-mail: Anthony.Chalmers@glasgow.ac.uk



shown to interact with RNA polymerases which direct Top IA localization to the negatively supercoiled transcription region [35, 36]. Top IB is also required for the removal of negative supercoiling and of RNA-DNA hybrids (R-loops) [37, 38]. In addition, Topoisomerases have been implicated in the regulation of promoter activity and nucleosome remodelling. In eukaryotes, Top IB plays an important role in the control of gene expression [39, 40]. Inactivation of Top IB in *S. cerevisiae* leads to histone-specific acetylation and methylation which increases the transcription of telomere-proximal genes [41].

### DNA Topoisomerase Inhibitors

Topological modification of DNA mediated by topoisomerases involves the formation of a covalent phosphotyrosine intermediate in which the topoisomerase is covalently linked to DNA termini; this important structure is termed a 'cleavage complex'. Collision of cleavage complexes with the replication machinery, DNA polymerases and/or DNA repair proteins prevents religation of the DNA ends, generating clastogenic DNA lesions that, if unrepaired, can induce cell death. Agents that poison topoisomerase activity are cytotoxic and have been widely used in the treatment of cancer: a degree of tumour-specificity arises from the increased replication activity that is an inherent feature of many cancer cells.

Topoisomerase inhibitors are assigned to one of two classes on the basis of their mode of action: inhibitors, which inhibit enzyme activity, and poisons which stabilize DNA cleavage complexes [42]. The natural product camptothecin was first discovered as a poison because of its potent antitumor activity [43]. Top I poisoning by the camptothecin derivatives topotecan and irinotecan has been widely used in the treatment of cancer. The mechanism of Top I poisoning by camptothecin derivatives is mediated by their capacity to stabilise the covalent enzyme-DNA complex and block religation of the two broken DNA ends [44, 45]. In rapidly dividing cells, the cytotoxic effects of Top I poisons are S phase specific and are mediated through collision of DNA replication forks with trapped Top I-DNA complexes, converting DNA single-strand breaks into potentially lethal, irreversible double strand DNA breaks, and ultimately promoting apoptotic cell death [46, 47]. The DNA breaks induced by irinotecan cause cell cycle arrest in S and G2 phase. Inefficient repair of the replication-associated breaks arising from Top I inhibition promotes apoptosis.

The second class of topoisomerase inhibitors induce their effect by impairing enzyme activity. Bisdioxopiperazines and radicicol belong to the group of anticancer agents that associate with ATP-bound eukaryotic Top II and convert the enzyme into an inactive, salt-stable clamp around DNA [48, 49]. Topoisomerase activity is regulated by post translational modification such as phosphorylation [50], acetylation [51], sumoylation [52] and ubiquitylation [53]. Topoisomerase poisoning promotes sumoylation and ubiquitylation of Top I and Top II in response to DNA damage and targets these enzymes for processing and/or degradation. Disruption of these modifications results in impaired repair of topoisomerase-induced DNA breaks. The regulation of eukaryotic topoisomerases and their processing enzymes by posttranslational modification is the subject of ongoing investigation, and promising new insights into the action of these enzymes may enable the development of novel anti-cancer drugs.

### Current Clinical Utility of Topoisomerase Poisons

The topoisomerase I poison irinotecan is widely used in metastatic colorectal cancer (mCRC) and is the subject of ongoing trials (concurrent with radiotherapy) in locally advanced rectal cancer. There is growing interest in its use in small cell lung cancer (with evidence of increased efficacy over etoposide regimens) and a number of other tumour types. It is less appreciated that the widely used anthracyclines (doxorubicin, idarubicin, mitoxantrone) also

function as Top I inhibitors amongst a range of other mechanisms of action.

### History and Efficacy of Irinotecan in Colorectal Cancer

Landmark clinical trials reported in 2000 demonstrated the efficacy of Irinotecan-containing chemotherapy regimens in metastatic colorectal cancer [54, 55]. Colorectal cancer is responsible for 16,000 deaths per year in the UK and 58,000 in the US (GLOBOCAN 2008: <http://globocan.iarc.fr/>). Outcomes for patients with metastatic disease at presentation or relapse remain poor – despite the improvements in surgical metastasectomy (for example resection of liver metastases) the majority of patients succumb to disseminated disease. Until the last decade only the fluoropyrimidine 5-fluorouracil (5FU – typically given with leucovorin) had proven efficacy in bowel cancer. The turn of the century saw the introduction of combination regimens utilising one of two novel drugs: either irinotecan or the third generation platinum compound oxaliplatin [56], with extension of overall median survival in some studies to 24 months [57].

A number of studies have subsequently compared the efficacy of these treatment options. The MRC Fluorouracil, Oxaliplatin, and CPT11 (irinotecan)—Use and Sequencing (FOCUS) study recruited 2135 previously untreated patients with mCRC and tested combinations of irinotecan or oxaliplatin with 5FU against 5FU alone in first line therapy and found broadly similar responses to each combination, with both giving improved response rates (though not statistically different median survival) over single agent 5FU [58]. The Dutch CAIRO study [59] randomly assigned 820 patients with mCRC to either sequential treatment (capecitabine – the oral pro-drug of 5FU, irinotecan at progression and then combination capecitabine and oxaliplatin) or combination treatment (capecitabine-irinotecan then capecitabine-oxaliplatin at progression). Again responses were seen after progression on the other drugs and no significant differences in survival were observed when these strategies were applied to the overall population. In both studies, response rates to combination treatment were around 40%, with disease control rates (including patients whose measurable tumours stabilised) of up to 80% in the first line setting and 60% subsequently. These findings present patients and clinicians with a dilemma: the existence of two combination treatment regimes with equal efficacy (albeit with differing toxicity profiles) and evidence of a lack of complete cross-resistance (to irinotecan and oxaliplatin) within individuals suggests that specific tumours may differ in their sensitivity to these drugs. Predictive markers of response (and ideally toxicity) are therefore required to optimise and individualise patient treatment.

### Irinotecan in the Adjuvant Treatment of Colorectal Cancer

Unlike oxaliplatin-5FU combinations, where six months of chemotherapy after apparently curative resections of high risk (node positive) colorectal cancer improves overall survival [60], it has been harder to demonstrate benefit for irinotecan in the adjuvant setting [61]. This is somewhat surprising given the apparent equivalence between the two combinations in the setting of advanced disease. Again, a better understanding of the molecular determinants of treatment response may yet identify a role for Irinotecan in the adjuvant setting. Early reports that Top I expression might identify a group of tumours that benefit from irinotecan regimens [62] and the observation that mismatch repair status might predict for improved efficacy [63] require further study and will be discussed elsewhere within this review.

### Concurrent Irinotecan and Radiotherapy in Locally Advanced Rectal Cancer

Rectal cancers present multidisciplinary teams with an additional challenge, namely the difficulty of obtaining complete surgical resection with clear margins. Failure to achieve this goal is

associated with high rates of debilitating local recurrence and distant relapse. The introduction of Magnetic Resonance Imaging (MRI) pre-operative staging [64] now allows identification of locally advanced tumours for which immediate surgery would not be expected to achieve complete clearance. In these situations, pre-operative radiotherapy is used to reduce the risk of local recurrence. Administration of concurrent 5FU chemotherapy further improves outcomes and is now considered standard of care [65, 66]. Up to 25% of rectal cancers present with an MRI-defined threat to the circumferential resection margin; in these patients surgical resection with clear margins is achieved in only 65% of cases after 5FU based pre-operative chemo-radiotherapy [67]. Prospective clinical trials have investigated whether these treatment paradigms can be improved by the addition of either oxaliplatin or irinotecan. Phase I/II studies incorporating irinotecan, 5FU and radiotherapy in rectal cancer have indicated improved efficacy over 5FU chemo-radiotherapy alone and have proved to be deliverable in terms of acute toxicity [68-70]. The currently recruiting UK ARISTOTLE study is a phase III randomised trial testing the addition of irinotecan to standard 5FU-based chemo-radiotherapy for the treatment of locally advanced rectal cancer. Even if this trial confirms that overall outcomes are improved by the use of irinotecan, the existing data indicate strongly that not all patients will benefit and that predictive markers of efficacy will be required to optimise treatment choices for individual patients and their tumours.

#### Irinotecan in Small Cell Lung Cancer

Current standard treatment protocols consist of radical chemo-radiotherapy for limited stage SCLC and chemotherapy for extensive stage disease with consolidation radiotherapy where possible. Chemotherapy regimens have for many years combined the Top II poison etoposide with a platinum compound (either cisplatin or carboplatin). More recently, attention has shifted to replacing etoposide with irinotecan.

One of the first randomised trial comparing irinotecan-cisplatin with etoposide-cisplatin in extensive stage SCLC was stopped early owing to a significant improvement in survival in the irinotecan-containing arm [71]. Improved outcomes for irinotecan combinations over etoposide based regimens were also reported by Hermes and co-workers [72]. However subsequent studies have failed to confirm these findings [73-75]. On balance the current view is that both regimens have similar efficacy in the first line setting, but differing toxicity profiles.

#### Anthracyclines as Topoisomerase Inhibitors

Anthracyclines (e.g. daunorubicin, doxorubicin, idarubicin) are widely used in the treatment of a range of cancers, in particular breast and haematological malignancies. They exert their cytotoxic effect through a number of mechanisms, primarily DNA intercalation [76, 77], with the capacity of anthracyclines to inhibit Top I function has also been described [78] although recently their effects on Top II have gained prominence both in terms of mediating cardiotoxicity and second malignancy risks but also because genomic amplification of Top II within tumours has been proposed as a biomarker of response to anthracycline chemotherapy in breast cancer [79-82]. Effects of this group of agents on Top I function will not be considered further in this review.

#### The Repair of Topoisomerase-Mediated DNA Damage

DNA breaks induced by topoisomerase activity are deleterious to cells and their inefficient repair can cause cell death. Impaired repair of Top1-mediated DNA breaks has been linked to human neurological disorders including cerebellar degeneration [83], mental retardation [84] and microcephaly [85], (reviewed in El-

Khamisy [86]). There are two main pathways by which cells remove protein-linked DNA breaks in order to initiate subsequent repair. One of the mechanisms involves the nucleolytic cleavage of DNA to remove topoisomerases and a fragment of DNA [87]. This non-specific nucleolytic cleavage of DNA can be achieved by double strand break repair proteins such as the MRN complex, XPF/ERCC1, Mus81, SLX1/SLX4, CtIP and ARTEMIS [87-91]. Double stranded DNA breaks arising from topoisomerase activity can be repaired by the homologous recombination and/or non-homologous end joining pathways. In cycling cells, most unrepaired Top1-SSBs are converted to Top1-DSBs and repaired by homologous recombination during DNA replication. Non-homologous end joining has been proposed to process overlapping Top1-SSBs outside S phase. The relative contribution of these two pathways is not clearly understood and is likely dictated by a variety of cellular factors including cell cycle status.

Removal of trapped topoisomerase from DNA can also be achieved by a more specific, error-free mechanism. The covalent linkage between DNA and topoisomerase can be hydrolysed enzymatically by tyrosyl-DNA phosphodiesterases. The prototype activity was assigned to the yeast tyrosyl DNA phosphodiesterase 1 (Tdp1) and the human homologue of the yeast enzyme has been associated with defects in the repair of Top1 DNA breaks [92-94]. Mutations of Tdp1 and the consequent defect in repairing Top I breaks is associated with the neurological disease Spinocerebellar Ataxia and Axonal Neuropathy 1 "SCAN1" [83, 92, 93, 95]. More recently, Top II mediated breaks have been shown to be processed by an enzyme acting in a similar manner, named Tdp2 [96, 97].

Tdp1 repair capacity has been associated with the proteins involved in single stranded DNA break repair and recent work has shown that Tdp1 function in human cells is regulated by posttranslational modifications, such as phosphorylation, and SUMOylation [98,99,100]. This is intriguing since SUMOylation has also been shown to regulate Top I activity in response to exogenous DNA damage. Thus modulating key players in the SUMO pathway may provide an attractive strategy for therapeutic intervention in conjunction with Top I and/or Tdp1 inhibitors.

Another form of protein modification is the attachment of poly(ADP-ribose) polymers in response to DNA damage. Poly ADP ribose polymerase 1 (PARP-1) plays a role in DNA repair through interactions with XRCC1 [98, 99], DNA ligase III [100], and Werner syndrome protein [101]. PARP-1 has also been reported to bind to Top I [102, 103] and it has been suggested that PARP-1 automodification functions to regulate the interaction between PARP-1 and Top I and hence can modify Top I activity in response to DNA damage [104]. Inhibition of PARP-1 causes a delay in the repair of camptothecin induced DNA breaks [105], but in Tdp1 deficient cells PARP inhibition appears not to affect sensitivity to camptothecin, suggesting that these two enzymes function in the same pathway [106]. A more recent study has shown that expression of a dominant-negative PARP-1 construct in cells with reduced expression of Tdp1 (due to a constitutively expressed microRNA that targets Tdp1) did not modulate cell sensitivity to camptothecin [107]. These findings support the hypothesis that Tdp1 and PARP interact closely and mediate their repair action through a common pathway; this will be explored in more detail in the next section.

#### PRE-CLINICAL EVIDENCE FOR THESE MOLECULES MODULATING EFFECT OF TOPOISOMERASE INHIBITORS

The repair mechanisms involved in resolving DNA lesions induced by inhibition of Top I are complex and involve a degree of overlap and/or redundancy. The initial processing of the Top I cleavage complex is clearly of critical importance in determining cellular responses to Top I inhibitors. However, failure to resolve

this complex generates DNA strand breaks that can subsequently be resolved by downstream repair pathways. In replicating tumour cells the key event appears to be collision of unresolved cleavage complexes with DNA replication forks, a process that generates complex double stranded lesions that require processing and repair by the homologous recombination repair (HRR) [108, 109]. In this section the various proteins and pathways that modulate sensitivity to Top1 inhibitors will be discussed, and the clinical implications considered. Pre-clinical studies have shown that inhibition or knockdown of a variety of repair proteins can increase the cytotoxic effects of Top I inhibitors, but the results have not always been consistent and do not always correlate with the clinical biomarker data that will be discussed later.

As the target, Top I is clearly required for the cytotoxic effects of these drugs to be manifest. Top I is frequently upregulated in cancers including colorectal tumours, while loss of Top I has not been reported. However a number of mutations in Top I have been shown to confer resistance to camptothecin and/or irinotecan *in vitro* [110, 111]; these mutations have generally either been located close to the catalytic site of the enzyme or have been proposed to affect the flexibility of its linker domain and hence the interaction with the SN38 species. However, these experimental findings probably have limited clinical relevance: there has only been one reported finding of mutated Top I in a clinical specimen, and this was in a patient with non-small cell lung cancer [112].

There is robust pre-clinical evidence that Tdp1 levels and activity influence cellular sensitivity to Top I inhibitors [92]. As described earlier, Tdp1 catalyses the removal of Top I from DNA, generating a single stranded break that is a suitable substrate for repair by the XRCC1 dependent single strand break repair (SSBR) pathway. XRCC1 defective cells, such as the EM9 Chinese hamster cell line, are hypersensitive to Top I inhibitors, and restoration of XRCC1 function reverses this sensitivity both by facilitating SSBR and by enhancing activity of Tdp1 itself [113]. Other components of the SSBR pathway such as polynucleotide kinase (PNK), DNA polymerase  $\beta$  and DNA ligase III are thought to contribute to the processing and repair of breaks arising from Top I inhibition, but there is little data available to illustrate the extent to which sensitivity is dependent on these factors. While aprataxin has been demonstrated to contribute to repair of DNA single strand breaks generated by oxidative damage or alkylating agents, deletion of this gene did not appear to interfere with resolution of DNA breaks induced by camptothecin in mouse neural cells [114]. This observation is at odds with the findings of an earlier study in colorectal cancer cell lines [115] in which camptothecin sensitivity correlative inversely with aprataxin expression and with the clinical observation that low levels of aprataxin in colorectal cancer specimens are associated with increased irinotecan sensitivity [116]. These discrepancies might be explained by an increased dependency on the DNA end-processing activity of aprataxin in rapidly proliferating cancer cells, which may also have impaired cell cycle checkpoints and hence be more susceptible to subtle repair defects that delay rather than abolish DNA repair function.

Staying with the SSBR pathway, there has been a huge amount of interest in the effects of chemical inhibitors of PARP-1 on cellular responses to Top I inhibitors. The precise role of PARP-1 and the related protein PARP-2 in the detection, processing and repair of Top I-associated DNA damage is still under investigation, but there is wealth of pre-clinical data illustrating the ability of PARP inhibitors to potentiate the cytotoxicity of agents including topotecan, camptothecin and irinotecan [105, 117, 118]. The mechanisms involved are complex and do not appear to be restricted to the involvement of PARP-1 in SSBR.

PARP-1 and PARP-2 bind to breaks and nicks in DNA, a process that activates their catalytic function, which is the addition of long, branching chains of poly(ADP-ribose) molecules to a range of nuclear target proteins. Among these targets are Top I and PARP-1 itself – automodification of PARP-1 causes its release from DNA, a process that is critical both for recycling of PARP-1 and to allow access of effector repair proteins to the damaged site [119]. In the context of a Top I-DNA cleavage complex stabilised by camptothecin, poly(ADP-ribosylation) of Top I appears to destabilise the complex, increasing the probability of resolution of the associated DNA break [120, 121]. Repair of the Top I-associated lesion may be further enhanced by the capacity of activated PARP-1 to promote recruitment and activity of the SSBR complex *via* interactions with XRCC1 [105, 113]. Finally, there is evidence that PARP activity promotes reactivation of stalled replication forks [122] a process that is necessary for cells to recover from Top I inhibition [109].

It is important to differentiate between the functional effects of deletion or knockdown of the PARP-1 protein and chemical inhibition of the enzyme. The vast majority of chemical inhibitors act by competing with NAD<sup>+</sup> at the catalytic site that is common to PARP-1 and PARP-2. While this abrogates the catalytic function of these proteins, it does not impair their ability to bind to DNA breaks. Indeed by preventing auto modification of PARP, chemical inhibitors are thought to prolong its binding to damaged sites, thus impeding repair by obstructing access to downstream repair factors as well as by blocking the repair-promoting effects of PARP activity [119]. Support for this model is provided by a recent paper in which the effects of the PARP inhibitor veliparib (ABT-888, Abbot Pharmaceuticals) and camptothecin (CPT) were tested on PARP-1 proficient and deficient mouse embryonic fibroblasts (MEFs). *Parp-1*<sup>-/-</sup>MEFs were no more sensitive to CPT than wild type (WT) parental controls, indicating that PARP-1 is not required for resolution of DNA damage induced by Top I inhibition. In contrast, veliparib treatment was associated with a significant increase in CPT sensitivity [123]. Sensitisation was also achieved by transfecting *Parp-1*<sup>-/-</sup>MEFs with truncated PARP-1 constructs that retained DNA binding capacity but lacked catalytic function.

Consistent with these mechanistic findings, the capacity of PARP inhibitors to increase the cytotoxic effects of Top I inhibitors is well established. *In vitro* potentiation is striking, and the pre-clinical data from *in vivo* models have also been compelling. Tumour growth delay studies using the HT29, LoVo and SW620 colorectal cancer xenograft models have shown enhancement of the anti-tumour effects of irinotecan by four different PARP inhibitors [118, 124-126]. In two of these studies, evidence was presented to indicate that the normal tissue toxicities associated with irinotecan were either unaffected (bone marrow toxicity, [125]) or reduced (intestinal damage, [126]) by concomitant treatment with a PARP inhibitor. These observations were extremely exciting because the first attempt to combine a PARP inhibitor with systemic chemotherapy in patients (AGO14699 plus temozolomide in metastatic melanoma) was complicated by exacerbation of bone marrow toxicity [127]. Unfortunately, these observations in animal studies have not been replicated in patients: early clinical experience of the combination of veliparib and topotecan indicates that addition of the PARP inhibitor exacerbates bone marrow toxicity and necessitates significant dose reductions of the cytotoxic agent [128].

As mentioned previously, the SSBR pathway is intimately involved in detection and repair of DNA single strand breaks that are induced either by Top1 inhibition or by ionising radiation. Not surprisingly, several factors implicated in determining sensitivity to Top1 inhibition have also been shown to influence the cellular response to radiation. This will be of increasing clinical relevance

as combination therapies comprising radiation and irinotecan gain an established place in treatment schedules. The radiosensitising effects of PARP inhibitors have been widely documented and a number of clinical trials testing the toxicity and efficacy of PARP inhibitors and radiation are in development [129]. The triple combination of irinotecan, radiation and PARP inhibition is an exciting prospect, and *in vitro* data in glioblastoma cell lines predict a supra-additive interaction in terms of tumour response [130]. With such a potent combination, however, the risk of enhanced toxicity is also significant.

While the role of Tdp1 in determining radiation sensitivity has received much less attention, the published *in vitro* data suggest that inhibition of this enzyme is also likely to enhance the cytotoxic effects of ionising radiation (IR) [131]. Specifically, cells deficient in Tdp1 exhibit delayed repair of single-stranded DNA breaks (SSB) induced by IR [95, 132]. This has two possible clinical implications: the first is that specific Tdp1 inhibitors might exert dual sensitising effects when combined with irinotecan/radiation regimes; the second is that expression levels of Tdp1 in rectal tumour specimens might be powerful predictors of response to chemoradiation regimes comprising irinotecan.

Recent studies have shed some light on the relationship between PARP-1 and Tdp1 in the context of Top 1 inhibition. *In vitro* experiments testing the effects of the PARP inhibitor ABT-888 on Tdp1 wild type and Tdp1<sup>-/-</sup> MEFs showed that, while PARP inhibition exacerbated camptothecin sensitivity in wild type cells, no additional enhancement of camptothecin induced cytotoxicity was observed in the Tdp1 deficient cells [106]. This indicates that the effect of PARP inhibition on sensitivity to Top1 inhibitors is mediated by an effect on Tdp1 and/or that PARP and Tdp1 participate in a common repair pathway. The observation that the sensitising effects of ABT-888 to camptothecin were not mediated via an increase in Top I cleavage complexes further support a model in which PARP inhibition blocks resolution of DNA repair intermediates that are generated by Tdp1 dependent cleavage of the Top I-DNA complex.

As mentioned earlier, a further possible mechanism by which PARP inhibition might act to increase sensitivity to Top I inhibitors is by interfering with repair of the double stranded DNA lesions that arise when unresolved cleavage complexes encounter DNA replication forks. While this hypothesis remains speculative with regard to the role of PARP, there is convincing data to support the importance of downstream repair pathways in determining cellular outcomes after Top I inhibition. Homologous recombination repair (HRR) is the key pathway responsible for resolving many types of damage associated with DNA replication, and is a complex process that is initiated by resection of damaged DNA to generate a single stranded region of overhang. CtIP plays a key role in this resection step and has been shown to interact with the MRN complex to initiate HRR [133]. BRCA1, another HRR protein, binds to CtIP and this complex appears to promote resolution of camptothecin mediated DNA double strand breaks both by promoting HRR and by resecting regions of single stranded DNA that are bound to Top I cleavage complexes [90].

Multiple proteins contribute to the activation and execution of HR repair, and a number of recent studies have reported that down regulation of known HR factors increases sensitivity to Top I poisons. These include Rad18 and FANCD2 [134] in addition to Rad17 and BRCA1 as described above and confirmed in human ovarian cancer cells [107]. The latter study showed that, unlike the situation for PARP, additive sensitizing effects were observed when BRCA1 was silenced in Tdp1 defective cells. Taken together these data indicate that functional HR is required for resolution of DNA double strand breaks that arise when unresolved Top I cleavage complexes collide with DNA replication forks, and that CtIP and BRCA1 play fundamental roles in initiating this process.

## EVIDENCE FOR CLINICAL EFFECTS OF DNA REPAIR PROTEINS

The broadest experience of Top I inhibitors in clinical practice has been the use of Irinotecan in mCRC, and the majority of biomarker data has been derived from this patient group.

It is reasonable to predict that cellular sensitivity to these agents will be modulated by absolute Top I levels given that the cytotoxic effects of topoisomerase poisons are dependent on stabilisation of the topoisomerase-DNA complex. However it is also becoming apparent that Top I levels can be modulated by chemotherapy treatment. Repeated exposure of colorectal cancer xenografts to camptothecin has been shown to down regulate Top I levels [135] and the same effect has been observed in peripheral blood mononuclear cells after treatment with topotecan [136]. These pre-clinical observations appear to have clinical relevance: tumour expression of Top I has been shown to decrease (between pre-treatment biopsy and subsequent surgical resection) following neoadjuvant treatment of rectal cancer with chemo-radiation comprising irinotecan and 5FU [137]. Whether this effect impacts on clinical responses to irinotecan, and whether it should influence treatment-scheduling remains to be established.

In general, Top I is highly expressed in many colorectal cancers, with one study demonstrating particularly elevated levels in rectal tumours [138]. There is considerable variation between tumours, however, an observation that supports the hypothesis that Top I expression levels will be useful in predicting response to irinotecan. The clinical data on this topic are mixed, however. High Top I levels have been demonstrated to correlate with response of rectal cancers to irinotecan containing neoadjuvant chemo-radiation [137], and the results of the MRC FOCUS study of 1313 patients with metastatic colorectal cancer indicated that tumours with moderate or high levels of Top I expression as determined by immunohistochemistry showed the greatest benefit from adding irinotecan or oxaliplatin to 5FU in the first line metastatic setting [139]. However, data from the contemporary 'CAIRO' study conducted by the Dutch Colorectal Cancer Group [59], failed to replicate these findings: no association between Top I expression (by immunohistochemistry) and response to irinotecan and capecitabine was observed in the 545 patients studied [140]. These apparently contradictory findings indicate that, while absolute Top I expression levels may play a part, it is likely that additional molecules contribute to irinotecan sensitivity in the clinic. The disagreement between studies also indicates the lack of consistency between methods for immunohistochemical analysis of clinical specimens.

As described earlier, cell lines harbouring Top I mutations that alter Top I-DNA or camptothecin interactions can exhibit camptothecin resistance [111, 141] but as yet only one case of mutated Top I in a clinical specimen has been reported, so this is unlikely to be a common cause of Top I resistance.

In contrast with the mechanistic studies that failed to demonstrate a role for aprataxin in modulating sensitivity of mouse neural cells to Top I inhibition [114], *in vitro* studies of colon cancer cell lines have shown an association between aprataxin expression levels and sensitivity to camptothecin [115]. There is also clinical evidence to suggest that aprataxin modulates response to irinotecan in metastatic colorectal cancer, with higher protein expression associated with a lower likelihood of response. Tumour blocks from 135 patients with metastatic disease treated with a variety of irinotecan/5FU combination regimens were probed for aprataxin using immunohistochemistry [116]. With a median follow up of 4.6 years, patients with low levels of aprataxin had improved progression free and overall survival (PFS 9.2 vs 5.5 months,  $p=0.03$ ; OS 36.7 vs 19 months  $p=0.008$ ). Taken together, these observations indicate that mechanisms of repair of Top I associated DNA damage may differ between malignant and non-malignant

cells, with differing rates of DNA replication offering a potential explanation. The promising clinical data require prospective validation but clearly demonstrate the potential value of this class of biomarker in predicting whether patients are likely to benefit from the addition of irinotecan to a therapeutic regime.

The difficulties inherent in attempting to quantify protein expression in heterogeneous tumour specimens have been touched on earlier. An alternative approach to identifying potential biomarkers is to interrogate patient and/or tumours at the genetic level. A number of studies have looked for associations between response to treatment and polymorphisms in genes involved in Top I related DNA repair. In one such study, 107 patients with advanced colorectal cancer treated with irinotecan were screened for host single nucleotide polymorphisms (SNPs) in a panel of six genes including PARP-1, Tdp1, TOP I, and XRCC1 [142]. Univariate analysis indicated that specific polymorphisms in TDP1 and XRCC1 were linked with both toxicity (grade 3-4 neutropenia) and response to irinotecan, but on multivariate analysis the only significant association was between the XRCC1 SNP and an increased likelihood of clinical response. While associations between host germ line SNPs and toxicity have been reported for a variety of cytotoxic agents, associations with response are much less common and the validity of such an observation is perhaps more difficult to assess. Nonetheless, these data combined with the established roles of Tdp1 and XRCC1 in determining cellular responses to irinotecan makes this a promising area of investigation.

Considering gene expression in tumour specimens, the available data indicate that *Tdp1* expression is increased in colorectal tumour samples compared with paired normal tissue [143]. In the most relevant study to date, 52 metastatic colorectal cancer specimens were analysed by RT-PCR for expression of 24 genes hypothesized to be associated with response to irinotecan. *Tdp1* was one of 8 genes that showed significantly higher levels of expression in tumours than in normal tissue. Expression of *Tdp1* grouped with other genes involved in DNA repair. Interrogation of Oncomine ([www.oncomine.org](http://www.oncomine.org)) supports this finding, with *Tdp1* expression levels appearing to be broadly increased in colorectal cancer specimens. Several microarray expression profiles for rectal adenocarcinomas have been published (NCBI GEO, EBI), but only one of these used a platform that included a probe for *Tdp1* [144]. Analysis of this data demonstrates increased levels of *Tdp1* in rectal cancers compared with normal tissues.

As detailed above, it has also been shown that Tdp1 has a role in the repair of single-strand DNA breaks induced by ionising radiation [131]. Whilst the cytotoxic effects of IR are predominately mediated through double strand breaks, unrepaired SSB can be converted to DSB during DNA replication. This raises the intriguing possibility that Tdp1 could be a dual biomarker for sensitivity to both Irinotecan and radiotherapy. While there is no published data to substantiate this claim, high quality tissue is available from several clinical trials that have tested irinotecan based chemo radiation regimes and these samples are currently being analysed for expression of Tdp1 and other relevant DNA repair genes and proteins.

The observation that PARP inhibition causes [106], no further enhancement of camptothecin cytotoxicity in cell lines lacking Tdp1 indicates that PARP and Tdp1 participate in the same repair pathway and has been discussed earlier. While this supports the rationale for either enzyme (but not both together) as a therapeutic target in combination with topoisomerase poisons, it also raises the possibility that tumours with high Tdp1 expression levels might derive particular benefit from the addition of a PARP inhibitor to treatment regimes comprising irinotecan and/or radiotherapy. This proposal is highly speculative, and the relationship between Tdp1 expression and sensitivity to combination therapies is likely to be

complex, but it provides an example of how the rational combination of biomarkers and small molecule, targeted agents might enhance the individualised treatment of patients with colorectal cancer.

Inherited deficiencies in mismatch repair (MMR) pathways are the causative factor in the hereditary non-polyposis colon cancer (HNPCC) Lynch syndrome [145] that accounts for approximately 3% of colorectal tumours. However an additional 15 to 17% of sporadic colorectal cancers exhibit loss of expression of one or more mismatch repair proteins when analysed by immunohistochemistry [146, 147]. MMR deficient colorectal cancers have been reported to be resistant to 5FU [148], but more recent evidence indicates that they may exhibit enhanced sensitivity to irinotecan. In the adjuvant setting, the CALGB 89803 trial randomised 1,264 patients with stage III colon cancer to weekly 5FU/leucovorin +/- irinotecan. 723 cases were retrospectively genotyped for microsatellite instability (MSI) and MMR protein expression was analysed by immunohistochemistry [63]. Tumours with evidence of MMR deficiency showed improved 5-year disease free survival when treated with irinotecan (0.76 vs 0.59,  $p=0.03$ ), a difference that was not observed in the patients receiving 5FU/leucovorin alone. This effect has also been documented in the metastatic setting [149]. Here, 72 patients treated with irinotecan containing regimens were analysed for loss of expression of hMLH1 and hMSH2 and genotyped for microsatellite instability. 4 out of 7 tumours with high levels of MSI responded to irinotecan as opposed to 7 out of 65 patients with low level MSI ( $p=0.009$ ). However, MLH1/MSH2 immunohistochemical analysis was not able to predict response to irinotecan (or oxaliplatin) within the FOCUS study [139], although with only 4.4% samples showing evidence of impaired mismatch repair the statistical power was low. Similarly a recent study of 197 evaluable mCRC patients treated with irinotecan regimens in the first line setting failed to show a significant difference in response between MMR deficient and intact tumours (Kim et al, 2011). Again, only 23/197 (12%) tumours were MMR deficient and there was a trend towards improved response rate (56.5% vs 46.5% in mismatch repair intact) and median progression free survival (8.85 months vs 6.82 months,  $p=0.089$ ).

As molecular subtyping of colorectal cancer improves it is likely that MMR deficient tumours will acquire specific treatment protocols. The current information indicates a likely role for irinotecan in these protocols, but more clinical data is required before this can be confirmed.

## DNA REPAIR PROTEINS AS BIOMARKERS PREDICTING RESPONSE

A biomarker is a measurable biological variable that informs on the state of disease or response to treatment. Within the field of cancer research and treatment an understanding of the molecular characteristics and likely clinical behaviour of a tumour can be derived from makers pertaining to the host or to the tumour. With regard to treatment responses, biomarkers are sought that will predict toxicity (host) or efficacy (tumour). Host biomarkers can include polymorphisms in DNA (SNPs) or plasma levels of circulating peptides. Tumour related biomarkers typically measure the constituents of biopsy material (DNA, RNA, proteins by e.g. immunohistochemistry) but there is increasing interest in circulating tumour cells or cell-free tumour DNA that can be extracted from plasma and allow less invasive and more frequent monitoring of response.

As detailed above, Top I inhibitors (in the form of irinotecan) have found most widespread clinical use in the treatment of mCRC, where response rates in an unselected population are broadly equivalent to the alternative drug, oxaliplatin. Biomarkers that predict response to these drugs would therefore revolutionise

decision-making for both clinicians and patients in this situation. No less relevant would be validated biomarkers predicting levels of toxicity for individual patients. Since the drugs have approximately equivalent efficacy in the palliative setting, maintaining quality of life by minimising treatment related morbidity is an important goal. Validated biomarkers are also required to optimise the development of treatment protocols combining irinotecan with radiotherapy for locally advanced rectal cancer.

Indeed, investigation of irinotecan in the neoadjuvant (before surgery) treatment of rectal cancer [69] may provide opportunities for testing a range of the potential biomarkers discussed in this review. MRI and pathological response at definitive surgery provide robust and quantitative early outcome measures, and the availability of pre- and post-treatment tissue samples makes this an ideal setting in which to investigate the efficacy of new drug combinations in so-called 'window studies' [150] and associated biomarkers.

In any tumour type, prospective validation of potential factors predicting response is required before they can be applied to define treatment in clinical practice. For patients with metastatic colorectal cancer, the process of validating a range of potential biomarkers is currently underway in clinical trials sponsored by the UK Medical Research Council (MRC). FOCUS 3 [151] represented a feasibility study investigating the practicalities of assessing a range of molecular biomarkers within the timescales required to allocate treatment: personalised cancer medicine. 332 patients with mCRC were registered in the study and pathological tumour specimens were analysed at 2 central laboratories for KRAS and BRAF mutation status and for Top I expression by immunohistochemistry

(the latter drawing from the previously described results from the initial FOCUS trial [139]). Standard treatment was a combination of irinotecan and fluorouracil and the molecular testing results were used to define entry into a number of different randomisations. Patients whose tumours expressed wild type KRAS and BRAF were randomised to receive additional cetuximab or control; for KRAS/BRAF mutant tumours, the addition of bevacizumab was tested; the addition of oxaliplatin was tested in the setting of high Top I expression; and finally the omission of Irinotecan was tested in the context of low Top I expression. This ingenious design (Fig. 1) acknowledged that more than one biomarker is likely to be relevant when optimising treatment selection.

Initial feasibility data from the study revealed that molecular biomarker results were available to the treating physicians within 10 working days (the study aim) in 72% of patients and within 20 days in 99% of cases. In this cohort of patients, KRAS mutations were identified in 36% of cases and BRAF mutations in 6%, with 2 tumours harbouring both mutations. 77% of samples showed strong expression of Top I by immunohistochemistry with 19% low and 4% inconclusive.

FOCUS 3 was designed to assess the feasibility of performing prospective assessment of several molecular factors that would allow simultaneously testing of multiple hypotheses relating to predictive markers of treatment response. The study itself was not powered to answer these hypotheses. However, the key output of the trial however is the demonstration that validated biomarker assessment can be performed in a timely fashion that paves the way for subsequent studies. Building on this success, FOCUS 4 is currently in development and aims to recruit patients with mCRC to

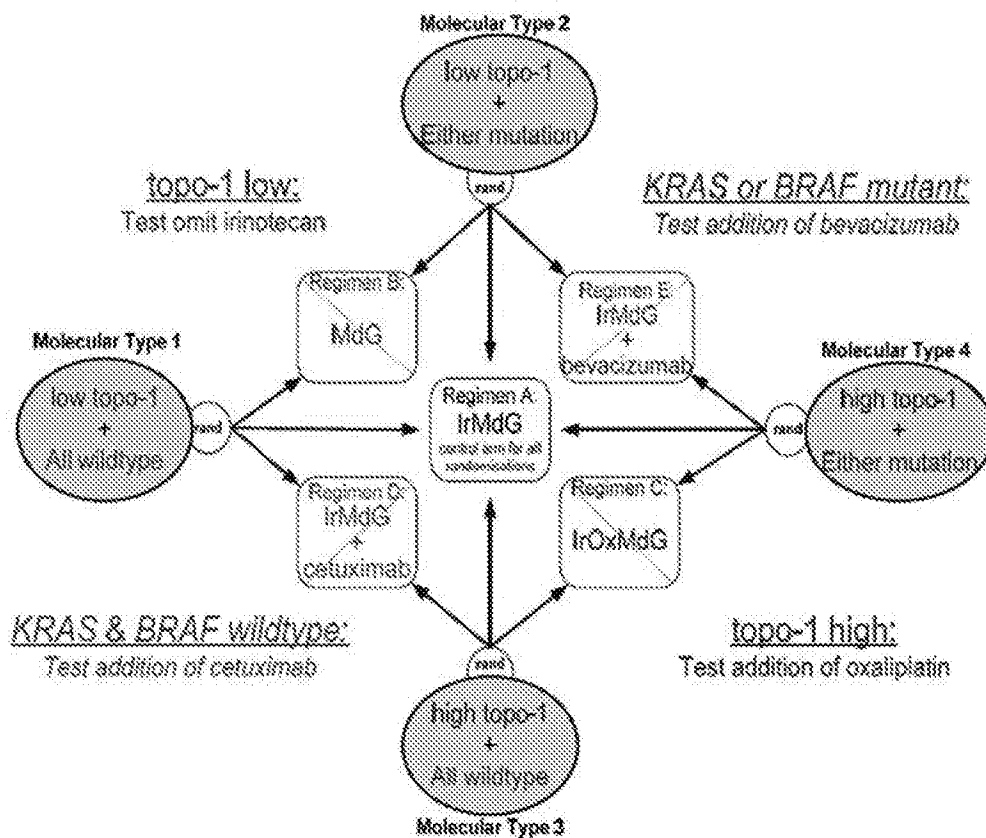


Fig. (1). FOCUS 3; an example of biomarker driven clinical trial design [151]. The reference treatment regime is irinotecan and modified de Gramont (MdG) 5-FU. Patients with high topoisomerase I expression are randomised between addition of oxaliplatin or cetuximab (if KRAS/BRAF wildtype) or bevacizumab (if KRAS/BRAF mutated). In patients with low topoisomerase I expression, the study tested the omission of irinotecan against the addition of cetuximab (wildtype) or bevacizumab (KRAS/BRAF mutated).



multiple arms of therapy determined by prospective biomarker assessments. Validated biomarkers predictive of response to Top I inhibition could form an important pathway within this and subsequently studies.

Given the equivalent first line efficacy of oxaliplatin and irinotecan regimens and lack of validated markers to predict treatment response, the ability to predict toxicity would also be of value in individualising treatment decisions. In this regard, germ line polymorphisms in the genes discussed may be more relevant than variations in tumour expression. Hoskins and co-workers [142] genotyped 107 metastatic CRC patients treated with irinotecan regimens and tested single nucleotide polymorphisms (SNP) in TOP I, CDC45L, NFKB1, PARP1, TDP1 and XRCC1 for association with the most frequent and significant side effects of irinotecan (significant diarrhoea and neutropenia). In univariate analysis, SNPs in both TOP1 and TDP1 were associated with grade 3/4 neutropenia. However multivariate analysis failed to demonstrate significant associations, and the same authors failed to replicate these findings in a separate sample set [152]. Small differences in toxicity however would have been lost in the relatively small sample sizes of the study; considering the overlapping pathways involved in responses to irinotecan at a cellular level, any modulation of toxicity is likely to be multifactorial.

#### THERAPEUTIC TARGETS IN COMBINATION WITH TOPOISOMERASE INHIBITION

Beyond their utility as biomarkers predicting response, a number of components of DNA repair pathways make compelling targets for therapeutic intervention, with the main aim of overcoming resistance to Top I poisons. PARP inhibitors e.g. veliparib (Abbot), iniparib (Sanofi-Aventis) and olaparib (AstraZeneca) are currently the subject of phase I studies in combination with irinotecan. Given the well documented radiosensitising effects of PARP inhibition [124, 129, 153], clinical trials of these agents in combination with radiotherapy are also in development [154]. For the reasons described above (evidence of efficacy, accessible biopsy material, early radiological outcome measures) locally advanced rectal cancer may provide an ideal opportunity to test combinations of irinotecan, radiotherapy and PARP inhibitors. Whether meaningful improvements in tumour response can be achieved without unacceptable exacerbation of normal tissue toxicities, particularly bone marrow suppression and diarrhoea, is very difficult to predict from pre-clinical findings, so cautious phase I dose escalation studies will be required.

The rationale for developing inhibitors of Tdp1 for subsequent combination with Topoisomerase I poisons is similarly robust. *In vitro*, cells deficient in Tdp1 accumulate an excess of DNA strand breaks when incubated with camptothecin [92, 93] or exposed to ionising radiation [131]. Tdp1 is therefore a compelling target for clinical studies in the treatment of cancer in combination with Top I inhibitors and radiotherapy. Again avoiding unacceptable exacerbation of normal tissues toxicities is likely to be the main challenge, although with improving radiotherapy technology this at least gives a degree of spatial targeting.

The recently demonstrated activity of irinotecan in small cell lung cancer and, more speculatively, glioblastoma may give Tdp1 a broader utility beyond CRC. Tdp1 inhibitors could also be combined with topotecan in the management of metastatic ovarian cancer. The close interactions between PARP and Tdp1, in particular the reports that they function within the same pathway, indicate that dual inhibition might not be advantageous. The ideal inhibitor would demonstrate tumour-specific potentiation of the cytotoxic effects of Top I inhibitors, both alone and in combination with radiotherapy. Whether this is a realistic aim will only become

apparent if high quality clinical trials are conducted using potent and specific inhibitors of PARP and Tdp1, using appropriate biomarkers for patient selection.

#### SUMMARY AND PROSPECTS

In this review we have provided an overview of the mode of action of topoisomerase I inhibitors and the various mechanisms by which the DNA damage that these agents induce is recognised and repaired. It is becoming increasingly apparent that a multitude of proteins is involved in this process, and that several recognised DNA repair pathways are represented. Relationships between the different repair proteins are complex and may vary between cell types. In particular, rapidly proliferating tumour cells with defective cell cycle checkpoints may be susceptible to inhibition of elements of the DNA damage response that are dispensable in non-replicating cells. This raises the prospect of tumour specific chemosensitisation, which is the ultimate goal of this research field. However, it must be acknowledged that the dose limiting toxicities associated with Top I inhibitors are also manifest in the rapidly proliferating cells of the bone marrow and the intestinal epithelium.

There is increasing evidence to support the combination of Top I inhibitors such as irinotecan with radiotherapy in the treatment of cancer. There is significant overlap between the repair pathways required for processing and resolution of DNA breaks induced by these agents, and hence a potential for synergistic effects of compounds that target these pathways. To date, PARP and Tdp1 have been demonstrated to modulate sensitivity to both Top I inhibitors and radiation and are thus credible targets. PARP inhibitors are widely available and have entered clinical practice as single agents. Early phase testing of these agents in combination with irinotecan is underway, and studies in combination with radiotherapy are in development. Tdp1 inhibitors are still in the laboratory phase of development, but it will be intriguing to observe how the pre-clinical effects of these compounds differ from those of PARP inhibitors, and in particular whether they enhance sensitivity to radiation as well as to Top I inhibition.

The variety of molecules involved in determining sensitivity to these agents also provides a panel of potential predictive biomarkers. Early clinical data have identified a number of proteins associated with the DNA damage response for which expression levels might predict clinical outcomes. The complex interactions between these factors indicate that it is probably unrealistic to aspire to a single biomarker. Whereas the concept of 'Ogene signatures' is well established and widely accepted, a methodology for combining multiple biomarkers at the level of protein expression has yet to emerge. Biomarker driven clinical trials such as FOCUS 3 and FOCUS 4 are leading the way in testing both the biomarkers themselves and the methodologies by which they can be evaluated in clinical practice.

#### CONFLICT OF INTEREST

The author(s) confirm that this article content has no conflicts of interest.

#### ACKNOWLEDGEMENT

We would like to thank colleagues in the Chalmers and El-Khamisy laboratories for useful discussions. This work is funded by an MRC Senior Clinical Fellowship to AC [G0802755], MA is funded by Wellcome Trust grants [085284 and 091043] to SEK.

#### REFERENCES

- [1] Wang, J.C., Interaction between DNA and an Escherichia coli protein omega, *Journal of molecular biology*, 1971, 55, (3), 523-533.
- [2] Koster, D.A.; Croquette, V.; Dekker, C.; Shuman, S.; Dekker, N.H., Friction

- and torque govern the relaxation of DNA supercoils by eukaryotic topoisomerase IB, *Nature*, 2005, 434, (7033), 671-674.
- [3] Liu, L.F.; Liu, C.C.; Alberts, B.M., Type II DNA topoisomerases: enzymes that can unknot a topologically knotted DNA molecule via a reversible double-strand break, *Cell*, 1980, 19, (3), 697-707.
- [4] Kim, R.A.; Wang, J.C., Function of DNA topoisomerases as replication swivels in *Saccharomyces cerevisiae*, *Journal of molecular biology*, 1989, 208, (2), 257-267.
- [5] Kornberg, A., Enzyme studies of replication of the *Escherichia coli* chromosome, *Advances in experimental medicine and biology*, 1984, 179, 3-16.
- [6] Hiasa, H.; Marians, K.J., Topoisomerase IV can support oriC DNA replication in vitro, *The Journal of biological chemistry*, 1994, 269, (23), 16371-16375.
- [7] Kaguni, J.M.; Kornberg, A., Topoisomerase I confers specificity in enzymatic replication of the *Escherichia coli* chromosomal origin, *The Journal of biological chemistry*, 1984, 259, (13), 8578-8583.
- [8] Halmer, L.; Vestner, B.; Gruss, C., Involvement of topoisomerases in the initiation of simian virus 40 minichromosome replication, *The Journal of biological chemistry*, 1998, 273, (52), 34792-34798.
- [9] Kawanishi, M., Topoisomerase I and II activities are required for Epstein-Barr virus replication, *The Journal of general virology*, 1993, 74 ( Pt 10), 2263-2268.
- [10] Hu, Y.; Clower, R.V.; Melendy, T., Cellular topoisomerase I modulates origin binding by bovine papillomavirus type 1 EI, *Journal of virology*, 2006, 80, (9), 4363-4371.
- [11] Abdurashidova, G.; Danailov, M.B.; Ochem, A.; Triolo, G.; Djeliova, V.; Radulescu, S.; Vindigni, A.; Riva, S.; Falaschi, A., Localization of proteins bound to a replication origin of human DNA along the cell cycle, *The EMBO journal*, 2003, 22, (16), 4294-4303.
- [12] Baguley, B.C.; Ferguson, L.R., Mutagenic properties of topoisomerase-targeted drugs, *Biochimica et biophysica acta*, 1998, 1400, (1-3), 213-222.
- [13] Grue, P.; Grasser, A.; Sehested, M.; Jensen, P.B.; Uhse, A.; Straub, T.; Ness, W.; Boege, F., Essential mitotic functions of DNA topoisomerase IIalpha are not adopted by topoisomerase Ibeta in human H69 cells, *The Journal of biological chemistry*, 1998, 273, (50), 33660-33666.
- [14] Hong, G.; Kreuzer, K.N., Endonuclease cleavage of blocked replication forks: An indirect pathway of DNA damage from antitumor drug-topoisomerase complexes, *Proceedings of the National Academy of Sciences of the United States of America*, 2003, 100, (9), 5046-5051.
- [15] Osheroff, N.; Zechiedrich, E.L., Calcium-promoted DNA cleavage by eukaryotic topoisomerase II: trapping the covalent enzyme-DNA complex in an active form, *Biochemistry*, 1987, 26, (14), 4303-4309.
- [16] McClendon, A.K.; Rodriguez, A.C.; Osheroff, N., Human topoisomerase IIalpha rapidly relaxes positively supercoiled DNA: implications for enzyme action ahead of replication forks, *The Journal of biological chemistry*, 2005, 280, (47), 39337-39345.
- [17] Adams, D.E.; Shekhtman, E.M.; Zechiedrich, E.L.; Schmid, M.B.; Cozzarelli, N.R., The role of topoisomerase IV in partitioning bacterial replicons and the structure of catenated intermediates in DNA replication, *Cell*, 1992, 71, (2), 277-288.
- [18] Baxter, J.; Diffley, J.F., Topoisomerase II inactivation prevents the completion of DNA replication in budding yeast, *Molecular cell*, 2008, 30, (6), 790-802.
- [19] DiNardo, S.; Voelkel, K.; Sternglanz, R., DNA topoisomerase II mutant of *Saccharomyces cerevisiae*: topoisomerase II is required for segregation of daughter molecules at the termination of DNA replication, *Proceedings of the National Academy of Sciences of the United States of America*, 1984, 81, (9), 2616-2620.
- [20] Holm, C.; Stearns, T.; Botstein, D., DNA topoisomerase II must act at mitosis to prevent nondisjunction and chromosome breakage, *Molecular and cellular biology*, 1989, 9, (1), 159-168.
- [21] Uemura, T.; Ohkura, H.; Adachi, Y.; Morino, K.; Shiozaki, K.; Yanagida, M., DNA topoisomerase II is required for condensation and separation of mitotic chromosomes in *S. pombe*, *Cell*, 1987, 50, (6), 917-925.
- [22] Branzei, D.; Sollier, J.; Liberi, G.; Zhao, X.; Maeda, D.; Seki, M.; Enomoto, T.; Ohta, K.; Foiani, M., Ubc9- and mms21-mediated sumoylation counteracts recombinogenic events at damaged replication forks, *Cell*, 2006, 127, (3), 509-522.
- [23] Chan, K.L.; Palmal-Pallag, T.; Ying, S.; Hickson, I.D., Replication stress induces sister-chromatid bridging at fragile site loci in mitosis, *Nature cell biology*, 2009, 11, (6), 753-760.
- [24] Cuvier, O.; Stanojic, S.; Lemaître, J.M.; Mechali, M., A topoisomerase II-dependent mechanism for resetting replicons at the S-M-phase transition, *Genes & development*, 2008, 22, (7), 860-865.
- [25] Suski, C.; Marians, K.J., Resolution of converging replication forks by RecQ and topoisomerase III, *Molecular cell*, 2008, 30, (6), 779-789.
- [26] Fachinetti, D.; Bermejo, R.; Cocito, A.; Minardi, S.; Katou, Y.; Kanoh, Y.; Shirahige, K.; Azvolinsky, A.; Zakian, V.A.; Foiani, M., Replication termination at eukaryotic chromosomes is mediated by Top2 and occurs at genomic loci containing pausing elements, *Molecular cell*, 2009, 39, (4), 595-605.
- [27] Drolet, M., Growth inhibition mediated by excess negative supercoiling: the interplay between transcription elongation, R-loop formation and DNA topology, *Molecular microbiology*, 2006, 59, (3), 723-730.
- [28] Fisher, L.M., DNA supercoiling and gene expression, *Nature*, 1984, 307, (5953), 686-687.
- [29] Gartenberg, M.R.; Wang, J.C., Positive supercoiling of DNA greatly diminishes mRNA synthesis in yeast, *Proceedings of the National Academy of Sciences of the United States of America*, 1992, 89, (23), 11461-11465.
- [30] Peter, B.J.; Arsuaga, J.; Breier, A.M.; Khodursky, A.B.; Brown, P.O.; Cozzarelli, N.R., Genomic transcriptional response to loss of chromosomal supercoiling in *Escherichia coli*, *Genome biology*, 2004, 5, (11), R87.
- [31] Travers, A.; Muskhelishvili, G., DNA supercoiling - a global transcriptional regulator for enterobacterial growth?, *Nature reviews*, 2005, 3, (2), 157-169.
- [32] Merino, A.; Madden, K.R.; Lane, W.S.; Champoux, J.J.; Reinberg, D., DNA topoisomerase I is involved in both repression and activation of transcription, *Nature*, 1993, 365, (6443), 227-232.
- [33] Mondal, N.; Zhang, Y.; Jonsson, Z.; Dhar, S.K.; Kannapiran, M.; Parvin, J.D., Elongation by RNA polymerase II on chromatin templates requires topoisomerase activity, *Nucleic acids research*, 2003, 31, (17), 5016-5024.
- [34] Zechiedrich, E.L.; Cozzarelli, N.R., Roles of topoisomerase IV and DNA gyrase in DNA unlinking during replication in *Escherichia coli*, *Genes & development*, 1995, 9, (22), 2859-2869.
- [35] Zechiedrich, E.L.; Khodursky, A.B.; Bachellier, S.; Schneider, R.; Chen, D.; Lilley, D.M.; Cozzarelli, N.R., Roles of topoisomerases in maintaining steady-state DNA supercoiling in *Escherichia coli*, *The Journal of biological chemistry*, 2000, 275, (11), 8103-8113.
- [36] Cheng, B.; Zhu, C.X.; Ji, C.; Ahumada, A.; Tse-Dinh, Y.C., Direct interaction between *Escherichia coli* RNA polymerase and the zinc ribbon domains of DNA topoisomerase I, *The Journal of biological chemistry*, 2003, 278, (33), 30705-30710.
- [37] Drolet, M.; Phoenix, P.; Menzel, R.; Masse, E.; Liu, L.F.; Crouch, R.J., Overexpression of RNase H partially complements the growth defect of an *Escherichia coli* delta topA mutant: R-loop formation is a major problem in the absence of DNA topoisomerase I, *Proceedings of the National Academy of Sciences of the United States of America*, 1995, 92, (8), 3526-3530.
- [38] Tuduri, S.; Crabbe, L.; Conti, C.; Tourriere, H.; Holtgreve-Grez, H.; Jauch, A.; Pantescio, V.; De Vos, J.; Thomas, A.; Theillet, C.; Pommier, Y.; Tazi, J.; Coquelle, A.; Pasero, P., Topoisomerase I suppresses genomic instability by preventing interference between replication and transcription, *Nature cell biology*, 2009, 11, (11), 1315-1324.
- [39] Juge, F.; Fernando, C.; Fic, W.; Tazi, J., The SR protein B52/SRp55 is required for DNA topoisomerase I recruitment to chromatin, mRNA release and transcription shutdown, *PLoS genetics*, 2010, 6, (9).
- [40] Rossi, F.; Labouirie, E.; Fome, T.; Divita, G.; Derancourt, J.; Riou, J.F.; Antoine, E.; Cathala, G.; Brunel, C.; Tazi, J., Specific phosphorylation of SR proteins by mammalian DNA topoisomerase I, *Nature*, 1996, 381, (6577), 80-82.
- [41] Lotito, L.; Russo, A.; Chillemi, G.; Bueno, S.; Cavalieri, D.; Capranico, G., Global transcription regulation by DNA topoisomerase I in exponentially growing *Saccharomyces cerevisiae* cells: activation of telomere-proximal genes by TOP1 deletion, *Journal of molecular biology*, 2008, 377, (2), 311-322.
- [42] Staker, B.L.; Feese, M.D.; Cushman, M.; Pommer, Y.; Zembower, D.; Stewart, L.; Burgin, A.B., Structures of three classes of anticancer agents bound to the human topoisomerase I-DNA covalent complex, *Journal of medicinal chemistry*, 2005, 48, (7), 2336-2345.
- [43] Wall, M.E., The isolation and structure of camptothecin, a novel alkaloidal leukemia and tumor inhibitor from *Camptotheca acuminata*, *J. Am. Chem. Soc.*, 1966, 88, 3888-3890.
- [44] Hsiang, Y.H.; Hertzberg, R.; Hecht, S.; Liu, L.F., Camptothecin induces protein-linked DNA breaks via mammalian DNA topoisomerase I, *The Journal of biological chemistry*, 1985, 260, (27), 14873-14878.
- [45] Pommer, Y.; Kohlhagen, G.; Kohn, K.W.; Leteurtre, F.; Wani, M.C.; Wall, M.E., Interaction of the alkylating camptothecin derivative with a DNA base at topoisomerase I-DNA cleavage sites, *Proceedings of the National Academy of Sciences of the United States of America*, 1995, 92, (19), 8861-8865.
- [46] Li, T.K.; Liu, L.F., Tumor cell death induced by topoisomerase-targeting drugs, *Annual review of pharmacology and toxicology*, 2001, 41, 53-77.
- [47] Sordet, O.; Khan, Q.A.; Kohn, K.W.; Pommer, Y., Apoptosis induced by topoisomerase inhibitors, *Current medicinal chemistry*, 2003, 3, (4), 271-290.
- [48] Classen, S.; Olland, S.; Berger, J.M., Structure of the topoisomerase II ATPase region and its mechanism of inhibition by the chemotherapeutic agent ICRF-187, *Proceedings of the National Academy of Sciences of the United States of America*, 2003, 100, (19), 10629-10634.
- [49] Corbett, K.D.; Berger, J.M., Structural basis for topoisomerase VI inhibition by the anti-Hsp90 drug radicicol, *Nucleic acids research*, 2006, 34, (15), 4269-4277.
- [50] Wells, N.J.; Addison, C.M.; Fry, A.M.; Ganapathi, R.; Hickson, I.D., Serine 1524 is a major site of phosphorylation on human topoisomerase II alpha protein in vivo and is a substrate for casein kinase II in vitro, *The Journal of biological chemistry*, 1994, 269, (47), 29746-29751.
- [51] Choudhary, C.; Kumar, C.; Gnad, F.; Nielsen, M.L.; Rehman, M.; Walther, T.C.; Olsen, J.V.; Mann, M., Lysine acetylation targets protein complexes and co-regulates major cellular functions, *Science (New York, N.Y.)*, 2009, 325, (5942), 834-840.
- [52] Mao, Y.; Sun, M.; Desai, S.D.; Liu, L.F., SUMO-1 conjugation to



- topoisomerase I: A possible repair response to topoisomerase-mediated DNA damage, *Proceedings of the National Academy of Sciences of the United States of America*, 2000, 97, (8), 4046-4051.
- [53] Mao, Y.; Desai, S.D.; Ting, C.Y.; Hwang, J.; Liu, L.F., 26 S proteasome-mediated degradation of topoisomerase II cleavable complexes, *The Journal of biological chemistry*, 2001, 276, (44), 40652-40658.
- [54] Douillard, J.Y.; Cunningham, D.; Roth, A.D.; Navarro, M.; James, R.D.; Karasek, P.; Jaudik, P.; Iveson, T.; Carmichael, J.; Alakl, M.; Gruija, G.; Awad, L.; Rougier, P., Irinotecan combined with fluorouracil compared with fluorouracil alone as first-line treatment for metastatic colorectal cancer: a multicentre randomised trial, *Lancet*, 2000, 355, (9209), 1041-1047.
- [55] Saltz, L.B.; Cox, J.V.; Blanke, C.; Rosen, L.S.; Fehrenbacher, L.; Moore, M.J.; Maroun, J.A.; Ackland, S.P.; Locker, P.K.; Pirotta, N.; Elfring, G.L.; Miller, L.L., Irinotecan plus fluorouracil and leucovorin for metastatic colorectal cancer. Irinotecan Study Group, *The New England journal of medicine*, 2000, 343, (13), 905-914.
- [56] de Gramont, A.; Figer, A.; Seymour, M.; Homerin, M.; Hmissi, A.; Cassidy, J.; Boni, C.; Cortes-Funes, H.; Cervantes, A.; Freyer, G.; Papamichael, D.; Le Bail, N.; Louvet, C.; Hendler, D.; de Braud, F.; Wilson, C.; Morvan, F.; Bonetti, A., Leucovorin and fluorouracil with or without oxaliplatin as first-line treatment in advanced colorectal cancer, *J Clin Oncol*, 2000, 18, (16), 2938-2947.
- [57] Fuchs, C.S.; Marshall, J.; Mitchell, E.; Wierzbiicki, R.; Ganju, V.; Jeffery, M.; Schulz, J.; Richards, D.; Soufi-Mahjoubi, R.; Wang, B.; Barrueco, J., Randomized, controlled trial of irinotecan plus infusional, bolus, or oral fluoropyrimidines in first-line treatment of metastatic colorectal cancer: results from the BICC-C Study, *J Clin Oncol*, 2007, 25, (30), 4779-4786.
- [58] Seymour, M.T.; Maughan, T.S.; Ledermann, J.A.; Topham, C.; James, R.; Gwyther, S.J.; Smith, D.B.; Shepherd, S.; Maraveyas, A.; Ferry, D.R.; Mcade, A.M.; Thompson, L.; Griffiths, G.O.; Parmar, M.K.; Stephens, R.J., Different strategies of sequential and combination chemotherapy for patients with poor prognosis advanced colorectal cancer (MRC FOCUS): a randomised controlled trial, *Lancet*, 2007, 370, (9582), 143-152.
- [59] Koopman, M.; Antonini, N.F.; Douma, J.; Wals, J.; Honkoop, A.H.; Erdkamp, F.L.; de Jong, R.S.; Rodenburg, C.J.; Vreugdenhil, G.; Loosveld, O.J.; van Bochove, A.; Simige, H.A.; Creemers, G.J.; Tesselar, M.E.; Slee, P.H.; Werter, M.J.; Mol, L.; Dalesio, O.; Punt, C.J., Sequential versus combination chemotherapy with capecitabine, irinotecan, and oxaliplatin in advanced colorectal cancer (CAIRO): a phase III randomised controlled trial, *Lancet*, 2007, 370, (9582), 135-142.
- [60] Andre, T.; Boni, C.; Mounedji-Boudiaf, L.; Navarro, M.; Taberero, J.; Hickish, T.; Topham, C.; Zaninelli, M.; Clingan, P.; Bridgewater, J.; Tabah-Fisch, I.; de Gramont, A., Oxaliplatin, fluorouracil, and leucovorin as adjuvant treatment for colon cancer, *The New England journal of medicine*, 2004, 350, (23), 2343-2351.
- [61] Saltz, L.B.; Niedzwiecki, D.; Hollis, D.; Goldberg, R.M.; Hantel, A.; Thomas, J.P.; Fields, A.L.; Mayer, R.J., Irinotecan fluorouracil plus leucovorin is not superior to fluorouracil plus leucovorin alone as adjuvant treatment for stage III colon cancer: results of CALGB 89803, *J Clin Oncol*, 2007, 25, (23), 3456-3461.
- [62] Kostopoulos, I.; Karavasilis, V.; Karina, M.; Bobos, M.; Xiros, N.; Pentheroudakis, G.; Kafiri, G.; Papakostas, P.; Vrettou, E.; Fountzilas, G., Topoisomerase I but not thymidylate synthase is associated with improved outcome in patients with resected colorectal cancer treated with irinotecan containing adjuvant chemotherapy, *BMC cancer*, 2009, 9, 339.
- [63] Bertagnoli, M.M.; Niedzwiecki, D.; Compton, C.C.; Hahn, H.P.; Hall, M.; Damas, B.; Jewell, S.D.; Mayer, R.J.; Goldberg, R.M.; Saltz, L.B.; Warren, R.S.; Redston, M., Microsatellite instability predicts improved response to adjuvant therapy with irinotecan, fluorouracil, and leucovorin in stage III colon cancer: Cancer and Leukemia Group B Protocol 89803, *J Clin Oncol*, 2009, 27, (11), 1814-1821.
- [64] Diagnostic accuracy of preoperative magnetic resonance imaging in predicting curative resection of rectal cancer: prospective observational study, *BMJ (Clinical research ed)*, 2006, 333, (7572), 779.
- [65] Bosset, J.F.; Collette, L.; Calais, G.; Mineur, L.; Maingon, P.; Radosevic-Jelic, L.; Daban, A.; Bardet, E.; Beny, A.; Ollier, J.C., Chemotherapy with preoperative radiotherapy in rectal cancer, *The New England journal of medicine*, 2006, 355, (11), 1114-1123.
- [66] Gerard, J.P.; Conroy, T.; Bonnetain, F.; Bouche, O.; Chapet, O.; Closon-Dejardin, M.T.; Untereiner, M.; Leduc, B.; Francois, E.; Maurel, J.; Seitz, J.F.; Buecher, B.; Mackiewicz, R.; Ducreux, M.; Bedenne, L., Preoperative radiotherapy with or without concurrent fluorouracil and leucovorin in T3-4 rectal cancers: results of FFC0 9203, *J Clin Oncol*, 2006, 24, (28), 4620-4625.
- [67] Mawdsley, S.; Glynne-Jones, R.; Grainger, J.; Richman, P.; Makris, A.; Harrison, M.; Ashford, R.; Harrison, R.A.; Osborne, M.; Livingstone, J.I.; MacDonald, P.; Mitchell, I.C.; Meyrick-Thomas, J.; Northover, J.M.; Windsor, A.; Novell, R.; Wallace, M., Can histopathologic assessment of circumferential margin after preoperative pelvic chemoradiotherapy for T3-T4 rectal cancer predict for 3-year disease-free survival?, *International journal of radiation oncology, biology, physics*, 2005, 63, (3), 745-752.
- [68] Glynne-Jones, R.; Falk, S.; Maughan, T.S.; Meadows, H.M.; Sebag-Montefiore, D., A phase I/II study of irinotecan when added to 5-fluorouracil and leucovorin and pelvic radiation in locally advanced rectal cancer: a Colorectal Clinical Oncology Group Study, *British journal of cancer*, 2007, 96, (4), 551-558.
- [69] Gollins, S.; Myint, A.S.; Haylock, B.; Wise, M.; Saunders, M.; Neupane, R.; Essapen, S.; Samuel, L.; Dougal, M.; Lloyd, A.; Morris, J.; Topham, C.; Susnerwal, S., Preoperative Chemoradiotherapy Using Concurrent Capecitabine and Irinotecan in Magnetic Resonance Imaging-Defined Locally Advanced Rectal Cancer: Impact on Long-Term Clinical Outcomes, *J Clin Oncol*, 2011.
- [70] Willeke, F.; Horisberger, K.; Kraus-Tiefenbacher, U.; Wenz, F.; Leitner, A.; Hochhaus, A.; Grobholz, R.; Willer, A.; Kahler, G.; Post, S.; Hofheinz, R.D., A phase II study of capecitabine and irinotecan in combination with concurrent pelvic radiotherapy (CapRI-RT) as neoadjuvant treatment of locally advanced rectal cancer, *British journal of cancer*, 2007, 96, (6), 912-917.
- [71] Noda, K.; Nishiwaki, Y.; Kawahara, M.; Negoro, S.; Sugiura, T.; Yokoyama, A.; Fukuoka, M.; Mori, K.; Watanabe, K.; Tamura, T.; Yamamoto, S.; Saijo, N., Irinotecan plus cisplatin compared with etoposide plus cisplatin for extensive small-cell lung cancer, *The New England journal of medicine*, 2002, 346, (2), 85-91.
- [72] Hermes, A.; Bergman, B.; Bremnes, R.; Ek, L.; Fluge, S.; Sederholm, C.; Sundstrom, S.; Thaning, L.; Vilsvik, J.; Aasebo, U.; Sorenson, S., Irinotecan plus carboplatin versus oral etoposide plus carboplatin in extensive small-cell lung cancer: a randomized phase III trial, *J Clin Oncol*, 2008, 26, (26), 4261-4267.
- [73] Lara, P.N., Jr.; Natale, R.; Crowley, J.; Lenz, H.J.; Redman, M.W.; Carleton, J.E.; Jett, J.; Langer, C.J.; Kuebler, J.P.; Dakhlil, S.R.; Chansky, K.; Gandara, D.R., Phase III trial of irinotecan/cisplatin compared with etoposide/cisplatin in extensive-stage small-cell lung cancer: clinical and pharmacogenomic results from SWOG S0124, *J Clin Oncol*, 2009, 27, (15), 2530-2535.
- [74] Schmittel, A.; Sebastian, M.; Fischer von Weikersthal, L.; Martus, P.; Gauler, T.C.; Kaufmann, C.; Hortig, P.; Fischer, J.R.; Link, H.; Binder, D.; Fischer, B.; Caca, K.; Eberhardt, W.E.; Keilholz, U., A German multicenter, randomized phase III trial comparing irinotecan-carboplatin with etoposide-carboplatin as first-line therapy for extensive-disease small-cell lung cancer, *Ann Oncol*, 2011, 22, (8), 1798-1804.
- [75] Zatloukal, P.; Cardenal, F.; Szczesna, A.; Gorbunova, V.; Moiseyenko, V.; Zhang, X.; Cisar, L.; Soria, J.C.; Domine, M.; Thomas, M., A multicenter international randomized phase III study comparing cisplatin in combination with irinotecan or etoposide in previously untreated small-cell lung cancer patients with extensive disease, *Ann Oncol*, 2010, 21, (9), 1810-1816.
- [76] Gewirtz, D.A., A critical evaluation of the mechanisms of action proposed for the antitumor effects of the anthracycline antibiotics adriamycin and daunorubicin, *Biochemical pharmacology*, 1999, 57, (7), 727-741.
- [77] Swift, L.P.; Rephaeli, A.; Nudelman, A.; Phillips, D.R.; Cutts, S.M., Doxorubicin-DNA adducts induce a non-topoisomerase II-mediated form of cell death, *Cancer research*, 2006, 66, (9), 4863-4871.
- [78] Crow, R.T.; Crothers, D.M., Inhibition of topoisomerase I by anthracycline antibiotics: evidence for general inhibition of topoisomerase I by DNA-binding agents, *Journal of medicinal chemistry*, 1994, 37, (19), 3191-3194.
- [79] Cardoso, F.; Durbecq, V.; Larsimont, D.; Paesmans, M.; Leroy, J.Y.; Rouas, G.; Sotiriou, C.; Renard, N.; Richard, V.; Piccart, M.J.; Di Leo, A., Correlation between complete response to anthracycline-based chemotherapy and topoisomerase II-alpha gene amplification and protein overexpression in locally advanced/metastatic breast cancer, *International journal of oncology*, 2004, 24, (1), 201-209.
- [80] Di Leo, A.; Desmedt, C.; Bartlett, J.M.; Piette, F.; Ejlertsen, B.; Pritchard, K.I.; Larsimont, D.; Poole, C.; Isola, J.; Earl, H.; Mouridsen, H.; O'Malley, F.P.; Cardoso, F.; Tanner, M.; Munro, A.; Twelves, C.J.; Sotiriou, C.; Shepherd, L.; Cameron, D.; Piccart, M.J.; Buysc, M., HER2 and TOP2A as predictive markers for anthracycline-containing chemotherapy regimens as adjuvant treatment of breast cancer: a meta-analysis of individual patient data, *The lancet oncology*, 2011, 12, (12), 1134-1142.
- [81] Di Leo, A.; Gancberg, D.; Larsimont, D.; Tanner, M.; Jarvinen, T.; Rouas, G.; Dolci, S.; Leroy, J.Y.; Paesmans, M.; Isola, J.; Piccart, M.J., HER-2 amplification and topoisomerase IIalpha gene aberrations as predictive markers in node-positive breast cancer patients randomly treated either with an anthracycline-based therapy or with cyclophosphamide, methotrexate, and 5-fluorouracil, *Clin Cancer Res*, 2002, 8, (5), 1107-1116.
- [82] Du, Y.; Zhou, Q.; Yin, W.; Zhou, L.; Di, G.; Shen, Z.; Shao, Z.; Lu, J., The role of topoisomerase IIalpha in predicting sensitivity to anthracyclines in breast cancer patients: a meta-analysis of published literatures, *Breast cancer research and treatment*, 2011, 129, (3), 839-848.
- [83] Takashima, H.; Boerkoel, C.F.; John, J.; Saifi, G.M.; Salih, M.A.; Armstrong, D.; Mao, Y.; Quijcho, F.A.; Roa, B.B.; Nakagawa, M.; Stockton, D.W.; Lupski, J.R., Mutation of TDP1, encoding a topoisomerase I-dependent DNA damage repair enzyme, in spinocerebellar ataxia with axonal neuropathy, *Nature genetics*, 2002, 32, (2), 267-272.
- [84] Kerzendorfer, C.; Whibley, A.; Carpenter, G.; Outwin, E.; Chiang, S.C.; Turner, G.; Schwartz, C.; El-Khamisy, S.; Raymond, F.L.; O'Driscoll, M., Mutations in Cullin 4B result in a human syndrome associated with increased camptothecin-induced topoisomerase I-dependent DNA breaks, *Human molecular genetics*, 2010, 19, (7), 1324-1334.
- [85] Shen, J.; Gilmore, E.C.; Marshall, C.A.; Haddadin, M.; Reynolds, J.J.; Eyaid, W.; Bodell, A.; Barry, B.; Gleason, D.; Allen, K.; Ganesh, V.S.; Chang, B.S.; Grix, A.; Hill, R.S.; Topcu, M.; Caldecott, K.W.; Barkovich, A.J.; Walsli, C.A., Mutations in PNKP cause microcephaly, seizures and defects in DNA

- repair, *Nature genetics*, 2010, 42, (3), 245-249.
- [86] El-Khamisy, S.F., To live or to die: a matter of processing damaged DNA termini in neurons, *EMBO molecular medicine*, 2011, 3, (2), 78-88.
- [87] Connelly, J.C.; Leach, D.R., Repair of DNA covalently linked to protein, *Molecular cell*, 2004, 13, (3), 307-316.
- [88] Eid, W.; Steger, M.; El-Shemerly, M.; Ferretti, L.P.; Pena-Diaz, J.; Konig, C.; Valtorta, E.; Sartori, A.A.; Ferrari, S., DNA end resection by CtIP and exonuclease 1 prevents genomic instability, *EMBO reports*, 2010, 11, (12), 962-968.
- [89] Hamilton, N.K.; Maizels, N., MRE11 function in response to topoisomerase poisons is independent of its function in double-strand break repair in *Saccharomyces cerevisiae*, *PLoS one*, 2010, 5, (10), e15387.
- [90] Nakamura, K.; Kogame, T.; Oshiumi, H.; Shinohara, A.; Sumitomo, Y.; Agama, K.; Pommier, Y.; Tsutsui, K.M.; Tsutsui, K.; Hartsuiker, E.; Ogi, T.; Takeda, S.; Taniguchi, Y., Collaborative action of Brc1 and CtIP in elimination of covalent modifications from double-strand breaks to facilitate subsequent break repair, *PLoS genetics*, 2010, 6, (1), e1000828.
- [91] Pommier, Y.; Barcelo, J.M.; Rao, V.A.; Sordet, O.; Jobson, A.G.; Thibaut, L.; Miao, Z.H.; Seiler, J.A.; Zhang, H.; Marchand, C.; Agama, K.; Nitiss, J.L.; Redon, C., Repair of topoisomerase I-mediated DNA damage, *Progress in nucleic acid research and molecular biology*, 2006, 81, 179-229.
- [92] El-Khamisy, S.F.; Saiji, G.M.; Weinfeld, M.; Johansson, F.; Helleday, T.; Lupski, J.R.; Caldecott, K.W., Defective DNA single-strand break repair in spinocerebellar ataxia with axonal neuropathy-1, *Nature*, 2005, 434, (7029), 108-113.
- [93] Interthal, H.; Chen, H.J.; Kehl-Fie, T.E.; Zotzmann, J.; Leppard, J.B.; Champoux, J.J., SCAN1 mutant Tdp1 accumulates the enzyme-DNA intermediate and causes camptothecin hypersensitivity, *The EMBO journal*, 2005, 24, (12), 2224-2233.
- [94] Yang, S.W.; Burgin, A.B., Jr.; Huizenga, B.N.; Robertson, C.A.; Yao, K.C.; Nash, H.A., A eukaryotic enzyme that can disjoin dead-end covalent complexes between DNA and type I topoisomerases, *Proceedings of the National Academy of Sciences of the United States of America*, 1996, 93, (21), 11534-11539.
- [95] Katyal, S.; el-Khamisy, S.F.; Russell, H.R.; Li, Y.; Ju, L.; Caldecott, K.W.; McKinnon, P.J., TDP1 facilitates chromosomal single-strand break repair in neurons and is neuroprotective in vivo, *The EMBO journal*, 2007, 26, (22), 4720-4731.
- [96] Cortes Ledesma, F.; El Khamisy, S.F.; Zuma, M.C.; Osborn, K.; Caldecott, K.W., A human 5'-tyrosyl DNA phosphodiesterase that repairs topoisomerase-mediated DNA damage, *Nature*, 2009, 461, (7264), 674-678.
- [97] Zeng, Z.; Cortes-Ledesma, F.; El Khamisy, S.F.; Caldecott, K.W., TDP2/TTRAP is the major 5'-tyrosyl DNA phosphodiesterase activity in vertebrate cells and is critical for cellular resistance to topoisomerase II-induced DNA Damage, *The Journal of biological chemistry*, 2011, 286, (1), 403-409.
- [98] Das B. B.; Antony S.; Gupta S.; Dexheimer T. S.; Redon C. E.; Garfield S.; Shiloh Y.; Pommier Y., Optimal function of the DNA repair enzyme TDP1 requires its phosphorylation by ATM and/or DNA-PK, *The EMBO Journal*, 2009, 28, 3667-3680.
- [99] Chiang S. C.; Carroll J.; El-Khamisy S. F., TDP1 serine 81 promotes interaction with DNA ligase IIIalpha and facilitates cell survival following DNA damage, *Cell Cycle*, 2010, 9, (3), 588-595.
- [100] Hudson JJ, Shih-Chieh Chiang SC, Wells OS, Rookyard C, El-Khamisy SF, SUMO modification of the neuroprotective protein TDP1 facilitates chromosomal single-strand break repair, *Nature Communications*, 2012, doi:10.1038/ncomms1739.
- [101] Caldecott, K.W.; Aoufouchi, S.; Johnson, P.; Shall, S., XRCC1 polypeptide interacts with DNA polymerase beta and possibly poly (ADP-ribose) polymerase, and DNA ligase III is a novel molecular 'nick-sensor' in vitro, *Nucleic acids research*, 1996, 24, (22), 4387-4394.
- [102] Masson, M.; Niedergang, C.; Schreiber, V.; Muller, S.; Menissier-de Murcia, J.; de Murcia, G., XRCC1 is specifically associated with poly(ADP-ribose) polymerase and negatively regulates its activity following DNA damage, *Molecular and cellular biology*, 1998, 18, (6), 3563-3571.
- [103] Leppard, J.B.; Dong, Z.; Mackey, Z.B.; Tomkinson, A.E., Physical and functional interaction between DNA ligase IIIalpha and poly(ADP-Ribose) polymerase 1 in DNA single-strand break repair, *Molecular and cellular biology*, 2003, 23, (16), 5919-5927.
- [104] von Kobbe, C.; Harrigan, J.A.; May, A.; Opresko, P.L.; Dawut, L.; Cheng, W.H.; Bohr, V.A., Central role for the Werner syndrome protein/poly(ADP-ribose) polymerase 1 complex in the poly(ADP-ribosylation) pathway after DNA damage, *Molecular and cellular biology*, 2003, 23, (23), 8601-8613.
- [105] Bauer, P.L.; Chen, H.J.; Kenesi, E.; Kenessey, I.; Buki, K.G.; Kirsten, E.; Hakam, A.; Hwang, J.L.; Kun, E., Molecular interactions between poly(ADP-ribose) polymerase (PARP I) and topoisomerase I (Topo I): identification of topology of binding, *FEBS letters*, 2001, 506, (3), 239-242.
- [106] Jongstra-Bilen, J.; Ittel, M.E.; Niedergang, C.; Vosberg, H.P.; Mandel, P., DNA topoisomerase I from calf thymus is inhibited in vitro by poly(ADP-ribosylation), *European journal of biochemistry / FEBS*, 1983, 136, (2), 391-396.
- [107] Yung, T.M.; Sato, S.; Satoh, M.S., Poly(ADP-ribosylation) as a DNA damage-induced post-translational modification regulating poly(ADP-ribose) polymerase-1-topoisomerase I interaction, *The Journal of biological chemistry*, 2004, 279, (38), 39686-39696.
- [108] Smith, L.M.; Willmore, E.; Austin, C.A.; Curtin, N.J., The novel poly(ADP-Ribose) polymerase inhibitor, AG14361, sensitizes cells to topoisomerase I poisons by increasing the persistence of DNA strand breaks, *Clin Cancer Res*, 2005, 11, (23), 8449-8457.
- [109] Zhang, Y.W.; Regairaz, M.; Seiler, J.A.; Agama, K.K.; Doroshow, J.H.; Pommier, Y., Poly(ADP-ribose) polymerase and XPF-ERCC1 participate in distinct pathways for the repair of topoisomerase I-induced DNA damage in mammalian cells, *Nucleic acids research*, 2011.
- [110] Perego, P.; Cossa, G.; Tinelli, S.; Corna, E.; Carenini, N.; Gatti, L.; De Cesare, M.; Ciusani, E.; Zunino, F.; Luison, E.; Canevari, S.; Zaffaroni, N.; Beretta, G.L., Role of tyrosyl-DNA phosphodiesterase 1 and inter-players in regulation of tumor cell sensitivity to topoisomerase I inhibition, *Biochemical pharmacology*, 2012, 83, (1), 27-36.
- [111] Hsiang, Y.H.; Liu, L.F.; Wall, M.E.; Wani, M.C.; Nicholas, A.W.; Manikumar, G.; Kirschenbaum, S.; Silber, R.; Potmesil, M., DNA topoisomerase I-mediated DNA cleavage and cytotoxicity of camptothecin analogues, *Cancer research*, 1989, 49, (16), 4385-4389.
- [112] Ryan, P.C.; Draper, D.E., Detection of a key tertiary interaction in the highly conserved GTPase center of large subunit ribosomal RNA, *Proceedings of the National Academy of Sciences of the United States of America*, 1991, 88, (14), 6308-6312.
- [113] Fiorani, P.; Bruselles, A.; Falconi, M.; Chillemi, G.; Desideri, A.; Benedetti, P., Single mutation in the linker domain confers protein flexibility and camptothecin resistance to human topoisomerase I, *The Journal of biological chemistry*, 2003, 278, (44), 43268-43275.
- [114] Gongora, C.; Vezzio-Vie, N.; Tuduri, S.; Denis, V.; Causse, A.; Auzauneau, C.; Collod-Beroud, G.; Coquelle, A.; Pasero, P.; Pourquier, P.; Martineau, P.; Del Rio, M., New Topoisomerase I mutations are associated with resistance to camptothecin, *Molecular cancer*, 2011, 10, 64.
- [115] Tsurutani, J.; Nitta, T.; Hirashima, T.; Komiya, T.; Uejima, H.; Tada, H.; Syunichi, N.; Tohda, A.; Fukuoaka, M.; Nakagawa, K., Point mutations in the topoisomerase I gene in patients with non-small cell lung cancer treated with irinotecan, *Lung cancer (Amsterdam, Netherlands)*, 2002, 35, (3), 299-304.
- [116] Plo, I.; Liao, Z.Y.; Barcelo, J.M.; Kohlhagen, G.; Caldecott, K.W.; Weinfeld, M.; Pommier, Y., Association of XRCC1 and tyrosyl DNA phosphodiesterase (Tdp1) for the repair of topoisomerase I-mediated DNA lesions, *DNA repair*, 2003, 2, (10), 1087-1100.
- [117] El-Khamisy, S.F.; Katyal, S.; Patel, P.; Ju, L.; McKinnon, P.J.; Caldecott, K.W., Synergistic decrease of DNA single-strand break repair rates in mouse neural cells lacking both Tdp1 and aprataxin, *DNA repair*, 2009, 8, (6), 760-766.
- [118] Mariadason, J.M.; Arango, D.; Shi, Q.; Wilson, A.J.; Corner, G.A.; Nicholas, C.; Aranes, M.J.; Lesser, M.; Schwartz, E.L.; Augenlicht, L.H., Gene expression profiling-based prediction of response of colon carcinoma cells to 5-fluorouracil and camptothecin, *Cancer research*, 2003, 63, (24), 8791-8812.
- [119] Dopazo, H.; Mateo-Lozano, S.; Elez, E.; Landolfi, S.; Ramos Pascual, F.J.; Hernandez-Losa, J.; Mazzolini, R.; Rodriguez, P.; Bazzocco, S.; Carreras, M.J.; Espin, E.; Armengol, M.; Wilson, A.J.; Mariadason, J.M.; Ramon, Y.C.S.; Taberner, J.; Schwartz, S., Jr.; Arango, D., Aprataxin tumor levels predict response of colorectal cancer patients to irinotecan-based treatment, *Clin Cancer Res*, 2010, 16, (8), 2375-2382.
- [120] Delaney, C.A.; Wang, L.Z.; Kyle, S.; White, A.W.; Calvert, A.H.; Curtin, N.J.; Durkacz, B.W.; Hostomsky, Z.; Newell, D.R., Potentiation of temozolomide and topotecan growth inhibition and cytotoxicity by novel poly(adenosine diphosphoribose) polymerase inhibitors in a panel of human tumor cell lines, *Clin Cancer Res*, 2000, 6, (7), 2860-2867.
- [121] Miknyoczki, S.J.; Jones-Bolin, S.; Pritchard, S.; Hunter, K.; Zhao, H.; Wan, W.; Ator, M.; Bihovsky, R.; Hudkins, R.; Chatterjee, S.; Klein-Szanto, A.; Dionne, C.; Ruggeri, B., Chemopotentiation of temozolomide, irinotecan, and cisplatin activity by CEP-6800, a poly(ADP-ribose) polymerase inhibitor, *Molecular cancer therapeutics*, 2003, 2, (4), 371-382.
- [122] Godon, C.; Cordeliers, F.P.; Biard, D.; Giocanti, N.; Meguin-Chanet, F.; Hall, J.; Favaudon, V., PARP inhibition versus PARP-1 silencing: different outcomes in terms of single-strand break repair and radiation susceptibility, *Nucleic acids research*, 2008, 36, (13), 4454-4464.
- [123] Malanga, M.; Althaus, F.R., Poly(ADP-ribose) reactivates stalled DNA topoisomerase I and induces DNA strand break resealing, *The Journal of biological chemistry*, 2004, 279, (7), 5244-5248.
- [124] Park, S.Y.; Cheng, Y.C., Poly(ADP-ribose) polymerase-1 could facilitate the religation of topoisomerase I-linked DNA inhibited by camptothecin, *Cancer research*, 2005, 65, (9), 3894-3902.
- [125] Bryant, H.E.; Petermann, E.; Schultz, N.; Jemth, A.S.; Loseva, O.; Issaeva, N.; Johansson, F.; Fernandez, S.; McGlynn, P.; Helleday, T., PARP is activated at stalled forks to mediate Mre11-dependent replication restart and recombination, *The EMBO journal*, 2009, 28, (17), 2601-2615.
- [126] Patel, A.G.; Flatten, K.S.; Schneider, P.A.; Dai, N.T.; McDonald, J.S.; Poirier, G.G.; Kaufmann, S.H., Enhanced killing of cancer cells by poly(ADP-ribose) polymerase inhibitors and topoisomerase I inhibitors reflects poisoning of both enzymes, *The Journal of biological chemistry*, 2012, 287, (6), 4198-4210.
- [127] Calabrese, C.R.; Almasy, R.; Barton, S.; Batey, M.A.; Calvert, A.H.; Canan-Koch, S.; Durkacz, B.W.; Hostomsky, Z.; Kumpf, R.A.; Kyle, S.; Li, J.; Maelgley, K.; Newell, D.R.; Notarianni, E.; Stratford, I.J.; Skaltitzky, D.; Thomas, H.D.; Wang, L.Z.; Webber, S.B.; Williams, K.J.; Curtin, N.J.,

- Anticancer chemosensitization and radiosensitization by the novel poly(ADP-ribose) polymerase-1 inhibitor AG14361, *Journal of the National Cancer Institute*, 2004, 96, (1), 56-67.
- [128] Miknyoczki, S.; Chang, H.; Grobelyni, J.; Pritchard, S.; Worrell, C.; McGann, N.; Aitor, M.; Husten, J.; Deibold, J.; Hudkins, R.; Zulli, A.; Parchment, R.; Ruggeri, B., The selective poly(ADP-ribose) polymerase-1(2) inhibitor, CEP-8983, increases the sensitivity of chemoresistant tumor cells to temozolomide and irinotecan but does not potentiate myelotoxicity, *Molecular cancer therapeutics*, 2007, 6, (8), 2290-2302.
- [129] Tentori, L.; Leonetti, C.; Scarsella, M.; Muzi, A.; Mazzon, E.; Vergati, M.; Forini, O.; Lapidus, R.; Xu, W.; Dorio, A.S.; Zhang, J.; Cuzzocrea, S.; Graziani, G., Inhibition of poly(ADP-ribose) polymerase prevents irinotecan-induced intestinal damage and enhances irinotecan/temozolomide efficacy against colon carcinoma, *Faseb J*, 2006, 20, (10), 1709-1711.
- [130] Plummer, R.; Jones, C.; Middleton, M.; Wilson, R.; Evans, J.; Olsen, A.; Curtin, N.; Boddy, A.; McHugh, P.; Newell, D.; Harris, A.; Johnson, P.; Steinfeldt, H.; Dewji, R.; Wang, D.; Robson, L.; Calvert, H., Phase I study of the poly(ADP-ribose) polymerase inhibitor, AG014699, in combination with temozolomide in patients with advanced solid tumors, *Clin Cancer Res*, 2008, 14, (23), 7917-7923.
- [131] Kumar, S.; Chen, A.; Ji, J.; Zhang, Y.; Reid, J.M.; Ames, M.; Jia, L.; Weil, M.; Speranza, G.; Murgo, A.J.; Kinders, R.; Wang, L.; Parchment, R.E.; Carter, J.; Stotler, H.; Rubinstein, L.; Hollingshead, M.; Melillo, G.; Pommier, Y.; Bonner, W.; Tomaszewski, J.E.; Doroshow, J.H., Phase I study of PARP inhibitor ABT-888 in combination with topotecan in adults with refractory solid tumors and lymphomas, *Cancer research*, 2011, 71, (17), 5626-5634.
- [132] Chalmers, A.J.; Lakshman, M.; Chan, N.; Bristow, R.G., Poly(ADP-ribose) polymerase inhibition as a model for synthetic lethality in developing radiation oncology targets, *Seminars in radiation oncology*, 2010, 20, (4), 274-281.
- [133] Chalmers, A.J., Overcoming resistance of glioblastoma to conventional cytotoxic therapies by the addition of PARP inhibitors, *Anti-cancer agents in medicinal chemistry*, 2010, 10, (7), 520-533.
- [134] El-Khamisy, S.F.; Hartsuiker, E.; Caldecott, K.W., TDP1 facilitates repair of ionizing radiation-induced DNA single-strand breaks, *DNA repair*, 2007, 6, (10), 1485-1495.
- [135] Chiang, S.C.; Carroll, J.; El-Khamisy, S.F., TDP1 serine 81 promotes interaction with DNA ligase IIIalpha and facilitates cell survival following DNA damage, *Cell cycle (Georgetown, Tex)*, 2010, 9, (3), 588-595.
- [136] Huertas, P.; Jackson, S.P., Human CtIP mediates cell cycle control of DNA end resection and double strand break repair, *The Journal of biological chemistry*, 2009, 284, (14), 9558-9565.
- [137] Palte, K.; Vaziri, C., Rad18 E3 ubiquitin ligase activity mediates Fanconi anemia pathway activation and cell survival following DNA Topoisomerase I inhibition, *Cell cycle (Georgetown, Tex)*, 2011, 10, (10), 1625-1638.
- [138] Giovanella, B.C.; Stehlin, J.S.; Wall, M.E.; Wani, M.C.; Nicholas, A.W.; Liu, L.F.; Silber, R.; Potmesil, M., DNA topoisomerase I-targeted chemotherapy of human colon cancer in xenografts, *Science (New York, N.Y)*, 1989, 246, (4933), 1046-1048.
- [139] Hochster, H.; Liebes, L.; Speyer, J.; Sorich, J.; Taubes, B.; Oratz, R.; Wernz, J.; Chachoua, A.; Blum, R.H.; Zeleniuch-Jacquotte, A., Effect of prolonged topotecan infusion on topoisomerase I levels: a phase I and pharmacodynamic study, *Clin Cancer Res*, 1997, 3, (8), 1245-1252.
- [140] Horisberger, K.; Erben, P.; Muessle, B.; Woernle, C.; Stroebel, P.; Kaehler, G.; Wenz, F.; Hochhaus, A.; Post, S.; Willeke, F.; Hofheinz, R.D., Topoisomerase I expression correlates to response to neoadjuvant irinotecan-based chemoradiation in rectal cancer, *Anti-cancer drugs*, 2009, 20, (6), 519-524.
- [141] Boonsong, A.; Curran, S.; McKay, J.A.; Cassidy, J.; Murray, G.I.; McLeod, H.L., Topoisomerase I protein expression in primary colorectal cancer and lymph node metastases, *Human pathology*, 2002, 33, (11), 1114-1119.
- [142] Braun, M.S.; Richman, S.D.; Quirke, P.; Daly, C.; Adlard, J.W.; Elliott, F.; Barrett, J.H.; Selby, P.; Meade, A.M.; Stephens, R.J.; Parmar, M.K.; Seymour, M.T., Predictive biomarkers of chemotherapy efficacy in colorectal cancer: results from the UK MRC FOCUS trial, *J Clin Oncol*, 2008, 26, (16), 2690-2698.
- [143] Koopman M, K.N., Richman S, et al. , The correlation between topoisomerase-I (Topo1) expression and outcome of treatment with capecitabine and irinotecan in advanced colorectal cancer (ACC) patients (pts) treated in the CAIRO study of the Dutch Colorectal Cancer Group (DCCG), *Eur J Cancer Suppl*, 2009, 7, 321.
- [144] Li, X.G.; Haluska, P., Jr.; Hsiang, Y.H.; Bharti, A.; Kufe, D.W.; Rubin, E.H., Identification of topoisomerase I mutations affecting both DNA cleavage and interaction with camptothecin, *Annals of the New York Academy of Sciences*, 1996, 803, 111-127.
- [145] Hoskins, J.M.; Marcuello, E.; Altes, A.; Marsh, S.; Maxwell, T.; Van Booven, D.J.; Pare, L.; Culverhouse, R.; McLeod, H.L.; Baiget, M., Irinotecan pharmacogenetics: influence of pharmacodynamic genes, *Clin Cancer Res*, 2008, 14, (6), 1788-1796.
- [146] Yu, J.; Shannon, W.D.; Watson, M.A.; McLeod, H.L., Gene expression profiling of the irinotecan pathway in colorectal cancer, *Clin Cancer Res*, 2005, 11, (5), 2053-2062.
- [147] Snipstad, K.; Fenton, C.G.; Kjaeve, J.; Cui, G.; Anderssen, E.; Paulsen, R.H., New specific molecular targets for radio-chemotherapy of rectal cancer, *Molecular oncology*, 2010, 4, (1), 52-64.
- [148] Ionov, Y.; Peinado, M.A.; Malkhosyan, S.; Shibata, D.; Perucho, M., Ubiquitous somatic mutations in simple repeated sequences reveal a new mechanism for clonic carcinogenesis, *Nature*, 1993, 363, (6429), 558-561.
- [149] Imai, K.; Yamamoto, H., Carcinogenesis and microsatellite instability: the interrelationship between genetics and epigenetics, *Carcinogenesis*, 2008, 29, (4), 673-680.
- [150] Popat, S.; Hubner, R.; Houlston, R.S., Systematic review of microsatellite instability and colorectal cancer prognosis, *J Clin Oncol*, 2005, 23, (3), 609-618.
- [151] Ribic, C.M.; Sargent, D.J.; Moore, M.J.; Thibodeau, S.N.; French, A.J.; Goldberg, R.M.; Hamilton, S.R.; Laurent-Puig, P.; Gryfe, R.; Shepherd, L.E.; Tu, D.; Redston, M.; Gallinger, S., Tumor microsatellite-instability status as a predictor of benefit from fluorouracil-based adjuvant chemotherapy for colon cancer, *The New England journal of medicine*, 2003, 349, (3), 247-257.
- [152] Fallik, D.; Borroni, F.; Boige, V.; Viguier, J.; Jacob, S.; Miquel, C.; Sabourin, J.C.; Ducreux, M.; Praz, F., Microsatellite instability is a predictive factor of the tumor response to irinotecan in patients with advanced colorectal cancer, *Cancer research*, 2003, 63, (18), 5738-5744.
- [153] Harrington, K.J.; Billingham, L.J.; Brunner, T.B.; Burnet, N.G.; Chan, C.S.; Hoskin, P.; Mackay, R.I.; Maughan, T.S.; Macdougall, J.; McKenna, W.G.; Nutting, C.M.; Oliver, A.; Plummer, R.; Stratford, I.J.; Illidge, T., Guidelines for preclinical and early phase clinical assessment of novel radiosensitisers, *British journal of cancer*, 2011, 105, (5), 628-639.
- [154] Tim Maughan, R.H.W., Geraint T Williams, Matthew T. Seymour, Susan D. Richman, Philip Quirke, Janet Pope, Malcolm Pope, Mahesh Parmar, Anumarie Nelson, Angela M. Meade, Laura L Nichols, Bharat Jasani, Elizabeth Hodgkinson, David Fisher, Rachel Butler, John A. Bridgewater, Richard A. Adams, Richard S. Kaplan; , FOCUS 3: A study to determine the feasibility of molecular selection of therapy using K-RAS, B-RAF, and topo-1 in patients with advanced colorectal cancer (ACRC), *J Clin Oncol* 30, 2012 (suppl 4; abstr 563) 2012.
- [155] Hoskins, J.M.; Rosner, G.L.; Ratain, M.J.; McLeod, H.L.; Innocenti, F., Pharmacodynamic genes do not influence risk of neutropenia in cancer patients treated with moderately high-dose irinotecan, *Pharmacogenomics*, 2009, 10, (7), 1139-1146.
- [156] Efimova, E.V.; Mauerer, H.J.; Golden, D.W.; Labay, E.; Bindokas, V.P.; Darga, T.E.; Chakraborty, C.; Barreto-Andrade, J.C.; Crawley, C.; Sutton, H.G.; Kron, S.J.; Weichselbaum, R.R., Poly(ADP-ribose) polymerase inhibitor induces accelerated senescence in irradiated breast cancer cells and tumors, *Cancer research*, 2010, 70, (15), 6277-6282.
- [157] Verheij, M.; Vens, C.; van Triest, B., Novel therapeutics in combination with radiotherapy to improve cancer treatment: rationale, mechanisms of action and clinical perspective, *Drug Resist Updat*, 2010, 13, (1-2), 29-43.

PROCEEDINGS  
OF THE  
NATIONAL ACADEMY OF SCIENCES



Volume 39

October 15, 1953

Number 10

*A SELECTIVE STAINING METHOD FOR THE BASIC PROTEINS  
OF CELL NUCLEI*

BY MAX ALFERT\* AND IRVING I. GESCHWIND†

DEPARTMENT OF ZOOLOGY; AND HORMONE RESEARCH LABORATORY, DEPARTMENT OF  
BIOCHEMISTRY, UNIVERSITY OF CALIFORNIA, BERKELEY

Communicated by W. M. Stanley, August 26, 1953

Histochemical staining methods combined with specific enzymatic hydrolysis and chemical substitution procedures have permitted the cytologist to visualize, and in some instances to quantitate by microphotometric methods, many cellular constituents. Methods for histochemical detection of specific proteins or of characteristic groups in proteins are few, and some of those presently available are somewhat cumbersome for routine histological use, or result in formation of highly unstable color complexes whose quantitative relationship to the substances tested is often unknown. As far as the distinction between histones and non-histones, or, in general, between proteins of different isoelectric points, is concerned, the methods previously used have included u.v. absorption-spectroscopy,<sup>1</sup> a modification of the Millon reaction,<sup>2</sup> and staining with acid and basic dyes at a series of different pH's.<sup>3</sup> The last-named method, which makes use of the amphoteric nature of proteins and their resulting ability to form salts with acid and basic dye ions, has been used extensively in the past. However, up to now it has not been possible to define any set of conditions under which a particular type of protein could be visualized selectively by a single staining operation involving only one dye. The procedure described herein represents an empirical method which grew out of a series of staining experiments at controlled pH. It is believed to afford a simple, stable, and specific staining procedure for histones and, when present, protamines in cell nuclei, since other proteins with high isoelectric points (such as cytochrome *C*), which were found to stain under the specified conditions, do not occur in cells in sufficient concentration to affect the staining picture. Moreover, this method permits relative quantitation of the stainable material by microphotometric procedures.

The method consists of the following steps:

1. Tissues are fixed for three to six hours in 10% neutral formalin, washed overnight in running water, dehydrated, and embedded in paraffin.

2. Sections on slides are rehydrated and immersed for 15 minutes in a 5% solution of trichloroacetic acid (TCA) in a boiling water-bath, for removal of nucleic acids. The TCA is subsequently washed out by three changes of 70% alcohol for ten minutes each, followed by distilled water.

3. Slides are stained at room temperature for 30 minutes in a 0.1% aqueous solution of the acid dye Fast green FCF (National Aniline Division; 96% dye content) adjusted to pH 8.0–8.1 with a minimum of NaOH; the sections are then washed for five minutes in distilled water, followed directly by 95% alcohol, and mounted after complete dehydration and clearing.

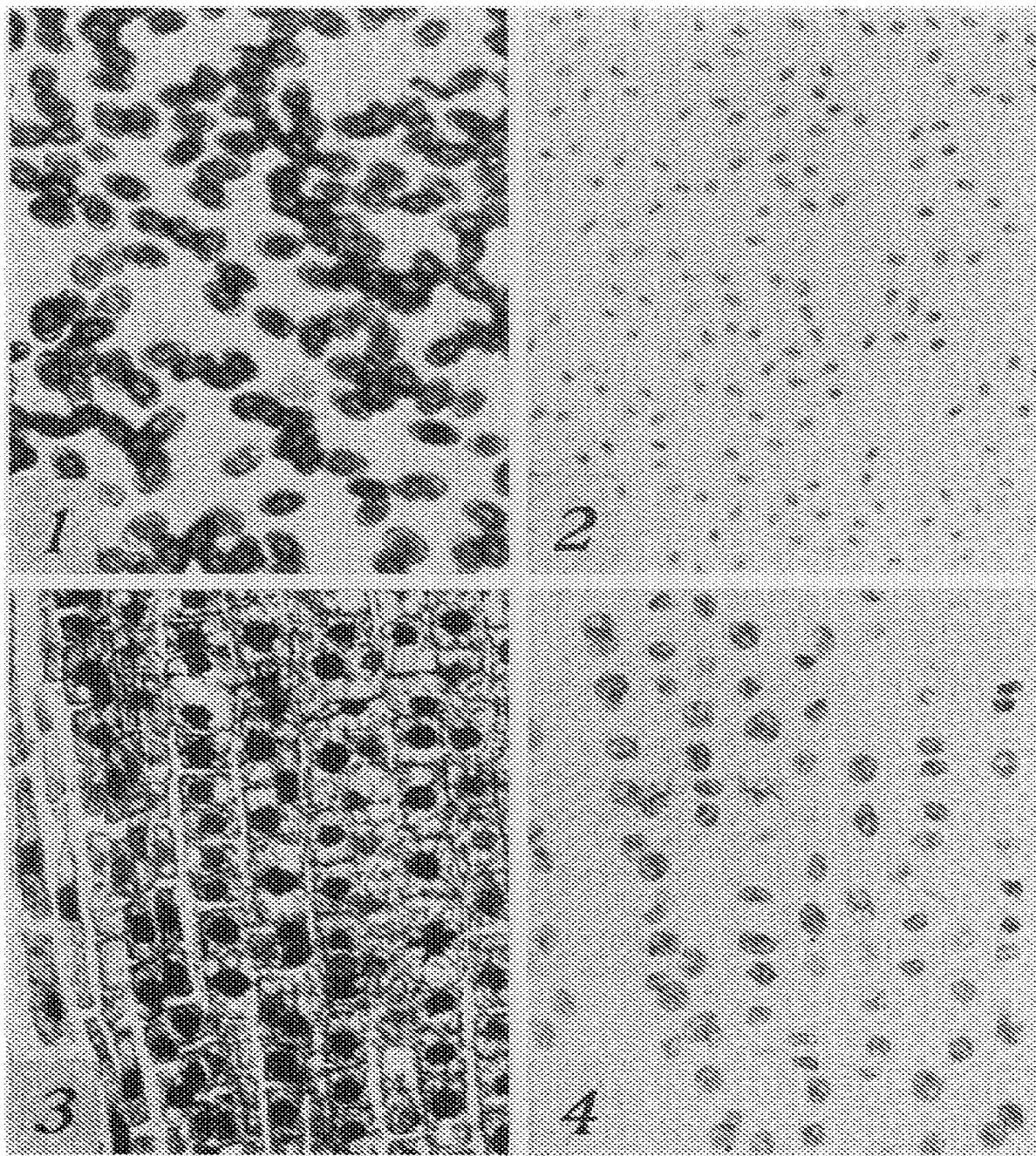
By this method a specific nuclear, i.e., chromosomal stain, has been obtained in a variety of vertebrate tissues and in onion root tips. The following comments to this technique are relevant:

1. A number of routine histological fixatives such as Zenker's, Susa's, and Carnoy's do not allow specific nuclear staining. The presence of mercuric chloride in Zenker's and Susa's fluids is apt to introduce a staining artifact since a divalent metal ion might serve as a link between carboxyl groups and acid dye ions. Carnoy's fluid, on the other hand, has been claimed<sup>4</sup> to cause a shift in the isoelectric point favoring acid dye uptake.

2. No stain is retained by the tissues unless nucleic acids are extracted prior to staining. Desoxyribonuclease can replace TCA in this respect, but ribonuclease is ineffective. It is a well-known fact that nucleic acids can interfere competitively with the staining of proteins,<sup>5</sup> and vice versa.<sup>6</sup>

3. Variations of the staining conditions were attempted in several ways: Increase of the dye concentration to 0.25% and, independently, of the time of staining and differentiation to two hours, produced no noticeably different results. Only freshly prepared and unbuffered dye solutions (to avoid interference by buffer ions) were used. The pH of the solution did not change during the staining procedure. Although the dye solution at pH 8 is distinctly bluish in color and its absorption curve is shifted to lower wave-lengths, the dye bound by nuclei appears green and has an absorption peak close to 635 m $\mu$ , similar to that of tissue elements stained at pH 2.2.

Figures 1 to 4 illustrate the difference in the staining picture between routine Fast green staining at low pH (in *N*/100 HCl, pH 2.2) and at pH 8, both after extraction of nucleic acids by hot TCA. It will be noted that the basic hemoglobin, formerly classified as a histone, does not stain at high pH, that the stain is restricted to chromosomes in dividing cells, and that nucleoli fail to stain. This last fact is of special interest. Although nucleoli were said by Caspersson<sup>1</sup> to contain histones on the basis of spectrophotometric analysis, this claim has not been substantiated by the histochemical studies of Pollister and Ris,<sup>2</sup> nor by direct chemical analysis of isolated nucleoli by Vincent.<sup>7</sup> That only chromatin stains in cells where



FIGURES 1-4

Photomicrographs of animal and plant cells stained with Fast green at pH 2.2 (Figs. 1 and 3) and at pH 8 (Figs. 2 and 4).  $\times 550$ . Figures 1 and 2 are blood smears of the lizard *Sceloporus occidentalis* prefixed in absolute methanol to prevent hemolysis; figures 3 and 4 are sections of onion root tips.



mitotic figures are evident (which aside from the onion root tips was also the case in activated rat thyroid glands) is of considerable importance since chromosomes are mainly composed of nucleic acid, histone and "residual protein," or "chromosomine." Hamer<sup>8</sup> has recently reviewed the available evidence for the acidic nature of nuclear and chromosomal non-histone proteins. On the basis of the model experiments reported below, proteins of this type would not be expected to stain.

In order to test this staining procedure model experiments on known proteins, protamine (salmine), desoxyribonucleic acid (DNA) and protamine-nucleate were undertaken. Commercial crystalline proteins and edestine were dissolved in suitable aqueous media in amounts calculated to provide solutions containing the same concentrations of total basic groups (6  $\mu$ M basic groups/ml.). Six  $\mu$ l. drops of these were spotted on filter paper, fixed in 80% alcohol followed by formalin, washed and stained with Fast green at pH 2.2 or 8. Typical results are summarized in figure 5.

It appears evident that the ability to bind acid dye at high pH is correlated with a high isoelectric point of the protein itself, rather than with the presence of any particular basic group: Protamine, histone, lysozyme, and cytochrome *C* (not illustrated) are able to stain at pH 8 although, with the exception of protamine, considerably less intensely than at pH 2.2. Globulins and albumins do not retain dye at high pH but they become stainable following methylation of carboxyl groups,<sup>9</sup> a procedure which results in a considerable shift of the isoelectric point into the alkaline range. The fact that globin and edestine (a seed protein of unusually high arginine content) fail to stain, or retain at most only traces of dye, at pH 8 indicates that the absolute number and type of basic groups present are of less importance than the over-all balance of acid to basic groups, i.e., the net positive charge of the protein.

At pH 8 the groups mainly responsible for staining by acid dye ions are the guanidine groups of arginine and the  $\epsilon$ -amino groups of lysine. Only about one-third of the terminal  $\alpha$ -amino groups and less than one-tenth of the imidazole groups of histidine can be expected to bind dye. The binding is further dependent upon the number and position of carboxylate ions which may exert a force opposing the approach of dye anions, and upon the degree of hydrogen bonding in the protein.<sup>10</sup>

Competitive interference with acid dye binding can be demonstrated by alternately spotting a solution of protamine and a solution of DNA (2.3 mg./ml.), thereby allowing formation of a precipitate of protamine-nucleate on the filter paper. Such a precipitate retains considerably less dye at pH 8 than a spot containing an equivalent amount of protamine alone. Protamine is also able to combine with and precipitate less basic proteins such as insulin. A protamine-insulin complex formed on filter paper in the same manner as the protamine nucleate was found to stain at pH 8 with

almost undiminished intensity when compared to an equivalent amount of protamine alone. It appears thus that the dye at high pH is able to compete successfully with insulin but not as well with DNA for binding sites on the protamine. The inhibitory effect of DNA is not as pronounced in these model systems when protamine nucleate is stained at low pH. How-

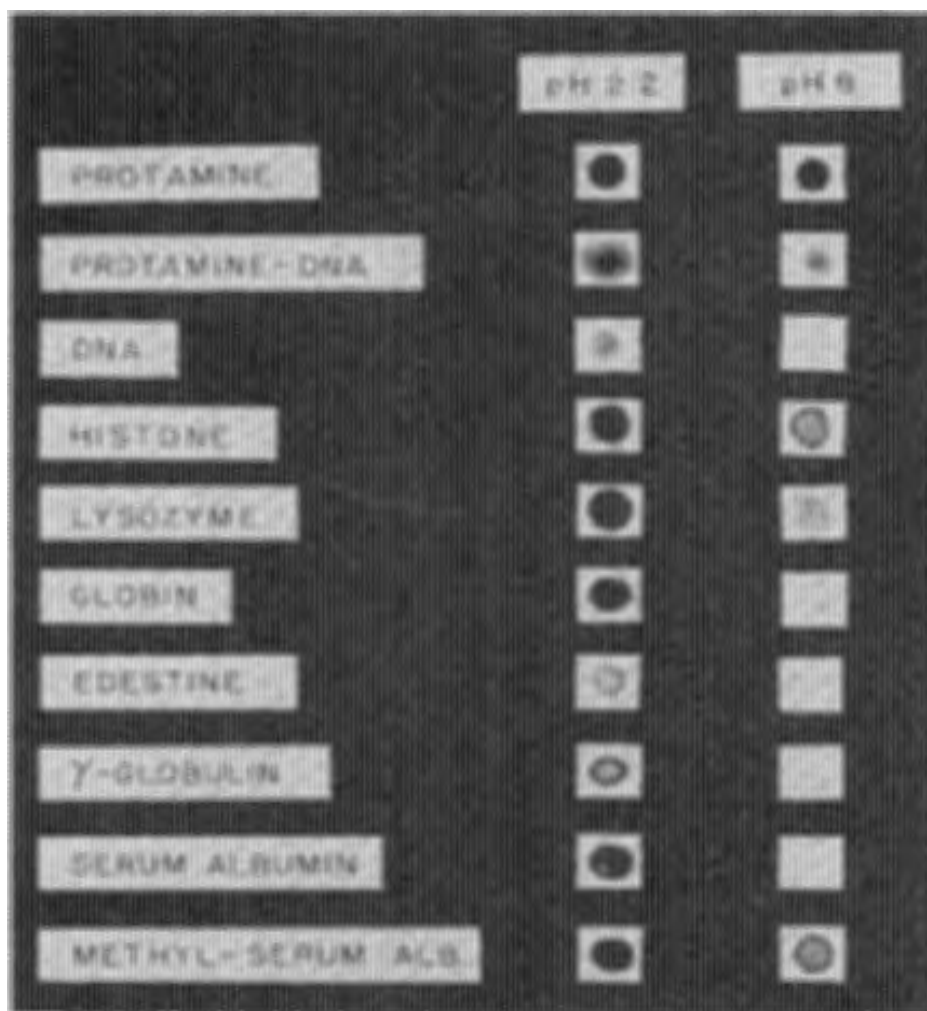


FIGURE 5

A series of drops of model-proteins stained with Fast green at pH 2.2 and pH 8. Photographed in red light, reduced (actual size of filter paper squares 13 × 13 mm.).

ever, we have observed that two different samples of DNA tested on filter paper were themselves able to bind dye at pH 2.2. (Two samples of ribonucleic acid could not be tested since they diffused from the filter paper during the staining procedure.) It is not known whether nucleic acids in fixed tissues retain acid dye when staining is performed, as custom-



ary, at low pH. If this were the case, it would be exceedingly difficult to detect since this phenomenon can be expected to be overcompensated by a stronger opposite effect, namely, the partial inhibition of protein staining in presence of nucleic acid.<sup>5</sup> Although the results of the model experiments reported here may not apply exactly to observations made on fixed and stained tissues, they still make it doubtful whether acid staining at low pH can be used for quantitative determination of basic protein groups in tissue sections unless nucleic acids were removed prior to staining.

It should be added that the staining of model proteins has proved to be quite reproducible. In all instances was it possible to demonstrate by re-staining at pH 2.2 that the failure to stain at pH 8 was not due to elution of the stainable material. Exposure of the paper strips to hot TCA, as is done in the histological application of the procedure, does not alter the results except that protamine is almost totally extracted. Since no protamine containing fish sperm was available to us, we do not know whether protamine would be lost from cell structures during this procedure. If this were found to be the case, it might be circumvented by enzymatic removal of DNA in such cases.

The assumption that histones or histone-like proteins are mainly responsible for the histological staining picture is thus supported by the model experiments and can be subjected to some further verification based on known analytical findings. Recent biochemical data<sup>11</sup> indicate that histones occur in a constant quantitative ratio to DNA in cell nuclei; neither of these compounds varies in amount when cells undergo physiological changes that bring about considerable variations in nuclear non-histone protein content. We have consequently determined the "DNA-histone ratios" of several series of tissue nuclei by microphotometric estimations of Feulgen-dye, and of Fast green bound at pH 8. The methods used have been described previously<sup>12</sup> and the results are summarized in table I.

It is evident that the Feulgen-Fast green ratios are quite similar in the somatic mammalian and two of the reptilian tissues tested. The polyploid series of liver nuclei as indicated by their DNA content is equally well detectable on the basis of Fast green measurements. The three series of thyroid nuclei represent cells in very different physiological states whose nuclei exhibit striking differences in size; the same is also true for the three types of mouse kidney nuclei which are reported here, but there is no detectable change of Feulgen dye or Fast green content within either series.<sup>13</sup> Lizard erythrocyte nuclei exhibit a markedly lower Feulgen-Fast green ratio and onion root tip nuclei show an intermediate ratio.

Vendrely and Vendrely<sup>14</sup> have recently reported an unusually high arginine-DNA ratio in certain fish sperm, as well as in beef sperm, when compared to other types of nuclei. By our method beef sperm has been

TABLE 1

ORGAN AND SAMPLE			AVERAGE NUCLEAR VOLUME OF	FEULGEN DYE* PER NUCLEUS: MEAN $\pm$ S.E.	FAST GREEN* PER NUCLEUS: MEAN $\pm$ S.E.	RATIO† FEULGEN FAST GREEN
			FEULGEN SAMPLE MEASURED			
Rat	Liver	2n	...	537 $\pm$ 9 (30)	282 $\pm$ 18 (19)	1.9
		4n	...	1057 $\pm$ 19 (30)	555 $\pm$ 18 (23)	1.9
		8n	...	1987 $\pm$ 37 (20)	1247 $\pm$ 63 ( 8)	1.6
Thyroid	(a) normal	68 $\mu^3$	525 $\pm$ 9 (28)	272 $\pm$ 14 (20)	1.9	
	(b) hypophysectomized (inactive)	44 $\mu^3$	522 $\pm$ 6 (30)	266 $\pm$ 13 (19)	2.0	
	(c) thiouracil treated ("activated")	95 $\mu^3$	523 $\pm$ 11 (24)	256 $\pm$ 11 (18)	2.0	
Mouse	Kidney	(a) collecting duct	60 $\mu^3$	514 $\pm$ 7 (20)	333 $\pm$ 9 (20)	1.5
		(b) proximal tubule of castrate	103 $\mu^3$	502 $\pm$ 10 (20)	308 $\pm$ 18 (20)	1.6
		(c) proximal tubule of androgen-treated castrate	149 $\mu^3$	530 $\pm$ 11 (20)	313 $\pm$ 15 (20)	1.7
Beef	Sperm <sup>a</sup>	...	Em = 0.153 $\pm$ 0.002 (15)	Em = 0.369 $\pm$ 0.009 (15)	0.42	
Lizard	Erythro- cytes <sup>b</sup>	1st sample	...	335 $\pm$ 6 (20)	538 $\pm$ 12 (20)	0.62
		2nd sample	...	350 $\pm$ 10 (15)	536 $\pm$ 14 (15)	0.65
	Liver	...	371 $\pm$ 7 (20)	214 $\pm$ 11 (20)	1.7	
	Kidney	...	394 $\pm$ 7 (20)	208 $\pm$ 11 (20)	1.9	
Onion	Root tip	...	3140 $\pm$ 60 (20)	3340 $\pm$ 80 (20)	0.94	

Optical conditions of microphotometric measurements: Beckman B spectrophotometer used as light source; animal nuclei were measured at 550  $m\mu$  for Feulgen-, and at 630  $m\mu$  for Fast green determinations, with 0.3 mm. slit width. To avoid stray light error in measuring the very dense root tip nuclei, measurements were conducted at 600  $m\mu$ , close to 50% of peak absorption for both dyes.

\* Amounts of dye are given in arbitrary units calculated according to the formula: amount = (0.6 average nuclear diameter)<sup>2</sup>  $\times$  optical density  $\times$  100. Numbers in parentheses are numbers of measurements.

† Since these ratios are based on arbitrary units of dye content, they do not indicate the ratios of actual amounts of DNA and histone and are only of value for relative comparison.

<sup>a</sup> The Feulgen-Fast green ratio of sperm was calculated on the basis of average optical density (Em) of central 2  $\mu$  cores. Since these sperm cells are of very regular size and shape, unaffected by the treatments used, this method results in a ratio directly comparable to all the others given.

<sup>b</sup> Blood smears, prefixed in methanol, were used. In these the nuclei are flattened to various extents. The computation of amounts of dye will in such a case result in values which are low compared to those obtained on spherical nuclei. Consequently the Feulgen values of erythrocytes cannot be compared to those of liver and kidney cells. Fast green values are affected to the same extent so that the Feulgen-Fast green ratio remains directly comparable to that of other nuclear types. Two different samples, stained at different occasions, were measured to test the reproducibility of the results.

found to possess the lowest Feulgen-Fast green ratio of all tissues tested, which agrees with these findings. Preliminary observations on mouse sperm tend to indicate a similar situation.

Assuming the Feulgen reaction to allow a correct quantitative estimate of nuclear DNA content even among different organisms, a change in the Feulgen-Fast green ratio may indicate a difference in the amount of nuclear basic protein, a different composition of the basic protein, or both. The exact significance of changes in this ratio will only be understood when more extensive analytical data on histones from different sources become available.

As has been pointed out earlier, this staining procedure cannot serve to titrate all basic groups that occur in the proteins which can be visualized by it. However, the results of the photometric measurements make it likely that a constant proportion of the available groups is stained when nuclei of related cell types are compared. This method should consequently prove to be of value for such relative quantitative comparisons, as well as provide a simple routine procedure for visualization of histones.

*Summary.*—Treatment of formalin-fixed tissue sections with Fast green at pH 8 after extraction of nucleic acids results in a selective chromatin stain. Model experiments were undertaken on a series of proteins to determine the specificity of the staining procedure, and microphotometric determinations of the Feulgen-Fast green ratios in nuclei of various cell types were made. All experiments indicate that histones or protamines are responsible for the histological staining picture.

*Acknowledgments.*—The authors are indebted to Mrs. E. Alfert for technical assistance, and wish to express their gratitude for gifts of materials used in this study to the following: Dr. H. Jordan for the reptilian tissues, Mr. M. Gordon for the beef sperm, Dr. D. M. Greenberg for the edestine, Armour Research Laboratories for samples of beef serum albumin and lysozyme, Eli Lilly & Co. for the insulin and protamine, and Cutter Laboratories for the  $\gamma$ -globulin.

\* Supported by Cancer Research Funds of the University of California.

† Supported in part by a grant from the Rockefeller Foundation.

<sup>1</sup> Caspersson, T., *Cell Growth and Cell Function*, Norton, New York, 1950.

<sup>2</sup> Pollister, A. W., and Ris, H., *Cold Spring Harbor Symp. Quant. Biol.*, **12**, 147–157 (1947).

<sup>3</sup> Singer, M., *Int. Rev. Cytology*, **1**, 211–255 (1952).

<sup>4</sup> Schwantes, H. O., *Protoplasma*, **41**, 382–414 (1952).

<sup>5</sup> Kaufmann, B. P., McDonald, M. R., and Gay, H., *J. Cellular Comp. Physiol.*, **38**, Suppl. 1, 71–99 (1951).

<sup>6</sup> Alfert, M., *Biol. Bull.*, **103**, 145–156 (1952).

<sup>7</sup> Vincent, W. S., these PROCEEDINGS, **38**, 139–145 (1952).

<sup>8</sup> Hamer, D., *Brit. J. Cancer*, **5**, 130–139 (1951).

<sup>9</sup> Fraenkel-Conrat, H., and Olcott, H. S., *J. Biol. Chem.*, **161**, 259–268 (1945).

..., *Cold Spring Harbor Symp. Quant. Biol.*, **14**, 97-112 (1950).  
 Mrs. E., and Ris, H., *J. Gen. Physiol.*, **34**, 475-492 (1951).  
 J., *Exp. Cell Research*, Suppl. 2, 75-94 (1952).  
 ... cytochemical studies on these cell types will be published elsewhere, by  
 and Alfer, and by Alfer, Bern, and Kahn.  
 R., and Vendrely, C., *Nature*, **172**, 30-31 (1953).

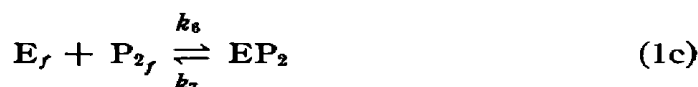
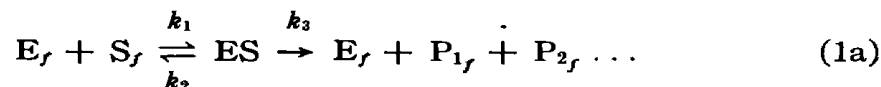
## THE EVALUATION OF THE KINETIC CONSTANTS OF ENZYME CATALYZED REACTIONS

BY ROBERT J. FOSTER AND CARL NIEMANN

GATES AND CRELLIN LABORATORIES OF CHEMISTRY,\* CALIFORNIA INSTITUTE OF TECHNOLOGY

Communicated July 27, 1953

For an enzyme-catalyzed reaction that can be described by equations (1a), (1b), (1c), etc., and where the experimental conditions are such that



the course of the reaction is given, within the limits of experimental error, by the integrated rate equation (2), the evaluation of the kinetic

$$k_3[E]t = K_S \left( 1 + [S]_0 \sum_{j=1}^n 1/K_{P_j} \right) \ln [S]_0/[S]_t + \left( 1 - K_S \sum_{j=1}^n 1/K_{P_j} \right) ([S]_0 - [S]_t) \quad (2)$$

constants  $K_S = (k_2 + k_3)/k_1$  and  $k_3$ , and eventually of  $K_{P_1} = k_5/k_4$ ,  $K_{P_2} = k_7/k_6$ , etc., is a problem of considerable practical importance which is complicated not only by the possible competitive interaction of the free enzyme with one or more of the reaction products but also by the fact that the integrated rate equation contains both a zero and a first order term.

The traditional solution of this problem has been to study the reaction in its initial stages so as to minimize the difficulties arising from the possible interaction of the free enzyme with one or more of the reaction products and to estimate the initial velocities, at the various initial specific substrate

# Topotecan, a New Active Drug in the Second-Line Treatment of Small-Cell Lung Cancer: A Phase II Study in Patients With Refractory and Sensitive Disease

By Andrea Ardizzoni, Heine Hansen, Per Dombernowsky, Teresa Gamucci, Shoshana Kaplan, Pieter Postmus, Giuseppe Giaccone, Brigitte Schaefer, Jantien Wanders, and Jaap Verweij for the European Organization for Research and Treatment of Cancer Early Clinical Studies Group and New Drug Development Office, and the Lung Cancer Cooperative Group

**Purpose:** To assess activity and toxicity of topotecan in previously treated small-cell lung cancer (SCLC) patients.

**Patients and Methods:** Patients with measurable SCLC, progressive after one first-line regimen, were eligible for the study. Two groups of patients were selected: (1) patients who failed first-line treatment  $\leq$  3 months from chemotherapy discontinuation (refractory group); and (2) patients who responded to first-line treatment and progressed greater than 3 months after chemotherapy discontinuation (sensitive group). Topotecan was administered as a 30-minute daily infusion at a dose of 1.5 mg/m<sup>2</sup> for 5 consecutive days, every 3 weeks.

**Results:** One hundred one patients were entered onto the study and 403 courses were administered. Ninety-two patients (47 refractory and 45 sensitive) were eligible and assessable for response. Among refractory patients, there were two partial responses (PRs) and one complete response (CR), for an overall response rate of 6.4% (95% confidence interval [CI], 1.3% to 17.6%),

whereas in the sensitive group, there were 11 PRs and six CRs, for an overall response rate of 37.8% (95% CI, 23.8% to 53.5%). Overall median duration of response was 7.6 months. Median survival was 5.4 months; median survival of refractory patients was 4.7 months, whereas that of sensitive patients was 6.9 months ( $P = .002$ ). Median survival of responding patients was 12.5 months. Toxicity was mainly hematologic. Leukopenia, although short-lived, was universal, with grade III and IV neutropenia occurring in 28% and 46.8% of cycles, respectively. Nonhematological toxicity was mild. Fatigue/malaise was reported in 39.3% of cycles and transient elevation of liver enzymes in 17%.

**Conclusion:** Topotecan has significant activity in SCLC, particularly in patients sensitive to prior chemotherapy, with predictable and manageable toxicity. The incorporation of topotecan in combination chemotherapy regimens for future treatment of SCLC is warranted. *J Clin Oncol 15:2090-2096. © 1997 by American Society of Clinical Oncology.*

**A**LTHOUGH small-cell lung cancer (SCLC) is highly responsive to initial chemotherapy, most patients experience tumor progression within a year after completion of first-line treatment.<sup>1</sup> Results of second-line chemotherapy are poor. The most active single agents yield response rates in the range of 10% to 30%,<sup>2</sup> and response rates with combination chemotherapy regimens are usually below 40%.<sup>3,4</sup> In addition, duration of response to second-line chemotherapy is short, with a median survival that rarely exceeds 4 months.<sup>5</sup>

Two categories of previously treated SCLC patients can be identified according to their different probability of responding to second-line chemotherapy: refractory patients are those who have never responded to first-line treatment or who responded but progressed within 3 months from the end of treatment; sensitive patients are defined as those who responded to first-line treatment and relapsed after a treatment-free interval of 3 or more months.<sup>6</sup> Refractory SCLC patients rarely respond to second-line single-agent chemotherapy and may only respond to true non-cross-resistant combination chemotherapy,<sup>7</sup> whereas sensitive patients have a reasonable chance of responding to second-line chemotherapy or even to first-line chemotherapy rechallenge.<sup>8</sup> In this latter category of patients, the probability of seeing a response for an active agent or regimen is similar to that achievable in untreated patients.<sup>3</sup>

Among new active agents in the treatment of SCLC, camptothecin analogs have emerged as most promising. Topotecan is a semisynthetic water-soluble analog of camptothecin with specific targeting to topoisomerase-I and remarkable preclinical antitumor activity in a broad range of tumors.<sup>9</sup> Phase I studies, involving many different schedules of administration, have identified neutropenia as the dose-limiting toxicity and enabled identifica-

---

Principal investigators and their affiliations are listed in the Appendix.

Submitted November 4, 1996; accepted February 5, 1997.

Presented in part at the 30th Annual Meeting of the American Society of Clinical Oncology, Dallas, TX, May 14-17, 1994.

This study was conducted by the Early Clinical Studies Group (J. Verweij, Chairman) and Lung Cancer Cooperative Group (G. Giaccone, Chairman) of the European Organization for Research and Treatment of Cancer and was supported by SmithKline Beecham Pharmaceuticals, Philadelphia, PA.

Address reprint requests to Andrea Ardizzoni, MD, Department of Medical Oncology I, Istituto Nazionale per la Ricerca sul Cancro, Largo Rosanna Benzi 10, 16132 Genova, Italy.

© 1997 by American Society of Clinical Oncology.  
0732-183X/97/1505-0029\$3.00/0

tion of 1.5 mg/m<sup>2</sup>/d intravenously daily for 5 days, repeated every 21 days, as the recommended dose and schedule for phase II studies.<sup>10</sup> The aim of the present phase II study was to assess the antitumor activity of topotecan in patients with both refractory and sensitive previously treated SCLC, and to further characterize its toxicity in this group of patients.

## PATIENTS AND METHODS

### Eligibility

Patients eligible for the trial were required to have all of the following: histologically or cytologically confirmed diagnosis of SCLC, presence of at least one bidimensionally measurable target lesion outside areas of prior radiotherapy, age  $\leq$  75 years, World Health Organization (WHO) performance status  $\leq$  2, a life expectancy greater than 3 months, and evidence of progressive disease after one first-line chemotherapy regimen that did not include camptothecin analogs. Patients treated twice with the same first-line chemotherapy regimen were also eligible. Patients must have been off all previous systemic therapy at least 3 weeks before study entry and must have recovered from the side effects of prior therapy. Patients with brain metastases were eligible provided that neurologic symptoms were under control with radiotherapy or steroid treatment, and that the brain was not the only site of assessable disease. At entry, eligible patients were required to have adequate hematologic, renal, and hepatic functions as defined by WBC count  $\geq$   $3.5 \times 10^9/L$ , absolute neutrophil count (ANC)  $\geq$   $1.5 \times 10^9/L$ , platelet count  $\geq$   $100 \times 10^9/L$ , hemoglobin level  $\geq$  9 g/dL, total bilirubin level  $\leq$  1.5 mg/dL, ALT and AST  $\leq$  two times the upper normal limit in absence of liver metastases or  $\leq$  five times the upper normal limit in case of documented liver metastases, and creatinine level  $\leq$  1.6 mg/dL. Informed consent was required from all patients according to the local regulatory requirements.

### Pretreatment and Follow-Up Studies

Within 2 weeks before the start of treatment, patients underwent a complete medical history and physical examination, assessment of vital signs, performance status and weight, 12-lead ECG, bone marrow biopsy, chest X-ray and computed tomography (CT) scan, brain CT, abdominal CT scan or ultrasound, complete blood count (CBC), blood chemistry, and urine analysis. Blood counts were repeated twice per week during the first course and weekly from the second course onward. Blood chemistry was obtained weekly. Vital signs were recorded daily during each first course. History, physical examination, assessment of performance status and weight, and urine analysis were repeated before each course. ECG, chest X-ray, CT scans, and ultrasounds, along with all other tests necessary to assess response, were performed every other cycle.

### Treatment

Topotecan (SmithKline Beecham Pharmaceuticals, Philadelphia, PA) was supplied in vials containing 5 mg of the free base as lyophilized cake with no antibacterial preservatives. The lyophilized formulation was reconstituted with 2 mL of sterile water for injection before dilution with 5% dextrose solution (final dilution between 3  $\mu$ g/mL and 500  $\mu$ g/mL). Topotecan was administered as a 30-minute intravenous infusion at a dose of 1.5 mg/m<sup>2</sup>/d for 5 consecutive days. Treatment cycles were repeated every 3 weeks if complete

hematologic recovery (WBC count  $>$   $3.5 \times 10^9/L$ , ANC  $\geq$   $1.5 \times 10^9/L$ , and platelet count  $>$   $100 \times 10^9/L$ ) and recovery to at least Common Toxicity Criteria (CTC) grade I nonhematologic toxicity had occurred. In case of incomplete hematologic recovery on day 22, treatment was delayed 1 or 2 weeks. Topotecan dose reduction of 0.25 mg/m<sup>2</sup>/d was to be performed in case of febrile neutropenia (ANC  $<$   $0.5 \times 10^9/L$  with fever or infection) or grade IV neutropenia lasting 7 to 14 days, grade III to IV thrombocytopenia associated with bleeding or lasting 7 to 14 days, and in case of grade II nonhematologic toxicity (except for nausea, vomiting, and alopecia) at recycle. A 0.5-mg/m<sup>2</sup>/d dose reduction was performed in case of ANC  $\leq$   $0.5 \times 10^9/L$  or platelet count  $\leq$   $50 \times 10^9/L$  lasting more than 14 days and in case of grade III to IV nonhematologic toxicity (except for nausea, vomiting, and alopecia). In any case, the minimum topotecan dose had to be 1.0 mg/m<sup>2</sup>/d.

Additional antineoplastic agents, including drugs that modulate the endocrine and/or immunologic response to cancer, had not to be given. Prophylactic use of hematopoietic growth factors was not allowed. Palliative radiotherapy not including the target lesions was allowed.

Decisions regarding continuation of treatment were made on the basis of tumor reassessments at the beginning of each cycle. A minimum of two courses had to be given before response evaluation; treatment was continued in case of response or stable disease, at the discretion of the responsible investigator, or until progression or severe cumulative toxicity or for a maximum of 6 months after the maximal response.

### Criteria for Evaluation of Response, Toxicity, and Survival

Response and toxicity were evaluated according to WHO and CTC criteria, respectively.<sup>11,12</sup> All responses had to be confirmed by two observations made not less than 4 weeks apart and had to be validated by a committee, including the study chairmen, study monitor, and an expert radiologist. Time to progression and survival were calculated from the start of treatment to progression or death, respectively, using the Kaplan-Meier method. Differences in response rates were calculated according to the Fisher's exact test (two-sided).

### Study Design and Statistical Considerations

The study was made up of two different phase II trials, one for the sensitive group and the other for the refractory group. The primary aim of the study was to assess the antitumor activity of topotecan and to further define its toxicity in the two groups of patients. Secondary aims were to evaluate time to progression and survival. Parallel to this study a population pharmacokinetic study was performed, which will be published separately.

The sample size was calculated according to Gehan,<sup>13</sup> which entailed that accrual in both groups was to be stopped if no response was seen in the first 14 assessable patients. If at least one response was observed, additional patients (to a total of 40 assessable patients in each group) were to be entered to allow a reliable estimate of response rate.

## RESULTS

### Patient Demographics

From July 1992 to September 1994, a total of 101 SCLC patients were entered onto the study from 22 Euro-

Table 1. Patient Characteristics

	Refractory		Sensitive		Total	
	No.	%	No.	%	No.	%
Eligible	47	100	46	100	93	100
Sex						
Female	17	36.2	12	26.1	29	31.2
Male	30	63.8	34	73.9	64	68.8
Age, years						
< 60	25	53.2	22	47.8	47	50.5
≥ 60	22	46.8	24	52.2	46	49.5
WHO performance status						
0	8	17.0	15	32.6	23	24.7
1	29	61.7	24	52.2	53	57.0
2	10	21.3	7	15.2	17	18.3
Disease extent						
Limited	15	31.9	20	43.5	35	37.6
Extensive	32	68.1	26	56.5	58	62.4
Prior treatment						
Surgery	6	12.8	5	10.9	11	11.8
Immunotherapy	2	4.2	4	8.7	6	6.4
Radiotherapy	9	19.1	25	54.3	34	36.5
Chemotherapy						
≤ 3 drugs	34	72.3	20	43.5	54	58.1
> 3 drugs	13	27.7	26	56.5	39	41.9
≤ 6 months	39	83.0	37	80.4	76	81.7
> 6 months	8	17.0	9	19.6	17	18.3

pean institutions. Eight patients were not eligible: two had no measurable lesions, one refused treatment before the start, two had a mixed non-SCLC (NSCLC) and SCLC histology, one had symptomatic brain metastases, and two had abnormal baseline blood tests. Therefore, 47 and 46 patients in the refractory and sensitive groups, respectively, were eligible. A total of 403 courses (154 refractory and 249 sensitive), with a mean of four courses (range, one to 14) per eligible patient, were administered. Main patient characteristics are listed in Table 1. Most patients were men (69%), with a median age of 58 years and a median performance status of 1. Sixty-two percent of the patients had extensive disease: sites of metastatic disease were liver in 31.9%, brain in 10.6%, and bone in 4.3%. The majority of patients had received extensive prior treatment, including radiotherapy in one third and chemotherapy in all cases. The mean number of drugs received during first-line chemotherapy was three, for a mean treatment duration of 4 months. Some of the patients received as many as 10 drugs within first-line alternating chemotherapy regimens that lasted up to 10 months. Seven patients were rechallenged at first relapse with the same first-line chemotherapy regimen before being treated with topotecan; four were enrolled among refractory and three among sensitive patients based on the type of response achieved with the second first-line challenge.

Table 2. Response Evaluation

	Refractory		Sensitive		Total	
	No.	%	No.	%	No.	%
Eligible	47	100	46	100	93	100
Not assessable	—		1	2.1	1	1.0
Assessable	47	100	45	100	92	100
CR	1	2.1	6	13.3	7	7.6
PR	2	4.2	11	24.0	13	14.1
OR	3	6.4	17	37.8	20	21.7
NC	19	40.4	14	31.1	33	35.9
PD	20	42.6	13	28.9	33	35.9
Early death	5	10.6	1	2.2	6	6.5

Abbreviations: OR, objective response; NC, no change; PD, progressive disease.

### Response to Treatment

Of 93 eligible patients, one could not be evaluated for response because of inadequate radiologic assessment. Of the 92 assessable patients (47 in the refractory and 45 in the sensitive groups, respectively), six died early (five because of tumor-related complications and one because of cardiac failure) and were recorded as treatment failures. Early deaths occurred mainly among refractory patients (five of six), reflecting the poor prognosis of this category of patients (Table 2). There were 13 (14.1%) partial responses (PRs) and seven (7.6%) complete responses (CRs): two PRs (4.2%) and one CR (2.1%) were found among refractory patients, while 11 PRs (24%) and six CRs (13.3%) occurred among sensitive patients. The overall response rate was 21.7% (95% confidence interval [CI], 13.8% to 31.6%): 6.4% (95% CI, 1.3% to 17.5%) in patients refractory and 37.8% (95% CI, 23.7% to 53.5%) in patients sensitive to first-line chemotherapy (Table 2).

There were 11 patients with brain metastases at registration: seven had bidimensionally measurable disease on brain CT or magnetic resonance imaging (MRI) and were assessable for response to topotecan. Three patients obtained a complete remission and one a partial remission. Another patient had a 42% tumor shrinkage of the target lesion with disappearance of another nonmeasurable lesion. All of the CRs occurred in patients with sensitive disease, while the only PR was obtained in a refractory patient. All patients with brain metastases who responded to topotecan outside the brain achieved an objective response also at the level of brain metastases.

A number of pretreatment variables were analyzed for their possible influence on response to second-line topotecan (Table 3). The type of response to prior chemotherapy along with the time elapsing from the end

**Table 3. Univariate Analysis of Prognostic Factors for Response to Topotecan**

	No. Responders/ Eligible	%	P
Performance status			
0-1	16/76	21.0	NS
2	4/17	23.5	
Sex			
Male	16/64	25.0	NS
Female	4/29	13.8	
Age, years			
< 60	11/47	23.4	NS
≥ 60	9/46	19.6	
Sensitivity to prior CT			
Sensitive	17/46	37.0	.0008
Refractory	3/47	6.4	
No. of drugs in prior CT regimen			
≤ 3	11/54	20.3	NS
> 3	9/39	23.0	
Duration of prior CT, months			
≤ 6	15/76	19.7	NS
> 6	5/17	29.4	
Prior CT including			
Anthracyclines			
Yes	17/68	25.0	NS
No	3/25	12.0	
Etoposide			
Yes	20/86	23.2	NS
No	0/7	—	
Platinum compounds			
Yes	8/39	20.5	NS
No	12/54	22.2	
Interval between end of prior CT and start of topotecan, months			
≤ 6	8/72	11.1	.00001
> 6	12/21	57.1	
Response to prior CT			
CT + PR	19/70	27.1	.002
No response	1/23	4.3	

Abbreviations: CT, chemotherapy; NS, not significant.

of first-line to the start of second-line treatment were confirmed to be the most important predictors of response. On the contrary, the type of prior chemotherapy did not appear to influence treatment outcome in a statistically significant manner. However, it can be observed that none of the few patients who had not received prior etoposide-containing chemotherapy responded to topotecan and that response rate in patients who had not had prior anthracycline-containing chemotherapy was halved compared with that of patients who had received this type of prior chemotherapy.

Overall median duration of response was 7.6 months (95% CI, 5.1 to 12.2 months). Overall median time to progression was 2.8 months (95% CI, 2.2 to 3.9 months), and overall survival was 5.4 months (95% CI,

4.8 to 6.3 months); median survival of sensitive patients was 6.9 months (95% CI, 5.4 to 9.9 months), while that of refractory patients was 4.7 months (95% CI, 2.7 to 5.4 months) ( $P < .0027$ ) (Fig 1). Median survival of responding patients was 12.5 months (95% CI, 6.3 to 17.4 months).

### Toxicity

The main toxicity was hematologic (Table 4). Leukopenia was almost universal, with severe (grade III to IV) neutropenia occurring in 75% of courses. Infections were recorded in 6% of courses, and one patient died of this complication. Both anemia and thrombocytopenia were frequent but usually not severe. Topotecan hematologic toxicity was predictable and manageable, and it did not appear to be cumulative. One hundred twenty-six blood transfusions were given to 52 patients (55.3%), and 12 platelet transfusions were given to five patients (5.3%). Nonhematologic toxicity was generally mild with nausea/vomiting, stomatitis, and diarrhea being rare. The most common complaint was fatigue/malaise, which occurred during nearly one third of courses. Toxicity, especially myelosuppression, required dose reductions and treatment delays in 18.6 and 26.5% of courses, respectively (Table 5). The median delivered dose-intensities of topotecan were 2.1 and 2.2 mg/m<sup>2</sup>/wk in refractory and sensitive patients, respectively.

### DISCUSSION

The results of SCLC treatment remain unsatisfactory. In fact, most patients with SCLC, despite high response rates to initial treatment, will eventually die of tumor progression. Results of second-line chemotherapy are poor because of the emergence of acquired drug resistance. Chemotherapeutic agents such as cisplatin, etoposide, and doxorubicin, which are currently incorporated into first-line chemotherapy regimens, yield only 5% to 20% response rates when used in previously treated patients.<sup>2</sup> The response rate to a number of Southwest Oncology Group salvage chemotherapy programs, including nearly 200 patients, was only 4.5% to 13.3%, with a disappointing median survival of 2.5 to 3.9 months.<sup>5</sup>

Therefore, the identification of new active agents for the treatment of SCLC represents one of the priority research issues. Unfortunately, the search for new active compounds in both pretreated and untreated SCLC patients has been, until recently, disappointing.<sup>13</sup> The present study, which is one of the largest phase II trial ever conducted with a single agent in the second-line treatment of this disease and the only study in which



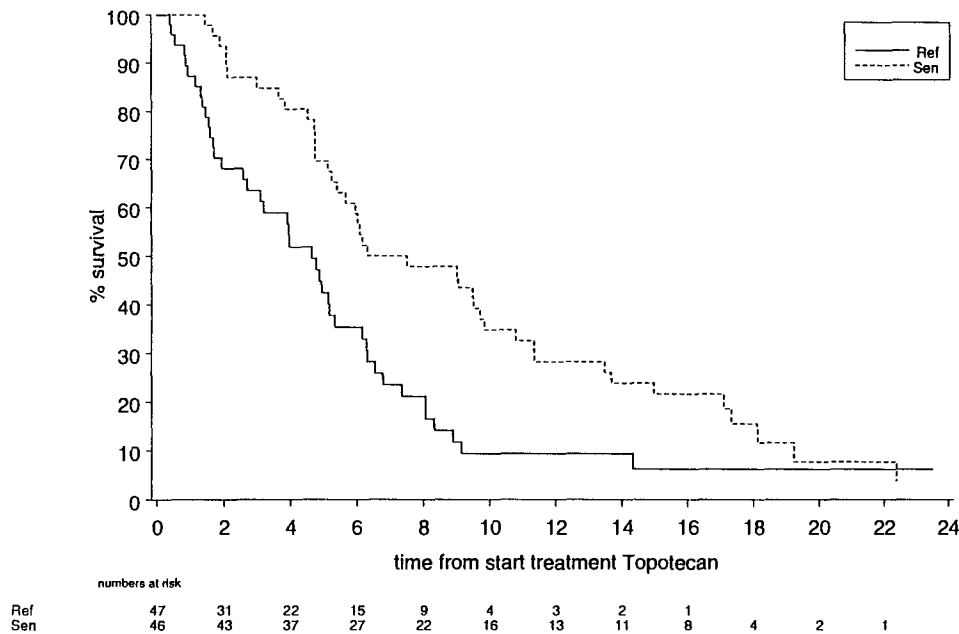


**Fig 1. Actuarial survival according to prior treatment results. (—) Actuarial survival of refractory patients (median survival, 4.7 months). (---) Actuarial survival of sensitive patients (median survival, 6.9 months). Difference in survival between refractory and sensitive patients:  $P = .0027$  (log-rank test of equality).**

a prospective distinction between refractory and sensitive patients has been made, provides evidence that topotecan is a new active agent for the treatment of SCLC. The 22% overall response rate obtained is among the highest reported in previously treated patients with single agents that are currently considered first choice in the treatment of SCLC.<sup>2</sup> This result should be interpreted in light of the heavy prior treatment of the patients enrolled onto the present study (two CRs and one PR were observed even among the patients who had been treated twice with the same first-line chemotherapy) and the strict criteria used for

response assessment and verification. In addition, the duration of response (7.6 months) as well as the median survival of responding patients (12.5 months) were considerably long. Both figures are almost superimposable to those achieved with first-line treatments. Finally, responses were observed at all disease sites, including the CNS, where five of seven patients with measurable CNS involvement achieved an objective response.

The response rate was, as expected, higher in the group of sensitive patients than in those who were refractory, being nearly 40% among 45 assessable pa-

**Table 4. Toxicity During All Courses (n = 403)**

Toxicity	CTC Grade							
	1		2		3		4	
	No.	%	No.	%	No.	%	No.	%
Leukopenia	22	5.4	93	23.0	236	58.5	40	9.9
Neutropenia	19	4.7	51	12.6	113	28.0	189	46.9
Thrombocytopenia	150	37.2	86	21.3	71	17.6	48	11.9
Anemia	143	35.5	208	51.6	36	8.9	12	2.9
Nausea	79	19.6	20	4.9	3	0.7	—	—
Vomiting	31	7.7	13	3.2	1	0.2	—	—
Alopecia	90	22.3	154	38.2	3	0.7	—	—
Fatigue/malaise	86	21.3	59	14.6	11	2.7	3	0.7
Infection	12	2.9	7	1.7	4	1.0	2	0.5
Diarrhea	9	2.2	4	1.0	1	0.2	—	—
Stomatitis	10	2.5	7	1.7	—	—	—	—
Liver	51	12.6	14	3.5	4	1.0	—	—

Note. There was 1 toxic death of neutropenia and infection.

**Table 5. Drug Administration**

	Refractory		Sensitive		Total	
	No.	%	No.	%	No.	%
Patients with reductions	10	21.3	13	28.3	23	24.7
Courses with reductions	37	24.0	38	15.3	75	18.6
Delayed courses	45	29.2	62	24.9	107	26.5

tients. This level of second-line activity approaches that obtained in first-line by most active single agents.<sup>14</sup> On the contrary, of the 47 refractory patients, only three had a major response to treatment. However, it is worth noting that the duration of response in the three refractory patients was similar to that achieved in sensitive patients, suggesting that responses obtained in the two groups of patients are qualitatively similar. It must be stressed that the subgroup of refractory SCLC patients have a bleak prognosis with a negligible chance of responding to any second-line single-agent chemotherapy and a short life expectancy.<sup>6</sup>

In the present study, the response to prior chemotherapy along with the treatment-free interval, which the definition of refractory/sensitive refers to, were found to be the only parameters to affect the probability of response to topotecan (Table 3). Instead, the type of prior chemotherapy did not appear to significantly influence treatment outcome. However, it is interesting to note that the response rate to topotecan was higher in patients who had been given prior topoisomerase II-directed agents (epipodophyllotoxins and anthracyclines) than in those who had not. This difference, although not statistically significant probably because of the small number of patients in each subgroup, would be in agreement with pre-clinical data that suggest that resistance to topoisomerase II-targeting agents may induce collateral sensitivity to topoisomerase I drugs.<sup>15</sup>

Our results are difficult to compare with that of other second-line single-agent studies because the distinction between refractory and sensitive patients is rarely made, and information about prior treatment is often unreported. There have been only two other topotecan studies in SCLC published in full. The Eastern Cooperative Oncology Group has tested the dose of 2 mg/m<sup>2</sup> daily for 5 days in 48 previously untreated patients with extensive-stage disease. The objective response rate was 39%, with a median response duration of 4.8 months and a median survival of 10 months.<sup>16</sup> It is interesting to note that the response rate obtained by the American group in untreated patients is identical to that achieved in the present study in previously treated sensitive patients. The other topotecan study has been conducted by the

M.D. Anderson group in 32 patients who were refractory to first-line cisplatin-etoposide therapy. Similar to our study, the response rate in this poor-risk group of patients was only 11%.<sup>17</sup>

The best strategy for testing new agents in SCLC has long been debated.<sup>14</sup> The use of new drugs in second-line therapy has been questioned because, given the low response rate achievable in pretreated patients, several potentially active new agents might be missed. On the other hand, the advocated testing of new agents in first-line therapy poses ethical problems, because potentially inactive agents are given to patients who are likely to benefit from standard chemotherapy.<sup>18-20</sup> The present study provides further evidence that results of new drug testing in sensitive pretreated SCLC patients are reliable and similar to those obtained in first-line treatment without ethical drawbacks. The identification of agents with activity in refractory patients remains the real challenge for future new drug research in SCLC.

So far, CPT-11 has been the only other camptothecin analog tested in SCLC. Masuda et al<sup>21</sup> reported a 47% response rate among 16 previously treated SCLC patients. The results of the Japanese study can only be compared with those obtained with topotecan in the group of sensitive patients in the present study. In fact, 14 of the 15 patients treated with CPT-11 belonged to this category. In any case, the results of the two trials are difficult to compare because of the small number of patients in the CPT-11 study, which is responsible for a wide CI for the response rate (21.4% to 71.9%). However, it should be noted that there were no CRs in the CPT-11 study, whereas there were six (13.6%) CRs among sensitive patients treated with topotecan in the present study. In addition, the median duration of response was only 2 months in the CPT-11 study versus 7.6 months in our topotecan study. The toxicity profile of the two camptothecin derivatives also turned out to be different. While leukopenia was the most common side effect for both agents, CPT-11 was, in addition, responsible for diarrhea in 70% of the patients and for pulmonary toxicity in 13%. On the contrary, with topotecan, diarrhea occurred in only 3.4% of cases and no pulmonary toxicity was registered.

Results of topotecan also compare favorably with those recently obtained with other new-generation agents such as Taxol (Bristol-Myers Squibb, Princeton, NJ) and gemcitabine, which, evaluated in untreated patients, have yielded response rates in the range of 30% to 40%.<sup>22-24</sup>

In conclusion, topotecan has significant activity in the second-line treatment of SCLC, particularly in the category of sensitive patients. Toxicity of topotecan is mainly hematologic, with predictable and manageable

grade III to IV leukopenia/neutropenia. Further studies of topotecan in combination chemotherapy of both first- and second-line treatment of SCLC are warranted.

#### APPENDIX

*Participating institutions (principal investigator):* National Institute for Cancer Research, Genoa, Italy (A. Ardizzoni); Finsen Center, Copenhagen, Denmark (H. Hansen); Herlev University Hospital, Copenhagen, Denmark (P. Dombernowsky); Regina Elena Institute, Rome, Italy (T. Gamucci); Kantonsspital, Basel, Switzerland (S. Kaplan); Free University, Amsterdam, The Netherlands (P. Postmus, G. Giaccone, J. Vermorken); Rotterdam Cancer Institute, Rotterdam, The Netherlands (J. Verweij); Netherlands Cancer Institute, Amsterdam, The Netherlands (W.W. ten Bokkel Huinink, N. Van Zandwijk); 12 de Octubre Hospital, Madrid, Spain (H. Cortes-Funes); Thoracic Clinic, Heidelberg, Germany (P. Drings); University of Turin, Turin, Italy (G. Scagliotti); University of Ioannina, Ioannina, Greece (N. Pavlidis); University of Newcastle, Newcastle, United Kingdom (J.H. Calvert); S. Giovanni Hospital, Bellinzona, Switzerland (C. Sessa); University of Glasgow, Glasgow, United Kingdom (S. Kaye); Kantonsspital, St Gallen, Switzerland (H. Senn); University of Edinburgh, Edinburgh, United Kingdom (J. Smyth); Medicine Clinic, Nurnberg, Germany (U. Bruntsch); Medicine Clinic, Klinikum rechts der Isar, Munich, Germany (A.R. Hanauske); University Hospital, Maastricht, The Netherlands (G. ten Velde); University Hospital, Nymegen, The Netherlands (D.J. Wagener); and University Hospital, Groningen, The Netherlands (H.J.M. Groen).

#### REFERENCES

- Hansen HH: Management of small-cell lung cancer. *Lancet* 339:846-849, 1992
- Grant SC, Gralla RJ, Kriss MG, et al: Single agent chemotherapy trials in small cell lung cancer, 1970-1990: The case for studies in previously treated patients. *J Clin Oncol* 10:484-498, 1992
- Giaccone G: Second line chemotherapy in small cell lung cancer. *Lung Cancer* 5:207-213, 1989
- Figoli F, Veronesi A, Ardizzoni A, et al: Cisplatin and etoposide as second line chemotherapy in patients with small cell lung cancer. *Cancer Invest* 6:1-5, 1988
- Albain KS, Crowley JJ, Hutchins L, et al: Predictors of survival following relapse or progression of small cell lung cancer. *Cancer* 72:1184-1191, 1993
- Giaccone G, Donadio M, Bonardi G, et al: Teniposide in the treatment of small-cell lung cancer: The influence of prior chemotherapy. *J Clin Oncol* 6:1264-1270, 1988
- Postmus PE, Smit EF, Kirkpatrick A, et al: Testing the possible non-cross resistance of two equipotent combination chemotherapy regimens against small-cell lung cancer: A phase II study of the EORTC Lung Cancer Cooperative Group. *Eur J Cancer Clin Oncol* 29A:204-207, 1993
- Postmus PE, Berendsen HH, Van Zandwijk N, et al: Retreatment with the induction regimen in small cell lung cancer relapsing after an initial response to short term chemotherapy. *Eur J Cancer Clin Oncol* 23:1409-1411, 1987
- Kingsbury WD, Boehm JC, Jakas DR, et al: Synthesis of water-soluble (aminoalkyl)camptothecin analogues: Inhibition of topoisomerase I and antitumor activity. *J Med Chem* 34:98-107, 1991
- Rowinsky EK, Grochow LB, Hendricks CB, et al: Phase I and pharmacologic study of topotecan: A novel topoisomerase I inhibitor. *J Clin Oncol* 10:647-656, 1992
- Miller AB, Hoogstraten B, Staquet M, et al: Reporting results of cancer treatment. *Cancer* 47:207-214, 1990
- National Cancer Institute: Guidelines for Reporting of Adverse Drug Reactions. Bethesda, MD, Division of Cancer Treatment, National Cancer Institute, 1988
- Gehan E: The determination of the number of patients required in a preliminary and a follow-up trial of a new chemotherapeutic agent. *J Chron Dis* 13:346-353, 1961
- Aisner J: Strategies for new drug identification in small cell lung cancer. *Lung Cancer* 9:S99-S107, 1993 (suppl 1)
- Kauffman SH: Antagonism between camptothecin and topoisomerase II-directed chemotherapeutic agents in a human leukemia cell line. *Cancer Res* 51:1129-1136, 1991
- Shiller JH, Kim K, Hutson P, et al: Phase II study of topotecan in patients with extensive-stage small-cell carcinoma of the lung: An Eastern Cooperative Oncology Group trial. *J Clin Oncol* 14:2345-2352, 1996
- Perez-Soler R, Glisson BS, Lee JS, et al: Treatment of patients with small-cell lung cancer refractory to etoposide and cisplatin with the topoisomerase I poison topotecan. *J Clin Oncol* 14:2785-2790, 1996
- Cullen MH, Smith SR, Benfield GFA, et al: Testing new agents may prejudice treatment: A phase II study of oral idarubicin in extensive disease small cell lung cancer. *Cancer Treat Rep* 71:1227-1230, 1987
- Lund B, Hansen F, Hansen M, et al: Phase II study of 1, 2, 4 triglycidylaruzol (TGU) in previously untreated and treated patients with small cell lung cancer. *Eur J Cancer Clin Oncol* 23:1031-1033, 1987
- Ardizzoni A, Pennucci C, Fusco V, et al: Oral chemotherapy for poor risk small-cell lung cancer patients with combined idarubicin and etoposide. *Anticancer Res* 9:937-940, 1989
- Masuda N, Fukuoka M, Kusunoki Y, et al: CPT-11: A new derivative of camptothecin for the treatment of refractory or relapsed small-cell lung cancer. *J Clin Oncol* 10:1225-1229, 1992
- Ettlinger DS, Finkelstein DM, Sarma R, et al: Phase II study of Taxol in patients (pts) with extensive-stage small cell lung cancer (SCLC): An Eastern Cooperative Oncology Group study. *Proc Am Soc Clin Oncol* 12:329, 1993 (abstr 1094)
- Kirshling RJ, Jung SH, Jett JR: A phase II trial of Taxol and G-CSF in previously untreated patients with extensive-stage small cell lung cancer (SCLC). *Proc Am Soc Clin Oncol* 13:326, 1994 (abstr)
- Cormier Y, Eisenhauer EA, Muldal A, et al: Gemcitabine is an active new agent in previously untreated extensive small cell lung cancer (SCLC). *Ann Oncol* 5:283-285, 1994

## Postfractionation for Enhanced Proteomic Analyses: Routine Electrophoretic Methods Increase the Resolution of Standard 2D-PAGE

R. Hussain Butt<sup>†</sup> and Jens R. Coorsen<sup>\*†‡</sup>

*Departments of Physiology & Biophysics, and Biochemistry & Molecular Biology, Hotchkiss Brain Institute, Faculty of Medicine, University of Calgary, Calgary, Alberta, Canada*

Received March 6, 2005

Here we have addressed common issues of resolution in two-dimensional polyacrylamide gel electrophoresis (2DE) experiments including proteins 'stacked' at pH extremes, unresolved peptides migrating at the front of separation, and areas of the 2D gel obscured by high abundance proteins. Postfractionation, by selective application of well-established electrophoretic separations immediately following standard 2DE, yields markedly improved resolution in these traditional problem areas using no more specialized equipment or techniques than SDS-PAGE itself.

**Keywords:** proteomics • membrane proteins • gradient gels • third separation • peptides

### Introduction

2D-PAGE (2DE) continues to offer itself as an excellent tool for high-resolution separations of proteins from complex biological samples. Nonetheless, it has often been reported that 2DE analyses are primarily suited to proteins of relatively neutral *pI* (e.g., 5–8), intermediate molecular weight (e.g., ~20–100 kDa), and intermediate abundance. The general belief is that high-resolution analyses of proteins falling outside these general ranges are practically difficult to achieve.

Poor resolution of proteins at the pH extremes of immobilized pH gradients during IEF has been attributed to protein precipitation,<sup>1</sup> a reduction in local reducing agent concentration,<sup>2</sup> and other, related endo-osmotic effects.<sup>1,3,4</sup> In part, these effects have been addressed by the application of more or different detergents,<sup>5</sup> nonionic or zwitterionic reducing agents such as tributyl phosphine<sup>2</sup> or hydroxyethyl-disulfide<sup>6</sup> and the application of wetting agents such as 2-propanol, glycerol,<sup>4</sup> and tergitol<sup>7</sup> in the 1st dimension. Narrow range immobilized pH gradients have been demonstrated to improve the overall resolving power of 2DE, across the entire pH range.<sup>8</sup> Wider gradients, beyond the common pH 3–10, have been utilized in order to improve the resolution of proteins at the pH extremes, demonstrating the critical resolving power of 2DE even for proteins with *pI* > 10.<sup>1,3,9</sup> However, systematic analyses using narrow range IPGs require multiple gels to rigorously resolve the entire proteome of a given sample, coupled with effective prefractionation techniques to ensure optimal resolution.<sup>10,11</sup>

Traditional SDS-PAGE analysis is generally unsuited to the resolution of proteins of either very low or high molecular

weight. Yet the tris-buffered system introduced by Laemmli<sup>12</sup> is still widely used for the 2nd dimension of separation in 2DE, sometimes with minor modifications<sup>13</sup>. Using this system, proteins of ≤10 kDa are poorly resolved, migrating with the dye front.<sup>12,13</sup> To address this concern, tris-tricine SDS-PAGE was developed by Schagger and von Jagow<sup>14</sup> to resolve oligopeptides with molecular weights approaching 3 kDa; literature values of as low as 1 kDa have been reported.<sup>15</sup>

Biological samples contain a range of protein abundances beyond what can be easily or directly resolved, detected, and quantified by current methods, including standard 2DE protocols.<sup>16</sup> In most experiments, proteins of low abundance fall below the detection range of even the most sensitive total protein stains, and thereby remain undetected. Conversely, proteins of extremely high abundance exceed the tolerance of the system, causing distortion and poor resolution, tending to saturate available detection methods; this renders quantification difficult, and obscures the analysis of all proteins having a similar *pI* and molecular weight. These effects are quite prominent in 2DE analysis of sera and muscle, in which the abundance of albumins and actins, respectively, are so extreme as to create a significant technical challenge.<sup>17,18</sup>

Increasing resolution in the 1st dimension has greatly improved this situation,<sup>11,19</sup> albeit with the caveats noted above. In our own experience, increasing the spatial resolution in the 2nd dimension, by the application of large format and/or gradient gels has also proven successful. However, here too there are limits to what can be practically achieved; eventually, increasing theoretical plate numbers by increasing the size of the gel provides for only limited gains in actual resolution. At present, sample prefractionation provides a viable solution when the high abundance protein(s) can be clearly identified and effectively separated from the sample.<sup>17,20</sup> These affinity based strategies are neither practical nor cost-effective for every sample and certainly do not offer a general solution to this

\* To whom correspondence should be addressed. Dr. Jens R. Coorsen, Room 174 Heritage Medical Research Building, 3330 Hospital Drive NW, Calgary Alberta, Canada, T2N 4N1. 403-220-2422. E-mail: jcoorsse@ucalgary.ca.

<sup>†</sup> Departments of Physiology & Biophysics.

<sup>‡</sup> Biochemistry & Molecular Biology.

problem. Moreover, there is mounting evidence indicating the widespread and nonspecific loss of other proteins during available prefractionation strategies; thus, although general concentration of the sample may be achieved, critical evaluation of potentially important protein losses must also be considered.<sup>21</sup>

Here, we have addressed these different resolution issues by alternative means, critically and selectively applying refined, well-established electrophoretic protocols. We thus describe simple, fast and cost-effective methods for separating proteins poorly resolved by traditional 2DE, including proteins 'stacked' at pH extremes, unresolved small proteins/oligopeptides migrating at the front of separation, and areas of the 2D gel obscured by high abundance proteins. In effect, these are postfractionation strategies. Our goal was a series of logical, practical solutions involving no more complicated or specialized technology than SDS-PAGE itself.

### Materials and Methods

**Chemicals.** All consumables used in this study were of electrophoresis grade or higher quality. CHAPS was purchased from Anatrace (Maumee OH). PBS, glycerol and DTT were from BioBasic (Toronto Ont., Canada). All IPGs, as well as acrylamide, bisacrylamide, low melting agarose, Precision Plus broad range molecular weight markers, broad range (3–10) ampholyte solutions, tris-glycine SDS buffer, reversible Zinc-imidazole staining kit, and Sypro Ruby total protein stain were from BioRad Laboratories (Hercules CA). Narrow range ampholytes were purchased from Fluka (Buchs, Switzerland). All other chemicals, including urea, thiourea, HEPES, tris, tricine, tributyl phosphine, SDS, ultralow range molecular weight markers, and components of the protease inhibitor cocktail<sup>22</sup> were purchased from Sigma (St. Louis, MO).

**Preparation of Total Protein Samples.** Fresh whole liver or myocardium excised from adult 192-SV-EV mice was briefly washed twice with cold PBS to remove blood and debris from the surface. The washed myocardium was diced into 4 mm cubes, and then washed twice again in cold PBS. The washed tissue was homogenized on ice with a polyethylene pestle in a 1.5 mL microcentrifuge tube with 500  $\mu$ L 2-DE solubilization buffer containing 8 M urea, 2 M thiourea, 4% CHAPS and 1 $\times$  concentration of a broad spectrum protease inhibitor cocktail.<sup>22</sup>

**Preparation of Membrane Protein Samples.** Whole brain excised from adult SV 192-SV-EV mice was briefly washed and dissected as described. Cubed tissue was manually homogenized for 3 min on ice in a hypotonic lysis medium consisting of 20 mM HEPES (pH = 7.4) supplemented with protease inhibitor cocktail and 4  $\mu$ M staurosporine, 4  $\mu$ M cantharidin and 1mM sodium orthovanadate to provide broad spectrum kinase and phosphatase inhibition.

An equal volume of 2 $\times$  PBS was added to the homogenate to restore isotonicity. To ensure thorough homogenization, up to 3 subsequent rounds of hypotonic lysis and manual homogenization were applied. All cellular membranes were collected from the homogenate by ultracentrifugation at 120 000 g for 3 h at 4  $^{\circ}$ C using an Optima-Max E Ultracentrifuge with the TLS-55 rotor (Beckman-Coulter, Fullerton CA). Thus, from the total brain tissue the cellular membrane/membrane associated proteins were separated from the soluble/cytosolic proteins. The membrane pellet was gently resuspended in ice-cold 1 $\times$  PBS supplemented with protease and kinase/phosphatase inhibitors as a wash, and the membranes isolated by a 2nd

ultracentrifugation step. Washed membranes were solubilized directly in 2-DE solubilization buffer.

**Sample Pretreatment, Rehydration and 1st Dimension Isoelectric Focusing.** The solubilized samples were vortexed thoroughly before removal of any small insoluble fraction by centrifugation at 16 000  $\times$  g for 10 min (4  $^{\circ}$ C) in a Mikro 20 microcentrifuge (Hettich, Tuttlingen, Germany). A portion of the solubilized sample was assayed for total protein using the RC DC Total Protein Assay (BioRad); the remainder was aliquoted and flash frozen in a dry ice/methanol slurry prior to storage at  $-80^{\circ}$  C.

For mini gels 100  $\mu$ g of total solubilized protein was diluted to a final concentration of 2 mg mL<sup>-1</sup> with solubilization buffer prior to mixing 1:1 (v/v) with solubilization buffer containing carrier ampholytes: 1% broad range 3–10 ampholytes and 0.2% each of 5 narrow range ampholytes, 3.5–4.0, 3.5–5.0, 5.0–7.0, 7.0–9.0, and 8.0–9.5. In this way, the protein sample was diluted to a final concentration of 1 mg mL<sup>-1</sup> in a working concentration of carrier ampholytes. Ampholytes were introduced at this stage to eliminate their false-positive contribution to the total protein assay. For large format gels, the process was carried out starting with 300  $\mu$ g of total protein.

Sequential post-harvest disulfide reduction and alkylation were carried out essentially according to Herbert and colleagues<sup>23,24</sup> with the following modifications: tributyl phosphine and DTT were added to final concentrations of 2.3 and 45 mM, respectively, and the sample was incubated for 60 min at 25  $^{\circ}$ C; acrylamide monomer (230 mM) was then applied as an alkylating agent for an additional 60 min at 25  $^{\circ}$ C. Samples were passively hydrated into mini-format (7 cm) or large-format (17 cm) IPG strips for 12 h at 25  $^{\circ}$ C.

Isoelectric focusing of mini-format strips was carried out at 15  $^{\circ}$ C using the Protean IEF Cell (BioRad), with a tray designed to accommodate 11 cm IPG strips. Large format strips were focused at 15  $^{\circ}$ C using the Investigator Electrophoresis system (Genomic Solutions, Ann Arbor MI) with a tray designed to accommodate 20 cm IPG strips. The longer electrode wicks accommodated by these larger-format trays enhance the removal of salts. Voltage was ramped to 250 for 15 min, and then ramped linearly to 4000 V at 50  $\mu$ A per gel over the course of 2 h, during which the electrode wicks were changed as necessary to remove salts from the circuit and promote unhindered ramping<sup>1</sup>. Isoelectric focusing was allowed to proceed at 4000 V (constant) for a total of 37 500 Vh for 7 cm gels, and 75 000 Vh for 17 cm gels. Focused 1st dimension gels were routinely either frozen for brief storage at  $-35^{\circ}$  C, or immediately equilibrated for the 2nd dimension.

**Equilibration and 2nd Dimension PAGE.** Focused IPG strips were equilibrated as routinely described; strips were immersed in 6 M urea, 20% glycerol, 2% SDS, 375 mM Tris (pH 8.8) containing 130 mM DTT for 10 min at room temperature, prior to immersion in equilibration buffer containing 350 mM acrylamide monomer for an additional 10 min, to ensure full disulfide reduction and alkylation of the SDS-denatured sample.

The equilibrated IPG strip was placed on the stacking surface of the 1 mm thick 2nd dimension gel and SDS-PAGE was carried out essentially as described by Laemmli<sup>12</sup> with minor modifications,<sup>13,24</sup> using the MiniProtein II (BioRad) for mini format gels, or the Protean II xi (BioRad) for large format gels. All 2nd dimension gels were buffered with 375 mM Tris (pH 8.8), and 5% T, 3.6% C stacking gels ( $\sim$ 8 mm tall) were cast on top of 12.5% T, 3.6% C separating gels. A 0.5% low melting agarose overlay, containing 0.1% SDS and 375 mM Tris (pH

8.8), was warmed to its melting point and used to seal the IPG to the surface of the stacking gel. Electrophoresis was carried out at 4 °C<sup>24</sup> using pre-chilled tris-glycine-SDS electrode buffer with constant voltage; to rapidly drive proteins out of the IPG and through the stacking gel, 150 V was briefly applied, after which the voltage was reduced to 90 V for completion of the separation.<sup>24</sup>

**Third Electrophoretic Separations.** To maximize resolution in areas empirically identified as cluttered or poorly resolved, we applied a 3rd electrophoretic separation following the 2nd dimension. Briefly, the area of interest (e.g., gel edge, containing proteins at the *pI* extreme of the 1st dimension) was excised from the 2nd dimension with a razor blade. In all cases, handling steps between the end of the 2nd dimension separation and the 3rd electrophoretic separation were carried out as rapidly as possible so as to minimize the effects of diffusion and maximize the resolving potential of the techniques.

To make excision as precise as possible the gel was routinely negative-stained using the standard reversible zinc-imidazole protocol<sup>25</sup> to facilitate direct visualization of the area of interest. We employed a commercially available kit for reversible Zinc-imidazole staining, according to the manufacturer's instructions. The excised area of interest (destained, in the case of slabs excised from zinc-imidazole stained gels) was turned 90° orthogonal to the 2nd dimension direction of separation, where possible, and applied to the top surface of another gel of the same thickness. For convenience, gels of the same composition as the 2nd dimension gel may be used. However, for even greater final resolution, linear gradient gels, cast with the Model 475 Gradient Delivery System (BioRad), were used; 10–15% T, 3.6% C separating gels, with 5% stacking gels produced excellent results. The excised area of interest was sealed to the top surface of the 3rd gel with a melted agarose overlay and separation was carried out as for the 2nd dimension.

For even greater resolution, we used the proven 10–15% acrylamide gradient in a large format (18 cm) Protean II Xi gel (BioRad) for 3rd electrophoretic separations. In this large format, electrophoresis was carried out at 4 °C using constant voltage; 200 V initially for ~20 min to rapidly drive protein through the stacking gel, and then 150 V to completion of the separation.

For the improved resolution of very small proteins or oligopeptides in the area of interest between ~3 and 15 kDa, an alternate 3rd gel system was used. Briefly, a modified Tris-tricine gel system was employed, consisting of a linear 15–20% T, 6% C<sup>16</sup> gradient separating gel buffered with 1 M Tris (pH 8.8), 10% T spacer gels prescribed by Schagger and von Jagow<sup>14</sup> were omitted as the area of interest contained almost exclusively unresolved oligopeptides with few or no larger proteins. The stacking gel consisted of a 5% T, 3.6% C layer buffered with 375 mM Tris (pH 6.8). Electrophoresis was carried out essentially as was described for traditional SDS-PAGE, using the electrode buffers recommended by Schagger and von Jagow.<sup>14</sup>

Extremely high abundance proteins (e.g., actin) in 2-D separations prevent the detection of lower abundance proteins of similar *pI*/MW. Following 2DE, the area immediately surrounding a high abundance protein spot was identified by zinc-imidazole staining and excised with a razor. The rectangular area was cut into vertical segments, each corresponding to a narrow (1 mm) *pI* range. Each vertical segment was turned 90° orthogonally, and applied to the surface of a 3rd gel for

electrophoretic separation; a linear 10–15% T, 3.6% C acrylamide gradient gel was cast in large format (18 cm) with a 5% T stacking gel cast with 5 mm wide wells, to readily accommodate 2nd dimension gel slices. Electrophoresis in the large format gradient was carried out as described above for gradient gels in this format.

**Detection, Image Analysis, Spot Picking, and Mass Spectrometry.** Final gels were fixed in 10% methanol, 7% acetic acid for 1–2 h with continuous mixing. Fixative was washed from the gel with 3–4 water exchanges over 1–2 h. Gels were stained in Sypro Ruby (BioRad) for 12 h, before destaining with fixative solution for 15 min. Destained gels were washed with water to remove methanol and acetic acid, and allow the gel to return to its normal hydrated size.

For selective staining of hydrophobic proteins we used the ProQ Amber Transmembrane Protein Stain reagent (Molecular Probes, Eugene OR) essentially according to the manufacturer's specifications. Final destaining steps were increased 3-fold to ensure a minimum of false-positive, nonspecific staining.

Stained gels were imaged using the ProXpress Proteomic Imaging System (Perkin-Elmer, Boston MA). Gel images were then analyzed using the automated spot detection paradigms of Progenesis Workstation (Nonlinear Dynamics, Newcastle, UK). Vertical or horizontal streaks (~5% of total staining pattern) were removed from the analysis by use of a spot circularity filter. In all cases, spot count differences noted in the text were all statistically significant ( $p < 0.05$ ; paired, two-tailed Student's T-test).

Protein spots of interest were excised from the gel using the Investigator ProPic (Genomic Solutions, Ann Arbor MI) using a standard 1.5 mm picking tool. Standard protocols of sample washing, elution, tryptic digestion, and tandem mass spectrometry (LC-MS-MS) were carried out in the Southern Alberta Mass Spectrometry Facility at the University of Calgary Faculty of Medicine.

## Results

Although  $760 \pm 40$  ( $n = 3$ ) proteins were resolved and detected in the total mouse liver extract (Figure 1A), we observed a characteristic limit in the resolution of extremely alkaline proteins ( $pI \approx 10$ ) in this sample (Highlight I, Figure 1A). A third electrophoretic separation was carried out in order to resolve proteins 'piled up' at this limiting range of the IPG strip (Figure 1B). In the highlighted region (Figure 1A, I), although clearly smeared, automated detection estimated  $31 \pm 4$  protein spots ( $n = 3$ ), whereas a third electrophoretic separation of this region resolved  $48 \pm 3$  ( $n = 3$ ) clearly detectable and well-separated protein spots (Figure 1B).

The total, unfractionated mouse liver contained a large number of proteins in the neutral range of the gel (Figure 1A). Thus, it is not surprising that when the unfractionated sample was applied to a narrow range (pH 5–8) IPG a very large number of proteins were resolved in mini format gels (Figure 1C); in total  $855 \pm 14$  proteins were indicated by automated analysis. However, the broad range (pH 3–10) gel contained a number of proteins beyond this neutral range (Figure 1A), and consequently we observed a large number of poorly resolved proteins at the pH extremes of the narrow range (pH 5–8) gel (Figure 1C). Automated detection indicated  $38 \pm 3$  proteins ( $n = 3$ ) in this region of the gel (Highlighted, Figure 1C). In parallel 3rd electrophoretic separations of this region (Figure 1D) fully  $58 \pm 3$  protein spots were resolved and detected ( $n = 3$ ).

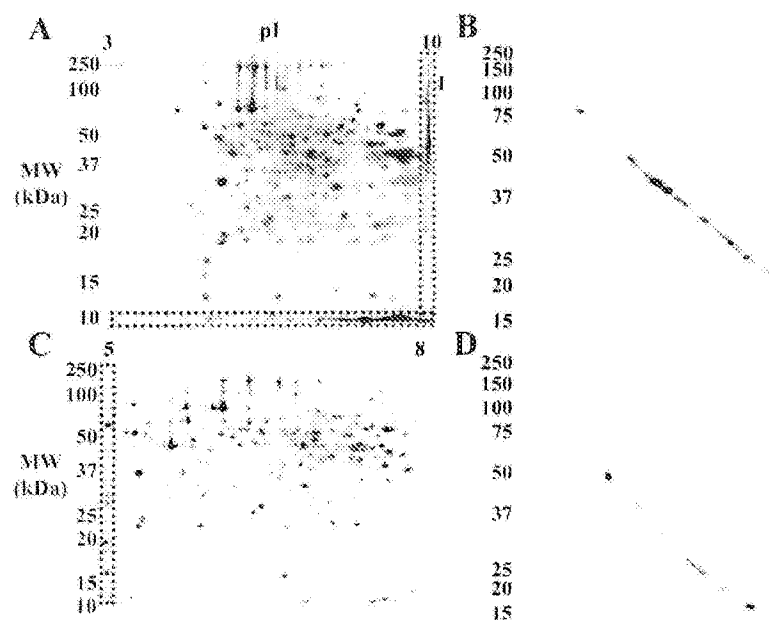


**Figure 1.** Whole mouse liver extract separated by standard 2DE in mini format, with specific areas of interest excised and resolved in 3rd electrophoretic separations; A, 2DE with 3–10 IPG; B, Orthogonal separation of 'stacked' proteins at the alkaline extreme ( $\text{pH} \approx 10$ ) highlighted in A; C, 2DE with 5–8 IPG; D, Orthogonal separation of 'stacked' protein at the acidic ( $\text{pH} \approx 5$ ) extreme highlighted in C.

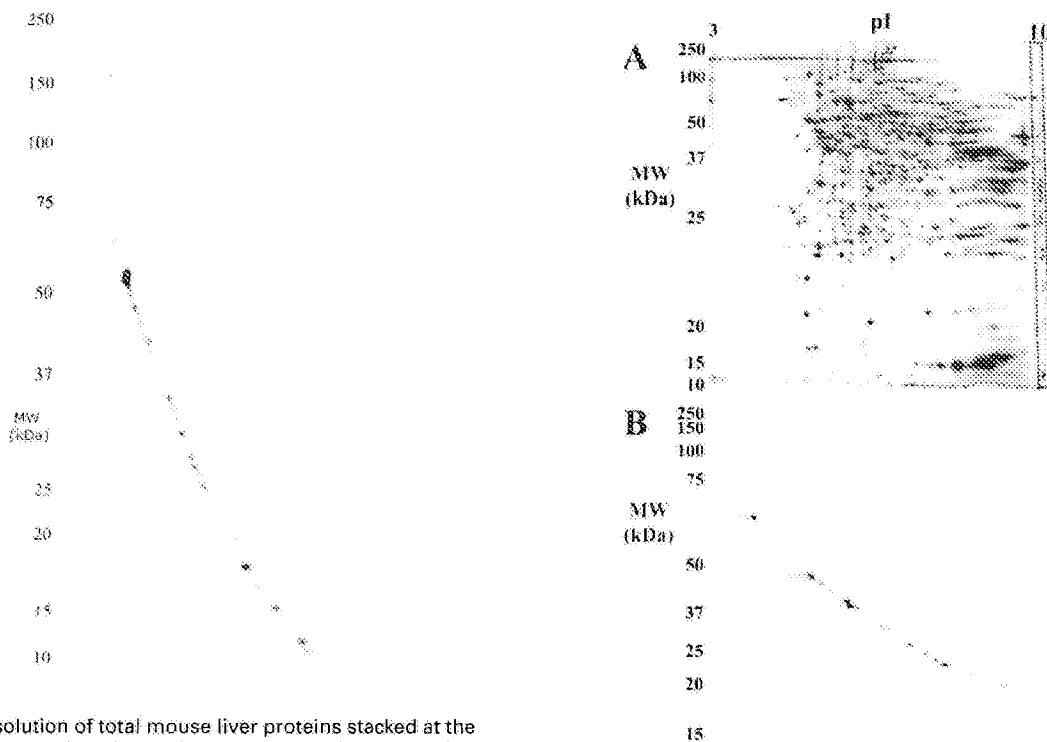


**Figure 2.** Resolution of total mouse liver proteins stacked at the alkaline extreme ( $\text{pH} \approx 10$ ) was further enhanced by increasing the length of separation. A 3rd separation was carried out as in Figure 1D, using a large format (18 cm) gradient gel for optimal resolution.

By using a large (18 cm) gel format for the 3rd electrophoretic separation, still more protein spots were resolved from this region of the narrow range 2nd dimension gel in Figure 1C; fully 65 protein spots were resolved and detected from those proteins stacked at  $\text{pI} \leq 5$  (Figure 2).

**Figure 3.** Improving resolution in standard 2DE by using large gel formats did not obviate the utility of a 3rd electrophoretic separation. A, In whole mouse liver extract separated by 2DE in large gel format, proteins remain stacked at the alkaline extreme ( $\text{pH} \approx 10$ ). B, Orthogonal 3rd electrophoretic separation of stacked alkaline proteins highlighted in A.

Although  $2500 \pm 100$  ( $n = 3$ ) proteins were resolved and detected when large format gels were used in 1st and 2nd

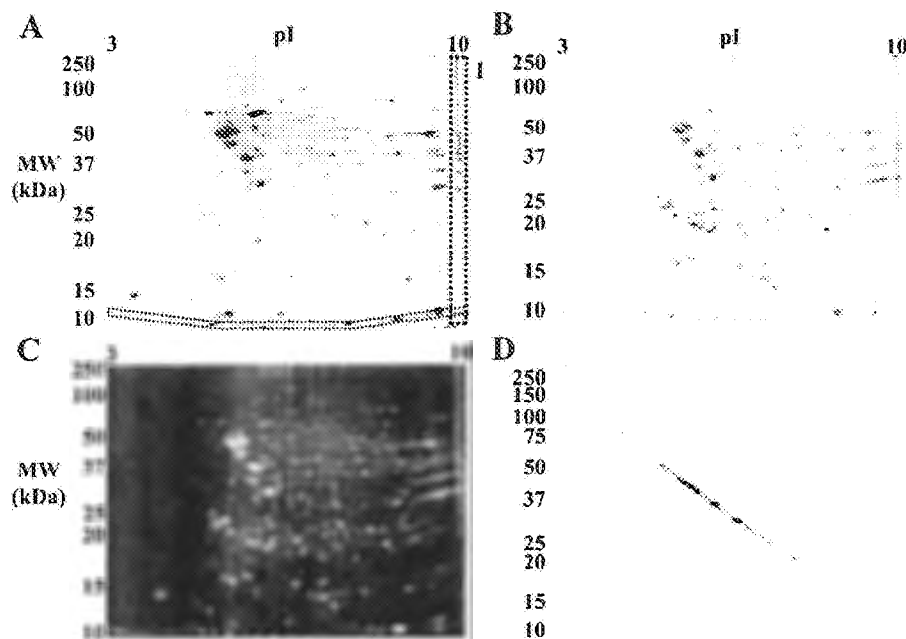


**Figure 4.** Mouse brain membrane protein isolate separated by standard 2DE in mini format, with specific areas of interest excised and resolved in 3rd electrophoretic separations. A. 2DE with 3–10 IPG; B. Parallel hydrophobic domain staining; C. Digital overlay of Sypro Ruby total protein staining (from A) in red with ProQ Amber hydrophobic domain staining (from B) in green. D. A 3rd electrophoretic separation to improve the separation of poorly resolved mouse membrane proteins stacked at the alkaline ( $pI \approx 10$ ) region of the 2nd dimension gel in A.

dimension separations of the mouse liver extract, proteins at the  $pI$  extreme remained poorly resolved (Figure 3A). The markedly improved resolution of this larger 2DE format does not obviate the utility of a 3rd electrophoretic separation of proteins at the alkaline extreme. In this region of the gel, automated spot detection estimated  $66 \pm 2$  protein spots ( $n = 3$ ). In a subsequent large format 3rd electrophoretic separation of this region fully  $78 \pm 4$  proteins were resolved and detected ( $n = 3$ ).

These improvements in effective resolution of proteins “stacked” at the  $pI$  extremes were not limited to the mouse liver extract sample. We resolved  $700 \pm 23$  ( $n = 3$ ) proteins from a mouse brain total membrane isolate in mini gel format 2DE (Figure 4A). Parallel transmembrane (e.g., hydrophobic domain) selective staining visually shared a great deal of similarity with total protein stained gel (Figure 4B); this similarity was most striking when the parallel stained gels were digitally overlaid (Figure 4C). Comparative image analysis indicated >98% overlap between the two staining formats. Included in this membrane proteome were notably poorly resolved proteins “stacked” at the alkaline extreme of the gel (Figure 4A–C). Automated spot detection estimated  $39 \pm 2$  ( $n = 3$ ) such proteins, whereas  $46 \pm 2$  ( $n = 3$ ) proteins were more cleanly resolved in 3rd electrophoretic separations of this region (Figure 4D).

Oligopeptides migrating with the dye front in 2DE of total mouse liver and mouse brain membrane isolates (highlighted in Figures 1A and 4A, respectively) were resolved by 3rd electrophoretic separations on mini format tris-tricine gels (Figure 5A,B). Capitalizing on the integration power of the ProXpress Imaging system, compared to scanner-based systems, fully  $53 \pm 4$  ( $n = 3$ ) previously unresolved peptides were counted in the total mouse liver sample, while  $63 \pm 3$  ( $n = 3$ ) previously unresolved peptides were counted in the mouse

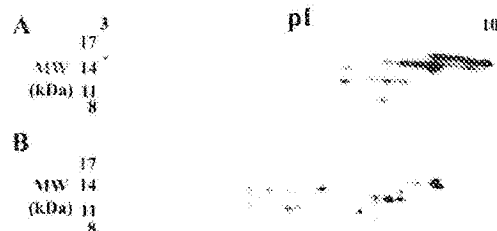


**Figure 5.** Tris-tricine SDS-PAGE for the high resolution 3rd electrophoretic separation of oligopeptides migrating at the 2nd dimension dye front of traditional 2DE. Tris-tricine 3rd electrophoretic separations of oligopeptides from; A. Total mouse liver (Highlighted, Figure 1A) and; B. Mouse brain membrane (Highlighted, Figure 4A).

brain membrane proteome (Figure 5A,B). Notably, these detectable small proteins were found across the entire 3–10  $pI$  range, and principally resolved in the 8–15 kDa range of apparent molecular weights.

In mini format 2DE separations of mouse cardiac muscle, we detected  $650 \pm 40$  ( $n = 3$ ) proteins (Figure 6A). These included several proteins of characteristically high abundance corresponding to the approximate  $pI$  and molecular weight of actin (Figure 6A). Proteins in narrow  $pI$  slices excised from these areas (Figure 6A) were separated orthogonally in 3rd electrophoretic separations (Figure 6B). From each slice, several proteins that were fully obscured in the 2nd dimension gels were clearly resolved from their over-abundant neighbors following the 3rd electrophoretic separation. These included proteins of slightly higher and lower molecular weight and a select number of very low abundance yet exceptionally well resolved proteins. Through this additional electrophoretic separation, enough spatial resolution was achieved to cleanly



**Table 1.** LC-MS/MS Identification of a Select Number of Mouse Cardiac Muscle Proteins Co-migrating with Actin in 2DE, but Distinctly Resolved by a 3rd Electrophoretic Separation as Shown in Figure 6<sup>a</sup>

spot	MOWSE score	sequence coverage (%)	accession no.	identified protein
1	51	9	NP_598623	fibrinogen, $\gamma$ polypeptide
2	543	26	Q9CZ13	ubiquinol-cytochrome <i>c</i> reductase core protein 1
3	522	28	AAC64398	ATP-specific succinyl-CoA synthetase $\beta$ subunit
4	45	1	NP_599162	myosin IXA
5	46	5	XP_228531	similar to hepatocellular carcinoma-associated protein HCA1
6	66	1	XP_237042	similar to bullous pemphigoid antigen 1-b
7	88	22	P04270	Actin, $\alpha$ cardiac

<sup>a</sup> Scores > 45 are statistically significant ( $p < 0.05$ ).

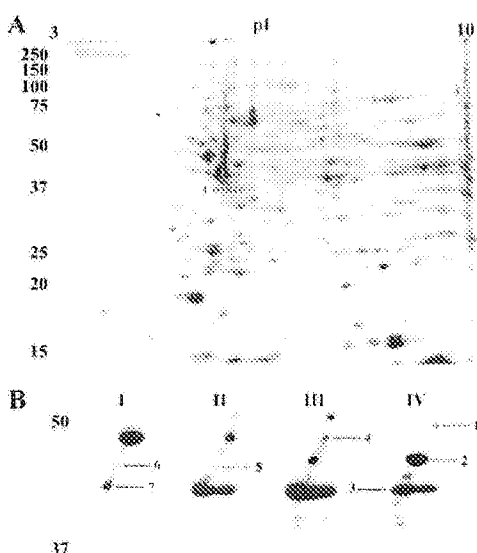


**Figure 6.** Use of a 3rd electrophoretic separation to effectively resolve multiple low abundance proteins obscured by neighboring high abundance proteins following standard 2DE. A. Whole mouse cardiac muscle protein was separated by standard 2DE. B. High abundance protein spots in A were excised and orthogonally resolved in parallel 3rd electrophoretic separations.

excise the protein spots using a 1.5 mm spot picking tool on a robotic picking apparatus. LC-MS-MS of select spots (Figure 6B) identified several metabolic enzymes that were resolved from high abundance, comigrating actin (Table 1).

## Discussion

Application of a 3rd electrophoretic separation to specific areas of poor resolution in 2nd dimension gels, rapidly improved protein detection in these regions. In each case the composition, size and direction of separation of the 3rd electrophoretic system were carefully selected to maximize final resolution beyond what can routinely be achieved by 2DE alone. In each example, objective analysis by automated spot detection indicated a substantial increase in the number of resolved proteins. Additionally, spatial resolution was increased to fully enable effective spot picking for subsequent mass spectrometric analyses. Use of postfractionation strategies in the form of 3rd electrophoretic separations provide simple, fast, and effective means of recovering data and thus enhancing proteomic analyses.

**Zinc-Imidazole Fixation Prior to 3rd Electrophoretic Separations.** Excision and transfer/sealing to a 3rd gel were carried out as rapidly as possible so as to minimize the effects of

diffusion and maximize the resolving potential of the final electrophoretic separation. For the most precise excision possible, the area of interest can be rapidly visualized immediately following completion of the 2nd dimension by staining with the well-characterized Zn-imidazole reversible fixation/staining protocol.<sup>25</sup> As a practical matter the entire 2nd dimension gel can be Zn-imidazole fixed and any areas of interest can be excised, destained, and then subjected to analysis by 3rd separations (or other methods); once reversed, prior Zn fixation did not affect the quality of subsequent high sensitivity Sypro Ruby staining. However, it should be noted that the time involved in Zn fixing/staining then reversing/destaining increases the opportunity for proteins to diffuse through the gel matrix. Naturally, diffusion will only serve to reduce resolution. Thus, Zn-imidazole staining should be limited to those situations that most warrant its use, so as to maximize the resolving power of the 3rd electrophoretic separation, and to preserve the high-resolution already achieved throughout the remainder of the 2nd dimension. For instance, visualization of oligopeptides migrating with the dye front of the 2nd dimension can be achieved simply by including trace bromophenol blue in the agarose overlay solution or stacking gel, negating the necessity for Zn-staining. Alternately, Zn<sup>2+</sup> fixation of the entire gel is typically required to identify areas in the center of 2D gels that would substantially benefit from 3rd separations, as excising these areas without such a visual aid proves quite difficult.

**Enhanced Resolution at pH Extremes.** Our attempts to improve resolution at the alkaline extreme of broad range (3–10) gel separations (Figure 1A) by modifying the hydration and IEF environment using 2-propanol (20% v/v), glycerol (5%, w/v) and tergitol (0.1%, w/v)<sup>4,7</sup> met with quite limited success (data not shown). It appeared that small gains in resolution of the alkaline extreme by the application of these reagents were achieved at the cost of resolution in all other regions of the gel. Manipulating 1st dimension conditions in order to improve resolution in a specific pH range, without adversely affecting resolution in the rest of the gel thus proved difficult in practice, if not completely ineffective. However, following 2nd dimension separation, poorly resolved proteins ‘stacked’ at the pH extremes, were easily isolated by careful excision from the 2nd dimension gel. Separated in a 3rd SDS-PAGE gel, the resolution of these traditionally poorly separated regions was substantially improved (Figure 1). Moreover, while the excised area of interest was subjected to a 3rd electrophoretic separation, the well-resolved bulk of the gel was left undisturbed and thus available for standard high-sensitivity staining, analysis, and spot picking. In these 3rd electrophoretic separations, although proteins were resolved in a direction orthogonal to that of the 2nd dimension, the parameter by which proteins were sepa-

rated (i.e., MW) was not altered. Thus, the third separation is not a true third dimension. However, here the sample represents a very select number of proteins that are already partially resolved. Naturally, then, in this 3rd separation, proteins migrate across the diagonal of the gel (Figure 1B). Increased resolution is therefore largely achieved by substantially increasing the linear distance over which proteins are separated in the 3rd gel relative to the 2nd (Figure 1B), and enhanced further by the use of gradient gels. Both these parameters can obviously be further optimized depending on the complexity of the protein mixture occurring at a given pH extreme. For example, by simply extending the length of the 3rd gel, thereby expanding the separation distance, even greater final resolution can be achieved (Figure 2).

It appears that many research groups routinely separate unfractionated samples on neutral, narrow range IPG strips (e.g., 5–8), rather than on broad range IPG strips; as the majority of proteins in many samples do fall in this near-neutral range, this is perhaps understandable. However, there are always poorly resolved proteins at the extremes of such gels.<sup>3</sup> We tested the application of a routine 3rd electrophoretic separation by first using 2DE to resolve a total mouse liver extract on narrow range IPG strips of pH 5–8 (Highlighted, Figure 1C). The poor resolution of proteins at the acidic extremes of these gels was immediately evident (Figures 1C). However, very high-resolution separations of these stacked proteins were quickly and effectively achieved using a 3rd electrophoretic separation (Figure 1D). A substantial number of proteins were resolved that were not distinguishable by eye, or by automated spot detection in the 2nd dimension gel (Figure 1C).

Presumably, in instances where unfractionated samples are applied to narrow range IPGs, it is felt that the benefit of improved spatial resolution of the majority of a given sample outweighs the benefit of separating all possible resolvable proteins. The simple addition of a 3rd electrophoretic separation then proves quite valuable; poorly resolved proteins at the pH extremes, that perhaps warrant neither complicated prefractionation strategies nor the use of wider range IPGs, can be simply and routinely separated, enhancing the rigor of the proteomic analysis. In this way, proteins falling outside the immediate area of interest on a narrow range IPG, and often ignored or quite poorly handled by image analysis software, can be routinely resolved, and potentially important data rescued.

It should be noted that many groups routinely employ large format ( $\geq 17$  cm) gels in the first and second dimension of 2DE separations for greater resolution than can be achieved in mini gel formats. Indeed, using large gels we were able to resolve and detect more proteins from the mouse liver sample than with mini gels. However, this increase in detection is additionally a result of increased loading; larger gels accommodate larger optimal loads, increasing the quantity of many low abundance proteins to the level of minimal detection. As a result, areas of the mini gel that were poorly resolved due to crowding, such as the alkaline extreme ( $pI = 10$ ) tend to remain poorly resolved in a large format separation if the increase in resolution is not sufficient to overcome the increase in loading. Most frequently, accepted protocols prescribe increasing load in direct proportion to the increased size of the gel when moving from mini to larger formats. Thus it is not surprising that poorly resolved liver proteins at the alkaline extreme remain poorly resolved whether separated on mini gels or on

large format gels with a larger load (Figure 1A, 3A). Nonetheless, a 3rd separation of this subset of proteins was a very successful means of improving the effective resolution of this region of the gel (Figure 3A,B).

Our findings were not limited to total mouse liver proteins. We have observed similar stacking of unresolved proteins at the pH extremes in many biological samples. Of particular note, is the occurrence of this phenomenon in membrane protein isolates from mouse brain (Figure 4A). We have described a simple physical prefractionation protocol, to rapidly isolate the total membrane/membrane associated protein complement from the total soluble/cytosolic protein content of cells or tissue. This rigorous application of purely physical parameters provides a rapid and reproducible prefractionation strategy. Importantly, this method renders both fractions completely available for processing by 2DE; the membrane/membrane associated proteins are directly solubilized in the detergent/chaotrope system of choice whereas soluble proteins can be rapidly concentrated and dialyzed using centrifugal concentration devices. This is accomplished with minimal operator input, relatively few consumables, and completely avoids the addition of contaminants which may confound subsequent gel separations. Moreover, prefractionated in this way, both membrane/membrane associated (Figure 4A) and soluble/cytosolic protein fractions (data not shown) produce excellent, high quality proteomic maps by 2DE. Staining the membrane isolate for hydrophobic domains in parallel with total protein staining indicated that  $>98\%$  of the resolved proteins contained large hydrophobic/transmembrane domains (Figure 4A–C). Although several proteins in the two-color overlay either appear entirely red (Sypro Ruby) or green (Pro-Q Amber), for the most part this is the result of differing fluorescence intensities between stains. It should be noted when Pro-Q Amber transmembrane selective stain is used, there is not necessarily a correlation between fluorescence intensity and protein (domain) quantity; this stain is not quantitative per se. Nonetheless, close inspection using the Progenesis Workstation image analysis software indicates that the majority of these proteins indeed have overlapping centers with the quantitatively stained (Sypro Ruby) spots (Figure 4C). Thus the general belief that proteins having hydrophobic stretches do not easily enter IPG strips appears to be unsubstantiated. Membrane proteomes can be quite effectively analyzed using the simple optimized 2DE protocols described here.

Even after prefractionation of the mouse brain tissue, however, proteins at the alkaline extreme remained characteristically piled-up (Highlighted, Figure 4A). Nonetheless, the highly hydrophobic nature of the sample (Figure 4A–C) did not impede or prevent the resolution of this troublesome region by 3rd electrophoretic separation (Figure 4D). Thus, it appears that this improvement in effective resolution is not limited to the total mouse liver extract specifically, but rather can be broadly applied to a wide variety of samples/sample types, including highly hydrophobic membrane proteins.

**Enhanced Resolution of Peptides.** Smaller proteins/peptides at the separation front always remain unresolved in standard 2DE protocols. Here a simple 3rd electrophoretic separation to enhance the overall rigor of the protein analysis would also be beneficial. Applying a tris-tricine gradient gel in a 3rd electrophoretic separation enabled detection of a large number of oligopeptides from both the total mouse liver extract and the mouse brain membrane isolate (Figure 5A and B, respectively), which go unresolved in traditional 2DE analyses (Figures

1A, 4A). Although automated spot detection suggested the presence of a number of spots (e.g., peaks) in the dye/lipid front of 2nd dimension gels (Figures 1A, 4A), these certainly do not represent distinct, resolved protein spots of the quality found in the 2D gel as a whole.

It should additionally be noted that despite advances in the field, current detection methods for low abundance proteins, and for small proteins/oligopeptides are less than optimal.<sup>26</sup> We were unable to improve our detection of the resolved oligopeptides (Figure 5) by the application of other common stains including mass spectrometry-compatible silver stain,<sup>27</sup> high sensitivity colloidal Coomassie (BioRad), or coupled BismarckBrown R-Coomassie staining<sup>28</sup> (data not shown). Nonetheless, the resolution of SyproRuby-stained peptides was improved to a level minimally required for high confidence spot picking operations. Such detection was only possible by fully utilizing the inherent fluorescence integration capabilities of the imaging system, and are impossible with scanner-based technologies. That said, the question remains as to how many peptides were actually resolved, as these are notoriously difficult to detect by any standard staining methods. Our data quite likely represent underestimates of the total number of resolved oligopeptides. Enhanced detection protocols should thus further compliment the enhanced resolution provided by these 3rd electrophoretic separations.

**Separation of Low Abundance Proteins from Comigrating High Abundance Proteins.** Our 2DE separation of total mouse cardiac muscle proteins resolved a very large number of proteins across the entire  $pI/MW$  range (Figure 6A). Very high abundance proteins, readily recognized by their pronounced saturating fluorescent signals, were detected at  $pI/MW$  corresponding to actin (Figure 6A). Poor resolution in both dimensions and characteristic distortions generally associated with overloading gels were observed in this specific region of the 2nd dimension gel (Figure 6A). Both phenomena obscure low abundance proteins in the affected areas of the 2nd dimension gel, but these proteins were successfully resolved by subsequent postfractionation using a 3rd electrophoretic separation (Figure 6B).

Thus, we observed a number of low abundance proteins that were obscured in the 2nd dimension gel due to their comigration with more abundant molecules (Figure 6). Although the high abundance protein spots in the area of interest (Figure 6A) could be picked from the 2nd dimension gel, the presence of co-resolved low abundance contaminants, as evidenced by higher resolution analysis (Figure 6B) indicate that this practice should clearly be discouraged. Although with careful analysis, simple mixtures can be resolved by MS/MS, more complex mixtures could conceivably compromise effective identification. In this way, a 3rd electrophoretic separation may be used as a tool to determine the quality of 2DE separations, and as a simple, effective cleanup step prior to mass spectrometric analyses.

In part, the improved resolution that was achieved here was the result of the careful transition from 2nd dimension to the 3rd electrophoretic separation. Slicing the gel into narrow  $pI$  segments effectively partitioned the dominant high abundance protein in this region of the gel (Figure 6). Partitioned in this way, the load of total protein per unit area of the gel was reduced in the orthogonal 3rd separation. As a result, the characteristic distortions attributed to overloading, as observed in the 2nd dimension gel, were absent from the 3rd separation (Figure 6). Subdividing the high abundance spot(s) in this way

further served to reduce signal saturation during fluorescent detection. Thus, using a 3rd separation, negative local effects interfering with the detection of neighboring low abundance spots were substantially reduced. When coupled with the enhanced resolution of an orthogonal 3rd separation, these improvements enable the detection of a number of previously undetected/unresolved protein spots (Figure 6).

Newly resolved protein spots were sufficiently separated that we were able to cleanly excise them from the gel using a standard 1.5 mm cutting tool and an automated picking robot. Among these "rescued" protein spots, newly resolved by postfractionation using a third electrophoretic separation (Figure 6B), LC-MS/MS identified several metabolic enzymes normally rendered undetectable by highly abundant albumins and cytoskeletal actin (Table 1). This is the essence of the 3rd electrophoretic separation as we apply it; we capitalize on the tremendous experience of the field in producing excellent, high quality, high resolution separations by 2DE, and then selectively apply additional resolving power in regions where resolution suffers as a result of characteristics inherent to the sample or method. Thus the majority of the sample, which is well resolved by 2DE, remains well resolved (Figure 6A) and more rigorous postfractionation can then be applied to areas where prohibitive comigration with high abundance proteins occurs (Figure 6B). Indeed, even after the additional handling required for a 3rd separation, low abundance proteins separated from actin appear as tight, round, well-resolved spots (Figure 6B). The migration of these proteins was thus apparently not impeded by the comigrating actin; removing actin from the mixture is not required for these molecules to be cleanly resolved. Thus, we regard this method as a novel means of sample postfractionation to achieve an effective level of resolution in biological samples with a very large dynamic range of protein abundance. As such the method provides a simple and effective alternative to commonly applied and commercialized affinity prefractionation techniques.<sup>17-19</sup> Nonquantitative losses of proteins, due to their possible binding with more abundant protein molecules,<sup>21</sup> can thus be simply, routinely, and cost-effectively avoided by applying a 3rd electrophoretic separation as a postfractionation strategy. Postfractionation offers a convenient means of generating more thorough proteomic maps, enabling us to quantitatively account for as much biological complexity as possible.

## Conclusions

Proteins of extreme isoelectric points, molecular masses, and relative abundance currently represent the analytical 'edge' of what can be achieved by 2DE technology. There is substantial effort being devoted to the development of techniques that optimize our capacity to resolve these proteins, and thereby further enhance and refine ongoing proteomic analyses. Our introduction of simple 3rd separation steps for improving resolution is but one example of such efforts. In each example described here, the additional resolution afforded by a simple 3rd electrophoretic separation was minimally sufficient to enable clean excision of newly detected spots using a standard 1.5 mm spot-picking tool.

It may very well be that there remain unresolved/undetected proteins even following the highest resolution electrophoretic separations. These not only represent lost data, but remain potential contaminants that can interfere with effective mass spectrometric analyses. Nonetheless techniques involving 3rd electrophoretic separations provide a means of analyzing

regions of inherently low resolution as rigorously as current separation and detection technologies allow, and provide for enhanced confidence in the quality of excised protein spots.

Importantly, this is accomplished without any re-tooling or additional consumables, in a manner that is routine, simple and cost-effective. In this vein, although the resolving power of large gels is obviously greater than mini-format gels, simply doubling the size of the gel does not proportionally improve effective resolution. In fact, mini-gel formats provide for excellent proteomic maps, with resolution that is perfectly acceptable for methods development, demonstration/training, or initial 1st pass comparative proteomic analyses. For any of these purposes, mini gel formats offer a significant cost advantage, with the knowledge that large format gels are always available for added resolution.

There was an additional impetus to provide a technique that completely preserves the well-resolved areas of the 2nd dimension separation, thus capitalizing on the tremendous experience of the field as a whole in producing excellent, high resolution, high quality separations from biological samples. By selectively removing only areas of poor resolution from the 2nd dimension separation and subjecting these to 3rd electrophoretic separations, the well-resolved bulk of the gel was left intact and available for standard analyses.

While this method does not substitute for the marked resolving power of narrow range IPGs,<sup>8</sup> it is anticipated that 3rd electrophoretic separations can form part of a combined, complementary analysis. Applied as described, this approach ultimately represents a means of rescuing potentially critical proteomic data. In the end, proteomic approaches are only as useful as their ability to account for as much of the underlying native complexity of the biological sample as possible. As such, methodological integrations and adaptations will always lie at the core of the most effective protein analyses.

**Acknowledgment.** The authors would like to thank Tiffany Rice, Tammy Wilson, and Dr. V. Wee Yong for their kind support in supplying the mouse tissue samples used in this work. We acknowledge Morgan Hughes and Dr. David C. Schriemer of the Southern Alberta Mass Spectrometry Centre for mass spectrometric identification services. Special thanks to Matthew Churchward for assistance with image analysis and preparation, and Marlies Ernst and Kendra L. Furber for helpful discussions and input throughout development of these methods. J.R.C. acknowledges support from the Canadian Institutes of Health Research, the Alberta Network for Proteomics Innovation, the Canada Foundation for Innovation, the Alberta Heritage Foundation for Medical Research, and the Heart and Stroke Foundation of Canada.

## References

- (1) Gorg, A.; Obermaier, C.; Boguth, G.; Harder, A.; Scheibe, B.; Wildgruber, R.; Weiss, W. The current state of two-dimensional electrophoresis with immobilized pH gradients. *Electrophoresis* **2000**, *21*, 1037–1053.
- (2) Herbert, B. R.; Molloy, M. P.; Gooley, A. A.; Walsh, B. J.; Bryson, W. G.; Williams, K. L. Improved protein solubility in two-dimensional electrophoresis using tributyl phosphine as reducing agent. *Electrophoresis* **1998**, *19*, 845–851.
- (3) Gorg, A.; Obermaier, C.; Boguth, G.; Csordas, A.; Diaz, J. J.; Madjar, J. J. Very alkaline immobilized pH gradients for two-dimensional electrophoresis of ribosomal and nuclear proteins. *Electrophoresis* **1997**, *18*, 328–337.

- (4) Hoving, S.; Gerrits, B.; Voshol, H.; Muller, D.; Roberts, R. C.; van Oostrum, J. Preparative two-dimensional gel electrophoresis at alkaline pH using narrow range immobilized pH gradients. *Proteomics* **2002**, *2*, 127–134.
- (5) Luche, S.; Santoni, V.; Rabilloud, T. Evaluation of nonionic and zwitterionic detergents as membrane protein solubilizers in two-dimensional electrophoresis. *Proteomics* **2003**, *3*, 249–253.
- (6) Olsson, I.; Larsson, K.; Palmgren, R.; Bjellqvist, B. Organic disulfides as a means to generate streak-free two-dimensional maps with narrow range basic immobilized pH gradient strips as first dimension. *Proteomics* **2002**, *2*, 1630–1632.
- (7) Laoudj-Chenivresse, D.; Marin, P.; Bennes, R.; Tronel-Peyroz, E.; Leterrier, F. High performance two-dimensional gel electrophoresis using a wetting agent Tergitol NP7. *Proteomics* **2002**, *2*, 481–485.
- (8) Wildgruber, R.; Harder, A.; Obermaier, C.; Boguth, G.; Weiss, W.; Fey, S. J.; Larsen, P. M.; Gorg, A. Towards higher resolution: two-dimensional electrophoresis of *Saccharomyces cerevisiae* proteins using overlapping narrow immobilized pH gradients. *Electrophoresis* **2000**, *21*, 2610–2616.
- (9) Gorg, A.; Obermaier, C.; Boguth, G.; Weiss, W. Recent developments in two-dimensional gel electrophoresis with immobilized pH gradients: wide pH gradients up to pH 12, longer separation distances and simplified procedures. *Electrophoresis* **1999**, *20*, 712–717.
- (10) Herbert, B.; Righetti, P. G. A turning point in proteome analysis: sample prefractionation via multicompartiment electrolyzers with isoelectric membranes. *Electrophoresis* **2000**, *21*, 3639–3648.
- (11) Zuo, X.; Speicher, D. W. A method for global analysis of complex proteomes using sample prefractionation by solution isoelectrofocusing prior to two-dimensional electrophoresis. *Anal. Biochem.* **2000**, *284*, 266–278.
- (12) Laemmli, U. K. Cleavage of structural proteins during the assembly of the head of bacteriophage T4. *Nature* **1970**, *227*, 680–685.
- (13) Cannon-Carlson, S.; Tang, I. Modification of the Laemmli sodium dodecyl sulfate-polyacrylamide gel electrophoresis procedure to eliminate artifacts on reducing and nonreducing gels. *Anal. Biochem.* **1997**, *246*, 146–148.
- (14) Schagger, H.; von J. G. Tricine-sodium dodecyl sulfate-polyacrylamide gel electrophoresis for the separation of proteins in the range from 1 to 100 kDa. *Anal. Biochem.* **1987**, *166*, 368–379.
- (15) Judd, R. C. Electrophoresis of peptides. *Methods Mol. Biol.* **1994**, *32*, 49–57.
- (16) Zhou, F.; Johnston, M. V. Protein characterization by on-line capillary isoelectric focusing, reversed-phase liquid chromatography, and mass spectrometry. *Anal. Chem.* **2004**, *76*, 2734–2740.
- (17) Pieper, R.; Gatlin, C. L.; Makusky, A. J.; Russo, P. S.; Schatz, C. R.; Miller, S. S.; Su, Q.; McGrath, A. M.; Estock, M. A.; Parmar, P. P.; Zhao, M.; Huang, S. T.; Zhou, J.; Wang, F.; Esquer-Blasco, R.; Anderson, N. L.; Taylor, J.; Steiner, S. The human serum proteome: display of nearly 3700 chromatographically separated protein spots on two-dimensional electrophoresis gels and identification of 325 distinct proteins. *Proteomics* **2003**, *3*, 1345–1364.
- (18) Pang, L.; Fryksdale, B. G.; Chow, N.; Wong, D. L.; Gaertner, A. L.; Miller, B. S. Impact of prefractionation using Gradiflow on two-dimensional gel electrophoresis and protein identification by matrix assisted laser desorption/ionization-time-of-flight-mass spectrometry. *Electrophoresis* **2003**, *24*, 3484–3492.
- (19) Sabounchi-Schutt, F.; Astrom, J.; Olsson, I.; Eklund, A.; Grunewald, I.; Bjellqvist, B. An immobilized DryStrip application method enabling high-capacity two-dimensional gel electrophoresis. *Electrophoresis* **2000**, *21*, 3649–3656.
- (20) Ahmed, N.; Barker, G.; Oliva, K.; Garfin, D.; Talmadge, K.; Georgiou, H.; Quinn, M.; Rice, G. An approach to remove albumin for the proteomic analysis of low abundance biomarkers in human serum. *Proteomics* **2003**, *3*, 1980–1987.
- (21) Zhou, M.; Lucas, D. A.; Chan, K. C.; Issaq, H. J.; Petricoin, E. F.; Liotta, L. A., III; Veenstra, T. D.; Conrads, T. P. An investigation into the human serum "interactome". *Electrophoresis* **2004**, *25*, 1289–1298.
- (22) Coorsen, J. R.; Blank, P. S.; Tahara, M.; Zimmerberg, J. Biochemical and functional studies of cortical vesicle fusion: the SNARE complex and Ca<sup>2+</sup> sensitivity. *J. Cell Biol.* **1998**, *143*, 1845–1857.
- (23) Herbert, B.; Galvani, M.; Hamdan, M.; Olivieri, E.; MacCarthy, J.; Pedersen, S.; Righetti, P. G. Reduction and alkylation of proteins in preparation of two-dimensional map analysis: why, when, and how? *Electrophoresis* **2001**, *22*, 2046–2057.

- (24) Coorssen, J. R.; Blank, P. S.; Albertorio, F.; Bezrukov, L.; Kolosova, I.; Backlund, P. S., Jr.; Zimmerberg, J. Quantitative femto- to attomole immunodetection of regulated secretory vesicle proteins critical to exocytosis. *Anal. Biochem.* **2002**, *307*, 54–62.
- (25) Fernandez-Patron, C.; Castellanos-Serra, L.; Rodriguez, P. Reverse staining of sodium dodecyl sulfate polyacrylamide gels by imidazole-zinc salts: sensitive detection of unmodified proteins. *Biotechniques* **1992**, *12*, 564–573.
- (26) Kang, C.; Kim, H. J.; Kang, D.; Jung, D. Y.; Suh, M. Highly sensitive and simple fluorescence staining of proteins in sodium dodecyl sulfate-polyacrylamide-based gels by using hydrophobic tail-mediated enhancement of fluorescein luminescence. *Electrophoresis* **2003**, *24*, 3297–3304.
- (27) Sinha, P.; Poland, J.; Schnolzer, M.; Rabilloud, T. A new silver staining apparatus and procedure for matrix-assisted laser desorption/ionization-time-of-flight analysis of proteins after two-dimensional electrophoresis. *Proteomics* **2001**, *1*, 835–840.
- (28) Choi, J. K.; Yoon, S. H.; Hong, H. Y.; Choi, D. K.; Yoo, G. S. A modified Coomassie blue staining of proteins in polyacrylamide gels with Bismark brown R. *Anal. Biochem.* **1996**, *236*, 82–84.

PR050054D

# Cancer Research

Experimental and Molecular Therapeutics

## Abstract 4626: Evaluating the pharmacodynamics and pharmacokinetic effects of MM-398, a nanoliposomal irinotecan (nal-IRI) in subcutaneous xenograft tumor models of human squamous cell carcinoma and small cell lung cancers

Daniel C. Chan, Ashish Kalra, Zhiyong Zhang, Nancy Paz, Dmitri Kirpotin, Daryl Drummond, Ulrik Nielsen, Paul A. Bunn, and Jonathan Fitzgerald

DOI: 10.1158/1538-7445.AM2014-4626 Published October 2014

Article

Info & Metrics

Proceedings: AACR Annual Meeting 2014; April 5-9, 2014; San Diego, CA

### Abstract

**Background:** MM-398 is a novel nanoliposomal encapsulation of irinotecan (nal-IRI), a topoisomerase I inhibitor. In preclinical studies, nal-IRI has been shown to greatly modify the pharmacokinetics and biodistribution of CPT-11 and its active metabolite, SN-38, thereby improving its activity. In this report, we evaluate the in vivo activity of nal-IRI in the two xenograft models of lung cancer. A pharmacodynamics (PD) study was performed to measure the drug activation and deposition parameters in these tumor models. In addition we investigated the effects of nal-IRI on tumor growth, tumor-associated macrophages (TAM's), vasculature, cell proliferation, and apoptosis.

**Methods:** Xenograft models of subcutaneous H157 squamous cell carcinoma (SCC) and H841 small cell lung cancer (SCLC) were established in mice. A short pharmacodynamics (PD) study was performed, wherein, 24 hours after a single dose, animals were euthanized and tumors collected. PD analysis included profiling for carboxylesterase (CES) levels, vasculature (CD31), macrophage (F4/80), and metabolite (CPT-11 and SN-38) levels. For the tumor activity study, animals (5 per group) were treated by weekly i.v. injections with placebo liposome, free irinotecan at 25 mg/kg/wk, or nal-IRI at 30 and 50 mg/kg/wk for three weeks. Tumor volumes were

measured with digital calipers. IHC analysis was performed for TAM content, tumor proliferation (Ki67), apoptosis, and vasculature.

**Results:** (1) The carboxylesterase enzyme (activation) and CPT-11 (deposition) tumor levels resulted in extended intratumor SN38 duration, as predicted by the model simulation; (2) nal-IRI suppressed H157 tumor growth in a dose dependent manner, much more efficiently than free irinotecan. On day 25, nal-IRI, at 30 and 50 mg/kg/wk, inhibited tumor growth by 92.6% and 96.3%, respectively, when compared with placebo liposome. In contrast, free irinotecan inhibited tumor growth by 55.7%; (3) For the SCLC H841 xenograft, on day 35, nal-IRI at 30 and 50 mg/kg/wk, also inhibited tumor growth by 84.9% and 93.4% respectively, greater than free irinotecan by 32.7%, when compared with placebo liposome. No obvious toxicities or weight loss were noted in the nal-IRI treated groups; (4) TAM levels were significantly ( $p < 0.05$ ) higher in tumors treated with nal-IRI (30mg/kg and 50mg/kg), as compared to control or free irinotecan treated tumors.

**Conclusion:** nal-IRI inhibited tumor growth in lung tumor xenograft models, suggesting the treatment of human SCC and SCLC, in which there are high unmet medical needs, as a potential target for clinical investigation.

**Citation Format:** Daniel CF Chan, Ashish Kalra, Zhiyong Zhang, Nancy Paz, Dmitri Kirpotin, Daryl Drummond, Ulrik Nielsen, Paul A. Bunn, Jonathan Fitzgerald. Evaluating the pharmacodynamics and pharmacokinetic effects of MM-398, a nanoliposomal irinotecan (nal-IRI) in subcutaneous xenograft tumor models of human squamous cell carcinoma and small cell lung cancers. [abstract]. In: Proceedings of the 105th Annual Meeting of the American Association for Cancer Research; 2014 Apr 5-9; San Diego, CA. Philadelphia (PA): AACR; Cancer Res 2014;74(19 Suppl):Abstract nr 4626. doi:10.1158/1538-7445.AM2014-4626

©2014 American Association for Cancer Research.

[← Previous](#)

[^ Back to top](#)



October 2014  
Volume 74, Issue 19 Supplement  
[Table of Contents](#)  
[Index by Author](#)

[Search this issue](#)



## Evaluating the pharmacodynamics and pharmacokinetic effects of MM-398, a nanoliposomal irinotecan (nal-IRI), in subcutaneous xenograft tumor models of human squamous cell carcinoma and small cell lung cancers

Daniel C. Chan<sup>1</sup>, Ashish Kalra<sup>2</sup>, Zhiyong Zhang<sup>1</sup>, Nancy Pazz, Dmitri Kirpolin<sup>2</sup>, Daryl Drummond<sup>2</sup>, Ulrik Nielsen<sup>2</sup>, Paul A. Bunn, Jr.<sup>1</sup>, and Jonathan Fitzgerald<sup>2</sup>

<sup>1</sup>University of Colorado, Denver, CO, USA, and <sup>2</sup>Merrimack Pharmaceuticals, Cambridge, MA, USA

#Abstract 4626

**Background:** MM-398 is a novel nanoliposomal encapsulation of irinotecan (nal-IRI), a topoisomerase I inhibitor. In preclinical studies, nal-IRI has been shown to greatly modify the pharmacokinetics and biodistribution of CPT-11 and its active metabolite, SN-38, thereby improving its activity. In this report, we evaluate the *in vivo* activity of nal-IRI in the two xenograft models of lung cancer. A pharmacodynamics (PD) study was performed to measure the drug activation and deposition parameters in these tumor models. In addition we investigated the effects of nal-IRI on tumor growth, tumor-associated macrophages (TAM's), vasculature, cell proliferation, and apoptosis.

**Methods:** Xenograft models of subcutaneous H157 squamous cell carcinoma (SCC) and H841 small cell lung cancer (SCLC) were established in mice. A short pharmacodynamics (PD) study was performed, wherein, 24 hours after a single dose, animals were euthanized and tumors collected. PD analysis included profiling for carboxylesterase (CES) levels, vasculature (CD31), macrophage (F4/80), and metabolite (CPT-11 and SN-38) levels. For the tumor activity study, animals (5 per group) were treated by weekly i.v. injections with placebo liposome, free irinotecan at 25 mg/kg/wk, or nal-IRI at 30 and 50 mg/kg/wk for three weeks. Tumor volumes were measured with digital calipers. IHC analysis was performed for TAM content, tumor proliferation (Ki67) and DNA damage (H2AX).

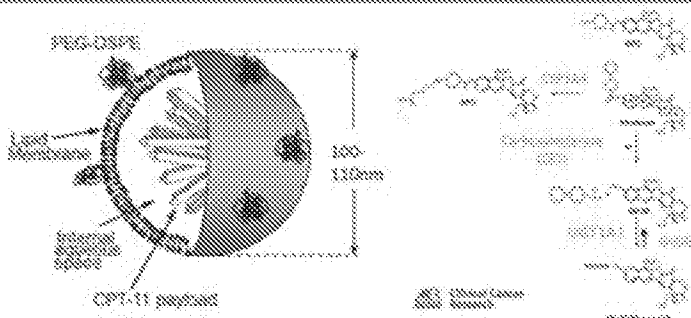
**Results:** (1) The carboxylesterase enzyme (activation) and CPT-11 (deposition) tumor levels resulted in extended intratumor SN-38 duration, as predicted by the model simulation; (2) nal-IRI suppressed H157 tumor growth in a dose dependent manner, much more efficiently than free irinotecan. On day 25, nal-IRI, at 30 and 50 mg/kg/wk, inhibited tumor growth by 92.6% and 96.3%, respectively, when compared with placebo liposome. In contrast, free irinotecan inhibited tumor growth by 55.7%; (3) For the SCLC H841 xenograft, on day 35, nal-IRI at 30 and 50 mg/kg/wk, also inhibited tumor growth by 84.9% and 93.4% respectively, greater than free irinotecan by 32.7%, when compared with placebo liposome. No obvious toxicities or weight loss were noted in the nal-IRI treated groups; (4) TAM levels were significantly ( $p < 0.05$ ) higher in tumors treated with nal-IRI (30mg/kg and 50mg/kg), as compared to control or free irinotecan treated tumors.

**Conclusion:** nal-IRI inhibited tumor growth in lung tumor xenograft models, suggesting that the treatments of human SCC and SCLC, in which there are high unmet medical needs, are potential targets for clinical investigation.



# Results

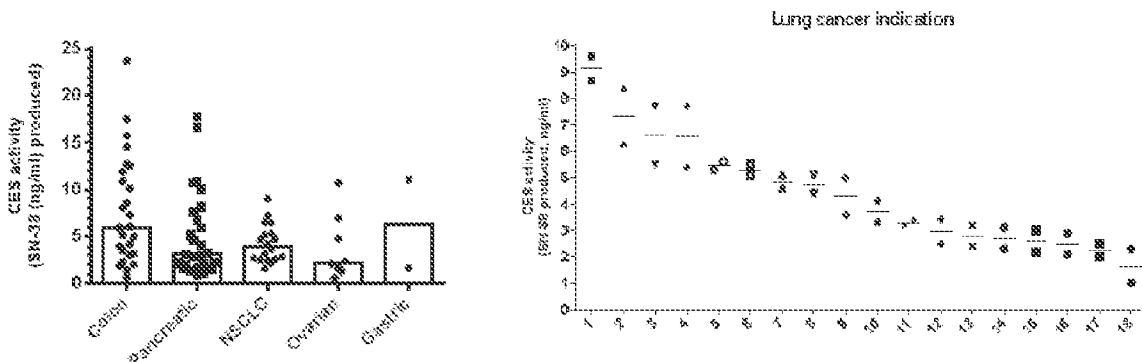
## nal-IRI background



- Liposomal formulation of irinotecan
- Topoisomerase inhibitor
- high levels of pro-drug CPT-11 uptake and SN-38 tumor levels

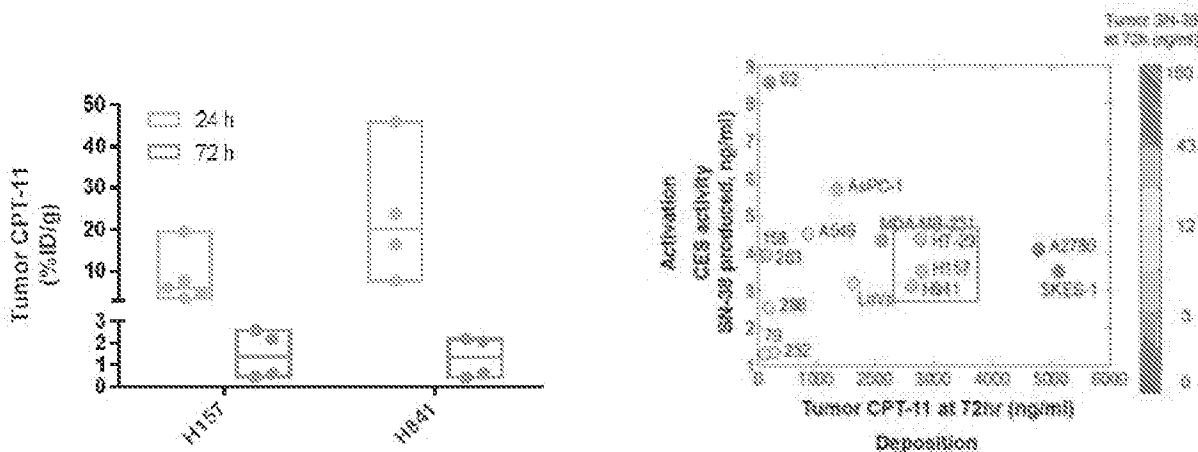
## Profiling panel of tumors models for CES enzyme activity and tumor pro-drug CPT-11 uptake

### Ex vivo CES enzyme conversion assay on PDX tumor xenografts



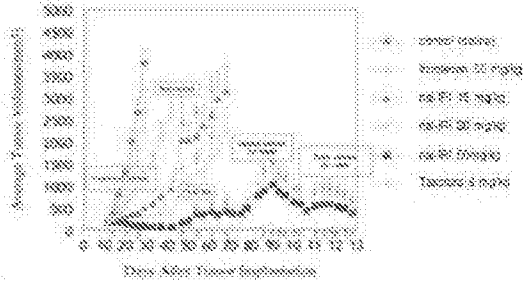
### Tumor CPT-11 at 24h and 72h post single dose of nal-IRI (10mg/kg)

### Profiling cell-line derived and patient-derived tumors for nal-IRI activation and deposition

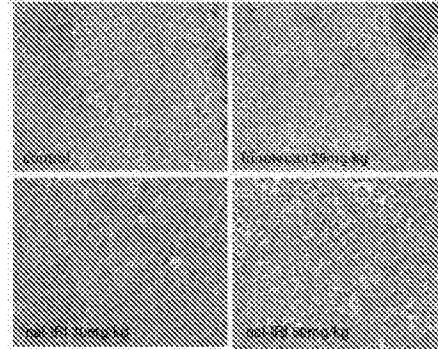


# In vivo activity of nal-IRI in H157 and H841 subcutaneous xenograft tumor models

H157

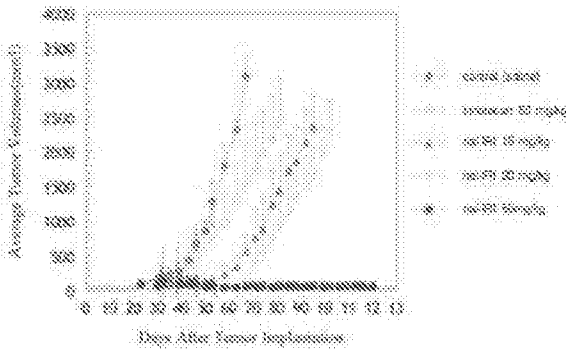


Tumor morphology at end of efficacy study (H&E staining)

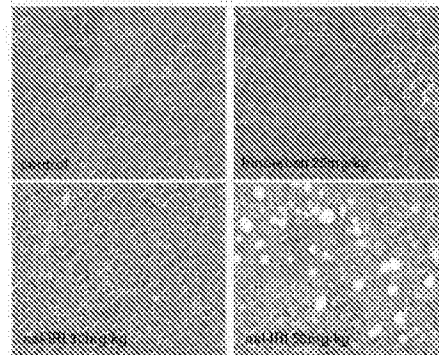


## Results

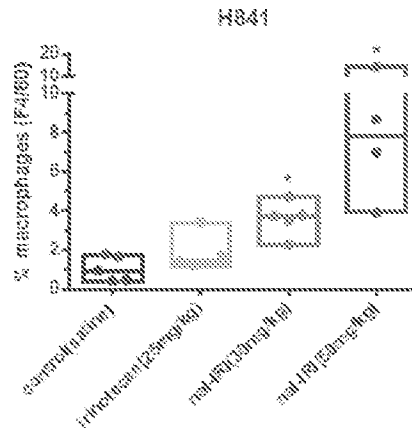
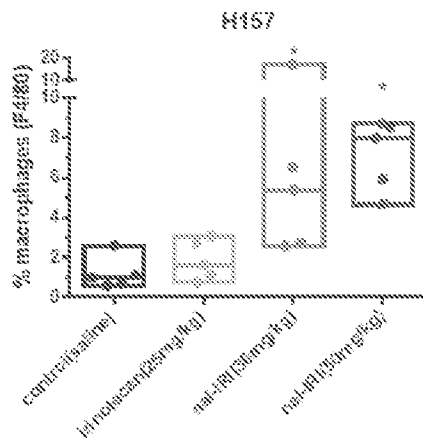
H841

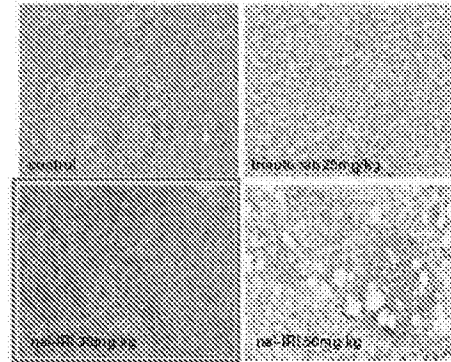
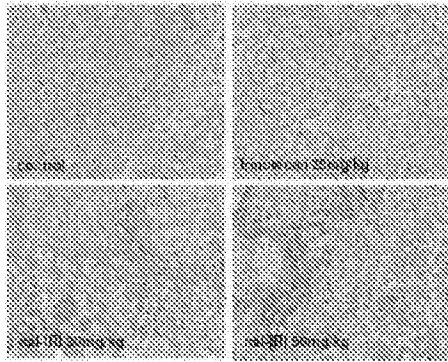


Tumor morphology at end of efficacy study (H&E staining)



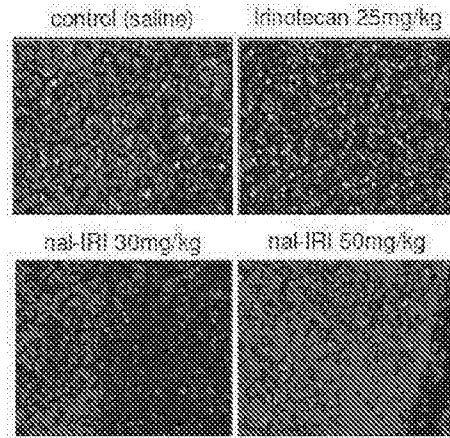
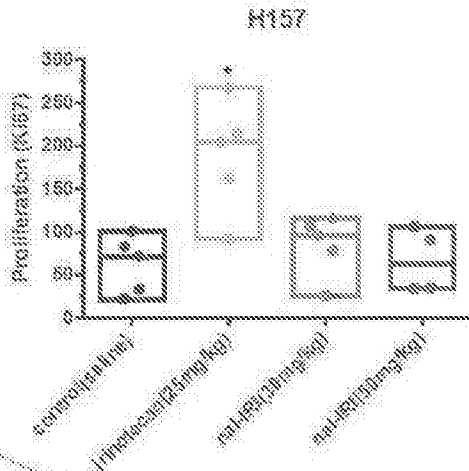
## Influx of tumor associated macrophages observed in tumors treated with nal-IRI





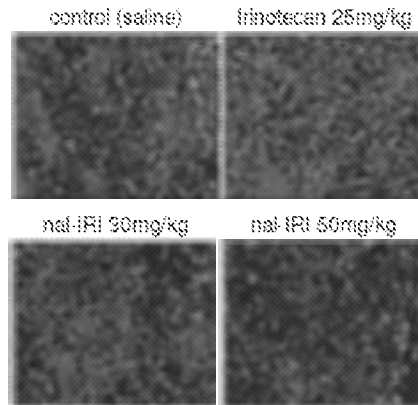
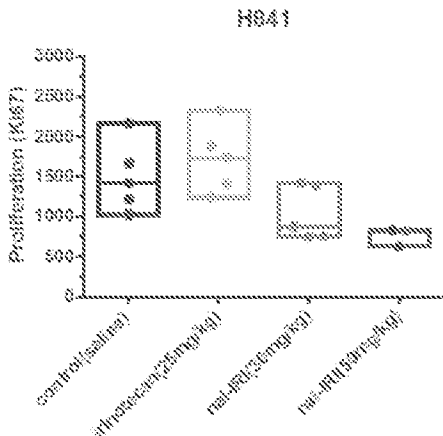
Tumor cell proliferation in H841 model was reduced following nal-IRI administration

Proliferation index at end of efficacy study (Ki67 staining)



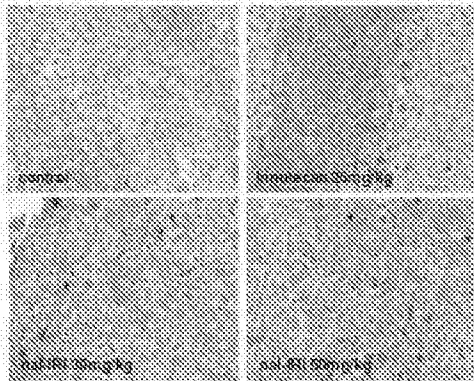
## Results

Proliferation index at end of efficacy study (Ki67 staining)

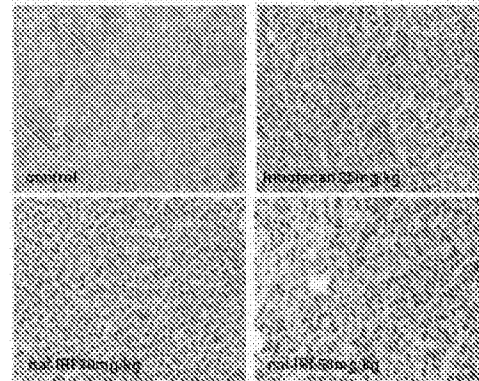


nal-IRI treatment leads to DNA damage as observed by increased gammaH2AX in tumors

H157

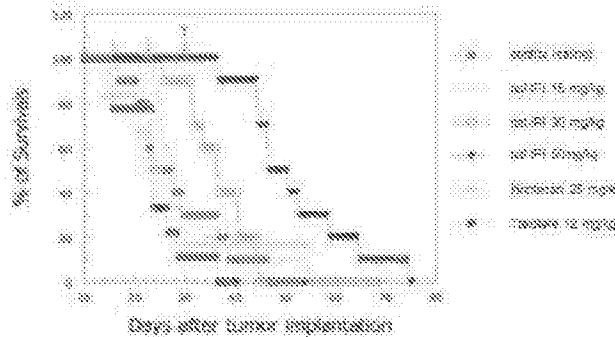


H841

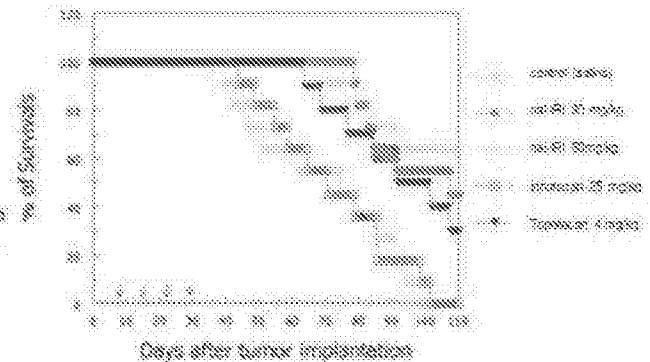


nal-IRI in vivo activity confirmed in rat orthotopic H157 and H841 lung models

H157



H841

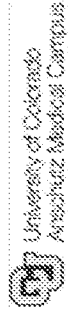
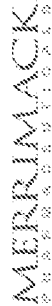


## Summary

- H157(SCC) and H841(SCLC) tumor models displayed high levels of pro-drug CPT-11 uptake and SN-38 tumor levels
- Tumor growth inhibition with nal-IRI in both models (H157 and H841) was associated with an increase in tumor macrophages, DNA damage, and a decrease in tumor cell proliferation
- These data support human lung SCC and SCLC as a potential therapeutic targets for clinical investigation of nal-IRI

# Evaluating the pharmacodynamics and pharmacokinetic effects of MM-398, a nanoliposomal irinotecan (nal-IRI), in subcutaneous xenograft tumor models of human squamous cell carcinoma and small cell lung cancers

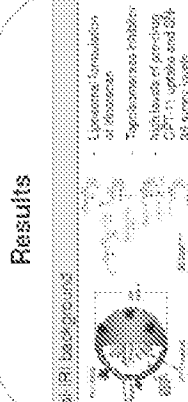
Daniel C. Chan<sup>1</sup>, Ashish Kaira<sup>2</sup>, Zhiyong Zhang<sup>3</sup>, Nancy Paz<sup>4</sup>, Dmin Kirpourn<sup>5</sup>, Dany Drummond<sup>6</sup>, Ulrik Nielsen<sup>6</sup>, Paul A. Bunn, Jr.<sup>7</sup>, and Jonathan Fitzgerald<sup>8</sup>  
<sup>1</sup>University of Colorado, <sup>2</sup>University of Colorado, <sup>3</sup>University of Colorado, <sup>4</sup>University of Colorado, <sup>5</sup>University of Colorado, <sup>6</sup>University of Colorado, <sup>7</sup>University of Colorado, <sup>8</sup>University of Colorado



Abstract #4626

**Background:** MM-398 is a novel nanoliposomal formulation of irinotecan (nal-IRI), a topoisomerase I inhibitor. In preclinical studies, nal-IRI has been shown to greatly improve the pharmacokinetics and bioavailability of CPT-11 and its active metabolite, SN-38, thereby improving its activity in the tumor. We evaluate the *in vivo* activity of nal-IRI in two xenograft models of lung cancer. A pharmacokinetic (PK) study was performed to measure the drug activation and degradation parameters in these tumor models. In addition we investigated the effects of nal-IRI on tumor growth, tumor-associated macrophages (TAMs), vascularization, cell proliferation, and apoptosis. **Methods:** Xenograft models of squamous cell carcinoma (SCC) and small cell lung cancer (SCLC) were established *in vivo*. A short pharmacokinetic (PK) study was performed, wherein 24 hours after a single dose, animals were sacrificed and tumor sections (TSS) were collected for analysis of irinotecan (CPT-11) levels, vascularization (CD31), macrophages (F4/80), and metalloproteinase (MMP-11 and SN-38) levels. For the tumor activity study, animals (6 per group) were treated by weekly *ip* injections with placebo (placebo), nal-IRI at 25 mg/kg, or nal-IRI at 50 and 100 mg/kg for three weeks. Tumor volumes were measured with digital calipers. PK analysis was performed by TAM content, tumor proliferation (Ki67) and DNA damage (γ-H2AX).

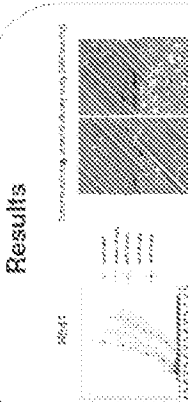
**Results:** (1) The subcutaneous enzyme activation of CPT-11 (liposomal tumor levels resulted in elevated irinotecan SN-38 flux) was improved by the novel formulation (2) nal-IRI suppressed HIF-1 $\alpha$  tumor levels in a dose dependent manner, much more effectively than free irinotecan. On Day 25, nal-IRI at 50 and 100 mg/kg reduced tumor growth by 52.6% and 84.3%, respectively, when compared with placebo (placebo). In contrast, free irinotecan inhibited tumor growth by 55.7%, 57.1% and 91.4%, respectively, on Day 25, nal-IRI at 50 and 100 mg/kg respectively. Tumor growth was inhibited by 22.7% when compared with placebo (placebo). In previous studies of weight loss were noted in the nal-IRI treated groups. (3) TAM levels were significantly (p<0.05) higher in tumors treated with nal-IRI (50mg/kg and 100mg/kg), as compared to control or free irinotecan treated tumors. **Conclusions:** nal-IRI inhibited tumor growth in lung tumor xenograft models, suggesting that the treatments of human SCLC and SCC, in which there are high tumor vascularization, are potential targets for clinical investigation.



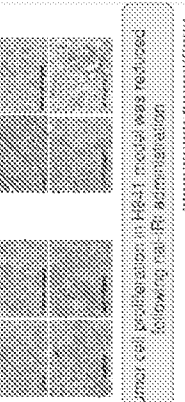
**Results**  
 - Upstream stimulation of downstream tyrosinase inhibits CPT-11 uptake and SN-38 tumor levels  
 - Profiling panel of tumors models for CPT-11 activity and tumor pro-drug CPT-11 uptake  
 - In vivo CPT-11 activity was measured in SCC and SCLC xenograft models at 24, 48, and 72 hours post-injection (25 mg/kg)



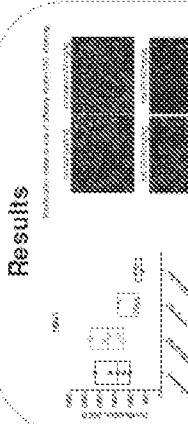
**Results**  
 - *In vivo* activity of nal-IRI in H157 and H461 subcutaneous xenograft tumor models  
 - TAM levels were significantly higher in tumors treated with nal-IRI (50mg/kg and 100mg/kg), as compared to control or free irinotecan treated tumors



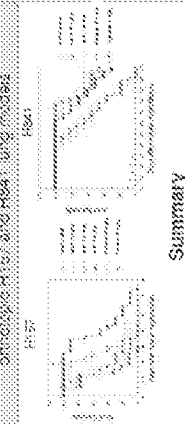
**Results**  
 - Profiling panel of tumors models for CPT-11 activity and tumor pro-drug CPT-11 uptake  
 - In vivo CPT-11 activity was measured in SCC and SCLC xenograft models at 24, 48, and 72 hours post-injection (25 mg/kg)



**Results**  
 - Tumor cell proliferation in H461 model was reduced following nal-IRI administration  
 - TAM levels were significantly higher in tumors treated with nal-IRI (50mg/kg and 100mg/kg), as compared to control or free irinotecan treated tumors



**Results**  
 - HIF-1 $\alpha$  tumor levels in H157 and H461 xenograft models were significantly reduced following nal-IRI administration  
 - HIF-1 $\alpha$  *in vivo* activity continued in H157 xenograft H157 and H461 lung models



**Summary**  
 - H157 (SCLC) and H461 (SCC) tumor models received high levels of pro-drug CPT-11 uptake and 80-38 tumor levels  
 - Tumor growth inhibition with nal-IRI in both models (H157 and H461) was associated with an increase in tumor macrophages (TAM) levels, and a decrease in tumor cell proliferation  
 - These data support ongoing SCLC and SCC, as a potential therapeutic target for clinical investigation of nal-IRI

vorinostat (1-5 $\mu$ M) for 2 or 4 days to investigate growth inhibitory and apoptotic effects. Expression of the cell cycle proteins cyclin D1, cyclin E and p27 were examined after vorinostat treatments. For in vivo studies, cyclin E transgenic mice were treated with vorinostat to investigate effects on cyclin D1, cyclin E and ki-67 expression in lung cancers. FVB mice harboring transplanted syngeneic murine lung cancer cells were treated with vorinostat to evaluate effects on lung cancer formation. For the window of opportunity clinical trial, patients with resectable non-small cell lung cancer (NSCLC) were treated with vorinostat (400mg) orally once daily for 7 days before surgical resection. Paired pre-treatment and post-treatment tumor biopsies were scored for immunohistochemical changes in cyclin D1, cyclin E and Ki-67.

**Results:** Among a panel of drugs that caused growth inhibition of lung cancer cells and repression of cyclin D1 protein, vorinostat was found as most potent. Vorinostat treatment caused dose-dependent and time-dependent growth inhibition and apoptosis induction in murine and human lung cancer cells. Effects were reversed by washouts of vorinostat.

Vorinostat treatments repressed cyclin D1 and cyclin E proteins, but increased p27 expression in ED-1 cells. Notably, vorinostat treatments of cyclin E transgenic mice substantially repressed cyclin D1 expression in pre-malignant and malignant lung tissues. Vorinostat treatment significantly reduced lung tumor formation ( $P = 0.047$ ) in the murine transplantation lung cancer model. To translate these studies into the clinic, 10 patients were recruited for the vorinostat window of opportunity clinical trial. Among 7 of the paired tumor specimens examined, 3 had decreased Ki-67 and cyclin E levels, 2 had decreased cyclin D1 expression, and 4 showed necrosis in post-treatment biopsies.

**Conclusion:** Substantial anti-neoplastic effects of vorinostat occurred in cultured lung cancer cells and in vivo in murine transgenic and transplantable lung cancer models. Findings were validated in the clinic through a vorinostat window of opportunity trial. These studies underscore the value of clinically-relevant murine lung cancer models for guiding clinical trials in lung cancer patients.

**Keywords:** window of opportunity trial, NSCLC, Vorinostat, murine lung cancer model

Preclinical Models | Wednesday, 6 July 2011 14:30-16:00

### O33.03 PEP02 (LIPOSOME IRINOTECAN) EFFECTIVELY INHIBITS HUMAN LUNG SQUAMOUS CELL CARCINOMA AND SMALL CELL LUNG CANCERS IN SUBCUTANEOUS AND ORTHOTOPIC XENOGRAFT TUMOR MODELS

Daniel C. Chan<sup>1</sup>, Zhiyong Zhang<sup>1</sup>, Paul A. Bunn<sup>1</sup>, Grace Yeh<sup>2</sup>

<sup>1</sup>Medical Oncology, University Of Colorado Denver/ United States Of America, <sup>2</sup>Pharmaengine, INC/ Taiwan

**Background:** PEP02 is a nanoparticle liposome formulation of irinotecan (CPT-11), a topoisomerase I inhibitor, used for the treatment of various tumor types including lung cancers. In preclinical and clinical studies, PEP02 has been shown to greatly modify the pharmacokinetics and biodistribution of CPT-11 and its active metabolite, SN-38, thereby improving its therapeutic efficacy. In this report, we evaluated the in vivo efficacy of PEP02 in three xenograft models of human lung tumors.

**Methods:** Xenograft models of subcutaneous H157 squamous cell carcinoma (SCC), known to be resistant to various EGFR inhibitors, and H841 small cell lung cancer (SCLC), known to be resistant to several conventional therapeutic agents, were established in mice and rats. Animals (10-12 per group) were treated by weekly iv injections after the tumor reached 200 cubic mm in size with placebo liposome, CPT-11 at 50 (mouse) or 25 (rat) mg/kg/wk, docetaxel at 8 (mouse) or 12 (rat) mg/kg/wk, or PEP02 at 15, 30 and 50 mg/kg/wk for three or four weeks. Tumor volumes were measured with digital calipers. For the orthotopic model, Kaplan-Meier survival curves were generated.

**Results:** (1) PEP02 effectively suppressed H157 subcutaneous SCC tumor growth in a dose dependent manner, much more efficient than CPT-11 or docetaxel. PEP02 at 15, 30 and 50 mg/kg/wk inhibited tumor growth by 86.7%, 92.9% and 97.6%, respectively when compared with that of placebo liposome, and the suppressions persisted for 12 to 15 days after the last treatment. In contrast, CPT-11 and docetaxel only inhibited tumor growth by 29.8% and 71.4%, respectively. Retreatment of the regrowth was achieved with PEP02 at 50 mg/kg/wk which extended the tumor suppression until 130 days. (2) For the SCLC H841 xenograft, PEP02 at 15, 30 and 50 mg/kg/wk also impressively inhibited tumor growth by 81.7%, 96.3% and 98.3% respectively, much better than CPT-11 by

51.6%, when compared with that of placebo liposome. Inhibition of tumor growth persisted more than 20 days after the last treatment with PEP02 at 15 and 30 mg/kg/wk before tumor grew again. In contrast, complete tumor regression was achieved at 50 mg/kg/wk. (3) When implanted orthotopically in the left lung of athymic nude rats, H157 SCC tumor grew aggressively and metastasized contra-laterally to right lungs, and eventually rats died from tumor burden with a median survival of 24 days in the placebo liposome group. At the maximum tolerated dose, CPT-11 at 25 mg/kg/wk or docetaxel at 12 mg/kg/wk did not extend rat survival at all. However, PEP02 at 15, 30 and 50 mg/kg/wk prolonged median survivals by 4, 12 and 26 days, respectively. In all three models, no obvious side effects or weight loss were noted in the PEP02 treated groups. **Conclusion:** PEP02 effectively inhibited tumor growth, regrowth, and prolonged survival in subcutaneous and orthotopic lung tumor xenograft models. PEP02 has great clinical potential for the treatment of human lung SCC and SCLC in which there are high unmet medical needs.

**Keywords:** Liposomal irinotecan, subcutaneous and orthotopic models, Squamous carcinoma and SCLC

A revised/updated abstract may be included in the Late Breaking Abstract Supplement, available at the 14<sup>th</sup> World Conference on Lung Cancer.

Preclinical Models | Wednesday, 6 July 2011 14:30-16:00

### O33.05 ANAPLASTIC LYMPHOMA KINASE (ALK) DEPENDENT AND CO-DEPENDENT MECHANISMS OF RESISTANCE TO ALK KINASE INHIBITORS IN EML4-ALK NON-SMALL CELL LUNG CANCER

Takaaki Sasaki<sup>1</sup>, Jussi Koivunen<sup>2</sup>, Atsuko Ogino<sup>3</sup>, Katsuhiko Okuda<sup>4</sup>, Masahiko Yanagita<sup>5</sup>, Marzia Cappelletti<sup>6</sup>, Keith Wilner<sup>4</sup>, James Christensen<sup>4</sup>, Michael Eck<sup>3</sup>, Natanael Gray<sup>3</sup>, Pasi A. Janne<sup>5</sup>

<sup>1</sup>Respiratory Center, Asahikawa Medical University Hospital/Japan, <sup>2</sup>Department Of Oncology And Hematology, Oulu University Hospital/Finland,

<sup>3</sup>Medical Oncology, Dana-Farber Cancer Institute/United States Of America, <sup>4</sup>Department Of Research Pharmacology, Pfizer Global Research And Development/United States Of America, <sup>5</sup>Lowie Center For Thoracic Oncology, Dana Farber Cancer Institute/United States Of America

**Background:** Lung cancers harboring anaplastic lymphoma kinase (ALK) rearrangements represent a unique subpopulation of patients. Crizotinib, an ALK tyrosine kinase inhibitor (TKI) is clinically effective in this genomically defined patient subset. However, the clinical success of treatment with ALK-TKIs is often limited by the development of acquired drug resistance. In this study, we examined resistance mechanisms to ALK-TKIs. The understanding of resistance mechanism(s) is critical to the development of effective subsequent treatments.

**Methods:** We examined tumor biopsies from patients treated with crizotinib that had developed acquired resistance to crizotinib. We also generated an ALK-TKI resistant H3122 cell (H3122TR3) by exposing the increasing dose of TAE684. Finally we generated a cell line (DFCI076) from a pleural effusion of a NSCLC patient that developed acquired resistance to crizotinib. We examined whether genomic changes (mutations or copy number changes) were present in the ALK TKI resistant tumors and cells. In addition, we evaluated for the presence of co-activated signaling pathways.

**Results:** We identified a secondary mutation in ALK, F1174L (also detected in neuroblastoma), in a patient with an inflammatory myofibroblastic tumor (IMT) harboring a RANBP2-ALK translocation who progressed while on crizotinib therapy. When present in cis with an ALK translocation, the F1174L mutation causes an increase in ALK phosphorylation, cell growth and downstream signaling. This mutation likely promotes the active conformation of ALK which disfavors crizotinib binding as it binds the inactive conformation of ALK. Treatment with a structurally distinct ALK inhibitor, TAE684, or with 3-fold above the current efficacious concentrations of crizotinib was sufficient to inhibit the growth of Ba/F3 cells harboring the F1174L mutation. In contrast the DFCI076 cells (EML4-ALK), were resistant to both crizotinib and TAE684. These cells contained a novel L1152R ALK secondary mutation. Ba/F3 cells with EML4-ALK L1152R were also resistant to crizotinib and the L1152R mutation diminished crizotinib mediated inhibition of downstream phosphorylation. In addition, we determined that the DFCI076 cells had evidence of significant Epidermal Growth Factor Receptor (EGFR) phosphorylation. Infection of an ALK shRNA inhibited the growth of DFCI076 cells to 40% of control; however the combination of ALK knockdown and PF00299804, an irreversible pan-ERBB inhibitor, led to further growth inhibition (19% of control). The H3122TR3



PEP02 (liposome irinotecan) effectively  
inhibits human squamous cell carcinoma and  
small cell lung cancers in subcutaneous and  
orthotopic xenograft tumor models

Daniel C. Chan\*, Zhiyong Zhang, Paul A. Bunn, Jr.,  
and C. Grace Yeh

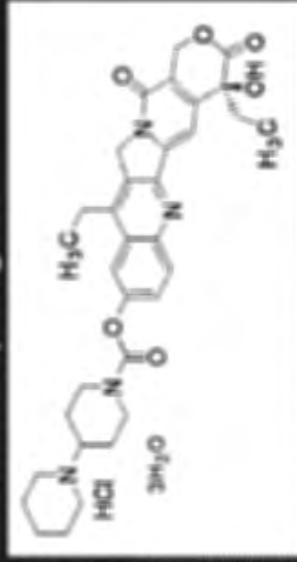
University of Colorado, Denver, CO, USA, and  
PharmaEngine, Inc., Taipei, Taiwan

This project was supported by a grant from PharmaEngine to DC, the presenting author.  
PEP02 is designated as MM-398 by Merrimack Pharmaceuticals, Inc.

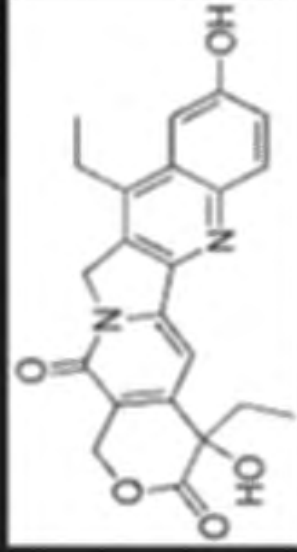


# Irinotecan (CPT-11)

- ◆ **Mechanism of Action**
  - Topoisomerase I inhibitor – induces single-strand DNA breaks
  - Irinotecan (CPT-11) is a prodrug, when converted by carboxylesterase to its active metabolite (SN-38), elicits 100-1000 fold higher potency
  - Carboxylesterase is commonly expressed in lung cancer cells and in tumor-associated macrophages



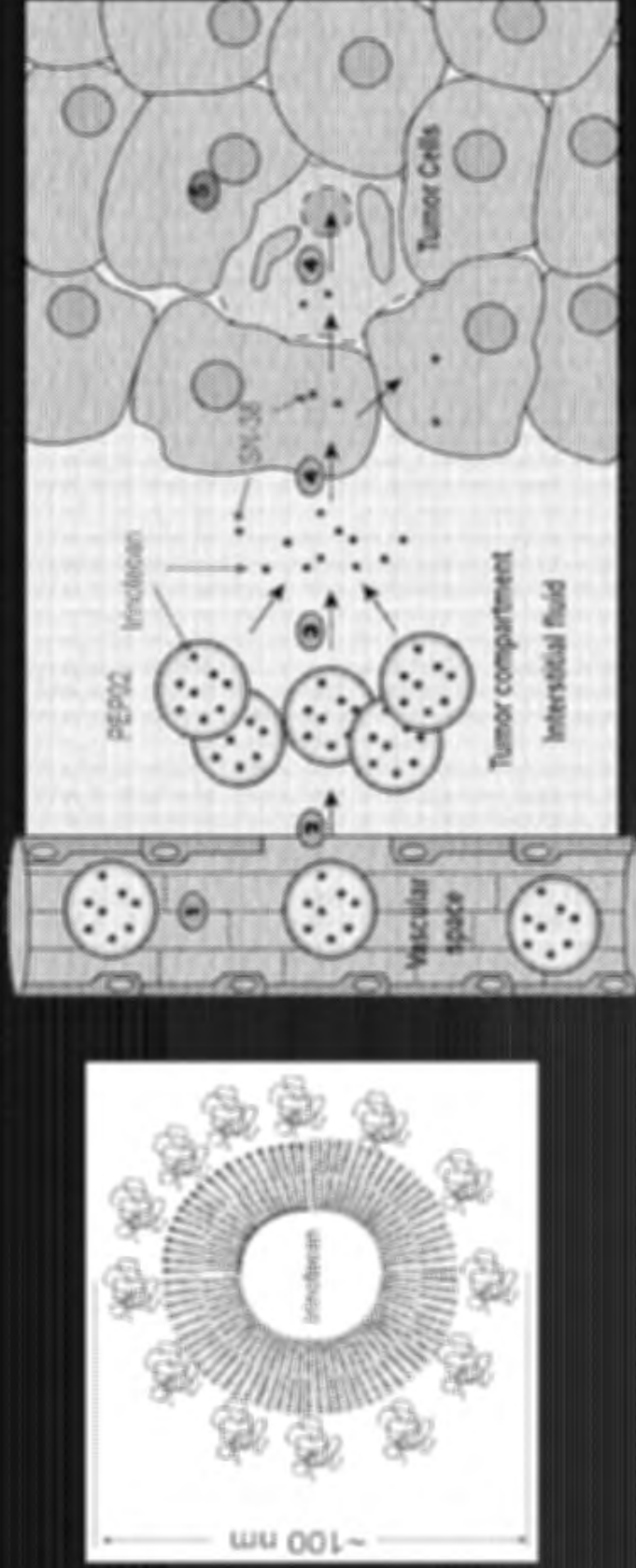
CPT-11



SN-38

- ◆ **Clinical Indications**
  - Approved for 1<sup>st</sup> and 2<sup>nd</sup> lines in metastatic colorectal cancer worldwide
  - Other cancer indications approved in Japan (NSCLC, SCLC, gastric, cervical, ovarian, breast, lymphoma)
- ◆ **Limitations**
  - Diarrhea and neutropenia

# PEP02/MM-398 (Liposome Irinotecan)



- ◆ Irinotecan is encapsulated in PEG-liposomes (PEP02/MM-398)
- ◆ Improved PK profile over free irinotecan in preclinical and clinical studies
- ◆ Enhanced permeability retention (EPR) effect - with the diameters adjusted at about 100 nm penetrating easily around tumor tissues
- ◆ Macrophages in tumors aid in converting CPT-11 to SN-38 to reach hypoxic tumor microenvironment

# Tumor Uptake of CPT-11 & SN-38

Tumor Uptake of Free Irinotecan and PEP02 in a Bioluminescent Orthotopic Human Pancreas Cancer Xenograft Model in Nude Mice\*

Mice with tumors were given a single i.v. injection of free CPT-11 or PEP02 at a dose of 20 mg CPT-11/kg.

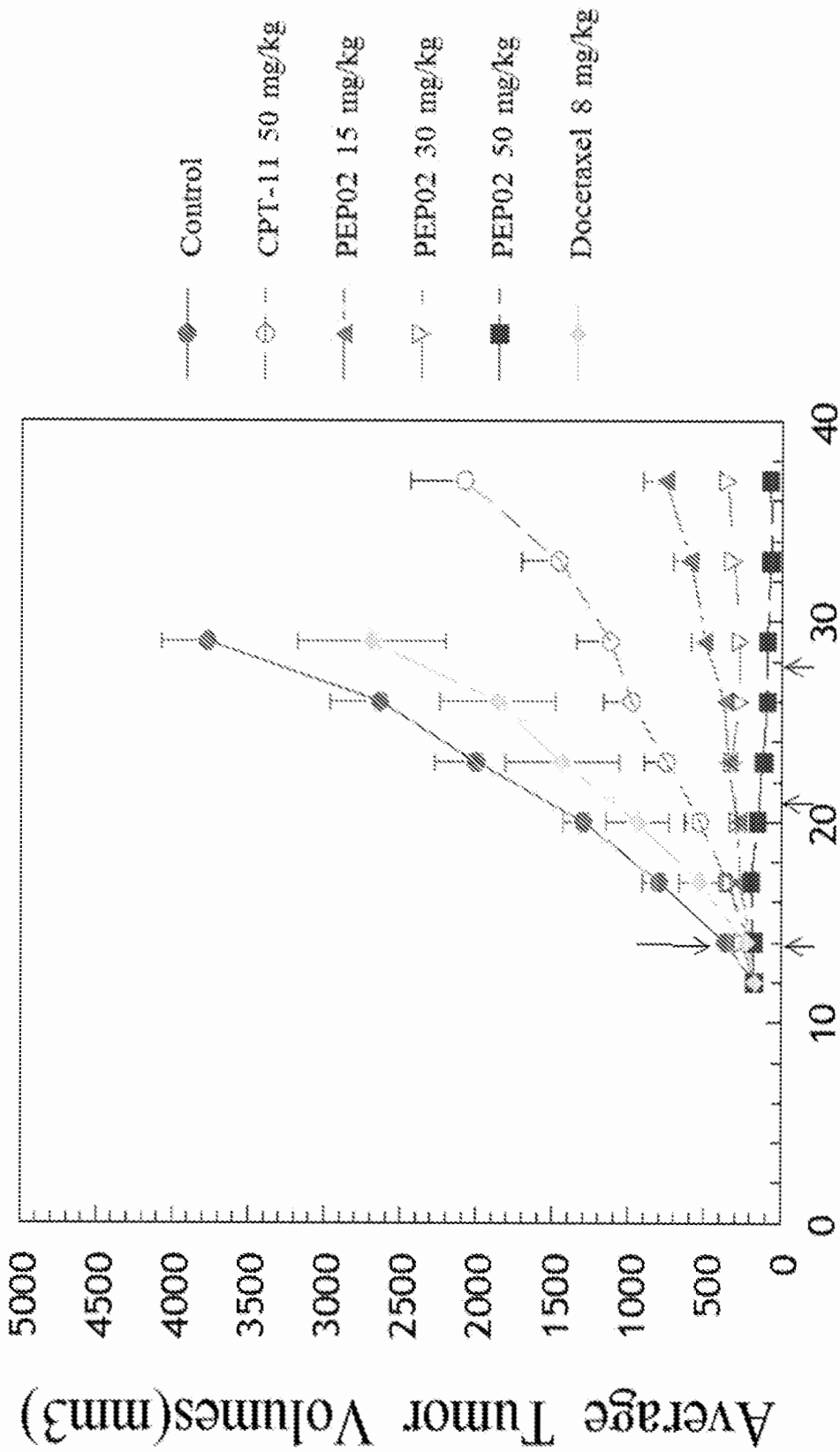
	CPT-11 ( $\mu\text{g/g}$ tumor)	SN-38 ( $\mu\text{g/g}$ tumor)
Free CPT-11 (24 h)	$0.043 \pm 0.11$	$0.019 \pm 0.011$
PEP02 (24 h)	$6.1 \pm 0.2$	$0.17 \pm 0.007$
PEP02 (72h)	$1.6 \pm 0.74$	$0.093 \pm 0.019$

\*Hann B. et al., 98<sup>th</sup> AACR Annual Meeting, Abstract #5648, 2007

## Rodent Lung Cancer Models

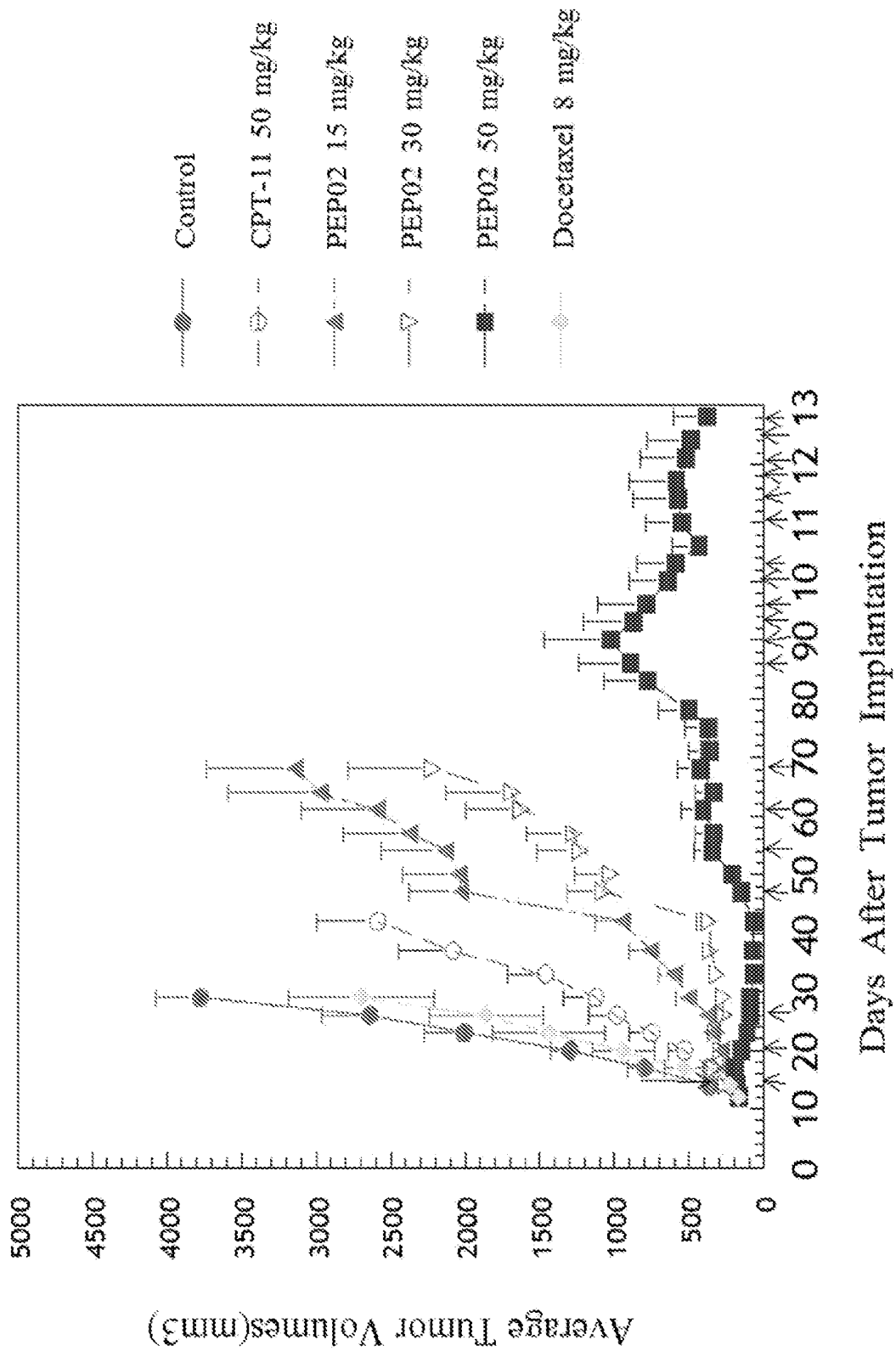
- ◆ Human lung squamous carcinoma NCI-H157 cells or human small cell lung cancer NCI-H841 implanted subcutaneously (in the rear flank) or orthotopically (intra-trachea to left lung) in athymic nude mice or nude rats, respectively.
- ◆ Treatment groups (n = 10 - 12 per group):
  - Control (placebo liposome), PEP02 (15, 30, 50 mg/kg), CPT-11 (25 or 50 mg/kg), docetaxel (8 or 12 mg/kg), or topotecan (4 or 5 mg/kg).
  - When the tumors reached ~150 mm<sup>3</sup>, the mice or rats were treated with 3 or 4 weekly iv injections.
- ◆ Endpoints: tumor volume, body weight, survival.

# Efficacy of PEP02/MM-398 in Human Lung SCC H157 Heterotopic Xenograft in Nude Mice



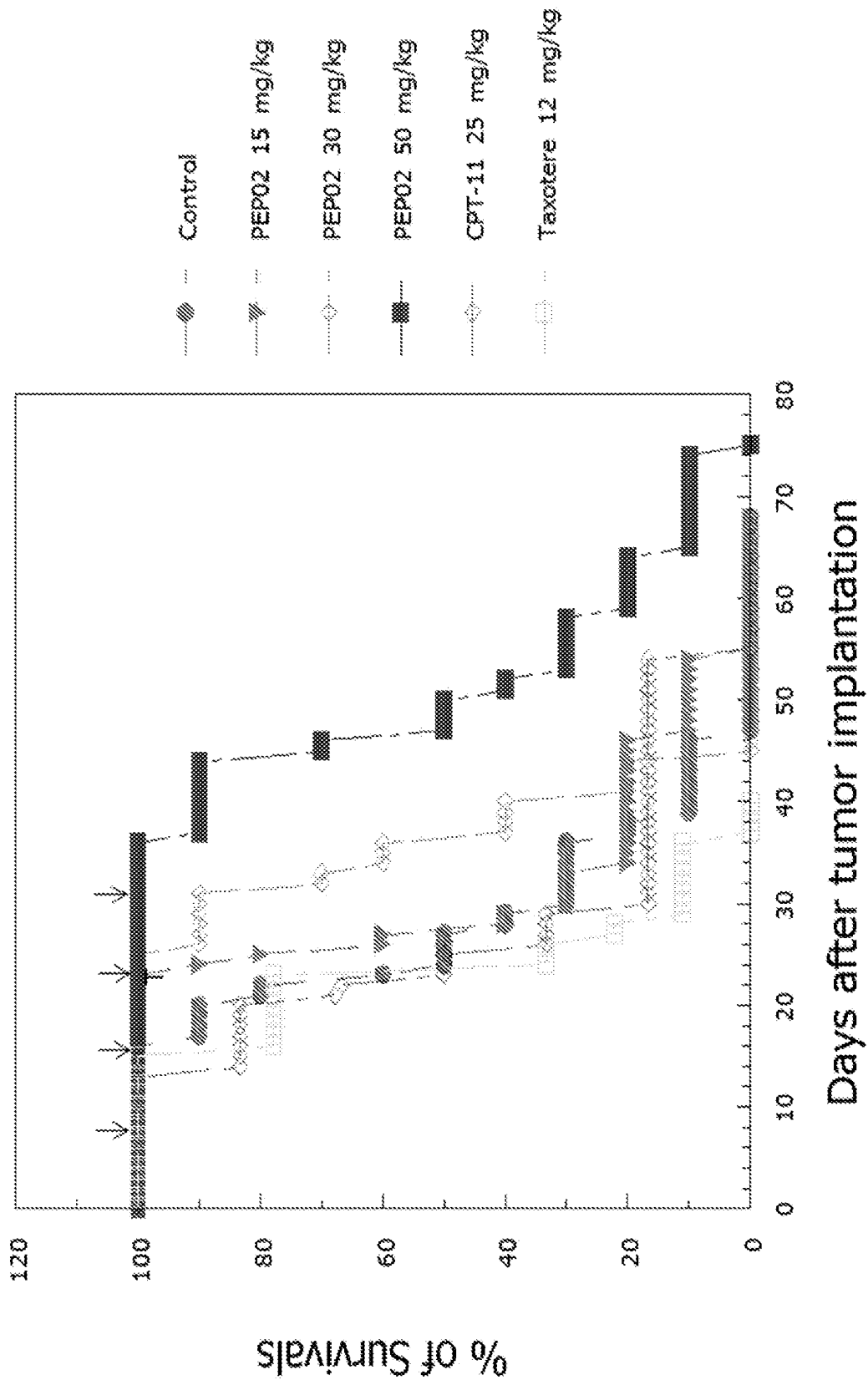
Days After Tumor Implantation

# Efficacy of PEP02/MM-398 in Human Lung SCC H157 Heterotopic Xenograft in Nude Mice

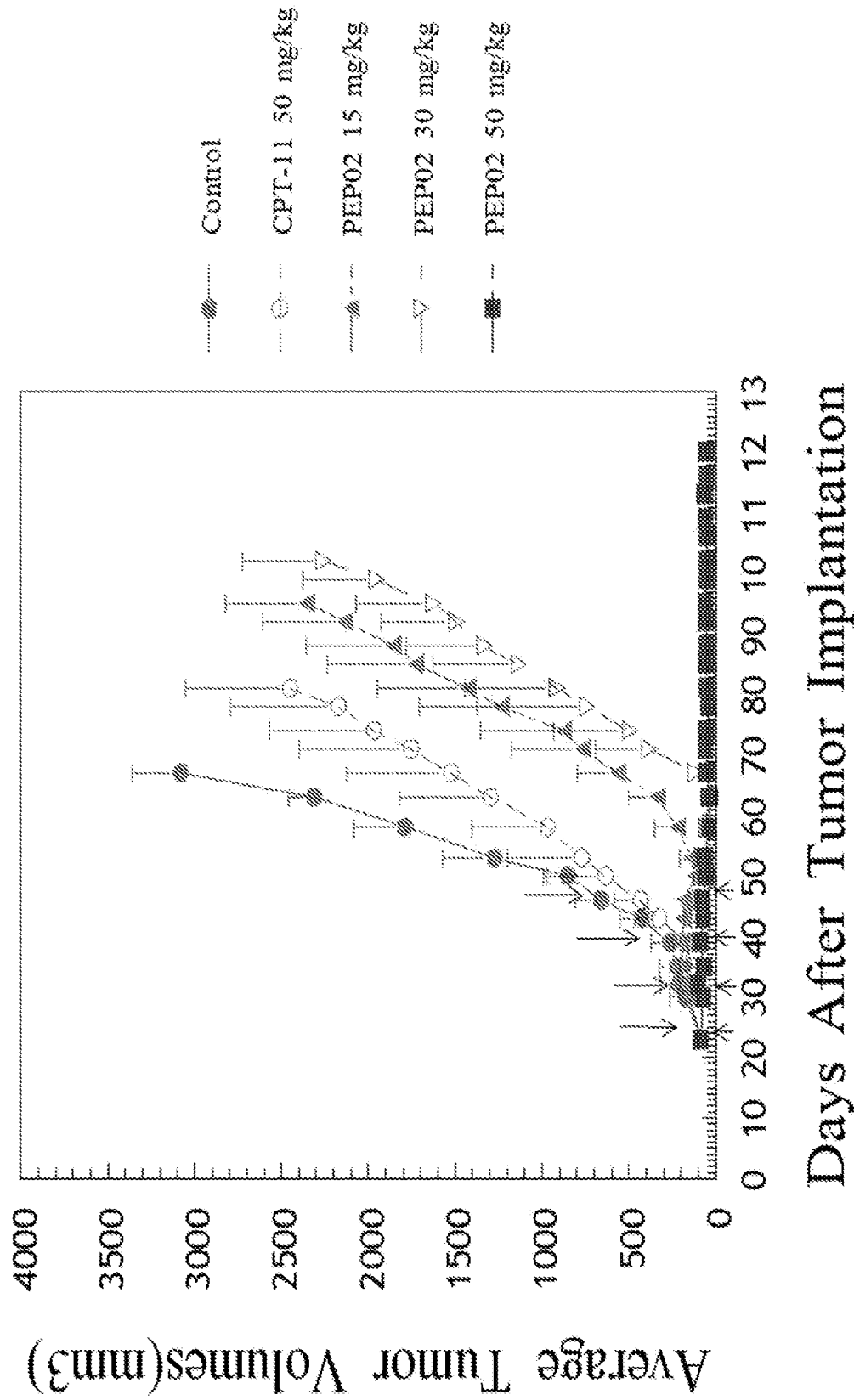




# Efficacy of PEP02/MM-398 in Human Lung SCC H157 Orthotopic Xenograft in Nude Rats

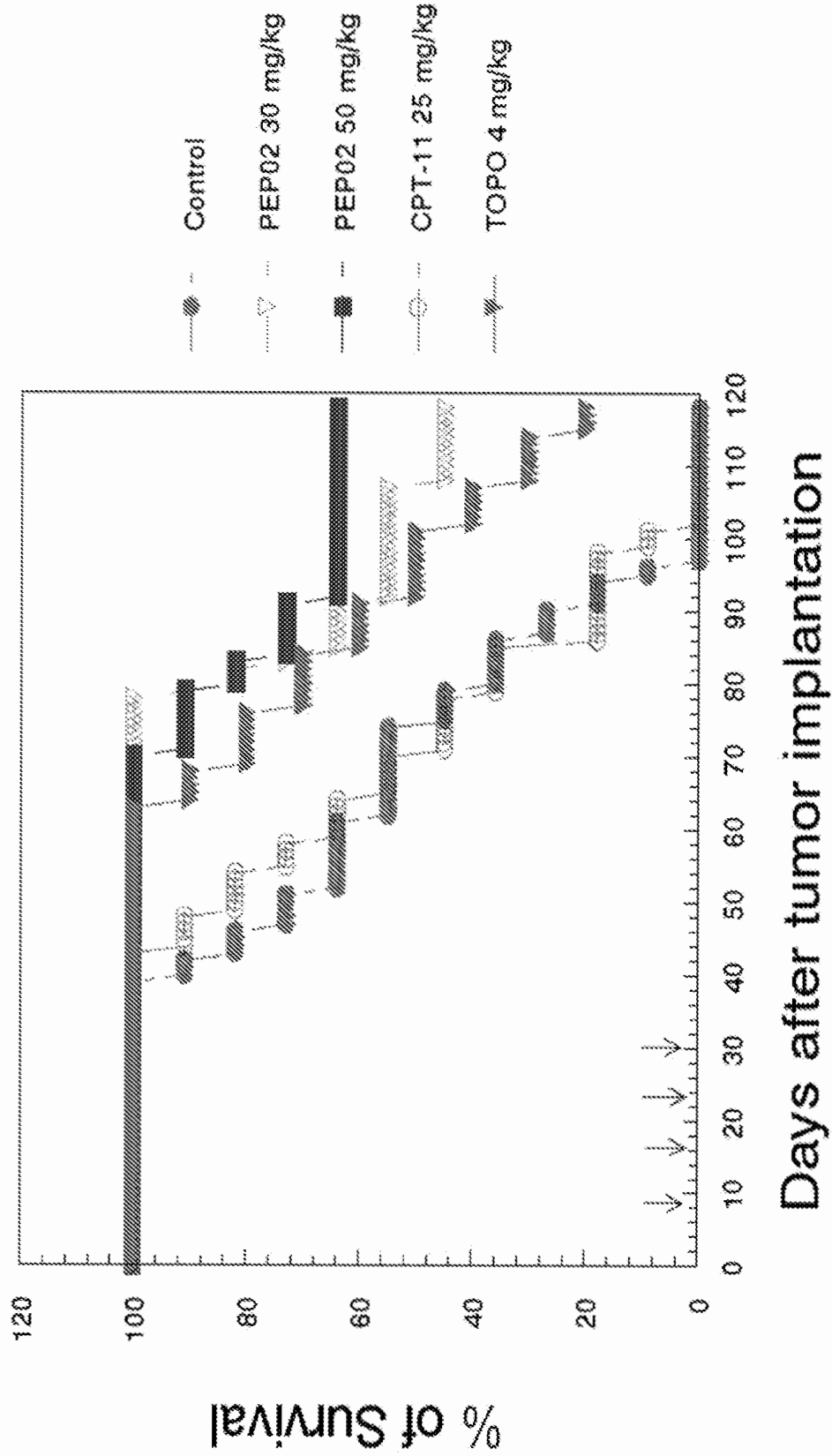


# Efficacy of PEP02/MM-398 in Human SCLC H841 Heterotopic Xenograft in Nude Mice





# Efficacy of PEP02/MM-398 in Human SCLC H841 Orthotopic Xenograft in Nude Rats



# Conclusions

- ◆ PEP02 (nanoparticle liposome irinotecan) has favorable PK profiles over free irinotecan, with enhanced permeability retention (EPR) effect in tumors.
- ◆ PEP02 shows impressive therapeutic effects against subcutaneous or orthotopic xenograft models of human lung SCC and SCLC in athymic nude mice and nude rats, with minimal side effects.
- ◆ Re-growth of tumors can be inhibited by repeated treatments with PEP02.
- ◆ Preclinical studies support clinical evaluation of PEP02/MM-398 for the treatment of human lung cancers.

far Beyond The Ordinary



UNIVERSITY OF COLORADO  
CANCER CENTER

UNIVERSITY OF COLORADO  
HOSPITAL

UNIVERSITY OF COLORADO  
HEALTH SCIENCES CENTER

## MM398 for Small Cell Lung Cancer

Paul A. Bunn, Jr, MD, Dudley Professor, Univ. of Colorado Cancer Center,  
Aurora, CO, USA



Consultant: Amgen, Allos, AstraZeneca, Abraxis, Bayer, Biodesix, Boehringer-  
Ingelheim, Bristol-Myers Squibb, Daiichi-Sankyo, Eli Lilly, GlaxoSmithKline,  
Merck, Novartis, OSI/Genentech/Roche, Poniard, Sanofi Aventis

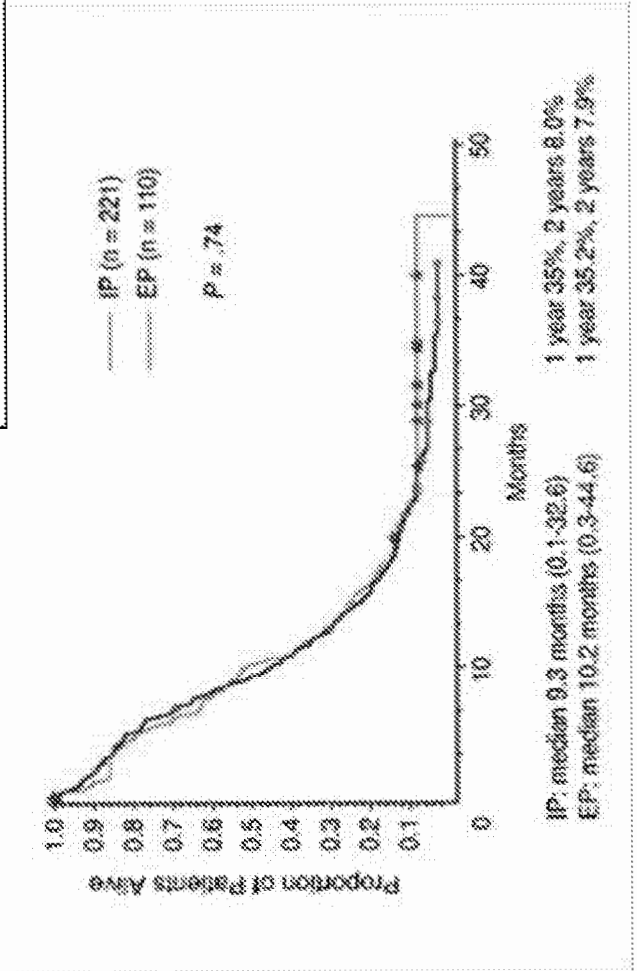
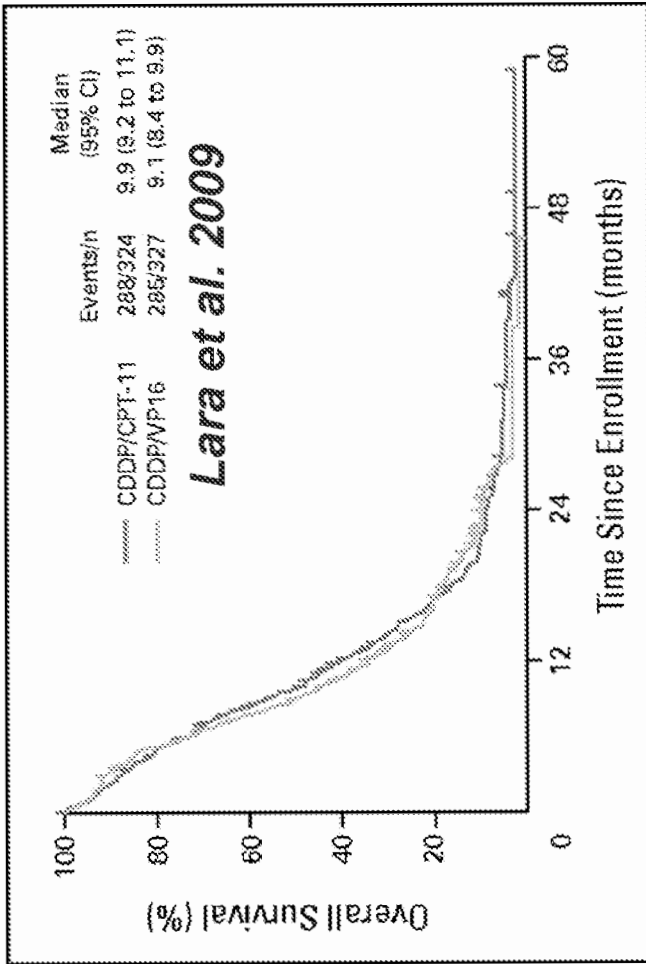
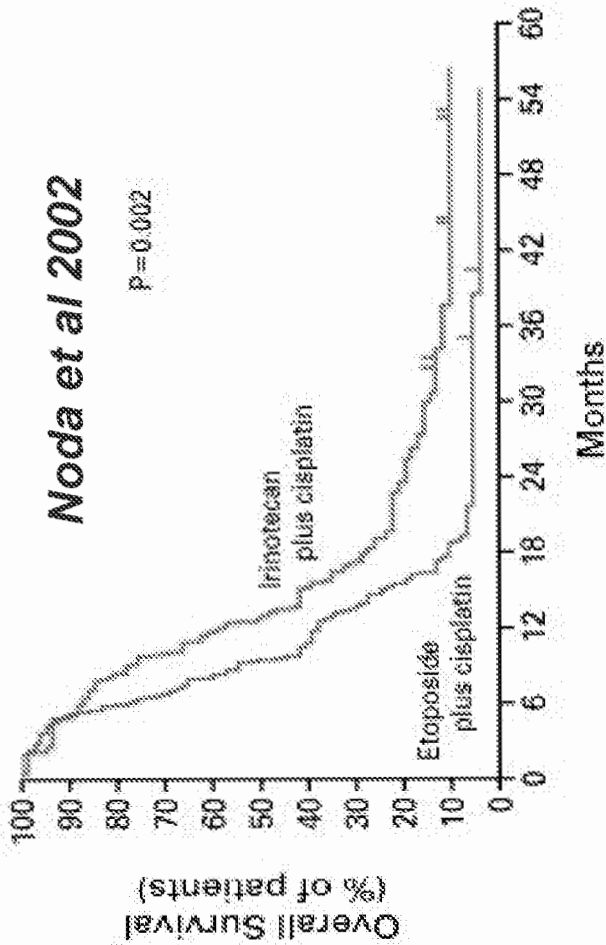
PEP02 (liposome irinotecan) effectively inhibits human squamous cell carcinoma and small cell lung cancers in subcutaneous and orthotopic xenograft tumor models

Daniel C. Chan\*, Zhiyong Zhang, Paul A. Bunn, Jr.,  
and C. Grace Yeh

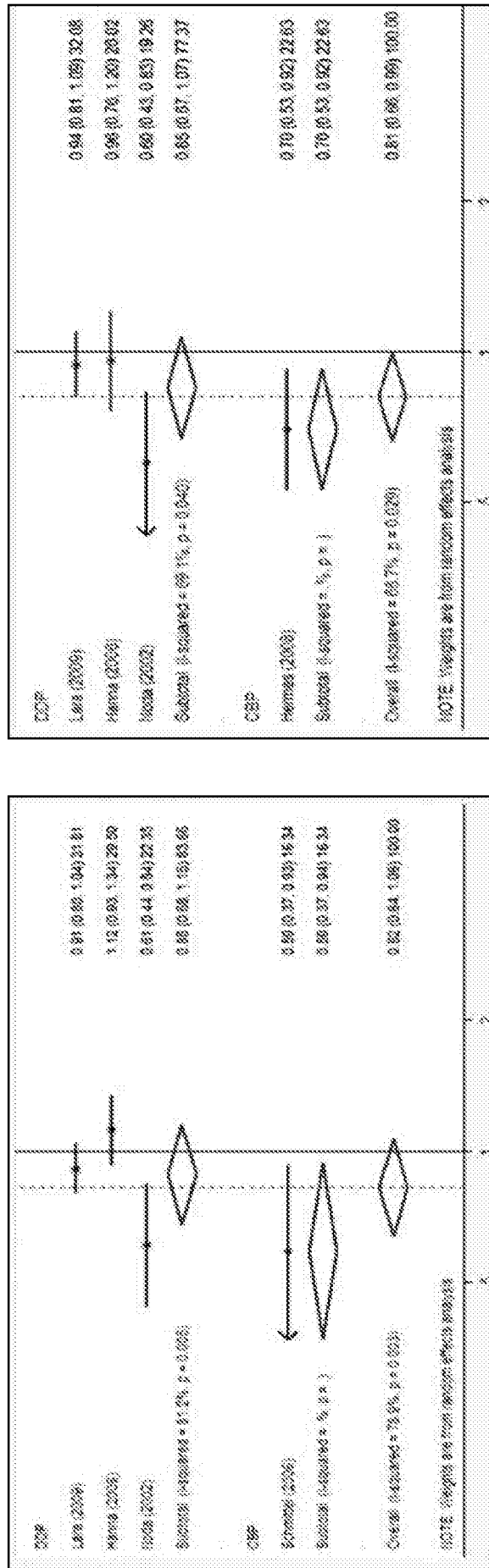
University of Colorado, Denver, CO, USA, and  
PharmaEngine, Inc., Taipei, Taiwan

This project was supported by a grant from PharmaEngine to DC, the presenting author.  
PEP02 is designated as MM-398 by Merrimack Pharmaceuticals, Inc.

# Irinotecan vs Etoposide & Cisplatin:ED SCLC



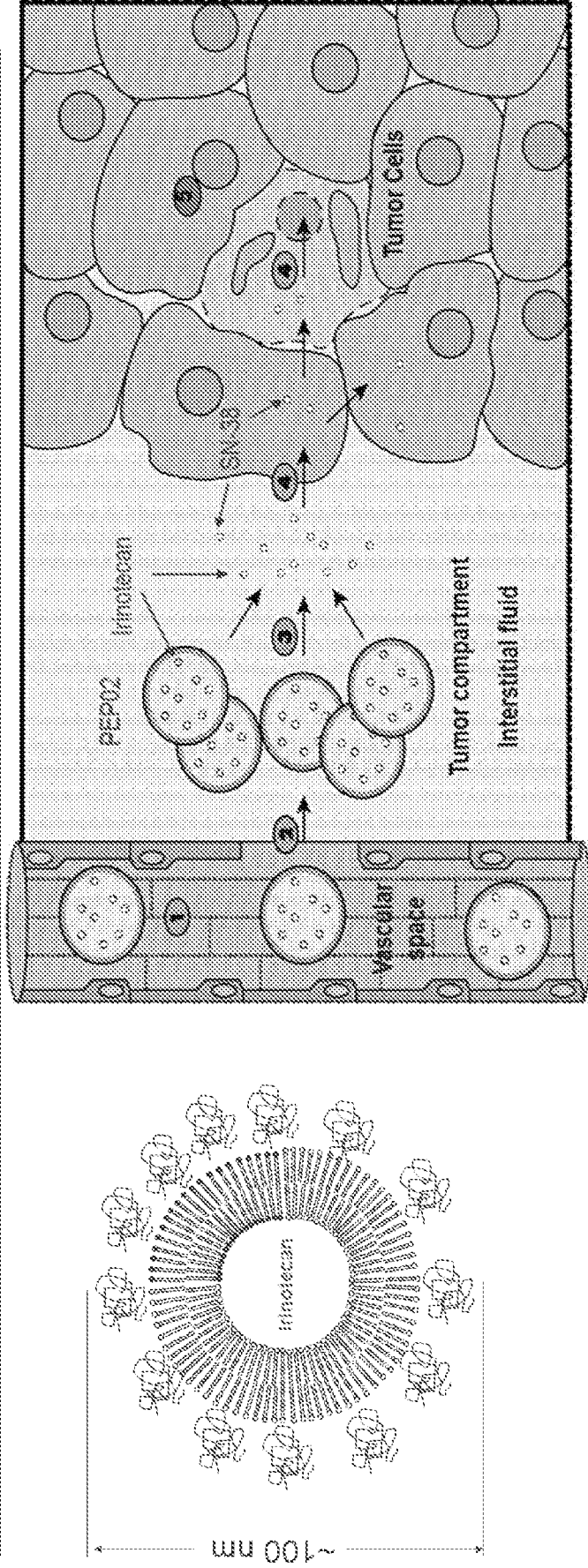
# Meta analysis EP vs IP



Study or Subgroup	Events	Total	Events	Total	O-E	Variance	Weight	Hazard Ratio	Exp(0-EI)/I, fixed, 95% CI
<b>1.1.1 Topotecan versus Etoposide</b>									
Evans 2006	303	369	230	395	7.3	149.62	21.7%	1.05 [0.69, 1.23]	1.05 [0.69, 1.23]
Hogener 2008	290	266	298	324	-10.03	140.22	21.3%	0.93 [0.79, 1.10]	0.93 [0.79, 1.10]
<b>Total events</b>	593	715	589	729					
<b>Heterogeneity:</b>	Chi <sup>2</sup> = 1.05, df = 1 (P = 0.31); I <sup>2</sup> = 5%								
<b>Test for overall effect:</b>	Z = 0.16 (P = 0.87)								
<b>1.1.2 Irinotecan versus Etoposide</b>									
Hanna 2004	101	105	101	104	-16.38	47.88	7.8%	0.71 [0.51, 0.94]	0.71 [0.51, 0.94]
Lava 2009	286	324	286	324	-10.03	147.23	21.4%	0.93 [0.79, 1.09]	0.93 [0.79, 1.09]
Koda 2003	58	77	65	77	-18.15	35.53	5.6%	0.69 [0.43, 0.93]	0.69 [0.43, 0.93]
Schmid 2002	49	106	50	110	-8.23	42.13	6.7%	0.82 [0.61, 1.11]	0.82 [0.61, 1.11]
<b>Total events</b>	745	833	652	726					
<b>Heterogeneity:</b>	Chi <sup>2</sup> = 7.25, df = 4 (P = 0.12); I <sup>2</sup> = 45%								
<b>Test for overall effect:</b>	Z = 3.28 (P = 0.001)								
<b>Total (95% CI)</b>	1968	1968	1497	1497			100.0%		
<b>Total events</b>	1344	1344	1281	1281					
<b>Heterogeneity:</b>	Chi <sup>2</sup> = 13.73, df = 6 (P = 0.26); I <sup>2</sup> = 53%								
<b>Test for overall effect:</b>	Z = 2.52 (P = 0.01)								
<b>Test for subgroup differences:</b>	Chi <sup>2</sup> = 4.44, df = 1 (P = 0.04), I <sup>2</sup> = 77.5%								

Journal of Thoracic Oncology. 5(12):1986-1993, 2010.

# PEP02/MM-398 (Liposome Irinotecan)



Irinotecan is encapsulated in PEG-liposomes (PEP02/MM-398)

Improved PK profile over free irinotecan in preclinical and clinical studies

Enhanced permeability retention (EPR) effect - with the diameters adjusted at about 100 nm penetrating easily around tumor tissues

Macrophages in tumors aid in converting CPT-11 to SN-38 to reach hypoxic tumor microenvironment



# Tumor Uptake of CPT-11 & SN-38

---

## Tumor Uptake of Free Irinotecan and PEP02 in a Bioluminescent Orthotopic Human Pancreas Cancer Xenograft Model in Nude

### Mice\*

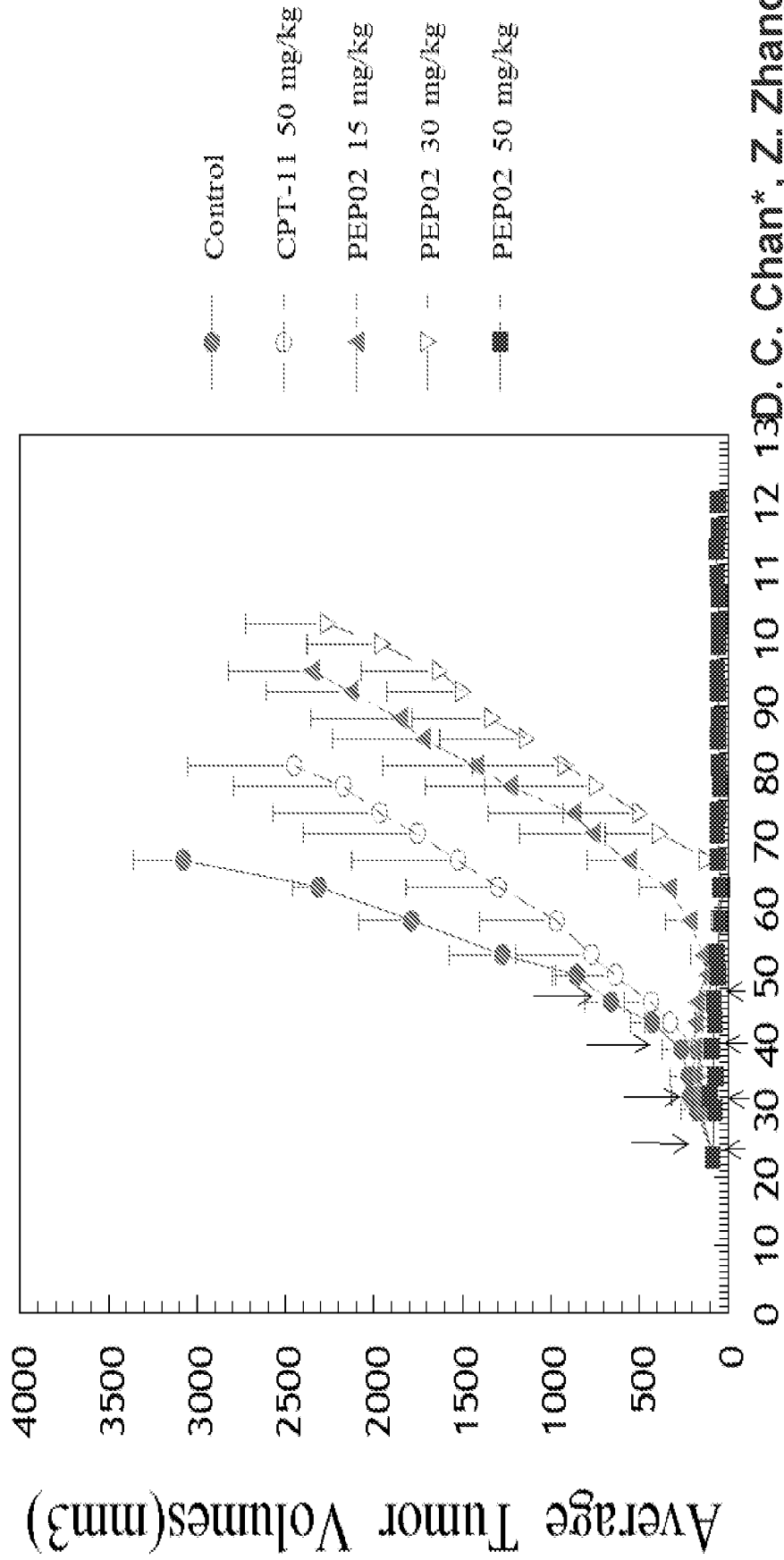
Mice with tumors were given a single i.v. injection of free CPT-11 or PEP02 at a dose of 20 mg CPT-11/kg.

	CPT-11 ( $\mu\text{g/g}$ tumor)	SN-38 ( $\mu\text{g/g}$ tumor)
Free CPT-11 (24 h)	$0.043 \pm 0.11$	$0.019 \pm 0.011$
PEP02 (24 h)	$6.1 \pm 0.2$	$0.17 \pm 0.007$
PEP02 (72h)	$1.6 \pm 0.74$	$0.093 \pm 0.019$

\*Hann B. et al., 98<sup>th</sup> AACR Annual Meeting, Abstract #5648, 2007

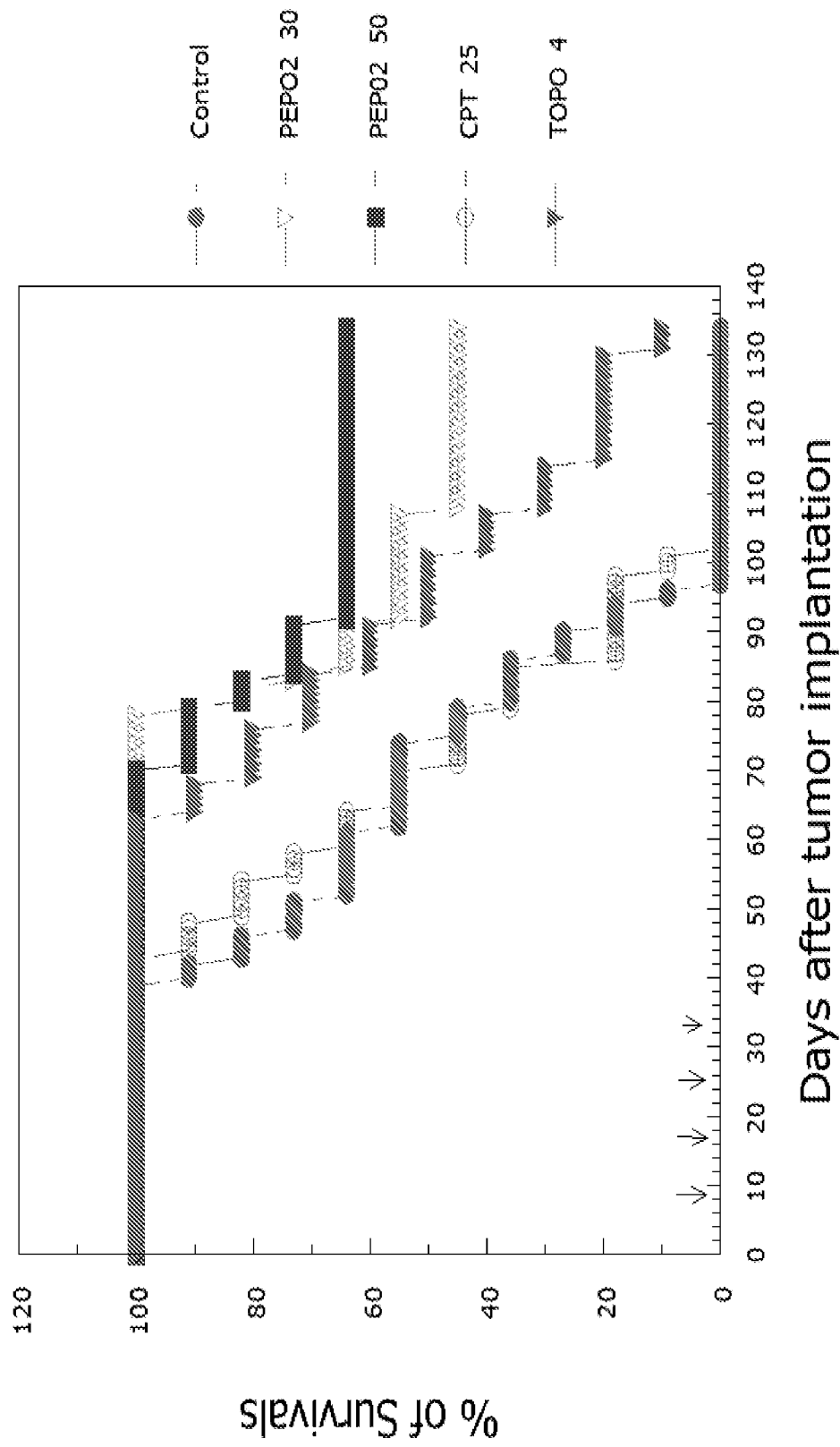


# Efficacy of PEP02/MM-398 in Human SCLC H841 Heterotopic Xenograft in Nude Mice



Days After Tumor Implantation

# Efficacy of PEP02/MM-398 in Human SCLC H841 Orthotopic Xenograft in Nude Rats



# Conclusions

---

**MM398 (PEP02) (nanoparticle liposome irinotecan) has favorable PK profiles over free irinotecan, with enhanced permeability retention (EPR) effect in tumors.**

**PEP02 shows impressive therapeutic effects against subcutaneous or orthotopic xenograft models of human SCLC in athymic nude mice and nude rats, with minimal side effects.**

**Re-growth of tumors can be inhibited by repeated treatments with PEP02.**

**Preclinical studies support clinical evaluation of PEP02/MM-398 for the treatment of human lung cancers.**

# Comparing routes of delivery for nanoliposomal irinotecan shows superior anti-tumor activity of local administration in treating intracranial glioblastoma xenografts

Pin-Yuan Chen<sup>†</sup>, Tomoko Ozawa<sup>†</sup>, Daryl C. Drummond, Ashish Kalra, Jonathan B. Fitzgerald, Dmitri B. Kirpotin, Kuo-Chen Wei, Nicholas Butowski, Michael D. Prados, Mitchel S. Berger, John R. Forsayeth, Krystof Bankiewicz, and C. David James

*Department of Neurological Surgery, University of California, San Francisco, California (P.-Y.C., T.O., N.B., M.D.P., M.S.B., J.R.F., K.B., C.D.J.); Department of Neurosurgery, Chang-Gung University and Memorial Hospital, Taoyuan, Taiwan (P.-Y.C., K.-C.W.); Graduate Institute of Clinical Medical Sciences, Chang-Gung University, Taoyuan, Taiwan (P.-Y.C.); Merrimack Pharmaceuticals, Cambridge, Massachusetts (D.D., A.K., J.B.F., D.B.K.)*

**Background.** Liposomal drug packaging is well established as an effective means for increasing drug half-life, sustaining drug activity, and increasing drug efficacy, whether administered locally or distally to the site of disease. However, information regarding the relative effectiveness of peripheral (distal) versus local administration of liposomal therapeutics is limited. This issue is of importance with respect to the treatment of central nervous system cancer, for which the blood-brain barrier presents a significant challenge in achieving sufficient drug concentration in tumors to provide treatment benefit for patients.

**Methods.** We compared the anti-tumor activity and efficacy of a nanoliposomal formulation of irinotecan when delivered peripherally by vascular route with intratumoral administration by convection-enhanced delivery (CED) for treating intracranial glioblastoma xenografts in athymic mice.

**Results.** Our results show significantly greater anti-tumor activity and survival benefit from CED of nanoliposomal irinotecan. In 2 of 3 efficacy experiments, there

were animal subjects that experienced apparent cure of tumor from local administration of therapy, as indicated by a lack of detectable intracranial tumor through bioluminescence imaging and histopathologic analysis. Results from investigating the effectiveness of combination therapy with nanoliposomal irinotecan plus radiation revealed that CED administration of irinotecan plus radiation conferred greater survival benefit than did irinotecan or radiation monotherapy and also when compared with radiation plus vascularly administered irinotecan.

**Conclusions.** Our results indicate that liposomal formulation plus direct intratumoral administration of therapeutic are important for maximizing the anti-tumor effects of irinotecan and support clinical trial evaluation of this therapeutic plus route of administration combination.

**Keywords:** convection-enhanced delivery, glioblastoma, irinotecan, liposome, xenograft.

Received September 7, 2012; accepted October 30, 2012.

<sup>†</sup>Authors contributed equally to this work.

Corresponding author: C. David James, PhD, Department of Neurological Surgery, University of California San Francisco, 1450 Third Street, Room HD-283, San Francisco, CA, 94158 (david.james@ucsf.edu).

The benefits of liposomal drug packaging have been well documented and include improved drug half-life, sustained drug activity, and increased drug efficacy. We and others have shown that liposomal formulation increases the activity of cytotoxic drugs when used in treating intracranial xenografts established

from human glioblastoma (GBM), the most common and malignant of primary brain tumors in adults, irrespective of whether the liposomal drug is administered directly into the tumor or peripherally by a vascular route.<sup>1–8</sup>

Prior studies, however, have not compared the relative efficacy of peripheral and local administration of liposomal therapeutics for treating brain tumors. Information from such comparisons would help increase understanding of the influence of the blood-brain barrier (BBB) in limiting drug access to tumors and the extent to which therapeutic benefit is affected by peripheral administration of liposomal drugs.<sup>9,10</sup> This understanding, in turn, could influence clinical trial design for testing novel therapeutics or therapeutic formulations in treating patients with brain tumors.

Although there is widespread understanding and appreciation of BBB-restricted access of therapy to intracranial tumors, this concern tends to be lessened with respect to the conduct of clinical trials by animal model studies, the results of which show activity of peripherally administered therapeutics against brain tumors. Such results, combined with the expectation of repeated administration of therapy through oral or vascular routes, to achieve comparable if not superior anti-tumor activity, relative to a single intratumoral administration of drug, have been instrumental in promoting the preferential use of peripheral administration of therapy for treating patients with brain tumor.

Convection-enhanced delivery (CED) for local administration of therapy is an alternative to vascular administration that bypasses the BBB and delivers therapeutic agents directly into the brain.<sup>11</sup> Previously, we have shown that the use of controlled pressure and a specially designed cannula are key to maximizing the distribution of CED-administered therapy in the brains of animal subjects,<sup>12,13</sup> which is a critically important issue for effective treatment of GBM, the majority of which grow in an infiltrative, disseminated manner.

Irinotecan has been extensively studied as a therapeutic agent for glioma (reviewed by Vredenburgh et al.<sup>14</sup>) based on promising *in vitro* and *in vivo* preclinical results, its BBB penetrance, and its distinct mechanism of action, as compared with other agents used in the treatment of these tumors. Clinical experience with irinotecan has been at least modestly promising, with this therapeutic showing activity both as a single agent and in combination with other modalities. However, the free drug is associated with complex pharmacologic interactions, less than ideal pharmacokinetic properties, and toxicity. Liposomal formulation improves on irinotecan's pharmacokinetics, reduces toxicity, and, if delivered locally, could be combined with other treatment approaches as an attractive addition to brain tumor therapy.<sup>3,4</sup>

In the current report, we present the results of a study in which we have conducted experiments for comparing peripheral intravascular and CED administration of nanoliposomal irinotecan for efficacy against 2 distinct orthotopic xenograft models of GBM. Our data reveal that a single administration of nanoliposomal irinotecan by CED is significantly more effective than multiple systemic intravascular

administrations of the same therapeutic and is safe for animal subjects. These results provide strong support for CED administration of nanoliposomal irinotecan in the investigational treatment of GBM.

## Materials and Methods

### *Investigational Agent*

Nanoliposomal irinotecan (MM-398) is a highly stabilized liposomal formulation containing nano-sized irinotecan crystals complexed with sucrose octasulfate in the liposome interior<sup>15</sup> and was generously provided by Merrimack Pharmaceuticals (Cambridge, MA). The preparation of nanoliposomal irinotecan, used in the experiments that follow, had a particle size of 111 nm, as determined by dynamic light scattering, and a drug-to-phospholipid (PL) ratio of 488 g irinotecan/mol PL.

### *GBM Xenografts*

Human GBM primary tissues, GBM43 and SF7796, are maintained as serially passaged subcutaneous xenografts in athymic mice.<sup>16,17</sup> Both GBM43 and SF7796 have been modified by lentiviral infection for stable expression of firefly luciferase to enable *in vivo* bioluminescence imaging, as previously described.<sup>18</sup>

To prepare tumor cells from subcutaneous xenografts for transfer to the intracranial compartment, excised subcutaneous tumors were placed in culture dishes and minced with a scalpel then mechanically dispersed by repetitive pipetting to create small cellular aggregates that were passed repeatedly through 40-micron nylon mesh filters to produce single-cell suspensions. Cell suspensions were centrifuged at a rate of 1000 rpm for 10 min at 4°C and supernatants aspirated before resuspending pellets in 1 mL of sterile DMEM media. Cells were counted and then diluted to  $1 \times 10^5$  cells/ $\mu$ L for intracranial injection.<sup>19</sup>

### *Intracranial Tumor Establishment in Athymic Mice*

Five-week-old female athymic mice (nu/nu, homozygous; Simonsen Laboratories, Gilroy, CA), housed under aseptic conditions, received intracranial tumor cell injection as previously described<sup>17</sup> and as approved by the University of California San Francisco Institutional Animal Care and Use Committee. In brief, mice were anesthetized by intraperitoneal injection of ketamine (100 mg/kg) and xylazine (10 mg/kg) and then were injected with 3  $\mu$ L of tumor cell suspension (300 000 cells total) into the right caudate putamen.

### *Bioluminescence Monitoring of Intracranial Tumor Growth*

In preparation for bioluminescence imaging (BLI), mice were anesthetized with ketamine (100 mg/kg) and xylazine (10 mg/kg), then administered 150 mg/kg of luciferin (D-luciferin potassium salt; Gold Biotechnology, St. Louis,

MO) via intraperitoneal injection. Ten minutes after luciferin injection, mice were examined for tumor bioluminescence with an IVIS Lumina imaging station (Caliper Life Sciences, Alameda, CA). Regions of interest, defined using Living Image software (Caliper Life Sciences, Alameda, CA), were recorded as photons per second per steradian per square centimeter.<sup>19</sup> Beginning at 1 week after intracranial tumor cell injection, mice were imaged twice weekly until deaths were observed in control (untreated) mice, with data from the last imaging session used to evaluate the effect of therapy on tumor growth.

#### *Vascular and Intratumoral Administration of Nanoliposomal Irinotecan*

For vascular administration of therapy,<sup>20</sup> mice were warmed for 5–10 min with either a heating pad or a heat lamp to dilate tail vasculature. Injection sites were then cleaned with an alcohol swab, after which a 28-g insulin syringe was inserted, with 50 or 100  $\mu$ L liposomal drug that had been diluted in 5 mM HEPES-buffered saline (pH, 6.5) to a concentration of 0.004 mg irinotecan per microliter, and injected with steady pressure over 5–10 s. For CED administration, our approach was similar to that previously described.<sup>21</sup> In brief, infusion cannulae were made with silica tubing (Polymicro Technologies, Phoenix, AZ) fused to a 0.1 mL syringe (Plastic One, Roanoke, VA) with a 0.5-mm stepped-tip needle that protruded from the silica guide base. Syringes were loaded with liposomal drug (0.04 mg per microliter) and attached to a microinfusion pump (Bioanalytical Systems, Lafayette, IN). The syringe with silica cannula was mounted onto a stereotactic holder then lowered through a puncture hole made in the skull<sup>19,20</sup> and to the same region in the caudate putamen at which tumor cells had been previously injected. Nanoliposomal irinotecan was infused at a rate of 1  $\mu$ L/min until a volume of 5 or 10  $\mu$ L had been delivered. Cannulae were removed 2 min after completion of infusion.

#### *Mouse Irradiation*

Mice were anesthetized via inhalation of 2.5% isoflurane with 1 L of oxygen per minute for 5 min prior to being positioned on an irradiation platform located 16.3 cm from a cesium-137 source (J. L. Shepherd & Associates, San Fernando, CA). Their eyes, respiratory tracts, and bodies were protected with lead shielding. Mice received whole brain irradiation at a dose rate of 247 cGy/min<sup>22</sup> until 1.5 Gy radiation had been administered. After irradiation, animals were monitored until recovery. For the experiment involving the analysis of combination therapy efficacy, mice were irradiated once daily for 5 consecutive days, Monday through Friday, with the first radiation treatment on day 7 following tumor cell implantation.

#### *Analysis of Irinotecan Content in Intracranial Tumors*

For the experiment involving analysis of tumor irinotecan content, athymic mice with intracranial GBM43

were administered 0.4 mg of irinotecan by tail vein or directly into the tumor mass on day 13 after implantation of tumor cells and 30 min after the fifth and final of radiation fractions that had been initiated on day 9. Mice were euthanized 24 h after nanoliposomal irinotecan administration, with brains immediately resected and tumor tissue dissected prior to snap-freezing by immersion in liquid nitrogen. Analysis of irinotecan levels in tumor tissues was as described previously.<sup>1</sup> In brief, water was added to tissues at a 20% (w/v) ratio, and tissues were then homogenized with a mechanical homogenizer in an ice bath. Homogenates were extracted for the lactone form of irinotecan with an acidic methanol solution by vortexing and centrifugation at 13 000 rpm for 10 min, with the supernatants then transferred to autosampler vials for Dionex high-pressure liquid chromatography (HPLC) analysis.

#### *Immunohistochemistry*

Resected mouse brains were fixed in 10% buffered formalin, then paraffin-embedded and sectioned for hematoxylin and eosin (H&E) staining and immunohistochemical (IHC) analysis. To determine cleaved caspase-3 reactivity, unstained sections were processed with a Ventana BenchMark XT automated system and a protocol consisting of pretreatment with 3% ethanolic hydrogen peroxide for 32 min at room temperature, epitope retrieval in Tris buffer (pH 8) for 8 min at 90°C, and incubation with primary antibody to cleaved caspase-3 (#9661, Cell Signaling Tech., Danvers, MA) at 0.2 mg/mL for 1 h at 37°C. Total and activated caspase-3–positive cells were counted in 5 high-powered fields within the tumor for each stained tissue section, with percent positive cells averaged for all fields associated with a specific treatment and subjected to statistical analysis as described below.

#### *Statistical Analysis*

PRISM 5, version 5.03 (GraphPad Software), was used to conduct all statistical analyses. For survival analysis, significance was determined by the log-rank (Mantel-Cox) test. Animals without tumor burden that died accidentally during anesthesia were excluded from the survival analysis. For all other statistical analyses, either a 2-tailed unpaired *t* test or Tukey's multiple comparison test was applied.

## Results

#### *Comparison of Intravascular Versus CED Administration of Nanoliposomal Irinotecan for Anti-Tumor Activity*

Our initial experiment for comparing intracranial GBM xenograft response to peripherally and CED administered nanoliposomal irinotecan used GBM43, which is maintained as a serially propagated subcutaneous

xenograft<sup>16,17</sup> and has been previously classified as a proneural GBM.<sup>23</sup> GBM43 cells, harvested from a disaggregated subcutaneous xenograft, produce rapidly growing intracranial tumors that have been shown to be relatively resistant to radiation therapy.<sup>24</sup>

Our experimental design included 3 CED and 2 intravascular administration treatment groups. CED administration was either once at 0.4 mg irinotecan, or twice at either 0.2 or 0.4 mg irinotecan each time. Intravascular administrations were 4 times at either 0.2 or 0.4 mg irinotecan administered each time. Thus, total irinotecan administered by CED was either 0.4 or 0.8 mg irinotecan, whereas total irinotecan administered by intravascular injection was either 0.8 or 1.6 mg. CED administrations were on day 5 only or on days 5 and 8, and intravascular administrations were on days 5, 8, 12, and 15 after tumor cell implantation. BLI of luciferase-modified GBM43 tumors showed an anti-tumor effect from irinotecan administration, regardless of amount or route of administration (Fig. 1A) and significantly ( $P < .05$ ) or near significantly greater anti-tumor effect of direct over intravascular administration, irrespective of the amounts of administered irinotecan being compared ( $P$  values for all 2-way comparisons shown in Table 1).

Survival analysis from these treatments showed that all irinotecan treatment groups experienced significant survival benefit relative to control (Fig. 1B). Of importance, comparisons of all CED and intravascular administration groups showed significantly greater benefit from direct administration of therapy, even when the

total amount of irinotecan administered by the vascular route was 4 times greater than that delivered directly into the tumor. More striking was the difference in number of mice that experienced apparent cure of tumor from CED of nanoliposomal irinotecan (6 of 7 in the group receiving 0.8 mg irinotecan, and a total of 4 of 18 in the 2 groups receiving 0.4 mg irinotecan), as indicated by a lack of detectable bioluminescence signal in mice at time of euthanasia. Serial sectioning of entire brains from 2 of the mice receiving CED administration of nanoliposomal irinotecan and showing lack of detectable bioluminescence at time of euthanasia revealed no detectable tumor on histopathologic analysis of H&E-stained tissues. None of the mice receiving intravascular administration of nanoliposomal irinotecan experienced cure of tumor.

Body weight monitoring of mice receiving vascular and CED of nanoliposomal irinotecan showed similar patterns of weight loss, irrespective of route of delivery (Fig. 1), with no animal losing >13% initial weight from treatment. All animals receiving liposomal therapy rapidly gained weight on completion of treatment and achieved weights comparable to or exceeding that of untreated control group mice prior to onset of symptoms indicative of tumor burden in control group mice, suggesting that administration of nanoliposomal irinotecan by either route of administration is without extended adverse effect and is well tolerated.

To investigate whether these results might prove to be generalizable to additional subtypes of GBM, we performed a second experiment with 5F7796, which was

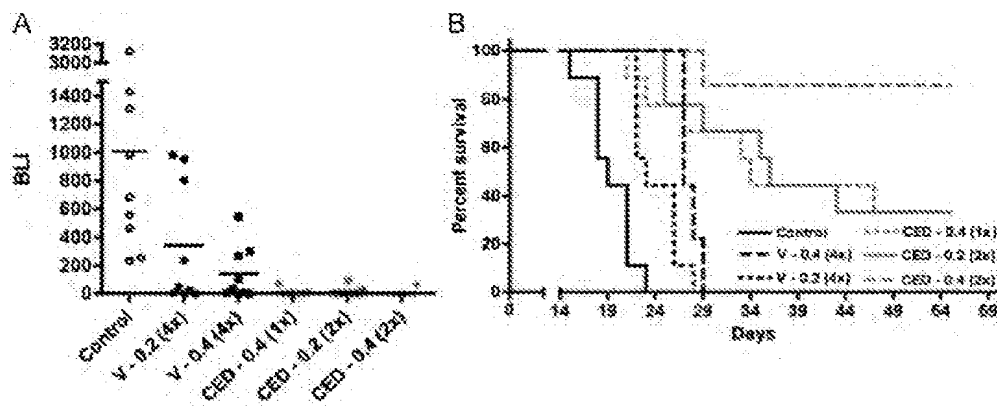


Fig. 1. Comparison of intravascular vs CED administration of nanoliposomal irinotecan for anti-tumor activity against intracranial GBM43 and corresponding survival benefit for animal subjects. (A) Treatment group day 15 normalized bioluminescence<sup>18</sup> (BLI) distributions (last imaging day in which all control group mice were alive). Route of administration identifiers: V, vascular administration; CED, convection enhanced delivery. Numbers following route of administration identifiers represent mg quantity of irinotecan administered with each dose; numbers in parentheses represent the number of administrations. Direct administrations were on day 5 or on days 5 and 8, and vascular administrations were on days 5, 8, 12, and 15. Student's *t*-test values for all 2-way comparisons are listed in Table 1s. (B) Corresponding survival plots for each treatment group. Log rank *P* values for all 2-way comparisons are listed in Table 2 and show that the survival benefit for mice receiving 2 CED administrations of 0.4 mg irinotecan was significantly greater ( $P < .05$ ) than for any other treatment. Mice surviving at day 60, all of which had no detectable tumor by bioluminescence imaging, were euthanized, with analysis of serial H&E-stained sections of entire brains from 2 of these mice showing no detectable tumor. Control group mice in this experiment were untreated, which were established as valid for comparison by determining, in a separate experiment, that CED of vehicle caused no adverse or beneficial effect on animal survival relative to no treatment (Supplementary Figure 2). Number of mice included in the survival analysis for each treatment group (see Materials and Methods): Control = 9; CED 0.2 (2x) = 9; CED 0.4 (1x) = 9; CED 0.4 (2x) = 7; V 0.2 (4x) = 9; and V 0.4 (4x) = 9.

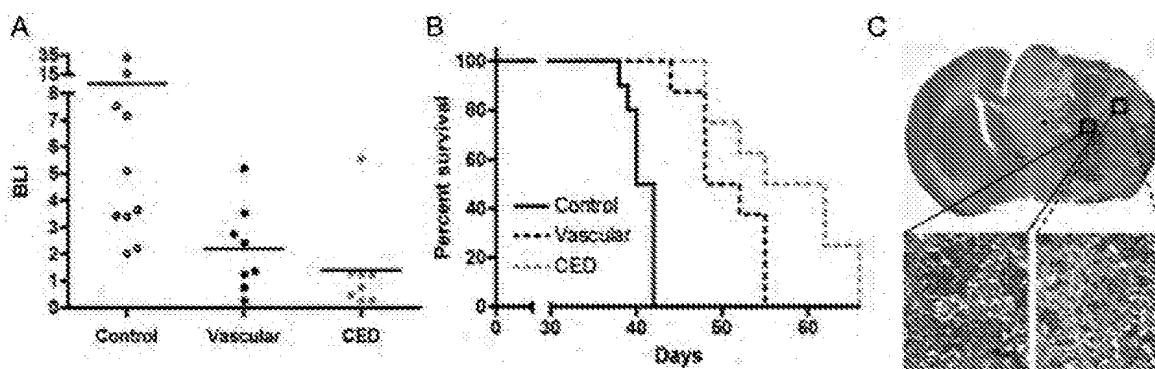


Fig. 2. Comparison of intravascular with CED administration of nanoliposomal irinotecan for anti-tumor activity and survival benefit for mice with intracranial SF7796. (A) Treatment group day 35 bioluminescence distributions (last imaging day for which all control group mice were alive). Mice receiving vascular administration received 0.4 mg doses of irinotecan on days 20 and 24 (0.8 mg total dose), whereas mice receiving CED administration were treated just once with 0.4 mg irinotecan on day 20 after tumor cell implantation. Student's *t*-test values for 2-way comparisons: 0.092 for control vs vascular; 0.061 for control vs CED; and 0.359 for vascular vs CED. (B) Corresponding survival plots for each treatment group. Log rank *P* values for 2-way comparisons: <0.001 for control vs vascular; <0.001 for control vs CED; and 0.048 for vascular vs CED. Number of mice included in the survival analysis for each treatment group: Control = 10; Vascular = 8; CED = 8. (C) 1.25x (upper) and 40x (lower) magnifications of an H&E-stained coronal section from the brain of a control group mouse that was euthanized on day 39 because of symptoms from increasing tumor burden. Lower left panel: high cellularity at the tumor core. Lower right panel: disseminated tumor cells at the tumor periphery.

established and has been maintained as a subcutaneous xenograft after initial implantation of a surgical specimen from a patient whose tumor had regrown after standard-of-care therapy (radiation + temozolomide<sup>25</sup>), which was followed by treatment of the recurrent tumor with bevacizumab<sup>26</sup> prior to second surgery. This GBM xenograft has been classified as mesenchymal using the classification scheme described by Verhaak et al.<sup>25</sup> For assessing SF7796 response to nanoliposomal therapy, we compared the anti-tumor effect and survival benefit of 0.4 mg irinotecan administered once by CED (day 20 after implantation) with 0.8 mg administered by intravascular route (0.4 mg administered twice: days 20 and 24). As for the previous experiment with GBM43, the results for SF7796 showed irinotecan anti-tumor activity by BLI (Fig. 2A) and significant survival benefit from treatment, irrespective of whether administered directly or intravascularly (Fig. 2B). SF7796 tumor cells produce a diffusely infiltrative intracranial tumor (Fig. 2C), and it is likely that this diffusely infiltrative nature, combined with the later time of treatment initiation for this experiment (day 20 vs day 5 for the initial experiment with GBM43), resulted in none of the mice with intracranial SF7796 experiencing cure of tumor from treatment. However, as before with the GBM43 model (Fig. 1), the survival benefit from one CED treatment was significantly greater than that resulting from multiple (2) intravascular administrations of liposomal irinotecan ( $P = .048$ ).

#### Effect of Radiation when Combined with Intravascular or Intratumoral Nanoliposomal Irinotecan Therapy

The design for the prior 2 experiments (Figs. 1 and 2) is consistent with that which might be used in a clinical

study for treating recurrent GBM and for which investigational therapies are often evaluated in isolation from co-treatment with other therapeutics and/or treatment modalities. To evaluate the activity of nanoliposomal irinotecan in a context consistent with a clinical trial for treating newly diagnosed GBM, we compared the anti-tumor activity of CED with intravascular administration of nanoliposomal irinotecan when used in combination with radiation therapy (RT). For this experiment, radiation was administered at 1.5 Gy/day  $\times$  5 (7.5 Gy total) beginning day 7 after implantation of GBM43 cells, with irinotecan administered once by CED (0.4 mg on day 7) or twice by the vascular route (0.4 mg on days 7 and 11). As with the previous GBM43 experiment (Fig. 1), CED of irinotecan outperformed intravascular administration, even though twice as much irinotecan was administered by the vascular route (Figs. 3A and B;  $P = .035$  for survival benefit comparison). RT, which as a monotherapy, provided modest, albeit statistically significant, survival benefit to mice with intracranial GBM43 (Fig. 3B;  $P = .011$  for RT vs control), further increased the anti-tumor effect and survival benefit from nanoliposomal irinotecan, with direct administration of irinotecan + RT providing the most extensive survival benefit of any treatment (Fig. 3B) and resulting in half (5 of 10) of the treatment group mice experiencing apparent cure of tumor. As for previous experiments, therapeutic regimens were well tolerated, with no animal subject experiencing >10% loss of pre-treatment body weight at completion of therapy (data not shown).

For this latter experiment, untreated mice were included for euthanasia at day 7 to obtain samples providing indication of extent of intracranial tumor at time of treatment initiation (Fig. 4A) and at day 12 for all treatment groups (Figs. 4B–F) to allow qualitative



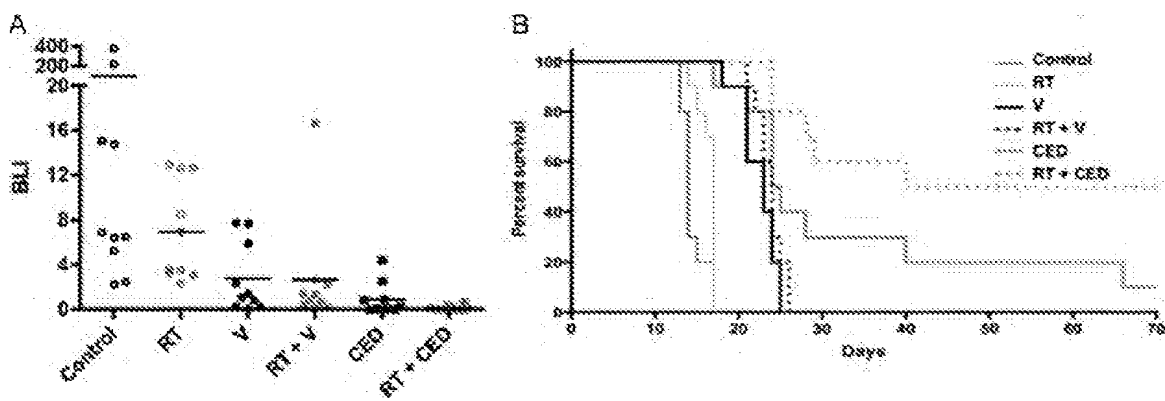


Fig. 3. Effect of radiation when combined with intravascular or CED administration of nanoliposomal irinotecan therapy. Radiation treatment for this experiment was 1.5 Gy/day  $\times$  5, beginning day 7 and ending day 11, for a total radiation dose of 7.5 Gy. Nanoliposomal irinotecan administration was 0.4 mg on day 7 for CED administration and was 0.4 mg on days 7 and 11 for intravascular administration. (A) Treatment group day 10 bioluminescence distributions (last imaging day at which all control group mice were alive). See Table 3 for all 2-way comparisons using the Student's *t*-test. (B) Corresponding survival plots for all treatment groups. Log rank *P* values for all 2-way comparisons are listed in Table 4 and show that CED administration of irinotecan as a monotherapy was significantly better than intravascular and RT monotherapies and that RT + CED of irinotecan was significantly better than all other therapies, including irinotecan monotherapy via CED. The experiment was terminated at 70 days, at which time there was no detectable bioluminescence signal in surviving mice. Ten mice included in the survival analysis for all treatment groups.

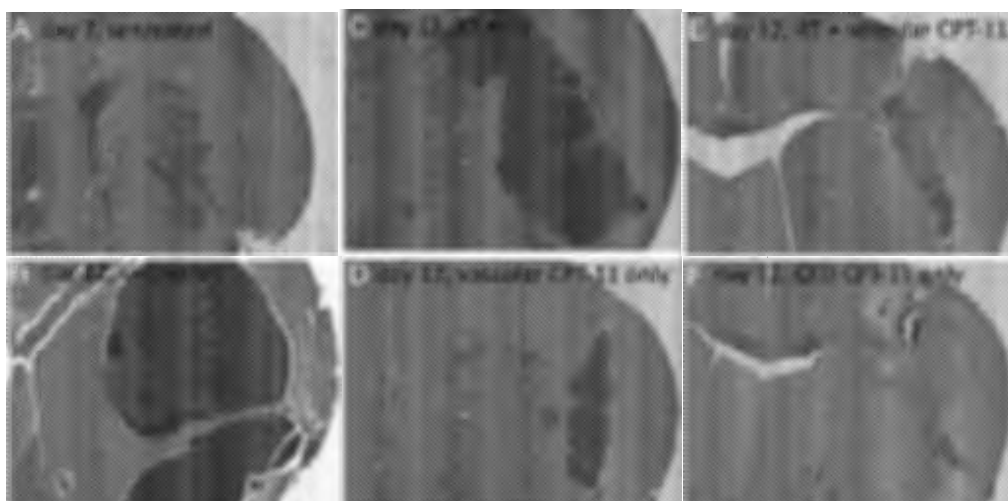


Fig. 4. H&E-stained coronal sections (2.5 $\times$  magnification) from the brain of an untreated mouse that was euthanized on the first day of therapy (A) and from the brains of mice that were euthanized from each treatment group one day after the last day of therapy (day 12: panels B-F). H&E-stained sections from the brain of a mouse receiving RT + CED administration of nanoliposomal irinotecan (not shown) appeared to be similar to those of the mouse receiving local administration of liposomal therapy only (F) and showed a lack of identifiable tumor from combination therapy at day 12 after tumor cell implantation.

comparison of relative tumor size among treatment groups and quantitative IHC analysis of activated caspase 3 staining for assessing the pro-apoptotic effect of different treatments at 1 day after completion of therapy (Fig. 5). Inspection of H&E-stained tissues for sections with the largest tumor areas showed reasonable consistency between treatment effect on amount of H&E-stained tumor at time of completing therapy (Figs. 4B-F) and eventual treatment group survival (Fig. 3B). This was also the case for the activated caspase 3 IHC analysis, which showed the most extensive apoptotic response in mice receiving direct administration of nanoliposomal irinotecan + radiation therapy

(Fig. 5;  $P < .05$  for CED + RT vs any other treatment group; Student's *t* test results for all Fig. 5G; 2-way comparisons are shown in supplementary Table 5).

#### *Analysis of Irinotecan Content in Intracranial Xenografts*

To obtain information addressing whether radiation alters access of peripherally administered nanoliposomal irinotecan to intracranial tumor or, alternatively, alters retention of irinotecan when therapy is administered locally, additional mice received intracranial

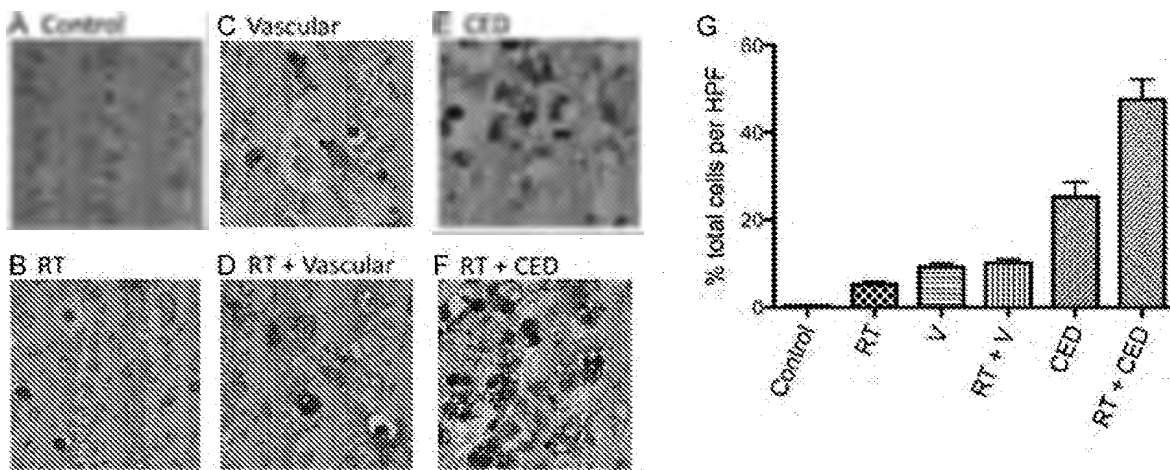


Fig. 5. (A–F) Examples of activated caspase 3 staining of tumors in the brains of mice from each of the treatment groups described in Fig. 3. Specimens were obtained from mice that were euthanized on the day after final treatments (day 12). (G) Histogram plot showing average values for percent positive cells from 5 high-powered fields examined in the brains of each of 3 mice from each treatment group: results are therefore based on a total of 15 high-powered fields per treatment group. Student's *t* test comparison of these values showed that radiation + CED administration of nanoliposomal irinotecan was significantly more effective in inducing apoptotic response, relative to all other treatment groups ( $P < .05$ ).

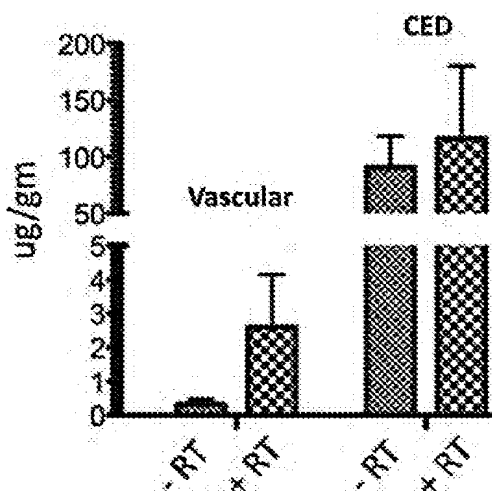


Fig. 6. Analysis of irinotecan content in intracranial GBM43 xenograft tumors 24 h after either vascular or CED administration of 0.4 mg nanoliposomal irinotecan and either in the presence or absence of radiation, with the last of 5 radiation treatments administered 30 min prior to the single irinotecan administration at day 13 subsequent to tumor cell implantation. The results show that RT does not cause a significant difference in tumor irinotecan, whether administered directly or by vascular route, but do show a significantly higher amount of irinotecan content in tumors receiving direct administration of therapy ( $P < .05$ ). Analyzable samples were 2–4 for each treatment group.

implantation of GBM43, with tumors allowed to grow until day 9, at which time mice began receiving daily radiation for 5 consecutive days (1.5 Gy/day, 7.5 Gy total), with 0.4 mg nanoliposomal irinotecan administered either by CED or by a vascular route on day 13, the last day of radiation treatment. Twenty-four hours later, the mice were euthanized and tumor was dissected

from surrounding normal brain of the euthanized mice, with dissected tumors subsequently examined for irinotecan content. The results of this analysis showed no significant difference in irinotecan content in tumors as a result of mice receiving pretreatment with radiation, although for mice receiving vascular administration of therapy, the mean value for tumor irinotecan was substantially higher in the group receiving radiation (Fig. 6). Not surprisingly, intratumoral irinotecan was substantially and significantly higher in mice receiving CED administration of liposomal therapy, irrespective of radiation pretreatment: 302-fold greater when comparing direct vs vascular administration in nonirradiated mice and 45-fold greater when comparing irinotecan content in mice from irradiated groups.

## Discussion

In the current report, we have presented results addressing the relative activity and efficacy of intravascular and CED administration of nanoliposomal irinotecan in treating mice with orthotopic GBM xenografts. To the best of our knowledge, there are no previously published reports involving a route of administration comparison for liposomal therapy in treating an experimental animal model of GBM. Although our study is not exhaustive with respect to potential experimental variations, we feel that there is sufficient consistency of results for the variables tested in 2 distinct intracranial xenograft models to support the interpretation of CED administration of irinotecan nanoliposomes as being the more effective administration for maximizing anti-tumor effect of this therapy. Our cumulative experience in this area of research indicates that it is the combined effects of nanoliposomal packaging for extending the biologic half-life of active drug<sup>1–5</sup> and

bypassing the limiting influence of the BBB through direct intratumoral administration of therapy<sup>1-4</sup> that are important for maximizing the anti-tumor effect of cytotoxic chemotherapy.

Our interpretation of these results is not at odds with clinical trial designs that use intravascular administration of liposomal therapy to treat GBM, which is an approach that, according to our results, could well provide benefit to patients with brain tumors. Our results do, however, support a clinical trial design in which nanoliposomal irinotecan is administered locally.

The advantage of CED is multifactorial. The combination of cannulae that minimize reflux<sup>21</sup> and the liposomal formulation of irinotecan allows for more robust and uniform distribution of the therapeutic. Catheter placement into an intact tumor, confirmed by neuro-navigational methods with direct imaging assessment of catheter position and subsequent convective infusion of the liposome using real-time imaging,<sup>13</sup> would be the optimal strategy for initial clinical studies of this agent. This clinical setting would eliminate the risk of drug reflux back into a surgical cavity seen when using CED strategies at the time of surgical resection and minimize the risk of improper placement of catheters, often seen after expected changes in the geometry of the cavity hours to days after resection.

The increased efficacy of CED administration of therapy is consistent with the substantial disparity in irinotecan content of xenograft tumors removed 24 h after treatment of animal subjects with equivalent vascular and intratumoral amounts of liposomal drug (Fig. 6). In a previous study, we showed that CED of nanoliposomal irinotecan sustains higher intracranial levels of irinotecan, relative to intracranial administration of free irinotecan, and that CED administration of nanoliposomal irinotecan outperforms direct intratumoral administration of equivalent-free irinotecan.<sup>1</sup> Thus, liposomal formulation is important to maximizing anti-tumor activity and, potentially, clinical benefit from CED administration of irinotecan.

For the present study, it is noteworthy that the nanoliposomal irinotecan preparation used for direct intracranial administration was the same as that used for intravascular administration, and this formulation was developed for intravascular administration of therapy. Thus, it is conceivable that alternative nanoliposomal irinotecan formulations may further improve on the intracranial distribution and efficacy of CED administration of nanoliposomal irinotecan. Despite the use of vascular-optimized nanoliposomal irinotecan, our results suggest the diffusion of locally administered liposomal therapy to an extent that is effective in eradicating, at least in some instances, tumor that occupies a substantial portion of total brain (Figs. 4A and F). Because mice experiencing apparent cure of intracranial tumor (Figs. 1 and 3) were treated with 5–10  $\mu$ L of liposomal therapy, our results support the concept that this therapeutic approach involving local administration of

therapy is sufficiently scalable to anticipate efficacy against brain tumor in patients with GBM.

In addition to the superior efficacy of local administration of nanoliposomal irinotecan, it is important to emphasize the apparent safety of direct intracranial administration of therapy, as indicated by body weight monitoring of treated mice (Fig. 1), and lack of an indication of neurologic deficit (e.g., ambulation, activity, and seizure) from CED of liposomal therapy. Future pre-clinical studies will focus on dose escalation experiments to identify maximum tolerable amounts of nanoliposomal irinotecan that can be administered directly into brain and the optimization of convection-enhanced delivery approaches for sustained CED administration of nanoliposomal irinotecan.

Finally, our results show that CED administration of nanoliposomal irinotecan can be used with radiation therapy for further improvement of anti-tumor effect and survival benefit, relative to either monotherapy, and thereby support the potential use of direct administration of liposomal therapy with subsequent standard-of-care therapy for treating GBM: RT + temozolomide.<sup>25</sup> With irinotecan being administered locally, one would anticipate a lack of adverse effects associated with the peripheral administration of 2 cytotoxic therapies and that local administration of nanoliposomal irinotecan could be used safely with conventional treatment for newly diagnosed GBM. Thus, our results support the clinical trial evaluation of direct intratumoral administration of nanoliposomal irinotecan, both as a single agent in the treatment of recurrent GBM and as part of a combination therapy for patients with newly diagnosed GBM.

## Supplementary Material

Supplementary material is available online at Neuro-Oncology (<http://neuro-oncology.oxfordjournals.org/>).

## Funding

This study was supported by National Cancer Institute (grant CA097257 to T. O., M. D. P., M. S. B., K. B., C. D. J.).

## Acknowledgments

We thank Raquel Santos, Edgar Lopez-Lepe, Jacqueline De La Torre, and Christina Ng for their expert technical assistance.

*Conflict of interest statement.* D. C. D., A. K., J. B. F., and D. B. K. are employees of Merrimack Pharmaceuticals, the supplier of the therapeutic investigated in the study reported herein. All other authors declare no conflict of interest.

## References

- Noble CO, Krauze MT, Drummond DC, et al. Novel nanoliposomal CPT-11 infused by convection-enhanced delivery in intracranial tumors: pharmacology and efficacy. *Cancer Res.* 2006;66:2801–2806.
- Saito R, Krauze MT, Noble CO, et al. Convection-enhanced delivery of LS-TPT enables an effective, continuous, low-dose chemotherapy against malignant glioma xenograft model. *Neuro Oncol.* 2006;8:205–214.
- Yamashita Y, Krauze MT, Kawaguchi T, et al. Convection-enhanced delivery of a topoisomerase I inhibitor (nanoliposomal topotecan) and a topoisomerase II inhibitor (pegylated liposomal doxorubicin) in intracranial brain tumor xenografts. *Neuro Oncol.* 2007;9:20–28.
- Krauze MT, Noble CO, Kawaguchi T, et al. Convection-enhanced delivery of nanoliposomal CPT-11 (irinotecan) and Pegylated liposomal doxorubicin (Doxil) in rodent intracranial brain tumor xenografts. *Neuro Oncol.* 2007;9:393–403.
- Serwer LP, Noble CO, Michaud K, et al. Investigation of intravenous delivery of nanoliposomal topotecan for activity against orthotopic glioblastoma xenografts. *Neuro Oncol.* 2011;13:1288–1295.
- Riondel J, Jacrot M, Fessi H, et al. Effects of free and liposome-encapsulated taxol on two brain tumors xenografted into nude mice. *In Vivo.* 1992;6:23–27.
- Sharma US, Sharma A, Chau RI, Straubinger RM. Liposome-mediated therapy of intracranial brain tumors in a rat model. *Pharm Res.* 1997;14:992–998.
- Grahn AY, Bankiewicz KS, Dugich-Djordjevic M, et al. Non-PEGylated liposomes for convection-enhanced delivery of topotecan and gadodiamide in malignant glioma: initial experience. *J Neurooncol.* 2009;95:185–197.
- Serwer LP, James CD. Challenges in drug delivery to tumors of the central nervous system: an overview of pharmacological and surgical considerations. *Adv Drug Deliv Rev.* 2012;64:590–597.
- de Vries NA, Beijnen JH, Boogerd W, van Tellingen O. Blood-brain barrier and chemotherapeutic treatment of brain tumors. *Expert Rev Neurother.* 2006;6:1199–1209.
- Bobo RH, Laske DW, Akbasak A, et al. Convection-enhanced delivery of macromolecules in the brain. *Proc Natl Acad Sci USA.* 1994;91:2076–2080.
- Mamot C, Nguyen JB, Pourdehnad M, et al. Extensive distribution of liposomes in rodent brains and brain tumors following convection-enhanced delivery. *J Neurooncol.* 2004;68:1–9.
- Dickinson PJ, LeCouteur RA, Higgins RJ, et al. Canine model of convection-enhanced delivery of liposomes containing CPT-11 monitored with real-time magnetic resonance imaging: laboratory investigation. *J Neurosurg.* 2008;108:989–996.
- Vredenburgh JJ, Desjardins A, Reardon DA, Friedman HS. Experience with irinotecan for the treatment of malignant glioma. *Neuro-Oncol.* 2009;12:80–91.
- Drummond DC, Noble CO, Guo Z, et al. Development of a highly active nanoliposomal irinotecan using a novel intraliposomal stabilization strategy. *Cancer Res.* 2006;66:3271–3277.
- Pandita A, Aldape KD, Zadeh G, Guha A, James CD. Contrasting in Vivo and in Vitro Fates of glioblastoma cell subpopulations with amplified EGFR. *Genes Chromosomes Cancer.* 2004;39:29–36.
- Giannini C, Sarkaria JN, Saito A, et al. Patient Tumor EGFR and PDGFRA Gene Amplifications Retained in an Invasive Intracranial Xenograft Model of GBM. *Neuro-Oncol.* 2005;7:164–176.
- Dinca EB, Sarkaria JN, Schroeder MA, et al. Bioluminescence Monitoring of Intracranial Glioblastoma Xenograft Response to Primary and Salvage Temozolomide Therapy. *J Neurosurg.* 2007;107:610–616.
- Ozawa T, James CD. Establishing Intracranial Brain Tumor Xenografts With Subsequent Analysis of Tumor Growth and Response to Therapy using Bioluminescence Imaging. *J Vis Exp.* 2010;41: doi:pil. 1986. 10.3791/1986.
- Serwer L, Hashizume R, Ozawa T, James CD. Systemic and Local Drug Delivery for Treating Diseases of the Central Nervous System in Rodent Models. *J Vis Exp.* 2010;42: doi:pil. 1992. 10.3791/1992.
- Yin D, Forsayeth J, Bankiewicz KS. Optimized cannula design and placement for convection-enhanced delivery in rat striatum. *J Neurosci Methods.* 2010;187:46–51.
- Ozawa T, Faddegon BA, Hu LJ, et al. Response of intracerebral human glioblastoma xenografts to multi-fraction radiation exposures. *Int J Radiat Oncol Biol Phys.* 2006;66:263–270.
- Verhaak RGW, Hoadley KA, Purdom E, et al. An integrated genomic analysis identifies clinically relevant subtypes of glioblastoma characterized by abnormalities in PDGFRA, IDH1, EGFR and NF1. *Cancer Cell.* 2010;17:98–110.
- Sarkaria JN, Carlson BL, Schroeder MA, et al. Use of an Orthotopic Xenograft Model for Assessing the Effect of EGFR Amplification on Glioblastoma Radiation Response. *Clin Cancer Res.* 2006;12:2264–2271.
- Stupp R, Mason WP, van den Bent MJ, et al. Radiotherapy plus concomitant and adjuvant temozolomide for glioblastoma. *N Engl J Med.* 2005;352:987–996.
- Chamberlain M. Bevacizumab for the treatment of recurrent glioblastoma. *Clin Med Insights Oncol.* 2011;5:117–129.

# A phase 1 trial of intravenous liposomal irinotecan in patients with recurrent high-grade glioma

Jennifer L. Clarke<sup>1,2</sup> · Annette M. Molinaro<sup>1</sup> · Juan R. Cabrera<sup>1</sup> · Ashley A. DeSilva<sup>1</sup> · Jane E. Rabbitt<sup>1</sup> · Joshua Prey<sup>3</sup> · Daryl C. Drummond<sup>4</sup> · Jaeyeon Kim<sup>4</sup> · Charles Noble<sup>4</sup> · Jonathan B. Fitzgerald<sup>4</sup> · Susan M. Chang<sup>1</sup> · Nicholas A. Butowski<sup>1</sup> · Jennie W. Taylor<sup>1,2</sup> · John W. Park<sup>5</sup> · Michael D. Prados<sup>1</sup>

Received: 12 October 2016 / Accepted: 23 November 2016 / Published online: 23 February 2017  
© Springer-Verlag Berlin Heidelberg 2017

## Abstract

**Purpose** Preclinical activity of irinotecan has been seen in glioma models, but only modest efficacy has been noted in clinical studies, perhaps related to drug distribution and/or pharmacokinetic limitations. In preclinical testing, irinotecan liposome injection (nal-IRI) results in prolongation of drug exposure and higher tissue levels of drug due to slower metabolism and the effect of enhanced permeability and retention. The objective of the current study was to assess the safety and pharmacokinetics (PK) of nal-IRI and to determine the maximum tolerated dose (MTD) in patients with recurrent high-grade glioma stratified based on UGT1A1 genotyping.

**Methods** This phase I study stratified patients with recurrent high-grade glioma into 2 groups by UGT1A1 status: homozygous WT (“WT”) vs heterozygous WT/\*28 (“HT”). Patients who were homozygous \*28 were ineligible. The

design was a standard 3+3 phase I design. WT patients were started at 120 mg/m<sup>2</sup> intravenously every 3 weeks with dose increases in 60 mg/m<sup>2</sup> increments. HT patients were started at 60 mg/m<sup>2</sup>, with dose increases in 30 mg/m<sup>2</sup> increments. The assessment period for dose-limiting toxicity was 1 cycle (21 days).

**Results** In the WT cohort ( $n=16$ ), the MTD was 120 mg/m<sup>2</sup>. In the HT cohort ( $n=18$ ), the MTD was 150 mg/m<sup>2</sup>. Dose-limiting toxicity in both cohorts included diarrhea, some with associated dehydration and/or fatigue. PK results were comparable to those seen in other PK studies of nal-IRI; UGT1A1\*28 genotype (WT vs. HT) did not affect PK parameters.

**Conclusions** Nal-IRI had no unexpected toxicities when given intravenously. Of note, UGT1A1 genotype did not correlate with toxicity or affect PK profile.

**Keywords** Glioblastoma · High-grade glioma · Chemotherapy · Irinotecan · Liposomes

✉ Jennifer L. Clarke  
clarkej@neurosurg.ucsf.edu

- <sup>1</sup> Division of Neuro-oncology, Department of Neurological Surgery, University of California, San Francisco (UCSF), 505 Parnassus Avenue M779, San Francisco, CA 94143, USA
- <sup>2</sup> Department of Neurology, University of California, San Francisco, 400 Parnassus Avenue, San Francisco, CA 94122, USA
- <sup>3</sup> Roswell Park Cancer Institute, Elm and Carlton Streets, Buffalo, NY 14263, USA
- <sup>4</sup> Merrimack Pharmaceuticals, One Kendall Square, 1 Kendall Square B7201, Cambridge, MA 02139, USA
- <sup>5</sup> Division of Hematology/Oncology, Helen Diller Family Comprehensive Cancer Center, University of California San Francisco, 1600 Divisadero St., San Francisco, CA 94115, USA

## Introduction

High-grade gliomas are the most common primary malignant brain tumor in adults; approximately 15,000 new cases are diagnosed in the US each year [1]. Despite progress made using combination therapies including surgery, radiation, and/or chemotherapy, the treatment of malignant gliomas remains problematic, and patients experience nearly universal recurrence. At the time of recurrence, effective treatment options are limited.

## Irinotecan liposome injection

Irinotecan, also known as CPT-11, is a topoisomerase I inhibitor used as an antineoplastic agent to treat colorectal, gastric, lung, cervical, and ovarian cancers; diarrhea and myelosuppression are the dose limiting toxicities. Liposomal encapsulation of chemotherapeutic agents is an approach used to improve the therapeutic ratio of antineoplastic agents; several anti-cancer drugs such as doxorubicin and vincristine have been encapsulated in liposomes, and have demonstrated therapeutic benefits over their unencapsulated counterparts. Nanoliposomal irinotecan (nal-IRI) is a proprietary liposomal formulation of irinotecan hydrochloride [2] that is approved in combination with 5-fluorouracil and leucovorin for the treatment of pancreatic cancer in patients who have previously been treated with gemcitabine.

## Preclinical development

Studies of human breast, colon, Ewing's sarcoma, and brain cancer xenograft rodent models have evaluated the efficacy of nal-IRI when administered intravenously, most using 4- or 7-day dosing regimens [3–5]. Results showed that nal-IRI enhanced anti-tumor efficacy, including inhibition of tumor growth and regression, over unencapsulated irinotecan without increasing irreversible toxicity (loss of body weight). The results of pharmacokinetic and metabolism studies in mice and rats demonstrated that encapsulation not only increased overall plasma concentrations of the parent drug (irinotecan) and its active metabolite, SN-38, but also prolonged its circulation in the blood, as well as increased and sustained exposure in tumors [2]. In glioma mouse models, nal-IRI has been tested both intravenously and with local delivery using convection-enhanced delivery (CED). Both routes of delivery demonstrated efficacy, but CED appeared particularly promising [3–6].

## Prior clinical experience

A phase 1 clinical study of nal-IRI administered every 3 weeks in patients with advanced solid tumor was conducted at 3 sites in Taiwan [7]. A total of 11 patients were recruited at 3 different dose levels (1 at 60 mg/m<sup>2</sup>, 6 at 120 mg/m<sup>2</sup>, and 4 at 180 mg/m<sup>2</sup>). The dose-limiting toxicities (DLT) that occurred in the study were grade 3 diarrhea and grade 4 leucopenia/neutropenia, and the maximum-tolerated dose (MTD) of single-agent nal-IRI found in the study was 120 mg/m<sup>2</sup>. Among the 11 patients treated, the most common types of adverse events were gastrointestinal, such as diarrhea. However, these events were mostly categorized as National Center Institute-Common Terminology Criteria for Adverse Events (NCI-CTCAE) grade 1

or 2, while most grade 3 and 4 adverse events were hematological toxicities. UGT1A1 genotyping was not prospectively performed prior to therapy for patients in that study.

Since initiation of the study we report here, plasma pharmacokinetics of nal-IRI have been compared with those of non-liposomal irinotecan in a phase 2 study of patients with gastric cancer [8]. Re-analysis of the supplementary data in this study showed that compared with irinotecan 300 mg/m<sup>2</sup> every 3 weeks ( $n=27$ ), nal-IRI 100 mg/m<sup>2</sup> every 3 weeks ( $n=37$ ) had a total irinotecan (tIRI) maximum concentration ( $C_{max}$ ) that was 13.4 times higher, a half-life ( $t_{1/2}$ ) that was 2.0 times longer, and an area under the concentration–time curve extrapolated to infinity (AUC<sub>0-∞</sub>) that was 46.2 times greater (D.C. Drummond, PhD, unpublished data). The  $t_{1/2}$  and AUC<sub>0-∞</sub> of SN-38, the active metabolite of irinotecan, were also increased relative to non-liposomal irinotecan (3.0-fold and 1.4-fold, respectively), while maintaining a 5.3-fold lower SN-38  $C_{max}$ .

Furthermore, in a separate clinical trial, nal-IRI-mediated tumor delivery of irinotecan and SN-38 were evaluated in tumor biopsies from 13 patients [9]. In this study, 70 mg/m<sup>2</sup> nal-IRI was administered and biopsies collected 72 h thereafter. The ratio of total SN-38 (tSN38) to total irinotecan (tIRI; a measure of the extent of conversion) was observed to be 8 times higher in tumor lesions than in plasma, providing evidence that the liposomal formulation of irinotecan increases delivery and conversion of irinotecan to SN-38 in the tumor.

Finally, the results of an open-label phase 3 clinical trial testing nal-IRI alone or in combination with fluorouracil and folinic acid in patients with metastatic pancreatic cancer after prior treatment with gemcitabine were recently published [10] and demonstrated improvement in overall survival for the combination, leading to FDA approval of the combination for this indication.

Of note, all nal-IRI doses in this manuscript are expressed as the irinotecan hydrochloride trihydrate salt, which was the convention at the time the study was written (120 mg/m<sup>2</sup> irinotecan trihydrate salt is equivalent to approximately 100 mg/m<sup>2</sup> irinotecan free base). Since approval in the US on October 22, 2015, per FDA guidance, the dose in the US is now expressed as the irinotecan free base. Conversion of a dose based on irinotecan salt to a dose based on irinotecan free base is accomplished by substituting the molecular weight of the salt (677.19 g/mol) with the molecular weight of the free base (586.68 g/mol), resulting in a conversion factor of 0.866.

## Pharmacogenetics of nal-IRI

It is now recognized that inherited differences in the metabolism and excretion of an agent or its metabolites can have a significant impact on toxicity and efficacy [11–13], and

this is particularly relevant for irinotecan. In humans, the ester bond of irinotecan is cleaved to form a primary pharmacologically active metabolite, SN-38, which is inactivated by the UGT enzyme system to its  $\beta$ -glucuronic acid conjugate, SN-38G. The metabolism of irinotecan is substantially influenced by a nucleotide polymorphism in the TATA-box sequences of *UGT1A1* [11–13]. This gene encodes the enzyme UGT1A1, which is responsible for the glucuronidation of SN-38. An extra (7th) repeat in 1 allele (designated UGT1A1\*28) results in an approximately 70% reduction in transcriptional activity compared with wild-type *UGT1A1*. The allelic frequency of UGT1A1 in Caucasians is approximately 45% homozygous wild-type, 45% heterozygous wild-type/\*28, and 10% homozygous \*28. Patients with either a 6/7 heterozygous or 7/7 homozygous UGT1A1\*28 have a reduced ability to metabolize SN-38, and as a result are at increased risk for significant drug-related toxicities [10–12]. However, the association between UGT1A1\*28, SN-38 concentrations, and hematologic toxicity is also dependent on the dose of irinotecan [13–15].

In the prior solid tumor phase 1 study of nal-IRI, the single patient who died from toxicity related to the agent had genotyping performed and was a heterozygote for the UGT1A1 \*28 allele [7]. As shown in the plasma concentration–time profile of SN-38 for this patient, there was prolonged elevation of the plasma concentration compared to the other patients. UGT1A1 genotyping was not performed in all patients in that study, however, so the relationship of UGT1A1 genotyping and the pharmacokinetic results remained unclear. Several years ago, UGT1A1 genotyping was made commercially available, and the available information regarding the role of UGT1A1 genotype as a predictor of toxicity of irinotecan was felt to warrant prospective evaluation and stratification in this phase 1 trial of nal-IRI.

## Materials and methods

### Study design

The primary objective of this study was to assess the safety and pharmacokinetics of nal-IRI in patients with recurrent malignant glioma stratified based on UGT1A1 genotype. The primary efficacy endpoint was 6-month progression-free survival (PFS-6). Eligibility criteria for this phase 1 clinical trial included unequivocal radiographic or pathologic confirmation of recurrent high-grade glioma (glioblastoma, gliosarcoma, anaplastic astrocytoma, anaplastic oligoastrocytoma, anaplastic oligodendroglioma, or malignant astrocytoma NOS); age  $\geq 18$ ; Karnofsky Performance Status score of  $\geq 60$ ;

adequate organ and bone marrow function; lack of other cancer, infection, or serious medical problem; and patients could not be on any enzyme-inducing drugs including enzyme-inducing anticonvulsants. There were no limits on number of prior recurrences or prior treatments aside from exclusion of patients who had previously been treated with irinotecan. Patients were stratified by UGT1A1 genotype; patients who were homozygous wild-type were enrolled in the wild-type (WT) cohort, while patients who were heterozygous wild-type/\*28 were enrolled into the heterotype (HT) cohort. Patients who were homozygous 7/7 \*28 were not eligible for study enrollment. Starting dose for the WT cohort was 120 mg/m<sup>2</sup>, the MTD from the unselected phase 1 solid tumor study. Starting dose for the HT cohort was 60 mg/m<sup>2</sup>, due to concern for potentially increased toxicity in these patients. Planned dose levels were as outlined in Table 1, with the plan to continue escalation if the MTD had not been reached at the highest dose levels.

Because the starting dose for the WT cohort was the MTD from the prior phase 1 study, enrollment was initially restricted to the WT cohort, and 6 patients were to be enrolled at dose level 0 before any dose escalation was attempted. If there were 0 or 1 DLTs in those patients, then the WT cohort could be escalated and the HT dose level 0 enrollment could begin.

Aside from the initial 6 patients enrolled within the WT cohort, the study was a standard 3+3 design. Drug was given on D1 of each 21-day cycle, for up to 12 months in the absence of progression or intolerable toxicity, and the DLT period was defined as the first 21-day cycle. The MTD was defined as the dose level at which 0 of 3 or 1 of 6 patients experienced DLT, with the next higher dose having at least 2 of 3 or 2 of 6 patients encountering DLT. Table 2 shows definitions for DLTs and recommended dose modifications; CTCAE v3.0 was used for this study. Informed consent was obtained from all individual participants included in the study.

**Table 1** Planned dose levels

Dose level	WT (mg/m <sup>2</sup> )	HT (mg/m <sup>2</sup> )
–1	60	30
0 (starting)	120	60
1	180	90
2	240	120
3		150

Dose expression of nal-IRI here is in the form of the trihydrate salt; as described in the manuscript text, the conversion factor from the trihydrate salt dose to the currently used free base dose is 0.866

**Table 2** Dose-limiting toxicities and recommended dose modifications

Dose-limiting toxicity		
Hematological	Grade 3+ thrombocytopenia persisting >5 days Grade 4 neutropenia persisting >5 days Grade 4 anemia of any duration	
Non-hematological	Any grade 3 or greater toxicity <sup>b</sup> except for grade 3 alopecia	
Other	Failure to recover from toxicities to be eligible for re-treatment with nal-IRI within 35 days of the first dose of nal-IRI	
Recommended dose modifications: hematological toxicity		
ANC Nadir	Platelet Nadir	Subsequent dose to be given
≥1000	≥75,000	Full dose (no dose reduction) <sup>a</sup>
750–999	50,000–74,000	Held, then single dose level reduction <sup>a</sup>
<750	<50,000	Held, then two-dose level reduction <sup>a</sup>
Recommended dose modifications: non-hematological toxicity		
Grade 0–2+		Full dose (no dose reduction) <sup>c</sup>
Grade 3		Hold, then single dose level reduction <sup>d</sup>
Grade 4		Hold, then two-dose level reduction <sup>e</sup>

Defined according to NCI CTCAE version 3.0

<sup>a</sup>To be given only once there had been recovery to ANC ≥1000 and platelets ≥100,000

<sup>b</sup>For nausea, vomiting or diarrhea, only if grade 3 or greater despite optimal medical management

<sup>c</sup>For intolerable Grade 2 toxicity, the dose could be held until recovery to CTCAE Grade 0–1, then resumed at one dose lower, at the investigator's discretion

<sup>d</sup>To be held until recovery to CTCAE Grade 0–1 (or to within 1 grade of starting values for pre-existing laboratory abnormalities), and then resumed at one dose level lower, unless toxicity was nausea/vomiting and patients were not on optimal antiemetic therapy

<sup>e</sup>To be held until recovery to CTCAE Grade 0–1 (or to within 1 grade of starting values for pre-existing laboratory abnormalities), and then resumed at two dose levels lower

## Pharmacokinetic analyses

Pharmacokinetics samples were to be drawn prior to the first dose of drug, and then immediately post-infusion, at 2, 4, 6, and 24 h post-infusion, and, if possible, at 48 h post-infusion. Samples were drawn again prior to the second infusion. Study samples (human plasma) were analyzed for 3 analytes [irinotecan (CPT-11), SN38, and SN38 glucuronide (SN38G)] using a modified version of a validated ultra performance liquid chromatographic (UPLC) assay. Authentic standards of CPT-11, SN38, and SN38G were obtained from Toronto Research Chemicals Inc. (Toronto, Ontario, Canada) and camptothecin, the internal standard (IS), was obtained from Sigma Aldrich (St. Louis, MO). Study samples were quantitated using calibration standards and quality control (QC) samples prepared by spiking CPT-11, SN38, and SN38G into human lithium heparin plasma (Bioreclamation, LLC, Westbury, New York). Calibration ranges were 0.200–1000 ng/mL for all analytes, and plasma QCs were prepared at 1.00, 100, and 750 ng/mL for all analytes.

Study samples were analyzed undiluted for SN38 and SN38G, but diluted for CPT-11 prior to extraction so the concentrations were within the range of the standard curve. Study samples were extracted by mixing a 200-μL aliquot

of a calibrator, QC, plasma blank, or study sample with 800 μL of ice cold, acidified methanol containing the IS camptothecin at 20 ng/mL in a 1.5-mL microcentrifuge tube. The tubes were capped, vortexed, and centrifuged at 14,000 rpm and 4 °C for 10 min. After centrifugation, 700 μL of the supernatant was transferred to a clean 16×100-mm glass culture tube, and the supernatant evaporated at 37 °C under nitrogen. The residue was reconstituted with 200 μL of a mixture of 85% mobile phase A (80.0% water containing 3.00% trimethylamine (TEA)/20.0% acetonitrile, pH 5.5) and 15% mobile phase B (100% acetonitrile). The suspension was centrifuged at 14,000 rpm and 4 °C for 10 min to separate insoluble materials. A 100-μL aliquot of the supernatant was transferred to a glass insert in an amber autosampler vial and a 15-μL aliquot injected.

UPLC analysis of the extracted samples was performed using an Acquity<sup>®</sup> UPLC System with fluorescence detection (Waters Corporation, Milford, MA, USA). Chromatographic separation was achieved using a Waters<sup>®</sup> Acquity<sup>®</sup> RP18, 2.1 mm×100 mm, 1.7 μm column (part number 186002854) preceded by a Waters<sup>®</sup> Acquity<sup>®</sup> BEH Shield RP18, 2.1 mm×5.0 mm, 1.7 μm guard column (part number 186003977). The HPLC column was maintained at 40 °C and a flow rate of 500 μL/min using a biphasic gradient (Mobile Phase A: 80.0% water containing 3.00% TEA/



20.0% acetonitrile pH 5.5; and Mobile Phase B: 100% acetonitrile).

Analytes were analyzed by fluorescence detection controlled by Waters® Empower™ 3 software, build 3471. Excitation wavelength was set at 370 nm for all three analytes with emission wavelengths at 510, 530, and 420 nm for CPT-11, SN38, and SN38G, respectively. Calibration curves were generated using analyte/IS peak area response ratios versus nominal concentrations (ng/mL) and weighted linear regressions with a weighting factor of  $1/\text{concentration}^2$ . Back-calculated concentrations were generated using the formula  $x = (y - b)/m$  where  $x$  is the back-calculated concentration,  $y$  is the analyte/IS peak area ratio,  $b$  is the  $y$  intercept, and  $m$  is the slope. Calibrator and QC acceptance criteria required all acceptable concentrations to have accuracy deviations of 15% or less from the nominal concentration with coefficients of variations (% CV) of 15% or less, except at the lower limit of quantitation, which was allowed a 20% deviation for both parameters.

The standard non-compartmental method was used to estimate the pharmacokinetic parameters of total irinotecan, SN-38, and SN-38G from the analyzed plasma concentration data in patients. The estimated pharmacokinetic parameters included maximum plasma concentrations ( $C_{\max}$ ), areas under the plasma concentration time curve ( $AUC_{0-t}$ ) and terminal half-life ( $t_{1/2}$ ).

## Results

### Patient demographics

Patients in the two groups had similar baseline characteristics. In the WT cohort, mean age was 50 years (range 28–65 years) and median Karnofsky Performance Status (KPS) was 80 (range 60–90); in the HT cohort mean age was 48 years (range 28–75 years) and median KPS was 90 (60–100). Of the 16 patients in the WT cohort, 12 patients had GBM and 4 had grade III oligoastrocytoma. Of the 18 patients in the HT cohort, 14 had GBM, 1 had grade III oligoastrocytoma, and 3 had grade III astrocytoma. The median number of relapses was 3 in both groups (WT, range 1–8; HT, range 1–5).

### Safety results

The MTD for the WT cohort was 120 mg/m<sup>2</sup> every 3 weeks. Six patients were enrolled at that dose, without any DLTs. Four patients were enrolled at 180 mg/m<sup>2</sup> without DLTs (patients #3 and #4 were consented and screened, including testing of UGT1A1 genotype, simultaneously, and an exception was granted to allow both patients to enroll when their genotypes were both WT). Three patients

were then enrolled at 240 mg/m<sup>2</sup>, but DLTs occurred in 2 of the 3 patients (diarrhea and dehydration). As a result, the dose was de-escalated to 180 mg/m<sup>2</sup>, and 3 additional patients were enrolled. Within these 3 patients, there were 2 DLTs (diarrhea in one patient, and diarrhea and fatigue in the other). As such, the MTD for the WT cohort was declared to be 120 mg/m<sup>2</sup>, to which 6 patients had already been enrolled without any DLTs.

In the HT cohort, 3 patients were treated at 60 mg/m<sup>2</sup>, with no DLTs. Six were treated at 90 mg/m<sup>2</sup> with 1 DLT. Three were treated at 120 mg/m<sup>2</sup> with no DLTs, and then 6 patients were treated at 150 mg/m<sup>2</sup> with 1 DLT (dehydration/diarrhea). Given the above-described experience with the WT cohort, further dose escalation to 180 mg/m<sup>2</sup> was not felt advisable, and as such, the MTD for the HT cohort was declared to be 150 mg/m<sup>2</sup>. Table 3 lists all grade 3 or greater toxicities that were possibly, probably or definitely related to the study medication.

### Efficacy results

PFS-6 was 2.9% for the intent-to-treat (ITT) cohort. Median PFS (Fig. 1a) was 42 days (95% CI 40–45 days), while median overall survival (Fig. 1b) was 107 days (95% CI 87–198 days).

### Pharmacokinetic analysis results

The pharmacokinetic parameters of nal-IRI were analyzed by each dose level for total irinotecan and the metabolites SN-38 and SN-38G (Table 4). Due to the limited sampling schedule, only  $C_{\max}$  was reported for SN-38 and SN-38G. The maximum concentration and  $AUC_{0-t}$  for total

**Table 3** Grade 3 or greater toxicities possibly related to drug

Toxicity	Grade <sup>a</sup>	Number of patients
Neutropenia	3	1
	4	1
Leukopenia	3	5
	4	1
Lymphopenia	3	4
	4	1
Fatigue (asthenia, lethargy, malaise)	3	2
Nausea	3	1
Dehydration	3	3
Diarrhea	3	3
Elevation of creatinine	3	1
Hypokalemia	4	1

<sup>a</sup>Defined according to NCI CTCAE version 3.0

**Fig. 1 a** Kaplan–Meier estimate (*solid line*) of progression-free survival for the intent-to-treat (ITT) cohort. 95% confidence interval bands are represented using *dashed lines*. **b** Kaplan–Meier estimate (*solid line*) of overall survival for the intent-to-treat (ITT) cohort. 95% confidence interval bands are represented using *dashed lines*

irinotecan proportionally increased with dose (Table 4). The terminal half-life for nal-IRI did not change with dose and was comparable to a prior study [8] (also D.C. Drummond, PhD, unpublished data). Interestingly, UGT1A1\*28 WT or HT genotype had no clear effect on nal-IRI PK parameters (Fig. 2a). In addition, the ratio of SN-38G to SN-38, the indicator of UGT1A1 activity did not show any difference (Fig. 2b).

## Discussion

In this phase 1 study, nal-IRI did not demonstrate any unexpected toxicities. The DLTs were diarrhea, dehydration and fatigue, all known toxicities of the parent drug irinotecan. Contrary to expectations, there was no clear difference in the pharmacokinetic parameters between the WT cohort and the HT cohort, and the clinical tolerability, as measured by the MTD achieved in the two cohorts, was not superior in the WT cohort. Moreover, these results are consistent with recent findings that similar SN-38 concentrations were observed for both 7/7 homozygous and non-7/7 homozygous UGT1A1\*28 (D.C. Drummond, MD, unpublished data). One limitation of the current study is the fact that the PK sampling time point in this study was limited to the first 24 h; therefore, the clearance of SN-38 cannot be estimated.

Although 150 mg/m<sup>2</sup> was not tested in the WT cohort within this study, given that the MTD in the prior (unselected genotype) phase 1 study was 120 mg/m<sup>2</sup> and that it was 120 mg/m<sup>2</sup> (WT cohort) and 150 mg/m<sup>2</sup> (HT cohort) in this study, we would suggest that 120 mg/m<sup>2</sup> be the recommended phase 2 dose going forward for glioma patients with either WT or HT genotype.

Preclinical testing of CED of nal-IRI has demonstrated efficacy in intracranial rodent models as a monotherapy [16], in combination with PEGylated liposomal doxorubicin [17], and in combination with radiation [6]. Antitumor activity was also observed in spontaneous canine brain tumors treated with nal-IRI administered by CED [18]. The study we report here on intravenous delivery of nal-IRI was required by the FDA prior to testing CED of nal-IRI in patients with gliomas, and the toxicity profile of the drug was acceptable to move forward. As such, we have initiated a phase 1 clinical trial testing CED of single-agent nal-IRI in humans with recurrent malignant glioma [NCT02022644], with the goal of moving to CED

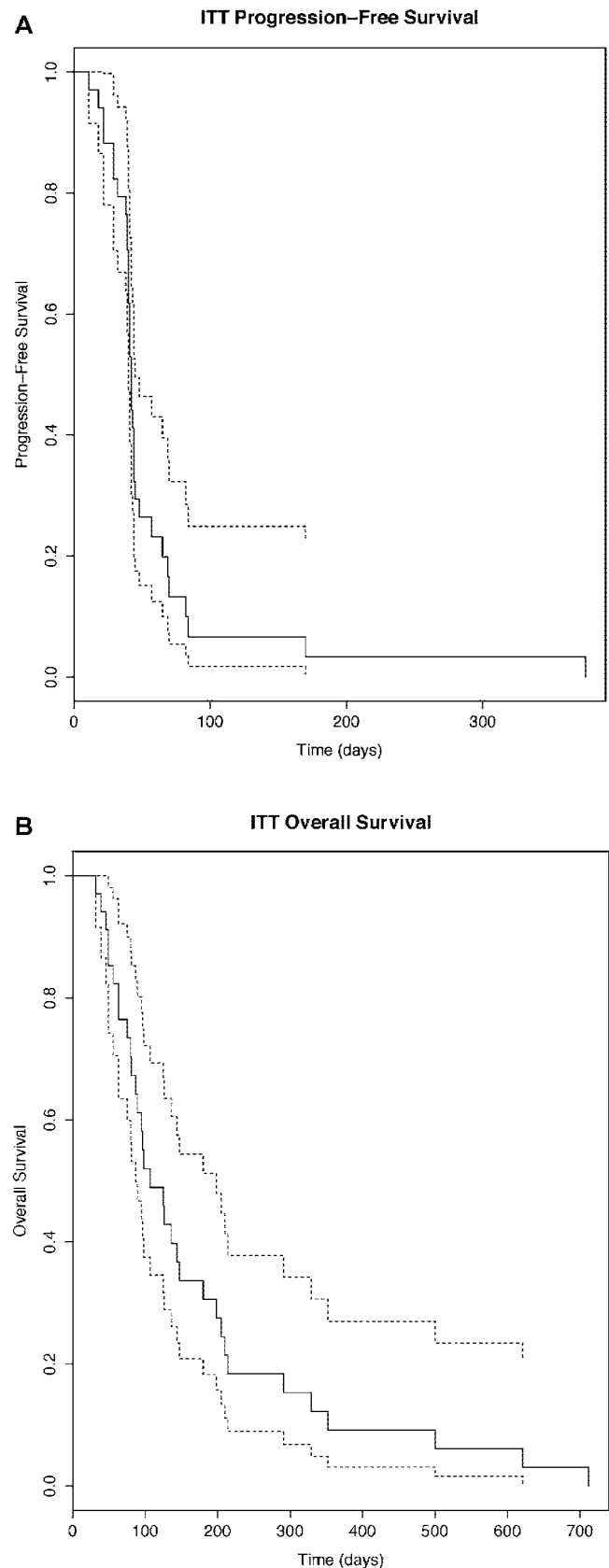


**Table 4** Mean pharmacokinetic parameters of nal-IRI

	Dose, mg/m <sup>2</sup>	60	90	120	150	180	240
Total irinotecan ( <i>N</i> =33)	<i>C</i> <sub>max</sub> , µg/mL	31.8 (2.3)	171.6 (61.6)	91.8 (12.7)	194.0 (57.0)	169.7 (14.5)	253.5 (70.5)
	AUC <sub>t</sub> , h·µg/mL	360.0 (117.1)	1848.6 (628.1)	1782.4 (409.6)	4152.2 (1341.2)	3786.2 (795.5)	9418.2 (7237.2)
	<i>t</i> <sub>1/2</sub> , h	11.5 (–)	13.4 (0.2)	28.4 (14.1)	32.1 (9.2)	42.2 (13.8)	37.2 (–)
SN-38 ( <i>N</i> =11) <sup>a</sup>	<i>C</i> <sub>max</sub> , ng/mL	15.5 (5.2)	3.6 (–)	11.8 (4.0)	(–)	3.2 (1.4)	(–)
SN-38G ( <i>N</i> =33)	<i>C</i> <sub>max</sub> , ng/mL	15.0 (1.2)	96.0 (63.6)	25.7 (5.1)	28.0 (7.4)	28.4 (5.6)	38.5 (26.0)

Standard error is reported within parenthesis

<sup>a</sup>Not all patients have SN-38 concentration data due to assay failure

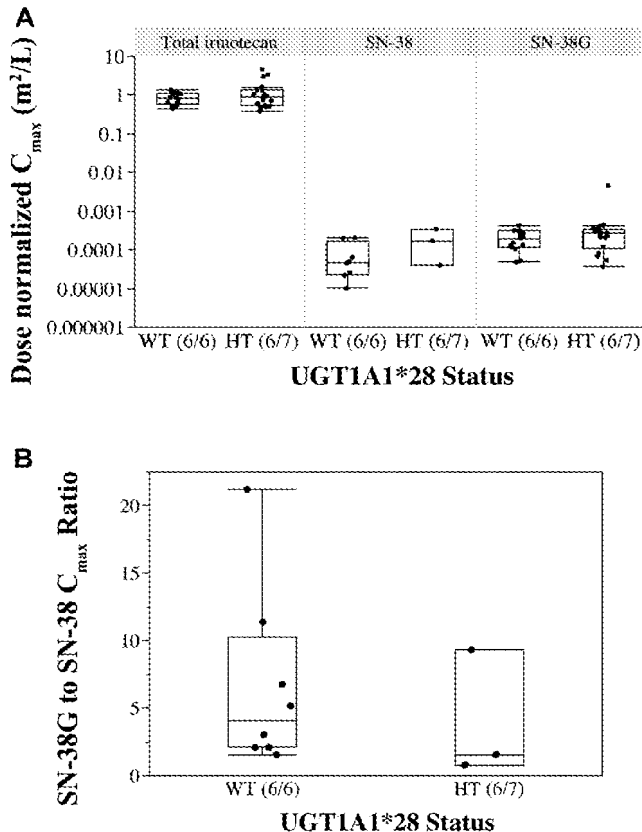


**Fig. 2** **a** Comparison of dose normalized *C*<sub>max</sub> in patients with different UGT1A1\*28 genotypes. **b** Comparison of SN-38G to SN-38 *C*<sub>max</sub> ratio in patients with different UGT1A1\*28 genotypes

of combination therapy if it is tolerated as a single-agent. Further development of intravenous delivery of nal-IRI in glioma patients is not planned at this time.

In this study, the patients with UGT1A1 heterozygosity showed similar pharmacokinetic properties for SN-38 and SN-38G relative to WT patients following the administration of nal-IRI. While the plasma levels of SN-38 can be affected by the activity of UGT enzymes, they also rely on the incoming load of SN-38 (ie, the amount of irinotecan conversion to SN-38). Indeed, the associations between UGT1A1\*28 7/7 homozygosity and hematological toxicity

were observed only in patients treated with higher irinotecan doses [15]. Furthermore, the plasma SN-38 concentrations from UGT1A1\*28 7/7 homozygous patients were higher only in patients administered with higher dose of irinotecan (300 mg/m<sup>2</sup>), not in patients with a low daily dose (15–75 mg/m<sup>2</sup> for 5 days) of irinotecan [13, 14]. Therefore, the lack of significant pharmacokinetic difference in our HT cohort relative to the WT cohort could be attributed to the fact that nal-IRI can lower the amount of SN-38 to be metabolized by UGT enzymes by preventing the rapid conversion of irinotecan to SN 38.

**Acknowledgements** The authors would like to thank Ms. Iiona Garner (UCSF) for her expert assistance with manuscript preparation and editing.

**Compliance with Ethical Standards**

**Funding** This clinical trial was funded by the UCSF Brain Tumor Research Center's Specialized Program of Research Excellence (SPORE) Grant from the NCI: P50 CA097257.

**Conflict of interest** Daryl C. Drummond is both an employee and stockholder in Merrimack, and is the inventor of Onivyde (liposomal irinotecan). Jonathan B. Fitzgerald is an employee of Merrimack. Charles Noble is a stockholder in Merrimack.

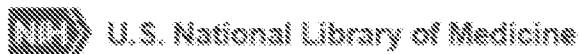
## References

- Ostrom QT, Gittleman H, Fulop J, Liu M, Blanda R, Kromer C et al (2015) CBTRUS statistical report: primary brain and central nervous system tumors diagnosed in the United States in 2008–2012. *Neurooncology* 17(Suppl 4):iv1–iv62
- Drummond DC, Noble CO, Guo Z, Hong K, Park JW, Kirpotin DB (2006) Development of a highly active nanoliposomal irinotecan using a novel intraliposomal stabilization strategy. *Cancer Res* 66(6):3271–3277
- Kalra AV, Kim J, Klinz SG, Paz N, Cain J, Drummond DC et al (2014) Preclinical activity of nanoliposomal irinotecan is governed by tumor deposition and intratumor prodrug conversion. *Cancer Res* 74(23):7003–7013
- Kang MH, Wang J, Makena MR, Lee JS, Paz N, Hall CP et al (2015) Activity of MM-398, nanoliposomal irinotecan (nal-IRI), in Ewing's family tumor xenografts is associated with high

- exposure of tumor to drug and high SLFN11 expression. *Clin Cancer Res Off J Am Assoc Cancer Res* 21(5):1139–1150
5. Noble CO, Krauze MT, Drummond DC, Forsayeth J, Hayes ME, Beyer J et al (2014) Pharmacokinetics, tumor accumulation and antitumor activity of nanoliposomal irinotecan following systemic treatment of intracranial tumors. *Nanomedicine (London, England)* 9(14):2099–2108
  6. Chen PY, Ozawa T, Drummond DC, Kalra A, Fitzgerald JB, Kirpotin DB et al (2013) Comparing routes of delivery for nanoliposomal irinotecan shows superior anti-tumor activity of local administration in treating intracranial glioblastoma xenografts. *Neurooncology* 15(2):189–197
  7. Chang TC, Shiah HS, Yang CH, Yeh KH, Cheng AL, Shen BN et al (2015) Phase I study of nanoliposomal irinotecan (PEP02) in advanced solid tumor patients. *Cancer Chemother Pharmacol* 75(3):579–586
  8. Roy AC, Park SR, Cunningham D, Kang YK, Chao Y, Chen LT et al (2013) A randomized phase II study of PEP02 (MM-398), irinotecan or docetaxel as a second-line therapy in patients with locally advanced or metastatic gastric or gastro-oesophageal junction adenocarcinoma. *Ann Oncol Off J Eur Soc Med Oncol ESMO* 24(6):1567–1573
  9. Ramanathan RK, Korn RL, Sachdev JC, Fetterly GJ, Jameson G, Marceau K et al (2014) Lesion characterization with ferumoxytol MRI in patients with advanced solid tumors and correlation with treatment response to MM-398, nanoliposomal irinotecan (nal-IRI). *Eur J Cancer* 50(Suppl 6):87 (**abstract 261**)
  10. Wang-Gillam A, Li CP, Bodoky G, Dean A, Shan YS, Jameson G et al (2016) Nanoliposomal irinotecan with fluorouracil and folinic acid in metastatic pancreatic cancer after previous gemcitabine-based therapy (NAPOLI-1): a global, randomised, open-label, phase 3 trial. *Lancet (London, England)* 387(10018):545–557
  11. Ando Y, Saka H, Ando M, Sawa T, Muro K, Ueoka H et al (2000) Polymorphisms of UDP-glucuronosyltransferase gene and irinotecan toxicity: a pharmacogenetic analysis. *Cancer Res* 60(24):6921–6926
  12. Innocenti F, Undevia SD, Iyer L, Chen PX, Das S, Kocherginsky M et al (2004) Genetic variants in the UDP-glucuronosyltransferase 1A1 gene predict the risk of severe neutropenia of irinotecan. *J Clin Oncol Off J Am Soc Clin Oncol* 22(8):1382–1388
  13. Iyer L, Das S, Janisch L, Wen M, Ramirez J, Karrison T et al (2002) UGT1A1\*28 polymorphism as a determinant of irinotecan disposition and toxicity. *Pharmacogenomics J* 2(1):43–47
  14. Stewart CF, Panetta JC, O'Shaughnessy MA, Throm SL, Fraga CH, Owens T et al (2007) UGT1A1 promoter genotype correlates with SN-38 pharmacokinetics, but not severe toxicity in patients receiving low-dose irinotecan. *J Clin Oncol Off J Am Soc Clin Oncol* 25(18):2594–2600
  15. Hoskins JM, Goldberg RM, Qu P, Ibrahim JG, McLeod HL (2007) UGT1A1\*28 genotype and irinotecan-induced neutropenia: dose matters. *J Natl Cancer Inst* 99(17):1290–1295
  16. Noble CO, Krauze MT, Drummond DC, Yamashita Y, Saito R, Berger MS et al (2006) Novel nanoliposomal CPT-11 infused by convection-enhanced delivery in intracranial tumors: pharmacology and efficacy. *Cancer Res* 66(5):2801–2806
  17. Krauze MT, Noble CO, Kawaguchi T, Drummond D, Kirpotin DB, Yamashita Y et al (2007) Convection-enhanced delivery of nanoliposomal CPT-11 (irinotecan) and PEGylated liposomal doxorubicin (Doxil) in rodent intracranial brain tumor xenografts. *Neurooncology* 9(4):393–403
  18. Dickinson PJ, LeCouteur RA, Higgins RJ, Bringas JR, Roberts B, Larson RF et al (2008) Canine model of convection-enhanced delivery of liposomes containing CPT-11 monitored with real-time magnetic resonance imaging: laboratory investigation. *J Neurosurg* 108(5):989–998

We updated the design of this site on September 25th. [Learn more.](#)

We will be updating this site in phases. This allows us to move faster and to deliver better services. [Show less](#)



**ClinicalTrials.gov**

- [Find Studies](#) ▼
- [About Studies](#) ▼
- [Submit Studies](#) ▼
- [Resources](#) ▼
- [About Site](#) ▼

## Liposomal SN-38 in Treating Patients With Small Cell Lung Cancer

This study has been withdrawn prior to enrollment.

**Sponsor:**

Alliance for Clinical Trials in Oncology

**ClinicalTrials.gov Identifier:**

NCT00104754

First Posted: March 4, 2005

Last Update Posted: July 20, 2016

**⚠** The safety and scientific validity of this study is the responsibility of the study sponsor and investigators. Listing a study does not mean it has been evaluated by the U.S. Federal Government. Read our [disclaimer](#) for details.

**Collaborator:**

National Cancer Institute (NCI)

**Information provided by (Responsible Party):**

Alliance for Clinical Trials in Oncology

[Full Text View](#)

[Tabular View](#)

[No Study Results Posted](#)

[Disclaimer](#)

[How to Read a Study Record](#)

### ► Purpose

**RATIONALE:** Drugs used in chemotherapy, such as liposomal SN-38, work in different ways to stop the growth of tumor cells, either by killing the cells or by stopping them from dividing.

**PURPOSE:** This phase II trial is studying how well liposomal SN-38 works in treating patients with small cell lung cancer.

<u>Condition</u>	<u>Intervention</u>	<u>Phase</u>
Lung Cancer	Drug: liposomal SN-38	Phase 2

Study Type: Interventional

Study Design: Masking: None (Open Label)

Primary Purpose: Treatment

Official Title: Phase II Trial of Liposome Encapsulated SN38 (LE-SN38) in the Treatment of Small Cell Lung Cancer

**Resource links provided by NLM:**

Genetics Home Reference related topics: lung cancer

MedlinePlus related topics: Lung Cancer

Drug Information available for: Irinotecan Irinotecan hydrochloride

U.S. FDA Resources

**Further study details as provided by Alliance for Clinical Trials in Oncology:**

Primary Outcome Measures:

- Tumor response measured by number of responses [ Time Frame: Up to 3 years ]

Secondary Outcome Measures:

- Time to disease progression [ Time Frame: Up to 3 years ]
- Survival time [ Time Frame: Up to 3 years ]
- Change in quality of life (QOL) score over time [ Time Frame: Up to 3 years ]

Enrollment: 0

<u>Arms</u>	<u>Assigned Interventions</u>
<p><b>Experimental: liposomal SN-38</b></p> <p>Patients receive SN-38 liposome IV over 90 minutes on day 1. Treatment repeats every 21 days for 2 courses in the absence of disease progression or unacceptable toxicity. Patients achieving a complete or partial response or patients with stable disease (SD) who were previously treated before study enrollment receive up to 4 additional courses of treatment. Patients with CNS-only disease progression receive whole brain radiotherapy (WBRT). After completion of WBRT, these patients also receive up to 4 additional courses of treatment. Patients with disease progression to sites other than the CNS or patients with SD who were previously untreated before study enrollment are removed from the study.</p> <p>Quality of life is assessed at baseline, before each treatment course, and then annually for 3 years.</p> <p>After completion of study treatment, patients are followed every 3 months for 1 year and then every 6 months for 2 years.</p>	<p><b>Drug:</b> liposomal SN-38</p>

**Detailed Description:****OBJECTIVES:**

- Determine the response rate in patients with small cell lung cancer treated with SN-38 liposome that is dosed according to a UGT1A1-specific genotype.
- Determine the toxicity of this drug in these patients.
- Determine, preliminarily, overall and progression-free survival of patients treated with this drug.
- Determine the quality of life of patients treated with this drug.
- Correlate UGT1A1-specific haplotypes with toxicity of this drug in these patients.
- Correlate UGT1A1-specific haplotypes with outcomes of patients treated with this drug.

**OUTLINE:** This is a multicenter study. Patients are stratified according to length of time since prior treatment (previously untreated disease OR chemosensitive disease and  $\geq 3$  months since prior treatment vs refractory disease OR chemoresistant disease and  $< 3$  months since prior treatment).

Patients receive SN-38 liposome IV over 90 minutes on day 1. Treatment repeats every 21 days for 2 courses in the absence of disease progression or unacceptable toxicity. Patients achieving a complete or partial response or patients with stable disease (SD) who were previously treated

before study enrollment receive up to 4 additional courses of treatment. Patients with CNS-only disease progression receive whole brain radiotherapy (WBRT). After completion of WBRT, these patients also receive up to 4 additional courses of treatment. Patients with disease progression to sites other than the CNS or patients with SD who were previously untreated before study enrollment are removed from the study.

Quality of life is assessed at baseline, before each treatment course, and then annually for 3 years. After completion of study treatment, patients are followed every 3 months for 1 year and then every 6 months for 2 years.

PROJECTED ACCRUAL: Approximately 73 patients (40 for stratum I and 33 for stratum II) will be accrued for this study within 16-19 months.

## ► Eligibility

### Information from the National Library of Medicine



*Choosing to participate in a study is an important personal decision. Talk with your doctor and family members or friends about deciding to join a study. To learn more about this study, you or your doctor may contact the study research staff using the contacts provided below. For general information, [Learn About Clinical Studies](#).*

Ages Eligible for Study: 18 Years and older (Adult, Senior)  
 Sexes Eligible for Study: All  
 Accepts Healthy Volunteers: No

### Criteria

#### DISEASE CHARACTERISTICS:

- Histologically or cytologically confirmed small cell lung cancer meeting 1 of the following criteria:
  - Previously untreated disease
    - Extensive stage disease, as defined by any of the following:
      - Metastatic disease outside of the chest
      - Contralateral supraclavicular or contralateral hilar nodes that cannot be included in a single radiation port



- Malignant pleural effusion
- Previously treated disease
  - Limited or extensive stage disease
- Measurable disease
  - Lesions  $\geq 1$  cm and  $< 2$  cm must be measured by spiral CT scan for pre- and post-treatment tumor assessment
- UGT1A1\*28 genotype wt/wt (6/6 promoter TA repeats) OR wt/\*28 (6/7 promoter TA repeats)
  - No \*28/\*28 (7/7 promoter TA repeats) genotype
- No mixed histology
- No uncontrolled CNS metastasis
  - Previously treated, stable CNS metastasis allowed
- No superior vena cava syndrome
- No malignant pericardial effusion
- No near obstruction of the trachea or main stem bronchi

#### PATIENT CHARACTERISTICS:

##### Age

- 18 and over

##### Performance status

- ECOG 0-2

##### Life expectancy

- Not specified

##### Hematopoietic

- Absolute neutrophil count  $\geq 1,500/\text{mm}^3$
- Platelet count  $\geq 100,000/\text{mm}^3$

##### Hepatic

- Total bilirubin  $< 1.5$  times upper limit of normal (ULN) OR
- Direct bilirubin normal

##### Renal

- Creatinine  $< 1.5$  times ULN

#### Cardiovascular

- No unstable angina pectoris
- No uncontrolled congestive heart failure
- No myocardial infarction within the past 3 months

#### Other

- Not pregnant or nursing
- Negative pregnancy test
- Fertile patients must use effective contraception during and for 6 months after study participation
- No syndrome of inappropriate antidiuretic hormone secretion
- No ectopic adrenocorticotrophic syndrome
- No Lambert-Eaton myasthenic syndrome
- No other severe paraneoplastic syndrome
- No active infection requiring oral or parenteral antibiotics
- No other life threatening disease
- No other malignancy except basal cell or squamous cell skin cancer, localized prostate cancer, superficial bladder cancer, or carcinoma in situ of the cervix

#### PRIOR CONCURRENT THERAPY:

##### Biologic therapy

- No concurrent filgrastim (G-CSF) during course 1 of study treatment

##### Chemotherapy

- No more than 1 prior chemotherapy regimen for this malignancy
  - Prior cyclophosphamide, doxorubicin, and vincristine (CAV) alternating with etoposide and cisplatin (EP) allowed
- More than 21 days since prior chemotherapy

##### Endocrine therapy

- Not specified

##### Radiotherapy

- More than 14 days since prior radiotherapy

- Concurrent palliative radiotherapy allowed except radiotherapy to a solitary measured index lesion

#### Surgery

- More than 21 days since prior major surgery

#### Other

- No other concurrent treatment for this malignancy
- No other concurrent investigational treatment

## ► Contacts and Locations

### Information from the National Library of Medicine



*To learn more about this study, you or your doctor may contact the study research staff using the contact information provided by the sponsor.*

*Please refer to this study by its ClinicalTrials.gov identifier (NCT number):*

***NCT00104754***

### Sponsors and Collaborators

Alliance for Clinical Trials in Oncology

National Cancer Institute (NCI)

### Investigators

Study Chair: James R. Jett, MD Mayo Clinic

## ► More Information

Responsible Party:	Alliance for Clinical Trials in Oncology
ClinicalTrials.gov Identifier:	<a href="#">NCT00104754</a> <a href="#">History of Changes</a>
Other Study ID Numbers:	NCCTG-N0322 CDR0000415847 ( Registry Identifier: PDQ (Physician Data Query) )
First Submitted:	March 3, 2005
First Posted:	March 4, 2005
Last Update Posted:	July 20, 2016

Last Verified: July 2016

Keywords provided by Alliance for Clinical Trials in Oncology:

extensive stage small cell lung cancer

limited stage small cell lung cancer

recurrent small cell lung cancer

Additional relevant MeSH terms:

Lung Neoplasms

Small Cell Lung Carcinoma

Respiratory Tract Neoplasms

Thoracic Neoplasms

Neoplasms by Site

Neoplasms

Lung Diseases

Respiratory Tract Diseases

Carcinoma, Bronchogenic

Bronchial Neoplasms

Irinotecan

Antineoplastic Agents, Phytogetic

Antineoplastic Agents

Topoisomerase I Inhibitors

Topoisomerase Inhibitors

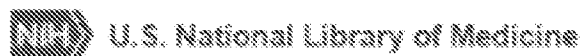
Enzyme Inhibitors

Molecular Mechanisms of Pharmacological

Action

We updated the design of this site on September 25th. [Learn more.](#)

We will be updating this site in phases. This allows us to move faster and to deliver better services. [Show less](#)



**ClinicalTrials.gov**

- [Find Studies](#) ▼
- [About Studies](#) ▼
- [Submit Studies](#) ▼
- [Resources](#) ▼
- [About Site](#) ▼

---

---

## Liposomal SN-38 in Treating Patients With Metastatic Colorectal Cancer

This study has been completed.

**Sponsor:**

Alliance for Clinical Trials in Oncology

**ClinicalTrials.gov Identifier:**

NCT00311610

First Posted: April 6, 2006

Last Update Posted: June 29, 2016

**⚠** The safety and scientific validity of this study is the responsibility of the study sponsor and investigators. Listing a study does not mean it has been evaluated by the U.S. Federal Government. Read our [disclaimer](#) for details.

**Collaborator:**

National Cancer Institute (NCI)

**Information provided by (Responsible Party):**

Alliance for Clinical Trials in Oncology

[Full Text View](#)

[Tabular View](#)

[No Study Results Posted](#)

[Disclaimer](#)

[How to Read a Study Record](#)

---

### ► Purpose

**RATIONALE:** Drugs used in chemotherapy, such as liposomal SN-38, work in different ways to stop the growth of tumor cells, either by killing the cells or by stopping them from dividing.

**PURPOSE:** This phase II trial is studying how well liposomal SN-38 works in treating patients with metastatic colorectal cancer.

<u>Condition</u>	<u>Intervention</u>	<u>Phase</u>
Colorectal Cancer	Drug: SN-38 liposome	Phase 2

**Study Type:** Interventional

**Study Design:** Intervention Model: Single Group Assignment

Masking: None (Open Label)

Primary Purpose: Treatment

**Official Title:** Phase II Trial of LE SN38 in Patients With Metastatic Colorectal Cancer After Progression on Oxaliplatin

**Resource links provided by NLM:**

MedlinePlus related topics: [Colorectal Cancer](#)

Drug Information available for: [Irinotecan](#) [Irinotecan hydrochloride](#)

U.S. FDA Resources

**Further study details as provided by Alliance for Clinical Trials in Oncology:**

**Primary Outcome Measures:**

- Objective response rate [ Time Frame: q 2 cycles during tx ]

**Secondary Outcome Measures:**

- Toxicity [ Time Frame: q cycle during tx ]
- Progression-free survival [ Time Frame: 3 years ]
- Overall survival [ Time Frame: 3 years ]

**Enrollment:** 30

**Study Start Date:** January 2006

**Study Completion Date:** June 2010

Primary Completion Date: January 2007 (Final data collection date for primary outcome measure)

Arms	Assigned Interventions
<p>Experimental: SN-38 liposome</p> <p>Patients receive SN-38 liposome IV over 90 minutes on day 1. Treatment repeats every 21 days in the absence of disease progression or unacceptable toxicity.</p> <p>After completion of study treatment, patients are followed every 3 months for up to 3 years.</p>	<p>Drug: SN-38 liposome</p> <p>38 mg/sq m IV infusion over 30 min q 21 days (1 cycle) until progression</p>

### Detailed Description:

#### OBJECTIVES:

##### Primary

- Determine the objective response rate following treatment with SN-38 liposome as a second-line treatment in patients with metastatic colorectal cancer.

##### Secondary

- Determine the toxicity profile of this drug in these patients.
- Determine the proportion of patients treated with this drug who experience any grade 3 or greater toxicity.
- Determine progression-free survival and overall survival for patients treated with this drug.

OUTLINE: This is a multicenter study.

Patients receive SN-38 liposome IV over 90 minutes on day 1. Treatment repeats every 21 days in the absence of disease progression or unacceptable toxicity.

After completion of study treatment, patients are followed every 3 months for up to 3 years.

### ► Eligibility

#### Information from the National Library of Medicine



*Choosing to participate in a study is an important personal decision. Talk with your doctor and family members or friends about deciding to join a study. To learn more about this study, you or your doctor may contact the*

*study research staff using the contacts provided below. For general information, [Learn About Clinical Studies](#).*

Ages Eligible for Study: 18 Years to 120 Years (Adult, Senior)

Sexes Eligible for Study: All

Accepts Healthy Volunteers: No

### Criteria

#### DISEASE CHARACTERISTICS:

- Histologically or cytologically determined metastatic colorectal cancer\*
  - Primary lesion confirmed endoscopically, surgically, or radiologically NOTE: \* Patients with a history of colorectal cancer treated by surgical resection who develop radiological or clinical evidence of metastatic cancer do not require separate histological or cytological confirmation of metastatic disease, unless more than 5 years between primary surgery and development of metastatic disease OR primary cancer was stage I
- Measurable disease, defined as  $\geq 1$  unidimensionally measurable lesion  $\geq 20$  mm by conventional techniques OR  $\geq 10$  mm by spiral CT scan
  - Nonmeasurable lesions include the following:
    - Bone lesions
    - Leptomeningeal disease
    - Ascites
    - Pleural/pericardial effusion
    - Lymphangitis cutis/pulmonis
    - Abdominal masses not confirmed and followed by imaging techniques
    - Cystic lesions
- UGT1A1\*1 homozygous or UGT1A1\*28 heterozygous genotype status
  - Patients with homozygous UGT1A1\*28 genotype not eligible
- Received at least 1 prior regimen with oxaliplatin for metastatic disease
- Recurrent disease following prior adjuvant therapy allowed

#### PATIENT CHARACTERISTICS:

- ECOG performance status 0-1



- Granulocyte count  $\geq 1,500/\text{mm}^3$
- Platelet count  $\geq 100,000/\text{mm}^3$
- Creatinine normal
- Bilirubin normal
- Not pregnant or nursing
- Negative pregnancy test
- Fertile patients must use effective contraception duration and for 3 months after completion of study treatment
- No known Gilbert's disease or other chronic liver disease
- No colonic or small bowel disorders (e.g., inflammatory bowel disease, Crohn's disease, or ulcerative colitis) that predispose the patients to uncontrolled diarrhea (i.e.,  $> 3$  watery or soft stools daily at baseline in patients without a colostomy or ileostomy)

#### PRIOR CONCURRENT THERAPY:

- See Disease Characteristics
- Recovered from prior therapy
- No prior irinotecan
- Prior pelvic radiotherapy allowed as long as measurable lesion is outside irradiated field
- No concurrent palliative radiotherapy
- No other concurrent chemotherapy
- No concurrent steroids except those given for adrenal failure, hormones for non-disease-related conditions (e.g., insulin for diabetes), or intermittent dexamethasone as an antiemetic or for prevention of infusion reaction

## ► Contacts and Locations

### Information from the National Library of Medicine



*To learn more about this study, you or your doctor may contact the study research staff using the contact information provided by the sponsor.*

*Please refer to this study by its ClinicalTrials.gov identifier (NCT number):*

**NCT00311610**

## Locations

### United States, California

Kaiser Permanente Medical Office -Vandever Medical Office  
San Diego, California, United States, 92120

### United States, Delaware

Tunnell Cancer Center at Beebe Medical Center  
Lewes, Delaware, United States, 19958

CCOP - Christiana Care Health Services  
Newark, Delaware, United States, 19713

### United States, Maryland

Union Hospital Cancer Program at Union Hospital  
Elkton MD, Maryland, United States, 21921

### United States, Nevada

University Medical Center of Southern Nevada  
Las Vegas, Nevada, United States, 89102

CCOP - Nevada Cancer Research Foundation  
Las Vegas, Nevada, United States, 89106

### United States, New Jersey

Cancer Institute of New Jersey at Cooper - Voorhees  
Voorhees, New Jersey, United States, 08043

### United States, North Carolina

Lineberger Comprehensive Cancer Center at University of North Carolina - Chapel Hill  
Chapel Hill, North Carolina, United States, 27599-7295

Kinston Medical Specialists  
Kinston, North Carolina, United States, 28501

### United States, Ohio

Arthur G. James Cancer Hospital and Solove Research Institute at Ohio State University Me  
Columbus, Ohio, United States, 43210-1240



## Sponsors and Collaborators

Alliance for Clinical Trials in Oncology

National Cancer Institute (NCI)

### Investigators

Study Chair: Allyson Ocean, MD Weill Medical College of Cornell University

### ► More Information

#### Publications:

Ocean AJ, Niedzwiecki D, Atkins JN, et al.: LE-SN38 for metastatic colorectal cancer after progression on oxaliplatin: results of CALGB 80402. [Abstract] J Clin Oncol 26 (Suppl 15): A-4109, 2008.

Responsible Party: Alliance for Clinical Trials in Oncology  
 ClinicalTrials.gov Identifier: [NCT00311610](#) [History of Changes](#)  
 Other Study ID Numbers: CALGB-80402  
[U10CA031946 \( U.S. NIH Grant/Contract \)](#)  
 CDR0000467234 ( Registry Identifier: NCI Physician Data Query )  
 First Submitted: April 5, 2006  
 First Posted: April 6, 2006  
 Last Update Posted: June 29, 2016  
 Last Verified: June 2016

#### Keywords provided by Alliance for Clinical Trials in Oncology:

recurrent colon cancer  
 stage IV colon cancer  
 recurrent rectal cancer  
 stage IV rectal cancer

#### Additional relevant MeSH terms:

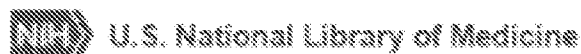
Colorectal Neoplasms	Intestinal Diseases
Intestinal Neoplasms	Rectal Diseases
Gastrointestinal Neoplasms	Irinotecan
Digestive System Neoplasms	Antineoplastic Agents, Phytogetic
Neoplasms by Site	Antineoplastic Agents
Neoplasms	Topoisomerase I Inhibitors
Digestive System Diseases	Topoisomerase Inhibitors
	Enzyme Inhibitors

Gastrointestinal Diseases  
Colonic Diseases

Molecular Mechanisms of Pharmacological  
Action

We updated the design of this site on September 25th. [Learn more.](#)

We will be updating this site in phases. This allows us to move faster and to deliver better services. [Show less](#)



**ClinicalTrials.gov**

- [Find Studies](#) ▼
- [About Studies](#) ▼
- [Submit Studies](#) ▼
- [Resources](#) ▼
- [About Site](#) ▼

---

## Safety Study of IHL-305 (Irinotecan Liposome Injection) to Treat Advanced Solid Tumors

---

The recruitment status of this study is unknown. The completion date has passed and the status has not been verified in more than two years.

Verified January 2012 by Yakult Honsha Co., LTD.

Recruitment status was: *Recruiting*

**Sponsor:**

Yakult Honsha Co., LTD

**ClinicalTrials.gov Identifier:**

NCT00364143

First Posted: August 15, 2006

Last Update Posted: January 26, 2012

**⚠** The safety and scientific validity of this study is the responsibility of the study sponsor and investigators. Listing a study does not mean it has been evaluated by the U.S. Federal Government. Read our [disclaimer](#) for details.

**Information provided by:**

Yakult Honsha Co., LTD

[Full Text View](#)

[Tabular View](#)

[No Study Results Posted](#)

[Disclaimer](#)

[How to Read a Study Record](#)

## ► Purpose

The purpose of this study is to determine whether IHL-305 (irinotecan liposome injection) is safe and effective in the treatment of advanced solid tumors.

Condition	Intervention	Phase
Cancer	Drug: IHL-305 (irinotecan liposome injection)	Phase 1

**Yakult Honsha Co., LTD has indicated that access to an investigational treatment associated with this study is available outside the clinical trial.**

Study Type: Interventional

Study Design: Allocation: Non-Randomized

Intervention Model: Single Group Assignment

Masking: None (Open Label)

Primary Purpose: Treatment

Official Title: A Phase I Study of IHL-305 (Irinotecan Liposome Injection) in Patients With Advanced Solid Tumors

### Resource links provided by NLM:

Drug Information available for: Irinotecan Irinotecan hydrochloride

U.S. FDA Resources

### Further study details as provided by Yakult Honsha Co., LTD:

#### Primary Outcome Measures:

- Incidence of dose-limiting toxicity within 28 days of treatment administration for patients with UGT1A1\*28 genotype (wt/wt and wt/\*28)
- determination of maximum tolerated dose (MTD) and recommended Phase 2 dose for patients with UGT1A1\*28 genotype (wt/wt and wt/\*28)

#### Secondary Outcome Measures:

- Tumor shrinkage per Response Evaluation Criteria in Solid Tumors (RECIST) every 8 weeks/2 cycles while receiving study drug for patients with UGT1A1\*28 genotype (wt/wt and wt/\*28)
- limited pharmacokinetics (PK) for patients with UGT1A1\*28 genotype (wt/wt and wt/\*28)
- limited incidence and severity of adverse events (AEs) and PK for UGT1A1 homozygous (\*28/\*28) patients

Estimated Enrollment: 40

Study Start Date: September 2006

#### Detailed Description:

This is a Phase I dose-escalation study of intravenous administration of IHL-305 in patients with advanced solid tumors. Patients will receive IHL-305 as an intravenous infusion over 60 minutes on Day 1 followed by a 27-day observation period for a total of 28 days (4 weeks) per cycle. Two patient populations will be evaluated separately; patients with UGT1A1\*28 genotype homozygous wild-type (wt/wt) and heterozygous (wt/\*28) variants as one group, and patients with UGT1A1\*28 homozygous variant (\*28/\*28) as another group.

#### ► Eligibility

##### Information from the National Library of Medicine



*Choosing to participate in a study is an important personal decision. Talk with your doctor and family members or friends about deciding to join a study. To learn more about this study, you or your doctor may contact the study research staff using the contacts provided below. For general information, [Learn About Clinical Studies](#).*

Ages Eligible for Study: 18 Years and older (Adult, Senior)

Sexes Eligible for Study: All

Accepts Healthy Volunteers: No

#### Criteria

##### Inclusion Criteria:

1. Histologically confirmed malignant solid tumor and not a candidate for known regimens or protocol treatments of higher efficacy or priority

2. Failed conventional therapy for their cancer or have a malignancy for which a conventional therapy does not exist
3. Recovered from all acute adverse effects of prior therapies, excluding alopecia (hair loss)
4. ECOG performance status of 0, 1, or 2
5. 18 years of age or older
6. Normal organ and bone marrow function as defined by:
  - absolute neutrophil count greater than or equal to 1,500 cells/microliter
  - platelets greater than or equal to 100,000 cells/microliter
  - total bilirubin within normal institutional limits
  - AST (SGOT)/ALT (SGPT) less than or equal to 2.5 x institutional upper limit of normal (ULN) or less than or equal to 5.0 x ULN in patients with liver metastases
  - plasma creatinine less than or equal to 1.5 x institutional ULN OR
  - creatinine clearance greater than or equal to 60 mL/min/1.73 m<sup>2</sup> for patients with creatinine levels above institutional normal
7. Ability to understand and the willingness to sign a written informed consent document

Exclusion Criteria:

1. Previously treated with irinotecan, or had chemotherapy or radiotherapy within 4 weeks (6 weeks for nitrosoureas or mitomycin C) prior to entering the study, or not recovered from adverse effects due to agents administered more than 4 weeks earlier
2. Receiving any other investigational agent
3. Known brain metastases
4. History of allergic reactions attributed to compounds of similar chemical composition to IHL-305
5. Concurrent serious infections (i.e., requiring an intravenous antibiotic)
6. Pregnant women or women of childbearing potential and not using methods to avoid pregnancy; a negative pregnancy test (urine or serum) must be documented at baseline for women of childbearing potential; no breast-feeding while on study.
7. Uncontrolled intercurrent illness including, but not limited to, ongoing or active infection, unstable angina pectoris, or psychiatric illness/social situations that would limit compliance with study requirements
8. Significant cardiac disease including heart failure that meets New York Heart Association (NYHA) class III and IV definitions; history of myocardial infarction within one year of study entry; uncontrolled dysrhythmias; or poorly controlled angina.



9. History of serious ventricular arrhythmia (ventricular tachycardia [VT] or ventricular fibrillation [VF], greater than or equal to 3 beats in a row); QTc greater than or equal to 450 msec for men and 470 msec for women; or left ventricular ejection fraction (LVEF) less than or equal to 40% by multi-gated acquisition scan (MUGA).

## ► Contacts and Locations

### Information from the National Library of Medicine



*To learn more about this study, you or your doctor may contact the study research staff using the contact information provided by the sponsor.*

*Please refer to this study by its ClinicalTrials.gov identifier (NCT number):*  
**NCT00364143**

### Contacts

Contact: Christina A Weaver, BS 609-799-7580 ext 406 [cweaver@theradex.com](mailto:cweaver@theradex.com)  
 Contact: Brad Davis 609-799-7580 ext 394 [bdavis@theradex.com](mailto:bdavis@theradex.com)

### Locations

#### United States, Tennessee

Sarah Cannon Cancer Center **Recruiting**  
 Nashville, Tennessee, United States, 37203  
 Principal Investigator: Howard Burris, MD

Vanderbilt-Ingram Cancer Center **Recruiting**  
 Nashville, Tennessee, United States, 37232-6307  
 Contact: Wendy L. VerMeulen, RN, BSN 615-343-0798  
[wendy.vermeulen@vanderbilt.edu](mailto:wendy.vermeulen@vanderbilt.edu)  
 Contact: Wendy Cooper, RN, BSN, OCN 615-936-5869  
[wendy.cooper@vanderbilt.edu](mailto:wendy.cooper@vanderbilt.edu)  
 Principal Investigator: Mace Rothenberg, MD

### Sponsors and Collaborators

Yakult Honsha Co., LTD

## Investigators

Principal Investigator: Mace L Rothenberg, M.D. Vanderbilt University

## ► More Information

ClinicalTrials.gov Identifier: [NCT00364143](#) [History of Changes](#)

Other Study ID Numbers: IHL-PRT001

First Submitted: August 11, 2006

First Posted: August 15, 2006

Last Update Posted: January 26, 2012

Last Verified: January 2012

Keywords provided by Yakult Honsha Co., LTD:

Cancer

Advanced Solid Tumor

Oncology

Additional relevant MeSH terms:

Irinotecan

Camptothecin

Antineoplastic Agents, Phytogenic

Antineoplastic Agents

Topoisomerase I Inhibitors

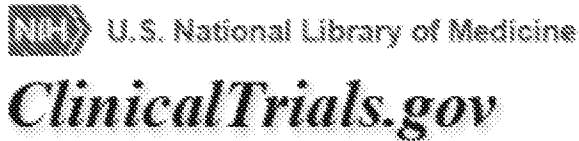
Topoisomerase Inhibitors

Enzyme Inhibitors

Molecular Mechanisms of Pharmacological  
Action

We updated the design of this site on September 25th. [Learn more.](#)

We will be updating this site in phases. This allows us to move faster and to deliver better services. [Show less](#)



- [Find Studies](#) ▼
- [About Studies](#) ▼
- [Submit Studies](#) ▼
- [Resources](#) ▼
- [About Site](#) ▼

## A Phase I Trial of Nanoliposomal CPT-11 (NL CPT-11) in Patients With Recurrent High-Grade Gliomas

This study has been completed.

**Sponsor:**

University of California, San Francisco

**ClinicalTrials.gov Identifier:**

NCT00734682

First Posted: August 14, 2008

Last Update Posted: January 7, 2015

**⚠** The safety and scientific validity of this study is the responsibility of the study sponsor and investigators. Listing a study does not mean it has been evaluated by the U.S. Federal Government. Read our [disclaimer](#) for details.

**Information provided by (Responsible Party):**

Michael Prados, University of California, San Francisco

[Full Text View](#)

[Tabular View](#)

[No Study Results Posted](#)

[Disclaimer](#)

[How to Read a Study Record](#)

### ► Purpose

This is a Phase I study of Nanoliposomal CPT-11 in patients with Recurrent high-grade gliomas. Patients must have a histologically proven intracranial malignant glioma, which includes glioblastoma multiforme (GBM), gliosarcoma (GS), anaplastic astrocytoma (AA), anaplastic oligodendroglioma (AO), anaplastic mixed oligoastrocytoma (AMO), or malignant astrocytoma NOS (not otherwise specified). Patients who are wild type or heterozygous for the UGT1A1\*28 gene will received Nanoliposomal CPT-11. The total

CSPC Exhibit 1094  
Page 287 of 512

anticipated accrual will be approximately 36 patients (depending upon the actual MTD). The investigators hypothesis is that this new formulation of CPT-11 will increase survival over that seen in historical controls who have recurrent gliomas because CPT-11 will be encapsulated in a liposome nanoparticle, which has been seen to reduce toxicities from the drug.

<u>Condition</u>	<u>Intervention</u>	<u>Phase</u>
Glioblastoma Gliosarcoma Anaplastic Astrocytoma Anaplastic Oligodendroglioma	Drug: Nanoliposomal CPT-11	Phase 1

Study Type: Interventional

Study Design: Intervention Model: Single Group Assignment

Masking: None (Open Label)

Primary Purpose: Treatment

Official Title: A Phase I Trial of Nanoliposomal CPT-11 (NL CPT-11) in Patients With Recurrent High-Grade Gliomas

**Resource links provided by NLM:**

Drug Information available for: [Irinotecan](#) [Irinotecan hydrochloride](#)

Genetic and Rare Diseases Information Center resources: [Glioma](#) [Glioblastoma](#) [Gliosarcoma](#) [Anaplastic Astrocytoma](#) [Oligodendroglioma](#) [Oligoastrocytoma](#) [Anaplastic Oligodendroglioma](#) [Neuroepithelioma](#)

U.S. FDA Resources

**Further study details as provided by Michael Prados, University of California, San Francisco:**

Primary Outcome Measures:

- To assess the safety and pharmacokinetics of NL CPT-11 in patients with recurrent malignant glioma stratified based on UGT1A1 genotyping. [ Time Frame: 1-2 years ]

Secondary Outcome Measures:

- To determine the maximum tolerated dose of NL CPT-11 in these patient populations.  
[ Time Frame: 1-2 years ]

Enrollment: 34  
 Study Start Date: August 2008  
 Study Completion Date: December 2014  
 Primary Completion Date: December 2014 (Final data collection date for primary outcome measure)

Arms	Assigned Interventions
<p>Experimental: Nanoliposomal CPT-11</p> <p>All patients are treated with nanoliposomal CPT-11</p>	<p>Drug: Nanoliposomal CPT-11</p> <p>Depending on UGT1A1 genotyping status, patients are either given a starting dose of 120 mg/m<sup>2</sup> (wild type) or 60 mg/m<sup>2</sup> IV q3 weeks.</p> <p>Other Names:</p> <ul style="list-style-type: none"> <li>• NL CPT-11</li> <li>• liposomal irinotecan</li> </ul>

**Detailed Description:**

Patients with recurrent malignant glioma will receive Nanoliposomal CPT-11 at the time of relapse. The dose will be adjusted according to a phase-1 dose escalation scheme. Patients will receive drug intravenously every 3 weeks until tumor progression or excessive toxicity. Weekly follow up will occur to assess toxicities during the DLT phase of the trial. Patients will have different dose escalation if UGT1A1 is 6/6 versus UGT1A1 is 6/7. Patients with UGT 1A1 of 7/7 will not be eligible. All patients must have UGT 1A1 status know as an eligibility requirement. Patients will be followed for both toxicity and progression, and progression will be evaluated by MR imaging every 6 weeks. Pharmacokinetics will be obtained in the first treatment cycle.

**► Eligibility**

**Information from the National Library of Medicine**



*Choosing to participate in a study is an important personal decision. Talk with your doctor and family members or friends about deciding to join a study. To learn more about this study, you or your doctor may contact the*

*study research staff using the contacts provided below. For general information, [Learn About Clinical Studies](#).*

Ages Eligible for Study: 18 Years and older (Adult, Senior)

Sexes Eligible for Study: All

Accepts Healthy Volunteers: No

### Criteria

#### Inclusion Criteria:

- Patients with histologically proven intracranial malignant glioma are eligible . -All patients must sign an informed consent
  - Patients must be > 18 years old, and with a life expectancy > 8 weeks.
  - Patients must have a Karnofsky performance status of > 60.
- Patients must have recovered from the toxic effects of prior therapy
- Patients must have adequate bone marrow function (WBC > 3,000/ $\mu$ l, ANC > 1,500/mm<sup>3</sup>, platelet count of > 100,000/mm<sup>3</sup>, and hemoglobin > 10 gm/dl), adequate liver function (SGOT and bilirubin < 2 times ULN), and adequate renal function (creatinine < 1.5 mg/dL and/or creatinine clearance > 60 cc/min) Patients must have shown radiographic evidence for tumor progression by MRI or CT scan. A scan should be performed within 14 days prior to registration and on a steroid dose that has been stable for at least 5 days. -Patients having undergone recent resection of recurrent or progressive tumor will be eligible as long as all of the following conditions apply:
  - They have recovered from the effects of surgery.
  - Residual disease following resection of recurrent malignant glioma is not mandated for eligibility into the study.
- Patients must have failed prior radiation therapy
- Patients with prior therapy that included interstitial brachytherapy or stereotactic radiosurgery must have confirmation of true progressive disease
- Women of childbearing potential must have a negative  $\beta$ -HCG pregnancy test documented within 14 days prior to registration.
- Patients may have had treatment for any number of prior relapses.

#### Exclusion Criteria:

- Patients must not have any significant medical illnesses that in the investigator opinion cannot be adequately controlled
- Patients with a history of any other cancer (except non-melanoma skin cancer or carcinoma in-situ of the cervix), unless in complete remission and off of all therapy for that disease for a minimum of 3 years are ineligible.
- Patients must not have active infection or serious intercurrent medical illness.
- Patients must not be pregnant/breast feeding and must agree to practice adequate contraception.
- Patients must not have any disease that will obscure toxicity or dangerously alter drug metabolism.
- Patients must not have received prior therapy with irinotecan.
- Patients with 7/7 (homozygous) UGT1A1\*28 genotyping will be excluded from the study.
- Patients receiving enzyme-inducing anticonvulsants or other enzyme inducing drugs are excluded.

## ► Contacts and Locations

### Information from the National Library of Medicine



*To learn more about this study, you or your doctor may contact the study research staff using the contact information provided by the sponsor.*

*Please refer to this study by its ClinicalTrials.gov identifier (NCT number):*

***NCT00734682***

### Locations

#### United States, California

University of California, San Francisco  
San Francisco, California, United States, 94143

### Sponsors and Collaborators

University of California, San Francisco

### Investigators

Principal Investigator: Michael Prados, MD University of California, San Francisco

**► More Information**

Responsible Party: Michael Prados, Professor, University of California, San Francisco  
 ClinicalTrials.gov Identifier: [NCT00734682](#) [History of Changes](#)  
 Obsolete Identifiers: NCT00745082  
 Other Study ID Numbers: 08103  
 First Submitted: August 13, 2008  
 First Posted: August 14, 2008  
 Last Update Posted: January 7, 2015  
 Last Verified: December 2014

Keywords provided by Michael Prados, University of California, San Francisco:

Glioblastoma	Anaplastic Mixed Oligoastrocytoma
Gliosarcoma	Malignant Astrocytoma NOS
Anaplastic Astrocytoma	Nanoliposomal CPT-11
Anaplastic Oligodendroglioma	liposomal irinotecan

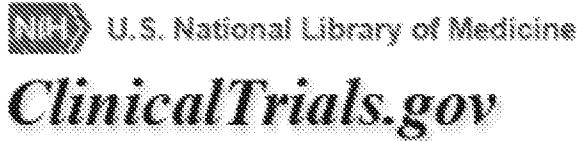
Additional relevant MeSH terms:

Glioblastoma	Neoplasms, Glandular and Epithelial
Astrocytoma	Neoplasms, Nerve Tissue
Gliosarcoma	Irinotecan
Oligodendroglioma	Camptothecin
Glioma	Antineoplastic Agents, Phytogenic
Neoplasms, Neuroepithelial	Antineoplastic Agents
Neuroectodermal Tumors	Topoisomerase I Inhibitors
Neoplasms, Germ Cell and Embryonal	Topoisomerase Inhibitors
Neoplasms by Histologic Type	Enzyme Inhibitors
Neoplasms	Molecular Mechanisms of Pharmacological Action



We updated the design of this site on September 25th. [Learn more.](#)

We will be updating this site in phases. This allows us to move faster and to deliver better services. [Show less](#)



- [Find Studies](#) ▼
- [About Studies](#) ▼
- [Submit Studies](#) ▼
- [Resources](#) ▼
- [About Site](#) ▼

## Study of PEP02, Irinotecan or Docetaxel in Gastric or Gastroesophageal Junction Adenocarcinoma

This study has been completed.

**Sponsor:**  
PharmaEngine

**ClinicalTrials.gov Identifier:**

NCT00813072

First Posted: December 22, 2008

Last Update Posted: March 2, 2012

**⚠** The safety and scientific validity of this study is the responsibility of the study sponsor and investigators. Listing a study does not mean it has been evaluated by the U.S. Federal Government. Read our [disclaimer](#) for details.

**Information provided by (Responsible Party):**

PharmaEngine

[Full Text View](#)

[Tabular View](#)

[No Study Results Posted](#)

[Disclaimer](#)

[How to Read a Study Record](#)

### ► Purpose

The purpose of this study is to assess objective tumor response in the single agent treatment of PEP02, irinotecan, or docetaxel for locally advanced or metastatic gastric or gastroesophageal junction adenocarcinoma

<u>Condition</u>	<u>Intervention</u>	<u>Phase</u>
Stomach Neoplasms	Drug: PEP02	Phase 2
Esophageal Neoplasms	Drug: irinotecan	
	Drug: docetaxel	

Study Type: Interventional  
Study Design: Allocation: Randomized  
Intervention Model: Parallel Assignment  
Masking: None (Open Label)  
Primary Purpose: Treatment

Official Title: A Randomized Phase II Study of PEP02, Irinotecan or Docetaxel as a Second Line Therapy in Patients With Locally Advanced or Metastatic Gastric or Gastroesophageal Junction Adenocarcinoma

**Resource links provided by NLM:**

Drug Information available for: [Irinotecan](#) [Irinotecan hydrochloride](#) [Docetaxel](#)

Genetic and Rare Diseases Information Center resources: [Stomach Cancer](#) [Esophageal Cancer](#)

U.S. FDA Resources

**Further study details as provided by PharmaEngine:**

Primary Outcome Measures:

- objective tumor response

Secondary Outcome Measures:

- progression-free survival, duration of tumor response, time to progression, time to treatment failure, disease control rate, 1-year survival rate, and overall survival; pharmacokinetics and pharmacogenetics of PEP02 and irinotecan

Enrollment: 135  
Study Start Date: November 2007  
Study Completion Date: December 2010

Primary Completion Date: July 2010 (Final data collection date for primary outcome measure)

Arms	Assigned Interventions
Experimental: 1. PEP02 liposome irinotecan	Drug: PEP02 120 mg/m <sup>2</sup> , IV infusion for 90 minutes on day 1 of each 21 day as a treatment cycle. Number of Cycles: until progression or unacceptable toxicity develops. Other Name: liposome irinotecan
Active Comparator: 2. irinotecan	Drug: irinotecan 300 mg/m <sup>2</sup> , IV infusion on day 1 of each 21 day as a treatment cycle. Number of Cycles: until progression or unacceptable toxicity develops. Other Name: Campto
Active Comparator: 3. docetaxel	Drug: docetaxel 75 mg/m <sup>2</sup> , IV infusion for 60 minutes on day 1 of each 21 day as a treatment cycle. Number of Cycles: until progression or unacceptable toxicity develops. Other Name: Taxetere

#### Detailed Description:

Palliative chemotherapy has been shown to improve survival compared with best supportive care alone in patients with unresectable or recurrent gastric cancer. There is no standard second-line chemotherapy for advanced gastric cancer and no randomized-controlled trial data suggest a benefit of second-line chemotherapy compared with supportive care alone. Response rates of second-line therapy in phase II trials are similar to those seen for other cancers that are more commonly retreated. Combination therapy may achieve higher response rates than single agents, however, the survival outcome are the same. In addition, data suggest that patients may obtain symptomatic benefits from second-line therapy. In comparison to the toxicity profile of single agent with combination regimen, patients are more tolerable to single agent therapy than combination.

Based on the previous clinical experience in second line chemotherapy of advanced gastric cancer, the single agent of PEP02, irinotecan and docetaxel are selected as the regimens for this

randomized phase II study. The efficacy and toxicity outcome of the three-arm design will be a valuable reference for future combination therapy or phase III study design.

## ► Eligibility

### Information from the National Library of Medicine



*Choosing to participate in a study is an important personal decision. Talk with your doctor and family members or friends about deciding to join a study. To learn more about this study, you or your doctor may contact the study research staff using the contacts provided below. For general information, [Learn About Clinical Studies](#).*

Ages Eligible for Study: 18 Years and older (Adult, Senior)

Sexes Eligible for Study: All

Accepts Healthy Volunteers: No

### Criteria

#### Inclusion Criteria:

- Histologically or cytologically confirmed locally advanced (unresectable) or metastatic adenocarcinoma of gastric or gastroesophageal junction
- Failed to only one systemic chemotherapy for locally advanced or metastatic disease, including patients whose diseases recur within 6 months after (neo)adjuvant chemotherapy. Chemotherapy administered with concurrent radiotherapy is NOT considered as systemic chemotherapy.
- Have at least one measurable lesion according to the RECIST criteria
- Aged above or equal to 18 years, at the time of acquisition of informed consent
- With ECOG performance status 0, 1, or 2
- Life expectancy equal to or more than 3 months
- With adequate organ and marrow function as defined below:
- With ability to understand and the willingness to sign a written Informed Consent Form

#### Exclusion Criteria:

- Had systemic chemotherapy within 3 weeks before the commencement of study treatment
- Had radiotherapy within 4 weeks before the commencement of study treatment

- With known brain metastasis
- With active multiple cancers or had treatment for other carcinomas within the last five years, except cured non-melanoma skin and treated in-situ cervical cancer
- With prior irinotecan or taxane (paclitaxel, docetaxel) treatment
- Have received irradiation affecting > 30% of the active bone marrow
- Had major surgery within 4 weeks of the start of study treatment (laparotomy, line placement is not considered major surgery)
- Have not recovered from prior treatments
- With preexisting peripheral neuropathy > grade 2
- With history of allergic reaction to liposome product or other drugs formulated with polysorbate
- With uncontrolled intercurrent illness including, but not limited to, ongoing or active infection, symptomatic congestive heart failure, active gastrointestinal bleeding, watery stools, central nervous system disorders or psychiatric illness/social situation that would limit compliance with study requirements or judged to be ineligible for the study by the investigator
- Have received any investigational agents within 3 weeks preceding the start of study treatment
- Pregnant or breastfeeding females (a pregnancy test must be performed on all female patients who are of child-bearing potential before entering the study, and the result must be negative)
- With intestinal obstruction
- Have received St. John's Wort, CYP3A4 inducing anticonvulsants (phenytoin, phenobarbital, and carbamazepine), rifampin and rifabutin within two weeks, or ketoconazole, itraconazole, troleandomycin, erythromycin, diltiazem and verapamil within one week before the administration of study medications

## ► Contacts and Locations

### Information from the National Library of Medicine



*To learn more about this study, you or your doctor may contact the study research staff using the contact information provided by the sponsor.*

*Please refer to this study by its ClinicalTrials.gov identifier (NCT number):*

**NCT00813072**

## Locations

### **Bosnia and Herzegovina**

Clinical Hospital Mostar  
Mostar, Bosnia and Herzegovina, 36 000

Clinical Centre University of Sarajevo  
Sarajevo, Bosnia and Herzegovina, 71 000

### **Croatia**

University Hospital Centre Rijeka  
Rijeka, Croatia, 51 000

University Hospital Centre Dubrava  
Zagreb, Croatia, 10 000

University Hospital Centre Zagreb  
Zagreb, Croatia, 10 000

### **Korea, Republic of**

Samsung Medical Center  
Seoul, Korea, Republic of, 135-710

Asan Medical Center  
Seoul, Korea, Republic of, 138-736

National Cancer Center  
Seoul, Korea, Republic of, 410-769

### **Spain**

Hospital Universitario Vall d'Hebron  
Barcelona, Spain, 08035

Hospital General Universitario de Elche  
Elche, Spain, 03203

Hospital Clínico San Carlos  
Madrid, Spain, 28040

Hospital Universitario Marques de Valdecilla  
Santander, Spain, 39008

### Taiwan

Chang Gung Memorial Hospital - Chiayi  
Chiayi, Taiwan

Chang Gung Memorial Hospital - LinKou  
LinKou, Taiwan

National Cheng Kung University Hospital  
Tainan, Taiwan, 704

Taipei Veterans General Hospital  
Taipei, Taiwan, 112

Mackay Memorial Hospital  
Taipei, Taiwan, 25115

### United Kingdom

Addenbrookes Hospital Oncology Center  
Cambridge, United Kingdom, CB2 2QQ

Guy's & St Thomas' NHS Foundation Trust  
London, United Kingdom, SE19RT

Kent Oncology Centre, Maidstone Hospital  
Maidstone, United Kingdom, ME16 9QQ

Southampton University Hospital  
Southampton, United Kingdom, SO16 6YD

The Royal Marsden Hospital  
Surrey, United Kingdom, SM2 5PT

### Sponsors and Collaborators

PharmaEngine

### Investigators

Principal Investigator: David Cunningham The Royal Marsden Hospital, London & Surrey, UK



### ▶ More Information

Publications automatically indexed to this study by ClinicalTrials.gov Identifier (NCT Number):

Roy AC, Park SR, Cunningham D, Kang YK, Chao Y, Chen LT, Rees C, Lim HY, Tabernero J, Ramos FJ, Kujundzic M, Cardic MB, Yeh CG, de Gramont A. A randomized phase II study of PEP02 (MM-398), irinotecan or docetaxel as a second-line therapy in patients with locally advanced or metastatic gastric or gastro-oesophageal junction adenocarcinoma. Ann Oncol. 2013 Jun;24(6):1567-73. doi: 10.1093/annonc/mdt002. Epub 2013 Feb 13.

Responsible Party: PharmaEngine  
 ClinicalTrials.gov Identifier: [NCT00813072](#) [History of Changes](#)  
 Other Study ID Numbers: PEP0206  
 EudraCT number: 2006-006452-35  
 First Submitted: December 18, 2008  
 First Posted: December 22, 2008  
 Last Update Posted: March 2, 2012  
 Last Verified: March 2012

Keywords provided by PharmaEngine:

Gastric Cancer	randomization
Stomach Cancer	randomisation
Gastroesophageal	adenocarcinoma
Gastroesophageal Junction	locally advanced
Esophageal Cancer	metastatic
phase II	simon's two
PEP02	

Additional relevant MeSH terms:

Neoplasms	Esophageal Diseases
Adenocarcinoma	Docetaxel
Stomach Neoplasms	Irinotecan
Esophageal Neoplasms	Camptothecin
Carcinoma	Antineoplastic Agents
Neoplasms, Glandular and Epithelial	Tubulin Modulators
Neoplasms by Histologic Type	Antimitotic Agents
Gastrointestinal Neoplasms	Mitosis Modulators
Digestive System Neoplasms	Molecular Mechanisms of Pharmacological Action
Neoplasms by Site	Antineoplastic Agents, Phytogetic
Digestive System Diseases	Topoisomerase I Inhibitors
Gastrointestinal Diseases	



Stomach Diseases

Head and Neck Neoplasms

Topoisomerase Inhibitors

Enzyme Inhibitors

# ClinicalTrials.gov archive

A service of the U.S. National Institutes of Health

Developed by the National Library of Medicine

[← History of this study](#)    [↑ Current version of this study](#)

## View of NCT01770353 on 2013\_08\_09

**ClinicalTrials Identifier:** NCT01770353**Updated:** 2013\_08\_09

### Descriptive Information

**Brief title** Pilot Study to Determine Biodistribution of MM-398 and Feasibility of Ferumoxytol as a Tumor Imaging Agent

**Official title** A Pilot Study in Patients Treated With MM-398 to Determine Tumor Drug Levels and to Evaluate the Feasibility of Ferumoxytol Magnetic Resonance Imaging to Measure Tumor Associated Macrophages

#### Brief summary

This is a Phase I Pilot study to understand the biodistribution of MM-398 and to determine the feasibility of using Ferumoxytol as a tumor imaging agent.

#### Detailed description

**Phase** Phase 1

**Study type** Interventional

**Study design** Other

**Study design** Open Label

**Study design** Single Group Assignment

**Study design** Pharmacokinetics Study

**Primary outcome** Measure: Measure tumor levels of irinotecan and SN-38 (in ng/mL)  
Time Frame: 12 months  
Safety Issue? No

**Secondary outcome** Measure: Safety profile of MM-398 in the presence of ferumoxytol (number and type of Adverse Events compared with histological control)  
Time Frame: 12 months  
Safety Issue? No

**Secondary outcome** Measure: Tumor response Rate measured by RECIST (Response Evaluation Criteria in Solid Tumors) 1.1 guidelines  
Time Frame: 12 months  
Safety Issue? No

**Secondary outcome** Measure: Half-life of the drug (t 1/2) in number of hours  
Time Frame: 12 months  
Safety Issue? No  
Description:

	50% of total time of drug in plasma
<b>Secondary outcome</b>	Measure: Maximum concentration of drug in plasma (Cmax) in ng/mL Time Frame: 12 months Safety Issue? No
<b>Secondary outcome</b>	Measure: Measure of drug availability in the plasma (AUC) in ng/mL x hours Time Frame: 12 months Safety Issue? No Description:
<b>Enrollment</b>	Area under the plasma drug concentration versus time curve 12 (Anticipated)
<b>Condition</b>	Solid Tumors
<b>Condition</b>	Triple Negative Breast Cancer
<b>Condition</b>	Non Small Cell Lung Cancer
<b>Condition</b>	Colorectal Cancer
<b>Condition</b>	ER/PR Positive Breast Cancer
<b>Condition</b>	Pancreatic Cancer
<b>Condition</b>	Ovarian Cancer
<b>Condition</b>	Gastric Cancer
<b>Condition</b>	Gastro-Esophageal Junction Adenocarcinoma
<b>Condition</b>	Head and Neck Cancer
<b>Arm/Group</b>	Arm Label: Ferumoxytol followed by MM-398 Experimental
	Ferumoxytol 5 mg/kg IV at the rate of 1 mL/sec, given once on Day 1. MM-398 80 mg/m <sup>2</sup> IV over 90 min on Days 1 and 15 of every 4 weekly cycle
<b>Intervention</b>	Drug: Ferumoxytol followed by MM-398      Arm Label: Ferumoxytol followed by MM-398
	Ferumoxytol 5 mg/kg IV at 1mL/sec, given once. MM-398 80 mg/m <sup>2</sup> IV over 90 min every 2 weeks, until progressive disease or intolerable toxicity

---

## Recruitment Information

<b>Status</b>	Recruiting
<b>Start date</b>	2012-11
<b>Last follow-up date</b>	2013-11 (Anticipated)
<b>Primary completion date</b>	2013-11 (Anticipated)
<b>Criteria</b>	

**Inclusion Criteria:**

- Pathologically confirmed diagnosis of solid tumors, CRC, TNBC, ER/PR Breast Cancer, NSCLC, Pancreatic Cancer, Ovarian Cancer, Gastric Cancer, GEJ adenocarcinoma, Head and Neck Cancer
- Metastatic disease
- ECOG Performance Status 0 to 2
- Adequate bone marrow, hepatic and renal function
- Normal ECG
- 18 years of age or above
- Able to understand and sign informed consent

**Exclusion Criteria:**

- Active CNS metastasis
- Clinically significant GI disorders
- Prior irinotecan or bevacizumab therapy within last 6 months
- Known hypersensitivity to MM-398 or ferumoxytol
- Inability to undergo MRI
- Active infection
- Pregnant or breast feeding

<b>Gender</b>	Both
<b>Minimum age</b>	18 Years
<b>Healthy volunteers</b>	No

---

**Administrative Data**

<b>Organization name</b>	Merrimack Pharmaceuticals
<b>Organization study ID</b>	MM-398-01-01-02
<b>Sponsor</b>	Merrimack Pharmaceuticals
<b>Health Authority</b>	United States: Food and Drug Administration

# ClinicalTrials.gov archive

A service of the U.S. National Institutes of Health

Developed by the National Library of Medicine

[← History of this study](#)    [↑ Current version of this study](#)

## View of NCT01770353 on 2015\_04\_26

**ClinicalTrials Identifier:** NCT01770353**Updated:** 2015\_04\_26

---

### Descriptive Information

**Brief title** Pilot Study to Determine Biodistribution of MM-398 and Feasibility of Ferumoxytol as a Tumor Imaging Agent**Official title** A Pilot Study in Patients Treated With MM-398 to Determine Tumor Drug Levels and to Evaluate the Feasibility of Ferumoxytol Magnetic Resonance Imaging to Measure Tumor Associated Macrophages**Brief summary**

This is a Phase I Pilot study to understand the biodistribution of MM-398 and to determine the feasibility of using Ferumoxytol as a tumor imaging agent.

**Detailed description**

This study will enroll approximately 12 patients, up to 20 in total in the Pilot Phase and 30 patients in the Expansion Phase. The first three patients that are enrolled can have any solid tumor type; however subsequent patients must have NSCLC, CRC, TNBC, ER/PR positive breast cancer, pancreatic cancer, ovarian cancer, gastric cancer, gastro-oesophageal junction adenocarcinoma or head and neck cancer. No more than three patients with ER/PR positive breast cancer can be enrolled in the Pilot Phase and similar restrictions may be placed on other tumor types to ensure a heterogeneous population.

An Expansion Phase will enroll cohorts of single indications of patients with metastatic breast cancer in 3 cohorts:

Cohort 1: ER and/or PR-positive breast cancer

Cohort 2: TNBC

Cohort 3: BC with active brain metastasis

<b>Phase</b>	Phase 1
<b>Study type</b>	Interventional
<b>Study design</b>	Other
<b>Study design</b>	Non-Randomized
<b>Study design</b>	Open Label
<b>Study design</b>	Single Group Assignment
<b>Study design</b>	Pharmacokinetics Study
<b>Primary outcome</b>	Measure: Measure tumor levels of irinotecan and SN-38 (in ng/mL)

	Time Frame: 12 months Safety Issue? No
<b>Secondary outcome</b>	Measure: Safety profile of MM-398 in the presence of ferumoxytol (number and type of Adverse Events compared with histological control) Time Frame: 12 months Safety Issue? No
<b>Secondary outcome</b>	Measure: Tumor response Rate measured by RECIST (Response Evaluation Criteria in Solid Tumors) 1.1 guidelines Time Frame: 12 months Safety Issue? No
<b>Secondary outcome</b>	Measure: Half-life of the drug (t 1/2) in number of hours Time Frame: 12 months Safety Issue? No Description:
	50% of total time of drug in plasma
<b>Secondary outcome</b>	Measure: Maximum concentration of drug in plasma (Cmax) in ng/mL Time Frame: 12 months Safety Issue? No
<b>Secondary outcome</b>	Measure: Measure of drug availability in the plasma (AUC) in ng/mL x hours Time Frame: 12 months Safety Issue? No Description:
	Area under the plasma drug concentration versus time curve
<b>Enrollment</b>	45 (Anticipated)
<b>Condition</b>	Solid Tumors
<b>Condition</b>	Triple Negative Breast Cancer
<b>Condition</b>	Non Small Cell Lung Cancer
<b>Condition</b>	Colorectal Cancer
<b>Condition</b>	ER/PR Positive Breast Cancer
<b>Condition</b>	Pancreatic Cancer
<b>Condition</b>	Ovarian Cancer
<b>Condition</b>	Gastric Cancer
<b>Condition</b>	Gastro-Esophageal Junction Adenocarcinoma
<b>Condition</b>	Head and Neck Cancer
<b>Arm/Group</b>	Arm Label: Pilot Phase: Ferumoxytol followed by MM-398      Experimental
	Ferumoxytol 5 mg/kg IV at the rate of 1 mL/sec, given once on Day 1.

<b>Arm/Group</b>	MM-398 80 mg/m <sup>2</sup> IV over 90 min on Days 1 and 15 of every 4 weekly cycle Arm Label: Expansion Phase: Ferumoxytol followed by MM-398      Experimental
<b>Intervention</b>	Ferumoxytol 5 mg/kg IV at the rate of 1 mL/sec, given once on Day 1. MM-398 80 mg/m <sup>2</sup> IV over 90 min on Days 1 and 15 of every 4 weekly cycle Cohort 1: ER and/or PR-positive breast cancer Cohort 2: TNBC Cohort 3: BC with active brain metastasis Drug: Ferumoxytol followed by MM-398      Arm Label: Pilot Phase: Ferumoxytol followed by MM-398  Ferumoxytol 5 mg/kg IV at 1mL/sec, given once. MM-398 80 mg/m <sup>2</sup> IV over 90 min every 2 weeks, until progressive disease or intolerable toxicity

---

## Recruitment Information

<b>Status</b>	Recruiting
<b>Start date</b>	2012-11
<b>Last follow-up date</b>	2016-03 (Anticipated)
<b>Primary completion date</b>	2016-01 (Anticipated)

### Criteria

#### Inclusion Criteria:

- Pathologically confirmed diagnosis of solid tumors, CRC, TNBC, ER/PR Breast Cancer, NSCLC, Pancreatic Cancer, Ovarian Cancer, Gastric Cancer, GEJ adenocarcinoma, Head and Neck Cancer
- Metastatic disease
- ECOG Performance Status 0 to 2
- Adequate bone marrow, hepatic and renal function
- Normal ECG
- 18 years of age or above
- Able to understand and sign informed consent

#### Expansion Phase Additional Criteria:

The following invasive breast cancer tumor sub-types are required:

- Cohort 1: hormone receptor positive breast cancer patients with ER-positive and/or PR-positive tumors defined as  $\geq 1\%$  of tumor nuclei that are immunoreactive for ER and/or PR and HER2 negative
- Cohort 2: triple negative breast cancer (TNBC) patients with ER-negative, PR-negative tumors defined as  $< 1\%$  of tumor nuclei that are immunoreactive for ER and PR and HER2 negative
- Cohort 3: Any sub-type of metastatic breast cancer and active brain metastases

- Documented metastatic disease with at least two radiologically measurable lesions as defined by RECIST v1.1 (except Cohort 3, see inclusion criterion o below)
  - Received at least one cytotoxic therapy in the metastatic setting, with exception of TNBC patients who progressed within 12 months of adjuvant therapy
  - Received  $\leq 3$  prior lines of chemotherapy in the metastatic setting (no limit to prior lines of hormonal therapy in Cohort 1)
  - At least one lesion amenable to multiple pass core biopsy (exception: Cohort 3 patients)
- Expansion Phase Cohort 3 additional inclusion criteria:
- Radiographic evidence of new or progressive brain metastases after prior radiation therapy with at least one brain metastasis measuring  $\geq 1$  cm in longest diameter on gadolinium-enhanced MRI (note: progressive brain lesions are not required to meet RECIST criteria in order to be eligible; extra-cranial metastatic disease is also allowed)

Exclusion Criteria:

- Active CNS metastasis (applies to pilot phase and expansion phase cohort 1 and 2 only)
- Clinically significant GI disorders
- Prior irinotecan or bevacizumab therapy within last 6 months
- Known hypersensitivity to MM-398 or ferumoxytol
- Inability to undergo MRI
- Active infection
- Pregnant or breast feeding

<b>Gender</b>	Both
<b>Minimum age</b>	18 Years
<b>Healthy volunteers</b>	No

---

### Administrative Data

<b>Organization name</b>	Merrimack Pharmaceuticals
<b>Organization study ID</b>	MM-398-01-01-02
<b>Sponsor</b>	Merrimack Pharmaceuticals
<b>Health Authority</b>	United States: Food and Drug Administration



# ClinicalTrials.gov archive

A service of the U.S. National Institutes of Health

Developed by the National Library of Medicine

[← History of this study](#)    [↑ Current version of this study](#)

## View of NCT01770353 on 2015\_05\_06

**ClinicalTrials Identifier:** NCT01770353**Updated:** 2015\_05\_06

---

### Descriptive Information

**Brief title** Pilot Study to Determine Biodistribution of MM-398 and Feasibility of Ferumoxytol as a Tumor Imaging Agent**Official title** A Pilot Study in Patients Treated With MM-398 to Determine Tumor Drug Levels and to Evaluate the Feasibility of Ferumoxytol Magnetic Resonance Imaging to Measure Tumor Associated Macrophages**Brief summary**

This is a Phase I Pilot study to understand the biodistribution of MM-398 and to determine the feasibility of using Ferumoxytol as a tumor imaging agent.

**Detailed description**

This study is conducted over two phases. The pilot phase of this trial is closed. The expansion phase of this trial is currently open to enrollment.

**Pilot Phase:** This study will enroll approximately 12 patients, up to 20 in total in the Pilot Phase and 30 patients in the Expansion Phase. The first three patients that are enrolled can have any solid tumor type; however subsequent patients must have NSCLC, CRC, TNBC, ER/PR positive breast cancer, pancreatic cancer, ovarian cancer, gastric cancer, gastro-oesophageal junction adenocarcinoma or head and neck cancer. No more than three patients with ER/PR positive breast cancer can be enrolled in the Pilot Phase and similar restrictions may be placed on other tumor types to ensure a heterogeneous population.

**Expansion Phase:** The expansion will enroll cohorts of single indications of patients with metastatic breast cancer in 3 cohorts:

Cohort 1: ER and/or PR-positive breast cancer

Cohort 2: TNBC

Cohort 3: BC with active brain metastasis

<b>Phase</b>	Phase 1
<b>Study type</b>	Interventional
<b>Study design</b>	Other
<b>Study design</b>	Non-Randomized
<b>Study design</b>	Open Label

<b>Study design</b>	Single Group Assignment
<b>Study design</b>	Pharmacokinetics Study
<b>Primary outcome</b>	Measure: Measure tumor levels of irinotecan and SN-38 (in ng/mL) Time Frame: 12 months Safety Issue? No
<b>Secondary outcome</b>	Measure: Safety profile of MM-398 in the presence of ferumoxytol (number and type of Adverse Events compared with histological control) Time Frame: 12 months Safety Issue? No
<b>Secondary outcome</b>	Measure: Tumor response Rate measured by RECIST (Response Evaluation Criteria in Solid Tumors) 1.1 guidelines Time Frame: 12 months Safety Issue? No
<b>Secondary outcome</b>	Measure: Half-life of the drug (t 1/2) in number of hours Time Frame: 12 months Safety Issue? No Description:
<b>Secondary outcome</b>	50% of total time of drug in plasma Measure: Maximum concentration of drug in plasma (Cmax) in ng/mL Time Frame: 12 months Safety Issue? No
<b>Secondary outcome</b>	Measure: Measure of drug availability in the plasma (AUC) in ng/mL x hours Time Frame: 12 months Safety Issue? No Description:
<b>Enrollment</b>	45 (Anticipated)
<b>Condition</b>	Solid Tumors
<b>Condition</b>	Triple Negative Breast Cancer
<b>Condition</b>	ER/PR Positive Breast Cancer
<b>Condition</b>	Metastatic Breast Cancer With Active Brain Metastasis
<b>Arm/Group</b>	Arm Label: Pilot Phase: Ferumoxytol followed by MM-398 (closed)      Experimental
<b>Arm/Group</b>	Ferumoxytol 5 mg/kg IV at the rate of 1 mL/sec, given once on Day 1. MM-398 80 mg/m <sup>2</sup> IV over 90 min on Days 1 and 15 of every 4 weekly cycle

<b>Intervention</b>	Arm Label: Expansion Phase: Ferumoxytol followed by MM-398      Experimental
	Ferumoxytol 5 mg/kg IV at the rate of 1 mL/sec, given once on Day 1. MM-398 80 mg/m <sup>2</sup> IV over 90 min on Days 1 and 15 of every 4 weekly cycle Cohort 1: ER and/or PR-positive breast cancer Cohort 2: TNBC Cohort 3: BC with active brain metastasis
	Drug: Ferumoxytol followed by MM-398      Arm Label: Pilot Phase: Ferumoxytol followed by MM-398 (closed)
	Ferumoxytol 5 mg/kg IV at 1mL/sec, given once. MM-398 80 mg/m <sup>2</sup> IV over 90 min every 2 weeks, until progressive disease or intolerable toxicity

---

## Recruitment Information

<b>Status</b>	Recruiting
<b>Start date</b>	2012-11
<b>Last follow-up date</b>	2016-03 (Anticipated)
<b>Primary completion date</b>	2016-01 (Anticipated)

### Criteria

#### Inclusion Criteria:

- Pathologically confirmed diagnosis of solid tumors, CRC, TNBC, ER/PR Breast Cancer, NSCLC, Pancreatic Cancer, Ovarian Cancer, Gastric Cancer, GEJ adenocarcinoma, Head and Neck Cancer
- Metastatic disease
- ECOG Performance Status 0 to 2
- Adequate bone marrow, hepatic and renal function
- Normal ECG
- 18 years of age or above
- Able to understand and sign informed consent

#### Expansion Phase Additional Criteria:

The following invasive breast cancer tumor sub-types are required:

- Cohort 1: hormone receptor positive breast cancer patients with ER-positive and/or PR-positive tumors defined as  $\geq 1\%$  of tumor nuclei that are immunoreactive for ER and/or PR and HER2 negative
- Cohort 2: triple negative breast cancer (TNBC) patients with ER-negative, PR-negative tumors defined as  $< 1\%$  of tumor nuclei that are immunoreactive for ER and PR and HER2 negative
- Cohort 3: Any sub-type of metastatic breast cancer and active brain metastases
- Documented metastatic disease with at least two radiologically measurable lesions as defined by RECIST v1.1 (except Cohort 3, see inclusion criterion o

below)

- Received at least one cytotoxic therapy in the metastatic setting, with exception of TNBC patients who progressed within 12 months of adjuvant therapy
- Received  $\leq 3$  prior lines of chemotherapy in the metastatic setting (no limit to prior lines of hormonal therapy in Cohort 1)
- At least one lesion amenable to multiple pass core biopsy (exception: Cohort 3 patients)

Expansion Phase Cohort 3 additional inclusion criteria:

- Radiographic evidence of new or progressive brain metastases after prior radiation therapy with at least one brain metastasis measuring  $\geq 1$  cm in longest diameter on gadolinium-enhanced MRI (note: progressive brain lesions are not required to meet RECIST criteria in order to be eligible; extra-cranial metastatic disease is also allowed)

Exclusion Criteria:

- Active CNS metastasis (applies to pilot phase and expansion phase cohort 1 and 2 only)
- Clinically significant GI disorders
- Prior irinotecan or bevacizumab therapy within last 6 months
- Known hypersensitivity to MM-398 or ferumoxytol
- Inability to undergo MRI
- Active infection
- Pregnant or breast feeding

<b>Gender</b>	Both
<b>Minimum age</b>	18 Years
<b>Healthy volunteers</b>	No

---

### Administrative Data

<b>Organization name</b>	Merrimack Pharmaceuticals
<b>Organization study ID</b>	MM-398-01-01-02
<b>Sponsor</b>	Merrimack Pharmaceuticals
<b>Health Authority</b>	United States: Food and Drug Administration

# ClinicalTrials.gov archive

A service of the U.S. National Institutes of Health

Developed by the National Library of Medicine

[← History of this study](#)    [↑ Current version of this study](#)

## View of NCT01770353 on 2016\_03\_22

**ClinicalTrials Identifier:** NCT01770353**Updated:** 2016\_03\_22

---

### Descriptive Information

**Brief title** Pilot Study to Determine Biodistribution of MM-398 and Feasibility of Ferumoxytol as a Tumor Imaging Agent

**Official title** A Pilot Study in Patients Treated With MM-398 to Determine Tumor Drug Levels and to Evaluate the Feasibility of Ferumoxytol Magnetic Resonance Imaging to Measure Tumor Associated Macrophages and to Predict Patient Response to Treatment

#### Brief summary

This is a Phase I Pilot study to understand the biodistribution of MM-398 and to determine the feasibility of using Ferumoxytol as a tumor imaging agent.

#### Detailed description

This study is conducted over two phases. The pilot phase of this trial is closed. The expansion phase of this trial is currently open to enrollment.

**Pilot Phase:** This study will enroll approximately 12 patients, up to 20 in total in the Pilot Phase and 30 patients in the Expansion Phase. The first three patients that are enrolled can have any solid tumor type; however subsequent patients must have NSCLC, CRC, TNBC, ER/PR positive breast cancer, pancreatic cancer, ovarian cancer, gastric cancer, gastro-oesophageal junction adenocarcinoma or head and neck cancer. No more than three patients with ER/PR positive breast cancer can be enrolled in the Pilot Phase and similar restrictions may be placed on other tumor types to ensure a heterogeneous population.

**Expansion Phase:** The expansion will enroll patients with advanced metastatic breast cancer into three cohorts:

Cohort 1: ER and/or PR-positive breast cancer

Cohort 2: TNBC

Cohort 3: BC with active brain metastasis

<b>Phase</b>	Phase 1
<b>Study type</b>	Interventional
<b>Study design</b>	Other
<b>Study design</b>	Non-Randomized
<b>Study design</b>	Open Label

<b>Study design</b>	Single Group Assignment
<b>Study design</b>	Pharmacokinetics Study
<b>Primary outcome</b>	Measure: Measure tumor levels of irinotecan and SN-38 (in ng/mL) Time Frame: 12 months Safety Issue? No
<b>Secondary outcome</b>	Measure: Safety profile of MM-398 in the presence of ferumoxytol (number and type of Adverse Events compared with histological control) Time Frame: 12 months Safety Issue? No
<b>Secondary outcome</b>	Measure: Tumor response Rate measured by RECIST (Response Evaluation Criteria in Solid Tumors) 1.1 guidelines Time Frame: 12 months Safety Issue? No
<b>Secondary outcome</b>	Measure: Half-life of the drug (t 1/2) in number of hours Time Frame: 12 months Safety Issue? No Description:
<b>Secondary outcome</b>	50% of total time of drug in plasma Measure: Maximum concentration of drug in plasma (Cmax) in ng/mL Time Frame: 12 months Safety Issue? No
<b>Secondary outcome</b>	Measure: Measure of drug availability in the plasma (AUC) in ng/mL x hours Time Frame: 12 months Safety Issue? No Description:
<b>Enrollment</b>	45 (Anticipated)
<b>Condition</b>	Solid Tumors
<b>Condition</b>	ER/PR Positive Breast Cancer
<b>Condition</b>	Triple Negative Breast Cancer
<b>Condition</b>	Metastatic Breast Cancer With Active Brain Metastasis
<b>Arm/Group</b>	Arm Label: Pilot Phase: Ferumoxytol followed by MM-398 (CLOSED)      Experimental
<b>Arm/Group</b>	Ferumoxytol 5 mg/kg IV at the rate of 1 mL/sec, given once on Day 1. MM-398 80 mg/m <sup>2</sup> IV over 90 min on Days 1 and 15 of every 4 week cycle

<b>Intervention</b>	<p>Arm Label: Expansion Phase: Ferumoxytol followed by MM-398      Experimental</p> <p>Ferumoxytol 5 mg/kg IV at the rate of 1 mL/sec, given once on Day 1. MM-398 80 mg/m<sup>2</sup> IV over 90 min on Days 1 and 15 of every 4 week cycle Cohort 1: ER and/or PR-positive BC Cohort 2: TNBC Cohort 3: BC with active brain metastasis</p> <p>Drug: Ferumoxytol followed by MM-398      Arm Label: Pilot Phase: Ferumoxytol followed by MM-398 (CLOSED)</p> <p>Ferumoxytol 5 mg/kg IV at 1mL/sec, given once. MM-398 80 mg/m<sup>2</sup> IV over 90 min every 2 weeks, until progressive disease or intolerable toxicity</p>
---------------------	--

---

## Recruitment Information

<b>Status</b>	Recruiting
<b>Start date</b>	2012-11
<b>Last follow-up date</b>	2017-10 (Anticipated)
<b>Primary completion date</b>	2017-06 (Anticipated)

### Criteria

#### Inclusion Criteria:

- Pathologically confirmed diagnosis of solid tumors, CRC, TNBC, ER/PR Breast Cancer, NSCLC, Pancreatic Cancer, Ovarian Cancer, Gastric Cancer, GEJ adenocarcinoma, Head and Neck Cancer
- Metastatic disease
- ECOG Performance Status 0 to 2
- Adequate bone marrow, hepatic and renal function
- Normal ECG
- 18 years of age or above
- Able to understand and sign informed consent

#### Expansion Phase Additional Criteria:

The following invasive breast cancer tumor sub-types are required:

- Cohort 1: hormone receptor positive breast cancer patients with ER-positive and/or PR-positive tumors defined as  $\geq 1\%$  of tumor nuclei that are immunoreactive for ER and/or PR and HER2 negative
- Cohort 2: triple negative breast cancer (TNBC) patients with ER-negative, PR-negative tumors defined as  $< 1\%$  of tumor nuclei that are immunoreactive for ER and PR and HER2 negative
- Cohort 3: Any sub-type of metastatic breast cancer and active brain metastases
- Documented metastatic disease with at least two radiologically measurable lesions as defined by RECIST v1.1 (except Cohort 3, see inclusion criterion o

below)

- Received at least one cytotoxic therapy in the metastatic setting, with exception of TNBC patients who progressed within 12 months of adjuvant therapy
- Received  $\leq 3$  prior lines of chemotherapy in the metastatic setting (no limit to prior lines of hormonal therapy in Cohort 1)
- At least one lesion amenable to multiple pass core biopsy (exception: Cohort 3 patients)

Expansion Phase Cohort 3 additional inclusion criteria:

- Radiographic evidence of new or progressive brain metastases after prior radiation therapy with at least one brain metastasis measuring  $\geq 1$  cm in longest diameter on gadolinium-enhanced MRI (note: progressive brain lesions are not required to meet RECIST criteria in order to be eligible; extra-cranial metastatic disease is also allowed)

Exclusion Criteria:

- Active CNS metastasis (applies to pilot phase and expansion phase cohort 1 and 2 only)
- Clinically significant GI disorders
- Prior irinotecan or bevacizumab therapy within last 6 months
- Known hypersensitivity to MM-398 or ferumoxytol
- Inability to undergo MRI
- Active infection
- Pregnant or breast feeding

<b>Gender</b>	Both
<b>Minimum age</b>	18 Years
<b>Healthy volunteers</b>	No

---

### Administrative Data

<b>Organization name</b>	Merrimack Pharmaceuticals
<b>Organization study ID</b>	MM-398-01-01-02
<b>Sponsor</b>	Merrimack Pharmaceuticals
<b>Health Authority</b>	United States: Food and Drug Administration



**ClinicalTrials.gov**

A service of the U.S. National Institutes of Health

Try our beta test site

Trial record **1 of 1** for: Pilot Study to Determine Biodistribution of MM-398 and Feasibility of Ferumoxytol as a Tumor Imaging Agent[Previous Study](#) | [Return to List](#) | [Next Study](#)**Pilot Study to Determine Biodistribution of MM-398 and Feasibility of Ferumoxytol as a Tumor Imaging Agent**This study is currently recruiting participants. (see [Contacts and Locations](#))

Verified July 2016 by Merrimack Pharmaceuticals

**Sponsor:**Merrimack **Pharmaceuticals****Information provided by (Responsible Party):**

Merrimack Pharmaceuticals

**ClinicalTrials.gov Identifier:**

NCT01770353

First received: December 19, 2012

Last updated: July 7, 2016

Last verified: July 2016

[History of Changes](#)[Full Text View](#)[Tabular View](#)[No Study Results Posted](#)[Disclaimer](#)[How to Read a Study Record](#)**Purpose**This is a Phase I **Pilot study** to understand the **biodistribution of MM-398** and to **determine** the **feasibility** of using **Ferumoxytol as a tumor imaging agent**.

Condition	Intervention	Phase
Solid <b>Tumors</b> ER/PR Positive Breast <b>Cancer</b> Triple Negative Breast <b>Cancer</b> Metastatic Breast <b>Cancer</b> With Active Brain Metastasis	<b>Drug: Ferumoxytol</b> followed by <b>MM-398</b>	Phase 1

Study Type: **Interventional**Study Design: **Allocation: Non-Randomized****Intervention Model: Single Group Assignment****Masking: Open Label**Official Title: **A Pilot Study** in Patients Treated With **MM-398** to **Determine Tumor Drug** Levels and to Evaluate the **Feasibility of Ferumoxytol** Magnetic Resonance **Imaging** to Measure **Tumor** Associated Macrophages and to Predict Patient Response to Treatment**Resource links provided by NLM:**[Genetics Home Reference](#) related topics: [breast cancer](#)[MedlinePlus](#) related topics: [Cancer](#)[Drug Information](#) available for: [Ferumoxytol](#)[Genetic and Rare Diseases information Center](#) resources: [Ovarian Cancer](#) [Stomach Cancer](#)[U.S. FDA Resources](#)**Further study details as provided by Merrimack Pharmaceuticals:**

## Primary Outcome Measures:

- Measure **tumor** levels of irinotecan and SN-38 (in ng/mL) [ Time Frame: 12 months ]

## Secondary Outcome Measures:

CSPC Exhibit 1094

Page 317 of 512

- Safety profile of **MM-398** in the presence of **ferumoxytol** (number and type of Adverse Events compared with histological control) [ Time Frame: 12 months ]
- **Tumor** response Rate measured by RECIST (Response Evaluation Criteria in Solid **Tumors**) 1.1 guidelines [ Time Frame: 12 months ]
- Half-life of the **drug** (t 1/2) in number of hours [ Time Frame: 12 months ]  
50% of total time of drug in plasma
- Maximum concentration of **drug** in plasma (Cmax) in ng/mL [ Time Frame: 12 months ]
- Measure of **drug** availability in the plasma (AUC) in ng/mL x hours [ Time Frame: 12 months ]  
Area under the plasma drug concentration versus time curve

Estimated Enrollment: 45  
 Study Start Date: November 2012  
 Estimated Study Completion Date: October 2017  
 Estimated Primary Completion Date: June 2017 (Final data collection date for primary outcome measure)

Arms	Assigned Interventions
Experimental: <b>Pilot Phase: Ferumoxytol</b> followed by <b>MM-398</b> (CLOSED) <b>Ferumoxytol</b> 5 mg/kg IV at the rate of 1 mL/sec, given once on Day 1. <b>MM-398</b> 80 mg/m2 IV over 90 min on Days 1 and 15 of every 4 week cycle	<b>Drug: Ferumoxytol</b> followed by <b>MM-398</b> <b>Ferumoxytol</b> 5 mg/kg IV at 1mL/sec, given once. <b>MM-398</b> 80 mg/m2 IV over 90 min every 2 weeks, until progressive disease or intolerable toxicity
Experimental: Expansion Phase: <b>Ferumoxytol</b> followed by <b>MM-398</b> <b>Ferumoxytol</b> 5 mg/kg IV at the rate of 1 mL/sec, given once on Day 1. <b>MM-398</b> 80 mg/m2 IV over 90 min on Days 1 and 15 of every 4 week cycle Cohort 1: ER and/or PR-positive BC Cohort 2: TNBC Cohort 3: BC with active brain metastasis	<b>Drug: Ferumoxytol</b> followed by <b>MM-398</b> <b>Ferumoxytol</b> 5 mg/kg IV at 1mL/sec, given once. <b>MM-398</b> 80 mg/m2 IV over 90 min every 2 weeks, until progressive disease or intolerable toxicity

**Detailed Description:**

This study is conducted over two phases. The pilot phase of this trial is closed. The expansion phase of this trial is currently open to enrollment.  
 Pilot Phase: This study will enroll approximately 12 patients, up to 20 in total in the Pilot Phase and 30 patients in the Expansion Phase. The first three patients that are enrolled can have any solid tumor type; however subsequent patients must have NSCLC, CRC, TNBC, ER/PR positive breast cancer, pancreatic cancer, ovarian cancer, gastric cancer, gastro-oesophageal junction adenocarcinoma or head and neck cancer. No more than three patients with ER/PR positive breast cancer can be enrolled in the Pilot Phase and similar restrictions may be placed on other tumor types to ensure a heterogeneous population.  
 Expansion Phase: The expansion will enroll patients with advanced metastatic breast cancer into three cohorts:  
 Cohort 1: ER and/or PR-positive breast cancer Cohort 2: TNBC Cohort 3: BC with active brain metastasis

**Eligibility**

Ages Eligible for Study: 18 Years and older (Adult, Senior)  
 Sexes Eligible for Study: All  
 Accepts Healthy Volunteers: No

**Criteria**

Inclusion Criteria:

- Pathologically confirmed diagnosis of solid tumors, CRC, TNBC, ER/PR Breast Cancer, NSCLC, Pancreatic Cancer, Ovarian Cancer, Gastric Cancer, GEJ adenocarcinoma, Head and Neck Cancer
- Metastatic disease
- ECOG Performance Status 0 to 2
- Adequate bone marrow, hepatic and renal function
- Normal ECG
- 18 years of age or above
- Able to understand and sign informed consent

Expansion Phase Additional Criteria:

The following invasive breast cancer tumor sub-types are required:

- Cohort 1: hormone receptor positive breast cancer patients with ER-positive and/or PR-positive tumors defined as ≥1% of tumor nuclei that are immunoreactive for ER and/or PR and HER2 negative

- ◊ Cohort 2: triple negative breast cancer (TNBC) patients with ER-negative, PR-negative tumors defined as < 1% of tumor nuclei that are immunoreactive for ER and PR and HER2 negative
- ◊ Cohort 3: Any sub-type of metastatic breast cancer and active brain metastases
- ◊ Documented metastatic disease with at least two radiologically measurable lesions as defined by RECIST v1.1 (except Cohort 3, see inclusion criterion o below)
- ◊ Received at least one cytotoxic therapy in the metastatic setting, with exception of TNBC patients who progressed within 12 months of adjuvant therapy
- ◊ Received ≤ 3 prior lines of chemotherapy in the metastatic setting (no limit to prior lines of hormonal therapy in Cohort 1)
- ◊ At least one lesion amenable to multiple pass core biopsy (exception: Cohort 3 patients)

Expansion Phase Cohort 3 additional inclusion criteria:

- Radiographic evidence of new or progressive brain metastases after prior radiation therapy with at least one brain metastasis measuring ≥ 1 cm in longest diameter on gadolinium-enhanced MRI (note: progressive brain lesions are not required to meet RECIST criteria in order to be eligible; extra-cranial metastatic disease is also allowed)

Exclusion Criteria:

- ◊ Active CNS metastasis (applies to pilot phase and expansion phase cohort 1 and 2 only)
- ◊ Clinically significant GI disorders
- ◊ Prior irinotecan or bevacizumab therapy within last 6 months
- ◊ Known hypersensitivity to MM-398 or ferumoxytol
- ◊ Inability to undergo MRI
- ◊ Active infection
- ◊ Pregnant or breast feeding

## 📍 Contacts and Locations

Choosing to participate in a study is an important personal decision. Talk with your doctor and family members or friends about deciding to join a study. To learn more about this study, you or your doctor may contact the study research staff using the Contacts provided below. For general information, see [Learn About Clinical Studies](#).

Please refer to this study by its ClinicalTrials.gov identifier: NCT01770353

### Contacts

Contact: Istvan Molnar, MD 617-441-1000 ext 7649 [imolnar@merimack.com](mailto:imolnar@merimack.com)

### Locations

#### United States, Arizona

Mayo Clinic **Not yet recruiting**  
 Scottsdale, Arizona, United States, 85159-5499  
 Contact: Clinical Trials Office All Mayo Clinic Locations 855-776-0015

HonorHealth **Recruiting**  
 Scottsdale, Arizona, United States, 85258

#### United States, California

UCSF Helen Diller Family Comprehensive **Cancer** Center **Recruiting**  
 San Francisco, California, United States, 94115

#### United States, Florida

Moffitt **Cancer** Center **Recruiting**  
 Tampa, Florida, United States, 33607

#### United States, Michigan

University of Michigan Comprehensive **Cancer** Center **Not yet recruiting**  
 Ann Arbor, Michigan, United States, 48109

#### United States, Missouri

Washington University **Not yet recruiting**  
 Saint Louis, Missouri, United States, 63110

#### United States, North Carolina

UNC- Lineberger Comprehensive **Cancer** Center  
 Chapel Hill, North Carolina, United States, 27599

**Recruiting**

**Sponsors and Collaborators**

Merrimack **Pharmaceuticals**

**Investigators**

**Study Director:** Istvan Molnar, MD Merrimack **Pharmaceuticals**

 **More Information**

Responsible Party: Merrimack Pharmaceuticals  
 ClinicalTrials.gov Identifier: [NCT01770353](#) [History of Changes](#)  
 Other Study ID Numbers: **MM-398-01-01-02**  
 Study First Received: December 19, 2012  
 Last Updated: July 7, 2016

Keywords provided by Merrimack Pharmaceuticals:

solid <b>tumors</b>	Ovarian <b>Cancer</b>
Triple Negative Breast <b>Cancer</b>	Gastric <b>Cancer</b>
Colorectal <b>Cancer</b>	Head and Neck <b>Cancer</b>
<b>MM-398</b>	nanoliposomal irinotecan
<b>Ferumoxytol</b>	Gastro-Esophageal Junction Adenocarcinoma
ER/PR positive Breast <b>Cancer</b>	TNBC
Pancreatic <b>Cancer</b>	

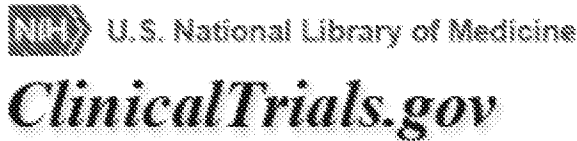
Additional relevant MeSH terms:

Breast <b>Neoplasms</b>	Ferrosferric Oxide
Triple Negative Breast <b>Neoplasms</b>	Camptothecin
<b>Neoplasms</b> by Site	Hematinics
<b>Neoplasms</b>	Parenteral Nutrition Solutions
<b>Pharmaceutical</b> Solutions	Topoisomerase I Inhibitors
Antineoplastic <b>Agents</b> , Phytogetic	Topoisomerase Inhibitors
Antineoplastic <b>Agents</b>	Enzyme Inhibitors
Breast Diseases	Molecular Mechanisms of Pharmacological Action
Skin Diseases	

ClinicalTrials.gov processed this record on January 31, 2017

We updated the design of this site on September 25th. [Learn more.](#)

We will be updating this site in phases. This allows us to move faster and to deliver better services. [Show less](#)



- [Find Studies](#) ▼
- [About Studies](#) ▼
- [Submit Studies](#) ▼
- [Resources](#) ▼
- [About Site](#) ▼

## Phase 1 Study of MM-398 Plus Cyclophosphamide in Pediatric Solid Tumors

This study is currently recruiting participants.

**See [▶ Contacts and Locations](#)**

*Verified February 2017 by South Plains Oncology Consortium*

**Sponsor:**

South Plains Oncology Consortium

**ClinicalTrials.gov Identifier:**

NCT02013336

First Posted: December 17, 2013

Last Update Posted: February 6, 2017

**⚠** The safety and scientific validity of this study is the responsibility of the study sponsor and investigators. Listing a study does not mean it has been evaluated by the U.S. Federal Government. [Know the risks and potential benefits](#) of clinical studies and talk to your health care provider before participating. Read our [disclaimer](#) for details.

**Information provided by (Responsible Party):**

South Plains Oncology Consortium

[Full Text View](#)

[Tabular View](#)

[No Study Results Posted](#)

[Disclaimer](#)

[How to Read a Study Record](#)

### ▶ Purpose

This is a Phase 1 study of the combination of two drugs: MM-398 and Cyclophosphamide. The goal is to find the highest dose of MM-398 that can be given safely when it is used together with the chemotherapy drug Cyclophosphamide.

<u>Condition</u>	<u>Intervention</u>	<u>Phase</u>
Recurrent or Refractory Solid Tumors Ewing Sarcoma Rhabdomyosarcoma Neuroblastoma Osteosarcoma	Drug: MM-398 (Irinotecan Sucrosfate Liposome Injection) plus cyclophosphamide	Phase 1

Study Type: Interventional

Study Design: Intervention Model: Single Group Assignment

Masking: None (Open Label)

Primary Purpose: Treatment

Official Title: Phase 1 Dose-escalating Study of MM-398 (Irinotecan Sucrosfate Liposome Injection) Plus Intravenous Cyclophosphamide in Recurrent or Refractory Pediatric Solid Tumors

**Resource links provided by NLM:**

Genetics Home Reference related topics: [Ewing sarcoma](#) [neuroblastoma](#)

Drug Information available for: [Cyclophosphamide](#) [Irinotecan](#) [Irinotecan hydrochloride](#)

Genetic and Rare Diseases Information Center resources: [Osteosarcoma](#) [Soft Tissue Sarcoma](#) [Neuroblastoma](#) [Ewing Sarcoma](#) [Ewing's Family of Tumors](#) [Neuroepithelioma](#)

U.S. FDA Resources

**Further study details as provided by South Plains Oncology Consortium:**

Primary Outcome Measures:

- To determine the Maximum Tolerated Dose (MTD) of MM-398 in combination with intravenous cyclophosphamide by assessing the occurrence of dose limiting toxicities [ Time Frame: 12 months ]

**Secondary Outcome Measures:**

- Measurement of plasma levels of study drug to determine the pharmacokinetic properties of MM-398 in combination with cyclophosphamide [ Time Frame: 12 months ]

Estimated Enrollment: 30  
 Study Start Date: December 2013  
 Estimated Study Completion Date: December 2017  
 Estimated Primary Completion Date: December 2017 (Final data collection date for primary outcome measure)

<u>Arms</u>	<u>Assigned Interventions</u>
Experimental: MM-398 + cyclophosphamide	Drug: MM-398 (Irinotecan Sucrosfate Liposome Injection) plus cyclophosphamide

## ► Eligibility

### Information from the National Library of Medicine



*Choosing to participate in a study is an important personal decision. Talk with your doctor and family members or friends about deciding to join a study. To learn more about this study, you or your doctor may contact the study research staff using the contacts provided below. For general information, [Learn About Clinical Studies](#).*

Ages Eligible for Study: 12 Months to 20 Years (Child, Adult)  
 Sexes Eligible for Study: All  
 Accepts Healthy Volunteers: No

**Criteria****Inclusion Criteria:**

- Histologically or cytologically-confirmed Ewing sarcoma, rhabdomyosarcoma, neuroblastoma, or osteosarcoma
- Disease progression after prior therapy in locally advanced or metastatic setting

- Measurable or evaluable disease based on the Response Evaluation Criteria in Solid Tumors (RECIST v1.1) criteria
- Age 12 months to <21 years
- Adequate bone marrow reserves, hepatic function, and renal function
- Recovered from effects of any prior surgery or cancer therapy
- Patients 18 years or older will provide written consent. A parent or legal guardian of a patient <18 years of age will provide informed consent and patients 11 to 18 years of age will provide written assent or as per participating institutional policy.

#### Exclusion Criteria:

- Clinically significant gastrointestinal disorders
- NYHA Class III or IV congestive heart failure, ventricular arrhythmias or uncontrolled blood pressure
- Active infection or unexplained fever
- Known hypersensitivity to any of the components of MM-398 or other liposomal products
- Recent Investigational therapy
- Pregnant or breast feeding; females of child-bearing potential must test negative for pregnancy at the time of enrollment

## ► Contacts and Locations

### Information from the National Library of Medicine



*To learn more about this study, you or your doctor may contact the study research staff using the contact information provided by the sponsor.*

*Please refer to this study by its ClinicalTrials.gov identifier (NCT number):*

***NCT02013336***

#### Contacts

Contact: Amanda Knight, RN, BSN, CCRP 806-743-2690 [amanda.knight@ttuhsc.edu](mailto:amanda.knight@ttuhsc.edu)

#### Locations



**United States, Oklahoma**

University Of Oklahoma Health Sciences Center **Recruiting**  
 Oklahoma City, Oklahoma, United States  
 Contact: Susan Heavner

**United States, Texas**

UT Southwestern **Recruiting**  
 Dallas, Texas, United States  
 Contact: Alison Patterson

**Not yet recruiting**

Houston, Texas, United States

Texas Tech University Health Sciences Center **Not yet recruiting**  
 Lubbock, Texas, United States, 79430

**United States, Wisconsin**

Midwest Children's Hospital **Recruiting**  
 Milwaukee, Wisconsin, United States, 53226  
 Contact: Adam Fiebelkorn

**Sponsors and Collaborators**

South Plains Oncology Consortium

**Investigators**

Study Chair: Paul Harker-Murray, MD Midwest Children's Hospital

**► More Information**

Responsible Party: South Plains Oncology Consortium  
 ClinicalTrials.gov Identifier: [NCT02013336](#) [History of Changes](#)  
 Other Study ID Numbers: SPOC-2012-001  
 First Submitted: December 11, 2013  
 First Posted: December 17, 2013  
 Last Update Posted: February 6, 2017  
 Last Verified: February 2017

Studies a U.S. FDA-regulated Drug Product: Yes

Studies a U.S. FDA-regulated Device Product: No

Keywords provided by South Plains Oncology Consortium:

pediatric

MM-398

cyclophosphamide

irinotecan

Additional relevant MeSH terms:

Neuroblastoma

Osteosarcoma

Rhabdomyosarcoma

Sarcoma, Ewing

Neuroectodermal Tumors, Primitive, Peripheral

Neuroectodermal Tumors, Primitive

Neoplasms, Neuroepithelial

Neuroectodermal Tumors

Neoplasms, Germ Cell and Embryonal

Neoplasms by Histologic Type

Neoplasms

Neoplasms, Glandular and Epithelial

Neoplasms, Nerve Tissue

Neoplasms, Bone Tissue

Neoplasms, Connective Tissue

Neoplasms, Connective and Soft Tissue

Sarcoma

Myosarcoma

Neoplasms, Muscle Tissue

Cyclophosphamide

Irinotecan

Camptothecin

Immunosuppressive Agents

Immunologic Factors

Physiological Effects of Drugs

Antirheumatic Agents

Antineoplastic Agents, Alkylating

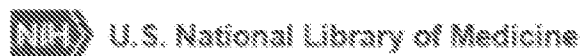
Alkylating Agents

Molecular Mechanisms of Pharmacological  
Action

Antineoplastic Agents

We updated the design of this site on September 25th. [Learn more.](#)

We will be updating this site in phases. This allows us to move faster and to deliver better services. [Show less](#)



**ClinicalTrials.gov**

- [Find Studies](#) ▼
- [About Studies](#) ▼
- [Submit Studies](#) ▼
- [Resources](#) ▼
- [About Site](#) ▼

## Study of Convection-Enhanced, Image-Assisted Delivery of Liposomal-Irinotecan In Recurrent High Grade Glioma

This study is enrolling participants by invitation only.

**Sponsor:**

University of California, San Francisco

**ClinicalTrials.gov Identifier:**

NCT02022644

First Posted: December 30, 2013

Last Update Posted: May 8, 2017

**⚠** The safety and scientific validity of this study is the responsibility of the study sponsor and investigators. Listing a study does not mean it has been evaluated by the U.S. Federal Government. Read our [disclaimer](#) for details.

**Collaborators:**

Merrimack Pharmaceuticals

National Institutes of Health (NIH)

**Information provided by (Responsible Party):**

Nicholas Butowski, University of California, San Francisco

[Full Text View](#)

[Tabular View](#)

[No Study Results Posted](#)

[Disclaimer](#)

[How to Read a Study Record](#)

### ► Purpose

This is a dose-toleration study designed to investigate and determine the maximum tolerated dose of nanoliposomal irinotecan in adults with recurrent high-grade glioma when administered directly into the tumor using a process called convection-enhanced delivery. (CED)

<u>Condition</u>	<u>Intervention</u>	<u>Phase</u>
High Grade Glioma	Drug: nanoliposomal irinotecan	Phase 1

Study Type: Interventional

Study Design: Allocation: Non-Randomized

Intervention Model: Single Group Assignment

Masking: None (Open Label)

Primary Purpose: Treatment

Official Title: A Phase I Study of Convection-Enhanced Delivery of Liposomal-Irinotecan Using Real-Time Imaging With Gadolinium In Patients With Recurrent High Grade Glioma

**Resource links provided by NLM:**

Drug Information available for: [Irinotecan](#) [Irinotecan hydrochloride](#)

Genetic and Rare Diseases Information Center resources: [Glioma](#) [Neuroepithelioma](#)

U.S. FDA Resources

**Further study details as provided by Nicholas Butowski, University of California, San Francisco:**

**Primary Outcome Measures:**

- Maximum tolerated dose [ Time Frame: 30 Days post-dose ]

Dose limiting toxicity (DLT) will be defined as any grade-3 or higher neurological toxicity felt to be attributable to the CED infusion of liposomal-irinotecan with gadolinium, as well as any systemic grade-3 or higher hematologic or non-hematologic toxicity (after maximal medical management of nausea/vomiting/diarrhea), over a period of 30 days after CED infusion.

**Secondary Outcome Measures:**

- Tumor Response Rate [ Time Frame: 12 Months ]

To determine the objective tumor response rate, based upon MR imaging using RANO criteria, at 4 weeks post CED, then every 8 weeks thereafter for 12 months.

- Time to Progression (TTP) [ Time Frame: Until progression of disease up to 12 months from dosing. ]

Estimated time to progression measured from the date of CED administration.

- Overall Survival (OS) [ Time Frame: Up to 12 months from time of dosing. ]

Other Outcome Measures:

- Pre-infusion modeling of the drug distribution vs. post-infusion imaging. [ Time Frame: Up to 48 hours pre-infusion and up to 48 hours post-infusion ]
- Ratio of the Volume of distribution (Vd) to volume infused (Vi) [ Time Frame: Up to 24 hours from time of dosing ]
- Effect of Nano CED on tumor histology [ Time Frame: Up to 12 months from date of surgery ]

Assessed by comparing pre-treatment tumor samples to post-treatment tumor samples in patients who undergo subsequent repeat surgical procedures. (If applicable)

Estimated Enrollment: 30  
 Study Start Date: February 2014  
 Estimated Study Completion Date: January 2019  
 Estimated Primary Completion Date: September 2018 (Final data collection date for primary outcome measure)

Arms	Assigned Interventions
Experimental: Group 1 - 20 mg Tumor volume: 1-4 cm <sup>3</sup> , Infusion Volume: 1.0 ml, Irinotecan conc.: 20 mg/ml, Infusion Time: 2-3h	Drug: nanoliposomal irinotecan  Other Name: MM-398
Experimental: Group 2 - 40 mg	Drug: nanoliposomal irinotecan

Tumor volume: 1-4 cm <sup>3</sup> , Infusion Volume: 1.0 ml, Irinotecan conc.: 40 mg/ml, Infusion Time: 2-3h	Other Name: MM-398
Experimental: Group 3 - 60 mg Tumor volume: 2-5 cm <sup>3</sup> , Infusion Volume: 1.5 ml, Irinotecan conc.: 40 mg/ml, Infusion Time: 3-4h	Drug: nanoliposomal irinotecan Other Name: MM-398
Experimental: Group 4 - 80 mg Tumor volume: 2-6 cm <sup>3</sup> , Infusion Volume: 2.0 ml, Irinotecan conc.: 40 mg/ml, Infusion Time: 3-4h	Drug: nanoliposomal irinotecan Other Name: MM-398

### Detailed Description:

High grade gliomas (HGG) are the most common brain tumor in adults, with 15,000 new cases/year in the USA. Despite progress made using combination therapies including surgery, radiation and/or chemotherapy, the treatment of HGG remains challenging with a typical median survival of 6-12 months for patients with newly diagnosed glioblastoma multiforme (GB) and 24-36 months for patients with anaplastic astrocytoma. The time to tumor progression of patients with recurrent GBM is nine weeks and the median survival is 25 weeks, while for recurrent anaplastic astrocytomas (AA), the time to tumor progression is 13 weeks and the median survival is 47 weeks. More recently, single-agent Avastin has been seen to improve 6-month progression-free survival (PFS-6) to 42.6% as well as increase Median Overall Survival to 9.3 months in patients with recurrent GBM. However, chemotherapy treatment for malignant gliomas has limitations given the low activity of available antineoplastic agents, the emergence or de-novo presence of resistance to such agents, the sensitivity of the brain to irreversible damage from a therapeutic modality, and the compromised delivery of these agents to partially privileged intracranial sites. Effective agents with novel mechanisms of action need to be evaluated in HGG which account for these limitations.

With these limitations in mind, this study directs attention to two particularly appealing delivery modalities which may improve the efficacy of neuro-oncologic chemotherapeutic agents: liposomes (liposomal irinotecan) and convection enhanced delivery (CED). Liposomes are typically composed of double chain phospholipid amphiphiles (chemical compounds with combined hydrophilic and lipophilic properties) in combination with cholesterol, forming spheroidal bilayer membrane structures that encompass an aqueous internal domain. Based on structural/pharmacologic features, distinct liposome classes have been developed to package various therapeutic agents for the treatment of cancer. From the circulating bloodstream,

liposomes are able to diffuse across the blood brain barrier (BBB) due to their lipophilic characteristics. An example is liposomal irinotecan which may reduce the toxicity of irinotecan to healthy tissues while maintaining or increasing its anti-tumor potency.

CED improves chemotherapeutic delivery to brain tumors intraparenchymally by utilizing bulk flow, or fluid convection, established as a result of a pressure gradient, rather than a concentration gradient. As such, CED offers markedly improved distribution of infused therapeutics within the central nervous system (CNS) compared to direct injection or via drug eluting polymers, both of which depend on diffusion for parenchymal distribution. Additionally, CED obviates the challenges of systemic agents crossing the blood brain barrier while minimizing systemic exposure and toxicity. Through the maintenance of a pressure gradient from the delivery cannula tip to the surrounding tissues, CED is able to distribute small and large molecules, including high molecular weight proteins, to clinically significant target volumes centimeters rather than millimeters in diameter. Although developed independently, work combining the two delivery options, liposomes and CED, is presently underway in an effort to improve treatment efficacy in the treatment of CNS malignancies. This clinical trial is a step in this direction with a prospective, single-arm, open-label trial that delivers liposomal-irinotecan and gadolinium (which provided real time imaging of delivery) by CED in patients with recurrent malignant glioma.

Added to this logic is support from a recent preclinical study at the University of California, San Francisco (UCSF) which compared routes of delivery for liposomal irinotecan (CED versus IV) and showed superior anti-tumor activity of CED administration in treating mice with intracranial glioblastoma xenografts. In total, such results indicate that liposomal formulation plus direct intratumoral administration of therapeutic are important for maximizing the anti-tumor effects of irinotecan and support the current clinical trial evaluation of this therapeutic plus CED route of administration combination.

## ► Eligibility

### Information from the National Library of Medicine



*Choosing to participate in a study is an important personal decision. Talk with your doctor and family members or friends about deciding to join a study. To learn more about this study, you or your doctor may contact the study research staff using the contacts provided below. For general information, [Learn About Clinical Studies](#).*

Ages Eligible for Study: 18 Years and older (Adult, Senior)

Sexes Eligible for Study: All

Accepts Healthy Volunteers: No

### Criteria

#### Inclusion Criteria:

- Patients with radiographically proven recurrent, intracranial high grade glioma will be eligible for this protocol. Patients must have evidence of tumor progression as determined by the Revised Assessment in Neuro-Oncology RANO criteria following standard therapy.
- High grade glioma includes glioblastoma multiforme (GBM), Gliosarcoma (GS), anaplastic astrocytoma (AA), anaplastic oligodendroglioma (AO), anaplastic mixed oligoastrocytoma (AMO), or malignant astrocytoma not otherwise specified. (NOS)
- Magnetic resonance imaging (MRI) must be performed within 21 days prior to enrollment, and patients who are receiving steroids must be stable or decreasing for at least 5 days prior to imaging. If the steroid dose is increased between the date of imaging and enrollment, a new baseline MRI is required.
- Patients must have completed only 1 prior course of radiation therapy and must have experienced an interval of greater than 12 weeks from the completion of radiation therapy to study entry.
- Patients will be eligible if the original histology was low-grade glioma and a subsequent histological diagnosis of a high grade glioma is made.
- There is no limit as to the number of prior treatments but patients must have radiographic evidence of progressive disease
- Recurrent tumor must be a solid, single, supratentorial, contrast-enhancing HGG which conforms to the following volume according to the relevant treatment group Group Tumor volume
  - 1 - 1-4 cm<sup>3</sup>
  - 2 - 1-4 cm<sup>3</sup>
  - 3 - 2-5 cm<sup>3</sup>
  - 4 - 2-6 cm<sup>3</sup>
- All patients must sign an informed consent indicating that they are aware of the investigational nature of this study. Patients must be registered prior to treatment with study drug.
- Patients must be > 18 years old, and with a life expectancy > 8 weeks
- Patients with Karnofsky performance status of > 70.



- At the time of registration: Patients must have recovered from the toxic effects of prior therapy: > 10 days from any noncytotoxic investigational agent, >28 days from prior cytotoxic therapy or Avastin, >14 days from vincristine, >42 days from nitrosoureas, >21 days from procarbazine administration, and >7 days for non-cytotoxic agents, e.g., interferon, tamoxifen, thalidomide, cis-retinoic acid, etc. (radiosensitizer does not count). Any questions related to the definition of non-cytotoxic agents should be directed to the Study Chair.
- requirements for organ and marrow function as follows:
  - Adequate bone marrow function:
    - leukocytes > 3,000/mcL
    - absolute neutrophil count > 1,500/mcL
    - platelets > 100,000/mcL
  - Adequate hepatic function:
    - total bilirubin within normal institutional limits
    - aspartate aminotransferase (AST) < 2.5 X institutional upper limit of normal
    - alanine aminotransferase (ALT) < 2.5 X institutional upper limit of normal
  - Adequate renal function:
    - creatinine within normal institutional limits OR
    - creatinine clearance > 60 mL/min/1.73 m<sup>2</sup> for patients with creatinine levels above institutional normal
- The effects of nano liposomal irinotecan on the developing human fetus are unknown. For this reason, women of child-bearing potential and men must agree to use adequate contraception: hormonal or barrier method of birth control; abstinence, etc. prior to study entry, for the duration of study participation, and for 6 months post drug administration. Should a woman become pregnant or suspect she is pregnant while she or her partner is participating in this study, she should inform her treating physician immediately
- Women of childbearing potential must have a negative beta-human chorionic gonadotropin (beta-HCG) pregnancy test documented within 14 days prior to treatment.
- Patients with prior therapy that included interstitial brachytherapy, or Gliadel wafers must have confirmation of true progressive disease rather than radiation necrosis based upon either PET or Thallium scanning, MR spectroscopy or surgical documentation of disease
- Patients must be able to have MRI brain imaging.
- Patients must not have any significant medical illnesses that in the investigator's opinion cannot be adequately controlled with appropriate therapy or would compromise the patient's ability to tolerate this therapy

- Patients with a history of any other cancer (except non-melanoma skin cancer or carcinoma in-situ of the cervix), unless in complete remission and off of all therapy for that disease for a minimum of 3 years are ineligible.
- Patients must not have an active infection or serious intercurrent medical illness.
- Patients must not be pregnant/breast feeding and must agree to practice adequate contraception.
- HIV-positive patients on combination antiretroviral therapy are ineligible
- Contrast-enhancing tumor which crosses the midline.
- Multi-focal disease
- Nonparenchymal tumor dissemination (e.g., subependymal or leptomeningeal)
- History of hypersensitivity reactions to products containing irinotecan (irinotecan), topotecan or other topoisomerase inhibitors, gadolinium contrast agents or lipid products
- Ongoing treatment with cytotoxic therapy
- Patients may not be on an enzyme-inducing anti-epileptic drug (EIAED). If previously on an EIAED, patient must be off for at least 10 days prior to CED infusion.

## ► Contacts and Locations

### Information from the National Library of Medicine



*To learn more about this study, you or your doctor may contact the study research staff using the contact information provided by the sponsor.*

*Please refer to this study by its ClinicalTrials.gov identifier (NCT number):*

***NCT02022644***

### Locations

#### United States, California

University of California, San Francisco  
San Francisco, California, United States, 94143

### Sponsors and Collaborators

University of California, San Francisco

Merrimack Pharmaceuticals

National Institutes of Health (NIH)

### Investigators

Principal Investigator: Nicholas Butowski, MD University of California, San Francisco

Study Director: Susan Chang, MD University of California, San Francisco

### ► More Information

Responsible Party: Nicholas Butowski, Assistant Professor of Neurological Surgery;  
Director of Clinical Services, Division of Neuro-Oncology, University  
of California, San Francisco

ClinicalTrials.gov Identifier: [NCT02022644](#) [History of Changes](#)

Other Study ID Numbers: Nano CED  
13-12025 ( Other Identifier: University of California, San Francisco )

First Submitted: December 11, 2013

First Posted: December 30, 2013

Last Update Posted: May 8, 2017

Last Verified: May 2017

#### Additional relevant MeSH terms:

Glioma	Irinotecan
Neoplasms, Neuroepithelial	Camptothecin
Neuroectodermal Tumors	Antineoplastic Agents, Phytogenic
Neoplasms, Germ Cell and Embryonal	Antineoplastic Agents
Neoplasms by Histologic Type	Topoisomerase I Inhibitors
Neoplasms	Topoisomerase Inhibitors
Neoplasms, Glandular and Epithelial	Enzyme Inhibitors
Neoplasms, Nerve Tissue	Molecular Mechanisms of Pharmacological Action

# ClinicalTrials.gov archive

A service of the U.S. National Institutes of Health

Developed by the National Library of Medicine

[← History of this study](#)    [↑ Current version of this study](#)

## View of NCT02631733 on 2015\_12\_15

**ClinicalTrials Identifier:** NCT02631733**Updated:** 2015\_12\_15

---

### Descriptive Information

**Brief title** Liposomal Irinotecan and Veliparib in Treating Patients With Solid Tumors That Are Metastatic or Cannot Be Removed by Surgery**Official title** A Phase I Study of a Combination of MM-398 and Veliparib in Solid Tumors**Brief summary**

This phase I trial studies the side effects and best dose of veliparib when given together with liposomal irinotecan in treating patients with solid tumors that have spread to other parts of the body (metastatic) or cannot be removed by surgery. Liposomal irinotecan and veliparib may stop the growth of tumor cells by blocking some of the enzymes needed for cell growth.

**Detailed description****PRIMARY OBJECTIVES:**

- I. To evaluate the safety and tolerability of escalating doses of MM-398 (liposomal irinotecan) + veliparib combination.
- II. To determine the maximum tolerated dose (MTD) and recommended phase 2 dose (RP2D) of the combination of MM-398 + veliparib.

**SECONDARY OBJECTIVES:**

- I. To observe and record anti-tumor activity.
- II. To characterize the preliminary efficacy of the combination using key efficacy indicators, such as objective response rate, clinical benefit rate defined as complete response (CR), partial response (PR), or stable disease (SD) at 24 weeks, and progression free survival (PFS).

**EXPLORATORY OBJECTIVES**

- I. Imaging, tumor, and blood biomarkers to assess the sensitivity or resistance to each drug and correlation with clinical response.

**OUTLINE:** This is a dose-escalation of veliparib.

Patients receive liposomal irinotecan intravenously (IV) over 90 minutes on days 1 and 15 and veliparib orally (PO) on days 5-12 and 19-25 or 3-12 and 17-25. Courses repeat every 28 days in the absence of disease progression or unacceptable toxicity.

After completion of study treatment, patients are followed up for 4 weeks.

<b>Phase</b>	Phase 1
<b>Study type</b>	Interventional
<b>Study design</b>	Treatment
<b>Study design</b>	Open Label
<b>Study design</b>	Single Group Assignment
<b>Study design</b>	Safety Study
<b>Primary outcome</b>	Measure: Incidence of adverse events, graded using the NCI Common Terminology Criteria for Adverse Events (CTCAE) version 4.0 Time Frame: Up to 4 weeks Safety Issue? Yes
<b>Primary outcome</b>	Measure: MTD and RP2D of liposomal irinotecan in combination with veliparib determined by incidence of dose limiting toxicities, graded using the NCI CTCAE version 4.0 Time Frame: 28 days Safety Issue? Yes
<b>Secondary outcome</b>	Measure: Clinical benefit rate defined as CR, PR, or SD assessed using RECIST version 1.1 Time Frame: At 24 weeks Safety Issue? No
<b>Secondary outcome</b>	Measure: Objective response rate assessed using RECIST version 1.1 Time Frame: At 24 weeks Safety Issue? No
<b>Secondary outcome</b>	Measure: PFS Time Frame: Duration of time from start of treatment to time of progression or death, whichever occurs first, assessed up to 4 weeks after completion of study treatment Safety Issue? No
<b>Secondary outcome</b>	Measure: Tumor response assessed using the revised Response Evaluation Criteria in Solid Tumors (RECIST) guideline (version 1.1) Time Frame: Up to 4 weeks after completion of study treatment Safety Issue? No
<b>Enrollment</b>	48 (Anticipated)
<b>Condition</b>	Estrogen Receptor Negative
<b>Condition</b>	HER2/Neu Negative
<b>Condition</b>	Neuroendocrine Neoplasm
<b>Condition</b>	Progesterone Receptor Negative
<b>Condition</b>	Stage IIB Cervical Cancer
<b>Condition</b>	Stage IIIA Cervical Cancer

<b>Condition</b>	Stage IIIB Cervical Cancer
<b>Condition</b>	Stage IIIB Non-Small Cell Lung Cancer
<b>Condition</b>	Stage IIIC Breast Cancer
<b>Condition</b>	Stage IV Breast Cancer
<b>Condition</b>	Stage IV Cervical Cancer
<b>Condition</b>	Stage IV Gastric Cancer
<b>Condition</b>	Stage IV Non-Small Cell Lung Cancer
<b>Condition</b>	Stage IV Ovarian Cancer
<b>Condition</b>	Stage IV Small Cell Lung Carcinoma
<b>Condition</b>	Triple-Negative Breast Carcinoma
<b>Arm/Group</b>	Arm Label: Treatment (liposomal irinotecan, veliparib) Experimental
	Patients receive liposomal irinotecan IV over 90 minutes on days 1 and 15 and veliparib PO on days 5-12 and 19-25 or 3-12 and 17-25. Courses repeat every 28 days in the absence of disease progression or unacceptable toxicity.
<b>Intervention</b>	Drug: Ferumoxytol Non-Stoichiometric Magnetite Arm Label: Treatment (liposomal irinotecan, veliparib)
	Correlative studies
<b>Intervention</b>	Other: Laboratory Biomarker Analysis      Arm Label: Treatment (liposomal irinotecan, veliparib)
	Correlative studies
<b>Intervention</b>	Drug: Liposomal Irinotecan      Arm Label: Treatment (liposomal irinotecan, veliparib)
	Given IV
<b>Intervention</b>	Procedure/Surgery: Magnetic Resonance Imaging Arm Label: Treatment (liposomal irinotecan, veliparib)
	Correlative studies
<b>Intervention</b>	Drug: Veliparib      Arm Label: Treatment (liposomal irinotecan, veliparib)
	Given PO

---

### Recruitment Information

<b>Status</b>	Not yet recruiting
<b>Start date</b>	2016-05
<b>Primary completion date</b>	2018-01 (Anticipated)
<b>Criteria</b>	

#### Inclusion Criteria:

- Patients must have pathologically confirmed diagnosis of one of the following

solid tumors: cervical cancer, ovarian cancer, triple negative breast cancer (TNBC), non-small cell lung cancer (NSCLC), small cell lung cancer (SCLC), gastric cancer, and neuroendocrine tumors that is metastatic or unresectable and for which standard curative or palliative measures do not exist or are no longer effective

- Prior poly ADP ribose polymerase (PARP) inhibitor therapy is allowed
- Patients at the National Cancer Institute (NCI) site must be willing to undergo a pre-treatment ferumoxytol magnetic resonance imaging (MRI) (patients will be excluded from undergoing ferumoxytol MRI if they have evidence of iron overload, a known hypersensitivity to ferumoxytol or any other IV iron product, a documented history of multiple drug allergies, or those for whom MRI is otherwise contraindicated, including claustrophobia or anxiety related to undergoing MRI); this eligibility criterion applies only to patients enrolling at NCI
- Eastern Cooperative Oncology Group (ECOG) performance status  $\leq$  2 (Karnofsky  $\geq$  60%)
- Life expectancy of greater than 3 months
- Hemoglobin  $>$  9 g/dL
- Leukocytes  $\geq$  3,000/mcL
- Absolute neutrophil count  $\geq$  1,500/mcL without the use of hematopoietic growth factors
- Platelets  $\geq$  100,000/mcL
- Total bilirubin within normal institutional limits
- Aspartate aminotransferase (AST)(serum glutamic oxaloacetic transaminase [SGOT])/alanine aminotransferase (ALT)(serum glutamate pyruvate transaminase [SGPT])  $\leq$  2.5 x institutional upper limit of normal ( $\leq$  5 x upper limit of normal [ULN] is acceptable if liver metastases are present)
- Creatinine  $\leq$  1.5 x ULN OR creatinine clearance  $\geq$  60 mL/min/1.73 m<sup>2</sup> for patients with creatinine levels above institutional normal
- Women of child-bearing potential and men must agree to use adequate contraception (hormonal or barrier method of birth control; abstinence) prior to study entry and for the duration of study participation; should a woman become pregnant or suspect she is pregnant while she or her partner is participating in this study, she should inform her treating physician immediately; men and women treated or enrolled on this protocol must also agree to use adequate contraception prior to the study, for the duration of study participation, and 4 months after completion of veliparib, MM-398 and ferumoxytol MRI administration
- Ability to understand and the willingness to sign a written informed consent document
- IMAGING CORRELATIVE STUDY: Patients will be eligible to participate in the ferumoxytol (FMX) imaging study if they do not meet any of the following criteria
  - Evidence of iron overload as determined by:
    - \* Fasting transferrin saturation of  $>$  45% and/or
    - \* Serum ferritin levels  $>$  1000 ng/ml
  - A history of allergic reactions to any of the following:
    - \* Compounds similar to ferumoxytol or any of its components as described in full prescribing information for ferumoxytol injection
    - \* Any IV iron replacement product (e.g. parenteral iron, dextran, iron-dextran, or parenteral iron polysaccharide preparations)

## \* Multiple drugs

- Unable to undergo MRI or for whom MRI is otherwise contraindicated (e.g. presence of errant metal, cardiac pacemakers, pain pumps or other MRI incompatible devices; or history claustrophobia or anxiety related to undergoing MRI)

## Exclusion Criteria:

- Patients who have had chemotherapy or radiotherapy within 4 weeks (6 weeks for nitrosoureas or mitomycin C) prior to entering the study or those who have not recovered from adverse events due to agents administered more than 4 weeks earlier; patients must have completed prior biological therapies and/or targeted therapies  $\geq$  2 weeks prior to study enrollment; patients who have had radiation to the pelvis or other bone marrow-bearing sites will be considered on a case by case basis and may be excluded if the bone marrow reserve is not considered adequate (i.e. radiation to  $>$  25% of bone marrow)
- Patients who are receiving any other investigational agents
- Patients with active brain metastases should be excluded from this clinical trial
- History of allergic reactions attributed to compounds of similar chemical or biologic composition to veliparib, MM-398 and ferumoxytol
- Clinically significant gastrointestinal (GI) disorders, including history of small bowel obstruction unless the obstruction was a surgically treated remote episode
- Active infection
- Uncontrolled intercurrent illness including, but not limited to, ongoing or active infection, symptomatic congestive heart failure, unstable angina pectoris, cardiac arrhythmia, or psychiatric illness/social situations that would limit compliance with study requirements
- Pregnant women are excluded from this study; breastfeeding should be discontinued if the mother is treated with any of these agents
- Human immunodeficiency virus (HIV)-positive patients on combination antiretroviral therapy are ineligible
- Patients who are taking medications which are strong inhibitors or inducers of cytochrome P450, family 3, subfamily A, polypeptide 4 (CYP3A4)

<b>Gender</b>	Both
<b>Minimum age</b>	18 Years
<b>Healthy volunteers</b>	No

**Administrative Data**

<b>Organization name</b>	National Cancer Institute (NCI)
<b>Organization study ID</b>	NCI-2015-02125
<b>Secondary ID</b>	NCI-2015-02125 (CTRP (Clinical Trial Reporting Program))
<b>Secondary ID</b>	9914 (National Cancer Institute LAO)
<b>Secondary ID</b>	9914 (CTEP)
<b>Sponsor</b>	National Cancer Institute (NCI)
<b>Collaborator</b>	National Cancer Institute (NCI)
<b>Health Authority</b>	United States: Food and Drug Administration





# ClinicalTrials.gov archive

A service of the U.S. National Institutes of Health

Developed by the National Library of Medicine

[← History of this study](#)    [↑ Current version of this study](#)

## View of NCT02631733 on 2016\_02\_16

**ClinicalTrials Identifier:** NCT02631733**Updated:** 2016\_02\_16

---

### Descriptive Information

**Brief title** Liposomal Irinotecan and Veliparib in Treating Patients With Solid Tumors That Are Metastatic or Cannot Be Removed by Surgery**Official title** A Phase I Study of a Combination of MM-398 and Veliparib in Solid Tumors**Brief summary**

This phase I trial studies the side effects and best dose of veliparib when given together with liposomal irinotecan in treating patients with solid tumors that have spread to other parts of the body (metastatic) or cannot be removed by surgery. Liposomal irinotecan and veliparib may stop the growth of tumor cells by blocking some of the enzymes needed for cell growth.

**Detailed description****PRIMARY OBJECTIVES:**

- I. To evaluate the safety and tolerability of escalating doses of MM-398 (liposomal irinotecan) + veliparib combination.
- II. To determine the maximum tolerated dose (MTD) and recommended phase 2 dose (RP2D) of the combination of MM-398 + veliparib.

**SECONDARY OBJECTIVES:**

- I. To observe and record anti-tumor activity.
- II. To characterize the preliminary efficacy of the combination using key efficacy indicators, such as objective response rate, clinical benefit rate defined as complete response (CR), partial response (PR), or stable disease (SD) at 24 weeks, and progression free survival (PFS).

**EXPLORATORY OBJECTIVES**

- I. Imaging, tumor, and blood biomarkers to assess the sensitivity or resistance to each drug and correlation with clinical response.

**OUTLINE:** This is a dose-escalation of veliparib.

Patients receive liposomal irinotecan intravenously (IV) over 90 minutes on days 1 and 15 and veliparib orally (PO) on days 5-12 and 19-25 or 3-12 and 17-25. Courses repeat every 28 days in the absence of disease progression or unacceptable toxicity.

After completion of study treatment, patients are followed up for 4 weeks.

<b>Phase</b>	Phase 1
<b>Study type</b>	Interventional
<b>Study design</b>	Treatment
<b>Study design</b>	Open Label
<b>Study design</b>	Single Group Assignment
<b>Study design</b>	Safety Study
<b>Primary outcome</b>	Measure: Incidence of adverse events, graded using the NCI Common Terminology Criteria for Adverse Events (CTCAE) version 4.0 Time Frame: Up to 4 weeks Safety Issue? Yes
<b>Primary outcome</b>	Measure: MTD and RP2D of liposomal irinotecan in combination with veliparib determined by incidence of dose limiting toxicities, graded using the NCI CTCAE version 4.0 Time Frame: 28 days Safety Issue? Yes
<b>Secondary outcome</b>	Measure: Clinical benefit rate defined as CR, PR, or SD assessed using RECIST version 1.1 Time Frame: At 24 weeks Safety Issue? No
<b>Secondary outcome</b>	Measure: Objective response rate assessed using RECIST version 1.1 Time Frame: At 24 weeks Safety Issue? No
<b>Secondary outcome</b>	Measure: PFS Time Frame: Duration of time from start of treatment to time of progression or death, whichever occurs first, assessed up to 4 weeks after completion of study treatment Safety Issue? No
<b>Secondary outcome</b>	Measure: Tumor response assessed using the revised Response Evaluation Criteria in Solid Tumors (RECIST) guideline (version 1.1) Time Frame: Up to 4 weeks after completion of study treatment Safety Issue? No
<b>Enrollment</b>	48 (Anticipated)
<b>Condition</b>	Estrogen Receptor Negative
<b>Condition</b>	HER2/Neu Negative
<b>Condition</b>	Neuroendocrine Neoplasm
<b>Condition</b>	Progesterone Receptor Negative
<b>Condition</b>	Stage IIB Cervical Cancer
<b>Condition</b>	Stage IIIA Cervical Cancer

<b>Condition</b>	Stage IIIB Cervical Cancer
<b>Condition</b>	Stage IIIB Non-Small Cell Lung Cancer
<b>Condition</b>	Stage IIIC Breast Cancer
<b>Condition</b>	Stage IV Breast Cancer
<b>Condition</b>	Stage IV Cervical Cancer
<b>Condition</b>	Stage IV Gastric Cancer
<b>Condition</b>	Stage IV Non-Small Cell Lung Cancer
<b>Condition</b>	Stage IV Ovarian Cancer
<b>Condition</b>	Stage IV Small Cell Lung Carcinoma
<b>Condition</b>	Triple-Negative Breast Carcinoma
<b>Arm/Group</b>	Arm Label: Treatment (liposomal irinotecan, veliparib) Experimental
	Patients receive liposomal irinotecan IV over 90 minutes on days 1 and 15 and veliparib PO on days 5-12 and 19-25 or 3-12 and 17-25. Courses repeat every 28 days in the absence of disease progression or unacceptable toxicity.
<b>Intervention</b>	Drug: Ferumoxytol      Arm Label: Treatment (liposomal irinotecan, veliparib)
	Correlative studies
<b>Intervention</b>	Other: Laboratory Biomarker Analysis      Arm Label: Treatment (liposomal irinotecan, veliparib)
	Correlative studies
<b>Intervention</b>	Drug: Liposomal Irinotecan      Arm Label: Treatment (liposomal irinotecan, veliparib)
	Given IV
<b>Intervention</b>	Procedure/Surgery: Magnetic Resonance Imaging Arm Label: Treatment (liposomal irinotecan, veliparib)
	Correlative studies
<b>Intervention</b>	Drug: Veliparib      Arm Label: Treatment (liposomal irinotecan, veliparib)
	Given PO

---

## Recruitment Information

<b>Status</b>	Not yet recruiting
<b>Start date</b>	2016-05
<b>Primary completion date</b>	2018-01 (Anticipated)
<b>Criteria</b>	

### Inclusion Criteria:

- Patients must have pathologically confirmed diagnosis of one of the following

solid tumors: cervical cancer, ovarian cancer, triple negative breast cancer (TNBC), non-small cell lung cancer (NSCLC), small cell lung cancer (SCLC), gastric cancer, and neuroendocrine tumors that is metastatic or unresectable and for which standard curative or palliative measures do not exist or are no longer effective

- Prior poly ADP ribose polymerase (PARP) inhibitor therapy is allowed
- Patients at the National Cancer Institute (NCI) site must be willing to undergo a pre-treatment ferumoxytol magnetic resonance imaging (MRI) (patients will be excluded from undergoing ferumoxytol MRI if they have evidence of iron overload, a known hypersensitivity to ferumoxytol or any other IV iron product, a documented history of multiple drug allergies, or those for whom MRI is otherwise contraindicated, including claustrophobia or anxiety related to undergoing MRI); this eligibility criterion applies only to patients enrolling at NCI
- Eastern Cooperative Oncology Group (ECOG) performance status  $\leq$  2 (Karnofsky  $\geq$  60%)
- Life expectancy of greater than 3 months
- Hemoglobin  $>$  9 g/dL
- Leukocytes  $\geq$  3,000/mcL
- Absolute neutrophil count  $\geq$  1,500/mcL without the use of hematopoietic growth factors
- Platelets  $\geq$  100,000/mcL
- Total bilirubin within normal institutional limits
- Aspartate aminotransferase (AST)(serum glutamic oxaloacetic transaminase [SGOT])/alanine aminotransferase (ALT)(serum glutamate pyruvate transaminase [SGPT])  $\leq$  2.5 x institutional upper limit of normal ( $\leq$  5 x upper limit of normal [ULN] is acceptable if liver metastases are present)
- Creatinine  $\leq$  1.5 x ULN OR creatinine clearance  $\geq$  60 mL/min/1.73 m<sup>2</sup> for patients with creatinine levels above institutional normal
- Women of child-bearing potential and men must agree to use adequate contraception (hormonal or barrier method of birth control; abstinence) prior to study entry and for the duration of study participation; should a woman become pregnant or suspect she is pregnant while she or her partner is participating in this study, she should inform her treating physician immediately; men and women treated or enrolled on this protocol must also agree to use adequate contraception prior to the study, for the duration of study participation, and 4 months after completion of veliparib, MM-398 and ferumoxytol MRI administration
- Ability to understand and the willingness to sign a written informed consent document
- IMAGING CORRELATIVE STUDY: Patients will be eligible to participate in the ferumoxytol (FMX) imaging study if they do not meet any of the following criteria
  - Evidence of iron overload as determined by:
    - \* Fasting transferrin saturation of  $>$  45% and/or
    - \* Serum ferritin levels  $>$  1000 ng/ml
  - A history of allergic reactions to any of the following:
    - \* Compounds similar to ferumoxytol or any of its components as described in full prescribing information for ferumoxytol injection
    - \* Any IV iron replacement product (e.g. parenteral iron, dextran, iron-dextran, or parenteral iron polysaccharide preparations)

## \* Multiple drugs

- Unable to undergo MRI or for whom MRI is otherwise contraindicated (e.g. presence of errant metal, cardiac pacemakers, pain pumps or other MRI incompatible devices; or history claustrophobia or anxiety related to undergoing MRI)

## Exclusion Criteria:

- Patients who have had chemotherapy or radiotherapy within 4 weeks (6 weeks for nitrosoureas or mitomycin C) prior to entering the study or those who have not recovered from adverse events due to agents administered more than 4 weeks earlier; patients must have completed prior biological therapies and/or targeted therapies  $\geq$  2 weeks prior to study enrollment; patients who have had radiation to the pelvis or other bone marrow-bearing sites will be considered on a case by case basis and may be excluded if the bone marrow reserve is not considered adequate (i.e. radiation to  $>$  25% of bone marrow)
- Patients who are receiving any other investigational agents
- Patients with active brain metastases should be excluded from this clinical trial
- History of allergic reactions attributed to compounds of similar chemical or biologic composition to veliparib, MM-398 and ferumoxytol
- Clinically significant gastrointestinal (GI) disorders, including history of small bowel obstruction unless the obstruction was a surgically treated remote episode
- Active infection
- Uncontrolled intercurrent illness including, but not limited to, ongoing or active infection, symptomatic congestive heart failure, unstable angina pectoris, cardiac arrhythmia, or psychiatric illness/social situations that would limit compliance with study requirements
- Pregnant women are excluded from this study; breastfeeding should be discontinued if the mother is treated with any of these agents
- Human immunodeficiency virus (HIV)-positive patients on combination antiretroviral therapy are ineligible
- Patients who are taking medications which are strong inhibitors or inducers of cytochrome P450, family 3, subfamily A, polypeptide 4 (CYP3A4)

<b>Gender</b>	Both
<b>Minimum age</b>	18 Years
<b>Healthy volunteers</b>	No

---

**Administrative Data**

<b>Organization name</b>	National Cancer Institute (NCI)
<b>Organization study ID</b>	NCI-2015-02125
<b>Secondary ID</b>	NCI-2015-02125 (CTRP (Clinical Trial Reporting Program))
<b>Secondary ID</b>	9914 (National Cancer Institute LAO)
<b>Secondary ID</b>	9914 (CTEP)
<b>Sponsor</b>	National Cancer Institute (NCI)
<b>Collaborator</b>	National Cancer Institute (NCI)
<b>Health Authority</b>	United States: Food and Drug Administration



# ClinicalTrials.gov archive

A service of the U.S. National Institutes of Health

Developed by the National Library of Medicine

[← History of this study](#)    [↑ Current version of this study](#)

## View of NCT02631733 on 2016\_06\_20

**ClinicalTrials Identifier:** NCT02631733**Updated:** 2016\_06\_20

---

### Descriptive Information

**Brief title** Liposomal Irinotecan and Veliparib in Treating Patients With Solid Tumors That Are Metastatic or Cannot Be Removed by Surgery**Official title** A Phase I Study of a Combination of MM-398 and Veliparib in Solid Tumors**Brief summary**

This phase I trial studies the side effects and best dose of veliparib when given together with liposomal irinotecan in treating patients with solid tumors that have spread to other parts of the body (metastatic) or cannot be removed by surgery. Liposomal irinotecan and veliparib may stop the growth of tumor cells by blocking some of the enzymes needed for cell growth.

**Detailed description****PRIMARY OBJECTIVES:**

- I. To evaluate the safety and tolerability of escalating doses of MM-398 (liposomal irinotecan) + veliparib combination.
- II. To determine the maximum tolerated dose (MTD) and recommended phase 2 dose (RP2D) of the combination of MM-398 + veliparib.

**SECONDARY OBJECTIVES:**

- I. To observe and record anti-tumor activity.
- II. To characterize the preliminary efficacy of the combination using key efficacy indicators, such as objective response rate, clinical benefit rate defined as complete response (CR), partial response (PR), or stable disease (SD) at 24 weeks, and progression free survival (PFS).

**EXPLORATORY OBJECTIVES**

- I. Imaging, tumor, and blood biomarkers to assess the sensitivity or resistance to each drug and correlation with clinical response.

**OUTLINE:** This is a dose-escalation of veliparib.

Patients receive liposomal irinotecan intravenously (IV) over 90 minutes on days 1 and 15 and veliparib orally (PO) on days 5-12 and 19-25 or 3-12 and 17-25. Courses repeat every 28 days in the absence of disease progression or unacceptable toxicity.



After completion of study treatment, patients are followed up for 4 weeks.

<b>Phase</b>	Phase 1
<b>Study type</b>	Interventional
<b>Study design</b>	Treatment
<b>Study design</b>	Open Label
<b>Study design</b>	Single Group Assignment
<b>Study design</b>	Safety Study
<b>Primary outcome</b>	Measure: Incidence of adverse events, graded using the NCI Common Terminology Criteria for Adverse Events (CTCAE) version 4.0 Time Frame: Up to 4 weeks Safety Issue? Yes
<b>Primary outcome</b>	Measure: MTD and RP2D of liposomal irinotecan in combination with veliparib determined by incidence of dose limiting toxicities, graded using the NCI CTCAE version 4.0 Time Frame: 28 days Safety Issue? Yes
<b>Secondary outcome</b>	Measure: Clinical benefit rate defined as CR, PR, or SD assessed using RECIST version 1.1 Time Frame: At 24 weeks Safety Issue? No
<b>Secondary outcome</b>	Measure: Objective response rate assessed using RECIST version 1.1 Time Frame: At 24 weeks Safety Issue? No
<b>Secondary outcome</b>	Measure: PFS Time Frame: Duration of time from start of treatment to time of progression or death, whichever occurs first, assessed up to 4 weeks after completion of study treatment Safety Issue? No
<b>Secondary outcome</b>	Measure: Tumor response assessed using the revised Response Evaluation Criteria in Solid Tumors (RECIST) guideline (version 1.1) Time Frame: Up to 4 weeks after completion of study treatment Safety Issue? No
<b>Enrollment</b>	48 (Anticipated)
<b>Condition</b>	Estrogen Receptor Negative
<b>Condition</b>	HER2/Neu Negative
<b>Condition</b>	Neuroendocrine Neoplasm
<b>Condition</b>	Progesterone Receptor Negative
<b>Condition</b>	Stage IIB Cervical Cancer
<b>Condition</b>	Stage IIIA Cervical Cancer

<b>Condition</b>	Stage IIIB Cervical Cancer
<b>Condition</b>	Stage IIIB Non-Small Cell Lung Cancer
<b>Condition</b>	Stage IIIC Breast Cancer
<b>Condition</b>	Stage IV Breast Cancer
<b>Condition</b>	Stage IV Cervical Cancer
<b>Condition</b>	Stage IV Gastric Cancer
<b>Condition</b>	Stage IV Non-Small Cell Lung Cancer
<b>Condition</b>	Stage IV Ovarian Cancer
<b>Condition</b>	Stage IV Small Cell Lung Carcinoma
<b>Condition</b>	Triple-Negative Breast Carcinoma
<b>Arm/Group</b>	Arm Label: Treatment (liposomal irinotecan, veliparib) Experimental
	Patients receive liposomal irinotecan IV over 90 minutes on days 1 and 15 and veliparib PO on days 5-12 and 19-25 or 3-12 and 17-25. Courses repeat every 28 days in the absence of disease progression or unacceptable toxicity.
<b>Intervention</b>	Drug: Ferumoxytol      Arm Label: Treatment (liposomal irinotecan, veliparib)
	Correlative studies
<b>Intervention</b>	Other: Laboratory Biomarker Analysis      Arm Label: Treatment (liposomal irinotecan, veliparib)
	Correlative studies
<b>Intervention</b>	Drug: Liposomal Irinotecan      Arm Label: Treatment (liposomal irinotecan, veliparib)
	Given IV
<b>Intervention</b>	Procedure/Surgery: Magnetic Resonance Imaging Arm Label: Treatment (liposomal irinotecan, veliparib)
	Correlative studies
<b>Intervention</b>	Drug: Veliparib      Arm Label: Treatment (liposomal irinotecan, veliparib)
	Given PO

---

### Recruitment Information

<b>Status</b>	Not yet recruiting
<b>Start date</b>	2016-05
<b>Primary completion date</b>	2018-01 (Anticipated)
<b>Criteria</b>	

Inclusion Criteria:

- Patients must have pathologically confirmed diagnosis of one of the following

solid tumors: cervical cancer, ovarian cancer, triple negative breast cancer (TNBC), non-small cell lung cancer (NSCLC), small cell lung cancer (SCLC), gastric cancer, and neuroendocrine tumors that is metastatic or unresectable and for which standard curative or palliative measures do not exist or are no longer effective

- Prior poly ADP ribose polymerase (PARP) inhibitor therapy is allowed
- Patients at the National Cancer Institute (NCI) site must be willing to undergo a pre-treatment ferumoxytol magnetic resonance imaging (MRI) (patients will be excluded from undergoing ferumoxytol MRI if they have evidence of iron overload, a known hypersensitivity to ferumoxytol or any other IV iron product, a documented history of multiple drug allergies, or those for whom MRI is otherwise contraindicated, including claustrophobia or anxiety related to undergoing MRI); this eligibility criterion applies only to patients enrolling at NCI
- Eastern Cooperative Oncology Group (ECOG) performance status  $\leq$  2 (Karnofsky  $\geq$  60%)
- Life expectancy of greater than 3 months
- Hemoglobin  $>$  9 g/dL
- Leukocytes  $\geq$  3,000/mcL
- Absolute neutrophil count  $\geq$  1,500/mcL without the use of hematopoietic growth factors
- Platelets  $\geq$  100,000/mcL
- Total bilirubin within normal institutional limits
- Aspartate aminotransferase (AST)(serum glutamic oxaloacetic transaminase [SGOT])/alanine aminotransferase (ALT)(serum glutamate pyruvate transaminase [SGPT])  $\leq$  2.5 x institutional upper limit of normal ( $\leq$  5 x upper limit of normal [ULN] is acceptable if liver metastases are present)
- Creatinine  $\leq$  1.5 x ULN OR creatinine clearance  $\geq$  60 mL/min/1.73 m<sup>2</sup> for patients with creatinine levels above institutional normal
- Women of child-bearing potential and men must agree to use adequate contraception (hormonal or barrier method of birth control; abstinence) prior to study entry and for the duration of study participation; should a woman become pregnant or suspect she is pregnant while she or her partner is participating in this study, she should inform her treating physician immediately; men and women treated or enrolled on this protocol must also agree to use adequate contraception prior to the study, for the duration of study participation, and 4 months after completion of veliparib, MM-398 and ferumoxytol MRI administration
- Ability to understand and the willingness to sign a written informed consent document
- IMAGING CORRELATIVE STUDY: Patients will be eligible to participate in the ferumoxytol (FMX) imaging study if they do not meet any of the following criteria
  - Evidence of iron overload as determined by:
    - \* Fasting transferrin saturation of  $>$  45% and/or
    - \* Serum ferritin levels  $>$  1000 ng/ml
  - A history of allergic reactions to any of the following:
    - \* Compounds similar to ferumoxytol or any of its components as described in full prescribing information for ferumoxytol injection
    - \* Any IV iron replacement product (e.g. parenteral iron, dextran, iron-dextran, or parenteral iron polysaccharide preparations)

## \* Multiple drugs

- Unable to undergo MRI or for whom MRI is otherwise contraindicated (e.g. presence of errant metal, cardiac pacemakers, pain pumps or other MRI incompatible devices; or history claustrophobia or anxiety related to undergoing MRI)

## Exclusion Criteria:

- Patients who have had chemotherapy or radiotherapy within 4 weeks (6 weeks for nitrosoureas or mitomycin C) prior to entering the study or those who have not recovered from adverse events due to agents administered more than 4 weeks earlier; patients must have completed prior biological therapies and/or targeted therapies  $\geq$  2 weeks prior to study enrollment; patients who have had radiation to the pelvis or other bone marrow-bearing sites will be considered on a case by case basis and may be excluded if the bone marrow reserve is not considered adequate (i.e. radiation to  $>$  25% of bone marrow)
- Patients who are receiving any other investigational agents
- Patients with active brain metastases should be excluded from this clinical trial
- History of allergic reactions attributed to compounds of similar chemical or biologic composition to veliparib, MM-398 and ferumoxytol
- Clinically significant gastrointestinal (GI) disorders, including history of small bowel obstruction unless the obstruction was a surgically treated remote episode
- Active infection
- Uncontrolled intercurrent illness including, but not limited to, ongoing or active infection, symptomatic congestive heart failure, unstable angina pectoris, cardiac arrhythmia, or psychiatric illness/social situations that would limit compliance with study requirements
- Pregnant women are excluded from this study; breastfeeding should be discontinued if the mother is treated with any of these agents
- Human immunodeficiency virus (HIV)-positive patients on combination antiretroviral therapy are ineligible
- Patients who are taking medications which are strong inhibitors or inducers of cytochrome P450, family 3, subfamily A, polypeptide 4 (CYP3A4)

<b>Gender</b>	Both
<b>Minimum age</b>	18 Years
<b>Healthy volunteers</b>	No

**Administrative Data**

<b>Organization name</b>	National Cancer Institute (NCI)
<b>Organization study ID</b>	NCI-2015-02125
<b>Secondary ID</b>	NCI-2015-02125 (CTRP (Clinical Trial Reporting Program))
<b>Secondary ID</b>	9914 (National Cancer Institute LAO)
<b>Secondary ID</b>	9914 (CTEP)
<b>Sponsor</b>	National Cancer Institute (NCI)
<b>Collaborator</b>	National Cancer Institute (NCI)
<b>Health Authority</b>	United States: Food and Drug Administration



# ClinicalTrials.gov archive

A service of the U.S. National Institutes of Health

Developed by the National Library of Medicine

[← History of this study](#)    [↑ Current version of this study](#)

## View of NCT02631733 on 2016\_06\_21

**ClinicalTrials Identifier:** NCT02631733**Updated:** 2016\_06\_21

---

### Descriptive Information

**Brief title** Liposomal Irinotecan and Veliparib in Treating Patients With Solid Tumors That Are Metastatic or Cannot Be Removed by Surgery**Official title** A Phase I Study of a Combination of MM-398 and Veliparib in Solid Tumors**Brief summary**

This phase I trial studies the side effects and best dose of veliparib when given together with liposomal irinotecan in treating patients with solid tumors that have spread to other parts of the body (metastatic) or cannot be removed by surgery. Liposomal irinotecan and veliparib may stop the growth of tumor cells by blocking some of the enzymes needed for cell growth.

**Detailed description****PRIMARY OBJECTIVES:**

- I. To evaluate the safety and tolerability of escalating doses of MM-398 (liposomal irinotecan) + veliparib combination.
- II. To determine the maximum tolerated dose (MTD) and recommended phase 2 dose (RP2D) of the combination of MM-398 + veliparib.

**SECONDARY OBJECTIVES:**

- I. To observe and record anti-tumor activity.
- II. To characterize the preliminary efficacy of the combination using key efficacy indicators, such as objective response rate, clinical benefit rate defined as complete response (CR), partial response (PR), or stable disease (SD) at 24 weeks, and progression free survival (PFS).

**EXPLORATORY OBJECTIVES**

- I. Imaging, tumor, and blood biomarkers to assess the sensitivity or resistance to each drug and correlation with clinical response.

**OUTLINE:** This is a dose-escalation of veliparib.

Patients receive liposomal irinotecan intravenously (IV) over 90 minutes on days 1 and 15 and veliparib orally (PO) on days 5-12 and 19-25 or 3-12 and 17-25. Courses repeat every 28 days in the absence of disease progression or unacceptable toxicity.

After completion of study treatment, patients are followed up for 4 weeks.

<b>Phase</b>	Phase 1
<b>Study type</b>	Interventional
<b>Study design</b>	Treatment
<b>Study design</b>	Open Label
<b>Study design</b>	Single Group Assignment
<b>Study design</b>	Safety Study
<b>Primary outcome</b>	Measure: Incidence of adverse events, graded using the NCI Common Terminology Criteria for Adverse Events (CTCAE) version 4.0 Time Frame: Up to 4 weeks Safety Issue? Yes
<b>Primary outcome</b>	Measure: MTD and RP2D of liposomal irinotecan in combination with veliparib determined by incidence of dose limiting toxicities, graded using the NCI CTCAE version 4.0 Time Frame: 28 days Safety Issue? Yes
<b>Secondary outcome</b>	Measure: Clinical benefit rate defined as CR, PR, or SD assessed using RECIST version 1.1 Time Frame: At 24 weeks Safety Issue? No
<b>Secondary outcome</b>	Measure: Objective response rate assessed using RECIST version 1.1 Time Frame: At 24 weeks Safety Issue? No
<b>Secondary outcome</b>	Measure: PFS Time Frame: Duration of time from start of treatment to time of progression or death, whichever occurs first, assessed up to 4 weeks after completion of study treatment Safety Issue? No
<b>Secondary outcome</b>	Measure: Tumor response assessed using the revised Response Evaluation Criteria in Solid Tumors (RECIST) guideline (version 1.1) Time Frame: Up to 4 weeks after completion of study treatment Safety Issue? No
<b>Enrollment</b>	48 (Anticipated)
<b>Condition</b>	Estrogen Receptor Negative
<b>Condition</b>	HER2/Neu Negative
<b>Condition</b>	Neuroendocrine Neoplasm
<b>Condition</b>	Progesterone Receptor Negative
<b>Condition</b>	Stage IIB Cervical Cancer
<b>Condition</b>	Stage IIIA Cervical Cancer

<b>Condition</b>	Stage IIIB Cervical Cancer
<b>Condition</b>	Stage IIIB Non-Small Cell Lung Cancer
<b>Condition</b>	Stage IIIC Breast Cancer
<b>Condition</b>	Stage IV Breast Cancer
<b>Condition</b>	Stage IV Cervical Cancer
<b>Condition</b>	Stage IV Gastric Cancer
<b>Condition</b>	Stage IV Non-Small Cell Lung Cancer
<b>Condition</b>	Stage IV Ovarian Cancer
<b>Condition</b>	Stage IV Small Cell Lung Carcinoma
<b>Condition</b>	Triple-Negative Breast Carcinoma
<b>Arm/Group</b>	Arm Label: Treatment (liposomal irinotecan, veliparib) Experimental
	Patients receive liposomal irinotecan IV over 90 minutes on days 1 and 15 and veliparib PO on days 5-12 and 19-25 or 3-12 and 17-25. Courses repeat every 28 days in the absence of disease progression or unacceptable toxicity.
<b>Intervention</b>	Drug: Ferumoxytol      Arm Label: Treatment (liposomal irinotecan, veliparib)
	Correlative studies
<b>Intervention</b>	Other: Laboratory Biomarker Analysis      Arm Label: Treatment (liposomal irinotecan, veliparib)
	Correlative studies
<b>Intervention</b>	Drug: Liposomal Irinotecan      Arm Label: Treatment (liposomal irinotecan, veliparib)
	Given IV
<b>Intervention</b>	Procedure/Surgery: Magnetic Resonance Imaging Arm Label: Treatment (liposomal irinotecan, veliparib)
	Correlative studies
<b>Intervention</b>	Drug: Veliparib      Arm Label: Treatment (liposomal irinotecan, veliparib)
	Given PO

---

### Recruitment Information

<b>Status</b>	Not yet recruiting
<b>Start date</b>	2016-05
<b>Primary completion date</b>	2018-01 (Anticipated)
<b>Criteria</b>	

Inclusion Criteria:

- Patients must have pathologically confirmed diagnosis of one of the following



solid tumors: cervical cancer, ovarian cancer, triple negative breast cancer (TNBC), non-small cell lung cancer (NSCLC), small cell lung cancer (SCLC), gastric cancer, and neuroendocrine tumors that is metastatic or unresectable and for which standard curative or palliative measures do not exist or are no longer effective

- Prior poly ADP ribose polymerase (PARP) inhibitor therapy is allowed
- Patients at the National Cancer Institute (NCI) site must be willing to undergo a pre-treatment ferumoxytol magnetic resonance imaging (MRI) (patients will be excluded from undergoing ferumoxytol MRI if they have evidence of iron overload, a known hypersensitivity to ferumoxytol or any other IV iron product, a documented history of multiple drug allergies, or those for whom MRI is otherwise contraindicated, including claustrophobia or anxiety related to undergoing MRI); this eligibility criterion applies only to patients enrolling at NCI
- Eastern Cooperative Oncology Group (ECOG) performance status  $\leq$  2 (Karnofsky  $\geq$  60%)
- Life expectancy of greater than 3 months
- Hemoglobin  $>$  9 g/dL
- Leukocytes  $\geq$  3,000/mcL
- Absolute neutrophil count  $\geq$  1,500/mcL without the use of hematopoietic growth factors
- Platelets  $\geq$  100,000/mcL
- Total bilirubin within normal institutional limits
- Aspartate aminotransferase (AST)(serum glutamic oxaloacetic transaminase [SGOT])/alanine aminotransferase (ALT)(serum glutamate pyruvate transaminase [SGPT])  $\leq$  2.5 x institutional upper limit of normal ( $\leq$  5 x upper limit of normal [ULN] is acceptable if liver metastases are present)
- Creatinine  $\leq$  1.5 x ULN OR creatinine clearance  $\geq$  60 mL/min/1.73 m<sup>2</sup> for patients with creatinine levels above institutional normal
- Women of child-bearing potential and men must agree to use adequate contraception (hormonal or barrier method of birth control; abstinence) prior to study entry and for the duration of study participation; should a woman become pregnant or suspect she is pregnant while she or her partner is participating in this study, she should inform her treating physician immediately; men and women treated or enrolled on this protocol must also agree to use adequate contraception prior to the study, for the duration of study participation, and 4 months after completion of veliparib, MM-398 and ferumoxytol MRI administration
- Ability to understand and the willingness to sign a written informed consent document
- IMAGING CORRELATIVE STUDY: Patients will be eligible to participate in the ferumoxytol (FMX) imaging study if they do not meet any of the following criteria
  - Evidence of iron overload as determined by:
    - \* Fasting transferrin saturation of  $>$  45% and/or
    - \* Serum ferritin levels  $>$  1000 ng/ml
  - A history of allergic reactions to any of the following:
    - \* Compounds similar to ferumoxytol or any of its components as described in full prescribing information for ferumoxytol injection
    - \* Any IV iron replacement product (e.g. parenteral iron, dextran, iron-dextran, or parenteral iron polysaccharide preparations)

## \* Multiple drugs

- Unable to undergo MRI or for whom MRI is otherwise contraindicated (e.g. presence of errant metal, cardiac pacemakers, pain pumps or other MRI incompatible devices; or history claustrophobia or anxiety related to undergoing MRI)

## Exclusion Criteria:

- Patients who have had chemotherapy or radiotherapy within 4 weeks (6 weeks for nitrosoureas or mitomycin C) prior to entering the study or those who have not recovered from adverse events due to agents administered more than 4 weeks earlier; patients must have completed prior biological therapies and/or targeted therapies  $\geq$  2 weeks prior to study enrollment; patients who have had radiation to the pelvis or other bone marrow-bearing sites will be considered on a case by case basis and may be excluded if the bone marrow reserve is not considered adequate (i.e. radiation to  $>$  25% of bone marrow)
- Patients who are receiving any other investigational agents
- Patients with active brain metastases should be excluded from this clinical trial
- History of allergic reactions attributed to compounds of similar chemical or biologic composition to veliparib, MM-398 and ferumoxytol
- Clinically significant gastrointestinal (GI) disorders, including history of small bowel obstruction unless the obstruction was a surgically treated remote episode
- Active infection
- Uncontrolled intercurrent illness including, but not limited to, ongoing or active infection, symptomatic congestive heart failure, unstable angina pectoris, cardiac arrhythmia, or psychiatric illness/social situations that would limit compliance with study requirements
- Pregnant women are excluded from this study; breastfeeding should be discontinued if the mother is treated with any of these agents
- Human immunodeficiency virus (HIV)-positive patients on combination antiretroviral therapy are ineligible
- Patients who are taking medications which are strong inhibitors or inducers of cytochrome P450, family 3, subfamily A, polypeptide 4 (CYP3A4)

<b>Gender</b>	Both
<b>Minimum age</b>	18 Years
<b>Healthy volunteers</b>	No

**Administrative Data**

<b>Organization name</b>	National Cancer Institute (NCI)
<b>Organization study ID</b>	NCI-2015-02125
<b>Secondary ID</b>	NCI-2015-02125 (CTRP (Clinical Trial Reporting Program))
<b>Secondary ID</b>	9914 (National Cancer Institute LAO)
<b>Secondary ID</b>	9914 (CTEP)
<b>Sponsor</b>	National Cancer Institute (NCI)
<b>Collaborator</b>	National Cancer Institute (NCI)
<b>Health Authority</b>	United States: Food and Drug Administration



# ClinicalTrials.gov archive

A service of the U.S. National Institutes of Health

Developed by the National Library of Medicine

[← History of this study](#)    [↑ Current version of this study](#)

## View of NCT02631733 on 2016\_07\_06

**ClinicalTrials Identifier:** NCT02631733**Updated:** 2016\_07\_06

---

### Descriptive Information

**Brief title** Liposomal Irinotecan and Veliparib in Treating Patients With Solid Tumors That Are Metastatic or Cannot Be Removed by Surgery**Official title** A Phase I Study of a Combination of MM-398 and Veliparib in Solid Tumors**Brief summary**

This phase I trial studies the side effects and best dose of veliparib when given together with liposomal irinotecan in treating patients with solid tumors that have spread to other parts of the body (metastatic) or cannot be removed by surgery. Liposomal irinotecan and veliparib may stop the growth of tumor cells by blocking some of the enzymes needed for cell growth.

**Detailed description****PRIMARY OBJECTIVES:**

- I. To evaluate the safety and tolerability of escalating doses of MM-398 (liposomal irinotecan) + veliparib combination.
- II. To determine the maximum tolerated dose (MTD) and recommended phase 2 dose (RP2D) of the combination of MM-398 + veliparib.

**SECONDARY OBJECTIVES:**

- I. To observe and record anti-tumor activity.
- II. To characterize the preliminary efficacy of the combination using key efficacy indicators, such as objective response rate, clinical benefit rate defined as complete response (CR), partial response (PR), or stable disease (SD) at 24 weeks, and progression free survival (PFS).

**EXPLORATORY OBJECTIVES**

- I. Imaging, tumor, and blood biomarkers to assess the sensitivity or resistance to each drug and correlation with clinical response.

**OUTLINE:** This is a dose-escalation of veliparib.

Patients receive liposomal irinotecan intravenously (IV) over 90 minutes on days 1 and 15 and veliparib orally (PO) on days 5-12 and 19-25 or 3-12 and 17-25. Courses repeat every 28 days in the absence of disease progression or unacceptable toxicity.

After completion of study treatment, patients are followed up for 4 weeks.

<b>Phase</b>	Phase 1
<b>Study type</b>	Interventional
<b>Study design</b>	Treatment
<b>Study design</b>	Open Label
<b>Study design</b>	Single Group Assignment
<b>Study design</b>	Safety Study
<b>Primary outcome</b>	Measure: Incidence of adverse events, graded using the NCI Common Terminology Criteria for Adverse Events (CTCAE) version 4.0 Time Frame: Up to 4 weeks Safety Issue? Yes
<b>Primary outcome</b>	Measure: MTD and RP2D of liposomal irinotecan in combination with veliparib determined by incidence of dose limiting toxicities, graded using the NCI CTCAE version 4.0 Time Frame: 28 days Safety Issue? Yes
<b>Secondary outcome</b>	Measure: Clinical benefit rate defined as CR, PR, or SD assessed using RECIST version 1.1 Time Frame: At 24 weeks Safety Issue? No
<b>Secondary outcome</b>	Measure: Objective response rate assessed using RECIST version 1.1 Time Frame: At 24 weeks Safety Issue? No
<b>Secondary outcome</b>	Measure: PFS Time Frame: Duration of time from start of treatment to time of progression or death, whichever occurs first, assessed up to 4 weeks after completion of study treatment Safety Issue? No
<b>Secondary outcome</b>	Measure: Tumor response assessed using the revised Response Evaluation Criteria in Solid Tumors (RECIST) guideline (version 1.1) Time Frame: Up to 4 weeks after completion of study treatment Safety Issue? No
<b>Enrollment</b>	48 (Anticipated)
<b>Condition</b>	Estrogen Receptor Negative
<b>Condition</b>	HER2/Neu Negative
<b>Condition</b>	Neuroendocrine Neoplasm
<b>Condition</b>	Progesterone Receptor Negative
<b>Condition</b>	Stage IIB Cervical Cancer
<b>Condition</b>	Stage IIIA Cervical Cancer

<b>Condition</b>	Stage IIIB Cervical Cancer
<b>Condition</b>	Stage IIIB Non-Small Cell Lung Cancer
<b>Condition</b>	Stage IIIC Breast Cancer
<b>Condition</b>	Stage IV Breast Cancer
<b>Condition</b>	Stage IV Cervical Cancer
<b>Condition</b>	Stage IV Gastric Cancer
<b>Condition</b>	Stage IV Non-Small Cell Lung Cancer
<b>Condition</b>	Stage IV Ovarian Cancer
<b>Condition</b>	Stage IV Small Cell Lung Carcinoma
<b>Condition</b>	Triple-Negative Breast Carcinoma
<b>Arm/Group</b>	Arm Label: Treatment (liposomal irinotecan, veliparib) Experimental
	Patients receive liposomal irinotecan IV over 90 minutes on days 1 and 15 and veliparib PO on days 5-12 and 19-25 or 3-12 and 17-25. Courses repeat every 28 days in the absence of disease progression or unacceptable toxicity.
<b>Intervention</b>	Drug: Ferumoxytol      Arm Label: Treatment (liposomal irinotecan, veliparib)
	Correlative studies
<b>Intervention</b>	Other: Laboratory Biomarker Analysis      Arm Label: Treatment (liposomal irinotecan, veliparib)
	Correlative studies
<b>Intervention</b>	Drug: Liposomal Irinotecan      Arm Label: Treatment (liposomal irinotecan, veliparib)
	Given IV
<b>Intervention</b>	Procedure/Surgery: Magnetic Resonance Imaging Arm Label: Treatment (liposomal irinotecan, veliparib)
	Correlative studies
<b>Intervention</b>	Drug: Veliparib      Arm Label: Treatment (liposomal irinotecan, veliparib)
	Given PO

---

### Recruitment Information

<b>Status</b>	Not yet recruiting
<b>Start date</b>	2016-05
<b>Primary completion date</b>	2018-01 (Anticipated)
<b>Criteria</b>	

#### Inclusion Criteria:

- Patients must have pathologically confirmed diagnosis of one of the following

solid tumors: cervical cancer, ovarian cancer, triple negative breast cancer (TNBC), non-small cell lung cancer (NSCLC), small cell lung cancer (SCLC), gastric cancer, and neuroendocrine tumors that is metastatic or unresectable and for which standard curative or palliative measures do not exist or are no longer effective

- Prior poly ADP ribose polymerase (PARP) inhibitor therapy is allowed
- Patients at the National Cancer Institute (NCI) site must be willing to undergo a pre-treatment ferumoxytol magnetic resonance imaging (MRI) (patients will be excluded from undergoing ferumoxytol MRI if they have evidence of iron overload, a known hypersensitivity to ferumoxytol or any other IV iron product, a documented history of multiple drug allergies, or those for whom MRI is otherwise contraindicated, including claustrophobia or anxiety related to undergoing MRI); this eligibility criterion applies only to patients enrolling at NCI
- Eastern Cooperative Oncology Group (ECOG) performance status  $\leq$  2 (Karnofsky  $\geq$  60%)
- Life expectancy of greater than 3 months
- Hemoglobin  $>$  9 g/dL
- Leukocytes  $\geq$  3,000/mcL
- Absolute neutrophil count  $\geq$  1,500/mcL without the use of hematopoietic growth factors
- Platelets  $\geq$  100,000/mcL
- Total bilirubin within normal institutional limits
- Aspartate aminotransferase (AST)(serum glutamic oxaloacetic transaminase [SGOT])/alanine aminotransferase (ALT)(serum glutamate pyruvate transaminase [SGPT])  $\leq$  2.5 x institutional upper limit of normal ( $\leq$  5 x upper limit of normal [ULN] is acceptable if liver metastases are present)
- Creatinine  $\leq$  1.5 x ULN OR creatinine clearance  $\geq$  60 mL/min/1.73 m<sup>2</sup> for patients with creatinine levels above institutional normal
- Women of child-bearing potential and men must agree to use adequate contraception (hormonal or barrier method of birth control; abstinence) prior to study entry and for the duration of study participation; should a woman become pregnant or suspect she is pregnant while she or her partner is participating in this study, she should inform her treating physician immediately; men and women treated or enrolled on this protocol must also agree to use adequate contraception prior to the study, for the duration of study participation, and 4 months after completion of veliparib, MM-398 and ferumoxytol MRI administration
- Ability to understand and the willingness to sign a written informed consent document
- IMAGING CORRELATIVE STUDY: Patients will be eligible to participate in the ferumoxytol (FMX) imaging study if they do not meet any of the following criteria
  - Evidence of iron overload as determined by:
    - \* Fasting transferrin saturation of  $>$  45% and/or
    - \* Serum ferritin levels  $>$  1000 ng/ml
  - A history of allergic reactions to any of the following:
    - \* Compounds similar to ferumoxytol or any of its components as described in full prescribing information for ferumoxytol injection
    - \* Any IV iron replacement product (e.g. parenteral iron, dextran, iron-dextran, or parenteral iron polysaccharide preparations)

## \* Multiple drugs

- Unable to undergo MRI or for whom MRI is otherwise contraindicated (e.g. presence of errant metal, cardiac pacemakers, pain pumps or other MRI incompatible devices; or history claustrophobia or anxiety related to undergoing MRI)

## Exclusion Criteria:

- Patients who have had chemotherapy or radiotherapy within 4 weeks (6 weeks for nitrosoureas or mitomycin C) prior to entering the study or those who have not recovered from adverse events due to agents administered more than 4 weeks earlier; patients must have completed prior biological therapies and/or targeted therapies  $\geq$  2 weeks prior to study enrollment; patients who have had radiation to the pelvis or other bone marrow-bearing sites will be considered on a case by case basis and may be excluded if the bone marrow reserve is not considered adequate (i.e. radiation to  $>$  25% of bone marrow)
- Patients who are receiving any other investigational agents
- Patients with active brain metastases should be excluded from this clinical trial
- History of allergic reactions attributed to compounds of similar chemical or biologic composition to veliparib, MM-398 and ferumoxytol
- Clinically significant gastrointestinal (GI) disorders, including history of small bowel obstruction unless the obstruction was a surgically treated remote episode
- Active infection
- Uncontrolled intercurrent illness including, but not limited to, ongoing or active infection, symptomatic congestive heart failure, unstable angina pectoris, cardiac arrhythmia, or psychiatric illness/social situations that would limit compliance with study requirements
- Pregnant women are excluded from this study; breastfeeding should be discontinued if the mother is treated with any of these agents
- Human immunodeficiency virus (HIV)-positive patients on combination antiretroviral therapy are ineligible
- Patients who are taking medications which are strong inhibitors or inducers of cytochrome P450, family 3, subfamily A, polypeptide 4 (CYP3A4)

<b>Gender</b>	Both
<b>Minimum age</b>	18 Years
<b>Healthy volunteers</b>	No

---

**Administrative Data**

<b>Organization name</b>	National Cancer Institute (NCI)
<b>Organization study ID</b>	NCI-2015-02125
<b>Secondary ID</b>	NCI-2015-02125 (CTRP (Clinical Trial Reporting Program))
<b>Secondary ID</b>	9914 (National Cancer Institute LAO)
<b>Secondary ID</b>	9914 (CTEP)
<b>Sponsor</b>	National Cancer Institute (NCI)
<b>Collaborator</b>	National Cancer Institute (NCI)
<b>Health Authority</b>	United States: Food and Drug Administration





# ClinicalTrials.gov archive

A service of the U.S. National Institutes of Health

Developed by the National Library of Medicine

[← History of this study](#)    [↑ Current version of this study](#)

## View of NCT02631733 on 2016\_07\_11

**ClinicalTrials Identifier:** NCT02631733**Updated:** 2016\_07\_11

---

### Descriptive Information

**Brief title** Liposomal Irinotecan and Veliparib in Treating Patients With Solid Tumors That Are Metastatic or Cannot Be Removed by Surgery**Official title** A Phase I Study of a Combination of MM-398 and Veliparib in Solid Tumors**Brief summary**

This phase I trial studies the side effects and best dose of veliparib when given together with liposomal irinotecan in treating patients with solid tumors that have spread to other parts of the body (metastatic) or cannot be removed by surgery. Liposomal irinotecan and veliparib may stop the growth of tumor cells by blocking some of the enzymes needed for cell growth.

**Detailed description****PRIMARY OBJECTIVES:**

- I. To evaluate the safety and tolerability of escalating doses of MM-398 (liposomal irinotecan) + veliparib combination.
- II. To determine the maximum tolerated dose (MTD) and recommended phase 2 dose (RP2D) of the combination of MM-398 + veliparib.

**SECONDARY OBJECTIVES:**

- I. To observe and record anti-tumor activity.
- II. To characterize the preliminary efficacy of the combination using key efficacy indicators, such as objective response rate, clinical benefit rate defined as complete response (CR), partial response (PR), or stable disease (SD) at 24 weeks, and progression free survival (PFS).

**EXPLORATORY OBJECTIVES**

- I. Imaging, tumor, and blood biomarkers to assess the sensitivity or resistance to each drug and correlation with clinical response.

**OUTLINE:** This is a dose-escalation of veliparib.

Patients receive liposomal irinotecan intravenously (IV) over 90 minutes on days 1 and 15 and veliparib orally (PO) on days 5-12 and 19-25 or 3-12 and 17-25. Courses repeat every 28 days in the absence of disease progression or unacceptable toxicity.

After completion of study treatment, patients are followed up for 4 weeks.

<b>Phase</b>	Phase 1
<b>Study type</b>	Interventional
<b>Study design</b>	Treatment
<b>Study design</b>	Open Label
<b>Study design</b>	Single Group Assignment
<b>Study design</b>	Safety Study
<b>Primary outcome</b>	Measure: Incidence of adverse events, graded using the NCI Common Terminology Criteria for Adverse Events (CTCAE) version 4.0 Time Frame: Up to 4 weeks Safety Issue? Yes
<b>Primary outcome</b>	Measure: MTD and RP2D of liposomal irinotecan in combination with veliparib determined by incidence of dose limiting toxicities, graded using the NCI CTCAE version 4.0 Time Frame: 28 days Safety Issue? Yes
<b>Secondary outcome</b>	Measure: Clinical benefit rate defined as CR, PR, or SD assessed using RECIST version 1.1 Time Frame: At 24 weeks Safety Issue? No
<b>Secondary outcome</b>	Measure: Objective response rate assessed using RECIST version 1.1 Time Frame: At 24 weeks Safety Issue? No
<b>Secondary outcome</b>	Measure: PFS Time Frame: Duration of time from start of treatment to time of progression or death, whichever occurs first, assessed up to 4 weeks after completion of study treatment Safety Issue? No
<b>Secondary outcome</b>	Measure: Tumor response assessed using the revised Response Evaluation Criteria in Solid Tumors (RECIST) guideline (version 1.1) Time Frame: Up to 4 weeks after completion of study treatment Safety Issue? No
<b>Enrollment</b>	48 (Anticipated)
<b>Condition</b>	Estrogen Receptor Negative
<b>Condition</b>	HER2/Neu Negative
<b>Condition</b>	Neuroendocrine Neoplasm
<b>Condition</b>	Progesterone Receptor Negative
<b>Condition</b>	Stage IIB Cervical Cancer
<b>Condition</b>	Stage IIIA Cervical Cancer

<b>Condition</b>	Stage IIIB Cervical Cancer
<b>Condition</b>	Stage IIIB Non-Small Cell Lung Cancer
<b>Condition</b>	Stage IIIC Breast Cancer
<b>Condition</b>	Stage IV Breast Cancer
<b>Condition</b>	Stage IV Cervical Cancer
<b>Condition</b>	Stage IV Gastric Cancer
<b>Condition</b>	Stage IV Non-Small Cell Lung Cancer
<b>Condition</b>	Stage IV Ovarian Cancer
<b>Condition</b>	Stage IV Small Cell Lung Carcinoma
<b>Condition</b>	Triple-Negative Breast Carcinoma
<b>Arm/Group</b>	Arm Label: Treatment (liposomal irinotecan, veliparib) Experimental
	Patients receive liposomal irinotecan IV over 90 minutes on days 1 and 15 and veliparib PO on days 5-12 and 19-25 or 3-12 and 17-25. Courses repeat every 28 days in the absence of disease progression or unacceptable toxicity.
<b>Intervention</b>	Drug: Ferumoxytol      Arm Label: Treatment (liposomal irinotecan, veliparib)
	Correlative studies
<b>Intervention</b>	Other: Laboratory Biomarker Analysis      Arm Label: Treatment (liposomal irinotecan, veliparib)
	Correlative studies
<b>Intervention</b>	Drug: Liposomal Irinotecan      Arm Label: Treatment (liposomal irinotecan, veliparib)
	Given IV
<b>Intervention</b>	Procedure/Surgery: Magnetic Resonance Imaging Arm Label: Treatment (liposomal irinotecan, veliparib)
	Correlative studies
<b>Intervention</b>	Drug: Veliparib      Arm Label: Treatment (liposomal irinotecan, veliparib)
	Given PO

---

### Recruitment Information

<b>Status</b>	Not yet recruiting
<b>Start date</b>	2016-07
<b>Primary completion date</b>	2019-07 (Anticipated)
<b>Criteria</b>	

Inclusion Criteria:

- Patients must have pathologically confirmed diagnosis of one of the following

CSPC Exhibit 1094

Page 368 of 512

solid tumors: cervical cancer, ovarian cancer, triple negative breast cancer (TNBC), non-small cell lung cancer (NSCLC), small cell lung cancer (SCLC), gastric cancer, and neuroendocrine tumors that is metastatic or unresectable and for which standard curative or palliative measures do not exist or are no longer effective

- Prior poly ADP ribose polymerase (PARP) inhibitor therapy is allowed
- Patients at the National Cancer Institute (NCI) site must be willing to undergo a pre-treatment ferumoxytol magnetic resonance imaging (MRI) (patients will be excluded from undergoing ferumoxytol MRI if they have evidence of iron overload, a known hypersensitivity to ferumoxytol or any other IV iron product, a documented history of multiple drug allergies, or those for whom MRI is otherwise contraindicated, including claustrophobia or anxiety related to undergoing MRI); this eligibility criterion applies only to patients enrolling at NCI
- Eastern Cooperative Oncology Group (ECOG) performance status  $\leq$  2 (Karnofsky  $\geq$  60%)
- Life expectancy of greater than 3 months
- Hemoglobin  $>$  9 g/dL
- Leukocytes  $\geq$  3,000/mcL
- Absolute neutrophil count  $\geq$  1,500/mcL without the use of hematopoietic growth factors
- Platelets  $\geq$  100,000/mcL
- Total bilirubin within normal institutional limits
- Aspartate aminotransferase (AST)(serum glutamic oxaloacetic transaminase [SGOT])/alanine aminotransferase (ALT)(serum glutamate pyruvate transaminase [SGPT])  $\leq$  2.5 x institutional upper limit of normal ( $\leq$  5 x upper limit of normal [ULN] is acceptable if liver metastases are present)
- Creatinine  $\leq$  1.5 x ULN OR creatinine clearance  $\geq$  60 mL/min/1.73 m<sup>2</sup> for patients with creatinine levels above institutional normal
- Women of child-bearing potential and men must agree to use adequate contraception (hormonal or barrier method of birth control; abstinence) prior to study entry and for the duration of study participation; should a woman become pregnant or suspect she is pregnant while she or her partner is participating in this study, she should inform her treating physician immediately; men and women treated or enrolled on this protocol must also agree to use adequate contraception prior to the study, for the duration of study participation, and 4 months after completion of veliparib, MM-398 and ferumoxytol MRI administration
- Ability to understand and the willingness to sign a written informed consent document
- IMAGING CORRELATIVE STUDY: Patients will be eligible to participate in the ferumoxytol (FMX) imaging study if they do not meet any of the following criteria
  - Evidence of iron overload as determined by:
    - \* Fasting transferrin saturation of  $>$  45% and/or
    - \* Serum ferritin levels  $>$  1000 ng/ml
  - A history of allergic reactions to any of the following:
    - \* Compounds similar to ferumoxytol or any of its components as described in full prescribing information for ferumoxytol injection
    - \* Any IV iron replacement product (e.g. parenteral iron, dextran, iron-dextran, or parenteral iron polysaccharide preparations)

## \* Multiple drugs

- Unable to undergo MRI or for whom MRI is otherwise contraindicated (e.g. presence of errant metal, cardiac pacemakers, pain pumps or other MRI incompatible devices; or history claustrophobia or anxiety related to undergoing MRI)

## Exclusion Criteria:

- Patients who have had chemotherapy or radiotherapy within 4 weeks (6 weeks for nitrosoureas or mitomycin C) prior to entering the study or those who have not recovered from adverse events due to agents administered more than 4 weeks earlier; patients must have completed prior biological therapies and/or targeted therapies  $\geq$  2 weeks prior to study enrollment; patients who have had radiation to the pelvis or other bone marrow-bearing sites will be considered on a case by case basis and may be excluded if the bone marrow reserve is not considered adequate (i.e. radiation to  $>$  25% of bone marrow)
- Patients who are receiving any other investigational agents
- Patients with active brain metastases should be excluded from this clinical trial
- History of allergic reactions attributed to compounds of similar chemical or biologic composition to veliparib, MM-398 and ferumoxytol
- Clinically significant gastrointestinal (GI) disorders, including history of small bowel obstruction unless the obstruction was a surgically treated remote episode
- Active infection
- Uncontrolled intercurrent illness including, but not limited to, ongoing or active infection, symptomatic congestive heart failure, unstable angina pectoris, cardiac arrhythmia, or psychiatric illness/social situations that would limit compliance with study requirements
- Pregnant women are excluded from this study; breastfeeding should be discontinued if the mother is treated with any of these agents
- Human immunodeficiency virus (HIV)-positive patients on combination antiretroviral therapy are ineligible
- Patients who are taking medications which are strong inhibitors or inducers of cytochrome P450, family 3, subfamily A, polypeptide 4 (CYP3A4)

<b>Gender</b>	Both
<b>Minimum age</b>	18 Years
<b>Healthy volunteers</b>	No

---

**Administrative Data**

<b>Organization name</b>	National Cancer Institute (NCI)
<b>Organization study ID</b>	NCI-2015-02125
<b>Secondary ID</b>	NCI-2015-02125 (CTRP (Clinical Trial Reporting Program))
<b>Secondary ID</b>	TBD
<b>Secondary ID</b>	9914 (National Cancer Institute LAO)
<b>Secondary ID</b>	9914 (CTEP)
<b>Sponsor</b>	National Cancer Institute (NCI)
<b>Collaborator</b>	National Cancer Institute (NCI)

**Health Authority**

United States: Food and Drug Administration

# ClinicalTrials.gov archive

A service of the U.S. National Institutes of Health

Developed by the National Library of Medicine

[← History of this study](#)    [↑ Current version of this study](#)

## View of NCT02631733 on 2016\_07\_19

**ClinicalTrials Identifier:** NCT02631733**Updated:** 2016\_07\_19

---

### Descriptive Information

**Brief title** Liposomal Irinotecan and Veliparib in Treating Patients With Solid Tumors That Are Metastatic or Cannot Be Removed by Surgery**Official title** A Phase I Study of a Combination of MM-398 and Veliparib in Solid Tumors**Brief summary**

This phase I trial studies the side effects and best dose of veliparib when given together with liposomal irinotecan in treating patients with solid tumors that have spread to other parts of the body (metastatic) or cannot be removed by surgery. Liposomal irinotecan and veliparib may stop the growth of tumor cells by blocking some of the enzymes needed for cell growth.

**Detailed description****PRIMARY OBJECTIVES:**

- I. To evaluate the safety and tolerability of escalating doses of MM-398 (liposomal irinotecan) + veliparib combination.
- II. To determine the maximum tolerated dose (MTD) and recommended phase 2 dose (RP2D) of the combination of MM-398 + veliparib.

**SECONDARY OBJECTIVES:**

- I. To observe and record anti-tumor activity.
- II. To characterize the preliminary efficacy of the combination using key efficacy indicators, such as objective response rate, clinical benefit rate defined as complete response (CR), partial response (PR), or stable disease (SD) at 24 weeks, and progression free survival (PFS).

**EXPLORATORY OBJECTIVES**

- I. Imaging, tumor, and blood biomarkers to assess the sensitivity or resistance to each drug and correlation with clinical response.

**OUTLINE:** This is a dose-escalation of veliparib.

Patients receive liposomal irinotecan intravenously (IV) over 90 minutes on days 1 and 15 and veliparib orally (PO) on days 5-12 and 19-25 or 3-12 and 17-25. Courses repeat every 28 days in the absence of disease progression or unacceptable toxicity.



After completion of study treatment, patients are followed up for 4 weeks.

<b>Phase</b>	Phase 1
<b>Study type</b>	Interventional
<b>Study design</b>	Treatment
<b>Study design</b>	Open Label
<b>Study design</b>	Single Group Assignment
<b>Study design</b>	Safety Study
<b>Primary outcome</b>	Measure: Incidence of adverse events, graded using the NCI Common Terminology Criteria for Adverse Events (CTCAE) version 4.0 Time Frame: Up to 4 weeks Safety Issue? Yes
<b>Primary outcome</b>	Measure: MTD and RP2D of liposomal irinotecan in combination with veliparib determined by incidence of dose limiting toxicities, graded using the NCI CTCAE version 4.0 Time Frame: 28 days Safety Issue? Yes
<b>Secondary outcome</b>	Measure: Clinical benefit rate defined as CR, PR, or SD assessed using RECIST version 1.1 Time Frame: At 24 weeks Safety Issue? No
<b>Secondary outcome</b>	Measure: Objective response rate assessed using RECIST version 1.1 Time Frame: At 24 weeks Safety Issue? No
<b>Secondary outcome</b>	Measure: PFS Time Frame: Duration of time from start of treatment to time of progression or death, whichever occurs first, assessed up to 4 weeks after completion of study treatment Safety Issue? No
<b>Secondary outcome</b>	Measure: Tumor response assessed using the revised Response Evaluation Criteria in Solid Tumors (RECIST) guideline (version 1.1) Time Frame: Up to 4 weeks after completion of study treatment Safety Issue? No
<b>Enrollment</b>	48 (Anticipated)
<b>Condition</b>	Estrogen Receptor Negative
<b>Condition</b>	HER2/Neu Negative
<b>Condition</b>	Neuroendocrine Neoplasm
<b>Condition</b>	Progesterone Receptor Negative
<b>Condition</b>	Stage IIB Cervical Cancer
<b>Condition</b>	Stage IIIA Cervical Cancer

<b>Condition</b>	Stage IIIB Cervical Cancer
<b>Condition</b>	Stage IIIB Non-Small Cell Lung Cancer
<b>Condition</b>	Stage IIIC Breast Cancer
<b>Condition</b>	Stage IV Breast Cancer
<b>Condition</b>	Stage IV Cervical Cancer
<b>Condition</b>	Stage IV Gastric Cancer
<b>Condition</b>	Stage IV Non-Small Cell Lung Cancer
<b>Condition</b>	Stage IV Ovarian Cancer
<b>Condition</b>	Stage IV Small Cell Lung Carcinoma
<b>Condition</b>	Triple-Negative Breast Carcinoma
<b>Arm/Group</b>	Arm Label: Treatment (liposomal irinotecan, veliparib) Experimental
	Patients receive liposomal irinotecan IV over 90 minutes on days 1 and 15 and veliparib PO on days 5-12 and 19-25 or 3-12 and 17-25. Courses repeat every 28 days in the absence of disease progression or unacceptable toxicity.
<b>Intervention</b>	Drug: Ferumoxytol      Arm Label: Treatment (liposomal irinotecan, veliparib)
	Correlative studies
<b>Intervention</b>	Other: Laboratory Biomarker Analysis      Arm Label: Treatment (liposomal irinotecan, veliparib)
	Correlative studies
<b>Intervention</b>	Drug: Liposomal Irinotecan      Arm Label: Treatment (liposomal irinotecan, veliparib)
	Given IV
<b>Intervention</b>	Procedure/Surgery: Magnetic Resonance Imaging Arm Label: Treatment (liposomal irinotecan, veliparib)
	Correlative studies
<b>Intervention</b>	Drug: Veliparib      Arm Label: Treatment (liposomal irinotecan, veliparib)
	Given PO

---

### Recruitment Information

<b>Status</b>	Recruiting
<b>Start date</b>	2016-07
<b>Primary completion date</b>	2019-07 (Anticipated)
<b>Criteria</b>	

Inclusion Criteria:

- Patients must have pathologically confirmed diagnosis of one of the following

solid tumors: cervical cancer, ovarian cancer, triple negative breast cancer (TNBC), non-small cell lung cancer (NSCLC), small cell lung cancer (SCLC), gastric cancer, and neuroendocrine tumors that is metastatic or unresectable and for which standard curative or palliative measures do not exist or are no longer effective

- Prior poly ADP ribose polymerase (PARP) inhibitor therapy is allowed
- Patients at the National Cancer Institute (NCI) site must be willing to undergo a pre-treatment ferumoxytol magnetic resonance imaging (MRI) (patients will be excluded from undergoing ferumoxytol MRI if they have evidence of iron overload, a known hypersensitivity to ferumoxytol or any other IV iron product, a documented history of multiple drug allergies, or those for whom MRI is otherwise contraindicated, including claustrophobia or anxiety related to undergoing MRI); this eligibility criterion applies only to patients enrolling at NCI
- Eastern Cooperative Oncology Group (ECOG) performance status  $\leq$  2 (Karnofsky  $\geq$  60%)
- Life expectancy of greater than 3 months
- Hemoglobin  $>$  9 g/dL
- Leukocytes  $\geq$  3,000/mcL
- Absolute neutrophil count  $\geq$  1,500/mcL without the use of hematopoietic growth factors
- Platelets  $\geq$  100,000/mcL
- Total bilirubin within normal institutional limits
- Aspartate aminotransferase (AST)(serum glutamic oxaloacetic transaminase [SGOT])/alanine aminotransferase (ALT)(serum glutamate pyruvate transaminase [SGPT])  $\leq$  2.5 x institutional upper limit of normal ( $\leq$  5 x upper limit of normal [ULN] is acceptable if liver metastases are present)
- Creatinine  $\leq$  1.5 x ULN OR creatinine clearance  $\geq$  60 mL/min/1.73 m<sup>2</sup> for patients with creatinine levels above institutional normal
- Women of child-bearing potential and men must agree to use adequate contraception (hormonal or barrier method of birth control; abstinence) prior to study entry and for the duration of study participation; should a woman become pregnant or suspect she is pregnant while she or her partner is participating in this study, she should inform her treating physician immediately; men and women treated or enrolled on this protocol must also agree to use adequate contraception prior to the study, for the duration of study participation, and 4 months after completion of veliparib, MM-398 and ferumoxytol MRI administration
- Ability to understand and the willingness to sign a written informed consent document
- IMAGING CORRELATIVE STUDY: Patients will be eligible to participate in the ferumoxytol (FMX) imaging study if they do not meet any of the following criteria
  - Evidence of iron overload as determined by:
    - \* Fasting transferrin saturation of  $>$  45% and/or
    - \* Serum ferritin levels  $>$  1000 ng/ml
  - A history of allergic reactions to any of the following:
    - \* Compounds similar to ferumoxytol or any of its components as described in full prescribing information for ferumoxytol injection
    - \* Any IV iron replacement product (e.g. parenteral iron, dextran, iron-dextran, or parenteral iron polysaccharide preparations)

## \* Multiple drugs

- Unable to undergo MRI or for whom MRI is otherwise contraindicated (e.g. presence of errant metal, cardiac pacemakers, pain pumps or other MRI incompatible devices; or history claustrophobia or anxiety related to undergoing MRI)

## Exclusion Criteria:

- Patients who have had chemotherapy or radiotherapy within 4 weeks (6 weeks for nitrosoureas or mitomycin C) prior to entering the study or those who have not recovered from adverse events due to agents administered more than 4 weeks earlier; patients must have completed prior biological therapies and/or targeted therapies  $\geq$  2 weeks prior to study enrollment; patients who have had radiation to the pelvis or other bone marrow-bearing sites will be considered on a case by case basis and may be excluded if the bone marrow reserve is not considered adequate (i.e. radiation to  $>$  25% of bone marrow)
- Patients who are receiving any other investigational agents
- Patients with active brain metastases should be excluded from this clinical trial
- History of allergic reactions attributed to compounds of similar chemical or biologic composition to veliparib, MM-398 and ferumoxytol
- Clinically significant gastrointestinal (GI) disorders, including history of small bowel obstruction unless the obstruction was a surgically treated remote episode
- Active infection
- Uncontrolled intercurrent illness including, but not limited to, ongoing or active infection, symptomatic congestive heart failure, unstable angina pectoris, cardiac arrhythmia, or psychiatric illness/social situations that would limit compliance with study requirements
- Pregnant women are excluded from this study; breastfeeding should be discontinued if the mother is treated with any of these agents
- Human immunodeficiency virus (HIV)-positive patients on combination antiretroviral therapy are ineligible
- Patients who are taking medications which are strong inhibitors or inducers of cytochrome P450, family 3, subfamily A, polypeptide 4 (CYP3A4)

<b>Gender</b>	Both
<b>Minimum age</b>	18 Years
<b>Healthy volunteers</b>	No

---

**Administrative Data**

<b>Organization name</b>	National Cancer Institute (NCI)
<b>Organization study ID</b>	NCI-2015-02125
<b>Secondary ID</b>	NCI-2015-02125 (CTRP (Clinical Trial Reporting Program))
<b>Secondary ID</b>	TBD
<b>Secondary ID</b>	9914 (National Cancer Institute LAO)
<b>Secondary ID</b>	9914 (CTEP)
<b>Sponsor</b>	National Cancer Institute (NCI)
<b>Collaborator</b>	National Cancer Institute (NCI)

**Health Authority**

United States: Food and Drug Administration

# ClinicalTrials.gov archive

A service of the U.S. National Institutes of Health

Developed by the National Library of Medicine

[← History of this study](#)    [↑ Current version of this study](#)

## View of NCT02631733 on 2016\_08\_07

**ClinicalTrials Identifier:** NCT02631733**Updated:** 2016\_08\_07

---

### Descriptive Information

**Brief title** Liposomal Irinotecan and Veliparib in Treating Patients With Solid Tumors That Are Metastatic or Cannot Be Removed by Surgery

**Official title** A Phase I Study of a Combination of MM-398 and Veliparib in Solid Tumors

#### Brief summary

This phase I trial studies the side effects and best dose of veliparib when given together with liposomal irinotecan in treating patients with solid tumors that have spread to other parts of the body (metastatic) or cannot be removed by surgery. Liposomal irinotecan and veliparib may stop the growth of tumor cells by blocking some of the enzymes needed for cell growth.

#### Detailed description

##### PRIMARY OBJECTIVES:

- I. To evaluate the safety and tolerability of escalating doses of MM-398 (liposomal irinotecan) + veliparib combination.
- II. To determine the maximum tolerated dose (MTD) and recommended phase 2 dose (RP2D) of the combination of MM-398 + veliparib.

##### SECONDARY OBJECTIVES:

- I. To observe and record anti-tumor activity.
- II. To characterize the preliminary efficacy of the combination using key efficacy indicators, such as objective response rate, clinical benefit rate defined as complete response (CR), partial response (PR), or stable disease (SD) at 24 weeks, and progression free survival (PFS).

##### EXPLORATORY OBJECTIVES

- I. Imaging, tumor, and blood biomarkers to assess the sensitivity or resistance to each drug and correlation with clinical response.

**OUTLINE:** This is a dose-escalation of veliparib.

Patients receive liposomal irinotecan intravenously (IV) over 90 minutes on days 1 and 15 and veliparib orally (PO) on days 5-12 and 19-25 or 3-12 and 17-25. Courses repeat every 28 days in the absence of disease progression or unacceptable toxicity.

After completion of study treatment, patients are followed up for 4 weeks.

<b>Phase</b>	Phase 1
<b>Study type</b>	Interventional
<b>Study design</b>	Treatment
<b>Study design</b>	Open Label
<b>Study design</b>	Single Group Assignment
<b>Study design</b>	Safety Study
<b>Primary outcome</b>	Measure: Incidence of adverse events, graded using the NCI Common Terminology Criteria for Adverse Events (CTCAE) version 4.0 Time Frame: Up to 4 weeks Safety Issue? Yes
<b>Primary outcome</b>	Measure: MTD and RP2D of liposomal irinotecan in combination with veliparib determined by incidence of dose limiting toxicities, graded using the NCI CTCAE version 4.0 Time Frame: 28 days Safety Issue? Yes
<b>Secondary outcome</b>	Measure: Clinical benefit rate defined as CR, PR, or SD assessed using RECIST version 1.1 Time Frame: At 24 weeks Safety Issue? No
<b>Secondary outcome</b>	Measure: Objective response rate assessed using RECIST version 1.1 Time Frame: At 24 weeks Safety Issue? No
<b>Secondary outcome</b>	Measure: PFS Time Frame: Duration of time from start of treatment to time of progression or death, whichever occurs first, assessed up to 4 weeks after completion of study treatment Safety Issue? No
<b>Secondary outcome</b>	Measure: Tumor response assessed using the revised Response Evaluation Criteria in Solid Tumors (RECIST) guideline (version 1.1) Time Frame: Up to 4 weeks after completion of study treatment Safety Issue? No
<b>Enrollment</b>	48 (Anticipated)
<b>Condition</b>	Estrogen Receptor Negative
<b>Condition</b>	HER2/Neu Negative
<b>Condition</b>	Neuroendocrine Neoplasm
<b>Condition</b>	Progesterone Receptor Negative
<b>Condition</b>	Stage IIB Cervical Cancer
<b>Condition</b>	Stage IIIA Cervical Cancer

<b>Condition</b>	Stage IIIB Cervical Cancer
<b>Condition</b>	Stage IIIB Non-Small Cell Lung Cancer
<b>Condition</b>	Stage IIIC Breast Cancer
<b>Condition</b>	Stage IV Breast Cancer
<b>Condition</b>	Stage IV Cervical Cancer
<b>Condition</b>	Stage IV Gastric Cancer
<b>Condition</b>	Stage IV Non-Small Cell Lung Cancer
<b>Condition</b>	Stage IV Ovarian Cancer
<b>Condition</b>	Stage IV Small Cell Lung Carcinoma
<b>Condition</b>	Triple-Negative Breast Carcinoma
<b>Arm/Group</b>	Arm Label: Treatment (liposomal irinotecan, veliparib) Experimental
	Patients receive liposomal irinotecan IV over 90 minutes on days 1 and 15 and veliparib PO on days 5-12 and 19-25 or 3-12 and 17-25. Courses repeat every 28 days in the absence of disease progression or unacceptable toxicity.
<b>Intervention</b>	Drug: Ferumoxytol      Arm Label: Treatment (liposomal irinotecan, veliparib)
	Correlative studies
<b>Intervention</b>	Other: Laboratory Biomarker Analysis      Arm Label: Treatment (liposomal irinotecan, veliparib)
	Correlative studies
<b>Intervention</b>	Drug: Liposomal Irinotecan      Arm Label: Treatment (liposomal irinotecan, veliparib)
	Given IV
<b>Intervention</b>	Procedure/Surgery: Magnetic Resonance Imaging Arm Label: Treatment (liposomal irinotecan, veliparib)
	Correlative studies
<b>Intervention</b>	Drug: Veliparib      Arm Label: Treatment (liposomal irinotecan, veliparib)
	Given PO

---

### Recruitment Information

<b>Status</b>	Recruiting
<b>Start date</b>	2016-07
<b>Primary completion date</b>	2019-07 (Anticipated)
<b>Criteria</b>	

Inclusion Criteria:

- Patients must have pathologically confirmed diagnosis of one of the following



solid tumors: cervical cancer, ovarian cancer, triple negative breast cancer (TNBC), non-small cell lung cancer (NSCLC), small cell lung cancer (SCLC), gastric cancer, and neuroendocrine tumors that is metastatic or unresectable and for which standard curative or palliative measures do not exist or are no longer effective

- Prior poly ADP ribose polymerase (PARP) inhibitor therapy is allowed
- Patients at the National Cancer Institute (NCI) site must be willing to undergo a pre-treatment ferumoxytol magnetic resonance imaging (MRI) (patients will be excluded from undergoing ferumoxytol MRI if they have evidence of iron overload, a known hypersensitivity to ferumoxytol or any other IV iron product, a documented history of multiple drug allergies, or those for whom MRI is otherwise contraindicated, including claustrophobia or anxiety related to undergoing MRI); this eligibility criterion applies only to patients enrolling at NCI
- Eastern Cooperative Oncology Group (ECOG) performance status  $\leq$  2 (Karnofsky  $\geq$  60%)
- Life expectancy of greater than 3 months
- Hemoglobin  $>$  9 g/dL
- Leukocytes  $\geq$  3,000/mcL
- Absolute neutrophil count  $\geq$  1,500/mcL without the use of hematopoietic growth factors
- Platelets  $\geq$  100,000/mcL
- Total bilirubin within normal institutional limits
- Aspartate aminotransferase (AST)(serum glutamic oxaloacetic transaminase [SGOT])/alanine aminotransferase (ALT)(serum glutamate pyruvate transaminase [SGPT])  $\leq$  2.5 x institutional upper limit of normal ( $\leq$  5 x upper limit of normal [ULN] is acceptable if liver metastases are present)
- Creatinine  $\leq$  1.5 x ULN OR creatinine clearance  $\geq$  60 mL/min/1.73 m<sup>2</sup> for patients with creatinine levels above institutional normal
- Women of child-bearing potential and men must agree to use adequate contraception (hormonal or barrier method of birth control; abstinence) prior to study entry and for the duration of study participation; should a woman become pregnant or suspect she is pregnant while she or her partner is participating in this study, she should inform her treating physician immediately; men and women treated or enrolled on this protocol must also agree to use adequate contraception prior to the study, for the duration of study participation, and 4 months after completion of veliparib, MM-398 and ferumoxytol MRI administration
- Ability to understand and the willingness to sign a written informed consent document
- IMAGING CORRELATIVE STUDY: Patients will be eligible to participate in the ferumoxytol (FMX) imaging study if they do not meet any of the following criteria
  - Evidence of iron overload as determined by:
    - \* Fasting transferrin saturation of  $>$  45% and/or
    - \* Serum ferritin levels  $>$  1000 ng/ml
  - A history of allergic reactions to any of the following:
    - \* Compounds similar to ferumoxytol or any of its components as described in full prescribing information for ferumoxytol injection
    - \* Any IV iron replacement product (e.g. parenteral iron, dextran, iron-dextran, or parenteral iron polysaccharide preparations)

## \* Multiple drugs

- Unable to undergo MRI or for whom MRI is otherwise contraindicated (e.g. presence of errant metal, cardiac pacemakers, pain pumps or other MRI incompatible devices; or history claustrophobia or anxiety related to undergoing MRI)

## Exclusion Criteria:

- Patients who have had chemotherapy or radiotherapy within 4 weeks (6 weeks for nitrosoureas or mitomycin C) prior to entering the study or those who have not recovered from adverse events due to agents administered more than 4 weeks earlier; patients must have completed prior biological therapies and/or targeted therapies  $\geq$  2 weeks prior to study enrollment; patients who have had radiation to the pelvis or other bone marrow-bearing sites will be considered on a case by case basis and may be excluded if the bone marrow reserve is not considered adequate (i.e. radiation to  $>$  25% of bone marrow)
- Patients who are receiving any other investigational agents
- Patients with active brain metastases should be excluded from this clinical trial
- History of allergic reactions attributed to compounds of similar chemical or biologic composition to veliparib, MM-398 and ferumoxytol
- Clinically significant gastrointestinal (GI) disorders, including history of small bowel obstruction unless the obstruction was a surgically treated remote episode
- Active infection
- Uncontrolled intercurrent illness including, but not limited to, ongoing or active infection, symptomatic congestive heart failure, unstable angina pectoris, cardiac arrhythmia, or psychiatric illness/social situations that would limit compliance with study requirements
- Pregnant women are excluded from this study; breastfeeding should be discontinued if the mother is treated with any of these agents
- Human immunodeficiency virus (HIV)-positive patients on combination antiretroviral therapy are ineligible
- Patients who are taking medications which are strong inhibitors or inducers of cytochrome P450, family 3, subfamily A, polypeptide 4 (CYP3A4)

<b>Gender</b>	Both
<b>Minimum age</b>	18 Years
<b>Healthy volunteers</b>	No

---

**Administrative Data**

<b>Organization name</b>	National Cancer Institute (NCI)
<b>Organization study ID</b>	NCI-2015-02125
<b>Secondary ID</b>	NCI-2015-02125 (CTRP (Clinical Trial Reporting Program))
<b>Secondary ID</b>	9914 (National Cancer Institute LAO)
<b>Secondary ID</b>	9914 (CTEP)
<b>Sponsor</b>	National Cancer Institute (NCI)
<b>Collaborator</b>	National Cancer Institute (NCI)
<b>Health Authority</b>	United States: Food and Drug Administration



# ClinicalTrials.gov archive

A service of the U.S. National Institutes of Health

Developed by the National Library of Medicine

[← History of this study](#)    [↑ Current version of this study](#)

## View of NCT02631733 on 2016\_09\_21

**ClinicalTrials Identifier:** NCT02631733**Updated:** 2016\_09\_21

---

### Descriptive Information

**Brief title** Liposomal Irinotecan and Veliparib in Treating Patients With Solid Tumors That Are Metastatic or Cannot Be Removed by Surgery**Official title** A Phase I Study of a Combination of MM-398 and Veliparib in Solid Tumors**Brief summary**

This phase I trial studies the side effects and best dose of veliparib when given together with liposomal irinotecan in treating patients with solid tumors that have spread to other parts of the body (metastatic) or cannot be removed by surgery. Liposomal irinotecan and veliparib may stop the growth of tumor cells by blocking some of the enzymes needed for cell growth.

**Detailed description****PRIMARY OBJECTIVES:**

- I. To evaluate the safety and tolerability of escalating doses of MM-398 (liposomal irinotecan) + veliparib combination.
- II. To determine the maximum tolerated dose (MTD) and recommended phase 2 dose (RP2D) of the combination of MM-398 + veliparib.

**SECONDARY OBJECTIVES:**

- I. To observe and record anti-tumor activity.
- II. To characterize the preliminary efficacy of the combination using key efficacy indicators, such as objective response rate, clinical benefit rate defined as complete response (CR), partial response (PR), or stable disease (SD) at 24 weeks, and progression free survival (PFS).

**EXPLORATORY OBJECTIVES**

- I. Imaging, tumor, and blood biomarkers to assess the sensitivity or resistance to each drug and correlation with clinical response.

**OUTLINE:** This is a dose-escalation of veliparib.

Patients receive liposomal irinotecan intravenously (IV) over 90 minutes on days 1 and 15 and veliparib orally (PO) on days 5-12 and 19-25 or 3-12 and 17-25. Courses repeat every 28 days in the absence of disease progression or unacceptable toxicity.

After completion of study treatment, patients are followed up for 4 weeks.

<b>Phase</b>	Phase 1
<b>Study type</b>	Interventional
<b>Study design</b>	Treatment
<b>Study design</b>	Open Label
<b>Study design</b>	Single Group Assignment
<b>Study design</b>	Safety Study
<b>Primary outcome</b>	Measure: Incidence of adverse events, graded using the NCI Common Terminology Criteria for Adverse Events (CTCAE) version 4.0 Time Frame: Up to 4 weeks Safety Issue? Yes
<b>Primary outcome</b>	Measure: MTD and RP2D of liposomal irinotecan in combination with veliparib determined by incidence of dose limiting toxicities, graded using the NCI CTCAE version 4.0 Time Frame: 28 days Safety Issue? Yes
<b>Secondary outcome</b>	Measure: Clinical benefit rate defined as CR, PR, or SD assessed using RECIST version 1.1 Time Frame: At 24 weeks Safety Issue? No
<b>Secondary outcome</b>	Measure: Objective response rate assessed using RECIST version 1.1 Time Frame: At 24 weeks Safety Issue? No
<b>Secondary outcome</b>	Measure: PFS Time Frame: Duration of time from start of treatment to time of progression or death, whichever occurs first, assessed up to 4 weeks after completion of study treatment Safety Issue? No
<b>Secondary outcome</b>	Measure: Tumor response assessed using the revised Response Evaluation Criteria in Solid Tumors (RECIST) guideline (version 1.1) Time Frame: Up to 4 weeks after completion of study treatment Safety Issue? No
<b>Enrollment</b>	48 (Anticipated)
<b>Condition</b>	Estrogen Receptor Negative
<b>Condition</b>	HER2/Neu Negative
<b>Condition</b>	Neuroendocrine Neoplasm
<b>Condition</b>	Progesterone Receptor Negative
<b>Condition</b>	Stage IIB Cervical Cancer
<b>Condition</b>	Stage IIIA Cervical Cancer

<b>Condition</b>	Stage IIIB Cervical Cancer
<b>Condition</b>	Stage IIIB Non-Small Cell Lung Cancer
<b>Condition</b>	Stage IIIC Breast Cancer
<b>Condition</b>	Stage IV Breast Cancer
<b>Condition</b>	Stage IV Cervical Cancer
<b>Condition</b>	Stage IV Gastric Cancer
<b>Condition</b>	Stage IV Non-Small Cell Lung Cancer
<b>Condition</b>	Stage IV Ovarian Cancer
<b>Condition</b>	Stage IV Small Cell Lung Carcinoma
<b>Condition</b>	Triple-Negative Breast Carcinoma
<b>Arm/Group</b>	Arm Label: Treatment (liposomal irinotecan, veliparib) Experimental
	Patients receive liposomal irinotecan IV over 90 minutes on days 1 and 15 and veliparib PO on days 5-12 and 19-25 or 3-12 and 17-25. Courses repeat every 28 days in the absence of disease progression or unacceptable toxicity.
<b>Intervention</b>	Drug: Ferumoxytol      Arm Label: Treatment (liposomal irinotecan, veliparib)
	Correlative studies
<b>Intervention</b>	Other: Laboratory Biomarker Analysis      Arm Label: Treatment (liposomal irinotecan, veliparib)
	Correlative studies
<b>Intervention</b>	Drug: Liposomal Irinotecan      Arm Label: Treatment (liposomal irinotecan, veliparib)
	Given IV
<b>Intervention</b>	Procedure/Surgery: Magnetic Resonance Imaging Arm Label: Treatment (liposomal irinotecan, veliparib)
	Correlative studies
<b>Intervention</b>	Drug: Veliparib      Arm Label: Treatment (liposomal irinotecan, veliparib)
	Given PO

---

### Recruitment Information

<b>Status</b>	Suspended
<b>Start date</b>	2016-07
<b>Primary completion date</b>	2019-07 (Anticipated)

**Criteria**

Inclusion Criteria:

- Patients must have pathologically confirmed diagnosis of one of the following

solid tumors: cervical cancer, ovarian cancer, triple negative breast cancer (TNBC), non-small cell lung cancer (NSCLC), small cell lung cancer (SCLC), gastric cancer, and neuroendocrine tumors that is metastatic or unresectable and for which standard curative or palliative measures do not exist or are no longer effective

- Prior poly ADP ribose polymerase (PARP) inhibitor therapy is allowed
- Patients at the National Cancer Institute (NCI) site must be willing to undergo a pre-treatment ferumoxytol magnetic resonance imaging (MRI) (patients will be excluded from undergoing ferumoxytol MRI if they have evidence of iron overload, a known hypersensitivity to ferumoxytol or any other IV iron product, a documented history of multiple drug allergies, or those for whom MRI is otherwise contraindicated, including claustrophobia or anxiety related to undergoing MRI); this eligibility criterion applies only to patients enrolling at NCI
- Eastern Cooperative Oncology Group (ECOG) performance status  $\leq$  2 (Karnofsky  $\geq$  60%)
- Life expectancy of greater than 3 months
- Hemoglobin  $>$  9 g/dL
- Leukocytes  $\geq$  3,000/mcL
- Absolute neutrophil count  $\geq$  1,500/mcL without the use of hematopoietic growth factors
- Platelets  $\geq$  100,000/mcL
- Total bilirubin within normal institutional limits
- Aspartate aminotransferase (AST)(serum glutamic oxaloacetic transaminase [SGOT])/alanine aminotransferase (ALT)(serum glutamate pyruvate transaminase [SGPT])  $\leq$  2.5 x institutional upper limit of normal ( $\leq$  5 x upper limit of normal [ULN] is acceptable if liver metastases are present)
- Creatinine  $\leq$  1.5 x ULN OR creatinine clearance  $\geq$  60 mL/min/1.73 m<sup>2</sup> for patients with creatinine levels above institutional normal
- Women of child-bearing potential and men must agree to use adequate contraception (hormonal or barrier method of birth control; abstinence) prior to study entry and for the duration of study participation; should a woman become pregnant or suspect she is pregnant while she or her partner is participating in this study, she should inform her treating physician immediately; men and women treated or enrolled on this protocol must also agree to use adequate contraception prior to the study, for the duration of study participation, and 4 months after completion of veliparib, MM-398 and ferumoxytol MRI administration
- Ability to understand and the willingness to sign a written informed consent document
- IMAGING CORRELATIVE STUDY: Patients will be eligible to participate in the ferumoxytol (FMX) imaging study if they do not meet any of the following criteria
  - Evidence of iron overload as determined by:
    - \* Fasting transferrin saturation of  $>$  45% and/or
    - \* Serum ferritin levels  $>$  1000 ng/ml
  - A history of allergic reactions to any of the following:
    - \* Compounds similar to ferumoxytol or any of its components as described in full prescribing information for ferumoxytol injection
    - \* Any IV iron replacement product (e.g. parenteral iron, dextran, iron-dextran, or parenteral iron polysaccharide preparations)

## \* Multiple drugs

- Unable to undergo MRI or for whom MRI is otherwise contraindicated (e.g. presence of errant metal, cardiac pacemakers, pain pumps or other MRI incompatible devices; or history claustrophobia or anxiety related to undergoing MRI)

## Exclusion Criteria:

- Patients who have had chemotherapy or radiotherapy within 4 weeks (6 weeks for nitrosoureas or mitomycin C) prior to entering the study or those who have not recovered from adverse events due to agents administered more than 4 weeks earlier; patients must have completed prior biological therapies and/or targeted therapies  $\geq$  2 weeks prior to study enrollment; patients who have had radiation to the pelvis or other bone marrow-bearing sites will be considered on a case by case basis and may be excluded if the bone marrow reserve is not considered adequate (i.e. radiation to  $>$  25% of bone marrow)
- Patients who are receiving any other investigational agents
- Patients with active brain metastases should be excluded from this clinical trial
- History of allergic reactions attributed to compounds of similar chemical or biologic composition to veliparib, MM-398 and ferumoxytol
- Clinically significant gastrointestinal (GI) disorders, including history of small bowel obstruction unless the obstruction was a surgically treated remote episode
- Active infection
- Uncontrolled intercurrent illness including, but not limited to, ongoing or active infection, symptomatic congestive heart failure, unstable angina pectoris, cardiac arrhythmia, or psychiatric illness/social situations that would limit compliance with study requirements
- Pregnant women are excluded from this study; breastfeeding should be discontinued if the mother is treated with any of these agents
- Human immunodeficiency virus (HIV)-positive patients on combination antiretroviral therapy are ineligible
- Patients who are taking medications which are strong inhibitors or inducers of cytochrome P450, family 3, subfamily A, polypeptide 4 (CYP3A4)

<b>Gender</b>	Both
<b>Minimum age</b>	18 Years
<b>Healthy volunteers</b>	No

---

**Administrative Data**

<b>Organization name</b>	National Cancer Institute (NCI)
<b>Organization study ID</b>	NCI-2015-02125
<b>Secondary ID</b>	NCI-2015-02125 (CTRP (Clinical Trial Reporting Program))
<b>Secondary ID</b>	TBD
<b>Secondary ID</b>	9914 (National Cancer Institute LAO)
<b>Secondary ID</b>	9914 (CTEP)
<b>Sponsor</b>	National Cancer Institute (NCI)
<b>Collaborator</b>	National Cancer Institute (NCI)

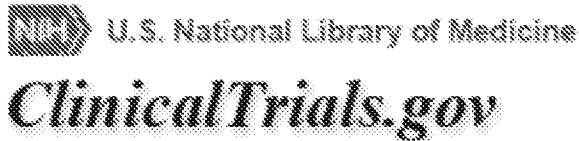


**Health Authority**

United States: Food and Drug Administration

We updated the design of this site on September 25th. [Learn more.](#)

We will be updating this site in phases. This allows us to move faster and to deliver better services. [Show less](#)



- [Find Studies](#) ▼
- [About Studies](#) ▼
- [Submit Studies](#) ▼
- [Resources](#) ▼
- [About Site](#) ▼

---

## Liposomal Irinotecan and Veliparib in Treating Patients With Solid Tumors

---

This study is currently recruiting participants.

**See [▶ Contacts and Locations](#)**

Verified August 2017 by National Cancer Institute (NCI)

**Sponsor:**

National Cancer Institute (NCI)

**ClinicalTrials.gov Identifier:**

NCT02631733

First Posted: December 16, 2015

Last Update Posted: October 4, 2017

**⚠** The safety and scientific validity of this study is the responsibility of the study sponsor and investigators. Listing a study does not mean it has been evaluated by the U.S. Federal Government. [Know the risks and potential benefits](#) of clinical studies and talk to your health care provider before participating. Read our [disclaimer](#) for details.

**Information provided by (Responsible Party):**

National Cancer Institute (NCI)

[Full Text View](#)

[Tabular View](#)

[No Study Results Posted](#)

[Disclaimer](#)

[How to Read a Study Record](#)

---

**▶ Purpose**

This phase I trial studies the side effects and best dose of veliparib when given together with liposomal irinotecan in treating patients with solid tumors. Liposomal irinotecan and veliparib may stop the growth of tumor cells by blocking some of the enzymes needed for cell growth.

<u>Condition</u>	<u>Intervention</u>	<u>Phase</u>
Malignant Solid Neoplasm	Drug: Ferumoxytol Other: Laboratory Biomarker Analysis Drug: Liposomal Irinotecan Procedure: Magnetic Resonance Imaging Drug: Veliparib	Phase 1

Study Type: Interventional

Study Design: Intervention Model: Single Group Assignment

Masking: None (Open Label)

Primary Purpose: Treatment

Official Title: A Phase I Study of a Combination of MM-398 and Veliparib in Solid Tumors

**Resource links provided by NLM:**

Drug Information available for: [Irinotecan](#) [Irinotecan hydrochloride](#)

U.S. FDA Resources

**Further study details as provided by National Cancer Institute (NCI):**

**Primary Outcome Measures:**

- Incidence of adverse events, graded using the National Cancer Institute Common Terminology Criteria for Adverse Events version 4.0 [ Time Frame: Up to 4 weeks ]

Safety and tolerability of escalating doses of liposomal irinotecan and veliparib combination will be evaluated.

- Maximum tolerated dose and recommended phase II dose of liposomal irinotecan in combination with veliparib evaluated according to the National Cancer Institute Common Terminology Criteria for Adverse Events version 4.0 [ Time Frame: 28 days ]

Maximum tolerated dose and recommended phase II dose of liposomal irinotecan in combination with veliparib will be determined by incidence of dose limiting toxicities, graded

using the National Cancer Institute Common Terminology Criteria for Adverse Events version 4.0.

Secondary Outcome Measures:

- Clinical benefit rate defined as complete response, partial response, or stable disease assessed using Response Evaluation Criteria in Solid Tumors version 1.1 [ Time Frame: At 24 weeks ]

Will be evaluated according to Response Evaluation Criteria in Solid Tumors version 1.1.

- Objective response rate assessed using Response Evaluation Criteria in Solid Tumors version 1.1 [ Time Frame: At 24 weeks ]

Will be evaluated according to Response Evaluation Criteria in Solid Tumors version 1.1.

- Progression free survival [ Time Frame: Duration of time from start of treatment to time of progression or death, whichever occurs first, assessed up to 4 weeks after completion of study treatment ]

Progression free survival is defined as the duration of time from start of treatment to time of progression or death, whichever occurs first.

- Tumor response assessed using the revised Response Evaluation Criteria in Solid Tumors guideline (version 1.1) [ Time Frame: Up to 4 weeks after completion of study treatment ]

Will be evaluated according to Response Evaluation Criteria in Solid Tumors version 1.1.

Other Outcome Measures:

- Biomarker levels [ Time Frame: Up to 4 weeks after completion of study treatment ]

Will be studied to assess the sensitivity or resistance to each drug and correlated with clinical response.

Estimated Enrollment: 48  
Actual Study Start Date: July 15, 2016  
Estimated Study Completion Date: July 1, 2019

Estimated Primary Completion Date: July 1, 2019 (Final data collection date for primary outcome measure)

Arms	Assigned Interventions
<p>Experimental: Treatment (liposomal irinotecan, veliparib)</p> <p>Patients receive liposomal irinotecan IV over 90 minutes on days 1 and 15 and veliparib PO BID on days 5-12 and 19-25 or 3-12 and 17-25. Courses repeat every 28 days in the absence of disease progression or unacceptable toxicity. Within 2-6 days prior to beginning liposomal irinotecan treatment, patients may optionally receive FMX IV and undergo MRI at baseline and 24 hours after FMX infusion.</p>	<p>Drug: Ferumoxytol</p> <p>Given IV</p> <p>Other Names:</p> <ul style="list-style-type: none"> <li>• Feraheme</li> <li>• Ferumoxytol Non-Stoichiometric Magnetite</li> </ul> <p>Other: Laboratory Biomarker Analysis</p> <p>Correlative studies</p> <p>Drug: Liposomal Irinotecan</p> <p>Given IV</p> <p>Other Names:</p> <ul style="list-style-type: none"> <li>• Irinotecan Liposome</li> <li>• Onivyde</li> <li>• PEP02</li> </ul> <p>Procedure: Magnetic Resonance Imaging</p> <p>Undergo MRI</p> <p>Other Names:</p> <ul style="list-style-type: none"> <li>• Magnetic Resonance Imaging Scan</li> <li>• Medical Imaging, Magnetic Resonance / Nuclear Magnetic Resonance</li> <li>• MRI</li> <li>• MRI Scan</li> <li>• NMR Imaging</li> </ul>

- NMRI
- Nuclear Magnetic Resonance Imaging

Drug: Veliparib

Given PO

Other Names:

- ABT-888
- PARP-1 inhibitor  
ABT-888

### Detailed Description:

#### PRIMARY OBJECTIVES:

- I. To evaluate the safety and tolerability of escalating doses of liposomal irinotecan (MM-398) + veliparib combination.
- II. To determine the maximum tolerated dose (MTD) and recommended phase 2 dose (RP2D) of the combination of MM-398 + veliparib.

#### SECONDARY OBJECTIVES:

- I. To observe and record anti-tumor activity.
- II. To characterize the preliminary efficacy of the combination using key efficacy indicators, such as objective response rate, clinical benefit rate defined as complete response (CR), partial response (PR), or stable disease (SD) at 24 weeks, and progression free survival (PFS).

EXPLORATORY OBJECTIVES I. Imaging, tumor, and blood biomarkers to assess the sensitivity or resistance to each drug and/or correlation with clinical response.

OUTLINE: This is a dose-escalation study of veliparib.

Patients receive liposomal irinotecan intravenously (IV) over 90 minutes on days 1 and 15 and veliparib orally (PO) twice daily (BID) on days 5-12 and 19-25 or 3-12 and 17-25. Courses repeat every 28 days in the absence of disease progression or unacceptable toxicity. Within 2-6 days prior to beginning liposomal irinotecan treatment, patients may optionally receive ferumoxytol (FMX) IV and undergo magnetic resonance imaging (MRI) at baseline and 24 hours after FMX infusion.

After completion of study treatment, patients are followed up for 4 weeks.

## ► Eligibility

### Information from the National Library of Medicine



*Choosing to participate in a study is an important personal decision. Talk with your doctor and family members or friends about deciding to join a study. To learn more about this study, you or your doctor may contact the study research staff using the contacts provided below. For general information, [Learn About Clinical Studies](#).*

Ages Eligible for Study: 18 Years and older (Adult, Senior)

Sexes Eligible for Study: All

Accepts Healthy Volunteers: No

### Criteria

#### Inclusion Criteria:

- Patients must have pathologically confirmed diagnosis of a solid tumor cancer for which there is no known standard therapy capable of extending life expectancy
- Prior poly ADP ribose polymerase (PARP) inhibitor therapy is allowed; patients with ovarian cancer and a BRCA mutation should have had prior treatment with olaparib per guidelines for standard of care treatment
- Eastern Cooperative Oncology Group (ECOG) performance status  $\leq 2$  (Karnofsky  $\geq 60\%$ )
- Hemoglobin  $> 9$  g/dL
- Leukocytes  $\geq 3,000$ /mcL
- Absolute neutrophil count  $\geq 1,500$ /mcL without the use of hematopoietic growth factors
- Platelets  $\geq 100,000$ /mcL
- Total bilirubin below normal institutional upper limit of normal (ULN)
- Aspartate aminotransferase (AST) (serum glutamic oxaloacetic transaminase [SGOT])/alanine aminotransferase (ALT) (serum glutamate pyruvate transaminase [SGPT])  $\leq 2.5$  x institutional upper limit of normal ( $\leq 5$  x ULN is acceptable if liver metastases are present)
- Creatinine  $\leq 1.5$  x ULN OR creatinine clearance  $\geq 60$  mL/min/1.73 m<sup>2</sup> for patients with creatinine levels above institutional normal

- Women of childbearing potential and male patients should use effective contraception during treatment with MM-398 and for 90 days following the final dose of veliparib and MM-398 for both female and male patients; should a woman become pregnant or suspect she is pregnant while she or her partner is participating in this study, she should inform her treating physician immediately
- Ability to understand and the willingness to sign a written informed consent document
- IMAGING CORRELATIVE STUDY: Patients will be eligible to participate in the FMX imaging study if the participating study center offers this test and they do not meet any of the following criteria:
  - Evidence of iron overload as determined by:
    - Fasting transferrin saturation of > 45% and/or
    - Serum ferritin levels > 1000 ng/ml
  - A history of allergic reactions to any of the following:
    - Compounds similar to ferumoxytol or any of its components as described in full prescribing information for ferumoxytol injection
    - Any IV iron replacement product (e.g. parenteral iron, dextran, iron-dextran, or parenteral iron polysaccharide preparations)
    - Multiple drugs
  - Unable to undergo MRI or for whom MRI is otherwise contraindicated (e.g. presence of errant metal, cardiac pacemakers, pain pumps or other MRI incompatible devices; or history claustrophobia or anxiety related to undergoing MRI)

#### Exclusion Criteria:

- Patients who have had chemotherapy or radiotherapy within 4 weeks (6 weeks for nitrosoureas or mitomycin C) prior to entering the study or those who have not recovered from adverse events due to agents administered more than 4 weeks earlier; patients must have completed prior biological therapies and/or targeted therapies  $\geq$  2 weeks prior to study enrollment; patients who have had radiation to the pelvis or other bone marrow-bearing sites will be considered on a case by case basis and may be excluded if the bone marrow reserve is not considered adequate (i.e. radiation to > 25% of bone marrow)
- Patients who are receiving any other investigational agents
- Subjects with symptomatic brain metastases will be excluded from trial secondary to poor prognosis; however, subjects who have had treatment for their brain metastasis and whose brain disease is stable without steroid therapy for at least 3 months may be enrolled



- History of allergic reactions attributed to compounds of similar chemical or biologic composition to veliparib and MM-398; if patients have a history of allergic reactions to compounds resembling MM-398, they will be excluded from participating in the FMX MRI study, if applicable
- Patients who have severe hypersensitivity to irinotecan hydrochloride (HCl)
- Patients with known and confirmed diagnosis of interstitial lung disease (ILD)
- Clinically significant gastrointestinal (GI) disorders, including history of small bowel obstruction unless the obstruction was a surgically treated remote episode
- Patient is unable to swallow or keep down oral medication
- Patients at the National Cancer Institute (NCI) site and other selected centers who are willing to undergo an optional pre-treatment ferumoxytol MRI must not have evidence of iron overload, a known hypersensitivity to ferumoxytol or any other IV iron product, a documented history of multiple drug allergies, or those for whom MRI is otherwise contraindicated, including claustrophobia or anxiety related to undergoing MRI; this exclusion criterion applies only to patients enrolling at NCI and other selected sites; of note, the principal investigator (PI) will allow other centers to offer FMX MRI scans if the site in question is willing and the site PI can identify the necessary resources and expertise at their center
- Active infection
- Uncontrolled intercurrent illness including, but not limited to, ongoing or active infection, symptomatic congestive heart failure, unstable angina pectoris, cardiac arrhythmia, or psychiatric illness/social situations that would limit compliance with study requirements
- Pregnant women are excluded from this study; breastfeeding should be discontinued if the mother is treated with any of these agents
- Human immunodeficiency virus (HIV)-positive patients on combination antiretroviral therapy are ineligible; appropriate studies will be undertaken in patients receiving combination antiretroviral therapy when indicated
- Patients who need chronic use of medications or substances that are strong inhibitors or inducers of CYP3A4 are ineligible
- Patients with a high risk of seizures should be excluded from the protocol (e.g. those patients with an uncontrolled seizure disorder, and/or patients who have had a focal or generalized seizure within the last 12 months)

## ► **Contacts and Locations**

**Information from the National Library of Medicine**

*To learn more about this study, you or your doctor may contact the study research staff using the contact information provided by the sponsor.*

*Please refer to this study by its ClinicalTrials.gov identifier (NCT number):*  
**NCT02631733**

**Locations****United States, Maryland**

Johns Hopkins University/Sidney Kimmel Cancer Center **Suspended**  
Baltimore, Maryland, United States, 21287

National Cancer Institute LAO **Recruiting**  
Bethesda, Maryland, United States, 20892  
Contact: Anish Thomas 301-451-8418 [thomasa6@mail.nih.gov](mailto:thomasa6@mail.nih.gov)  
Principal Investigator: Anish Thomas

National Institutes of Health Clinical Center **Recruiting**  
Bethesda, Maryland, United States, 20892  
Contact: Anish Thomas 800-411-1222  
Principal Investigator: Anish Thomas

**United States, Minnesota**

Mayo Clinic **Recruiting**  
Rochester, Minnesota, United States, 55905  
Contact: Ciara C. O'Sullivan 855-776-0015  
Principal Investigator: Ciara C. O'Sullivan

**United States, New York**

Columbia University/Herbert Irving Cancer Center **Recruiting**  
New York, New York, United States, 10032  
Contact: Susan E. Bates 212-305-8615  
Principal Investigator: Susan E. Bates

**Sponsors and Collaborators**

National Cancer Institute (NCI)

**Investigators**

Principal Investigator: Anish Thomas National Cancer Institute LAO

**► More Information**

Responsible Party: National Cancer Institute (NCI)  
 ClinicalTrials.gov Identifier: [NCT02631733](#) [History of Changes](#)  
 Other Study ID Numbers: NCI-2015-02125  
 NCI-2015-02125 ( Registry Identifier: CTRP (Clinical Trial Reporting Program) )  
 17-C-0012  
 9914 ( Other Identifier: National Cancer Institute LAO )  
 9914 ( Other Identifier: CTEP )  
[ZIABC011078 \( U.S. NIH Grant/Contract \)](#)  
 First Submitted: December 15, 2015  
 First Posted: December 16, 2015  
 Last Update Posted: October 4, 2017  
 Last Verified: August 2017

## Additional relevant MeSH terms:

Irinotecan	Topoisomerase Inhibitors
Camptothecin	Enzyme Inhibitors
Veliparib	Molecular Mechanisms of Pharmacological Action
Ferrosferric Oxide	Poly(ADP-ribose) Polymerase Inhibitors
Antineoplastic Agents, Phytogetic	Hematinics
Antineoplastic Agents	Parenteral Nutrition Solutions
Topoisomerase I Inhibitors	Pharmaceutical Solutions



## Study of Irinotecan Liposome Injection (ONIVYDE®) in Patients With Small Cell Lung Cancer




The safety and scientific validity of this study is the responsibility of the study sponsor and investigators. Listing a study does not mean it has been evaluated by the U.S. Federal Government. Know the risks and potential benefits of clinical studies and talk to your health care provider before participating. Read our [disclaimer](#) for details.

ClinicalTrials.gov Identifier: NCT03088813

Recruitment Status  : Recruiting

First Posted  : March 23, 2017

Last Update Posted  : September 30, 2019

See [Contacts and Locations](#)

### Sponsor:

Ipsen

### Information provided by (Responsible Party):

Ipsen

[Study Details](#)

[Tabular View](#)

[No Results Posted](#)

[Disclaimer](#)

[How to Read a Study Record](#)

## Study Description

Go to 

### Brief Summary:

A Randomized, Open Label Phase 3 Study of Irinotecan Liposome Injection (ONIVYDE®) versus Topotecan in Patients with Small Cell Lung Cancer Who Have Progressed on or after Platinum-based First-Line Therapy

The study will be conducted in two parts:

1. Dose determination of irinotecan liposome injection

CSPC Exhibit 1094

Page 400 of 512

## 2. A randomized, efficacy study of irinotecan liposome injection versus topotecan

Condition or disease	Intervention/treatment	Phase
Small Cell Lung Cancer	Drug: Irinotecan liposome injection	Phase 2
	Drug: Topotecan	Phase 3

### Detailed Description:

The study will be conducted in two parts:

Part 1: Open-label dose-finding study of irinotecan liposome injection. 30 patients were enrolled.

#### Part 1 Primary Objectives:

- Describe the safety and tolerability of irinotecan liposome injection monotherapy administered every 2 weeks
- Determine the optimal irinotecan liposome injection monotherapy dose for Part 2 of this study

Part 2: A randomized, efficacy study of irinotecan liposome injection versus IV topotecan.

Approximately 450 patients will be enrolled in part 2.

Part 2 objectives: Detailed in the Primary & Secondary outcome measure sections.

## Study Design

Go to 

### Study Type :

Interventional (Clinical Trial)

### Estimated Enrollment :

480 participants

### Allocation:

Randomized

### Intervention Model:

Parallel Assignment

### Masking:

None (Open Label)

### Masking Description:

Open Label

### Primary Purpose:

Treatment

**Official Title:**

RESILIENT: A Randomized, Open Label Phase 3 Study of Irinotecan Liposome Injection (ONIVYDE®) Versus Topotecan in Patients With Small Cell Lung Cancer Who Have Progressed on or After Platinum-based First-Line Therapy

**Actual Study Start Date** ⓘ :

April 25, 2018

**Estimated Primary Completion Date** ⓘ :

September 2022

**Estimated Study Completion Date** ⓘ :

December 2022

**Resource links provided by the National Library of Medicine**

[Genetics Home Reference](#) related topics: [Lung cancer](#)

[MedlinePlus](#) related topics: [Lung Cancer](#)

[Drug Information](#) available for: [Irinotecan](#) [Irinotecan hydrochloride](#) [Topotecan hydrochloride](#)  
[Topotecan](#)

[Genetic and Rare Diseases Information Center](#) resources: [Small Cell Lung Cancer](#)

[U.S. FDA Resources](#)

**Arms and Interventions**

Go to

<b>Arm</b> ⓘ	<b>Intervention/treatment</b> ⓘ
Experimental: Experimental Arm Irinotecan liposome injection	Drug: Irinotecan liposome injection IV Other Name: ONIVYDE®
Active Comparator: Control Arm Topotecan	Drug: Topotecan IV

**Outcome Measures**

Go to

CSPC Exhibit 1094  
Page 402 of 512

### Primary Outcome Measures :

#### 1. Overall survival (OS) [ Time Frame: 40 months ]

Overall survival is defined as the time from randomization to date of death. The primary hypothesis will test whether OS is increased in patients treated with irinotecan liposome injection

### Secondary Outcome Measures :

#### 1. Progression-free survival [ Time Frame: 40 months ]

Progression-free survival is the time from randomization to the first documented objective disease progression (PD) using RECIST v1.1 or death due to any cause, whichever occurs first

#### 2. Objective Response [ Time Frame: 40 months ]

Objective response is defined as the time from randomization to date of progression or death. Objective response rate (ORR) is the proportion of patients who achieve partial response or complete response according to RECIST v1.1 guidelines

#### 3. Proportion of Patients with Symptom Improvement [ Time Frame: Randomization to 30 Days after permanent treatment termination ]

Patient-reported EORTC-QLQ symptom scales for cough, dyspnea, and fatigue

#### 4. Incidence of treatment-emergent adverse events, serious adverse events and laboratory abnormalities [ Time Frame: Enrollment to 30 days after permanent treatment termination ]

Safety analyses (adverse events and laboratory analyses) will be performed using the safety population, defined as all patients receiving any study drug.

## Eligibility Criteria

Go to 

### Information from the National Library of Medicine



*Choosing to participate in a study is an important personal decision. Talk with your doctor and family members or friends about deciding to join a study. To learn more about this study, you or your doctor may contact the study research staff using the contacts provided below. For general information, [Learn About Clinical Studies](#).*

CSPC Exhibit 1094  
Page 403 of 512

**Ages Eligible for Study:**

18 Years and older (Adult, Older Adult)

**Sexes Eligible for Study:**

All

**Accepts Healthy Volunteers:**

No

**Criteria****Inclusion Criteria:**

- At least 18 years of age.
- Able to understand and provide an informed consent
- Eastern Cooperative Oncology Group (ECOG) performance status of 0 or 1.
- Life expectancy >12 weeks
- Histopathologically or cytologically confirmed small cell lung cancer
- Evaluable disease as defined by RECIST Version 1.1 guidelines (patients with non measurable lesions only are eligible).
- Radiologically confirmed progression on or after first-line platinum based chemotherapy (carboplatin or cisplatin), immunotherapy, or chemo-radiation including platinum-based chemotherapy for treatment of limited or extensive stage Small Cell Lung Cancer (SCLC).
- Recovered from the effects of any prior chemotherapy, surgery, radiotherapy or other anti-neoplastic therapy (recovered to Grade 1 or better, with the exception of alopecia).
- Adequate bone marrow reserves
- Adequate hepatic function Adequate renal function
- Electrocardiogram during the Screening period without any clinically significant findings, per investigator's assessment

**Exclusion Criteria**

- Any medical or social condition deemed by the Investigator to be likely to interfere with a patient's ability to sign informed consent, cooperate and participate in the study, or interfere with the interpretation of the results
- Pregnant or breast feeding;
- Patients with large cell neuroendocrine lung carcinoma.
- Patients who have received prior topoisomerase I inhibitor treatment, retreatment with e platinum-based regimen, antibody-drug conjugates or molecular targeted agents, more than one line of immunotherapy, or any other additional regimen of prior cytotoxic chemotherapy.



- Patients with the symptomatic Central Nervous System (CNS) metastasis and/or who have developed new or progressive brain metastasis following prophylactic and/or therapeutic cranial radiation (whole brain stereotactic radiation).
- Patients with carcinomatous meningitis.
- Unable to discontinue the use of strong CYP3A4 or UGT1A1 inhibitors at least 1 week or strong CYP3A4 inducers at least 2 weeks prior to receiving the first dose of irinotecan liposome injection.
- Have a previous or concurrent cancer that is distinct in primary (non-pulmonary) site or SCLC histology
- Investigational therapy administered within 4 weeks, or within a time interval less than at least 5 half-lives of the investigational agent, whichever is less, prior to the first scheduled day of dosing in this study.
- Severe cardiovascular and pulmonary diseases
- New York Heart Association Class III or IV congestive heart failure, ventricular arrhythmias, or uncontrolled blood pressure.
- Active infection
- Known hypersensitivity to any of the components of irinotecan liposome injection, other liposomal products, or topotecan.
- Clinically significant gastrointestinal disorder including hepatic disorders, bleeding, inflammation, occlusion, or diarrhea > grade 1.

## Contacts and Locations

Go to 

### Information from the National Library of Medicine



*To learn more about this study, you or your doctor may contact the study research staff using the contact information provided by the sponsor.*

*Please refer to this study by its ClinicalTrials.gov identifier (NCT number): **NCT03088813***

### Contacts

Contact: Ipsen Recruitment Enquiries [clinical.trials@ipson.com](mailto:clinical.trials@ipson.com)

 [Show 39 Study Locations](#)

### Sponsors and Collaborators

Ipsen

### Investigators

CSPC Exhibit 1094  
Page 405 of 512

Study Director: Ipsen Medical Director Ipsen

## More Information

Go to 

---

### Responsible Party:

Ipsen

### ClinicalTrials.gov Identifier:

[NCT03088813](#) [History of Changes](#)

### Other Study ID Numbers:

MM-398-01-03-04

### First Posted:

March 23, 2017 [Key Record Dates](#)

### Last Update Posted:

September 30, 2019

### Last Verified:

September 2019

### Studies a U.S. FDA-regulated Drug Product:

Yes

### Studies a U.S. FDA-regulated Device Product:

No

### Additional relevant MeSH terms:

Lung Neoplasms  
Small Cell Lung Carcinoma  
Respiratory Tract Neoplasms  
Thoracic Neoplasms  
Neoplasms by Site  
Neoplasms  
Lung Diseases  
Respiratory Tract Diseases  
Carcinoma, Bronchogenic  
Bronchial Neoplasms  
Irinotecan  
Topotecan  
Topoisomerase I Inhibitors  
Topoisomerase Inhibitors  
Enzyme Inhibitors  
Molecular Mechanisms of Pharmacological Action  
Antineoplastic Agents

## The PARP inhibitor ABT-888 synergizes irinotecan treatment of colon cancer cell lines

David Davidson · Yunzhe Wang · Raquel Aloyz · Lawrence Panasci

Received: 9 August 2012 / Accepted: 26 September 2012  
© Springer Science+Business Media New York 2012

**Summary** Poly [ADP-ribose] polymerase-1 (PARP-1) localizes rapidly to sites of DNA damage and has been associated with various repair mechanisms including base excision repair (BER) and homologous recombination/non-homologous end joining (HRR/NHEJ). PARP-1 acts by adding poly-ADP ribose side chains to target proteins (PARylation) altering molecular interactions and functions. Recently small molecule inhibitors of PARP-1 have been shown to have significant clinical potential and third generation PARP inhibitors are currently being investigated in clinical trials. These drugs alone or in combination with radio/chemotherapy have resulted in meaningful patient responses and an increase in survival in metastatic breast cancer cases bearing BRCA-deficient or triple negative tumors and BRCA-deficient ovarian cancer patients. ABT-888, a potent PARP-1 inhibitor, sensitizes many cancer cells *in-vitro* and *in-vivo* to temozolomide. As such, we hypothesized that colon cancers would be sensitized to the DNA damaging chemotherapeutic agents, oxaliplatin and irinotecan, by ABT-888. Using colon cancer cell lines significant synergy was observed between ABT-888 and irinotecan at concentrations of ABT-888 as low as 0.125  $\mu$ M. The level of synergy observed correlated with the degree of PARP1 inhibition as measured biochemically in cell lysates. ABT-888 at concentrations of 0.5–4  $\mu$ M resulted in synergy with oxaliplatin. Furthermore, 24 h post treatment combinations of ABT-888/irinotecan generally resulted in increased G2/M cell cycle arrest and increased levels of DNA damage, followed by increased levels of apoptosis 48 h post treatment. In conclusion this study suggests that ABT-888 may

be a clinically effective adjuvant to current colon cancer therapies that include the use of irinotecan and/or oxaliplatin.

**Keywords** PARP · PARP inhibitor · VE-821 · Irinotecan · SN38 · Colon cancer

### Introduction

Metastatic colon cancer related mortality remains high due to the development of drug resistance over the course of treatment [1]. Current chemotherapeutic regimens for the treatment of metastatic colon cancer include the DNA damaging drugs, oxaliplatin or irinotecan, in combination with the nucleotide analog 5FU [1]. Although these treatments are initially effective in many patients, all patients eventually become resistant. A major cause of this resistance is increased levels of DNA repair [2–5]. As such an effective strategy to overcome chemotherapy resistance may be the use of small molecule inhibitors of DNA repair networks. We and others have used this strategy to show that inhibition of DNA-PK, a critical modulator of NHEJ, effectively synergizes with irinotecan to kill colon cancer cells and doxorubicin in killing breast cancer cells [6–9]. The present work focuses on a different inhibitor, 2-((R)-2-Methylpyrrolidin-2-yl)-1H-benzimidazole-4-carboxamide (ABT-888), an Abbott laboratories lead compound, that interacts reversibly with PARP1 and 2 inhibiting the formation of poly-ADP ribose side chains [10–13]. PARP1 is a potential target to synergize DNA damaging drugs because of its' important role in the modulation of DNA damage repair. Specifically, PARP1 has been associated with the repair of single strand breaks. It is speculated that inhibition of PARP1 leads to increased single strand breaks in DNA and if left unrepaired that these eventually lead to the formation of increased double strand breaks and in turn increased levels of cell death [14–22]. Currently, as many as 55

D. Davidson · Y. Wang · R. Aloyz (✉) · L. Panasci (✉)  
Montreal Centre for Experimental Therapeutics in Cancer—Segal  
Cancer Center—Lady Davis Institute—Jewish General Hospital,  
McGill University,  
3755, Côte Sainte Catherine Road,  
Montréal, Québec H3T 1E2, Canada  
e-mail: raquel.aloyz@mcgill.ca  
e-mail: lpanasci@hotmail.com

clinical trials are in progress using ABT-888 in combination with chemotherapy against a variety of cancers [18, 23, 24]. Prominent among these are clinical studies treating breast cancer patients with ABT-888 in combination with temozolomide. In addition to being a potent inhibitor of PARP-1 and PARP-2, ABT-888 has good oral bioavailability, can cross the blood–brain barrier, and has been shown to potentiate a variety of DNA damaging anti-cancer therapies including: temozolomide, platinum agents, cyclophosphamide, and radiation in syngenic and xenograft tumor models [10, 11, 13].

Due to the clinical potential of ABT-888, we hypothesized that concurrent treatment of colon cancer cell lines with oxaliplatin or SN38 (the active metabolite of irinotecan) and ABT-888 would synergize the DNA damaging and cytotoxic effects of these drugs. These studies were performed in chemotherapy resistant (p53 mutated) and sensitive (p53 wild type) colon cancer cell lines to demonstrate efficacy in different genetic backgrounds.

## Materials and methods

### Cell culture and reagents

HCT-116 and HT-29 colon cancer cell lines were obtained from the American Type Culture Collection and were maintained at 37 °C in 5 % CO<sub>2</sub> in RPMI or McCoy's medium supplemented with 10 % fetal bovine serum and penicillin/streptomycin. Chemicals and reagents were obtained from Sigma-Aldrich or Invitrogen. ABT-888 was kindly provided by Abbott Laboratories.

### Sulforhodamine (SRB) cytotoxicity assays

SRB assays were performed according to the method of Vichai et al. 2006 [25]. In this assay, SRB stain binds to basic amino acid moieties under mildly acidic conditions facilitating total protein quantification and by implication cell density determination. The assay is amenable to high throughput screening, is linear over a 20 fold range of cell numbers and has sensitivity similar to fluorescence based assays making it an ideal tool for cytotoxicity studies. Briefly, cells were seeded at low density (final density within the linear range of the assay) in 96 well culture dishes and incubated overnight. Cells were subsequently treated with oxaliplatin or SN38 alone, the PARP inhibitor, ABT-888, alone or combinations of oxaliplatin or SN38 and ABT-888 (concentrations indicated in results) as previously described [7, 8]. Five days post drug treatment cells were fixed with trichloroacetic acid (10 %), stained with SRB, and analyzed for percent growth on a 96 well plate reader. Efficacies of the various drug treatments were determined by calculating

50 % inhibitory concentrations (IC<sub>50</sub>) and synergy values. Synergy values (I values) were calculated using the equation of Berenbaum [26] as previously used in our laboratory [6–8]. Using this equation, I values significantly less than 1 indicate synergy, equal to 1 indicate additive behavior, and greater than 1 indicate inhibitory drug interactions. Each experiment was comprised of triplicate drug treatments and experiments were repeated at least 5 times.

### Flow cytometric analyses

These experiments were performed as described [6–8]. Briefly, cells were treated with drugs as described in the results section and analyzed for cell cycle distribution (stained with 5 µg/mL 7AAD and 0.2 mg/mL RNase A) or γH2AX (anti-phospho-Ser139, Upstate, Lake Placid NY). The mean fluorescence intensity was measured to determine levels of phosphorylation of histone H2AX. Alexa488 conjugated secondary antibodies were used to detect the antigens of interest.

### PARP inhibition assay

Levels of PARP inhibition were measured using the Universal PARP assay from Trevigen inc. Cells were plated in 6 well cluster plates at a density of  $5 \times 10^5$  cells per well. After 24 h, cells were treated with SN38 (IC<sub>50</sub> level) alone or in combination with various concentrations of ABT-888. Cells were harvested 1 h and 24 h post drug treatment by scraping and suspending in the culture medium. After spinning at 2,000 rpm for 5 min, medium was removed and the resulting pellet suspended in 100 µL of lysis buffer. After homogenization and incubating on ice for 15 min lysates were centrifuged for 5 min at 13,000 rpm. The resulting supernatant was removed and assayed for protein content. The Trevigen PARP assay was immediately performed on all samples using aliquots with equivalent protein content.

### Western blot analysis

Western blot analyses were performed to determine the relative amount of PARP in each of the treated samples [27]. PARP protein levels were normalized to actin and subsequently used to normalize levels of PARP activity to protein levels.

### Apoptosis assay

Levels of apoptotic cell death were evaluated by monitoring drug treated cultures for membrane permeabilization and Annexin V content using flow cytometry as described [27]. Cells were treated with the stated drug combinations and concentrations for 24 or 48 h and assayed using the PE Annexin V Apoptosis Detection Kit I (BD Pharmingen) according to the manufacturers protocol.

## Statistical analysis

There were at least 5 replicates for all SRB experiments and at least 3 replicates for all other experiments. Means were calculated and compared using Students *T*-test analysis (significance determined at  $p \leq 0.05$ ) employing Graphpad incorporated's "Quickclac" software.

## Results

The ability of ABT-888 to synergize the effect of the anti-cancer agents, SN38 or oxaliplatin, was determined using the SRB assay (Tables 1 and 2). In brief the combined treatment of ABT-888 and SN38 significantly decreased  $IC_{50}$  values of SN38 at ABT-888 concentrations as low as 250 nM compared to SN38 alone in HCT-116 cells. In a similar fashion, ABT-888 concentrations as low as 125 nM, resulted in significant decreases of  $IC_{50}$  values (39 % reduction) in HT29 cells. ABT-888 was also effective in combination with oxaliplatin but required concentrations of 1 to 2  $\mu$ M to produce significant decreases in the  $IC_{50}$  values of oxaliplatin for HCT-116 and HT-29 cell lines. Significantly, *I* values for ABT-888 and SN38 were less than 1 even at concentrations of 0.125  $\mu$ M indicating a strong synergistic effect.

## PARP activity assays and PARP protein expression

PARP activity was measured in HCT-116 cell lysates grown for 24 h in the presence or absence of 10nM SN38 and increasing concentrations of ABT-888 (Fig. 1a). PARP activity was significantly increased over basal levels by the

**Table 1**  $IC_{50}$  values of colon cancer cell lines treated with SN38 alone or combined with the PARP inhibitor ABT-888 determined using the SRB assay

Cell line	[ABT-888] ( $\mu$ M)	SN38 (nM) $IC_{50} \pm SE$	<i>I</i> value	<i>P</i> value $IC_{50}$
HCT-116	0	11.9 $\pm$ 0.4		
	4	6.3 $\pm$ 0.3	0.63	$\leq 0.007$
	2	7.1 $\pm$ 0.7	0.62	$\leq 0.001$
	1	7.3 $\pm$ 1.2	0.65	$\leq 0.001$
	0.5	7.3 $\pm$ 0.4	0.63	$\leq 0.001$
	0.25	8.5 $\pm$ 0.8	0.73	$\leq 0.03$
	0.125	9.1 $\pm$ 0.8	0.76	NS
HT-29	0	23.3 $\pm$ 0.9		
	4	10.7 $\pm$ 0.9	0.56	$\leq 0.001$
	2	12.1 $\pm$ 1.2	0.64	$\leq 0.001$
	1	13.0 $\pm$ 1.1	0.67	$\leq 0.001$
	0.5	13.4 $\pm$ 0.7	0.64	$\leq 0.001$
	0.25	13.6 $\pm$ 1.1	0.72	$\leq 0.001$
	0.125	14.1 $\pm$ 1.7	0.57	$\leq 0.001$

**Table 2**  $IC_{50}$  values of colon cancer cell lines treated with Ox alone or combined with the PARP inhibitor ABT-888 determined using the SRB assay

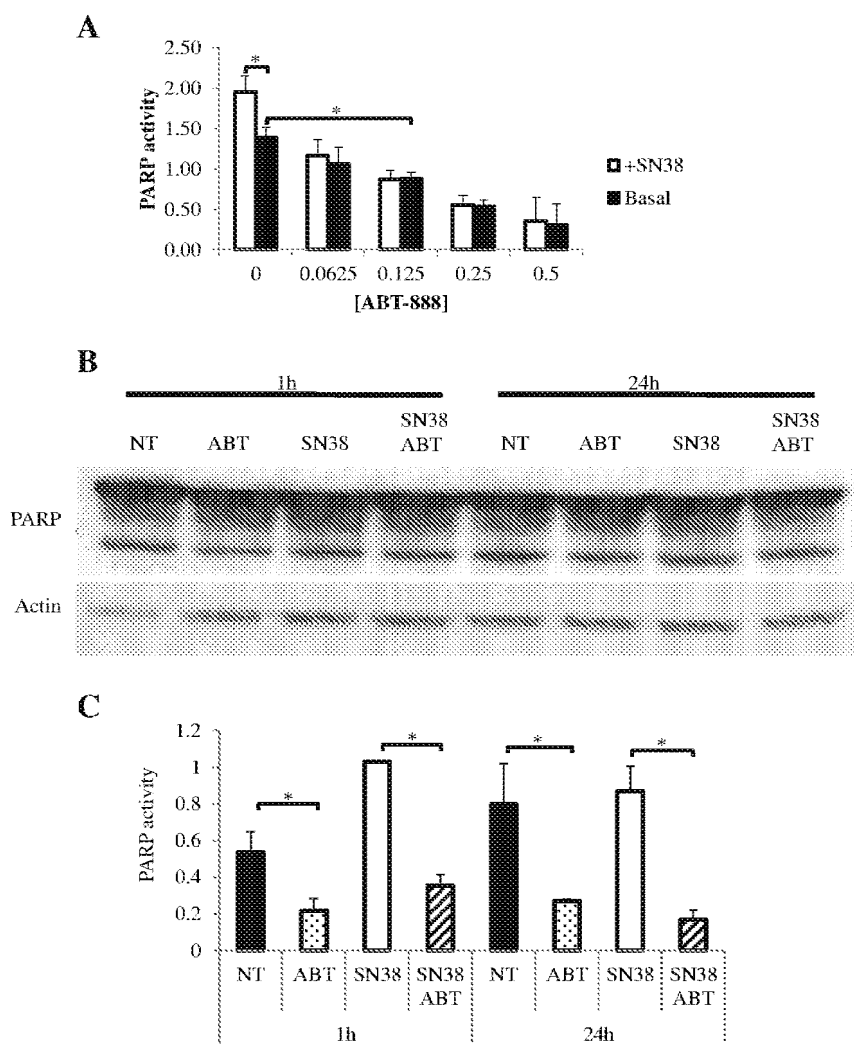
Cell line	[ABT-888] ( $\mu$ M)	Oxali ( $\mu$ M) $IC_{50} \pm SE$	<i>I</i> value	<i>P</i> value $IC_{50}$
HCT-116	0	0.34 $\pm$ 0.07		
	4	0.19 $\pm$ 0.02	0.54	$\leq 0.05$
	2	0.19 $\pm$ 0.01	0.55	$\leq 0.05$
	1	0.23 $\pm$ 0.03	0.67	NS
	0.5	0.24 $\pm$ 0.04	0.71	NS
HT-29	0	1.59 $\pm$ 0.12		
	4	1.12 $\pm$ 0.08	0.70	$\leq 0.05$
	2	1.16 $\pm$ 0.07	0.72	$\leq 0.05$
	1	1.27 $\pm$ 0.08	0.83	$\leq 0.05$
	0.5	1.30 $\pm$ 0.06	0.81	NS

addition of SN38 (2.2 fold increase). In contrast, addition of ABT-888 resulted in a concentration dependent decrease in PARP activity. In the presence of SN38 in combination with ABT-888, PARP activity was not significantly higher than with the equivalent concentration of ABT-888 alone. To demonstrate that this change in activity was not due to altered protein expression, western blot analysis was performed on samples treated for 1 h or 24 h with 0.5  $\mu$ M ABT-888, 10 nM SN38 or combinations of these two (Fig. 1b). Levels of total PARP protein normalized to actin were consistent from sample to sample. However, activity measured in the same protein samples and normalized to total PARP protein demonstrated the highest PARP activity in samples treated with SN38 alone (Fig. 1c). PARP activity was significantly reduced in samples treated with SN38 in combination with ABT-888 (>4 fold at 24 h).

To understand the mechanism underlying the drug effects on colon cancer cells, levels of  $\gamma$ H2AX were measured in both HCT-116 and HT-29 cells treated with oxaliplatin or SN38 alone or in combination with ABT-888.  $\gamma$ H2AX, an indicator of DNA double strand breaks, was significantly increased in cells treated with SN38 or SN38 in combination with ABT-888 (Fig. 2) ( $p \leq 0.05$ ). The highest levels of  $\gamma$ H2AX were detected in the presence of SN38 combined with ABT-888. An increase in  $\gamma$ H2AX was observed with oxaliplatin or oxaliplatin in combination with ABT-888 but these differences were not significant.

Cell cycle analysis was also determined (Fig. 3). At a 24 h time point no change in cell cycle progression was observed for either HCT-116 or HT-29 cells treated with ABT-888, oxaliplatin or the combinations of ABT-888 with oxaliplatin. In contrast, treatment with SN38 alone caused significant G2M arrest in both cell lines and this effect was increased by the addition of ABT-888, being most prominent in p53 wild type HCT-116 cells. To demonstrate that DNA damage observed at 24 h was not due to DNA

**Fig. 1** **a** PARP activity in HCT-116 cells treated with increasing concentrations of ABT-888 alone (Basal) or in combination with 10 nM SN38 (24 h), **b** total PARP expression in HCT-116 cell culture at 1 and 24 h after treatment with 10nM SN38, 0.5  $\mu$ M ABT-888 or the combination of SN38 and ABT-888, **c** PARP activity normalized to total PARP expression in HCT-116 cells 1 and 24 h post treatment with 10nM SN38, 0.5  $\mu$ M ABT-888 or the combination of these drugs. (\* = significant at  $p \leq 0.01$ )



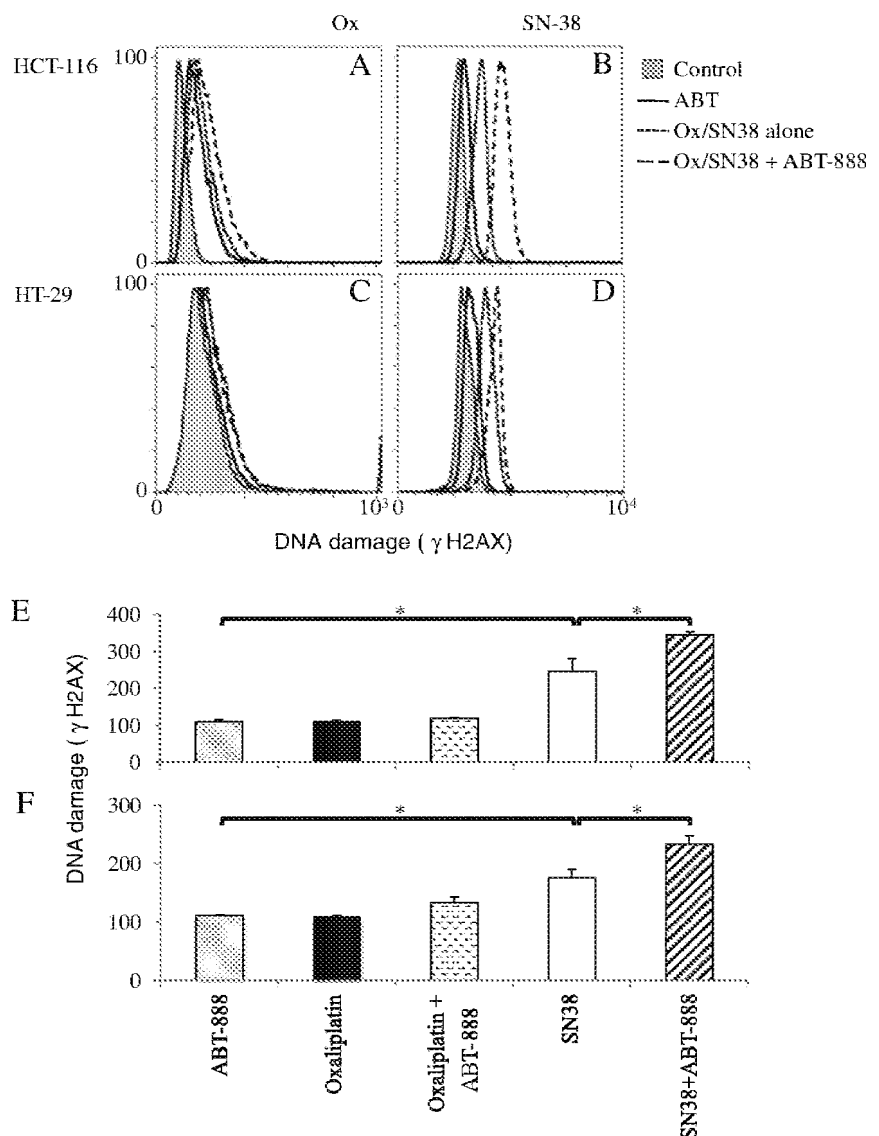
degradation associated with induction of apoptosis, Annexin V expression was analyzed at both 24 and 48 h. Although little apoptosis was detected at the 24 h time point, a significant increase in apoptosis was observed at 48 h in the presence of SN38 or SN38 plus ABT-888 for both cell lines (Fig. 4) indicating that  $\gamma$ H2AX preceded drug-induced-apoptosis.

## Discussion

Ideally, DNA repair inhibitors will improve the therapeutic index of chemotherapeutic drugs by targeting cancer cells over healthy cells. The PARP inhibitor, ABT-888, has significant potential in this regard [28]. Typically, cancer cells have one or more mutations affecting DNA repair pathways and as such there is the possibility to exploit synthetic lethality using drugs that target DNA repair [29–31]. The efficacy of this approach has been demonstrated in BRCA1/2 deficient breast cancers (mutations affecting HRR) were PARP inhibitors including ABT-888 were shown to improve

treatment with temozolomide [16, 32–38]. Interestingly, it was shown using mono-therapy that the a PARP inhibitor, AGO14669, increased double stand breaks in all cells but primarily effected those with deficiencies in HRR that were unable to repair the damage [39]. Here we show that treatment with ABT-888, at concentrations well below clinically achievable levels [10, 12, 13], sensitized both p53 wild type and mutant colon cancer cells lines to SN38 induced death in vitro. SN38, the active metabolite of irinotecan, is a potent topoisomerase I (topo 1) inhibitor that through its' interaction inhibits the separation of topo 1 from the DNA strand and can result in the formation of DSBs [40, 41]. In healthy cells, this damage can be rapidly repaired via the major DNA damage repair pathways, HR and NHEJ. Here, sensitization was achieved in both cell lines tested although more pronounced in the p53 inactive HT-29 cells. This synergy was associated with increased DNA damage and was also reflected in dramatic cell cycle arrest in both cell lines. G2/M arrest observed with SN38 treatment alone was enhanced most prominently by the addition of ABT-888 in p53 functional HCT-116 cells. Other investigators have

**Fig. 2**  $\gamma$ H2AX expression (double stand breaks) in HCT-116 (a, b) or HT-29 (c, d) cells treated with the  $[IC_{50}]$  of oxaliplatin (a, c) or SN38 (b, d) alone or in combination with ABT-888 (0.5 $\mu$ M). Cells were fixed and stained with a  $\gamma$ H2AX specific antibody 24 h post drug treatment. Mean  $\gamma$ H2AX in HCT-116 (e) or HT-29 (f) cells 24 h post drug treatment. (\* = significant at  $p \leq 0.05$ )



shown that a major effect of SN38 treatment is G2/M arrest [42]. In HT-29 cells, G2/M arrest was almost complete with SN38 treatment alone suggesting that in the face of DNA damage cells arrest in G2/M to facilitate repair and that although functional p53 is not required for this arrest, it is needed for cells to leave G2/M efficiently. It is likely SN38 treated p53 inactive HT29 cells were unable to progress in the cell cycle due to p53 inactivity [43]. In contrast, the inability to progress in the cell cycle might in part explain the higher level of resistance to SN38 of these cells, with active replication forks being required for the creation of DSBs. Alternatively, a lack of functional p53 in the face of overwhelming DNA damage might confer resistance by inhibiting apoptotic signaling. These data suggest that the presence of active p53 facilitates cell cycle progression in the presence of DNA damage and that this progression is inhibited by ABT-888. One possible explanation for this is that p53 is PARylated in response to PARP activation

preventing nuclear export. Thus, it is possible that the presence of the PARP inhibitor abrogates p53 PARylation preventing normal functionality. PARP has a number of diverse cellular functions including: regulation of cell survival and death pathways, transcription regulation, telomere cohesion, mitotic spindle formation, intracellular energy metabolism and trafficking of signaling proteins such as p53, p63 and NF $\kappa$ B. In this context PARylation prevents interaction of these molecules with exportin-1 (XPO-1), a mediator of nuclear export, and as such inhibits normal trafficking to the cytoplasm [44]. Our results are in keeping with that of others that showed the PARP inhibitor, veliparib, synergized the topoisomerase I poisons topotecan and camptothecin [31]. Like many of the PARP inhibitors (including ABT-888) veliparib is an NAD<sup>+</sup> analogue small molecule inhibitor of PARP and may function by preventing cross PARylation (PARylation of PARP by PARP) and subsequent release of PARP from DNA damage sites. As such DNA



**Fig. 3** Cell cycle analysis of HCT-116 and HT29 colon cancer cells 24 h post treatment with [IC<sub>50</sub>] of oxaliplatin or SN38 alone or in combination with 0.5  $\mu$ M ABT-888

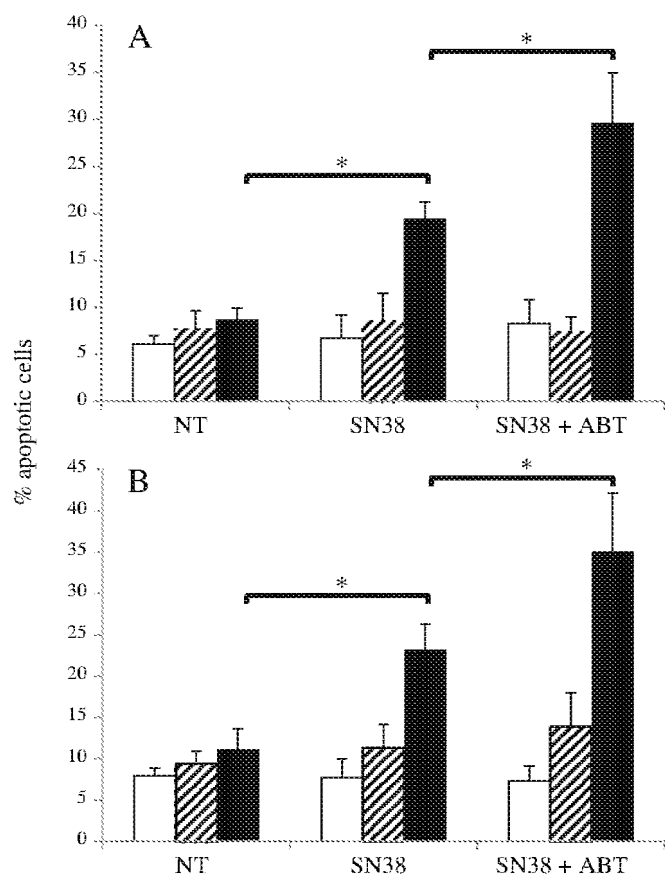
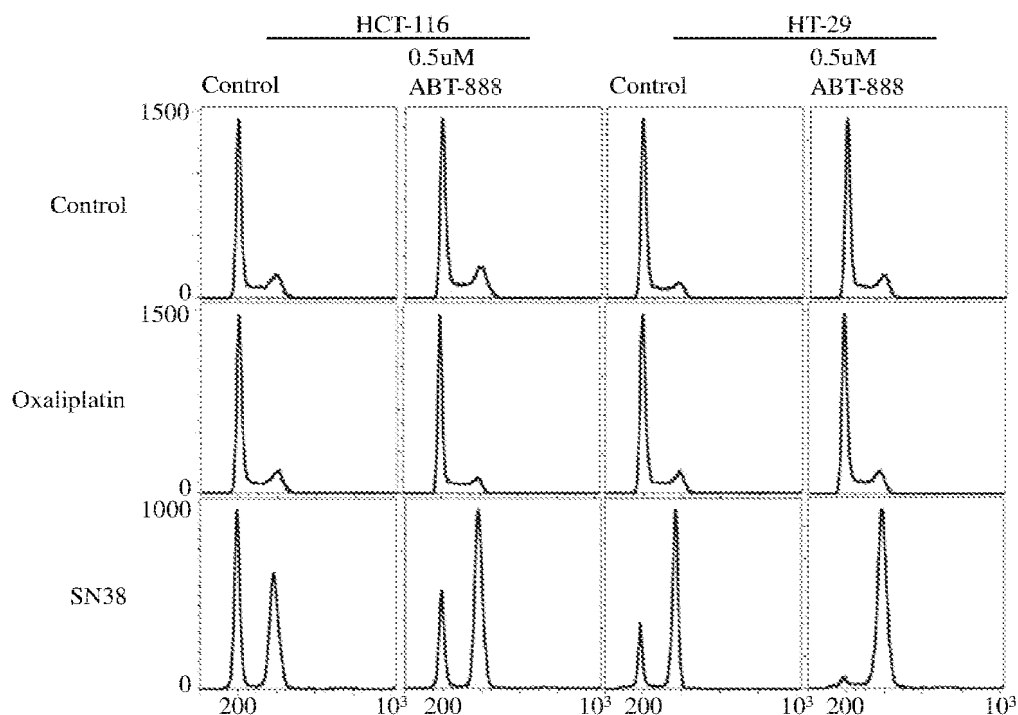


**Fig. 4** Annexin V apoptosis assay of HCT-116 (a) or HT-29 (b) cells treated with SN38 (10 nM (HCT-116), 20 nM (HT-29)) or SN38 in combination with ABT-888 (0.5  $\mu$ M) for 4 h, 24 h or 48 h. (\* = significant at  $p \leq 0.05$ )

bound PARP would induce cell death by interfering with transcription and the progress of replication forks [31]. Furthermore, it has been shown that ABT-888 potentiates temozolomide, platinum based drugs, cyclophosphamide and radiation [10]. Here we report a synergistic effect for combined treatment with oxaliplatin and ABT-888 but at higher concentrations of ABT-888 than with SN38. The platinum analogues function by forming complex DNA adducts including intrastrand and interstrand crosslinks (ICLs) [4]. Repair of these lesions is mediated by multiple DNA repair systems. The synergy seen with ABT-888 and oxaliplatin suggests that inhibition of PARP results in inhibition of many DNA repair pathways and thus sensitizes cells to this agent [19].

Although much work with PARP inhibitors has focused on BRCA1/2 deficient cancers, other investigators have shown that other DNA repair phenotypes may be sensitive to PARP inhibitor therapy. For example, recently it was shown that ATM deficient tumors are effectively targeted with PARP inhibitors. This response was even more pronounced when tumors were deficient in both ATM and p53 [45]. PARP inhibition has also been shown to result in extreme sensitization to methyl methane sulfonate (MMS) in mouse embryonic fibroblasts (MEFs). Here, PARP inhibition was accompanied by accumulation of S-phase cells that required ATR signaling. This study showed interaction of PARP and ATR by co-IP that required active PARylation of ATR [46]. Finally, microarray analysis showed that the DDR pathways elicited by ABT-888 and topotecan are the G1/S checkpoint, ATM and p53 in p53 wild type cells and

BRCA1/2 and ATR in p53 mutant cell lines. Topotecan alone caused induction of the G1/S checkpoint and the combination of drugs enhanced G2 arrest, apoptosis and cell death. Cell death was further enhanced by the checkpoint kinase inhibitor UCN-01 that abolished G2 arrest [47]. Our data indicate that levels of PARP expression were not significantly affected by drug treatments and, in spite of this, a large increase in PARP activity with SN38 treatment alone was observed. However, in the presence of ABT-888, PARP activity was dramatically reduced.

Most importantly, the results of a Phase I clinical trial of ABT-888 and irinotecan demonstrated that a full dose of irinotecan can be given with doses of ABT-888 that suppress PARP activity [48] suggesting that an increase in the therapeutic index will be seen with this combination in the treatment of patients with metastatic colon cancer.

**Acknowledgements** We gratefully acknowledge Abbott laboratories for providing the PARP inhibitor ABT-888 used in this study.

**Grant support** This work was supported by research grants to Lawrence Panasci and Raquel Aloyz from the Canadian Institute of Health Research (CIHR) and CIHR and the Leukemia, Lymphoma Society (USA), respectively. David Davidson received salary support from the Quebec-Clinical Research Organization in Cancer (Q-CROC).

**Conflict of interest** The authors declare they have no conflict of interest.

## References

- Raftery L, Goldberg RM (2010) Optimal delivery of cytotoxic chemotherapy for colon cancer. *Cancer J* 16:214–219
- Edwards SL (2008) Resistance to therapy caused by intragenic deletion in BRCA2. *Nature* 451:1111–1115
- Gottesman MM (2002) Mechanisms of cancer drug resistance. *Annu Rev Med* 53:615–627
- Rabik CA, Dolan ME (2007) Molecular mechanisms of resistance and toxicity associated with platinating agents. *Cancer Treat Rev* 33:9–23
- Spanwick VI, Craddock C, Sekhar M, Mahendra P, Shankaranarayana P, Hughes RG (2002) Repair of DNA interstrand crosslinks as a mechanism of clinical resistance to melphalan in multiple myeloma. *Blood* 100:224–229
- Amrein L, Loignon M, Goulet A-C, Dunn M, Jean-Claude B, Aloyz R et al (2007) Chlorambucil cytotoxicity in malignant B lymphocytes is synergistically increased by 2-(morpholin-4-yl)-benzo[h]chomen-4-one (NU7026)-mediated inhibition of DNA double-strand break repair via inhibition of DNA-dependent protein kinase. *J Pharmacol Exp Ther* 321:848–855
- Davidson D, Coulombe Y, Martinez-Marignac V, Amrein L, Grenier J, Hodgkinson K et al (2012) Irinotecan and DNA-PKcs inhibitors synergize in killing of colon cancer cells. *Invest New Drugs* 30:1248–1256
- Davidson D, Grenier J, Martinez-Marignac V, Amrein L, Shawi M, Tokars M et al (2012) Effects of the novel DNA dependent protein kinase inhibitor, IC486241, on the DNA damage response to doxorubicin and cisplatin in breast cancer cells. *Invest New Drugs* 30:1736–1742
- Nutley BP, Smith NF, Hayes A, Kelland LR, Brunton L, Golding BT et al (2005) Preclinical pharmacokinetics and metabolism of a novel prototype DNA-PK inhibitor NU7026. *Br J Cancer* 93:1011–1018
- Donawho CK, Luo Y, Luo Y, Penning TD, Bauch JL, Bouska JJ et al (2007) ABT-888, an Orally Active Poly(ADP-Ribose) Polymerase Inhibitor that Potentiates DNA-Damaging Agents in Preclinical Tumor Models. *Clin Cancer Res* 13:2728–2737
- Horton TM, Jenkins G, Pati D, Zhang L, Dolan ME, Ribes-Zamora A et al (2009) Poly(ADP-ribose) polymerase inhibitor ABT-888 potentiates the cytotoxic activity of temozolomide in leukemia cells: influence of mismatch repair status and O6-methylguanine-DNA methyltransferase activity. *Mol Cancer Ther* 8:2232–2242
- Ji J, Lee M, Kadota M, Zhang Y, Parchment R, Tomaszewski JE et al (2011) Pharmacodynamic and pathway analysis of three presumed inhibitors of poly (ADP-ribose) polymerase: ABT-888, AZD2281, and BSI201. Proceedings of the 102nd Annual Meeting of the American Association for Cancer Research; 2011 April 2–6; Orlando, FL. Philadelphia, PA: American Association of Cancer Research
- Kummar S, Kinders R, Gutierrez ME, Rubinstein L, Parchment RE, Phillips LR et al (2009) Phase 0 clinical trial of the poly (ADP-ribose) polymerase inhibitor ABT-888 in patients with advanced malignancies. *J Clin Oncol* 27:2705–2711
- Curtin NJ (2005) PARP inhibitors for cancer therapy. *Expert Rev Mol Med* 7:1–20
- Heacock ML, Stefanick DF, Horton JK, Wilson SH (2010) Alkylation DNA damage in combination with PARP inhibition results in formation of S-phase-dependent double-strand breaks. *DNA Repair* 9:929–936
- Helleday T. The underlying mechanism for the PARP and BRCA synthetic lethality: Clearing up the misunderstandings. *Molecular Oncology*; 5:387–393.
- Javle M, Curtin NJ (2011) The role of PARP in DNA repair and its therapeutic exploitation. *Br J Cancer* 105:1114–1122
- Kummar S, Chen A, Parchment R, Kinders R, Ji J, Tomaszewski J et al (2012) Advances in using PARP inhibitors to treat cancer. *BMC Med* 10:25
- Rouleau M, Patel A, Hendzel MJ, Kaufmann SH, Poirier GG (2010) PARP inhibition: PARP1 and beyond. *Nat Rev Cancer* 10:293–301
- Sousa FG, Matuo R, Soares DG, Escargueil AE, Henriques JAP, Larsen AK et al (2012) PARPs and the DNA damage response. *Carcinogenesis*
- Tentori L, Graziani G (2005) Chemopotential by PARP inhibitors in cancer therapy. *Pharmacol Res* 52:25–33
- Zaremba T, Thomas HD, Cole M, Coulthard SA, Plummer ER, Curtin NJ (2011) Poly(ADP-ribose) polymerase-1 (PARP-1) pharmacogenetics, activity and expression analysis in cancer patients and healthy volunteers. *Biochem J* 436:671–679
- Bedikian AY, Papadopoulos NE, Kim KB, Hwu WJ, Homsy J, Glass MR et al (2009) A phase IB trial of intravenous INO-1001 plus oral temozolomide in subjects with unresectable stage-III or IV melanoma. *Cancer Invest* 27:756–763
- Plummer R, Jones C, Middleton M, Wilson R, Evans J, Olsen A et al (2008) Phase I study of the poly(ADP-ribose) polymerase inhibitor, AG014699, in combination with temozolomide in patients with advanced solid tumors. *Clin Cancer Res* 14:7917–7923
- Vichai V, Kirtikara K (2006) Sulforhodamine B colorimetric assay for cytotoxicity screening. *Nat Protoc* 1:1112–1116
- Berenbaum M (1992) Letter Correspondence re: “Greco et al., Applications of a New Approach for the Quantitation of Drug Synergism to the Combination of c/s-Diamminedichloroplatinum and 1-tf-D-Arabinofuranosylecytosine. *Cancer Res* 50: 5318–5327, 1990.”. *Cancer Res* 52:4558–4565

27. Xu Z-Y, Loignon M, Han F-Y, Panasci L, Aloyz R (2005) Xrcc3 Induces cisplatin resistance by stimulation of Rad51-related recombinational repair, S-phase checkpoint activation, and reduced apoptosis. *J Pharmacol Exp Ther* 314:495–505
28. Tentori L, Leonetti C, Scarsella M, Muzi A, Mazzon E, Vergati M et al (2006) Inhibition of poly(ADP-ribose) polymerase prevents irinotecan-induced intestinal damage and enhances irinotecan/temozolomide efficacy against colon carcinoma. *FASEB J* 20:1709–1711
29. Smith J, Mun Tho L, Xu N, A. Gillespie D. The ATM-Chk2 and ATR-Chk1 Pathways in DNA Damage Signaling and Cancer. In: George FVW, George K, editors. *Advances in Cancer Research*: Academic Press; 2010. p. 73–112.
30. Shaheen M, Allen C, Nickoloff JA, Hromas R (2011) Synthetic lethality: exploiting the addiction of cancer to DNA repair. *Blood* 117:6074–6082
31. Patel AG, Flatten KS, Schneider PA, Dai NT, McDonald JS, Poirier GG et al (2012) Enhanced killing of cancer cells by poly(ADP-ribose) polymerase inhibitors and topoisomerase I inhibitors reflects poisoning of both enzymes. *J Biol Chem* 287:4198–4210
32. Tutt A, Robson M, Garber JE, Domchek SM, Audeh MW, Weitzel JN et al (2010) Oral poly(ADP-ribose) polymerase inhibitor olaparib in patients with BRCA1 or BRCA2 mutations and advanced breast cancer: a proof-of-concept trial. *Lancet* 376:235–244
33. Rottenberg S, Jaspers JE, Kersbergen A, van der Burg E, Nygren AO, Zander SA et al (2008) High sensitivity of BRCA1-deficient mammary tumors to the PARP inhibitor AZD2281 alone and in combination with platinum drugs. *Proc Natl Acad Sci USA* 105:17079–17084
34. Fong PC, Yap TA, Boss DS, Carden CP, Mergui-Roelvink M, Gourley C et al (2009) Poly(ADP)-ribose polymerase inhibition: frequent durable responses in BRCA carrier ovarian cancer correlating with platinum-free interval. *J Clin Oncol* 28:2512–2519
35. Fong PC, Boss DS, Yap TA, Tutt A, Wu P, Mergui-Roelvink M et al (2009) Inhibition of poly(ADP-ribose) polymerase in tumors from BRCA mutation carriers. *N Engl J Med* 361:123–134
36. Farmer H, McCabe N, Lord CJ, Tutt AN, Johnson DA, Richardson TB et al (2005) Targeting the DNA repair defect in BRCA mutant cells as a therapeutic strategy. *Nature* 434:917–921
37. Drew Y, Mulligan EA, Vong WT, Thomas HD, Kahn S, Kyle S et al (2010) Therapeutic potential of Poly(ADP-ribose) polymerase inhibitor AG014699 in human cancers with mutated or methylated BRCA1 or BRCA2. *J Natl Cancer Inst* 103:334–346
38. Bryant HE, Schultz N, Thomas HD, Parker KM, Flower D, Lopez E et al (2005) Specific killing of BRCA2-deficient tumours with inhibitors of poly(ADP-ribose) polymerase. *Nature* 434:913–917
39. Drew Y, Mulligan EA, Vong W-T, Thomas HD, Kahn S, Kyle S et al (2011) Therapeutic Potential of Poly(ADP-ribose) Polymerase Inhibitor AG014699 in Human Cancers With Mutated or Methylated BRCA1 or BRCA2. *J Natl Cancer Inst* 103:334–346
40. Rudolf E, Rudolf K, Cervinka M (2011) Camptothecin induces p53-dependent and -independent apoptogenic signaling in melanoma cells. *Apoptosis* 16:1–12
41. Zuco V, Benedetti V, Zunino F (2010) ATM- and ATR-mediated response to DNA damage induced by a novel camptothecin, ST1968. *Cancer Lett* 292:186–196
42. Schwartz GK (2005) Development of cell cycle active drugs for the treatment of gastrointestinal cancers: a new approach to cancer therapy. *J Clin Oncol* 23:4499–4508
43. Poele RH, Joel SP (1999) Schedule-dependent cytotoxicity of SN-38 in p53 wild-type and mutant colon adenocarcinoma cell lines. *Br J Cancer* 81:1285–93
44. Elmageed A, Zakaria Y, Amarjit NS, Errami Y, Zerfaoui M (2012) The Poly(ADP-ribose) polymerases (PARPs): New roles in intracellular transport. *Cell Signal* 24:1–8
45. Williamson CF, Kubota E, Hamill JD, Klimowicz A, Ye R, Muzik H et al (2012) Enhanced cytotoxicity of PARP inhibition in mantle cell lymphoma harbouring mutations in both ATM and p53. *EMBO Mol Med* 4:515–527
46. Kedar PS, Stefanick DF, Horton JK, Wilson SH (2008) Interaction between PARP-1 and ATR in mouse fibroblasts is blocked by PARP inhibition. *DNA Repair* 7:1787–1798
47. Nguyen D, Zajac-Kaye M, Rubinstein L, Voeller D, Tomaszewski JE, Kummar S et al (2011) Poly(ADP-ribose) polymerase inhibition enhances p53-dependent and -independent DNA damage responses induced by DNA damaging agent. *Cell Cycle* 10:4074–4082
48. LoRusso JJ, Heilbrun LK, Shapiro G, Sausville EA, Boerner SA, Smith DW et al (2011) Phase I study of the safety, pharmacokinetics (PK), and pharmacodynamics (PD) of the poly(ADP-ribose) polymerase (PARP) inhibitor veliparib (ABT-888; V) in combination with irinotecan (CPT-11; Ir) in patients (pts) with advanced solid tumors. *Proceedings of the 102nd Annual Meeting of the American Association for Cancer Research*; 2011 April 2–6; Orlando, FL. Philadelphia, PA: American Association of Cancer Research

# Canine model of convection-enhanced delivery of liposomes containing CPT-11 monitored with real-time magnetic resonance imaging

## Laboratory investigation

PETER J. DICKINSON, B.V.Sc., Ph.D.,<sup>1</sup> RICHARD A. LECOUREUR, B.V.Sc., Ph.D.,<sup>1</sup>  
 ROBERT J. HIGGINS, B.V.Sc., Ph.D.,<sup>2</sup> JOHN R. BRINGAS, Ph.D.,<sup>3</sup> BYRON ROBERTS, M.S.,<sup>1</sup>  
 RICHARD F. LARSON, B.S.,<sup>1</sup> YOJI YAMASHITA, M.D.,<sup>3</sup> MICHAL KRAUZE, M.D.,<sup>3</sup>  
 CHARLES O. NOBLE, Ph.D.,<sup>4</sup> DARYL DRUMMOND, Ph.D.,<sup>4</sup> DMITRI B. KIRPOTIN, Ph.D.,<sup>4</sup>  
 JOHN W. PARK, M.D.,<sup>5</sup> MITCHEL S. BERGER, M.D.,<sup>3</sup>  
 AND KRYSZTOF S. BANKIEWICZ, M.D., Ph.D.<sup>3</sup>

Departments of <sup>1</sup>Surgical and Radiological Sciences, and <sup>2</sup>Pathology, Microbiology and Immunology, School of Veterinary Medicine, University of California, Davis; <sup>3</sup>Department of Neurosurgery, Brain Tumor Research Center, University of California, San Francisco; <sup>4</sup>Hermes Biosciences, Inc., San Francisco; and <sup>5</sup>University of California at San Francisco Comprehensive Cancer Center, San Francisco, California

**Object.** Many factors relating to the safety and efficacy of convection-enhanced delivery (CED) into intracranial tumors are poorly understood. To investigate these factors further and establish a more clinically relevant large animal model, with the potential to investigate CED in large, spontaneous tumors, the authors developed a magnetic resonance (MR) imaging-compatible system for CED of liposomal nanoparticles into the canine brain, incorporating real-time MR imaging. Additionally any possible toxicity of liposomes containing Gd and the chemotherapeutic agent irinotecan (CPT-11) was assessed following direct intraparenchymal delivery.

**Methods.** Four healthy laboratory dogs were infused with liposomes containing Gd, rhodamine, or CPT-11. Convection-enhanced delivery was monitored in real time by sequential MR imaging, and the volumes of distribution were calculated from MR images and histological sections. Assessment of any toxicity was based on clinical and histopathological evaluation. Convection-enhanced delivery resulted in robust volumes of distribution in both gray and white matter, and real-time MR imaging allowed accurate calculation of volumes and pathways of distribution.

**Results.** Infusion variability was greatest in the gray matter, and was associated with leakage into ventricular or sub-arachnoid spaces. Complications were minimal and included mild transient proprioceptive deficits, focal hemorrhage in 1 dog, and focal, mild perivascular, nonsuppurative encephalitis in 1 dog.

**Conclusions.** Convection-enhanced delivery of liposomal Gd/CPT-11 is associated with minimal adverse effects in a large animal model, and further assessment for use in clinical patients is warranted. Future studies investigating real-time monitored CED in spontaneous gliomas in canines are feasible and will provide a unique, clinically relevant large animal translational model for testing this and other therapeutic strategies. (DOI: 10.3171/JNS.2008.108.5.0989)

**KEY WORDS** • brain • convection-enhanced delivery • dog • irinotecan • magnetic resonance imaging

**C**ONVECTION enhanced delivery is a local delivery technique that uses a bulk-flow mechanism to deliver and distribute macromolecules over clinically relevant volumes of targeted tissue.<sup>2,3</sup> Unlike local injection techniques, CED uses a pressure gradient established at the tip of an infusion catheter that literally pushes the infusate

through the interstitial space. Volumes of distribution of infused molecules are significantly increased compared with local injection or surgical implantation methods that rely primarily on diffusion and are limited by concentration gradients and the molecular weight of the delivered substance. Distribution of infusates over centimeters, rather than millimeters, have been reported in a variety of experimental models of CED.<sup>2,10,17,27</sup> Real-time in vivo imaging of CED is an essential consideration if adequate drug distribution is to be confirmed antemortem. Additionally, the ability to detect and minimize drug distribution or leakage to normal tissues during delivery has the potential to decrease toxicity significantly and increase the therapeutic index.

Abbreviations used in this paper: CED = convection-enhanced delivery; CSF = cerebrospinal fluid; MR = magnetic resonance; TEA-SOS = triethylammonium sucrose octasulphate; V<sub>d</sub> = volume of distribution; V<sub>i</sub> = volume of infusion.

Several surrogate marker systems have been described that facilitate image-guided CED. These have included MR imaging systems with T2-weighted imaging correlated with  $^{125}\text{I}$ -labeled serum albumin single photon emission computed tomography,<sup>29,30</sup> and liposomes colabeled with Gd.<sup>13,21,26,27,35</sup> Liposomes are phospholipid nanoparticles composed of a bilayered membrane capable of encapsulating a variety of therapeutic molecules. Liposomal encapsulation of a variety of drugs, including chemotherapeutics, has been shown to result in prolonged half-life, sustained release, and decreased toxicity.<sup>7,18,22</sup> Convection-enhanced delivery of drug-containing liposomes directly into targeted brain tissue offers several advantages over systemic delivery of unencapsulated drugs, including bypassing of the blood-brain barrier, an increased  $V_d$  within the target tissue, and an increased therapeutic index as a result of both liposomal encapsulation and minimal systemic exposure. Irinotecan/CPT-11 is a camptothecin derivative and topoisomerase I inhibitor with activity against a variety of cancer types, including brain tumors. We previously reported on the efficacy and safety of direct delivery of liposome-encapsulated camptothecin analogs in rodent models of glioma.<sup>22,28</sup> Translation of this promising therapeutic approach into clinical trials will require demonstration of the safety and efficacy of combined real-time Gd-based imaging and liposome-encapsulated CPT-11 treatment in a large animal model. There are several advantages of a canine model over the established rodent and primate models, including the ability to investigate aspects of feasibility and toxicity on a scale relevant to human patients, and the unique potential to investigate CED efficacy and adverse effects in large, spontaneously occurring tumors. The occurrence of primary brain tumors in dogs, ~ 14.5 per 100,000 (Vandeveld, unpublished data) or 1–3% of all primary neoplasias recorded at necropsy,<sup>23</sup> is comparable to the incidence of primary brain tumors in humans. The biological behavior, clinical imaging results, and histological and molecular characteristics of primary gliomas in canines have many similarities to their counterparts in humans.<sup>4,5,8,11,12,16,32,33</sup>

We hypothesized that CED of liposomes containing a Gd marker was a feasible and safe strategy for guiding local delivery of nanoliposomal CPT-11 to clinically significant areas of the canine brain, and that real-time MR imaging would be predictive of the actual  $V_d$ . The goals of this study were to develop a large animal translational model for real-time imaged CED, with the potential for investigations into spontaneously occurring tumors, and to assess in detail, both clinically and histologically, any potential adverse effects of liposomal Gd and CPT-11 in large animal brains.

## Materials and Methods

### Experimental Animals

Four female hound/cross dogs (20–22 kg, 8 months to 3 years of age) were obtained from Marshall Farms Inc. Experimental protocols were performed in accordance with the National Institutes of Health laboratory animal guidelines and the Animal Welfare Act. The experimental protocol was reviewed and approved by the Institutional Animal Care and Use Committee at the University of California at Davis. All dogs were individually housed in concrete runs and maintained on a 12-hour light/dark cycle with a room temperature of 20–22°C. A standard commercial maintenance dry food diet was provided on a daily basis with water provided ad libitum, and

chew toys for environmental enrichment. All animals were held for 1 week prior to CED procedures, and all underwent complete physical and neurological examinations prior to the procedure and daily thereafter until completion of the study.

### Liposome Preparation

Separate liposomes were prepared for detection on MR imaging, on histological examination, and for delivery of CPT-11. Liposomes that contained the MR imaging contrast agent were composed of 1,2-dioleoyl-sn-glycero-3-phosphocholine (DOPG, Avanti Polar Lipids), cholesterol (Calbiochem), and 1,2-distearoyl-sn-glycero-3-[methoxy(polyethylene glycol)-2000 (PEG-DSG, NOF Corporation) with a molar ratio of 3:2:0.3. The lipids were dissolved in chloroform/methanol solution (90:10, vol/vol) and then the solvent was removed by rotary evaporation, resulting in a thin lipid film. The lipid film was dissolved in ethanol and heated to 60°C. A commercial United States Pharmacopoeia solution of 0.5 M gadoteridol (ProHance, Bracco Diagnostics) was heated to 60°C and injected rapidly into the ethanol/lipid solution. Unilamellar liposomes were formed by extrusion (Lipex, Northern Lipids) with 15 passes through double-stacked polycarbonate membranes (Whatman Nucleopore) with a pore size of 100 nm, resulting in a liposome diameter of  $124 \pm 24.4$  nm as determined by quasielastic light scattering (N4Plus Particle Size Analyzer, Beckman Coulter). Unencapsulated gadoteridol was removed with a Sephadex G-75 (Amersham Biosciences) size-exclusion column eluted with HEPES-buffered saline (5 mM HEPES and 135 mM NaCl at pH 6.5, adjusted with NaOH).

Liposomes, loaded with rhodamine for histological studies, were formulated with the same lipid composition and preparation method as the gadoteridol-containing liposomes except that the lipids were hydrated directly with 20 mM sulforhodamine B (Sigma) in HEPES-buffered saline (pH 6.5) by 6 successive cycles of rapid freezing and thawing rather than by ethanol injection. The sulforhodamine B liposomes had a diameter of  $115 \pm 40.1$  nm (used for coinjection with the gadoteridol-containing liposomes).

### Quantification of Liposome-Entrapped Gadoteridol on MR Imaging

The concentration of gadoteridol entrapped in the liposomes was determined from nuclear MR relaxivity measurements. The relationship between the change in the intrinsic relaxation rate imposed by a paramagnetic agent ( $\Delta R$ ), also known as “T1 shortening,” and the concentration of the agent is defined by the equation:  $\Delta R = r_1[\text{agent}]$ , in which  $r_1$  = relaxivity of the paramagnetic agent and  $\Delta R = (1/T1_{\text{observed}} - 1/T1_{\text{intrinsic}})$ . Because gadoteridol was encapsulated within the liposome, we corrected for the change in the observed T1 imposed by the lipid by measuring the T1 of solubilized liposomes, with and without gadoteridol, by means of an iterative inversion-recovery MR imaging sequence on a 2-T Bruker Omega unit (Bruker Medical). The relaxivity of gadoteridol had been empirically derived previously on the same system, and had a value of  $4.07 \text{ mM}^{-1}\text{sec}^{-1}$ . The concentration of the encapsulated gadoteridol was then calculated with the following equation:  $[\text{gadoteridol}] = [(1/T1_{\text{with gadoteridol}}) - (1/T1_{\text{without gadoteridol}})]/4.07$ .

### Preparation of CPT-11 Liposomes

The CPT-11 (gift from PharmaEngine Inc.) was loaded into liposomes using the drug trapping agent TEA-SOS as previously described.<sup>22</sup> The CPT-11/HCl was incubated with TEA-SOS-containing liposomes at 60°C (pH 6.0) for 45 minutes and then quenched in ice for 15 minutes. Unencapsulated CPT-11 was removed by Sephadex G75 size-exclusion chromatography, and the nanoliposomal CPT-11 was concentrated on a stirred cell concentrator containing a regenerated cellulose  $10^5$  K nominal molecular weight limit membrane (Amicon, Millipore Corp.) and sterilized by passage through a 0.2- $\mu\text{m}$  polyethersulfone syringe filter. The concentration of CPT-11 was determined by measuring absorbance at 375 nm of a solubilized sample.

### Stereotactic Frame

After general anesthesia was induced, the dogs were mounted in

## Canine model of CED of liposomal CPT-11

an MR imaging-compatible stereotactic primate head frame that was modified by the addition of a bite plate holder. The frame components were constructed of either perspex, aluminum, or brass. A dental impression mold was made for each animal in situ using vinyl-polysiloxane impression material putty (Express STD, 3M ESPE Dental Products), and the dogs' heads were stabilized using the bite plate, ear bars, and foam padding placed ventral to the rami of the mandibles.

### Magnetic Resonance Image Acquisition

With the animals secured in the head frame, transverse T1-weighted images of the dogs' brains were acquired prior to catheter placement. A 1.5-T Signa LX unit (GE Medical Systems) and 5-in circular surface coil were used to obtain baseline spoiled gradient echo images: TR 28 msec, TE 8 msec, flip angle 40°, slice thickness 1 mm, number of excitations 3, matrix 256 × 192, field of view 16 × 16 cm. After catheter placement, spoiled gradient echo imaging scans were taken consecutively throughout the infusion. The number of slices varied depending on the location and extent of infusions (50–70 slices), and the scan time varied from 13 to 15 minutes. Stereotactic coordinates for the target implant sites were determined from MR images. Rostral/caudal coordinates were determined based on linear reference markers (vegetable oil) located within the ear bars. Medial/lateral and dorsal/ventral coordinates were measured directly from MR images using bone landmarks including the external sagittal crest and skull surface, respectively.

### Convection-Enhanced Delivery Procedure

**Cannula Design.** The infusion cannula system (Fig. 1) consisted of 4 components: 1) a 22-gauge fused silica guide cannula molded to a threaded cylindrical plastic pedestal (Plastics One Inc.); 2) a 28-gauge fused silica infusion cannula (Plastics One Inc.); 3) a sterile Teflon loading line (0.02-in inner diameter) containing the liposomes (Upchurch Scientific); and 4) a nonsterile infusion line containing olive oil (Upchurch Scientific). The lengths of the cannulae were determined such that the inner infusion cannula was 2-mm longer than the outer guide cannula, resulting in a step design. Based on the MR imaging coordinates, each guide cannula was mounted onto a stereotactic arm (David Kopf Instruments), attached to the head frame, and manually guided to the targeted region of brain through bur holes made in the skull after sterile surgical exposure of the cannula insertion site. The guide cannulae were secured to the skull using brass screws and ultraviolet curing urethane dimethacrylate gel (Triad Gel, Dentsply International Inc.), and sealed prior to infusions using a solid nylon filament dummy cannula (Plastics One Inc). All guide cannulae were left in place for the duration of the study, allowing for repeated infusions. Following initial infusions, the surgical site was closed routinely over the guide cannulae after replacement of the

dummy stylets. All dogs received intraoperative antibiotic treatment (intravenous cephazolin 22 mg/kg, every 4 hours) and a postoperative 2-week course of oral antibiotics (cephalexin 22 mg/kg, every 12 hours).

**Infusions.** Convection-enhanced delivery infusions were done by previously established techniques.<sup>1</sup> Briefly, the dogs were placed in the MR imaging unit and infusion cannulae were inserted and secured following attachment of drug loading and infusion lines. Infusion pressure was generated by a 1-ml syringe, loaded with oil, mounted on a microinfusion pump (BeeHive, Bioanalytical Systems) located outside of the unit. Infusion rates were started at 0.1  $\mu\text{l}/\text{min}$ , and increased at 10-minute intervals to 0.2, 0.5, 0.8, 1.0, 1.5, 2.0, and 2.5  $\mu\text{l}/\text{min}$ , and then to a maximum of 3.0  $\mu\text{l}/\text{min}$  for ~ 1 hour. A total of 300  $\mu\text{l}$  of infusate was delivered over ~ 2.5 hours.

The initial infusions were at 2 sites, either the corona radiata or the rostral thalamus, with liposomes containing Gd (1.85–3.7 mM) and the chemotherapeutic agent irinotecan (CPT-11) (48.2 mg/ml), or liposomes containing Gd alone. Four weeks after the initial infusion, the Gd-only site was reinfused with liposomes containing both Gd and rhodamine in 3 dogs, and the animals were killed immediately after the second infusion.

### Volume Quantification From MR images

The  $V_d$  within gray and white matter regions was determined using 3D cranial image analysis software (BrainLab). Volumes of infusion, determined from rates and times of infusion, were correlated with MR images at specified time points. Briefly, following definition of a threshold pixel value for liposomal Gd signal, all signal above the threshold value was calculated and a 3D volume of distribution was determined at any given time point.

### Volume Quantification From Fluorescent Images

Immediately after the second infusion, the dogs were killed, and the brains were removed and sectioned along the median plane. Half brains containing the rhodamine/Gd liposome infusion were sectioned transversely into 6-mm slices that were immediately frozen in  $-70^\circ\text{C}$  isopentane and stored at  $-80^\circ\text{C}$ . Brain sections containing rhodamine/Gd liposomes were sequentially sectioned on a cryostat at a thickness of 40  $\mu\text{m}$  and interval of 400  $\mu\text{m}$ . Images of fluorescence distribution from rhodamine-containing liposomes were obtained using a charged-coupled device camera with a fixed aperture and an ultraviolet light source. The volume of fluorescent liposome distribution was calculated using an image analysis system (NIH Image 1.62, National Institutes of Health).

### Neuropathological Examination

The brain halves infused with liposomes containing Gd or Gd and

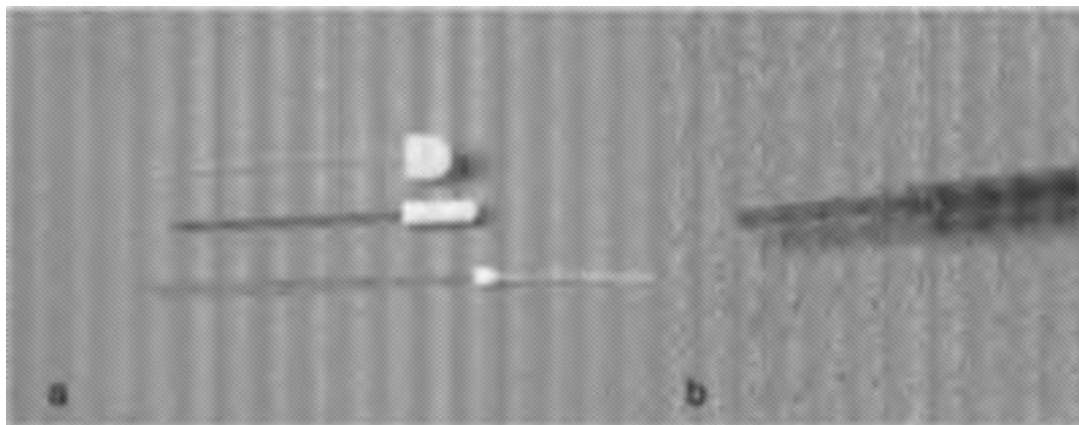


FIG. 1. a: Photograph of the infusion system with 28-gauge fused silica infusion cannula (lower), 22-gauge guide cannula (center), and dummy stylet (upper). b: Photograph showing the insertion of the infusion cannula beyond the tip of the guide cannula. This provides a step configuration resulting in decreased reflux of infusates during delivery.

irinotecan were immersed in 10% buffered formalin for 10 days, sectioned transversely into 3-mm-thick sections, and gross lesions were digitally photographed. Sections were processed for routine paraffin embedding and then 5- $\mu$ m-thick sections were routinely stained with H & E and Luxol fast blue-H & E. Selected 5- $\mu$ m-thick sections were also immunostained using a modified streptavidin-biotin unlabeled immunoperoxidase technique with aminoethylcarbazide as the chromogen essentially as previously described.<sup>9</sup> Antibodies used included a mouse monoclonal to glial fibrillary acidic protein, vimentin, and a standard panel of antibodies for canine cell-specific immunophenotypic markers—including CD3, CD18, CD45, CD79a, CD20, CD31, and factor VIII—with antibody dilutions, pretreatments, and positive controls performed as previously described.<sup>19</sup>

#### *Ancillary Diagnostic Procedures*

Complete blood counts, serum biochemical analyses, and CSF analyses were done in all animals immediately prior to both CED procedures. Blood samples were collected via jugular puncture and CSF was obtained via cerebellomedullary cisternal puncture (with the animals in a state of general anesthesia). The CSF was analyzed for cellular and total protein content within 30 minutes of collection.

## Results

### *Detection of Liposomal Gd After CED*

To assess the feasibility of real-time imaging of liposome distribution during CED in dogs, liposomal Gd was infused into either the corona radiata or the thalamus in 4 dogs. Apparent  $V_a$  values were clearly defined in all animals and were seen to increase consistently with infusion volumes during the infusion period (Fig. 2). Gadolinium-impregnated liposomes were detected in all animals at the first scan time, ~13–15 minutes after the start of the infusions. An unsuccessful infusion was monitored in 1 dog during infusion into the left thalamus. The apparent  $V_a$  was small and reached a maximum value early in the infusion. The contrast material was clearly seen leaking into the subarachnoid space due to inappropriate placement of the infusion cannula too close to the left lateral ventricle (Fig. 3).

### *Distribution of Liposomes After CED Detected on MR Imaging*

Liposomes containing either Gd alone, Gd and rhodamine, or Gd and the chemotherapeutic agent CPT-11 were infused into the corona radiata or thalamus in 4 dogs. Eleven infusions were done using up to 300- $\mu$ l liposomes per infusion. Robust infusions were seen in 10 of 11 cases, and MR imaging volume data points were acquired for 7 corona radiata infusions and 3 thalamic infusions. The  $V_a$  values were calculated and plotted against  $V_i$  values (Fig. 4), and the correlation between  $V_a$  and  $V_i$  was calculated. Linear trend lines revealed a strong correlation between  $V_a$  and  $V_i$  for both corona radiata and thalamic infusions ( $R^2 \geq 0.89$ ). The  $V_a/V_i$  ratio for corona radiata infusions was ~2.8. The  $V_a/V_i$  ratio for thalamic infusions was more variable due to a higher incidence of leakage into ventricular or subarachnoid spaces; this ratio varied from ~1.2 to 3.4.

### *Correlation of Volume of Administration and Distribution*

Three animals received infusions of liposomes containing Gd and rhodamine 3–4 weeks after the initial infusions of liposomes containing Gd alone. No evidence of the previously used contrast agent was present at the time of the

second infusion. Two infusions were directed to the corona radiata and 1 into the thalamus. The animals were killed immediately after the infusion, and the brains were processed for histological detection of the fluorescence generated from the rhodamine-containing liposomes that were coinjected with the liposomes containing Gd.

Fusion images generated from equivalent MR images and fluorescent histological slices demonstrated a close correlation of areas of distribution for both modalities, suggesting that real-time MR imaging gives an accurate measurement of the true tissue distribution of infused liposomes (Fig. 5). Bivariate fit of rhodamine volumes by MR imaging volumes produced an  $R^2$  value of 0.98.

### *Evaluation of Liposomal CED Toxicity*

All dogs that received CED of liposomes containing Gd or rhodamine showed no major evidence of adverse clinical effects over the 3–4 week study period. Mild transient neurological deficits were seen immediately after the infusions that consisted of conscious proprioceptive deficits on the side contralateral to the infusion. These were present only after thalamic infusions. In 1 dog (Dog 3) the corona radiata infusion was associated with an intraparenchymal hemorrhage. Neurological deficits resolved after 7–10 days in all dogs other than Dog 3, in which subtle conscious proprioceptive deficits remained 3 weeks after the infusion.

The results of CSF analysis were unremarkable in all animals both before and 3–4 weeks after the infusions. Normal reference values for cisternal CSF analysis were a total nucleated cell count of  $< 5/\mu$ l, and a total protein content of  $< 25$  mg/dl. Serum biochemical analysis was also unremarkable in all animals both before and after the infusions.

Histologically, minimal changes were present in 3 animals (Dogs 1, 2, and 4) associated with cannula placement and liposomal CPT-11 infusions. A thin track of hemorrhagic necrosis bordered by a mild gemistocytic astrogliosis, a few hemosiderin-containing macrophages, and prominent capillaries were generally present along the line of the indwelling infusion cannulae (Fig. 6). Variable small areas of malacia of up to  $1.5 \times 4$  mm in size were also present at the cannula tip. In Dog 1, which received only Gd-containing liposomes, no morphological lesions were seen in the overlying cortex or in the surrounding white matter that corresponded to the area of infusion as delineated on imaging. In the white matter 1-mm adjacent to the cannula track lesion, there were increased numbers of prominent blood vessels with perivascular cuffs of CD18-positive macrophages, a few CD3-positive lymphocytes, and a very mild peripheral astrogliosis in otherwise morphologically normal white matter. Other than minimal cannulae track lesions, no morphological lesions were associated with infusion areas of Gd/CPT-11 liposomes in either gray or white matter (thalamus/corona radiata). A mild, multifocal angiocentric nonsuppurative encephalitis was present in Dog 4, which was confined to the corona radiata in the region of the infusion (as defined on MR imaging) and was less severe in the overlying cortex. The predominant perivascular cells were CD18-positive macrophages, with some CD20-positive B lymphocytes and occasional 3C6- and CD3-positive T lymphocytes.

In Dog 3, infusion of Gd/CPT-11 into the corona radiata



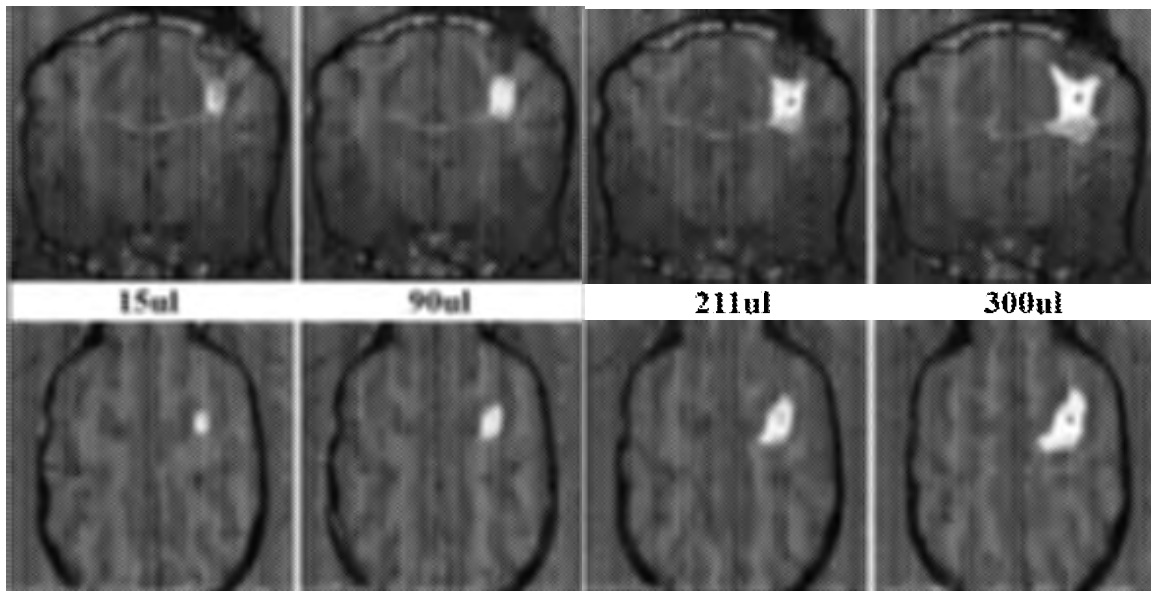


FIG. 2. Dog 4. Selected sequential transverse (*upper*) and dorsal (*lower*) MR images obtained during a corona radiata infusion in which 300  $\mu$ l liposomal Gd was infused over a 2-hour period. The extent and anatomical location of the infusion is clearly demarcated. ul =  $\mu$ l.

was associated with acute hemorrhagic leucoencephalomalacia. This hemorrhagic malacia was restricted to the corona radiata whose outline corresponded closely to the limits of the prior infusion as delineated on MR imaging. The malacic area contained predominantly active phagocytic macrophages, and was bordered by mild reactive astrogliosis, prominent blood vessels, axonal necrosis, demyelination, and peripheral edema. The presence of active erythrophagocytosis without hemosiderosis suggested a recent hemorrhage into the malacic lesion.

### Discussion

Successful systemic delivery of therapeutic agents to abnormal brain tissue is restricted by the blood-brain barrier, resulting in poor penetration of drugs into the target tissue, and limiting adverse effects due to the high drug concentrations necessary to overcome this otherwise protective barrier. Convection-enhanced delivery techniques, developed to overcome this problem, have been shown to be both safe and efficacious in a variety of animal models in which many therapeutic approaches were used.<sup>1-3,10,15,17</sup> In the present study, we have shown that CED can be used to deliver liposomal nanoparticles containing Gd/CPT-11 to clinically significant volumes of both gray and white matter in healthy canine brains with minimal adverse effects, and that delivery can be monitored using real-time MR imaging.

#### *Efficacy of Liposomal CED*

The robust nature of the described technique was reflected in the consistently high, clinically relevant  $V_e$  values seen after the infusions in all animals. Minimal convection of liposomes was seen in only 1 of 11 infusions due to early leakage of infusate into a lateral ventricle.

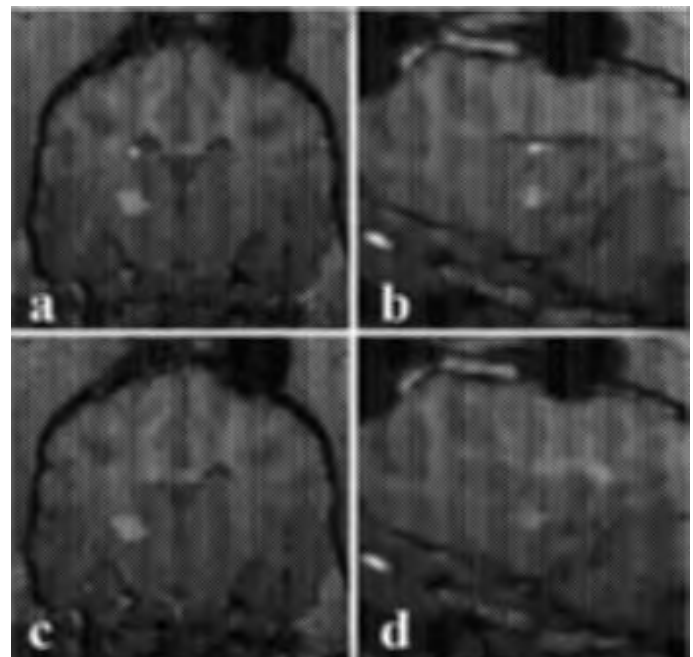


FIG. 3. Dog 4. Real-time MR images demonstrating suboptimal thalamic infusion associated with leakage of infusate into the lateral ventricle. Transverse (a) and sagittal (b) T1-weighted images acquired early in the infusion showing a small  $V_e$  within the target site and the early onset of leakage into the lateral ventricle. The cannula track can be seen dorsal to the infusion. Continued infusion (c and d) results in an increased volume of infusate within the ventricles with no increase in  $V_e$  within the target tissue.



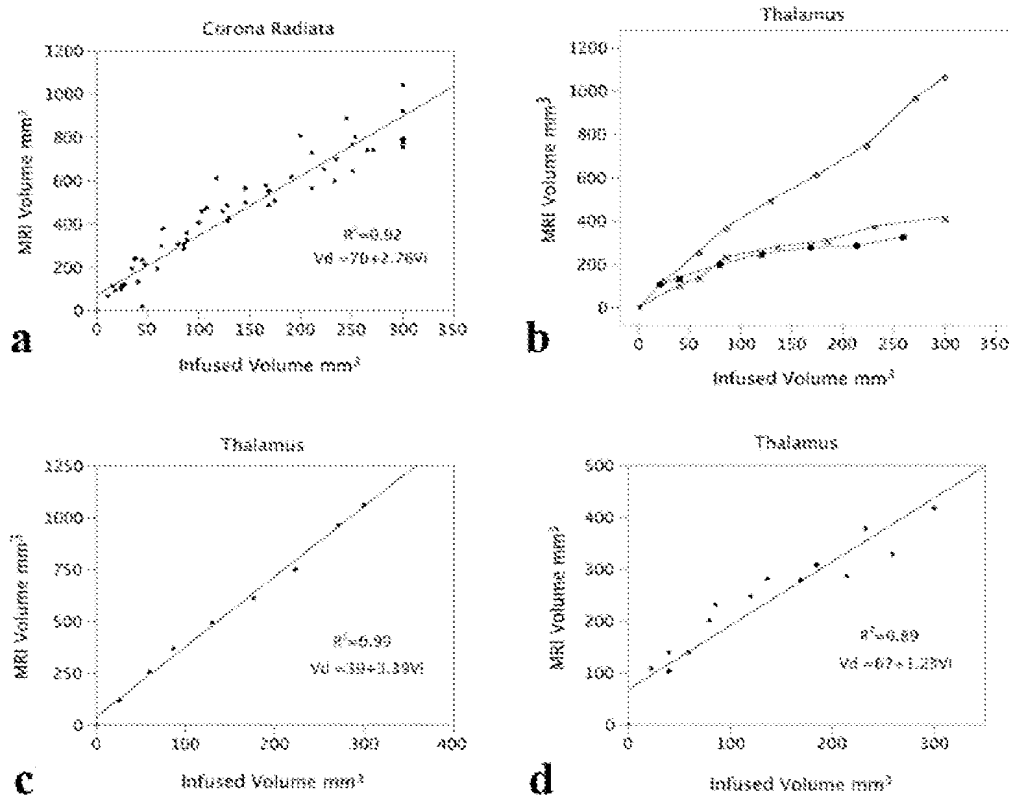


FIG. 4. Graphs of  $V_d/V_i$  data for CED of liposomal Gd/CPT-11 in the corona radiata and thalamus in 4 dogs. The most consistent infusions were seen in the corona radiata (a), where the target sites were farthest from ventricular structures. Infusions into the thalamus (b) were more variable, and demonstrated different target  $V_d/V_i$  ratios depending on the degree of leakage into nontarget tissues (c and d).

The overall  $V_d/V_i$  ratios of liposomes for corona radiata and thalamic infusions were  $\sim 2.8$  and  $1.2\text{--}3.4$ , respectively, and are similar to those found in rats and nonhuman primates using similar techniques.<sup>13,26,27</sup> Ratios of up to 8.7 have been reported for CED of nonliposomal infusates in other studies, probably reflecting the different physicochemical properties of the agents infused compared with the liposomal infusions we used in the present study. Even with the lower  $V_d$  seen in our study, clinically relevant volumes of tissue were infused, and the consistent relationship between  $V_d$  and  $V_i$  over a wide volume range suggests that prospective clinical planning of infusions is possible. Convection-enhanced delivery has been described previously in normal dogs,<sup>6,15</sup> and in an experimental model of brain tumors in dogs.<sup>24</sup> The infusates consisted of either cytosine arabinoside or water soluble iodinated contrast agent infused into the white matter. Using infusion rates of  $3\text{--}7 \mu\text{l}/\text{minute}$  for up to 3 months allowed  $V_d$  values of up to 80% of the ipsilaterally infused hemisphere. Extensive edema was reported after infusion in 1 study,<sup>6</sup> and  $V_d$  values were calculated postmortem. The results of these studies suggest that CED of therapeutic agents, particularly when monitored with in vivo imaging techniques, may be possible for time periods well beyond those investigated in the current study.

The use of the same liposomal carriers for both the therapeutic agent and the surrogate marker has many advantages. As shown in the current study and in others,<sup>13,26,27</sup> the

convective properties of the infusate are related to the liposomal carrier, regardless of its content. Magnetic resonance imaging-determined  $V_d$  values are therefore highly predictive of true tissue distribution, as demonstrated by the colocalization of Gd on MR imaging and rhodamine on histological analysis. Free Gd or other surrogate marker systems may have significantly different convective properties than the therapeutic agent they are being used to track, resulting in inaccurate estimation of tissue distribution. Liposomal delivery of both the therapeutic agent and a surrogate marker offers many other advantages in addition to an accurate assessment of distribution volume, including increased stability of therapeutic agents, decreased clearance, increased therapeutic index, decreased immunogenicity, and the potential for immunotargeting of modified liposomes.<sup>17</sup>

#### Advantages of Real-Time Imaging

Reflux and leakage of infusate are important CED phenomena that have been studied extensively<sup>3,14,20,24</sup> and have been related to several factors including catheter size, catheter design, infusion rate, and catheter placement. The step design catheter<sup>14</sup> used in this study together with the small cannula size and relatively slow infusion rates were probably the major factors contributing to successful infusion. Avoidance of potential low-pressure sinks such as large blood vessels, ventricles, and sulci, or tumor resection cavities is recommended in the placement of catheters for

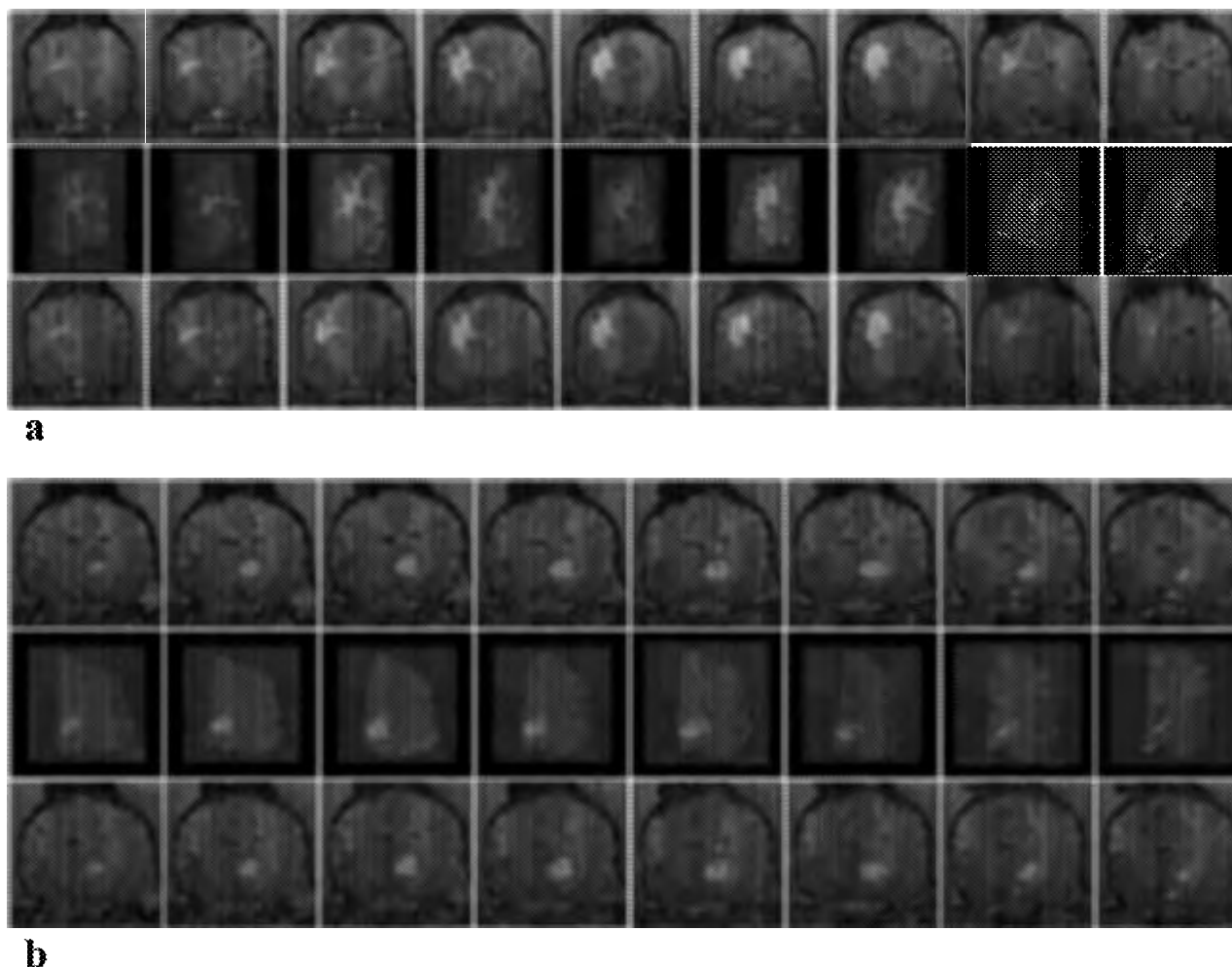


**Fig. 5.** Dog 2 (a) and Dog 3 (b). Colocalization of infusion volumes determined on MR imaging and histological analysis. Dogs infused with liposomes containing both Gd and rhodamine were killed immediately after infusion. Accurate colocalization of MR imaging contrast signal and fluorescent signal in tissue sections demonstrates the accurate measurement of true tissue distribution based on MR imaging.

CED,<sup>29,30,34</sup> and loss of infusate into these structures with subsequent poor delivery to target structures is common following poor placement. All infusions in which suboptimal  $V_e$  values were attained were readily detectable and quantifiable during real-time imaging, and successful infusion was predictable based on the degree and time of onset of leakage into nontargeted tissues. A clear definition of the extent of any clinical therapeutic delivery is essential, not only to provide a realistic framework on which to base assessment of therapeutic efficacy, but also to minimize potential toxicity related to inappropriate continued infusion into normal tissues after leakage or excessive infusion volumes. Ideally, therefore, CED should be managed in real time and based on dynamic imaging of the infusion as it occurs.

Convection-enhanced delivery in abnormal brains, particularly in neoplastic tissue, is likely to present additional barriers to successful delivery as demonstrated by the suboptimal infusions documented in both experimental models<sup>24</sup> and in ongoing clinical trials.<sup>25,29-31,34</sup> Factors including high interstitial tumor pressures, heterogenous distribution of vasculature, peritumoral edema, and heterogeneity of

the tumor tissue itself are likely to play important roles in determining infusion characteristics. Modeling of infusion parameters based on a combination of known tissue characteristics, MR imaging findings, retrospective analysis of infusion data, and real-time infusion data will probably be necessary for optimization of CED as a therapeutic delivery system in this context. Rodent, primate, and mathematical models have major limitations relating to clinical relevance based on factors of scale, and either availability of orthotopic tumor systems or similarity of induced tumors to their human counterparts. Canines are the only species in which primary brain tumors arise spontaneously and with a frequency and histological and molecular profile similar to that found in humans. The establishment of a CED model in canines will provide the unique potential for investigating CED in spontaneous intracranial tumors in a large animal model with more direct relevance to human patients than either rodent or primate models.

*Toxicity Associated With Liposomal Gd/CPT-11*

The adverse effects of infusion of liposomes containing

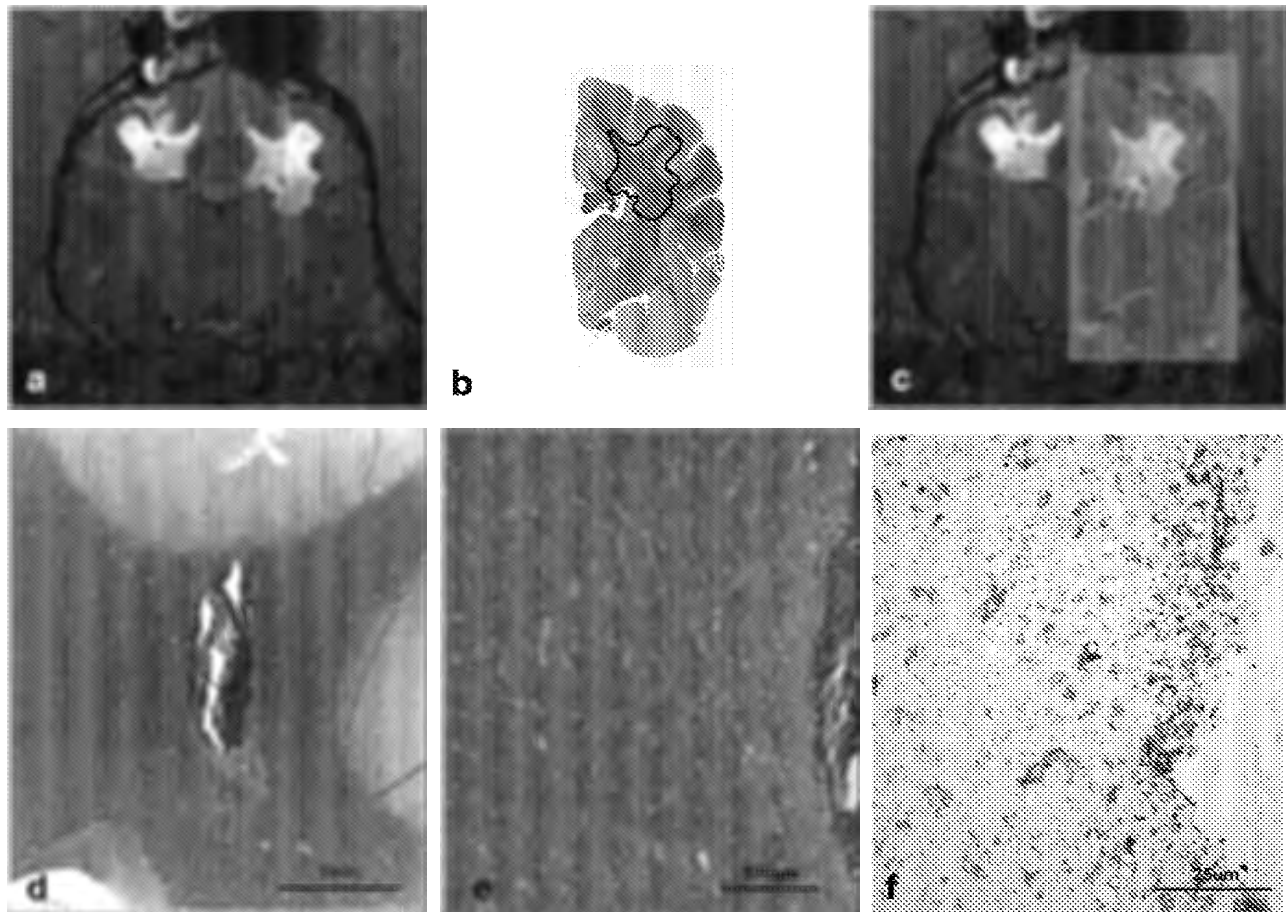


FIG. 6. Dog 1. a: Real-time MR image of bilateral corona radiata infusion. b: H & E- and Luxol fast-blue-stained section through the catheter tip site demonstrating focal malacia. The area of infusion as defined on MR imaging is outlined in black. c: Superimposed MR image and Luxol fast blue and H & E-stained section. d: Photomicrograph demonstrating site of catheter tip with border of normal gray and white matter. e: Photomicrograph showing normal white matter within 200  $\mu\text{m}$  of the edge of the catheter tip. f: Photomicrograph showing the site of catheter tip bordered by a thin rim of CD18-positive macrophages.

Gd and/or CPT-11 were mild in all animals, and the associated neurological deficits were transient over the period studied. These transient deficits may be related to edema secondary to the infusion, or due to the mild perivascular inflammatory response noted in 1 dog. Although T2-weighted images were not routinely acquired in all dogs, increased T2 signal (suggestive of edema) was not present beyond the boundaries of infused Gd liposomes in 2 cases. The cause of the hemorrhage after 1 corona radiata infusion was not determined but was suspected to be related to traumatic injury during cannula placement. No clinically apparent adverse effects were associated with leaving infusion cannulae in situ during the 3–4 week study period, and second infusions were successful in all cases (3/3), suggesting that multiple infusions using indwelling cannulae may be practicable in the clinical setting. Based on both the clinical and histological data in the present study, liposomal Gd and liposomal CPT-11 appear to be associated with minimal adverse effects over a 1-month time period when administered via CED. Limited toxicity was probably related both to the liposomal encapsulation of the Gd and the chemotherapeutic agent, and the ability to accurately define

appropriately targeted delivery based on real-time imaging. The safety of liposomal Gd has been documented previously in both rodents and primates,<sup>13,26,27</sup> however the use of Gd as a surrogate marker for CED in humans is still a major concern. The clinical and histological data in the dogs in the present study further support the development and use of Gd, at least as a liposomal formulation. No data are available relating to therapeutic efficacy and adverse effects of intraparenchymal liposomal CPT-11 in species other than rodents.<sup>22</sup> Minimal toxicity documented in dogs suggests that liposomal CPT-11 is likely to be well tolerated in human patients, and supports further assessment in spontaneous canine tumors as a more realistic translational model.

### Conclusions

Convection-enhanced delivery has not yet become a standard treatment for human diseases, and optimization will probably require more potent therapeutic agents and a strategy for image guidance. The pronounced efficacy of CED of liposomal camptothecin analogs in rodent brain

tumor models suggests that this therapeutic approach may be effective in human patients with gliomas. However, translation from small rodent experimental xenograft models to spontaneous human tumors must address the problems associated with the scale of delivery, chemotherapeutic efficacy, and the potential for local and systemic toxicity. The consistent delivery and minimal adverse effects demonstrated in the present study suggests that intratumoral CED of liposomal Gd and CPT-11 monitored with real-time MR imaging is justified in canine therapeutic trials of spontaneously occurring gliomas. Such trials may provide a valuable model for future characterization and optimization of CED parameters and therapeutic strategies that will be applicable to both canine and human patients.

**Acknowledgment**

We are grateful to John Doval for assistance with the figures.

**References**

1. Bankiewicz KS, Eberling JL, Kohutnicka M, Jagust W, Pivrotto P, Bringas J, et al: Convection-enhanced delivery of AAV vector in parkinsonian monkeys; in vivo detection of gene expression and restoration of dopaminergic function using pro-drug approach. *Exp Neurol* **164**:2–14, 2000
2. Bobo RH, Laske DW, Akbasak A, Morrison PF, Dedrick RL, Oldfield EH: Convection-enhanced delivery of macromolecules in the brain. *Proc Natl Acad Sci U S A* **91**:2076–2080, 1994
3. Chen MY, Lonser RR, Morrison PF, Governale LS, Oldfield EH: Variables affecting convection-enhanced delivery to the striatum: a systematic examination of rate of infusion, cannula size, infusate concentration, and tissue-cannula sealing time. *J Neurosurg* **90**: 315–320, 1999
4. Dickinson PJ, Roberts BN, Higgins RJ, Leutenegger CM, Bollen AW, Kass PH, et al: Expression of receptor tyrosine kinases VEGFR-1 (FLT-1), VEGFR-2 (KDR), EGFR-1, PDGFR $\alpha$  and c-Met in canine primary brain tumors. *Vet Comp Oncol* **4**:132–140, 2006
5. Foster ES, Carrillo JM, Painak AK: Clinical signs of tumors affecting the rostral cerebrum in 43 dogs. *J Vet Intern Med* **2**:71–74, 1988
6. Groothuis DR, Benalcazar H, Allen CV, Wise RM, Dills C, Dobrescu C, et al: Comparison of cytosine arabinoside delivery to rat brain by intravenous, intrathecal, intraventricular and intraparenchymal routes of administration. *Brain Res* **856**:281–290, 2000
7. Harrington KJ: Liposomal cancer chemotherapy: current clinical applications and future prospects. *Expert Opin Investig Drugs* **10**:1045–1061, 2001
8. Heidner GL, Kornegay JN, Page RL, Dodge RK, Thrall DE: Analysis of survival in a retrospective study of 86 dogs with brain tumors. *J Vet Intern Med* **5**:219–226, 1991
9. Higgins RJ, LeCouteur RA, Vernau KM, Sturges BK, Obradovich JE, Bollen AW: Granular cell tumor of the canine central nervous system: two cases. *Vet Pathol* **38**:620–627, 2001
10. Kawakami K, Kawakami M, Kioi M, Husain SR, Puri RK: Distribution kinetics of targeted cytotoxin in glioma by bolus or convection-enhanced delivery in a murine model. *J Neurosurg* **101**: 1004–1011, 2004
11. Koestner A, Bilzer T, Fatzner R, Schulman FY, Summers BA, Van Winkle TJ: *Histological Classification of Tumors of the Nervous System of Domestic Animals*, ed 2. Washington, DC: The Armed Forces Institute of Pathology, 1999, Vol 5
12. Kraft SL, Gavin PR, DeHaan C, Moore M, Wendling LR, Leathers CW: Retrospective review of 50 canine intracranial tumors

- evaluated by magnetic resonance imaging. *J Vet Intern Med* **11**: 218–225, 1997
13. Krauze MT, McKnight TR, Yamashita Y, Bringas J, Noble CO, Saito R, et al: Real-time visualization and characterization of liposomal delivery into the monkey brain by magnetic resonance imaging. *Brain Res Brain Res Protoc* **16**:20–26, 2005
14. Krauze MT, Saito R, Noble C, Tamas M, Bringas J, Park JW, et al: Reflux-free cannula for convection-enhanced high-speed delivery of therapeutic agents. *J Neurosurg* **103**:923–929, 2005
15. Levy RM, Major E, Ali MJ, Cohen B, Groothuis D: Convection-enhanced intraparenchymal delivery (CEID) of cytosine arabinoside (AraC) for the treatment of HIV-related progressive multifocal leukoencephalopathy (PML). *J Neurovirol* **7**:382–385, 2001
16. Lipsitz D, Higgins RJ, Kortz GD, Dickinson PJ, Bollen AW, LeCouteur RA: Glioblastoma multiforme: clinical findings, magnetic resonance imaging and pathology in 5 dogs. *Vet Pathol* **40**: 659–669, 2003
17. Marnot C, Nguyen JB, Pourdehnad M, Hadaczek P, Saito R, Bringas JR, et al: Extensive distribution of liposomes in rodent brains and brain tumors following convection-enhanced delivery. *J Neurooncol* **68**:1–9, 2004
18. Moog R, Burger AM, Brandl M, Schuler J, Schubert R, Unger C, et al: Change in pharmacokinetic and pharmacodynamic behavior of gemcitabine in human tumor xenografts upon entrapment in vesicular phospholipid gels. *Cancer Chemother Pharmacol* **49**: 356–366, 2002
19. Moore PF, Affolter VK, Olivry T, Schrenzel MD: The use of immunological reagents in defining the pathogenesis of canine skin disease involving the proliferation of leucocytes, in Kwochka KW, Willemsen T, von Tscharner C (eds): *Advances in Veterinary Dermatology*. Oxford, UK: Butterworth Heinemann, 1998, Vol 3, pp 77–94
20. Morrison PF, Chen MY, Chadwick RS, Lonser RR, Oldfield EH: Focal delivery during direct infusion to brain: role of flow rate, catheter diameter, and tissue mechanics. *Am J Physiol* **277**: R1218–R1229, 1999
21. Nguyen TT, Pannu YS, Sung C, Dedrick RL, Walbridge S, Brechbiel MW, et al: Convective distribution of macromolecules in the primate brain demonstrated using computerized tomography and magnetic resonance imaging. *J Neurosurg* **98**:584–590, 2003
22. Noble CO, Krauze MT, Drummond DC, Yamashita Y, Saito R, Berger MS, et al: Novel nanoliposomal CPT-11 infused by convection-enhanced delivery in intracranial tumors: pharmacology and efficacy. *Cancer Res* **66**:2801–2806, 2006
23. Priester WA, Mantel N: Occurrence of tumors in domestic animals. Data from 12 United States and Canadian colleges of veterinary medicine. *J Natl Cancer Inst* **47**:1333–1344, 1971
24. Raghavan R, Brady ML, Rodríguez-Ponce MI, Hartlep A, Pedain C, Sampson JH: Convection-enhanced delivery of therapeutics for brain disease, and its optimization. *Neurosurg Focus* **20**(3): E12, 2006
25. Ren H, Bouliskas T, Lundstrom K, Soling A, Warnke PC, Rainov NG: Immunogene therapy of recurrent glioblastoma multiforme with a liposomally encapsulated replication-incompetent Semliki forest virus vector carrying the human interleukin-12 gene—a phase I/II clinical protocol. *J Neurooncol* **64**:147–154, 2003
26. Saito R, Bringas JR, McKnight TR, Wendland MF, Marnot C, Drummond DC, et al: Distribution of liposomes into brain and rat brain tumor models by convection-enhanced delivery monitored with magnetic resonance imaging. *Cancer Res* **64**:2572–2579, 2004
27. Saito R, Krauze MT, Bringas JR, Noble C, McKnight TR, Jackson P, et al: Gadolinium-loaded liposomes allow for real-time magnetic resonance imaging of convection-enhanced delivery in the primate brain. *Exp Neurol* **196**:381–389, 2005
28. Saito R, Krauze MT, Noble CO, Drummond DC, Kirpotin DB, Berger MS, et al: Convection-enhanced delivery of Ls-TPT enables an effective, continuous, low-dose chemotherapy against

- malignant glioma xenograft model. *Neuro-oncol* **8**:205–214, 2006
29. Sampson JH, Brady ML, Petry NA, Croteau D, Friedman AH, Friedman HS, et al: Intracerebral infusate distribution by convection-enhanced delivery in humans with malignant gliomas: descriptive effects of target anatomy and catheter positioning. *Neurosurgery* **60** (2 Suppl):ONS89–ONS99, 2007
  30. Sampson JH, Raghavan R, Provenzale JM, Croteau D, Reardon DA, Coleman RE, et al: Induction of hyperintense signal on T2-weighted MR images correlates with infusion distribution from intracerebral convection-enhanced delivery of a tumor-targeted cytotoxin. *AJR Am J Roentgenol* **188**:703–709, 2007
  31. Slevin JT, Gash DM, Smith CD, Gerhardt GA, Kryscio R, Chebrolu H, et al: Unilateral intraputaminar glial cell line-derived neurotrophic factor in patients with Parkinson disease: response to 1 year each of treatment and withdrawal. *Neurosurg Focus* **20**(5):E1, 2006
  32. Stoica G, Kim HT, Hall DG, Coates JR: Morphology, immunohistochemistry, and genetic alterations in dog astrocytomas. *Vet Pathol* **41**:10–19, 2004
  33. Summers BA, Cummings JF, de Lahunta A (eds): Tumors of the central nervous system, in *Veterinary Neuropathology*. St Louis: Mosby, 1995, pp 351–401
  34. Vandergrift WA, Patel SJ, Nicholas JS, Varma AK: Convection-enhanced delivery of immunotoxins and radioisotopes for treatment of malignant gliomas. *Neurosurg Focus* **20**(4):E13, 2006
  35. Voges J, Reszka R, Gossmann A, Dittmar C, Richter R, Garlip G, et al: Imaging-guided convection-enhanced delivery and gene therapy of glioblastoma. *Ann Neurol* **54**:479–487, 2003

---

Manuscript submitted January 11, 2007.

Accepted August 16, 2007.

This work was supported by the Paul C. and Borghild T. Petersen Foundation; the Center for Companion Animal Health, University of California, Davis; and the Brain Tumor SPOR Award (NCI).

Address correspondence to: Peter J. Dickinson, B.V.Sc., Ph.D., Department of Surgical and Radiological Sciences, Tupper Hall, School of Veterinary Medicine, University of California, Davis, California 95616. email: pjddickinson@ucdavis.edu.

# Canine spontaneous glioma: A translational model system for convection-enhanced delivery

Peter J. Dickinson, Richard A. LeCouteur, Robert J. Higgins, John R. Bringas, Richard F. Larson, Yoji Yamashita, Michal T. Krauze, John Forsayeth, Charles O. Noble, Daryl C. Drummond, Dmitri B. Kirpotin, John W. Park, Mitchel S. Berger, and Krystof S. Bankiewicz

*Departments of Surgical and Radiological Sciences (P.J.D., R.A.L., R.F.L.), Pathology, Microbiology, and Immunology (R.J.H.), School of Veterinary Medicine, University of California–Davis, Davis, California; Department of Neurosurgery, Brain Tumor Research Center (J.R.B., Y.Y., M.T.K., J.F., M.S.B., K.S.B.) and Division of Hematology-Oncology (C.O.N., J.W.P.), University of California–San Francisco, San Francisco, California; Merrimack Pharmaceuticals, Cambridge, Massachusetts (C.O.N., D.C.D., D.B.K.)*

Canine spontaneous intracranial tumors bear striking similarities to their human tumor counterparts and have the potential to provide a large animal model system for more realistic validation of novel therapies typically developed in small rodent models. We used spontaneously occurring canine gliomas to investigate the use of convection-enhanced delivery (CED) of liposomal nanoparticles, containing topoisomerase inhibitor CPT-11. To facilitate visualization of intratumoral infusions by real-time magnetic resonance imaging (MRI), we included identically formulated liposomes loaded with Gadoteridol. Real-time MRI defined distribution of infusate within both tumor and normal brain tissues. The most important limiting factor for volume of distribution within tumor tissue was the leakage of infusate into ventricular or subarachnoid spaces. Decreased tumor volume, tumor necrosis, and modulation of tumor phenotype correlated with volume of distribution of infusate (Vd), infusion location, and leakage as determined by real-time MRI and histopathology. This study demonstrates the potential for canine spontaneous gliomas as a model system for the validation and development of novel therapeutic strategies for human brain tumors. Data obtained from infusions monitored in real time in a large, spontaneous

tumor may provide information, allowing more accurate prediction and optimization of infusion parameters. Variability in Vd between tumors strongly suggests that real-time imaging should be an essential component of CED therapeutic trials to allow minimization of inappropriate infusions and accurate assessment of clinical outcomes.

**Keywords:** brain tumors, canine, CPT-11, convection-enhanced delivery, magnetic resonance imaging.

The long-term prognosis for patients with malignant gliomas after conventional therapy is poor, and has remained relatively static over the last 30 years. Many novel strategies have been developed for the treatment of malignant gliomas; however, few have progressed beyond early-phase clinical trials. One of the major reasons for the failure to reproduce the dramatic results seen in preclinical therapeutic development is the large “translational distance” between spontaneous, large invasive tumors in people, and the classical immunologically compromised, small, clonal, rodent xenograft tumor model systems typically used in preclinical development and testing. Recent development of transgenic models of glioma promise to provide a more realistic testing ground, at least at the molecular level,<sup>1</sup> and some characterized orthotopic rodent models have been shown to mimic clinical reality relating to therapeutic issues such as 1p19q status and the use of surgery and chemotherapy combinations.<sup>2</sup> However, the significant limitations of rodent models, particularly

Received October 28, 2009; accepted March 15, 2010.

**Corresponding Author:** Peter J. Dickinson, PhD, BVSc, Department of Surgical and Radiological of Sciences, UC Davis School of Veterinary, One Shields Avenue, 2112 Tupper Hall, Davis, CA 95616-8745 (pjdickinson@ucdavis.edu).



relating to the mechanistics of delivery and tumor heterogeneity, remain.

Naturally occurring cancers in pet dogs, including tumors of the nervous system, are as diverse as the cancers seen in humans and have many similarities to their human tumor counterparts.<sup>3,4</sup> Specific cancers are often overrepresented in certain breeds, within which exists a limited degree of genetic variation. This homogeneity provides an ideal background for the identification of underlying genetic abnormalities. A number of factors make canine cancers attractive from a drug development vantage. These include the relatively rapid cancer progression rates relative to humans, and the opportunity to treat over long periods of time (relative to rodent models), in “large” spontaneous tumors that exhibit both heterogeneity and genomic instability. All these factors together may provide a rapid and more realistic approach to preclinical therapeutic assessment of novel strategies developed and proven in rodent model systems.<sup>5,6</sup>

The incidence of primary brain and central nervous system (CNS) tumors in humans is approximately 6–12 of 100 000 person-years,<sup>7,8</sup> with a necropsy frequency of brain tumors of approximately 2%.<sup>9</sup> Although the true incidence of canine gliomas is unknown, the frequency of brain tumors in dogs, based on necropsy data, is similar to humans (ie, approximately 3%), with primary intracranial tumors accounting for approximately 2%.<sup>10</sup> The prevalence of nervous system tumors in the general population of pet dogs is also similar and has been estimated at 14.5 of 100 000 animal-years.<sup>11,12</sup> In addition to the similar frequency of occurrence, a parallel spectrum of canine tumor types arise that bear striking similarities to their human tumor counterparts in terms of histopathology<sup>4,13–18</sup> and neuroimaging.<sup>16,18–22</sup> Molecular and cytogenetic characterization of canine primary brain tumors, though preliminary, is advancing rapidly since the publication of the canine genome. Many similarities to human tumors have already been described, relating to chromosomal instability, expression profiles, the presence of stem-like tumor cells, expression of growth factors and their receptors such as EGF, PDGF, VEGF, as well as other markers frequently described in human tumors such as IL-13R $\alpha$ 2, IGFBP2, and telomerase activity.<sup>17,22–31</sup> Limited data are available relating to the efficacy of standard therapeutic modalities in canine gliomas, and it is likely that some significant differences will be present between human and canine gliomas, as has already been described for meningiomas.<sup>30,32</sup> However, as the number of molecular similarities are further defined, spontaneous canine tumors, with their relatively large size and heterogeneous nature, are becoming attractive for translational investigation of both targeted and nontargeted novel therapies in a tumor environment more representative of the human clinical situation.

Convection-enhanced delivery (CED) of therapeutic agents into brain is a promising treatment strategy, allowing direct infusion of high concentrations of therapeutic drugs, while essentially eliminating systemic toxicity.<sup>33</sup>

However, our current inability to accurately define the extent and location of infusions in real-time considerably limits the therapeutic efficacy at the individual level, and reduces our ability to objectively assess the outcome in clinical trials. CPT-11 (Irinotecan) is a water-soluble derivative of the potent alkaloid anticancer agent camptothecin and acts as a specific inhibitor of topoisomerase I.<sup>34</sup> It has been shown to be one of the most active agents against a variety of CNS xenograft tumors when delivered systemically.<sup>35</sup> On the basis of this experimental data, CPT-11 has progressed into clinical trials for a variety of primary brain tumors either alone or in combination therapies.<sup>36</sup> Because prognosis for canine intra-axial gliomas is generally poor with conventional therapy, we surmised that these tumors might provide a valuable translational model system to investigate the value of real-time MRI during intratumoral CED of novel therapeutic agents in a realistic large animal model system. We show here that CED of liposomal nanoparticles containing the topoisomerase I inhibitor CPT-11 and the surrogate marker Gadoteridol into spontaneously occurring, nonresected gliomas is feasible and potentially efficacious. Moreover, efficacy defined by decreased tumor volume and modulation of tumor phenotype correlated with volume of distribution of infusate (Vd), cannula location, and leakage of infusate as revealed by real-time magnetic resonance imaging (MRI). These data suggest that real-time imaging should be an essential component of CED therapeutic trials and that intratumoral CED may offer additional therapeutic options for nonresectable tumors. Further study of CED in canine spontaneous gliomas correlating infusion characteristics with real-time imaging and histopathology is likely to provide valuable data for the optimization of CED, as well as preliminary assessment of the efficacy and safety of novel therapeutic drugs.

## Materials and Methods

### Clinical Patients

Dogs receiving CED of liposomal CPT-11 were patients at the Veterinary Medical Teaching Hospital (VMTH), School of Veterinary Medicine, University of California, Davis. The clinical trial was reviewed and approved by the Institutional Animal Care and Use Committee (IACUC) at the University of California, Davis, and by the VMTH clinical trials review board. All dogs had spontaneous intra-axial gliomas confirmed histopathologically by stereotactic CT-guided biopsy. Dogs were considered suitable candidates for treatment if they had minimal neurological deficits at the time of presentation and tumors were located rostral-tentorially, involving either the cerebrum or thalamus. Complete blood counts, serum biochemical analyses, and cerebrospinal fluid (CSF) analyses were acquired from all animals immediately prior to the CED procedures, and at scheduled follow-up MRI after infusions. Blood samples were collected via jugular puncture and CSF was taken via cerebellomedullary cisternal puncture (under general anesthesia). CSF was analyzed for cellular

and total protein content within 30 minutes of collection. Animals were monitored throughout the clinical trial period by serial neurological examination and serial MRI.

#### Liposome Preparation

Separate liposomes were prepared for detection by MRI and for delivery of CPT-11. Gadoteridol (Gd) was obtained commercially as 0.5 M 10-(2-hydroxy-propyl)-1,4,7,10-tetraazacyclododecane-1,4,7-triacetic acid (Prohance; Bracco Diagnostics, Princeton, New Jersey). Liposome-encapsulated gadolinium (GDL) was prepared as described previously.<sup>37,38</sup> Briefly, the lipids were hydrated in Prohance followed by extrusion 5 times through a 0.2- $\mu$ m polycarbonate membrane then 8 times through a 0.1- $\mu$ m polycarbonate membrane. Unencapsulated gadoteridol was removed by purification on a Sephadex G-75 size-exclusion column eluted with HEPES-buffered saline (pH 7.25). The resulting GDL had a diameter ranging from 93.6 to 108 nm as determined by quasi-elastic light scattering (N4Plus particle size analyzer, Beckman Coulter, Fullerton, Louisiana) and was sterilized by passage through a 0.2- $\mu$ m polyethersulphone (PES) syringe filter. CPT-11 (gift from PharmaEngine, Inc., Taipei, Taiwan) was loaded into liposomes composed of 1,2-distearoyl-*sn*-glycero-3-phosphocholine, cholesterol, and 1,2-distearoyl-*sn*-glycero-3-phosphoethanolamine-*N*-[methoxy(polyethylene glycol)-2000] (PEG-DSPE) at the molar ratio of 3:2:0.015 with the drug-trapping agent triethylammonium sucrose octasulphate (TEA-SOS), as described previously.<sup>39</sup> CPT-11 HCl was incubated with TEA-SOS containing liposomes at 60°C (pH 6.0) for 45 minutes followed by quenching on ice for 15 minutes. Unencapsulated CPT-11 was removed by Sephadex G75 size-exclusion chromatography, and the liposomal CPT-11 was concentrated on a stirred cell concentrator containing a regenerated cellulose  $1 \times 10^5$  NMWL membrane (Amicon, Millipore Corp., Billerica, Massachusetts) and sterilized by passage through a 0.2- $\mu$ m PES syringe filter. The CPT-11 concentration was determined by measuring the absorbance at 375 nm of a solubilized sample. The final formulation contained nanoliposomal CPT-11 with the potency equivalent to 45 mg/mL CPT-11 HCl and nanoliposomal Gadoteridol with the potency equivalent to 2.0 mM Gadoteridol.

#### MRI Acquisition

Transverse T1- and T2-weighted images of the dogs' brains were acquired with animals secured in a stereotactic head frame. A 1.5T Signa LX scanner (GE Medical Systems, Waukesha, Wisconsin) and 5" circular surface coil were used to obtain baseline spoiled gradient echo (SPGR) images: repetition time (TR) = 28 ms, echo time (TE) = 8 ms, flip angle = 40°, slice thickness = 1 mm, number of excitations (NEX) = 3, matrix = 256  $\times$  192, field of view (FOV) = 16  $\times$  16 cm. SPGR scans were taken consecutively throughout the infusion.

T2-weighted images were acquired prior to and following infusions: TR = 2500 ms, TE = 110 ms, echo train length = 29, slice thickness = 2 mm, NEX = 4, matrix 256  $\times$  224, FOV = 16  $\times$  16 cm. The number of slices varied depending on the location and extent of the infusions (50–70 slices), and scan time varied from 13 to 15 minutes. Stereotactic coordinates for the target implant sites were determined from MR images. Rostral/caudal coordinates were determined based on linear (vegetable oil) reference markers located within the ear bars. Medial/lateral and dorsal/ventral coordinates were measured directly from bone landmarks on MR images that included the external sagittal crest and skull surface.

#### Stereotactic Frame/CED Infusion

Anesthetized dogs were placed in an MRI compatible stereotactic primate head frame that was modified by the addition of a bite plate holder. Components of the frame were constructed of either Plexiglass, aluminum, or brass. A dental impression mold was made for each animal in situ with vinyl polysiloxane impression material putty, (Express<sup>TM</sup> STD, 3 M ESPE Dental Products, St Paul, Minnesota) and the dogs' heads were stabilized with the bite plate and ear bars (Fig. 1).

The infusion cannula system consisted of four components (Fig. 1): (i) a 12-mm diameter (27 hole) or 8-mm diameter (6 hole) cylindrical plastic guide pedestal (Plastics One, Inc., Roanoke, Virginia), (ii) a fused silica infusion cannula consisting of a 22-gauge outer cannula with a 28-gauge inner cannula that was 2 mm longer than the outer guide cannula resulting in a stepped design, (iii) a sterile teflon loading line (0.508 mm inner diameter) containing the liposomes (Upchurch Scientific, Oak Harbor, Washington), and (iv) a nonsterile infusion line containing olive oil (Upchurch Scientific). On the basis of MRI coordinates, each guide pedestal was mounted onto a stereotactic arm (David Kopf Instruments, Tujunga, California) attached to the head frame, and manually guided to the targeted region of brain through burr holes made in the skull after sterile surgical exposure of the pedestal insertion site. The guide pedestals were secured to the skull with brass screws and ultraviolet curing urethane dimethacrylate gel (Triad Gel<sup>®</sup>, Dentsply International Inc., York, Pennsylvania). All guide pedestals were left in place for the duration of the treatment, thereby permitting repeated infusions. After infusions, the surgical site was closed over the guide pedestals that were sealed with plastic screw caps. All dogs received intraoperative antibiotics (Cephazolin 22 mg/kg, IV, q 4 hours) and a postoperative 2 week course of oral antibiotics (Cephalexin 22 mg/kg, PO, q 12 hours).

CED infusions were done by previously established techniques.<sup>40,41</sup> Briefly, dogs were placed in the MRI scanner; then infusion cannulae were inserted and secured after attachment of drug loading and infusion lines. Infusion pressure was generated by a 1-ml syringe loaded with oil and mounted on a microinfusion pump



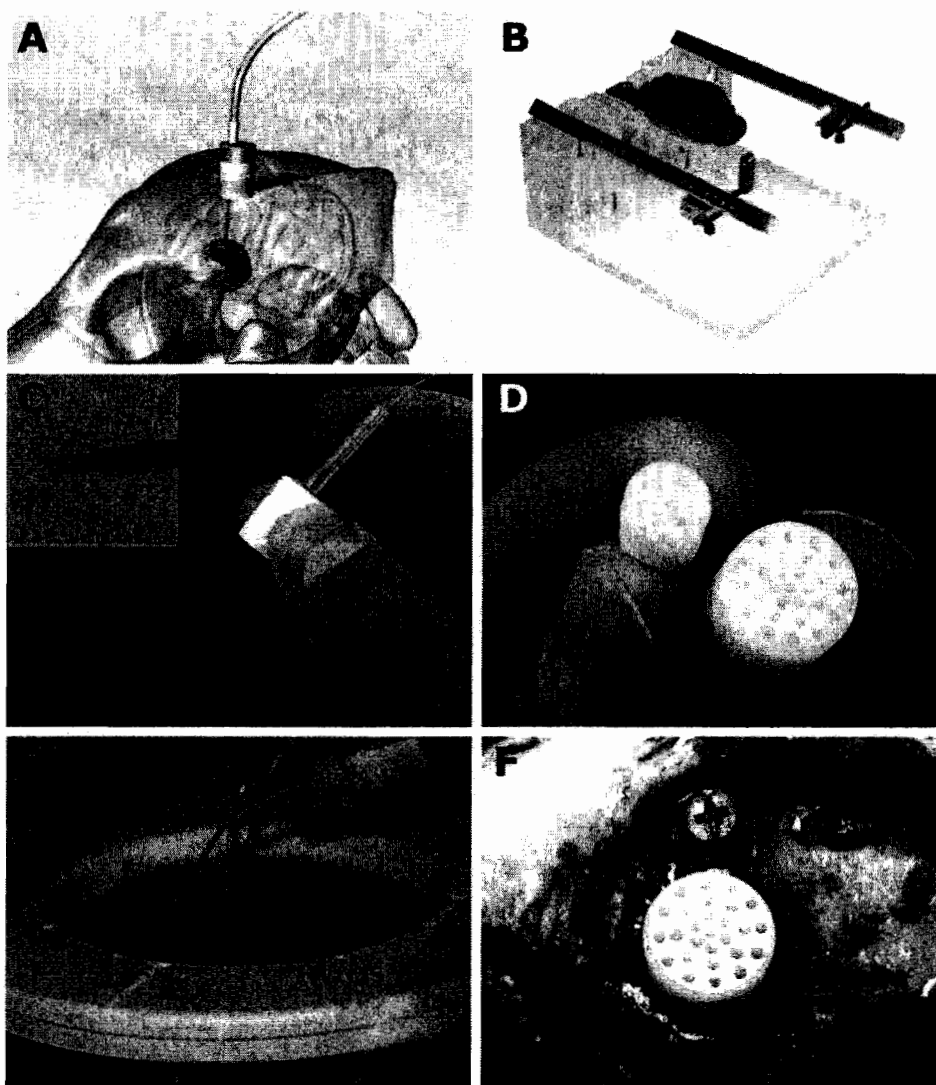


Fig. 1. Convection-enhanced delivery equipment used in the canine model system. (A) Schematic representation of indwelling guide pedestal system. (B) MRI compatible head frame utilizing ear bars and a dental bite plate. (C) Fused silica infusion cannulae with a reflux resistant step design are directed into the tumor site through the stereotactically placed guide pedestals. (D) Guide pedestals contain multiple ports to allow modification of targeting coordinates within the tumor. (E) Simultaneous infusion of liposomal infusate through 3 infusion cannulae. (F) Guide pedestals are secured *in situ* using rapid curing urethane dimethacrylate.

(BeeHive™, Bioanalytical Systems, West Lafayette, Indiana) located outside of the scanner. Infusion rates were started at 0.1  $\mu\text{L}/\text{min}$ , and increased at 10-minute intervals to 0.2, 0.5, 0.8, 1.0, 1.5, 2.0, 2.5  $\mu\text{L}/\text{min}$  and then to a maximum of 5.0  $\mu\text{L}/\text{min}$ . Up to 4 individual infusion cannulae were used for each CED infusion procedure depending on the size of the tumor and placement of guide pedestals. Infusion procedures were repeated based on evidence of increasing tumor volume (or poor infusions with subsequent poor response) determined by serial MRI at 6–8-week intervals.

#### Volume Quantification

The volume of the tumors and infusate distribution ( $V_d$ ) within tumor regions was determined using 3D image analysis software (OsiriX v.3.1, OsiriX Imaging

Software, Osirix Foundation, Geneva, Switzerland). Briefly, tumor volumes were defined from T2-weighted MRI, and infusate distribution was defined based on T1-weighted SPGR images. Regions of interest (ROIs) were defined manually for individual contiguous MR image slices and volumes calculated with ROI volume software.

#### Neuropathological Examination

After euthanasia, brains were immersed in 10% buffered formalin for 7 days, sectioned transversely into 3-mm thick sections, and gross lesions were digitally photographed. Selected tissues were processed for routine paraffin embedding and then 5- $\mu\text{m}$  thick sections were routinely stained with hematoxylin and eosin (HE) and Luxol-fast blue–HE (LFB–HE). Selected sections were also

immunostained by a modified streptavidin–biotin unlabeled immunoperoxidase technique with amino-ethyl-carbazide as the chromogen, essentially as described previously.<sup>42</sup> The polyclonal or monoclonal mouse antibodies used included a standard panel for canine cell-specific immunophenotypic markers, including CD3, CD18, CD45, CD 79a, as well as for CD20, CD31, Factor VIII RA, GFAP, caspase 3, triple neurofilament protein, synaptophysin, and Neu-N with antibody dilutions, pretreatments, and positive controls, as described previously.<sup>42</sup> The tumor proliferative index (in %) was calculated from MIB-1 immunoreactivity. All canine gliomas from both the initial CT-guided biopsy and at necropsy were histologically classified and graded according to the criteria established for the human WHO 2007 classification of tumors of the CNS.<sup>43</sup>

## Results

Nine dogs with intra-axial gliomas (1 grade II astrocytoma, 3 anaplastic astrocytomas, 2 oligodendrogliomas, 3 anaplastic oligodendrogliomas) were infused with liposomal CPT-11/Gadoteridol. Signalment and infusion summaries are presented in Table 1. Total infusion times ranged from 135 to 290 minutes. The maximum total infusion volume (administered between 3 catheters) during a single procedure was 2.125 mL.

### Tumor Volume/Infusion Volumes

One to four infusion cannulae per dog were used to infuse the tumors (Fig. 1), and direct infusion into non-resected tumors was achieved in all cases. All infusions were monitored approximately every 15 minutes by MRI. The infusions lasted from 1 to 4 hours, and the total volume of infusate varied from less than 50  $\mu$ L to approximately 2 mL. Tumor volumes were considered to be well defined on T2-weighted MR images in 7 of 8 dogs. Dog 3 had extensive T2-signal changes after treatment, which made assessment of tumor volumes unreliable, and this animal was excluded from volume

and distribution analysis. The distribution of tumor determined by MRI correlated well with histopathological tissue sections at necropsy in all dogs except Dog 3.

The range of maximal tumor volumes for the dogs was 1.29–7.13 cm<sup>3</sup> (mean 4.0 cm<sup>3</sup>, median 3.6 cm<sup>3</sup>, SD 2.3 cm<sup>3</sup>). Infusate distribution volumes (Vd) and percentage coverage of tumor volumes were calculated for a total of 27 infusion procedures. Vd varied considerably both between infusion procedures and between individual catheters within a procedure. The range of total percentage coverage for individual procedures was 0.02–90% (mean 38%, median 28%, SD 23%).

The clinical effect of the infusions in tumors responsive to CPT-11 chemotherapy assessed by repeat MRI and histopathology was subjectively correlated with the Vd determined by real-time imaging during the infusion procedure (Figs 2–4). Poor infusions with early leakage and poor Vd resulted in minimal changes in tumor volume or imaging characteristics (Fig. 3), whereas infusions with increasing Vd and percent coverage of the tumor volume resulted in an apparent reduction in tumor volume, necrosis, and decreased or static tumor growth.

### Leakage

The most common limitation in the procedure was the leakage of infusate into low pressure systems such as a ventricle or subarachnoid space (Figs 2, 3, and 6), which resulted in a poor volume of distribution within the target tissue, as previously described.<sup>44</sup> Leakage into necrotic cavities resulting from previous infusions, as well as into adjacent normal brain structures such as the internal capsule was also documented (Figs 4 and 6). The reflux of infusate along the cannula track was uncommon unless infusion rates exceeded 5  $\mu$ L/min. Infusion rates >5  $\mu$ L/min were only used once Vd had reached a plateau following leakage into a low pressure system (Figs 2, 3, and 6). Once leakage had occurred, a further increase in Vd was negligible regardless of infusion rate.

**Table 1.** Clinical case signalment

Patient	Breed/sex	Age (y)	Tumor type/grade	Survival (d) <sup>b</sup>	No. CED infusions	Cause of death
1	Jack Russell terrier FS	9	Astrocytoma II/III <sup>a</sup>	+331	3	Euthanasia (hemangiosarcoma) <sup>c</sup>
2	Boxer M	8	Astrocytoma II/III <sup>a</sup>	+560	6	Euthanasia (tumor progression)
3	French bulldog FS	10	Astrocytoma II/III <sup>a</sup>	+363	3	Euthanasia (tumor progression)
4	Labrador MC	10	Astrocytoma II	+190	3	Euthanasia (pancreatitis) <sup>c</sup>
5	Boston terrier MC	6	Oligodendroglioma II	+126	1	Died (status epilepticus) <sup>c</sup>
6	Boxer MC	7	Oligodendroglioma III	+147	2	Euthanasia (tumor progression)
7	English bulldog MC	5	Oligodendroglioma III	+190	3	Euthanasia (tumor progression)
8	Labrador FS	14	Oligodendroglioma II	+611	3	Alive
9	Boston terrier M	6	Oligodendroglioma III	+181	2	Alive

<sup>a</sup>Initial grade based on stereotactic/CT biopsy; final grade based on necropsy.

<sup>b</sup>Survival was determined from the time of initial MRI diagnosis.

<sup>c</sup>Cause of death was determined to be unrelated to tumor progression.

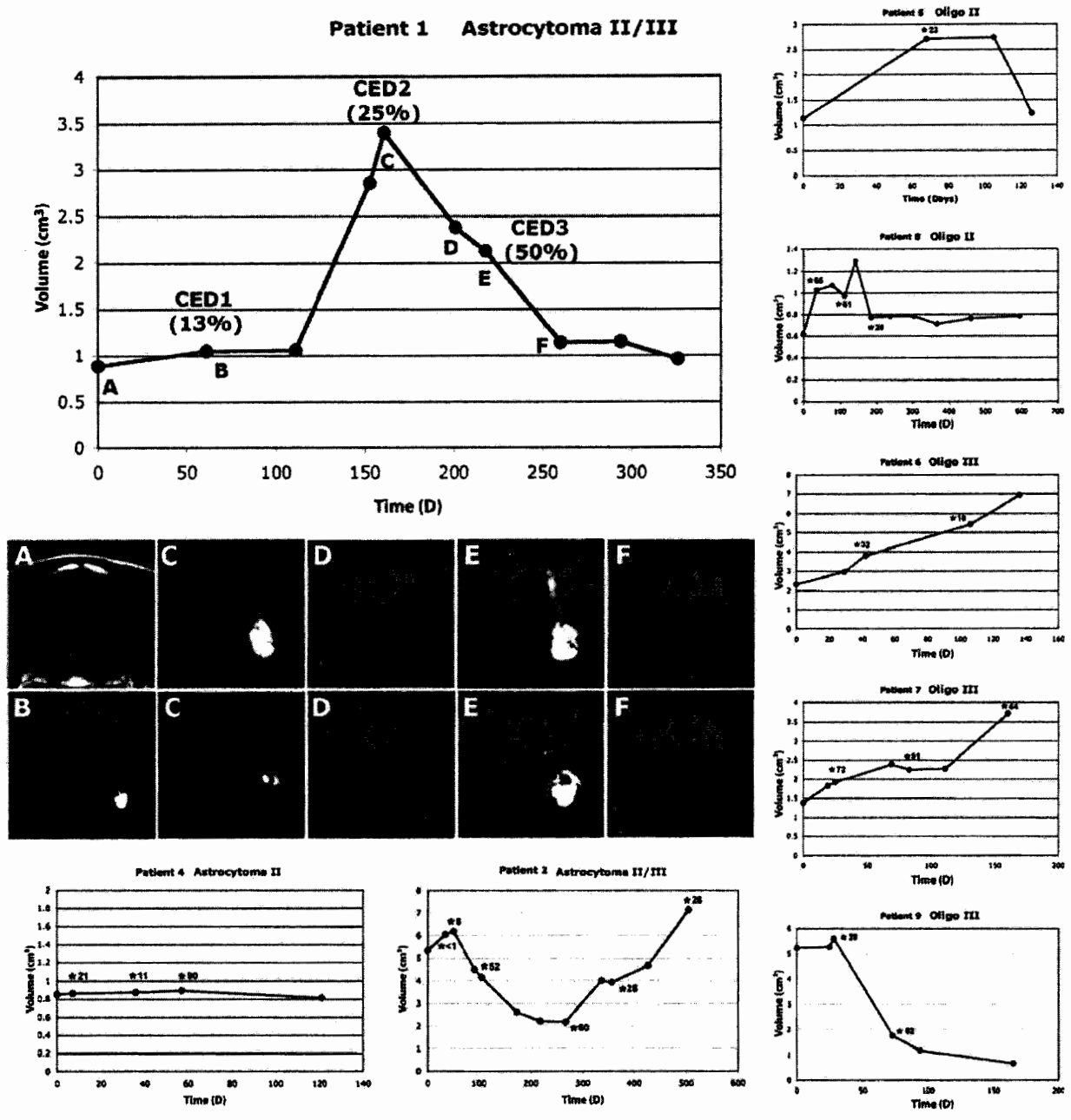


Fig. 2. Patient tumor volumes following intratumoral CED of liposomal CPT-11. CED infusions are represented by asterisks, with total percentage of tumor coverage for each infusion. Patient 1 is shown with associated MR imaging. MR images (T1 weighted) correlate to therapeutic or monitoring time points represented graphically. Real-time monitoring of infusions defined appropriate targeting and volume of distribution critical for objective assessment of therapeutic efficacy. (A) Initial MR imaging and tumor volume. (B) Initial single cannula infusion resulting in 13% Vd within the tumor and subsequent minimal effect on tumor growth. (C) Rapid tumor growth was followed by a second infusion, resulting in 25% Vd within the tumor and a subsequent decrease in tumor volume (D). (E) Third infusion, using two cannulae, resulted in 55% Vd within the tumor. A dramatic decrease in tumor volume was seen (F) followed by static disease before the animal was euthanized for disease unrelated to the primary tumor. Reflux of infusate (E, upper panel) and leakage into ventricles and the subarachnoid space (E, lower panel) were clearly visible on imaging, and dictated eventual infusion termination to minimize potential toxicity. In this apparently chemosensitive tumor, increasing real-time defined volume of distribution was associated with increasing response based on tumor volume.

**Clinical/MRI Response**

Maximum percentage decrease in tumor volume following therapy was 88% with 5 tumors having a decrease of

40% or greater (2 grade III astrocytomas 65%, 72%; 2 grade II oligodendrogliomas 40%, 55%; 1 grade III oligodendroglioma 88%). One grade II astrocytoma (Dog 4) was considered to have static disease. Two

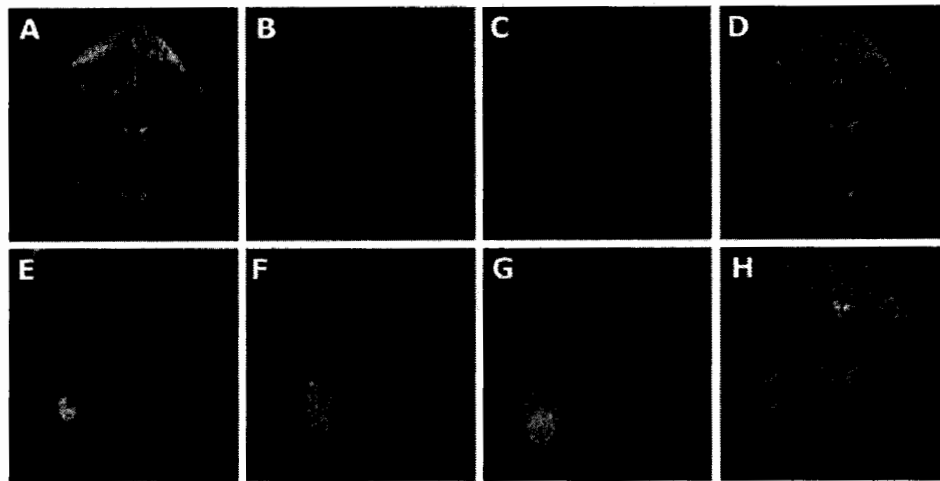


Fig. 3. MR images from a Boxer with a grade III astrocytoma. (A) Initial diagnostic MRI; the temporal/pyriform lobe tumor is most easily seen on T2-weighted images. (B and C) T1-weighted real-time images during two separate infusions (2 weeks apart) showing poor Vd within the tumor because of leakage into the subarachnoid space and lateral ventricle. Documented poor Vd was associated with minimal effect of tumor volume (D). Repositioning of guide pedestals to target different sites within the tumor resulted in improved Vd (>50%) using 3 infusion cannulae (E, F, G, T1-weighted images). (H) T2-weighted image 2 months following the successful infusion; improved Vd is associated with a decrease in tumor volume with associated decreased mass effect (an area of malacia is present within the tumor and the ipsilateral sulci and lateral ventricle are more prominent).

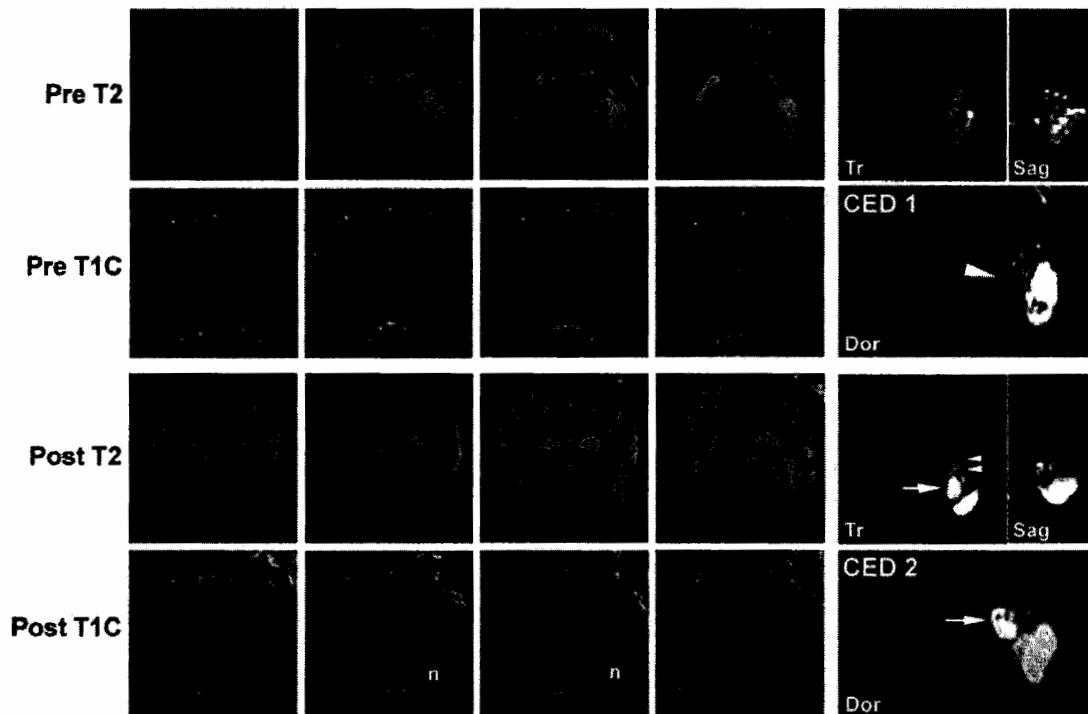


Fig. 4. MR images from a Boston Terrier with a grade III oligodendroglioma. Two infusion procedures (CED 1,2) achieved 28% and 62% Vd, respectively, within the tumor, resulting in an 88% total reduction in tumor volume 5 months following initial treatment. Decreased tumor volume, decreased mass effect, and presumed necrosis (n) of the tumor is seen on posttreatment MR images. Real-time imaging of the first CED procedure identified poor coverage of the medial aspect of the mass (arrow head). An infusion cannula was specifically targeted to this area in the second procedure resulting in good medial coverage (arrows). Suboptimal placement of this cannula superficially within the tumor eventually resulted in leakage into the internal capsule (double arrow heads). Real-time imaging allowed detection and termination of the infusion to limit potential toxicity. Tr, transverse plane image; Sag, sagittal plane image; Dor, dorsal plane image.

dogs (Dogs 1 and 8) had static disease after an initial decrease in tumor volume. Dog 1 had no increase in tumor volume for 2 months and was euthanized for an unrelated disease. Dog 8 is alive and has had no increase in tumor volume for 14 months. Dog 9 is alive 6 months post diagnosis with an 88% reduction in tumor volume. No apparent response to therapy was seen in 2 anaplastic grade III oligodendrogliomas.

#### Adverse Events

Cannula placement and infusion procedures were tolerated well by all patients except Dog 3. Animals were reported by the owners to appear quieter for 4–5 days after infusions, but returned to preinfusion activity levels thereafter. Dog 3 had prolonged anesthetic recovery after the initial infusion and had a decreased neurological status 8 weeks after treatment. MRI revealed ipsilateral diffuse white and grey matter hyperintensity on T2-weighted imaging consistent with vasogenic and cytotoxic edema. Both MRI abnormalities and clinical signs were responsive to corticosteroid therapy (prednisolone 0.5 mg/kg BID [Fig. 6]). Dog 8 had a mild decrease in neurological status 2 weeks after the second CED procedure associated with ipsilateral-increased T2 signal predominantly involving white matter that was also rapidly responsive to corticosteroid therapy.

CSF was collected sequentially from 8 dogs, and a mild, predominantly lymphocytic pleocytosis (range 4–

158 total nucleated cells/ $\mu\text{L}$ ; reference  $<3/\mu\text{L}$ ) was seen in 5 dogs. Seven of 9 dogs received anti-inflammatory doses of corticosteroids either for peritumoral edema present prior to treatment or following MRI evidence of posttreatment edema or CSF pleocytosis.

#### Pathology

A total of 7 brain tumors were evaluated after necropsy and assigned into 1 of 2 groups. Within the first group (5 dogs), lesions were present within tumors corresponding to sites of prior intratumoral CPT-11 infusion, based on infusion MR images. In these tumors (3 grade III astrocytomas, 1 grade II astrocytoma, 1 grade II oligodendroglioma) were variably sized areas of cystic malacia and intratumoral necrosis corresponding to sites of previous infusions (Figs 2, 3, and 5; Table 2). Immediately adjacent to this malacia, a zone of change in the tumor cell cytomorphology and pattern compared with that of the untreated tumor cell type was present in the 3 grade III astrocytomas and grade II oligodendroglioma (Fig. 5). In the astrocytomas, the modified GFAP-immunoreactive astrocytoma cells were much less dense, more uniformly spindloid, and with a proliferative index 15-fold lower (12–15% vs  $<1\%$ ) than the untreated areas of tumor. Although each of these tumors had been classified as grade II astrocytoma based on the initial stereotactic biopsy, there were now in all tumors substantial areas of untreated tumor, which were now classified as grade III. The grade II

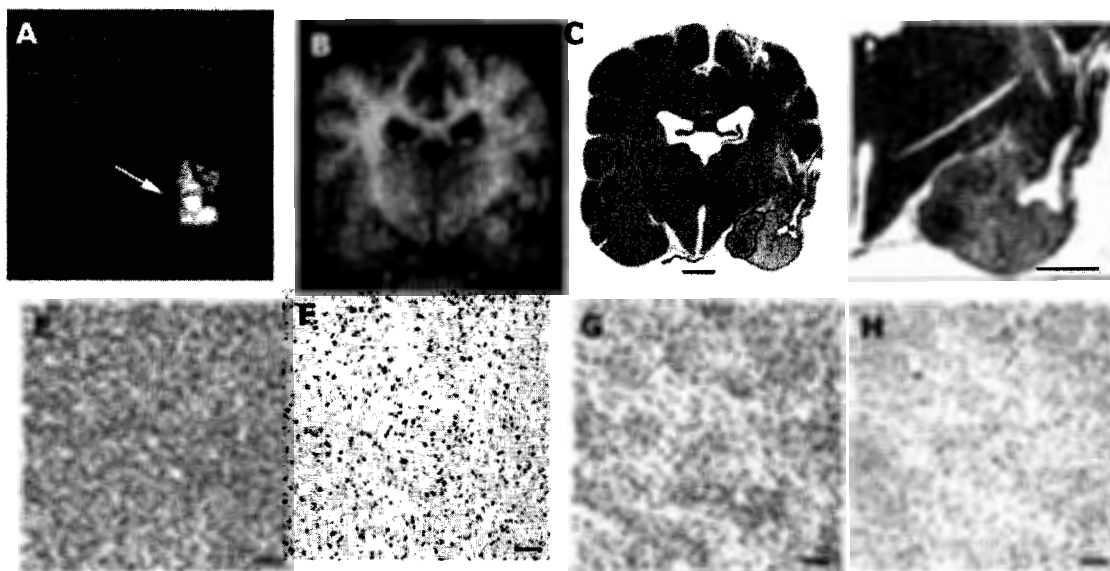


Fig. 5. Necropsy data from Patient 1. Real-time imaging of infusions and availability of necropsy in all clinical cases allowed histopathological data to be correlated with areas of infused and noninfused tumor and normal brain. (A) T1-weighted real-time imaging of the final CED showing poor infusion of tumor tissue medially (arrow). (B) Gross pathological specimen at the same level as the MRI (scale bar = 1 cm). (C) Whole brain section (hematoxylin and eosin) showing distinct areas consisting of infused tumor with malacia (M), infused tumor with modified tumor (I), and noninfused tumor (T) (scale bar = 500  $\mu\text{m}$ ). (D) Magnified view of infusion area (hematoxylin and eosin, scale bar = 500  $\mu\text{m}$ ). Modification of tumor phenotype was seen in areas of tumor that were infused (G, hematoxylin and eosin) compared with noninfused tumor (E, hematoxylin and eosin). Infused tumor was less cellular with a more homogenous cellular phenotype. MIB-1 index in infused tumor (H) was  $<1\%$  compared with 15% in noninfused tumor (E) (E, F, G, H, scale bar = 60  $\mu\text{m}$ ).

**Table 2.** Pathology summary

Patient no.	Tumor type/grade	Tumoral necrosis	Modified phenotype	MIB-1 decrease (infused tumor)	Adverse reaction <sup>a</sup>
1	Astrocytoma II/III	++	++	15% → <1%	–
2	Astrocytoma II/III	++	++	12% → <1%	–
3	Astrocytoma II/III	+	++	14% → <1%	++
4	Astrocytoma II	++	–	–	–
5	Oligodendroglioma II	++	+	4% → <1%	–
6	Oligodendroglioma III	–	–	–	–
7	Oligodendroglioma III	–	–	–	–
8	Oligodendroglioma II	+	ND	ND	+
9	Oligodendroglioma III	++	ND	ND	–

Abbreviation: ND, not done.

<sup>a</sup>Adverse reactions were defined by diffuse T2W hyperintensity beyond the margins of the tumor or infusion, not present on pretreatment MRI. Both adverse reactions were associated with decreased neurological status.

oligodendroglioma (Dog 5) had a large area of cystic malacia, also surrounded by cytologically modified tumor cells (GFAP immunonegative) exhibiting a much lower proliferative index (4% vs <1%) than the noninfused tumor. In the grade II astrocytoma (Dog 4), there was a small area of cystic malacia surrounded only by the same original grade II astrocytoma in the untreated area.

Dog 3 (grade III astrocytoma) was categorized as having an adverse reaction to the CPT-11 infusion. The tumor had an area of cystic malacia, again with more peripheral phenotypically modified astrocytoma cells and with multiple sites of an expansive and aggressive grade III astrocytoma. Additionally, outside of the tumor were widespread areas of encephalomalacia restricted to the shrunken left hemisphere and compatible in location with the adverse postinfusion response detected on MRI (Fig. 6).

In the second group of 2 high-grade (III) oligodendrogliomas, there were no apparent gross or microscopic lesions corresponding to the sites of infusion.

Within all tumors, and peritumorally, there was almost no detectable inflammatory cell response, suggesting the essential safety of CED and that the liposomal CPT-11/Gd does not evoke any detrimental toxicity apart from targeted tumor necrosis.

## Discussion

Direct delivery and liposomal encapsulation of CPT-11 have been shown to decrease local toxicity and allow much higher concentrations of drug to be achieved at the target site compared with either systemic or free drug delivery.<sup>39,45</sup> The efficacy of liposomal topoisomerase inhibitors delivered by CED in rodent glioma models has been previously documented,<sup>39,45–47</sup> as has our ability to monitor CED infusions by co-infusion of liposomes containing gadolinium as a surrogate marker.<sup>37,48</sup> We have also previously demonstrated that CED of liposomally encapsulated CPT-11 and gadoteridol results in negligible clinical and histopathological adverse effects in normal experimental dogs,<sup>40</sup> and the current study suggests that this is also true for

dogs with intra-axial gliomas. Although most animals exhibited mild lymphocytic pleocytosis in CSF analyzed after infusions, only 2 animals showed evidence of either histopathological or MRI changes consistent with an adverse reaction to the infusion. Both animals exhibited a deterioration in neurological status and both were rapidly responsive to corticosteroids (Fig. 5; Table 2); although marked atrophy/malacia involving both grey and white matter was seen in the most severely affected animal (Dog 3). While marked leakage of infusate into nontargeted peritumoral tissues was documented in this case, T2W hyperintensity in the second dog (Dog 8) occurred after infusions that were essentially limited to the tumor volume, and leakage of infusate in other animals was not associated with apparent adverse effects. The likelihood of adverse effects secondary to inappropriate targeting of liposomes to normal brain or CSF were minimized, since real-time imaging allowed for the termination of infusions, alteration of infusion rates, and/or redirection of infusion cannulae when leakage, distribution to normal brain, or static volumes of distribution were documented during the infusion process.

Although assessment of therapeutic efficacy was not a defined endpoint for the study, evidence for efficacy of intratumoral liposomal CPT-11 in these spontaneous tumors and indications of its potential mechanism of action were apparent in the study animals. The natural biology of canine spontaneous gliomas is poorly documented, as is response to conventional therapy such as radiation and chemotherapy. The endpoint for most animals is euthanasia rather than overall survival, and published “survival” data range from several days to several months for all treatment options. As such, any efficacy of direct intratumoral infusion of liposomal CPT-11 could only be assessed subjectively for individual cases on the basis of MRI evidence of static or decreasing tumor volumes and histopathology after euthanasia or death. Liposomal encapsulation has been shown to improve the pharmacokinetic properties and tissue residence time of CPT-11, which has been detected in rodent glioma models up to 2 months after a single CED administration.<sup>39,45</sup> Consistent with this experimental data, the efficacy of treatment in dogs

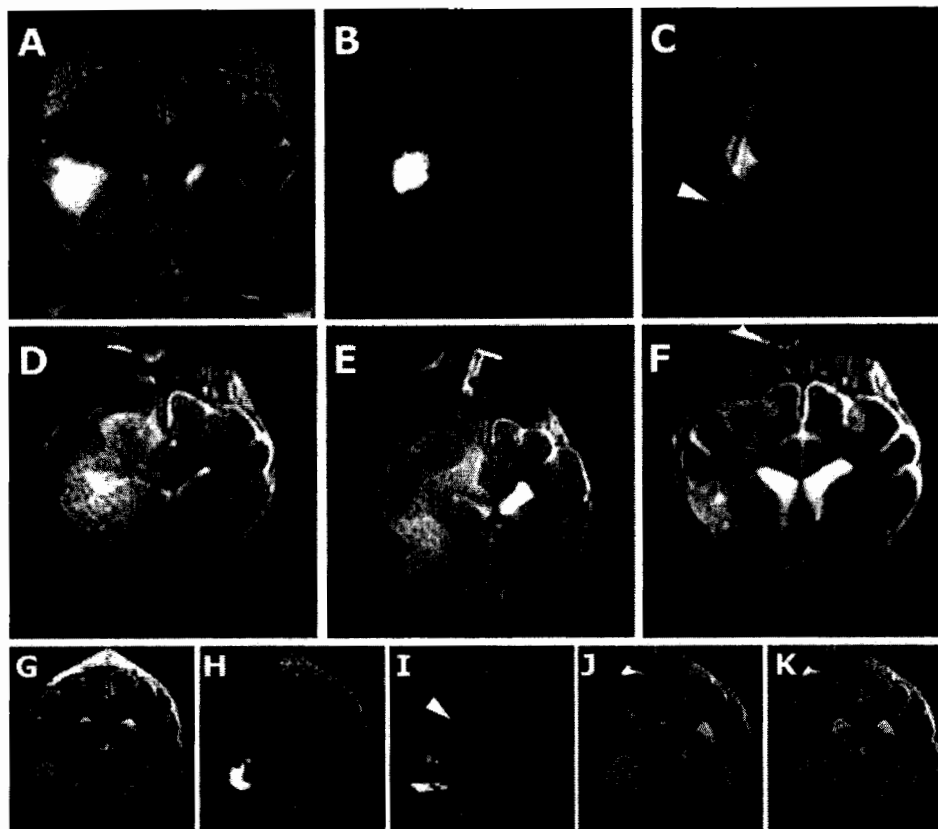


Fig. 6. Adverse effects associated with nanoliposomal CPT-11/gadoteridol infusions. (Patient 3, A–F; Patient 8, G–K.) (A) Preinfusion T2W MR image. (B and C) CED using 3 cannulae resulted in intratumoral delivery rostrally; however, reflux of infusate from the caudal cannula resulted in delivery into the internal capsule instead of the target site (arrowhead). (D and E) T2W MR images 8 weeks postinfusion; T2 hyperintensity is present predominantly affecting white matter, resulting in ventricular compression and effacement of sulci. (F) T2W MR image 6 weeks later following corticosteroid treatment with resolution of the majority of the white matter hyperintensity. (G) Preinfusion T2W MR image. First (H) and second (I) infusions (T1W MR images). The first infusion achieved good intratumoral Vd, whereas the second was restricted to the ventral aspect of the tumor. Both infusions were eventually limited by ventricular leakage (arrowhead). (J) Four weeks postinfusion, clinical deterioration was associated with T2 hyperintensity predominantly associated with white matter and also increased tumor volume. (K) Four weeks following corticosteroid treatment and rapid resolution of clinical signs, T2 hyperintensity and associated mass effect has resolved, and tumor volume is decreased.

receiving multiple infusions appeared to be present over several weeks, based on serial MRI (Fig. 2).

Five tumors decreased in volume ranging from 40% to 88%, and 1 dog with grade II astrocytoma (Dog 4) had apparently stable disease (Fig. 2). The small area of malacia present within this tumor was probably because of expansion of the CT-biopsy cavity since pooling of infusate was noted in this area during treatments. Malacia secondary to toxic effects in infused neuropil was considered less likely because this was not a finding in other cases or in previous experimental dogs.<sup>40</sup> Two tumors, both anaplastic oligodendrogliomas, had rapid growth progression and had no apparent response based either on MRI or histopathology. Importantly, the lack of response in these tumors was associated with successful intratumoral infusions, as defined by real-time imaging (Fig. 2). The percent coverage of tumor determined by real-time imaging varied from 32% to 72%, a degree of coverage associated with apparent positive responses in other tumors. These cases, therefore, suggested that there was a true

failure of the therapeutic drug rather than a failure of the delivery system. In contrast, the lack of response in Dog 2 (grade III astrocytoma) after the initial 2 infusions was clearly associated with poor Vd secondary to leakage and tumor coverage of <10% (Figs 2 and 3). Subsequent delivery of liposomal CPT-11 covering >50% of this tumor resulted in a marked decrease in tumor volume. Similar findings were apparent in Patient 1 (grade III astrocytoma) where limited infusions covering approximately 10% of tumor volume had only slight clinical effect compared with subsequent infusions where tumor coverage was 25% or greater (Fig. 2). Although the number of dogs in the study was small and tumor phenotype varied, the critical value of real-time imaging in defining Vd of infusions and subsequent assessment of therapeutic efficacy of a novel therapeutic delivered by CED is clearly demonstrated, as are the potential pitfalls of assessing therapeutic value in the absence of imaging.

The mechanism for the decreased sensitivity and lack of response in the 2 anaplastic oligodendrogliomas is



unclear. CPT-11, (7-ethyl-10-(4-[1-piperidinio]-1-piperidino) carbonyloxy)camptothecin) is a water-soluble derivative of the potent alkaloid anticancer agent camptothecin and acts as a specific inhibitor of topoisomerase I.<sup>34</sup> CPT-11 is converted into a more active metabolite, SN-38 (7-ethyl-10-hydroxycamptothecin), by carboxylesterase (CES) activity, predominantly in the liver and serum.<sup>49</sup> The precise contribution of SN-38 to the anti-neoplastic effect of CPT-11 compared with Irinotecan hydrochloride is unclear, as is the necessity for systemic metabolism. Some data suggest that intratumoral or neuropil activation of Irinotecan might be as important as systemic/hepatic activation and is an important factor when considering direct intratumoral infusion.<sup>50–60</sup> One of the largest decreases in tumor volume (~90%) following therapy was seen in the third anaplastic oligodendroglioma, suggesting, not surprisingly, that factors influencing therapeutic efficacy are not consistent across individual tumors of similar histological type and grade. Further investigation of factors such as carboxylesterase and topoisomerase expression in individual treated tumors may be more informative regarding the sensitivity when tumor infusion has been documented by MRI.

A major advantage of the canine spontaneous tumor model is the availability of necropsy (all nonsurviving animals in this study), providing valuable correlative data often unavailable from human clinical trials. Two major responses were noted in tumors examined histopathologically: necrosis and a modulation of the tumor phenotype. Consistent with the predictive value of real-time imaging in relation to clinical response, histological findings after necropsy were also closely correlated with real-time infusion images. Overlay of MR infusion images and histological sections showed areas of tumor necrosis and/or modulation of tumor phenotype in areas of infused tumor, with residual/new tumor present beyond the margins of infusion exhibiting a more aggressive phenotype (Fig. 5). Modulation of tumor phenotype was seen in 4 of 5 necropsied animals that displayed a decreased tumor volume or static disease. Modulation was characterized by more benign, less anaplastic cellular characteristics, and a decrease in the MIB-1 proliferative index (Fig. 5; Table 2). The mechanism for this altered phenotype following exposure to CPT-11 is unclear, but may involve selective targeting of a more proliferative compartment of tumor cells, leaving terminally differentiated tumor cells as a residual population. The authors have also seen this tumor modulation after CED of liposomal CPT-11 in orthotopic murine tumor models with a canine glioma cell line. The presence of essentially non-dividing, yet apparently viable, tumor tissue after therapy has important implications for both the prognosis and assessment of efficacy simply measured in terms of reduction in tumor volume. Routine MRI did not discriminate between untreated tumor and tumor with

modified phenotype, and additional imaging approaches such as diffusion-weighted imaging and spectroscopy may be beneficial in defining this modified compartment of the tumor.

In summary, we have shown that canine spontaneous gliomas may provide a valuable large animal, spontaneous tumor model for the investigation of novel delivery, and novel therapeutic strategies for intracranial tumors. It is hoped that retrospective analysis of MRI parameters and infusion data in this more clinically realistic spontaneous model may help to further optimize cannula and infusion parameters. CED of a chemotherapeutic agent (liposomal CPT-11) directly into spontaneous gliomas in a large volume brain is feasible and well tolerated clinically. On the basis of responses in canine patients, intratumoral liposomal CPT-11 should be considered as a potential therapeutic option, particularly in nonresectable or recurrent tumors. As was the case with these spontaneous gliomas in dogs, assessment and optimization of any therapy delivered by CED in future human glioma clinical trials will depend critically on the ability to accurately define infusions in real time. In addition to providing an appropriate mechanistic and biological environment to assess CED parameters more realistically, the canine model has provided an equally realistic system to assess potential adverse effects associated with the infusion procedure, the delivery system, therapeutic agent, and surrogate marker in the context of a large immunocompetent mammal with ongoing intracranial disease.

*Conflict of interest statement.* D.B.K., C.O.N., and D.C.D. both hold stock and stock options in Merrimack Pharmaceuticals, the company working to develop this novel drug formulation. D.B.K. was previously the Vice President of Pharmaceutical Research and Development for Hermes Biosciences, a company working to develop the product that was recently merged with Merrimack Pharmaceuticals. D.B.K. and D.C.P. are the inventors on a patent application that describes the highly stabilized nanoliposome formulation of CPT-11 used in this manuscript. D.C.P. is the Senior Director of Research for Merrimack Pharmaceuticals. J.W.P. is a Board member, officer in Hermes Biosciences, Inc. and also has equity in the same company. The University of California–San Francisco has a patent related to this work.

## Funding

This work was supported by the National Institutes of Health [1P01 CA-118816-0102 and P50 CA097257] and The Paul C. and Borghild T. Petersen Foundation.



## References

1. Fomchenko EI, Holland EC. Mouse models of brain tumors and their applications in preclinical trials. *Clin Cancer Res*. 2006;12:5288–5297.
2. Branle F, Lefranc F, Cambry I, et al. Evaluation of the efficiency of chemotherapy in *in vivo* orthotopic models of human glioma cells with and without 1p19q deletions and in C6 rat orthotopic allografts serving for the evaluation of surgery combined with chemotherapy. *Cancer*. 2002;95:641–655.
3. Vail DM, MacEwen EG. Spontaneously occurring tumors of companion animals as models for human cancer. *Cancer Invest*. 2000;18:781–792.
4. Koestner A, Bilzer T, Fatzner R, Schulman FY, Summers BA, Van Winkle TJ. *Histological Classification of Tumors of the Nervous System of Domestic Animals*. 2nd ed, vol. 5. Washington, D.C: The Armed Forces Institute of Pathology; 1999.
5. Paoloni M, Khanna C. Translation of new cancer treatments from pet dogs to humans. *Nat Rev Cancer*. 2008;8:147–156.
6. Kimmelman J, Nalbantoglu J. Faithful companions: a proposal for neurooncology trials in pet dogs. *Cancer Res*. 2007;67:4541–4544.
7. Surawicz TS, McCarthy BJ, Kupelian V, Jukich PJ, Bruner JM, Davis FG. Descriptive epidemiology of primary brain and CNS tumors: results from the Central Brain Tumor Registry of the United States, 1990–1994. *Neuro Oncol*. 1999;1:14–25.
8. McKinney PA. Brain tumours: incidence, survival, and aetiology. *J Neurol Neurosurg Psychiatry*. 2004;75(suppl 2):ii12–ii17.
9. Klotz M. Incidence of brain tumors in patients hospitalized for chronic mental disorders. *Psychiatr Q*. 1957;31:669–680.
10. McGrath JT. Intracranial pathology of the dog. *Acta Neuropathol (Berl)*. 1962;1(suppl 1):3–4.
11. Schneider R. General considerations. In: Moulton, JE ed. *Tumors in Domestic Animals*. 2nd ed. Berkeley: University of California Press; 1978:1–15.
12. Priester WA, McKay FW. The occurrence of tumors in domestic animals. In: Ziegler, JL ed. *National Cancer Institute Monograph*. Bethesda, MD: U.S. Department of Health and Human Services; 1980:1–210.
13. Candolfi M, Curtin JF, Nichols WS, et al. Intracranial glioblastoma models in preclinical neuro-oncology: neuropathological characterization and tumor progression. *J Neurooncol*. 2007;85:133–148.
14. Summers BA, Cummings JF, de Lahunta A. *Tumors of the Central Nervous System*. Veterinary Neuropathology St Louis: Mosby; 1995:351–401.
15. Vandevelde M, Fankhauser R, Luginbühl H. Immunocytochemical studies in canine neuroectodermal brain tumors. *Acta Neuropathol (Berl)*. 1985;66:111–116.
16. Sturges BK, Dickinson PJ, Bollen AW, et al. Magnetic resonance imaging and histological classification of intracranial meningiomas in 112 dogs. *J Vet Intern Med*. 2008;22:586–595.
17. Stoica G, Kim HT, Hall DG, Coates JR. Morphology, immunohistochemistry, and genetic alterations in dog astrocytomas. *Vet Pathol*. 2004;41:10–19.
18. Westworth DR, Dickinson PJ, Vernau W, et al. Choroid plexus tumors in 56 dogs (1985–2007). *J Vet Intern Med*. 2008;22:1157–1165.
19. Snyder JM, Shofer FS, Van Winkle TJ, Massicotte C. Canine intracranial primary neoplasia: 173 cases (1986–2003). *J Vet Intern Med*. 2006;20:669–675.
20. Thomas WB, Wheeler SJ, Robert K, Kornegay JN. Magnetic resonance imaging features of primary brain tumors in dogs. *Vet Radiol Ultrasound*. 1996;37:20–27.
21. Kraft SL, Gavin PR, DeHaan C, Moore M, Wendling LR, Leathers CW. Retrospective review of 50 canine intracranial tumors evaluated by magnetic resonance imaging. *J Vet Intern Med*. 1997;11:218–225.
22. Lipsitz D, Higgins RJ, Kortz GD, Dickinson PJ, Bollen AW, LeCouteur RA. Glioblastoma multiforme: clinical findings, magnetic resonance imaging and pathology in 5 dogs. *Vet Pathol*. 2003;40:659–669.
23. Dickinson PJ, Roberts BN, Higgins RJ, et al. Expression of receptor tyrosine kinases VEGFR-1 (FLT-1), VEGFR-2 (KDR), EGFR-1, PDGFR $\alpha$  and c-Met in canine primary brain tumors. *Vet Comp Oncol*. 2006;4:132–140.
24. Dickinson PJ, Sturges BK, Higgins RJ, et al. Vascular endothelial growth factor mRNA expression and peritumoral edema in canine primary central nervous system tumors. *Vet Pathol*. 2008;45:131–139.
25. Debinski W, Gibo DM, Wykosky J, Stanton C, Rossmeisl J, Robertson J. Canine gliomas over-express IL-13R $\alpha$ 2, EphA2 and Fra-1 in common with human high-grade astrocytomas. *Neuro Oncol*. 2007;9:535.
26. Stoica G, Lungu G, Stoica H, Waghela S, Levine J, Smith R, 3rd. Identification of cancer stem cells in dog glioblastoma. *Vet Pathol*. 2009;
27. Thomson SA, Kennerly E, Olby N, et al. Microarray analysis of differentially expressed genes of primary tumors in the canine central nervous system. *Vet Pathol*. 2005;42:550–558.
28. Platt SR, Scase TJ, Adams V, et al. Vascular endothelial growth factor expression in canine intracranial meningiomas and association with patient survival. *J Vet Intern Med*. 2006;20:663–668.
29. Long S, Argyle DJ, Nixon C, et al. Telomerase reverse transcriptase (TERT) expression and proliferation in canine brain tumours. *Neuropathol Appl Neurobiol*. 2006;32:662–673.
30. Thomas R, Duke SE, Wang HJ, et al. 'Putting our heads together': insights into genomic conservation between human and canine intracranial tumors. *J Neurooncol*. 2009;94:333–349.
31. Higgins RJ, Dickinson PJ, Lecouteur RA, et al. Spontaneous canine gliomas: overexpression of EGFR, PDGFR $\alpha$  and IGF2 demonstrated by tissue microarray immunophenotyping [published online ahead of print December 5, 2009]. *J Neurooncol*. 2009.
32. Dickinson PJ, Surace EI, Cambell M, et al. Expression of the tumor suppressor genes NF2, 4.1B, and TSLC1 in canine meningiomas. *Vet Pathol*. 2009;46:884–892.
33. Debinski W, Tatter SB. Convection-enhanced delivery for the treatment of brain tumors. *Expert Rev Neurother*. 2009;9:1519–1527.
34. Potmesil M. Camptothecins: from bench research to hospital wards. *Cancer Res*. 1994;54:1431–1439.
35. Hare CB, Elion GB, Houghton PJ, et al. Therapeutic efficacy of the topoisomerase I inhibitor 7-ethyl-10-(4-[1-piperidino]-1-piperidino)-carbonyloxy-camptothecin against pediatric and adult central nervous system tumor xenografts. *Cancer Chemother Pharmacol*. 1997;39:187–191.
36. Feun L, Savaraj N. Topoisomerase I inhibitors for the treatment of brain tumors. *Expert Rev Anticancer Ther*. 2008;8:707–716.
37. Saito R, Krauze MT, Bringas JR, et al. Gadolinium-loaded liposomes allow for real-time magnetic resonance imaging of convection-enhanced delivery in the primate brain. *Exp Neurol*. 2005;196:381–389.
38. Krauze MT, McKnight TR, Yamashita Y, et al. Real-time visualization and characterization of liposomal delivery into the monkey brain by magnetic resonance imaging. *Brain Res Brain Res Protoc*. 2005;16:20–26.
39. Noble CO, Krauze MT, Drummond DC, et al. Novel nanoliposomal CPT-11 infused by convection-enhanced delivery in intracranial tumors: pharmacology and efficacy. *Cancer Res*. 2006;66:2801–2806.

40. Dickinson PJ, LeCouteur RA, Higgins RJ, et al. Canine model of convection-enhanced delivery of liposomes containing CPT-11 monitored with real-time magnetic resonance imaging: laboratory investigation. *J Neurosurg.* 2008;108:989–998.
41. Bankiewicz KS, Eberling JL, Kohutnicka M, et al. Convection-enhanced delivery of AAV vector in parkinsonian monkeys; *in vivo* detection of gene expression and restoration of dopaminergic function using pro-drug approach. *Exp Neurol.* 2000;164:2–14.
42. Higgins RJ, LeCouteur RA, Vernau KM, Sturges BK, Obradovich JE, Bollen AW. Granular cell tumor of the canine central nervous system: two cases. *Vet Pathol.* 2001;38:620–627.
43. Louis DN, Ohgaki H, Wiestler OD, Cavenee WK. WHO classification of tumors of the central nervous system. 4th ed. Geneva: WHO Press; 2007.
44. Varenika V, Dickinson P, Bringas J, et al. Detection of infusate leakage in the brain using real-time imaging of convection-enhanced delivery. *J Neurosurg.* 2008;109:874–880.
45. Krauze MT, Noble CO, Kawaguchi T, et al. Convection-enhanced delivery of nanoliposomal CPT-11 (irinotecan) and PEGylated liposomal doxorubicin (Doxil) in rodent intracranial brain tumor xenografts. *Neuro Oncol.* 2007;9:393–403.
46. Saito R, Krauze MT, Noble CO, et al. Convection-enhanced delivery of Ls-TPT enables an effective, continuous, low-dose chemotherapy against malignant glioma xenograft model. *Neuro-oncology.* 2006;8:205–214.
47. Yamashita Y, Krauze MT, Kawaguchi T, et al. Convection-enhanced delivery of a topoisomerase I inhibitor (nanoliposomal topotecan) and a topoisomerase II inhibitor (pegylated liposomal doxorubicin) in intracranial brain tumor xenografts. *Neuro-oncology.* 2007;9:20–28.
48. Saito R, Bringas JR, McKnight TR, et al. Distribution of liposomes into brain and rat brain tumor models by convection-enhanced delivery monitored with magnetic resonance imaging. *Cancer Res.* 2004;64:2572–2579.
49. Kaneda N, Nagata H, Furuta T, Yokokura T. Metabolism and pharmacokinetics of the camptothecin analogue CPT-11 in the mouse. *Cancer Res.* 1990;50:1715–1720.
50. Atsumi R, Okazaki O, Hokusui H. Metabolism of irinotecan to SN-38 in a tissue-isolated tumor model. *Biol Pharm Bull.* 1995;18:1024–1026.
51. Guichard S, Terret C, Hennebelle I, et al. CPT-11 converting carboxylesterase and topoisomerase activities in tumour and normal colon and liver tissues. *Br J Cancer.* 1999;80:364–370.
52. Kawato Y, Furuta T, Aonuma M, Yasuoka M, Yokokura T, Matsumoto K. Antitumor activity of a camptothecin derivative, CPT-11, against human tumor xenografts in nude mice. *Cancer Chemother Pharmacol.* 1991;28:192–198.
53. Ohtsuka K, Inoue S, Kameyama M, et al. Intracellular conversion of irinotecan to its active form, SN-38, by native carboxylesterase in human non-small cell lung cancer. *Lung Cancer.* 2003;41:187–198.
54. Nagai S, Yamauchi M, Andoh T, et al. Establishment and characterization of human gastric and colonic xenograft lines resistant to CPT-11 (a new derivative of camptothecin). *J Surg Oncol.* 1995;59:116–124.
55. Niimi S, Nakagawa K, Sugimoto Y, et al. Mechanism of cross-resistance to a camptothecin analogue (CPT-11) in a human ovarian cancer cell line selected by cisplatin. *Cancer Res.* 1992;52:328–333.
56. Hu ZP, Yang XX, Chen X, Chan E, Duan W, Zhou SF. Simultaneous determination of irinotecan (CPT-11) and SN-38 in tissue culture media and cancer cells by high performance liquid chromatography: application to cellular metabolism and accumulation studies. *J Chromatogr B Analyt Technol Biomed Life Sci.* 2007;850:575–580.
57. Sanghani SP, Quinney SK, Fredenburg TB, et al. Carboxylesterases expressed in human colon tumor tissue and their role in CPT-11 hydrolysis. *Clin Cancer Res.* 2003;9:4983–4991.
58. Zhang W, Xu G, McLeod HL. Comprehensive evaluation of carboxylesterase-2 expression in normal human tissues using tissue array analysis. *Appl Immunohistochem Mol Morphol.* 2002;10:374–380.
59. Yamada T, Hosokawa M, Satoh T, et al. Immunohistochemistry with an antibody to human liver carboxylesterase in human brain tissues. *Brain Res.* 1994;658:163–167.
60. Furihata T, Hosokawa M, Satoh T, Chiba K. Synergistic role of specificity proteins and upstream stimulatory factor 1 in transactivation of the mouse carboxylesterase 2/microsomal acylcarnitine hydrolase gene promoter. *Biochem J.* 2004;384:101–110.

# Magnetic resonance imaging of intracranial tumors: intra-patient comparison of gadoteridol and ferumoxytol

Edit Dósa, Daniel J. Guillaume, Marianne Haluska, Cynthia A. Lacy, Bronwyn E. Hamilton, Jeffrey M. Njus, William D. Rooney, Dale F. Kraemer, Leslie L. Muldoon, and Edward A. Neuwelt

Department of Neurology (E.D., M.H., C.A.L., L.L.M., E.A.N.), Department of Neurosurgery (D.J.G., E.A.N.), Department of Radiology (B.E.H.), Department of Public Health and Preventive Medicine (D.F.K.), Department of Medical Informatics and Clinical Epidemiology (D.F.K.), Advanced Imaging Research Center (J.M.N., W.D.R.), Oregon Health and Science University, Portland, Oregon Department of Pharmacy Practice, Oregon State University, Portland, Oregon (D.F.K.); Portland Veterans Affairs Medical Center, Portland, Oregon (E.A.N)

This study aims to compare gadoteridol with ferumoxytol for contrast-enhanced and perfusion-weighted (PW) MRI of intracranial tumors. The final analysis included 26 patients, who underwent 3 consecutive days of 3T MRI. Day 1 consisted of anatomical pre- and post-contrast images, and PW MRI was acquired using gadoteridol (0.1 mmol/kg). On Day 2, the same MRI sequences were obtained with ferumoxytol (510 mg) and on Day 3, the anatomical images were repeated to detect delayed ferumoxytol-induced signal changes. The  $T_1$ -weighted images were evaluated qualitatively and quantitatively for enhancement volume and signal intensity (SI) changes; PW data were used to estimate the relative cerebral blood volume (rCBV). All 26 lesions showed 24-hour  $T_1$ -weighted ferumoxytol enhancement; 16 also had  $T_2$ -weighted hypointensities. In 6 patients, ferumoxytol-induced signal changes were noted in areas with no gadoteridol enhancement. Significantly greater ( $P < .0001$ ) SI changes were seen with gadoteridol, and qualitative analyses (lesion border delineation, internal morphology, contrast enhancement) also showed significant preferences ( $P = .0121$ ;  $P = .0015$ ;  $P < .0001$ , respectively) for this agent. There was no significant difference in lesion enhancement volumes between contrast materials. The ferumoxytol-rCBV values were significantly higher ( $P = .0016$ ) compared

with the gadoteridol-rCBV values. In conclusion, ferumoxytol provides important information about tumor biology that complements gadoteridol imaging. The rCBV measurements indicate areas of tumor undergoing rapid growth, whereas the 24-hour scans mark the presence of inflammatory cells. Both of these functions provide useful information about tumor response to treatment. We suggest that dynamic and anatomical imaging with ferumoxytol warrant further assessment in brain tumor therapy.

**Keywords:** brain tumors, ferumoxytol, magnetic resonance imaging, ultrasmall superparamagnetic iron oxide nanoparticles.

The most commonly used gadolinium-based contrast agents (GBCAs) are low-molecular-weight extracellular substances with a short plasma half-life. GBCAs are relatively safe when administered in clinically recommended doses (0.1–0.3 mmol/kg). However, emerging evidence linking GBCAs to nephrogenic systemic fibrosis has changed medical practice patterns toward avoiding gadolinium-enhanced MRI in patients with glomerular filtration rates (GFR)  $< 30$  mL/min/1.73m<sup>2</sup>.<sup>1</sup>

Ultrasmall superparamagnetic iron oxide nanoparticles (USPIOs), such as ferumoxytol (Feraheme, AMAG Pharmaceuticals Inc.), developed for iron-replacement therapy primarily in patients with kidney disease, are promising contrast materials for brain tumor MRI due to their  $T_1$  and  $T_2$  relaxation time—shortening effects.<sup>2,3</sup> The semisynthetic carbohydrate-coated

Received June 8, 2010; accepted September 30, 2010.

Corresponding Author: Edward A. Neuwelt, MD, Oregon Health and Science University, 3181 S.W. Sam Jackson Park Road, L603, Portland, OR 97239-3098 (neuwelte@ohsu.edu).

ferumoxytol, which has a hydrodynamic diameter of 30 nm, shows little uptake by circulating monocytes, resulting in a long blood half-life (14 hours).<sup>4</sup> Ferumoxytol can be safely given as a short intravenous bolus for dynamic MRI where it serves as a true blood pool agent at early time points (minutes) and is useful for measurement of the relative cerebral blood volume (rCBV).<sup>5,6</sup> Over a period of hours, ferumoxytol undergoes uptake in reactive astrocytes and tissue macrophages.<sup>7</sup> Consequently, ferumoxytol has the potential for imaging of both tumor vasculature and inflammation in central nervous system (CNS) malignancies.<sup>7,8</sup>

A 1.02-g treatment course of ferumoxytol (2 × 510 mg) was used for iron-replacement therapy in a large number of patients without significant adverse effects.<sup>9</sup> So far, the highest given dose of ferumoxytol as an MRI contrast agent was 4 mg/kg (280 mg for a 70-kg patient).<sup>3</sup> A total dose of 510 mg (the maximum FDA-approved dose) of ferumoxytol administered in this study has not been investigated for MR imaging before. This study aims to qualitatively and quantitatively compare gadoteridol (ProHance, Bracco Diagnostic Inc.) with high-dose ferumoxytol for contrast-enhanced and perfusion-weighted (PW) MRI in patients with intracranial tumors.

## Subjects and Methods

### Study Population

Between March 2008 and February 2010, 36 patients with intracranial tumors were enrolled in this prospective study. Patients who were younger than 18 years; were pregnant or lactating; showed clinical symptoms and signs of herniation (e.g. acute pupillary enlargement, rapidly developing motor changes, rapidly decreasing level of consciousness) or hemodynamic instability; had contraindications to MRI procedures (e.g. pacemaker); or had known allergic or hypersensitivity reactions to parenteral iron, dextran, iron-dextran or iron-polysaccharide preparations; had known or suspected iron overload (e.g. hemochromatosis, history of multiple transfusions); or had hepatic insufficiency or liver cirrhosis were excluded. HIV-positive patients on combination antiretroviral therapy were also ineligible because of the potential for pharmacokinetic interactions with ferumoxytol.

The study was sponsored by the National Institutes of Health and was approved by the Oregon Health and Science University Institutional Review Board (eIRB #1562). All participants provided written informed consent.

### MRI Examination

All MRI scans were performed on a 3T whole-body MRI system (TIM Trio, Siemens) with a body radio frequency (RF) coil transmit and a 12-channel phased-array head RF receiver coil. The imaging protocol consisted of 3 consecutive days. On the first day, localizer scout images,

axial  $T_1$ - and  $T_2$ -weighted pre- and 18.5-minute (range, 16–21 minutes) postcontrast images, and first-pass dynamic susceptibility-weighted contrast-enhanced (DSC) perfusion MRI were acquired using gadoteridol gadolinium (III) chelate. On the following day, the same MRI sequences were obtained with ferumoxytol. On the third day, at least 22 hours (mean, 24.3 hours; range, 22–28 hours) after the USPIO agent administration, the anatomical images were repeated in identical spatial orientations to detect delayed ferumoxytol-induced signal changes. Subjects with renal insufficiency (GFR < 30 mL/min/1.73m<sup>2</sup>) underwent only a 2-day MRI with USPIO, without gadoteridol.

Gadoteridol was injected at a dose of 0.1 mmol/kg of body weight. Ferumoxytol was given over 20 minutes in a constant volume of 17 mL (510 mg) diluted with 17 mL of saline regardless of body weight, from which a separate 5-mL bolus was used for DSC MRI. After contrast agent administration, the patients were monitored closely for 2 hours and were followed up for 1 month.

### MRI Acquisition Parameters

To minimize possible differences, the inter-day MRI acquisitions were carefully repositioned using consistent and clearly visualized anatomical landmarks from high-quality scout MRI scans.

For  $T_1$ -weighted spin echo (SE) images, a repetition time (TR)/echo time (TE) of 900/10 was used, and up to 44 slices with a 2-mm<sup>2</sup> slice thickness without gap were obtained. A field of view (FOV) of 240 × 240 mm<sup>2</sup> and an acquisition matrix of 256 × 256 were chosen. For  $T_2$ -weighted turbo SE images, we used 9000/93 at a slice thickness of 2 mm<sup>2</sup> without gap. The TSE factor was 9, while the FOV was 240 × 240 mm<sup>2</sup> with an acquisition matrix of 256 × 256. For DSC MRI, dynamic  $T_2^*$ -weighted images were acquired using a gradient-echo echo-planar imaging pulse sequence (TR, 1500 ms; TE, 20 ms; FA, 45°; FOV, 192 × 192 mm<sup>2</sup>; matrix, 64 × 64; and 27 interleaved slices with 3-mm<sup>2</sup> thickness and 0.9-mm<sup>2</sup> gap). After an initial baseline period of 7 series of 27 image slices (11 seconds), a rapid bolus of contrast agent was administered intravenously using a power injector (Spectris Solaris, Medrad Inc.) through an 18-gauge intravenous line at a rate of 3 mL/s, followed immediately by 20 mL of saline flush at the same rate. DSC data collection was continued for 90 series (2 minutes 21 seconds).

### Image Analysis

All images from each patient were evaluated in a matched-pair fashion and were analyzed by two neuroradiologists in consensus. The image assessment consisted of the following steps:

- (i) The total number of enhancing brain lesions as visualized on  $T_1$ -weighted gadoteridol-enhanced,  $T_1$ - and  $T_2$ -weighted ferumoxytol-enhanced images was recorded for each patient. In the case

of multiple lesions, only the largest, most conspicuous lesion was selected for further evaluation.

- (ii)  $T_1$ -weighted gadoteridol and  $T_1$ -weighted 24-hour ferumoxytol enhancement patterns were compared in a descriptive manner. In addition, the images were scored in terms of the following: (1) lesion border delineation, (2) visualization of lesion internal morphology, and (3) lesion contrast enhancement compared with surrounding normal tissue. These assessments were performed by using 3-point scales from  $-1$  (gadoteridol superior) through  $0$  (both contrast agents equal) to  $+1$  (ferumoxytol superior).
- (iii)  $T_1$ -weighted postcontrast (gadoteridol, 24-hour ferumoxytol) MR images were uploaded in MIPAV (Medical Image Processing, Analysis, and Visualization, BIRSS; NIH). The enhancing lesion was outlined on each MR image and the software calculated the enhancement volume. Volumetric analysis was expressed in units of cubic centimeter.
- (iv) By using user-defined regions of interests (ROIs) in the lesion, contralateral normal brain parenchyma, and background noise, lesion-to-brain contrast-to-noise measurements for  $T_1$ -weighted pre- and postcontrast images were calculated as follows:  $(SI_{\text{lesion}} - SI_{\text{brain}})/SI_{\text{noise}}$ . On the basis of values recorded on  $T_1$ -weighted pre- and postcontrast (gadoteridol, 24-hour ferumoxytol) images, the percentage of signal intensity (SI) change in the lesion was calculated as follows:  $[(SI_{\text{postcontrast}} - SI_{\text{precontrast}}) \times 100]/SI_{\text{precontrast}}$ . ROIs of equal size were positioned at identical coordinates on all corresponding image sets. The ROIs were placed to encompass as much of the enhancing lesion as possible while avoiding necrosis or scarring within the lesion. The ROIs larger than  $20 \text{ mm}^2$  were used to measure the SI of contralateral normal brain parenchyma and background noise. All SI measurements were made using ImageJ software (NIH).
- (v) All first-pass DSC MRI data were processed using Lupe (Lund) perfusion image analysis software. The arterial input function was determined from the middle cerebral artery contralateral to the enhancing lesion. Color-coded rCBV maps were created on a voxel-wise basis uncorrected for contrast leakage and were overlaid onto  $T_1$ -weighted gadoteridol-enhanced images. Within the enhancing lesion, a single voxel ( $3 \times 3 \times 3 \text{ mm}$ ) ROI with the highest rCBV value was chosen on the ferumoxytol-rCBV parametric map. An ROI of equal size was positioned at identical coordinates on the gadoteridol-rCBV parametric map. ROI analyses were performed in native image space—an approach that is more labor-intensive but avoids interpolation errors frequently associated with rigid-body coregistration methods—using ImageJ software (NIH). Areas depicting major vessels were excluded from ROIs. Normal white matter within the contralateral hemisphere was

used as the internal reference standard; rCBV values were calculated by dividing the maximal rCBV of the lesion by that of contralateral normal-appearing white matter.

### Statistical Analysis

Categorical variables were presented as numbers. Continuous variables were expressed as means (standard errors), unless otherwise stated. The normality of distribution for all continuous variables was determined by the Kolmogorov–Smirnov test. The distribution of preferences for gadoteridol or ferumoxytol in various diagnostic information end-points (border delineation, visualization of lesion internal morphology, contrast enhancement) was tested using the Wilcoxon signed rank test. For enhancement volumes, SI changes, and rCBV ratios, the differences between the value using gadoteridol and the value using ferumoxytol were compared using paired  $t$ -tests. For contrast-to-noise ratios (CNRs), there were 3 groups of values (precontrast, gadoteridol, ferumoxytol) to compare; therefore, a mixed model, repeated measures analysis of variance (ANOVA) was performed, and multiple comparisons were made using the Tukey–Kramer adjustment if there was a significant difference among these values. All statistical computations were performed using SAS Version 9.2 for Windows (SAS Institute Inc.), and the results were declared significant at the two-sided 5% comparison-wise significance level ( $P < .05$ ).

## Results

Among 36 patients considered for inclusion in the study, no enhancing lesion was seen in 3 subjects with either gadoteridol or ferumoxytol. In 7 participants with end-stage renal disease or history of kidney transplantation, only ferumoxytol was used as a contrast agent. Therefore, 26 patients (18 men, 8 women; mean age, 47 years; age range, 19–72 years) were included for final comparative analysis. Twenty-three patients had histologically verified malignant brain tumors, including primary glial tumor ( $n = 19$ ), angiocentric T-cell lymphoma ( $n = 1$ ), and secondary metastasis ( $n = 3$ ). Three patients had benign brain tumors [meningioma ( $n = 2$ ), pituitary adenoma ( $n = 1$ )] (Table 1). All patients underwent surgery or biopsy 39.6 (3–255) [mean (range)] months before the study and 24 of them received 53.8 (0.5–61.5) [mean (range)] Gy fractionated external beam radiation therapy 31.7 (1–309) [mean (range)] months prior to study enrollment (Table 1). Ten out of 26 patients were treated with chemotherapy, 5 with bevacizumab (Avastin, Genentech; 5 or 10 mg/kg) alone or in combination with chemotherapeutic agents, and 11 were taking steroids (4–20 mg/day dexamethasone) at the time of the study (Table 1).

There were no adverse events attributed to either contrast material.

**Table 1.** Demographics and treatments

Patient No./ Gender/Age (years)	Histological Diagnosis	Treatment						
		Surgery		Radiation		Chemotherapeutic Agents	Steroids (mg/day)	Bevacizumab (mg/kg)
		Type	Time Interval (months)	Dose (Gy)	Time Interval (months)			
1/M/50	Glioblastoma multiforme	GTR	6	59.4	4	—	—	—
2/M/50	Glioblastoma multiforme	BX	9	59.4	7	C, T	4	10
3/F/46	Glioblastoma multiforme	STR	14	59.4	13	L	12	—
4/M/19	Glioblastoma multiforme	GTR	5	59.4	2	—	12	—
5/M/19	Glioblastoma multiforme	GTR	8	59.4	5	T	12	5
6/M/56	Glioblastoma multiforme	PR	32	59.4	29	T	—	—
7/F/57	Glioblastoma multiforme	GTR	9	59.4	6	T	—	—
8/F/57	Glioblastoma multiforme	GTR	12	59.4	9	T	—	—
9/M/54	Glioblastoma multiforme	PR	3	59.4	1	—	12	—
10/M/62	Glioblastoma multiforme	GTR	5	60	2	—	4	—
11/M/62	Glioblastoma multiforme	GTR	6	60	4	T	—	5
12/F/62	Glioblastoma multiforme	PR	7	60	3	T	8	—
13/M/32	Anaplastic oligodendroglioma	GTR	54	—	—	—	—	—
14/F/58	Anaplastic ependymoma	GTR	8	57.5	7	C	20	5
15/M/51	Anaplastic astrocytoma	BX	5	59.4	3	—	16	—
16/F/33	Anaplastic astrocytoma	BX	71	59.4	70	I	16	5
17/M/26	Pilocytic astrocytoma	PR	153	50.4	11	—	—	—
18/M/31	Astroblastoma	GTR	21	54	20	—	—	—
19/M/44	Pineoblastoma	GTR	87	50.4	72	—	—	—
20/M/46	Angiocentric T-cell lymphoma	BX	3	—	—	—	—	—
21/M/40	Nasopharyngeal carcinoma metastasis	BX	44	61.5	24	—	—	—
22/M/35	Melanoma metastasis	STR	28	48	28	—	—	—
23/F/72	Non small cell lung carcinoma metastasis	GTR	25	35	12	—	16	—
24/F/49	Meningioma	PR	255	50.4	309	—	—	—
25/M/53	Meningioma	STR	44	50.4	10	—	—	—
26/M/59	Non secreting pituitary adenoma	GTR	115	0.5	110	—	—	—

BX, biopsy; PR, partial resection; STR, subtotal resection; GTR, gross total resection; C, carboplatin; I, irinotecan; L, lomustine; T, temozolomide.

### Lesion Detection

All of the image sets from each of the 26 evaluated patients were technically adequate for assessment. Except for 2 patients, all participants had unifocal disease; in the 2 subjects with multifocal disease, only the largest most prominent lesion was assessed.  $T_1$ -weighted enhancement and/or  $T_2$  signal dropout consistent with iron accumulation was detected in only 4 lesions within 29 minutes (mean, 25.2 minutes; range, 23–29 minutes) after ferumoxytol administration. All lesions showed 24-hour  $T_1$  SI changes, but only 16 of them had  $T_2$  hypointensities in the approximate region where gadoteridol enhancement was seen (Fig. 1A–H). The SI changes were more prominent and extended into a larger area on the 24-hour ferumoxytol-enhanced images compared with the 25-minute studies (Fig. 1C, D, G, and H). Six patients

had ferumoxytol enhancement in areas that did not correspond to gadoteridol enhancement (Fig. 2).

### Qualitative Image Assessment

Side-by-side analysis of  $T_1$ -weighted postcontrast images revealed that in 20 cases the lesions appeared more clearly after gadoteridol administration and the morphology of gadoteridol enhancement was more homogeneous compared with the hazy, punctate pattern of ferumoxytol enhancement (Fig. 3). In general, the ferumoxytol-induced hyperintense  $T_1$  SI changes were readily detectable, while the hypointense  $T_2$  SI changes were modest and more variable, but their volumes were relatively equivalent.

Comparison of  $T_1$ -weighted postcontrast images showed highly significant preferences ( $P = .0121$ ;

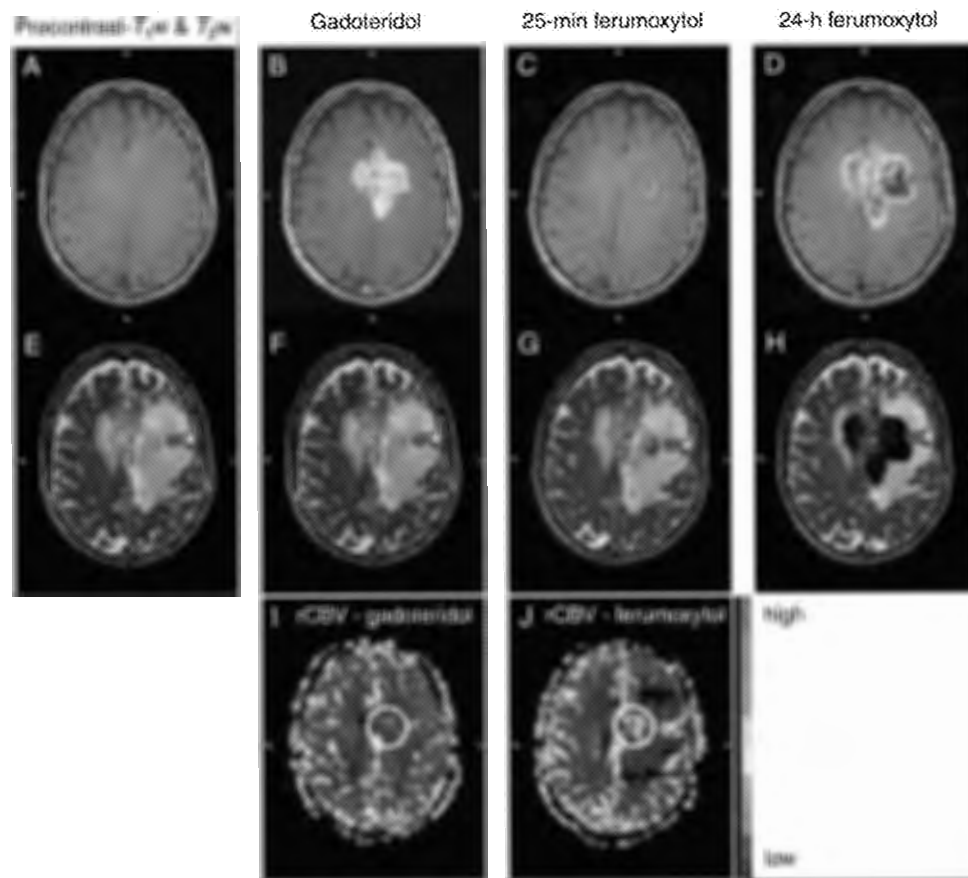


Fig. 1. Patient 8 with glioblastoma multiforme. (A and B) Nonenhanced (A) and gadoteridol-enhanced (B)  $T_1$ -weighted images of a left frontoparietal mass, which crosses the midline. The gadoteridol-enhanced image shows evidence of strong enhancement. (C) Twenty-five minutes after ferumoxytol administration, the  $T_1$ -weighted image demonstrates some faint, mainly punctate, enhancement within the mass. (D) Twenty-four hours after ferumoxytol injection, mixed SI changes are seen in the approximate region where gadoteridol enhancement is noted. (E–H)  $T_2$ -weighted images obtained before (E) and after gadoteridol (F), 25 minutes (G), and 24 hours after ferumoxytol injection (H). Twenty-five minutes after ferumoxytol administration, the  $T_2$ -weighted image shows some punctate and a curvilinear hypointensity within the mass. Twenty-four hours after ferumoxytol injection, strong lobulated areas of decreased signal are observed. The distribution of low SI areas is similar to that of mixed high and low SI areas on the  $T_1$ -weighted image in (D). (I and J) Color-coded rCBV parametric maps. The ferumoxytol-rCBV parametric map (J) shows high blood volume within the tumor, while the gadoteridol-rCBV parametric map (I) does not.

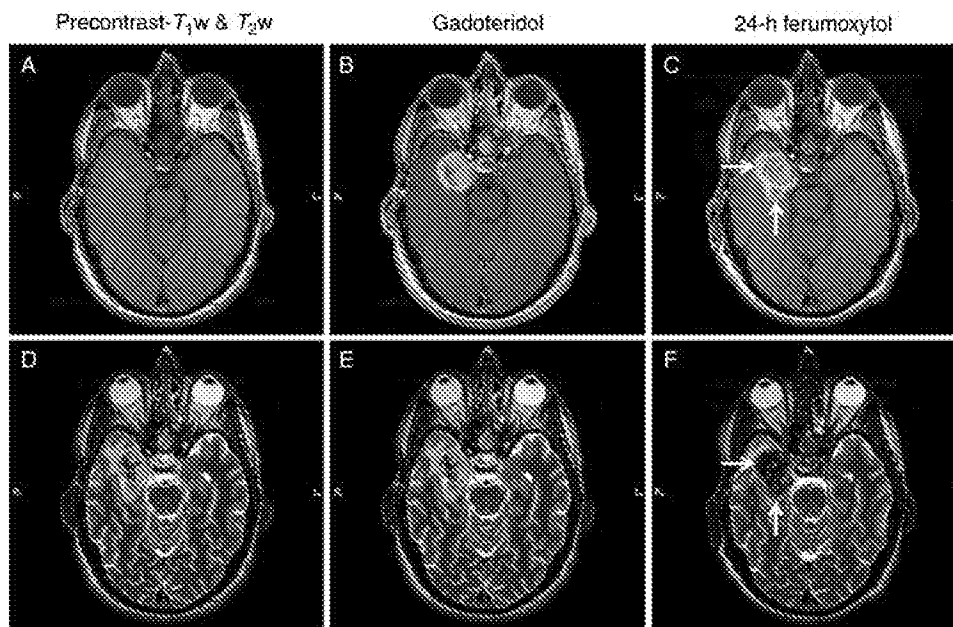


Fig. 2. Patient 6 with glioblastoma multiforme. (A–C) Nonenhanced (A), gadoteridol- (B), and ferumoxytol-enhanced (C)  $T_1$ -weighted images of a right medial temporal tumor. A linear intrinsic  $T_1$  signal is seen in the lateral portion of the mass. The gadoteridol-enhanced image shows evidence of strong enhancement. Twenty-four hours after ferumoxytol administration, additional area of enhancement is noted around the mass (arrows), compared with the gadoteridol-enhanced images. (D–F)  $T_2$ -weighted images obtained before (D) and after gadoteridol (E) and 24 hours after ferumoxytol injection (F). Hypointense signal is demonstrated on the precontrast images in the same area where an intrinsic  $T_1$  signal is seen. Twenty-four hours after ferumoxytol injection, strong decreased signal is observed within and around the tumor (arrows). The distribution of the low SI area is similar to that of the high SI area on the  $T_1$ -weighted image in (C).

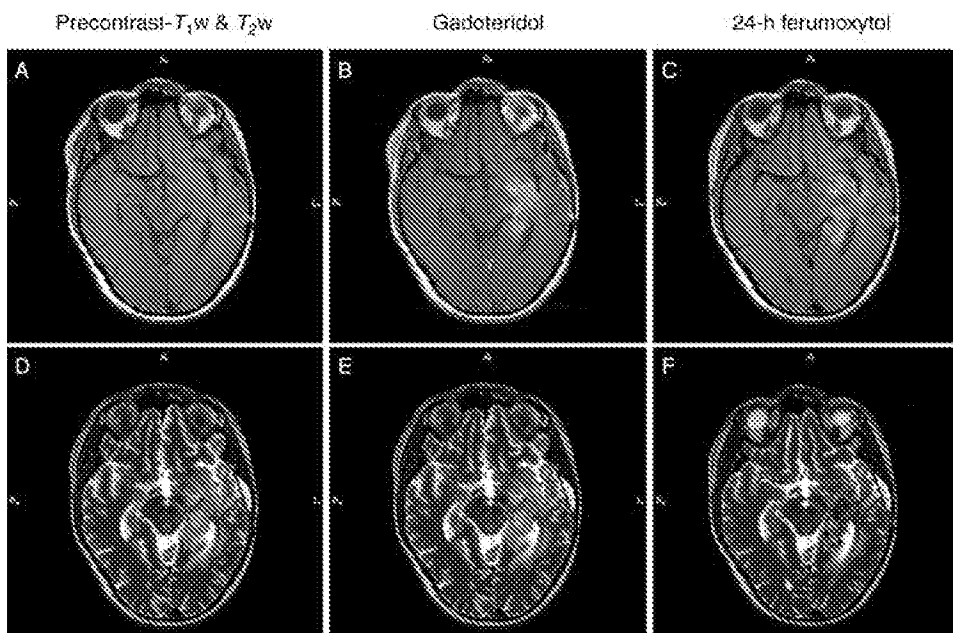


Fig. 3. Patient 3 with glioblastoma multiforme. (A–C) Nonenhanced (A), gadoteridol- (B), and ferumoxytol-enhanced (C)  $T_1$ -weighted images of a left temporal tumor. The mass is enhancing both with gadoteridol and ferumoxytol. The gadoteridol enhancement is more homogeneous compared with the punctate pattern of the 24-hour ferumoxytol enhancement. (D–F)  $T_2$ -weighted images obtained before (D) and after gadoteridol (E) and 24 hours after ferumoxytol injection (F). The ferumoxytol-enhanced image shows punctate hypointensities within the mass.



$P = .0015$ ;  $P < .0001$ , respectively) for gadoteridol compared with ferumoxytol for border delineation, visualization of internal morphology, and lesion contrast enhancement (Fig. 4).

**Enhancement Volume**

There was no significant difference ( $P = .4471$ ) in enhancement volumes of the lesions [ $24.5 (5.0) \text{ cm}^3$ ,  $22.3 (4.7) \text{ cm}^3$ , respectively] measured on  $T_1$ -weighted gadoteridol- and 24-hour ferumoxytol-enhanced images.

**CNR and SI Change**

A significant difference ( $P < .0001$ ) was demonstrated among the CNRs obtained on  $T_1$ -weighted precontrast, gadoteridol-enhanced and 24-hour ferumoxytol-enhanced images. The CNR least square means (standard errors) were 0.90 (0.04) for precontrast, 1.58

(0.04) for gadoteridol, and 1.29 (0.04) for ferumoxytol (Fig. 5A).

The mean percentages of SI changes induced by contrast agent administration on  $T_1$ -weighted images are shown in Fig. 5B. Significantly greater ( $P < .0001$ ) SI changes were seen with gadoteridol [ $58.3 (5.1)\%$ ] than with ferumoxytol [ $28.7 (3.8)\%$ ].

**Relative Cerebral Blood Volume**

All 26 patients showed significant  $T_2^*$ -weighted SI decreases during each contrast agent first-pass in both lesion and normal-appearing brain tissue areas.

The ferumoxytol-rCBV values [ $3.73 (0.68)$ ] were significantly higher ( $P = .0016$ ) than the gadoteridol-rCBV values [ $2.52 (0.56)$ ] (Fig. 6A).

A threshold rCBV ratio of the highest lesion blood volume to the normal-appearing contralateral white matter blood volume, measured by DSC MRI using GBCA of 1.75, has been shown to predict time to progression or survival.<sup>10,11</sup> Therefore, in our study, rCBV > 1.75 was considered high and rCBV < 1.75 low. The rCBV values were elevated both with ferumoxytol and gadoteridol in 14 subjects (patients 1, 2, 3, 6, 9, 11, 13, 14, 15, 16, 18, 24, 25, and 26; Table 1), although in 8 subjects the Gd-rCBV ratios were only slightly elevated compared with the 1.75 cutoff (Fig. 6B). The rCBV values were low with both contrast agents in 10 subjects (patients 5, 7, 10, 12, 17, 19, 20, 21, 22, and 23). There was a discordance between rCBV values in 2 GBM patients (subjects 4 and 8) who had elevated rCBV with ferumoxytol, but had low rCBV on the gadoteridol-rCBV parametric map (Figs 1I, J and 6B). Both participants showed worsening clinical condition and increased areas of enhancement on gadoteridol-enhanced  $T_1$ -weighted images 3 months after the study. Among those 5 patients who were treated with bevacizumab at the time of the study, 4 had low rCBV values, while 1 had elevated rCBV values with both contrast materials reflecting resistance to treatment.

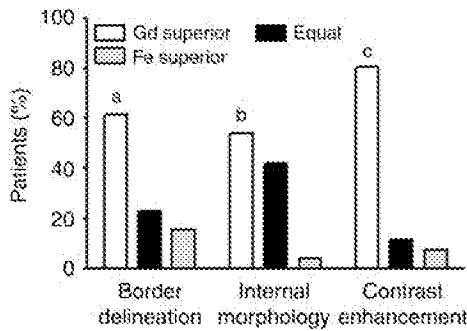


Fig. 4. Qualitative evaluation of  $T_1$ -weighted postcontrast MR images. Neuroradiologists expressed significant preferences (a,  $P = .0121$ ; b,  $P = .0015$ ; c,  $P < .0001$ , respectively) for gadoteridol compared with ferumoxytol for border delineation, internal morphology, and contrast enhancement of the lesions. The Wilcoxon signed rank test was used. Gd, gadoteridol; Fe, ferumoxytol.

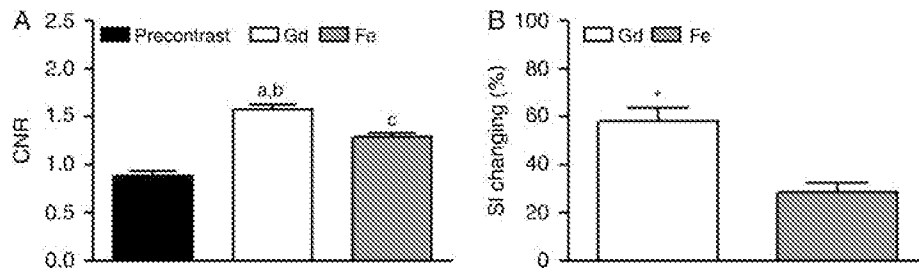


Fig. 5. Quantitation of  $T_1$ -weighted MR images. (A) A significant difference ( $P < .0001$ ) was demonstrated among the CNRs obtained on  $T_1$ -weighted precontrast, gadoteridol-, and 24-hour ferumoxytol-enhanced images. a,  $P < .0001$  for gadoteridol enhancement compared with precontrast images; b,  $P < .0001$  for gadoteridol enhancement compared with ferumoxytol enhancement; c,  $P < .0001$  for ferumoxytol enhancement compared with precontrast images. ANOVA and Tukey-Kramer adjustment were used. CNR, contrast-to-noise ratio; Gd, gadoteridol; Fe, ferumoxytol. (B) Significantly greater (\*,  $P < .0001$ ) SI changes were noted with gadoteridol than with ferumoxytol. The paired  $t$ -test was used. SI, signal intensity; Gd, gadoteridol; Fe, ferumoxytol.

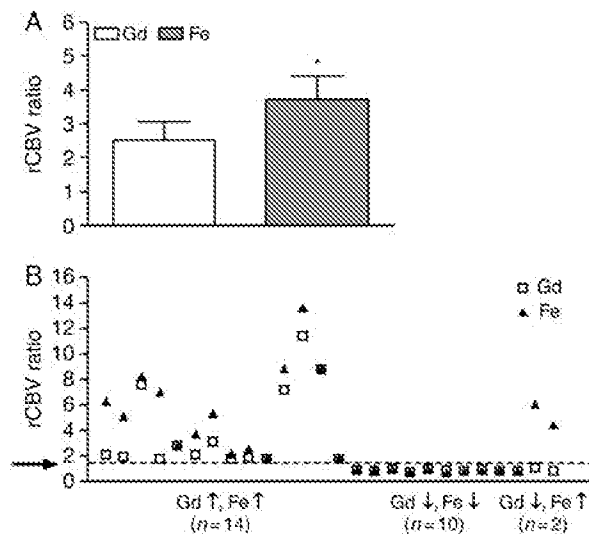


Fig. 6. Analysis of dynamic susceptibility contrast MR images. (A) The ferumoxytol-rCBV values were significantly higher (\*,  $P = .0016$ ) compared with the gadoteridol-rCBV values. The paired  $t$ -test was used. rCBV, relative cerebral blood volume; Gd, gadoteridol; Fe, ferumoxytol. (B) The rCBV values were elevated both with ferumoxytol and with gadoteridol in 14 patients, they were low with both contrast agents in 10, and there was a discordance between them in 2 participants. The arrow indicates a threshold rCBV ratio of 1.75. rCBV, relative cerebral blood volume; Gd, gadoteridol; Fe, ferumoxytol.

## Discussion

Cerebral neoplasms are characterized by the leakiness of aberrant blood vessels and macrophage infiltration within and around the lesions, in addition to the presence of neoplastic cells. In this study, gadoteridol was used to detect vascular leakage and ferumoxytol to provide a more accurate measurement of rCBV and as a molecular agent to determine intracellular uptake within inflammatory cells in patients with intracranial tumors. These data provide insights into tumor biology and treatment effects. Elevated rCBV and minimal intracellular uptake suggest a predominance of residual or recurrent tumor, while low rCBV and increased intracellular accumulation of USPIOs would be expected within areas of suspected treatment effects.

Ferumoxytol was injected in the amount of 510 mg for all patients regardless of body weight. The intent of using a standard maximal administration was to achieve the highest possible plasma levels of ferumoxytol and thereby maximize its tissue uptake. We did not investigate the effect of ferumoxytol dose in this study. Three fundamentally different MRI sequences were used to compare gadoteridol with ferumoxytol: (1)  $T_1$ -weighted anatomical MRI, (2)  $T_2$ -weighted anatomical MRI, and (3)  $T_2^*$ -weighted DSC MRI scan. We emphasize that  $T_2^*$ -weighted SI decreases always were observed during gadoteridol and ferumoxytol first-pass DSC measurements.

USPIOs produce a hypointense signal on  $T_2$ - or  $T_2^*$ -weighted MR images in addition to  $T_1$

enhancement.<sup>12,13</sup> In our study all lesions had gadoteridol and 24-hour ferumoxytol enhancement on  $T_1$ -weighted SE images.  $T_2$  shortening consistent with iron accumulation was detected in 16 patients 24 hours after ferumoxytol administration; among them 4 showed 25-minute  $T_2$  SI change. The USPIO-induced SI changes are known to be dose dependent. Whereas iron uptake results in  $T_2$  shortening at higher concentrations,  $T_1$  shortening effect peaks at lower concentrations.<sup>12,13</sup> Thus, at doses applied in this study, the iron accumulation was not concentrated enough to cause a decreased signal on  $T_2$ -weighted TSE images in all lesions. It is unknown whether this means that there was ferumoxytol uptake in phagocytic cells but at low concentrations or that there were not very many macrophages to endocytose USPIOs, because no histopathological analyses were performed in this study.

The exact route of USPIO entry into the CNS is not fully established. Both passive leakage of iron oxides over an impaired blood-brain barrier (BBB) and their active transcytosis through the CNS capillary membranes have been suggested to contribute to USPIO enhancement in the brain.<sup>14,15</sup> Although most of the nanoparticles are concentrated intracellularly according to immunohistochemical results of biopsy specimens, a small amount can also be present in the extracellular space.<sup>7,16</sup> This observation might explain why in 4 cases SI changes were detected as early as 25 minutes, because it is unlikely that phagocytic cells can incorporate iron nanoparticles within such a short time frame.

The 24-hour ferumoxytol enhancement covered a larger area compared with the 25-minute studies and in 6 patients extended beyond the border of the lesions delineated by gadoteridol on  $T_1$ -weighted SE images. The mechanism for this additional MRI signal change of USPIOs is most likely to be the result of intracellular trapping of iron oxides by microglia and macrophages. It should be noted that accurate brain tumor delineation is a challenging task, especially in patients with highly infiltrative tumor. Posttreatment changes may further complicate the interpretation of MR images; therefore, the true boundary of any tumor is possibly not specified by either contrast agent.

Some histopathological studies have suggested a direct association between tumor grade and number as well as location of iron-loaded microglia.<sup>7,17</sup> Parallel with these observations, the intensity and morphology of USPIO enhancement on MR images were found to be correlated to tumor malignancy: malignant lesions, such as high-grade gliomas, showed prominent enhancement both within and around the tumor, and particularly prominently around the necrotic areas, whereas low-grade gliomas and benign lesions, like pituitary adenomas and meningiomas, demonstrated minimal SI changes mainly at the tumor margin or showed no enhancement.<sup>7,18</sup> Although we noted similar tendencies in benign intracranial lesions, in patients with malignant brain tumors the morphology and intensity of ferumoxytol enhancement varied widely, presumably because of treatment-related effects.

Conventional MRI has limited ability to detect therapy-associated changes in tumor viability. Surgery

and radiochemotherapy are known to cause increased contrast enhancement due to the alteration of vascular permeability and activation of microglial cells.<sup>19–21</sup> On the other hand, the human antivascular endothelial growth factor monoclonal antibody bevacizumab has been shown to prune abnormal vessels and normalize existing vasculature, thus decreasing GBCA enhancement.<sup>22</sup> Besides its added value as a corroborative approach for achieving a diagnosis and guiding biopsies, PW MRI has also proven to be beneficial for mapping response to treatment with antiangiogenic agents.<sup>23</sup> Moreover, it has an essential role in differentiating tumor progression from radiochemotherapy-induced pseudoprogression as radiation necrosis typically reveals decreased rCBV within the area of abnormal enhancement, whereas high-grade tumor recurrence results in increased rCBV values.<sup>6,24,25</sup> Relative quantification of CBV has been found to correlate with both conventional angiographic assessments of tumor vascular density and histologic evaluation of tumor neoangiogenesis.<sup>26,27</sup> Despite a positive association existing between the degree of vascularity and tumor aggressiveness, some of the benign lesions (e.g. meningioma) also can be highly vascular.

The application of USPIOs may be most useful for studying tumor microvasculature. We have previously reported that rCBV estimation using ferumoxytol is reliable and does not require leakage correction.<sup>5,8</sup> The observed lower gadoteridol rCBV values in comparison with the ferumoxytol results in the present study are not surprising. In the case of disrupted BBB, the rapid extravasation of GBCAs from capillaries to the interstitial space leads to inaccurate CBV estimation using modeling approaches that assume contrast agents are localized only within the vascular compartment. In contrast to gadoteridol, USPIOs have a low leakage rate due to their large particle size, which makes them suitable for first-pass as well as steady-state measurements and allows precise quantification of perfusion images.

## Conclusions

We have shown here that the 24-hour ferumoxytol enhancement differed from the gadoteridol enhancement in morphology and intensity. Ferumoxytol has 2 important uses that can provide additional information for brain tumor assessment either alone or in conjunction with GBCA. First, conventional MRI with ferumoxytol can detect an inflammatory component, because these nanoparticles are taken up by phagocytic cells. Second, as ferumoxytol is a blood pool agent at early time points, rCBV measurement with USPIO provides a better indicator of tumor progression than with typical GBCA, which is essential for diagnostic purposes and assessment of treatment efficacy. Beyond that, ferumoxytol has a good biocompatibility profile and has no known long-term toxicity, which makes it an attractive contrast agent for MR imaging, especially in patients with decreased renal function.

## Acknowledgments

This work was supported by National Institutes of Health grants CA137488, NS53468, and ARRA CA137488-1551, and an NCI-Fredrick Cancer Research and Development Center Contract to EAN. NIHRO1 EB007258 and NSO4801 to WDR.

*Conflict of interest statement.* None declared.

## Funding

OHSU has received a sponsored research agreement from AMAG Pharmaceuticals to conduct clinical trials of MRI with ferumoxytol. None of the authors has financial interest in this agent or in its developer AMAG Pharmaceuticals.

## References

- Weinreb JC, Kuo PH. Nephrogenic systemic fibrosis. *Magn Reson Imaging Clin N Am.* 2009;17(1):159–167.
- Neuwelt EA, Hamilton BE, Varallyay CG, et al. Ultrasmall superparamagnetic iron oxides (USPIOs): a future alternative magnetic resonance (MR) contrast agent for patients at risk for nephrogenic systemic fibrosis (NSF)? *Kidney Int.* 2009;75(5):465–474.
- Weinstein JS, Varallyay CG, Dosa E, et al. Superparamagnetic iron oxide nanoparticles: diagnostic magnetic resonance imaging and potential therapeutic applications in neurooncology and central nervous system inflammatory pathologies, a review. *J Cereb Blood Flow Metab.* 2010;30(1):15–35.
- Wu YJ, Muldoon LL, Varallyay C, et al. In vivo leukocyte labeling with intravenous ferumoxides/protamine sulfate complex and in vitro characterization for cellular magnetic resonance imaging. *Am J Physiol Cell Physiol.* 2007;293(5):C1698–1708.
- Varallyay CG, Muldoon LL, Gahramanov S, et al. Dynamic MRI using iron oxide nanoparticles to assess early vascular effects of antiangiogenic versus corticosteroid treatment in a glioma model. *J Cereb Blood Flow Metab.* 2009;29(4):853–860.
- Gahramanov S, Raslan AM, Muldoon LL, et al. Potential for differentiation of pseudoprogression from true tumor progression with dynamic susceptibility-weighted contrast-enhanced magnetic resonance imaging using ferumoxytol vs. gadoteridol: a pilot study. *Int J Radiat Oncol Biol Phys.* 2010.
- Muldoon LL, Sandor M, Pinkston KE, et al. Imaging, distribution, and toxicity of superparamagnetic iron oxide magnetic resonance nanoparticles in the rat brain and intracerebral tumor. *Neurosurgery.* 2005;57(4):785–796, discussion: 785–796.
- Neuwelt EA, Varallyay CG, Manninger S, et al. The potential of ferumoxytol nanoparticle magnetic resonance imaging, perfusion, and angiography in central nervous system malignancy: a pilot study. *Neurosurgery.* 2007;60(4):601–611, discussion: 611–602.
- Spinowitz BS, Kausz AT, Baptista J, et al. Ferumoxytol for treating iron deficiency anemia in CKD. *J Am Soc Nephrol.* 2008;19(8):1599–1605.
- Cao Y, Tsien CI, Nagesh V, et al. Survival prediction in high-grade gliomas by MRI perfusion before and during early stage of RT [corrected]. *Int J Radiat Oncol Biol Phys.* 2006;64(3):876–885.

11. Law M, Young RJ, Babb JS, et al. Gliomas: predicting time to progression or survival with cerebral blood volume measurements at dynamic susceptibility-weighted contrast-enhanced perfusion MR imaging. *Radiology*. 2008;247(2):490–498.
12. Chambon C, Clement O, Le Blanche A, et al. Superparamagnetic iron oxides as positive MR contrast agents: in vitro and in vivo evidence. *Magn Reson Imaging*. 1993;11(4):509–519.
13. Muller RN, Gillis P, Moyny F, et al. Transverse relaxivity of particulate MRI contrast media: from theories to experiments. *Magn Reson Med*. 1991;22(2):178–182; discussion 195–176.
14. Dousset V, Delalande C, Ballarino L, et al. In vivo macrophage activity imaging in the central nervous system detected by magnetic resonance. *Magn Reson Med*. 1999;41(2):329–333.
15. Rausch M, Hiestand P, Baumann D, et al. MRI-based monitoring of inflammation and tissue damage in acute and chronic relapsing EAE. *Magn Reson Med*. 2003;50(2):309–314.
16. Neuwelt EA, Varallyay P, Bago AC, et al. Imaging of iron oxide nanoparticles by MR and light microscopy in patients with malignant brain tumours. *Neuropathol Appl Neurobiol*. 2004;30(5):456–471.
17. Roggendorf W, Strupp S, Paulus W. Distribution and characterization of microglia/macrophages in human brain tumors. *Acta Neuropathol*. 1996;92(3):288–293.
18. Varallyay P, Nesbit G, Muldoon LL, et al. Comparison of two superparamagnetic viral-sized iron oxide particles ferumoxides and ferumoxtran-10 with a gadolinium chelate in imaging intracranial tumors. *AJNR Am J Neuroradiol*. 2002;23(4):510–519.
19. de Wit MC, de Bruin HG, Eijkenboom W, et al. Immediate post-radiotherapy changes in malignant glioma can mimic tumor progression. *Neurology*. 2004;63(3):535–537.
20. Kumar AJ, Leeds NE, Fuller GN, et al. Malignant gliomas: MR imaging spectrum of radiation therapy- and chemotherapy-induced necrosis of the brain after treatment. *Radiology*. 2000;217(2):377–384.
21. Vos MJ, Uitdehaag BM, Barkhof F, et al. Interobserver variability in the radiological assessment of response to chemotherapy in glioma. *Neurology*. 2003;60(5):826–830.
22. Jain RK. Normalizing tumor vasculature with anti-angiogenic therapy: a new paradigm for combination therapy. *Nat Med*. 2001;7(9):987–989.
23. Cha S, Knopp EA, Johnson G, et al. Dynamic contrast-enhanced T2-weighted MR imaging of recurrent malignant gliomas treated with thalidomide and carboplatin. *AJNR Am J Neuroradiol*. 2000;21(5):881–890.
24. Covarrubias DJ, Rosen BR, Lev MH. Dynamic magnetic resonance perfusion imaging of brain tumors. *Oncologist*. 2004;9(5):528–537.
25. Sugahara T, Korogi Y, Tomiguchi S, et al. Posttherapeutic intraaxial brain tumor: the value of perfusion-sensitive contrast-enhanced MR imaging for differentiating tumor recurrence from nonneoplastic contrast-enhancing tissue. *AJNR Am J Neuroradiol*. 2000;21(5):901–909.
26. Aronen HJ, Gazit IE, Louis DN, et al. Cerebral blood volume maps of gliomas: comparison with tumor grade and histologic findings. *Radiology*. 1994;191(1):41–51.
27. Sugahara T, Korogi Y, Kochi M, et al. Correlation of MR imaging-determined cerebral blood volume maps with histologic and angiographic determination of vascularity of gliomas. *AJR Am J Roentgenol*. 1998;171(6):1479–1486.

## Phase III Study of Oral Compared With Intravenous Topotecan As Second-Line Therapy in Small-Cell Lung Cancer

John R. Eckardt, Joachim von Pawel, Jean-Louis Pujol, Zsolt Papai, Elisabeth Quoix, Andrea Ardizzoni, Ruth Poulin, Alaknanda J. Preston, Graham Dane, and Graham Ross

### ABSTRACT

#### Purpose

Single-agent intravenous (IV) topotecan is an effective treatment for small-cell lung cancer (SCLC) after failure of first-line chemotherapy. This open-label, randomized, phase III study compared oral and IV topotecan in patients with SCLC sensitive to initial chemotherapy.

#### Patients and Methods

Patients with limited- or extensive-disease SCLC, documented complete or partial response to first-line therapy, Eastern Cooperative Oncology Group performance status  $\leq 2$ , and measurable recurrent disease (WHO criteria) with a treatment-free interval of  $\geq 90$  days were assigned to treatment with either oral topotecan 2.3 mg/m<sup>2</sup>/d on days 1 through 5 or IV topotecan 1.5 mg/m<sup>2</sup>/d on days 1 through 5 every 21 days. Primary end point was response rate as confirmed by an external reviewer blinded to treatment.

#### Results

A total of 309 patients were randomly assigned. In intent-to-treat analysis, response rates were 18.3% with oral topotecan (n = 153) and 21.9% with IV topotecan (n = 151), with a difference (oral – IV) of –3.6% (95% CI, –12.6% to 5.5%). Median survival time was 33.0 weeks for oral and 35.0 weeks for IV topotecan; 1- and 2-year survival rates were 32.6% and 12.4% for oral topotecan, respectively, and 29.2% and 7.1% for IV topotecan, respectively. Third-line chemotherapy was similar for both groups (33% for oral; 35% for IV). Incidence of grade 4 toxicity in patients who received oral and IV topotecan was as follows: neutropenia in 47% and 64%, thrombocytopenia in 29% and 18%, grade 3 or 4 anemia in 23% and 31%, and sepsis in 3% and 3%, respectively. The most frequent nonhematologic adverse events (all grades) included nausea (43% oral; 42% IV), alopecia (26% oral; 30% IV), fatigue (31% oral; 36% IV), and diarrhea (36% oral; 20% IV).

#### Conclusion

Oral topotecan demonstrates activity and tolerability similar to IV topotecan in chemotherapy-sensitive SCLC patients and offers patients a convenient alternative to IV therapy.

*J Clin Oncol* 25:2086-2092. © 2007 by American Society of Clinical Oncology

### INTRODUCTION

Small-cell lung cancer (SCLC) is an aggressive pulmonary tumor comprising approximately 13% of lung cancers.<sup>1</sup> Prognosis for patients with SCLC who have experienced relapse is poor; expected survival in untreated patients is 2 to 3 months.<sup>2</sup> New, non-cross-resistant therapeutic options in SCLC are needed.

Topotecan is a topoisomerase I inhibitor widely available as an intravenous (IV) formulation for the treatment of patients with sensitive SCLC after failure of first-line therapy. Three phase II studies of single-agent IV topotecan have shown re-

sponse rates of 14% to 38% among sensitive patients.<sup>3-5</sup> Among refractory patients, response rates were 2% to 6%. Median survival time was 26 to 28 weeks for sensitive patients compared with 16 to 20 weeks for refractory patients. A meta-analysis of sensitive patients in all three studies reported an 18% response rate and a median survival time of 30 weeks.<sup>6</sup>

A randomized phase II study comparing oral versus IV topotecan as second-line treatment in sensitive SCLC patients showed response rates of 23% for oral topotecan and 15% for IV topotecan; median survival times were 32 and 25 weeks, respectively.<sup>7</sup> We hypothesized that similar response rates

From the Center for Cancer Care and Research, St Louis, MO; Asklepios Klinik, Gauting bei Muenchen, Germany; Hôpital Arnaud de Villeneuve, Montpellier; University Hospital, Strasbourg, France; St George County Hospital, Székesfehérvár, Hungary; University Hospital, Parma, Italy; GlaxoSmithKline, Collegeville, PA; and GlaxoSmithKline, Harlow, United Kingdom.

Submitted July 24, 2006; accepted February 20, 2007.

Research funded by GlaxoSmithKline, Middlesex, United Kingdom.

Presented in part at the 39th Annual Meeting of the American Society of Clinical Oncology, Chicago, IL, May 31 to June 3, 2003.

Authors' disclosures of potential conflicts of interest and author contributions are found at the end of this article.

Address reprint requests to John R. Eckardt, MD, Center for Cancer Care and Research, 12855 N Outer Fourty Rd, Ste 200, St Louis, MO 63141; e-mail: jeckardt@cccr.com.

© 2007 by American Society of Clinical Oncology

0732-183X/07/2515-2086/\$20.00

DOI: 10.1200/JCO.2006.08.3998

would be seen with oral topotecan in this randomized phase III study. Oral topotecan 2.3 mg/m<sup>2</sup>/d for 5 days every 3 weeks was selected based on a phase I study using this schedule.<sup>8</sup> Reported oral bioavailability for topotecan is 30% to 40%.<sup>9-11</sup>

## PATIENTS AND METHODS

### Patient Selection

Patients were recruited from 83 centers in North America, Europe, the Southeast Asia, and Australia, randomly assigned in a 1:1 ratio, and stratified according to duration of response to first-line therapy (progression  $\leq$  6 months or  $>$  6 months), sex, and presence or absence of liver metastases. Eligible patients were those with limited or extensive-stage SCLC who had documented complete or partial response to first-line therapy with disease recurrence after  $\geq$  90 days and met the following inclusion criteria:  $\geq$  18 years old, only one prior chemotherapy regimen, bidimensionally measurable disease, an Eastern Cooperative Oncology Group performance status  $\leq$  2, WBC count  $\geq$  3,500/ $\mu$ L, neutrophils  $\geq$  1,500/ $\mu$ L, platelets  $\geq$  100,000/ $\mu$ L, hemoglobin  $\geq$  9.0 g/dL, serum creatinine  $\leq$  1.5 mg/dL, bilirubin  $\leq$  2.0 mg/dL, and alkaline phosphatase, AST, and ALT  $\leq$  2 $\times$  the upper limit of normal or  $\leq$  5 $\times$  the upper limit of normal with liver metastases. Patients with CNS metastases were eligible only if they were asymptomatic without corticosteroids. Prior surgery was allowed if  $\geq$  4 weeks had passed, as was immunotherapy ( $\geq$  3 months) and radiotherapy ( $\geq$  24 hours). Concurrent chemotherapy, immunotherapy, or radiotherapy was not permitted. Concurrent radiation for palliation of bone or brain lesions was not allowed unless discussed with the medical monitor.

The protocol was approved by the institutional review board at each site. Each patient provided written informed consent.

### Chemotherapy Regimens

Oral topotecan 2.3 mg/m<sup>2</sup>/d or IV topotecan 1.5 mg/m<sup>2</sup>/d (as a 30-minute infusion) was administered on days 1 through 5, every 3 weeks. Patients with complete or partial response continued treatment until disease progression or for two courses beyond best response. Patients with stable disease were recommended to receive at least four courses<sup>12</sup> because some responses have not been noted until completion of four to eight courses. Oral topotecan was supplied as capsules containing topotecan hydrochloride equivalent to 0.25 mg or 1.00 mg of the anhydrous free base (GlaxoSmithKline, Middlesex, United Kingdom).

During course 1, patients randomly assigned to oral topotecan were administered capsules under clinical supervision for each of the 5 days. During subsequent courses, only day 1 was orally administered in the clinic; capsules were dispensed for the remaining 4 days to be taken at home. Compliance was documented through pill counts.

### Dose Modifications

After course 1, dose escalation was permitted if no toxicity more than grade 2 occurred during the previous course. Oral topotecan dose was increased in increments of 0.4 mg/m<sup>2</sup> to a maximum of 3.1 mg/m<sup>2</sup>/d, and IV topotecan was increased in increments of 0.25 mg/m<sup>2</sup> to a maximum of 2.0 mg/m<sup>2</sup>/d. Severe or prolonged neutropenia or severe thrombocytopenia was managed via dose reduction. Minimum doses permitted were 1.5 mg/m<sup>2</sup>/d for oral topotecan and 1.0 mg/m<sup>2</sup>/d for IV topotecan; delays of more than 2 weeks at these doses resulted in study withdrawal.

### Assessments

Patients had to have lesions that were bidimensionally measurable according to WHO criteria.<sup>13</sup> After baseline evaluation, lesions were assessed either at the end of each course (if evaluated by photography or physical examination) or at the end of alternate courses (if evaluated by computed topography or magnetic resonance imaging, x-ray, or ultrasound). The same method of evaluation was to be used throughout the study.

All responses were verified by a central radiologist independent of patient management decisions and blinded to study treatment. By implementing

these stringent criteria, treatment responses have been shown to correlate with outcomes.<sup>14</sup>

Time to response was measured from first topotecan dose to first documented complete or partial response in patients who achieved a response; duration of response was measured from when response was first documented to disease progression. Time to progression was measured from first topotecan dose to progression; survival was measured from first dose until death. Follow-up was conducted at each study site to document dates of disease progression, any poststudy therapies administered, and date of death.

Blood counts were obtained on days 8 and 15 and before initiation of each subsequent course. Blood chemistry was evaluated on day 15, and if there was deterioration from baseline values, the evaluation was repeated before the next course. Toxicities (graded according to the National Cancer Institute Common Toxicity Criteria) were used to assess whether dose adjustments were indicated.

Health-related quality of life (HRQOL) was assessed using the Functional Assessment of Cancer Therapy–Lung (FACT-L).<sup>15</sup> FACT-L is a 44-item self-report instrument that includes four generic dimensions of HRQOL and a subscale that measures symptoms specific to lung cancer (Lung Cancer Subscale [LCS]). Generic dimensions include functional well-being, physical well-being, social and family well-being, and emotional well-being. LCS measures the severity of the following seven common symptoms: shortness of breath, cough, tightness in chest, difficulty breathing, appetite loss, weight loss, and lack of clear thinking. The Trial Outcome Index (TOI) is derived by adding the physical and functional well-being LCS subscale scores. FACT-L has been well validated, translated for use in many different countries,<sup>15-17</sup> and used extensively in clinical trial and other study settings. Patients completed the FACT-L as the initial event of their first clinic visit (eg, before course 1, or at baseline), before each subsequent course, and at study end.

Primary end point was response rate. Secondary end points were response duration, time to progression, time to response, survival, quality of life (QOL), and toxicities.

### Statistical Methods

Response rate was compared between treatments, and the estimated percent difference in response rates between regimens was calculated with 95% CIs. Sample size was not based on formal statistical criteria; rather, it was based on the feasibility of patient accrual and study completion. A study population of 150 patients per treatment arm provided 71% power that the 95% CI would exclude more than 10% difference in favor of IV treatment.

Time to event data (time to response, response duration, time to progression, and survival) were summarized using Kaplan-Meier survival methods. A hazard ratio for treatment in the presence of covariates (ie, duration of prior response, sex, and liver metastases) using Cox's proportional hazards model was generated for the survival end point.

QOL data were evaluated by calculating the total FACT-L score and the 21-item TOI.<sup>15</sup> Scores recorded before each course of treatment after the first course were compared with baseline scores. A repeated measures analysis was performed to compare the rate of change between the two treatment groups for each dimension or subscale.

## RESULTS

### Patients

Between January 25, 1999, and October 20, 2001, 309 patients were randomly assigned (Fig 1); 153 patients were assigned to oral topotecan, and 151 patients were assigned to IV topotecan (five patients received no treatment). Because there was no predetermined treatment duration, all patients who had least one full course of treatment were considered to have completed the study unless withdrawn as a result of an adverse event, protocol deviation, patient request, or loss to follow-up. Proportions of patients completing therapy were similar for both oral (124 patients, 81%) and IV topotecan (128 patients, 85%) treatment arms. Withdrawals for adverse events were

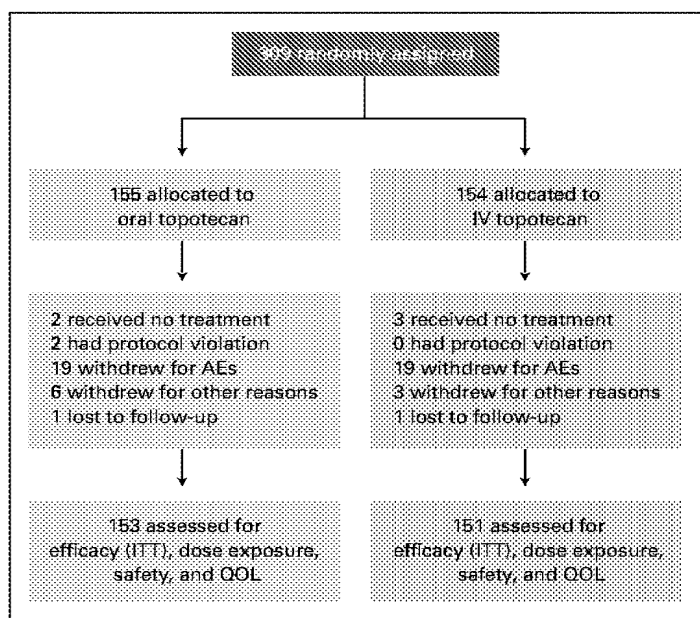


**Fig 1.** CONSORT diagram. IV, intravenous; AEs, adverse events; ITT, intent-to-treat; QOL, quality of life.

also similar in both groups (12% and 13% of patients on oral and IV topotecan, respectively).

Demographics and baseline characteristics were well matched between groups (Table 1). A majority of patients (approximately 70%) had extensive disease, and liver metastases were present in approximately 28% of patients. Forty-three patients had documented baseline brain or leptomeningeal metastases (18 patients on oral topotecan, and 25 patients on IV topotecan). All patients had responded to previous cancer chemotherapy; 129 patients (84.3%) in the oral topotecan arm and 125 patients (82.8%) in the IV topotecan arm had received prior combination chemotherapy that included platinum (cisplatin or carboplatin). Approximately 10% of patients in both treatment groups had a treatment-free interval of less than 90 days at study entry.

### Delivered Chemotherapy

In each treatment group, patients received a median of four courses of topotecan, with at least 40% of patients in either group continuing to receive treatment beyond course 4. Median dose-intensity was 3.74 mg/m<sup>2</sup> for the oral topotecan arm and 2.31 mg/m<sup>2</sup> for the IV topotecan arm (ratio = 1.61), which reflects the difference in oral and IV doses (ratio = 1.53).

Dose escalations above the starting dose occurred for 36% of patients treated with oral topotecan and 19% of patients receiving the IV regimen. More than 90% of initial dose escalations were made at the end of courses 1 or 2. Dose reductions were made for 31% of patients in the oral group and 35% of patients in the IV group. A majority of the dose reductions were made at the end of course 1, primarily as a result of hematologic toxicity. Of the 55 patients (36%) who had a dose escalation of oral topotecan to 2.7 mg/m<sup>2</sup>/d, 25 had a further dose escalation up to 3.1 mg/m<sup>2</sup>/d. For IV topotecan, of the 28 patients (19%) who were dose escalated to 1.75 mg/m<sup>2</sup>/d, 13 had a further dose escalation to 2.0 mg/m<sup>2</sup>/d. No patient was withdrawn from the study or excluded from any analysis as a result of lack of compliance.

**Table 1.** Demographic and Baseline Disease Characteristics

Characteristic	Oral Topotecan (n = 153)		IV Topotecan (n = 151)	
	No. of Patients	%	No. of Patients	%
Sex				
Male	96	64.1	96	63.6
Female	56	35.9	55	36.4
Age, years				
Mean	62.5		62.0	
Range	41-82		35-82	
Performance status				
0	48	31.4	35	23.2
1	95	65.6	98	64.9
2	20	13.1	18	11.8
Disease stage				
Extensive	102	66.7	106	70.2
Limited	51	33.3	45	29.8
Duration of response to first-line chemotherapy†				
< 3 months	15	9.8	13	8.6
3-6 months	50	32.7	51	35.8
> 6 months	84	54.9	83	55.0
Maximum lesion diameter‡				
< 2 cm	1	0.7	2	1.3
2 to < 5 cm	88	57.5	79	52.3
5 to 10 cm	54	35.3	65	43.0
> 10 cm	6	3.9	5	3.3
Liver metastases				
Present	44	28.8	43	28.5
Absent	109	71.2	108	71.5

Abbreviation: IV, intravenous.

†Data missing for four patients in the oral group and one patient in the IV group.

‡Prior chemotherapy included cisplatin or carboplatin + etoposide; vincristine + cisplatin or carboplatin + etoposide; or cyclophosphamide + epirubicin + cisplatin or carboplatin + etoposide.

‡Data missing for four patients in the oral group.

### Efficacy

The overall response rate was 18.3% (95% CI, 12.2% to 24.4%) for patients who received oral topotecan and 21.9% (95% CI, 15.3% to 28.5%) for patients who received IV topotecan (Table 2). Difference in response rates (oral – IV) was –3.6% (95% CI, –12.6% to 5.5%). In the oral topotecan group, median time to response was 6.1 weeks, and median duration of response was 18.3 weeks. In the IV topotecan group, median time to response was 6.1 weeks, and median duration of response was 25.4 weeks. Median time to progression was 11.9 weeks in the oral topotecan group compared with 14.6 weeks in the IV topotecan group (Table 3). A plot of the Kaplan-Meier product-limit estimates for time to progression is provided in Figure 2. Of the 43 patients with baseline brain or leptomeningeal metastases, one patient on the IV topotecan arm experienced a partial response.

Median survival time was 33.0 weeks (95% CI, 29.1 to 42.4 weeks) in the oral group and 35.0 weeks (95% CI, 31.0 to 37.4 weeks) in the IV group, with data censored for 13.7% and 10.6% of patients in the respective groups (Table 3). Cox proportional hazards regression showed no difference between the two groups (hazard ratio = 0.98; 95% CI, 0.77 to 1.25). A plot of the Kaplan-Meier product-limit estimates for survival is provided in Figure 3. Data collected during

**Table 2.** Best Response to Topotecan

Response	Oral Topotecan (n = 153)		IV Topotecan (n = 151)	
	No. of Patients	%	No. of Patients	%
<b>Responders</b>				
Complete response	2	1.3	0	
Partial response	26	17.0	33	21.9
Overall response*	28	18.3	33	21.9
95% CI, %	12.2 to 24.4		15.3 to 28.5	
<b>Nonresponders</b>				
Stable disease	27	17.6	35	23.2
Progressive disease	78	51.0	65	43.0
Not assessable†	20	13.1	18	11.9

Abbreviation: IV, intravenous.  
 \*Difference in response rates (oral-IV) was -3.6% (95% CI, -12.6% to 5.5%).  
 †The 32 patients who were not assessable for response were those who died, were withdrawn (as a result of an adverse experience or a protocol violation), withdrew consent after one or two courses of treatment, or were considered to have completed treatment after one or two courses. These patients received insufficient treatment to assign a response.

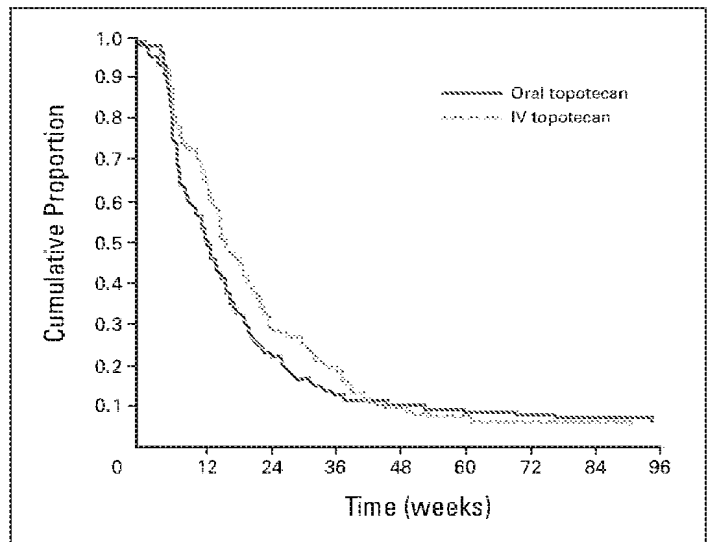


**Fig 2.** Kaplan-Meier plot for time to progression in the intent-to-treat population. IV, intravenous.

poststudy monitoring showed that similar proportions of patients in each group had received third-line chemotherapy (33% of patients in the oral group and 35% of patients in the IV group). At 1 year, the survival rate was 33% after treatment with oral topotecan and 29% after treatment with IV topotecan; the 2-year survival rates were 12% for oral topotecan and 7% for IV topotecan.

**Toxicity**

The principal toxicity was neutropenia for both groups (Table 4). Fever and/or infection of at least grade 2 associated with grade 4 neutropenia, together with sepsis, occurred in 5% of courses in both

groups. Antibiotic use was slightly higher for patients treated with IV topotecan compared with oral topotecan (56% v 41% of patients received a systemic antibiotic and 23% v 14% of patients received an IV antibiotic, respectively). Granulocyte colony-stimulating factor was administered to a higher proportion of patients in the oral than the IV group (25% v 16%, respectively), although the proportion of treatment courses was similar in both groups (9% v 7%, respectively). With the protocol-specified dose adjustments, there was no evidence of cumulative toxicity.

At time of analysis, 267 patients had died; 250 of these patients had died as a result of disease progression. Ten patients (six in the oral group and four in the IV group) died as a result of hematologic toxicity, septic shock related to treatment with topotecan, or of other causes where a relationship to topotecan could not be excluded. This treatment-related mortality is consistent with reports of deaths in

**Table 3.** Time to Response, Response Duration, Progression, and Survival

Event	Oral Topotecan	IV Topotecan
<b>Time to response, weeks</b>		
No. of patients	28	33
Median	6.1	6.3
Range	4.4-17.7	2.1-13.9
<b>Response duration, weeks</b>		
No. of patients	28	33
Median	18.3	25.4
Range	9.0-65.4	8.4-132.1*
<b>Time to progression, weeks</b>		
No. of patients	153	151
Median	11.9	14.6
95% CI	9.7 to 14.1	13.3 to 18.9
Range	0.3-149.0*	0.7-177.9*
<b>Survival time, weeks†</b>		
No. of patients	153	151
Median	33.0	35.0
95% CI	29.1 to 42.4	31.0 to 37.4
Range	0.3-185.3	0.7-205.3

Abbreviation: IV, intravenous.  
 \*Includes censored event(s).  
 †Cox proportional hazards regression showed no survival difference between the two groups (hazard ratio = 0.98; 95% CI, 0.77 to 1.25).

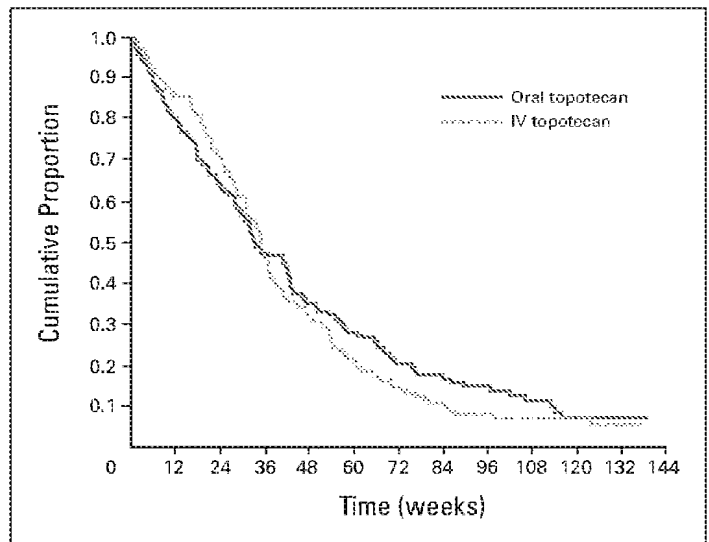


**Fig 3.** Kaplan-Meier plot for survival in the intent-to-treat population. IV, intravenous.



**Table 4.** Hematologic and Nonhematologic Toxicities\* by Treatment Group

Toxicity	Oral Topotecan (n = 153)		IV Topotecan (n = 151)	
	No. of Patients	%	No. of Patients	%
<b>Hematologic</b>				
Leukopenia				
Grade 3	64	42.7	74	49.3
Grade 4	34	22.7	39	26.0
Neutropenia				
Grade 3	39	26.2	39	23.6
Grade 4	70	47.0	95	64.2
Thrombocytopenia				
Grade 3	30	20.0	38	25.3
Grade 4	43	28.7	27	18.0
Anemia				
Grade 3	26	17.3	42	28.0
Grade 4	8	5.3	4	2.7
<b>Nonhematologic</b>				
Diarrhea				
Grade 3	11	7.2	3	2.0
Grade 4	1	0.7	1	0.7
Fatigue				
Grade 3	10	6.5	10	6.6
Grade 4	0	0	2	1.3
Dyspnea				
Grade 3	9	5.9	10	6.6
Grade 4	3	2.0	5	3.3
Anorexia				
Grade 3	8	5.2	3	2.0
Grade 4	0	0	1	0.7
Nausea				
Grade 3	6	3.9	3	2.0
Grade 4	0	0	1	0.7
Asthenia				
Grade 3	4	2.6	7	4.6
Grade 4	3	2.0	3	2.0
Fever				
Grade 3	3	2.0	4	2.6
Grade 4	3	2.0	6	4.0

Abbreviation: IV, intravenous.

\*Occurring with a frequency of  $\geq 10\%$  in either treatment group.

studies on second-line therapy for SCLC, in which deaths caused by hematologic toxicity or septic shock related to treatment ranged from 0% to 12%.<sup>18,19</sup>

Incidence of grade 4 thrombocytopenia was higher in the oral than in the IV group (Table 4), but platelet transfusions were used to a similar extent in both groups (oral group, 15%; IV group, 13%). Grade 3 or 4 anemia occurred in a slightly higher proportion of patients in the IV group; however, transfusions of RBCs were administered to a similar number of patients in each group (oral group, 37%; IV group, 43%).

Nonhematologic adverse events in the oral and IV groups involved mainly nausea (42.5% and 42.4%, respectively), fatigue (30.7% and 36.4%, respectively), and alopecia (25.5% and 29.8%, respectively). Diarrhea was one of the most commonly occurring events in the oral group; 35.9% of patients in the oral group experienced diarrhea (7.9% grade 3 or 4) compared with 19.9% of patients in the oral group (2.7% grade 3 or 4; Table 4). These events were predominantly

grade 1 or 2, and there were no suggestions of cumulative toxicity. Diarrhea in the oral topotecan group was self-limiting or manageable with treatment, primarily oral loperamide.

### HRQOL

All randomly assigned patients reported baseline HRQOL information using FACT-L and LCS, and 88% (oral) to 90% (IV) of patients reported HRQOL before at least one course of therapy. Questionnaire response was 75% and 78% for the oral and IV groups, respectively, after two courses of therapy. Rates at which patients failed to complete QOL assessment at one or more courses of therapy were similar in the two arms.

Least squares estimates for mean change from baseline indicated no statistical difference between treatment groups for subscale dimension scores and LCS, TOI, and FACT-L total scores. Only a small decline in HRQOL was noted for each treatment group compared with declines that may be expected in an untreated lung cancer population (ie, patients on best supportive care), which suggests that treatment (with oral or IV topotecan) may delay symptom progression, as was subsequently reported.<sup>20</sup> Mean change from baseline to last course also showed no statistical differences between the oral and IV topotecan arms.

### DISCUSSION

This study confirms results of the earlier phase II trial in which similar activity was demonstrated for both oral and IV topotecan in the treatment of relapsed, sensitive SCLC.<sup>7</sup> Response rates of 18% for oral topotecan and 22% for IV topotecan are comparable to the rates of the earlier study (23% for oral and 15% for IV) and consistent with the rate reported in a pooled analysis of patients with relapsed SCLC who received IV topotecan.<sup>6</sup>

Median survival time was 33.0 weeks in the oral topotecan group and 35.0 weeks in the IV group. Although survival was not the primary end point and the study was not powered to confirm noninferiority in survival outcomes, the hazard ratio seems to indicate that the treatments are similar. Median survival times of more than 8 months are comparable to those reported in the literature<sup>2</sup> and confirm that both oral and IV topotecan are active in patients with relapsed SCLC. These results were not confounded by poststudy treatment because third-line chemotherapy was similar in both groups.

Topotecan was generally well tolerated, with good compliance with the oral formulation. Hematologic toxicity was consistent with the drug's established profile. Most dose modifications occurred at the end of the first or second course of treatment. Decreased incidence of grade 4 neutropenia from course 1 to course 4 suggests that dose adjustments were successful in controlling risk of severe neutropenia. Reduction in occurrence of severe neutropenia in the oral arm may have been, in part, related to the slightly higher use of granulocyte colony-stimulating factor in that group.

Nonhematologic toxicities of both formulations of topotecan were consistent with previous trials of SCLC and in other indications<sup>6,21,22</sup> (ie, primarily diarrhea, dyspnea, and fatigue). Both oral and IV topotecan demonstrated acceptable tolerability, and there was no suggestion of specific organ toxicity, including neuropathy.

This study targeted 300 patients, with 150 patients per arm. Conservatively assuming a response rate after second-line IV topotecan treatment of 19% (pooled data, all second-line IV SCLC studies), 150 patients would provide 71% power that the upper limit of the 95% CI for the difference (IV – oral) between formulations would exclude values larger than 10 percentage points in favor of IV topotecan. These assumptions were based on experience with topotecan as second-line SCLC treatment and the magnitude of a clinically important difference in this population. Eventually, 304 patients received treatment. This study was not able to answer definitively whether oral topotecan was inferior or noninferior to IV topotecan because the lower boundary of the prespecified CI (oral – IV) was –12.6% (ie, 2.6% greater than the 10% needed), which did not meet the prespecified requirement for demonstrating noninferiority.

The importance of QOL is increasingly emphasized.<sup>23</sup> In this study, IV topotecan palliated disease-related symptoms. FACT-L corroborated this for oral topotecan, including in patients whose best response was progressive disease. Besides patient preference for oral therapy,<sup>24</sup> its advantages for patients include fewer clinic visits and venous line placements, a sense of control and participation in therapy, more time to spend time with loved ones, and less stress on caregivers. Aspects of decision making for optimal therapeutic management will be further evaluated in future studies.

This study confirms earlier results for oral topotecan in patients with relapsed sensitive SCLC. Given the antitumor activity demonstrated in both studies by response rate and overall survival, together with comparable safety profiles, oral topotecan may offer a useful, convenient, and compassionate treatment option for patients and their families in this palliative setting.

## REFERENCES

- Govindan R, Page N, Morgensztern D, et al: Changing epidemiology of small-cell lung cancer in the United States over the last 30 years: Analysis of the surveillance, epidemiologic, and end results database. *J Clin Oncol* 24:4539-4544, 2006
- Okuno SH, Jett JR: Small cell lung cancer: Current therapy and promising new regimens. *Oncologist* 7:234-238, 2002
- Ardizzoni A, Hansen H, Dombrowski P, et al: Topotecan, a new active drug in the second-line treatment of small-cell lung cancer SCLC: A phase II study in patients with refractory and sensitive disease. *J Clin Oncol* 15:2090-2096, 1997
- Depierre A, von Pawel J, Hans K et al: Evaluation of topotecan (Hycamtin) in relapsed small-cell lung cancer (SCLC): A multicentre phase II study. *Lung Cancer* 18:35, 1997 (abstr 126)
- Eckardt J, Gralla R, Palmer MC, et al: Topotecan (T) as second-line therapy in patients (Pts) with small cell lung cancer (SCLC): A phase II study. *Ann Oncol* 7:107, 1996 (abstr 523)
- Eckardt J, Depierre A, Ardizzoni A, et al: Pooled analysis of topotecan (T) in the second-line treatment of patients (pts) with sensitive small cell lung cancer. *Proc Am Soc Clin Oncol* 16:452a, 1997 (abstr 1624)

- von Pawel J, Gatzmeier U, Pujol J-L, et al: Phase II comparator study of oral versus intravenous topotecan in patients with chemosensitive small-cell lung cancer. *J Clin Oncol* 19:1743-1749, 2001
- Gerrits CJH, Schellens JHM, Burris H, et al: A comparison of clinical pharmacodynamics of different administration schedules of oral topotecan (Hycamtin). *Clin Cancer Res* 5:69-75, 1999
- Schellens J, Creemers GJ, Beijnen JH, et al: Bioavailability and pharmacokinetics of oral topotecan: A new topoisomerase I inhibitor. *Br J Cancer* 73:1268-1271, 1996
- Kruijtzter C, Beijnen J, Rosing H, et al: Increased oral bioavailability of topotecan in combination with the breast cancer resistance protein and P-glycoprotein inhibitor GF120918. *J Clin Oncol* 20:2943-2950, 2002
- Léger F, Loos WJ, Fourcade J, et al: Factors affecting pharmacokinetic variability of oral topotecan: A population analysis. *Br J Cancer* 90:343-347, 2004
- GlaxoSmithKline: Hycamtin: Package insert. Philadelphia, PA, GlaxoSmithKline, 2004
- World Health Organization: WHO Handbook for Reporting Results of Cancer Treatment. Geneva, Switzerland, World Health Organization, 1979

- Gwyther SJ, Ross G, Crofts T, et al: Correlation between response, treatment duration and median survival: Single agent intravenous (IV) topotecan in a population of 631 relapsed small cell lung cancer (SCLC) patients. *Lung Cancer* 41:S235, 2003 (suppl 2, abstr)
- Cella DF, Bonomi AE, Lloyd SR, et al: Reliability and validity of the Functional Assessment of Cancer Therapy–Lung (FACT-L) quality of life instrument. *Lung Cancer* 12:199-220, 1995
- Cella D, Eton DT, Fairclough DL, et al: What is a clinically meaningful change on the Functional Assessment of Cancer Therapy–Lung (FACT-L) Questionnaire? Results from Eastern Cooperative Oncology Group (ECOG) Study 5592. *J Clin Epidemiol* 55:285-295, 2002
- Cella DF: The Functional Assessment of Cancer Therapy–Lung (FACT-L) quality of life instrument, in Gralla RJ, Moirpour CM (eds): *Assessing Quality of Life in Patients with Lung Cancer: A Guide for Clinicians*. New York, NY, NCM Publishers Inc, 1995
- Stewart DJ, Dahrouge S, Soltys KM, et al: A phase II study of 5-fluorouracil plus high-dose folinic acid in the treatment of recurrent small cell lung cancer. *Am J Clin Oncol* 18:130-132, 1995
- Falk SJ, Maughan TS, Laurence VM, et al: Phase II study of carboplatin plus Adriamycin as second line chemotherapy in small cell lung cancer. *Clin Oncol (R Coll Radiol)* 5:85-88, 1993

## AUTHORS' DISCLOSURES OF POTENTIAL CONFLICTS OF INTEREST

Although all authors completed the disclosure declaration, the following authors or their immediate family members indicated a financial interest. No conflict exists for drugs or devices used in a study if they are not being evaluated as part of the investigation. For a detailed description of the disclosure categories, or for more information about ASCO's conflict of interest policy, please refer to the Author Disclosure Declaration and the Disclosures of Potential Conflicts of Interest section in Information for Contributors.

**Employment:** Ruth Poulin, GlaxoSmithKline; Alaknanda J. Preston, GlaxoSmithKline; Graham Dane, GlaxoSmithKline; Graham Ross, GlaxoSmithKline **Leadership:** N/A **Consultant:** John R. Eckardt, GlaxoSmithKline; Elisabeth Quoix, GlaxoSmithKline; Andrea Ardizzoni, GlaxoSmithKline **Stock:** Alaknanda J. Preston, GlaxoSmithKline; Graham Dane, GlaxoSmithKline; Graham Ross, GlaxoSmithKline **Honoraria:** John R. Eckardt, GlaxoSmithKline; Andrea Ardizzoni, GlaxoSmithKline **Research Funds:** John R. Eckardt, GlaxoSmithKline **Testimony:** N/A **Other:** N/A

## AUTHOR CONTRIBUTIONS

**Conception and design:** John R. Eckardt, Ruth Poulin, Graham Dane, Graham Ross  
**Provision of study materials or patients:** John R. Eckardt, Joachim von Pawel, Jean-Louis Pujol, Zsolt Papai, Elisabeth Quoix, Andrea Ardizzoni  
**Collection and assembly of data:** Jean-Louis Pujol, Zsolt Papai, Elisabeth Quoix, Andrea Ardizzoni, Ruth Poulin, Alaknanda J. Preston, Graham Dane, Graham Ross  
**Data analysis and interpretation:** John R. Eckardt, Zsolt Papai, Ruth Poulin, Alaknanda J. Preston, Graham Dane, Graham Ross  
**Manuscript writing:** John R. Eckardt, Ruth Poulin, Graham Ross  
**Final approval of manuscript:** John R. Eckardt, Joachim von Pawel, Jean-Louis Pujol, Zsolt Papai, Elisabeth Quoix, Andrea Ardizzoni, Ruth Poulin, Alaknanda J. Preston, Graham Dane, Graham Ross  
**Other:** Graham Ross [Ethics and regulatory submission; ongoing safety monitoring]

20. O'Brien MER, Ciuleanu TE, Tsekov H, et al: Phase III trial comparing supportive care alone with supportive care with oral topotecan in patients with relapsed small-cell lung cancer. *J Clin Oncol* 24: 5441-5447, 2006

21. von Pawel J, Schiller JH, Shepherd FA, et al: Topotecan versus cyclophosphamide, doxorubi-

cin and vincristine for the treatment of recurrent small cell lung cancer. *J Clin Oncol* 17:658-667, 1999

22. Gore M, Oza A, Rustin G, et al: A randomised trial of oral versus intravenous topotecan in patients with relapsed epithelial ovarian cancer. *Eur J Cancer* 38:57-63, 2002

23. Borner M, Scheithauer W, Twelves C, et al: Answering patient's needs: Oral alternative to intravenous therapy. *Oncologist* 6:12-16, 2001 (suppl 4)

24. Liu G, Franssen E, Fitch MI, et al: Patient preferences for oral versus intravenous palliative chemotherapy. *J Clin Oncol* 15:110-115, 1997

---

**Acknowledgment**

We acknowledge participation of other members of the European Small-Cell Lung Cancer Topotecan Study Group.



Systems Pharmacology Identification of Tumour Nanoparticle Permeability as Predictor of Clinical Anti-Cancer Activity of MM-398, Nanoliposomal Irinotecan, nal-IRI

Jonathan Fitzgerald<sup>1</sup>, Ron Korn<sup>2</sup>, Gerald Fetterly<sup>3</sup>, Jasjit Sachdev<sup>4</sup>, Jaeyeon Kim<sup>1</sup>, Natarajan Raghunand<sup>5</sup>, Joshua Prey<sup>3</sup>, Kimberley Clark<sup>3</sup>, Ashish Kalra<sup>1</sup>; Stephan Klinz<sup>1</sup>, Elieel Bayever<sup>1</sup>, Ramesh Ramanathan<sup>4</sup>

<sup>1</sup>Merrimack Pharmaceuticals, Inc., Cambridge, MA, USA, <sup>2</sup>Imaging Endpoints, Scottsdale, AZ, USA, <sup>3</sup>Roswell Park Cancer Institute, Buffalo, NY, USA, <sup>4</sup>Virginia G Piper Cancer Center, Scottsdale Healthcare, Scottsdale, AZ, USA, <sup>5</sup>Translational Cancer Imaging, Arizona Cancer Center, Tucson, AZ, USA

## ABSTRACT

**Background:** MM-398, nanoliposomal irinotecan (nal-IRI), is designed to extend the pharmacokinetic exposure of irinotecan, preferentially in tumours. Mechanistic PK model sensitivity analysis identified tumour permeability to nal-IRI (tumour deposition) as a key determinant of the tumour concentration of SN-38 (activated irinotecan), which we show correlates with in vivo activity. We have undertaken a clinical study to confirm the presence of SN-38 in tumours following nal-IRI treatment and to measure tumour nanoparticle permeability using magnetic resonance imaging (MRI).

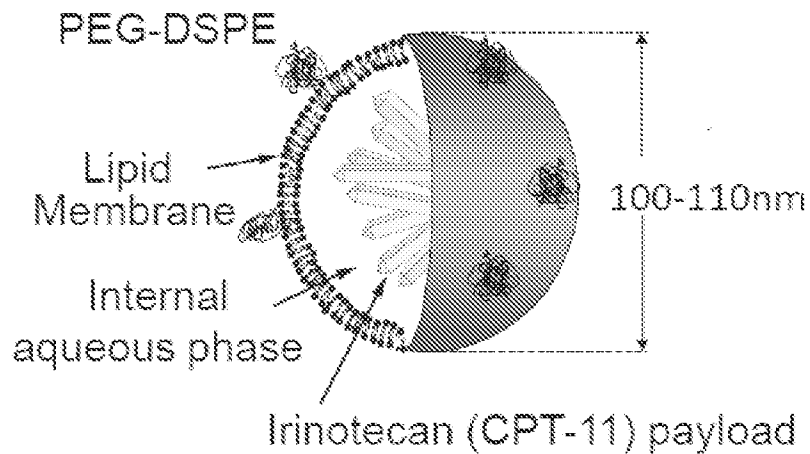
**Methods:** Eligible patients (n=12) with refractory solid tumours were treated with nal-IRI (80mg/m<sup>2</sup> q2w). Plasma PK was measured at multiple timepoints and tissue biopsies were collected 72hrs post-treatment, with drug metabolite levels measured by mass-spectrometry. Prior to nal-IRI treatment, patients underwent ferumoxytol-MRI to test the feasibility of non-invasively measuring tumour permeability in humans. Ferumoxytol is a 30nm iron-oxide, superparamagnetic nanoparticle.

**Results:** Patient-derived data showed that SN-38 concentrations in tumour were 3.6-fold higher (90% CI: 2.6~5.1) than in plasma 72h post-treatment consistent with our simulations incorporating the enhanced permeability and retention effect for tumour deposition of liposomes. A ferumoxytol PK model described both plasma and tumour ferumoxytol-MRI data (R<sup>2</sup>>0.9, n=9). Analyses indicated that tumour permeability to ferumoxytol contributed to MRI signals at 24h. Ferumoxytol levels above the median at 24h were significantly associated with better lesion responses as measured by change in lesion size resulting in receiver operating characteristics AUC>0.8 for lesion classification.

**Conclusion:** Tumour nanoparticle permeability, identified through systems pharmacology techniques, represents a promising biomarker strategy for nal-IRI.

# nal-IRI Background

Low-pegylated non-targeted liposomal irinotecan



## Systems pharmacology approach to identify MOA for nal-IRI

Figure 1. Mechanistic tumor PK model was developed and trained with plasma and tumor PK data in mice bearing HT-29 xenografts.

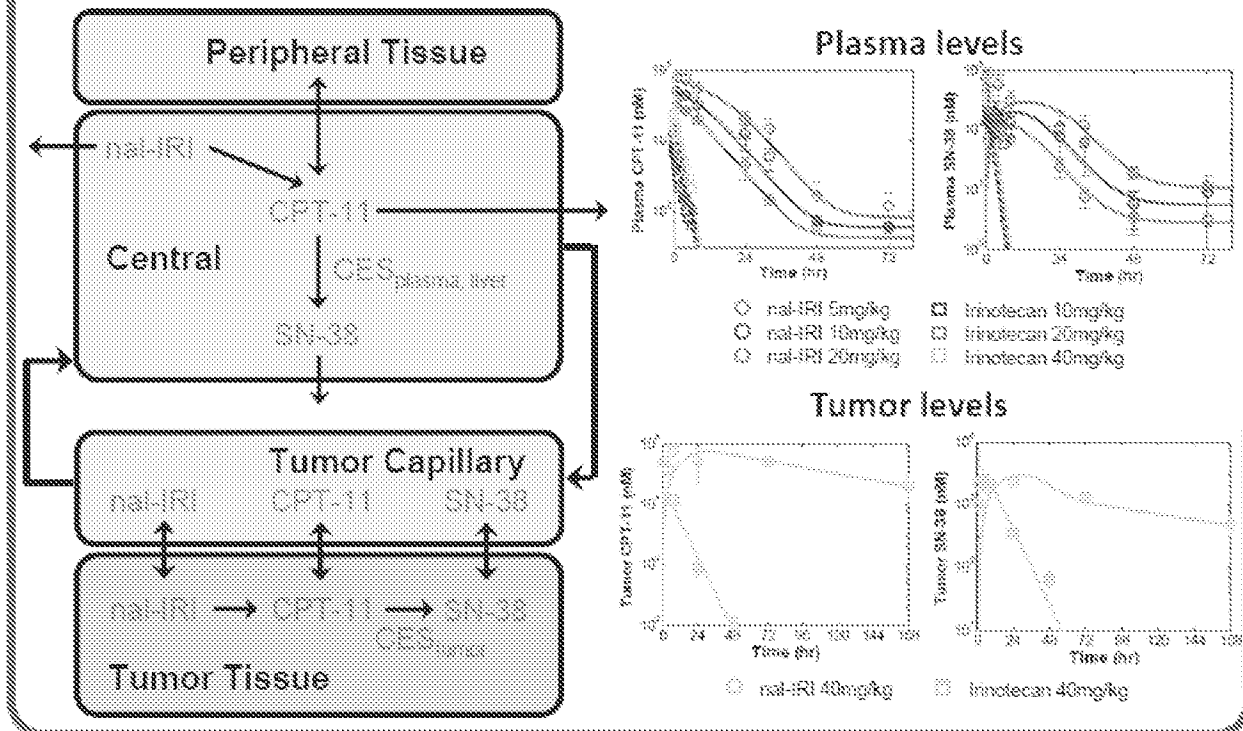
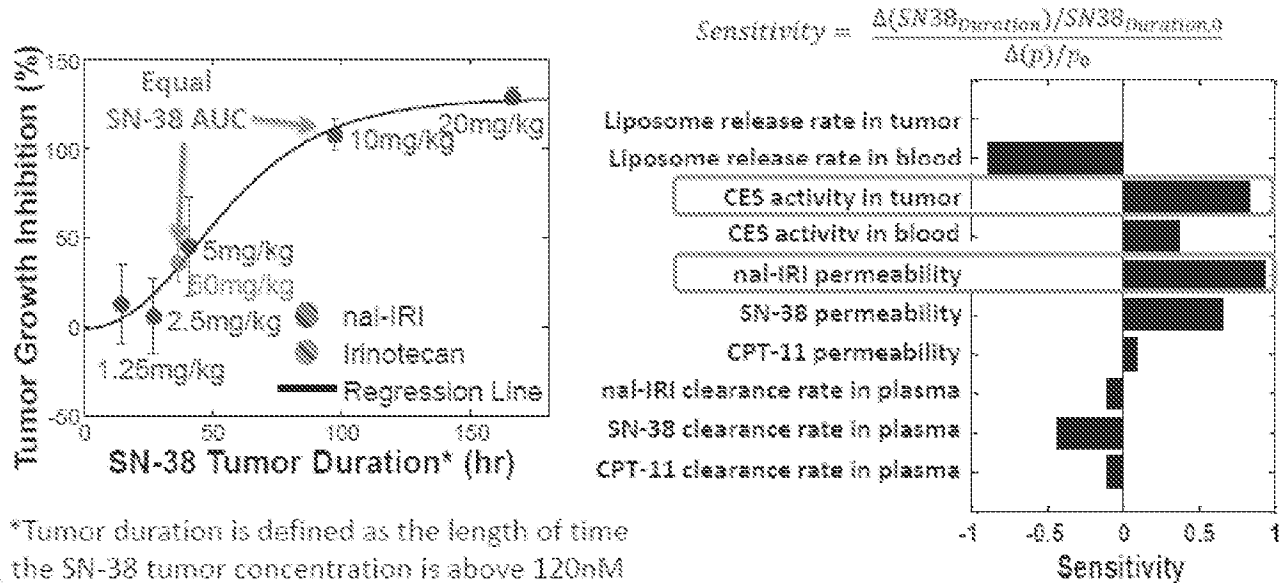


Figure 2. Mechanistic PK model identified that longer duration of SN-38 in tumor differentiates nal-IRI from free irinotecan for *in vivo* activity. Sensitivity analysis on the model parameters predicted critical processes to influence SN-38 tumor duration.



## Design of Clinical Translational Study

Figure 3. Eligible patients with refractory solid tumors were recruited. PK samples for FMX were collected at 0.5h, 2h, 24h and 72h. PK samples for nal-IRI were collected at 1.5h, 3.5h, 72h and 168h. RECIST v1.1 evaluation was done every 8 weeks.

Days	Week 1							Week 2						
	1	2	3	4	5	6	7	8	9	10	11	12	13	14
MRI (pre-FMX)														
FMX (5mg/kg)														
MRI (post-FMX)	1 hr	24 hr		72 hr										
nal-IRI (80mg/m <sup>2</sup> )														every 2 weeks
CT-guided Biopsies				2				2						
PK sampling														

# Ferumoxytol Imaging and Quantitation

Figure 4. Ferumoxytol (FMX) is a 30 nm size superparamagnetic iron oxide nanoparticle coated with polyglucose sorbitol carboxymethylether. FMX is approved for iron supplement in patients with chronic kidney disease and recently has been used as MRI contrast agent (off-label).

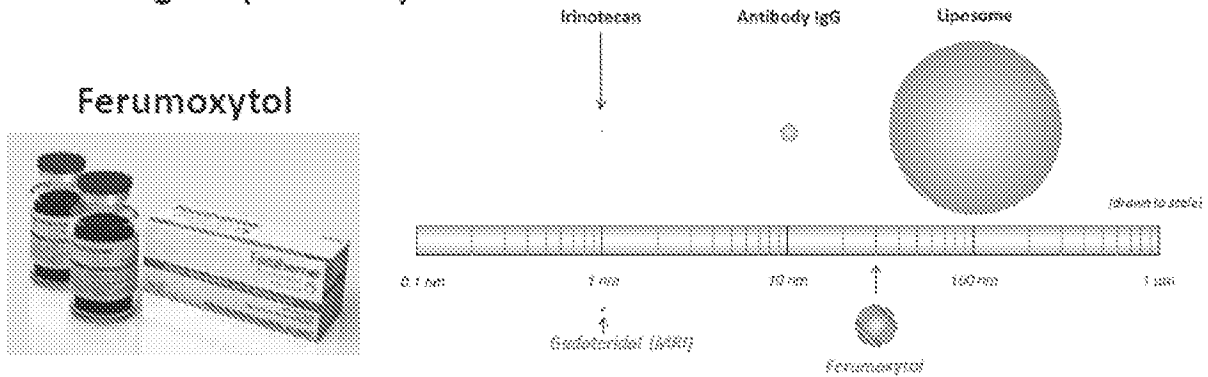
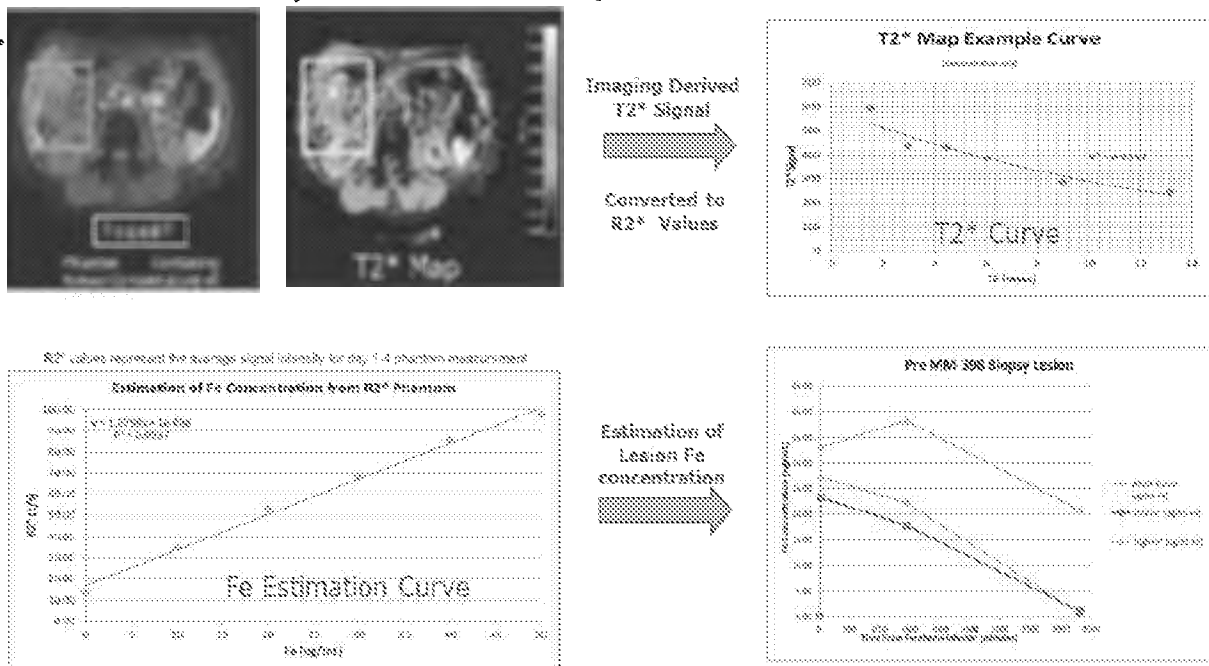
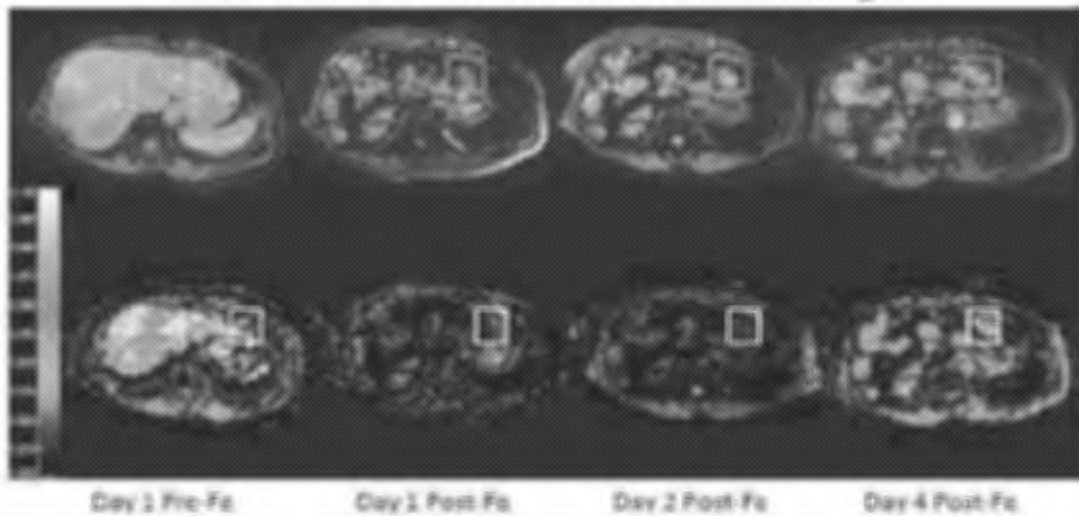


Figure 5. MR images were acquired on a GE 1.5T MRI instrument with a T1 FSPGR series with echo delay times from 1.5 – 13.2ms. Slice thickness and spacing was 6mmx1mm using a 256x256 matrix. T2\* values were extrapolated from each image series to construct a T2\* map. Phantom tubes containing known FMX concentrations from 10 – 200mg/ml was included during each MRI session and demonstrated a linear relationship between  $R2^* = 1/T2^*$  and FMX levels.

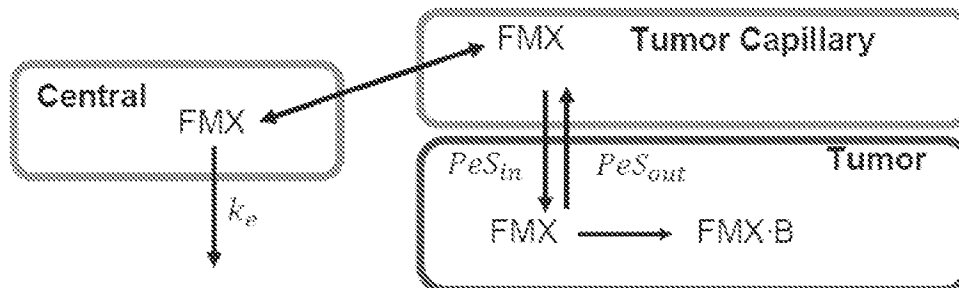


MRI FSPGR FatSat TE 13.2 ms Breathhold Images



## FMX Tumor PK model identifies the temporal characteristics of FMX signals

Figure 6. Plasma and tumor PK models were integrated to simulate FMX signals for each patient tumor lesion. FMX tumor PK model was developed by using SimBiology<sup>®</sup> toolbox in MATLAB<sup>®</sup>. Particle swarm optimization was used to estimate the model parameters.



$PeS_{in}$ (Ktrans): Responsible for vascular wall permeability

$v_e$ , Extravascular volume fraction,  $v_e = PeS_{in}/PeS_{out}$ : Responsible for permeability of extravascular tissue bed and distance that drug can diffuse out from the vascular wall

B: Number of tissue binding site (e.g., macrophages)



Figure 7. FMX tumor PK model could quantify the degree of tissue permeability and FMX binding activity across all tumor lesions

Low permeability and low signal retention model

$$v_p = 0.22, B = 1 \text{ (P7-Low-Pre)}$$

High permeability and high signal retention model

$$v_p = 0.56, B = 26 \text{ (P2-High-Pre)}$$

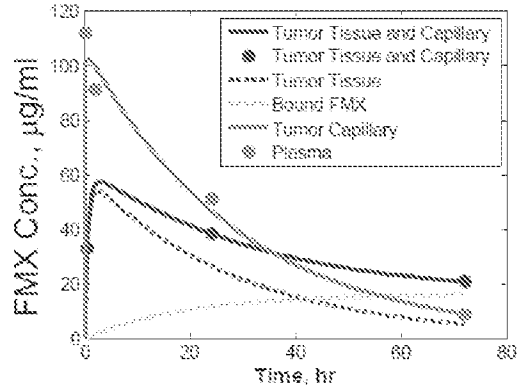
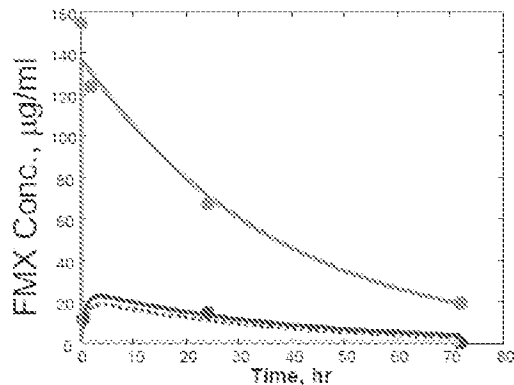
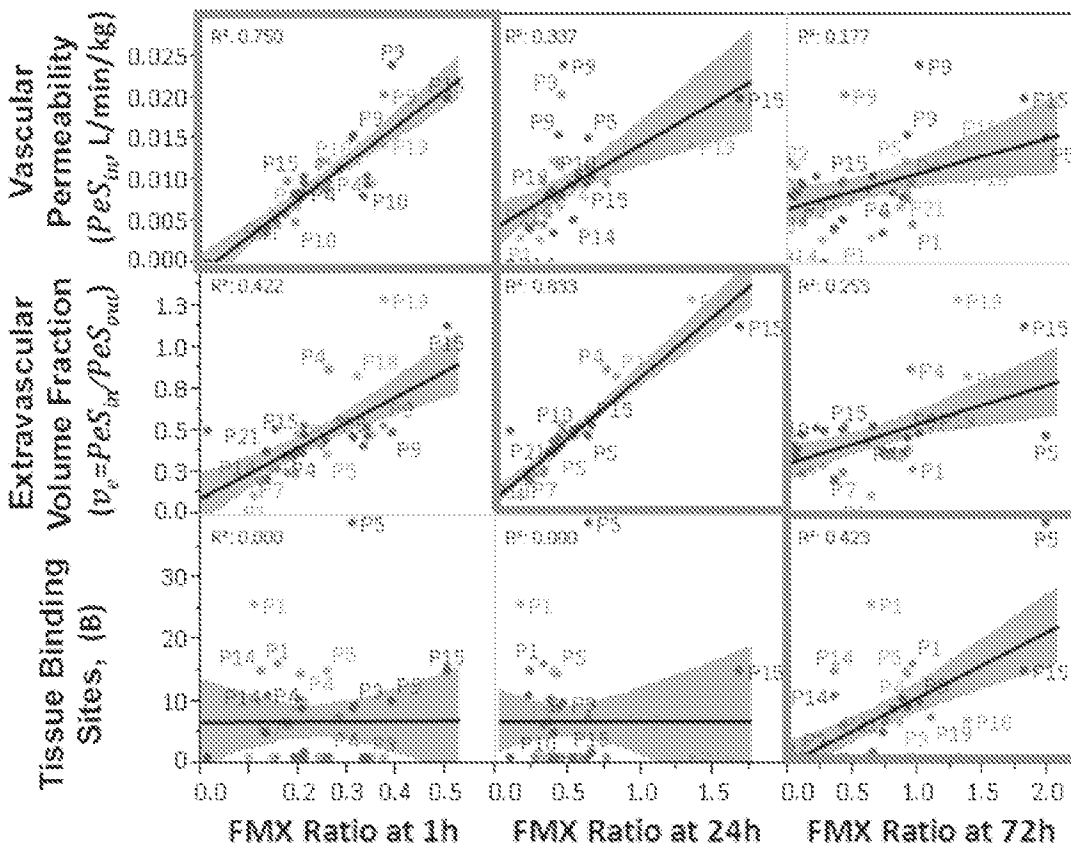
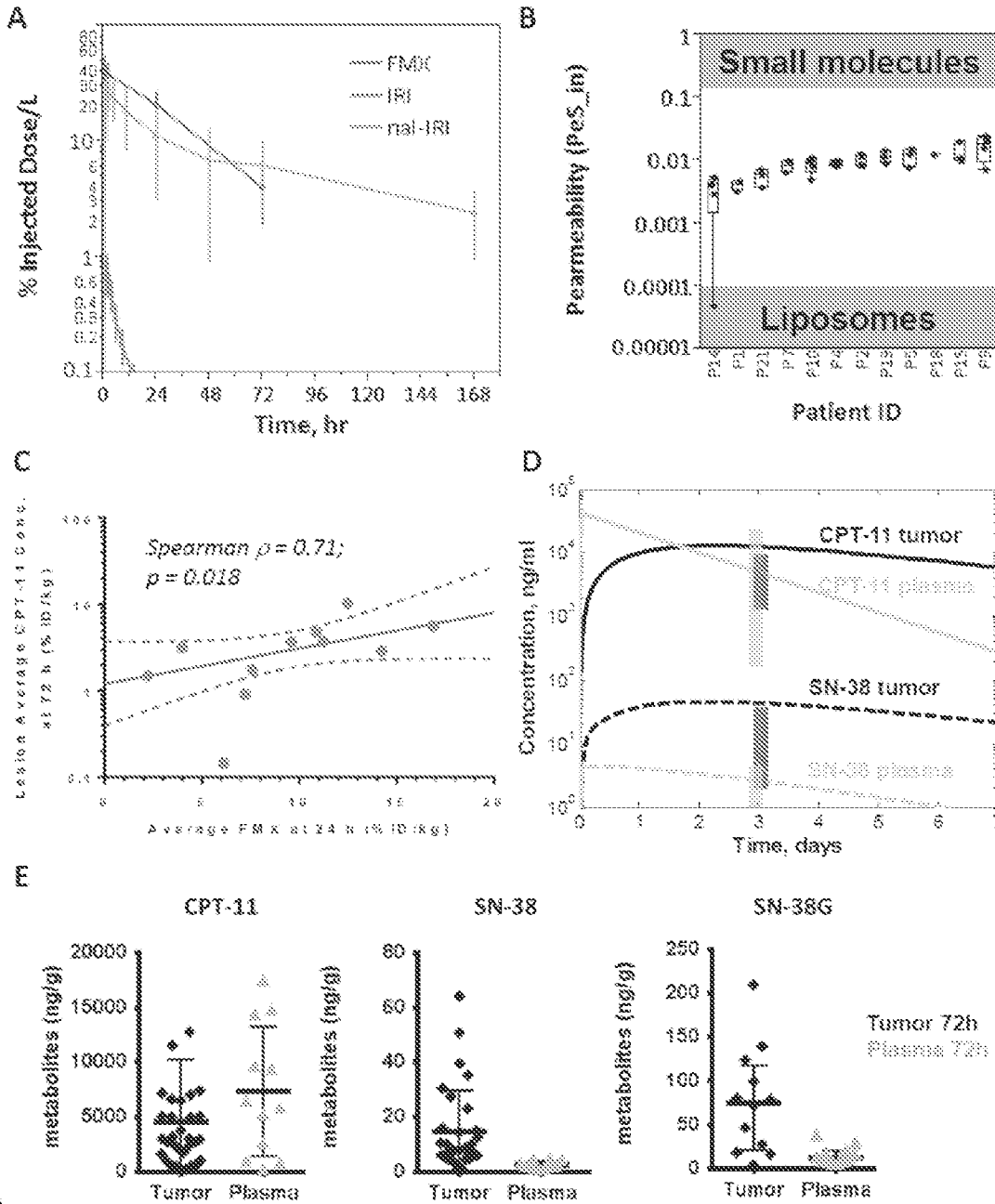


Figure 8. Earlier FMX signals (1h and 24h) were explained by the model parameters related to vascular permeability, whereas FMX signals at 72h were explained by the model parameter for FMX binding to tumor tissue.



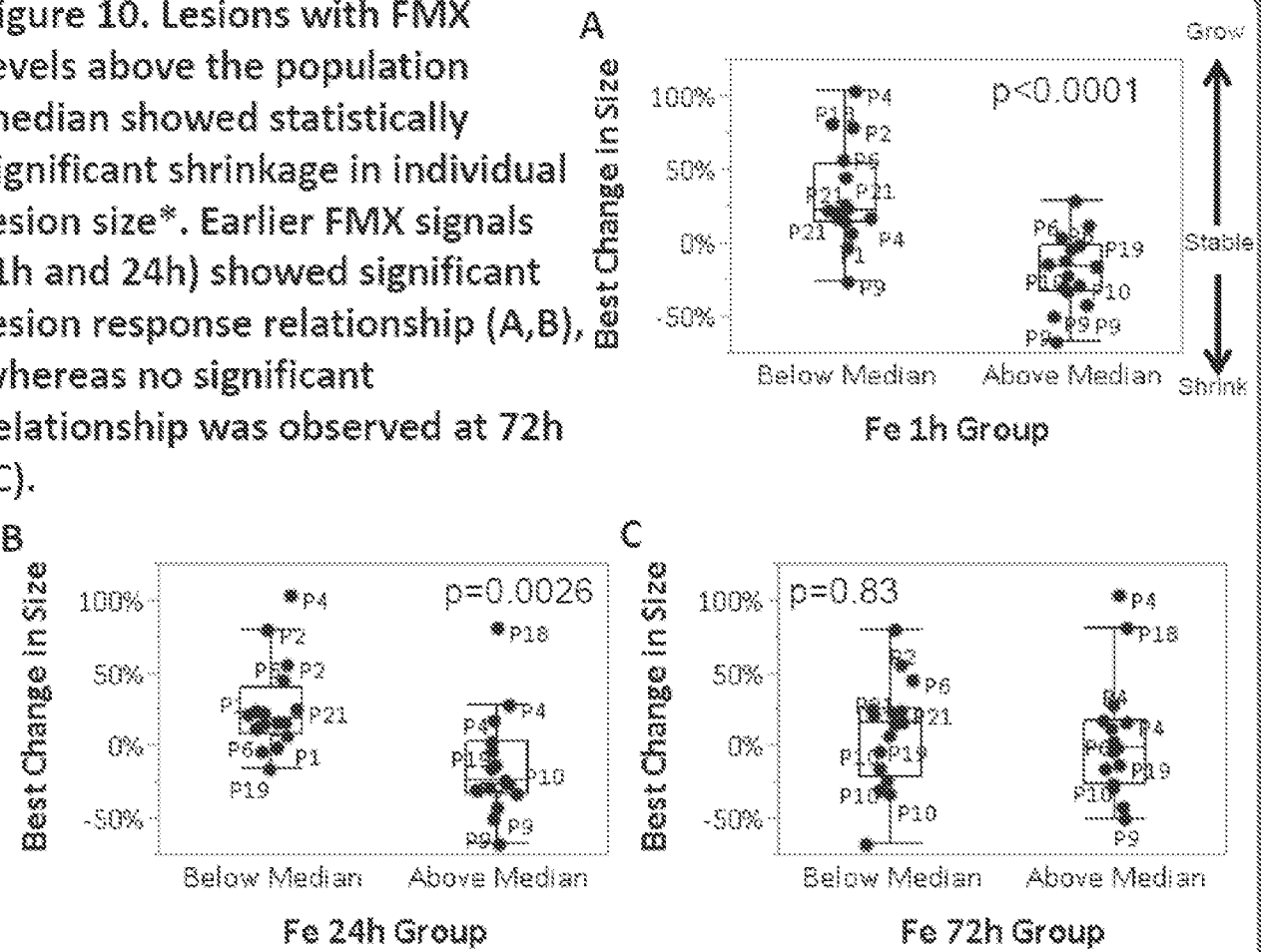
# Plasma and Tumor PK of FMX and nal-IRI

Figure 9. FMX plasma half-life was similar to nal-IRI as compared to free IRI (A). Even though the estimated tissue permeability parameters for FMX were in between small molecules and liposomes (B), average FMX tumor levels correlated well with nal-IRI deposition to tumor in each patient (C). The mechanistic tumor PK model of nal-IRI predicted higher SN-38 levels in tumor suggesting strong local conversion activity of nal-IRI (D). The predictions were confirmed by the metabolite data from tumor biopsy samples in patients (D, E).



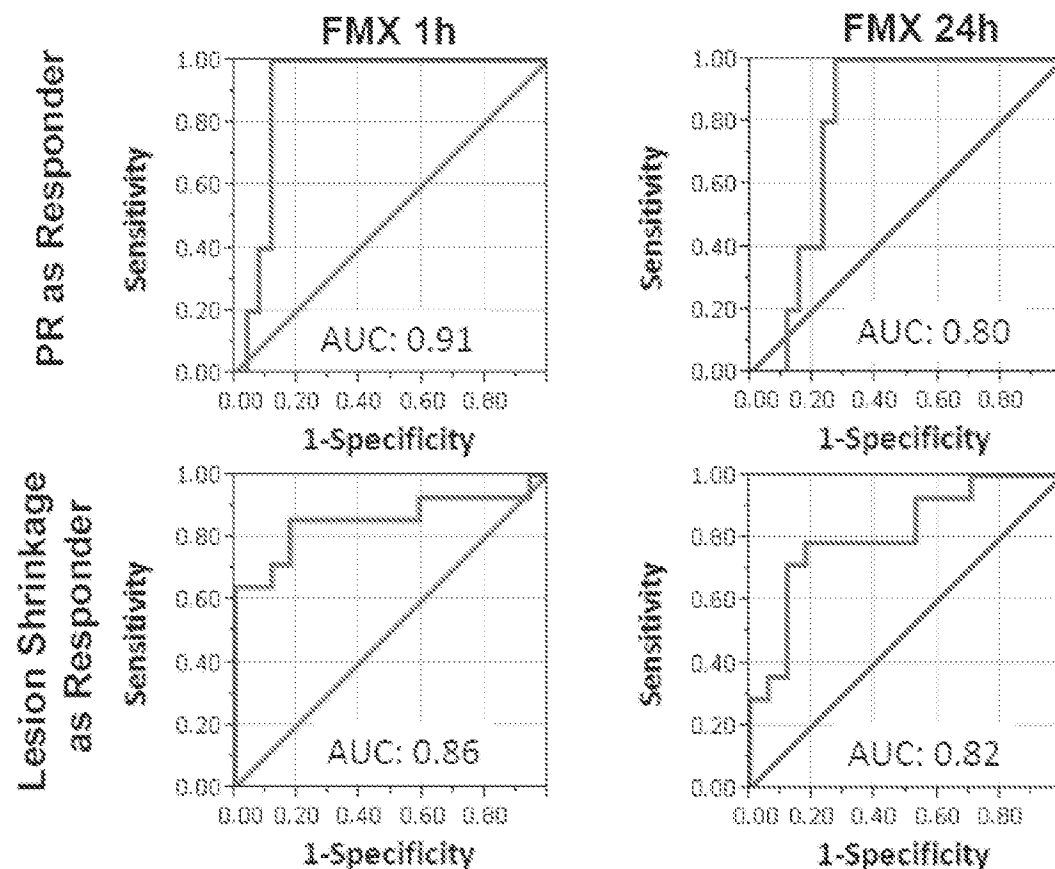
# FMX Signal and Lesion Response Relationship

Figure 10. Lesions with FMX levels above the population median showed statistically significant shrinkage in individual lesion size\*. Earlier FMX signals (1h and 24h) showed significant lesion response relationship (A,B), whereas no significant relationship was observed at 72h (C).



\*Lesions from one patient were treated as independent samples

Figure 11. FMX signals at 1h and 24h were used to explore the utility of FMX-MRI as a diagnostic test for nal-IRI *in vivo* activity in humans. Receiver operating characteristic (ROC) curves were calculated by using two different definitions for responders; 1. Partial Response (PR) in lesion size change (Size Change < -30%) and 2. Decrease in lesion size change (Size Change < 0%). Area under curves (AUC) for ROC curves at both time points (1h and 24h) were >0.8 suggesting the potential usefulness of FMX-MRI as a diagnostic tool for nal-IRI *in vivo* activity

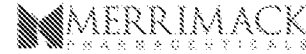


## Conclusions

- This phase I study demonstrated the feasibility of incorporating FMX-MRI into a clinical workflow
- FMX tumor PK model identified that early FMX signals at 1h and 24h contributed to tumor permeability of FMX
- FMX-MRI correlated well with nal-IRI delivery to tumor lesions
- Significantly higher SN-38 levels in tumor suggested strong local conversion activity of nal-IRI
- Early FMX signals showed significant relationship with lesion size change response suggesting the potential use as a diagnostic tool

# Systems Pharmacology Identification of Tumour Nanoparticle Permeability as Predictor of Clinical Anti-Cancer Activity of MM-398, Nanoliposomal Irinotecan, and IRI

Jonathan Fitzgerald<sup>1</sup>, Ron Korn<sup>2</sup>, Gerald Fetterly<sup>3</sup>, Jasjit Sachdev<sup>4</sup>, Jaeyoon Kim<sup>5</sup>, Natarajan Raghunand<sup>6</sup>, Vishnu Pray<sup>7</sup>, Kimberley Clark<sup>8</sup>, Ashish Kabra<sup>9</sup>, Stephan Hillz<sup>7</sup>, Eliel Bayever<sup>1</sup>, Ramesh Ramnathan<sup>1</sup>  
<sup>1</sup>Merrimack Pharmaceuticals, Inc., Cambridge, MA, USA, <sup>2</sup>Imaging Endpoints, Scottsdale, AZ, USA, <sup>3</sup>Roswell Park Cancer Institute, Buffalo, NY, USA, <sup>4</sup>Virginia G Piper Cancer Center, Scottsdale Healthcare, Scottsdale, AZ, USA, <sup>5</sup>Translational Cancer Imaging, Arizona Cancer Center, Tucson, AZ, USA



ABSTRACT	Pharmacovital Imaging and Quantification	Plasma and Tumor PK of FPMX and IRI
<p><b>Background:</b> MM-398, a novel oral kinase inhibitor, is designed to address the pharmacokinetic exposure of irinotecan, particularly in tumors. Pharmacovital PK model analysis identified tumor permeability as a key PK determinant of tumor deposition of IRI. In a phase 1b study, we have undertaken a clinical study to evaluate the presence of IRI in tumors following IRI treatment and to measure tumor nanoparticle permeability using magnetic resonance imaging (MRI). <b>Methods:</b> Eligible patients (n=12) with refractory solid tumors were treated with IRI (100mg/m<sup>2</sup> qd). Plasma PK was measured at multiple timepoints and tissue biopsies were collected 72h post-treatment, with drug metabolism levels measured by LC-MS/MS. PK data for IRI in tumors and plasma were analyzed to assess the feasibility of permeability measurement. <b>Results:</b> Patient-derived data showed that IRI concentrations in tumor were 2.6-fold higher (SD: 0.2-5.1) than in plasma 72h post-treatment consistent with our objective incorporating the enhanced permeability and retention effect for tumor deposition of liposomes. A pharmacovital PK model described both plasma and tumor pharmacovital PK data (R<sup>2</sup> 0.9, 0.9). Analysis indicated that tumor permeability to irinotecan contributed to MRI signals at 24h. Pharmacovital PK data above the detection of IRI were significantly associated with tumor lesion responses as measured by change in lesion size resulting in overall one-stage disease-free survival for lesion classification. <b>Conclusion:</b> Tumor nanoparticle permeability identified through without pharmacovital techniques, represents a promising biomarker strategy for IRI.</p>	<p><b>Figure 4:</b> Pharmacovital (FPMX) is a 30-minute pharmacovital PK model incorporating tumor and plasma PK data. Pharmacovital PK model analysis identified tumor permeability as a key PK determinant of tumor deposition of IRI. In a phase 1b study, we have undertaken a clinical study to evaluate the presence of IRI in tumors following IRI treatment and to measure tumor nanoparticle permeability using magnetic resonance imaging (MRI). <b>Methods:</b> Eligible patients (n=12) with refractory solid tumors were treated with IRI (100mg/m<sup>2</sup> qd). Plasma PK was measured at multiple timepoints and tissue biopsies were collected 72h post-treatment, with drug metabolism levels measured by LC-MS/MS. PK data for IRI in tumors and plasma were analyzed to assess the feasibility of permeability measurement. <b>Results:</b> Patient-derived data showed that IRI concentrations in tumor were 2.6-fold higher (SD: 0.2-5.1) than in plasma 72h post-treatment consistent with our objective incorporating the enhanced permeability and retention effect for tumor deposition of liposomes. A pharmacovital PK model described both plasma and tumor pharmacovital PK data (R<sup>2</sup> 0.9, 0.9). Analysis indicated that tumor permeability to irinotecan contributed to MRI signals at 24h. Pharmacovital PK data above the detection of IRI were significantly associated with tumor lesion responses as measured by change in lesion size resulting in overall one-stage disease-free survival for lesion classification. <b>Conclusion:</b> Tumor nanoparticle permeability identified through without pharmacovital techniques, represents a promising biomarker strategy for IRI.</p>	<p><b>Figure 5:</b> FPMX plasma half-life was similar to IRI as compared to free IRI. PK data through the estimated tissue permeability parameters for FPMX were as follows: tumor PK parameters (PK<sub>1</sub>, average FPMX tumor levels, correlated well with IRI PK deposition in tumor in 10 patients [1]. The pharmacovital PK model of IRI predicted higher PK data for tumor PK parameters (PK<sub>1</sub>) and PK<sub>2</sub> (PK<sub>2</sub> PK<sub>1</sub>) compared to IRI. The PK data were confirmed by the metabolite data from tumor biopsy samples in patients [1].</p>
<p><b>Figure 1:</b> Pharmacovital PK model was developed and tested with plasma and tumor PK data to assess drug PK PK parameters.</p>	<p><b>Figure 6:</b> Plasma and tumor PK models were integrated to create FPMX PK model for IRI. FPMX PK model was developed by using Simbiology™ toolbox in MATLAB™. Particle swarm optimization was used to estimate the model parameters.</p>	<p><b>Figure 10:</b> Lesions with PK data above the population median showed statistically significant shrinkage in lesion size. Earlier FPMX signals (1h and 24h) showed significant lesion response relationship (A, R), which was not significant relationship was observed at 72h (C).</p>
<p><b>Figure 2:</b> Pharmacovital PK model identified that longer duration of PK data in tumor offers evidence of IRI from free IRI. PK data for IRI in tumors and plasma were analyzed to assess the feasibility of permeability measurement.</p>	<p><b>Figure 7:</b> FPMX tumor PK model could quantify the degree of tumor permeability and PK data loading activity across all tumor lesions.</p>	<p><b>Figure 15:</b> FPMX signals at 1h and 24h were used to explain the ability of FPMX to predict a diagnostic biomarker for IRI. PK data for IRI in tumors and plasma were analyzed to assess the feasibility of permeability measurement.</p>
<p><b>Figure 3:</b> High PK data with refractory solid tumors were analyzed. PK data for IRI in tumors and plasma were analyzed to assess the feasibility of permeability measurement.</p>	<p><b>Figure 8:</b> Earlier FPMX signals (1h and 24h) were explained by the model parameters related to tumor permeability, whereas FPMX signals at 72h were explained by the model parameter for IRI binding to tumor tissue.</p>	<p><b>Figure 16:</b> PK data for IRI in tumors and plasma were analyzed to assess the feasibility of permeability measurement.</p>
<p><b>Design of Clinical Translational Study</b></p> <p><b>Figure 9:</b> High PK data with refractory solid tumors were analyzed. PK data for IRI in tumors and plasma were analyzed to assess the feasibility of permeability measurement.</p>	<p><b>Figure 11:</b> PK data for IRI in tumors and plasma were analyzed to assess the feasibility of permeability measurement.</p>	<p><b>Conclusions</b></p> <p>This phase 1 study demonstrated the feasibility of incorporating FPMX PK into a clinical workflow. FPMX tumor PK model identified that early FPMX signals at 1h and 24h contributed to tumor permeability of IRI. FPMX PK model correlated well with IRI PK data in tumor lesions. Significantly higher PK data for tumor PK parameters (PK<sub>1</sub>) and PK<sub>2</sub> (PK<sub>2</sub> PK<sub>1</sub>) compared to IRI. The PK data were confirmed by the metabolite data from tumor biopsy samples in patients [1].</p>

# Pseudoprogression of Glioblastoma after Chemo- and Radiation Therapy: Diagnosis by Using Dynamic Susceptibility-weighted Contrast-enhanced Perfusion MR Imaging with Ferumoxytol versus Gadoteridol and Correlation with Survival<sup>1</sup>

Seymur Gahramanov, MD  
 Leslie L. Muldoon, PhD  
 Csanad G. Varallyay, MD  
 Xin Li, PhD  
 Dale F. Kraemer, PhD  
 Rongwei Fu, PhD  
 Bronwyn E. Hamilton, MD  
 William D. Rooney, PhD  
 Edward A. Neuwelt, MD

## Purpose:

To compare gadoteridol and ferumoxytol for measurement of relative cerebral blood volume (rCBV) in patients with glioblastoma multiforme (GBM) who showed progressive disease at conventional magnetic resonance (MR) imaging after chemo- and radiation therapy (hereafter, chemoradiotherapy) and to correlate rCBV with survival.

## Materials and Methods:

Informed consent was obtained from all participants before enrollment in one of four institutional review board-approved protocols. Contrast agent leakage maps and rCBV were derived from perfusion MR imaging with gadoteridol and ferumoxytol in 19 patients with apparently progressive GBM on conventional MR images after chemoradiotherapy. Patients were classified as having high rCBV ( $>1.75$ ), indicating tumor, and low rCBV ( $\leq 1.75$ ), indicating pseudoprogression, for each contrast agent separately, and with or without contrast agent leakage correction for imaging with gadoteridol. Statistical analysis was performed by using Kaplan-Meier survival plots with the log-rank test and Cox proportional hazards models.

## Results:

With ferumoxytol, rCBV was low in nine (47%) patients, with median overall survival (mOS) of 591 days, and high rCBV in 10 (53%) patients, with mOS of 163 days. A hazard ratio of 0.098 ( $P = .004$ ) indicated significantly improved survival. With gadoteridol, rCBV was low in 14 (74%) patients, with mOS of 474 days, and high in five (26%), with mOS of 156 days and a nonsignificant hazard ratio of 0.339 ( $P = .093$ ). Five patients with mismatched high rCBV with ferumoxytol and low rCBV with gadoteridol had an mOS of 171 days. When leakage correction was applied, rCBV with gadoteridol was significantly associated with survival (hazard ratio, 0.12;  $P = .003$ ).

## Conclusion:

Ferumoxytol as a blood pool agent facilitates differentiation between tumor progression and pseudoprogression, appears to be a good prognostic biomarker, and unlike gadoteridol, does not require contrast agent leakage correction.

<sup>1</sup>From the Departments of Neurology (S.G., L.L.M., C.G.V., E.A.N.), Neurosurgery (E.A.N.), Public Health and Preventive Medicine (R.F.), Emergency Medicine (R.F.), Radiology (B.E.H.), and the Advanced Imaging Research Center (X.L., W.D.R.), Oregon Health & Science University, 3181 SW Sam Jackson Park Rd, L603, Portland, OR 97239-3090; Office of Research and Development, Department of Veterans Affairs Medical Center, Portland, Ore (E.A.N.); and Department of Medical Informatics and Clinical Epidemiology, Oregon State University, Portland, Ore (D.F.K.). Received July 25, 2011; revision requested September 8; revision received June 5, 2012; accepted June 25; final version accepted August 2. Address correspondence to E.A.N. (e-mail: [neuwelt@ohsu.edu](mailto:neuwelt@ohsu.edu)).

<sup>2</sup>Current address: Department of Neuroradiology, Universitätsklinikum Würzburg, Würzburg, Germany.



**R**adiation therapy in combination with temozolomide chemotherapy (hereafter, chemoradiotherapy) shows a significant survival benefit in patients with newly diagnosed glioblastoma multiforme (GBM) and has become the standard of care (1). However, radiologic deterioration is seen in patients more frequently after chemoradiotherapy than in those who receive radiation alone. Radiologic deterioration appears as an enlarged area of enhancement on contrast material-enhanced T1-weighted magnetic resonance (MR) images in up to 50% of all patients who have received chemoradiotherapy (2–4). Radiologic deterioration with or without clinical worsening can reflect either tumor progression or treatment-induced inflammatory change with increased permeability of the blood-brain barrier, which is known as pseudoprogression (5–8). Apparent tumor progression on MR images may actually represent pseudoprogression in up to 64% of cases (4). Patients with pseudoprogression, unlike those with

tumor progression, recover or stabilize spontaneously, generally without any changes in their treatment paradigm. Moreover, pseudoprogression is associated with a favorable prognosis and with O-6-methylguanine-DNA methyltransferase methylation status (4,5).

Conventional T2-weighted and contrast material-enhanced T1-weighted MR imaging sequences do not allow differentiation of tumor progression from pseudoprogression (5,9). Therefore, there is an urgent need to develop imaging tools that will assist clinicians in evaluating treatment effects and allow them to make appropriate therapeutic decisions. One of these imaging modalities is dynamic susceptibility-weighted contrast-enhanced (DSC) MR imaging measurement of relative cerebral blood volume (rCBV), which has been used for glioma grading (10–13), assessment of prognosis for patients with gliomas (13–17), and differentiation of recurrent tumor from radiation necrosis (18–20). High rCBV values indicate active neovascularization and a viable tumor (16,21,22). Accurate measurement of tumor rCBV by using standard DSC modeling approaches requires intravascular localization of contrast agent, which is compromised by the leaky blood-brain barrier present in patients with malignant brain tumors, especially after chemoradiotherapy. Rapid extravasation of a low-molecular-weight gadolinium-based contrast agent (GBCA) can result in underestimation of tumor rCBV (19–21,23).

Ferumoxytol, a very small superparamagnetic iron oxide nanoparticle that is approved by the U.S. Food and

Drug Administration for iron replacement therapy in adults with chronic kidney disease, has shown utility in brain imaging (24–26). Because ferumoxytol does not undergo renal elimination, it may serve as an alternative to GBCA in patients who are at risk for nephrogenic systemic fibrosis (27). Ferumoxytol acts as a blood pool agent shortly after administration because the iron nanoparticles are large (approximately 30 nanometers), and vascular localization is not compromised by the leaky blood-brain barrier (25). In addition, unlike other iron oxide nanoparticle contrast agents, ferumoxytol is administered as a fast bolus injection in therapeutic use (26). For these reasons, we hypothesized that ferumoxytol has the potential to allow measurement of rCBV more reliably than does GBCA.

The goal of this study was to compare gadoteridol versus ferumoxytol for measurement of relative cerebral blood volume (rCBV) in patients with glioblastoma multiforme who showed progressive disease at conventional magnetic resonance (MR) imaging after chemoradiotherapy and to correlate rCBV with survival.

#### Advances in Knowledge

- The results of this study confirm that brain tumor blood volume measurements are underestimated when gadoteridol, a low-molecular-weight gadolinium-based contrast agent, is used, most likely because of extravasation artifacts, and leakage correction is necessary to improve the accuracy of rCBV estimation.
- Ferumoxytol as a blood pool agent offers reliable and simplified modeling of tumor blood volume assessment with no need of leakage correction.
- Tumor blood volume estimated by using perfusion MR imaging with ferumoxytol or leakage-corrected perfusion MR imaging with gadoteridol, unlike nonleakage-corrected perfusion MR imaging with gadoteridol, may facilitate diagnosis of pseudoprogression and is significantly associated with survival.

#### Implication for Patient Care

- Perfusion MR imaging with ferumoxytol can assist clinicians in establishing which patients have active glioblastoma multiforme after chemoradiotherapy and should begin second line or experimental therapy without delay, and which patients have a better prognosis and would benefit from continuation of adjuvant temozolomide.

#### Published online before print

10.1148/radiol.12111472 Content code: NR

Radiology 2013; 266:842–852

#### Abbreviations:

CI = confidence interval  
 DSC = dynamic susceptibility-weighted contrast-enhanced  
 GBCA = gadolinium-based contrast agent  
 GBM = glioblastoma multiforme  
 mOS = median overall survival  
 rCBV = relative cerebral blood volume

#### Author contributions:

Guarantors of integrity of entire study, S.G., E.A.N.; study concepts/study design or data acquisition or data analysis/interpretation, all authors; manuscript drafting or manuscript revision for important intellectual content, all authors; approval of final version of submitted manuscript, all authors; literature research, S.G., L.L.M., X.L.; clinical studies, S.G., C.G.V., B.E.H., W.D.R.; experimental studies, S.G., X.L., W.D.R.; statistical analysis, S.G., D.F.K., R.F.; and manuscript editing, all authors

#### Funding:

This research was supported by the National Institutes of Health (grants 5 R01 NS053468, 5 R01 CA137488, 3 R01 CA137488-15S1, and 5 R01 NS044687)

Conflicts of interest are listed at the end of this article.

CSPC Exhibit 1094

### Materials and Methods

Between April 2007 and October 2009, 19 patients with GBM were prospectively studied in one of four different research imaging protocols that were sponsored by the National Institutes of Health and approved by the institutional review board. The four protocols were designed to compare anatomic and dynamic MR imaging by using GBCA versus ferumoxytol. The number of patients from each protocol that were included in our analysis and the objective of each protocol were as follows: six patients from protocol 2753 (<http://clinicaltrials.gov/ct2/show/NCT00660543?term=neuwell+and+portland&rank=3>), which was a study of serial imaging changes of GBM patients before and after chemoradiotherapy; five patients from protocol 2864 (<http://clinicaltrials.gov/ct2/show/NCT00659126?term=neuwell+and+portland&rank=8>), a study of sequential imaging with gadoteridol and ferumoxytol at 3-T and 7-T MR imaging in patients with primary or metastatic brain tumors either before or after therapy; seven patients from protocol 1562 (<http://clinicaltrials.gov/ct2/show/NCT00659776?term=neuwell+and+portland&rank=6>), a study of MR imaging of central nervous system inflammatory lesions with intravenous gadoteridol and ferumoxytol; and one patient from protocol 3678 (<http://clinicaltrials.gov/ct2/show/NCT00769093?term=neuwell+and+portland&rank=10>), a comparison of imaging changes induced by bevacizumab versus dexamethasone in patients with recurrent high-grade glioma. As of October 2009, 84 patients were imaged in these four protocols, 27 (32%) had a diagnosis of GBM, and 19 patients with GBM met the inclusion criteria for our study. Informed written consent was obtained from all patients.

Inclusion criteria for this analysis included histologically proved GBM (World Health Organization classification, grade IV) and apparent tumor progression at conventional MR imaging after standard postsurgical treatment of radiation therapy and chemotherapy with temozolomide. No patients who met the inclusion

criteria were excluded from analysis. Inclusion criteria common to all protocols were Karnofsky Performance Score greater than 50 and absence of contraindication for GBCA or ferumoxytol administration. Collected patient data included age, sex, extent of surgery, radiation dose, date of chemoradiotherapy, date of first conventional MR imaging examination that was suggestive of progression, date of DSC MR imaging examination of the study, ferumoxytol and gadoteridol dose, dexamethasone dose, and antiangiogenic treatment after study. The patients were followed up until death or the date of their last follow-up examination. Patients who were still alive at the time of analysis were treated as censored cases for the data analysis.

### Magnetic Resonance Imaging

Nineteen patients who underwent conventional MR imaging after chemoradiotherapy and received results that suggested progression of the disease were included. Patients underwent a total of 19 MR imaging sessions on two consecutive days. On the first day, unenhanced and contrast-enhanced T1-weighted images and DSC MR images were acquired by using gadoteridol gadolinium (III) chelate (ProHance, Bracco Diagnostic, Princeton, NJ). On the following day, the same MR imaging sequences were performed by using ferumoxytol (AMAG Pharmaceuticals, Cambridge, Mass). AMAG Pharmaceuticals provided ferumoxytol free of charge. The authors had full control of the data and the information submitted for publication. No patient had any complications during the MR imaging examinations.

MR imaging sessions for 18 of the 19 patients were conducted by using a 3-T whole-body MR imaging system (Tim Trio; Siemens, Erlangen, Germany) with a body radiofrequency coil transmitter and a 12-channel matrix head coil signal receiver. One patient underwent MR imaging sessions with a 7-T MR imaging system (Magnetom 7 T, Siemens) equipped with an eight-channel phased-array transmit-receive radiofrequency head coil (Rapid Biomedical, Rimpf, Germany).

For DSC MR imaging, dynamic T2\*-weighted images were acquired by using a gradient-echo echo-planar imaging pulse sequence (repetition time msec/echo time msec, 1500/20; flip angle, 45°; field of view, 192 × 192 mm; matrix, 64 × 64; and 27 interleaved sections at 3 T or 13 sections at 7 T; section thickness, 3 mm; and section gap, 0.9 mm). After patients underwent a baseline period of seven imaging volumes (11 seconds), a rapid bolus of contrast agent was administered intravenously through an 18-gauge intravenous catheter at a rate of 3 mL per second by using a power injector (Spectris Solaris-Medrad, Warrendale, Pa), immediately followed by 20 mL of saline flush at the same rate. DSC data collection comprised a total of 90 series (2 minutes 21 seconds). Gadoteridol was injected at a dose of 0.1 mmol/kg of body weight. The ferumoxytol dose was dependent on the protocol in which the patient was enrolled and was administered at either 2 mg/kg, 1 mg/kg, or in a constant volume of 2.5 mL diluted with 2.5 mL of saline (75 mg) regardless of body weight. T1-weighted anatomic MR imaging was performed before and 20 minutes after gadoteridol administration by using a two-dimensional spin-echo sequence (900/10; field of view, 180 × 240 mm; matrix, 256 × 192; sections, 44; section thickness, 2 mm, gapless).

### Imaging Analysis

All data were acquired (S.G. and C.V., with 4 and 8 years of experience, respectively), processed (S.G., C.V., and B.H., with 10 years of experience) and analyzed (D.K. and R.F., with 15 and 10 years of experience, respectively). The neuroradiologists (S.G., C.V., and B.H.) were blinded to survival data. All DSC MR imaging data were processed with a dedicated software package (NordicICE; NordicNeuroLab, Bergen, Norway). The rCBV maps were generated by using established tracer kinetic models applied to the first-pass data (28,29) without and with application of the mathematic leakage correction method (30). Leakage correction was applied only when gadoteridol was used



because ferumoxytol is an intravascular contrast agent and eliminates the need for correction, and all correction methods were developed for GBCAs. On a pixel-by-pixel basis, the rCBV maps were normalized by dividing every rCBV value by the unaffected white matter rCBV value. The normalized rCBV maps were coregistered and displayed as color overlays on gadoteridol-enhanced T1-weighted images. In the enhancing lesion, a  $2 \times 2$  pixel ( $6 \times 6$  mm) region of interest with the highest rCBV value on the ferumoxytol rCBV parametric map and the same region of interest on the gadoteridol rCBV parametric map were analyzed. Areas showing major vessels, obvious hemorrhage, and visible cystic and necrotic changes were excluded from regions of interest. Previous studies showed that a threshold rCBV ratio of 1.75, which was measured by using DSC MR imaging with GBCA, was predictive of time to progression or survival (14,16). Our prior study results showed the feasibility of this cutoff value for ferumoxytol as well (21). Therefore, in this study, we considered an rCBV greater than 1.75 to be high (active tumor) and rCBV less than or equal to 1.75 to be low (pseudoprogression). However, we also tested alternative cutoff values. By using the NordicICE software, we generated first-order estimates of vascular permeability or leakage maps, referred to as K2 in the Boxerman et al study (30), from DSC MR imaging data for both contrast agents for contrast agent extravasation visualization and assessment.

#### Statistical Analysis

To assess whether rCBV measurements allow differentiation of active tumor from pseudoprogression and to predict prognosis by using DSC MR imaging with ferumoxytol or GBCA, we classified each patient into one of two groups on the basis of rCBV value (rCBV > 1.75 and rCBV  $\leq$  1.75) for ferumoxytol, gadoteridol, and gadoteridol with leakage correction. Mean and standard deviation of rCBV measurements were obtained for each group. Differences between groups were assessed by using

the Student paired *t* test and were graphed by using Bland-Altman plots.

For each contrast agent, median overall survival (mOS) and 95% confidence interval (CI) were assessed in each group by using Kaplan-Meier product limit estimates, and the groups were compared by using the log-rank test. When the upper limit of the 95% CI was not estimable, the highest observed survival time was reported. In addition, Cox proportional hazards models were fitted to estimate the hazard ratios separately for each contrast agent. These survival analyses were performed by using four different rCBV cutoff values (1.5, 1.75, 2.0, 2.5) for ferumoxytol, gadoteridol, and gadoteridol with leakage correction. A *P* value less than .05 was considered to indicate a significant difference. All analyses were performed by using SAS Version 9.2 for Windows (SAS Institute, Cary, NC).

#### Results

Nineteen patients with GBM showed apparent tumor progression on conventional MR images obtained within one year of chemoradiotherapy. In 16 of 19 (84%) patients, DSC MR imaging studies were performed within 6 months after completion of chemoradiotherapy, and three (16%) patients underwent DSC MR imaging 9, 10, and 11 months after chemoradiotherapy.

The mean and standard deviation for rCBV values in the entire group measured by using ferumoxytol, gadoteridol, and gadoteridol with leakage correction were  $2.5 \pm 2.1$ ,  $1.38 \pm 1.73$ , and  $2.36 \pm 1.94$ , respectively, with a statistically significant difference between ferumoxytol and gadoteridol (*P* = .003), and between ferumoxytol and gadoteridol with leakage correction (*P* = .008). When leakage correction was applied, rCBV values measured with gadoteridol were not different from those measured with ferumoxytol (*P* = .33). On the basis of DSC MR imaging with ferumoxytol, nine (47%) patients had rCBV values less than or equal to 1.75 ( $0.6 \pm 0.19$ ) and 10 (53%) patients had rCBV values greater than 1.75 ( $4.21 \pm 1.38$ ) (Fig 1A and 1B). In the same patients, DSC MR imaging

by using gadoteridol without leakage correction showed rCBV less than or equal to 1.75 in 14 (74%) patients ( $0.41 \pm 0.36$ ) and rCBV greater than 1.75 in five (26%) patients ( $4.1 \pm 0.7$ ). With leakage correction, the rCBV was less than or equal to 1.75 in 10 (53%) patients ( $0.79 \pm 0.55$ ) and greater than 1.75 in nine (47%) patients ( $4.1 \pm 1.26$ ) (Fig 1A and 1B). All nine patients who had low rCBV with ferumoxytol also had low rCBV with gadoteridol without and with leakage correction. Figure 2 shows a representative patient in whom conventional MR imaging suggested tumor progression but in whom DSC MR imaging with both ferumoxytol and gadoteridol showed low rCBV. Such results were unambiguously classified as pseudoprogression. All five patients who had high rCBV with gadoteridol without leakage correction and nine patients with leakage correction also had high ferumoxytol rCBV (Fig 1A and 1B). Figure 3 shows a patient who had high rCBV with both contrast agents, particularly at the tumor margin, which is indicative of true tumor progression. In five patients, rCBV values for ferumoxytol and gadoteridol were mismatched, where rCBV was greater than 1.75 with ferumoxytol and less than 1.75 with gadoteridol. However, after leakage correction application, only one patient had mismatched values (Fig 1A and 1B). The representative patient images in Figure 4 show progression in the posterior lesion with ferumoxytol and pseudoprogression with gadoteridol. With the application of leakage correction, accuracy of gadoteridol rCBV estimation improved and was suggestive of tumor progression. Bland-Altman plots showed that the average of the differences between rCBV values obtained by using ferumoxytol and those obtained by using gadoteridol was 1.12, and between rCBV values with ferumoxytol and those with gadoteridol with leakage correction, the difference was reduced to 0.14 (Fig 1C and 1D).

At the time of analysis, 15 of 19 (79%) patients had died and four of 19 (21%) patients were still alive at the time of analysis (mean survival, 1049 days; range, 483–1331 days). The mOS in all patients from DSC MR imaging to

Figure 1

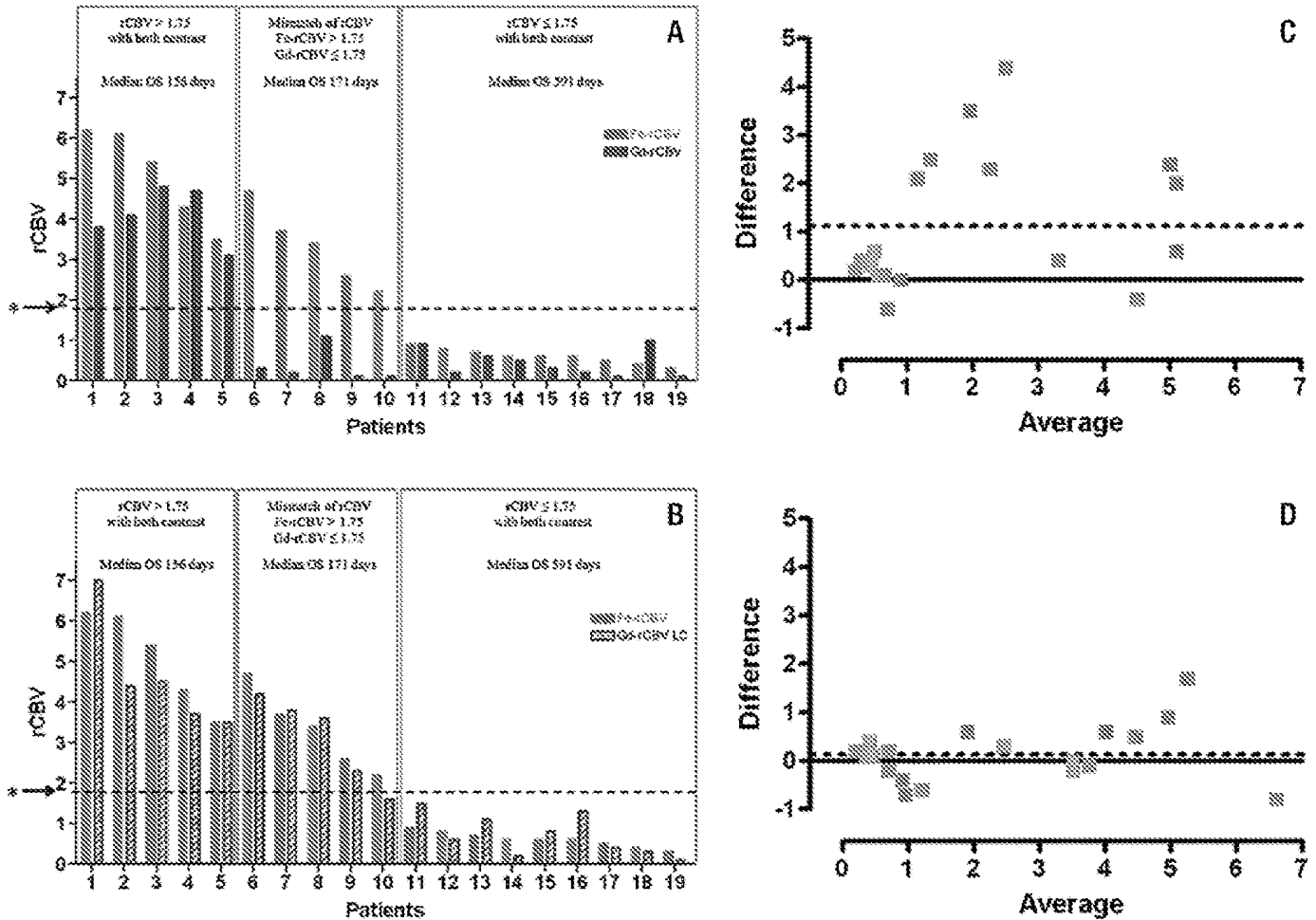


**Figure 1:** Bar graphs and scatterplots show summary of rCBV values estimated at perfusion MR imaging with both contrast agents. Bar graphs *A* and *B* show tumor rCBVs with ferumoxytol (red bars, *Fe-rCBV*), gadoteridol (blue bars, *Gd-rCBV*) and gadoteridol with leakage correction (striped blue bars, *Gd-rCBV LC*) for each patient. Patients with high rCBV ( $>1.75$ ) with both contrast agents had poor overall survival (OS). Patients with low rCBV ( $\leq 1.75$ ) with both contrast agents had significantly longer overall survival. Patients with high rCBV with ferumoxytol and low rCBV with gadoteridol had poor prognosis. Asterisks indicate rCBV cutoff value of 1.75. Bland-Altman plots show average differences between rCBV values for, *C*, ferumoxytol and gadoteridol as 1.12 and, *D*, ferumoxytol and gadoteridol with leakage correction as 0.14.

death or last follow-up examination was 314 days (95% CI: 156, 591 days). The Kaplan-Meier estimates of survival for patients with high and low rCBV values are shown in Figure 5.

For ferumoxytol, the mOS was 591 days (95% CI: 286, 1232 days) for patients with rCBV values less than or equal to 1.75 and 163 days (95% CI: 24, 295 days) for those with values greater than 1.75 (log-rank  $P$  value  $< .001$ ). The estimated hazard ratio for rCBV values less than or equal to 1.75 measured by using ferumoxytol was 0.098 (95% CI:

0.020, 0.481;  $P = .004$ ), indicating significantly improved survival in patients with rCBV values less than or equal to 1.75. The same results were obtained by using an rCBV cutoff value of 1.5 or 2.0 for ferumoxytol, but by using a cutoff of 2.5, the mOS was 576 days (95% CI: 286–1232 days) in patients with rCBV values less than or equal to 2.5 and 156 days (95% CI: 24, 295 days) in patients with rCBV values greater than 2.5 ( $P < .001$ ), with an estimated hazard ratio of 0.120 (95% CI: 0.030, 0.482;  $P = .003$ ) for rCBV values less than or equal to 2.5.

For gadoteridol without leakage correction, the mOS was 474 days (95% CI: 171, 1232 days) in patients with rCBV less than or equal to 1.75 and 156 days (95% CI: 24, 484 days) in patients with rCBV greater than 1.75 ( $P = .079$ ). The estimated hazard ratio for rCBV values less than or equal to 1.75 with gadoteridol was 0.339 (95% CI: 0.096, 1.197,  $P = .093$ ) also indicating improved survival in patients with rCBV values less than or equal to 1.75, but it was not a statistically significant difference. Testing rCBV cutoff values

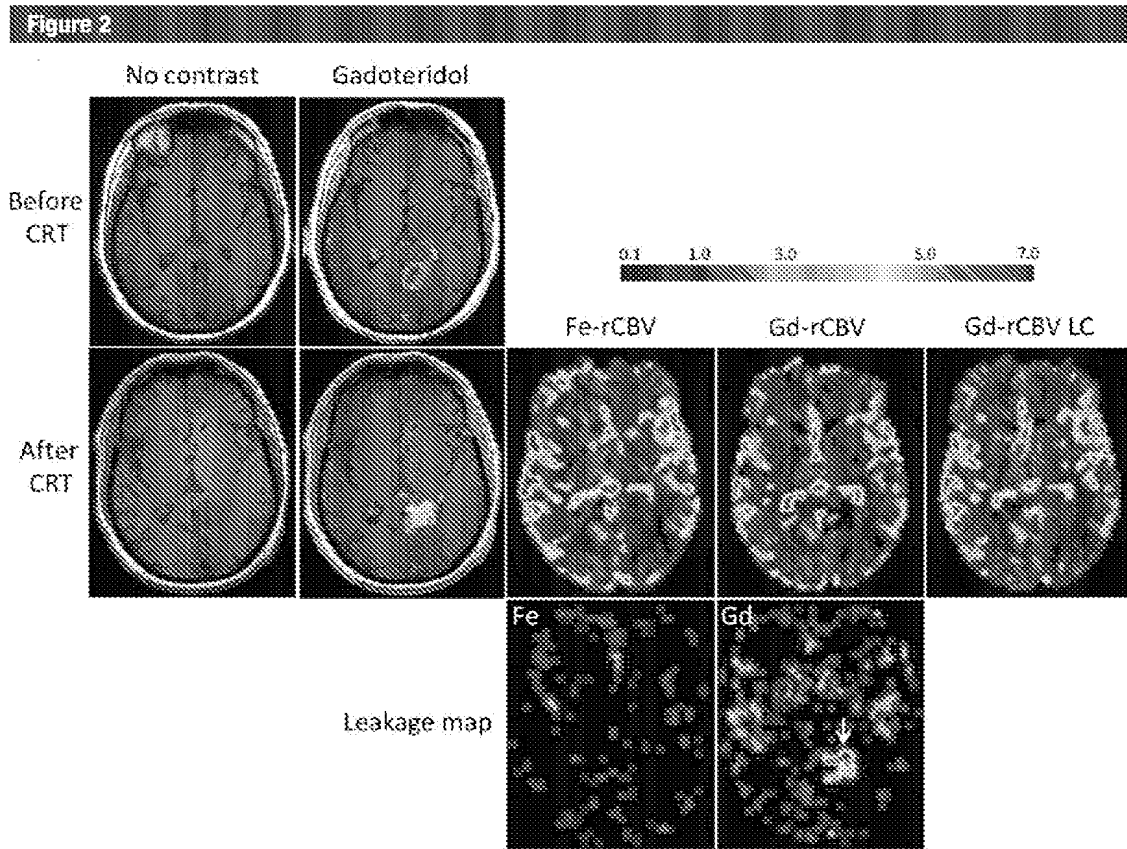


**Figure 2:** Axial images of 73-year-old man with GBM show pseudoprogression of disease. T1-weighted MR images without contrast enhancement and with gadoteridol (*Gd*) obtained before and 3 months after chemoradiotherapy (*CRT*) show increased contrast enhancement after treatment. Low rCBV ( $\leq 1.75$ ) is apparent on parametric maps obtained by using ferumoxytol (*Fe-rCBV*), gadoteridol (*Gd-rCBV*), and gadoteridol with leakage correction (*Gd-rCBV LC*), which indicates pseudoprogression. Leakage map shows absence of contrast extravasation when ferumoxytol (*Fe*) was used and contrast leakage with gadoteridol (arrow).

of 1.5, 2.0, and 2.5 for gadoteridol resulted in the same outcome as that for 1.75.

For gadoteridol with leakage correction, the mOS was 576 days (95% CI: 286, 1232 days) in patients with rCBV less than or equal to 1.75 and 156 days (95% CI: 24, 295 days) in patients with rCBV greater than 1.75 ( $P < .001$ ). The estimated hazard ratio for rCBV values less than or equal to 1.75 was 0.12 (95% CI: 0.030, 0.482;  $P = .003$ ) also indicating significantly improved survival in patients with rCBV less than or equal to 1.75. These were the same as they were when using a cutoff value of 2.0. The mOS was 561 days (95% CI: 286, 1232 days) in patients with rCBV less than or equal to 2.5 and 163 days (95% CI: 24, 295 days) in patients with rCBV greater than 2.5 ( $P = .004$ ) and

the estimated hazard ratio for rCBV less than or equal to 2.5 was 0.182 (95% CI: 0.050, 0.659;  $P = .009$ ), and by using the rCBV cutoff of 1.5, the mOS was 591 days (95% CI: 286, 1232 days) in patients with rCBV less than or equal to 1.5 and 163 days (95% CI: 24, 295 days) with rCBV greater than 1.5 ( $P < .001$ ) and the estimated hazard ratio for rCBV less than or equal to 1.5 was 0.098 (95% CI: 0.020, 0.481;  $P = .004$ ), which was the same as for rCBV measured with ferumoxytol with cutoff values between 1.5 and 2.0.

The mOS in five patients with discordance between ferumoxytol and gadoteridol rCBV was 171 days (95% CI: 73, 315 days) indicating poor survival due to tumor progression (Fig 1, A); however, after leakage correction application only one patient had rCBV mismatch, with

survival of 315 days. None of the leakage maps showed ferumoxytol extravasation, but gadoteridol leakage was apparent in all cases (Figs 2–4).

**Discussion**

Our study results showed the role of rCBV measurement in differentiating tumor progression from pseudoprogression and predicting survival in GBM patients who appeared to have progressive disease at conventional MR imaging after chemoradiotherapy. There is a significant difference in survival between patients with low versus high rCBV with ferumoxytol, and this binary cutoff set in a range between 1.5 and 2.0 returns the same prediction capacity. Absence of ferumoxytol extravasation shown on leakage maps indicated

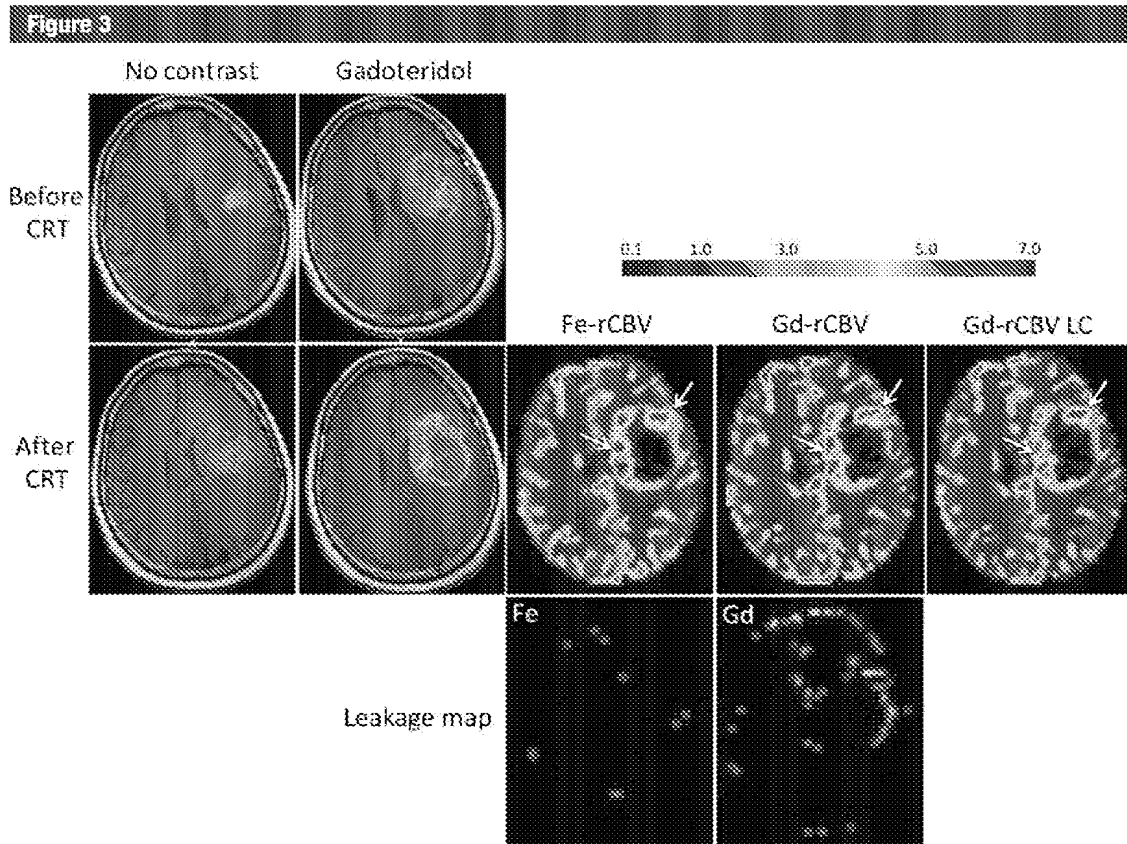


**Figure 3:** Axial images of 59-year-old woman with GBM show progression of disease. T1-weighted MR images without contrast agent and with gadoteridol (*Gd*) obtained before and 2 weeks after chemoradiotherapy (*CRT*) show increased contrast enhancement after treatment. High rCBV ( $> 1.75$ ) is apparent on parametric maps obtained by using ferumoxytol (*Fe-rCBV*), gadoteridol (*Gd-rCBV*), and gadoteridol with leakage correction (*Gd-rCBV LC*), which indicates true tumor progression (arrows). No contrast agent extravasation is seen on leakage map with ferumoxytol (*Fe*) but small leakage in the lateral aspect of the tumor is seen with gadoteridol.

that leakage correction is not necessary with ferumoxytol. The results based on rCBV with gadoteridol without leakage correction are similar but not statistically significant for all tested cutoff values. In addition, rCBV values obtained with gadoteridol that suggested pseudoprogression were not correct in five patients with a short survival, and rCBV with ferumoxytol indicated a progressive tumor in these patients. Use of leakage correction resulted in improvement of gadoteridol rCBV estimation, which was not significantly different from ferumoxytol rCBV values. Moreover, leakage-corrected gadoteridol rCBV values with a cutoff of 1.5 were significantly associated with survival and matched the ferumoxytol rCBV cutoff range of 1.5–2.0. This finding shows the effect of GBCA extravasation

and rCBV underestimation, which can potentially lead to incorrect diagnosis, treatment, and prognosis and necessity of leakage correction.

The issue of GBCA extravasation during perfusion MR imaging of lesions with a disrupted blood-brain barrier and the resulting underestimation of rCBV is well known and has been shown by multiple investigators (18–20). To improve the diagnostic accuracy of DSC MR imaging, several methods have been proposed for leakage correction, such as the use of small flip-angle gradient-echo (11,31,32) or dual-echo (33,34) perfusion acquisitions, a preload method (33,34), or postprocessing with multiple mathematic correction algorithms (30,35,36), but these still have a lack of consistency and reproducibility. Magnetic field strength differences and MR

pulse sequence details must be taken into account on correction methods for proper leakage correction with GBCA. Leakage correction works best with limited extravasation rates, above which the blood space and extravascular extracellular space becomes intrinsically indistinguishable when GBCA is used, and the derived rCBV value and leakage rate are no longer independent. The results of our preclinical rodent study also showed that brain tumor rCBV was underestimated when GBCA was used in a human high-grade glioma xenograft, and the accuracy of the measurement was improved by using the preload leakage correction method; however, rCBV values depended on the dose of contrast agent preload (37). By using ferumoxytol for DSC MR imaging in the same animals, we obtained consistent

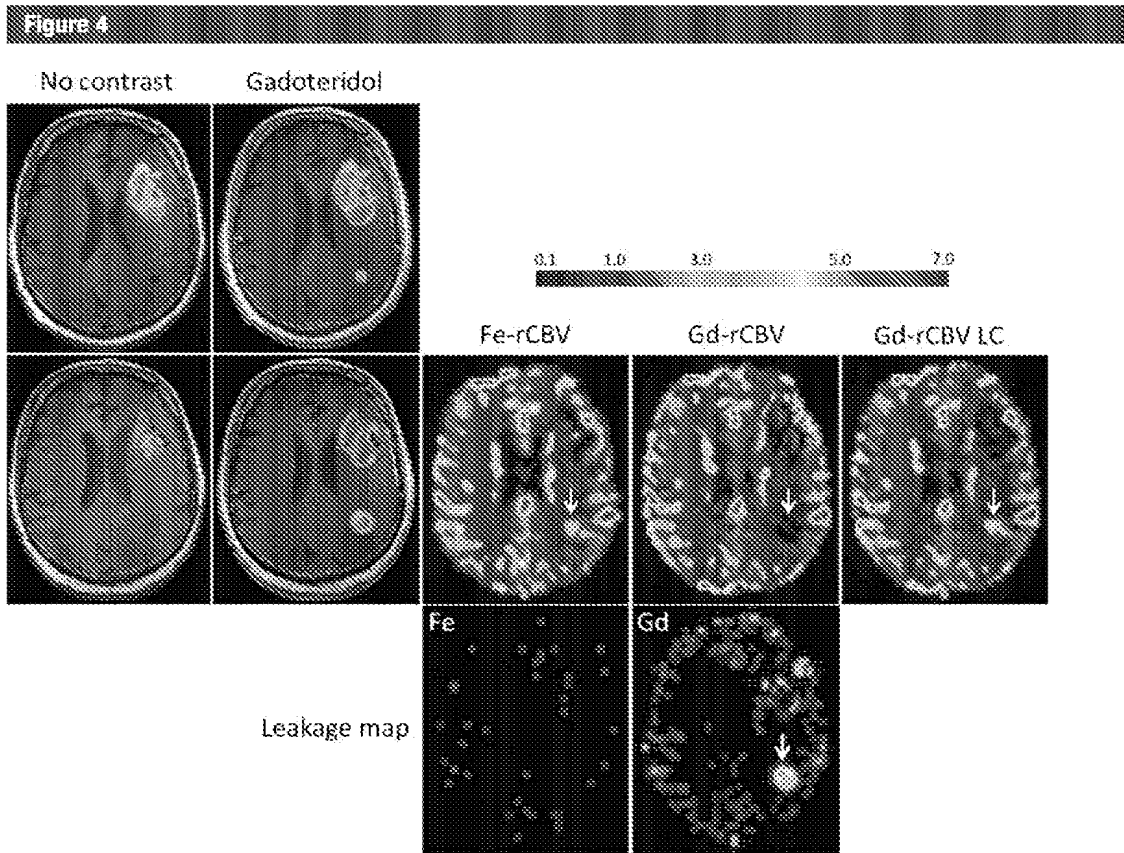


**Figure 4:** Axial images in 68-year-old man with GBM show discordance between rCBV values measured with ferumoxytol (*Fe*) and gadoteridol (*Gd*). T1-weighted MR images without contrast agent and with gadoteridol obtained before and 2 weeks after chemoradiotherapy (*CRT*) show increased contrast enhancement after treatment. High rCBV ( $> 1.75$ ) on parametric maps obtained by using ferumoxytol (*Fe-rCBV*) and gadoteridol with leakage correction (*Gd-rCBV*) indicates active tumor, and low rCBV ( $\leq 1.75$ ) on gadoteridol parametric map (*Gd-rCBV*) indicates pseudoprogression (arrows). Leakage map indicates absence of contrast extravasation when ferumoxytol was used and contrast extravasation with gadoteridol (arrow).

rCBV estimation regardless of the permeability of the tumor vasculature and independent of contrast agent preload.

Current treatment response evaluation criteria, such as the McDonald criteria, Response Evaluation Criteria in Solid Tumors, and Response Assessment in Neuro-Oncology (RANO) Working Group, are based on conventional MR imaging sequences and cannot allow reliable differentiation of progression from pseudoprogression (38–40). This is the major reason that there was no significant difference in survival shown in patients with progressive disease versus those with no progression (stable or partial response) based on McDonald criteria 1 month after chemoradiotherapy in two studies

(41,42). The current standard-of-practice recommendation in patients with increased or new enhancement within 3 months after completion of chemoradiotherapy is to continue adjuvant temozolomide treatment for one to three cycles (40,43,44). If repeated MR imaging 1–3 months after the first MR imaging examination shows no further progression or even a decrease of enhancement and the patient is on adjuvant temozolomide treatment with a stable dose of steroids and without antiangiogenic therapy, then diagnosis of pseudoprogression can be made retrospectively. This approach has limitations because (a) ineffective therapy may be continued in patients with true progressive disease; (b) patients with

true progressive disease may not be included in second line or experimental therapy without delay; (c) retrospective diagnosis of pseudoprogression cannot be made if a patient's condition required an increase in steroid dose or antiangiogenic therapy to decrease mass effect; (d) new or increased enhancement more than 3 months after chemoradiotherapy does not necessarily indicate true tumor progression because pseudoprogression can be seen beyond this time frame; (e) further increases of enhancement on the second follow-up MR imaging examination could be caused not only by tumor progression but also by continuation of treatment-related inflammatory reaction; (f) the inability to reliably



**Figure 5**

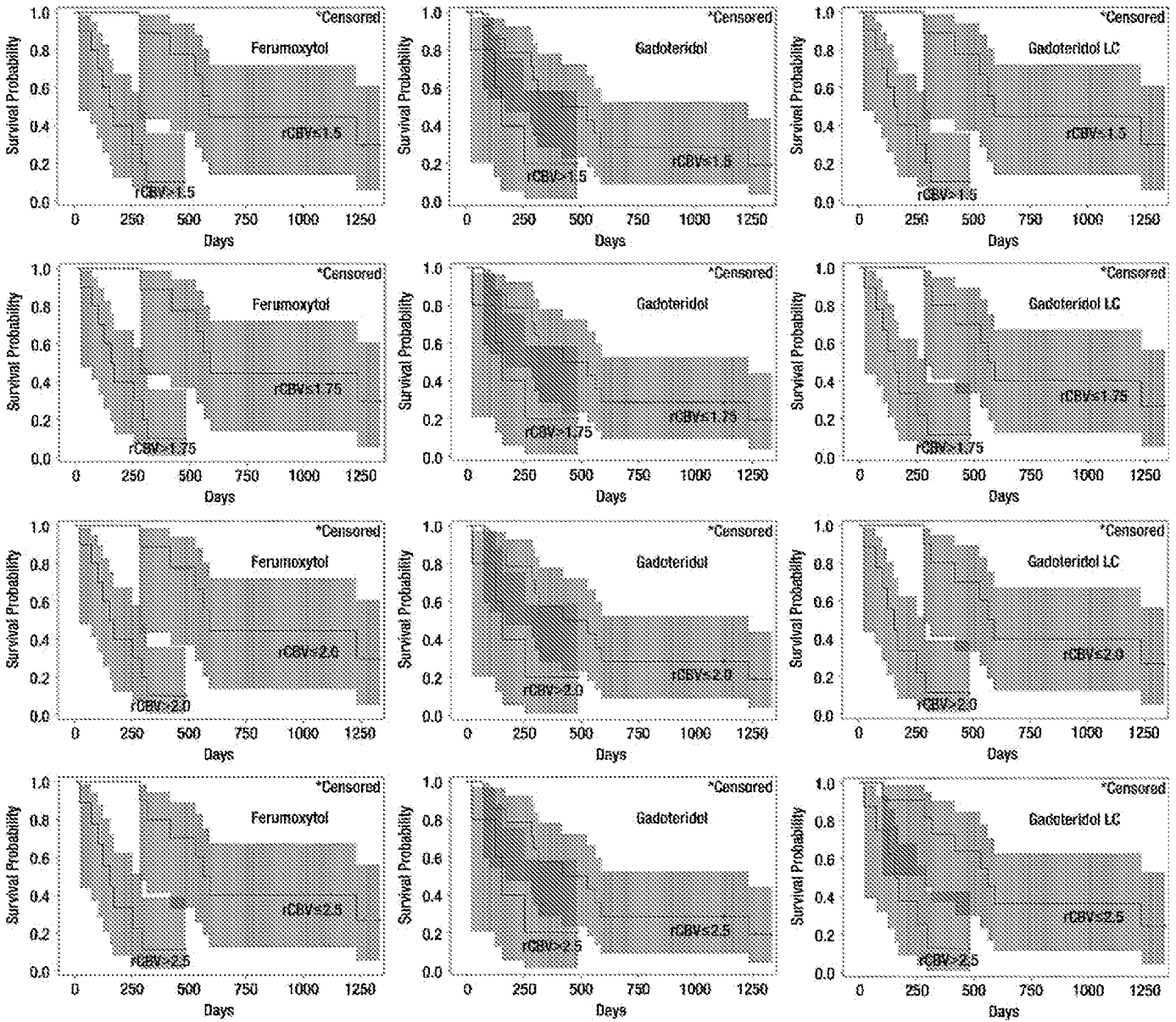


**Figure 5:** Charts show survival of GBM patients according to rCBV by using four cutoff values. Tumor rCBV was measured by using ferumoxytol versus gadoteridol and gadoteridol with leakage correction (LC). Kaplan-Meier survival curves show best survival prediction by using rCBV values obtained with ferumoxytol ( $P < .001$ ) when cutoff range is between 1.5 and 2.0, and the same result was achieved with gadoteridol leakage correction with cutoff of 1.5. By using gadoteridol, survival prediction is similar but not statistically significant ( $P = .079$ ) for all cutoff values. Colored areas indicate 95% CIs.

differentiate tumor progression from pseudoprogression can cause inclusion of patients with pseudoprogression in experimental protocols, with further false-positive response to experimental treatment.

Our study indicated that perfusion MR imaging in conjunction with

conventional MR imaging can assist clinicians in avoiding continuation of ineffective therapy, starting second line or experimental therapy without delay in patients with active tumors, and establishing the patients who have a better prognosis and who will benefit from continuation of adjuvant temozolomide.

These findings are in agreement with those of other investigations regarding the role of perfusion MR imaging in this dilemma (14,41). Unlike authors of other studies, we compared DSC MR imaging by using low-molecular-weight GBCA versus high-molecular-weight ferumoxytol in the patients with

apparent progression at conventional MR imaging after chemoradiotherapy and assessed the ability of mathematic leakage correction to improve accuracy of rCBV estimation.

One of the limitations of this study was the inclusion of only 19 patients. Even so, 70% of patients with high rCBV values with ferumoxytol died before the first death among patients with low rCBV with ferumoxytol. Thus, rCBV values with ferumoxytol appeared to be a strong predictor of prognosis and similar to rCBV values with leakage-corrected gadoteridol. In addition, survival prediction with rCBV with ferumoxytol was robust in a wide range of rCBV cutoff values. Larger confirmatory studies are required to validate the findings of this study. A second limitation is that only one type of leakage correction method was tested. Paulson et al (35) found variability in tumor rCBV depending on the choice of five different mathematic correction algorithms. Moreover, our preclinical study (37) results showed the inconsistency of preload methods for leakage correction. The most commonly used of these two methods required either sophisticated postprocessing or high contrast-agent dose exposure but was still inconsistent. The third potential limitation was the difference in the treatment after the study, which may have affected the overall survival rates. However, most of the patients in this study received antiangiogenic treatment, and there was no marked survival benefit from the use of different chemotherapy regimens in patients with recurrent GBM. The use of three different ferumoxytol doses for DSC MR imaging was the fourth limitation of our study. MR imaging signal intensity may be affected by ferumoxytol dose. Because there is not a recommended standard dose of ferumoxytol for DSC MR imaging, we tested a variety of doses in different protocols. Ferumoxytol has a greater apparent transverse relaxivity than GBCA and causes more signal decrease on T2\* sequences, and therefore less contrast agent is required for perfusion MR imaging. We found no

correlation between ferumoxytol dose and rCBV value. It is likely that within a detectable dosage range the findings of the study were independent of ferumoxytol dose. The fifth limitation of this study was the difference in timing of DSC MR imaging among patients. Although most patients (84%) were studied within 6 months after chemoradiotherapy, which is the time period when pseudoprogression is thought to occur, three patients were included in the study 9, 10, and 11 months after chemoradiotherapy. Nonetheless, ferumoxytol DSC MR images showed that one of these patients had pseudoprogression rather than true tumor progression. Although this study included only patients with GBM, the diagnostic dilemma of pseudoprogression may be valid for any brain tumor requiring radiation without or with concomitant chemotherapy.

On the basis of our findings, we propose that tumor blood volume assessment by using perfusion MR imaging with ferumoxytol may help clinicians to differentiate true tumor progression from pseudoprogression in patients with GBM who show radiologic progression at conventional MR imaging after chemoradiotherapy. Unlike GBCA, ferumoxytol does not require leakage correction application. The rCBV values obtained by using ferumoxytol and leakage-corrected gadoteridol appear to be good prognostic biomarkers and may improve disease management by allowing clinicians to choose the correct treatment strategy without delay. Leakage correction is necessary to improve accuracy of rCBV estimation when GBCA is used, and despite that misestimation of rCBV, still can occur in some cases. Furthermore, the effectiveness of leakage correction may depend on the rate constant of GBCA extravasation (ie,  $K^{trans}$ ), a dimension that we did not investigate. Ferumoxytol, because of the absence of extravasation during DSC acquisition, greatly simplifies modeling and holds promise for evaluation of tumor behavior and response to therapy in patients with brain tumors.

**Acknowledgments:** The authors thank Aliana Culp and Lisa Bennett for help with manuscript preparation.

**Disclosures of Conflicts of Interest:** S.G. No relevant conflicts of interest to disclose. L.L.M. No relevant conflicts of interest to disclose. C.G.V. No relevant conflicts of interest to disclose. X.L. No relevant conflicts of interest to disclose. D.E.K. No relevant conflicts of interest to disclose. R.E. No relevant conflicts of interest to disclose. B.E.H. Financial activities related to the present article: none to disclose. Financial activities not related to the present article: Received payment for consultancy and royalties from Amirsys. Other relationships: none to disclose. W.D.R. Financial activities related to the present article: none to disclose. Financial activities not related to the present article: Institution has patent pending related to DCE MR imaging for cancer. Author has stock/stock options for DeltaPoint in relation to patent. Other relationships: none to disclose. E.A.N. Financial activities related to the present article: none to disclose. Financial activities not related to the present article: none to disclose. Other relationships: none to disclose.

## References

1. Stupp R, Mason WP, van den Bent MJ, et al. Radiotherapy plus concomitant and adjuvant temozolomide for glioblastoma. *N Engl J Med* 2005;352(10):987-996.
2. Gerstner ER, McNamara MB, Norden AD, Lafrankie D, Wen PY. Effect of adding temozolomide to radiation therapy on the incidence of pseudo-progression. *J Neurooncol* 2009;94(1):97-101.
3. de Wit MC, de Bruin HG, Eijkenboom W, Sillevius Smitt PA, van den Bent MJ. Immediate post-radiotherapy changes in malignant glioma can mimic tumor progression. *Neurology* 2004;63(3):535-537.
4. Brandes AA, Franceschi E, Tosoni A, et al. MGMT promoter methylation status can predict the incidence and outcome of pseudoprogression after concomitant radiochemotherapy in newly diagnosed glioblastoma patients. *J Clin Oncol* 2008;26(13):2192-2197.
5. Brandsma D, Stalpers L, Taal W, Sminia P, van den Bent MJ. Clinical features, mechanisms, and management of pseudoprogression in malignant gliomas. *Lancet Oncol* 2008;9(5):453-461.
6. Tofilon PJ, Fike JR. The radioresponse of the central nervous system: a dynamic process. *Radiat Res* 2000;153(4):357-370.
7. Wong CS, Van der Kogel AJ. Mechanisms of radiation injury to the central nervous system: implications for neuroprotection. *Mol Interv* 2004;4(5):273-284.
8. Nordal BA, Nagy A, Pintilie M, Wong CS. Hypoxia and hypoxia-inducible factor-1 target genes in central nervous system radiation injury: a role for vascular en-

- dothelial growth factor. *Clin Cancer Res* 2004;10(10):3342-3353.
9. Brandes AA, Tosoni A, Spagnoli F, et al. Disease progression or pseudoprogression after concomitant radiochemotherapy treatment: pitfalls in neurooncology. *Neuro-oncol* 2008;10(3):361-367.
  10. Aronen HJ, Gazit IE, Louis DN, et al. Cerebral blood volume maps of gliomas: comparison with tumor grade and histologic findings. *Radiology* 1994;191(1):41-51.
  11. Knopp EA, Cha S, Johnson G, et al. Glial neoplasms: dynamic contrast-enhanced T2\*-weighted MR imaging. *Radiology* 1999;211(3):791-798.
  12. Sugahara T, Korogi Y, Kochi M, et al. Correlation of MR imaging-determined cerebral blood volume maps with histologic and angiographic determination of vascularity of gliomas. *AJR Am J Roentgenol* 1998;171(6):1479-1486.
  13. Lev MH, Ozsunar Y, Henson JW, et al. Glial tumor grading and outcome prediction using dynamic spin-echo MR susceptibility mapping compared with conventional contrast-enhanced MR: confounding effect of elevated rCBV of oligodendrogliomas [corrected]. *AJNR Am J Neuroradiol* 2004;25(2):214-221.
  14. Cao Y, Tsien CI, Nagesh V, et al. Survival prediction in high-grade gliomas by MRI perfusion before and during early stage of RT [corrected]. *Int J Radiat Oncol Biol Phys* 2006;64(3):876-885.
  15. Danchavijitr N, Waldman AD, Tozer DJ, et al. Low-grade gliomas: do changes in rCBV measurements at longitudinal perfusion-weighted MR imaging predict malignant transformation? *Radiology* 2008;247(1):170-178.
  16. Law M, Young RJ, Babb JS, et al. Gliomas: predicting time to progression or survival with cerebral blood volume measurements at dynamic susceptibility-weighted contrast-enhanced perfusion MR imaging. *Radiology* 2008;247(2):490-498.
  17. Oh J, Henry RG, Pirzkall A, et al. Survival analysis in patients with glioblastoma multiforme: predictive value of choline-to-N-acetylaspartate index, apparent diffusion coefficient, and relative cerebral blood volume. *J Magn Reson Imaging* 2004;19(5):546-554.
  18. Barajas RF Jr, Chang JS, Segal MR, et al. Differentiation of recurrent glioblastoma multiforme from radiation necrosis after external beam radiation therapy with dynamic susceptibility-weighted contrast-enhanced perfusion MR imaging. *Radiology* 2009;253(2):486-496.
  19. Hoefnagels FW, Lagerwaard FJ, Sanchez E, et al. Radiological progression of cerebral metastases after radiosurgery: assessment of perfusion MRI for differentiating between necrosis and recurrence. *J Neurol* 2009;256(6):878-887.
  20. Hu LS, Baxter LC, Smith KA, et al. Relative cerebral blood volume values to differentiate high-grade glioma recurrence from post-treatment radiation effect: direct correlation between image-guided tissue histopathology and localized dynamic susceptibility-weighted contrast-enhanced perfusion MR imaging measurements. *AJNR Am J Neuroradiol* 2009;30(3):552-558.
  21. Gahramanov S, Raslan AM, Muldoon LL, et al. Potential for differentiation of pseudoprogression from true tumor progression with dynamic susceptibility-weighted contrast-enhanced magnetic resonance imaging using ferumoxytol vs. gadoteridol: a pilot study. *Int J Radiat Oncol Biol Phys* 2011;79(2):514-523.
  22. Hu LS, Eschbacher JM, Dueck AC, et al. Correlations between perfusion MR imaging cerebral blood volume, microvessel quantification, and clinical outcome using stereotactic analysis in recurrent high-grade glioma. *AJNR Am J Neuroradiol* 2012;33(1):69-76.
  23. Sorensen AG. Perfusion MR imaging: moving forward. *Radiology* 2008;249(2):416-417.
  24. Neuwelt EA, Várallyay CG, Manninger S, et al. The potential of ferumoxytol nanoparticle magnetic resonance imaging, perfusion, and angiography in central nervous system malignancy: a pilot study. *Neurosurgery* 2007;60(4):601-611; discussion 611-612.
  25. Várallyay CG, Muldoon LL, Gahramanov S, et al. Dynamic MRI using iron oxide nanoparticles to assess early vascular effects of anti-angiogenic versus corticosteroid treatment in a glioma model. *J Cereb Blood Flow Metab* 2009;29(4):853-860.
  26. Weinstein JS, Várallyay CG, Dosa E, et al. Superparamagnetic iron oxide nanoparticles: diagnostic magnetic resonance imaging and potential therapeutic applications in neurooncology and central nervous system inflammatory pathologies, a review. *J Cereb Blood Flow Metab* 2010;30(1):15-35.
  27. Neuwelt EA, Hamilton BE, Várallyay CG, et al. Ultrasmall superparamagnetic iron oxides (USPIOs): a future alternative magnetic resonance (MR) contrast agent for patients at risk for nephrogenic systemic fibrosis (NSF)? *Kidney Int* 2009;75(5):465-474.
  28. Rosen BR, Belliveau JW, Vevea JM, Brady TJ. Perfusion imaging with NMR contrast agents. *Magn Reson Med* 1990;14(2):249-265.
  29. Ostergaard L, Weisskoff RM, Chesler DA, Gyldensted C, Rosen BR. High resolution measurement of cerebral blood flow using intravascular tracer bolus passages. Part I: Mathematical approach and statistical analysis. *Magn Reson Med* 1996;36(5):715-725.
  30. Boxerman JL, Schmainda KM, Weisskoff RM. Relative cerebral blood volume maps corrected for contrast agent extravasation significantly correlate with glioma tumor grade, whereas uncorrected maps do not. *AJNR Am J Neuroradiol* 2006;27(4):859-867.
  31. Maeda M, Itoh S, Kimura H, et al. Tumor vascularity in the brain: evaluation with dynamic susceptibility-contrast MR imaging. *Radiology* 1993;189(1):233-238.
  32. Cha S. Perfusion MR imaging of brain tumors. *Top Magn Reson Imaging* 2004;15(5):279-289.
  33. Heiland S, Benner T, Dehus J, Rempp K, Reith W, Sartor K. Simultaneous assessment of cerebral hemodynamics and contrast agent uptake in lesions with disrupted blood-brain-barrier. *Magn Reson Imaging* 1999;17(1):21-27.
  34. Uematsu H, Maeda M. Double-echo perfusion-weighted MR imaging: basic concepts and application in brain tumors for the assessment of tumor blood volume and vascular permeability. *Eur Radiol* 2006;16(1):180-186.
  35. Paulson ES, Schmainda KM. Comparison of dynamic susceptibility-weighted contrast-enhanced MR methods: recommendations for measuring relative cerebral blood volume in brain tumors. *Radiology* 2008;249(2):601-613.
  36. Hu LS, Baxter LC, Pinnaduwa DS, et al. Optimized preload leakage-correction methods to improve the diagnostic accuracy of dynamic susceptibility-weighted contrast-enhanced perfusion MR imaging in post-treatment gliomas. *AJNR Am J Neuroradiol* 2010;31(1):40-48.
  37. Gahramanov SML, Muldoon LL, Li X, Neuwelt EA. Improved perfusion MR imaging assessment of intracerebral tumor blood volume and antiangiogenic therapy efficacy in a rat model with ferumoxytol. *Radiology* 2011;261(3):796-804.
  38. Macdonald DR, Cascino TL, Schold SC Jr, Cairncross JG. Response criteria for phase II studies of supratentorial malignant glioma. *J Clin Oncol* 1990;8(7):1277-1280.
  39. Therasse P, Arbuck SG, Eisenhauer EA, et al. New guidelines to evaluate the response to treatment in solid tumors. European Organization for Research and Treatment of Cancer, National Cancer Institute of the United States, National Cancer Institute of Canada. *J Natl Cancer Inst* 2000;92(3):205-216.
  40. Wen PY, Macdonald DR, Reardon DA, et al. Updated response assessment criteria for high-grade gliomas: response assessment in neuro-oncology working group. *J Clin Oncol* 2010;28(11):1963-1972.
  41. Mangla R, Singh G, Ziegelitz D, et al. Changes in relative cerebral blood volume 1 month after radiation-temozolomide therapy can help predict overall survival in patients with glioblastoma. *Radiology* 2010;256(2):575-584.
  42. Taal W, Brandsma D, de Bruin HG, et al. Incidence of early pseudo-progression in a cohort of malignant glioma patients treated with chemoradiation with temozolomide. *Cancer* 2008;113(2):405-410.
  43. Mason WP, Maestro RD, Eisenstat D, et al. Canadian recommendations for the treatment of glioblastoma multiforme. *Curr Oncol* 2007;14(3):110-117.
  44. Roldán GB, Scott JN, McIntyre JB, et al. Population-based study of pseudoprogression after chemoradiotherapy in GBM. *Can J Neurol Sci* 2009;36(5):617-622.



PRIMARY RESEARCH

Open Access

# Treatment with the PARP inhibitor, niraparib, sensitizes colorectal cancer cell lines to irinotecan regardless of MSI/MSS status

Sybil M Genther Williams<sup>1\*</sup>, Apryle M Kuznicki<sup>2</sup>, Paula Andrade<sup>2</sup>, Brian M Dolinski<sup>1</sup>, Cem Elbi<sup>1,3</sup>, Ronan C O'Hagan<sup>1</sup> and Carlo Toniatti<sup>1,4</sup>

## Abstract

**Background:** Cells with homologous recombination (HR) deficiency, most notably caused by mutations in the *BRCA1* or *BRCA2* genes, are sensitive to PARP inhibition. Microsatellite instability (MSI) accounts for 10-15% of colorectal cancer (CRC) and is hypothesized to lead to HR defects due to altered expression of Mre11, a protein required for double strand break (DSB) repair. Indeed, others have reported that PARP inhibition is efficacious in MSI CRC.

**Methods:** Here we examine the response to niraparib, a potent PARP-1/PARP-2 inhibitor currently under clinical evaluation, in MSI versus microsatellite stable (MSS) CRC cell lines *in vitro* and *in vivo*. We compiled a large panel of MSI and MSS CRC cell lines and evaluated the anti-proliferative activity of niraparib. In addition to testing single agent cytotoxic activity of niraparib, we also tested irinotecan (or SN-38, the active metabolite of irinotecan) activity alone and in combination with niraparib *in vitro* and *in vivo*.

**Results:** In contrast to earlier reports, MSI CRC cell lines were not more sensitive to niraparib than MSS CRC cell lines, suggesting that the MSI phenotype does not sensitize CRC cell lines to PARP inhibition. Moreover, even the most sensitive MSI cell lines had niraparib EC50s greater than 10 fold higher than BRCA-deficient cell lines. However, MSI lines were more sensitive to SN-38 than MSS lines, consistent with previous findings. We have also demonstrated that combination of niraparib and irinotecan was more efficacious than either agent alone in both MSI and MSS cell lines both *in vitro* and *in vivo*, and that niraparib potentiates the effect of irinotecan regardless of MSI status.

**Conclusions:** Our results support the clinical evaluation of this combination in all CRC patients, regardless of MSI status.

## Introduction

Poly (ADP-ribose) polymerase (PARP) enzymes are involved in repair of single strand DNA lesions using the base excision repair (BER) pathway. Inhibition of PARP enzymes induces persistence of single strand breaks (SSBs) which can cause double strand breaks (DSBs) when the SSBs are encountered by a replication fork. The development of PARP inhibitors as agents to treat cancers with homologous recombination (HR) defects is based on the idea that cells with defects in DSB repair, such as BRCA-deficient cells, are more dependent on PARP and BER to maintain genomic integrity [1,2]. Indeed, preclinical

and clinical evidence have demonstrated that PARP inhibitors are synthetic lethal for tumors with mutations in the *BRCA1* and *BRCA2* genes and other genes involved in HR [1-5].

The instability of microsatellite repeated sequences, MSI, is found in tumors from the familial cancer syndrome hereditary nonpolyposis colorectal cancer (HNPCC) and in 10-15% of sporadic CRC. The MSI phenotype is a marker of an underlying mismatch repair (MMR) defect which stems from germline mutation in one of the MMR genes (principally *MLH1* or *MSH2*) or aberrant methylation of the *MLH1* promoter. One consequence of MSI is the reduced expression of the Mre11 protein resulting from mutation of the poly(T) 11 repeat within intron 4 of human *MRE11* [6]. Reduced expression of Mre11 is hypothesized

\* Correspondence: sybil\_williams@merck.com

<sup>1</sup>Department of Oncology, Merck Research Laboratories, 33 Avenue Louis Pasteur, Boston, MA 02115, USA

Full list of author information is available at the end of the article



to lead to defects in HR, due to Mre11's essential role in sensing DSBs and facilitating their repair [6-10].

PARP inhibition is effective in combination with irradiation and DNA-damaging agents [11]. In particular, PARP inhibitors have been shown to potentiate the effects of Topoisomerase 1 (Top 1) inhibitors both pre-clinically and clinically [12-17]. Top1 inhibition slows replication fork progression and induces the widespread formation of unusual replication intermediates, most notably reverse replication forks [12]. PARP activity is required for effective fork reversal, which limits the number of DSBs that result [12].

Irinotecan, a Top 1 inhibitor, is used as a therapy for CRC either alone or in combination with leucovorin and 5-Fluorouracil (5-FU). MSI is associated with increased sensitivity to irinotecan, both *in vitro* and in patients with advanced colon cancer [9,18,19]. The mechanism underlying this observation is not well understood.

Niraparib is a potent and selective orally available PARP-1/2 inhibitor [3]. *In vitro* and *in vivo*, niraparib displays outstanding monotherapy efficacy in a large panel of BRCA mutant cell lines with at least 10-fold selectivity over BRCA wild type cell lines [3]. In this study, the efficacy of niraparib was evaluated in the presence and absence of irinotecan in models of CRC with defects associated with the MSI phenotype as compared to MSS phenotype.

We demonstrate that the MSI phenotype does not overtly sensitize CRC cell lines to PARP inhibition and confirm that MSI CRC cell lines are more sensitive to SN-38 (active metabolite of irinotecan) than MSS cell lines. Niraparib potentiated the cytotoxic activity of irinotecan in both MSI and MSS CRC models. Our data suggests that both MSI and MSS patient populations will benefit from the combination of niraparib and irinotecan.

## Methods

### Microsatellite repeat analysis

DNA was extracted using standard methods from cells that were plated one day prior. Cell lines that were used in this study were described as being either MSI or MSS in previous publications [20-25]. The cell lines analyzed for MSI included: **MSI**- COLO205, DLD-1, HCT8, HCT15, HCT116, LOVO, LS411N, RKO, RKO-E6, SW48 and **MSS**-SW403, SW1417, WIDR. Primers used to amplify BAT-25 and BAT-26 were (BAT-25) 5'-6FAM-TCG CCT CCA AGA ATG TAA GT-3' and 5'-TCT GCA TTT TAA CTA TGG CTC-3' (BAT-26) 5'-HEX- TGA CTA CTT TTG ACT TCA GCC-3' and 5'-AAC CAT TCA ACA TTT TTA ACC-3'. PCR amplification was performed with primers at 200nM each with 1X concentration of colorless GoTaq Flexi buffer (Promega Cat. No. M8305), 2 mM MgCl<sub>2</sub>, 0.2 mM of each dNTP (PCR nucleotide Mix Promega cat. No. C1141), 1.25 u of GoTaq

DNA polymerase (5 u/μl; Promega cat. No. M8305), 50 ng of DNA, and nuclease free water to 50 μl. PCR conditions were: 95°C for 2 minutes followed by 35 cycles of 94°C for 1 minute, 55°C for 1 minute and 72°C for 1 minute, followed by a final extension of 72°C for 5 minutes and the 4°C. To analyze the PCR products the following mix was prepared: 10 μl Hi-Dri Formamide (Applied Biosystems Cat. No. 4311320) + 0.05 μl GeneScan 500 LIZ marker (Applied Biosystems Cat. No. 4322362). PCR product was diluted 1:400 in water. 1 μl of PCR product was added to 10 μl of Hi-Dri Formamide/Gene Scan 500 LIZ marker mix and samples were heated at 95°C for 5 minutes. The fluorescently labeled PCR products were detected using the Sequencer 3730 DNA analyzer (Applied Biosystems) and analyzed using Peak Scanner software (Applied Biosystems).

### Western analysis

10 cm dishes were lysed with 50–150 μl (depending on cell density) of boiling 1% SDS Lysis Buffer [50 ml-10% SDS (5 ml) 5 M NaCl (1 ml), 1 M Tris pH 7.5 (500 μl) dH<sub>2</sub>O (43.5 ml)] and put at 95°C for 5 minutes. Protein concentration was assessed in a 96 well format by BCA Protein assay Kit (PIERCE Catalog number: 23225). 30 μg of protein extract was loaded onto 10% Tris-Glycine SDS-PAGE gels and run at 100 Volts for 90 minutes. The gels were transferred onto PVDF membrane and incubated overnight at 4°C with primary antibody, 1:1000 rabbit Anti-MRE11 Antibody (NOVUS Biologicals Catalog number: NB100-276 diluted in 5% non fat dry milk/TBS-T. The secondary antibody used was a 1:5000 dilution of ECL Anti-rabbit IgG Horseradish Peroxidase-Linked Species specific F(ab')<sub>2</sub> Fragment (donkey) (Amersham Catalog number: NA9340). Membranes were incubated for 1 hour in secondary antibody and developed using Pierce Supersignal West Dura Extended Duration Substrate (Catalog number: 34705).

### Proliferation assays

All of the cell lines were obtained from ATCC (Manassas, VA). **MSI**- DLD-1, HCT-8, HCT-15, HCT116, LOVO, LS174T, LS180, LS411N, RKO, RKO-E6, SNUC2A, SW48. **MSS**- COLO205, HT29, NCI-H-508, SK-CO-1, SW403, SW480, SW620, SW837, SW948, SW1116, SW1417, SW1463, T84. To carry out 7 day monotherapy proliferation assays with the cell lines, 500–32,000 cells (cell line-dependent) were seeded in 96-well clear tissue culture plates (190 μl/well) in an appropriate tissue culture medium supplemented with FBS. The plate was incubated for 4 hours at 37°C, and niraparib was added in a 9 point titration, 3-fold dilutions starting at 10 μM for niraparib and starting at either 10 μM, 1 μM, or 100nM for SN-38 (in 9 point titration, 3-fold dilutions). The cells were then incubated for 7 days at 37°C, 5% CO<sub>2</sub> (except cell lines

grown in L-15 medium which were grown in at 37°C, 0% CO<sub>2</sub>, 100% air) and the cell viability was assessed by WST-1 assay (Roche) as described by the Manufacturer. To carry out 7 day combination proliferation assays with the cell lines, 500–32,000 cells (cell line-dependent) were seeded in 96-well clear tissue culture plates (180 µl/well) in an appropriate tissue culture medium supplemented with FBS. The plate was incubated for 4 hours at 37°C, and niraparib was added at 125 nM, 250 nM, or 1 µM and SN-38 was added in an 8 point titration, 3-fold dilutions, starting at 100 nM. The cells were then incubated for 7 days at 37°C, 5% CO<sub>2</sub> (except for the cell lines grown in L-15 medium which were grown in at 37°C, 0% CO<sub>2</sub>, 100% air) and the cell viability was assessed by WST-1 assay (Roche) as described by the Manufacturer. The number of living cells was determined by reading the plate at 450 nm on a spectrophotometer. The signal produced is directly proportional to the cell number as the cells convert tetrazolium salt due into a formazan end product. Each experiment was run in duplicate. Cell growth was expressed as the percentage growth with respect to vehicle treated cells. The concentration required to inhibit cell growth by 50% (EC<sub>50</sub>) was determined using the four-parameter fit in SoftMax Pro 5.2. The Wilcoxon rank sum test was performed to determine statistical significance. Excess Volume HSA combination index was calculated using a MATLAB algorithm as described previously [26].

#### ***In vivo* xenograft studies**

6 week old CD1 nu/nu mice were injected subcutaneously with either 5X10<sup>6</sup> HT29 cells in 50% matrigel or 5X10<sup>6</sup> HCT116 cells in 50% matrigel. When the average tumor size reached to 150 mm<sup>3</sup> for HT29 and HCT116, mice were randomized to form homogeneous groups, and treatment started. Tumor measurements were recorded bi-weekly throughout the course of each study. Animals were dosed orally (p.o.) with 50, 25, or 10 mg/kg (mpk) niraparib (5 ml/kg in 0.5% w/v methylcellulose) each day for 3, 5, or 7 days (according to individual study design) alone or in combination with 100 mpk irinotecan (10 ml/kg) dosed intraperitoneally (ip.), once per week (qwk), on day 3 for 4 weeks depending on treatment group. For tumor relapse studies, animals were treated for 4 weeks as described above, and then treatments were withdrawn and tumor relapse was monitored until the average tumor volume for each group reached 1000 mm<sup>3</sup>. Each animal study was conducted with 7–10 mice per individual treatment group. All animal studies were conducted in a specific pathogen-free environment in accordance with the internal Institutional Animal Care and Use Committee (IACUC) and other relevant standards.

#### **Results**

BAT-25 is a poly (T) tract intragenic to the c-kit proto-oncogene assigned to 4q12 and BAT-26 is a poly (A) tract located in the 5<sup>th</sup> intron of the hMSH2 gene. The BAT-25 and BAT-26 mononucleotide repeats are reported to be quasi-monomorphic meaning that there is not a significant size variation either between the alleles of one individual or between alleles of different individuals. This property permits the easy identification of MSI status without the use of a normal tissue control or on cell lines. MSI/MSS status across a CRC cell line panel was determined via PCR fragment analysis of the BAT-25 and BAT-26 mononucleotide repeats. MSS cell lines had longer and more uniform BAT-25 and BAT-26 alleles than MSI lines on average (Figure 1A and B). This data confirmed that the cell lines used in our cell line panel were MSI or MSS, as previously reported [20-25].

Cells with MSI are hypothesized to be HR-deficient due to reduced expression of Mre11 and subsequently the reduced expression of the Mre11-Nbs1-Rad50 complex. This reduction in expression has been shown to result from a mutation in the poly(T) 11 repeat within the human *MRE11* intron 4 [6]. Western analysis confirmed reduced Mre11 protein levels in MSI as compared to MSS cell lines (Figure 1C), consistent with previous reports [6,7,10,27].

Enhanced sensitivity to PARP inhibition was postulated for MSI CRC cell lines due to the reduction in Mre11 protein expression. To test this hypothesis, the cell line panel was expanded (12 MSI and 13 MSS) and 7-day proliferation assays were performed with niraparib. Although MSI cell lines on average did have lower 7 day proliferation EC<sub>50</sub> values (Ave = 1823 nM) than MSS cell lines (Ave = 6859 nM), this difference was not statistically significant (p = 0.15 Wilcoxon Rank Sum Test; Figure 2A and Table 1), in contrast to what has been previously reported [28,29]. A semi-quantitative assessment of the amount of Mre11 expression relative to GAPDH expression was also performed, and there was no correlation between the level of Mre11 expression and sensitivity to niraparib (data not shown).

Proliferation assays were also performed on the panel of cell lines with SN-38. In agreement with previous reports, MSI CRC cell lines were significantly more sensitive to SN-38 monotherapy than MSS cells (p = 0.02 Wilcoxon Rank Sum Test; Figure 2B and Table 1) [18]. All of the MSI cell lines were sensitive to SN-38 with EC<sub>50</sub>s less than 5 nM, and although on average the MSS cell lines were less sensitive, 6/13 cell lines did have EC<sub>50</sub>s less than 5 nM.

PARP inhibitors have been shown to potentiate the effects of Top1 inhibitors both preclinically and clinically [12-17]. In order to test if niraparib potentiates irinotecan in MSI and MSS CRC cell lines, *in vitro* combination

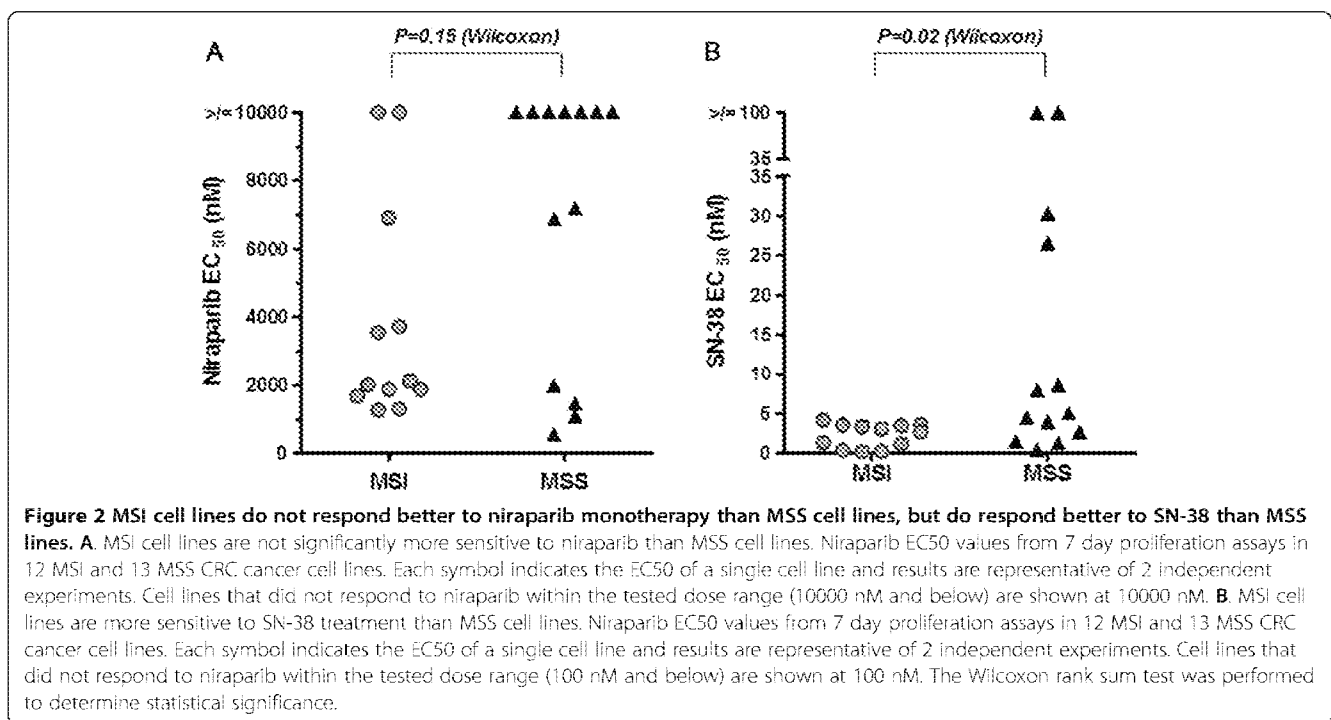
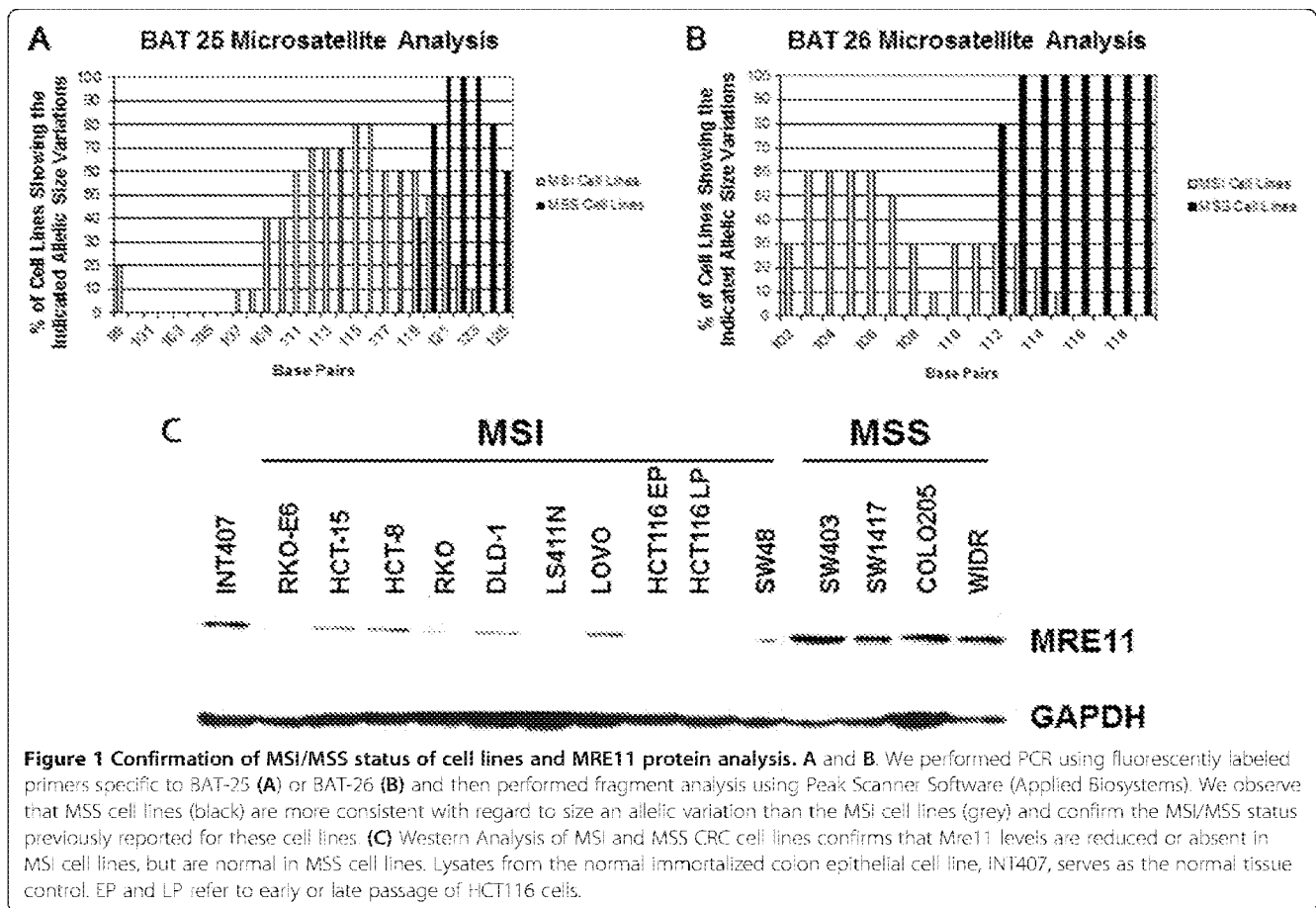


**Table 1 Niraparib potentiates the effects of SN-38 in MSI and MSS cell lines**

	Cell line	7 day EC50 (nM)		Combination EC50 (shift of SN-38 EC50 in presence of Niraparib)		
		Niraparib	SN-38	Niraparib		
				125 nM	250 nM	1000 nM
<b>MSI</b>	DLD1	3560	3.63	0.992	1.67	1.68
	HCT8	2130	3.60	2.07	1.54	1.35
	HCT15	1685	3.77	3.47	3.44	1.73
	HCT116	6915	0.180	0.125	0.155	0.0991
	LOVO	2010	3.43	2.3	3.53	2.4
	LS174T	1310	0.331	0.257	0.208	0.231
	LS180	3730	0.474	0.399	0.395	0.389
	LS411N	1875	3.57	1.21	1.11	0.729
	RKO	1870	0.958	0.593	0.778	0.184
	RKOE6	1270	0.730	0.426	0.422	0.464
	SNUC2A	>10000	3.23	3.04	2.72	2.52
	SW48	>10000	1.79	0.886	0.762	0.598
<b>MSS</b>	COLO205	1990	1.57	0.572	0.475	0.531
	HT29	6880	4.29	3.07	3.64	1.75
	NCI-H-508	>10000	3.63	1.70	3.31	1.41
	SK-CO-1	1090	0.416	0.178	0.334	0.143
	SW403	>10000	3.39	1.14	1.87	0.387
	SW480	>10000	29.0	11.9	11.6	8.7
	SW620	552	5.91	3.62	UR	UR
	SW837	>10000	UR	UR	UR	UR
	SW948	7195	6.67	3.85	4.47	2.80
	SW1116	>10000	UR	UR	UR	UR
	SW1417	>10000	27.7	29.2	28.3	31.0
	SW1463	>10000	26.4	22.2	UR	UR
T84	1460	1.01	0.491	0.352	0.210	

7 day EC50 data for niraparib alone, SN-38 alone, and the combination EC50 at 125, 250 and 1000 nM of niraparib in a panel of 25 MSI and MSS CRC cell lines. The niraparib EC50 values are the average of n=2 from previous experiments. The SN-38 EC50 values reported are for n=1 for the experiment done on that day. Values listed under 125, 250, and 1000nM niraparib are the EC50 values for SN-38 in the presence of 125, 250 or 1000 nM niraparib (combination EC50). EC50 data was calculated using the inflection point of the curve in a 4 parameter fit in SoftMax Pro 5.2. UR indicates that the data is unreportable due to an inadequate curve.

studies with niraparib (125 nM, 250 nM, and 1000 nM) and SN-38 (8 point dose response) were performed. As expected, we observed a shift of the SN-38 EC50 an average of 2-fold lower when niraparib was tested in combination with SN-38 as compared to when SN-38 was tested alone in both MSI and MSS CRC cell lines (Table 1). This data demonstrates that if a cell line responds to SN-38 monotherapy *in vitro*, niraparib potentiates that effect, regardless of MSI/MSS status. In addition, when Highest Single Agent (HSA) combinatorial analysis was applied to this data, we observe that combination of niraparib with SN-38 results in additive to synergistic inhibition of cell proliferation regardless of MSI/MSS status *in vitro* (Figure 3).

In order to extend these observations, xenograft studies employing MSI (HCT116) or MSS (HT29) models

were performed. HCT116 (MSI) or HT29 (MSS) xenograft tumor-bearing mice were dosed with niraparib at 10, 25, or 50 mpk (oral, daily) for 5 days per cycle (4 cycles) and efficacy at these doses was compared to irinotecan monotherapy (100 mpk, ip., qwk; 4 cycles). In both models, irinotecan monotherapy was more efficacious than niraparib monotherapy at the niraparib doses tested (Figure 4). In HCT116, the average tumor volume at day 28 for the irinotecan treated group was 225 mm<sup>3</sup> and the tumor volumes for the niraparib single agent treated groups were 605, 734 and 739 mm<sup>3</sup> for 10 mpk, 25 mpk and 50 mpk niraparib treated groups, respectively. When compared to vehicle control, only the average tumor volume of the irinotecan treated group was statistically different than the average of vehicle control (p = 0.0002 one-tailed homoscedastic student's T test). In

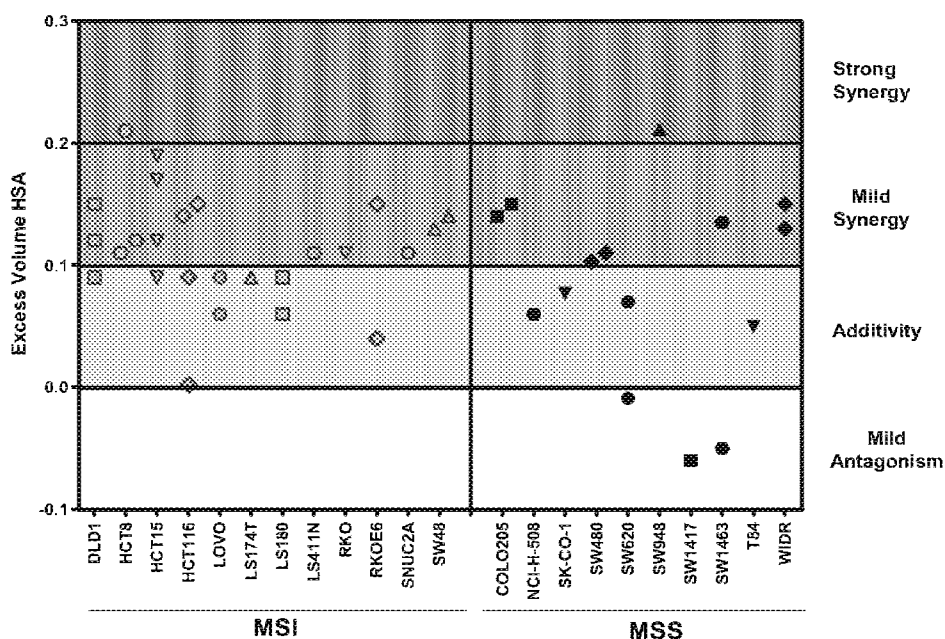


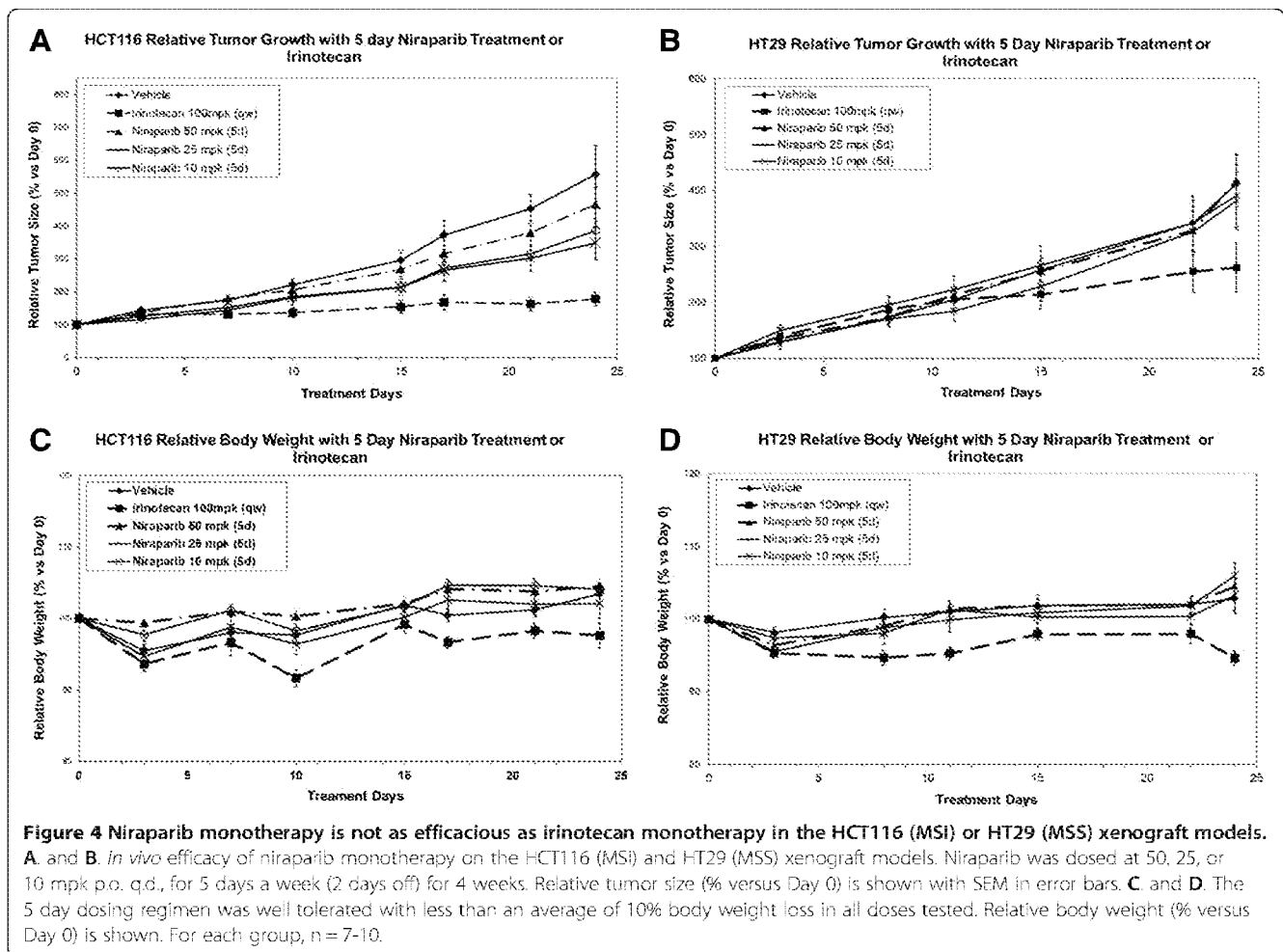
**Figure 3 Niraparib potentiates the effects of SN-38 in MSI and MSS cell lines.** Assessment of synergy with niraparib and SN-38 by excess volume HSA. Each symbol indicates a single experiment with the indicated cell lines. Data was generated from 7 day proliferation assay and excess volume HSA was calculated using a MATLAB algorithm. HSA values from 0.2-0.3 indicate strong synergy, 0.1-0.2 indicated mild synergy, 0.0-0.1 indicate additivity, and negative numbers indicate mild antagonism. Data points are from 1–3 experiments and are only shown if the p value associated with the excess volume HSA is equal to or less than 0.05.

HT29, the average tumor volume for the irinotecan treated group at day 24 was 542 mm<sup>3</sup> whereas the tumor volumes for the niraparib treated groups were 934, 802 and 768 mm<sup>3</sup>, for the 10 mpk, 25mpk and 50 mpk, niraparib treated groups, respectively. (Tumor volumes at day 24 were recorded for HT29 as compared to day 28 for HCT116 due to the day when vehicle control treated groups reached the maximum tumor volume of 1000 mm<sup>3</sup>). In the HT29 model, none of the single agent groups (including irinotecan) had average tumor volumes that were statistically different as compared to vehicle control (irinotecan versus vehicle control p value = 0.06 one-tailed homoscedastic student's T test). Niraparib was dosed no higher than 50 mpk in these studies because higher concentrations of niraparib were not tolerated in combination with irinotecan dosed at 100 mpk, qwk (data not shown). The maximum tolerated dose for niraparib as a single agent in mice is 100 mpk daily (data not shown). Doses of niraparib at 50 mpk (daily) gives approximately the same C min values as 40 mg/day in humans, the lowest dose that demonstrated clinical benefit (stable disease) in humans [30].

In the same studies, mice were also treated with niraparib (at 10, 25, and 50 mpk) in combination with irinotecan (100 mpk; qwk) to determine if niraparib could enhance irinotecan efficacy, and to determine if the combination would be tolerated. Niraparib significantly

enhanced irinotecan efficacy at the 25 and 50 mpk combination dosing regimens in the HCT116 model, but not in the 10 mpk combination dosing regimen. The average tumor volume at day 28 in the Irinotecan group was 225 mm<sup>3</sup>, in the 50 mpk combination group was 120 mm<sup>3</sup>, the 25 mpk combination group was 101 mm<sup>3</sup> and in the 10 mpk combination group was 166 mm<sup>3</sup>. Significance was determined using a one-tailed homoscedastic T test and p = 0.01, 0.02 and 0.06 for the 50 mpk, 25 mpk and 10 mpk combination groups as compared to irinotecan alone at day 28. In the HT29 model, the average tumor volumes for the combination groups were smaller at 24 days as compared to irinotecan, but these values were not statistically significant. The average tumor volume at day 24 in the Irinotecan group was 542 mm<sup>3</sup>, in the 50 mpk combination group was 363 mm<sup>3</sup>, the 25 mpk combination group was 438 mm<sup>3</sup> and in the 10 mpk combination group was 448 mm<sup>3</sup>. Significance was again determined using a one-tailed homoscedastic T test and p = 0.09, 0.15 and 0.18 for the 50 mpk, 25 mpk and 10 mpk combination groups as compared to irinotecan alone at day 24. 15% or less body weight loss was observed throughout the duration of the studies (Figures 4C, 4D, 5C and 5D).

In addition to assessing tumor growth inhibition during the 4 weeks with niraparib and irinotecan combination treatment, we also investigated tumor growth

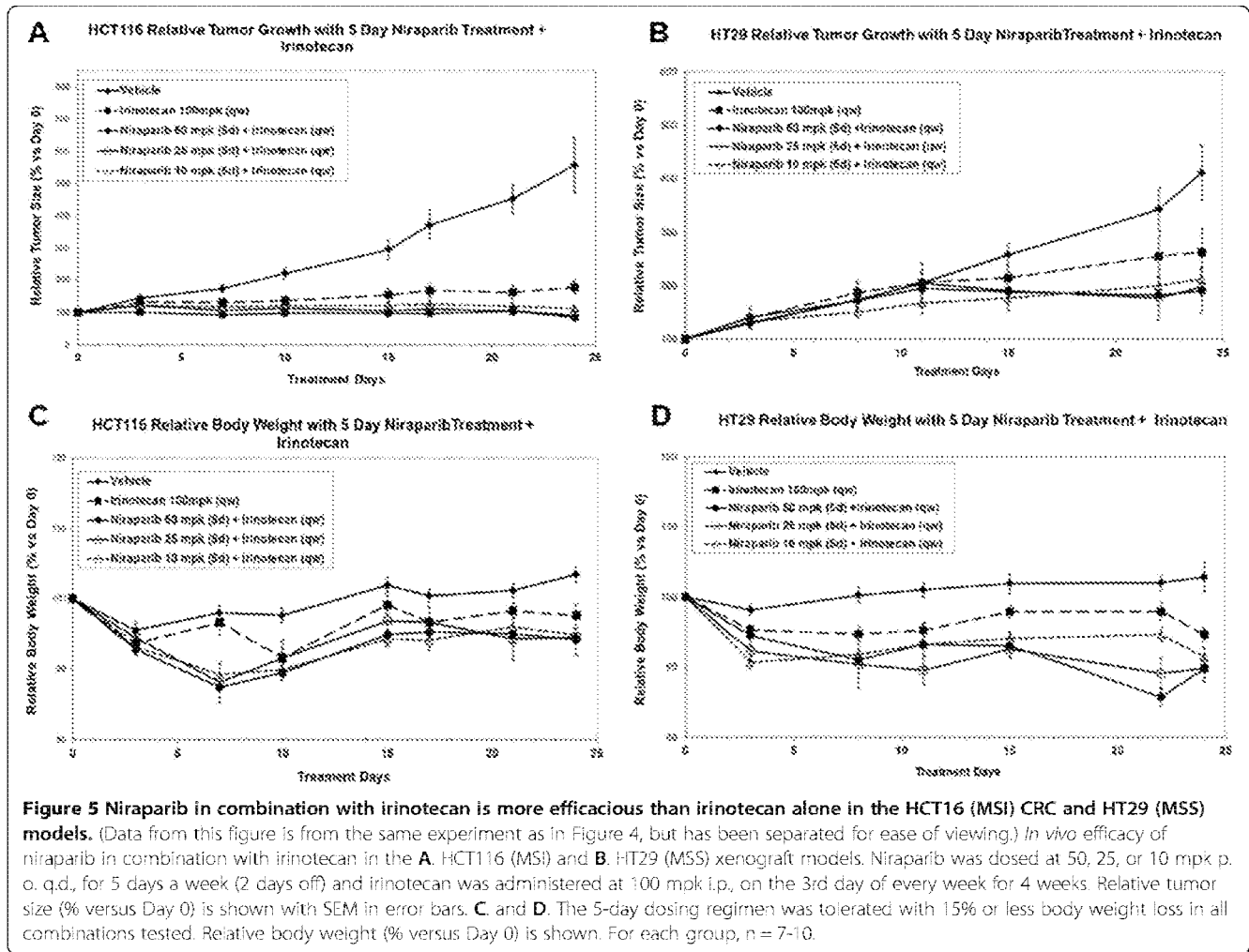


delay and relapse in the same studies after the withdrawal of treatments. The HCT116 and HT29 tumors treated with irinotecan alone relapsed sooner than tumors treated with niraparib in combination with irinotecan at all 3 niraparib doses tested (Figure 6). In the HCT116 study, the 50 mpk niraparib + irinotecan combination treatment group reached the 1000 mm<sup>3</sup> endpoint at day 99, whereas the irinotecan alone treatment group reached the 1000 mm<sup>3</sup> endpoint at day 70, demonstrating a 29-day tumor growth delay. Additionally, the average tumor volume for the 50, 25, and 10 mpk niraparib + irinotecan combination groups in the HCT116 model were significantly different from the irinotecan single agent group at day 70 when the average tumor size in the irinotecan single agent group reached the end-point of 1000 mm<sup>3</sup>. (P = .02, .02, and .03, respectively. P values generated using a homoscedastic Student's t-test.) (Figure 6A). Likewise, in the HT29 study, the 50 mpk niraparib + irinotecan combination treatment group reached the 1000 mm<sup>3</sup> endpoint at day 65, whereas the irinotecan only treatment group reached the end-point at day 49, demonstrating

a 16-day tumor growth delay. The average tumor volume for the 50, 25, and 10 mpk niraparib + irinotecan combination groups in the HT29 model were significantly different from the irinotecan single agent group at day 49 when the average tumor size in the irinotecan single agent group reached the end-point of 1000 mm<sup>3</sup>. (P-values of .05, .03, and .03, respectively. P value generated using a homoscedastic Student's t-test) (Figure 6B). Collectively, our *in vitro* and *in vivo* data demonstrate that combination of niraparib with irinotecan is efficacious in both MSI and MSS settings.

## Discussion

To determine if MSI is associated with increased sensitivity to the PARP inhibitor niraparib and to determine if niraparib potentiates the anti-proliferative effects of irinotecan, the efficacy of niraparib and irinotecan, both alone and in combination, was assessed in multiple MSI and MSS CRC models *in vitro* and *in vivo*. The studies detailed in this paper demonstrate that CRC MSI cell lines are not more sensitive than CRC MSS cell lines to niraparib, and that combination of niraparib with



irinotecan enhances the efficacy of irinotecan in both MSI and MSS CRC cell lines *in vitro* and *in vivo*.

We have demonstrated that MSI CRC cell lines have reduced levels of Mre11, a protein involved in the repair of DSBs, as compared to MSS cell lines, but that they are not significantly more sensitive to niraparib monotherapy than MSS cell lines (Figures 1 and 2A). Even the cell lines that had little or no detectable levels of Mre11 (RKO, LS411N, HCT116; Figure 1) did not respond to niraparib monotherapy in the EC50 ranges that BRCA deficient cell lines do (EC50s  $\geq 1000$  nM for MSI CRC cell lines and EC50s  $\leq 100$  nM for BRCA1/2 mutant cell lines using the same assay conditions) (Figure 2A and Table 1; [3]). This data demonstrates that reduction of Mre11 levels to the degree that they are reduced in the context of MSI, is not sufficient to induce sensitivity to PARP inhibition. The notion that Mre11 deficiency is fundamentally different from BRCA1/2 deficiency is supported by the observation that germline inactivation of Mre11 does not result in a cancer predisposition syndrome, whereas inactivation of BRCA1/2 does.

Our results differ from those published for the PARP inhibitor ABT-888 by Vilar et al., in 2011 and the PARP inhibitor BMN673 by Gaymes et al., in 2013 [28,29]. Vilar et al. reported that Mre11 deficiency increases sensitivity to PARP inhibition in MSI CRC. Discrepancies in our results are likely due to the size of the cell line panels that were used. The panel used in our study was larger than what Vilar et al., used. All of the MSI cell lines that were assayed in the Vilar manuscript were assayed in our panel with an additional 4 MSI lines. In addition, 7 out of the 9 of the MSS cell lines that were assayed in their panel were assayed in our panel with an additional 6 MSS lines. When statistical analysis is performed on our 7 day niraparib EC50 data using only the cell lines that were used in the Vilar study, we demonstrate that MSI cell lines are significantly more sensitive to niraparib than MSS cell lines ( $p = 0.02$ ). This data highlights the need to include large numbers of cell lines to evaluate biomarker hypotheses. Additionally, Vilar et al., describe the differences between MSI and MSS cell lines using 10  $\mu$ M (and 50  $\mu$ M) of ABT-888, which



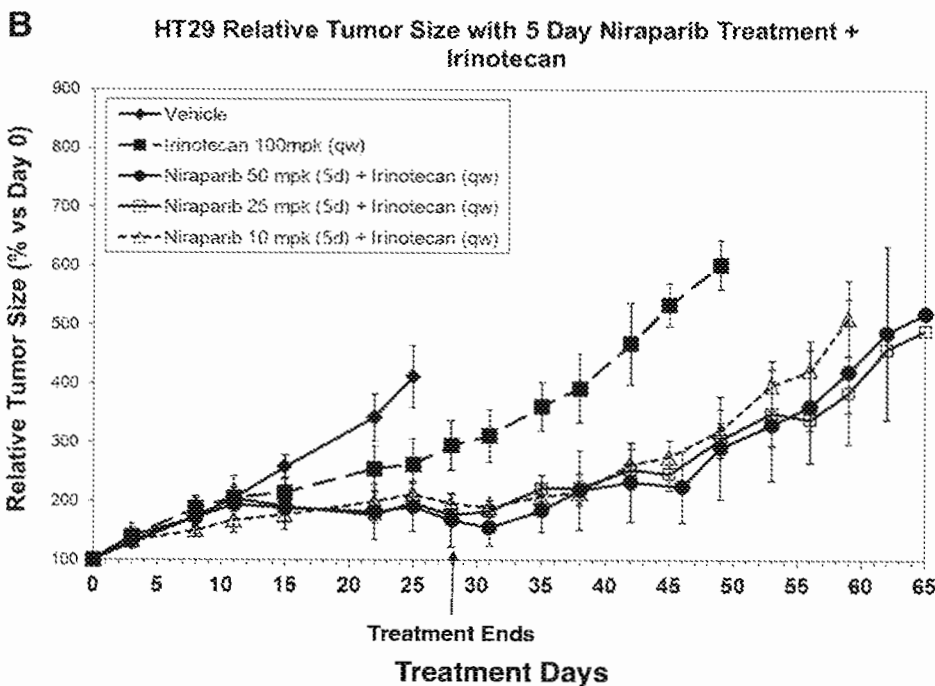
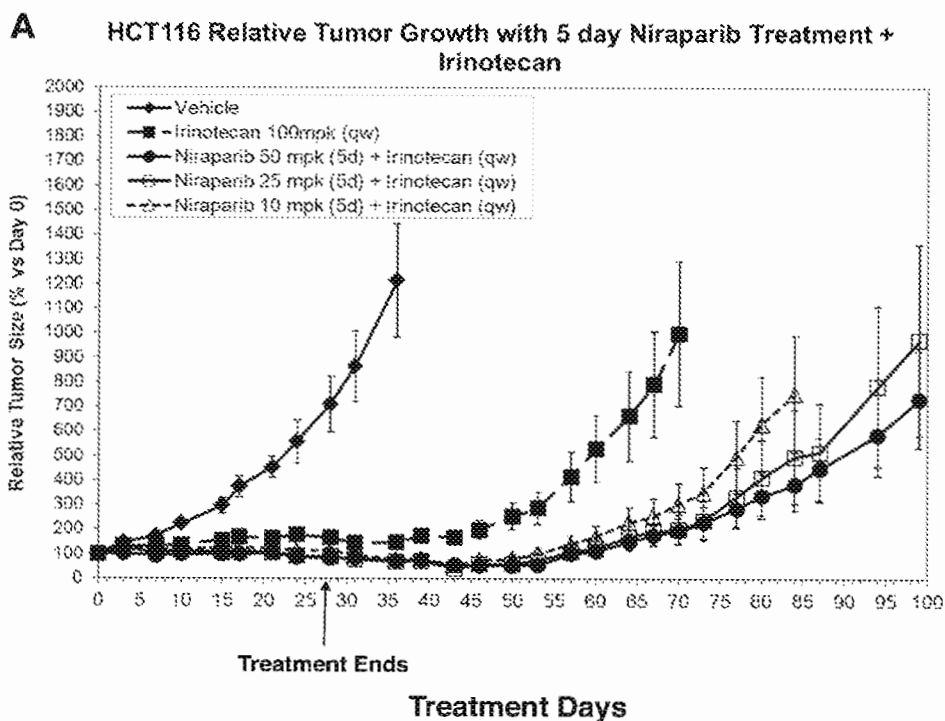


Figure 6 (See legend on next page.)

(See figure on previous page.)

**Figure 6 Tumor growth delay is extended significantly in niraparib + irinotecan combination treatment groups as compared to treatment with irinotecan alone.** (Data from this figure is from the same experiment as in Figures 4 and 5, but has been separated for ease of viewing). Tumor growth delay and relapse after the withdrawal of niraparib and irinotecan treatment in the **(A)** HCT116 (MSI) and **(B)** HT29 xenograft models. Niraparib was dosed at 50, 25, or 10 mpk p.o. q.d., for 5 days and irinotecan was administered at 100 mpk i.p. on the 3rd day of every week for 4 weeks. After the 4<sup>th</sup> week of dosing of both drugs, treatment was stopped and tumor growth was monitored bi-weekly until the average tumor volume for each group reached to an end-point of 1000 mm<sup>3</sup>. Relative tumor size (% versus Day 0) is shown with SEM in error bars. For each group, n = 7-10. **(A)** The average tumor volume for the 50, 25, and 10 mpk niraparib + irinotecan combination groups in the HCT116 model were significantly different from the irinotecan single agent group at day 70 when the average tumor size in the irinotecan single agent group reached the end-point of 1000 mm<sup>3</sup> with P-values of .02, .02, and .03, respectively. (P value generated using a homoscedastic Student's t-test.) **(B)** The average tumor volume for the 50, 25, and 10 mpk niraparib + irinotecan combination groups in the HT29 model were significantly different from the irinotecan single agent group at day 49 when the average tumor size in the irinotecan single agent group reached the end-point of 1000 mm<sup>3</sup> with P-values of .05, .03, and .03, respectively. (P value generated using a homoscedastic Student's t-test)

is more than 10 times the EC50 reported for ABT-888 in the BRCA mutant context [31]. Notably, the concentrations of compound used in those studies is unlikely a therapeutically relevant dose [32].

Gaymes et al., reported that MSI induced mutations in DNA repair genes confer hypersensitivity to the PARP inhibitor BMN673 in myeloid malignancies [29]. These authors were studying cell lines of myeloid lineage and we did not assay any of the same cell lines in our studies. Discrepancies in our results could stem from different cell line panels, the effects of MSI in other tissue types, or a difference in assay platform.

We have also confirmed previous reports that MSI CRC cell lines are more sensitive to irinotecan (SN-38) monotherapy than MSS CRC cell lines in a large cell line panel. (Figure 2B and Table 1) [18]. The average 7 day EC50 for SN-38 in MSI cell was 2.1 nM and for MSS cells was 10.0 nM. However, 6/13 MSS cell lines tested had EC50s less than 5nM (Figure 2B and Table 1). The data in Figure 2B. demonstrates that there are SN-38 sensitive and SN-38 insensitive subpopulations of MSS cell lines. Some of the MSS cell lines are quite sensitive to SN-38 and we have demonstrated that if a cell line responds to SN-38 monotherapy then niraparib will potentiate that effect, in both MSI and MSS cell lines (Table 1). We have also demonstrated that combination of niraparib with SN-38 results in additive to synergistic inhibition of cell proliferation in both MSI and MSS CRC cell lines *in vitro* (Figure 3). In addition, we demonstrate that while the doses of niraparib used in this study are not as efficacious as irinotecan in monotherapy, the combination of low doses of niraparib and irinotecan results in greater tumor growth inhibition in MSI and MSS tumor models *in vivo* (Figure 4.) In tumor growth delay and relapse studies, tumors treated with irinotecan alone relapsed earlier than tumors treated niraparib and irinotecan combination at all three niraparib doses tested (50, 25, 10 mpk) in both MSI and MSS CRC xenograft models.

Our *in vitro* and *in vivo* preclinical results demonstrate that in CRC cell lines, MSI does not render cells more

sensitive to niraparib, but that combination of niraparib with irinotecan enhances the efficacy of irinotecan in both MSI and MSS CRC cell lines. Our data suggests that both MSI and MSS patient populations will benefit from the combination of niraparib and irinotecan.

#### Competing interests

SW is an employee of Merck Research Laboratories. The authors declare that they have no competing interests.

#### Authors' contributions

SW contributed to study design and coordination, drafted the manuscript, constructed the figures, carried out the microsatellite repeat analysis, performed the Western analysis, and performed the *in vitro* proliferation assays (single agent and combination). AK and PA carried out *in vivo* studies. BD performed statistical analyses. RO contributed manuscript preparation. CE contributed to study design and coordination. CT contributed to study concept, design and coordination. All authors read and approved the final manuscript.

#### Acknowledgements

We thank Stuart Shumway, Leigh Zawel, and Keith Wilcoxon for critical reading of this manuscript.

#### Author details

<sup>1</sup>Department of Oncology, Merck Research Laboratories, 33 Avenue Louis Pasteur, Boston, MA 02115, USA. <sup>2</sup>Department of *In Vivo* Pharmacology, Merck Research Laboratories, 33 Avenue Louis Pasteur, Boston, MA 02115, USA. <sup>3</sup>Current address: Bayer HealthCare, 100 Bayer Road, Whippany, NJ 07891, USA. <sup>4</sup>Current address: Institute for Applied Cancer Science, 1901 East Road, Unit 1956, Room 4SCR6.1009, Houston, TX 77005, USA.

Received: 27 November 2013 Accepted: 14 January 2015

Published online: 04 February 2015

#### References

- Bryant HE, Schultz N, Thomas HD, Parker KM, Flower D, Lopez E, et al. Specific killing of BRCA2-deficient tumours with inhibitors of poly(ADP-ribose) polymerase. *Nature*. 2005;434:913-7.
- Farmer H, McCabe N, Lord CJ, Tutt AN, Johnson DA, Richardson TB, et al. Targeting the DNA repair defect in BRCA mutant cells as a therapeutic strategy. *Nature*. 2005;434:917-21.
- Jones P, Altamura S, Boueres J, Ferrigno F, Fonsi M, Giomini C, et al. Discovery of 2-[4-[(3S)-piperidin-3-yl]phenyl]-2H-indazole-7-carboxamide (MK-4827): a novel oral poly(ADP-ribose)polymerase (PARP) inhibitor efficacious in BRCA-1 and -2 mutant tumors. *J Med Chem*. 2009;52:7170-85.
- McCabe N, Turner NC, Lord CJ, Kluzek K, Bialkowska A, Swift S, et al. Deficiency in the repair of DNA damage by homologous recombination and sensitivity to poly(ADP-ribose) polymerase inhibition. *Cancer Res*. 2006;66:8109-15.
- Fong PC, Boss DS, Yap TA, Tutt A, Wu P, Mergui-Roelvink M, et al. Inhibition of poly(ADP-ribose) polymerase in tumors from BRCA mutation carriers. *N Engl J Med*. 2009;361:123-34.

6. Giannini G, Ristori E, Cerignoli F, Rinaldi C, Zani M, Viel A, et al. Human MRE11 is inactivated in mismatch repair-deficient cancers. *EMBO Rep*. 2002;3:248–54.
7. Duval A, Hamelin R. Mutations at coding repeat sequences in mismatch repair-deficient human cancers: toward a new concept of target genes for instability. *Cancer Res*. 2002;62:2447–54.
8. Koh KH, Kang HJ, Li LS, Kim NG, You KT, Yang E, et al. Impaired nonhomologous end-joining in mismatch repair-deficient colon carcinomas. *Lab Invest*. 2005;85:1130–8.
9. Fallik D, Borroni F, Boige V, Viguier J, Jacob S, Miquel C, et al. Microsatellite instability is a predictive factor of the tumor response to irinotecan in patients with advanced colorectal cancer. *Cancer Res*. 2003;63:5738–44.
10. Miquel C, Jacob S, Grandjouan S, Aime A, Viguier J, Sabourin JC, et al. Frequent alteration of DNA damage signalling and repair pathways in human colorectal cancers with microsatellite instability. *Oncogene*. 2007;26:5919–26.
11. Ratnam K, Low J. Current Development of Clinical Inhibitors of Poly (ADP-Ribose) Polymerase in Oncology. *Clin Cancer Res*. 2007;13:1383–8.
12. Ray CA, Hashimoto Y, Herrador R, Neelsen KJ, Fachinetti D, Bermejo R, et al. Topoisomerase I poisoning results in PARP-mediated replication fork reversal. *Nat Struct Mol Biol*. 2012;19:417–23.
13. Delaney CA, Wang LZ, Kyle S, White AW, Calvert AH, Curtin NJ, et al. Potentiation of temozolomide and topotecan growth inhibition and cytotoxicity by novel poly(adenosine diphosphoribose) polymerase inhibitors in a panel of human tumor cell lines. *Clin Cancer Res*. 2000;6:2860–7.
14. Smith LM, Willmore E, Austin CA, Curtin NJ. The novel poly(ADP-Ribose) polymerase inhibitor, AG14361, sensitizes cells to topoisomerase I poisons by increasing the persistence of DNA strand breaks. *Clin Cancer Res*. 2005;11:8449–57.
15. Patel AG, Flatten KS, Schneider PA, Dai NT, McDonald JS, Poirier GG, et al. Enhanced killing of cancer cells by poly(ADP-ribose) polymerase inhibitors and topoisomerase I inhibitors reflects poisoning of both enzymes. *J Biol Chem*. 2012;287:4198–210.
16. Kummur S, Chen A, Ji J, Zhang Y, Reid JM, Ames M, et al. Phase I study of PARP inhibitor ABT-888 in combination with topotecan in adults with refractory solid tumors and lymphomas. *Cancer Res*. 2011;71:5626–34.
17. Tentori L, Leonetti C, Scarsella M, Muzi A, Mazzone E, Vergati M, et al. Inhibition of poly(ADP-ribose) polymerase prevents irinotecan-induced intestinal damage and enhances irinotecan/temozolomide efficacy against colon carcinoma. *FASEB J*. 2006;20:1709–11.
18. Vilar E, Scaltriti M, Balmana J, Saura C, Guzman M, Arribas J, et al. Microsatellite instability due to hMLH1 deficiency is associated with increased cytotoxicity to irinotecan in human colorectal cancer cell lines. *Br J Cancer*. 2008;99:1607–12.
19. Bertagnolli MM, Niedzwiecki D, Compton CC, Hahn HP, Hall M, Damas B, et al. Microsatellite instability predicts improved response to adjuvant therapy with irinotecan, fluorouracil, and leucovorin in stage III colon cancer: Cancer and Leukemia Group B Protocol 89803. *J Clin Oncol*. 2009;27:1814–21.
20. Zhou XP, Hoang JM, Cottu P, Thomas G, Hamelin R. Allelic profiles of mononucleotide repeat microsatellites in control individuals and in colorectal tumors with and without replication errors. *Oncogene*. 1997;15:1713–8.
21. Hoang JM, Cottu PH, Thuille B, Salmon RJ, Thomas G, Hamelin R. BAT-26, an indicator of the replication error phenotype in colorectal cancers and cell lines. *Cancer Res*. 1997;57:300–3.
22. Efstathiou JA, Liu D, Wheeler JM, Kim HC, Beck NE, Ilyas M, et al. Mutated epithelial cadherin is associated with increased tumorigenicity and loss of adhesion and of responsiveness to the mitogenic trefoil factor 2 in colon carcinoma cells. *Proc Natl Acad Sci U S A*. 1999;96:2316–21.
23. Shibata D, Peinado MA, Ionov Y, Malkhosyan S, Perucho M. Genomic instability in repeated sequences is an early somatic event in colorectal tumorigenesis that persists after transformation. *Nat Genet*. 1994;6:273–81.
24. Umar A, Boyer JC, Thomas DC, Nguyen DC, Risinger JI, Boyd J, et al. Defective mismatch repair in extracts of colorectal and endometrial cancer cell lines exhibiting microsatellite instability. *J Biol Chem*. 1994;269:14367–70.
25. Koi M, Umar A, Chauhan DP, Cherian SP, Carethers JM, Kunkel TA, et al. Human chromosome 3 corrects mismatch repair deficiency and microsatellite instability and reduces N-methyl-N'-nitro-N-nitrosoguanidine tolerance in colon tumor cells with homozygous hMLH1 mutation. *Cancer Res*. 1994;54:4308–12.
26. Lehar J, Stockwell BR, Glaever G, Nislow C. Combination chemical genetics. *Nat Chem Biol*. 2008;4:674–81.
27. Ottini L, Falchetti M, Saieva C, De Marco M, Masala G, Zanna I, et al. MRE11 expression is impaired in gastric cancer with microsatellite instability. *Carcinogenesis*. 2004;25:2337–43.
28. Vilar E, Barnik CM, Stenzel SL, Raskin L, Ahn J, Moreno V, et al. MRE11 deficiency increases sensitivity to poly(ADP-ribose) polymerase inhibition in microsatellite unstable colorectal cancers. *Cancer Res*. 2011;71:2632–42.
29. Gaymes TJ, Mohamedali AM, Patterson M, Matto N, Smith A, Kulasekararaj A, et al. Microsatellite instability induced mutations in DNA repair genes CtIP and MRE11 confer hypersensitivity to poly (ADP-ribose) polymerase inhibitors in myeloid malignancies. *Haematologica*. 2013;98:1397–406.
30. Sandhu SK, Schelman WR, Wilding G, Moreno V, Baird RD, Miranda S, et al. The poly(ADP-ribose) polymerase inhibitor niraparib (MK4827) in BRCA mutation carriers and patients with sporadic cancer: a phase I dose-escalation trial. *Lancet Oncol*. 2013;14:882–92.
31. Clark CC, Weitzel JN, O'Connor TR. Enhancement of synthetic lethality via combinations of ABT-888, a PARP inhibitor, and carboplatin in vitro and in vivo using BRCA1 and BRCA2 isogenic models. *Mol Cancer Ther*. 2012;11:1948–58.
32. Huggins-Puhalla SL, Beumer JH, Appleman JL, Tawbi HA-H, Stoller RG, Lin Y, et al. A phase I study of chronically dosed, single-agent veliparib (ABT-888) in patients (pts) with either BRCA 1/2-mutated cancer (BRCA+), platinum-refractory ovarian cancer, or basal-like breast cancer (BRCA-w) [abstract]. *ASCO*. 2012;30s3054.

**Submit your next manuscript to BioMed Central  
and take full advantage of:**

- Convenient online submission
- Thorough peer review
- No space constraints or color figure charges
- Immediate publication on acceptance
- Inclusion in PubMed, CAS, Scopus and Google Scholar
- Research which is freely available for redistribution

Submit your manuscript at  
[www.biomedcentral.com/submit](http://www.biomedcentral.com/submit)





## Minireview

# Topoisomerase I inhibition in colorectal cancer: biomarkers and therapeutic targets

DC Gilbert<sup>\*1</sup>, AJ Chalmers<sup>2</sup> and SF El-Khamisy<sup>3,4</sup>

<sup>1</sup>Sussex Cancer Centre, Royal Sussex County Hospital, Eastern Road, Brighton BN2 5BE, UK; <sup>2</sup>Institute of Cancer Sciences, University of Glasgow, Glasgow G12 8QQ, UK; <sup>3</sup>Genome Damage and Stability Centre, University of Sussex, Falmer, Brighton BN1 9RQ, UK; <sup>4</sup>Department of Biochemistry, Faculty of Pharmacy, Ain Shams University, Cairo POB 11566, Egypt

The topoisomerase I (Top I) poison irinotecan is an important component of the modern treatment of colorectal cancer. By stabilising Top I-DNA complexes, irinotecan generates Top I-linked DNA single-strand breaks that can evolve into double-strand breaks and ultimately cause cell death. However, cancer cells may overcome cell killing by releasing the stalled topoisomerase from DNA termini, thereby reducing the efficacy of Top I poisons in clinics. Thus, understanding the DNA repair mechanisms involved in the repair of Top I-mediated DNA damage provides a useful tool to identify potential biomarkers that predict response to this class of chemotherapy. Furthermore, targeting these pathways could enhance the therapeutic benefits of Top I poisons. In this review, we describe the cellular mechanisms and consequences of targeting Top I activity in cells. We summarise preclinical data and discuss the potential clinical utility of small-molecule inhibitors of the key proteins.

*British Journal of Cancer* (2012) **106**, 18–24. doi:10.1038/bjc.2011.498 www.bjcancer.com

Published online 22 November 2011

© 2012 Cancer Research UK

**Keywords:** irinotecan; colorectal cancer; biomarkers; topoisomerase I; TDPI; PARP

## CLINICAL UTILITY OF TOPOISOMERASE I (TOP I) POISONS

Colorectal cancer remains a significant cause of morbidity and mortality worldwide, with 39 000 new cases per year in the UK and 16 000 deaths. In North America, the figures are 177 000 and 58 000, respectively (<http://globocan.iarc.fr/>). Despite the development of biological agents targeting EGFR and VEGF signalling, defining subgroups of patients that derive maximal benefit has proved difficult. Combination chemotherapy consisting of 5-fluorouracil paired with either the third-generation platinum compound oxaliplatin or the Top I poison irinotecan remains the mainstay of treatment for metastatic disease. The efficacy of irinotecan in metastatic colorectal cancer was demonstrated in clinical trials conducted over a decade ago (Douillard *et al*, 2000; Saltz *et al*, 2000), with response rates to combination regimens of 30–50% and overall survival in some studies approaching 24 months (Fuchs *et al*, 2007). In the treatment-naïve population, there is broad equivalence in tumour response between irinotecan and oxaliplatin when combined with 5-fluorouracil (Seymour *et al*, 2007). However, the observation that responses to both irinotecan and oxaliplatin occur in the second line setting after progression on the other drug indicates that individual tumours differ in their sensitivity to these drugs. Biomarkers are therefore required to optimise patient treatment.

Locally advanced rectal cancers are increasingly treated with neoadjuvant chemo-radiotherapy strategies to optimise surgical resection and reduce rates of local and distant relapse. Phase I/II

studies incorporating irinotecan, 5FU and radiotherapy in rectal cancer have indicated improved efficacy over 5FU chemo-radiotherapy alone, and have proved to be deliverable in terms of acute toxicity (Glynne-Jones *et al*, 2007; Willeke *et al*, 2007; Gollins *et al*, 2011). Neoadjuvant strategies incorporating oxaliplatin are also being developed, and thus robust predictive markers are required to optimise patient selection and maximise clinical benefit. Beyond its role in colorectal cancer, which will be the main focus of this review, there is also growing interest in the use of irinotecan in small-cell lung cancer, where there is evidence of increased efficacy over etoposide regimens (Lima *et al*, 2010), and a range of other tumour types including glioblastoma.

## CELLULAR BIOCHEMISTRY OF TOP I

The compact and supercoiled nature of the DNA double helix requires topological modification during important cellular processes such as transcription, replication and repair. This modification is conducted by DNA topoisomerases and involves transient cleavage and re-ligation of the double-stranded DNA molecule. Topoisomerases are enzymes that cleave one or both of the sugar-phosphate backbones of double-stranded DNA without altering its chemical composition (hence the term 'isomerase'). Type I topoisomerases (Top I, Wang, 1971) cut a single strand of DNA to allow relaxation of torsional stresses before re-annealing. Type II topoisomerases (Top II, Gellert *et al*, 1976) incise double-stranded DNA to facilitate the passage of an intact duplex through the gap before rejoining the cut DNA. This mode of catalysis involves an intermediate known as the cleavage complex, which comprises the topoisomerase enzyme attached to the cleaved DNA by a covalent phosphotyrosyl bond. Increased levels of Top I mRNA and protein are seen across human tumours (Husain *et al*,

\*Correspondence: Dr DC Gilbert;

E-mail: Duncan.Gilbert@bsuh.nhs.uk or duncan.gilbert@icr.ac.uk

Received 1 June 2011; revised 30 September 2011; accepted 21 October 2011; published online 22 November 2011

1994), suggesting increased transcription or mRNA stability, although genomic amplification of Top I in colorectal cancer has been described and correlates with increased RNA and protein expression (Yu *et al*, 2008).

Top I is the target of the camptothecin derivatives irinotecan and topotecan, whereas Top II is targeted by etoposide and anthracyclins. Camptothecin is a naturally occurring cytotoxic quinolone alkaloid (derived from the bark of *Camptotheca acuminata*) that binds to and stalls Top I on DNA. Irinotecan is a semisynthetic analogue of camptothecin that is activated by hydrolysis to the active metabolite SN38, which is subsequently metabolised through glucuronidation by uridine diphosphate glucuronosyltransferase 1A1 (UGT1A1) and excreted in the bile. Patients with specific polymorphisms in UGT1A1 (UGT1A1\*28) have impaired metabolism of SN38 and are predisposed to the major toxicities of irinotecan, which are diarrhoea and myelosuppression, particularly neutropenia (Innocenti *et al*, 2004; O'Dwyer and Catalano, 2006). More recently, it has been suggested that different polymorphisms in UGT1A might also modulate tumour response rates (Cecchin *et al*, 2009).

Irinotecan (predominantly in the form of SN38) binds to the Top I-DNA complex, stabilizing it and preventing re-ligation (Hsiang *et al*, 1985; Hsiang and Liu, 1988). Collision with advancing replication forks results in the formation of double-stranded DNA breaks. These breaks activate cell cycle arrest in G2 phase and, if unrepaired, can cause cell death (Figure 1). The requirement for DNA replication in this cytotoxic mechanism confers a degree of tumour specificity, with the major toxic effects arising in rapidly proliferating normal tissues. However, cell cycle-independent cytotoxicity may also occur through apoptosis, which is thought to be triggered by inhibition of Top I activity during DNA transcription (Morris and Geller, 1996). There is also recent evidence that activation of p38 MAPK may protect cells from irinotecan cytotoxicity (Paillas *et al*, 2011).

Repair of irinotecan-associated DNA damage requires removal of the stalled Top I peptide and resolution of the associated DNA break (Figure 1). A number of repair proteins are involved in this process, some of which have clinical potential either as predictive

biomarkers or as therapeutic targets. The most important factors will be briefly described in this section of the review.

Excision of the covalently linked topoisomerase is mandatory if subsequent repair steps are to be initiated; this can be achieved either by nonspecific nucleolytic cleavage of DNA, releasing the topoisomerase and a fragment of DNA, or by hydrolytic cleavage of the covalent phosphotyrosyl bond that links the topoisomerase to the DNA termini (reviewed in El-Khamisy, 2011). The prototype enzyme for the latter process was first identified in yeast and named tyrosyl DNA phosphodiesterase 1 (Yang *et al*, 1996). Tyrosyl DNA phosphodiesterase 1 (TDP1) catalyses hydrolysis of the phosphodiester bond between Top I and the 3'-phosphate of DNA, allowing resolution of the stalled Top I-DNA complexes (El-Khamisy *et al*, 2005; Interthal *et al*, 2005). In a similar manner, a second protein (TDP2) functions to remove Top II covalently bound to DNA double-strand breaks (Cortes Ledesma *et al*, 2009). Lack of TDP1 is associated with defects in the repair of Top I-associated DNA strand breaks, and cells deficient in TDP1 accumulate DNA strand breaks when incubated with camptothecin.

*In vitro*, TDP1 can process a variety of 3'-oxidative termini, including 3'-phosphoglycolate moieties that are a common feature of DNA breaks induced by ionising radiation (IR; Zhou *et al*, 2005, 2009; El-Khamisy *et al*, 2007; Chiang *et al*, 2010). This observation points to a requirement for TDP1 for effective resolution of DNA damage associated with both Top I inhibition and IR, and indicates a potentially critical role for TDP1 in the cellular response to irinotecan-based chemoradiation. The clinical implications of this will be discussed later.

Poly(ADP-ribose) polymerase (PARP) also influences repair of Top I-mediated DNA damage. Inhibition of PARP sensitises cells to camptothecin, primarily by delaying DNA repair (Smith *et al*, 2005). As PARP inhibition does not confer additional sensitivity to camptothecin in TDP1 knockout cells (Zhang *et al*, 2011), it has been suggested that PARP and TDP1 are components of a single repair pathway for Top I-DNA complexes. In the same study, XPF and ERCC1 were also shown to be involved in repair of camptothecin-induced DNA damage; however, unlike *TDP1*, knockdown of *XPF* was synergistic with PARP inhibition in terms of camptothecin cytotoxicity (Zhang *et al*, 2011). PARP/TDP1 and

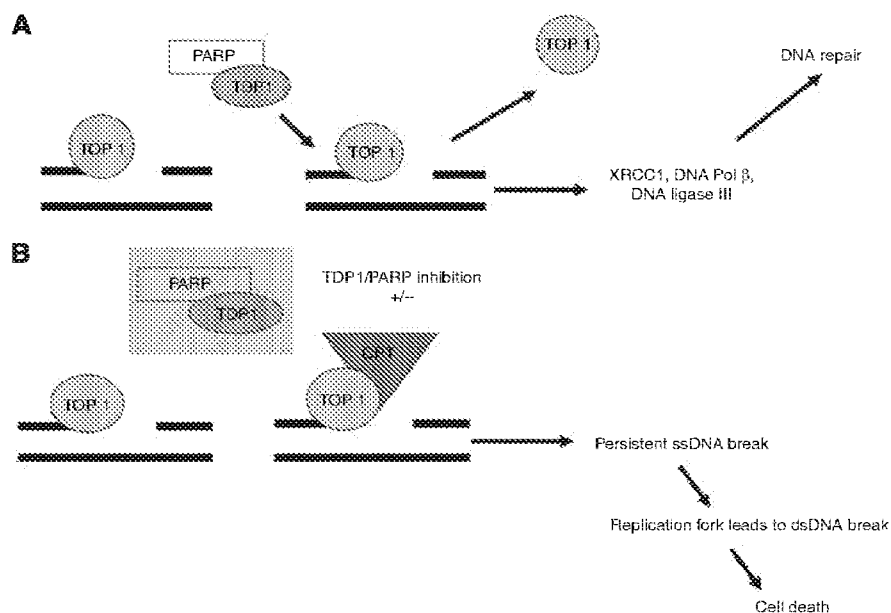


**Figure 1** (A) Top I cleavage complexes are ordinarily removed through TDP1- and PARP-dependent mechanisms, with the ssDNA breaks repaired through XRC1 and DNA through polymerases/ligases. (B) Camptothecin (and irinotecan via SN38) stabilises the cleavage complexes, with the persistent ssDNA breaks converting to dsDNA lesions causing cell death, and expected synergy with TDP1/PARP inhibition.

XPF-ERCC1 may therefore comprise alternative pathways for repairing Top 1-mediated DNA damage.

Another candidate that has a role during the repair of Top 1 breaks is Aprataxin (APTX). APTX is the gene mutated in ataxia-ocular apraxia 1 (Moreira *et al*, 2001) and encodes a protein involved in the repair of single- (SSB) and double-stranded (DSB) DNA breaks. There is evidence that APTX participates in the repair of CPT-induced DNA damage (Mosesso *et al*, 2005), and a synergy between the actions of TDP1 and APTX has also been reported during the repair of specific types of DNA breaks (El-Khamisy *et al*, 2009).

Approximately 5% of colorectal cancers are associated with hereditary non-polyposis colon cancer, an inherited cancer predisposition syndrome caused by germ-line alteration of mismatch repair genes (MMR). Moreover, around 15% of sporadic cases demonstrate somatic loss of function of one or more MMR genes (most commonly *MSH2* or *MLH1*). The MMR proteins recognise errors in the base sequence of DNA that occur during DNA replication (insertions, deletions or substitutions) and facilitate excision of the mismatched strand and restoration of base fidelity. Loss of function of one or more of these proteins results in microsatellite instability (MSI) – abnormally long or short microsatellites (repeated sequences of DNA) – which serves as a genetic signature for this phenotype. MMR-defective colorectal cancer lines exhibit increased sensitivity to CPT *in vitro*, which is reversed when wild-type gene expression is restored (Jacob *et al*, 2001). MMR proteins may also have additional roles in DSB repair and induction of apoptosis in response to DNA damage, and it is hypothesised that these actions may contribute to modulating the response to Top 1 response to topoisomerase poisons detailed below.

## THERAPEUTIC TARGETS IN THE CONTEXT OF TOP 1 INHIBITION

Much of our understanding of the proteins involved in repairing Top 1 cleavage complexes is derived from experimental strategies in which inhibition of those proteins potentiates the DNA damage sustained. Such proteins therefore constitute targets for therapeutic interventions aimed at improving the clinical efficacy of irinotecan.

Cell line and xenograft data demonstrate the potentiating effect of PARP inhibition on the cytotoxicity of irinotecan (Miknyoczki *et al*, 2003; Calabrese *et al*, 2004; Smith *et al*, 2005). Phase I studies of a number of PARP inhibitors, for example, veliparib (Abbott Laboratories, Abbott Park, IL, USA), iniparib (Sanofi-Aventis, Surrey, UK) and olaparib (AstraZeneca, London, UK), in combination with irinotecan are underway. The radiosensitising effects of PARP inhibition are also well documented (Calabrese *et al*, 2004; Chalmers *et al*, 2010; Efimova *et al*, 2010), and clinical trials in various tumour sites are in development (Verheij *et al*, 2010). Locally advanced rectal cancer may therefore provide an ideal opportunity to test combinations of irinotecan, radiotherapy and PARP inhibitors. Of critical importance will be whether meaningful improvements in tumour response can be achieved without unacceptable exacerbation of normal tissue toxicities, particularly bone marrow suppression and diarrhoea.

The rationale for developing inhibitors of TDP1 for subsequent combination with Top 1 poisons is similarly robust. *In vitro*, cells deficient in TDP1 accumulate an excess of DNA strand breaks when incubated with camptothecin (El-Khamisy *et al*, 2005; Interthal *et al*, 2005) or exposed to IR (El-Khamisy *et al*, 2007). This dual activity makes inhibition of TDP1 a compelling target for clinical studies in combination with Top 1 inhibitors and radiotherapy, especially when viewed in the context of the early success of PARP inhibition in clinical practice. Beyond its use in the management of colorectal cancer, the recently demonstrated

activity of irinotecan in small-cell lung cancer and glioblastoma may give TDP1 a broader utility. Combining TDP1 inhibitors with topotecan in ovarian cancer may also prove synergistic. However, given similarities in function and pathways at a cellular level, it remains to be seen how similar or different PARP and TDP1 inhibition will prove and whether inhibiting both together would prove synergistic or mutually redundant.

## POTENTIAL AS PREDICTIVE BIOMARKERS

As described previously, there are a number of therapeutic options available for patients with colorectal cancer, and patient selection is a critical process that is currently sub-optimal. Our increasing knowledge of the mechanisms determining sensitivity to Top 1 inhibitors raises the possibility that some of the key molecules described above will have utility as biomarkers that predict response of tumours to treatment.

### Top 1

As the cytotoxic effects of topoisomerase poisons are dependent on stabilisation of the topoisomerase-DNA complex, it is reasonable to predict that cellular sensitivity to these agents will be modulated by absolute Top 1 levels, although cell lines containing Top 1 mutations that alter Top 1 DNA or camptothecin interaction have been described that confer resistance to camptothecin (Li *et al*, 1996; Gongora *et al*, 2011). Repeated exposure of colorectal cancer xenografts to camptothecin resulted in downregulation of Top 1 levels (Giovannella *et al*, 1989) and the same effect has been observed in peripheral blood mononuclear cells after treatment with topotecan (Hochster *et al*, 1997). Clinically, tumour expression of Top 1 decreased (between pretreatment biopsy and subsequent surgical specimen) following neoadjuvant treatment of rectal cancer with chemoradiation comprising irinotecan and 5FU (Horisberger *et al*, 2009).

Top 1 is highly expressed in around half of the colorectal cancers, with one study demonstrating higher levels in rectal cancers (Boonsong *et al*, 2002). The observed broad range of expression supports the hypothesis that Top 1 expression will predict response to irinotecan. It has been suggested that higher levels of Top 1 expression may predict response to irinotecan-containing neoadjuvant chemoradiation in rectal cancer (Horisberger *et al*, 2009). In addition, the results of the MRC FOCUS study of 1313 patients with metastatic colorectal cancer indicated that tumours with moderate or high levels of Top 1 expression as determined by immunohistochemistry showed the greatest benefit from adding irinotecan or oxaliplatin to 5FU in the first-line metastatic setting (Braun *et al*, 2008). However, subsequent data from the similar 'CAIRO' study from the Dutch Colorectal Cancer Group (Koopman *et al*, 2007) failed to replicate these findings, with no association seen between Top 1 expression (by immunohistochemistry) and response to irinotecan and capecitabine in 545 patients (Koopman *et al*, 2009). These apparently contradictory findings suggest that although absolute Top 1 expression levels may play a part, it is likely that additional molecules contribute to irinotecan sensitivity in the clinic.

### TDP1

The critical role of TDP1 in determining cellular responses to irinotecan makes it a promising biomarker. A number of studies have investigated polymorphisms in genes involved in irinotecan/Top 1-related DNA repair and response to treatment, and some of these have included *TDP1*. In one such study, 107 patients treated with irinotecan were screened for host polymorphisms in *PARP*, *TDP1*, *Top 1* and *XRCC1* (Hoskins *et al*, 2008). Univariate analysis suggested that specific polymorphisms in *TDP1* and *XRCC1* were

linked with response to irinotecan, but on multivariate analysis only *XRCC1* remained significant.

The available data indicate that *TDP1* expression is increased in colorectal tumour samples compared with paired normal tissue (Yu *et al*, 2005). In the most relevant study to date, 52 metastatic colorectal cancer specimens were analysed by RT-PCR for expression of 24 genes hypothesised to be associated with response to irinotecan. *TDP1* was one of eight genes (including *ERCC1* – see above) that showed significantly higher levels of expression in tumours than in normal tissue. Expression of *TDP1* grouped with other genes involved in DNA repair. Interrogation of oncomine ([www.oncomine.org](http://www.oncomine.org)) supports this finding, with *TDP1* expression levels appearing to be broadly increased in colorectal cancer specimens. Several microarray expression profiles for rectal adenocarcinomas have been published (NCBI GEO, EBI), but only one of these used a platform that included a probe for *TDP1* (Snipstad *et al*, 2010). Our analysis of these data demonstrates increased levels of *TDP1* in rectal cancers compared with normal tissues.

As detailed above, it has also been shown that *TDP1* has a role in the repair of SSBs induced by IR (El-Khamisy *et al*, 2007). Specifically, cells deficient in *TDP1* exhibit delayed repair of SSBs induced by IR (Katyál *et al*, 2007; Chiang *et al*, 2010). Although the cytotoxic effects of IR are predominately mediated through double-strand breaks, unrepaired SSBs can be converted to DSBs during DNA replication. This raises the intriguing possibility that *TDP1* could be a dual biomarker for sensitivity to both irinotecan and radiotherapy. Although there is no published data to substantiate this claim, high quality tissue is available from several clinical trials that have tested irinotecan-based chemoradiation regimes, and these samples are currently being analysed for expression of *TDP1* and other relevant DNA repair genes and proteins.

Finally, *in vitro* experiments using the PARP inhibitor ABT-888 (Zhang *et al*, 2011) show no further enhancement of camptothecin cytotoxicity in cell lines lacking *TDP1*, suggesting that PARP and *TDP1* comprise a common repair pathway. Although this supports the rationale for either (but not both together) as therapeutic targets in potentiating topoisomerase poisons, it is possible that increased *TDP1* expression levels might prove a biomarker in predicting benefit from the addition of PARP inhibitors to irinotecan or radiotherapy.

## APT X

*In vitro* studies of colon cancer cell lines have shown an association between APTX expression levels and sensitivity to camptothecin (Mariadason *et al*, 2003), and there is also evidence to suggest that APTX modulates response to irinotecan in metastatic colorectal cancer, with higher protein expression associated with a lower likelihood of response. Tumour blocks from 135 patients with metastatic disease treated with a variety of irinotecan/5FU combination regimens were probed for APTX using immunohistochemistry (Dopeso *et al*, 2010). With a median follow-up of 4.6 years, patients with low levels of APTX had improved progression-free and overall survival (PFS 9.2 vs 5.5 months  $P=0.03$ , OS 36.7 vs 19 months  $P=0.008$ ). These promising data require validation, but demonstrates the potential value of this class of biomarker.

## MMR

Mismatch repair-deficient colorectal cancers have been reported to be resistant to 5FU (Ribic *et al*, 2003), but more recent evidence indicates that they may be sensitive to irinotecan. In the adjuvant setting, CALGB 89803 randomised 1264 patients with stage III colon cancer to weekly 5FU/leucovorin ± irinotecan. Of all, 723 cases were retrospectively genotyped for MSI, and MMR protein

expression was analysed by immunohistochemistry (Bertagnolli *et al*, 2009). Tumours with evidence of MMR deficiency showed improved 5-year disease-free survival when treated with irinotecan (0.76 vs 0.59,  $P=0.03$ ), a difference that was not observed in the 5FU-treated arm. This effect has also been documented in the metastatic setting (Fallik *et al*, 2003). Here, 72 patients treated with irinotecan-containing regimens were analysed for loss of expression of hMLH1 and hMSH2 and genotyped for microsatellite instability. Four out of seven tumours with high levels of MSI responded to irinotecan as opposed to seven out of sixty-five patients with low-level MSI ( $P=0.009$ ). However, unlike Top I, MLH1/MSH2 immunohistochemical analysis was not able to predict response to irinotecan (or oxaliplatin) within the FOCUS study (Braun *et al*, 2008), although with only 4.4% samples showing evidence of impaired mismatch repair the statistical power was low. As molecular subtyping of colorectal cancer improves, it is likely that MMR-deficient tumours will acquire specific treatment protocols. Current understanding of DNA repair mechanisms would place irinotecan at the centre of these, but more clinical data are required before such protocols are adopted.

## Biomarkers of toxicity

Given the equivalent first-line efficacy of oxaliplatin and irinotecan regimens, the ability to predict toxicity would be of value in individualising treatment decisions. Here, germ-line polymorphisms in the genes discussed in this review may be more relevant than variations in tumour expression. The previously described study (Hoskins *et al*, 2008) genotyped 107 metastatic CRC patients treated with irinotecan regimens for single-nucleotide polymorphisms (SNP) in *Top 1*, *CDC45L*, *NFKB1*, *PARP1*, *TDP1* and *XRCC1*. These SNPs were tested for association with the most frequent and significant side effects of irinotecan, namely grade three out of four diarrhoea and neutropenia. In univariate analysis, SNPs in both *Top 1* and *TDP1* were associated with grade three out of four neutropenia. However, multivariate analysis failed to demonstrate significant association, and the same authors failed to replicate these findings in a separate sample set (Hoskins *et al*, 2009). However, neither study was powered to detect relatively small effects, and consideration of the overlapping pathways involved in determining irinotecan response suggests that any modulation of toxicity is likely to be multifactorial.

## CLINICAL APPLICATION OF POTENTIAL BIOMARKERS

There is increasing awareness of the potential value of molecular pathology in clinical decision making, and colorectal cancer is at the forefront of this vogue. The MRC FOCUS 3 trial is currently testing the feasibility of such a strategy in a study that stratifies patients with metastatic colorectal cancer into treatment groups based on Top I I levels in their tumour specimens (<http://www.ctu.mrc.ac.uk/>). Drawing on molecular data from the FOCUS study described above (Braun *et al*, 2008), and using combination irinotecan and 5FU as a control regimen, patients with low Top I-expressing tumours will be randomised to omit the irinotecan (i.e., receive 5FU alone), whereas tumours with high Top I will be randomised to add oxaliplatin to irinotecan/5FU. A further randomisation will be determined by the mutation status of *KRAS* and *BRAF*, with the addition of cetuximab being tested if *KRAS/BRAF* are both wild type and bevacizumab if either are mutated. If successful, this ambitious study will be extremely informative both from a clinical perspective and as an indicator of the feasibility of individualising treatment by virtue of molecular testing.

Increasing application of irinotecan in the neoadjuvant treatment of rectal cancer (Gollins *et al*, 2011) may provide opportunities

**Table 1** Candidate therapeutic targets and biomarkers of response to irinotecan derived from an improved understanding of topoisomerase I activity and subsequent DNA repair mechanisms

Molecule	Potential clinical utility		
	Therapeutic target	Biomarker of response	Reference
Top I	Mechanism of action of Irinotecan	Yes	Braun <i>et al</i> , 2008
TDP1	Yes	Proposed	El-Khamisy <i>et al</i> , 2005, 2007
PARP	Yes	?	Smith <i>et al</i> , 2005; Zhang <i>et al</i> , 2011
Aprataxin	?	Yes	Dopeso <i>et al</i> , 2010
Mismatch repair	?	Yes	Bertagnolli <i>et al</i> , 2009

Abbreviations: PARP = poly(ADP-ribose) polymerase; TDP1 = tyrosyl DNA phosphodiesterase I; Top I = type I topoisomerases.

for testing a range of the potential biomarkers discussed in this review. MRI and pathological response at definitive surgery provide robust and quantitative early-outcome measures, and the availability of pre- and post-treatment tissue samples makes this an ideal setting in which to investigate new drug combinations and associated biomarkers.

## POTENTIAL UTILITY BEYOND TOPOISOMERASE INHIBITORS

There is increasing interest in the use of small-molecule inhibitors of DNA repair enzymes to overcome resistance to conventional cytotoxic agents that kill cells predominantly by damaging DNA. PARP inhibitors are at the forefront of this field, and several clinical trials combining PARP inhibitors with radiotherapy and/or cytotoxic drugs are either underway or in development. As previously highlighted, there are functional parallels between TDP1 and PARP, with TDP1 having a role in the resolution of SSBs induced by Top I poisons and by ionising radiation. Hence, there is a biological rationale for combining TDP1 inhibitors with radiotherapy (El-Khamisy *et al*, 2007), either alone or in the context of chemoradiation schedules. Although relatively little cancer-specific research has been conducted, TDP1 is known to be expressed in a variety of tumour types (Liu *et al*, 2007). In addition to the compelling evidence for TDP1 as a therapeutic target in the treatment of rectal cancer, it is reasonable to predict that ongoing research will identify whether additional therapeutic applications exist for combination treatments comprising TDP1 inhibitors.

## REFERENCES

- Bertagnolli MM, Niedzwiecki D, Compton CC, Hahn HP, Hall M, Damas B, Jewell SD, Mayer RJ, Goldberg RM, Saltz LB, Warren RS, Redston M (2009) Microsatellite instability predicts improved response to adjuvant therapy with irinotecan, fluorouracil, and leucovorin in stage III colon cancer: cancer and leukemia group B protocol 89803. *J Clin Oncol* 27: 1814–1821
- Boonsong A, Curran S, McKay JA, Cassidy J, Murray GI, McLeod HL (2002) Topoisomerase I protein expression in primary colorectal cancer and lymph node metastases. *Hum Pathol* 33: 1114–1119
- Braun MS, Richman SD, Quirke P, Daly C, Adlard JW, Elliott F, Barrett JH, Selby P, Meade AM, Stephens RJ, Parmar MK, Seymour MT (2008) Predictive biomarkers of chemotherapy efficacy in colorectal cancer: results from the UK MRC FOCUS trial. *J Clin Oncol* 26: 2690–2698
- Calabrese CR, Almasy R, Barton S, Batey MA, Calvert AH, Canan-Koch S, Durkacz BW, Hostomsky Z, Kumpf RA, Kyle S, Li J, Maegley K, Newell DR, Notarianni E, Stratford IJ, Skalitzky D, Thomas HD, Wang LZ, Webber SE, Williams KJ, Curtin NJ (2004) Anticancer chemosensitization and radiosensitization by the novel poly(ADP-ribose) polymerase-1 inhibitor AG14361. *J Natl Cancer Inst* 96: 56–67

## CONCLUSIONS

Although decades of basic scientific research has yielded a number of anti-cancer drugs that target signal transduction pathways, only recently has there been a resurgence of interest in understanding and exploiting the cellular mechanisms of DNA repair. This new knowledge promises to better explain clinical responses to conventional cytotoxic agents including radiotherapy, and to reveal biomarkers predictive of response and resistance (Table 1). Specifically, the mechanisms for repairing topoisomerase-associated DNA breaks that accumulate following treatment with Top I poisons, such as irinotecan, comprise proteins that can be targeted to modulate sensitivity to these agents. TDP1 has well-characterised roles in the repair of DNA-Top I intermediates and radiation-induced DNA breaks and shows significant promise as a biomarker. Furthermore, the clinical development of PARP inhibitors has demonstrated that this understanding can identify therapeutic targets, inhibitors of which might realistically be combined with irinotecan to yield clinically significant improvements in tumour response rates.

The promise of the biomarkers described in this review should be comprehensively assessed by translational work on the plethora of clinical studies that have used irinotecan in colorectal cancer (and beyond). Retrospective work, however, will require the cooperation of treating departments in collecting meaningful sample sets. The development of trials that begin to match treatment arms to underlying molecular characteristics (e.g., FOCUS3) should be widely supported and further developed. Combining an improved molecular understanding of individual tumours with specific adjunctive therapies, Top I will remain a key target in the treatment of colorectal cancer.

- Cecchin E, Innocenti F, D'Andrea M, Corona G, De Mattia E, Bionso P, Buonadonna A, Toffoli G (2009) Predictive role of the UGT1A1, UGT1A7, and UGT1A9 genetic variants and their haplotypes on the outcome of metastatic colorectal cancer patients treated with fluorouracil, leucovorin, and irinotecan. *J Clin Oncol* 27: 2457–2465
- Chalmers AJ, Lakshman M, Chan N, Bristow RG (2010) Poly(ADP-ribose) polymerase inhibition as a model for synthetic lethality in developing radiation oncology targets. *Semin Radiat Oncol* 20(4): 274–281
- Chiang SC, Carroll J, El-Khamisy SF (2010) TDP1 serine 81 promotes interaction with DNA ligase III alpha and facilitates cell survival following DNA damage. *Cell Cycle* 9: 588–595
- Cortes Ledesma F, El Khamisy SF, Zuma MC, Osborn K, Caldecott KW (2009) A human 5'-tyrosyl DNA phosphodiesterase that repairs topoisomerase-mediated DNA damage. *Nature* 461: 674–678
- Dopeso H, Mateo-Lozano S, Elez E, Landolfi S, Ramos Pascual FJ, Hernandez-Losa J, Mazzolini R, Rodrigues P, Bazzocco S, Carreras MJ, Espin E, Armengol M, Wilson AJ, Mariadason JM, Ramon YCS, Taberner J, Schwartz Jr S, Arango D (2010) Aprataxin tumor levels predict response of colorectal cancer patients to irinotecan-based treatment. *Clin Cancer Res* 16: 2375–2382





- Douillard JY, Cunningham D, Roth AD, Navarro M, James RD, Karasek P, Jandik P, Iveson T, Carmichael J, Alakl M, Gruia G, Awad L, Rougier P (2000) Irinotecan combined with fluorouracil compared with fluorouracil alone as first-line treatment for metastatic colorectal cancer: a multicentre randomised trial. *Lancet* 355: 1041–1047
- Efimova EV, Mauceri HJ, Golden DW, Labay E, Bindokas VP, Darga TE, Chakraborty C, Barreto-Andrade JC, Crowley C, Sutton HG, Kron SJ, Weichselbaum RR (2010) Poly(ADP-ribose) polymerase inhibitor induces accelerated senescence in irradiated breast cancer cells and tumors. *Cancer Res* 70: 6277–6282
- El-Khamisy SF (2011) To live or to die: a matter of processing damaged DNA termini in neurons. *EMBO Mol Med* 3: 78–88
- El-Khamisy SF, Hartsuiker E, Caldecott KW (2007) TDP1 facilitates repair of ionizing radiation-induced DNA single-strand breaks. *DNA Repair (Amst)* 6: 1485–1495
- El-Khamisy SF, Katyal S, Patel P, Ju L, McKinnon PJ, Caldecott KW (2009) Synergistic decrease of DNA single-strand break repair rates in mouse neural cells lacking both Tdp1 and aprataxin. *DNA Repair (Amst)* 8: 760–766
- El-Khamisy SF, Saifi GM, Weinfeld M, Johansson F, Helleday T, Lupski JR, Caldecott KW (2005) Defective DNA single-strand break repair in spinocerebellar ataxia with axonal neuropathy-1. *Nature* 434: 108–113
- Fallik D, Borriani F, Boige V, Viguier J, Jacob S, Miquel C, Sabourin JC, Ducreux M, Praz F (2003) Microsatellite instability is a predictive factor of the tumor response to irinotecan in patients with advanced colorectal cancer. *Cancer Res* 63: 5738–5744
- Fuchs CS, Marshall J, Mitchell E, Wierzbiicki R, Ganju V, Jeffery M, Schulz J, Richards D, Soufi-Mahjoubi R, Wang B, Barrueco J (2007) Randomized, controlled trial of irinotecan plus infusional, bolus, or oral fluoropyrimidines in first-line treatment of metastatic colorectal cancer: results from the BICC-C Study. *J Clin Oncol* 25: 4779–4786
- Gellert M, Mizuuchi K, O'Dea MH, Nash HA (1976) DNA gyrase: an enzyme that introduces superhelical turns into DNA. *Proc Natl Acad Sci USA* 73: 3872–3876
- Giovanella BC, Stehlin JS, Wall ME, Wani MC, Nicholas AW, Liu LF, Silber R, Potmesil M (1989) DNA topoisomerase I – targeted chemotherapy of human colon cancer in xenografts. *Science* 246: 1046–1048
- Glynn-Jones R, Falk S, Maughan TS, Meadows HM, Sebag-Montefiore D (2007) A phase I/II study of irinotecan when added to 5-fluorouracil and leucovorin and pelvic radiation in locally advanced rectal cancer: a Colorectal Clinical Oncology Group Study. *Br J Cancer* 96: 551–558
- Gollins S, Myint AS, Haylock B, Wise M, Saunders M, Neupane R, Essapen S, Samuel L, Dougal M, Lloyd A, Morris J, Topham C, Susnerwala S (2011) Preoperative chemoradiotherapy using concurrent capecitabine and irinotecan in magnetic resonance imaging-defined locally advanced rectal cancer: impact on long-term clinical outcomes. *J Clin Oncol* 29(8): 1042–1049
- Gongora C, Vezzio-Vie N, Tuduri S, Denis V, Causse A, Auzanneau C, Colod-Beroud G, Coquelle A, Passero P, Pourquier P, Martineau P, Del Rio M (2011) New topoisomerase I mutations are associated with resistance to camptothecin. *Mol Cancer* 10: 64
- Hochster H, Liebes L, Speyer J, Sorich J, Taubes B, Oratz R, Wernz J, Chachoua A, Blum RH, Zeleniuch-Jacquotte A (1997) Effect of prolonged topotecan infusion on topoisomerase 1 levels: a phase I and pharmacodynamic study. *Clin Cancer Res* 3: 1245–1252
- Horisberger K, Erben P, Muessle B, Woernle C, Stroebel P, Kaehler G, Wenz F, Hochhaus A, Post S, Willeke F, Hofheinz RD (2009) Topoisomerase I expression correlates to response to neoadjuvant irinotecan-based chemoradiation in rectal cancer. *Anticancer Drugs* 20: 519–524
- Hoskins JM, Marcuello E, Altes A, Marsh S, Maxwell T, Van Booven DJ, Pare L, Culverhouse R, McLeod HL, Baiget M (2008) Irinotecan pharmacogenetics: influence of pharmacodynamic genes. *Clin Cancer Res* 14: 1788–1796
- Hoskins JM, Rosner GL, Ratain MJ, McLeod HL, Innocenti F (2009) Pharmacodynamic genes do not influence risk of neutropenia in cancer patients treated with moderately high-dose irinotecan. *Pharmacogenomics* 10: 1139–1146
- Hsiang YH, Hertzberg R, Hecht S, Liu LF (1985) Camptothecin induces protein-linked DNA breaks via mammalian DNA topoisomerase I. *J Biol Chem* 260: 14873–14878
- Hsiang YH, Liu LF (1988) Identification of mammalian DNA topoisomerase I as an intracellular target of the anticancer drug camptothecin. *Cancer Res* 48: 1722–1726
- Husain I, Mohler JL, Seigler HF, Besterman JM (1994) Elevation of topoisomerase I messenger RNA, protein, and catalytic activity in human tumors: demonstration of tumor-type specificity and implications for cancer chemotherapy. *Cancer Res* 54: 539–546
- Innocenti F, Undevia SD, Iyer L, Chen PX, Das S, Kocherginsky M, Karrison T, Janisch L, Ramirez J, Rudin CM, Vokes EE, Ratain MJ (2004) Genetic variants in the UDP-glucuronosyltransferase 1A1 gene predict the risk of severe neutropenia of irinotecan. *J Clin Oncol* 22: 1382–1388
- Interthal H, Chen HJ, Kehl-Fie TE, Zotzmann J, Leppard JB, Champoux JJ (2005) SCAN1 mutant Tdp1 accumulates the enzyme – DNA intermediate and causes camptothecin hypersensitivity. *EMBO J* 24: 2224–2233
- Jacob S, Aguado M, Fallik D, Praz F (2001) The role of the DNA mismatch repair system in the cytotoxicity of the topoisomerase inhibitors camptothecin and etoposide to human colorectal cancer cells. *Cancer Res* 61: 6555–6562
- Katyal S, el-Khamisy SF, Russell HR, Li Y, Ju L, Caldecott KW, McKinnon PJ (2007) TDP1 facilitates chromosomal single-strand break repair in neurons and is neuroprotective *in vivo*. *EMBO J* 26: 4720–4731
- Koopman M, Antonini NF, Douma J, Wals J, Honkoop AH, Erdkamp FL, de Jong RS, Rodenburg CJ, Vreugdenhil G, Loosveld OJ, van Bochove A, Sinnige HA, Creemers GJ, Tesselar ME, Slee PH, Werter MJ, Mol L, Dalesio O, Punt CJ (2007) Sequential vs combination chemotherapy with capecitabine, irinotecan, and oxaliplatin in advanced colorectal cancer (CAIRO): a phase III randomised controlled trial. *Lancet* 370(9582): 135–142
- Koopman M, Knijn N, Richman S, Seymour M, Quirke P, van Tinteren H, van Krieken JHJM, Punt CJA, Nagtegaal ID (2009) The correlation between topoisomerase-I (Topo1) expression and outcome of treatment with capecitabine and irinotecan in advanced colorectal cancer (ACC) patients (pts) treated in the CAIRO study of the Dutch Colorectal Cancer Group (DCCG). *Eur J Cancer Suppl* 7: 321
- Li XG, Haluska Jr P, Hsiang YH, Bharti A, Kufe DW, Rubin EH (1996) Identification of topoisomerase I mutations affecting both DNA cleavage and interaction with camptothecin. *Ann NY Acad Sci* 803: 111–127
- Lima JP, dos Santos LV, Sasse EC, Lima CS, Sasse AD (2010) Camptothecins compared with etoposide in combination with platinum analog in extensive stage small cell lung cancer: systematic review with meta-analysis. *J Thorac Oncol* 5: 1986–1993
- Liu C, Zhou S, Begum S, Sidransky D, Westra WH, Brock M, Califano JA (2007) Increased expression and activity of repair genes TDP1 and XPF in non-small cell lung cancer. *Lung Cancer* 55(3): 303–311
- Mariadason JM, Arango D, Shi Q, Wilson AJ, Corner GA, Nicholas C, Aranes MJ, Lesser M, Schwartz EL, Augenlicht LH (2003) Gene expression profiling-based prediction of response of colon carcinoma cells to 5-fluorouracil and camptothecin. *Cancer Res* 63: 8791–8812
- Miknyoczki SJ, Jones-Bolin S, Pritchard S, Hunter K, Zhao H, Wan W, Ator M, Bihovsky R, Hudkins R, Chatterjee S, Klein-Szanto A, Dionne C, Ruggeri B (2003) Chemopotentiation of temozolomide, irinotecan, and cisplatin activity by CEP-6800, a poly(ADP-ribose) polymerase inhibitor. *Mol Cancer Ther* 2: 371–382
- Moreira MC, Barbot C, Tachi N, Kozuka N, Uchida E, Gibson T, Mendonca P, Costa M, Barros J, Yanagisawa T, Watanabe M, Ikeda Y, Aoki M, Nagata T, Coutinho P, Sequeiros J, Koenig M (2001) The gene mutated in ataxia-ocular apraxia 1 encodes the new HIT/Zn-finger protein aprataxin. *Nat Genet* 29(2): 189–193
- Morris EJ, Geller HM (1996) Induction of neuronal apoptosis by camptothecin, an inhibitor of DNA topoisomerase-I: evidence for cell cycle-independent toxicity. *J Cell Biol* 134: 757–770
- Mosesso P, Piane M, Palitti F, Pepe G, Penna S, Chessa L (2005) The novel human gene aprataxin is directly involved in DNA single-strand-break repair. *Cell Mol Life Sci* 62: 485–491
- O'Dwyer PJ, Catalano RB (2006) Uridine diphosphate glucuronosyltransferase (UGT) 1A1 and irinotecan: practical pharmacogenomics arrives in cancer therapy. *J Clin Oncol* 24: 4534–4538
- Paillass S, Boissiere F, Bibeau F, Denouel A, Mollevi C, Causse A, Denis V, Vezzio-Vie N, Marzi L, Cortijo C, Ait-Arsa I, Askari N, Pourquier P, Martineau P, Del Rio M, Gongora C (2011) Targeting the p38 MAPK pathway inhibits irinotecan resistance in colon adenocarcinoma. *Cancer Res* 71: 1041–1049
- Ribic CM, Sargent DJ, Moore MJ, Thibodeau SN, French AJ, Goldberg RM, Hamilton SR, Laurent-Puig P, Gryfe R, Shepherd LE, Tu D, Redston M, Gallinger S (2003) Tumor microsatellite-instability status as a predictor of benefit from fluorouracil-based adjuvant chemotherapy for colon cancer. *N Engl J Med* 349: 247–257



- Saltz LB, Cox JV, Blanke C, Rosen LS, Fehrenbacher L, Moore MJ, Maroun JA, Ackland SP, Locker PK, Pirotta N, Elfring GL, Miller LL (2000) Irinotecan plus fluorouracil and leucovorin for metastatic colorectal cancer. Irinotecan Study Group. *N Engl J Med* **343**: 905–914
- Seymour MT, Maughan TS, Ledermann JA, Topham C, James R, Gwyther SJ, Smith DB, Shepherd S, Maraveyas A, Ferry DR, Meade AM, Thompson L, Griffiths GO, Parmar MK, Stephens RJ (2007) Different strategies of sequential and combination chemotherapy for patients with poor prognosis advanced colorectal cancer (MRC FOCUS): a randomised controlled trial. *Lancet* **370**: 143–152
- Smith LM, Willmore E, Austin CA, Curtin NJ (2005) The novel poly(ADP-Ribose) polymerase inhibitor, AG14361, sensitizes cells to topoisomerase I poisons by increasing the persistence of DNA strand breaks. *Clin Cancer Res* **11**: 8449–8457
- Snipstad K, Fenton CG, Kjaeve J, Cui G, Anderssen E, Paulssen RH (2010) New specific molecular targets for radio-chemotherapy of rectal cancer. *Mol Oncol* **4**(1): 52–64
- Verheij M, Vens C, van Triest B (2010) Novel therapeutics in combination with radiotherapy to improve cancer treatment: rationale, mechanisms of action and clinical perspective. *Drug Resist Updat* **13**: 29–43
- Wang JC (1971) Interaction between DNA and an Escherichia coli protein omega. *J Mol Biol* **55**: 523–533
- Willeke F, Horisberger K, Kraus-Tiefenbacher U, Wenz F, Leitner A, Hochhaus A, Grobholz R, Willer A, Kahler G, Post S, Hofheinz RD (2007) A phase II study of capecitabine and irinotecan in combination with concurrent pelvic radiotherapy (CapTri-RT) as neoadjuvant treatment of locally advanced rectal cancer. *Br J Cancer* **96**: 912–917
- Yang SW, Burgin Jr AB, Huizenga BN, Robertson CA, Yao KC, Nash HA (1996) A eukaryotic enzyme that can disjoin dead-end covalent complexes between DNA and type I topoisomerases. *Proc Natl Acad Sci USA* **93**(21): 11534–11539
- Yu J, Miller R, Zhang W, Sharma M, Holtschlag V, Watson MA, McLeod HL (2008) Copy-number analysis of topoisomerase and thymidylate synthase genes in frozen and FFPE DNAs of colorectal cancers. *Pharmacogenomics* **9**: 1459–1466
- Yu J, Shannon WD, Watson MA, McLeod HL (2005) Gene expression profiling of the irinotecan pathway in colorectal cancer. *Clin Cancer Res* **11**: 2053–2062
- Zhang YW, Regairaz M, Seiler JA, Agama KK, Doroshov JH, Pommier Y (2011) Poly(ADP-ribose) polymerase and XPF-ERCC1 participate in distinct pathways for the repair of topoisomerase I-induced DNA damage in mammalian cells. *Nucleic Acids Res* **39**(9): 3607–3620
- Zhou T, Akopiants K, Mohapatra S, Lin PS, Valerie K, Ramsden DA, Lees-Miller SP, Povirk LF (2009) Tyrosyl-DNA phosphodiesterase and the repair of 3'-phosphoglycolate-terminated DNA double-strand breaks. *DNA Repair (Amst)* **8**: 901–911
- Zhou T, Lee JW, Tatavarthi H, Lupski JR, Valerie K, Povirk LF (2005) Deficiency in 3'-phosphoglycolate processing in human cells with a hereditary mutation in tyrosyl-DNA phosphodiesterase (TDP1). *Nucleic Acids Res* **33**: 289–297

## Randomized Phase III Trial Comparing Irinotecan/Cisplatin With Etoposide/Cisplatin in Patients With Previously Untreated Extensive-Stage Disease Small-Cell Lung Cancer

Nasser Hanna, Paul A. Bunn Jr, Corey Langer, Lawrence Einhorn, Troy Guthrie Jr, Thaddeus Beck, Rafat Ansari, Peter Ellis, Michael Byrne, Mark Morrison, Subramanian Hariharan, Benjamin Wang, and Alan Sandler

From Indiana University; Hoosier Oncology Group, Indianapolis; Michigan Hematology/Oncology, South Bend, IN; University of Colorado Cancer Center, Aurora, CO; Fox Chase Cancer Center, Philadelphia, PA; Baptist Cancer Institute, Jacksonville, FL; Highlands Oncology Group, Springdale, AR; Pfizer Inc, New York, NY; Vanderbilt-Ingram Cancer Center, Vanderbilt-Ingram Community Cancer Center Affiliate Network, Nashville, TN; Juravinski Cancer Centre, Hamilton, Canada; Sir Charles Gairdner Hospital, Nedlands, Australia.

Submitted November 7, 2005; accepted January 12, 2006.

Supported by Pfizer Inc, New York, NY.

Presented in part (abstract and oral presentation) at the 41st Annual Meeting of the American Society of Clinical Oncology, Orlando, FL, May 13-17, 2005, and at the 11th World Conference on Lung Cancer, Barcelona, Spain, July 3-6, 2005.

Authors' disclosures of potential conflicts of interest and author contributions are found at the end of this article.

Address reprint requests to Nasser Hanna, MD, Indiana University, 535 Barnhill Dr, RT 473, Indianapolis, IN 46202; e-mail: nhanna@iupui.edu.

© 2006 by American Society of Clinical Oncology

0732-183X/06/2413-2038/\$20.00

DOI: 10.1200/JCO.2005.04.8595

### ABSTRACT

#### Purpose

Etoposide and cisplatin (EP) has been a standard treatment for extensive-disease small-cell lung cancer (SCLC). An earlier phase III trial reported improved survival for patients receiving irinotecan plus cisplatin (IP) versus EP. Our trial was designed to determine if a modified weekly regimen of IP would provide superior survival with less toxicity than EP.

#### Patients and Methods

The primary objective was to compare overall survival in extensive-disease SCLC patients randomly assigned to receive IP (n = 221) or EP (n = 110). Patients were randomly assigned in 2:1 ratio to cisplatin 30 mg/m<sup>2</sup> intravenously (IV) + irinotecan 65 mg/m<sup>2</sup> IV on days 1 and 8 every 21 days, or cisplatin 60 mg/m<sup>2</sup> IV on day 1, and etoposide 120 mg/m<sup>2</sup> IV on days 1 to 3 every 21 days for at least four cycles, until progressive disease, or until intolerable toxicity resulted.

#### Results

Selected grade 3/4 toxicities for IP/EP were: neutropenia (36.2% v 86.5%; *P* < .01), febrile neutropenia (3.7% v 10.4%; *P* = .06), anemia (4.8% v 11.5%; *P* = .02), thrombocytopenia (4.3% v 19.2%; *P* < .01), vomiting (12.5% v 3.8%; *P* = .04), and diarrhea (21.3% v 0%; *P* < .01). There was no significant difference in response rates (48% v 43.6%), median time to progression (4.1 v 4.6 months), or overall survival (median survival time, 9.3 months v 10.2 months; *P* = .74).

#### Conclusion

Treatment with this dose and schedule of IP did not result in improved survival when compared with EP. Fewer patients receiving IP had grade 3/4 anemia, thrombocytopenia, neutropenia, and febrile neutropenia compared with patients receiving EP, but more had grade 3/4 diarrhea and vomiting.

*J Clin Oncol* 24:2038-2043. © 2006 by American Society of Clinical Oncology

### INTRODUCTION

In the United States, approximately 24,000 people are diagnosed with small-cell lung cancer (SCLC) each year, representing approximately 15% of all lung cancer cases.<sup>1,2</sup> More than half of these patients are diagnosed with extensive-stage disease (ED) and are most often treated with etoposide and a platinum agent, either carboplatin or cisplatin, resulting in a median survival of 8 to 10 months.<sup>3</sup> Newer agents, including the taxanes, vinorelbine, gemcitabine, topotecan, and irinotecan demonstrate significant single agent activity.<sup>4-8</sup> In the last decade, a variety of platinum-based combination therapies tested in phase III trials have failed to demonstrate an efficacy superior to that of etoposide plus cisplatin (EP).<sup>9-12</sup>

In 2002, Noda et al<sup>8</sup> reported the results of a phase III trial from the Japanese Cooperative Oncol-

ogy Group (JCOG) that randomly assigned 154 patients with ED SCLC to either EP (etoposide 100 mg/m<sup>2</sup> intravenously [IV] days 1 to 3 with cisplatin 80 mg/m<sup>2</sup> IV on day 1, once every 3 weeks) or irinotecan plus cisplatin (IP; irinotecan 60 mg/m<sup>2</sup> IV on days 1, 8, and 15 plus cisplatin 60 mg/m<sup>2</sup> IV on day 1, once every 4 weeks). Median survival and 1-year survival rates on the IP and EP arms were 12.8 months versus 9.4 months and 58.4% versus 37.7%, respectively. Patients in the EP arm experienced significantly higher rates of grade 3/4 neutropenia and thrombocytopenia, but lower rates of grade 3/4 diarrhea. Only 80.4% of the planned dose intensity of irinotecan was delivered and 50% of the day-15 irinotecan doses were never administered.

A confirmatory study was deemed necessary before a change in the standard of care could be recommended. The JCOG study represented a

single study with a small sample size (77 patients per arm) for a disease for which no significant survival gains had been seen in 20 years. Furthermore, it was postulated that pharmacogenomic differences might exist between patients in Japan and those in the United States. Therefore, our phase III study, comparing EP with IP in a larger number of ED SCLC patients, was undertaken in the United States, Australia, and Canada. Both the EP and IP regimens in this study were modified compared with the JCOG regimens to improve delivery and reduce toxicity, and to be more consistent with dose and schedules given in the United States, including in the cooperative groups.

## PATIENTS AND METHODS

### Patient Selection

Patients with histopathologically or cytologically confirmed ED SCLC were assessed for eligibility. Prior radiation therapy was allowed if the fields did not include the only sites of measurable disease. Patients met the following criteria to be eligible: measurable disease, adequate hematologic function (WBC > 3,000/ $\mu$ L, absolute neutrophil count  $\geq$  1,500/mm<sup>3</sup>, hemoglobin  $\geq$  9 g/dL, platelet count  $\geq$  100,000/mm<sup>3</sup>), hepatic function (bilirubin  $\leq$  1.5 mg/dL or  $\leq$  26  $\mu$ mol/L, AST  $\leq$  2.5 $\times$  the upper limit of normal [ULN] or  $\leq$  5 $\times$  ULN if liver metastases were present), and renal function (serum creatinine  $\leq$  1.7 mg/dL or  $\leq$  130  $\mu$ mol/L). Patients with an Eastern Cooperative Oncology Group (ECOG) performance status (PS) of 0 to 2 were eligible. Patients with known brain metastases were eligible if they were asymptomatic and on a stable or tapering steroid dose if they were on steroids. Patients were excluded if they had received any previous systemic anticancer therapy for SCLC, had a history of significant cardiovascular disease, serious active infection, known Gilbert's disease, National Cancer Institute Common Toxicity Criteria  $\geq$  grade 2 peripheral neuropathy, had impaired mental status, or if they were pregnant or breastfeeding. The protocol was approved through institutional ethics review boards, and all patients provided written informed consent before treatment.

### Treatment Plan

Patients were randomly assigned centrally by telephone after confirmation of eligibility. Patients were stratified by sex, lactate dehydrogenase (LDH;  $\leq$  ULN or  $>$  ULN), and age ( $<$  65 or  $\geq$  65 years) before treatment was assigned in a 2:1 ratio. Patients were assigned to either cisplatin 30 mg/m<sup>2</sup> IV plus irinotecan 65 mg/m<sup>2</sup> IV on days 1 and 8 every 21 days (IP), or cisplatin 60 mg/m<sup>2</sup> IV on day 1 plus etoposide 120 mg/m<sup>2</sup> IV on days 1 through 3 every 21 days (EP). Initially, patients were also stratified by PS (0/1 v 2), until a protocol amendment excluded PS 2 patients. Treatment in each arm was repeated for a minimum of four cycles, but additional cycles could be used at the discretion of the investigator. Re-treatment with the next cycle was permitted only if the absolute neutrophil count was at least 1,500/mm<sup>3</sup>, platelet count was at least 100,000/mm<sup>3</sup>, serum creatinine was no more than 1.7 mg/dL, and treatment-related nonhematologic toxicities (excluding alopecia) had resolved to grade 1 or lower. A delay of treatment of up to 2 weeks was permitted. Erythropoietin was allowed at the discretion of the treating physician. It was recommended that granulocyte colony-stimulating growth factors were to be used in accordance with their package inserts or the 1999 guidelines from the American Society of Clinical Oncology. Dose modifications were made for each agent per protocol guidelines.

Baseline assessment included a medical history and physical examination, CBC, comprehensive blood chemistries, serum pregnancy test (when applicable), adverse event assessment, and tumor assessment. Staging evaluations included chest x-ray or chest computed tomography (CT) or magnetic resonance imaging (MRI), abdominal CT or MRI (including liver and adrenals), and head CT or MRI. Bone scan and bone marrow evaluation were obtained only if clinically indicated. Tumor assessment was evaluated after every two cycles of therapy.

### Statistical Analysis

This was a multicenter, open-label, randomized phase III study. The primary objective of the study was to compare the overall survival associated with the use of IP with that associated with EP for the treatment of patients with previously untreated ED SCLC. Secondary objectives were to compare the antitumor efficacy as assessed by response rate and time to progression, and to evaluate the safety and tolerability of each regimen.

With a planned sample size of 300 patients (IP arm, 200 patients; EP arm, 100 patients), there was an 80% power of detecting a 30% improvement in survival (based on a 30% decrease in each of the hazard functions at 6-month intervals) using a log-rank test assuming that the EP arm hazard function was 0.3 for the first 6 months, 0.7 for the next 6 months, 0.8 for months 12 to 18, and 0.9 for months 18 to 24. A study amendment subsequently excluded PS-2 patients after the first 31 PS-2 patients were enrolled, due to high rates of neutropenic complications and treatment-related deaths. Therefore, the sample size was increased to achieve a total of 300 patients with either PS 0 or 1 only. The expected 1-year survival rates for the IP and EP arms were 50% and 37%, respectively, and the 2-year rates were 15% and 7%, respectively. The primary analysis was conducted 1.5 years after the last patient had been enrolled and when the 220th patient death was recorded.

Survival was defined from date of randomization to date of death and was reported on an intent-to-treat basis. In the absence of a confirmation of death, survival time was censored at the last date of follow-up. Kaplan-Meier method was used to estimate the survival curves of the two treatment arms. Unstratified log-rank test was performed to compare the two survival curves at the .05 level of significance. Survival was characterized in terms of the median and the probability of being alive at 6, 12, 18, and 24 months (based on Kaplan-Meier estimates). Ranges, 95% CI on the treatment estimates, and hazard ratios were computed. Response was measured based on the Response Evaluation Criteria in Solid Tumors guidelines and all responses were confirmed by repeat scans performed no fewer than 4 weeks after the criteria for response were first met. A  $\chi^2$  test was performed to compare the response rates between the two treatment groups. Time to progression was defined as the time from date of randomization to first documentation of progressive disease and was reported on an intent-to-treat basis. Treatment administration was recorded and dose intensity (in mg/m<sup>2</sup>/wk) was defined as the total dose per body-surface area divided by the number of weeks between the start of treatment and the first day of last treatment course plus 21 days.

Toxicity was evaluated using the National Cancer Institute common toxicity criteria version 2.0. An independent data safety monitoring board was implemented to monitor safety parameters during the study. Baseline patient characteristics were summarized with frequency tables for categorical variables and descriptive statistics for continuous variables. All efficacy analyses were done on an intent-to-treat population, whereas all safety analyses were done only on those patients who were actually treated with at least one dose.

## RESULTS

From December 2000 through June 2003, 331 patients were randomly assigned to receive either IP (n = 221) or EP (n = 110). The minimum follow-up for all patients was 18 months. The baseline patient and disease characteristics are listed in Table 1. Approximately 45% of patients were at least 65 years old, two thirds of patients had an LDH level higher than ULN, nearly 20% had metastatic disease to the CNS, more than 50% had metastases to the liver, and approximately 25% had metastases to the adrenal glands. More than 60% of patients had four or more sites of disease at baseline. All 331 randomly assigned patients were included in the analysis for response, time to disease progression, and overall survival. Only patients who received at least one cycle of study treatment (n = 322) were assessable for toxicity analysis.

**Table 1.** Baseline Patient and Disease Characteristics (N = 331)

Characteristic	% of Patients	
	IP (n = 221)	EP (n = 110)
<b>Sex</b>		
Male	57.5	57.3
Female	42.5	42.7
<b>Age, years</b>		
Median	63	62
Range	37-82	38-83
≥ 65	45.2	45.6
<b>Performance status</b>		
0 or 1	92.3	88.2
2	7.2	10.9
<b>Race/ethnicity</b>		
White	92.3	88.2
African American	2.3	5.5
Asian	0.9	0.9
<b>Lactose dehydrogenase</b>		
> Upper limits of normal	62	62.7
≤ Upper limits of normal	38	37.3
<b>Prior radiation</b>	8.6	11.8
<b>Metastatic site</b>		
Soft tissue	65.6	64.5
Bone	33.5	27.3
CNS	13.5	17.3
Liver	50.7	52.7
Adrenal	24.9	27.3
Bone marrow	1.8	1.8
Pleural/pericardial effusion	23.5	40.9
Other	21.7	29.1
<b>No. of disease sites</b>		
1-3	33.9	27.3
4-6	60.2	64.5
7-9	5.9	8.2

Abbreviations: IP, irinotecan/cisplatin; EP, etoposide/cisplatin.

### Treatment Administered

Table 2 lists the treatment administered. Two hundred sixteen of the 221 patients randomly assigned to the IP arm received at least one dose of study medication and 112 (50.7%) of the 221 treated patients completed at least four courses. The major reasons for not completing study included progressive disease (18.6%), more than a 2-week delay in treatment administration due to toxicities (5.9%), and unacceptable toxicity (9.0%). One hundred six of the 110 patients randomly assigned to the EP arm received at least one dose of the study medication. Sixty-one (55.5%) of the 110 patients completed study. The main reasons for not completing study included progressive disease (21.8%), more than a 2-week delay in treatment administration due to toxicities (3.6%), and unacceptable toxicity (5.5%). The median number of cycles of chemotherapy administered was four in each group; 25.9% of patients on the IP arm received at least one study treatment for six cycles versus 42.5% of patients on the EP arm. The dose intensity delivered on a mg/m<sup>2</sup>/wk basis exceeded 90% for all drugs. The dose-intensity regimen delivered for irinotecan was 94%, or 39 mg/m<sup>2</sup>/wk.

### Toxicity Results

Table 3 lists the toxicity data. Significantly higher rates of grade 3/4 neutropenia, anemia, and thrombocytopenia were observed in the

**Table 2.** Treatment Delivered

	IP (n = 216)		EP (n = 106)	
	No. of Patients	%	No. of Patients	%
<b>No. of cycles</b>				
Median	4		4	
Range	1-14		1-10	
<b>Cycles initiated</b>				
1	216	100	100	106
2	181	83.8	88	83
3	166	76.9	83	78.3
4	150	69.4	77	72.6
5	71	32.9	51	48.1
6	56	25.9	45	42.5
7	7	3.2	9	8.5
≥ 8	5	2.3	4	3.8
<b>Delivered dose of drug (mg/m<sup>2</sup>/wk), % planned</b>				
Cisplatin	18	94	18.4	92
Etoposide	—	—	113.9	94
Irinotecan	39	94	—	—

Abbreviations: IP, irinotecan/cisplatin; EP, etoposide/cisplatin.

EP arm compared with the IP arm. Higher rates of febrile neutropenia were also experienced in the EP arm compared with the IP arm. Rates of grade 3/4 dehydration, diarrhea, and vomiting were significantly higher on the IP arm compared with the EP arm. Seven patients (22.5%) with PS greater than 1 and 11 patients (3.6%) with PS 0 or 1 died due to treatment-related complications.

### Efficacy Results

There was no significant difference in response rates (IP, 48% v EP, 43.6%) or stable disease rates (IP, 4.1% v EP, 7.3%) between the IP and EP arms; 28.1% of patients on the IP arm and 29.1% of patients on the EP arm could not be evaluated for tumor response. There was no

**Table 3.** Select Grade 3 or 4 Toxicities

Toxicity	% of Patients		P
	IP (n = 216)	EP (n = 106)	
Neutropenia	36.2	66.5	< .01
Anemia	4.8	11.5	.03
Thrombocytopenia	4.3	19.2	< .01
Febrile neutropenia	3.7	10.4	.06
Dehydration	13	2.6	.02
Diarrhea	21.3	0	< .01
Vomiting	12.5	3.8	.04
Alopecia*	6.9	32.1	< .01
Infections	7.4	11.3	.50
Nausea	13	5.7	.13
Fatigue	13.6	6.6	.37
Asthenia	6	5.7	.99
Dyspnea	5.1	5.7	.98
Anorexia	5.6	1.9	.32

Abbreviations: IP, irinotecan/cisplatin; EP, etoposide/cisplatin.  
\*Grade 2.

significant difference between IP and EP in time to disease progression (median, 4.1 v 4.6 months;  $P = .37$ ; Fig 1), or survival ( $P = .68$ ; Fig 2). At the time of analysis, 305 (92.1%) of 331 patients had died. Median survival was similar in the two arms (9.3 v 10.2 months). Survival rates at selected time points were similar; 1-year survival rates were 34.95% versus 35.19% and 2-year survival rates were 8.0% versus 7.9%.

**Additional Treatment Given After Study**

More than 60% of patients on each arm of the study received additional treatment once off study (Table 4). More patients on the IP arm received subsequent treatment with etoposide (47.2% v 22.6%), whereas more patients on the EP arm received subsequent treatment with a topoisomerase I inhibitor (33% v 24.1%).

**DISCUSSION**

This open label, multicenter, randomized phase III study did not show a statistically significant difference in overall survival between the IP and EP regimens. Rather, the efficacy parameters were similar between the two combinations. The IP arm was associated with significantly lower rates of grade 3/4 neutropenia, anemia, and thrombocytopenia, and a lower rate of febrile neutropenia ( $P = .06$ ) that was not significant. In contrast, IP was associated with significantly higher rates of diarrhea, vomiting, and dehydration than the EP arm. Routine use of growth factor support and other supportive measures (adequate hydration, antidiarrhea medication) should be considered when treating the PS 2 patient with either regimen as high rates of neutropenia-related deaths were noted in this group.

Although both the JCOG study and this study treated patients with ED SCLC, there were significant differences in the disease characteristics between studies. Patients in our trial appeared to have more advanced disease because more than 60% of patients presented with four or more sites of disease at baseline. In the JCOG trial, only 6.5% had adrenal metastases and 18% had liver metastases compared with the 25% and 50% in our study.

Why did this study fail to confirm the positive JCOG results? One explanation might be that our study tested a different dose and schedule of IP. The IP regimen in this trial was chosen to increase the dose intensity (changing an every-4-week regimen to every 3 weeks) in response to the lower rates of drug compliance for irinotecan on the

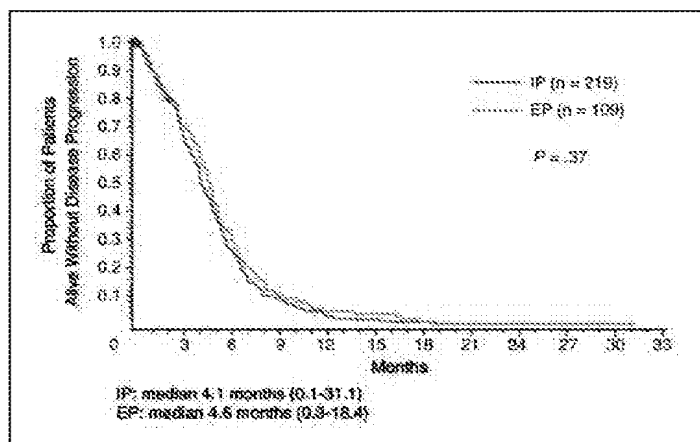


Fig 1. Time to disease progression. IP, irinotecan/cisplatin; EP, etoposide/cisplatin.

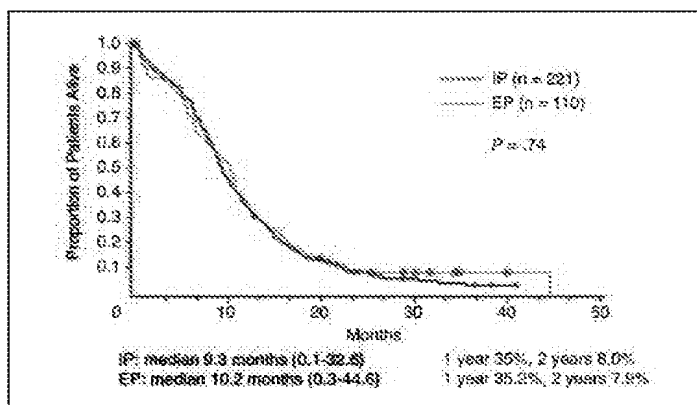


Fig 2. Overall survival. IP, irinotecan/cisplatin; EP, etoposide/cisplatin.

JCOG trial (80% of planned dose intensity of irinotecan was delivered with 50% of the day-15 doses omitted). The dose intensity delivered for irinotecan on this trial was 94% or 39 mg/m<sup>2</sup>/wk, which compares with 80% or 36.2 mg/m<sup>2</sup>/wk on the IP arm of the JCOG trial. Similar dose intensity delivered for cisplatin was observed in both studies. Cisplatin dose intensification has not yet resulted in significant differences in outcomes in ED SCLC.<sup>13</sup> A similar phase III trial recently reported that compared EP with cisplatin plus topotecan, another topoisomerase I inhibitor, also failed to demonstrate a survival difference between the arms.<sup>11</sup> It is, therefore, unlikely that the dose and schedule of IP had an adverse impact on outcomes. An ongoing trial by the Southwest Oncology Group in the United States comparing EP and IP using the same schedules from the JCOG study will address this issue.

Another possible reason why our study failed to demonstrate superiority for the IP regimen may be related to pharmacogenomic differences that may exist between North American and Japanese patient populations. Specifically, differences in polymorphisms of UDP-glucuronosyltransferase (*UGT1A1*), an enzyme that metabolizes irinotecan, are observed between patient populations. Low rates (2%) of Gilbert's syndrome, which results in a decreased level of gene transcription of *UGT1A1*, are recognized in the Asian population compared with European or African populations.<sup>14</sup> More or less effective metabolism of irinotecan may result in differences in toxicity, compliance, and chemosensitivity. For example, in one study in non-small-cell lung cancer (NSCLC), patients with Gilbert's syndrome

Table 4. Summary of Additional Treatment Given Off Study

	% of Patients	
	IP (n = 216)	EP (n = 106)
Any other chemotherapy*	69.9	60.4
Etoposide	47.2	22.6
Topotecan	13.4	19.8
Irinotecan	10.7	13.2
Taxane	12.5	7.5
Doxorubicin	7.4	5.7
Radiation therapy	16.7	14.2

Abbreviations: IP, irinotecan/cisplatin; EP, etoposide/cisplatin.  
\*Patients may have received ≥ one regimen of chemotherapy.

experienced significantly higher rates of severe toxicity when treated with irinotecan and inferior survival outcomes compared with those homozygous for a common allele.<sup>15</sup> The ongoing study by the Southwest Oncology Group (SWOG) that compares EP with IP in patients with ED SCLC will be evaluating differences in polymorphisms of *UGT1A1* as predictors for response and toxicity to irinotecan.

Molecular differences in lung cancer may also exist between Asian and US populations. It is known that a subset of patients with NSCLC have tumors that contain mutations in the epidermal growth factor receptor tyrosine kinase-binding domain.<sup>16,17</sup> These mutations predominate in bronchioloalveolar carcinoma type, female sex, never-smokers, and Asian patient populations.<sup>17,18</sup> Although the epidermal growth factor receptor does not play a significant role in SCLC, differences in other biologic characteristics may exist that predict for better or worse outcomes within the patient populations treated with the same regimens. One such example of this has recently been demonstrated in a study reported by Gandara et al.<sup>19</sup> In a joint effort with investigators from Japan, patients treated with a common arm, carboplatin plus paclitaxel for metastatic NSCLC, in separate but contemporaneous studies from the SWOG and Japan were analyzed. In that comparison, the study designs were very similar and response and toxicity criteria were the same. Despite similar patient characteristics (other than ethnicity), there were significantly higher rates of neutropenia, lower doses of paclitaxel delivered, and inferior survival for those patients treated in the SWOG study.

The JCOG trial was the only trial in more than 20 years to demonstrate any significant improvement in survival over the EP regimen. The study was closed early (based on the recommendation of

the monitoring committee after an interim analysis found a significant difference between the groups) after only 154 patients had been randomly assigned. Small differences in patient characteristics between the arms may result in differences in outcomes. There was an imbalance in the number of female and PS-2 patients in the JCOG study, thus favoring the IP arm. Furthermore, only 13% of patients on the IP arm had brain metastases versus 22% on the EP arm.

It is possible that IP is a better regimen for Japanese patients. In a phase III study reported by Kubota et al,<sup>20</sup> patients with advanced NSCLC were treated with one of four different platinum-based chemotherapy regimens. Patients on that trial receiving IP had a median survival of 14.2 months, which far exceeds efficacy seen in the United States, and is similar to what was reported in the JCOG SCLC trial. It is quite likely that in the United States, there are no significant differences in patient outcomes between those treated with IP and EP.

In conclusion, advances in the treatment of ED SCLC are clearly needed. Despite decreasing prevalence, SCLC still results in the deaths of approximately 20,000 patients in the United States each year. This figure exceeds that of cancers of the esophagus, stomach, liver, ovary, and bladder, as well as sarcomas, Hodgkin's disease, and most forms of leukemia.<sup>2</sup> Although the similar efficacy data from this trial do not suggest that the IP regimen will improve outcomes for the population of SCLC patients, our results suggest that IP represents an equally effective regimen with a different toxicity profile that can be used when it is anticipated that hematologic toxicity will be limiting or when the toxicity is found to be severe during the early cycles of EP.

#### REFERENCES

- Page N, Read W, Tierney R, et al: The epidemiology of small cell lung carcinoma. *Proc Am Soc Clin Oncol* 21:305a, 2002 (abstr 1216)
- Jemal A, Murray T, Samuels A, et al: Cancer statistics 2003. *CA Cancer J Clin* 53:5-26, 2003
- Roth B, Johnson D, Einhorn L, et al: Randomized study of cyclophosphamide, doxorubicin, and vincristine versus etoposide and cisplatin versus alternation of these two regimens in extensive small cell lung cancer: A phase III trial of the Southeastern Cancer Study Group. *J Clin Oncol* 10:282-291, 1992
- Kakolyris S, Mavroudis D, Tsavaris N, et al: Paclitaxel in combination with carboplatin as salvage treatment in refractory small cell lung cancer (SCLC): A multicenter phase II study. *Ann Oncol* 12:193-197, 2001
- Gridelli C, Perrone F, Ianniello G, et al: Carboplatin plus vinorelbine, a new well-tolerated and active regimen for the treatment of extensive-stage small cell lung cancer: A phase II study. *J Clin Oncol* 16:1414-1419, 1998
- Masters G, Declerck L, Blanke C, et al: Phase II trial of gemcitabine in refractory or relapsed small cell lung cancer: Eastern Cooperative Oncology Group Trial 1597. *J Clin Oncol* 21:1550-1555, 2003
- von Pawel J, Schiller J, Shepherd F, et al: Topotecan versus cyclophosphamide, doxorubicin, and vincristine for the treatment of recurrent small cell lung cancer. *J Clin Oncol* 17:658-667, 1999
- Noda K, Nishiwaki Y, Kawahara M, et al: Irinotecan plus cisplatin compared with etoposide plus cisplatin for extensive small cell lung cancer. *N Engl J Med* 346:85-91, 2002
- Mavroudis D, Papadakis E, Veslemes M, et al: A multicenter randomized clinical trial comparing paclitaxel-cisplatin-etoposide versus cisplatin-etoposide as first-line treatment in patients with small cell lung cancer. *Ann Oncol* 12:463-470, 2001
- Sundstrom S, Bremnes R, Kaasa S, et al: Cisplatin and etoposide regimen is superior to cyclophosphamide, epirubicin, and vincristine regimen in small cell lung cancer: Results from a randomized phase III trial with 5 years' follow-up. *J Clin Oncol* 20:4665-4672, 2002
- Eckhardt J, von Pawel J, Manikhas G, et al: Comparable activity with oral topotecan/cisplatin (TC) and IV etoposide/cisplatin (PE) as treatment for chemotherapy-naïve patients (pts) with extensive disease small cell lung cancer (ED-SCLC): Final results of a randomized phase III trial (389). *J Clin Oncol* 23:621s, 2005 (suppl; abstr 7003)
- Smit E, Groen H, Biesma B, et al: Phase III study comparing cyclophosphamide, doxorubicin, and etoposide (CDE) to carboplatin and paclitaxel (CP) in patients (pts) with extensive disease small cell lung cancer (ED SCLC). *J Clin Oncol* 23:631s, 2005 (suppl; abstr 7045)
- Ilde D, Mulshine J, Kramer B, et al: Prospective randomized comparison of high-dose and standard-dose etoposide and cisplatin chemotherapy in patients with extensive stage small cell lung cancer. *J Clin Oncol* 12:2022-2034, 1994
- Beutler E, Gelbart E, Demina A: Racial variability in the UDP-glucuronosyltransferase 1 (*UGT1A1*) promote, a balanced polymorphism for regulation of bilirubin metabolism? *Proc Natl Acad Sci U S A* 95:8170-8174, 1998
- Font A, Taron M, Rosell R, et al: *UGT1a1* genotyping correlates with toxicity and survival in non-small cell lung cancer (NSCLC) patients treated with second-line CPT-11/docetaxel. *Proc Am Soc Clin Oncol* 20:340a, 2001 (abstr 1357)
- Lynch T, Bell D, Sordella R, et al: Activating mutations in the epidermal growth factor receptor underlying responsiveness of non-small cell lung cancer to gefitinib. *N Engl J Med* 350:2129-2139, 2004
- Paez J, Janne P, Lee J, et al: EGFR mutations in lung cancer: Correlation with clinical response to gefitinib therapy. *Science* 304:1497-1500, 2004
- Shigematsu H, Lin L, Takahashi T, et al: Clinical and biological features associated with epidermal growth factor gene mutations in lung cancers. *J Natl Cancer Inst* 97:339-346, 2005
- Gandara D, Ohe Y, Kubota K, et al: Japan-SWOG common arm analysis of paclitaxel/carboplatin in advanced non-small cell lung cancer (NSCLC): A model for prospective comparison of cooperative group trials. *J Clin Oncol* 22:618s, 2004 (suppl; abstr 7007)
- Kubota K, Nishiwaki Y, Ohashi, et al: The four-arm cooperative study (FACS) for advanced non-small cell lung cancer (NSCLC). *J Clin Oncol* 22:618s, 2004 (suppl; abstr 7006)



**Authors' Disclosures of Potential Conflicts of Interest**

Although all authors completed the disclosure declaration, the following authors or their immediate family members indicated a financial interest. No conflict exists for drugs or devices used in a study if they are not being evaluated as part of the investigation. For a detailed description of the disclosure categories, or for more information about ASCO's conflict of interest policy, please refer to the Author Disclosure Declaration and the Disclosures of Potential Conflicts of Interest section in Information for Contributors.

Authors	Employment	Leadership	Consultant	Stock	Honoraria	Research Funds	Testimony	Other
Nasser Hanna						Bristol-Myers Squibb (C)		
Paul A. Bunn Jr			Pfizer (A)					
Corey Langer			Pfizer (A)		Pfizer (A)	Pfizer (B)		
Lawrence Einhorn			Bristol-Myers Squibb (A)	Amgen (C); GlaxoSmithKline (C); Biogenidec (C)				
Mark Morrison	Pfizer (N/R)			Pfizer (B)				
Subramanian Hariharan	Pfizer (N/R)			Pfizer (B)				
Benjamin Wang	Pfizer (N/R)			Pfizer (B)				
Alan Sandler			Bristol-Myers Squibb (A); Pfizer (A)		Bristol-Myers Squibb (A)	Pfizer (A)		

**Dollar Amount Codes** (A) < \$10,000 (B) \$10,000-99,999 (C) ≥ \$100,000 (N/R) Not Required

**Author Contributions**

**Conception and design:** Paul A. Bunn Jr, Corey Langer, Lawrence Einhorn, Alan Sandler

**Administrative support:** Subramanian Hariharan

**Provision of study materials or patients:** Nasser Hanna, Paul A. Bunn Jr, Corey Langer, Lawrence Einhorn, Troy Guthrie Jr, Thaddeus Beck, Rafat Ansari, Peter Ellis, Michael Byrne, Mark Morrison, Subramanian Hariharan, Benjamin Wang, Alan Sandler

**Collection and assembly of data:** Mark Morrison, Subramanian Hariharan, Benjamin Wang

**Data analysis and interpretation:** Mark Morrison, Subramanian Hariharan, Benjamin Wang

**Manuscript writing:** Nasser Hanna, Paul A. Bunn Jr, Corey Langer, Lawrence Einhorn, Troy Guthrie Jr, Thaddeus Beck, Rafat Ansari, Peter Ellis, Michael Byrne, Mark Morrison, Subramanian Hariharan, Benjamin Wang, Alan Sandler

**Final approval of manuscript:** Nasser Hanna, Paul A. Bunn Jr, Corey Langer, Lawrence Einhorn, Troy Guthrie Jr, Thaddeus Beck, Rafat Ansari, Peter Ellis, Michael Byrne, Mark Morrison, Subramanian Hariharan, Benjamin Wang, Alan Sandler



# Treatment of Colorectal Cancer Using a Combination of Liposomal Irinotecan (Irinophore C<sup>TM</sup>) and 5-Fluorouracil

Jennifer I. Hare<sup>1</sup>, Robert W. Neijzen<sup>2</sup>, Malathi Anantha<sup>3</sup>, Nancy Dos Santos<sup>3</sup>, Natasha Harasym<sup>4</sup>, Murray S. Webb<sup>4</sup>, Theresa M. Allen<sup>1,4</sup>, Marcel B. Bally<sup>3,4,5,6</sup>, Dawn N. Waterhouse<sup>3,6\*</sup>

**1** Department of Pharmacology, University of Alberta, Edmonton, Canada, **2** Department of Pharmaceutical Science, Universiteit Utrecht, Utrecht, Netherlands, **3** Experimental Therapeutics, BC Cancer Agency, Vancouver, Canada, **4** Centre for Drug Research and Development, Vancouver, Canada, **5** Department of Pathology and Laboratory Medicine, University of British Columbia, Vancouver, Canada, **6** Faculty of Pharmaceutical Sciences, University of British Columbia, Vancouver, Canada

## Abstract

**Purpose:** To investigate the use of liposomal irinotecan (Irinophore C<sup>TM</sup>) plus or minus 5-fluorouracil (5-FU) for the treatment of colorectal cancer.

**Experimental Design:** The effect of irinotecan (IRI) and/or 5-FU exposure times on cytotoxicity was assessed *in vitro* against HT-29 or LS174T human colon carcinoma cells. The pharmacokinetics and biodistribution of Irinophore C<sup>TM</sup> (IrC<sup>TM</sup>) and 5-FU, administered alone or in combination, were compared *in vivo*. A subcutaneous model of HT-29 human colorectal cancer in Rag2-M mice was utilized to assess the efficacy of IrC<sup>TM</sup> alone, and in combination with 5-FU.

**Results:** The cytotoxicity of IRI and 5-FU were strongly dependent on exposure time. Synergistic interactions were observed following prolonged exposure to IRI/5-FU combinations. Pharmacokinetics/biodistribution studies demonstrated that the 5-FU elimination rate was decreased significantly when 5-FU was co-administered intravenously with IrC<sup>TM</sup>, versus alone. Significant decreases in 5-FU elimination were also observed in plasma, with an associated increase of 5-FU in some tissues when 5-FU was given by intraperitoneal injection and IrC<sup>TM</sup> was given intravenously. The elimination of IrC<sup>TM</sup> was not significantly different when administered alone or in combination with 5-FU. Therapeutic studies demonstrated that single agent IrC<sup>TM</sup> was significantly more effective than the combination of IRI/5-FU; surprisingly, IrC<sup>TM</sup>/5-FU combinations were no more effective than IrC<sup>TM</sup> alone. The administration of combinations of 5-FU (16 mg/kg) and IrC<sup>TM</sup> (60 mg IRI/kg) showed increased toxicity when compared to IrC<sup>TM</sup> alone. Treatment with IrC<sup>TM</sup> alone (60 mg IRI/kg) delayed the time required for a 5-fold increase in initial tumor volume to day 49, compared to day 23 for controls. When IrC<sup>TM</sup> (40 mg IRI/kg) was used in combination with 5-FU (16 mg/kg), the time to increase tumor volume 5-fold was 43 days, which was comparable to that achieved when using IrC<sup>TM</sup> alone (40 mg IRI/kg).

**Conclusions:** Single agent IrC<sup>TM</sup> was well tolerated and has significant therapeutic potential. IrC<sup>TM</sup> may be a suitable replacement for IRI treatment, but its use with free 5-FU is complicated by IrC<sup>TM</sup>-engendered changes in 5-FU pharmacokinetics/biodistribution which are associated with increased toxicity when using the combination.

**Citation:** Hare JI, Neijzen RW, Anantha M, Dos Santos N, Harasym N, et al. (2013) Treatment of Colorectal Cancer Using a Combination of Liposomal Irinotecan (Irinophore C<sup>TM</sup>) and 5-Fluorouracil. PLoS ONE 8(4): e62349. doi:10.1371/journal.pone.0062349

**Editor:** Dimitris Fatouros, Aristotle University of Thessaloniki, Greece

**Received:** March 23, 2012; **Accepted:** March 22, 2013; **Published:** April 23, 2013

**Copyright:** © 2013 Hare et al. This is an open-access article distributed under the terms of the Creative Commons Attribution License, which permits unrestricted use, distribution, and reproduction in any medium, provided the original author and source are credited.

**Funding:** This work was supported by the Canadian Institutes of Health Research (Funding Reference Number 82583) and matching funds from the Terry Fox Research Institute (Project ID 2008-010). Funding for this research was also provided by Pfizer/Centre for Drug Research and Development Innovation Fund. The funders had no role in study design, data collection and analysis, decision to publish, or preparation of the manuscript.

**Competing Interests:** The authors have declared that no competing interests exist.

\* E-mail: dwater@bccrc.ca

## Introduction

Colorectal cancer (CRC) is a leading cause of cancer death worldwide [1,2,3]; in the United States, CRC is the third most common cause of cancer death and the third most commonly diagnosed cancer, with nearly 150,000 new cases estimated to be diagnosed in 2013 [4,5]. The chemotherapeutic drug irinotecan (IRI) is used in several first-line CRC treatment regimens. Although IRI itself is active, non-specific plasma, liver, gastrointestinal (GI), and tumor carboxylesterases [6,7,8] can metabolize IRI to SN-38, which is 100- to 1,000-fold more potent when tested using *in vitro* assays [9,10]. Gut carboxylesterases (CE) generate high local concentrations of SN-38 [11,12]. This conversion can

be associated with therapeutic activity, however, it has also been linked to the intestinal damage that is responsible for much of IRI's adverse GI toxicity [13,14,15]. A secondary drawback to the use of IRI and SN-38 is the pH-dependent hydrolytic conversion from an active lactone form, at acidic pH, to an inactive carboxylate form, at physiological pH, which limits the dose of active drug that reaches the target [16,17,18,19]. Some of the adverse toxicities and CE-mediated conversion of IRI can be ameliorated through the use of drug delivery systems [20,21,22,23,24,25]. Irinophore C<sup>TM</sup> (IrC<sup>TM</sup>) is a formulation of IRI encapsulated in unilamellar, 1,2-distearoyl-sn-glycero-3-phosphatidylcholine (DSPC)/cholesterol liposomes (100 nm diameter) containing an acidic aqueous interior of unbuffered CuSO<sub>4</sub>. IRI is

entrapped in the acidic aqueous interior of the liposomes when a pH gradient is generated in the presence of the divalent metal ionophore A23187, which is required for the stability and maintenance of the pH gradient [21,26]. The combination of the ionophore-generated pH gradient, together with the presence of encapsulated Cu<sup>2+</sup>, results in excellent drug retention properties for the formulation *in vivo* [26,27,28].

In preclinical studies, IrC<sup>TM</sup> demonstrated that the activity of IRI can be increased significantly in a wide range of tumor models [21,26,29,30], with an improved safety profile relative to the free drug [21]. The increase in therapeutic index for IrC<sup>TM</sup>, versus IRI, is thought to be due to several factors: i) maintenance of IRI in its active lactone form for extended time periods [21,27,30]; ii) increased delivery of IRI to sites of tumor growth [21]; iii) prolonged systemic exposure to the active lactone form of SN-38 [21]; and iv) the existence of an anti-vascular activity that is not observed following bolus administration of free IRI [29,31]. We hypothesized that the therapeutic impact of IrC<sup>TM</sup> will be most significant when it is used as part of a drug combination – for example, in the chemotherapy regimen FOLFIRI (leucovorin, 5-fluorouracil (5-FU), and IRI), where IrC<sup>TM</sup> would be substituted for free IRI. This hypothesis was tested in a pre-clinical setting here, where combinations of IrC<sup>TM</sup>/5-FU and IRI/5-FU were evaluated in a murine model of CRC. To our knowledge, this is the first research investigating the use of liposomal IRI formulations, including IrC<sup>TM</sup>, in combination with 5-FU for the treatment of CRC. The therapeutic results, surprisingly, demonstrated that the efficacy of this combination was no better than that achieved with IrC<sup>TM</sup> monotherapy. Additionally, in the model used here, there was an unexpected increase in the toxicity of the drug combination, which required a dose reduction of IrC<sup>TM</sup> to a level that was far less active than a higher dose of IrC<sup>TM</sup>, but could be administered safely when used as a single agent.

## Materials and Methods

### Materials

DSPC and cholesterol were obtained from Avanti Polar Lipids (Alabaster, Alabama, US). [<sup>3</sup>H]Cholesteryl hexadecylether (CHE) was purchased from PerkinElmer (Waltham, Massachusetts, US). [<sup>14</sup>C]5-FU was purchased from Moravak Biochemicals (Brea, California, US). A23187 was purchased from Sigma-Aldrich (Oakville, Ontario, CA). Saline, 5% dextrose in water (D5W), irinotecan (Camptosar, Sandoz), and 5-FU (Alfa Aesar) were obtained from the BC Cancer Agency (Vancouver, British Columbia, CA). The alamarBlue reagent, fetal bovine serum (FBS), L-glutamine, and sodium bicarbonate were purchased from Invitrogen (Burlington, Ontario, CA). Eagle's minimum essential medium (MEM) with Earle's balanced salt solution (BSS), McCoy's 5A medium, Hank's BSS (HBSS), non-essential amino acids, sodium pyruvate, and penicillin/streptomycin were purchased from StemCell Technologies (Vancouver, British Columbia, CA). All other chemicals were of analytical grade.

### Cell Culture

The human colorectal cell lines LS174T and HT-29 were obtained from ATCC (Manassas, Virginia, US). Stock cell lines were maintained in the absence of penicillin and streptomycin, and were screened for *Mycoplasma* prior to preparing a stock of cells that was frozen for use in experiments. Cells were re-suspended in freezing media (10% (vol/vol; v/v) dimethyl sulfoxide in FBS) and slowly frozen in Nalgene 1°C freezing containers (Rochester, New York, US) containing 100% isopropanol at -80°C for 24 h before storage in liquid nitrogen. Frozen cells were quickly thawed at

37°C, centrifuged to remove freezing media, plated and passaged twice before use in experiments. LS174T cells were cultured in Eagle's MEM with Earle's BSS supplemented with 2 mM L-glutamine, 1 mM sodium pyruvate, 0.1 mM non-essential amino acids, 1.5 g/L sodium bicarbonate, 1% (v/v) penicillin/streptomycin, and 10% (v/v) FBS, at 37°C in a 5% CO<sub>2</sub> environment. HT-29 cells were cultured in modified McCoy's 5A medium supplemented with 1.5 mM L-glutamine, 2.2 g/L sodium bicarbonate, 1% (v/v) penicillin/streptomycin, and 10% (v/v) FBS, at 37°C in a 5% CO<sub>2</sub> environment.

### Cytotoxicity Assays

The viability of human CRC cell lines following exposure to different concentrations of IRI and/or 5-FU was determined using the alamarBlue assay [32,33]. Cells (LS174T, 10,000 cells/well; HT-29, 5,000 cells/well) were seeded in flat-bottomed 96-well plates. After cell adherence had occurred, increasing concentrations of IRI or 5-FU were added to cells for 1–72 h, with drug washout as required at the indicated time point. In experiments to determine the time dependency of the exposure of the cells to drug combinations, HT-29 cells were exposed to IRI/5-FU at a 1:1 molar ratio for 1–48 h, with drug washout as required at the indicated time point(s). For all experiments, cell viability was assessed at 72 h after the initiation of drug exposure. The alamarBlue reagent was added to each well at a 1:10 dilution, and the cells were incubated for an additional 4–8 h before fluorescence was measured. For viability data, the fraction affected (FA) was a measure of the alamarBlue fluorescence normalized to the fluorescence of controls: a no cells control defining the 100% affect level and a drug-free control defining the 0% affect level. Interactions between IRI/5-FU when used in combination *in vitro* were determined on the basis of a single assay endpoint (alamarBlue viability assay, above), and the results were analyzed via the Median-Effect Principle [34], as estimated with CompuSyn software (ComboSyn, Inc.; Paramus, New Jersey, US) [35]. For each exposure time, dose-response curves were generated for the agents, alone and in combination, and, subsequently, combination index (CI) values were estimated at various affect levels (defined as fraction affected). A CI value of 0.8–1.2 represents an additive interaction, less than 0.8 represents a synergistic interaction, and greater than 1.2 represents an antagonistic interaction.

### Preparation of Irinophore C<sup>TM</sup>

IrC<sup>TM</sup> was prepared as described by Ramsay *et al.* [26]. DSPC:cholesterol (55:45 mol %) liposomes were prepared as previously outlined [36,37], using trace amounts of the non-metabolizable, non-exchangeable lipid tracer [<sup>3</sup>H]CHE [38]. The thin lipid film was hydrated with a 300 mM CuSO<sub>4</sub> solution at 65°C, the resulting lipid vesicles were subjected to 5 cycles of freeze-and-thaw, and the liposomes were extruded to a diameter of ~100 nm. Unencapsulated CuSO<sub>4</sub> was removed via chromatography using a Sephadex G-50 column, equilibrated with SHE buffer (300 mM sucrose, 20 mM HEPES, 15 mM EDTA; pH = 7.5). Liposomes were incubated with 0.5 µg A23187/mg total lipid for 30 min at 60°C. IRI was added to the liposomes at a molar drug-to-lipid ratio of 0.2:1, and the mixture was incubated at 50°C for 1 h. Unencapsulated drug was removed via chromatography on a Sephadex G-50 column, equilibrated with PBS (pH = 7.4), and drug loading efficiency was determined after measuring IRI absorbance at 370 nm. When required, IrC<sup>TM</sup> was concentrated at 3,000×g using centrifugal filter tubes (molecular weight cutoff 100 kDa).

## Animals and Ethics Statement

All *in vivo* experiments were conducted utilizing 129S6/SvEvTac-Rag2<sup>tm1Flua</sup> (Rag2-M) mice obtained from the BC Cancer Agency's Animal Resource Centre at the Vancouver Research Centre (Vancouver, British Columbia, CA). The studies were conducted in accordance with the Canadian Council on Animal Care Guidelines with oversight from the University of British Columbia's Animal Care Committee (protocols A10-0171 and A10-0206). Mice were housed under standard conditions with enrichment, with access to food and water *ad libitum*.

## Pharmacokinetics and Biodistribution

Experiments were completed to determine whether the simultaneous administration of IrC<sup>TM</sup>/5-FU, via intravenous (i.v.) or intraperitoneal (i.p.) injection, altered the PK/BD properties of either agent. Male Rag2-M mice (8–10 weeks old; 4 mice per time point) received i.v. injections, via the lateral tail vein, of [<sup>3</sup>H]CHE-labeled IrC<sup>TM</sup> (40 mg IRI/kg), [<sup>14</sup>C]5-FU (40 mg/kg), or co-administered [<sup>3</sup>H]CHE-labeled IrC<sup>TM</sup> and [<sup>14</sup>C]5-FU (40 mg IRI/kg and 40 mg/kg, respectively), in a total injection volume of 0.2 mL. The dose of 5-FU selected for these studies was based on previous experiments demonstrating that this dose was well tolerated when given on a once per week (Q7D) dosing schedule, comparable to that used for IrC<sup>TM</sup> (results not shown). At various time points post-injection, mice were euthanized via CO<sub>2</sub> asphyxiation. Blood was immediately collected via cardiac puncture, and centrifuged to separate the plasma. Organs were harvested and divided into 2 pieces; half of the plasma or organ was prepared for liquid scintillation counting (LSC) to determine the level of associated radioactivity (lipid and 5-FU), while the other half was processed for HPLC analysis to determine IRI and SN-38 levels. To limit conversion between the lactone and carboxylate forms, plasma samples and organs were kept on ice and transferred to -70°C within 1 h of collection.

A separate study was conducted to determine whether the PK/BD properties of 5-FU, administered QD×2 via i.p. injection, were affected by co-administration with IrC<sup>TM</sup> at a dose of 60 mg IRI/kg. This dosing was comparable to that used in the efficacy studies described below. The experiment was completed using male Rag2-M mice (7–10 weeks old; 3 mice per time point). Mice were injected i.p. with 16 mg/kg 5-FU on days 1 and 2, with or without co-administration of IrC<sup>TM</sup> (60 mg IRI/kg) via i.v. injection on day 1 at 2 hours after the injection of 5-FU. When repeated doses of 5-FU were administered, the final dose contained [<sup>14</sup>C]5-FU as a label to trace 5-FU levels. At various time points post-injection, mice were euthanized via CO<sub>2</sub> asphyxiation. Blood was immediately collected via cardiac puncture, and centrifuged to separate the plasma. Organs were harvested and stored on ice, and transferred to -70°C within 1 h of collection. Samples were prepared for LSC for measurement of the associated radioactivity.

In preparation for LSC, tissue homogenates (10% weight/volume) were prepared in saline using a Polytron homogenizer (Brinkmann Instruments; Rexdale, Ontario, CA), and 0.5 mL of each homogenate was then digested in 0.5 mL of Solvalex (DuPont Canada; Mississauga, Ontario, CA) for 1 h at 50°C. After cooling to room temperature, samples were decolorized by the addition of 0.2 mL of 30% H<sub>2</sub>O<sub>2</sub>. These samples were then incubated overnight at 4°C to prevent excessive foaming. Scintillation cocktail was added to samples, and following dark-equilibration the radioactivity ([<sup>3</sup>H]CHE and [<sup>14</sup>C]5-FU) associated with the plasma and organs was quantitated via LSC.

In preparation for HPLC analysis, the second half of each organ was homogenized in ice-cold water. Drug and metabolites were

extracted from the homogenate using ice-cold acetonitrile/methanol (1:1 v/v) solution, and centrifugation at 14,000×g for 15 min to precipitate proteins. The supernatant was collected, and the concentrations of IRI (lactone and carboxylate forms) and SN-38 (lactone and carboxylate forms) in the organ supernatant and plasma samples were determined via HPLC. HPLC separation of IRI and SN-38 lactone and carboxylate forms was performed using a 250×4.6 mm C18 Symmetryshield column and C18 Symmetryshield guard column (Waters; Mississauga, Ontario, CA). Gradient elution was used with mobile phase A, composed of 75 mM ammonium acetate and 7.5 mM tetrabutylammonium bromide, adjusted to pH 6.4 with glacial acetic acid (Fisher Scientific; Nepean, Ontario, CA), and mobile phase B, composed of acetonitrile. Gradient profile was as follows: time = 0 min: 78% A:22% B, time = 10 min: 64% A:36% B, time = 12 min: 78% A:22% B, time = 20 min: 78% A:22% B. A 0.01 mL sample was injected onto the column (column temperature of 35°C) and eluted at a flow rate of 1 mL/min. The lactone and carboxylate forms of both IRI and SN-38 were detected using a Waters 2475 multi-wavelength fluorescence detector (Waters; Mississauga, Ontario, CA), set with time program events of  $\lambda_{ex} = 370$  nm,  $\lambda_{em} = 425$  nm between 0 and 12.5 min for the IRI lactone and IRI carboxylate, and  $\lambda_{ex} = 370$  nm,  $\lambda_{em} = 535$  nm between 12.5 and 20 min for the SN-38 lactone and SN-38 carboxylate. Prior to injection, all samples were maintained at 4°C to reduce conversion between the lactone and carboxylate forms of IRI or SN-38. Standard curves of the IRI lactone and SN-38 lactone were prepared by serial dilutions in a 2:1:1 sodium acetate (100 mM):methanol:acetonitrile (pH 4.0) buffer. For the IRI carboxylate and SN-38 carboxylate, serial dilutions were prepared in a 2:1:1 sodium borate (100 mM):methanol:acetonitrile (pH 9.0) buffer. The limit of quantitation for IRI and SN-38 lactone and carboxylate forms was 10 ng/mL. Plasma and tissue AUC values were calculated from concentration versus time curves (mean +/- standard deviation) using GraphPad Prism 5.00 software (GraphPad Software; La Jolla, California, US). Statistical significance for the PK/BD study was calculated via two-way analysis of variance with Bonferroni post-test using GraphPad Prism 5.00 software.

## Therapeutic Efficacy

The HT-29 tumor model was used to determine therapeutic efficacy. HT-29 cells (5 × 10<sup>6</sup> cells in 0.05 mL media) were injected subcutaneously (s.c.) into the central lower backs of female Rag2-M mice (6–9 weeks old). Tumors appeared within 2 weeks following cell inoculation, and, at this time, mice were randomly separated into treatment groups of 6 mice per group, unless otherwise indicated. Treatments were initiated when tumors had reached an average volume of ~150 mm<sup>3</sup> (0.5–0.7 cm in diameter), which occurred around day 14 post-cell inoculation. Treatments were administered to mice as follows: saline+D5W, 5-FU (16 mg/kg), IRI (60 mg/kg), IrC<sup>TM</sup> (40 or 60 mg IRI/kg), IRI +5-FU (60 mg/kg+16 mg/kg), or IrC<sup>TM</sup> +5-FU (40 or 60 mg IRI/kg +16 mg/kg). D5W and 5-FU were administered daily for 5 days (QD×5) each week for 3 weeks via i.p. injection; all other treatments were administered once per week for 3 weeks (Q7D×3) via i.v. injection into the lateral tail vein. When mice received two different agents, either IRI and 5-FU or IrC<sup>TM</sup> and 5-FU, on the same day, 5-FU was injected at 2 h prior to IRI or IrC<sup>TM</sup> administration. In order to increase the total 5-FU exposure time, daily dosing of 5-FU was employed [39], based on the regimen described by Saltz *et al.* [40,41], and the 16 mg/kg dose was selected after a dose escalation study determined that it was the MTD in Rag2-M mice (unpublished results). The highest IrC<sup>TM</sup> dose (60 mg IRI/kg) utilized in this study is well tolerated and is

approximately 66% of the MTD determined by our group for Rag2-M mice. Intersecting tumor dimensions were measured 3 times per week; tumor volume was calculated using  $(ab^2)/2$  (a, larger dimension; b, smaller dimension). Mice were euthanized if body weight loss (BWL) exceeded 20%, if tumor volume exceeded 1000 mm<sup>3</sup>, if tumor ulceration was observed, or if significant deteriorations were observed in mouse health (clinical score as defined by an approved standard operating procedure). When assessing fold tumor volume increase, the tumor size on day 0 (day of treatment initiation) was defined as 1.

## Results

### 5-FU and IRI Show Exposure Time Dependency as Single Agents and in Combination

Drug combination effects are dependent on a number of factors, including drug-drug ratios, the orders and time sequences of administration, and exposure times. Previous studies have shown a drug ratio dependency for IRI/floxuridine combinations [42]; a similar drug ratio dependency was also shown in the current studies with combinations of IRI/5-FU (data not shown). However, the studies described here additionally considered the role of drug exposure times on drug combination effects. This might be achieved, for example, with the use of drug infusions, an optimized drug administration schedule, or through the use of nanoparticle anti-cancer drug formulations designed for optimized drug release rates and enhanced drug exposure times. The effect of exposure time on cytotoxicity/cytostasis was determined for combinations of IRI/5-FU, and these data are summarized in Fig. 1. The therapeutic effects of 5-FU and IRI, when used alone, were highly dependent on exposure time (Fig. 1A–D). For the LS174T cell line, the IC<sub>50</sub> for IRI (0.3 μM; Fig. 1A) and 5-FU (3.0 μM; Fig. 1B) were over 100-fold lower when the drug exposure time was 72 h, relative to an exposure time of 1 h (44 μM and 330 μM, respectively). For the HT-29 cells, the IC<sub>50</sub> for 5-FU was 9 μM for a drug exposure time of 72 h, compared to 4000 μM for an exposure time of 1 h (Fig. 1D). Further, the IC<sub>50</sub> for IRI was not measurable in the HT-29 cells when the exposure time was 1, 4, or 8 h (Fig. 1C). It should be noted (see Methods) that in these studies, the toxicity assessments were determined at 72 h, and thus only the drug exposure time was varied here.

The cytotoxic effects of combinations of IRI/5-FU were determined for HT-29 cells for different exposure times. Short exposure times (1 h) produced strong antagonism, with CI values of greater than 5 at FA values of greater than 0.1 (Fig. 1E). In contrast, synergism (CI values less than 0.8) was observed over a broad range of FA values when the exposure time was increased to 48 h. At an FA value of 0.9 (i.e., the alamarBlue assay indicated a value that was 90% lower than that detected for the drug-free controls), the CI values were >10, 0.8, 0.9, and 0.4 when the exposure times were 1, 8, 48, and 72 h, respectively (Fig. 1F). These results suggest that exposure time is an important variable to consider when trying to measure drug-drug interactions in cell-based screening assays.

### PK/BD Studies Following Administration of 5-FU and IrC<sup>TM</sup> Alone and in Combination

For *in vivo* studies assessing the combination effects of IrC<sup>TM</sup> with 5-FU, it is important to first determine if one of the drugs alters the pharmacokinetics or biodistribution behavior of the other drug when they are co-administered (Fig. 2–4). The plasma elimination curves for 5-FU administered alone or in combination with IrC<sup>TM</sup> are summarized in Fig. 2A. When administered alone, 5-FU was rapidly cleared and the plasma levels of 5-FU were less

than 3% of the injected dose within 15 min of injection. The plasma AUC<sub>0–24h</sub> for 5-FU, co-administered with IrC<sup>TM</sup>, was almost 10-fold higher than that seen for 5-FU administered alone, a result that is most evident at time points beyond 1 h (Fig. 3A). The higher plasma 5-FU levels were also associated with higher levels of 5-FU in the liver, spleen, and lungs, but not the kidneys (Fig. 3A). The results suggest that 5-FU elimination was reduced when the drug was co-administered (i.v.) with IrC<sup>TM</sup>.

The plasma elimination curves for IRI lactone following the administration of IrC<sup>TM</sup> alone, or in combination with 5-FU, are shown in Fig. 2B. At the early time points up to 4 h post-injection, there was a small, but significant, decrease in the plasma levels of IRI lactone for animals injected with IrC<sup>TM</sup> in combination with 5-FU, versus IrC<sup>TM</sup> alone; at the 8 and 24 h time points, a more pronounced decrease in plasma IRI lactone levels was observed for mice that were co-administered IrC<sup>TM</sup>/5-FU, compared to single agent IrC<sup>TM</sup>. However, when assessing the plasma AUC<sub>0–24h</sub> data calculated for liposomal lipid (Fig. 3B), IRI in the lactone form (Fig. 3C) or carboxylate form (Fig. 3D), and SN-38 in the lactone form (Fig. 3E) the values were essentially equivalent to the plasma AUC<sub>0–24h</sub> determined following the administration of IrC<sup>TM</sup> alone. This was also reflected in the tissue AUC<sub>0–24h</sub> data (Fig. 3B–E), with the exception of the spleen, where elevated levels of IRI lactone and IRI carboxylate were observed following co-administration (i.v.) of IrC<sup>TM</sup>/5-FU, relative to IrC<sup>TM</sup> alone. HPLC analysis of IRI and SN-38 in the liver could not be performed in animals given IrC<sup>TM</sup> or IrC<sup>TM</sup>/5-FU, due to spectral interference from an unknown molecule that was co-extracted with IRI and SN-38 from the liver homogenate. Although the assay used in these studies was capable of detecting SN-38 in the carboxylate form, it was not detected in any plasma or tissue samples above the HPLC limit of detection of 10 ng/mL.

The efficacy studies described below assessed the activity of 5-FU (alone and in combination) using a dose intense (daily) schedule, a schedule which made it necessary to administer the drug intraperitoneally. The change in PK/BD noted above, when the drugs were both given intravenously, was also expected to be less of a concern when IrC<sup>TM</sup> was given i.v. and 5-FU was given i.p. The results presented in Fig. 4 address this study design. Consistent with the results in Fig. 3, the data suggest, at least at the early time points, that the plasma and organ concentrations of 5-FU are higher when IrC<sup>TM</sup> is administered in combination with 5-FU. This effect was less evident than when dosing both drugs i.v., as the 5-FU concentrations were not statistically different at most time points beyond 2 h. However, at 0.5 h post-injection, the 5-FU concentrations were higher in the liver (P<0.001; Fig. 4A), lung (P<0.05; Fig. 4C), kidney (P<0.001; Fig. 4D), and plasma (P<0.05; Fig. 4E) of mice that were given IrC<sup>TM</sup>/5-FU, relative to those animals that were given 5-FU alone. Compared to animals injected with 5-FU as a single agent, when mice received the combination of IrC<sup>TM</sup>/5-FU, 2-fold higher concentrations of 5-FU were detected in the liver at 0.5 h (P<0.001) and 1 h (P<0.01) post-injection, and a corresponding increase in the liver AUC<sub>0–8h</sub> of 5-FU (Fig. 4F) was also observed. The AUC<sub>0–8h</sub> of 5-FU in plasma (Fig. 4F) was ~1.5-fold higher following the administration of IrC<sup>TM</sup>/5-FU, when compared to animals given 5-FU alone. A substantial increase in the AUC<sub>0–8h</sub> of 5-FU in kidney (Fig. 4F) was observed when animals received an i.v. dose of IrC<sup>TM</sup>, compared to mice given 5-FU alone.

### Efficacy of 5-FU and IrC<sup>TM</sup> Alone and in Combination

The results of mouse studies assessing the efficacy of IRI and IrC<sup>TM</sup>, with and without 5-FU, for the treatment of CRC are presented in Fig. 5. Maximum mean BWL was used as a measure

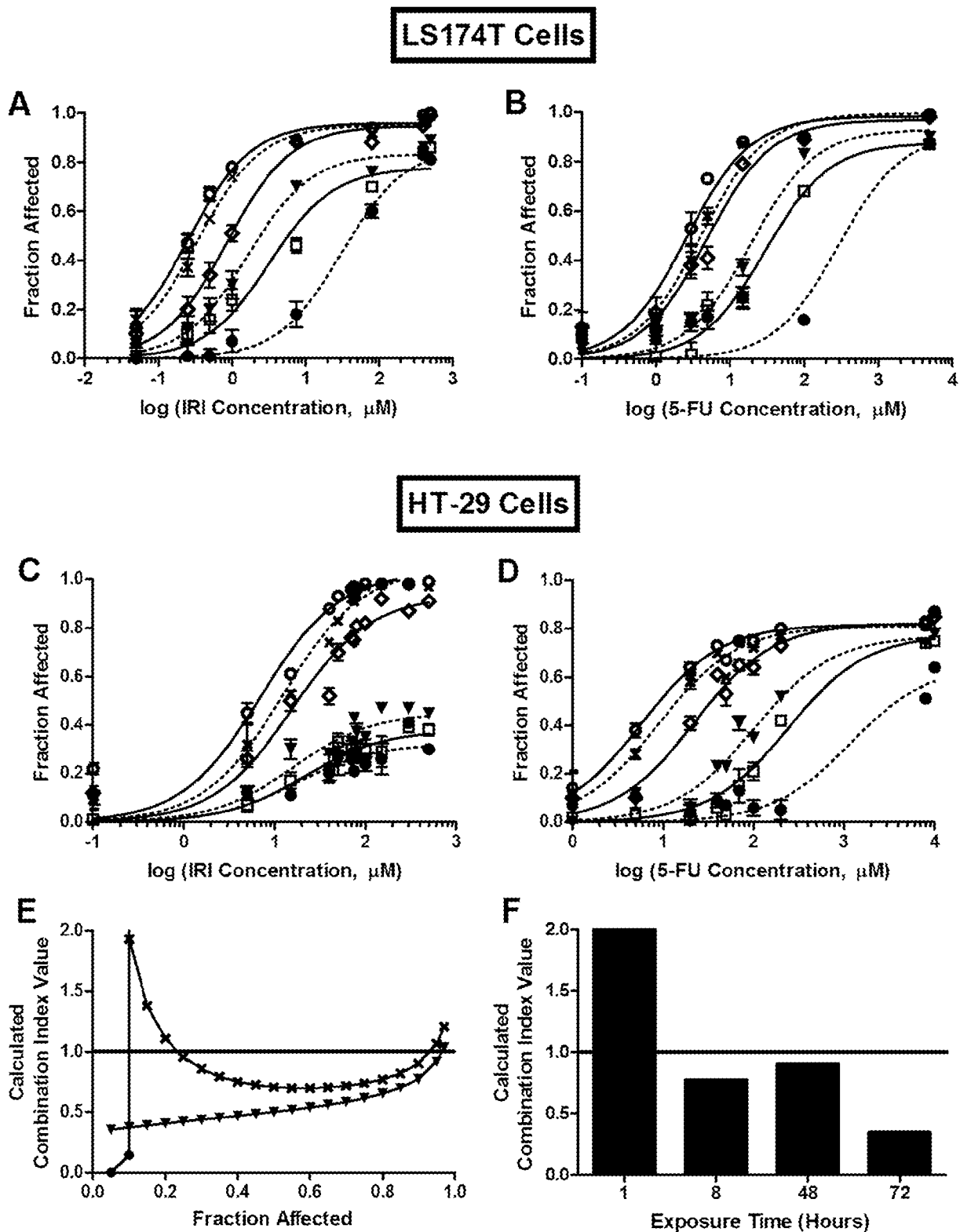


**Figure 1. Exposure time dependency of IRI and/or 5-FU cytotoxicity *in vitro*.** A–D) Single agent exposure time dependency. LS174T (A and B) and HT-29 (C and D) cells were exposed to IRI (A and C) or 5-FU (B and D) for 1 (●, dotted line), 4 (□, solid line), 8 (▼, dotted line), 24 (◇, solid line), 48 (X, dotted line), or 72 h (○, solid line). E) Combination exposure time dependency. HT-29 cells were exposed to IRI/5-FU (1:1 molar ratio) for 1 h (●), 8 h (▼), or 48 h (X). F) Calculated CI values at FA = 0.9 for HT-29 cells exposed to IRI/5-FU (1:1 molar ratio) for 1–72 h. A–D) Each point represents the mean  $\pm$  standard deviation ( $n = 3–9$ ) from 2–3 experiments, each completed in triplicate. E, F) Each point or bar represents a combination index value calculated from cytotoxicity data compiled from 2–4 separate experiments, each completed in triplicate. CI of 0.8 to 1.2 suggests additive interactions; CI < 0.8 suggests synergistic interactions; and CI > 1.2 suggests antagonistic interactions. doi:10.1371/journal.pone.0062349.g001

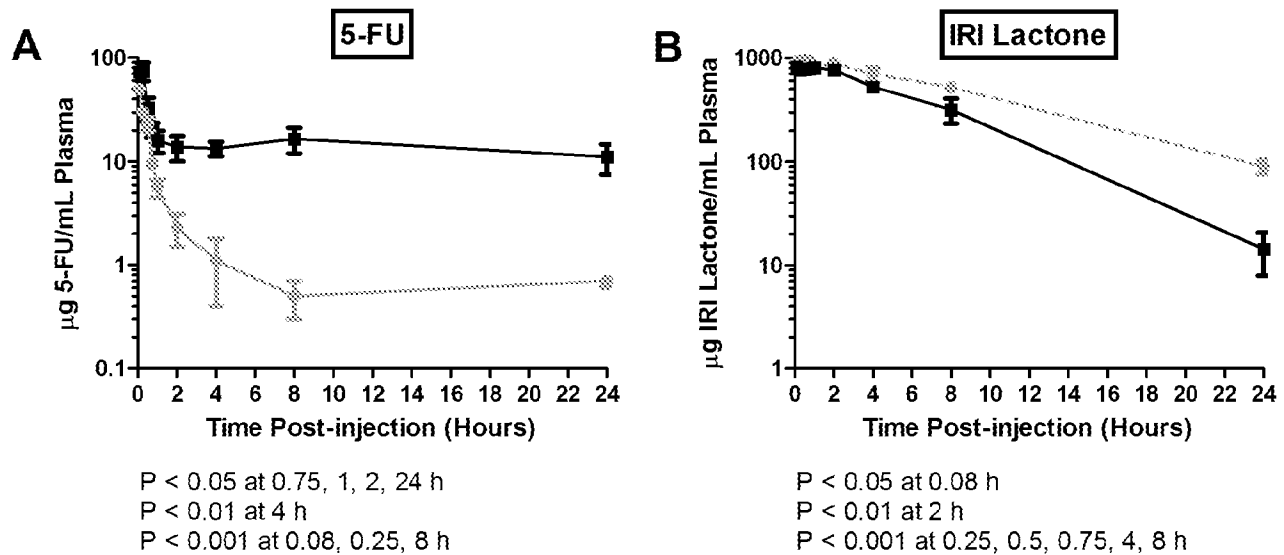


**Figure 2. Plasma clearance of 5-FU and IrC<sup>TM</sup> administered as single agents or co-administered.** Mice were injected i.v. with radio-labeled 5-FU (40 mg/kg) or IrC<sup>TM</sup> (40 mg IRI/kg), or both agents simultaneously. At various time points post-injection, the plasma concentrations of 5-FU and IRI (lactone) were determined. A) Mean plasma concentration of 5-FU  $\pm$  standard deviation ( $n=4$ ) after administration alone (solid gray line) or after co-administration with IrC<sup>TM</sup> (solid black line). B) Mean plasma concentration of IRI lactone  $\pm$  standard deviation ( $n=4$ ) after administration of IrC<sup>TM</sup> alone (dashed gray line) or after co-administration of IrC<sup>TM</sup> with 5-FU (solid black line). doi:10.1371/journal.pone.0062349.g002

of therapy-induced toxicity following treatment, and these data have also been summarized in Table 1. Free IRI was dosed at 60 mg/kg, which is the highest dose of free IRI that could be administered Q7D $\times$ 3 to Rag2-M mice without engendering greater than a 10% mean BWL, in addition to other changes in animal health status. The 5-FU dose of 16 mg/kg, administered QD $\times$ 5 each week for 3 weeks, was the maximum tolerated dose consistent with a maximum mean BWL of  $\sim$ 10%. As illustrated in Fig. 5, when used alone at this dose, 5-FU exhibited little therapeutic activity in this model. The time to reach a 5-fold increase in tumor volume was 23 days for control mice and 26 days for mice treated with 5-FU, a tumor growth delay of only 13%. The therapeutic benefits of free IRI given at 60 mg/kg were not substantially better; the time to reach a 5-fold increase in tumor size was 28 days (a growth delay of 22%). Single agent IrC<sup>TM</sup> (60 mg IRI/kg) exhibited substantial therapeutic effects, with some tumor regression noted shortly after the last treatment. The time to reach a 5-fold increase in tumor size was 49 days, a 113% tumor growth delay when compared to control.

When 5-FU (16 mg/kg) was combined with free IRI (60 mg/kg), there was a small, but not significant, improvement in therapeutic effect when compared to the effects of each drug used alone. The time to reach a 5-fold increase in tumor size was 30 days, compared to 23 days for control and 28 days for animals treated with IRI alone. The combination of IRI/5-FU resulted in an increase in toxicity that could be considered additive based on the effects of the agents when used alone. A maximum mean BWL of 16% was observed in animals treated with the combination. When used alone, each agent caused a maximum mean BWL of approximately 7% (IRI) or 9% (5-FU). When 5-FU (16 mg/kg) was combined with IrC<sup>TM</sup> (60 mg IRI/kg), a surprising increase in toxicity was observed. These animals showed dramatic weight loss ( $>20\%$ ) over the first week of dosing, and were euthanized prior to the start of the second treatment cycle. IrC<sup>TM</sup>, when given as a single agent at 60 mg IRI/kg, resulted in a mean BWL of 6.1% (Table 1). Due to increases in toxicity, the dose of IrC<sup>TM</sup> in the combination treatment was reduced to 40 mg IRI/kg. Treatment

with IrC<sup>TM</sup> (40 mg IRI/kg) alone resulted in a 91% tumor growth delay relative to control (a 5-fold increase in tumor volume by day 44). The toxicity at this dose, as judged by mean BWL, was comparable to that seen at the 60 mg IRI/kg dose (Table 1). Mice treated with the combination of 5-FU and IrC<sup>TM</sup> (40 mg IRI/kg) still showed an increase in toxicity (maximum mean BWL of 15.7%), but this dose was tolerated and allowed assessments of therapeutic activity. No further improvements in anti-tumor effects were observed when 40 mg IRI/kg IrC<sup>TM</sup> was combined with 5-FU. A 5-fold increase in tumor volume was observed on day 43. When compared to the equivalent dose of single agent IrC<sup>TM</sup> (40 mg IRI/kg), the same 5-fold increase was noted on day 44. Even with evidence suggesting that the combination resulted in increased toxicity, no gains in therapeutic activity were noted.

## Discussion

Evidence for the efficacy of IrC<sup>TM</sup> comes from a number of previous studies from our laboratory, which have demonstrated the significant therapeutic benefits of IrC<sup>TM</sup>, at doses that were 3- to 5-fold lower than the MTD of free IRI (60 mg/kg when given i.v. Q7D $\times$ 3 in Rag2-M mice (unpublished data)). These results were confirmed here using the HT-29 model of CRC, where single agent IrC<sup>TM</sup>, dosed at 40 or 60 mg IRI/kg, was well tolerated (causing less than 7% maximum mean BWL) and resulted in significant delays in tumor growth, including tumor regression at the higher dose. The objectives of the current studies, however, were to establish the therapeutic potential of prolonged exposure to IRI and 5-FU. This was assessed *in vitro* through evaluations of the cytotoxicity of free IRI and 5-FU, alone and in combination. Therapeutic activity was also measured *in vivo*, following treatment with IrC<sup>TM</sup> in combination with 5-FU administered via a dose-intensive daily schedule.

As noted above, the cytotoxicity assays were completed with free IRI to assess how the duration of IRI exposure affects its activity when used alone and in combination with 5-FU. Prolonged exposure to free IRI has been used to mimic the exposure to IRI

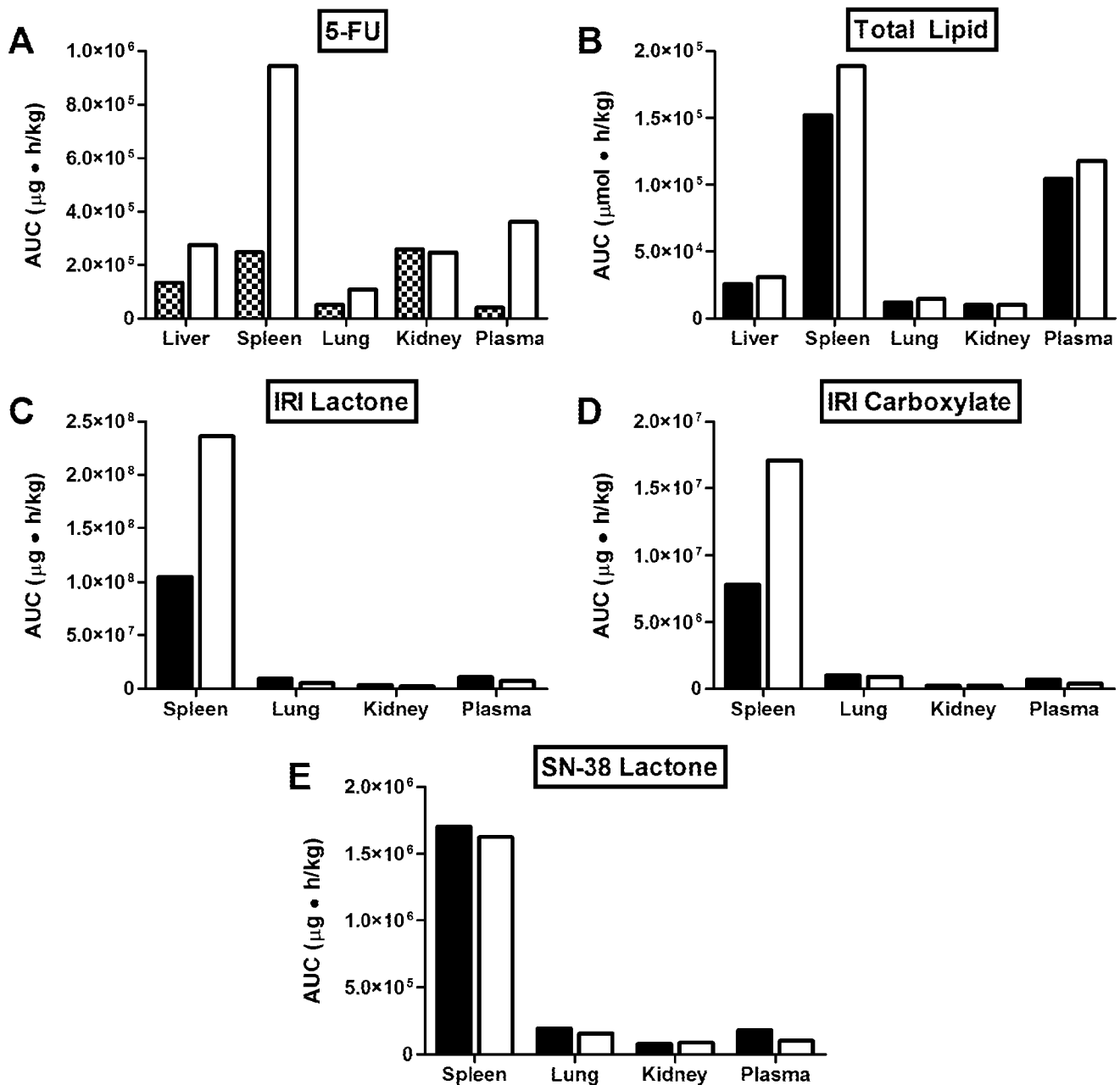


**Figure 3. Mean AUC<sub>0-24h</sub> of 5-FU and IrC<sup>TM</sup> administered i.v. as single agents or co-administered.** Mice were injected i.v. with radio-labeled 5-FU (40 mg/kg; hatched bars) or IrC<sup>TM</sup> (40 mg IRI/kg; black bars), or both agents simultaneously (white bars). At various time points post-injection, the plasma and organ concentrations of the lipid and drug species were determined, and AUC<sub>0-24h</sub> values were calculated from the resulting concentration-time curves. Data are presented as mean plasma and organ area under the curve (0–24 h) (n = 4) for 5-FU (A), total lipid (B), IRI lactone (C), IRI carboxylate (D), and SN-38 lactone (E).  
doi:10.1371/journal.pone.0062349.g003

achieved when administering the drug *in vivo*, in a well-designed drug carrier formulation, such as IrC<sup>TM</sup>. The *in vitro* results presented here (Fig. 1) show strong time-dependent cytotoxicity for both IRI and 5-FU against the target tumor cell population, and proved the synergistic activity of both drugs in combination, particularly when the drug exposure time was lengthened. These data helped to justify the *in vivo* investigations assessing the therapeutic potential of a combination of a sustained-release formulation of IRI (IrC<sup>TM</sup>) and 5-FU given via a dose-intense schedule (daily dosing). It could be argued that the ideal combination arising from the *in vitro* studies would include

a combination of a sustained-release formulation of 5-FU with IrC<sup>TM</sup>. Our lab has been developing a liposomal formulation of 5-FU [43] to pursue these studies in the future.

The studies summarized here are the first to assess the therapeutic potential of 5-FU combined with IrC<sup>TM</sup>. Nakajima *et al.* [22] have demonstrated therapeutic success in the treatment of HT-29 tumors when administering free 5-FU in combination with a micellar formulation of SN-38. These authors attribute the improved therapeutic effect of the combination (relative to free SN-38 and 5-FU) to prolonged drug exposure achieved when SN-38 is delivered via a polymeric formulation [22]. Previous research

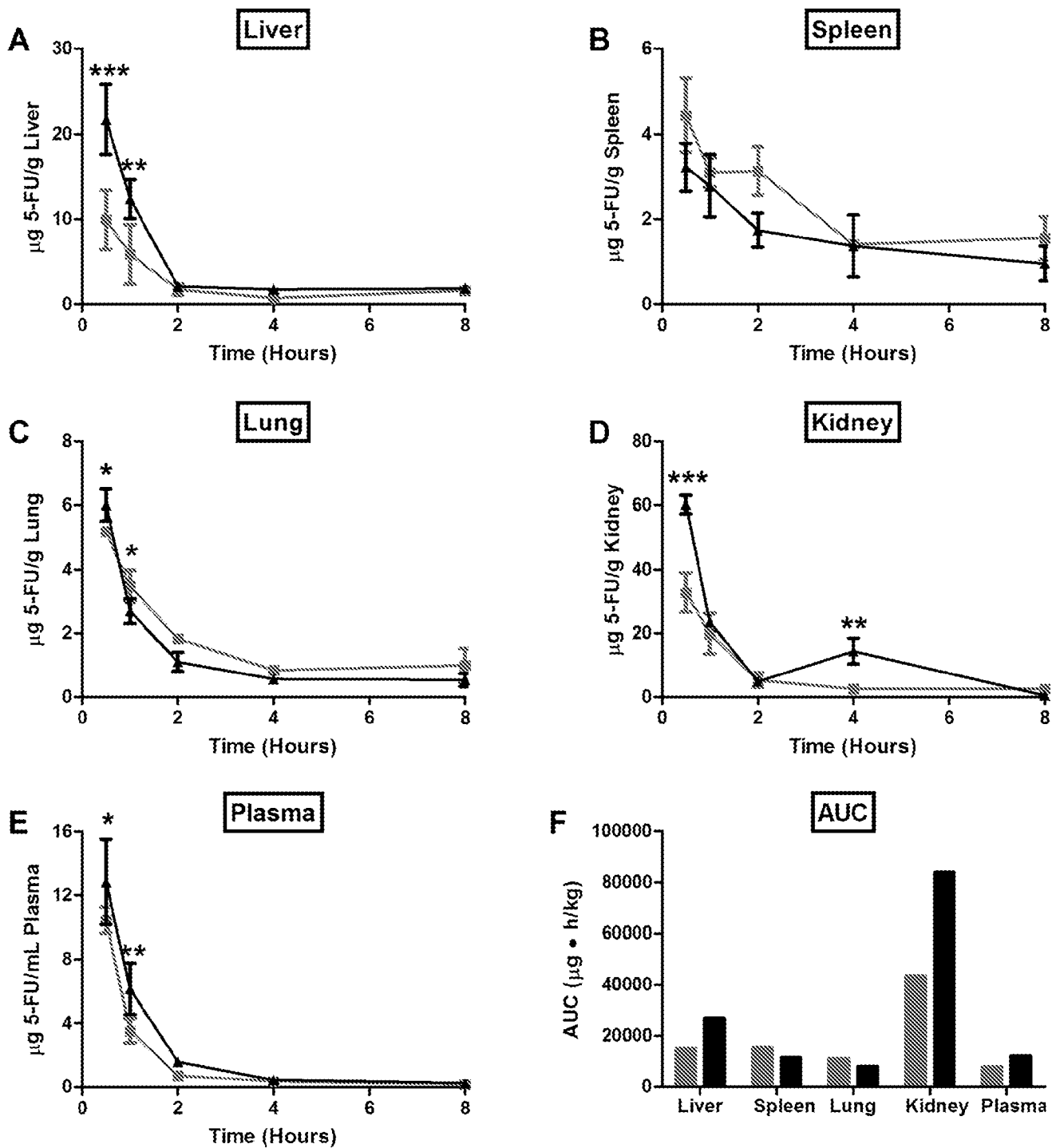


**Figure 4. PK/BD of 5-FU administered i.p. as a single agent or co-administered with IrC<sup>TM</sup>.** Mice were injected i.p. with 5-FU (16 mg/kg) on days 1 and 2 (gray line/bar); 5-FU was spiked with radio-labeled 5-FU on day 2. Half of the mice were also injected i.v. with IrC<sup>TM</sup> (60 mg IRI/kg) on day 1 (black line/bar), at 2 hours after the injection of 5-FU. At various time points post-injection, the plasma and tissue concentrations of 5-FU were determined, and AUC<sub>0-8h</sub> values were calculated from the resulting concentration-time curves. Data are presented as mean concentration of 5-FU in liver (A), spleen (B), lung (C), kidney (D), plasma (E) +/- standard deviation (n=3), or mean plasma and organ area under the curve (0-8 h) (n=3) for 5-FU (F).  
doi:10.1371/journal.pone.0062349.g004

from our lab has shown that animals that have been treated with IrC<sup>TM</sup> maintain SN-38 levels in the plasma compartment for extended time periods [21], and for this reason, it was reasonable

to expect that combinations of IrC<sup>TM</sup> and a dose-intense schedule of 5-FU would result in significant benefits.

Despite the clinical utility of the combination of IRI/5-FU [44], and the expectations of strong therapeutic activity for IrC<sup>TM</sup>/5-



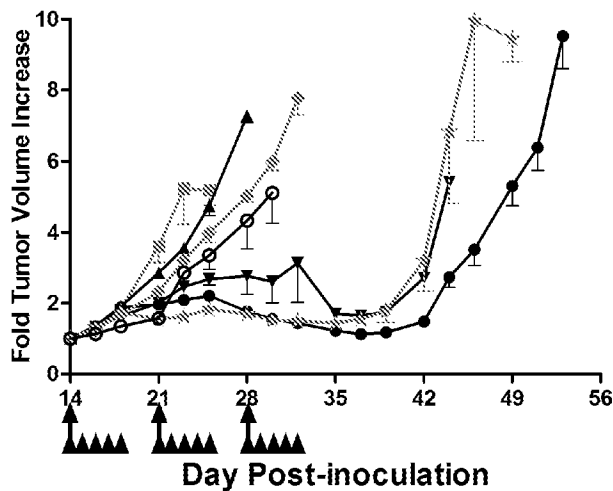


**Figure 5. Efficacy of IRI/5-FU and IrC<sup>TM</sup>/5-FU treatment in the HT-29 s.c. model of CRC.** Mice bearing s.c. HT-29 tumors were treated with saline+D5W (grey solid square), 5-FU (16 mg/kg; black solid upright triangle), IRI (60 mg/kg; grey solid diamond), IrC<sup>TM</sup> (40 or 60 mg IRI/kg; black solid inverted triangle or black solid circle, respectively), IRI +5-FU (60 mg/kg +16 mg/kg; black open circle), or IrC<sup>TM</sup> +5-FU (40 mg IRI/kg +16 mg/kg; grey solid star). Beginning on day 14, D5W and 5-FU were administered QD×5 (x 3 weeks) via i.p. injection (arrowheads); all other treatments were administered Q7D×3 via i.v. injection (full arrows). Data are presented as mean fold tumor volume increase ± standard error of the mean (n=6). doi:10.1371/journal.pone.0062349.g005

5-FU, our results convincingly demonstrated that the addition of 5-FU to IrC<sup>TM</sup> monotherapy provided no further benefit in the subcutaneous HT-29 model in mice. Increasing the exposure time of 5-FU has been shown by others to increase its efficacy [45,46]. However, the dose-intense schedule of 5-FU, while efficacious, resulted in only modest activity in the HT-29 model. In the clinic, systemic dosing of 5-FU via infusion is often preferred over i.v. bolus administration [45]. Infusions can mitigate toxicities associated with the peak plasma concentrations of 5-FU [47], and, more specifically, reduce the accumulation of 5-FU in bone marrow [48]. Interestingly, a number of recent clinical trials have investigated the therapeutic potential of post-operative biweekly i.p. injections of 5-FU in combination with systemically admin-

istered chemotherapy [49,50]. This type of adjunct 5-FU treatment has demonstrated good success. For example, Vaillant *et al.* [51] reported that treatment of post-operative stage II CRC patients with daily injections of i.p. 5-FU for 6 days, and no other chemotherapy, led to an increase in 5 year disease-free survival rates.

There are several possible explanations as to why there were no therapeutic benefits observed when using IrC<sup>TM</sup> in combination with daily injections of i.p. 5-FU. First, the choice of the HT-29 tumor model for *in vivo* studies may not have been ideal, as this model was reasonably insensitive to 5-FU, even when the drug was administered via a dose-intense daily schedule. It has been reported that the level of thymidylate synthase (TS) in tumor tissue may be correlated with response to 5-FU therapy [52]; thus, future studies should include careful consideration of the TS levels of different tumor models prior to experimentation. Another factor that should be considered here is the possibility of camptothecin-mediated down-regulation of dihydropyrimidine dehydrogenase (DPD) [53]. DPD is the enzyme primarily responsible for catabolising/detoxifying 5-FU [54]. Down-regulation of DPD can lead to fatal toxicities following 5-FU treatment, as has been observed clinically with DPD-deficient patients [55]. In addition, researchers have shown that treatment with SN-38 [56] or IRI [57] can lead to inhibition of TS, the target enzyme of 5-FU, thereby increasing cellular sensitivity to 5-FU and increasing the likelihood for toxicity. There is conflicting evidence about the effect of 5-FU on the metabolism of SN-38, with some studies showing no interaction between the drugs [58], and others suggesting that 5-FU may decrease the AUC of SN-38 [59] – although this may be dependent on the 5-FU dosing regimen [59] and/or the formulation used to enhance SN-38 exposure. At present, the interaction between the two drugs is not well understood.

Second, as highlighted by the results summarized in Fig. 2–4, the co-administration of IrC<sup>TM</sup>/5-FU changed the PK/BD properties of 5-FU, relative to the PK/BD of 5-FU when it was administered i.v. or i.p. as a single agent. Data revealed that, when given simultaneously with i.v. 5-FU, IrC<sup>TM</sup> engenders significant decreases in 5-FU elimination (Fig. 2A) and an associated increase in 5-FU plasma AUC<sub>0–24h</sub> (Fig. 3A). Similarly, when mice were treated with i.p. 5-FU (QD), with and without a single i.v. dose of IrC<sup>TM</sup> at 60 mg IRI/kg on day 1, there were significant changes in the PK/BD properties of 5-FU (Fig. 4). Specifically, statistically

**Table 1. Efficacy and toxicity of IRI, IrC<sup>TM</sup>, and 5-FU administered as single agents and in combination.**

Treatment	5-fold Tumor Volume Increase (Days)	Tumor Growth Delay vs. Control (%)	Mean Maximum BWL (+/- SEM) (%)
D5W+Saline	23	0	4.7+/- 0.3
5-FU (16 mg/kg) <sup>a</sup>	26	13.0	9.1+/- 3.4
IRI (60 mg/kg) <sup>a</sup>	28	21.7	7.0+/- 1.8
IrC <sup>TM</sup> (40 mg IRI/kg) <sup>b</sup>	44	91.3	6.9+/- 2.6
IrC <sup>TM</sup> (60 mg IRI/kg) <sup>b</sup>	49	113.0	6.1+/- 2.1
IRI +5-FU (60+16 mg/kg) <sup>a,b</sup>	30	30.4	15.7+/- 2.9
IrC <sup>TM</sup> +5-FU (40 mg IRI/kg +16 mg/kg) <sup>a,b</sup>	43	87.0	14.8+/- 1.2
IrC <sup>TM</sup> +5-FU (60 mg IRI/kg +16 mg/kg) <sup>a,b</sup>	N/A*	N/A*	21.4+/- 1.3

\*Unable to determine as treatment group euthanized early due to excessive BWL.

<sup>a</sup>Beginning on day 14 post-implantation, 5-FU was administered QD×5 for 3 weeks.

<sup>b</sup>Beginning on day 14 post-implantation, IRI and IrC<sup>TM</sup> were administered Q7D×3.

doi:10.1371/journal.pone.0062349.t001

significant increases in peak concentrations of 5-FU were observed in the plasma, kidney, and liver at 0.5 and/or 1 h post-injection, when 5-FU was co-administered with IrC<sup>TM</sup> at 60 mg IRI/kg when compared to mice who were administered 5-FU as a single agent. Associated changes in plasma and organ AUC<sub>0–8h</sub> values suggest that a drug-drug interaction occurs in mice when i.p. 5-FU is administered with IrC<sup>TM</sup>. It is not clear if similar increases in the 5-FU plasma AUC would be observed in a clinical setting following co-administration of IrC<sup>TM</sup>/5-FU.

Changes in the PK/BD of 5-FU are significant when considering the toxicity observed in the studies summarized here. Both 5-FU and IRI are known to be GI toxic agents [15,16,60,61,62]. GI toxicity is typically associated with BWL in mice and, unexpectedly, the combination of 5-FU (16 mg/kg) and IrC<sup>TM</sup> (60 mg IRI/kg) caused significant weight loss in the Rag2-M mice, even though the administered doses were well tolerated as monotherapies (see Table 1), suggestive of a synergistic toxicity. Clinical studies have noted increased adverse toxicities when employing dosing regimens where IRI is administered after 5-FU treatment [59]; thus, one could anticipate that the toxicities observed here may be mitigated by administering the two drugs in a different sequence. Importantly, when considering the mechanism of activity of these two drugs, changing the sequencing of when the drugs are administered may eliminate the drug-drug interactions that caused changes in PK/BD. This may in turn reduce toxicity while also enhancing therapeutic outcomes. Researchers have shown that the IRI treatment can cause an increase in the percentage of tumor cells in S-phase [56,63]. This, in turn, would increase the number of cells susceptible to the actions of 5-FU, which causes DNA damage to cells in S-phase following prolonged exposure. It has been suggested that this interaction between the effects of the drugs contributes to the synergistic efficacy observed in some tumor models when 5-FU and IRI were administered sequentially (IRI administered prior to 5-FU) [39,56,57,63,64]. Although these studies are beyond the scope of the objectives presented here, it will be important in future investigations to examine the effects of drug sequencing/timing on cell cycle progression to improve and optimize the therapeutic results for the combination of IrC<sup>TM</sup>/5-FU treatment.

Related to this point, it has been shown that IrC<sup>TM</sup> treatment can cause changes in tumor-associated blood vessels that are comparable to those observed when using anti-angiogenic drugs [29,31]. These changes have been described in the context of vascular normalization and it can be further suggested that

vascular normalization may promote enhanced delivery of small molecular weight drugs, such as 5-FU [31,65]. Thus, it could be anticipated that 5-FU should be administered after IrC<sup>TM</sup> has achieved normalization of tumor vasculature. This type of administration schedule is currently being tested in our lab. Further investigations of IRI/5-FU or IrC<sup>TM</sup>/5-FU combinations should also explore the use of 5-FU dosed in sustained-release formulations [43,66] or sustained-release formulations that contain both IRI and 5-FU at a fixed dose ratio [67,68]. Both of these dosing options may potentially have the advantage of making it possible to achieve synergistic drug ratios for an extended period of time at the target site [67,68,69], while minimizing exposure in sites of potential toxicities. This strategy has been shown to be important for producing synergistic anti-cancer effects with IRI/floxuridine [42] and other drug combinations [70,71]. Finally, it may be prudent to explore the use of leucovorin to potentiate the efficacy of 5-FU [72,73] in the HT-29 model.

## Conclusions

The importance of achieving prolonged exposure times to 5-FU and IRI, when used alone and in combination, was demonstrated through a series of *in vitro* cytotoxicity experiments evaluating drug synergies as a function of exposure time. *In vivo* studies revealed that 5-FU and IrC<sup>TM</sup>, when co-administered, caused significant changes in the PK/BD profile of 5-FU. Efficacy studies in a murine xenograft model of human CRC showed that single agent IrC<sup>TM</sup> was significantly more efficacious than the combination of free IRI/5-FU. Use of IrC<sup>TM</sup> alone resulted in a higher therapeutic index than the combination of IrC<sup>TM</sup>/5-FU, which caused significant increases in toxicities. Enhanced toxicity was likely due to IrC<sup>TM</sup>-engendered changes in the PK/BD of 5-FU. If 5-FU is to be used in combination with IrC<sup>TM</sup>, then studies exploring how efficacy and toxicity are influenced by different dose sequences need to be completed.

## Acknowledgments

The assistance of Dana Masin, Dita Strutt, Maryam Osooly, Christina Ostlund, and Hong Yan is gratefully acknowledged.

## Author Contributions

Conceived and designed the experiments: JH RN MW TA MB DW NDS. Performed the experiments: JH RN MA NH. Analyzed the data: JH MW MB DW. Wrote the paper: JH MW TA MB DW.

## References

- Jemal A, Bray F, Center MM, Ferlay J, Ward E, et al. (2011) Global cancer statistics. *CA Cancer J Clin* 61: 69–90.
- American Cancer Society (2008) *Global Cancer Facts & Figures 2nd Edition*. Atlanta: American Cancer Society.
- Ferlay J, Shin HR, Bray F, Forman D, Mathers C, et al. (2010) Estimates of worldwide burden of cancer in 2008: GLOBOCAN 2008. *Int J Cancer* 127: 2893–2917.
- American Cancer Society (2013) *Cancer Facts & Figures 2013*. Atlanta: American Cancer Society.
- American Cancer Society (2011) *Colorectal Cancer Facts & Figures 2011–2013*. Atlanta: American Cancer Society.
- Senter PD, Beam KS, Mixan B, Wahl AF (2001) Identification and activities of human carboxylesterases for the activation of CPT-11, a clinically approved anticancer drug. *Bioconjug Chem* 12: 1074–1080.
- Xu G, Zhang W, Ma MK, McLeod HL (2002) Human carboxylesterase 2 is commonly expressed in tumor tissue and is correlated with activation of irinotecan. *Clin Cancer Res* 8: 2605–2611.
- Humerickhouse R, Lohrbach K, Li L, Bosron WF, Dolan ME (2000) Characterization of CPT-11 hydrolysis by human liver carboxylesterase isoforms hCE-1 and hCE-2. *Cancer Res* 60: 1189–1192.
- Kawato Y, Aonuma M, Hirota Y, Kuga H, Sato K (1991) Intracellular roles of SN-38, a metabolite of the camptothecin derivative CPT-11, in the antitumor effect of CPT-11. *Cancer Res* 51: 4187–4191.
- Lavelle F, Bissery MC, Andre S, Roquet F, Riou JF (1996) Preclinical evaluation of CPT-11 and its active metabolite SN-38. *Semin Oncol* 23: 11–20.
- Khanna R, Morton CL, Danks MK, Potter PM (2000) Proficient metabolism of irinotecan by a human intestinal carboxylesterase. *Cancer Res* 60: 4725–4728.
- Guichard S, Terret C, Hennebelle I, Lochon I, Chevreau P, et al. (1999) CPT-11 converting carboxylesterase and topoisomerase activities in tumour and normal colon and liver tissues. *Br J Cancer* 80: 364–370.
- Rothenberg ML, Eckardt JR, Kuhn JG, Burris HA, 3rd, Nelson J, et al. (1996) Phase II trial of irinotecan in patients with progressive or rapidly recurrent colorectal cancer. *J Clin Oncol* 14: 1128–1135.
- Rothenberg ML, Cox JV, DeVore RF, Hainsworth JD, Pazdur R, et al. (1999) A multicenter, phase II trial of weekly irinotecan (CPT-11) in patients with previously treated colorectal carcinoma. *Cancer* 85: 786–795.
- Saliba F, Hagipantelli R, Misset JL, Bastian G, Vassal G, et al. (1998) Pathophysiology and therapy of irinotecan-induced delayed-onset diarrhea in patients with advanced colorectal cancer: a prospective assessment. *J Clin Oncol* 16: 2745–2751.
- Mathijssen RH, van Alphen RJ, Verweij J, Loos WJ, Nooter K, et al. (2001) Clinical pharmacokinetics and metabolism of irinotecan (CPT-11). *Clin Cancer Res* 7: 2182–2194.
- Fassberg J, Stella VJ (1992) A kinetic and mechanistic study of the hydrolysis of camptothecin and some analogues. *J Pharm Sci* 81: 676–684.

18. Rivory LP, Chatelut E, Canal P, Mathieu-Boue A, Robert J (1994) Kinetics of the in vivo interconversion of the carboxylate and lactone forms of irinotecan (CPT-11) and of its metabolite SN-38 in patients. *Cancer Res* 54: 6330–6333.
19. Burke TG, Mi Z (1994) The structural basis of camptothecin interactions with human serum albumin: impact on drug stability. *J Med Chem* 37: 40–46.
20. Drummond DC, Noble CO, Guo Z, Hong K, Park JW, et al. (2006) Development of a highly active nanoliposomal irinotecan using a novel intraliposomal stabilization strategy. *Cancer Res* 66: 3271–3277.
21. Ramsay EC, Anantha M, Zastre J, Meijs M, Zonderhuis J, et al. (2008) Irinophore C: a liposome formulation of irinotecan with substantially improved therapeutic efficacy against a panel of human xenograft tumors. *Clin Cancer Res* 14: 1208–1217.
22. Nakajima TE, Yasunaga M, Kano Y, Koizumi F, Kato K, et al. (2008) Synergistic antitumor activity of the novel SN-38-incorporating polymeric micelles, NK012, combined with 5-fluorouracil in a mouse model of colorectal cancer, as compared with that of irinotecan plus 5-fluorouracil. *Int J Cancer* 122: 2148–2153.
23. Hattori Y, Shi L, Ding W, Koga K, Kawano K, et al. (2009) Novel irinotecan-loaded liposome using phytic acid with high therapeutic efficacy for colon tumors. *J Control Release* 136: 30–37.
24. Ebrahimnejad P, Dinarvand R, Sajadi A, Jaafari MR, Nomani AR, et al. (2010) Preparation and in vitro evaluation of actively targetable nanoparticles for SN-38 delivery against HT-29 cell lines. *Nanomedicine* 6: 478–485.
25. Peng CL, Lai PS, Lin FH, Yueh-Hsiu Wu S, Shieh MJ (2009) Dual chemotherapy and photodynamic therapy in an HT-29 human colon cancer xenograft model using SN-38-loaded chlorin-core star block copolymer micelles. *Biomaterials* 30: 3614–3625.
26. Ramsay E, Alnajim J, Anantha M, Zastre J, Yan H, et al. (2008) A novel liposomal irinotecan formulation with significant anti-tumour activity: use of the divalent cation ionophore A23187 and copper-containing liposomes to improve drug retention. *Eur J Pharm Biopharm* 68: 607–617.
27. Ramsay E, Alnajim J, Anantha M, Taggar A, Thomas A, et al. (2006) Transition metal-mediated liposomal encapsulation of irinotecan (CPT-11) stabilizes the drug in the therapeutically active lactone conformation. *Pharm Res* 23: 2799–2808.
28. Patankar N, Anantha M, Ramsay E, Waterhouse D, Bally M (2011) The role of the transition metal copper and the ionophore A23187 in the development of Irinophore C. *Pharm Res* 28: 848–857.
29. Verreault M, Strutt D, Masin D, Anantha M, Yung A, et al. (2011) Vascular normalization in orthotopic glioblastoma following intravenous treatment with lipid-based nanoparticulate formulations of irinotecan (Irinophore C), doxorubicin (Caelyx(R)) or vincristine. *BMC Cancer* 11: 124–141.
30. Messerer CL, Ramsay EC, Waterhouse D, Ng R, Simms EM, et al. (2004) Liposomal irinotecan: formulation development and therapeutic assessment in murine xenograft models of colorectal cancer. *Clin Cancer Res* 10: 6638–6649.
31. Baker JH, Lam J, Kyle AH, Sy J, Oliver T, et al. (2008) Irinophore C, a novel nanoformulation of irinotecan, alters tumor vascular function and enhances the distribution of 5-fluorouracil and doxorubicin. *Clin Cancer Res* 14: 7260–7271.
32. Fields RD, Lancaster MV (1993) Dual-attribute continuous monitoring of cell proliferation/cytotoxicity. *Am Biotechnol Lab* 11: 48–50.
33. Page B, Page M, Noel C (1993) A new fluorometric assay for cytotoxicity measurements in vitro. *Int J Oncol* 3: 473–476.
34. Chou TC, Talalay P (1984) Quantitative analysis of dose-effect relationships: the combined effects of multiple drugs or enzyme inhibitors. *Adv Enzyme Regul* 22: 27–55.
35. Chou TC (2006) Theoretical basis, experimental design, and computerized simulation of synergism and antagonism in drug combination studies. *Pharmacol Rev* 58: 621–681.
36. Hope MJ, Bally MB, Mayer LD, Janoff AS, Cullis PR (1986) Generation of multilamellar and unilamellar phospholipid vesicles. *Chem Phys Lipids* 40: 89–96.
37. Hope MJ, Bally MB, Webb G, Cullis PR (1985) Production of large unilamellar vesicles by a rapid extrusion procedure. Characterization of size distribution, trapped volume and ability to maintain a membrane potential. *Biochim Biophys Acta* 812: 55–65.
38. Pool GL, French ME, Edwards RA, Huang L, Lumb RH (1982) Use of radiolabelled hexadecyl cholesterol ether as a liposome marker. *Lipids* 17: 445–452.
39. Guichard S, Cussac D, Hennebelle I, Bugat R, Canal P (1997) Sequence-dependent activity of the irinotecan-5FU combination in human colon-cancer model HT-29 in vitro and in vivo. *Int J Cancer* 73: 729–734.
40. Saltz LB, Cox JV, Blanke C, Rosen LS, Fehrenbacher L, et al. (2000) Irinotecan plus fluorouracil and leucovorin for metastatic colorectal cancer. *Irinotecan Study Group. N Engl J Med* 343: 905–914.
41. Saltz LB, Douillard JY, Pirotta N, Alakl M, Gruia G, et al. (2001) Irinotecan plus fluorouracil/leucovorin for metastatic colorectal cancer: a new survival standard. *Oncologist* 6: 81–91.
42. Harasym TO, Tardi PG, Harasym NL, Harvie P, Johnstone SA, et al. (2007) Increased preclinical efficacy of irinotecan and floxuridine coencapsulated inside liposomes is associated with tumor delivery of synergistic drug ratios. *Oncol Res* 16: 361–374.
43. Thomas AM, Kapanen AI, Hare JI, Ramsay E, Edwards K, et al. (2011) Development of a liposomal nanoparticle formulation of 5-fluorouracil for parenteral administration: formulation design, pharmacokinetics and efficacy. *J Control Release* 150: 212–219.
44. Hwang JJ (2004) Irinotecan and 5-FU/leucovorin in metastatic colorectal cancer: balancing efficacy, toxicity, and logistics. *Oncology (Williston Park)* 18: 26–34.
45. Meta-analysis Group In Cancer (1998) Efficacy of intravenous continuous infusion of fluorouracil compared with bolus administration in advanced colorectal cancer. *J Clin Oncol* 16: 301–308.
46. Liu C, Willingham M, Liu J, Gmeiner WH (2002) Efficacy and safety of FdUMP[10] in treatment of HT-29 human colon cancer xenografts. *Int J Oncol* 21: 303–308.
47. Sugarbaker PH, Gianola FJ, Speyer JL, Wesley R, Barofsky I, et al. (1985) Prospective randomized trial of intravenous v intraperitoneal 5-FU in patients with advanced primary colon or rectal cancer. *Semin Oncol* 12: 101–111.
48. Fraile RJ, Baker LH, Buroker TR, Horwitz J, Vaitkevicius VK (1980) Pharmacokinetics of 5-fluorouracil administered orally, by rapid intravenous and by slow infusion. *Cancer Res* 40: 2223–2228.
49. Fajardo AD, Tan B, Reddy R, Fleshman J (2012) Delayed repeated intraperitoneal chemotherapy after cytoreductive surgery for colorectal and appendiceal carcinomatosis. *Dis Colon Rectum* 55: 1044–1052.
50. Tan BR, Mutch M, Picus J, Dietz D, Birnbaum E, et al. (2005) Bi-weekly intraperitoneal (IP) 5FU chemotherapy with systemic oxaliplatin-based therapy in patients with pseudomyxoma peritonei (PP) and peritoneal carcinomatosis (PC) from colorectal cancer (CRC). *American Society of Clinical Oncology Meetings: Abstract #272*.
51. Vaillant JC, Nordlinger B, Deuffic S, Arnaud JP, Pelissier E, et al. (2000) Adjuvant intraperitoneal 5-fluorouracil in high-risk colon cancer: A multicenter phase III trial. *Ann Surg* 231: 449–456.
52. Leichman CG, Lenz HJ, Leichman L, Danenberg K, Baranda J, et al. (1997) Quantitation of intratumoral thymidylate synthase expression predicts for disseminated colorectal cancer response and resistance to protracted-infusion fluorouracil and weekly leucovorin. *J Clin Oncol* 15: 3223–3229.
53. Miyazaki K, Shibahara T, Sato D, Uchida K, Suzuki H, et al. (2006) Influence of chemotherapeutic agents and cytokines on the expression of 5-fluorouracil-associated enzymes in human colon cancer cell lines. *J Gastroenterol* 41: 140–150.
54. Heggie GD, Sommadossi JP, Cross DS, Huster WJ, Diasio RB (1987) Clinical pharmacokinetics of 5-fluorouracil and its metabolites in plasma, urine, and bile. *Cancer Res* 47: 2203–2206.
55. van Kuilenburg AB, Muller EW, Haasjes J, Meinsma R, Zoetekouw L, et al. (2001) Lethal outcome of a patient with a complete dihydropyrimidine dehydrogenase (DPD) deficiency after administration of 5-fluorouracil: frequency of the common IVS14+1G>A mutation causing DPD deficiency. *Clin Cancer Res* 7: 1149–1153.
56. Mullany S, Svingen PA, Kaufmann SH, Erlichman C (1998) Effect of adding the topoisomerase I poison 7-ethyl-10-hydroxycamptothecin (SN-38) to 5-fluorouracil and folinic acid in HCT-8 cells: elevated dTTP pools and enhanced cytotoxicity. *Cancer Chemother Pharmacol* 42: 391–399.
57. Guichard S, Hennebelle I, Bugat R, Canal P (1998) Cellular interactions of 5-fluorouracil and the camptothecin analogue CPT-11 (irinotecan) in a human colorectal carcinoma cell line. *Biochem Pharmacol* 55: 667–676.
58. Saltz LB, Kanowitz J, Kemeny NE, Schaaf L, Spriggs D, et al. (1996) Phase I clinical and pharmacokinetic study of irinotecan, fluorouracil, and leucovorin in patients with advanced solid tumors. *J Clin Oncol* 14: 2959–2967.
59. Falcone A, Di Paolo A, Masi G, Allegrini G, Danesi R, et al. (2001) Sequence effect of irinotecan and fluorouracil treatment on pharmacokinetics and toxicity in chemotherapy-naïve metastatic colorectal cancer patients. *J Clin Oncol* 19: 3456–3462.
60. Wiseman LR, Markham A (1996) Irinotecan. A review of its pharmacological properties and clinical efficacy in the management of advanced colorectal cancer. *Drugs* 52: 606–623.
61. Houghton JA, Houghton PJ, Wooten RS (1979) Mechanism of induction of gastrointestinal toxicity in the mouse by 5-fluorouracil, 5-fluorouridine, and 5-fluoro-2'-deoxyuridine. *Cancer Res* 39: 2406–2413.
62. Machover D (1997) A comprehensive review of 5-fluorouracil and leucovorin in patients with metastatic colorectal carcinoma. *Cancer* 80: 1179–1187.
63. Azrak RG, Cao S, Slocum HK, Toth K, Durrani FA, et al. (2004) Therapeutic synergy between irinotecan and 5-fluorouracil against human tumor xenografts. *Clin Cancer Res* 10: 1121–1129.
64. Mans DR, Grivicich I, Peters GJ, Schwartzmann G (1999) Sequence-dependent growth inhibition and DNA damage formation by the irinotecan-5-fluorouracil combination in human colon carcinoma cell lines. *Eur J Cancer* 35: 1851–1861.
65. Jain RK (2001) Normalizing tumor vasculature with anti-angiogenic therapy: a new paradigm for combination therapy. *Nat Med* 7: 987–989.
66. Barone C, Landriscina M, Quirino M, Basso M, Pozzo C, et al. (2007) Schedule-dependent activity of 5-fluorouracil and irinotecan combination in the treatment of human colorectal cancer: in vitro evidence and a phase I dose-escalating clinical trial. *Br J Cancer* 96: 21–28.
67. Mayer LD, Harasym TO, Tardi PG, Harasym NL, Shew CR, et al. (2006) Ratiometric dosing of anticancer drug combinations: controlling drug ratios after systemic administration regulates therapeutic activity in tumor-bearing mice. *Mol Cancer Ther* 5: 1854–1863.
68. Mayer LD, Janoff AS (2007) Optimizing combination chemotherapy by controlling drug ratios. *Mol Interv* 7: 216–223.

69. Pavillard V, Kherfella D, Richard S, Robert J, Montaudon D (2001) Effects of the combination of camptothecin and doxorubicin or etoposide on rat glioma cells and camptothecin-resistant variants. *Br J Cancer* 85: 1077–1083.
70. Tardi PG, Dos Santos N, Harasym TO, Johnstone SA, Zisman N, et al. (2009) Drug ratio-dependent antitumor activity of irinotecan and cisplatin combinations in vitro and in vivo. *Mol Cancer Ther* 8: 2266–2275.
71. Tardi P, Johnstone S, Harasym N, Xie S, Harasym T, et al. (2009) In vivo maintenance of synergistic cytarabine:daunorubicin ratios greatly enhances therapeutic efficacy. *Leuk Res* 33: 129–139.
72. Arbuck SG (1989) Overview of clinical trials using 5-fluorouracil and leucovorin for the treatment of colorectal cancer. *Cancer* 63: 1036–1044.
73. Advanced Colorectal Cancer Meta-Analysis Project (1992) Modulation of fluorouracil by leucovorin in patients with advanced colorectal cancer: evidence in terms of response rate. *Advanced Colorectal Cancer Meta-Analysis Project. J Clin Oncol* 10: 896–903.